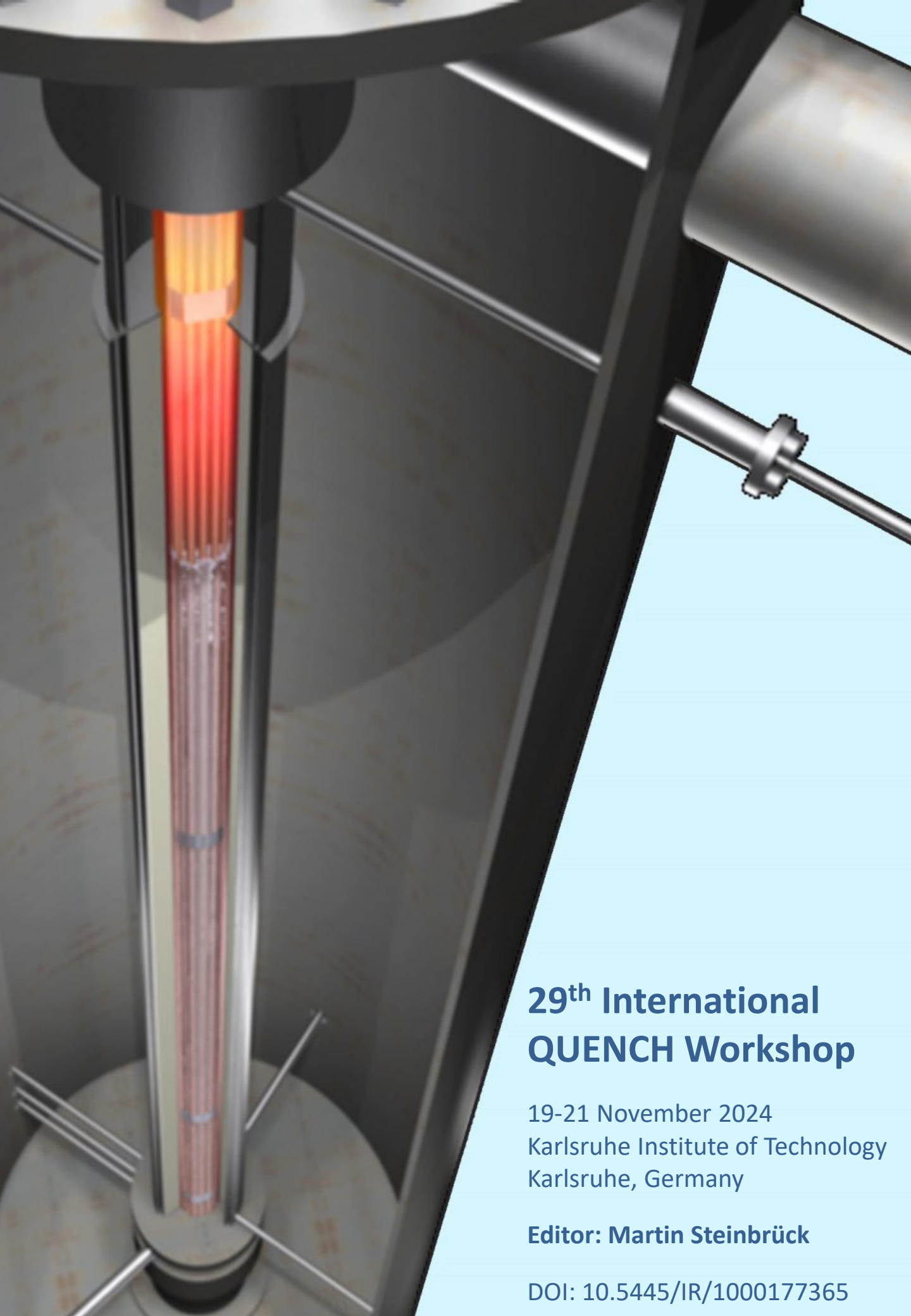

29th International QUENCH Workshop

19-21 November 2024
Karlsruhe Institute of Technology
Karlsruhe, Germany

Editor: Martin Steinbrück

DOI: 10.5445/IR/1000177365

AGENDA

29th International QUENCH Workshop

Karlsruhe Institute of Technology, Campus North, H.-von-Helmholtz-Platz 1, 76344 Egg.-Leopoldshafen, Germany
19-21 November 2024

Meeting Location: Fortbildungszentrum für Technik und Umwelt (FTU), Auditorium (Aula)

Tuesday, 19 Nov 2024

8:30	**Registration**	
9:00	Welcome	W. Tromm/M. Steinbrück, KIT
9:20	Update of the QUENCH Program	M. Steinbrück, KIT
	ATF CLADDING I (Chair: M. Grosse, KIT)	
9:50	Promising ATF cladding materials and their oxidation behavior at (very) high temperature	M. Steinbrück, KIT
10:20	Some illustrations of recent learnings and studies carried out at CEA on the behavior of Cr-coated Zr-based Claddings upon High Temperature Oxidation in relation with their Post-Quenching mechanical properties	J.-C. Brachet, CEA
10:50	**Coffee break (Group Photo)**	
11:20	Accident Tolerant Fuel: Cr Coated Cladding Development at Westinghouse	K. Frederick, WEC
11:40	Behaviour of Cr-coated cladding bundles under BDBA conditions at the DEGREE facility	K. Nakamura, CRIEPI
12:00	The CODEX-ATF-AIT integral air ingress experiment	R. Farkas, pres. by N. Ver, HUN-REN
12:30	**Lunch**	
	ATF CLADDING II (Chair: S. Weick, KIT)	
13:30	High-temperature single-rod tests on oxidation of Cr coated claddings, performed at KIT in the framework of the IAEA project ATF-TS	J. Stuckert, KIT
14:00	Behaviour of Fuel Cladding with Cr Coating during LOCA and Study of Cr Diffusion into Zr-alloy	A. Endrychova, UJP
14:20	Cr-Nb Coated Zr as a Suitable ATF Candidate for BWRs	M. Sevecek, CTU
14:40	High Temperature Steam Oxidation Tests in the Framework of the SCORPION Project	M. Grosse, KIT
15:10	**Coffee break**	

15:40	Integral LOCA Experiment to Investigate Comprehensive Accident Behavior of Cr-Coated Accident Tolerant Fuel (ATF)	Y. Lee, SNU
16:10	High temperature creep during LOCA conditions	J. Krejci, UJP
16:30	A Visual Experimental Study on Fuel Cladding Steam Oxidation and Ballooning	T. Liu, SJTU

Wednesday, 20 Nov 2024

9:00	***ATF-Session contd.:***	A. Charbal, CEA
	Chromium coating cracking quantification methods: recent developments and results	
	MODELLING AND CODE APPLICATION - ATF (Chair: E. Rouge, IRSN)	
9:30	Current Activities in PSS Research Projects: AC² Applications with a Focus on ATF	G. Stahlberg, RUB
9:50	ATF Modelling with AC2	L. Lovasz, GRS
10:10	FeCrAl Oxidation Model Development on the ASTEC Code and Preliminary Validation Against QUENCH Experiments	Z.E. Jiménez Balbuen, KIT
10:30	**Coffee break**	
11:00	Development and Assessment of ATF cladding materials for DBA and BDBA conditions using SCDAPSIM	C. Allison, ISS pres. by V. Martinez, ENSO
11:30	Results of the QUENCH-ATF-1 Benchmark within OECD/NEA QUENCH-ATF	T. Hollands, GRS
12:00	**Lunch**	
	MODELLING AND CODE APPLICATION (Chair: T. Hollands, GRS)	
13:30	Development and Assessment of ASYST SCDAPSIM modeling options for Lower Head Failure and Melt Relocation into the Reactor Cavity	C. Allison, ISS pres. by V. Martinez, ENSO
13:50	Integration and Preliminary Validation of a Thermal-Mechanical Fuel Rod Model for ATHLET	V.A. Di Nora, KIT
14:10	Evaluation of a BDBA Quench Sequence in a Generic iPWR with Natural Circulation: Application of the QUENCH-06 Experiment.	M.E. Cazado, KIT
14:30	Coffee break + Time for discussion/lab visits	
16:00	**Bus to Hambach for wine tasting and invited dinner**	

Thursday, 21 Nov 2024

8:30	**Pick-up at the hotel**	
	LONG-TERM DRY STORAGE – SYSTEM ZR-H (Chairs: J.-C- Brachet, CEA, M.Grosse, KIT))	
9:00	Conduction and analysis of the long-term SPIZWURZ bundle test	S. Weick, KIT
9:30	GRS Analytical Support to the SPIZWURZ Project	A. Rezchikova, GRS
9:50	Hydrogen diffusion and precipitation in nuclear cladding	J. Bertsch, PSI

10:20	**Coffee break**	
10:50	Hydrogen Quantification in Non-irradiated Zirconium Cladding after Various Oxidation Conditions	O. Yetik, PSI
11:10	Hydrogen diffusion in dependence of the grain size of Zircaloy-4 cladding tubes	S. Weick, KIT
11:30	Hydride orientation in fuel rod cladding: comparison of two competing simulation approaches	M. Kolesnik, KIT
11:50	**Closure of the Workshop**	M. Steinbrück, KIT


29th International QUENCH Workshop

Walter Tromm

KIT

Outlook Programme NUSAFE at KIT and Helmholtz Association

The NUSAFE program manager provided an overview on the nuclear safety research at KIT including reactor safety and safety for decommissioning and storage.

Welcome Address:

29th International QUENCH Workshop at KIT

Outlook Programme NUSAFE at KIT and Helmholtz Association

Th. Walter Tromm, Programme Nuclear Waste Management, Safety and Radiation Research




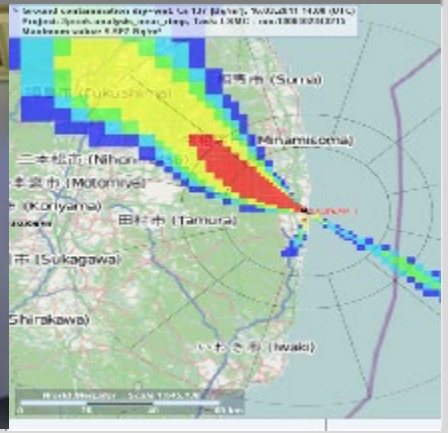

Program Nuclear Waste Management, Safety and Radiation Research (NUSAFE)

Topic 1 „Nuclear Waste Management

- Subtopic 1: Nuclear waste disposal
- Subtopic 2: Predisposal
- Subtopic 3: Fundamental scientific aspects

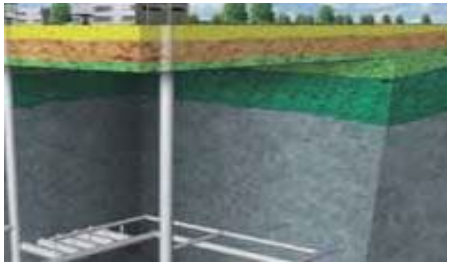

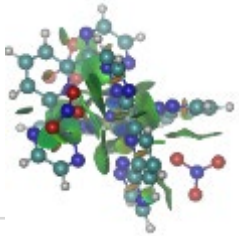

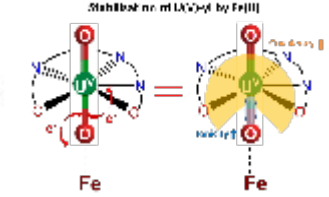

Work program and outlook

Subtopic 2: Predisposal

- Only chair in Germany dedicated to the decommissioning of nuclear facilities
  - Tool box for the development of tailored decommissioning concepts ready
  - Enhanced application of Building Information Modelling (BIM): interaction with industry

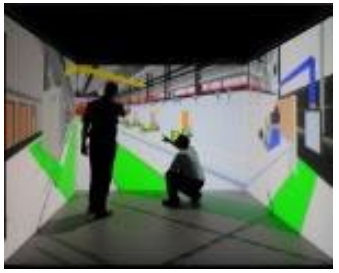

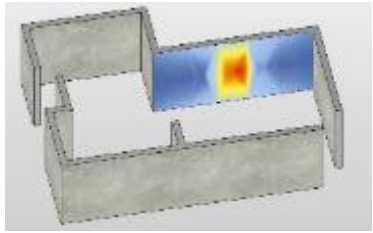

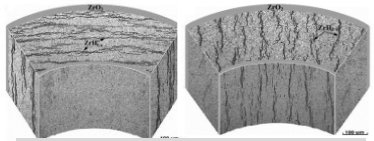

Cladding embrittlement by hydride reorientation and chemical reactions

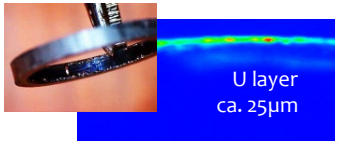

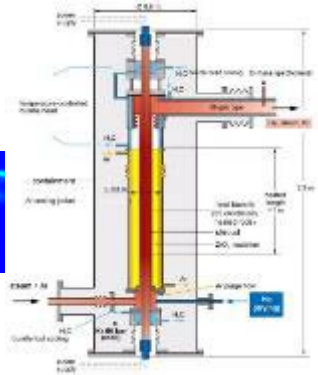

- SNF rod behavior under extended interim storage conditions examined and quantified (focus on physical/chemical embrittlement mechanisms): consequences for final disposal

Work program and outlook

HOVER Project: New Laboratory infrastructure investment at KIT (supported by the HELMHOLTZ association)

- Virtual laboratories for decommissioning activities (BIM) – *partly in operation*
- Facility for studies on fuel cladding under thermal conditions in an interim storage facility (Zr-hydride reorientation) - *in operation*
- Micro/spectroscopy laboratory to investigate RN behaviour in heterogeneous systems - *in operation*
- Ultrasensitive analysis of RN by Accelerator Mass Spectrometry (AMS) (URL experiments, environmental radioanalysis, status-quo-ante characterisation of nuclear sites (decommissioning, storage, disposal)) – *commissioning in 2025/26*

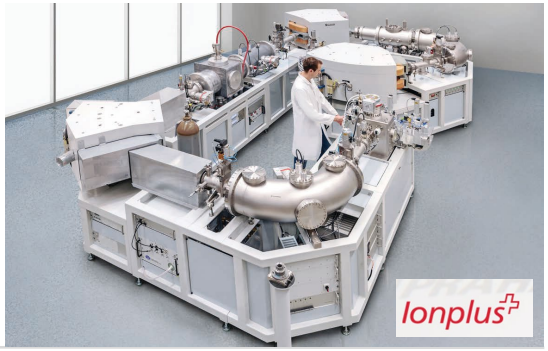

NUSAFE Program

Topic 2 Reactor Safety

- **Subtopic 1: Design Basis Accidents and Material Research**

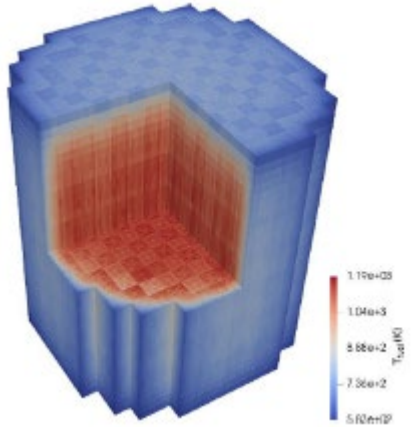

- **Subtopic 2: Beyond Design Basis Accidents and Emergency Management**

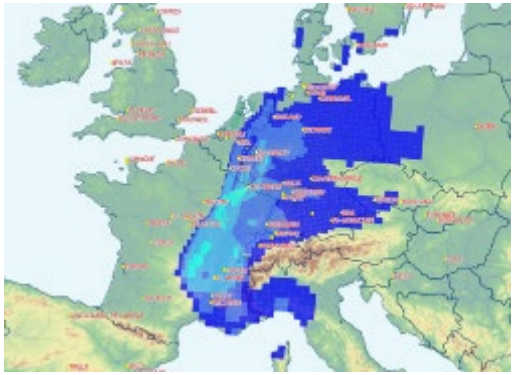

Motivation: Nuclear Technology Developments in LWRs

Karlsruhe Institute of Technology

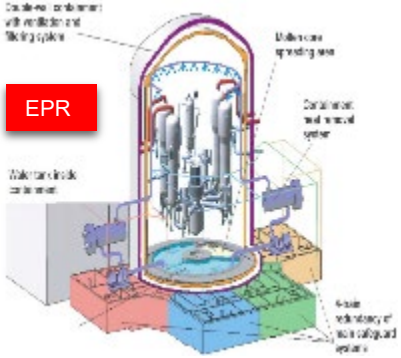

EPR

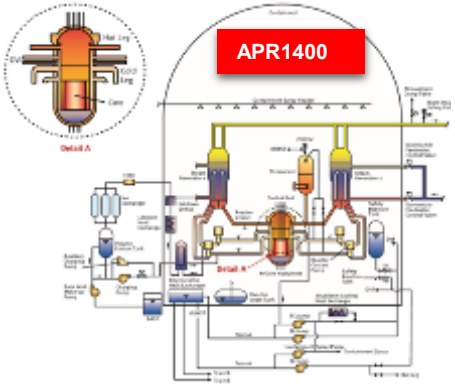

APR1400

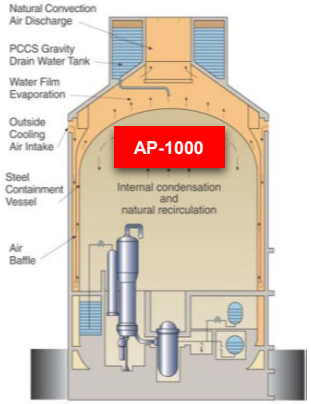

AP-1000

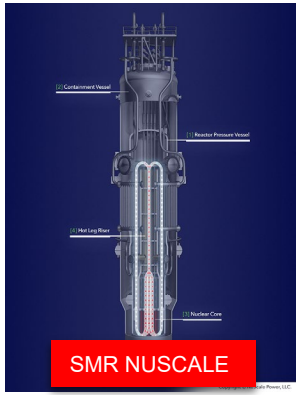

SMR NUSCALE

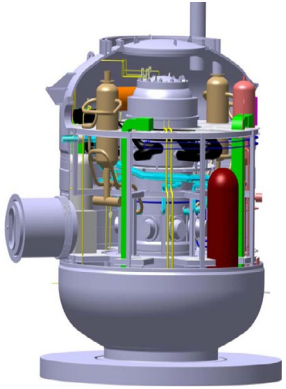

SMR NUWARD

SMR AP 300

SMR GE Hitachi

Multi-physics (core) and multi-scale (plant) analyses

- Increasing the prediction accuracy, the fidelity, and the spatial discretization of computational domains
- From pin-by-pin analysis up to plant analysis

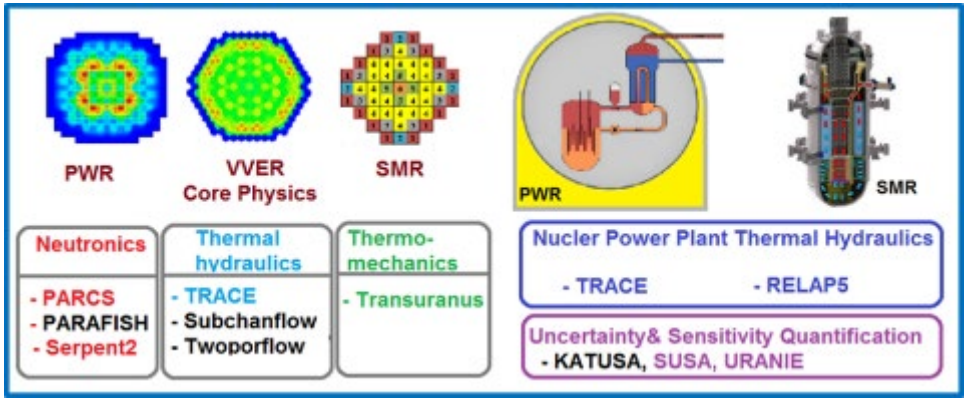

Pin-by-pin core analysis

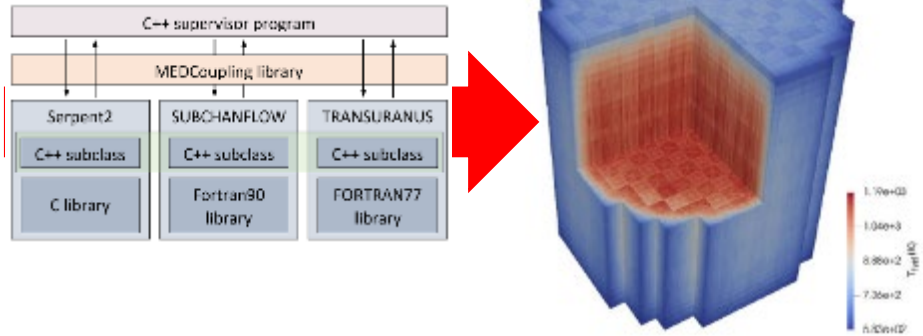

COSMOS-H facility

- Experimental investigation of, e.g.,
  - safety-relevant TH phenomena e.g. boiling, CHF, cross flow
  - natural circulation flow/forced convection transition

Outlook:

- New reactor concepts, SMRs:
  - Experiments under natural convection conditions
- New cladding materials, ATF
- Fundamental studies for code validation:
  - Generation of high-resolution (CFD-grade) data

COSMOS-H

QUENCH Facility: ATF-related Future Tests

Outlook:

- OECD/NEA QUENCH-ATF Joint Undertaking Phase II under discussion
- Experiments planned in the QUENCH- and COSMOS-H facility at KIT

‘The QUENCH facility hosted at KIT and the expertise of the associated staff are unique and unrivalled assets which provide the international community with invaluable data…... ‘

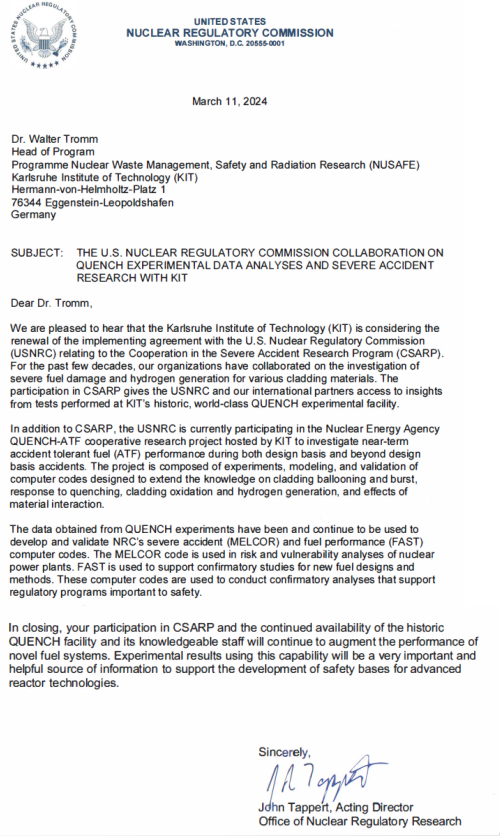

UNITED STATES
NUCLEAR REGULATORY COMMISSION
WASHINGTON, D.C. 20555-0001

March 11, 2024

Dr. Walter Tromm
Head of Program
Programme Nuclear Waste Management, Safety and Radiation Research (NUSAFE)
Karlsruhe Institute of Technology (KIT)
Hermann-von-Helmholtz-Platz 1
76344 Eggenstein-Leopoldshafen
Germany

SUBJECT: THE U.S. NUCLEAR REGULATORY COMMISSION COLLABORATION ON QUENCH EXPERIMENTAL DATA ANALYSES AND SEVERE ACCIDENT RESEARCH WITH KIT

Dear Dr. Tromm,

We are pleased to hear that the Karlsruhe Institute of Technology (KIT) is considering the renewal of the implementing agreement with the U.S. Nuclear Regulatory Commission (USNRC) relating to the Cooperation in the Severe Accident Research Program (CSARP). For the past few decades, our organizations have collaborated on the investigation of severe fuel damage and hydrogen generation for various cladding materials. The participation in CSARP gives the USNRC and our international partners access to insights from tests performed at KIT's historic, world-class QUENCH experimental facility.

In addition to CSARP, the USNRC is currently participating in the Nuclear Energy Agency QUENCH-ATF cooperative research project hosted by KIT to investigate near-term accident tolerant fuel (ATF) performance during both design basis and beyond design basis accidents. The project is composed of experiments, modeling, and validation of computer codes designed to extend the knowledge on cladding ballooning and burst, response to quenching, cladding oxidation and hydrogen generation, and effects of material interaction.

The data obtained from QUENCH experiments have been and continue to be used to develop and validate NRC's severe accident (MELCOR) and fuel performance (FAST) computer codes. The MELCOR code is used in risk and vulnerability analyses of nuclear power plants. FAST is used to support confirmatory studies for new fuel designs and methods. These computer codes are used to conduct confirmatory analyses that support regulatory programs important to safety.

In closing, your participation in CSARP and the continued availability of the historic QUENCH facility and its knowledgeable staff will continue to augment the performance of novel fuel systems. Experimental results using this capability will be a very important and helpful source of information to support the development of safety bases for advanced reactor technologies.

Sincerely,

John Tappert, Acting Director
Office of Nuclear Regulatory Research

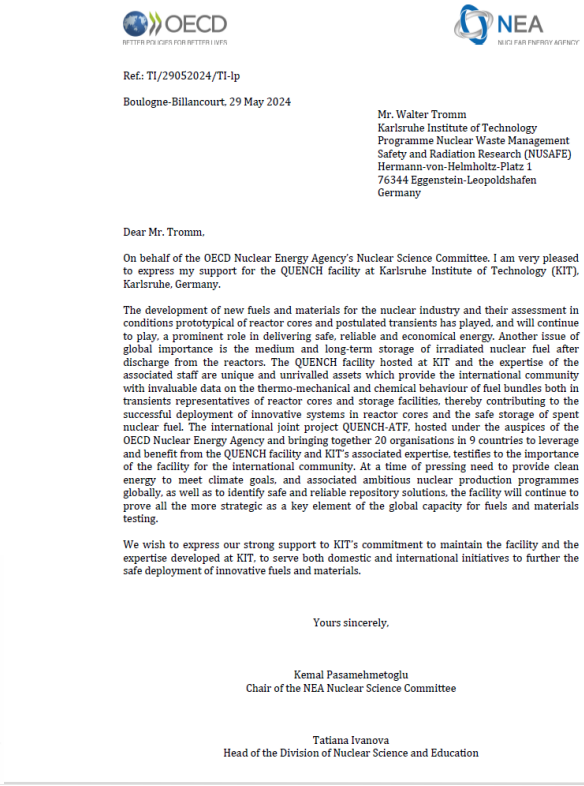

OECD
NEA

Ref.: TI/29052024/TI-lp

Boulogne-Billancourt, 29 May 2024

Mr. Walter Tromm
Karlsruhe Institute of Technology
Programme Nuclear Waste Management
Safety and Radiation Research (NUSAFE)
Hermann-von-Helmholtz-Platz 1
76344 Eggenstein-Leopoldshafen
Germany

Dear Mr. Tromm,

On behalf of the OECD Nuclear Energy Agency's Nuclear Science Committee. I am very pleased to express my support for the QUENCH facility at Karlsruhe Institute of Technology (KIT), Karlsruhe, Germany.

The development of new fuels and materials for the nuclear industry and their assessment in conditions prototypical of reactor cores and postulated transients has played, and will continue to play, a prominent role in delivering safe, reliable and economical energy. Another issue of global importance is the medium and long-term storage of irradiated nuclear fuel after discharge from the reactors. The QUENCH facility hosted at KIT and the expertise of the associated staff are unique and unrivalled assets which provide the international community with invaluable data on the thermo-mechanical and chemical behaviour of fuel bundles both in transients representatives of reactor cores and storage facilities, thereby contributing to the successful deployment of innovative systems in reactor cores and the safe storage of spent nuclear fuel. The international joint project QUENCH-ATF, hosted under the auspices of the OECD Nuclear Energy Agency and bringing together 20 organisations in 9 countries to leverage and benefit from the QUENCH facility and KIT's associated expertise, testifies to the importance of the facility for the international community. At a time of pressing need to provide clean energy to meet climate goals, and associated ambitious nuclear production programmes globally, as well as to identify safe and reliable repository solutions, the facility will continue to prove all the more strategic as a key element of the global capacity for fuels and materials testing.

We wish to express our strong support to KIT's commitment to maintain the facility and the expertise developed at KIT, to serve both domestic and international initiatives to further the safe deployment of innovative fuels and materials.

Yours sincerely,

Kemal Pasamehmetoglu
Chair of the NEA Nuclear Science Committee

Tatiana Ivanova
Head of the Division of Nuclear Science and Education

Motivation: Technology Developments in Innovative Reactor Concepts

Karlsruhe Institute of Technology

SAM SAFER

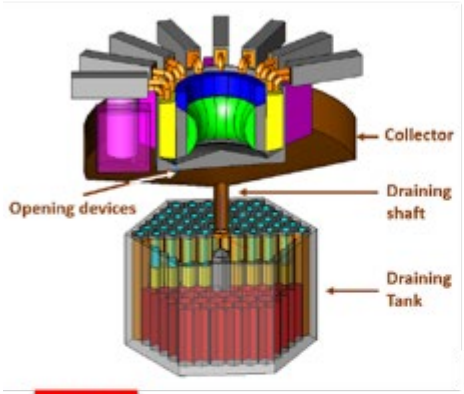

MSR

LFR

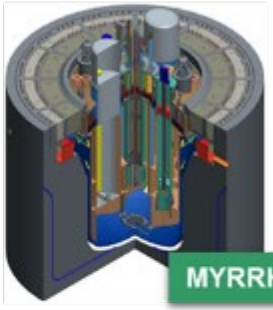

MYRRHA

ALFRED

ESFR-SMART

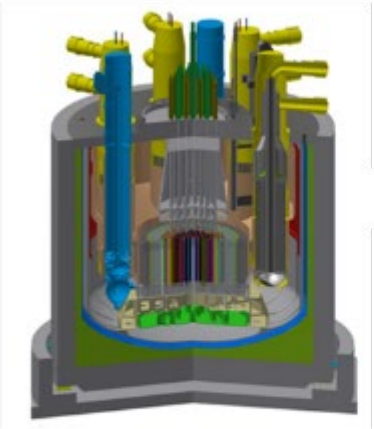

GFR

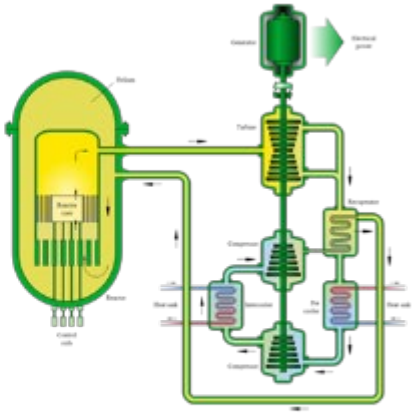

KALLA Laboratory
EU Project PATRICIA

- Partitioning And Transmuter Research Initiative Collaborative Innovation Action (2020-2024) (Lead: SCK-CEN)
- KIT: fuel rod bundle experiments with liquid metal Realistic blockage in 19-pin bundle

EU Project TRANSPARANT

- Technological Research Action Necessary for Safe PARtitioning And Nuclear Transmutation (2024-2028), (Lead: SCK-CEN)
- Testing of deformed bundle heated tests
  - Experiments on pin to wall and pin to pin contact

fuel rod bundle

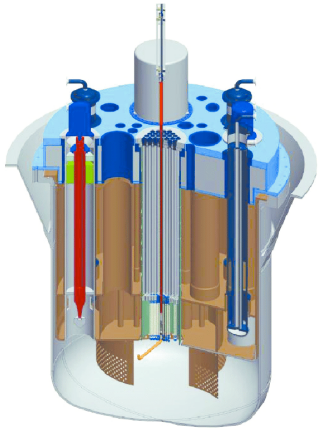

ADS MYRRHA reactor

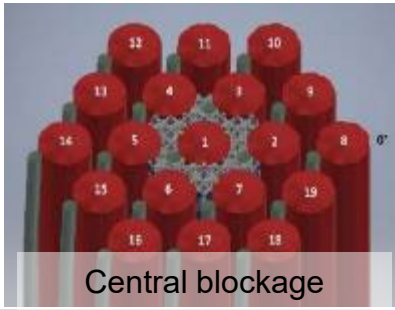

Central blockage

EU-project: INNUMAT - INNovative strUctural MATerials for fission and fusion (Coordinator: KIT)

- Development and qualification of innovative materials solutions for the increase of technology readiness level (TRL)
- Cross cutting aspects dealing with innovative materials for fission, fusion and also non-nuclear energies
- KIT involved in all major material research tracks

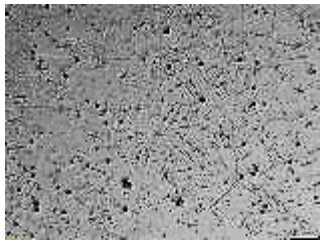

Austenitic microstructure after annealing at 1150°C

Materials:

- HEAs/CCAs
  (High entropy alloys / Compositionally complex alloys)
- AFA steels
  (Alumina forming Austenitic steels)
- Coated 15-15Ti
- Weld overlay

Reactor application

- Molten salt reactor
- Heavy metal cooled reactor
- Fusion DEMO

Materials Research: Outlook:

EU-projects LESTO and CONNECT-NM start in 2024:

- LESTO - LEad fast reactor Safety design and Tools
  - 24 European partners – 6Mill€ EU funding
- CONNECT-NM: Co-funded European partnership

Bilateral projects:

- NDA signed with NEWCLEO
  - first topics for cooperation are identified
- Informal relations with SEALER

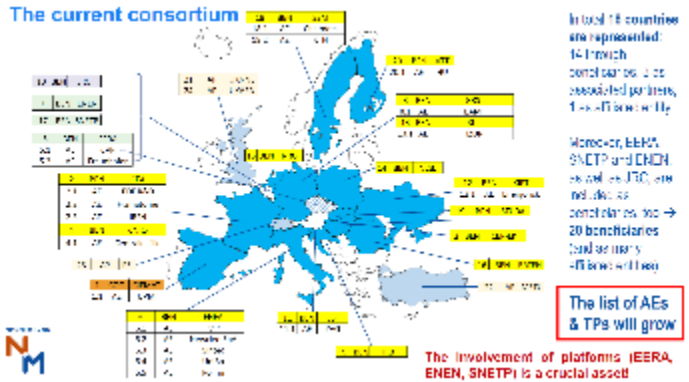

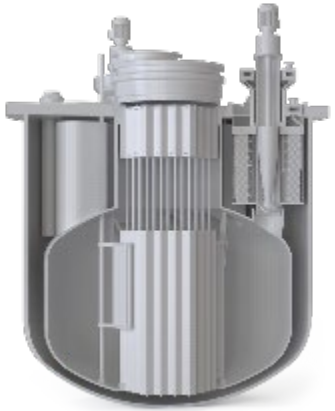

Subtopic 2: Beyond Design Basis Accidents

- Realistic assessments of fission product release and dispersion into the environment in case of severe accidents in NPPs, i.e. PWR, VVER-1000, BWR, SMRs, AMRs
- **Calculation platform:**
  - Status of the core when the SA occurs, i.e. burn-up (multiphysics analyses)
  - Analysis of accident scenarios for different initiators (integral codes)
  - ASTEC (KIT/IRSN agreement, including source-code shared with KIT)
  - MELCOR (USNRC/KIT Cooperative Severe Accident Research Program, CSARP)
  - Quantification of uncertainty and prediction accuracy (in-house KATUSA and FSTC tool)
  - Emergency management support for beyond-design-basis events (JRODOS)
  - Artificial intelligence algorithms to improve the performance of the ASTEC code and source term prediction (on-going)

Subtopic 2: BDBA, Outlook

- ‘Classical’ route: ASTEC + JRODOS (analysis of a single scenario)
- ‘Expanded’ route: ASTEC + KATUSA (UQ) + JRODOS
  → **improvement in the definition of the Emergency Planning Zones**

‘Classical’ Route

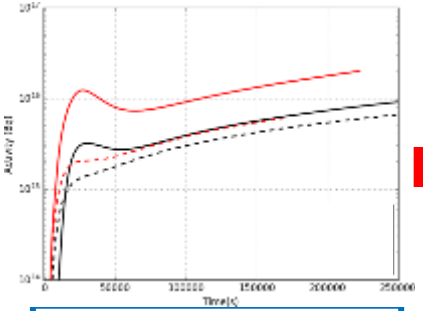

‘Expanded’ Route

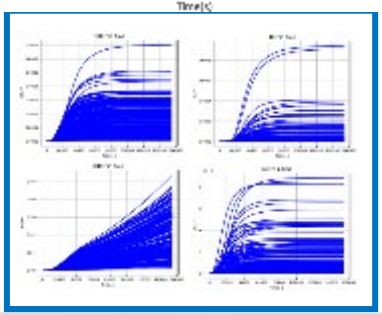

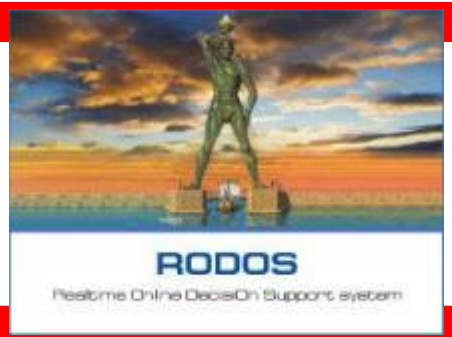

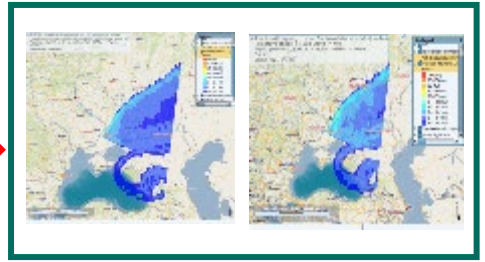

Outlook: Continuation of the work in HGF-PoF V

- Strong and internationally requested expertise in specific fields of nuclear safety research
- Strong cooperation within Europe and international
- Experimental facilities and infrastructures state-of-the-art
- Indispensable to be an attractive research platform for education and training of next generation experts

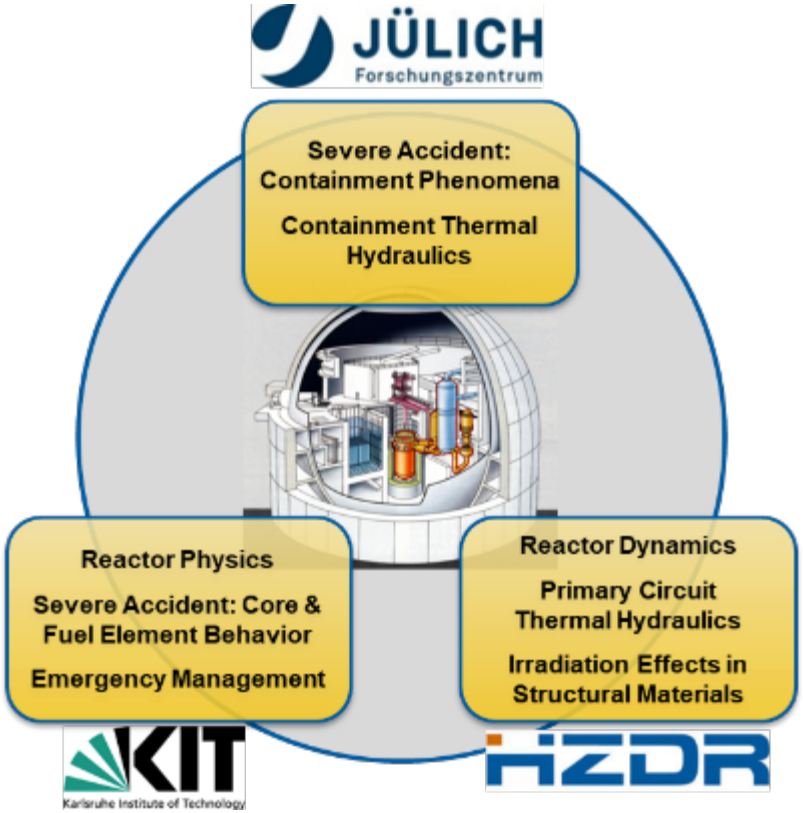

JRC Nuclear Foresight Workshop on Shaping the Future for Nuclear Safety, Security and Safeguards

First workshop conducted on 24th November 2023 at the JRC-Karlsruhe in conjunction with “60 Years of JRC Nuclear Safety and Security”

2nd Foresight Workshop:
Pilot project: Joint commitment to maintaining and developing nuclear capabilities and expertise in Germany
11th / 12 th November 2024
JRC Karlsruhe

- Young Italian perspectives on nuclear careers
- BMBF activities to maintain nuclear capabilities

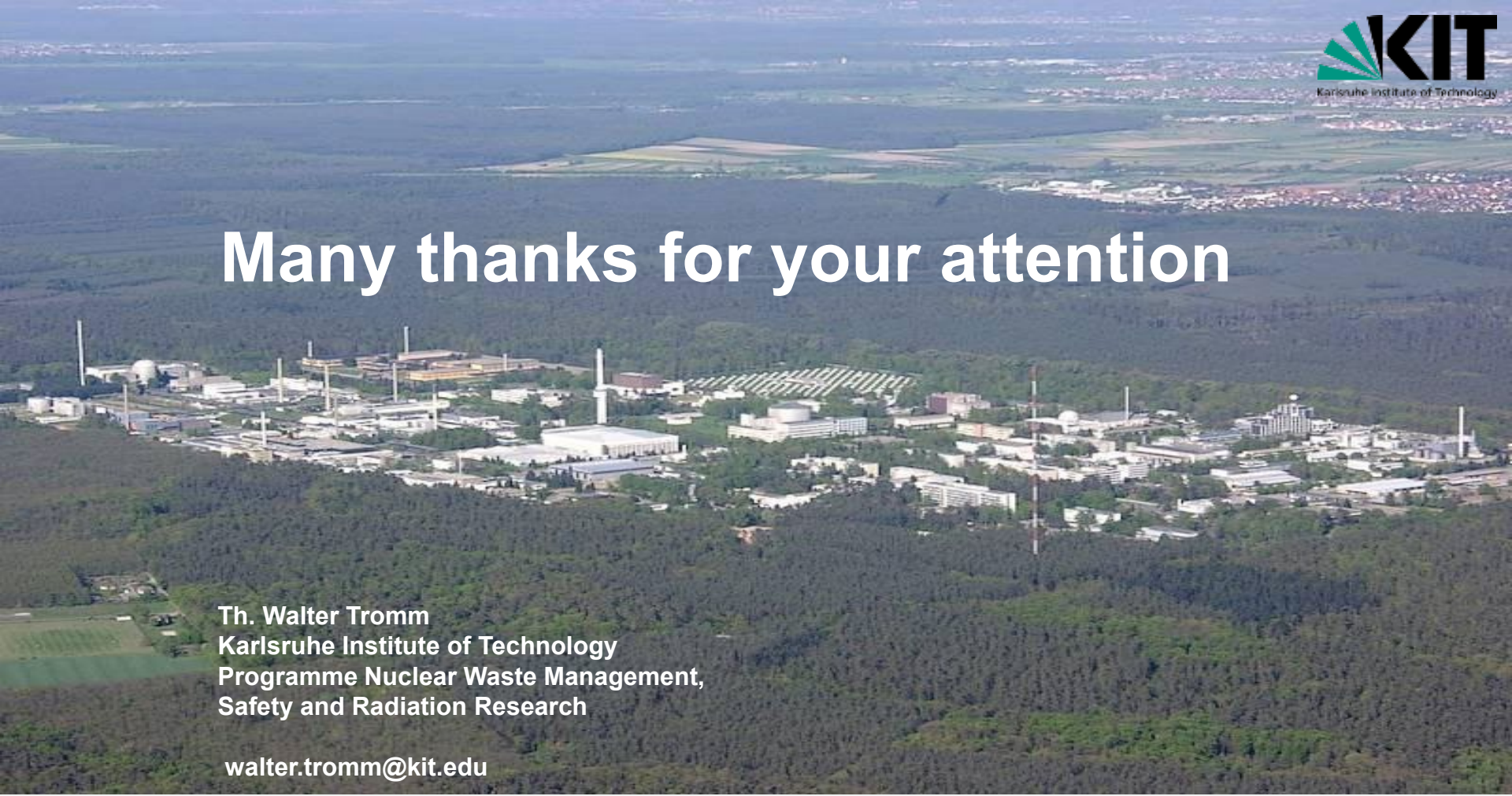

Many thanks for your attention

Th. Walter Tromm
Karlsruhe Institute of Technology
Programme Nuclear Waste Management,
Safety and Radiation Research

walter.tromm@kit.edu

Martin Steinbrück
KIT

Update of the QUENCH Program

The main objective of the QUENCH program at KIT is the investigation of the hydrogen source term and materials interactions during LOCA and the early phase of severe accidents including reflood. Bundle experiments as well as separate-effects tests are conducted to provide data for the development of models and the validation of severe fuel damage code systems.

The QUENCH bundle facility is a unique out-of-pile bundle facility with electrically heated fuel rod simulators and extensive instrumentation. So far, 21 experiments with various severe accident (SA) scenarios as well as a series of eight DBA LOCA experiments were conducted.

Two topics are currently in the focus of the QUENCH research activities:

1) Investigation of the high-temperature behavior of ATF cladding materials, and
2) Behavior of fuel cladding during (very) long-term dry storage, with the focus on the hydrogen/hydride effects on mechanical stability.

In the framework of the OECD-NEA Joint Undertaking QUENCH-ATF, the second bundle test with Cr-coated Zry cladding (from Westinghouse) was conducted with severe accident conditions. An 8-month lasting bundle experiment with pressurized and hydrogen preloaded fuel rod simulators was completed in January 2024 in the framework of the German SPIZWURZ project on long-term intermediate dry storage. Separate-effects tests during 2023/24 were focused also on the high-temperature behavior of various ATF cladding candidates as well as on the behavior of hydrogen in Zr alloys under long-term dry storage conditions.

QUENCH bundle tests are part of the validation matrices of most SFD code systems, which was also reflected during the session “Modelling and code validation”.

One remaining bundle experiment with ATF cladding in the framework of the NEA project is foreseen for 2025. Most activities of the QUENCH group are embedded in international cooperation in the framework of the EC, OECD-NEA and IAEA.

Finally, the status of reporting and publishing as well as the numerous national and international cooperations were briefly described and acknowledged.

Karlsruhe Institute of Technology

Update of the QUENCH program

M. Steinbrueck, J. Stuckert, M. Grosse

29th International QUENCH Workshop

Karlsruhe Institute of Technology, 19-21 Nov 2024

Outlook

- Current topics
- Experimental facilities
- ATF activities
- Long-term dry intermediate storage activities
- Modelling / Code validation
- Reporting
- Future planning

Current topics

- **Accident tolerant fuel (ATF) cladding**
  - ATF research after Fukushima Daiichi accidents
  - Characterization of promising ATF cladding concepts at (very) high temperatures
  - Degradation mechanisms and kinetic data
  - Max. temperature and coping time for AMMs
- **Long-term dry intermediate storage**
  - No final storage on the horizon in Germany and many other countries
  - Hydrogen/hydride behavior in Zr cladding during 50-100 years storage e.g. in CASTOR casks
  - Hydride reorientation and its effect on mechanical properties

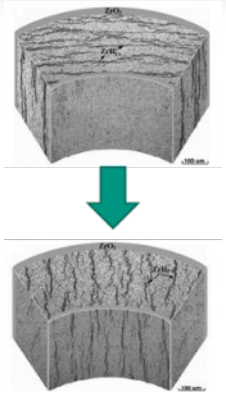

QUENCH program

Separate-effects tests

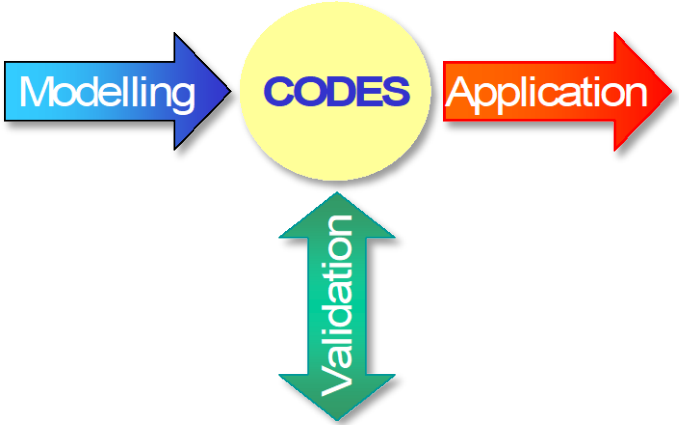

Bundle experiments

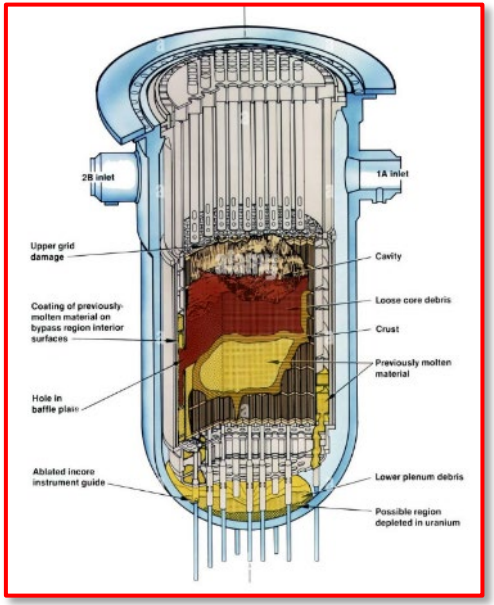

Application for simulation of nuclear accident scenarios

QUENCH/LICAS facility

- Unique out-of-pile bundle facility to investigate reflood of an overheated reactor core
- 21-31 electrically heated fuel rod simulators;
  T up to >2000°C
- Extensive instrumentation for T, p, flow rates, level, etc. + MS
- So far, 20+1 experiments on SA performed (1996-today)
  - Influence of pre-oxidation, initial temperature, flooding rate
  - B_4C, Ag-In-Cd control rods
  - Air ingress; debris formation
  - Advanced cladding alloys & ATF
- 7+1 DBA LOCA experiments with separately pressurized fuel rods

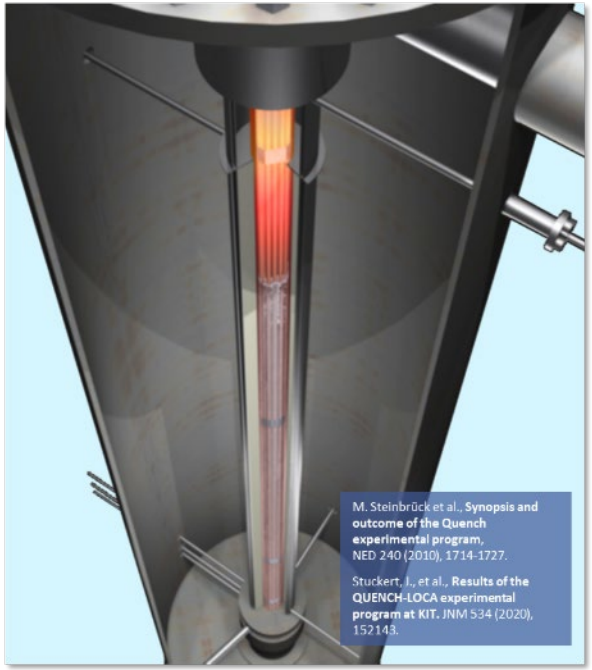

Experimental setup for ATF research

QUENCH-SR
- 10-15 cm cladding tube segments
- Fast inductive heating up to 2000°C
- Water quench

DTA-TG systems
- Max. temp. 1600°C (1250°C in steam)

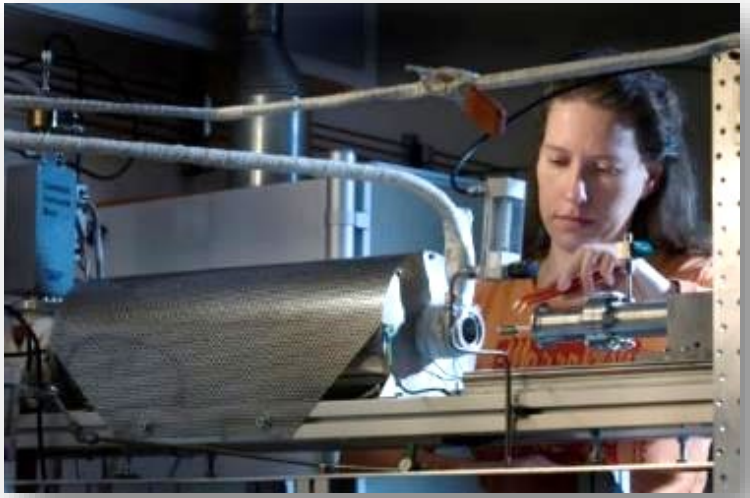

Tube furnaces
- Max. temp. 1600°C (all atmospheres)
- Sample airlock

All systems with water steam supply and mass spectrometer coupling

Test facilities for long-term storage research

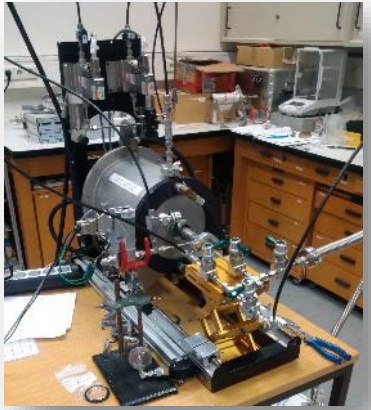

INCHAMEL

- Apparatus for in-situ neutron radiography experiments under defined mechanical load and temperature

SICHA

- Sieverts chamber for hydrogen loading of small Zry samples

HOKI

- 2.5 m long furnace for hydrogen pre-loading of cladding tubes for bundle tests

QUENCH activities on ATF cladding materials

- Bundle tests in the framework of OECD-NEA QUENCH-ATF
- Single-rod oxidation and quench tests of ATF cladding segment samples
- HT furnace tests with small samples in various atmospheres for analysis of oxidation kinetics and degradation mechanisms
- Tests on all promising ATF cladding concepts, including Cr-coated Zry, FeCrAl, SiC-based composites
- Data for model development, code validation and code application

International collaborations on ATF cladding

- OECD-NEA Joint Undertaking QUENCH-ATF
  - KIT is Operating Agent of the project
  - Three bundle experiments with Cr-coated ZIRLO provided by Westinghouse (USA)
- IAEA Coordinated Research Project ATF-TS
  - KIT coordinates two Work Packages
  - Experimental Round Robin exercises with various ATF cladding materials
  - Benchmark exercises on bundle tests conducted at KIT as well as in Hungary and Japan
- EC Projects IL TROVATORE and SCORPION
  - KIT coordinates WPs on fuel-cladding-coolant interaction
  - SCORPION devoted to sophisticated SiC-based composites
- EC Project OFFERR
  - KIT is proposer of the CODEX bundle test ATF-AIR at EK Budapest

OECD-NEA Joint Undertaking QUENCH-ATF

- **Three bundle experiments** with ATF cladding in the QUENCH facility
  - Focus on Cr-coated Zr alloys (CS & PVD)
  - Design basis and beyond design basis accident conditions
- Supporting **separate-effects tests**
  - at KIT
  - Complementary tests at IRSN and CEA (France)
- Code support for test preparation and **code benchmark exercises**, coordinated by GRS

Bundle test QUENCH-ATF1

- Scenario: Slightly beyond DBA-LOCA with QUENCH-LOCA3HT as reference test
- All non-destructive post-test examinations completed
- Destructive post-test examinations well progressed at KIT and IRSN
- KIT-NUSAFE data&analysis draft version distributed to project partners
- Benchmark exercises (blind&open) completed
  - Modelling of Cr/Zry cladding oxidation improved for all codes


Karlsruher Institut für Technologie
in der Helmholtz-Gemeinschaft
Wissenschaftliche Berichte

Results of the QUENCH-ATF1 bundle test
with Cr coated opt. ZIRLO claddings
under extended DBA conditions (NUSAFE-3584)

(DRAFT)

J. Stuckert, M. Große, C. Rössger, M. Steinbrück

Institut für Angewandte Materialien:
Angewandte Werkstoffphysik (IAM-AWP)

Programm Nukleare Entsorgung und Sicherheit

Karlsruher Institut für Technologie

2024

QUENCH-ATF2 bundle experiment

- Conducted in August 2024
- Severe accident test with cold sprayed Cr-coated ZIRLO cladding (Westinghouse)
- Max. temperature 1600°C, then initiation of quenching phase
- Reference test QUENCH-15 with uncoated ZIRLO
- Two ATCRs with pellets of Eu_2O_3-HfO_2 from CRIEPI (Japan)

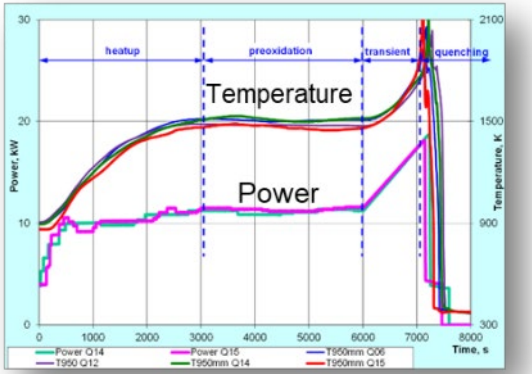

Test scenario (Q06/12/14/15 with non-coated Zr alloys)

QUENCH-ATF2 bundle assembly

- Finally successful after delays due to delivery problems and staff shortages in the KIT main workshop

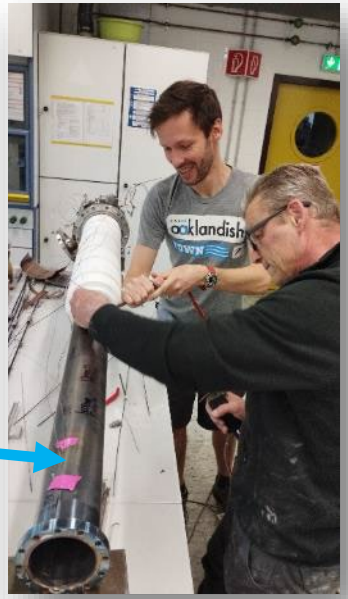

QUENCH-ATF2 results

- … are confidential (even for project members until completion of the blind phase of the code benchmark)

Anyway, what can be said:

- Power history (and consequently temperatures in the pre-transient phases) were the same as for the reference test QUENCH-15
- First analyses showed very interesting results

Why the QUENCH-ATF2 experiment was very exciting

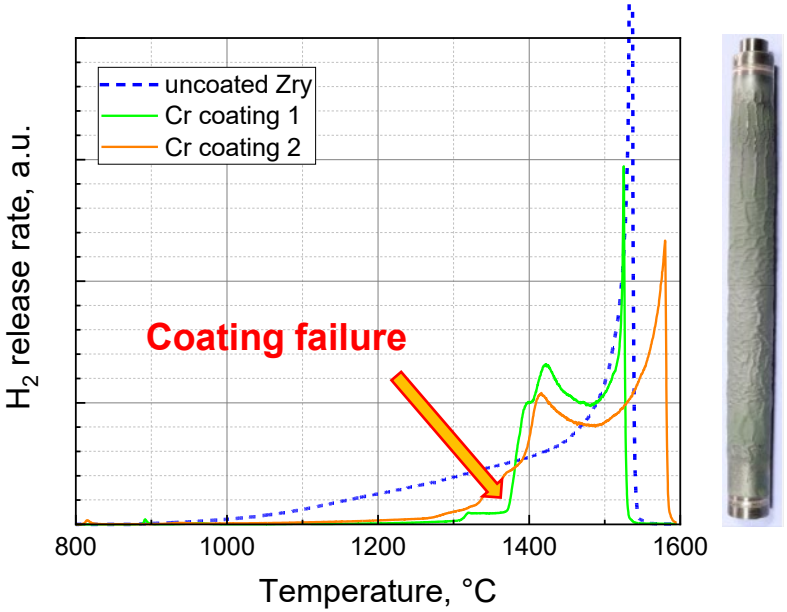

?

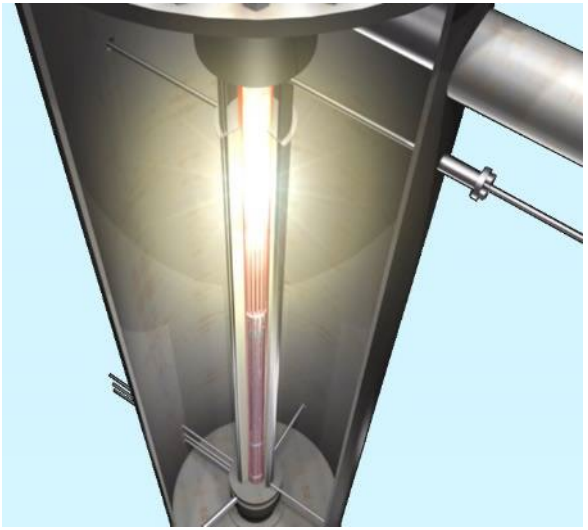

Faster oxidation of coated samples after coating failure compared to Zry in single-rod experiments with high heat losses!

What happened under almost adiabatic conditions in the bundle experiment?

QUENCH-ATF3 preparation

- ZIRLO cladding tubes at NNL for Cr coating by PVD
- Spacer grids have been shipped to KIT by WEC
- All other materials for bundle construction are available or have been ordered
- Test conduct planned for 2025 (as early as possible)
- Test scenario to be discussed during PRG and MB projects meetings end of this week

HT oxidation of Cr-coated Zry with varying thickness

1000°C

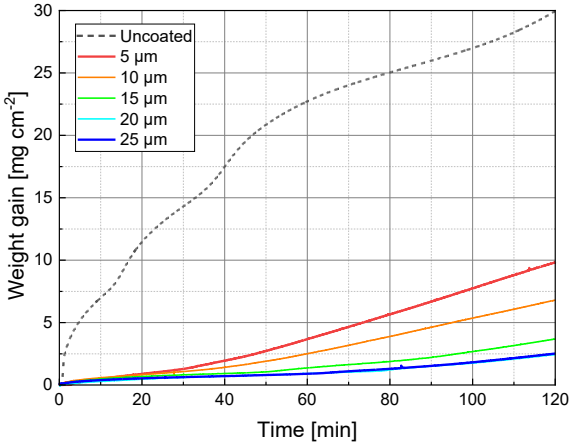

Protective effect of Cr coating below Zr-Cr eutectic temperature (1330°C)

1400°C

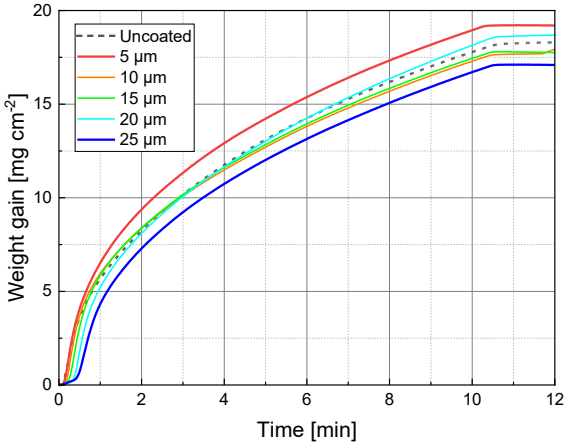

No protective effect of Cr coating above Zr-Cr eutectic temperature

500-1500°C

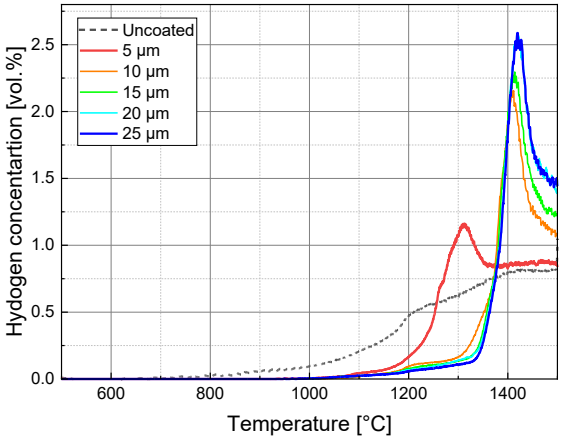

Loss of protective effect of Cr coating at Zr-Cr eutectic temperature

Activities on long-term intermediate storage

- Work embedded in the German project SPIZWURZ (GRS, KIT) and the HGF HOVER infrastructure program
- 8-month lasting bundle test successfully completed
  - Post-test analyses and benchmark exercises are progressing
- Various SETs on hydrogen dissolution and precipitation in zirconium alloys
- Follow-up project SPIZWURZ+ under preparation

SPIZWURZ bundle test

- Simulation of dry storage with pre-hydrided cladding
- 8 months (May 23 - Jan 24)
- Starting temperature 400°C
- Cool-down rate 1 K/day
- Cladding types: Zircaloy-4, DUPLEX, ZIRLO
- Hydrogen content 300/100 wppm
- Internal pressure 106/146 bar

SPIZWURZ bundle

SPIZWURZ separate-effects tests

H Diffusion in Zr single crystals in different directions

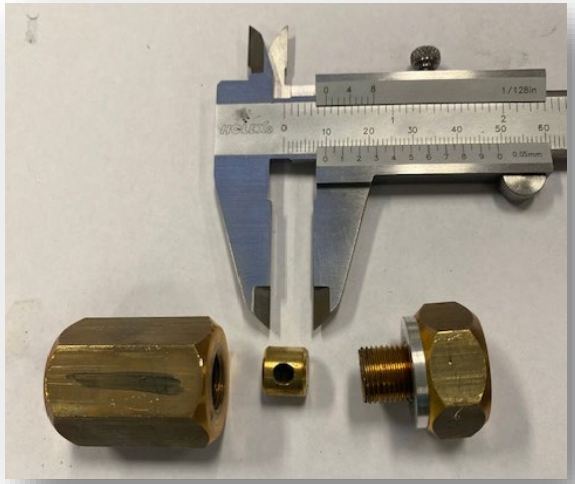

- Annealing in ZrH_2 bed in Ar filled leak tight capsule at $400°C \leq T \leq 500°C$
- Neutron radiography at IMAT (ISIS, RAL, Ditcot, UK) at Dec. 5-7, 2024

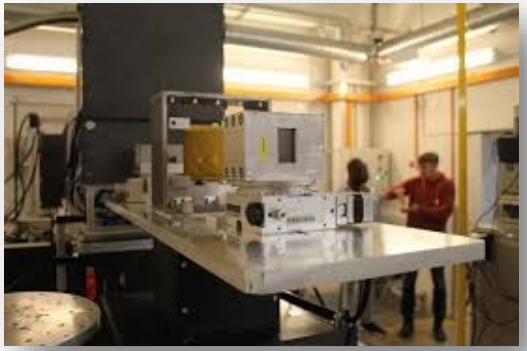

Modelling and code validation

- QUENCH bundle tests are part of validation matrices of most SFD code systems
- Post-test calculations of QUENCH-19 (24 FeCrAl claddings) and DEGREE (9 Cr-coated Zry-4 claddings) in the framework of the IAEA ATF-TS project
- Benchmark exercise (blind & open phase) on QUENCH-ATF2 test coordinated by GRS
- Benchmark exercise (blind & open phase) on SPIZWURZ bundle test coordinated by GRS
- Separate-effects test data are used by various institutions for model development

Reporting

High Temperature Corrosion of Materials (2024) 101:621–647
https://doi.org/10.1007/s11085-024-10229-y

REVIEW

Check for updates

An Overview of Mechanisms of the Degradation of Promising ATF Cladding Materials During Oxidation at High Temperatures

Martin Steinbrueck[1] · Mirco Grosse[1] · Chongchong Tang[1] · Juri Stuckert[1] · Hans Juergen Seifert[1]

Received: 20 June 2023 / Revised: 25 January 2024 / Accepted: 31 January 2024 /
Published online: 16 |

Nuclear Engineering and Technology 56 (2024) 824–831

Contents lists available at ScienceDirect

Nuclear Engineering and Technology

journal homepage: www.elsevier.com/locate/net

Original Article

The SPIZWURZ project – Experimental investigations and modeling of the behavior of hydrogen in zirconium alloys under long-term dry storage conditions

Mirco Grosse [a,*], Felix Boldt [b], Michel Herm [c], Conrado Roessger [a], Juri Stuckert [a], Sarah Weick [a], Daniel Nahm [d]

[a] Karlsruhe Institute of Technology, Institute for Applied Materials, Karlsruhe, Germany
[b] Bundesgesellschaft für Zwischenlagerung, Garching, Germany
[c] Karlsruhe Institute of Technology, Institute for Nuclear Waste Disposal, Karlsruhe, Germany
[d] Gesellschaft für Reaktorsicherheit, Garching, Germany

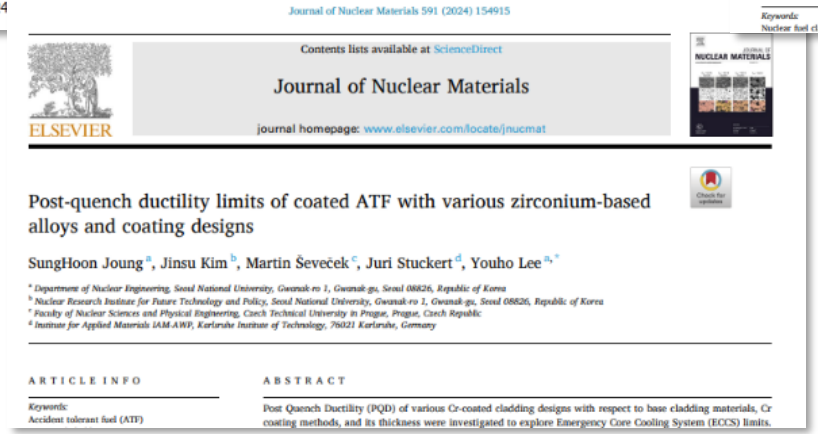

Journal of Nuclear Materials 591 (2024) 154915

Contents lists available at ScienceDirect

Journal of Nuclear Materials

journal homepage: www.elsevier.com/locate/jnucmat

Post-quench ductility limits of coated ATF with various zirconium-based alloys and coating designs

SungHoon Joung [a], Jinsu Kim [b], Martin Ševeček [c], Juri Stuckert [d], Youho Lee [a,*]

[a] Department of Nuclear Engineering, Seoul National University, Gwanak-ro 1, Gwanak-gu, Seoul 08826, Republic of Korea
[b] Nuclear Research Institute for Future Technology and Policy, Seoul National University, Gwanak-ro 1, Gwanak-gu, Seoul 08826, Republic of Korea
[c] Faculty of Nuclear Sciences and Physical Engineering, Czech Technical University in Prague, Prague, Czech Republic
[d] Institute for Applied Materials IAM-AWP, Karlsruhe Institute of Technology, 76021 Karlsruhe, Germany

ARTICLE INFO

Keywords:
Accident tolerant fuel (ATF)

ABSTRACT

Post Quench Ductility (PQD) of various Cr-coated cladding designs with respect to base cladding materials, Cr coating methods, and its thickness were investigated to explore Emergency Core Cooling System (ECCS) limits.

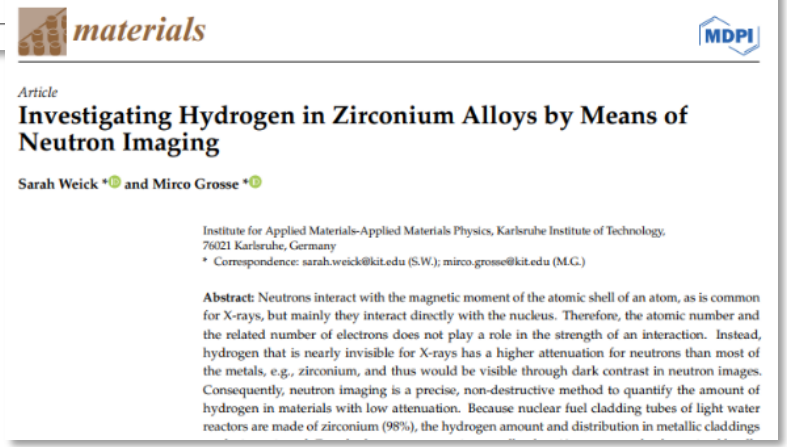

materials

MDPI

Article

Investigating Hydrogen in Zirconium Alloys by Means of Neutron Imaging

Sarah Weick * and Mirco Grosse *

Institute for Applied Materials-Applied Materials Physics, Karlsruhe Institute of Technology, 76021 Karlsruhe, Germany
* Correspondence: sarah.weick@kit.edu (S.W.); mirco.grosse@kit.edu (M.G.)

Abstract: Neutrons interact with the magnetic moment of the atomic shell of an atom, as is common for X-rays, but mainly they interact directly with the nucleus. Therefore, the atomic number and the related number of electrons does not play a role in the strength of an interaction. Instead, hydrogen that is nearly invisible for X-rays has a higher attenuation for neutrons than most of the metals, e.g., zirconium, and thus would be visible through dark contrast in neutron images. Consequently, neutron imaging is a precise, non-destructive method to quantify the amount of hydrogen in materials with low attenuation. Because nuclear fuel cladding tubes of light water reactors are made of zirconium (98%), the hydrogen amount and distribution in metallic claddings

QUENCH experiments 2025-2027 and beyond

- Commitment from the Federal Ministry of Education and Research (BMBF) and the Helmholtz Centers for the continuation of nuclear safety research for the current and next funding periods until 2035
- Future topics
  - Behavior of long-term ATF materials under DBA and SA conditions (QUENCH-ATF2?)
    - SiC-SiC CMC
    - Cr-coating with diffusion barrier
  - Safety research for SMRs (LWR- and GFR-type)
  - Safety research for long-term intermediate storage (Zr-H)
- Human resources remain a serious issue
  - Two job offers for the succession of two leading scientists of the project (Stuckert/Steinbrück)

Acknowledgement

- Helmholtz Association for funding program NUSAFE at KIT
- Program NUSAFE and IAM institute's management for broad support of our activities
- BMWK for funding of the SPIZWURZ project
- EC for funding the projects SEAKNOT, IL TROVATORE and SCORPION
- OECD-NEA and partners for support of QUENCH-ATF

- And last but not least the QUENCH team:
  M. Kolesnik, J. Laier, J. Moch, U. Peters, C. Roessger, U. Stegmaier, S. Weick

Martin Steinbrück
KIT

Promising ATF cladding materials and their oxidation behavior at high temperature

13 years after the Fukushima Daiichi accidents, three material systems are considered the most promising solutions for Accident Tolerant Fuel (ATF) cladding. These are (1) chromium-coated zirconium alloys, (2) FeCrAl alloys as an evolutionary short-term solution, and (3) SiC-based ceramic matrix composites (CMC) as a revolutionary long-term alternative to the classical Zr alloys.

The new cladding materials are expected to exhibit at least the same excellent properties as Zr alloys during operational and design-basis accidents, but the ATF materials are also expected to exhibit improved behavior in terms of high-temperature oxidation resistance during severe accidents, resulting in reduced hydrogen and chemical heat release and extended coping time for accident management measures.

This presentation briefly discussed the high-temperature degradation mechanisms for the three ATF cladding materials mentioned above that result in different maximum "survival" temperatures. Illustrative examples from recent experimental work at the Karlsruhe Institute of Technology were given for all systems.

Karlsruhe Institute of Technology

Promising ATF cladding materials and their oxidation behavior at (very) high temperature

M. Steinbrück, M. Große, J. Stuckert

29th International QUENCH Workshop, 19-21 Nov 2024, KIT, Karlsruhe, Germany

Institute for Materials Research IAM-AWP / Program Nuclear Safety

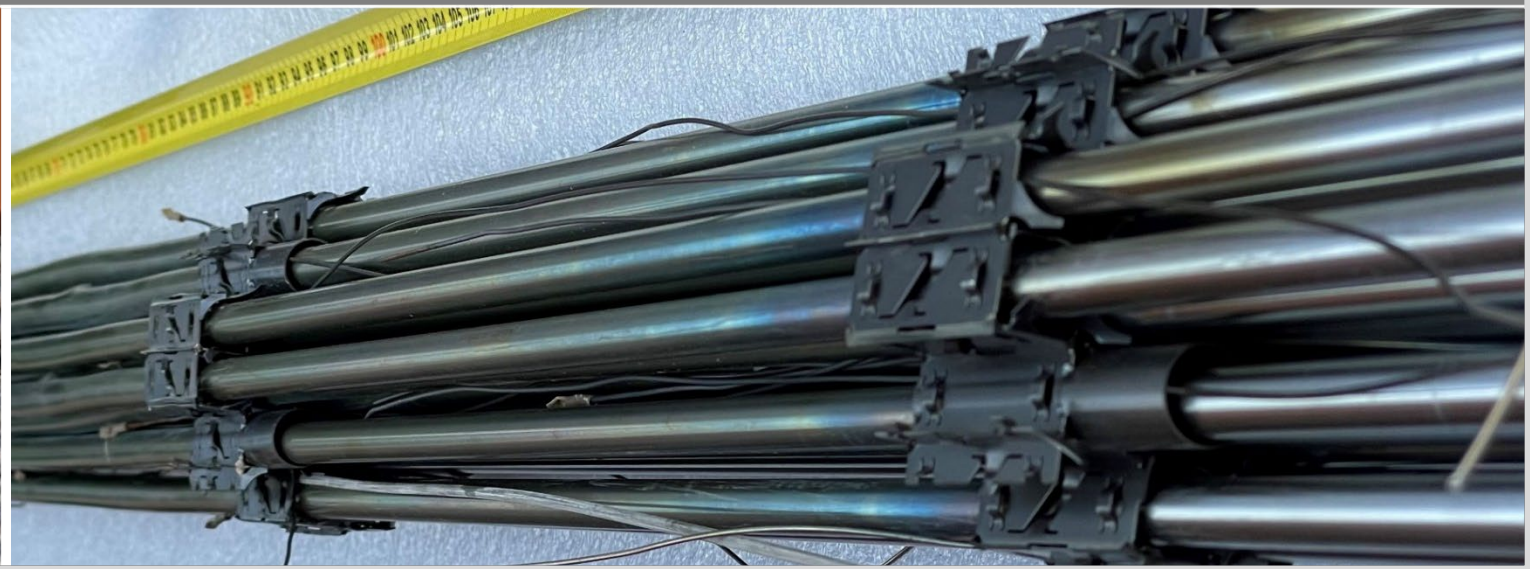

Hydrogen detonations in Fukushima Daiichi NPPs

- Ca. 1000 kg H_2 per reactor
- Main hydrogen source is Zry oxidation by steam: $Zr + 2H_2O = ZrO_2 + 2H_2$
- Chemical heat release
- Release of radioactive fission products

ATF cladding research and development

- Worldwide research on accident tolerant fuel (ATF) materials after Fukushima accidents
- ATF materials should reduce release of hydrogen and heat (oxidation kinetics) and increase coping time for accident management measures
- After more than ten years of international research, the most promising ATF cladding concepts are:
  - Cr-coated Zr alloys
  - FeCrAl alloys
  - SiC_f-SiC ceramic matrix composites

Publications on ATF cladding*

* Based on a SCOPUS search for “ATF cladding”

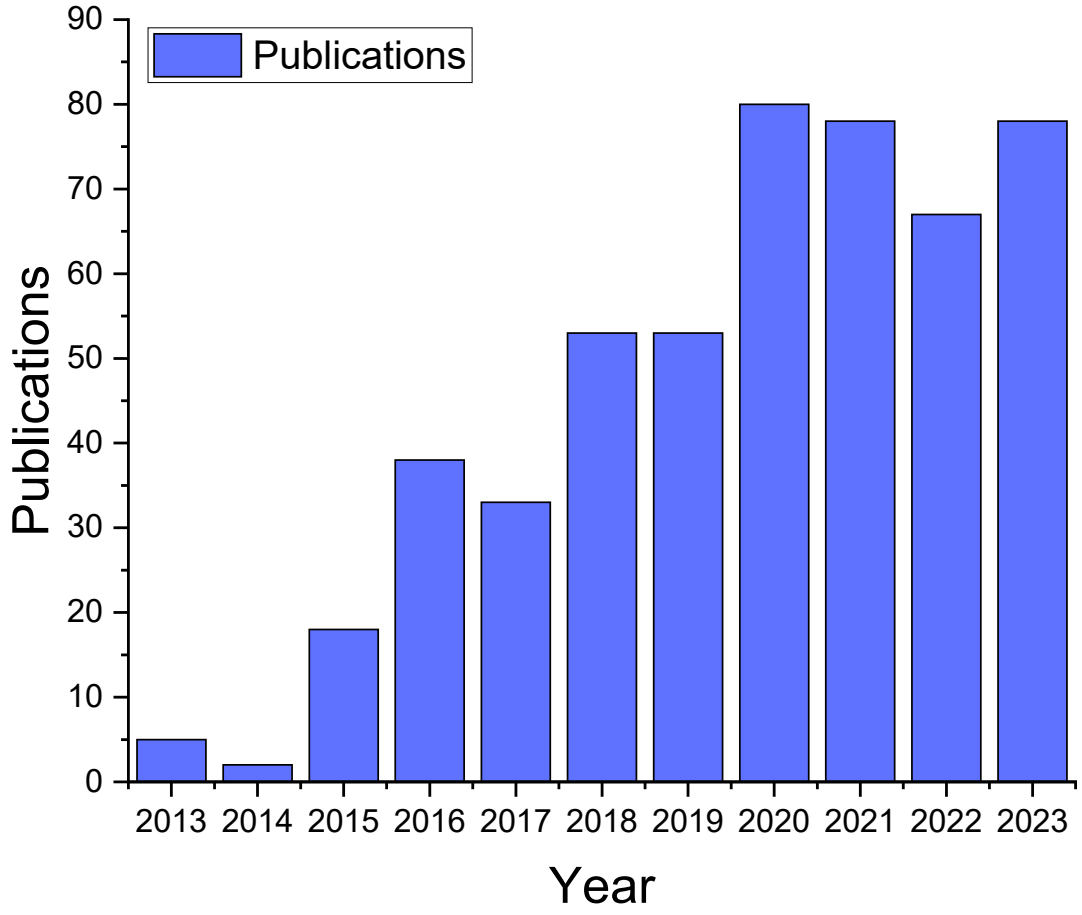

SCOPUS: >500 documents 2013-2023

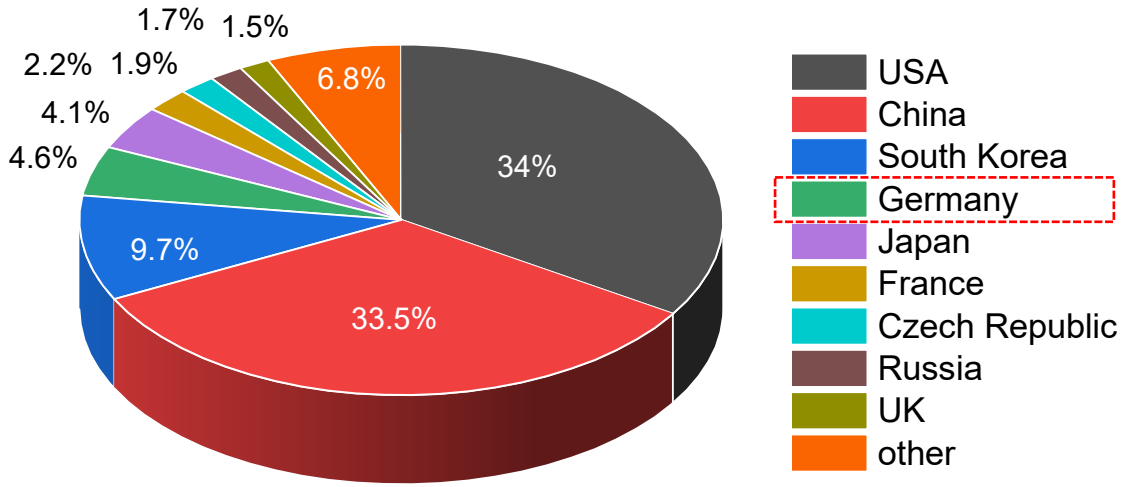

- 50% of German research is from KIT

Outline

- Basic information on oxidation and degradation at high temperature of promising ATF cladding materials
- Experimental setup used at KIT
- Cr-coated zirconium alloys
- FeCrAl alloys
- SiC-based ceramic composites
- Conclusion

  - Basics
  - Illustrative examples

Oxidation and degradation mechanisms at high temp.

- HT oxidation resistance relies on the formation of stable oxides with low diffusion constants of oxygen and/or metal ions
  - Al_2O_3, Cr_2O_3, SiO_2
- Degradation of these protective oxides may be caused by consumption of the oxide or oxidizing species due to:
  - Volatilization of the oxide in steam atmosphere
  - Diffusion
    - Depletion of oxidizing species in the bulk material (alloy)
    - of coating into bulk
- Melting of bulk material or oxide scale, eutectic interactions

Melting temperatures

- Determining the ultimate application/survival temperatures of the materials

Zry	**1850°C**	**ZrO_2**	**2715°C**
Cr	1907°C	Cr_2O_3	2435°C
FeCrAl	1425-1500°C	Al_2O_3 FeO	2072°C 1377°C*
SiC	2700°C (subl.)	SiO_2	1710°C

* Potential interaction with UO_2

Bechta, JNM 362 (2007) 46-52
Stuckert, Report NUSAFE 3574, KIT (2022)

Comparison of oxidation data

Gibbs enthalpy of reaction

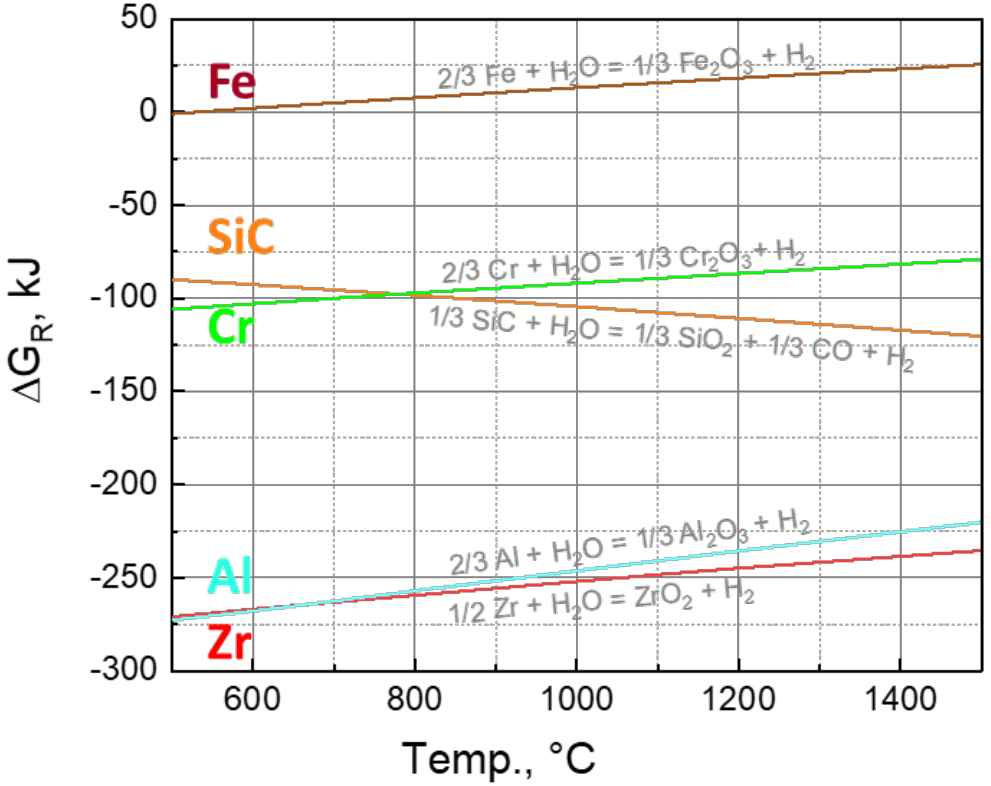

- Al_2O_3 and ZrO_2 are <u>thermo-dynamically</u> most stable

Parabolic rate constants of oxide growth

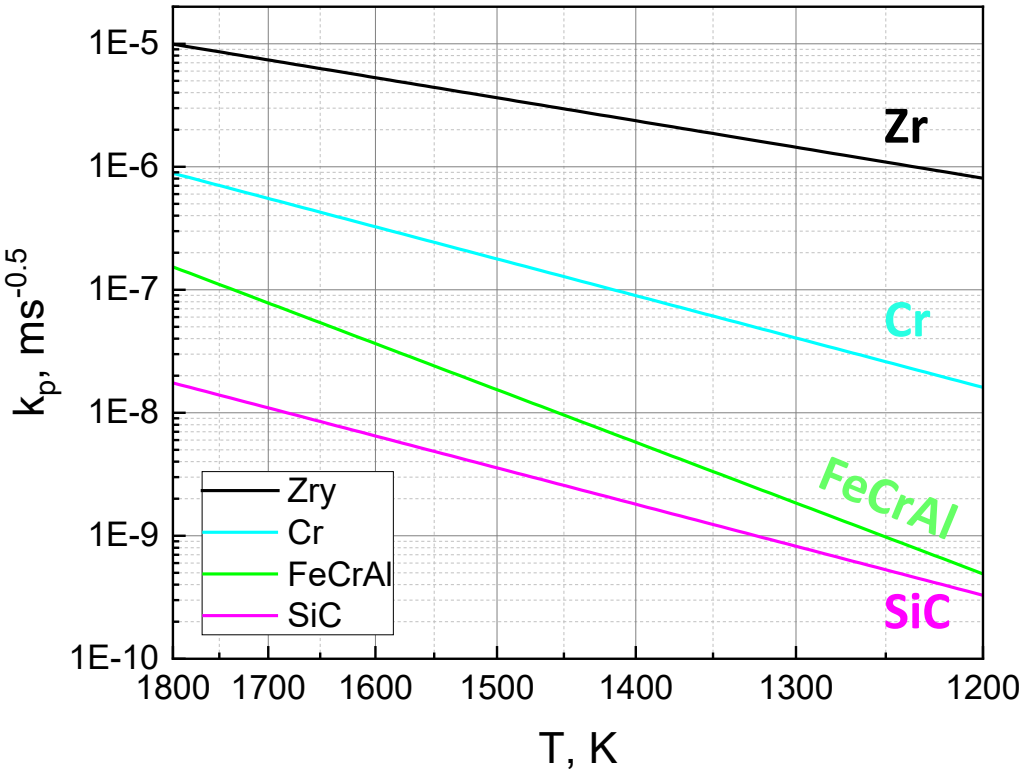

- Al_2O_3 and SiO_2 have the slowest growth <u>kinetics</u>

Calculated with HSC Chemistry 9
Steinbrueck, HTCM 101 (2024), 621

Experimental setup

Bundle tests

- 21-31 fuel rod simulators
- 2.5 m long
- Electrically heated
- Extensively instrumented

Separate-effects tests

- 10-15 cm cladding tube segments
- Inductive heating up to 2000°C
- Water quench

- DTA-TG systems
- Max. temp. 1600°C

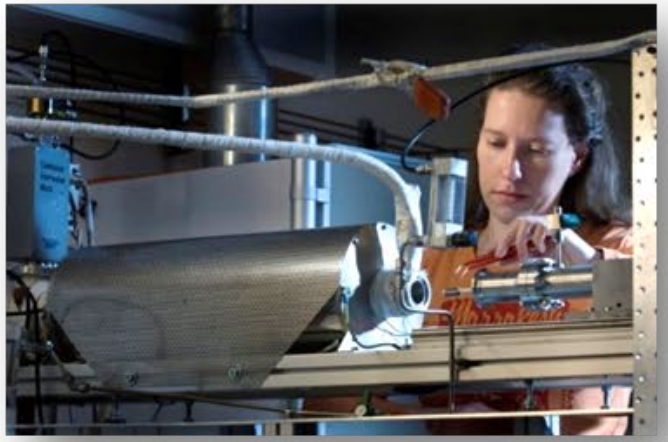

- Tube furnaces
- Max. temp. 1600°C
- Sample airlock

All systems with water steam supply and mass spectrometer coupling

Cr-coated Zr alloys

- $2\ Cr + 3\ H_2O \rightarrow Cr_2O_3 + 3\ H_2$
  - Adherent and well protective oxide scale
  - Consumption of Cr
- $Zr + 2\ Cr \rightarrow ZrCr_2$
  - Consumption of Cr coating by formation of an intermetallic layer
- Solubility of Cr in Zry bulk (and vice versa)
  - Consumption of Cr coating by diffusion into Zry bulk
- Zr-Cr eutectic melt formation at 1332°C
  - Ultimate upper limit of application

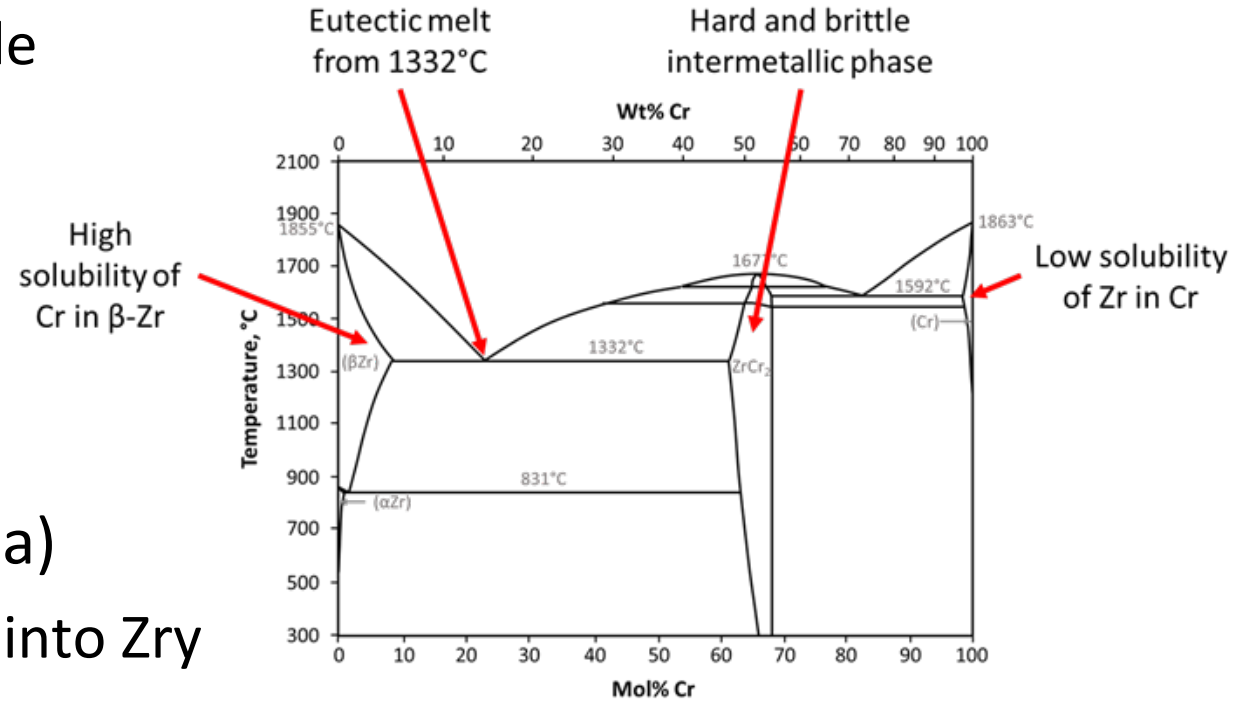

Zr-Cr phase diagram

Arias and Abriata, Bull. Alloy Phase Diagr. 7 (1986) 237-243

Oxidation of Cr-coating and interaction with Zry bulk

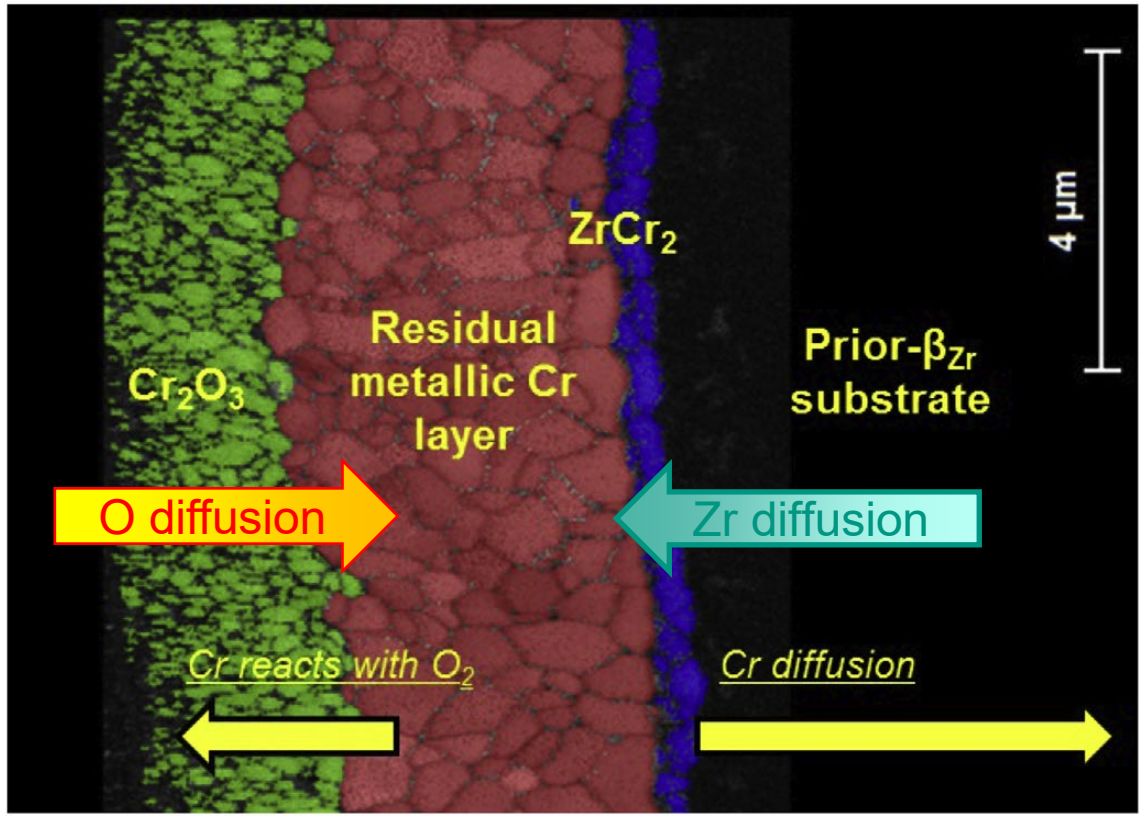

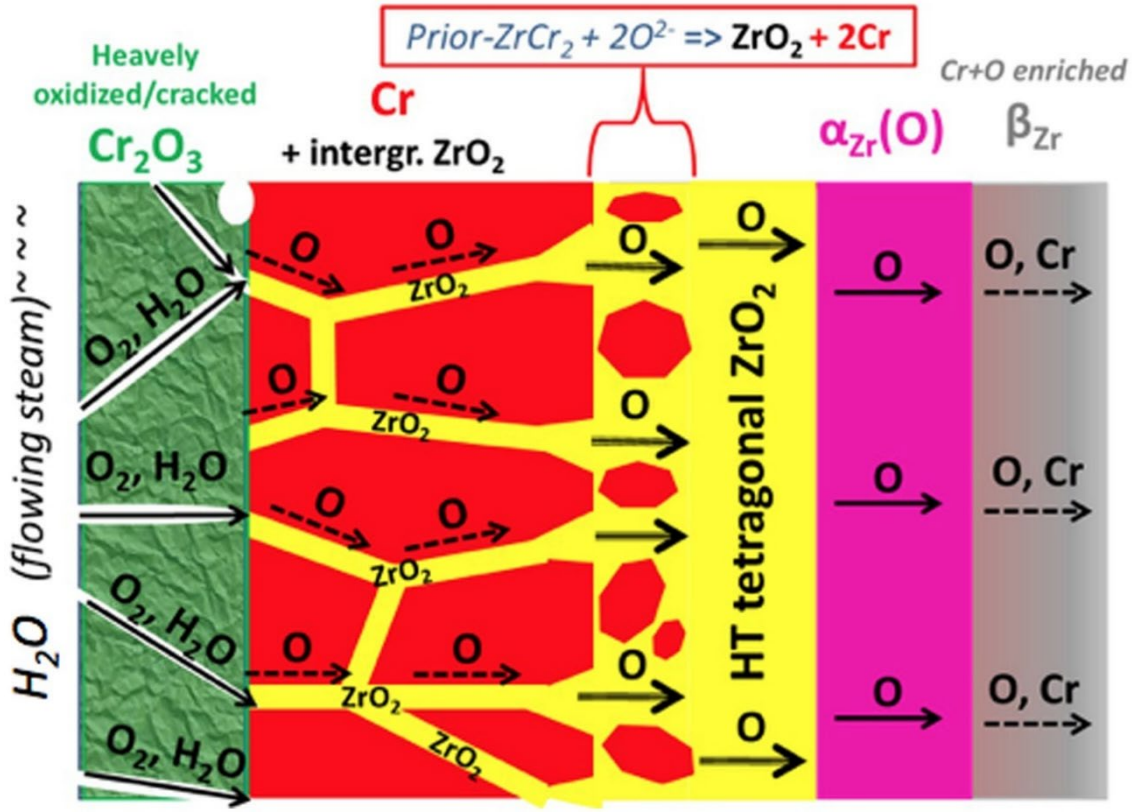

Protective coating → Non-protective coating

Due to the formation of O conducting ZrO_{2-x} channels along Cr grain boundaries

Brachet et al., JNM 517 (2019) 268-285
Brachet et al., Cor. Sci. 167 (2021), 108537

Volatility of chromia

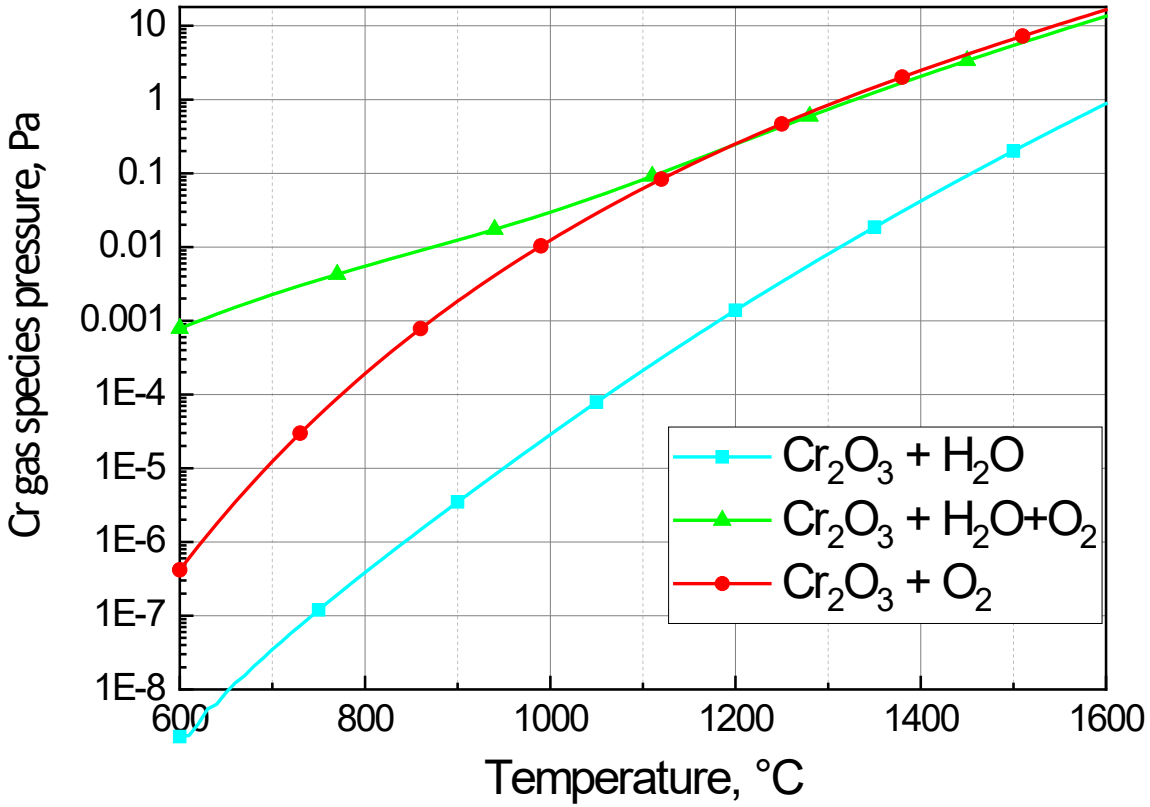

- Low volatility in pure water vapor
- Significant volatility only at temperatures >1300°C, i.e., after failure of Cr coating due to other reasons

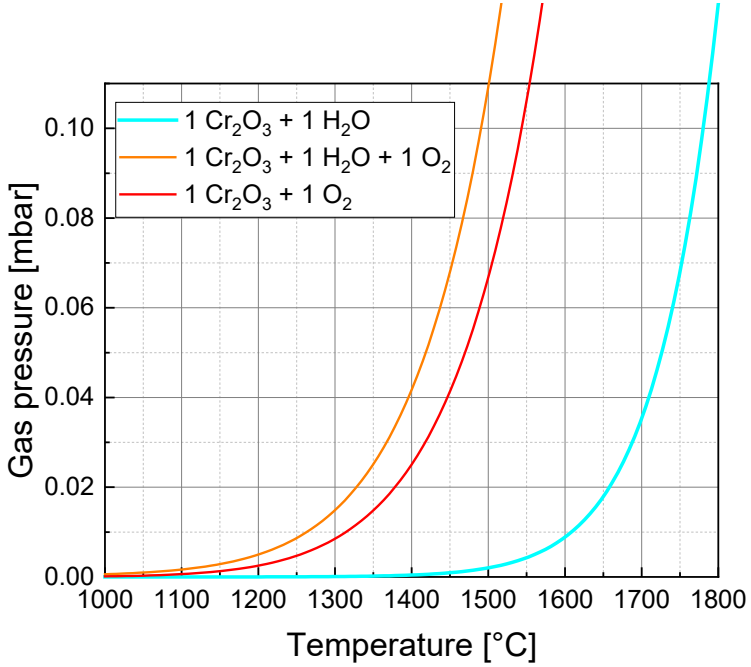

$$Cr_2O_3(s) + 2H_2O(g) + 1.5O_2(g) \rightarrow 2CrO_2(OH)_2(g)$$

$$Cr_2O_3(s) + 1.5O_2(g) \rightarrow 2CrO_3\ (g)$$

HT oxidation of Cr-coated Zry with varying thickness

Karlsruhe Institute of Technology

Isothermal 1200°C

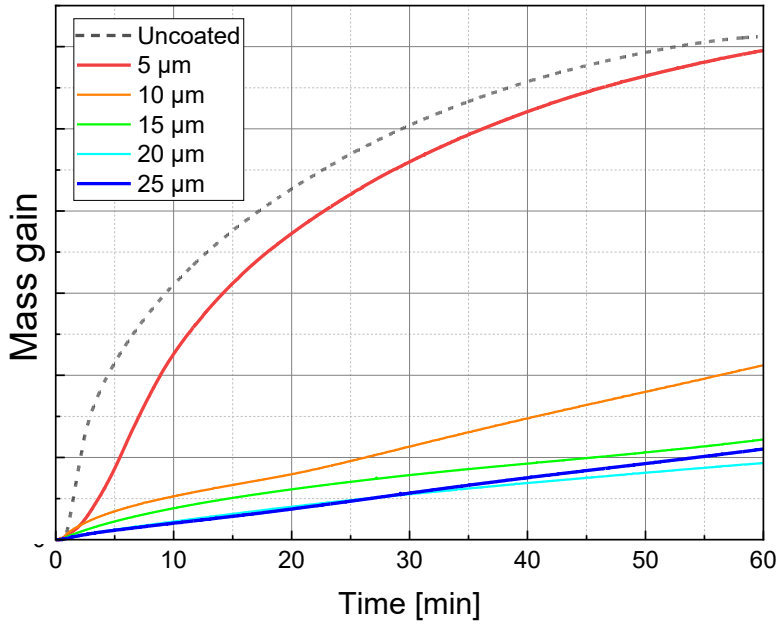

Increasing protective effect of Cr coating with thickness below Zr-Cr eutectic temperature (1330°C)

Isothermal 1400°C

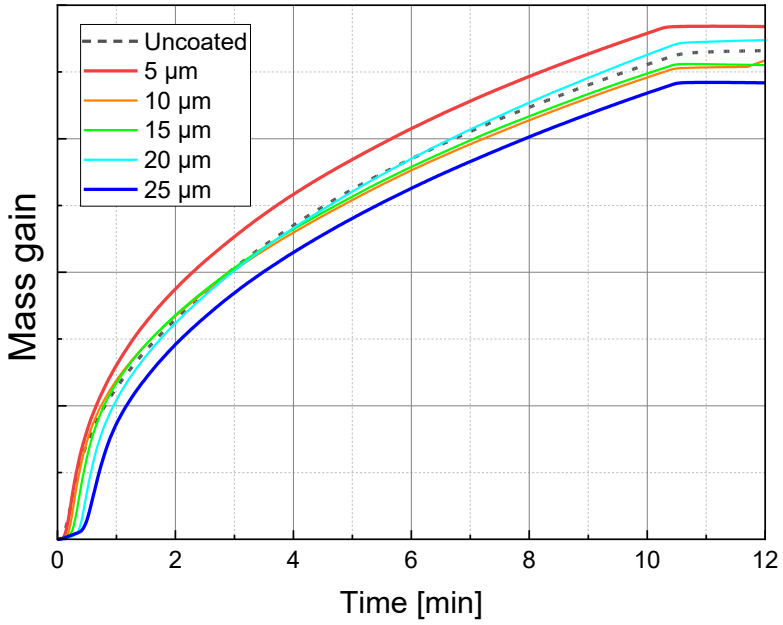

No protective effect of Cr coating above Zr-Cr eutectic temperature

Transient 500-1500°C

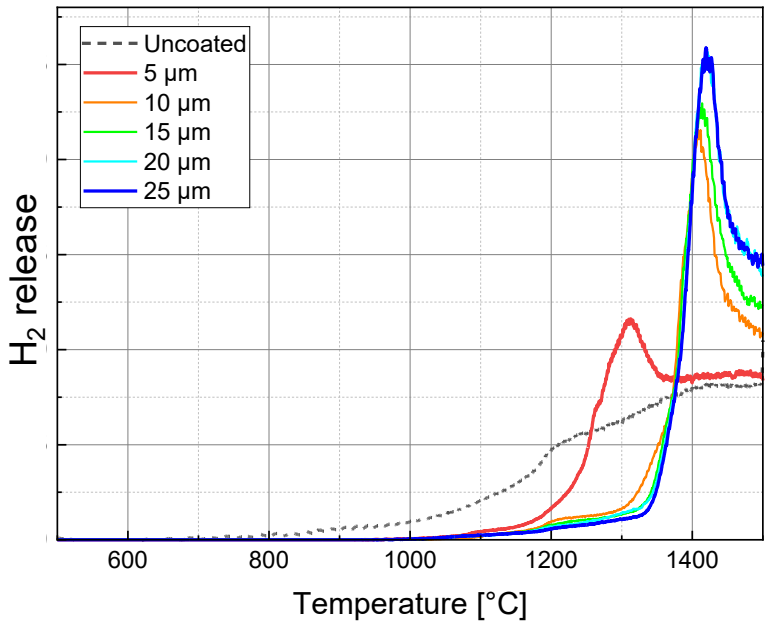

Loss of protective effect of Cr coating at Zr-Cr eutectic temperature

Post-test examination of 1200°C samples

- 5 µm Cr: Almost complete oxidation of sample
- 10 µm Cr: Degraded coating and significant α-Zr(O) formation
- 15-25 µm Cr: 4-layer structure with ZrO_2 paths along Cr GBs
- 25 µm Cr: local defects in coating
- ➡ Best protection for 15-20 µm Cr thickness

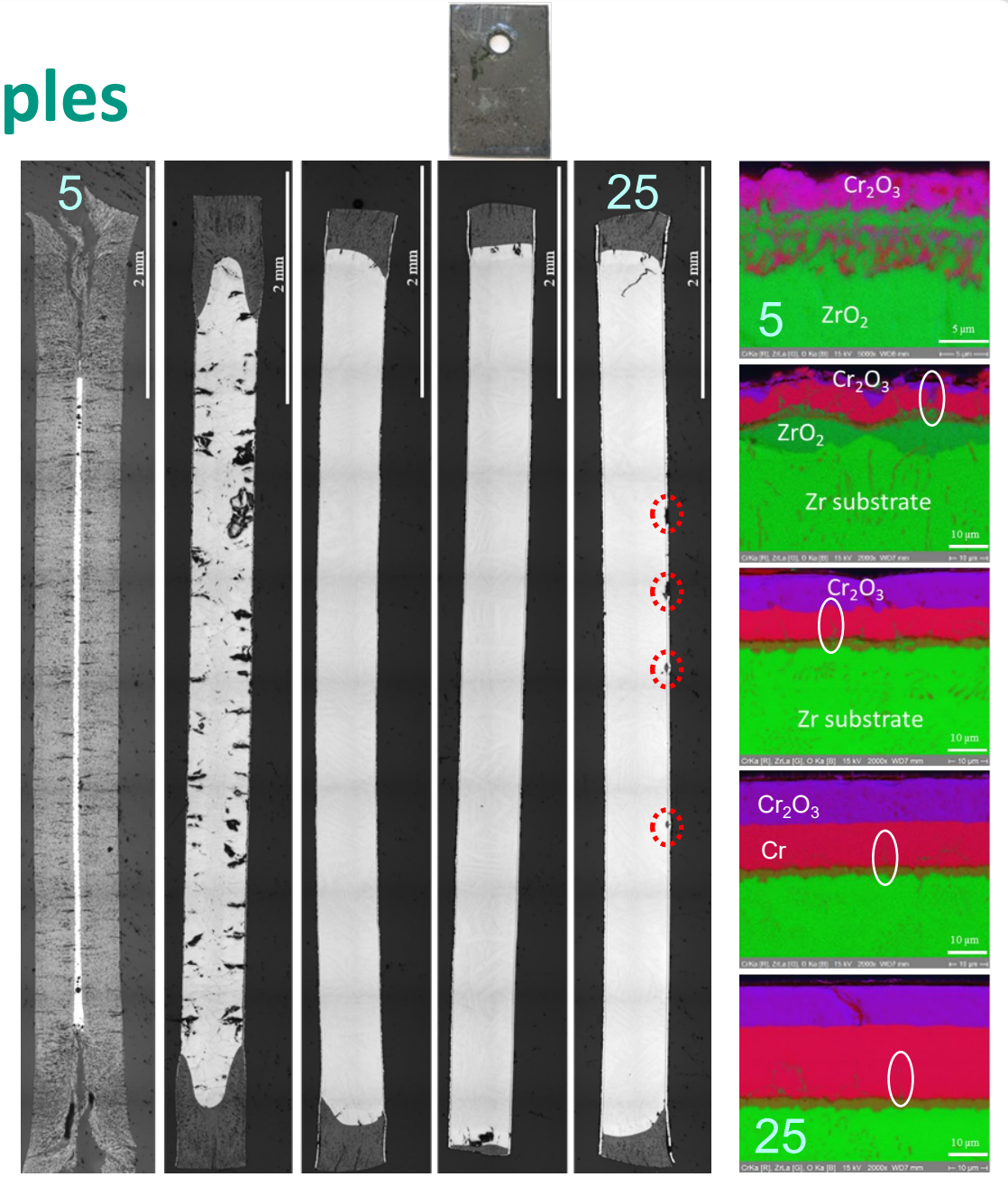

Crack formation in the coating for 25 µm samples at 1200°C

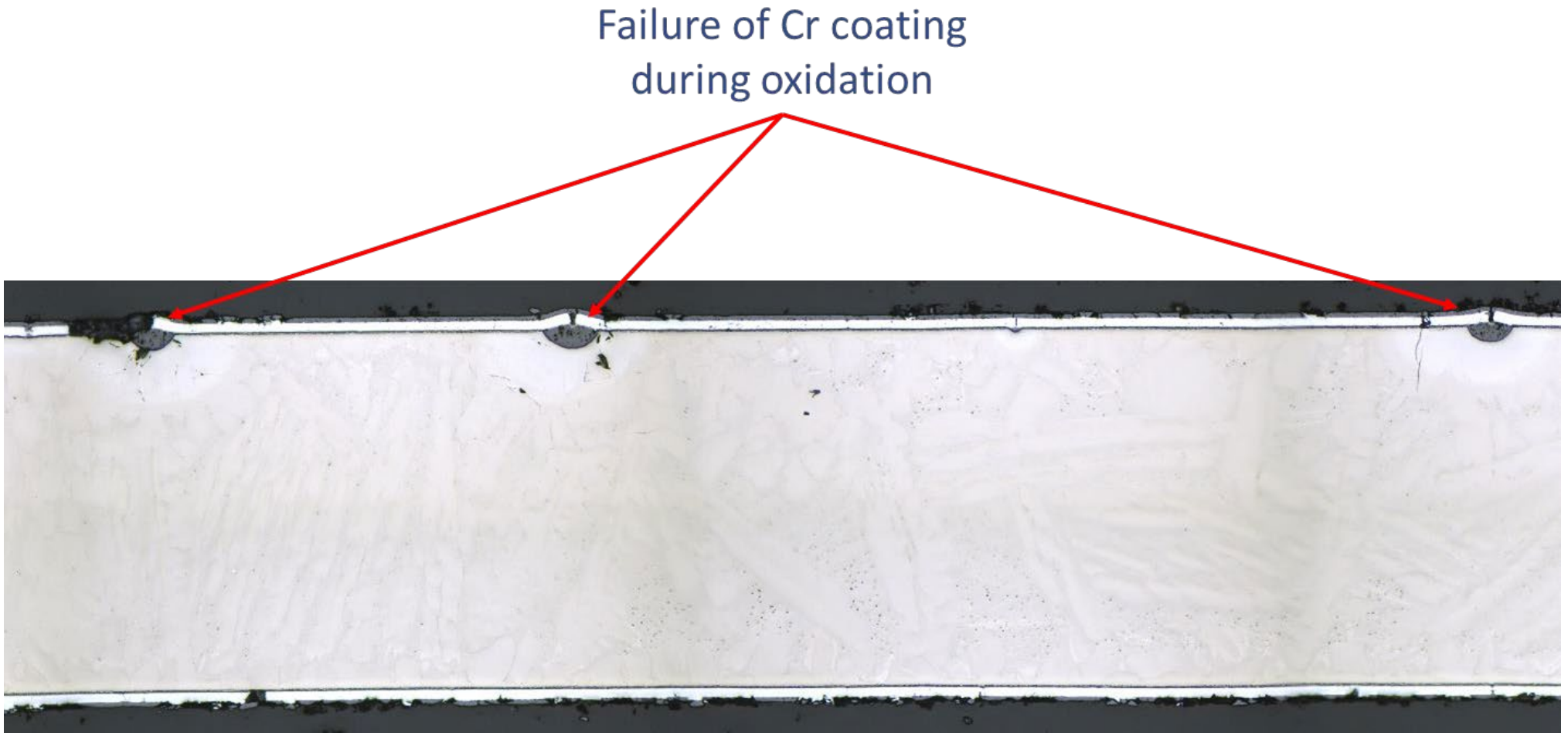

- Indication for too thick Cr coating resulting in thermo-mechanical mismatch?

Post-test examination of 1400°C samples

- Significant oxidation of all samples, almost independent on Cr thickness
- Increasing eutectic melt formation with thicker Cr coating
- $ZrCr_2$ precipitates in frozen melt
- Cr_2O_3 still on surface
- No protective effect of Cr coating above eutectic temperature (1330°C) - kinetics similar to uncoated Zry oxidation

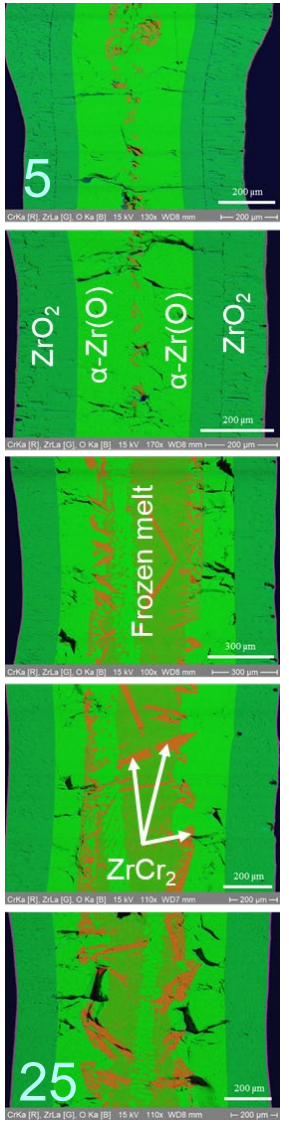

FeCrAl alloys

- $2\ M + 3\ H_2O \rightarrow M_2O_3 + 3\ H_2$
- Thermodynamic stability:
  $Al_2O_3 > Cr_2O_3 > FeO_x$
- Diffusion in metal: Al > Fe ≈ Cr
  Diffusion in oxide: $Fe^{3+} > Cr^{3+} > Al^{3+}$
- Formation of stable and very protective α-Al_2O_3 scale
  - At T > 800-1000°C
  - Depending on composition
  - "Third element effect" of Cr
- Nuclear grade FeCrAl with low Cr content (Fe13Cr6Al) and further minor alloying elements and ODS
- Volatility:
  $Cr_2O_3 >> Al_2O_3 \approx FeO_x$

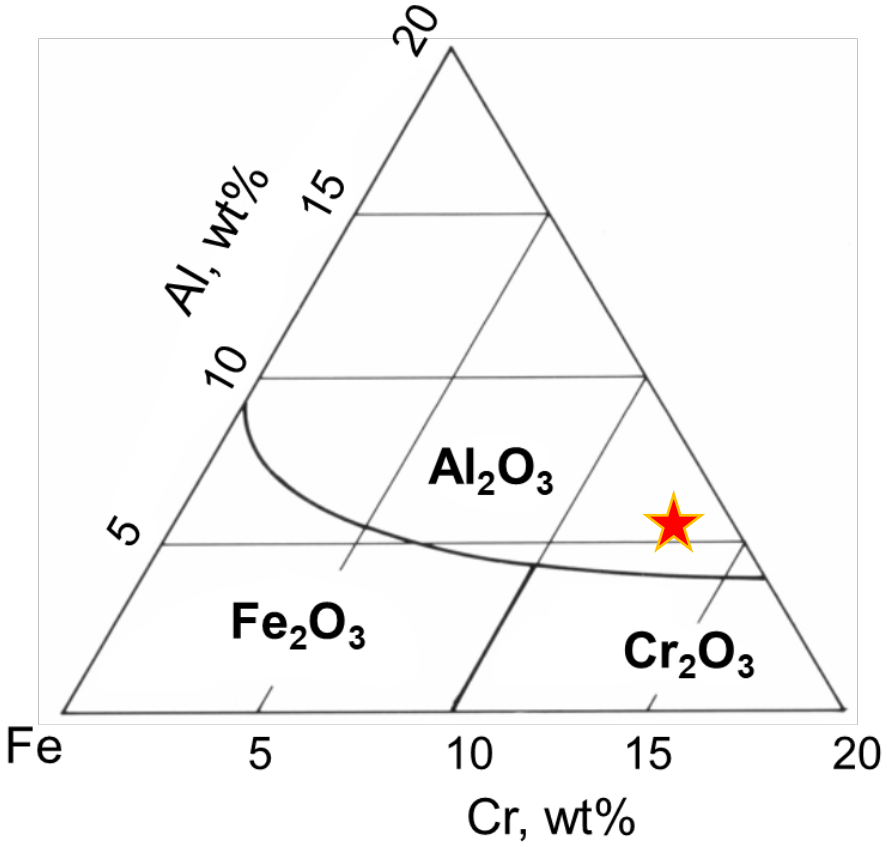

Oxide map at 1000°C

After Scheil and Schultz, Arch. Eisenhüttenwes.6 (1932) 155-160

HT oxidation mechanism of FeCrAl alloys

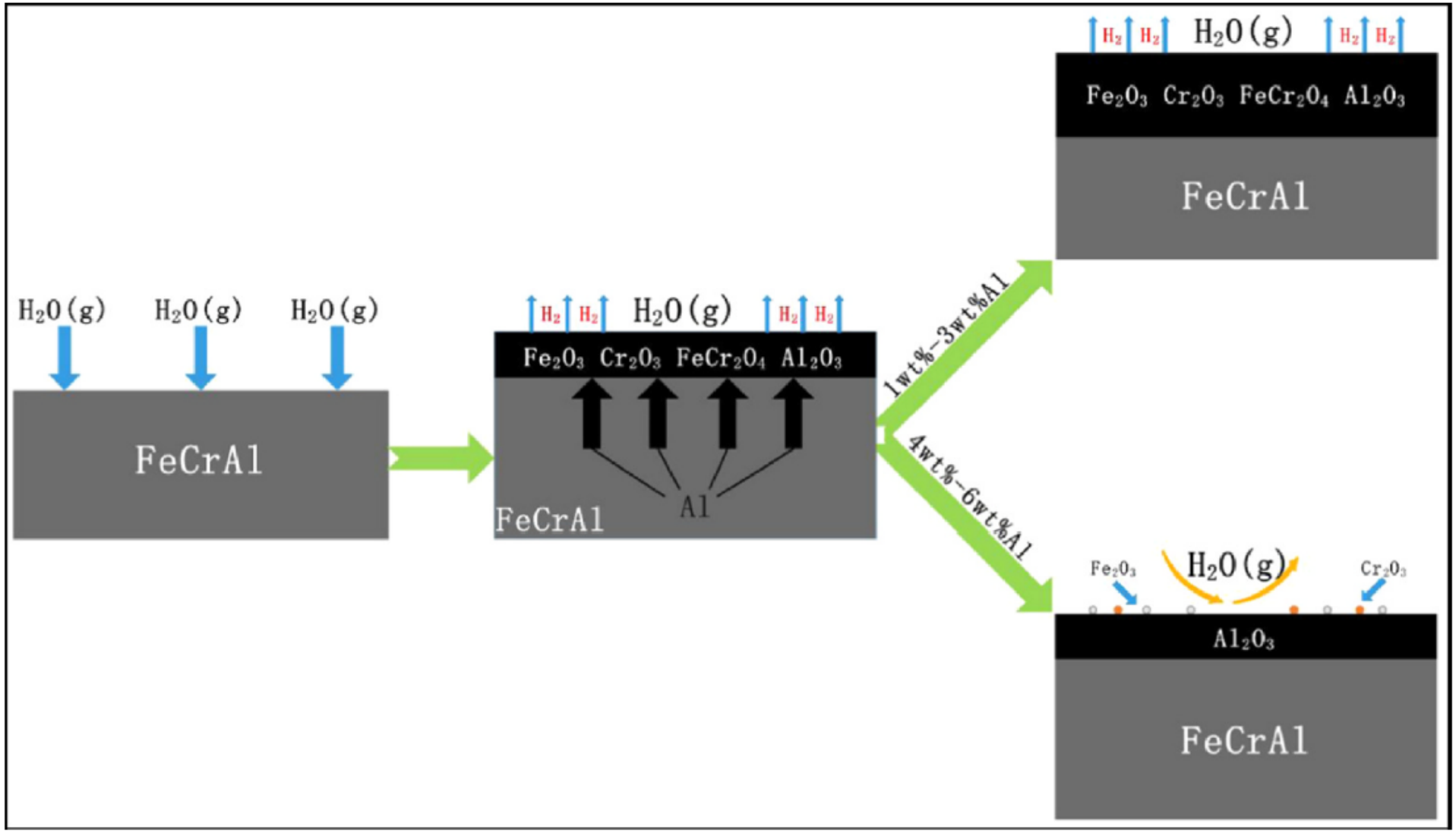

Oxidation of Kanthal APM (FeCrAl) in steam

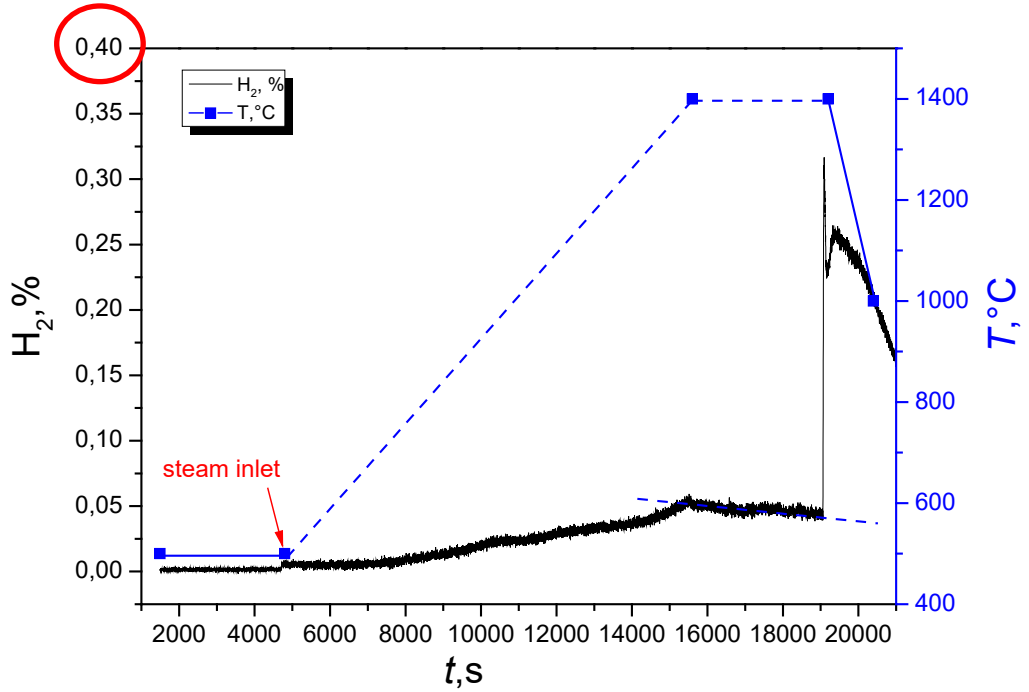

Heating with 5 K/min to 1400°C and subsequent isothermal annealing for 1 h in steam

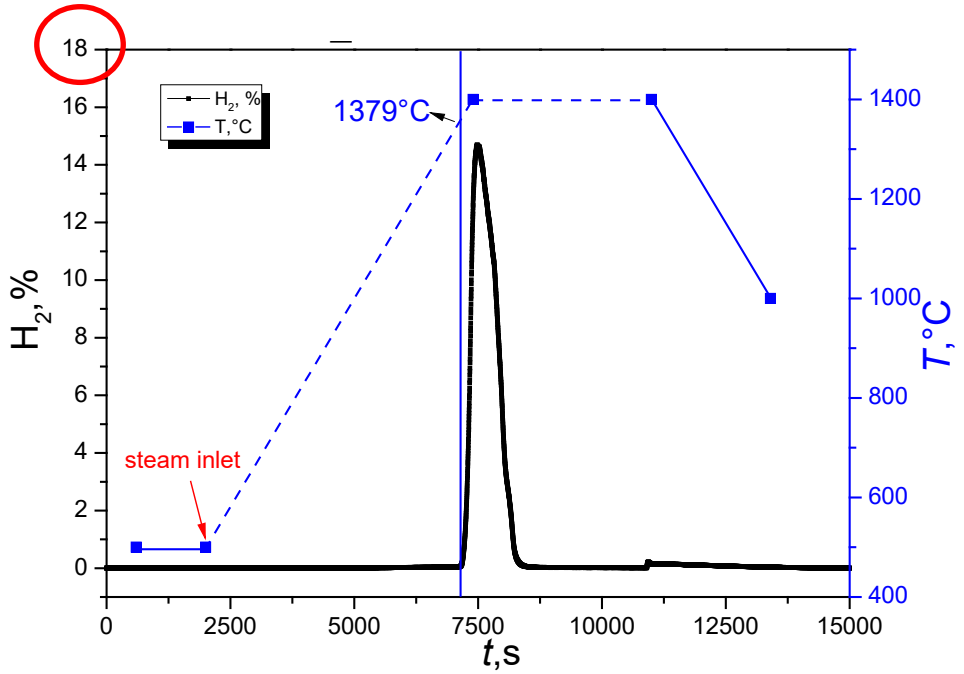

Heating with 10 K/min to 1400°C and subsequent isothermal annealing for 1 h in steam

- Formation of a protective alumina scale during slow heatup or pre-oxidation at lower temperatures
- Otherwise, rapid and complete oxidation of the FeCrAl alloy

Oxidation kinetics of nuclear grade FeCrAl alloys

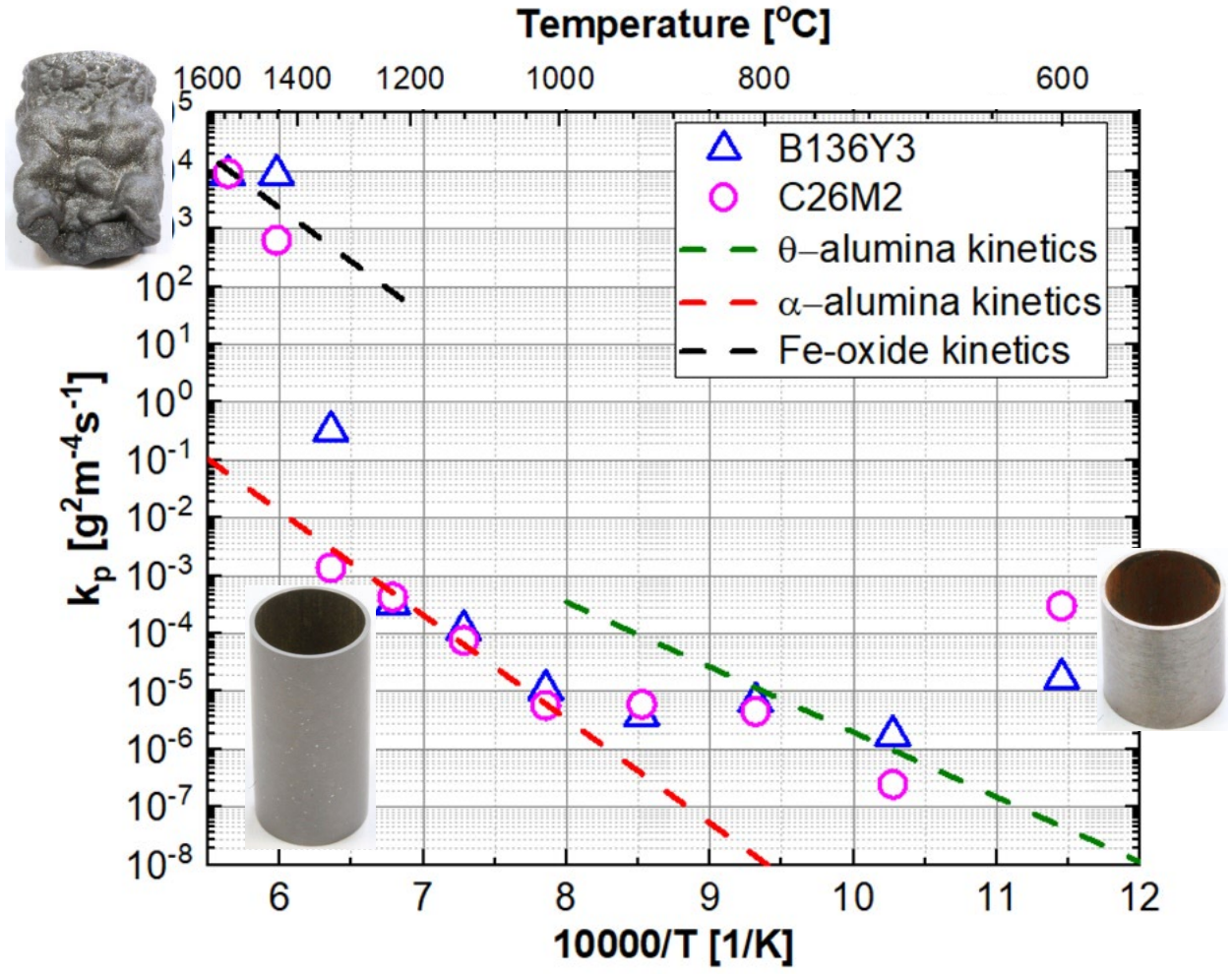

Steam oxidation kinetics of nuclear-grade FeCrAl alloys

- 700°C < T < 900°C:
  Transient oxide kinetics
- 1000°C < T < 1350°C:
  α-alumina kinetics (2-3 orders of magnitude lower than of Zry oxidation)
- T ≥ 1400°C:
  Catastrophic oxidation with kinetics similar to Fe oxidation
- Transition temperature from protective α-alumina kinetics to catastrophic oxidation is dependent on composition, surface finish and heating rate, etc.
- Three different correlations needed for code simulation of SA scenarios with FeCrAl cladding

C. Kim et al., JNM 564 (2022), 153696

QUENCH-19 bundle test with FeCrAl cladding

QUENCH Facility

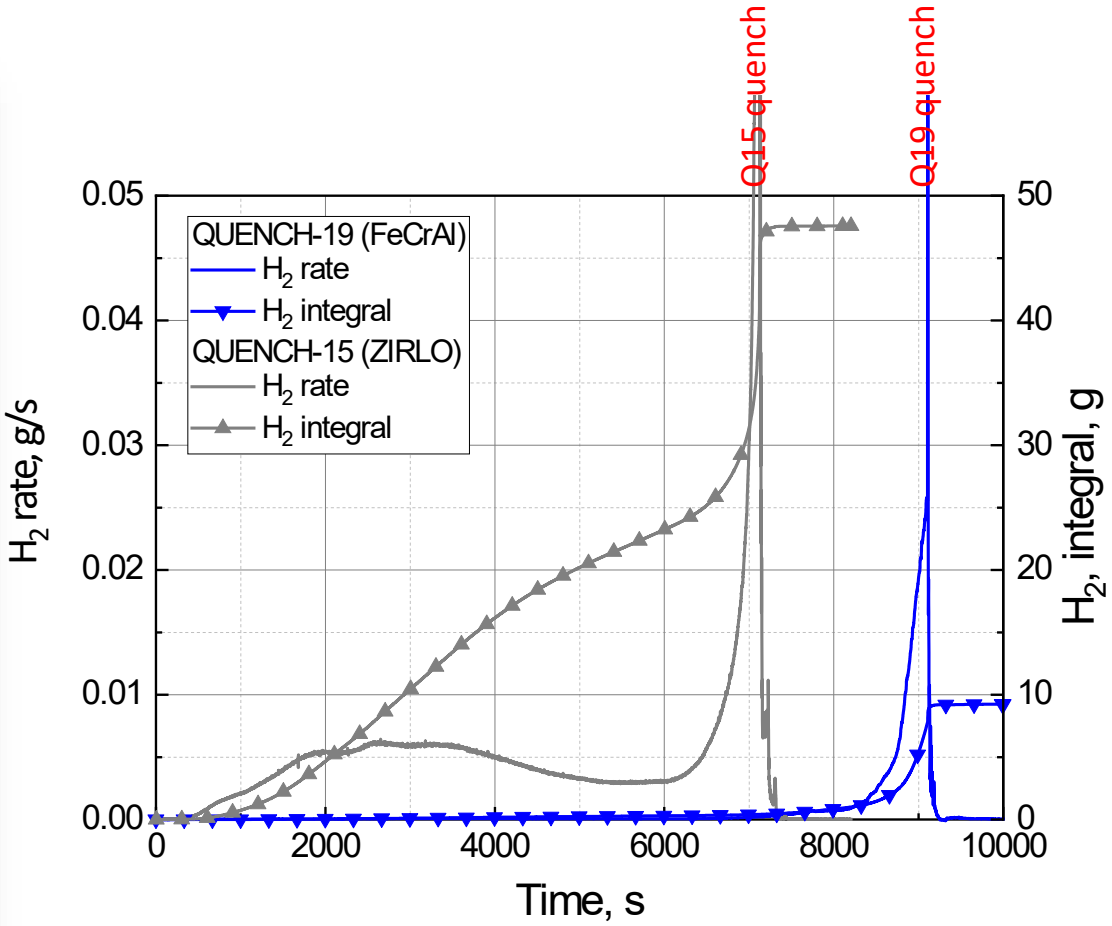

Hydrogen release during QU-19 test compared with reference test QU-15 with ZIRLO

QUENCH-19 bundle post-test

SiC reaction with steam at very high temperatures

$$SiC + 3H_2O \rightarrow SiO_2 + CO + 3H_2$$

Oxidation → scale growth (parabolic kinetics)

$$SiO_2 + 2H_2O \rightarrow Si(OH)_4$$

Volatilization → material loss (linear kinetics)

Paralinear kinetics

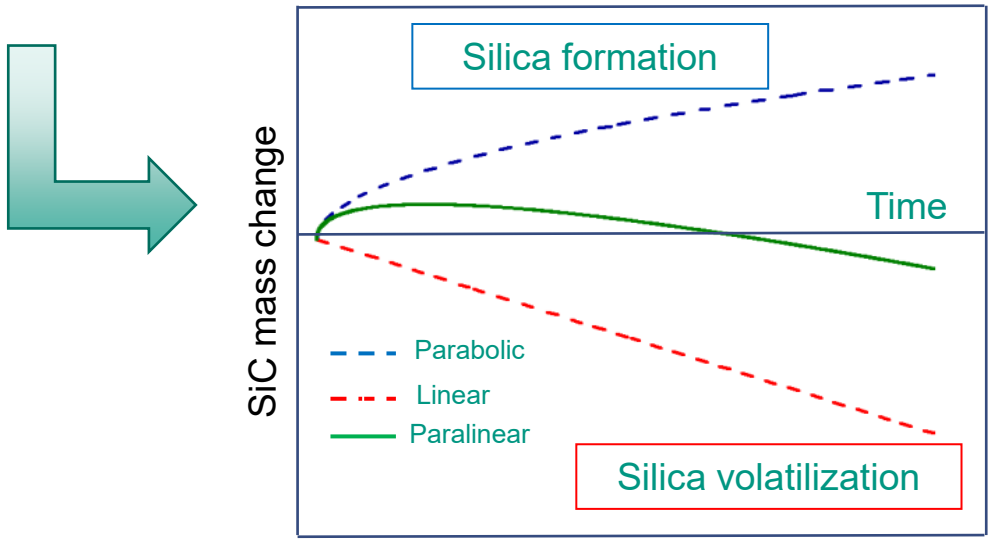

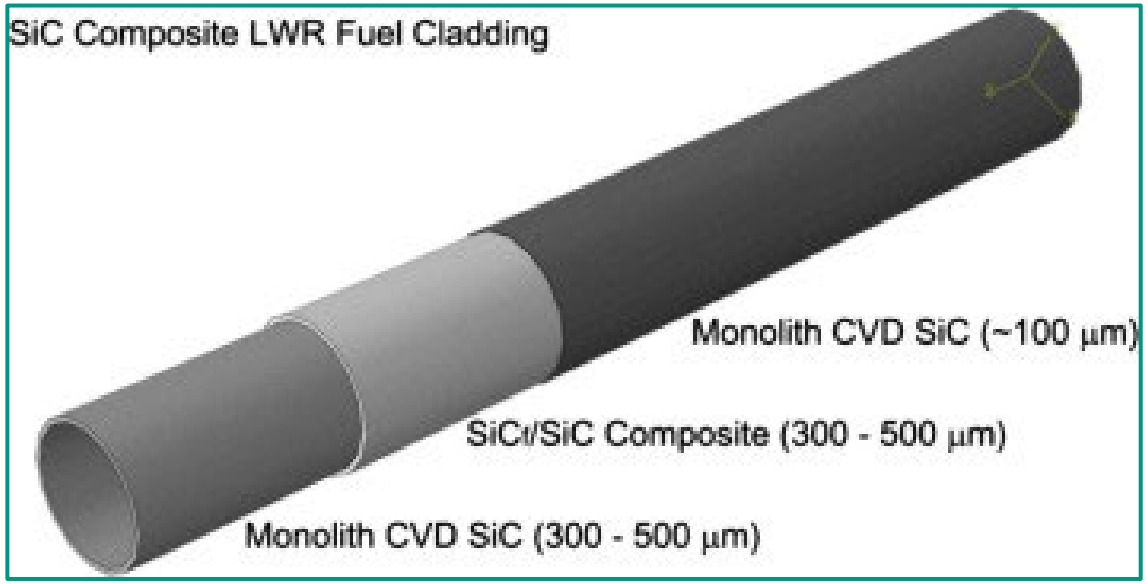

SiC oxidation in steam

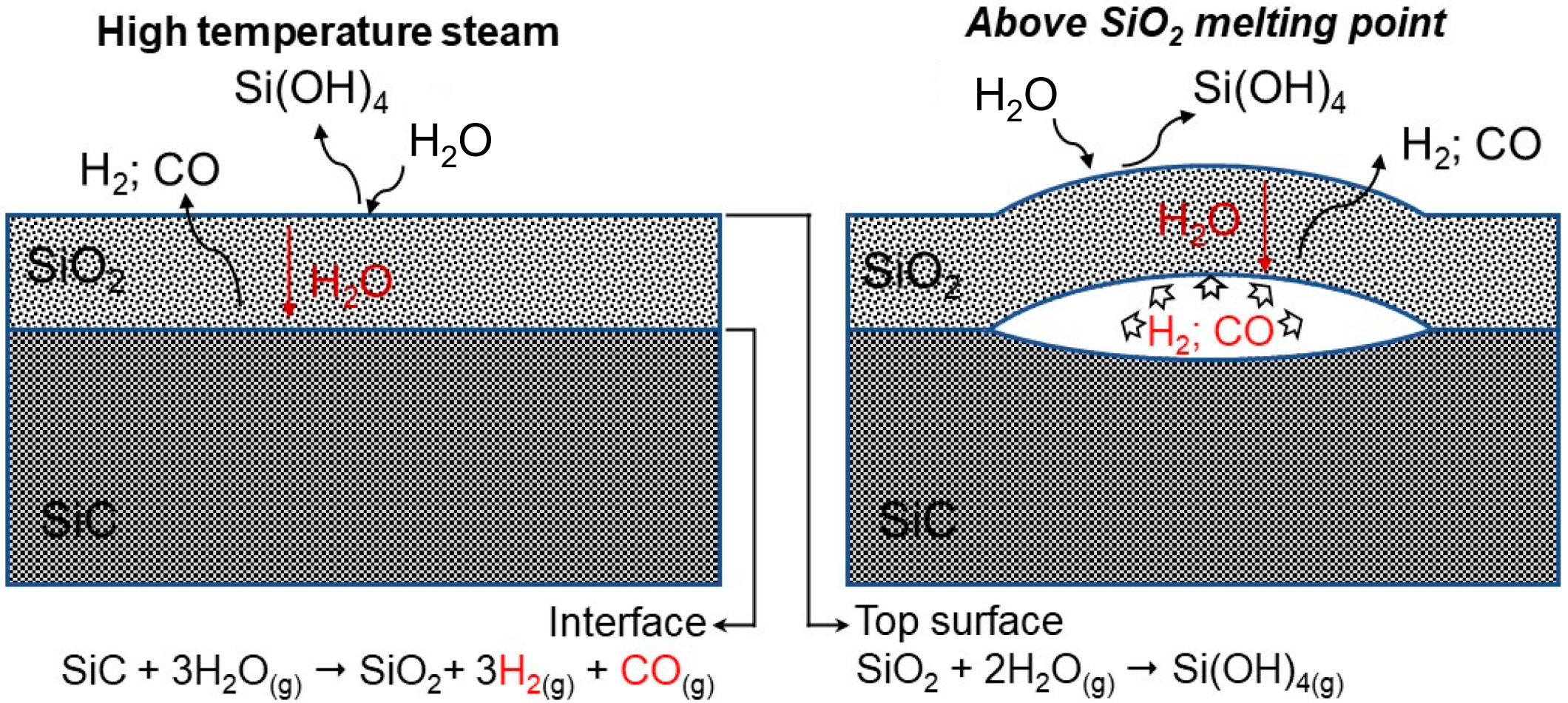

T>1800°C: $SiC + 2\ SiO_2 \rightarrow 3\ SiO_{(g)} + CO_{(g)}$

H.V. Pham et al., Thermo 1 (2021), 151-167

Isothermal test with SiC/SiC: 1 hour at 1700°C
Gas release and post-test appearance

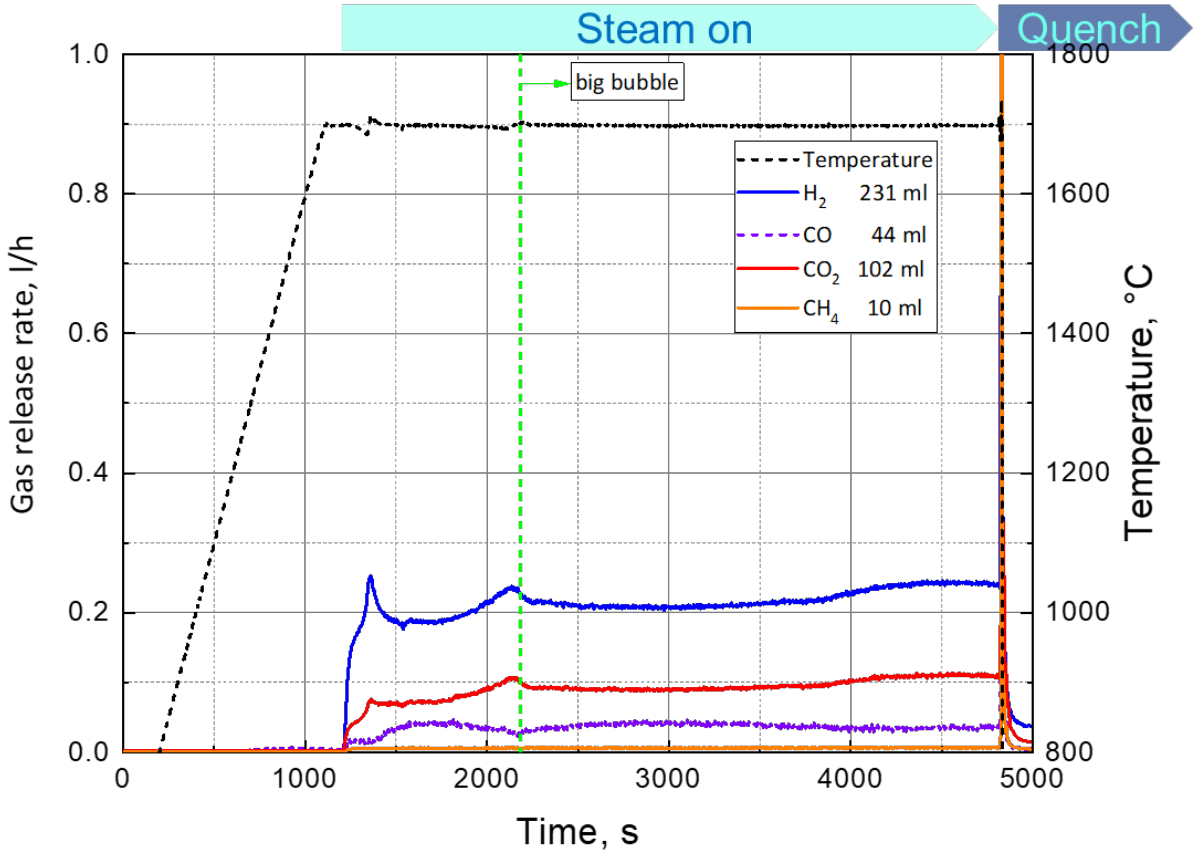

- Very limited oxidation of the SiC_f/SiC cladding at 1700°C
- Recession rate 15-25 µm/h
- Generally, strongly dependent on boundary conditions and impurities

Transient test with SiC: Conduct and MS results

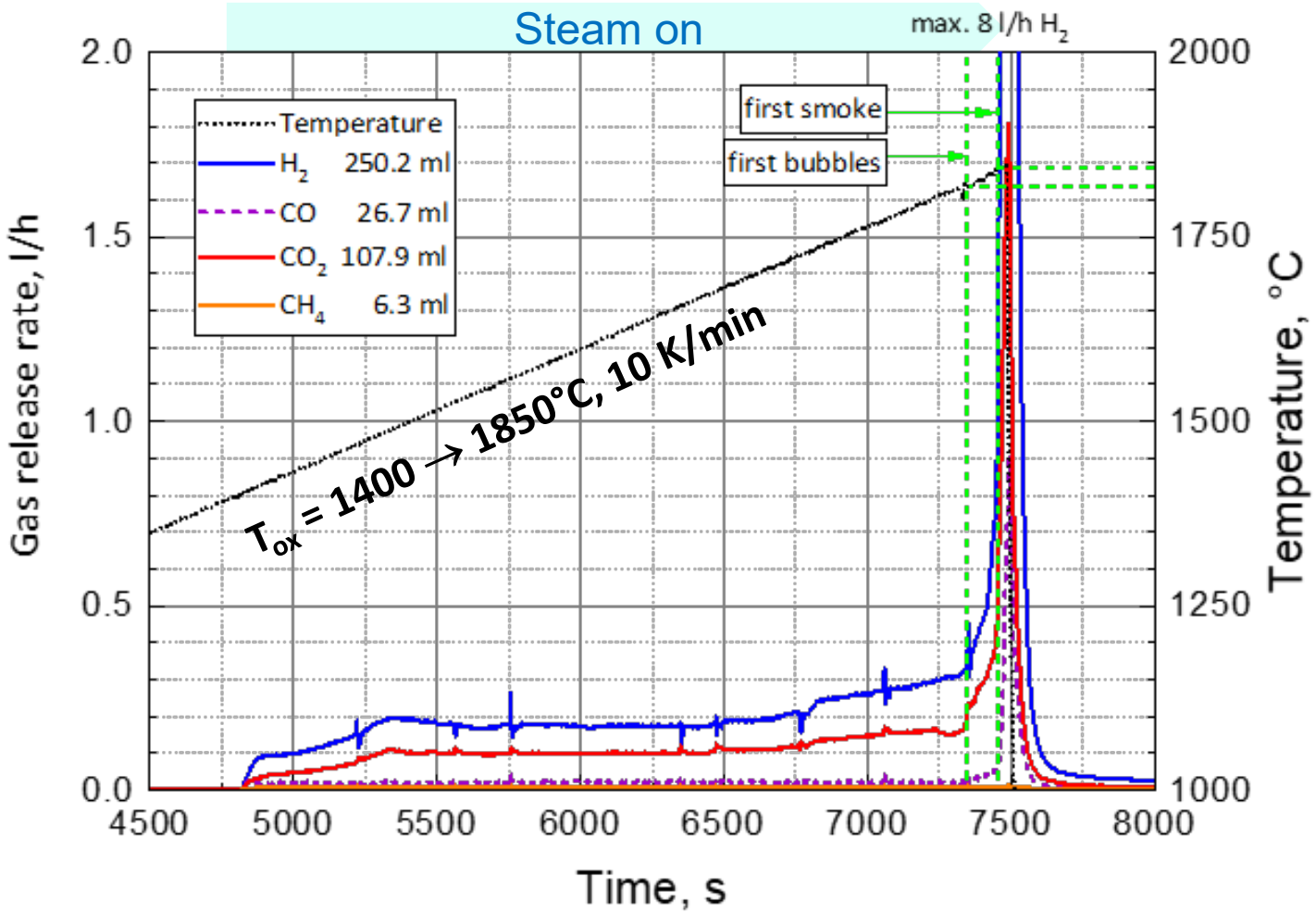

Video snapshot at 1845°C

- Low oxidation kinetics up to ca. 1750°C
- Bubble formation, strong gas release, SiO_x volatilization above ~1750°C

Transient tests: Post-test appearance

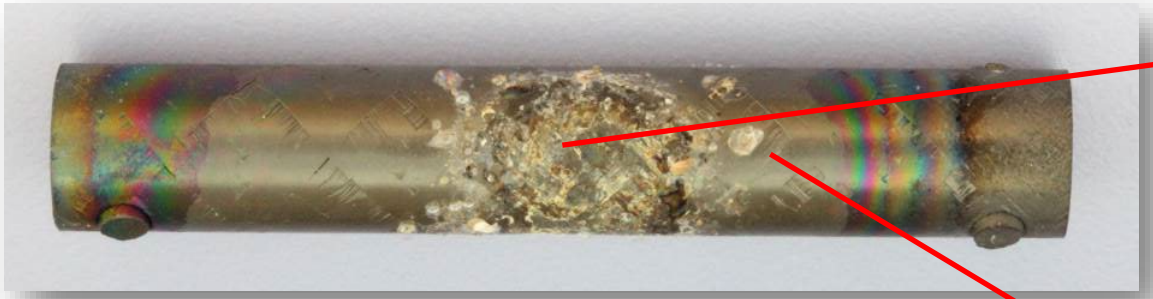

Sample after the transient test up to 1845°C

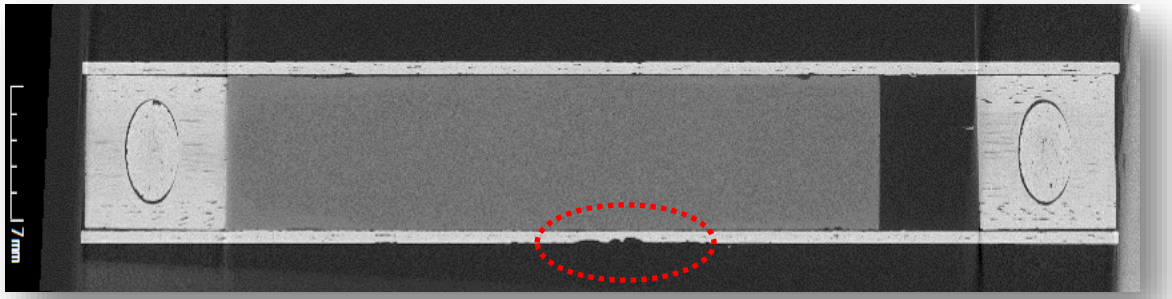

X-ray tomography, longitudinal cut

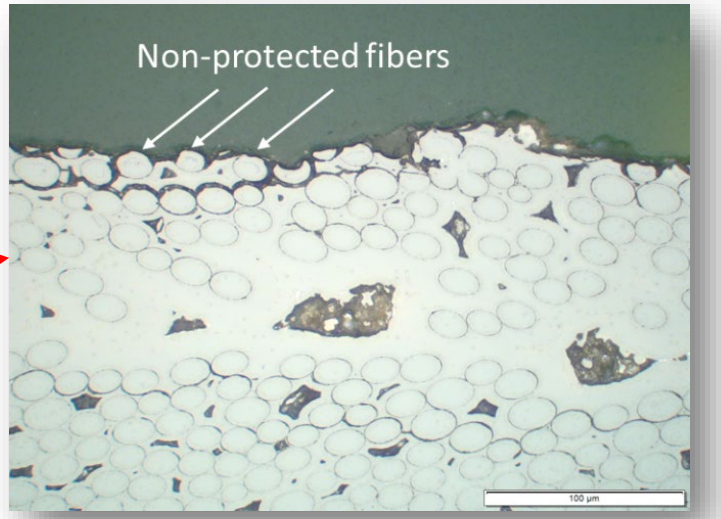

OM from the failure region

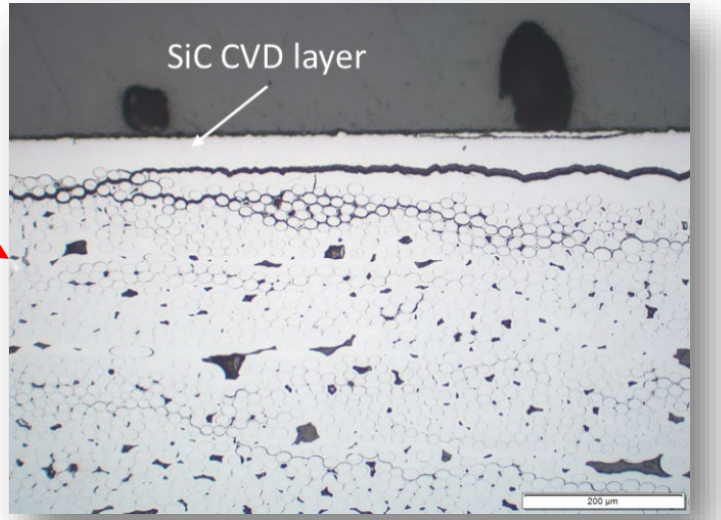

OM from the non-failure region

- Local failure of the CVI seal-coat above 1800°C and attack of SiC fibers

Conclusion I

- Up to a certain temperature, ATF claddings provide much lower HT oxidation rates compared to Zr alloys and therefore may decrease the risk of temperature escalation and hydrogen detonation during nuclear accidents as well as may increase the coping time for AMMs

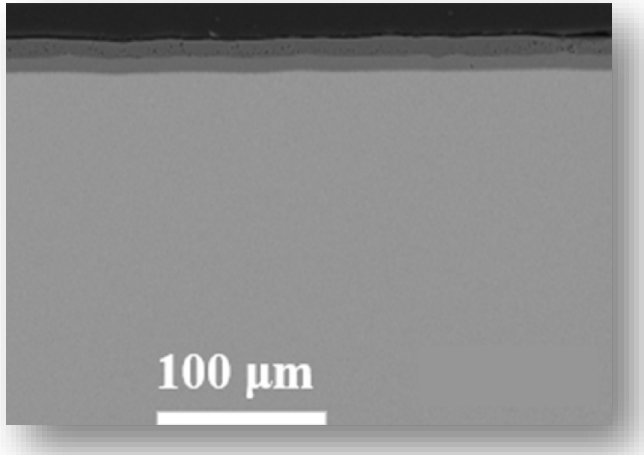

Cr-Zry
2 h 1200°C
steam
12 µm Cr_2O_3

ZrO_2: 250 µm

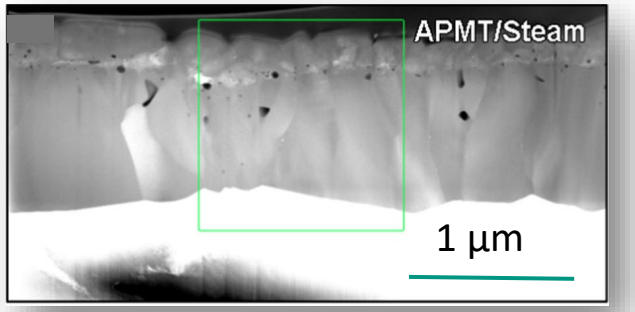

FeCrAl
4 h 1200°C
steam
1 µm Al_2O_3

ZrO_2: 350 µm

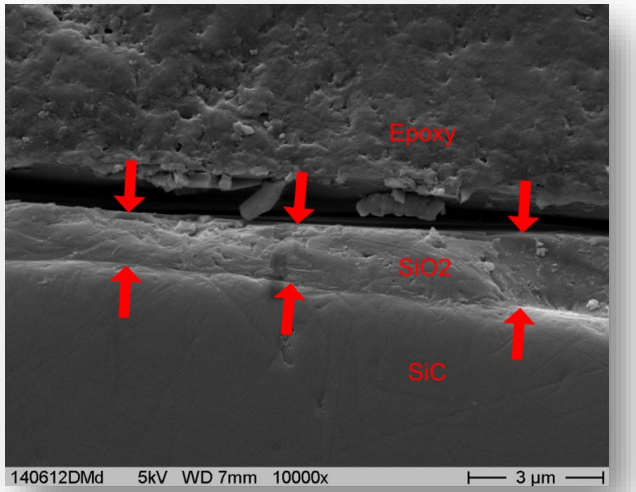

SiC
1 h 1700°C
steam
1 µm SiO_2

ZrO_2: 2400 µm

Chen, JMRT 30 (2024), 4412-4423
Unocic, OxMet 87 (2017), 431-441
Avincola, NED 295 (2015), 468-478

Conclusion II

- Degradation mechanisms of the three most promising ATF cladding concepts are different, they result in the following max. survival temperatures:
  - Cr-coated Zr-based cladding: 1200-1300°C
    - Determined mainly by Cr-Zr eutectic and diffusion processes leading to the loss of protective effect of coating
    - Depending on thickness (and quality) of Cr coating
  - FeCrAl alloys: 1350-1400°C
    - Determined mainly by the competition between bulk Al diffusion and the kinetics of α-alumina formation
    - Depending on composition and heating rate
  - SiC_f-SiC composites: 1700°C (with monolithic external layer)
    - Determined mainly by the volatilization kinetics of silica at HT in steam atmosphere
    - Depending on the thickness of the external monolithic SiC layer and thermo-hydraulic boundary conditions
- **Beyond these maximum temperatures, oxidation kinetics can increase rapidly, leading to an escalation in temperature and H_2 release**


рахмат
danke
謝謝
ngiyabonga
Баярлалаа
mersi
kia ora
barka
welalin
tack
spas
teşekkür ederim
mahalo
tapadh leat
спасибо
faafetai lava
vinaka
спасибі
blagodaram
dank je
misaotra
matondo
paldies
grazzi
gracias
хвала
kiitos
dankie
nanni
nandri
dhanyavad
thank you
asante
manana
obrigada
tenki
bedankt
bayarlalaa
gràçie
hvala
mauruuru
köszönöm
dankon
aciū
akun
djiere dieuf
tau
mochchakkeram
murakoze
enkosi
dziękuję
дякую
mamnun
chokrane
chnorakaloutioun
gratias ago
gràcies
sulpáy
go raibh maith agat
sobodi
dēkuji
sagolun
sukriya
kop khun krap
taiku
obrigado
mèsi
didi madloba
arigatô
takk
dakujem
trugarez
ありがとう
najis tuke
tanemirt
grazie
terima kasih
rahmet
kam sah hamnida
rahmat
diolch
dhanyavadagalu
shukriya
merce
мерси
ευχαριστώ
감사합니다
xièxie
merci

Jean-Christophe Brachet

CEA

Some illustrations of recent studies carried out at CEA on the behavior of Cr-coated Zr-based claddings upon high temperature oxidation, in relation with their post-quenching mechanical properties

The presentation will make an overview of some recent studies carried out at CEA on the behavior of Cr-coated Zr-based Claddings upon High Temperature (HT) steam oxidation in relation with their Post- Quenching (PQ) mechanical properties. The covered topics are:

- Development of simple but robust experimental methodologies to evaluate the overall protectiveness of Cr-based coated materials upon HT (one-sided) steam oxidation [1];

- Introduction of a new “Equivalent Cladding Reacted” parameter - called “Equivalent Chromium Reacted” (ECrR) – that is able to capture the influence of the initial Cr-coating thickness on the resultant cladding’s PQ mechanical strength and ductility [2];

- In-depth microstructural studies of the effect of HT Cr diffusion into the Zr-based substrate on the PQ prior-Zr hardening using in-situ and multiscale examinations of Cr-doped Zr1Nb(O) model alloys, for different cooling scenario from the HT βZr temperature range [3].

Acknowledgment: The presented works have been supported by the CEA-EDF-FRAMATOME “Innovation COMBustible” project.

References:

[1] J.-C. Brachet, et al., "*Some practical methodologies to assess the overall high temperature (onesided) steam oxidation protectiveness of chromium-based coatings on a zirconium-based substrate…*", to be published

[2] J.-C. Brachet et al., "*A new « ECR » parameter to support high-temperature (one-sided) steam oxidation behavior of Cr-coated Zr-based E-ATF claddings, in relation with their post-quenching mechanical strength and ductility…*", Proceedings of Topfuel-2024, Grenoble, France, (Sept. 29th. - Oct. 03rd. 2024)

[3] P. Gokelaere et al., "*Microstructural investigation of Cr coated Zr based alloys upon LOCA conditions*", Oral presentation at NUMAT-2024, Singapore, (14-17 October 2024)

Some illustrations of recent studies carried out at CEA on the behavior of Cr-coated Zr-based claddings upon high temperature steam oxidation, in relation with their post-quenching mechanical properties

J.-C. Brachet et al.,

Paris-Saclay University, CEA, Service de Recherche en Matériaux et procédés Avancés, 91191, Gif-sur-Yvette, France

References:

[1] J.-C. Brachet *et al.*, "*A new « ECR » parameter to support high-temperature (one-sided) steam oxidation behavior of Cr-coated Zr-based E-ATF claddings, in relation with their post-quenching mechanical strength and ductility*…", Proceedings of Topfuel-2024, Grenoble, France, (Sept. 29th - Oct. 03rd 2024);

[2] P. Gokelaere *et al.*, "*Microstructural investigation of Cr coated Zr based alloys upon LOCA conditions*", Oral presentation at NUMAT-2024, Singapore, (14-17 Oct. 2024).

[3] J.-C. Brachet, *et al.*, "*Some practical methodologies to assess the overall high temperature (one-sided) steam oxidation protectiveness of Cr-based coatings on a zirconium-based substrate*…", *to be published;*

jean-christophe.brachet@cea.fr

29th Int. QUENCH Workshop, KIT (Karlsruhe, Germany), 19-21 Nov. 2024

Outlines / recent R&D achievements at CEA:

(1) Find a better "ECR-like" metrics adapted for the Cr-coated Zr-based claddings
(cf. proceedings of Topfuel 2024)

(2) Derive some **relationship between Cr diffusion** *(from the coating)* **profiles** due to the HT incursion **with the residual Post-Quenching (PQ) prior-β_{Zr} hardening & embrittlement** and study more in depth **the underlying metallurgical evolutions**
(Paul Gokelaere PhD work, NUMAT 2024 presentation, more details to be published)

(3) Develop simple - but robust enough – **practical methodologies for overall Cr-coating protectiveness evaluation upon HT steam oxidation**
(to be published…)

Outlines / recent R&D achievements at CEA:

(1) Proposal of a new "ECrR", adapted for the Cr-coated Zr-based claddings…

(2) Relationship between Cr diffusion *(from the coating)* profiles upon HT incursion with the residual PQ prior-β_{Zr} hardening & embrittlement + underlying metallurgical evolutions…

(3) Overall Cr-coating protectiveness evaluation upon HT steam oxidation…

New « ECrR » / Introduction (1/2)

⇒ Following HT steam oxidation *(for LOCA and beyond conditions)*, **both experimental (based on measured Weight Gain) and calculated "$ECR_{BJ/CP}$"** (*used since the 70ties for the uncoated Zr-based claddings*) **are not adapted "metrics" to rely on the PQ mechanical properties of Cr-coated claddings**;

⇒ **Fundamentally due to the different underlying HT oxidation mechanisms** (*between uncoated & coated materials*) and the **different induced oxygen diffusion profiles and partitioning into the Zr-base (β_{Zr})** substrate

Materials	Oxidation time at 1200 °C (s)	WG (mg/cm²)	ECR_{WG} (%)	Fraction of ECR corresponding to oxygen which has diffused into the metallic substrate
Uncoated $M5_{Framatome}$	60 - 1420s	4 - 24	3 - 20	20-30 %
12-15µm Cr-coated $M5_{Framatome}$	9000	15 - 16	12 - 13	85 %

Brachet et al., JNM 2020

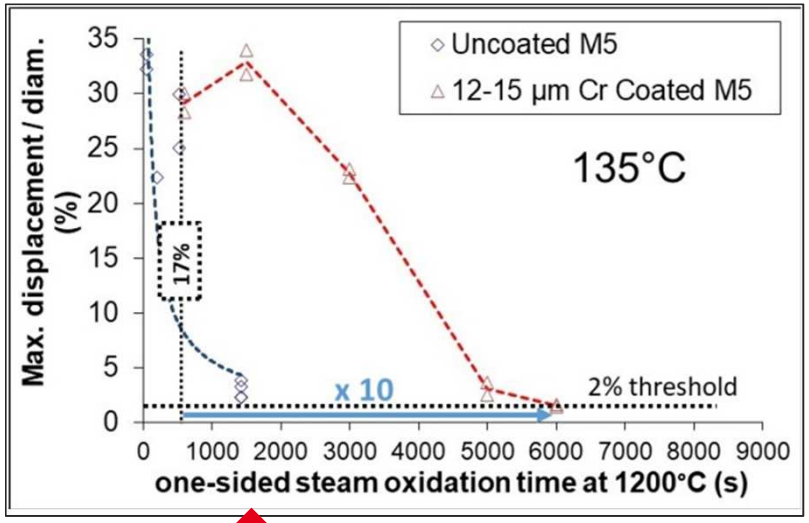

Seems to be contradictory?

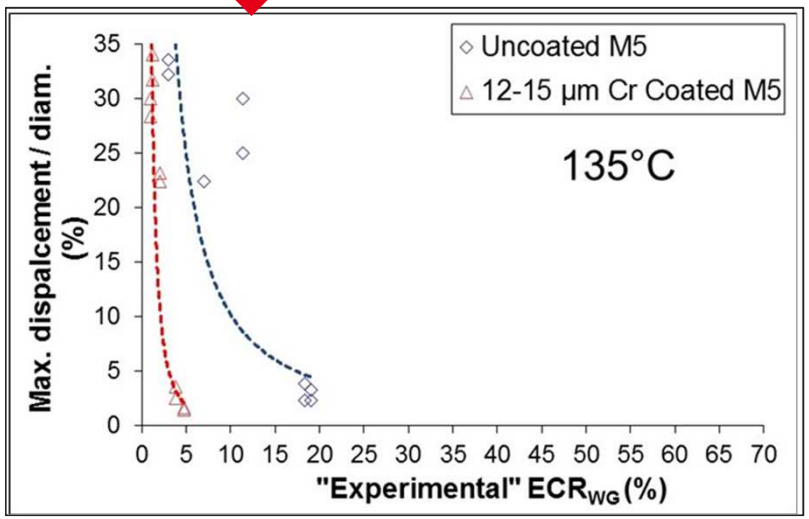

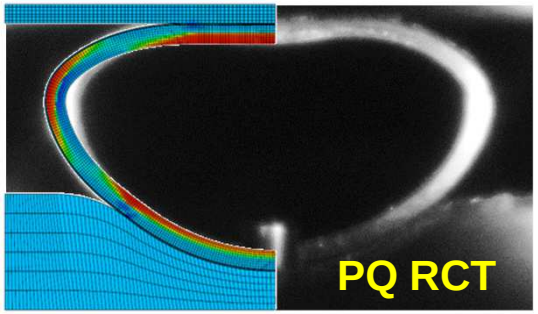

New « ECrR » / Introduction (2/2)

=> Additional limitation by using **conventional approaches** (*i.e., calculated Baker-Just or Cathcart-Pawel ECR correlations that have been derived for the uncoated reference claddings and/or experimental / WG ECR)* is that such parameters **are <u>not able to account for the influence of the initial Cr-coating thickness</u>**

Offset strain (~ « Residual ductility »)

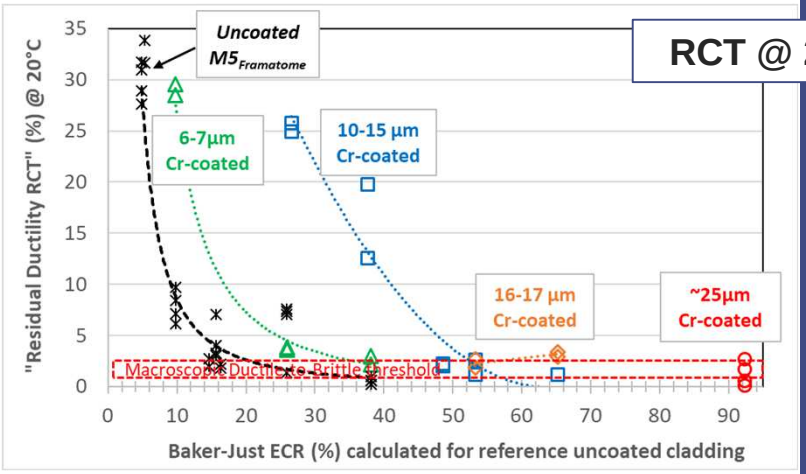

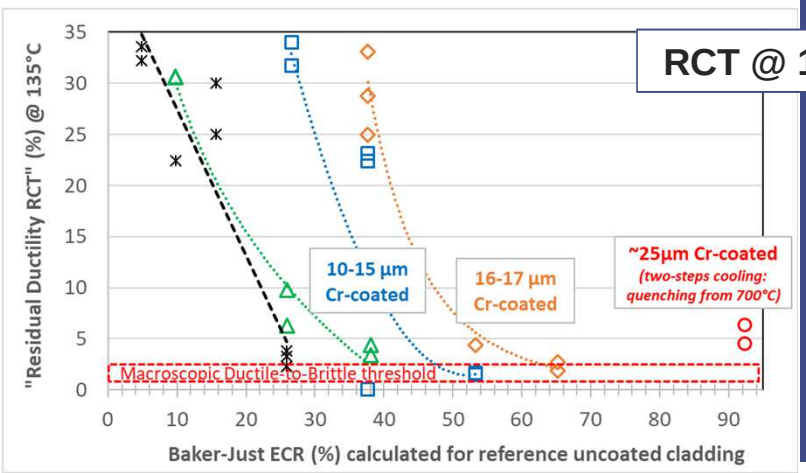

Max. Force (~ « Residual strength »)

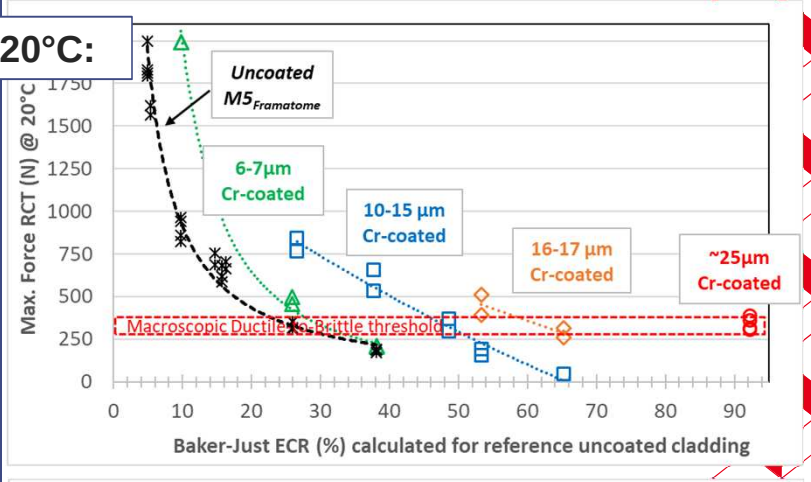

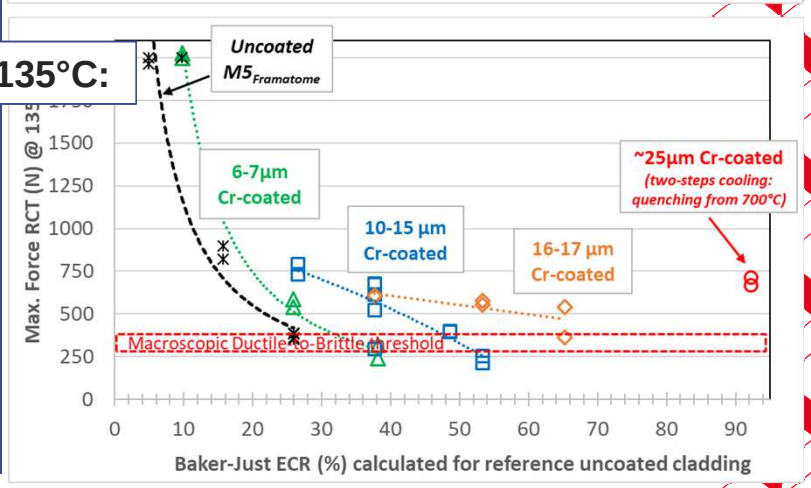

Recall: consumption kinetics of Cr coatings on Zr-based substrate upon HT steam oxidation (*1000-1300°C, LOCA and slightly beyond conditions*)

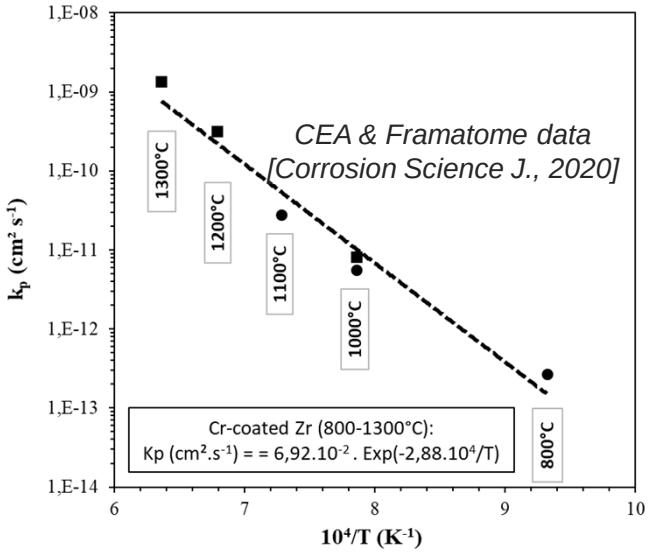

Arrhenius plot of the rate constant of the parabolic law describing the growth kinetics of Cr_2O_3 upon HT oxidation

$Kp(Cr_2O_3) = Kp_0 . Exp(-E/RT)$		$Kp'(Cr_2O_3) = Kp_0' . Exp(-E'/RT)$	
With **Cr_2O_3 thickness =** $\sqrt{Kp(Cr2O3).t}$		With **Cr_2O_3 thickness =** $Kp'(Cr2O3).\sqrt{t}$	
E (J/mol)	239493	E' (J/mol)	119747
Kp_0 (cm²/s)	$6,92.10^{-2}$	Kp_0' (m/s$^{1/2}$)	$2,63.10^{-03}$

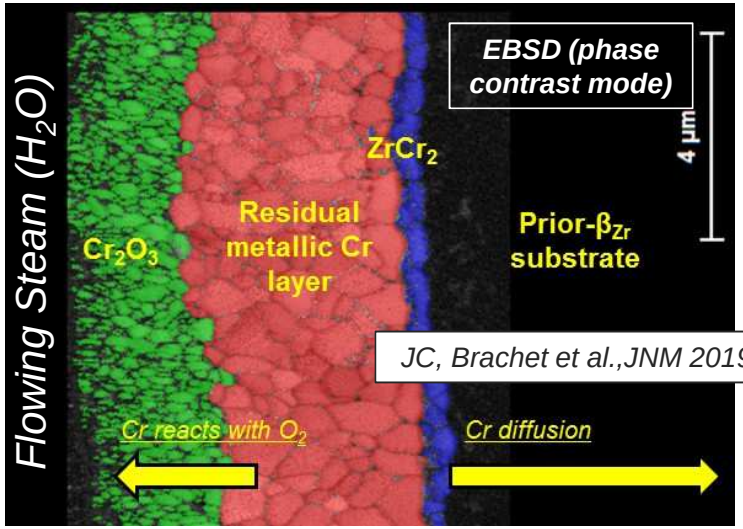

JC, Brachet et al.,JNM 2019

Consumption kinetics of the Cr coating at HT (steam environment) by:

(1) Outer Cr_2O_3 scale thickening

(2) Cr diffusion into the β_{Zr} substrate

which relies on **Cr thermal diffusivity and Cr solubility in β_{Zr}**

(3) Cr volatilization & Cr consumption due to the interlayer $ZrCr_2$ thickening can be neglected (< 2µm)

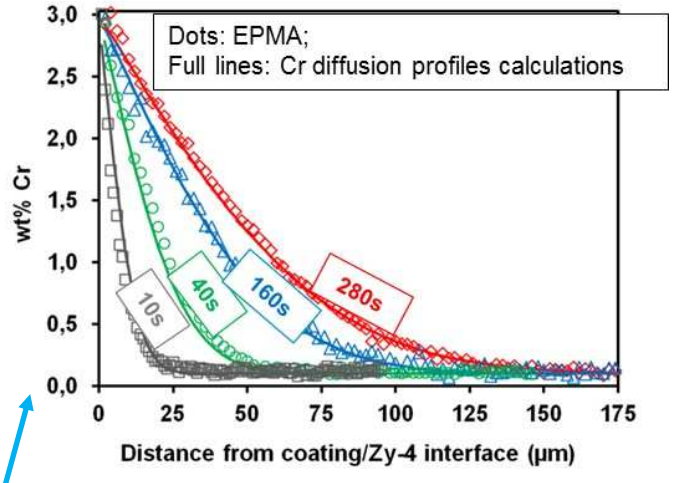

Thermocalc© + CEA-Zircobase-1995 calculations:

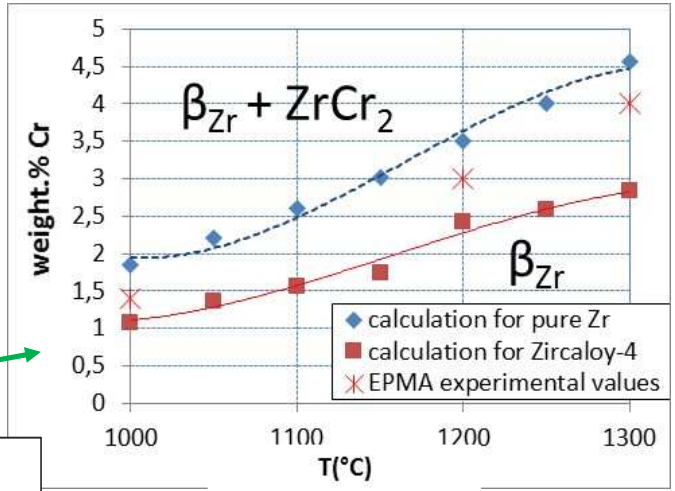

Overall Cr consumption of Cr coating by both (1) Cr_2O_3 outer scale thickening and (2) diffusion into β_{Zr} substrate:

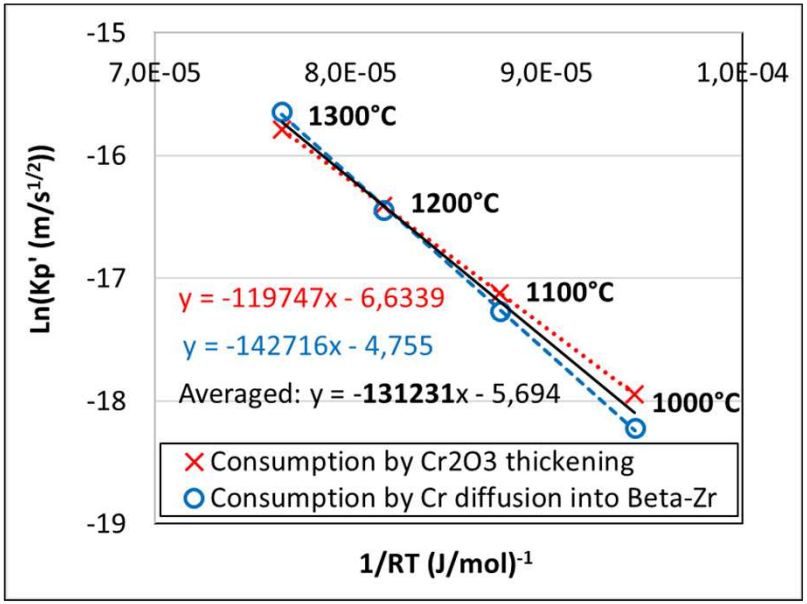

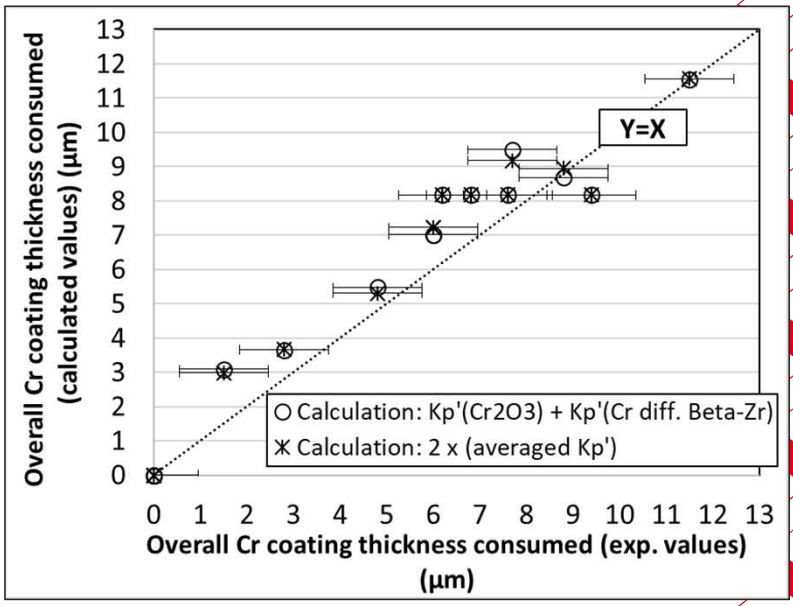

Due to similar parabolic rate constant (Kp') values upon HT steam oxidation, one can identify an **"averaged" Kp' describing the overall contributions of both Cr-coating consumption mechanisms**

<u>Overall</u> Cr consumption kinetics:

$$\Delta Cr_{(Cr2O3 + Cr\ diffusion\ into\ \beta\text{-}Zr)} = 2 \times Kp'_{Averaged}.(t)^{1/2} = 6{,}73.10^3.exp(-15784/T).(t)^{1/2}$$

*With: **ΔCr in µm**, T in Kelvin and t in seconds*

*Remarks: Due to occurrence of "eutectic Zr-Cr reaction" above 1300°C, overall parabolic kinetics is **only valid within the 1000-1300°C β_{Zr} temperatures range***

⇒This **simple overall (parabolic) Cr consumption kinetics** predictions **compare well with the experimental data**

More details in JC. Brachet et al. (Topfuel 2024)

New ECR parameter, *i.e.*, « *Equivalent Chromium Reacted* » proposed, taking into account the initial Cr-coating thickness (X_0):

$ECrR\ (\%) = 6{,}73.10^5.\exp(-15784/T).(t)^{1/2} / X_0$ *(X_0 in µm)* *(1/3)*

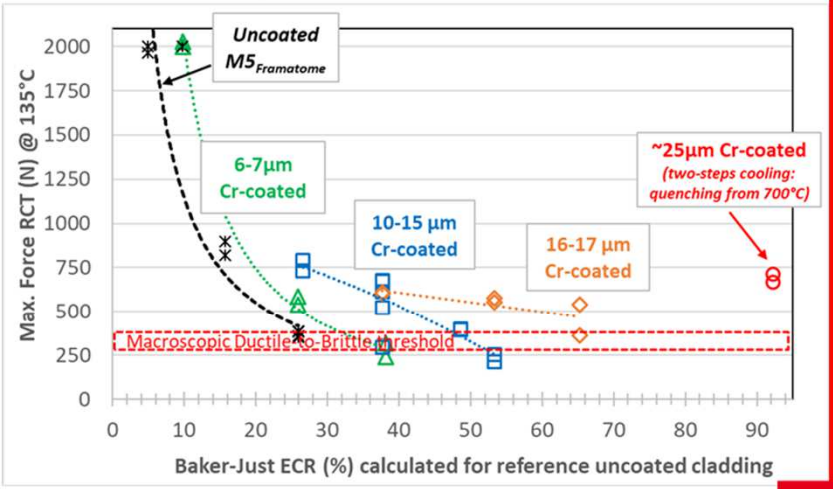

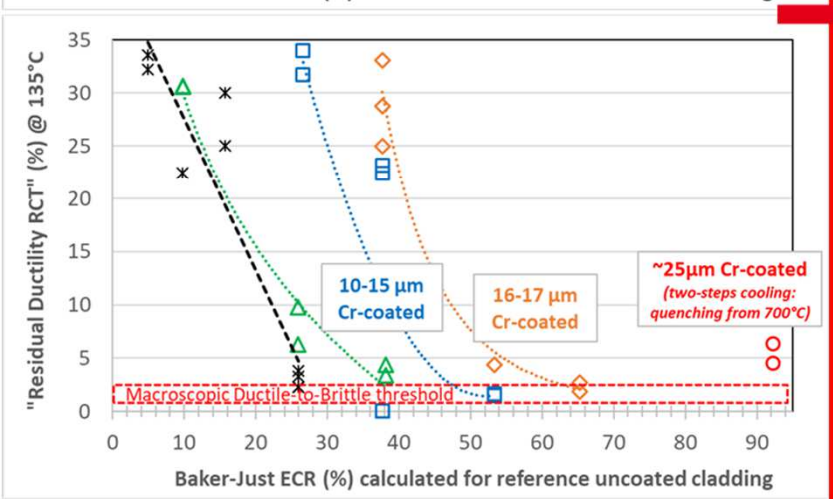

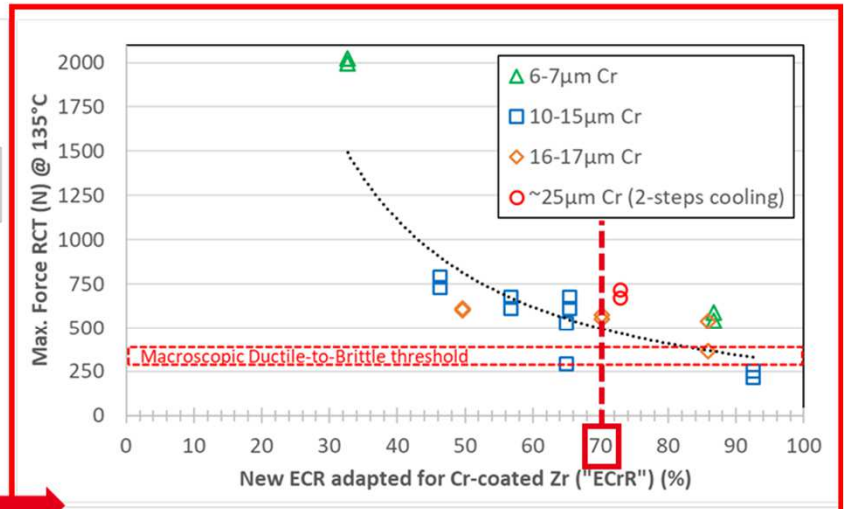

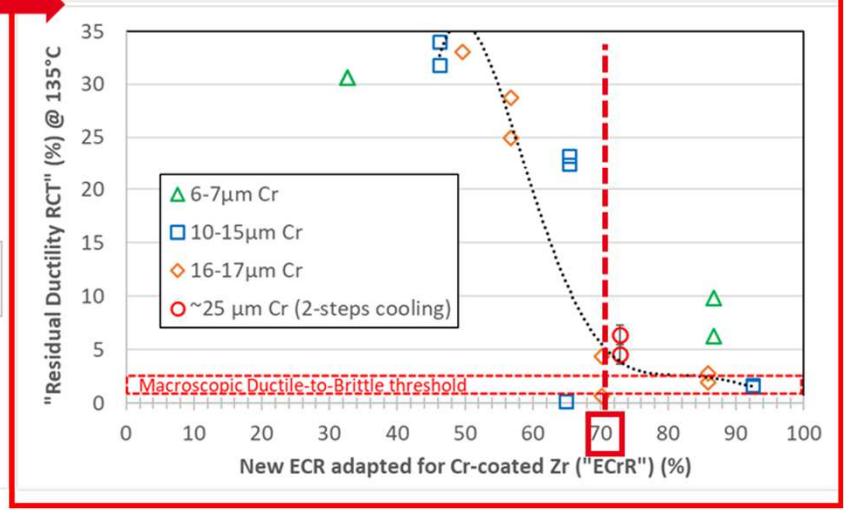

Partial Conclusion (1):

- **New "ECrR" parameter helps to "rationalize" the PQ clad mechanical properties of Cr-coated materials derived from RCT, by taking into account the initial Cr-coating thickness influence**

Partial Conclusion (2):

- **After 1sided steam oxidation & water quenching, determination of an apparent "critical ECrR" ~ 70% which *corresponds to Ductile-to-Brittle-Transition derived from RCT* @ 20 & 135°C**

Using the “critical” ECrR=70% threshold value, one can calculate typical “grace time” of Cr-coated Zr based claddings before reaching PQ Ductile-to-Brittle transition vs. initial Cr thickness
(*for <u>one-sided</u> steam oxidation and ~0.6 mm thick claddings*):

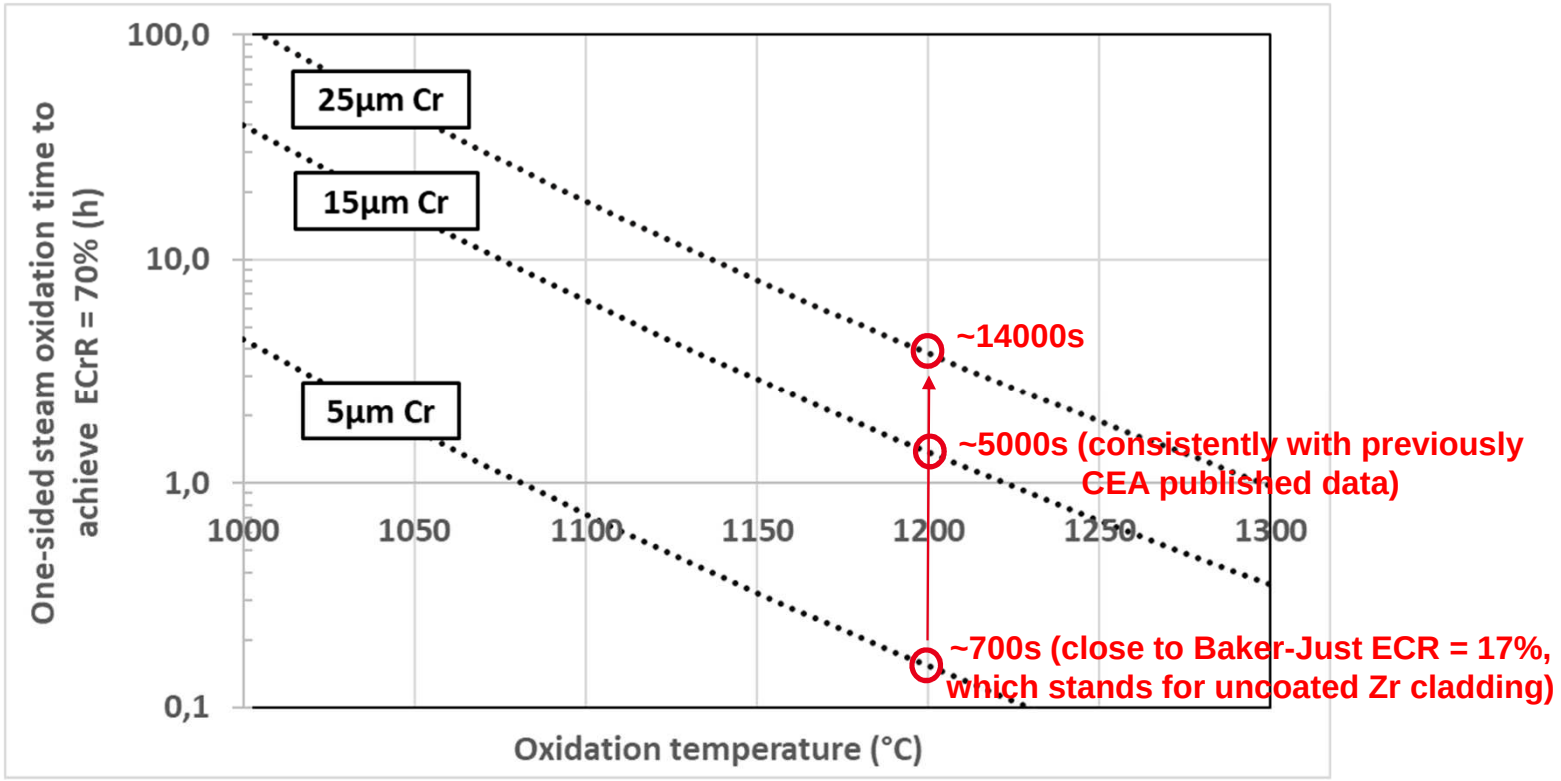

⇒ Among other results, such predictions confirm that **Cr-thickness lower than 10µm brings limited “grace time”**…

Outlines / recent R&D achievements at CEA:

(1) Proposal of a new “ECrR”, adapted for the Cr-coated Zr-based claddings…

(2) Relationship between Cr diffusion *(from the coating)* profiles upon HT incursion with the residual PQ prior-β_{Zr} hardening & embrittlement + underlying metallurgical evolutions…

(3) Overall Cr-coating protectiveness evaluation upon HT steam oxidation…

M5$_{Framatome}$ Cr coated behavior after direct quenching from 1200°C

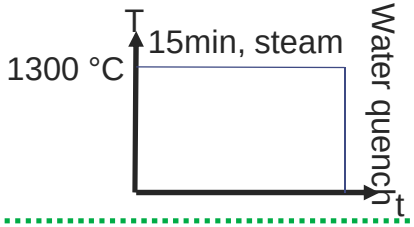

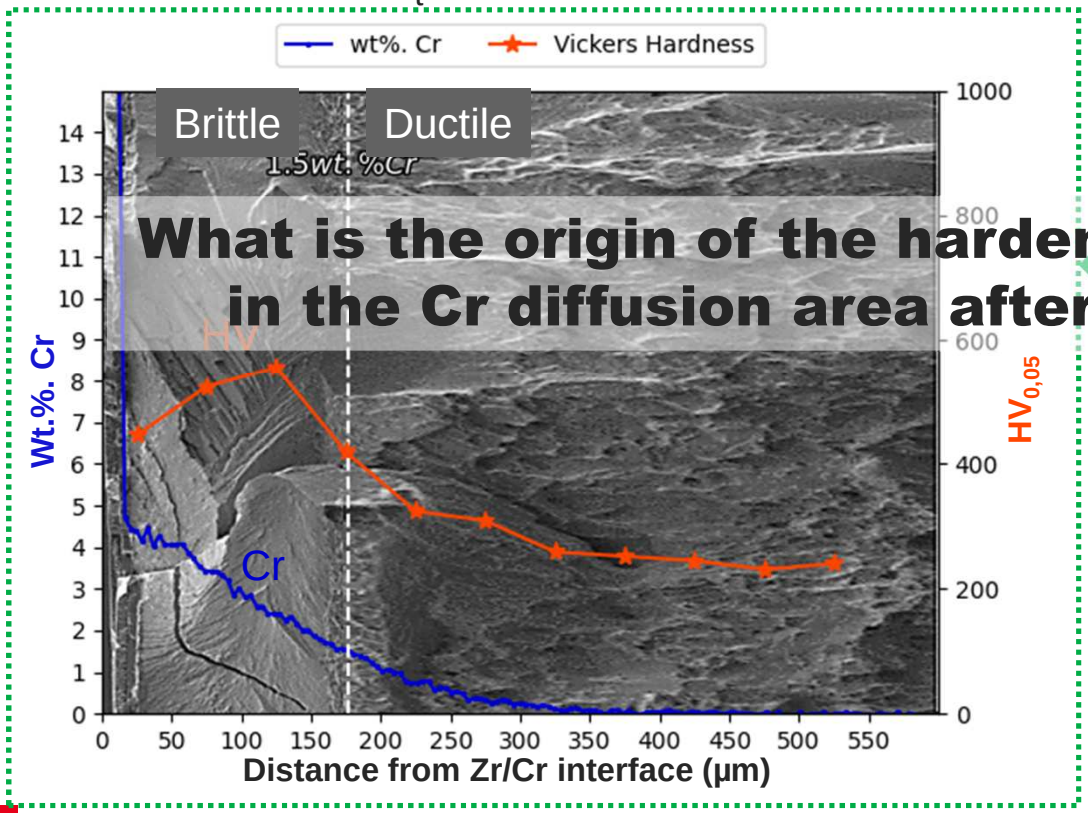

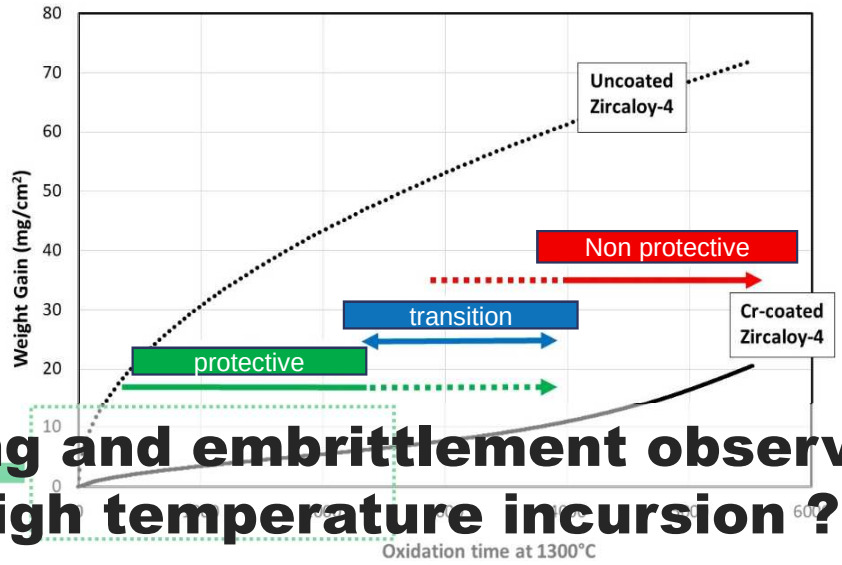

What is the origin of the hardening and embrittlement observed in the Cr diffusion area after high temperature incursion ?

- Upon HT transient, the Cr diffuses from the coating
- **After direct water quenching** following HT oxidation, **Cr enrichment in prior-β$_{Zr}$ induces PQ clad hardening and embrittlement beyond 1,5wt%**

Model material approach

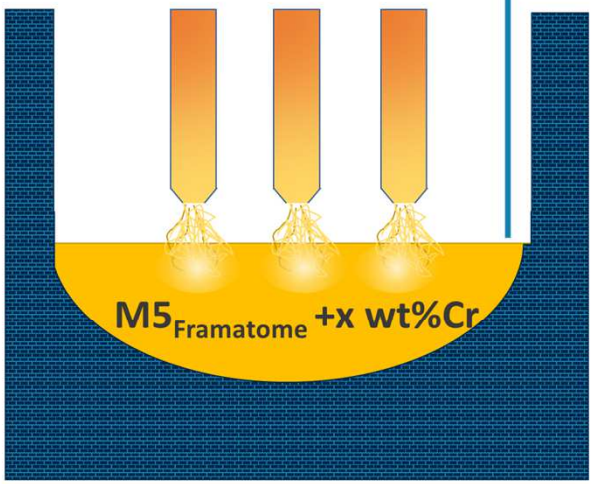

Arc furnace

M5 | 0,75 Cr | 1Cr | 1,25 Cr

2Cr | 2,5Cr | 3Cr | 4Cr

Heat treatment to reproduce LOCA like microstructure

characterisation

thermal

mechanical

microstructural

Thermodynamic modeling

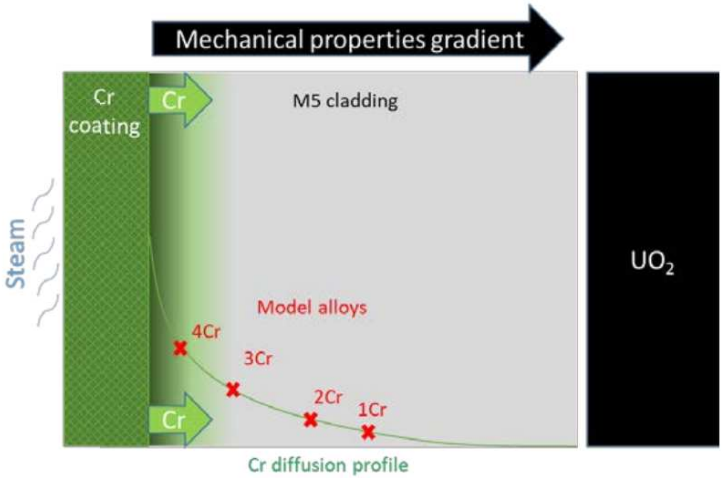

❖ Water quench

Origin of Cr embrittlement

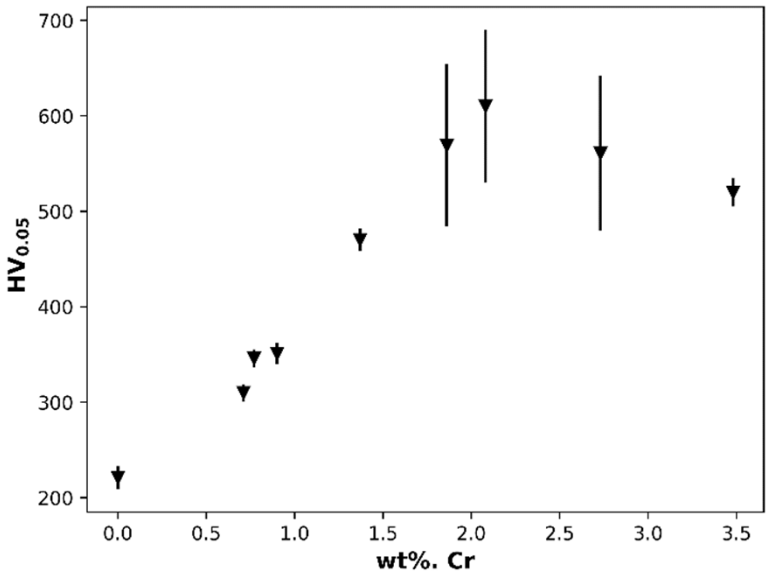

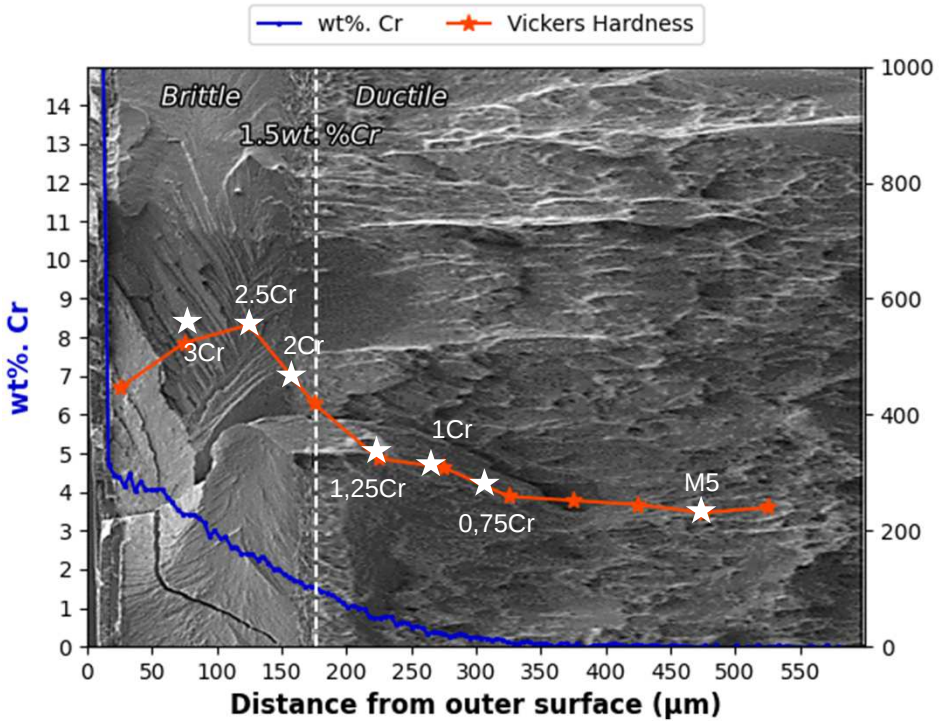

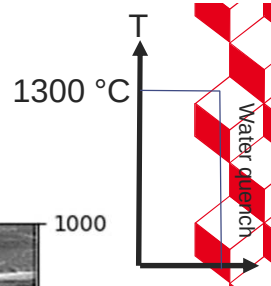

Model materials **reproduce** the hardening observed locally in Cr coated cladding;
When C_{Cr}<2 wt.%Cr: Linear hardening vs. % Cr
When C_{Cr}>2 wt.%Cr: Hardening plateau and then slight decrease are observed vs. % Cr

Numat 2024 *Paul.gokelaere@cea.fr*

❖ Water quench

Origin of hardening evolution for C_{cr}>2 wt.%.

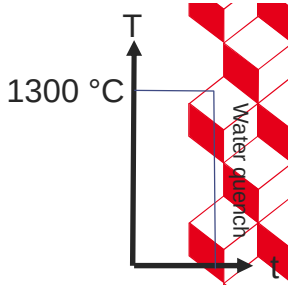

Zr1Nb(O)+3%wt.Cr

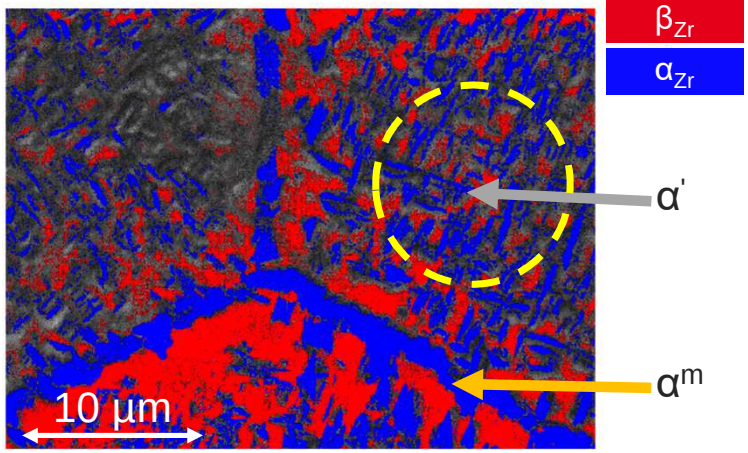

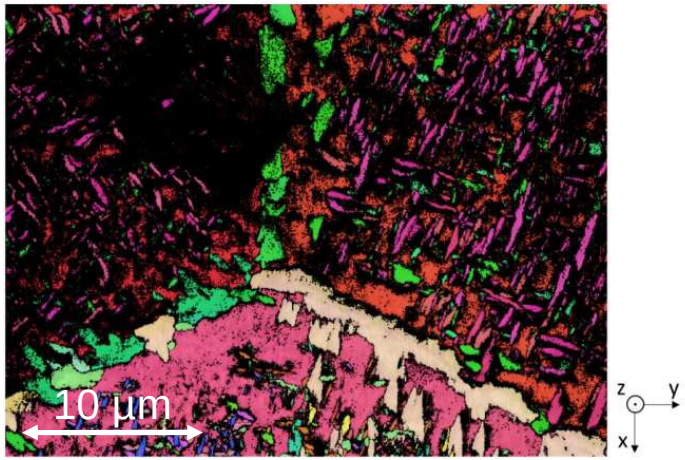

=> Deep multiscale metallurgical study…

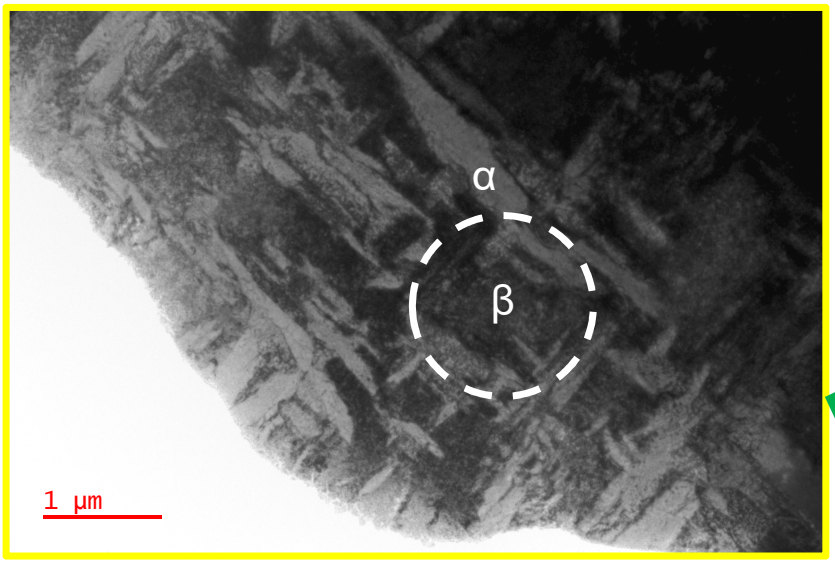

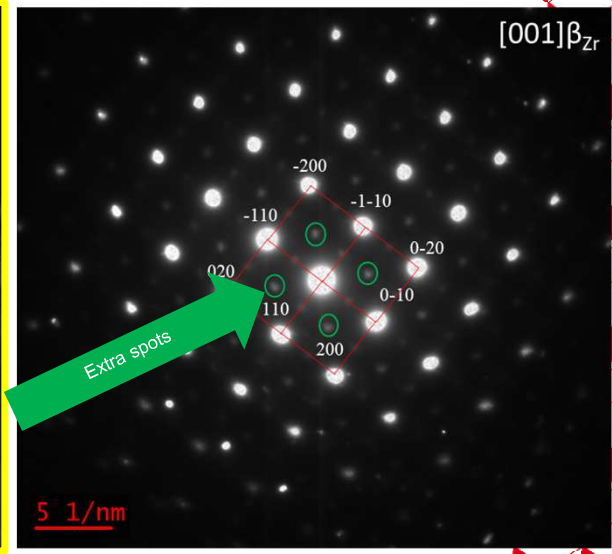

Numat 2024 Paul.gokelaere@cea.fr

❖ **Water quench**

Origin of hardening evolution for C_{cr}>2 wt.%.

Zr1Nb(O)+3%wt.Cr

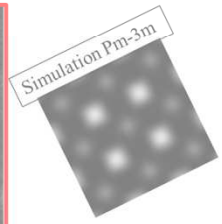

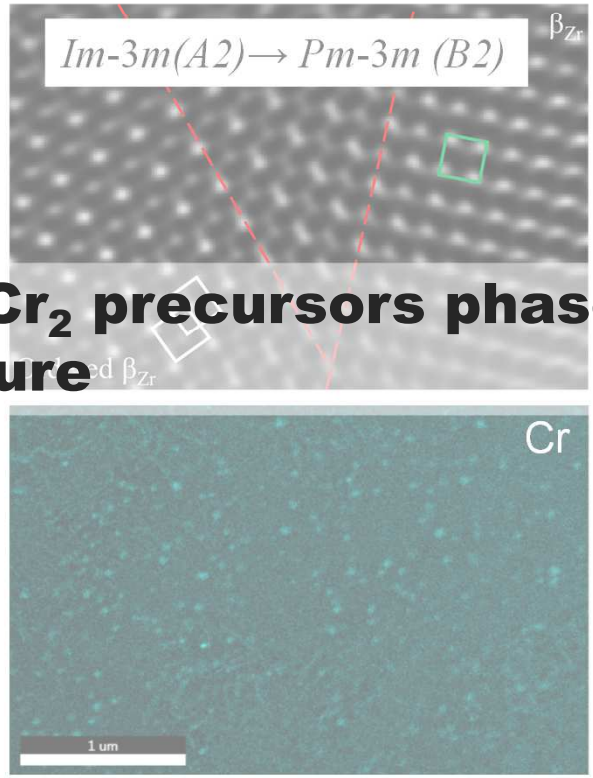

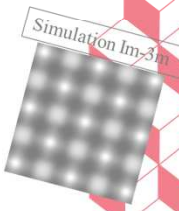

The ordered phases may correspond to $ZrCr_2$ precursors phase with a transitional structure

❖ Water quench

Origin of hardening evolution for C_{cr}>2 wt.%.

Zr1Nb(O)+3%wt.Cr

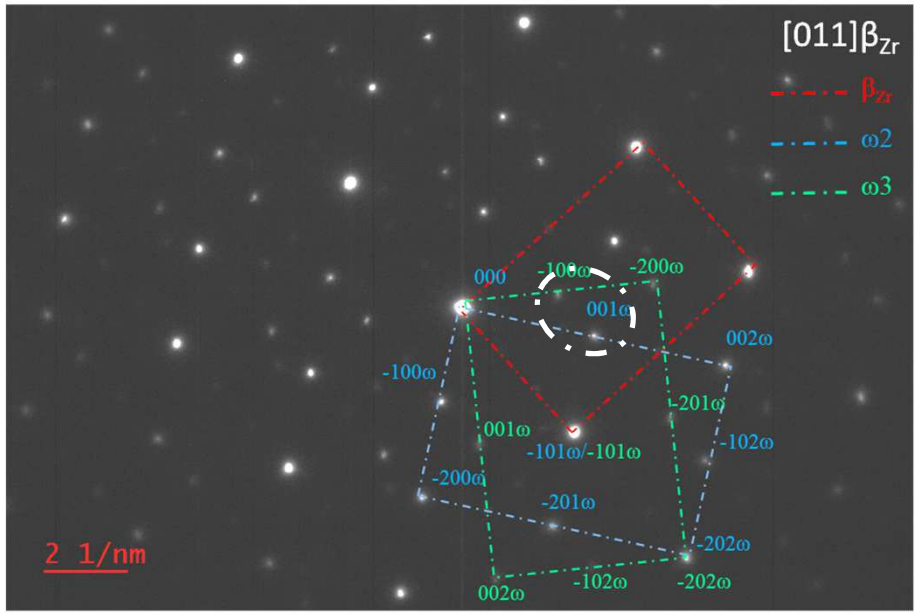

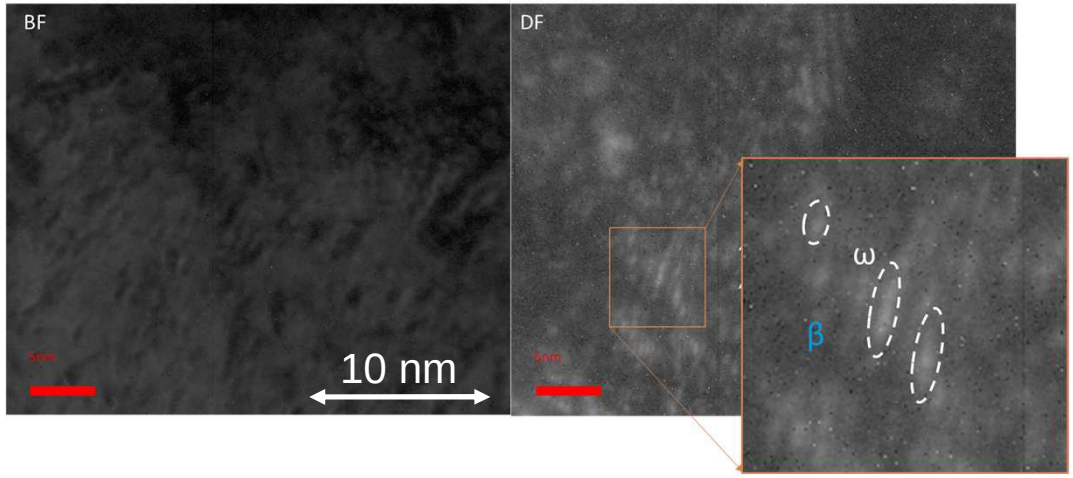

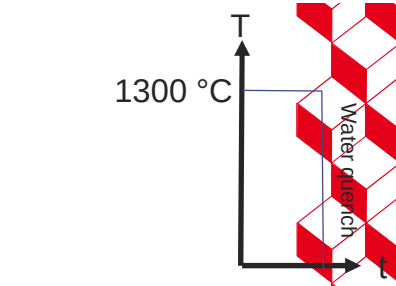

The **ω phase** is present, nanometric (0.5-2nm) and uniformly distributed in the untransformed β_{Zr} phases.

❖ Water quench

Origin of hardening evolution for C_{cr}>2 wt.%.

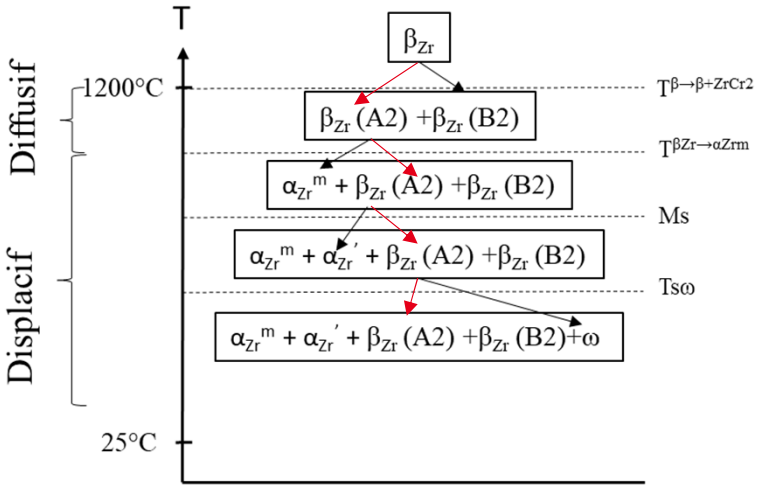

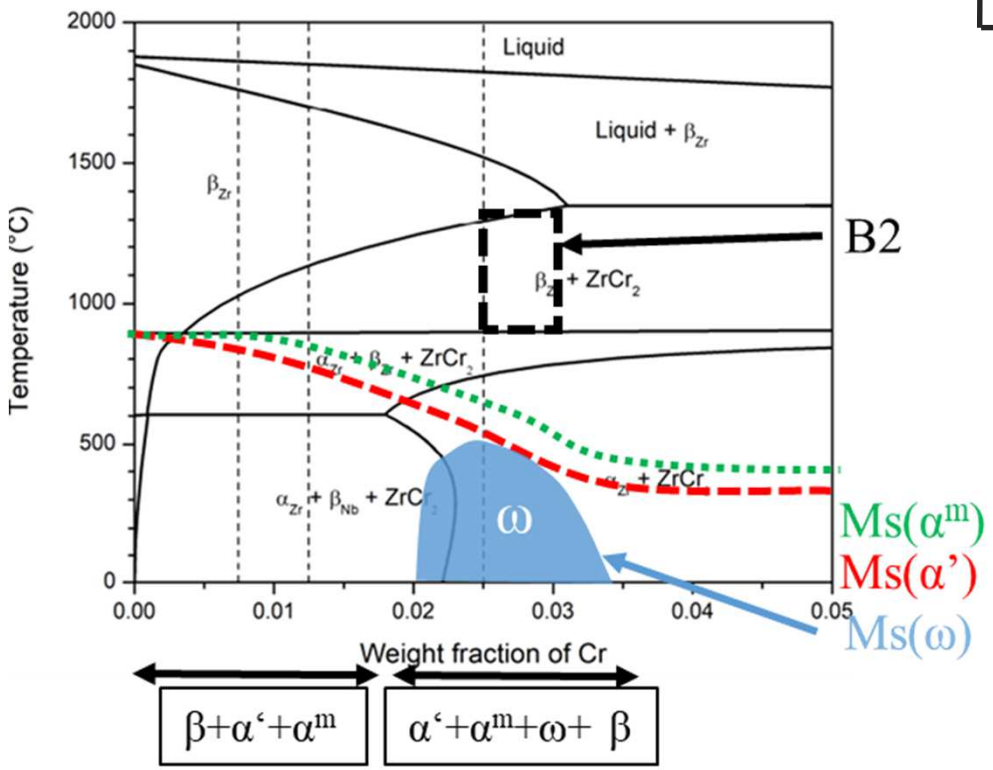

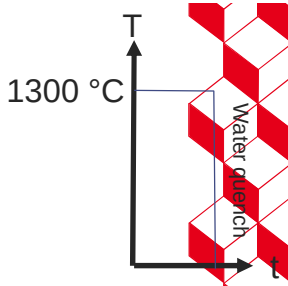

Change in μstructure at ~2 wt.% Cr could explain the change in hardening mode and the Ductile-to-Brittle failure mode occurrence

Numat 2024
Paul.gokelaere@cea.fr

Outlines / recent R&D achievements at CEA:

(1) Proposal of a new “ECrR”, adapted for the Cr-coated Zr-based claddings…

(2) Relationship between Cr diffusion *(from the coating)* profiles upon HT incursion with the residual PQ prior-β_{Zr} hardening & embrittlement + underlying metallurgical evolutions…

(3) Overall Cr-coating protectiveness evaluation upon HT steam oxidation…

Motivation: Most of the numerous papers published so far on the HT oxidation behavior of Cr-coated Zr claddings focused on detailed microstructural/microchemical examinations

⇒ However, there is still a need for some simple enough - but efficient - methodologies to evaluate the <u>overall</u> Cr-coating protectiveness upon HT steam oxidation, in relation with their PQ mechanical properties

⇒ Ideally, such methodologies have to be:

- **sensitive enough to detect the early oxidation time corresponding to partial loss of Cr-coating protectiveness inducing early oxygen diffusion into the prior-β_{Zr} substrate** (*before inducing under-coating $\alpha_{Zr}(O)$ & ZrO_2 thickening)*;

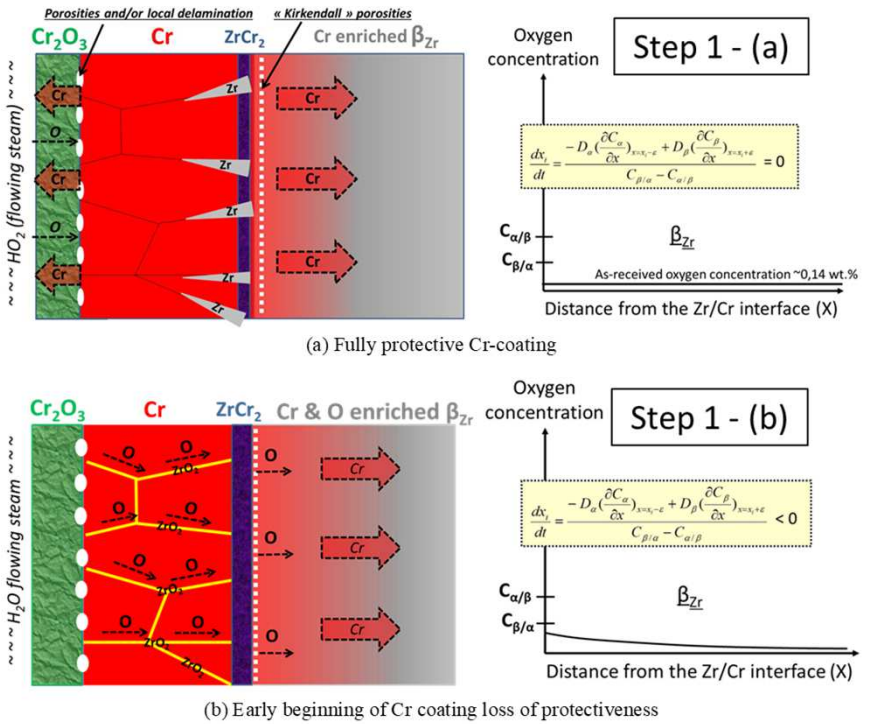

- **able to characterize the (under-coating) through-wall clad thickness oxygen (and chromium) diffusion profiles**, which could be further relied to the quenching resistance and PQ residual mechanical clad properties

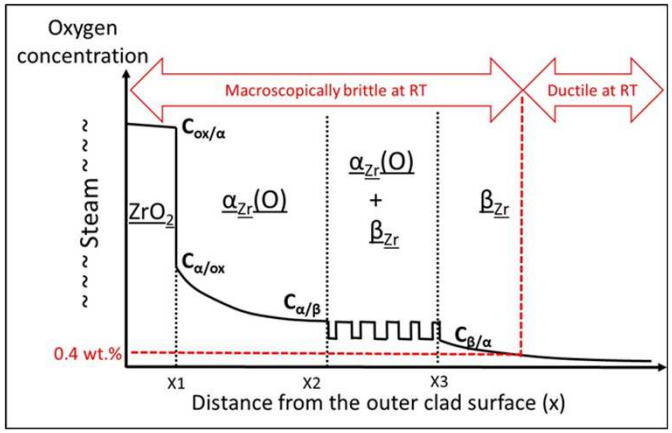

Ex. n°1: **Evaluation of the overall oxygen content that has diffused into the Zr-based metallic substrate following HT oxidation, by comparing their measured Weight Gain (WG) and their actual ZrO_2 or Cr_2O_3 outer scales thicknesses** (*for both uncoated and Cr-coated Zr*):

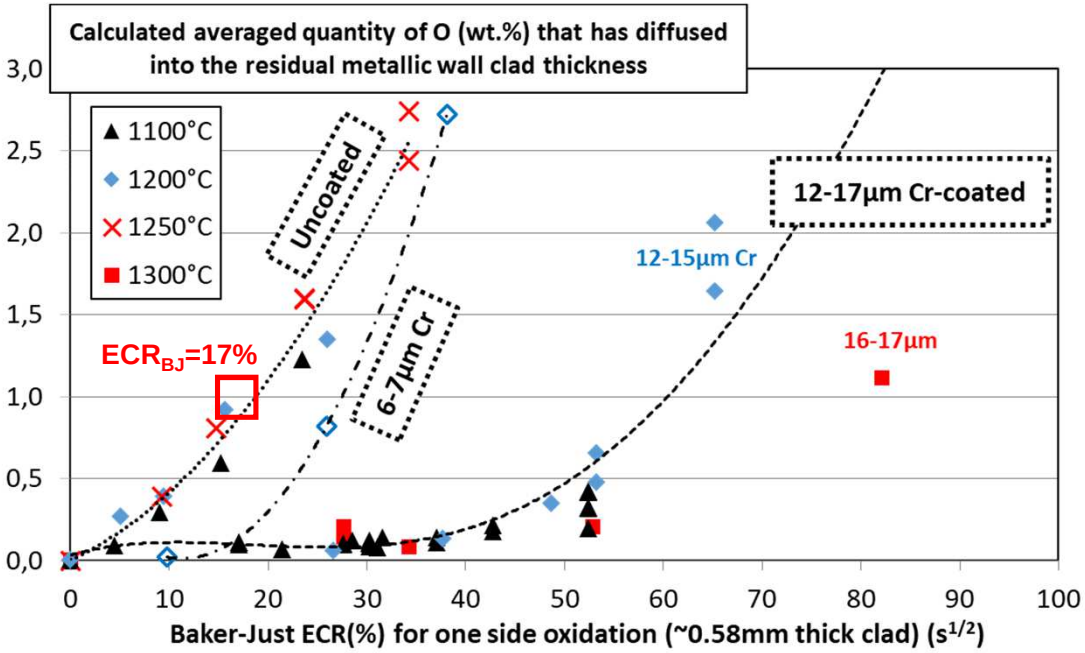

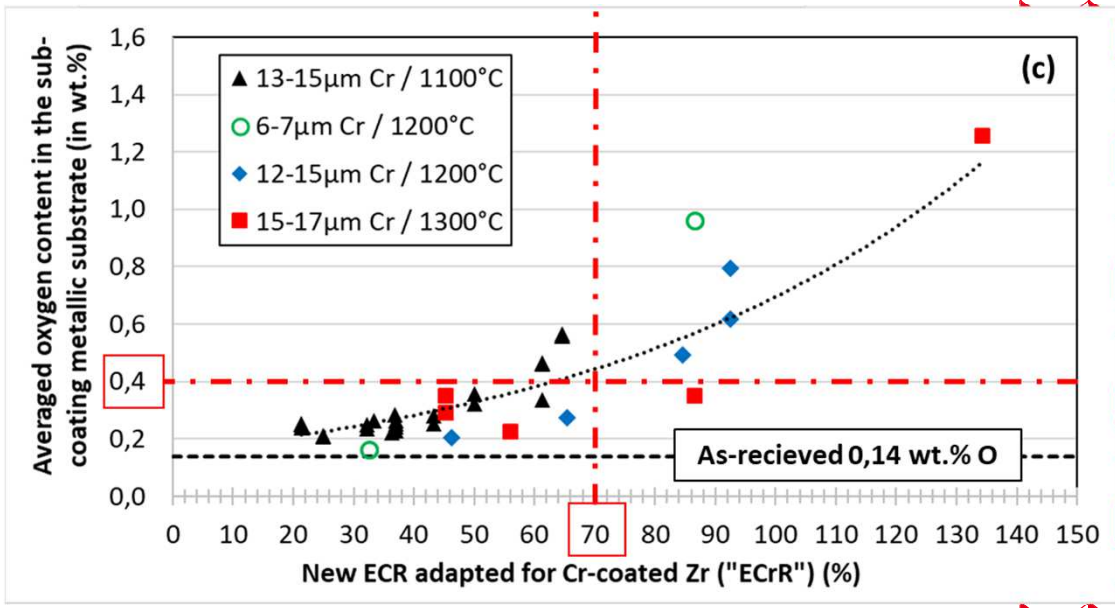

Relationship with the PQ residual Cr-coated cladding strength derived from RCT:

One-sided steam oxidation at **1100°C**:

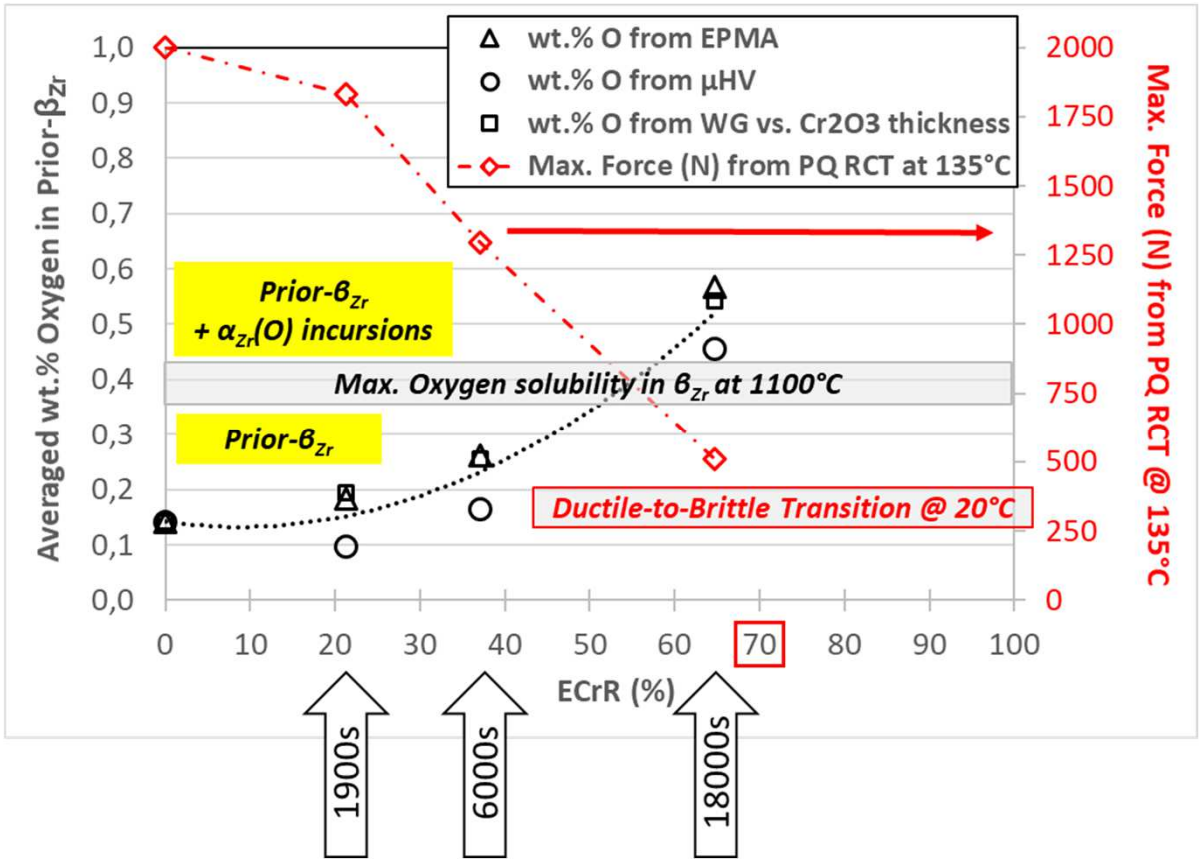

Ex. n°2: **Post-Quenching hydrogen uptake (≥ 100 wt.ppm) seems to be an indicator of the definitive loss of Cr-protectiveness** (*as already mentioned in Corrosion Sci. Journal paper, 2020*)

Note that a measured PQ hydrogen uptake of 200 wt.ppm (two-sided oxidation) has been previously proposed as an experimental indicator of the time for "breakaway" occurrence upon steam oxidation around 800°C and 1000°C on reference uncoated nuclear fuel claddings materials [M.C. Billone, et al., NUREG/CR-6967, (2008)]

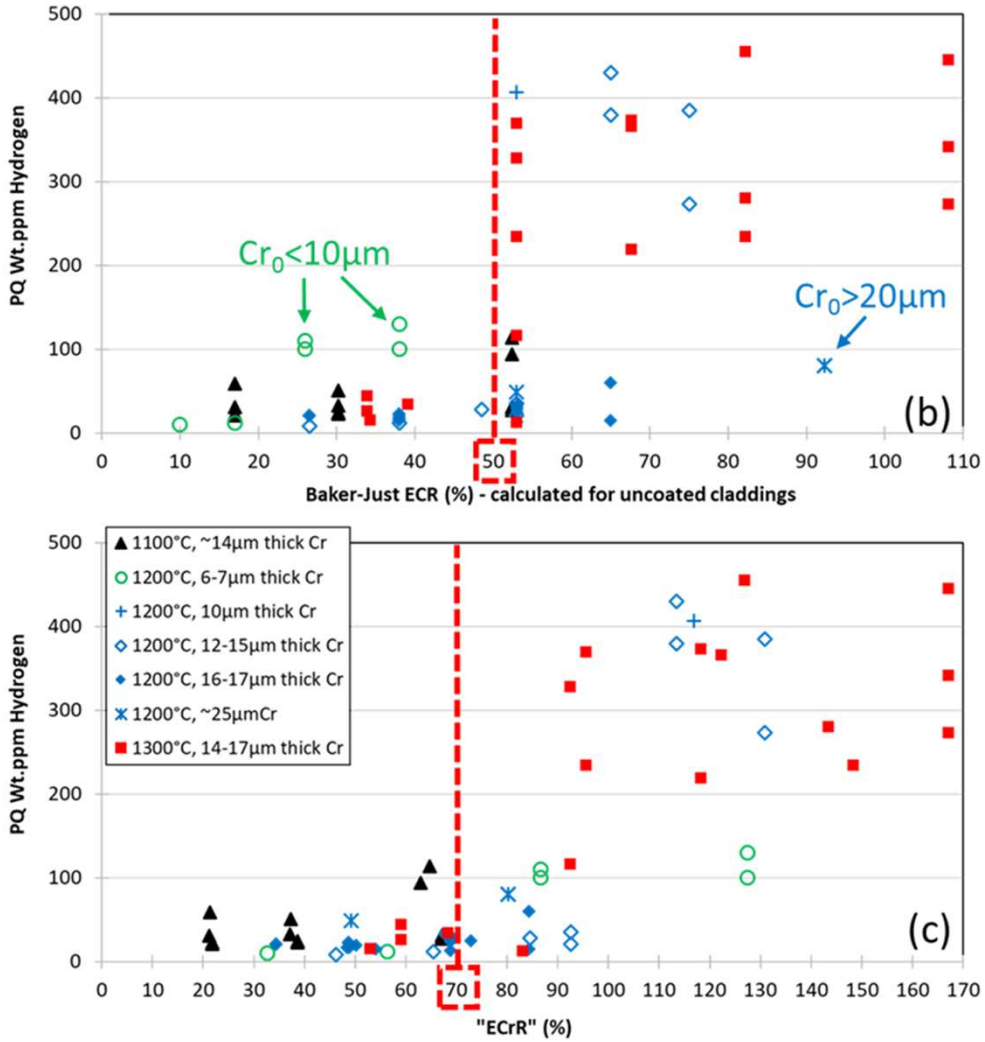

On-going and further work:

⇒ **Extend the approaches developed so far to last generation Cr-coated $M5_{Framatome}$ and to more complex (LOCA prototypical & slightly beyond) transients, *i.e., effect of 1st. temperature peak, influence of final "cooling scenario" / 2-steps cooling…***

⇒ **Account for the effect of ballooning and burst: *i.e., potential Cr-cracking at the balloon location (see A. Charbal et al., this conf.) + inner oxidation & 2ndary hydriding…***

⇒ **On-going and further efforts to derive more "physical" modelling of the quite complex oxidation mechanism of Cr-coated Zr (…)**

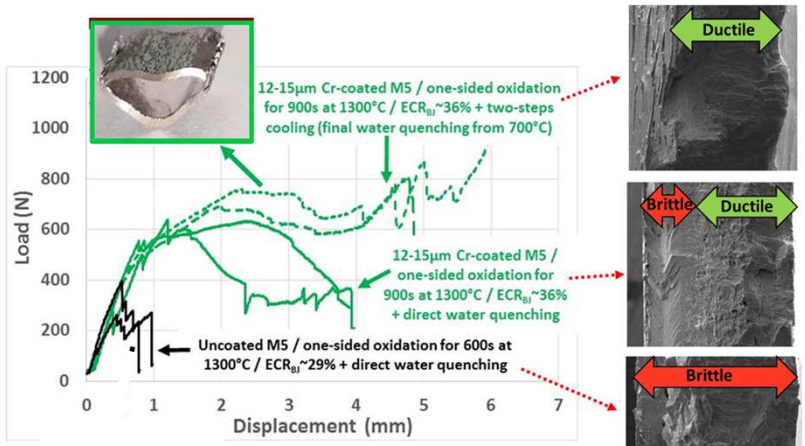

JC. Bachet, P. Gokelaere et.al., ASTM-STP, (2023)

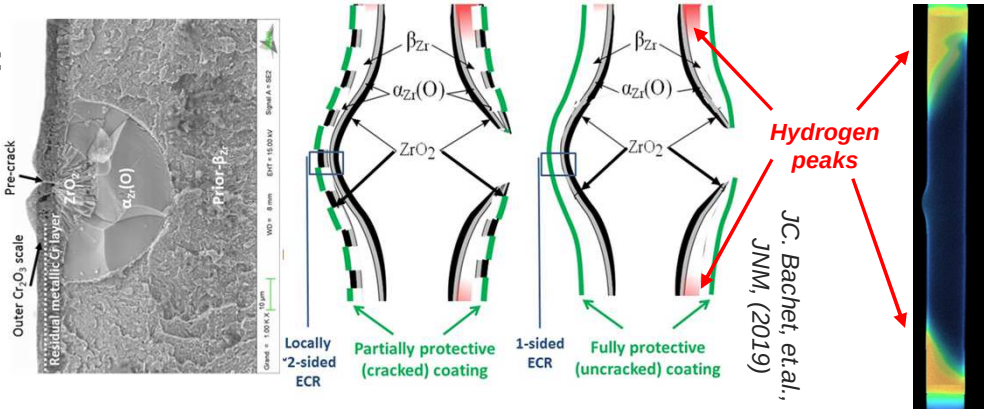

JC. Bachet, et.al., JNM, (2019)

F. Ott et al. (CEA/LLB), neutron tomography carried out at ILL (Grenoble, France)

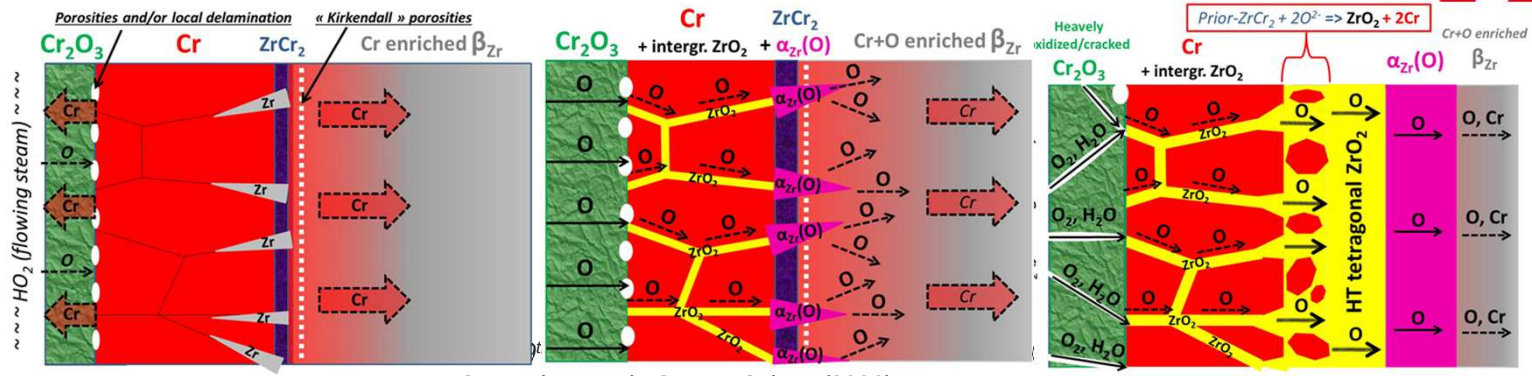

JC. Brachet, et.al., Corros. Sci. J., (2020)

jean-christophe.brachet@cea.fr

Thank you for your attention

This work has been funded by the French Nuclear Institute (I3P). Many thanks to the numerous colleagues and students at CEA who have contributed to the developement and evaluation of E-ATF Cr-coated Zr-based claddings over past ten years, and to our industrial partners for partial funding and fruitful discussions (and Framatome for providing the $M5_{Framatome}$ substrate)

jean-christophe.brachet@cea,fr

Photograph of an inscription on a french public works company metallic panel, corresponding likely to a **not-fully optimized coating** and/or that has been **corroded beyond its "critical ECR" value**

Back slides

(*from J.C. Brachet et al., “Evaluation of Equivalent Cladding Reacted parameters of Cr-coated claddings oxidized in steam at 1200°C in relation with oxygen diffusion/partitioning and post-quench ductility” / Journal of Nuclear Materials 533 (2020) 152106…)*

Uncoated:

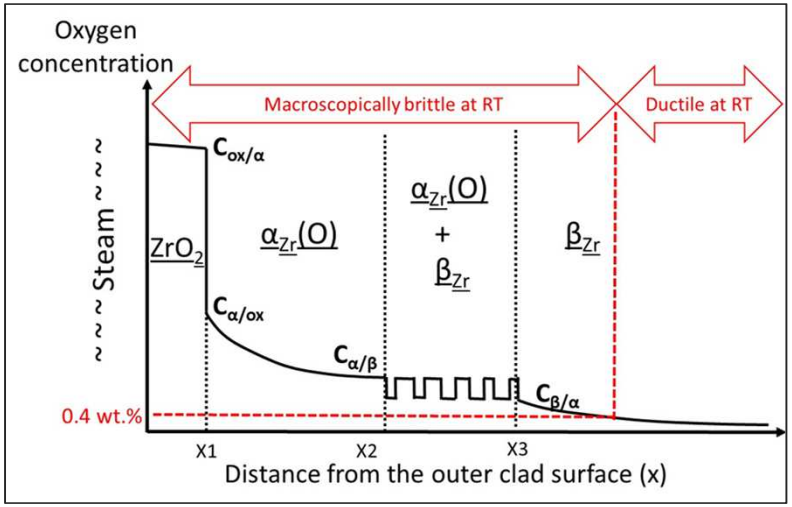

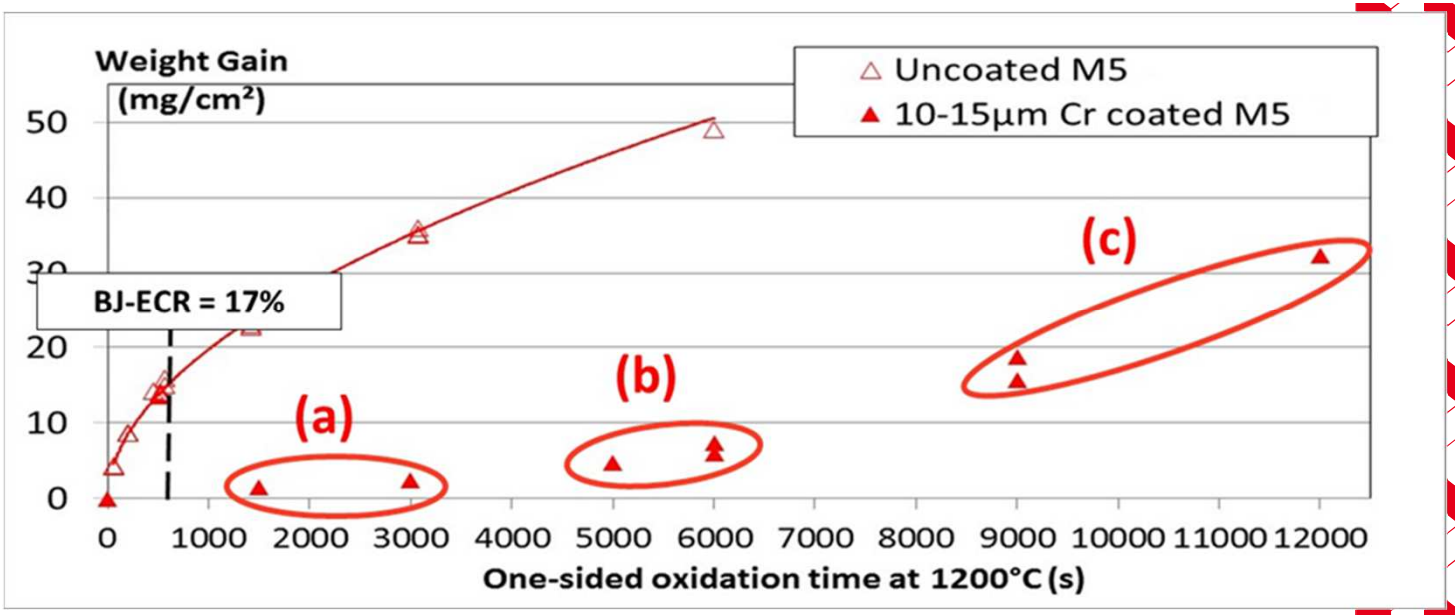

Cr-coated:

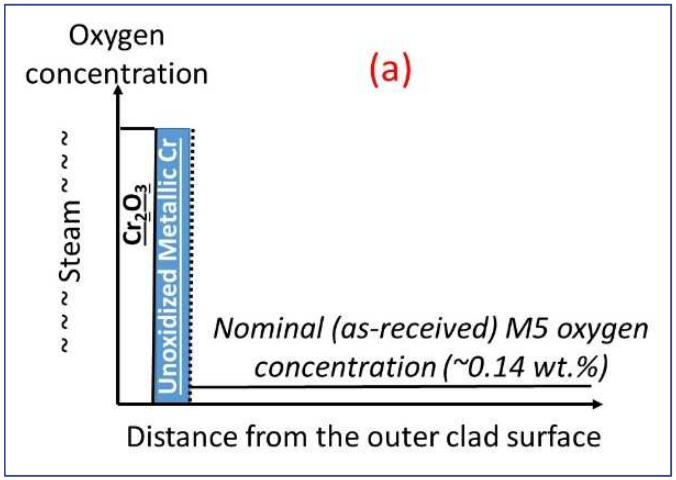

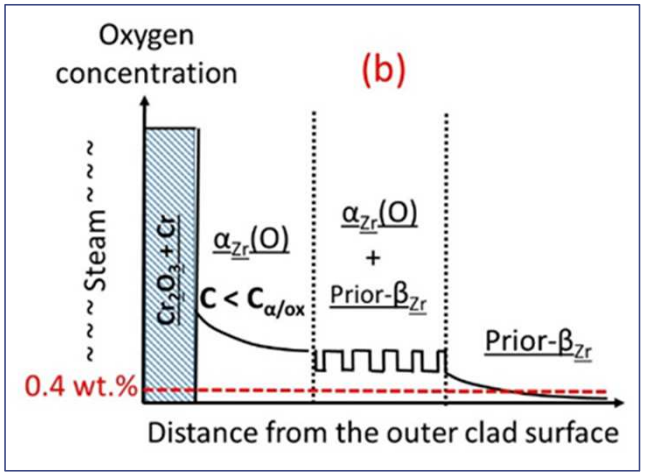

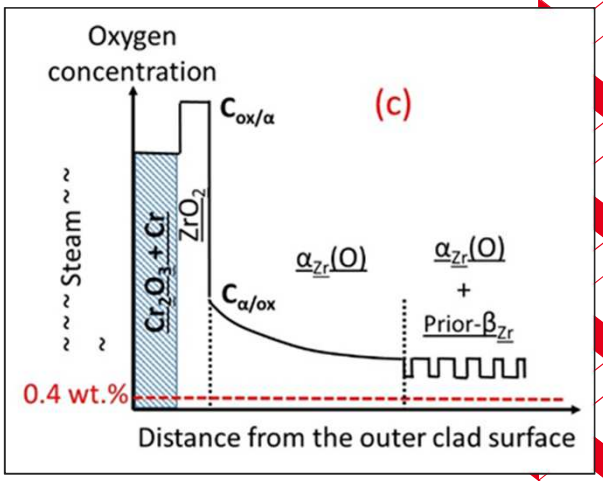

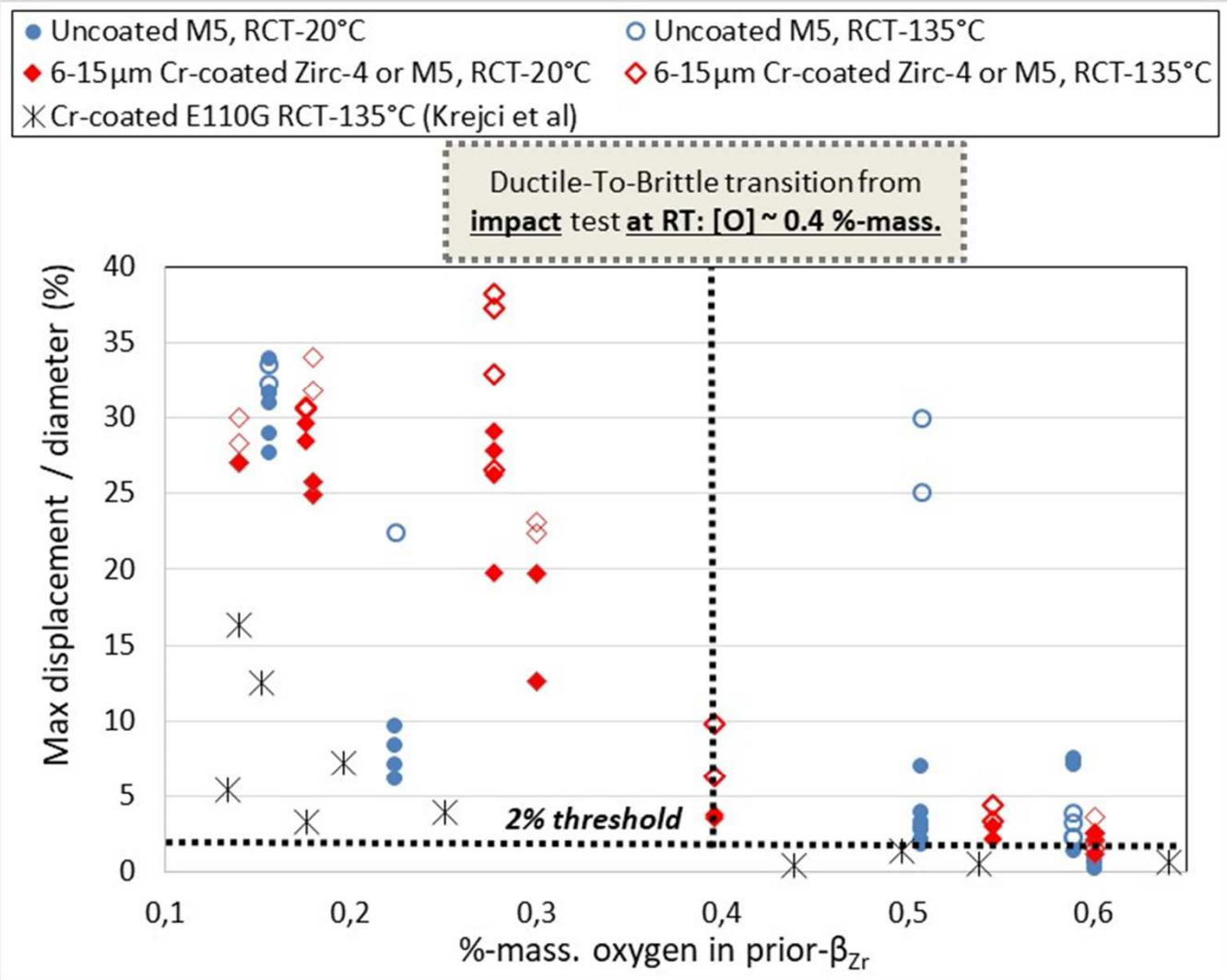

Figure 1 - Post-Quenching "residual ductility" derived from RCTs performed at 20 and 135 °C on uncoated and 6 to 15 µm thick Cr-coated zircaloy-4 or M5$_{Framatome}$, and from Krejci et al. on Cr-coated E110G substrate ***Erreur ! Source du renvoi introuvable.****, as a function of the mean oxygen content of the residual prior-β$_{Zr}$ layer*

Katerina Frederick

Westinghouse

Accident tolerant fuel: Cr coated cladding development at Westinghouse

In response to the nuclear industry's desire for longer coping times following the Fukushima accident in Japan in 2011, Westinghouse's **EnCore®*** accident tolerant fuel (ATF) program, is developing and commercializing an advanced fuel cladding and fuel pellet with the main goals of improving safety and economic performance. The program is a two-pathway approach, cladding and fuel, with each pathway having an intermediate product and long-term product; both of which are in testing and development phases. The cladding pathway will be the emphasis of this presentation as it is directly tied to the QUENCH testing being performed by Karlsruhe Institute of Technology (KIT). The chrome coated cladding has undergone testing in various environments and facilities to provide valuable results in the development of the design and specification of the chrome coating. Lead test rod (LTR) and lead test assembly (LTA) campaigns are currently underway with utility partners to provide real-world data on the irradiation performance of the coating. LTR post-irradiation examination (PIE) data as well as out-of-pile test data for current coatings will be presented and discussed.

This material is based upon work supported by the Department of Energy under Award Number DE-NE0009033.

Accident Tolerant Fuel: Cr Coated Cladding Development at Westinghouse

Katerina Frederick

29th International QUENCH Workshop

November 19-21, 2024

Westinghouse

Westinghouse **VISION & VALUES**

together

we advance technology
& services to power a
clean, carbon-free future.

- Customer Focus & Innovation
- Speed & Passion to Win
- Teamwork & Accountability

Safety • Quality • Integrity • Trust

Westinghouse

The following material is based upon work supported by the United Stated Department of Energy under Award Number DE-NE0009033

Outline

- Westinghouse **EnCore**® Fuel Program
- LTA and LTR Status
- Coated Cladding Testing
- 2nd and 3rd Test QUENCH-ATF Program

Westinghouse's EnCore® fuel program enables 24-month cycles and potential uprates for PWRs with advanced cladding and pellets

The EnCore® Fuel program is developing and commercializing advanced fuel products to improve safety and economic performance

Advanced Cladding

- Cr-Coated Zr – increases safety & operational margin, may enable high burnup
- Silicon Carbide Cladding – safety and operational benefits

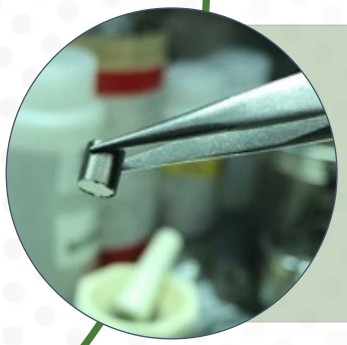

Advanced Fuel

- **ADOPT** fuel pellets – higher density
- Advanced Pellet (UN) - benefits to fuel cycle costs, may support high burnup, thermal properties, and lower operating temperatures

Chromium-Coated Zr Cladding

SiGA® Silicon Carbide (SiC) Composite Cladding

Photo courtesy of General Atomics

ATF Product Evolution → Enables HEF

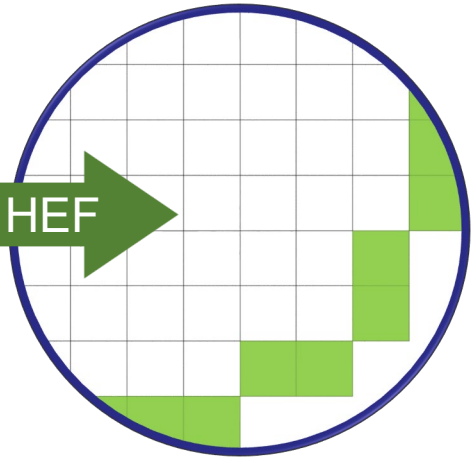

ADOPT Pellets

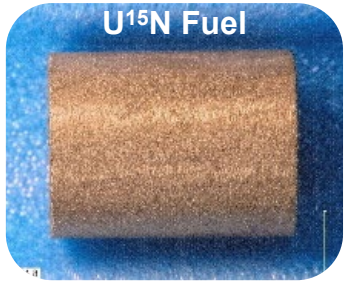

Uranium Nitride (UN) Pellets

Photo courtesy of Los Alamos National Lab

- Enables 24-month cycles, extended burnup
- Improves fuel cycle economics
- Supported through higher enrichment and ATF technologies

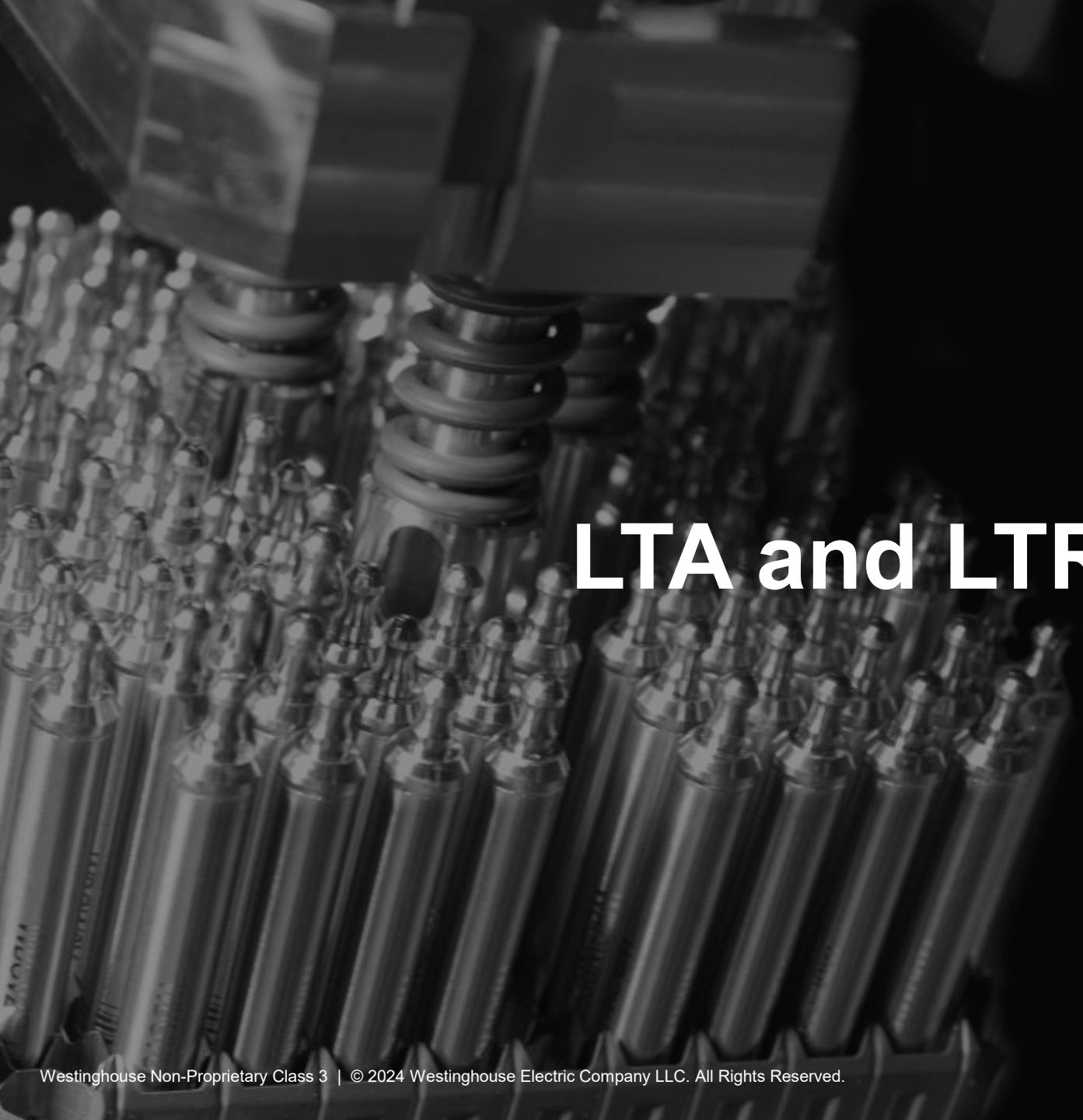

LTA and LTR Status

Lead Test Rod/Assembly (LTR/A) campaigns with utility partners provide critical data to support fuel qualification

	Cr Coated Cladding	ADOPT Pellets	High Density Pellets	High Enriched Pellets
Byron LTRs (2019)	✓	✓	✓	
Doel LTRs (2020)	✓		✓	
U.S. LTAs (Production)	✓	✓		✓
European LTRs (Planning)	✓	✓		

ATF rods appear "pristine" with excellent coating adherence and little indication of crud.

Byron Unit 2 LTRs

EOC 1

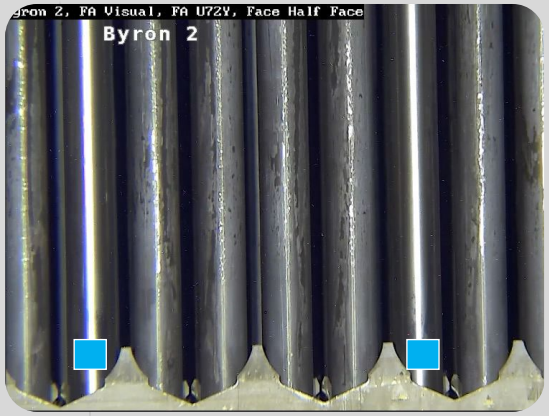

EOC 2

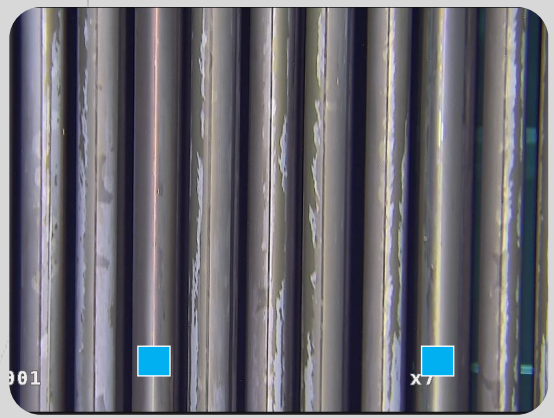

Doel Unit 4 LTRs

EOC 1

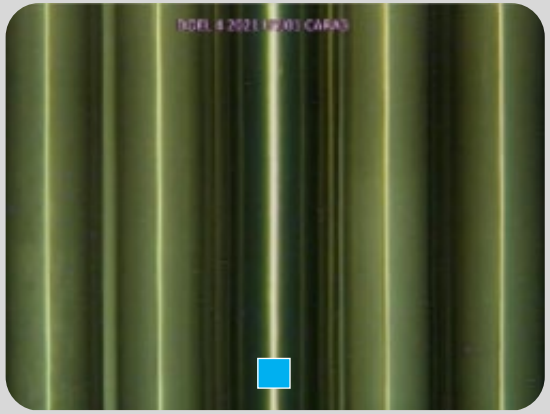

EOC 2

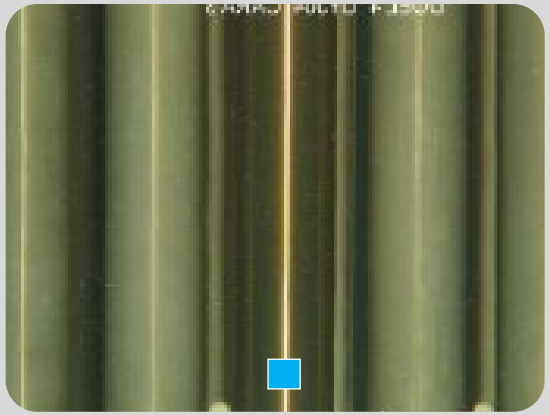

■ Cr Coated Rods

LTR: Lead Test Rod **LTA:** Lead Test Assemblies

Irradiated data collection supports licensing and accelerated fuel qualification of ATF materials

✓ Completed
❑ Planned

2023

- ✓ NDE (1 Cycle)
- ✓ Metallography, SEM/EDS (1 Cycle)
- ✓ Hydrogen Content (1 Cycle)
- ✓ Shipment 2 Cycle Rods to Hot Cell

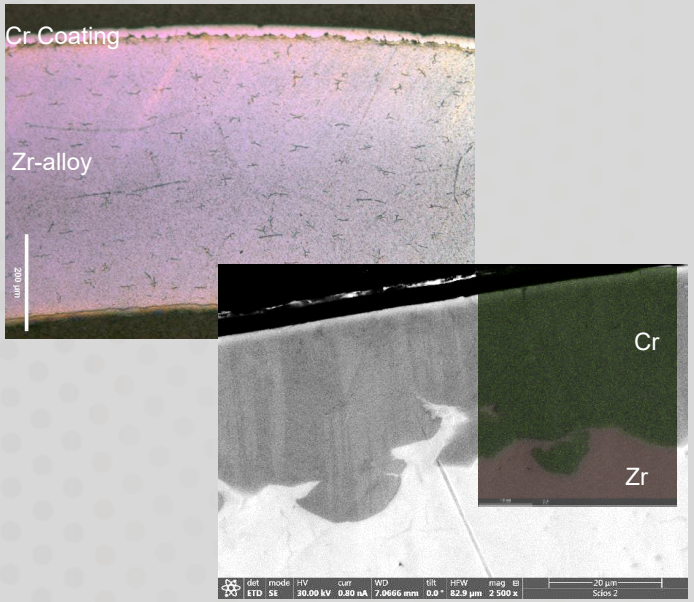

2024

- ✓ NDE (2 Cycles)
- ❑ Metallography, SEM/EDS (2 Cycles)
- ❑ LOCA Burst Testing Cr Coated Rods (1 Cycle)
- ❑ UN Modeling Underway (FGR, TCD, BISON)

2025

- ❑ Hydrogen Content (2 Cycles)
- ❑ Mechanical Testing (1 Cycle)
- ❑ Licensing Cr Coated Cladding
- ❑ Insertion Assemblies with High Enriched Pellets, Cr Coated Rods, ADOPT Pellets
- ❑ Poolside Inspection + Shipment HBU ATF Rods to Hot Cell (3 Cycles)
- ❑ Planned BR2 Irradiation of UN Mini-disks

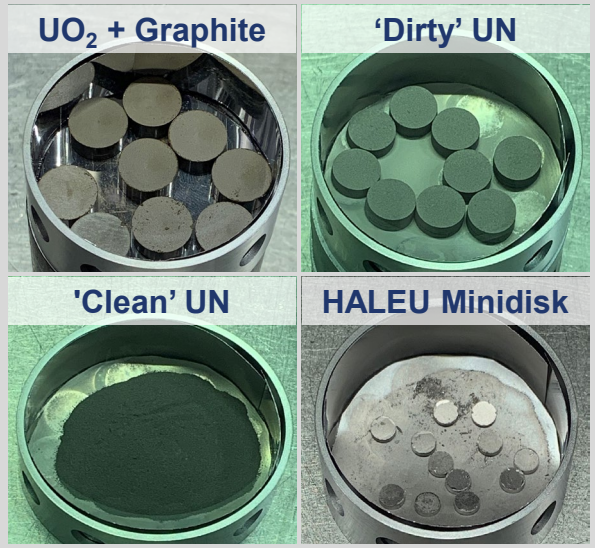

NDE: Non-Destructive Examinations **SEM:** Scanning Electron Microscopy **EDS:** Energy Dispersive X-ray Spectroscopy **LOCA:** Loss-of-Coolant Accident **FGR:** Fission Gas Release **TCD:** Thermal Conductivity Degradation **HBU:** High Burnup

Westinghouse

Hot cell examinations of one cycle irradiated **EnCore®** Cr coated rods confirm excellent fuel performance

3 ATF and 4 high burnup rods received mid-2021

Credit: ORNL Photographer Carlos Jones

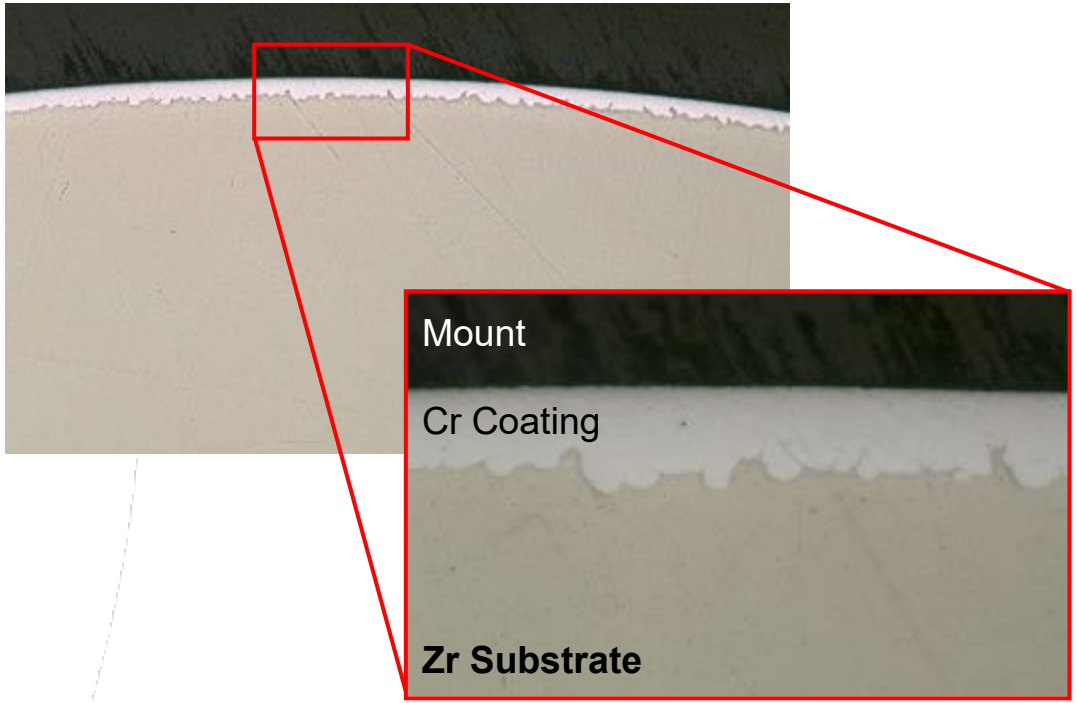

Excellent cold sprayed Cr coating integrity with complete protection of substrate

Hydride etched metallography shows no unfavorable hydride orientations or rim

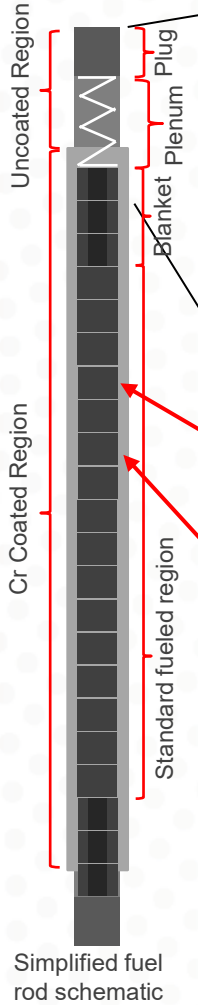

Simplified fuel rod schematic

~4in above coating
HPU: 26 ± 1 ppm

~1in above coating
HPU: 30 ± 5 ppm

at transition ~0.08in into coating
HPU: 20 ± 3 ppm

~2in into coating, ~0.4in above blanket
HPU: 11 ± 1 ppm

well into coating, ~4in above peak corrosion location for an uncoated rod
HPU: 24 ± 26 ppm & 16 ± 7 ppm

well into coating, near peak corrosion location for an uncoated rod
HPU: 19 ± 3 ppm

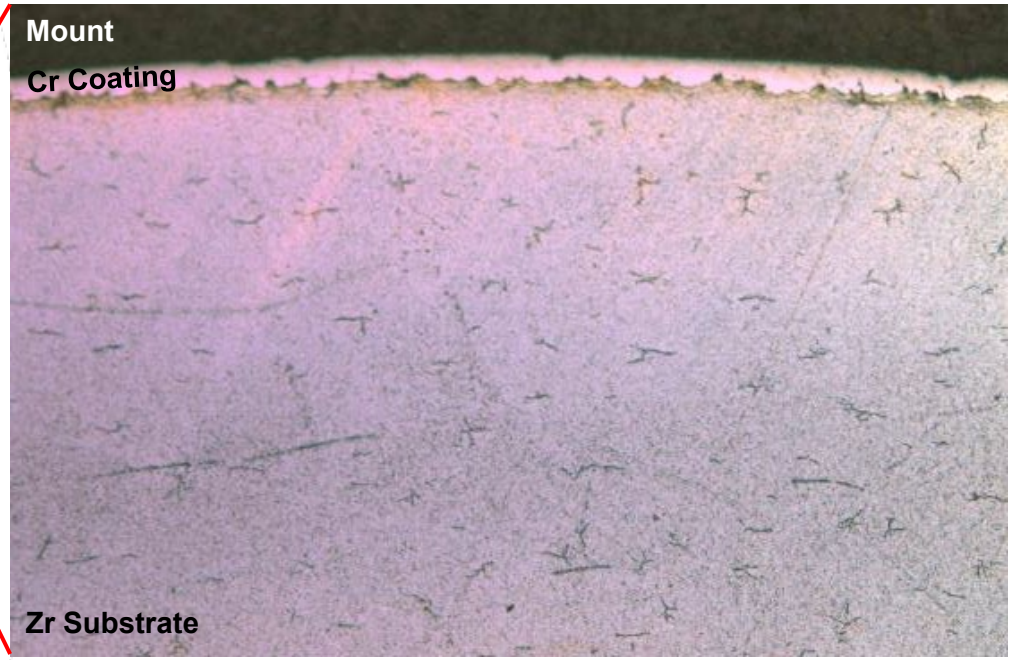

Second cycle rods shipment complete (~55 GWD/MTU)
Reactivity Insertion Accident and ramp testing planned at INL in 2026

Coated Cladding Testing

Hydrogen Uptake: Rodlet samples were encapsulated and charged with hydrogen at two pressures

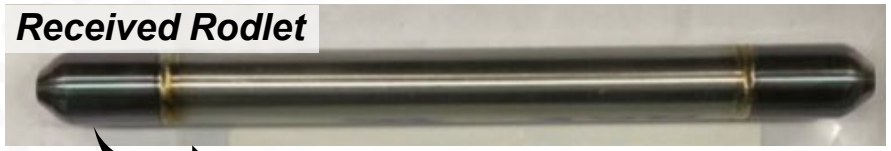

Quartz Tube Encapsulation
Low Pressure: 0.018 MPa
High Pressure: 0.028 MPa

Cladding Type	Cladding Condition	Hydrogen Fill Pressure
Uncoated Zr-Alloy	As-fabricated	Low, High
Cold Spray	As-fabricated, Scratched*	Low, High
PVD	As-fabricated, Scratched*	Low, High
PVD – Pulsed	As-fabricated, Scratched*	Low, High

*Scratched samples only tested at high fill pressures

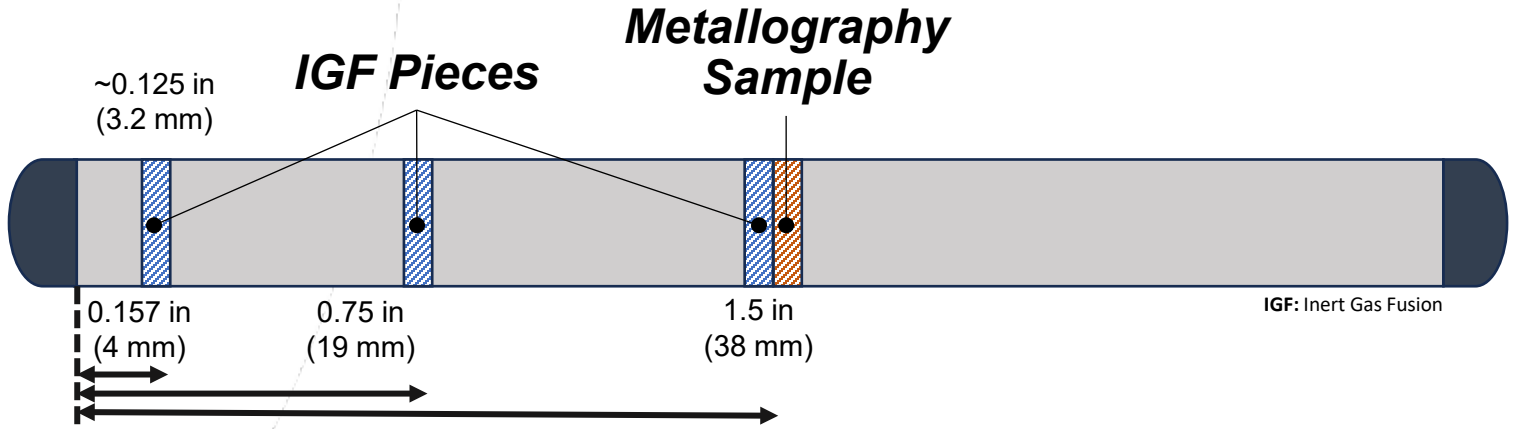

Hydrogen Uptake: Laboratory testing showed reduced H_2 pickup compared to unoxidized Zr-alloy cladding

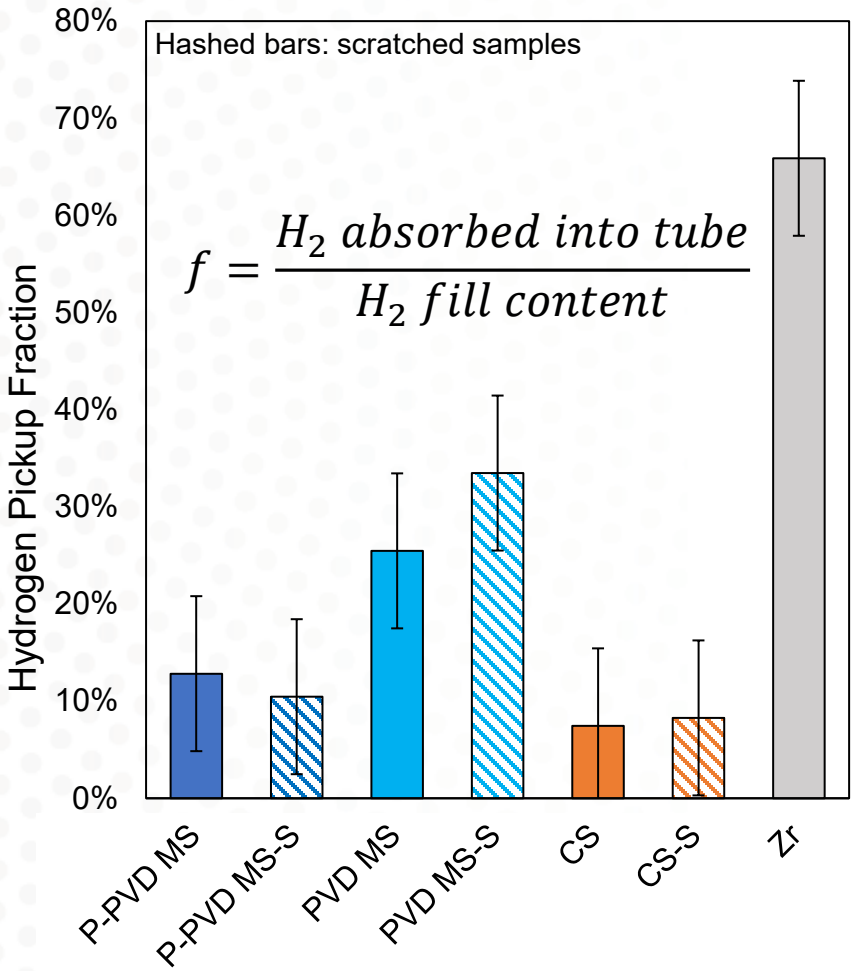

Flux of hydrogen atoms diffusing into cladding materials (function of coating thickness, L)

$$J_{Cr} = \phi \frac{\sqrt{P_{H_2}^f} - \sqrt{P_{H_2}^i}}{L}$$

$$J_{Zr} = \frac{mol\ H_2}{A * t}$$

Permeability normalizes for coating thickness

$$\phi = \frac{-2\left(\sqrt{P_{H_2}^f} - \sqrt{P_{H_2}^i}\right)LV}{tART}$$

$P_{H_2}^{f,i}$: fill pressure (final, initial)
L: coating thickness
V: free volume quartz tube
t: duration of test
A: surface area
R: universal gas constant
T: temperature (K)

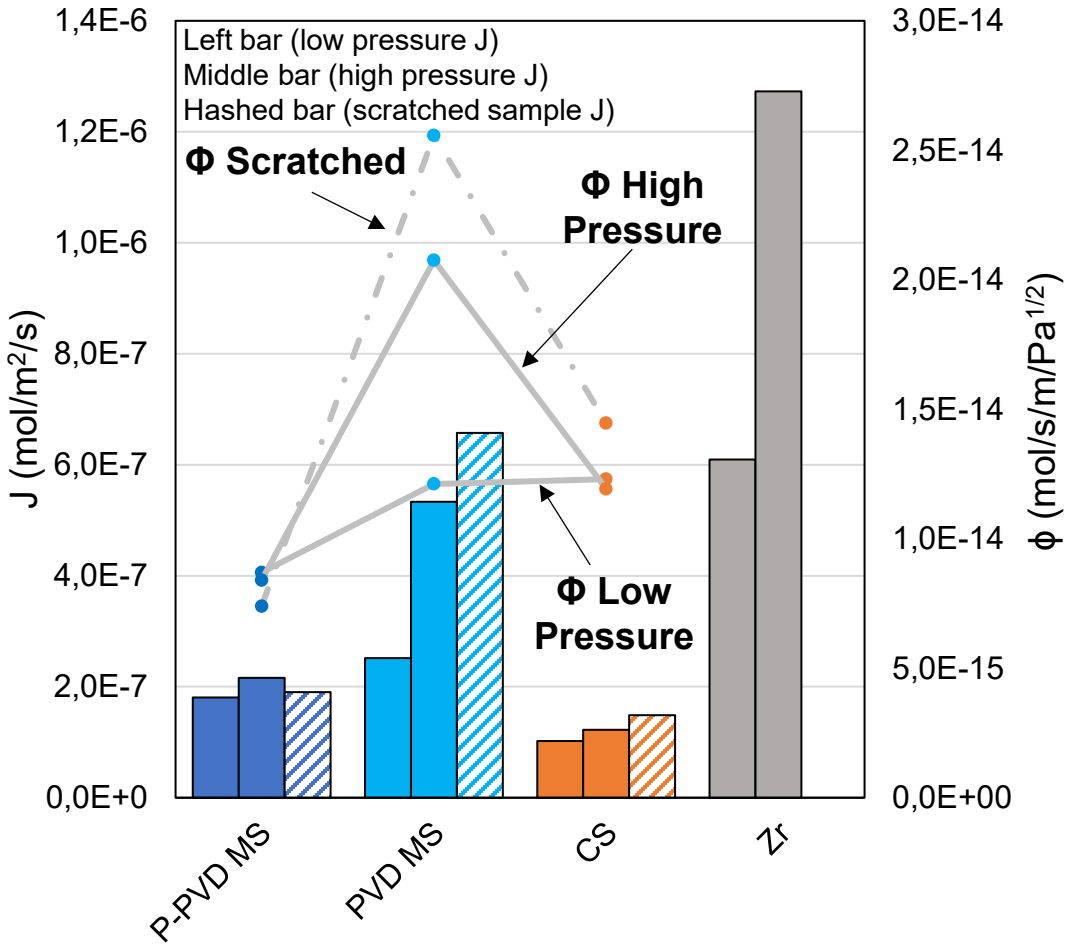

Out-of-Pile Corrosion: CS coatings improve corrosion resistance in simulated PWR water autoclave testing

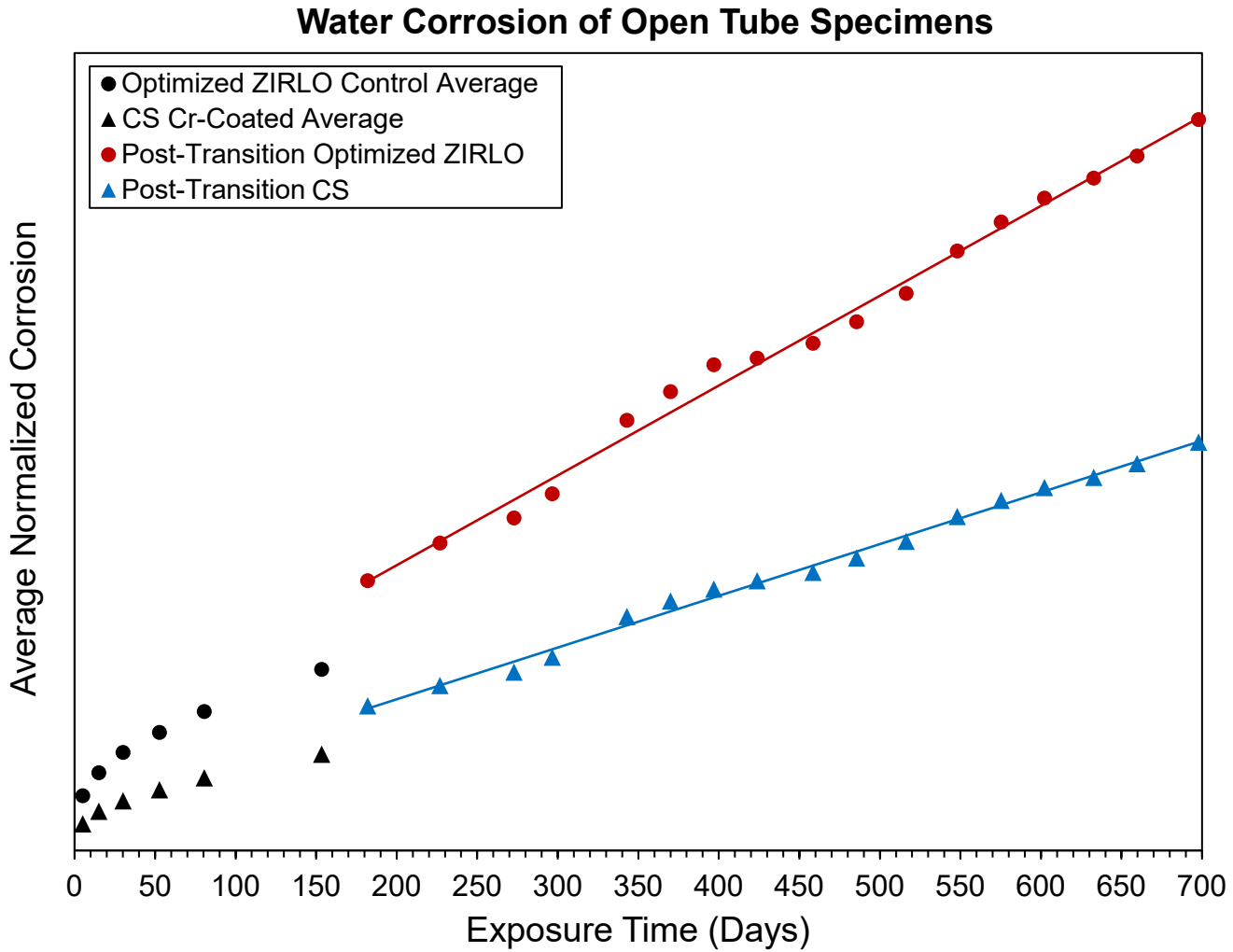

Tensile Testing: Coatings show slight increase in mechanical performance with same overall trend as uncoated substrate

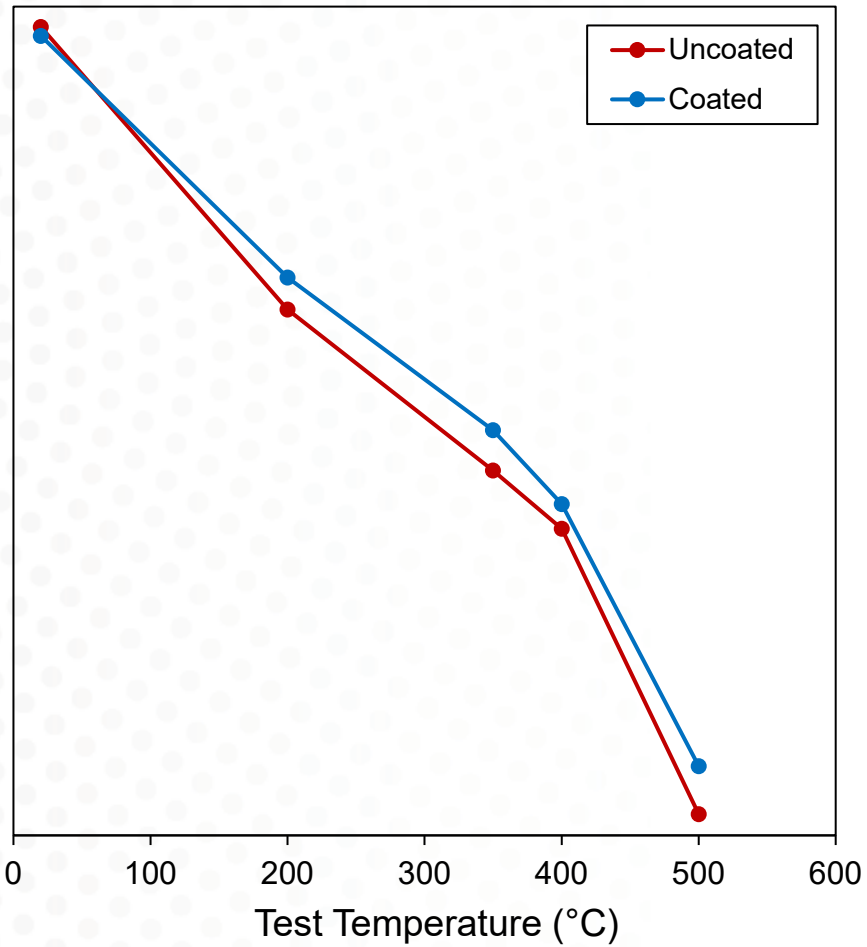

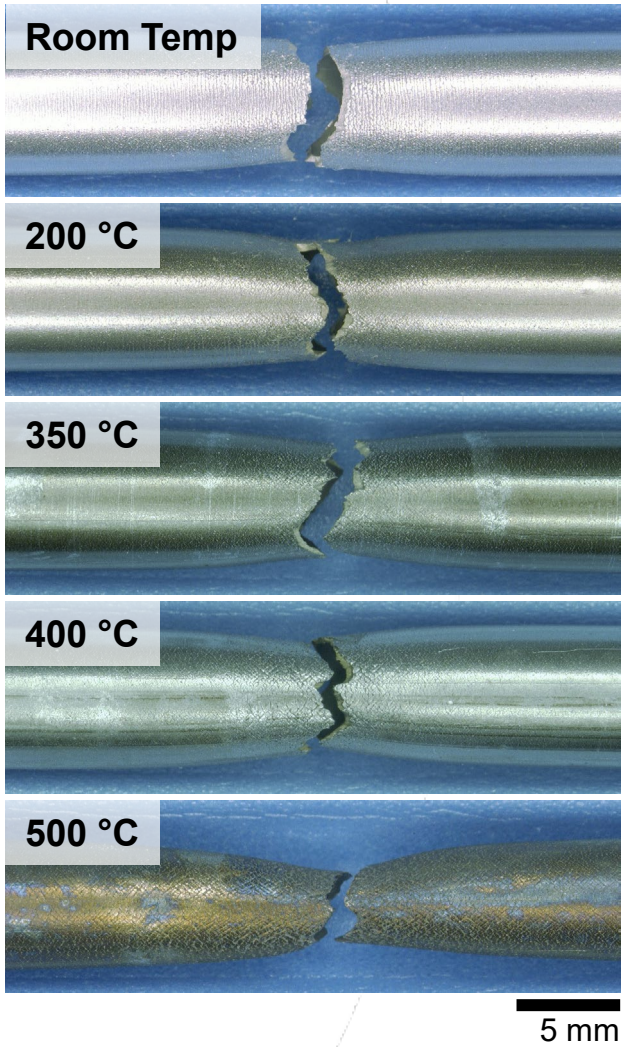

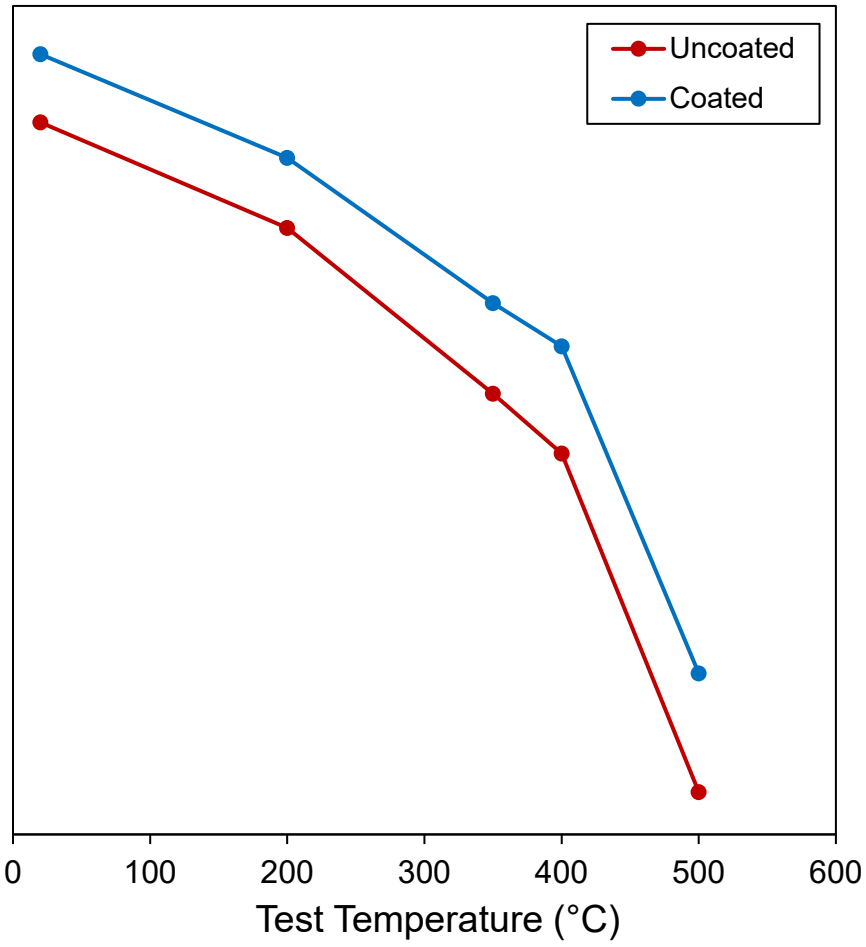

Coatings remain adhered to substrate

Continued development and testing supports licensing and CS coating improvements

Completed:

- Fatigue Testing
- Corrosion Studies
- High Temperature Oxidation
- Ring Compression Testing
- Burst Testing

In-Progress:

- Ultra-High Temperature Testing
- DNB Testing

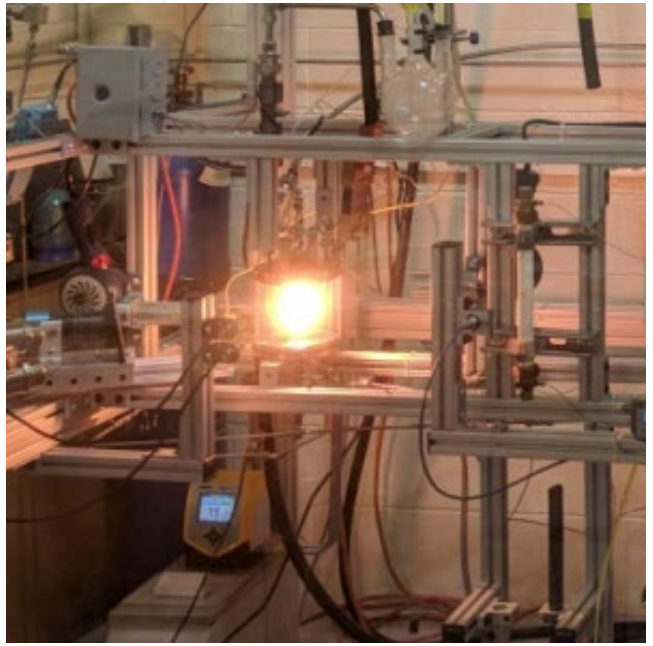

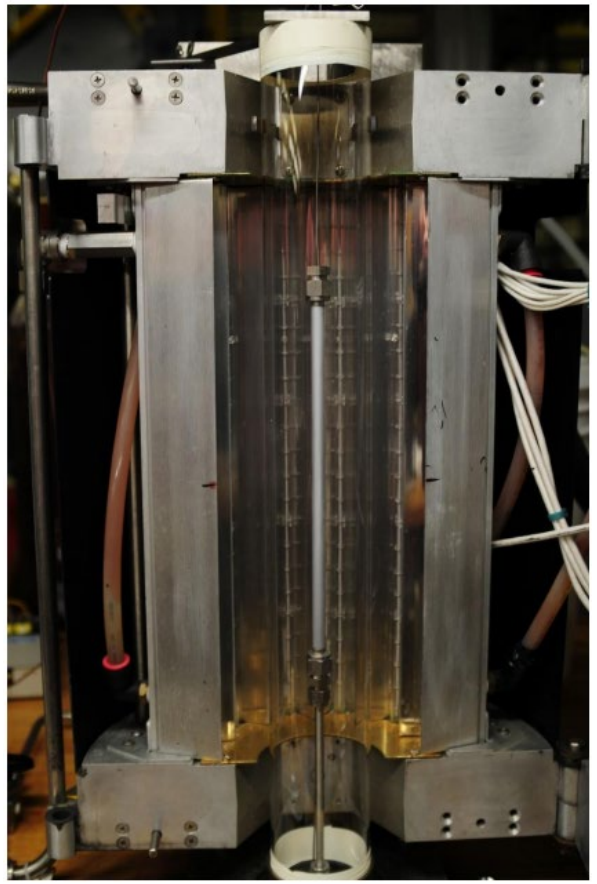

QUENCH-ATF Program

Second test with coated cladding was performed in August 2024

- Beyond Design Basis Accident Conditions
- Cold Spray Cr-Coated Cladding
- Max Temperature
  - 1600 °C
- Quench at 1600 °C
  - Cr-Zr eutectic: 1330 °C

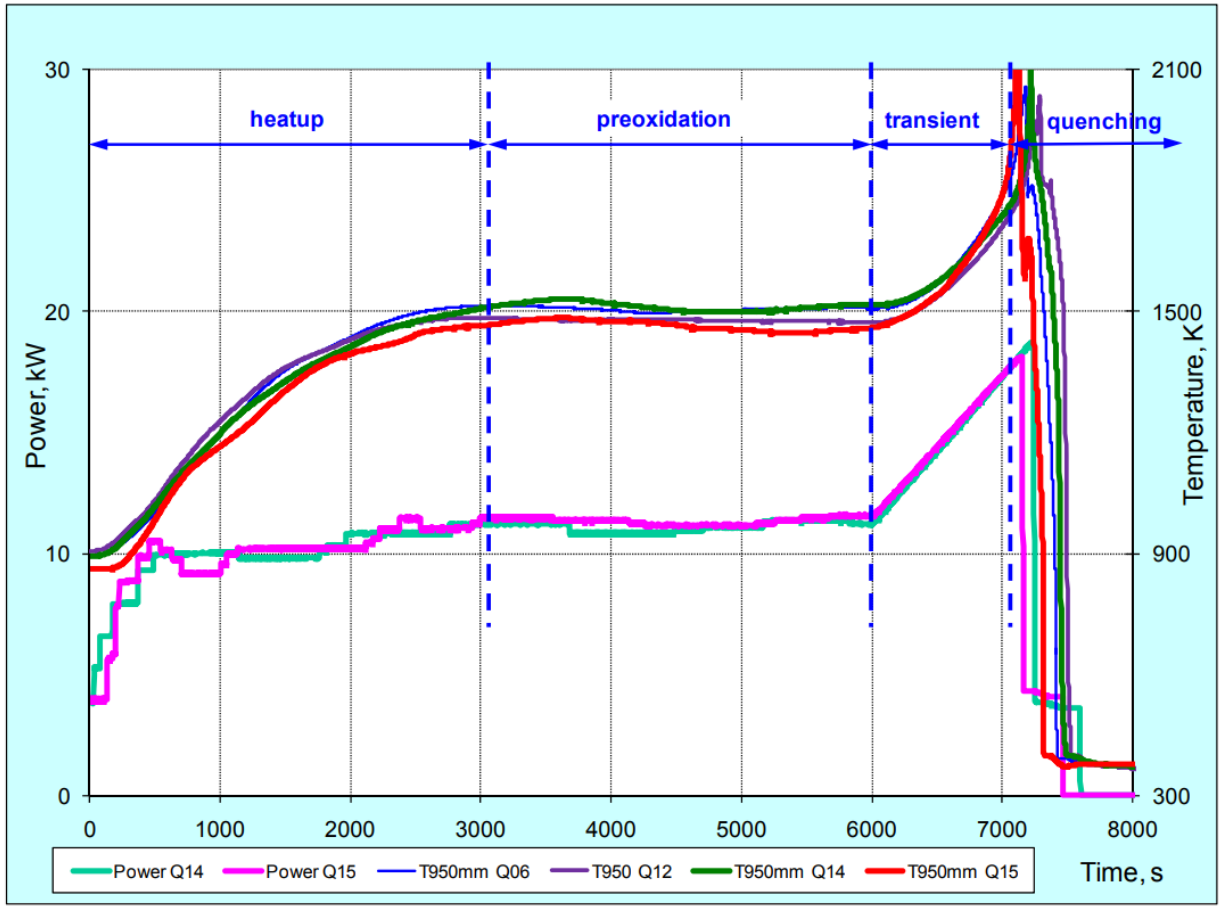

Tubes for 3rd test were shipped to NNL for PVD coating

- Tubes
  - 24 tubes (~2 m in length)
  - 15 µm PVD coating
- Grids
  - 17x17 grid construction
  - Standard mid-grid

Kinya Nakamura

CRIEPI

Behavior of Cr-coated cladding bundles under BDBA conditions at the DEGREE facility

Toward improvement of LWR core safety under accident conditions, efforts are underway to improve the accident tolerance of core materials that have a risk of promoting early core damage, such as not only fuel claddings but also control rods, grid spacers, and channel boxes. This paper focuses on the accident behavior of Cr-coated Zr alloy cladding, which is currently regarded as the near-term concept of ATF technology.

When the Cr coating on the outer surface of the Zr-based cladding no longer provides a protective barrier at high temperatures and Zr metal substrate oxidized, chemical reaction heat accompanying the Zr-water reaction may be generated rapidly. In this case, the temperature rise could be accelerated compared to the conventional uncoated cladding material, and the possibility of early core damage cannot be denied. Resolving this issue requires confirmation by bundle tests at different accident scenarios. CRIEPI is conducting series beyond design-basis accident (BDBA)-LOCA tests with Cr coated Zr-based claddings using an induction heating furnace at the CRIEPI's DEGREE facility. These tests were performed within the IAEA Coordinated Research Project on “Testing and Simulation for Advanced Technology and Accident Tolerant Fuels (ATF-TS)”.

Three types of fuel claddings (Zircaloy-4, Opt. ZIRLO, and E110) coated with single layer Cr and double or multi-layers Cr/CrN were applied to the single rod and bundle tests. These coated claddings were supplied by KIT, CTU, and AEOI. Test rods were assembled by loading the annular pellets made of Al_2O_3 or Y_2O_3 stabilized ZrO_2 and a tungsten rod as a susceptor into the cladding. The rod-internal-pressure was set to be 6 or 0.1 MPa of He gas at room temperature. Both tests were performed under simulated BDBA conditions in a high temperature steam-Ar environment. In the single rod tests, single ATF rod was placed in the center of the 3 × 3 type bundle with eight surrounding heater rods. In the bundle tests, the 3x3 type test bundle consisted of nine ATF test rods of the same specifications. After heating to the peak cladding surface temperature range of 1350 °C to 1600 °C at a heating rate of 3-5 K/s in a steam flow rate of 0.4 g/s, induction heating power supply was turned off and at the same time the atmosphere was switched from steam-Ar mixture to Ar gas only leading to cool down without quenching with water.

In addition to online measurements of cladding surface temperature, fuel rod internal pressure, and hydrogen generation amount, post-test analysis was conducted using EPMA, ToF-SIMS, and microhardness testing to reveal interdiffusion layer structure formed between the coating and the Zr-based materials, redistribution of the constituent elements, such as Cr, Zr, oxygen, hydrogen, and nitrogen, and radial profile of microhardness. Comparisons of accident behavior between different coating or cladding materials and between single rod and bundle tests are also discussed.

Behaviour of Cr-coated cladding bundles under BDBA conditions at the DEGREE facility

CRIEPI	Kinya Nakamura, Kenta Inagaki, Naoki Tarumi
KIT	Juri Stuckert
CTU	Martin Ševeček

29th International QUENCH Workshop

19-21 November 2024

Karlsruhe Institute of Technology, Campus North, Germany

IAEA International Atomic Energy Agency

CRIEPI Central Research Institute of Electric Power Industry

Outline

- Motivation
- Objective
- Experimental Results
  - Single Rod
  - Bundle
- Comparison between Single Rod and Bundle Tests
- Conclusion & Future Works

Motivation

Cr coated Zr-based alloy as near-term concept

- Cr_2O_3 diffusion barrier effect up to 1200 or 1300˚C [*1]
- Deterioration of barrier effect above the temp.
  - Pilling–Bedworth ratio 2.07 (Cr_2O_3)
  - Thinning of Cr_2O_3 layer by reduction with Zr
  - Increase in OD due to Cr-Zr eutectic above 1322˚C
  - Potential more intense temperature runaway[*2]
- Still lack of knowledge about the degradation behaviour

Coating materials under development

- Metal **Cr**, Mo, CrAl, FeCrAl, etc.
- Ceramic CrN, TiN, TiAlN, CrAlN, etc.
- Multi-layer **Cr/CrN**, Cr/FeCrAl, CrN–NbN, MAX, etc.

Resolving these issues require confirmation by integral tests at different accident scenarios with different coating materials.

International research project on material science-based ATF bundle behaviour under BDBA

QUECH-19 (2018)	OECD NEA QUENCH-ATF (2021-2026)	IAEA CRP ATF-TS (2021-2024)
FeCrAl	**Coated Zr alloy**	**Coated Zr alloy**
First ATF bundle test (QUENCH facility)	Three bundle tests under extended DBA and BDBA conditions (QUENCH facility)	Bundle tests and simulation (QUENCH, **DEGREE**, and CODEX facilities)

*[*1] M. Steinbrück, et. al., High Temperature Corrosion of Materials (2024) 101:621–647.*
*[*2] M. Steinbrück, et al., JNM 559 (2022) 153470.*

Objective of This Study

To improve knowledge of differences in behaviour of coating materials, their thickness, and cladding substrates under accident conditions,

- Series of **SINGLE ROD** tests
- Series of **BUNDLE** tests

ATF Test Rod

Coated Cladding Materials

Materials	Zircaloy-4	Opt. ZIRLO	E110
OD / Thickness (mm)	10.75 / 0.725	9.13 / 0.65	9.15 / 0.70
Length (mm)	235	235	235
Coating material and their thickness (Institution provided)	10 µm Cr (KIT) 20 µm Cr (CTU) 26 µm Cr/CrN (CTU)	20 µm Cr (CTU)	Total 6 µm Cr/CrN multi-layer (AEOI)
Coating method	PVD	PVD	PVD

KIT: *Karlsruhe Institute of Technology*
CTU: Czech Technical University in Prague
AEOI: Atomic Energy Organization of Iran

Cross-Sectional Microstructure

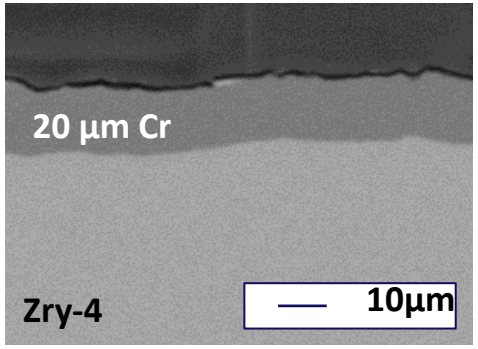

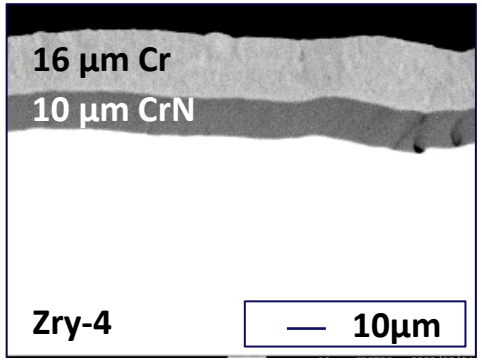

Structure of the Test Rod

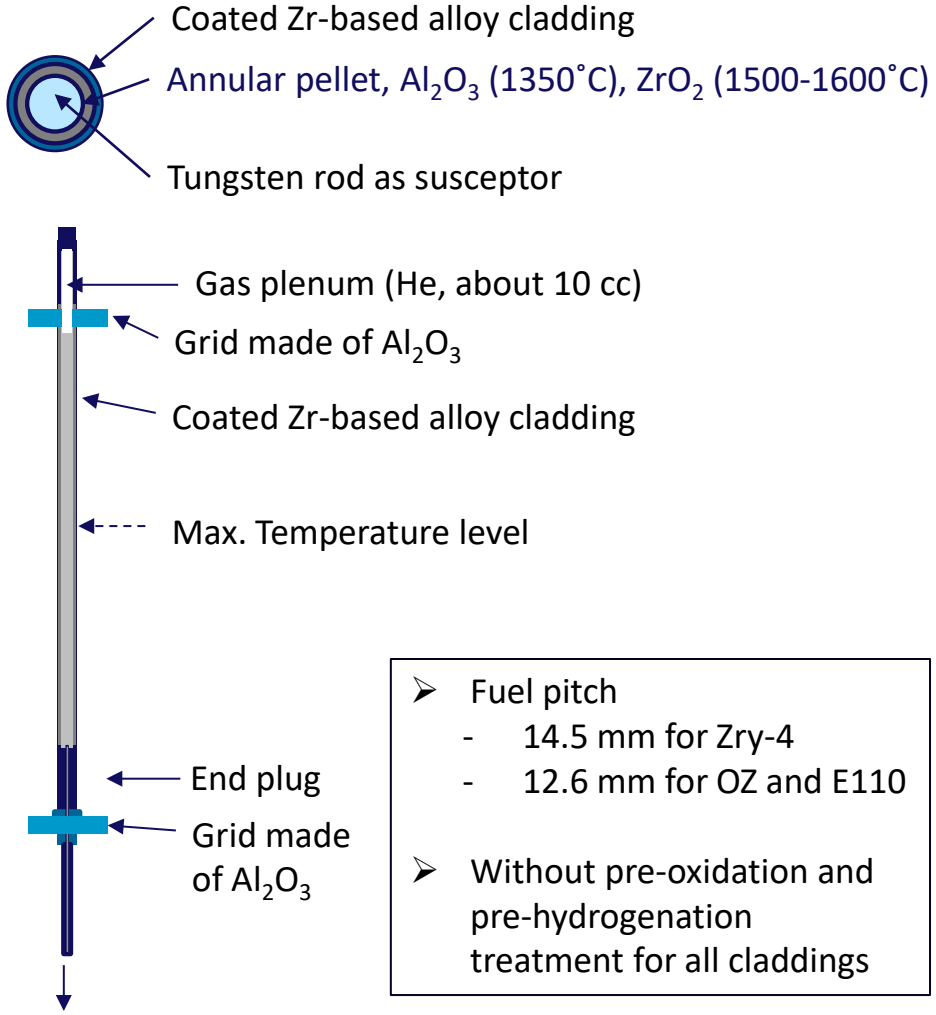

- Fuel pitch
  - 14.5 mm for Zry-4
  - 12.6 mm for OZ and E110
- Without pre-oxidation and pre-hydrogenation treatment for all claddings

Experimental Setup

Induction Heating Furnace (DEGREE)

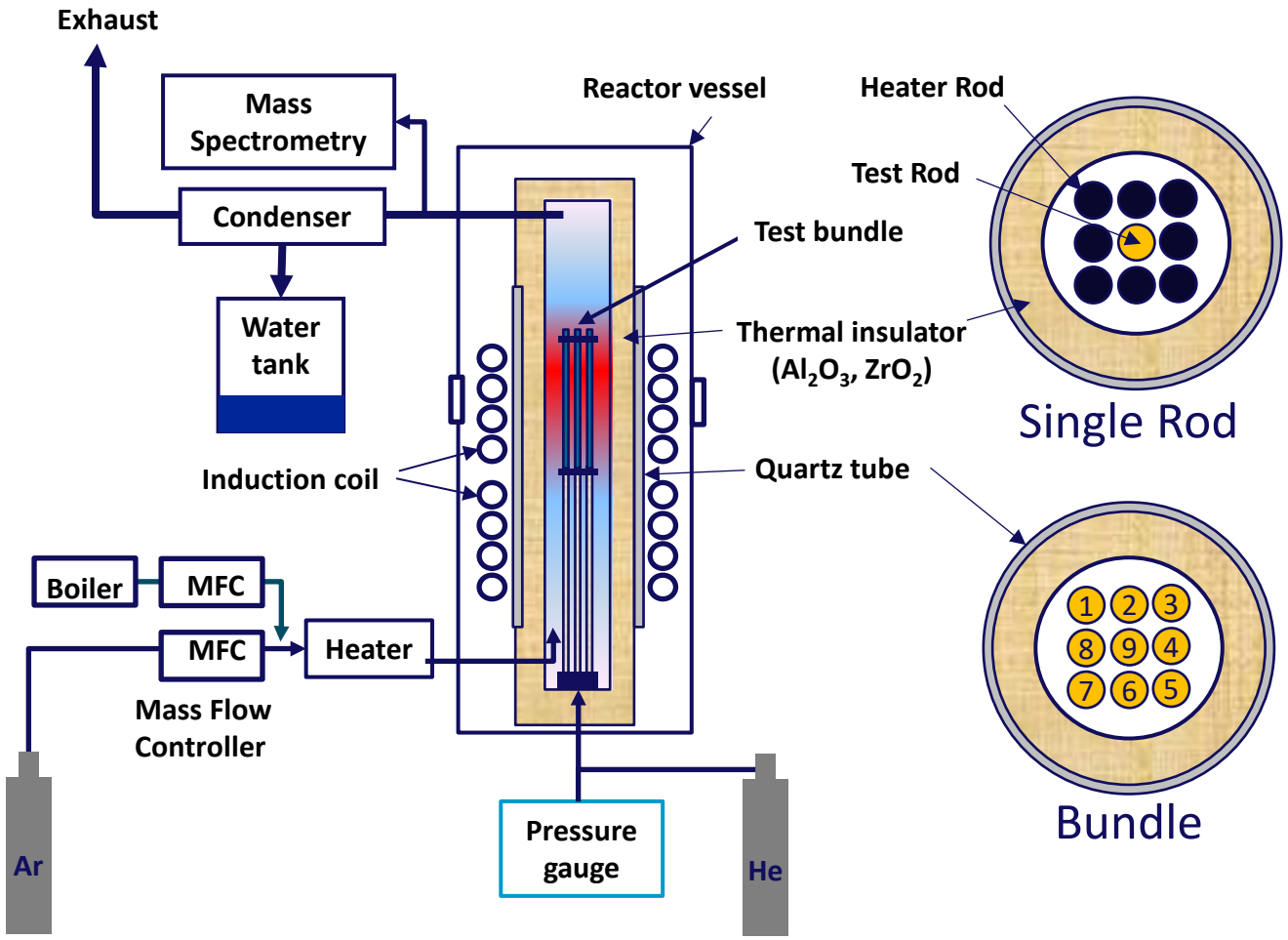

Test Scenario

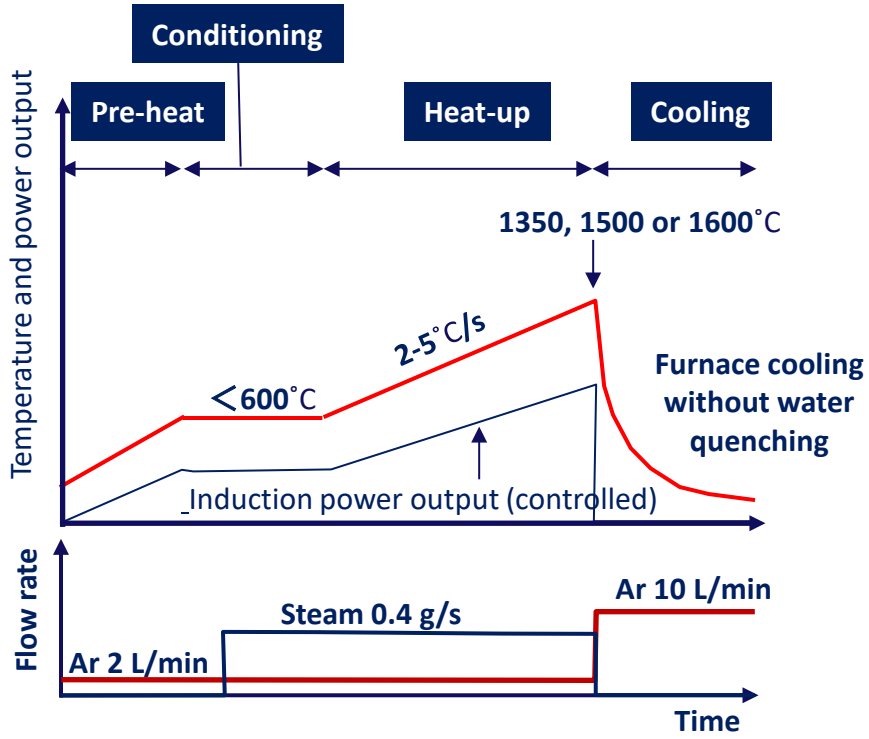

Test Matrix

Single Rod	S1	S2	S3	S4	S5	S6
Cladding materials	Zircaloy-4					
Coating materials	Uncoated	10 µm Cr	20 µm Cr	16 µm Cr/ 10 µm CrN	10 µm Cr	20 µm Cr
Max. temperature	1350 ˚C				1600 ˚C	
Rod inter. pressure	6.0 MPa					

Single Rod	S8	S9	S10	S11	S12	S13
Cladding materials	Opt. ZIRLO			E110		
Coating materials	Uncoated	20 µm Cr	20 µm Cr	Multi-layer Cr/CrN with 20 nm Cr and 20 nm CrN stacked to a total thickness of 6 µm		Uncoated
Max. temperature	1350 ˚C		1500 ˚C	1350 ˚C	1500 ˚C	1350 ˚C
Rod inter. pressure	6.0 MPa		0.1 MPa	6.0 MPa	0.1 MPa	6.0 MPa

Bundle	B1	B2	B3	B5	B6	B7
Cladding materials	Zircaloy-4					
Coating materials	Uncoated	10 µm Cr	20 µm Cr	20 µm Cr	16 µm Cr/ 10 µm CrN	20 µm Cr
Max. temperature	1350 ˚C					1500 ˚C
Rod inter. pressure	6.0 MPa	0.1 MPa	6.0 MPa	Nos. 4 and 8 with 6.0 MPa the rest with 0.1 MPa		

RIP layout in bundle

S1-S6, S8-S9, S10, S13

RIP 6.0 MPa

S10, S12

RIP 0.1 MPa

B1,B3

B2

B5-B7

RIP 6.0 MPa

RIP 0.1 MPa

Microstructure Heated to 1350˚C

(RIP=6.0 MPa)

Observation Region
- Circumferential cross sections
- 0 - 6 mm above burst opening

Single Rod

Zircaloy-4

20 µm Cr (S3)

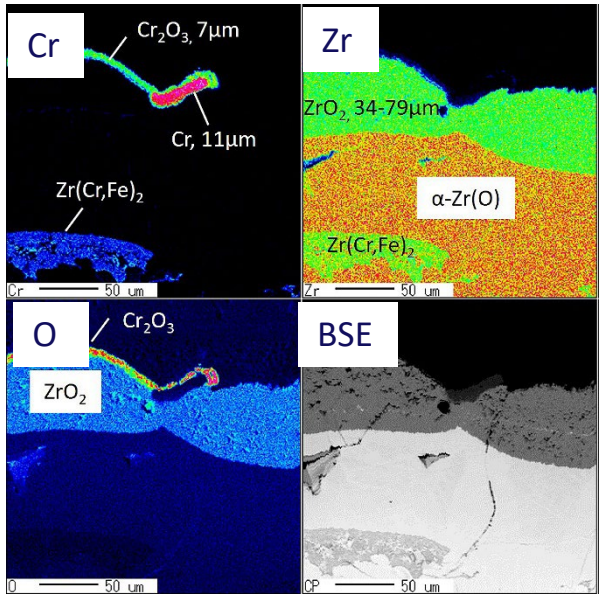

along the burst side

26 µm Cr/CrN (S4)

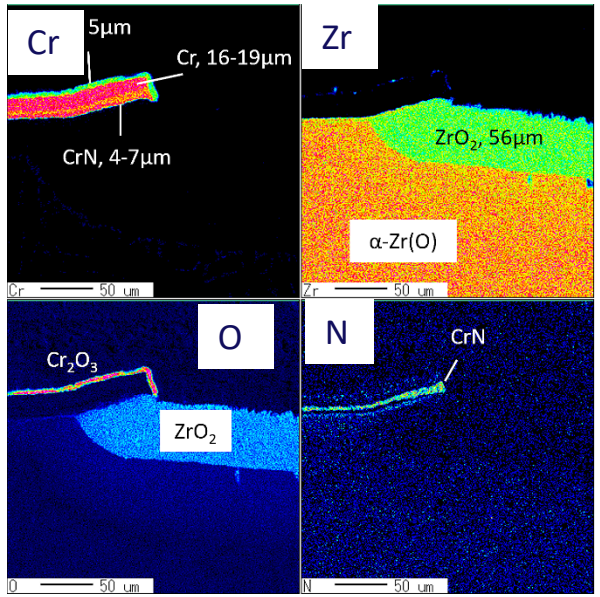

along the burst side

Opt. ZIRLO

20 µm Cr (S9)

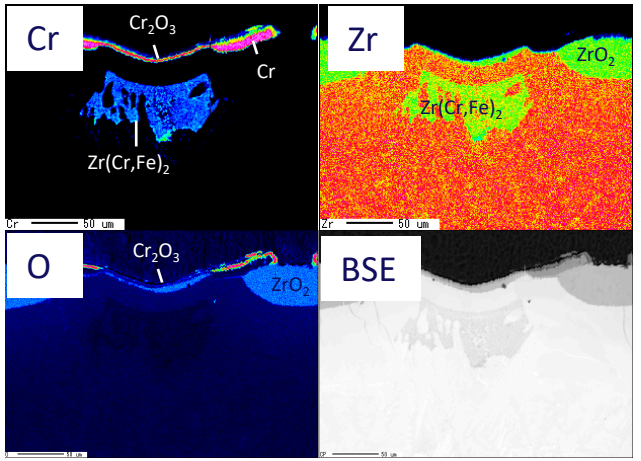

90 degree circumferential direction from the burst

E110

6 µm Cr/CrN (S11)

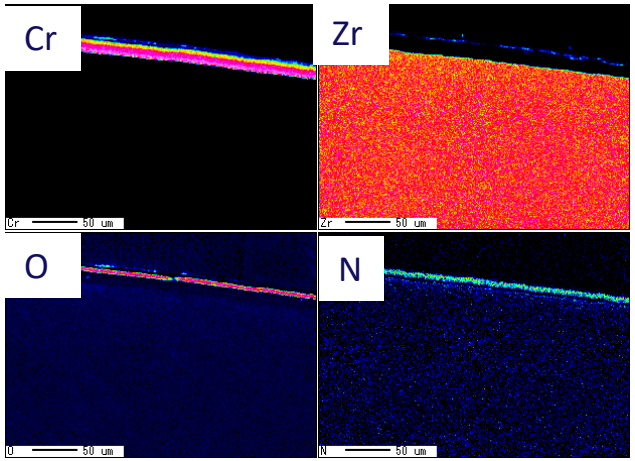

90 degree circumferential direction from the burst

- For the **Cr coatings (S3 and S9)**, formation of $ZrCr_2$ at the α-Zr(O)/prior β-Zr interface and disappearance of Cr layer
- For the **Cr/CrN coatings (S4 and S11)**, no formation of $ZrCr_2$ and remaining Cr and CrN layers

Suggested that the CrN layer has the function of suppressing the inward diffusion of Cr and oxygen and the outward diffusion of Zr.

Microstructure Heated to 1500˚C or 1600˚C

Observation Region
- longitudinal cross sections
- 24 mm above the burst

Single Rod

Zircaloy-4 (RIP = 6.0 MPa, 1600˚C)

10 µm Cr (S5)

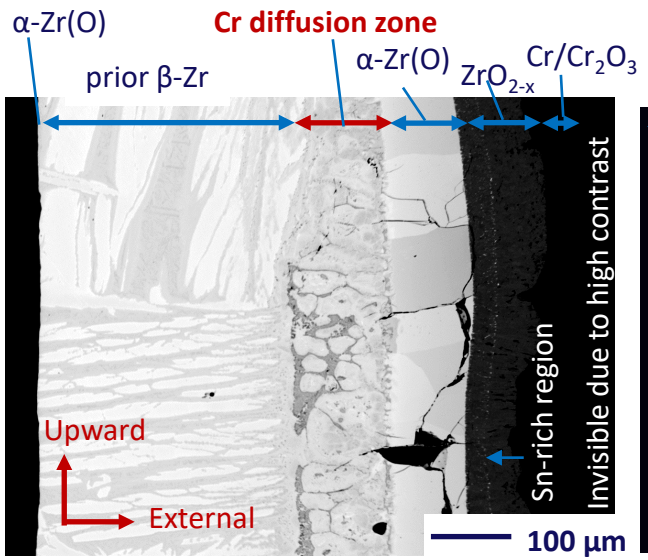

20 µm Cr (S6)

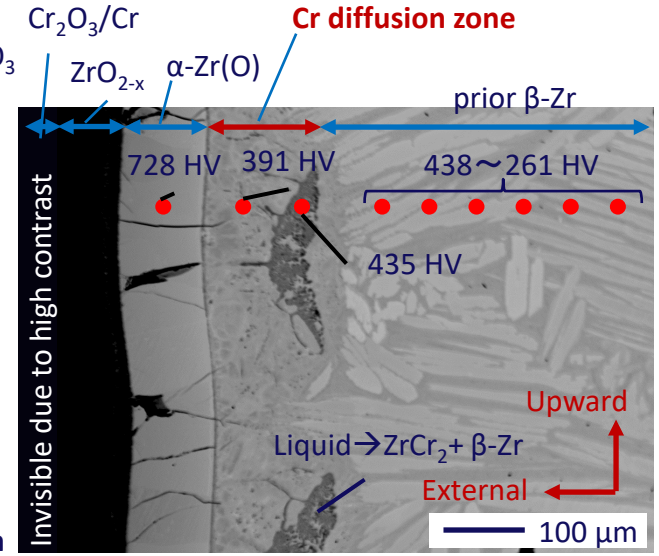

Opt. ZIRLO (RIP = 0.1 MPa, 1500˚C)

20 µm Cr (S10)

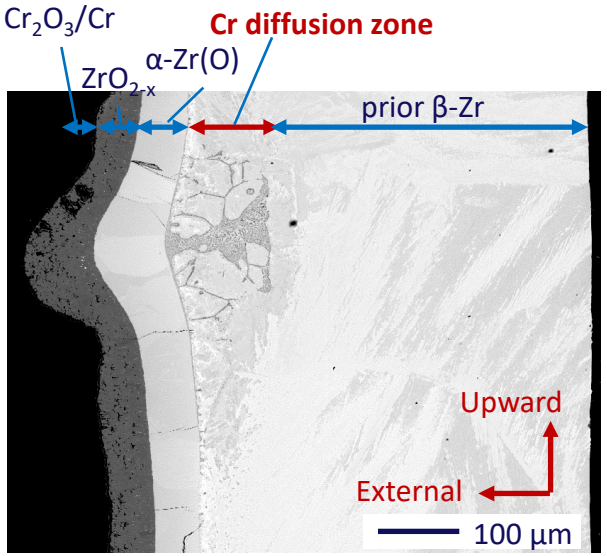

E110 (RIP = 0.1 MPa, 1500˚C)

6 µm Cr/CrN (S12)

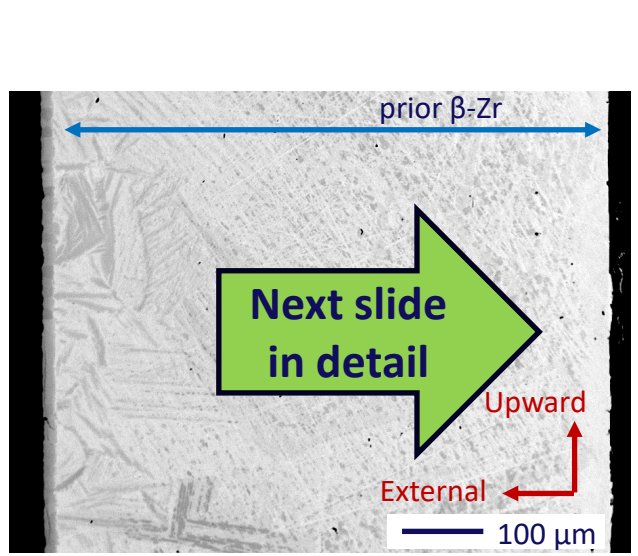

- Localized large strain due to formation of Cr-diffusion zone and liquefaction at the α-Zr(O)/prior β-Zr interface with or without rod internal pressurization
- Significant inward diffusion of Cr and oxygen and outward diffusion of Zr resulting in formation of interdiffusion structures including Cr-Zr eutectic melt
- Increasing trend of microhardness in the outward direction (● in BSE image of S6)

- Negligible inner diffusion of Cr and oxygen leading to no formation of Cr diffusion zone
- Smooth outer surface

Microstructure of Multilayer Cr/CrN coated E110

1350˚C
RIP 6.0 MPa (S11)

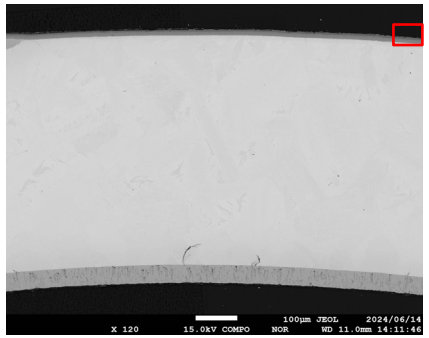

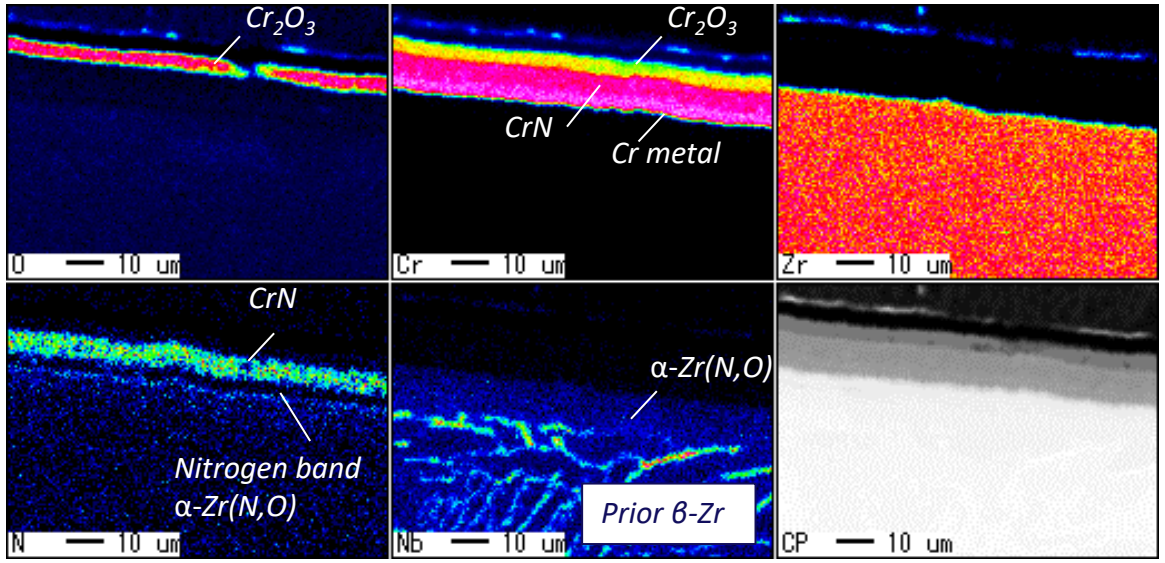

1500˚C
RIP 0.1 MPa (S12)

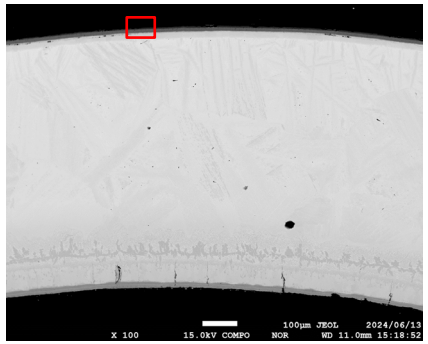

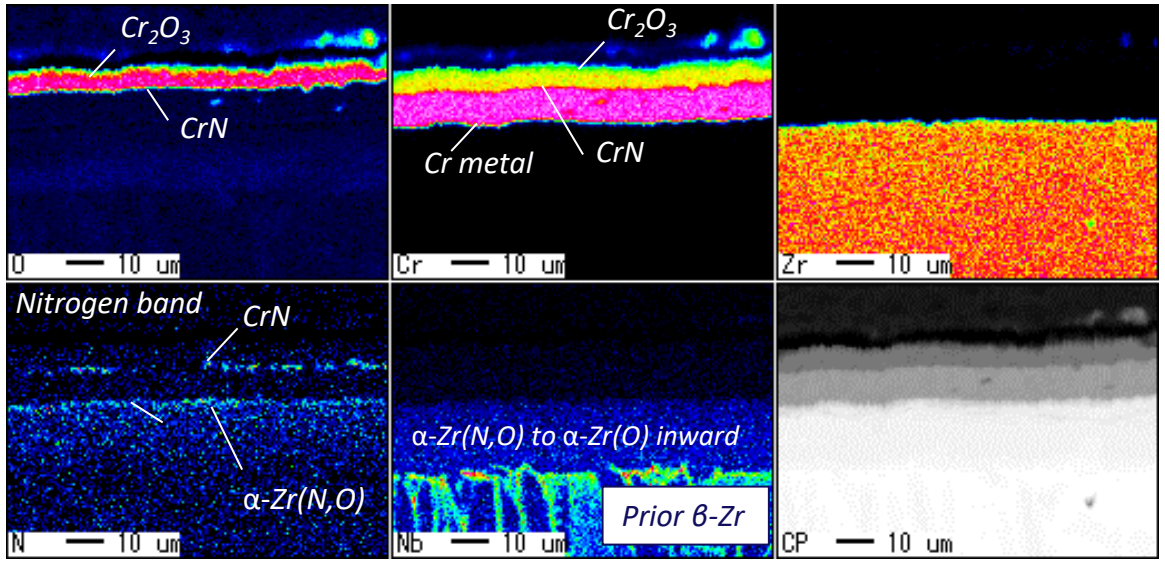

Observation Region

- **Burst level**
- **90 degrees circumferentially from the burst opening**

- The multi-layer Cr/CrN coating, initially 20 nm Cr and 20 nm CrN stacked to a total thickness of 6 µm, is transformed into another three layers: Cr_2O_3/CrN/Cr below 1350˚C .
- The CrN layer, which is likely to retard the inward diffusion of oxygen, reduces in thickness at HT to form Cr metal.
- Parts of nitrogen diffuses inward to form nitrogen-stabilized α-Zr(N,O), which is likely to retard the inward diffusion of Cr and the outward diffusion of Zr.

Hydrogen Concentration Distribution in Cladding

Vertical Distribution of Hydrogen Concentration Absorbed in the Cladding

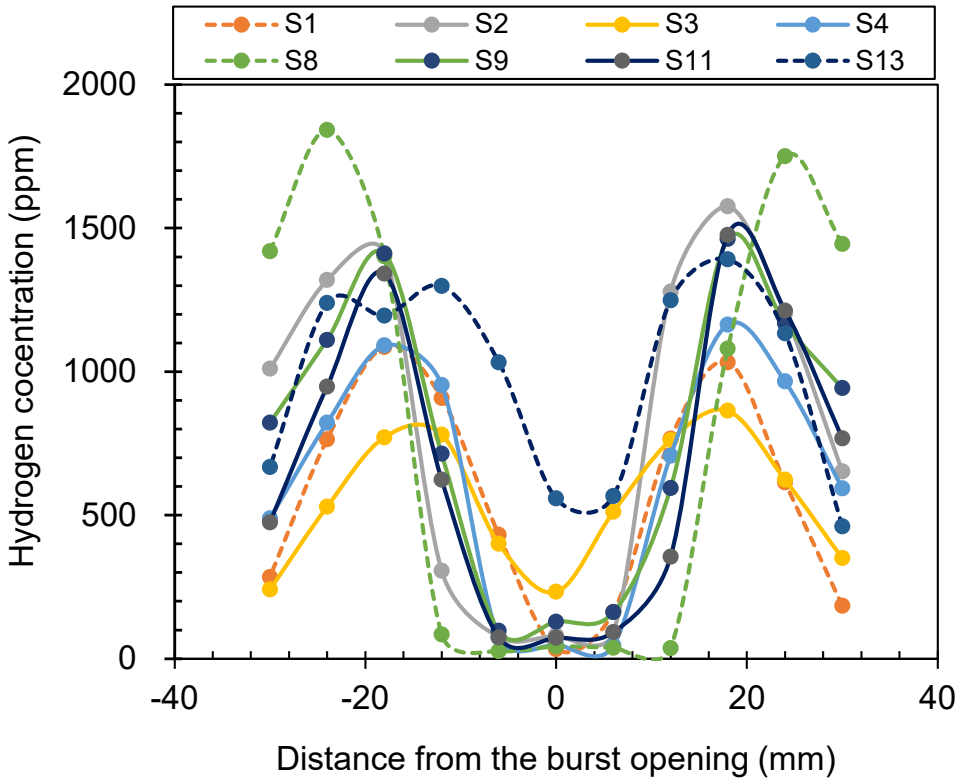

Radial Distribution of Hydrogen Concentration 24 mm above the Burst Opening (S6)

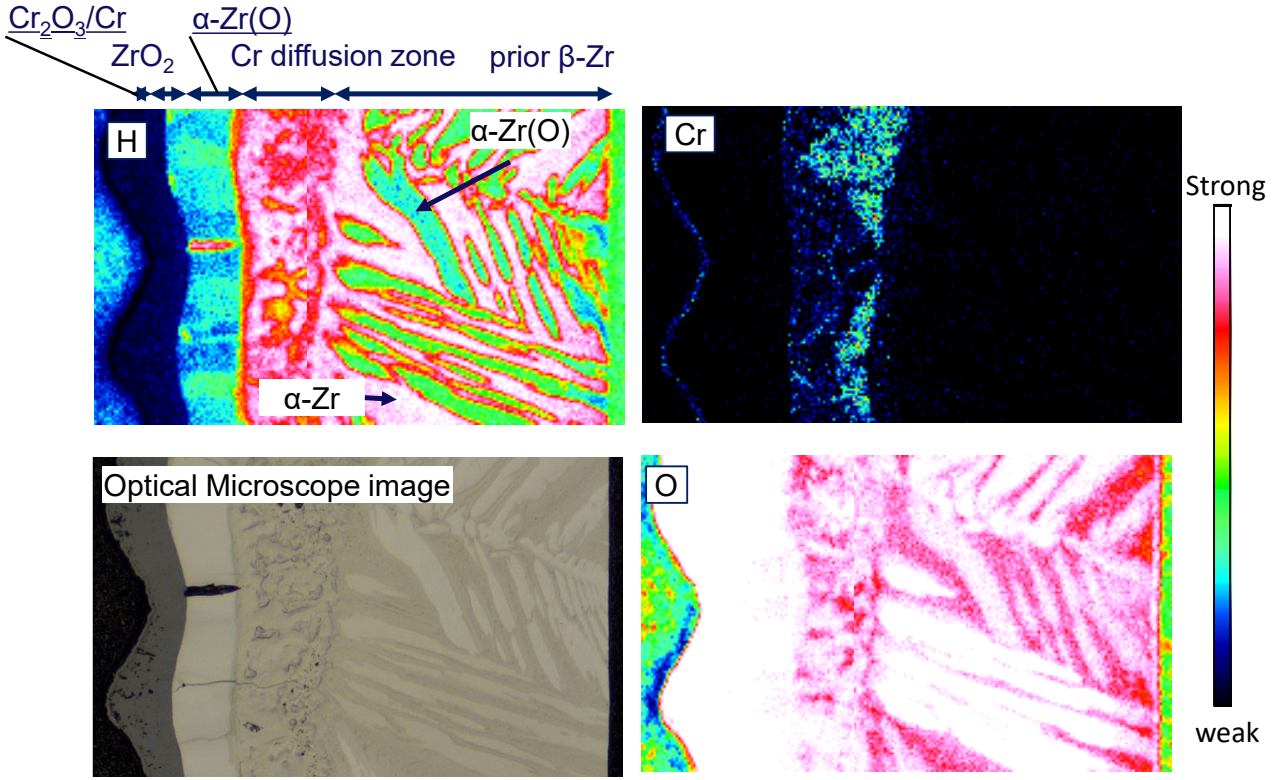

Hydrogen concentrates in the Cr diffusion zone and in the α-Zr phase that has transformed from the prior β-Zr layer.

obtained by ToF-SIMS

Bundle Test B6 (Cr/CrN coated Zry-4, 1350˚C)

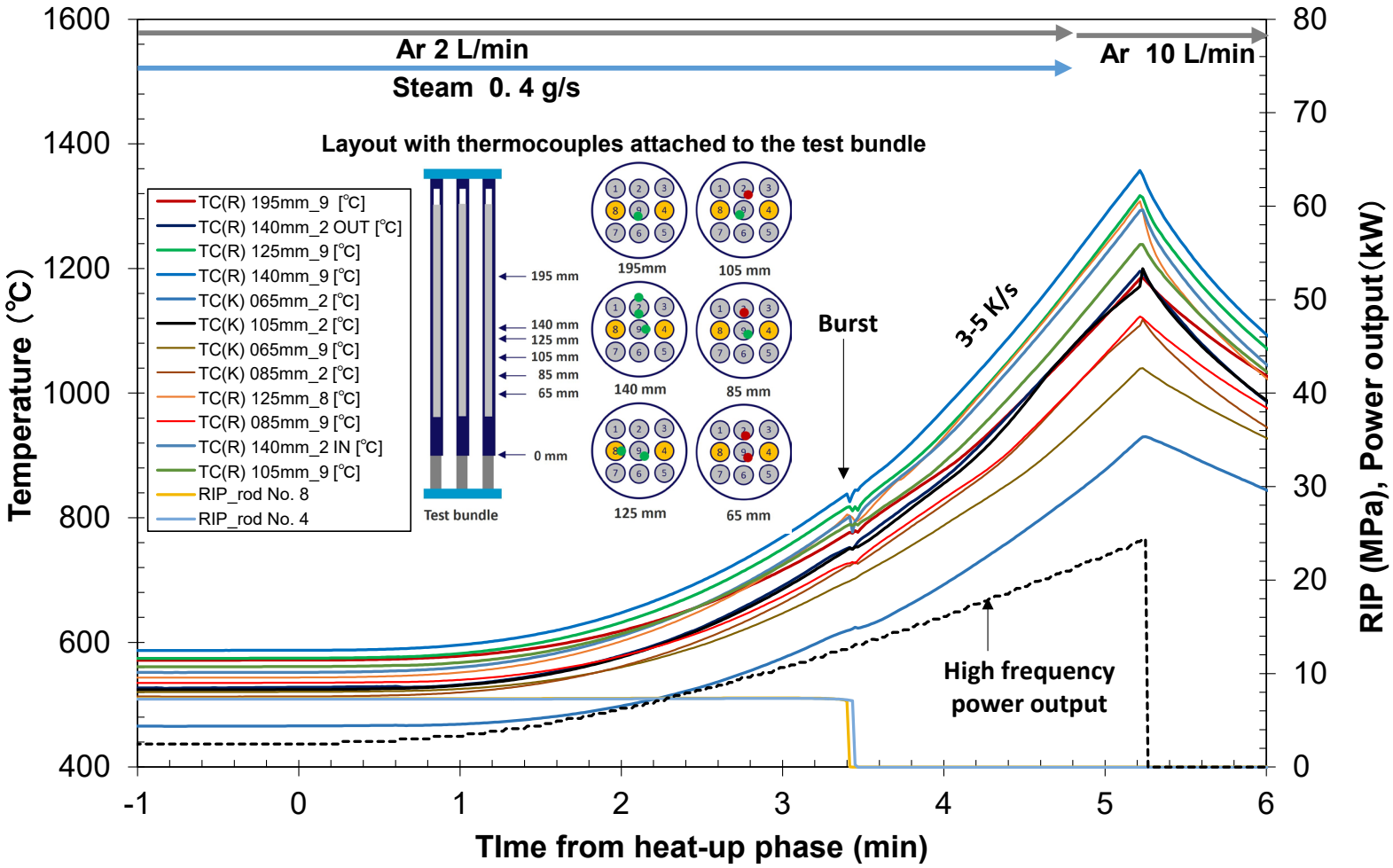

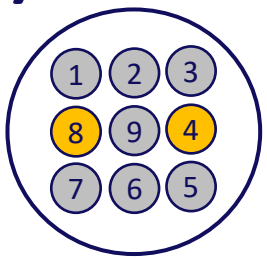

RIP 6.0 MPa No. 4 and No.8

RIP 0.1 MPa others

- Identical test conditions up to T=1350 ˚ C for bundle tests B5, B6, and B7
  - ➢Pressurized/non-pressurized fuel rod layout
  - ➢12 Thermocouple mounting positions (8 R-type and 4 K-type)
- The pressurized fuel rods (position No.4 and No.8) ballooned and burst at approximately 800˚ C, similar to the single rod tests.

Overview of Post-Test coated Zry-4 Bundle

Pressurized

Bundle

B5
20µm Cr
1350˚C

B6
Cr/CrN
1350˚C

B7
20µm Cr
1500˚C

1 2 3 4 5 6 7 8 9

B5

B6

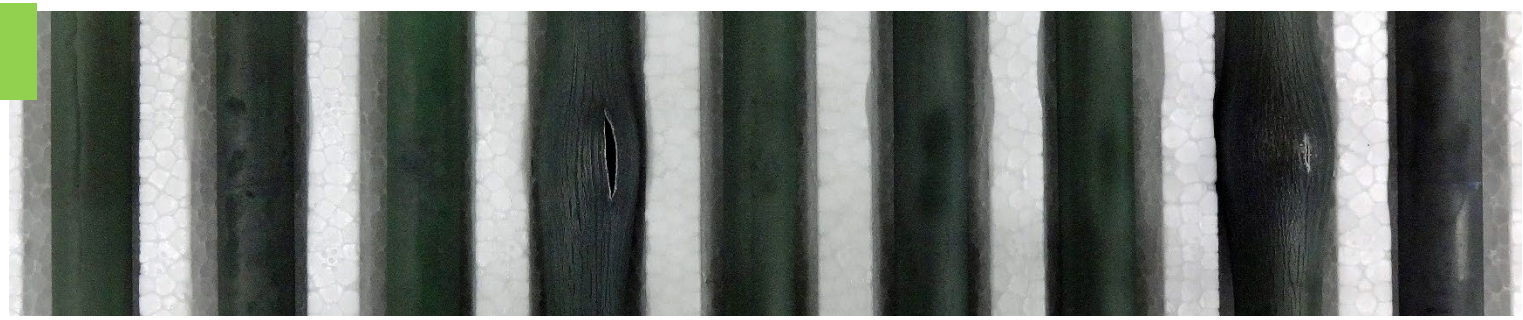

B7

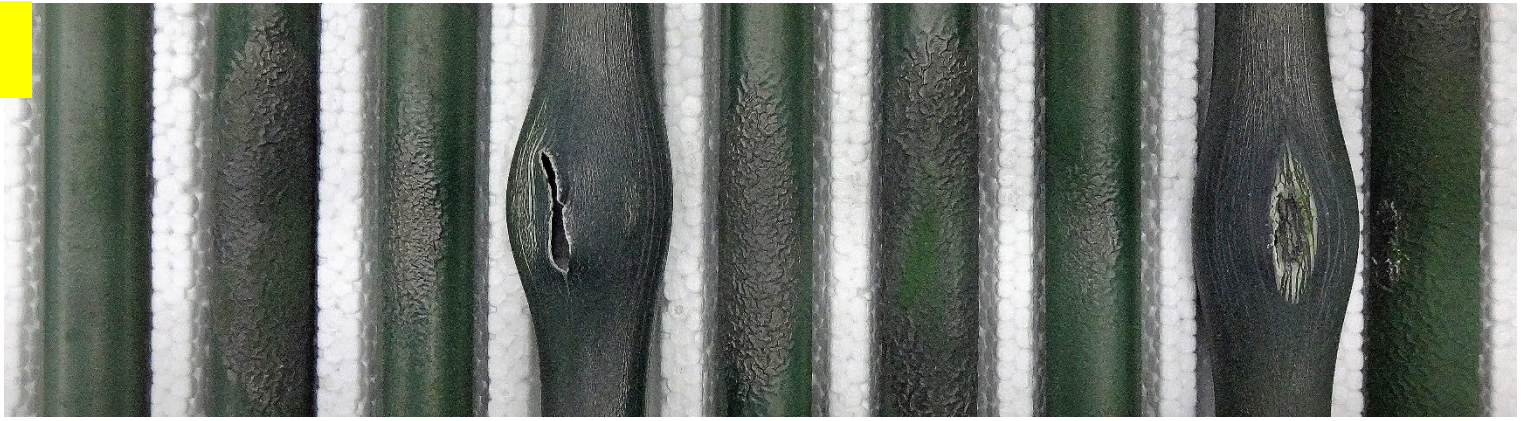

Cross Section at Burst Level

Bundle

Pressurized Rod (No. 4, RIP 6.0 MPa)

B5
20µm Cr
1350˚C

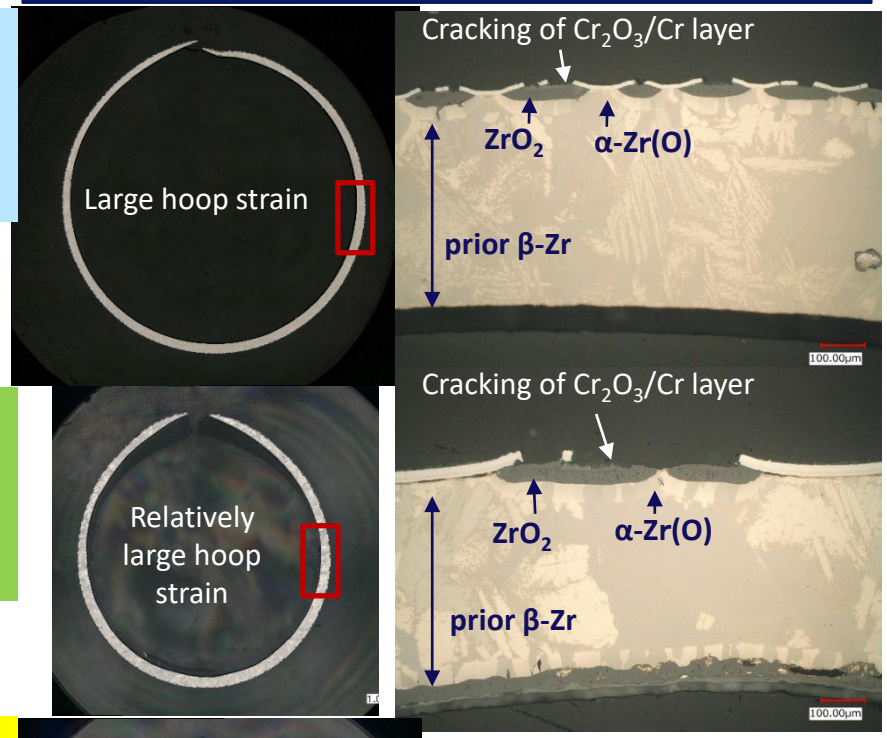

B6
Cr/CrN
1350˚C

B7
20µm Cr
1500˚C

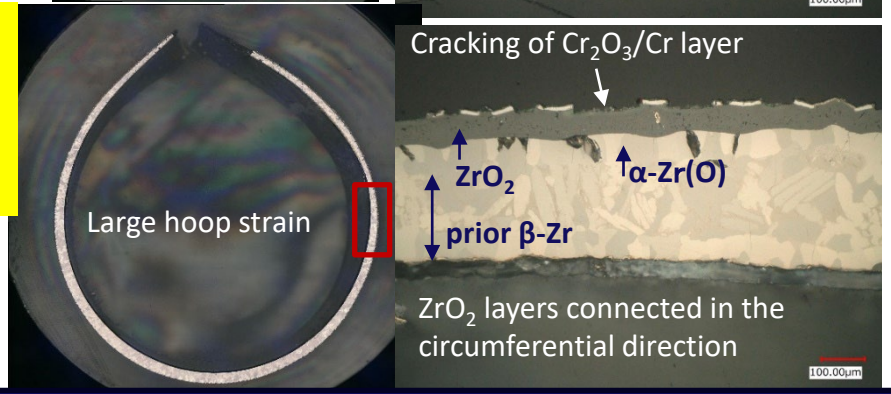

Unpressurized Rod (No. 9, RIP 0.1 MPa)

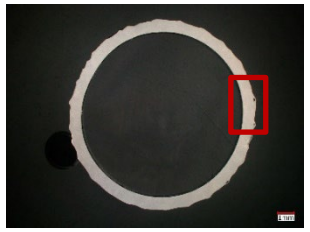

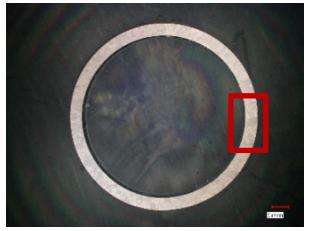

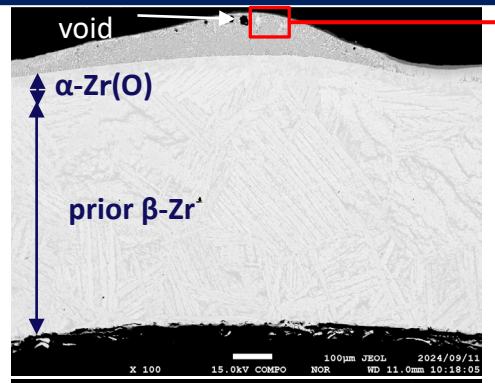

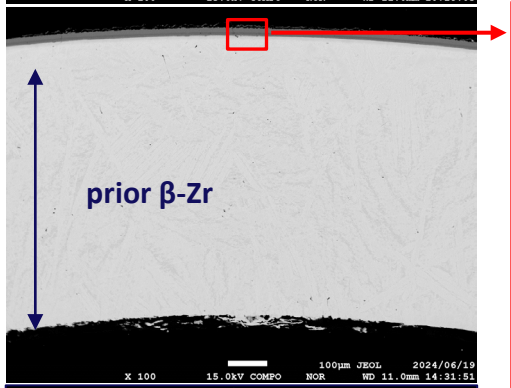

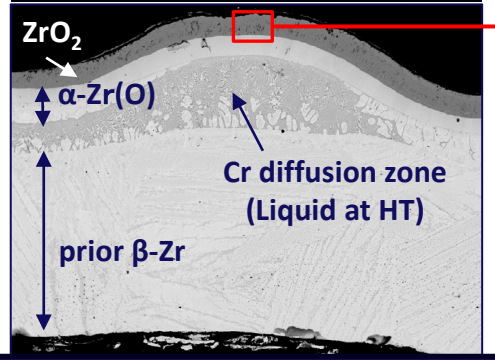

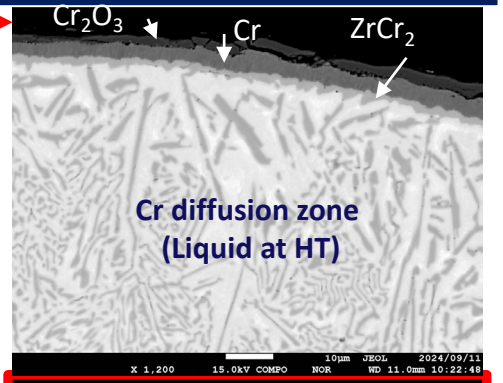

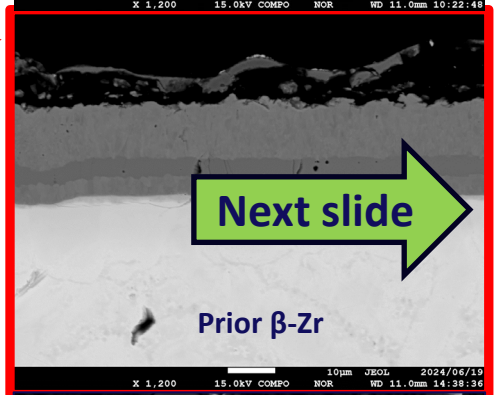

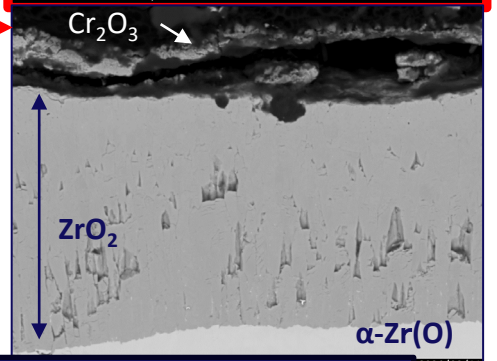

Cross section of Double-Layer Cr/CrN Coated Zry-4, 1350˚C

Bundle

Central Rod No. 9 at Burst Level (B6)

BSE Image

Elemental Map

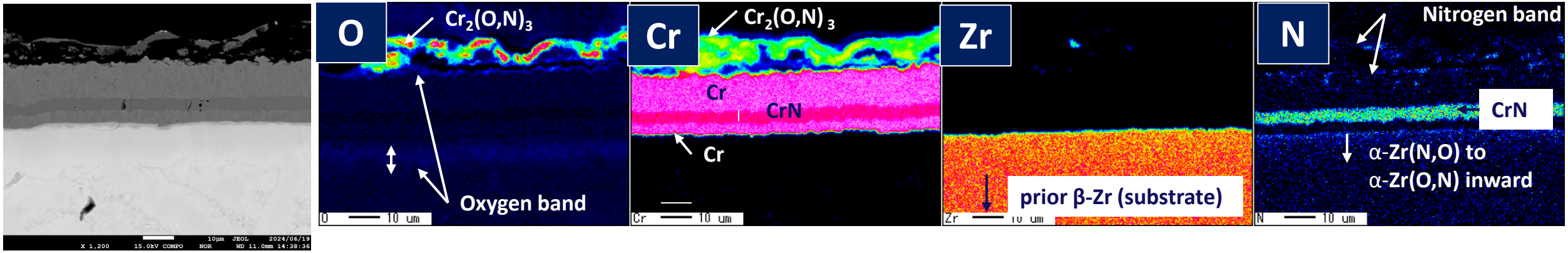

- The double-layer Cr/CrN was transformed into a four-layer structure: Cr_2O_3, Cr, CrN, Cr.
- The CrN layer was thinned from the original 10 µm to 4 µm.
- Formation of nitrogen-dissolved layers: likely $Cr_2(O,N)_3$ outward and α-Zr(N,O) inward.
- These layers appears to suppress the inward diffusion of Cr and Oxygen, and the outward diffusion of Zr.
- Similar microstructures are seen in the region at least 18 mm above the burst level.
- Expected properties of double- and multi-layer Cr/CrN coatings
  - Suppressing circumferential strain,
  - Reducing the oxidation kinetics, and
  - Retarding liquefaction due to the Cr-Zr eutectic.

- Could Nitrogen inventory be the key?
- Corrosion resistance?

Comparison of burst Behaviour between single rod and bundle tests

Burst Temp. and Hoop Strain

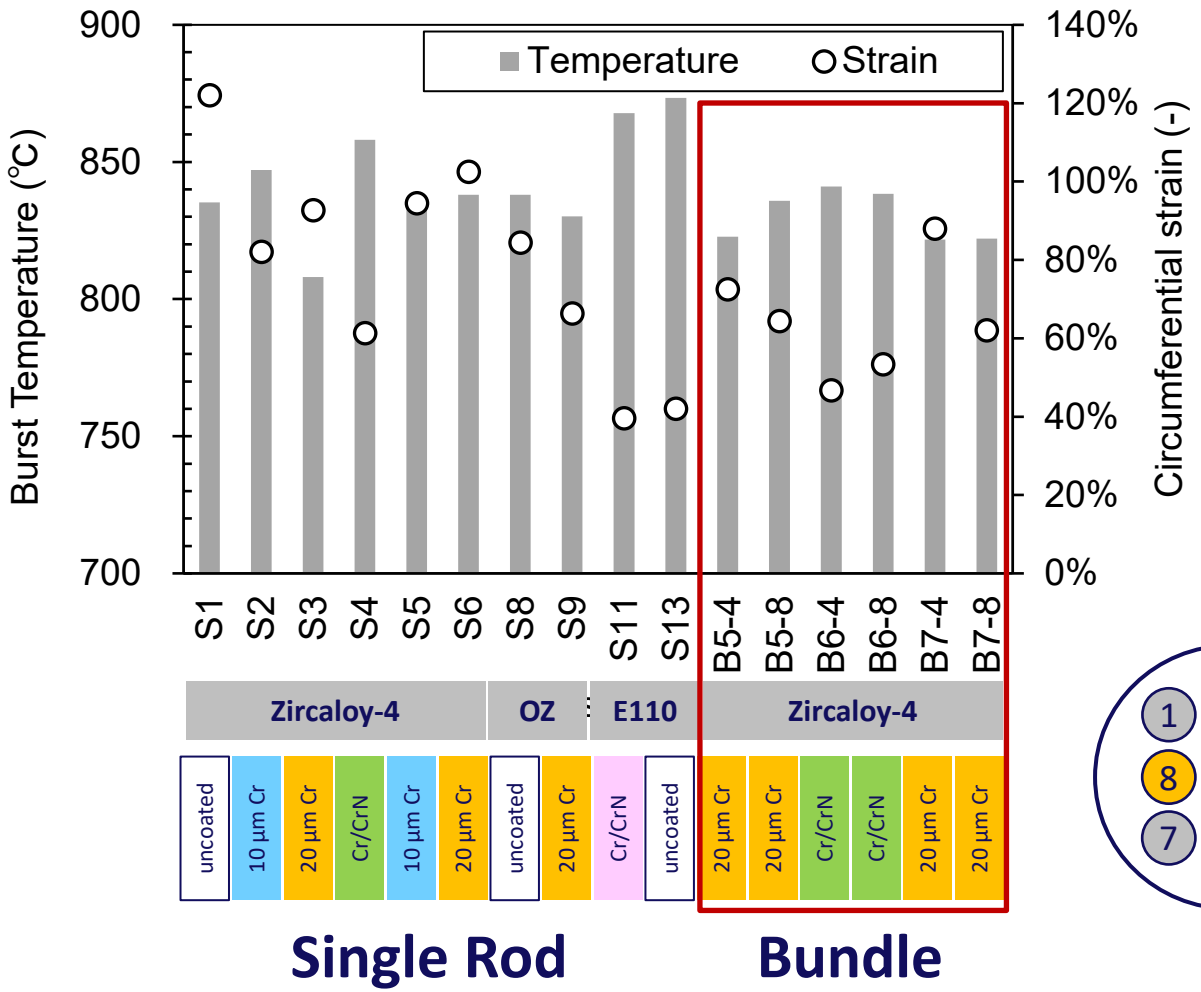

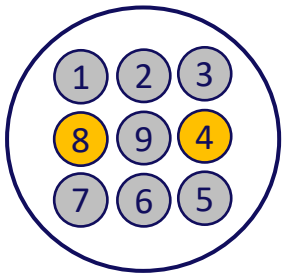

Single Rod Bundle

Burst Opening Size

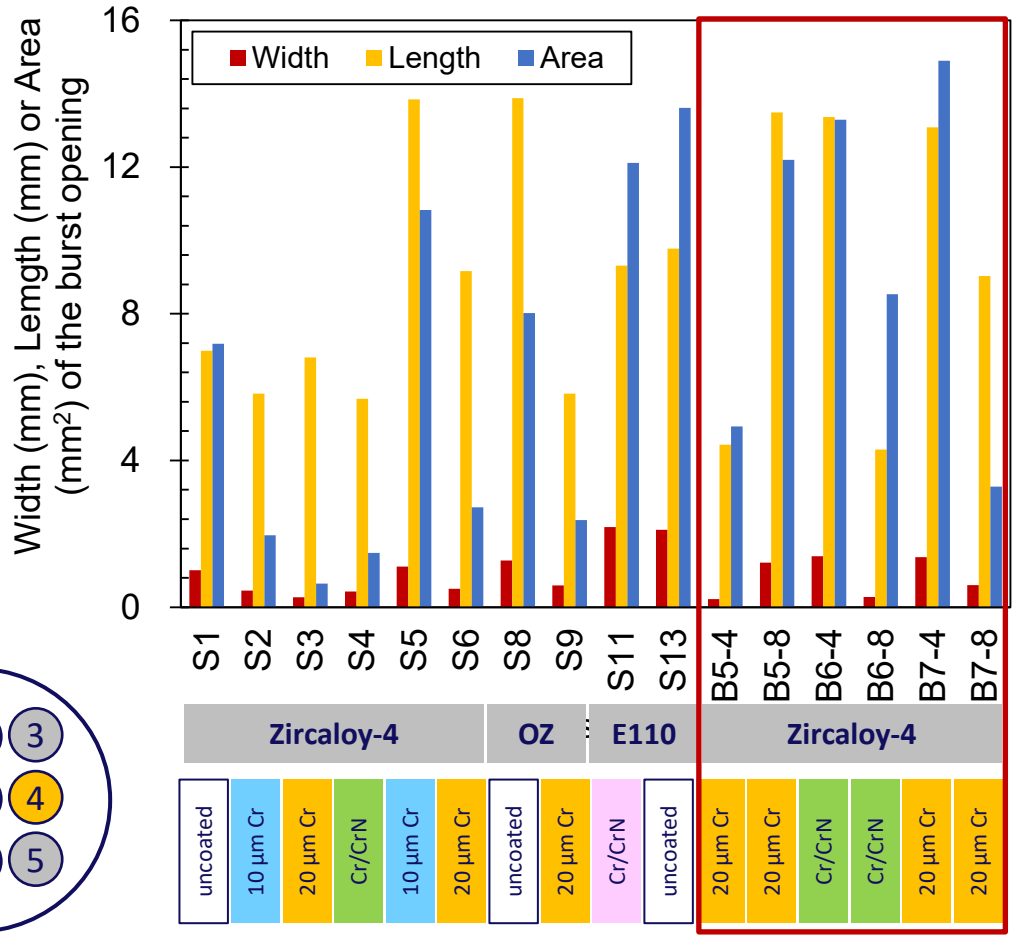

Single Rod Bundle

Conclusion & Future Works

Series of single rod and 3x3 bundle tests were successfully carried out using the DEGREE facility, where three types of fuel claddings coated with Cr or Cr/CrN, were heated up to 1350-1600˚C in a steam-Ar mixed atmosphere under simulated BDBA-LOCA conditions.

- The interdiffusion layer structure formed at the coating-substrate interface, the radial and vertical redistribution of the constituent elements including O, N, and H, the radial profile of the microhardness, and the ballooning and bursting behaviour were indicated.
- The accident behaviours of the different coating materials and their thicknesses or cladding materials, as well as between single rod and bundle tests, were also discussed.
- For the Cr coating, the Cr_2O_3 diffusion barrier effect is deteriorated at HT due to cracking in the coating layer, interdiffusion of the components, liquefaction due to Cr-Zr eutectic etc.
- For the Cr/CrN coating, regardless of whether it was a double- or multi-layer coating, the hoop strain was relatively small, and the nitrogen-containing layer caused by CrN might suppress the interdiffusion of the components, and the diffusion barrier effect was likely to be improved at HT compared with the Cr coating
- No temperature runaway was observed in bundle tests under non-adiabatic conditions (due to transparency of the quartz shroud for thermal radiation).

Further bundle tests should be conducted using different coating materials and different accident scenarios.

CRIEPI
Central Research Institute of Electric Power Industry

Acknowledgment

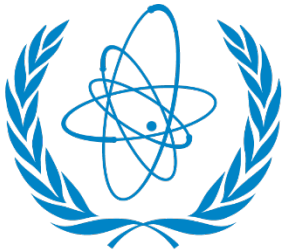

IAEA
International Atomic Energy Agency

Thank you for your attention!

Róbert Farkas, pres. by Nóra Vér

HUN-REN EK

The CODEX-ATF-AIT integral air ingress experiment

The introduction of accident tolerant fuel (ATF) at nuclear power plants needs testing under large variety of accident conditions. The most promising near-term ATF cladding solution are Cr-coated zirconium alloys. The access of air to the hot surface of fuel rods during accidents may significantly accelerate the core degradation after failure of the Cr coating due to the intense oxidation of zirconium alloys. The scenarios leading to air ingress (lower head failure, open reactor, spent fuel storage pool) can be critical from the point of view of radiological consequences, for the loss of cladding integrity can lead to the oxidation of ruthenium and formation of gaseous species of radionuclides. An integral bundle test with electrically heated Cr coated fuel rod simulators under air ingress conditions will be carried out in the CODEX facility. The design of the test section will be similar to the previous CODEX tests [1][2][3].

The fuel rods will be filled with zirconia pellets. The rods will be pressurized by kripton. Electrical heating with two tungsten heaters in each rod will be used. External heating will be also applied to the test section. The bundle will be covered by Cr coated Zr shroud and several thermal insulation layers. The proposed scenario will focus on covering several phenomena of fuel behavior during accidents (burst, oxidation, nitriding, eutectic formation). The steam generator will provide hot steam and argon to the test section. Air (or air/steam) injection will be started after some oxidation took place in steam. The data acquisition will include signals from large number of thermocouples and from the mass spectrometer used for the analyses of outlet gas composition. Post-test examinations (endoscopy, LOM, SEM, EDX) will focus on the identification of cladding degradation mechanisms.

The observations and the experimental data will provide direct information on the cladding degradation of ATF designs. The experiment will especially provide unique data on the effect of air containing atmosphere on high-temperature oxidation and degradation of Cr-coated zirconium alloy cladding as long as the coating keeps it protective effect and moreover after loss of the protective effect. The positive feedback of accelerated oxidation kinetics (connected with enhanced release of hydrogen and chemical energy) on the temperature course in the bundle can be only seen in such a more integral test. Furthermore, the formation of the Cr coating on nitride formation (as seen in air ingress experiments with uncoated cladding) will be analyzed.

[1] Farkas, R., Hózer, Z., Nagy, I., Vér, N., Szabó, P., Horváth, M., Kostka, P., Lajtha, G. (2023). Experimental simulation of selected design extension condition scenarios without core meltdown in the CODEX facility. *Progress in Nuclear Energy*, 161, 104720.

[2] Farkas, R., Hozer, Z., Nagy, I., Ver, N., Horvath, M., Steinbrück, M., Stuckert, J., Grosse, M. (2022). Effect of steam and oxygen starvation on severe accident progression with air ingress. *Nuclear Engineering and Design*, 396, 111884.

[3] Hózer, Z., Windberg, P., Nagy, I., Maróti, L., Matus, L., Horváth, M., Csordás, A., P., Balaskó, M., Jani, P. (2003). Interaction of failed fuel rods under air ingress conditions. *Nuclear Technology*, 141(3), 244-256.

HUN REN | Centre for Energy Research

HUN-REN Hungarian Research Network

The CODEX-ATF-AIT integral air ingress experiment

R. Farkas, N. Vér, B. Bürger, A. Pintér Csordás, L. Illés, Z. Hózer, U. Stegmaier*

*KIT, IAM-AWP

Quench Workshop
19-21th November 2024

Research. Innovation. Impact.

Objectives

Integral testing of accident tolerant fuel design under air ingress conditions (CODEX-ATF-AIT)

- The CODEX-ATF-AIT experiment was performed in the framework of the EU OFFERR project.
- The main objective of the proposed test was to check if Cr coating would have a protective role in case of NPP accidents with air ingress.
- The proposed scenario was focused on covering several phenomena of fuel behavior during accidents
  - burst,
  - oxidation,
  - nitriding,
  - eutectic formation.
- CODEX-AIT-3 experiment was chosen for reference test which was an air ingress test conducted with traditional Zr materials.

Test facility

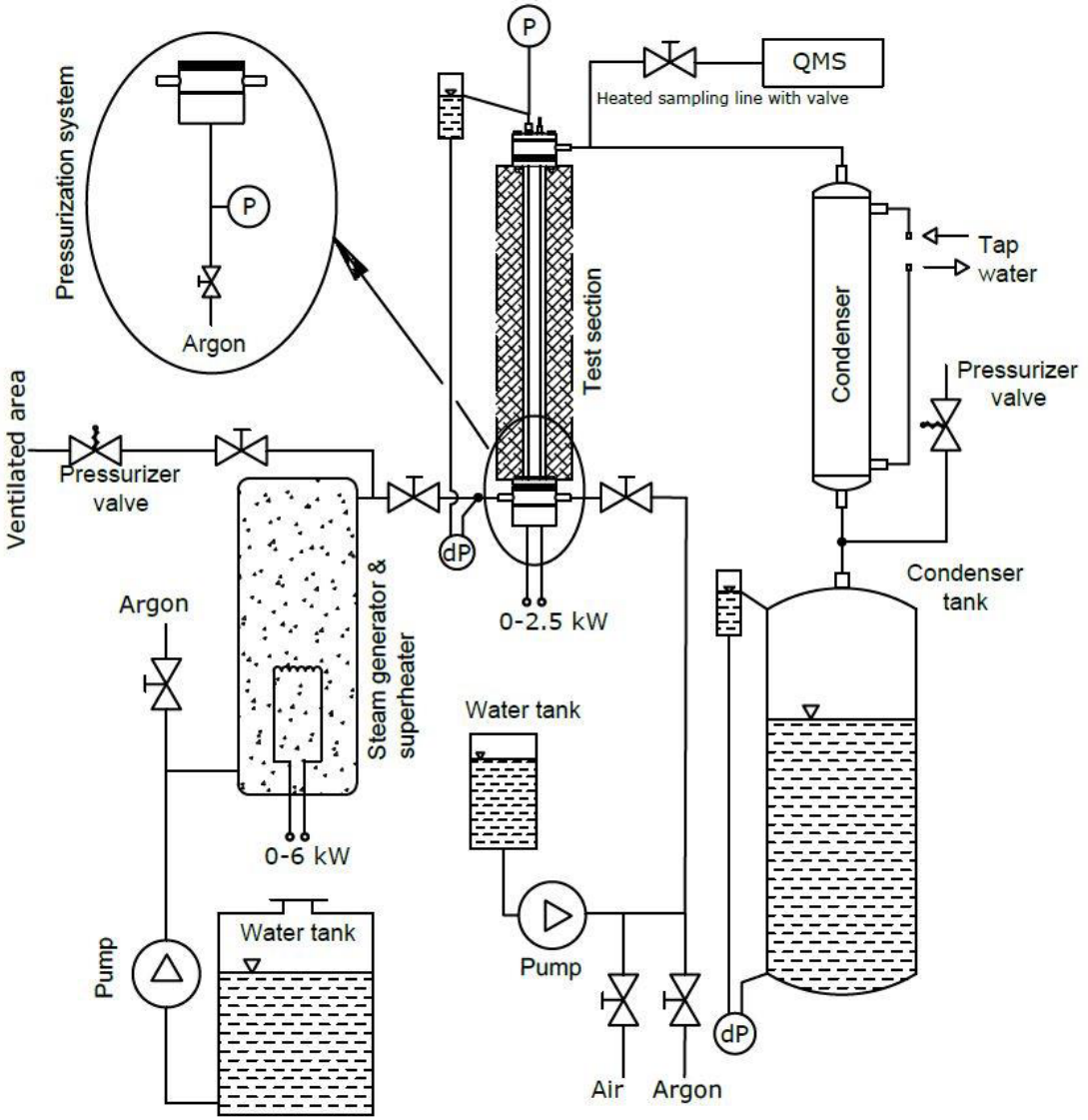

Schematic view of the CODEX facility

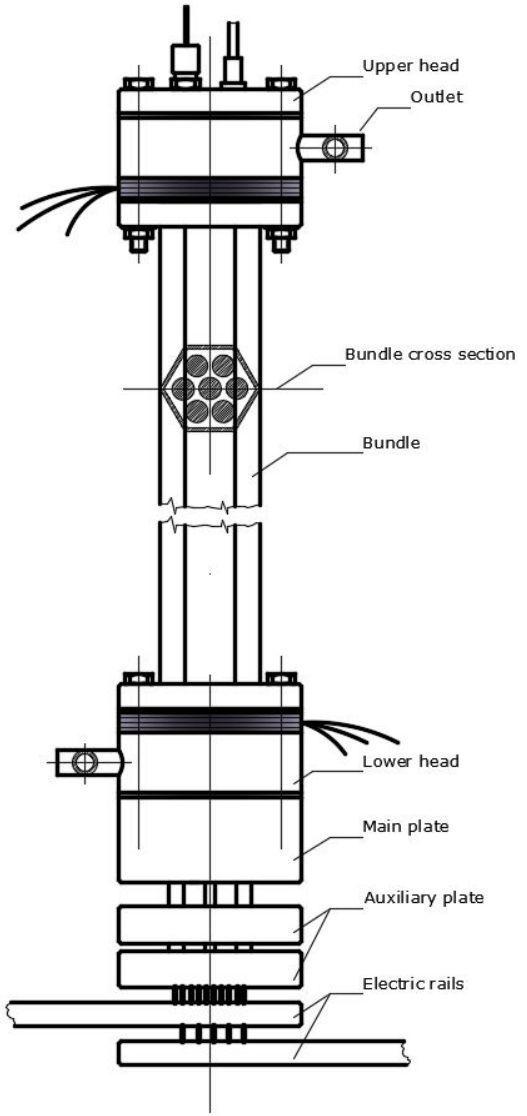

View of the test section with seven-rod bundle

Test section and bundle design

- VVER bundle type:
  hexagonal arrangement of 7 rods

- 6 rods electrically heated with tungsten heaters
  1 rod unheated
  - CODEX-AIT-3: rod No. 1. (in the center)
  - CODEX-ATF-AIT: rod No. 7. (periphery)

- Rods pressurized
  - CODEX-AIT-3: rod No. 1. (in the center) pressurized with Ar
  - CODEX-ATF-AIT: all 7 rods pressurized with Kr

- ZrO_2 ceramic pellets

- 3 spacer grids

- Hexagonal shroud

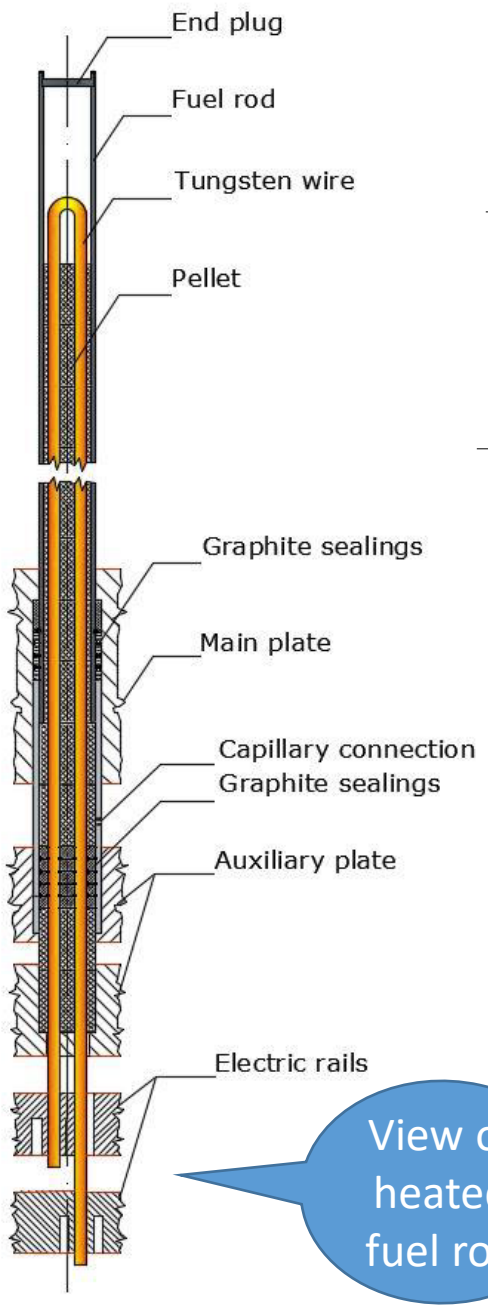

View of heated fuel rod

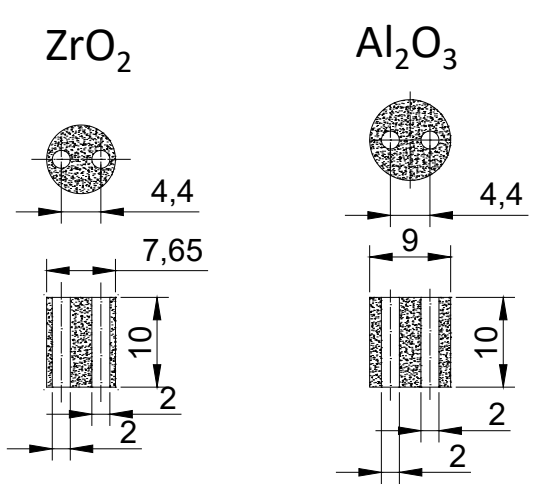

View of ceramic pellets

Cross section of the test section

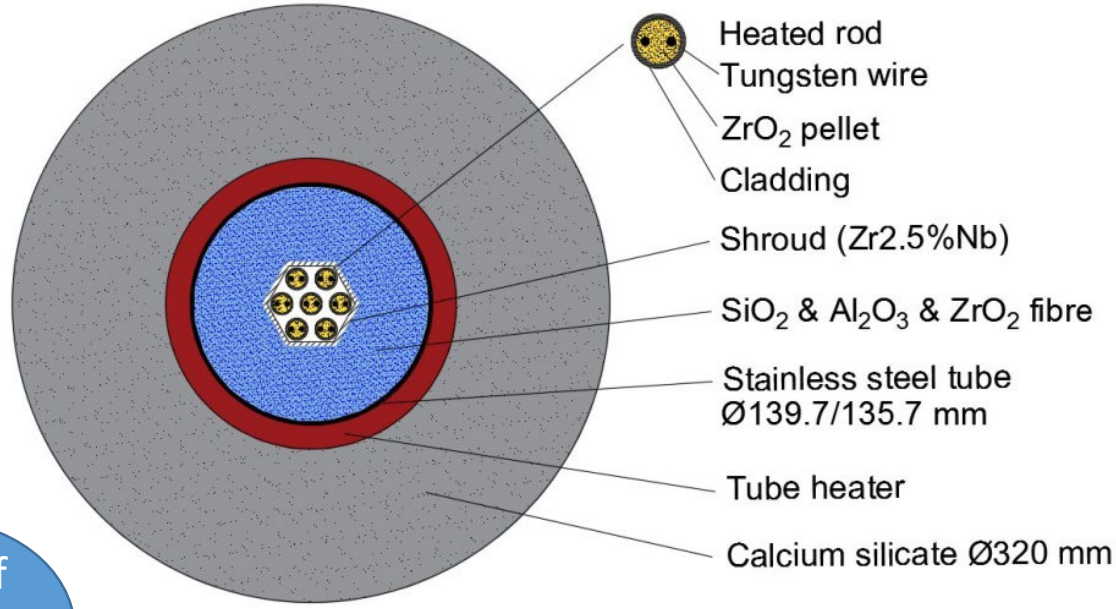

Main characteristics of the test section

CODEX-AIT-3

Number of fuel rods	7
Cladding of fuel rods	**E110G**
Length of fuel rods	**1000 mm**
External diameter of fuel rods	9.1 mm
Cladding wall thickness	0.69 mm
Pellet material	ZrO_2
Pellet material in the bottom of the rods	Al_2O_3
Height of pellet	10 mm
Diameter of pellet	7.65 mm
Hole diameter in the pellet	2 mm
Spacer grid material	**Zr1%Nb**
Height of spacer grid	10 mm
Thickness of spacer grid	0.4 mm
Number of spacer grids	3
Shroud material	**Zr2.5%Nb**
Shroud thickness	2 mm
Length of shroud	1000 mm

CODEX-ATF-AIT

Number of fuel rods	7
Cladding of fuel rods	**Cr-coated optZIRLO™**
Length of fuel rods	**900 mm**
External diameter of fuel rods	9.1 mm
Cladding wall thickness	0.57 mm
Pellet material	ZrO_2
Pellet material in the bottom of the rods	Al_2O_3
Height of pellet	10 mm
Diameter of pellet	7.65 mm
Hole diameter in the pellet	2 mm
Spacer grid material	**Cr-coated Zr1%Nb**
Height of spacer grid	10 mm
Thickness of spacer grid	0.4 mm
Number of spacer grids	3
Shroud material	**Cr-coated Zr2.5%Nb**
Shroud thickness	2 mm
Length of shroud	1000 mm

Cr coating: Czech Technical University in Prague, PVD technique

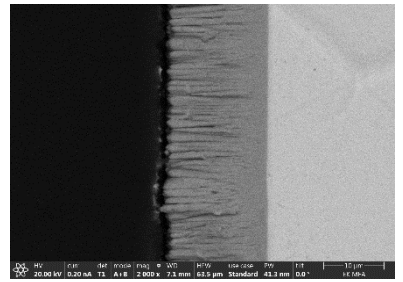

Uniform Cr coating layer around the circumference of the cladding ~**15.5 µm**

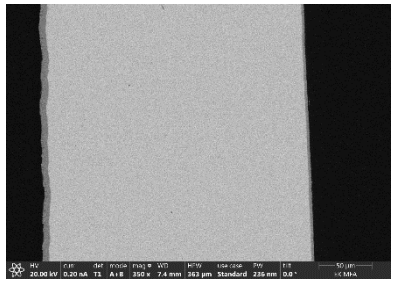

Thickness of the Cr layer on spacer grid

- at the straight sections almost uniform ~**10 – 12 µm**
- at the curved parts ~**2 – 3 µm**

Measurements

On-line measurements and data acquisition:

- **temperatures** (rod surfaces, others: shroud, stainless steel tube, coolant , off-gas, …)
- **pressures** (system and rods),
- **flowrates** (argon, air),
- **power**,
- **outlet gas composition**.

Thermocouple positions

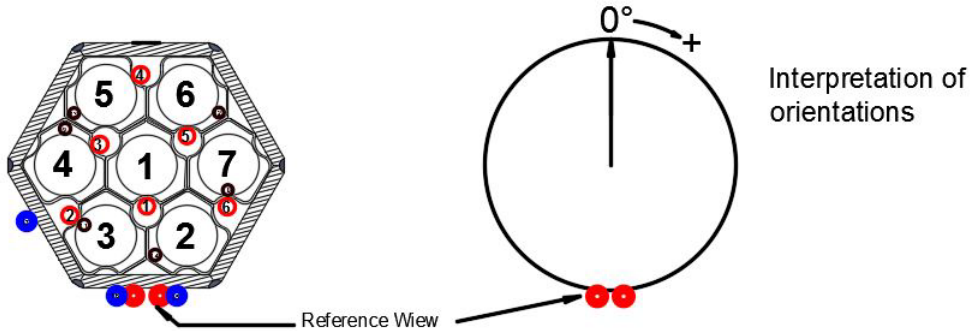

① W5Re/W26Re at elevation 850 mm with orientation of 180°
② W5Re/W26Re at elevation 650 mm with orientation of 300°
③ W5Re/W26Re at elevation 750 mm with orientation of 60°
④ W5Re/W26Re at elevation 650 mm with orientation of 60°
⑤ W5Re/W26Re at elevation 750 mm with orientation of 180°
⑥ W5Re/W26Re at elevation 500 mm with orientation of 180°

High temperature thermocouples (6 pieces)

⑦ "K" type at elevation 50 mm with orientation of 0°
⑩ "K" type at elevation 50 mm with orientation of 180°
⑪ "K" type at elevation 150 mm with orientation of 300°
⑫ "K" type at elevation 150 mm with orientation of 120°
⑬ "K" type at elevation 500 mm with orientation of 240°
⑭ "K" type at elevation 200 mm with orientation of 240°
"K" type at elevation 750 mm
"K" type at elevation 650 mm
"K" type at elevation 500 mm

K-type thermocouples (26 pieces)

Reference scenario – CODEX-AIT-3

CODEX-AIT-3

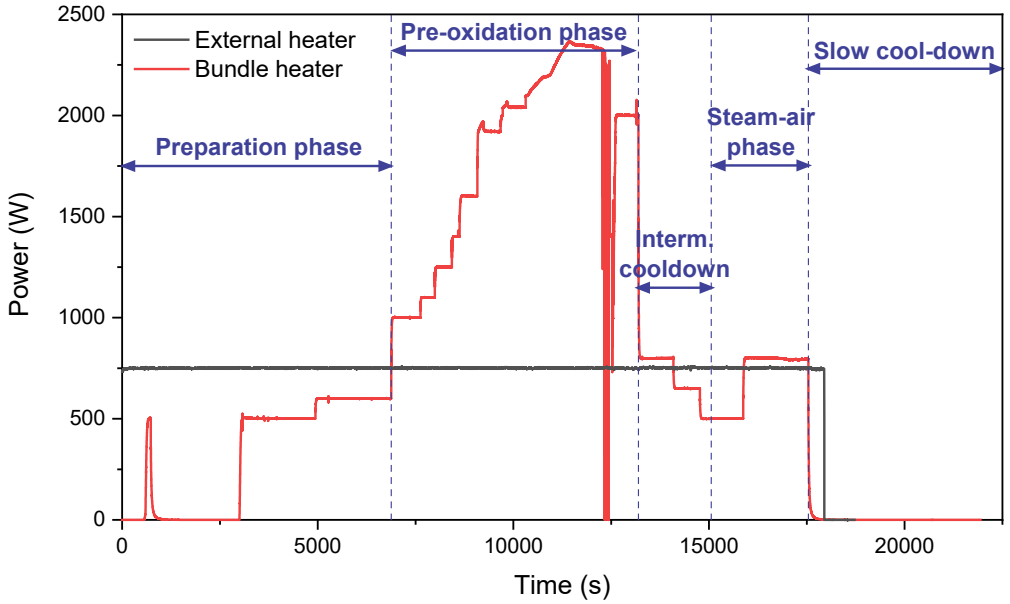

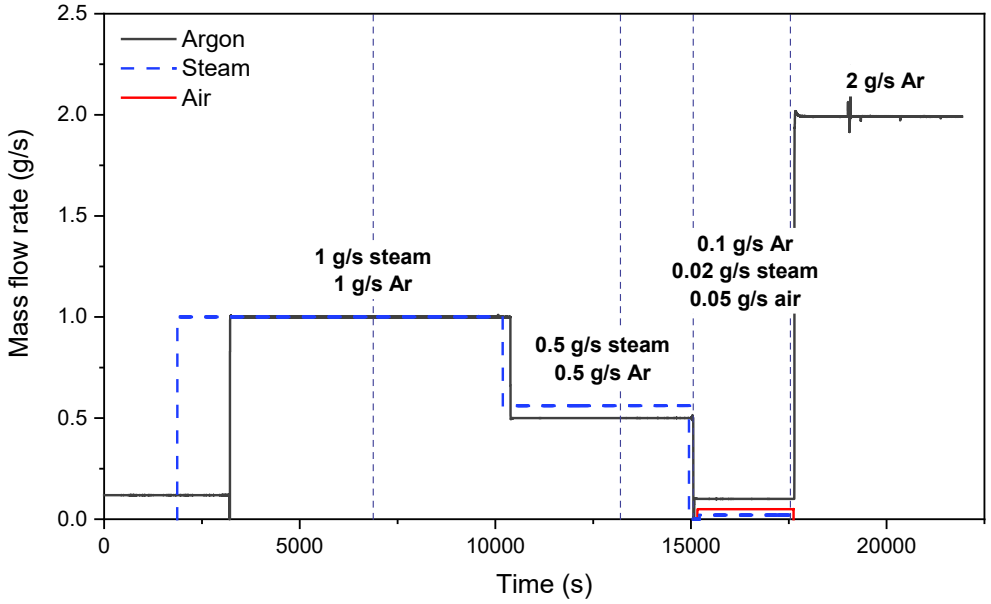

CODEX-ATF-AIT

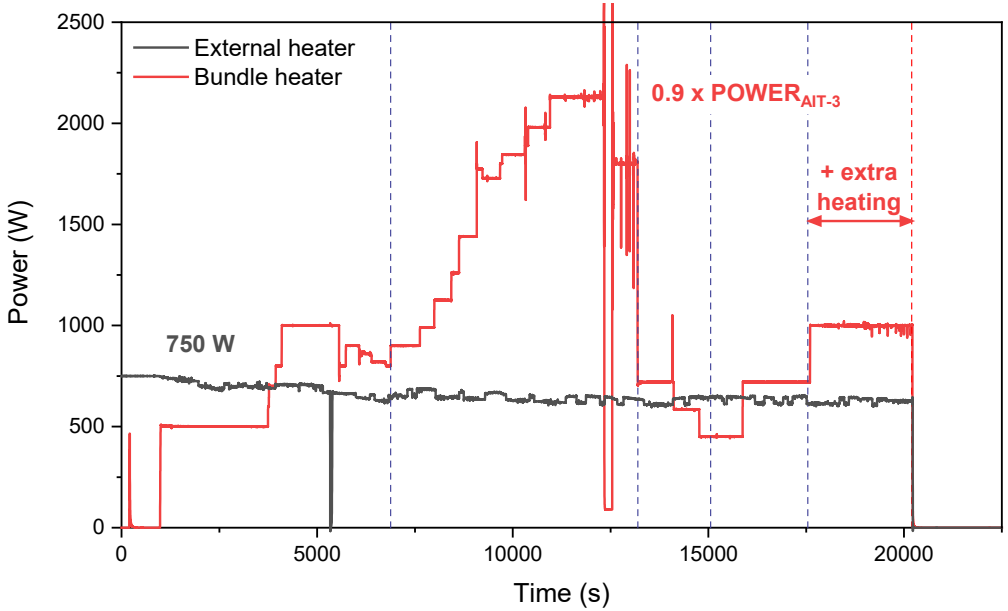

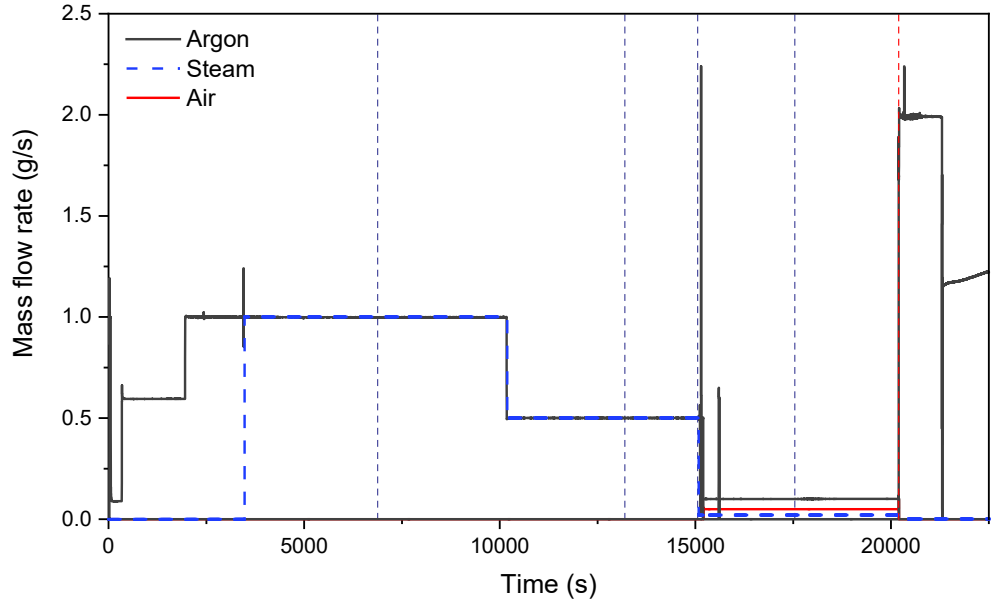

CODEX-ATF-AIT results – Temperatures

CODEX-AIT-3

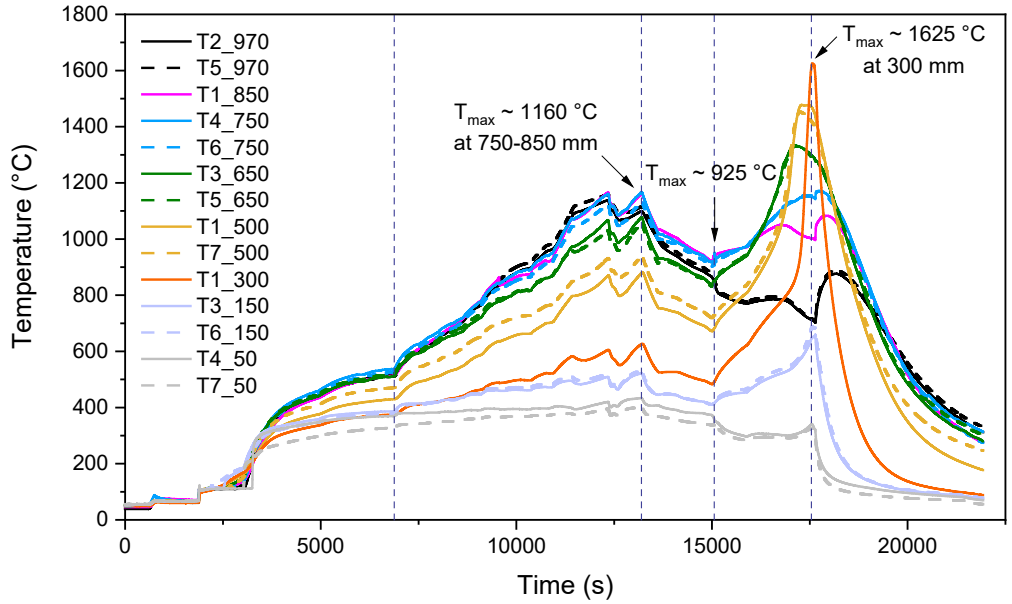

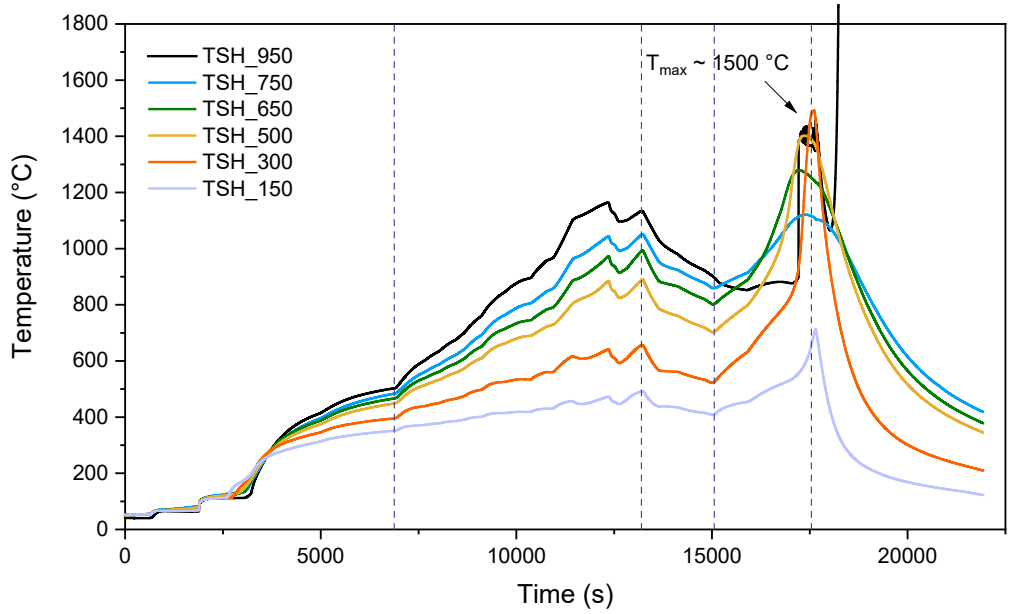

CODEX-ATF-AIT

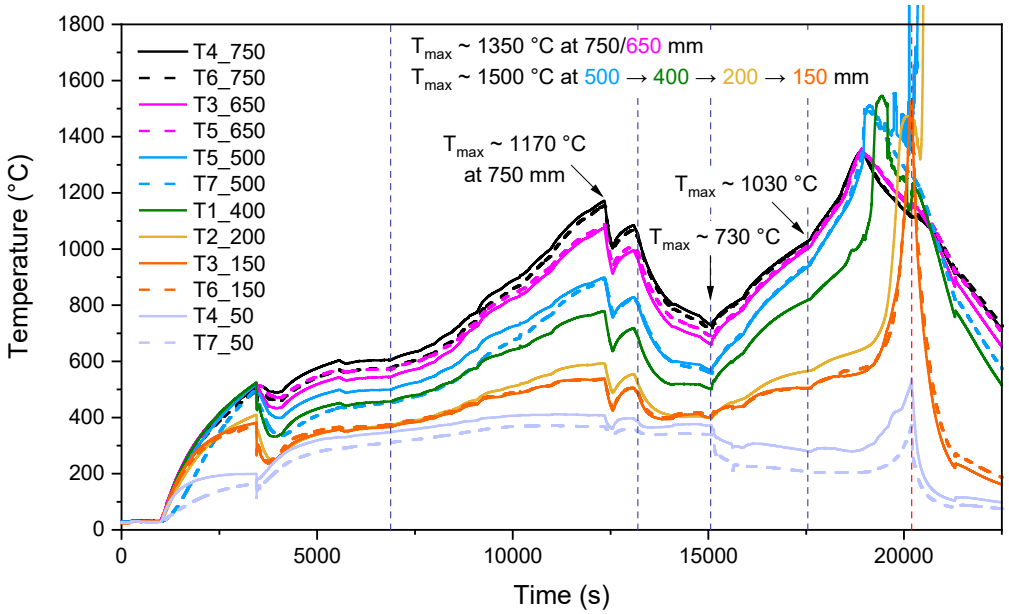

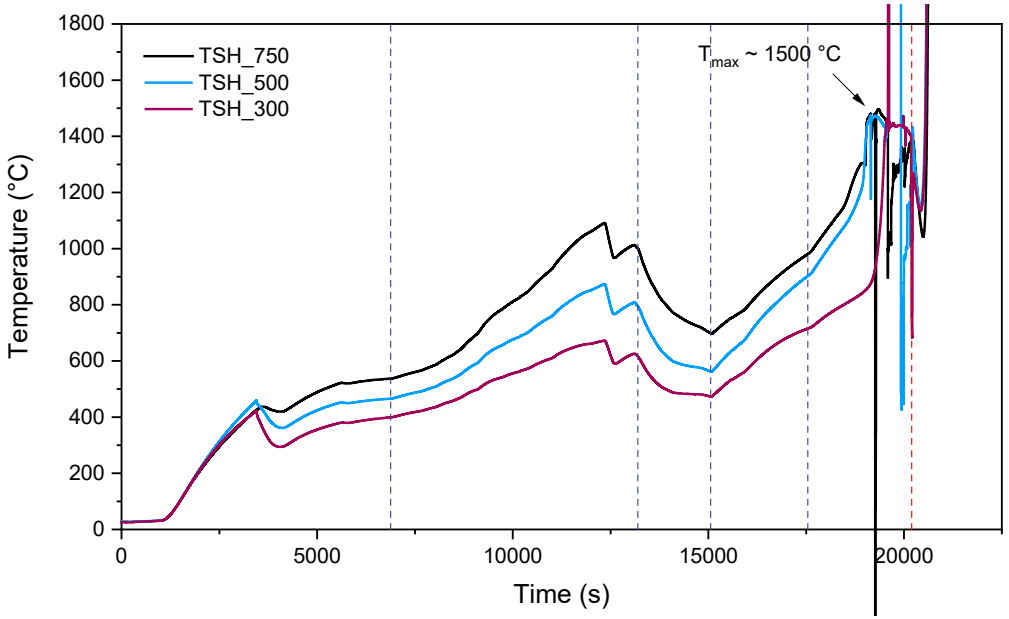

CODEX-ATF-AIT results – Temperatures

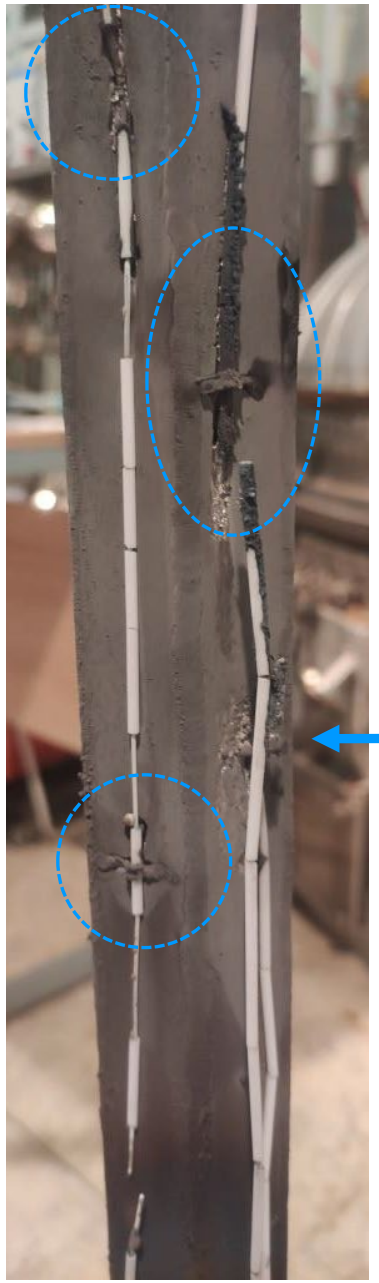

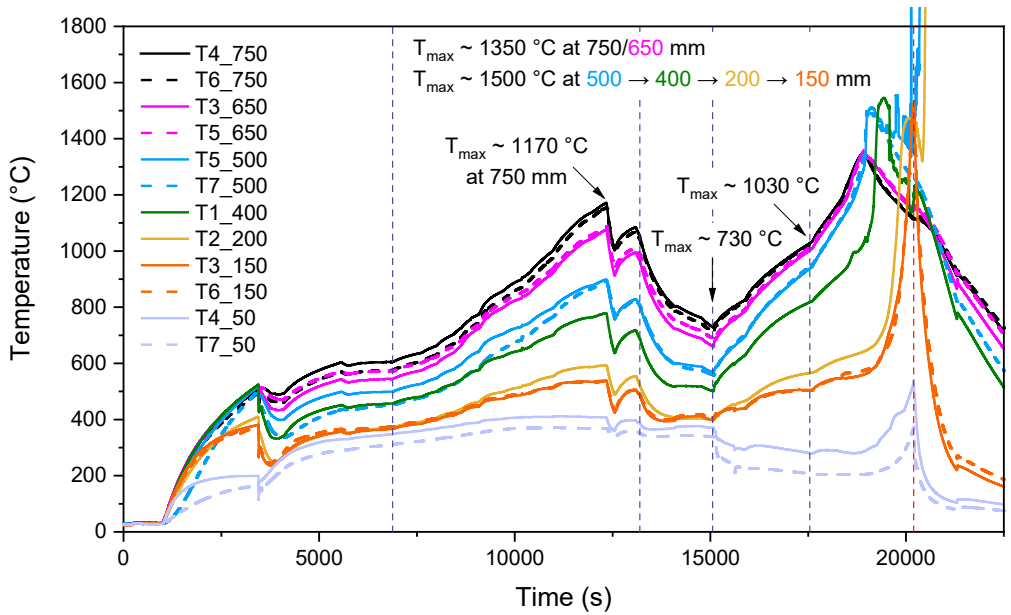

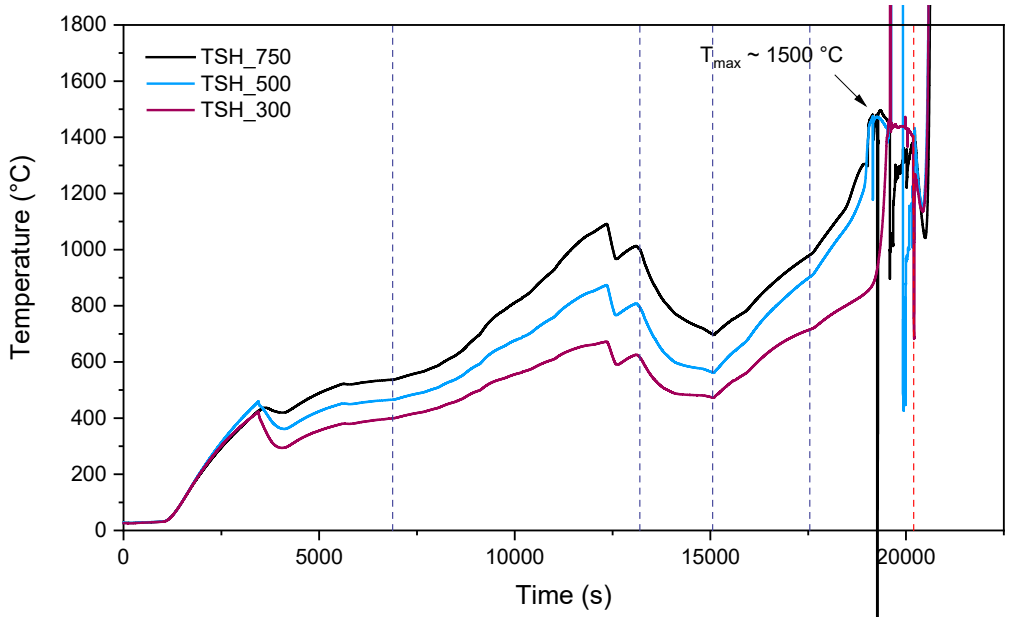

CODEX-ATF-AIT results – Pressures

CODEX-AIT-3

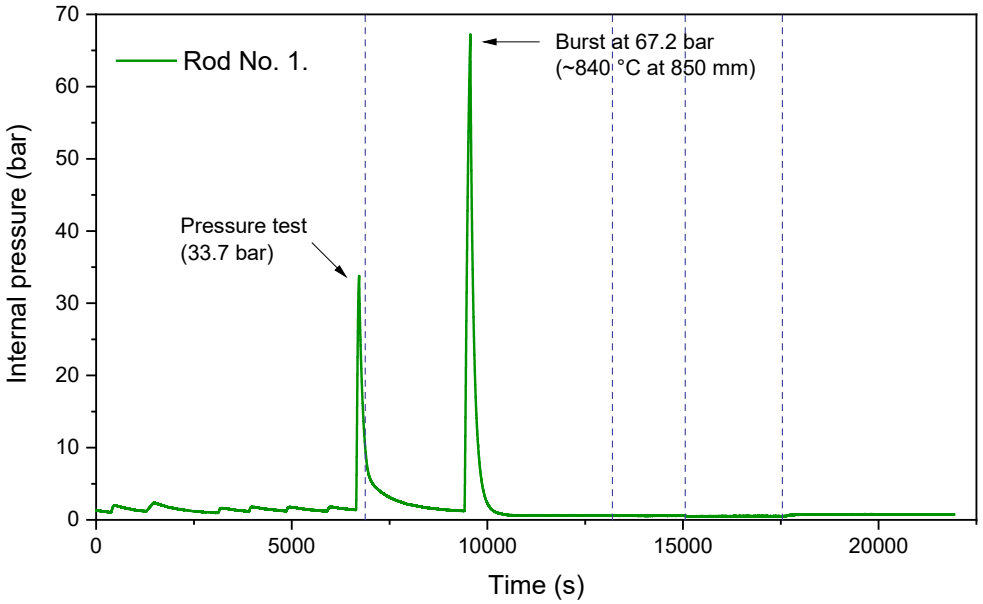

CODEX-ATF-AIT

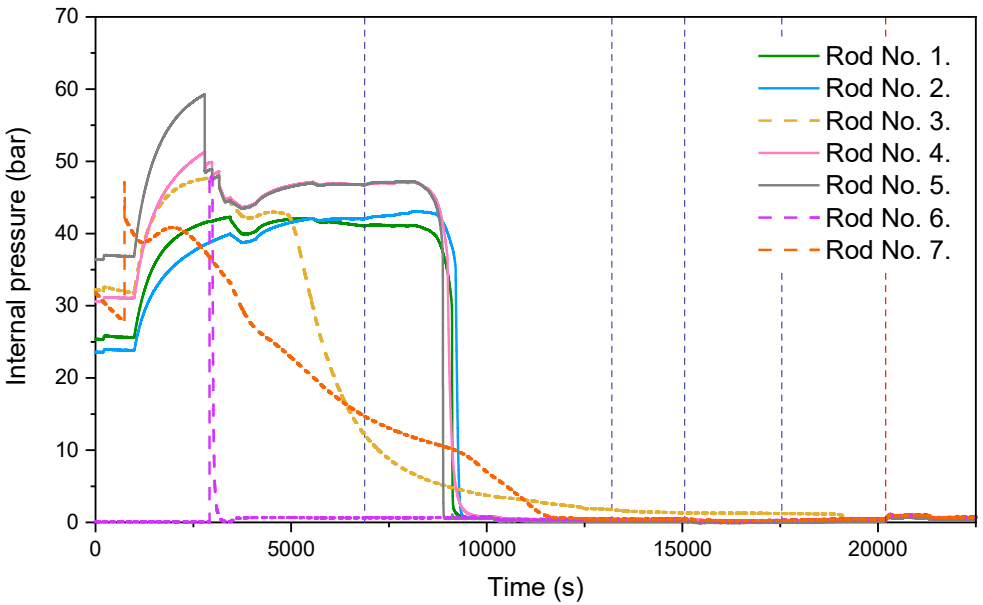

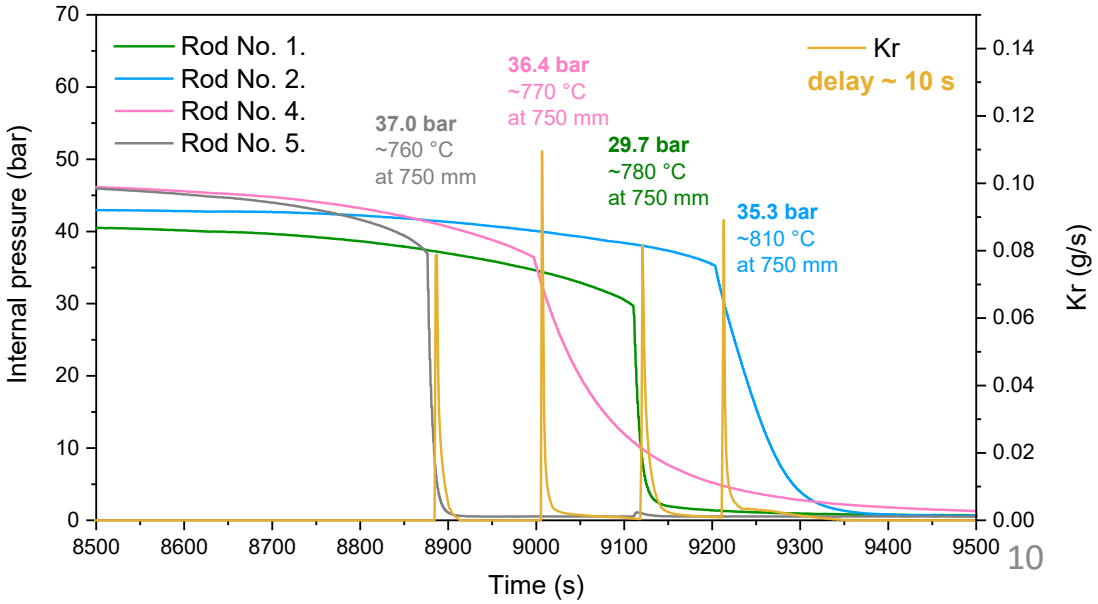

CODEX-ATF-AIT results – Pressures

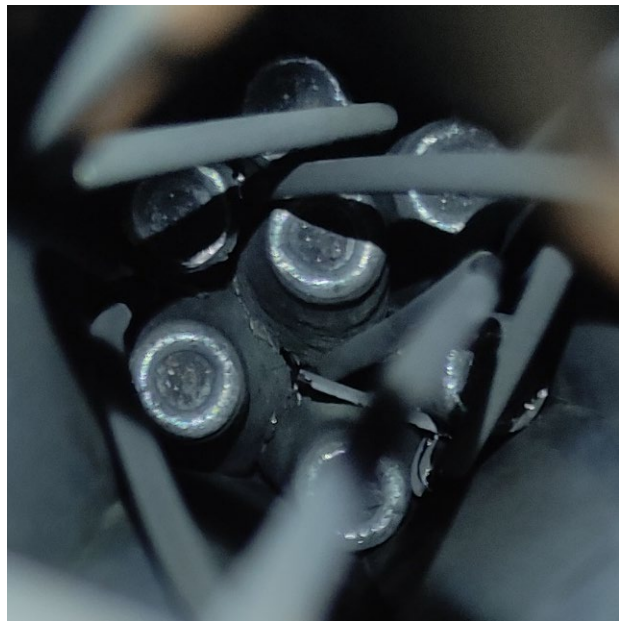

Top view of the CODEX-ATF-AIT bundle after experiment

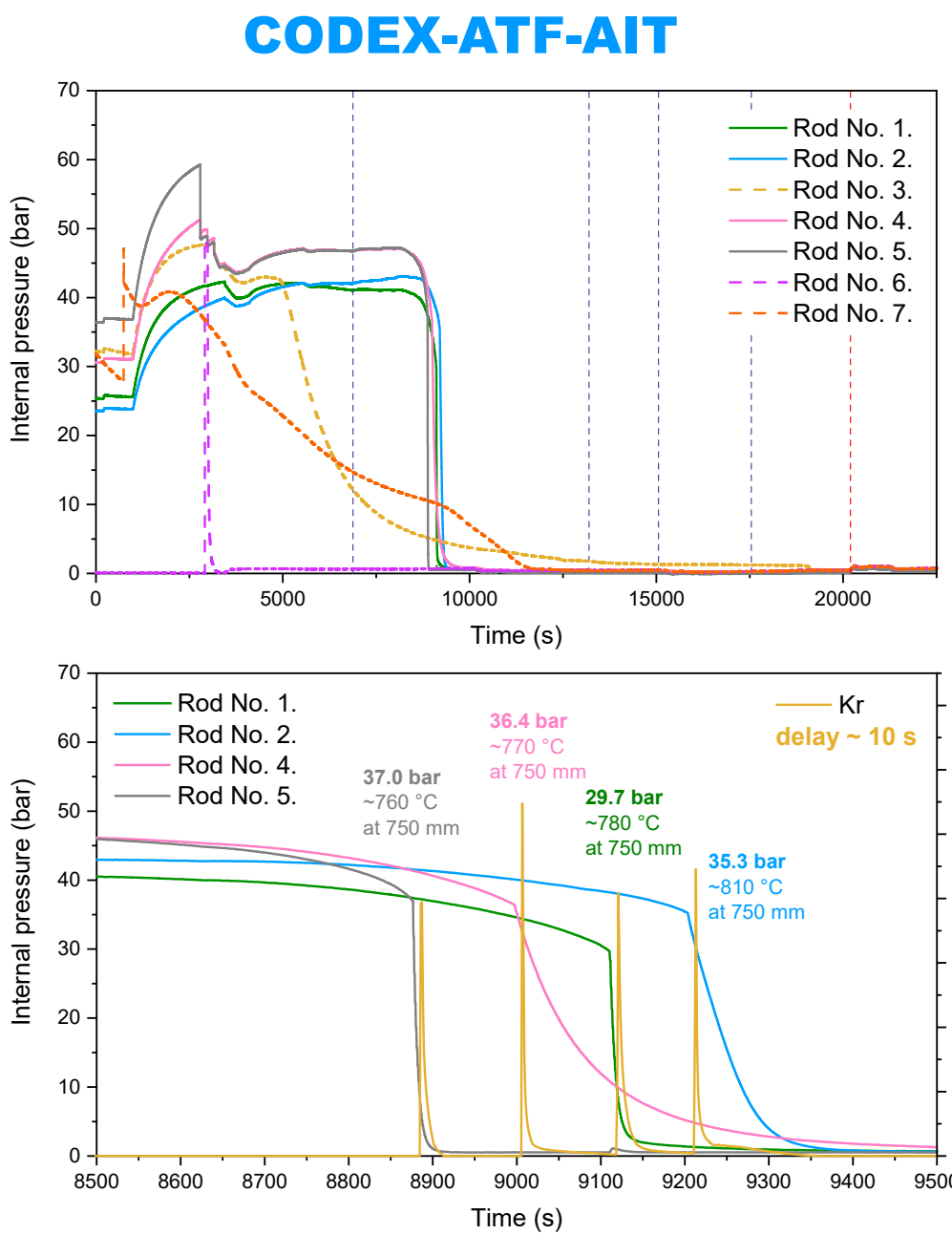

CODEX-ATF-AIT results – Outlet gas composition

CODEX-AIT-3

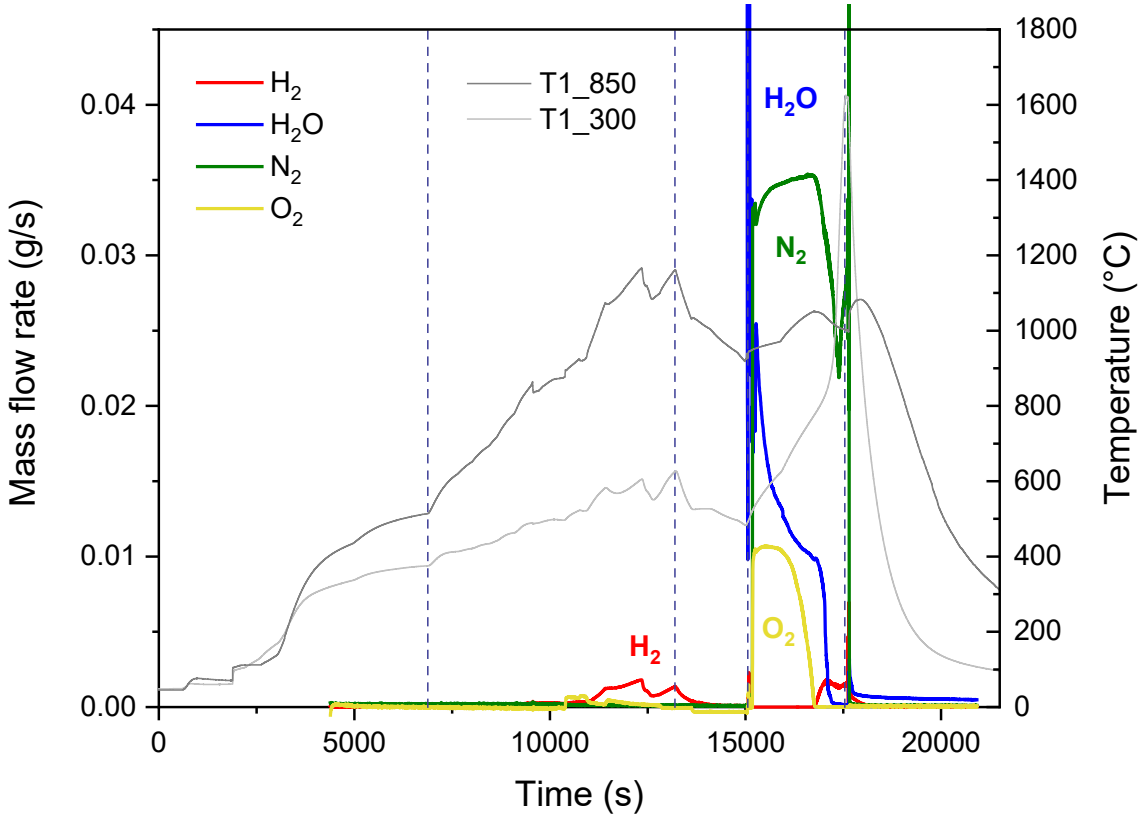

Total H_2 generation:

- Pre-oxidation phase: ~ 3.8 g
- Air-ingress phase: ~ 1.4 g

CODEX-ATF-AIT

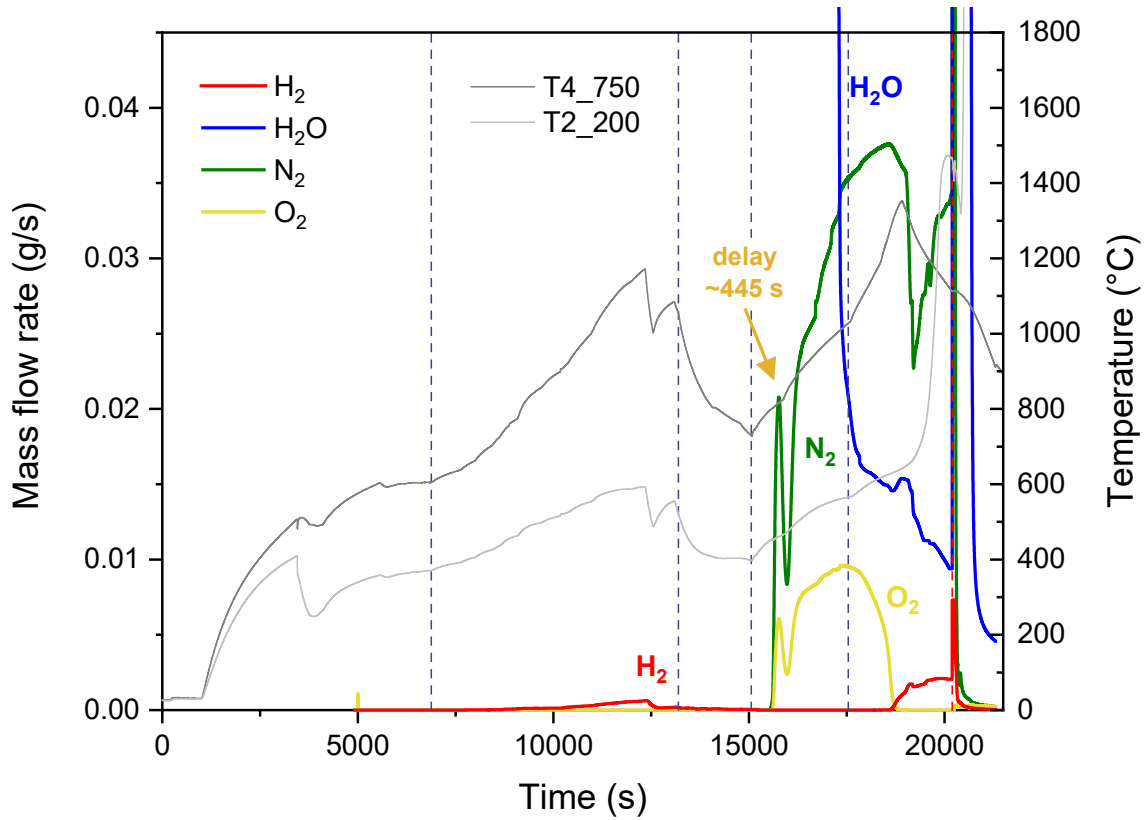

Total H_2 generation:

- Pre-oxidation phase: ~ 1.4 g
- Air-ingress phase: -
- Extra air-ingress phase: ~ 3.3 g

Images of the bundle (endoscopic)

Top of the bundle

Conclusions

- The comparison of results from the CODEX-AIT-3 and CODEX-ATF-AIT tests suggests that ATF materials can increase the coping time in the event of air ingress type reactor accidents.

- The ATF cladding reacted significantly less with high-temperature steam below 1200 °C than traditional Zr cladding material.

- In the reference test, air ingress led to a temperature excursion, with cladding temperatures reaching 1625 °C within 40 minutes. Under the same conditions in the CODEX-ATF-AIT test, the cladding temperature increased only to 1030 °C over the same period.

Further actions and schedule

- Release of experimental data report with on-line measurements

Mid-term report
31.12.2024

- Post-test examination of the bundle, and release of final report with post-test data

Final report
31.03.2025

Post-test examination results

CODEX-AIT-3

No. 1. at 350 mm

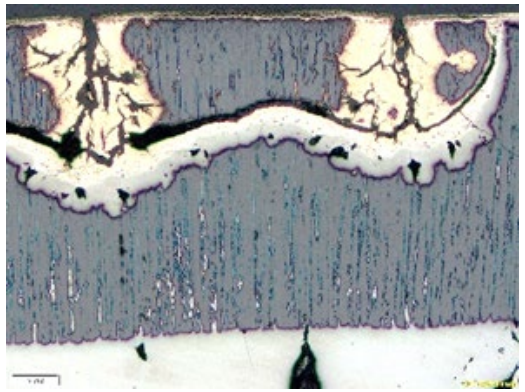

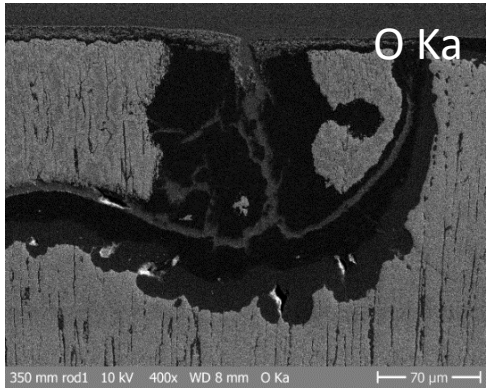

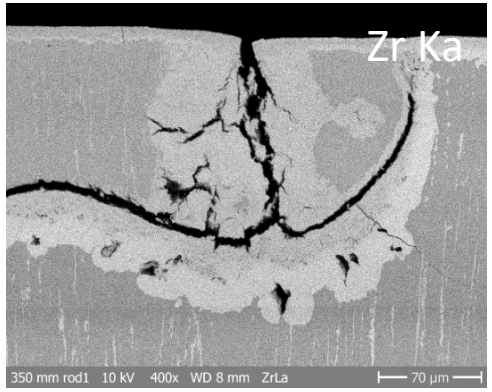

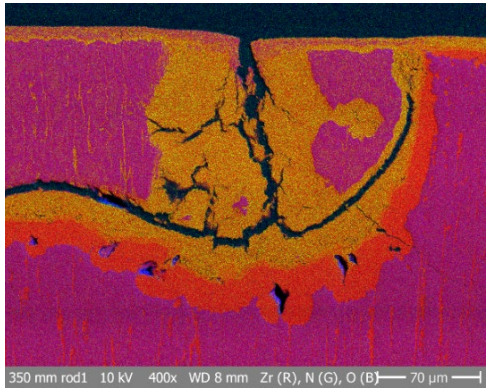

CODEX-ATF

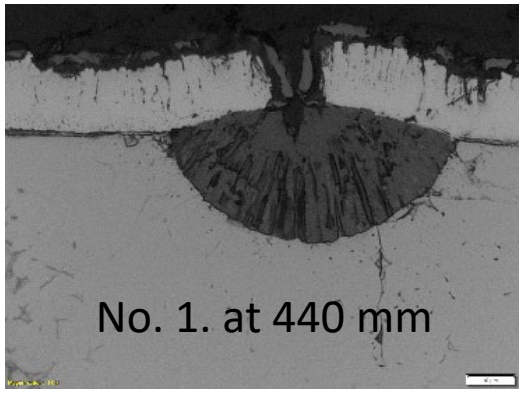

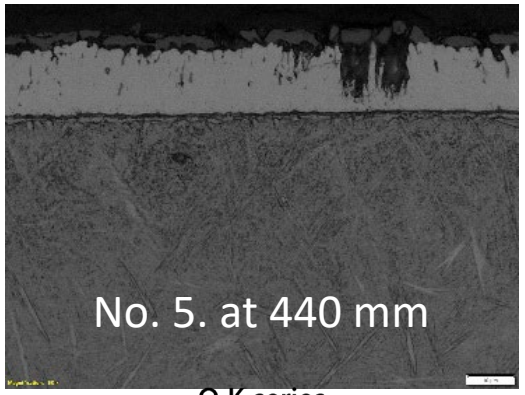

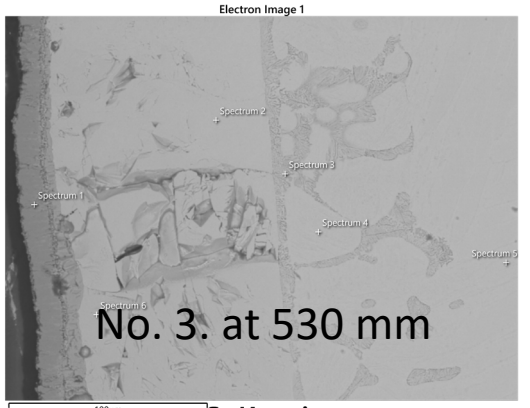

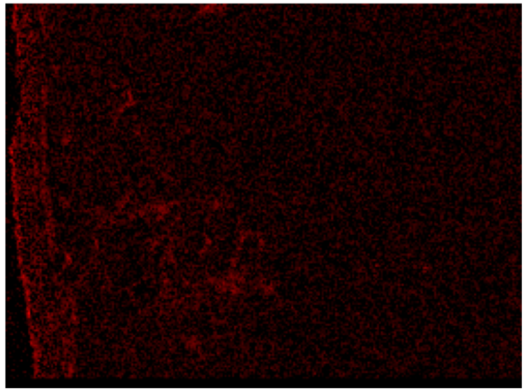

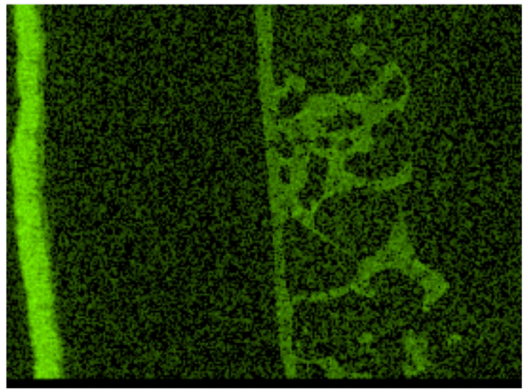

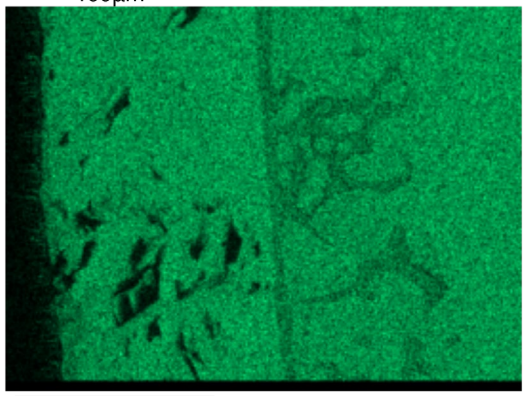

HUN REN | Centre for Energy Research

Thank you for your attention!

The CODEX-ATF-AIT experiment was supported by OFFERR.

Juri Stuckert

KIT

High-temperature single-rod tests on oxidation of Cr coated claddings, performed at KIT in the framework of the IAEA project ATF-TS

22 single rod oxidation tests with Cr coated zirconium alloy tubes were carried out within the framework of the IAEA project ATF-TS under DBA and BDBA transient conditions in an induction furnace. Eight M5® and four ZIRLO™ claddings PVD coated to 7 µm thick Cr layer, four E110 claddings with arc ion Cr plating to 8 µm thick Cr layer, six opt. ZIRLO™ claddings PVD coated to 5, 18 µm thick Cr layer and 18+8 µm thick Cr+CrN layer were tested.

The tests performed with ZIRLO claddings coated to 7 µm Cr layer showed that for Tmax<1300 °C, only small oxidation of Cr layer with low hydrogen release (factor 15 in comparison to not coated claddings) occurred. For higher temperatures, formation of numerous local swellings at the outer cladding surface due to Zr-Cr eutectic at 1350 °C occurred and significant hydrogen release due to oxidation of Zr substrate was measured.

The tests performed with E110 claddings coated to 8 µm Cr layer showed significant decrease of hydrogen release under extended LOCA conditions (max 1250 °C) in comparison to not coated samples (factor 15). For peak cladding temperature of 1350 °C, numerous local swellings at the outer cladding surface formed and intensive hydrogen release (factor 18 in comparison to 1250 °C) was measured.

The tests performed with opt. ZIRLO claddings coated to three different layer thicknesses showed that an increase in the thickness of the Cr layer by 3 times (from 6 to 18 µm) reduced the hydrogen release by 30% under DBA conditions (transient to 1200 °C), however, only by 3% under BDBA conditions (1400 °C). Barrier layer CrN has only moderate influence on hydrogen release under DBA, but strong reduced hydrogen release under BDBA (reduction factor 4). A local temperature escalation and formation and relocation of (Zr,Cr)+Zr melt for Cr/CrN coating occurred perhaps due to the lack of intermediate oxidation of part of the zirconium substrate, which could not react with steam due to the barrier effect of CrN layer.

Karlsruhe Institute of Technology

IAM
Institute for Applied Materials

HT single rod tests on oxidation of Cr coated claddings

J. Stuckert, U. Peters, U. Stegmaier, E. Vogel, K. Vizelkova

29th QWS

Institute for Applied Materials; Program NUSAFE

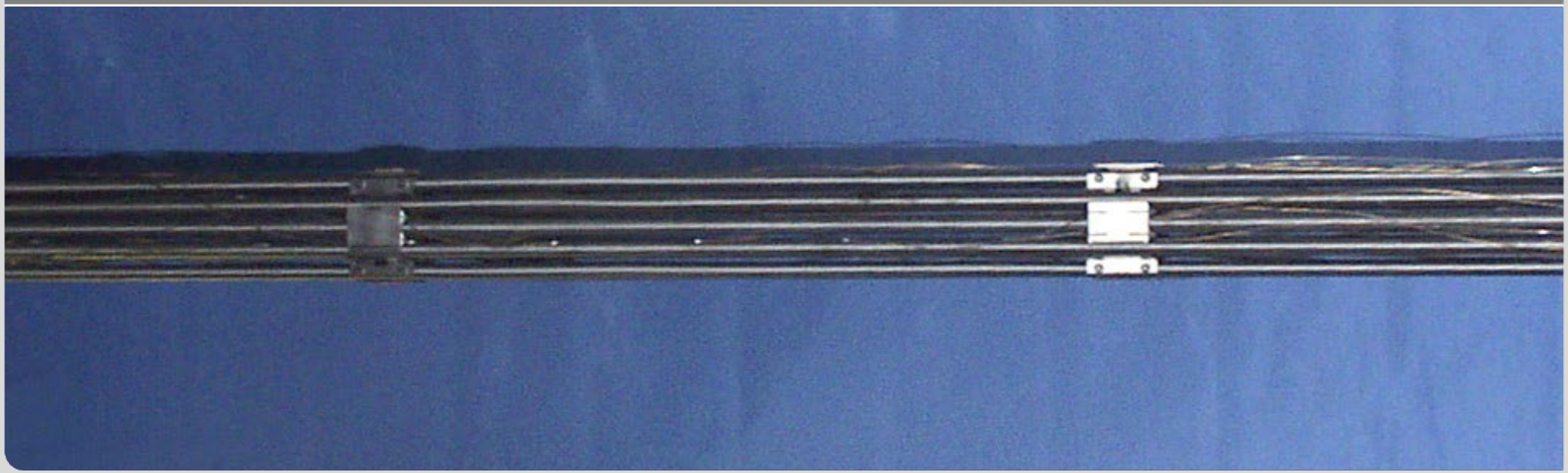

Three sets of HT oxidation tests

I. ZIRLO and M5® tubes, PVD coated by Oerlikon/Balzers GmbH with Cr to the layer thickness of 7 µm.

II. ZIRLO tubes, PVD coated by UPM/Prague with Cr to the layer thicknesses of 5 and 18 µm as well as with Cr/CrN to the layer thickness 18/8 µm (Cr/CrN.

III. E110 tubes, treated by AEOI with arc ion coated method to the Cr layer thickness of 8 µm.

Transient tests in inductive furnace: cladding oxidation in steam

mass spectrometer

H_2+Ar + steam

Ar (30 l/h) + steam (100 g/h)

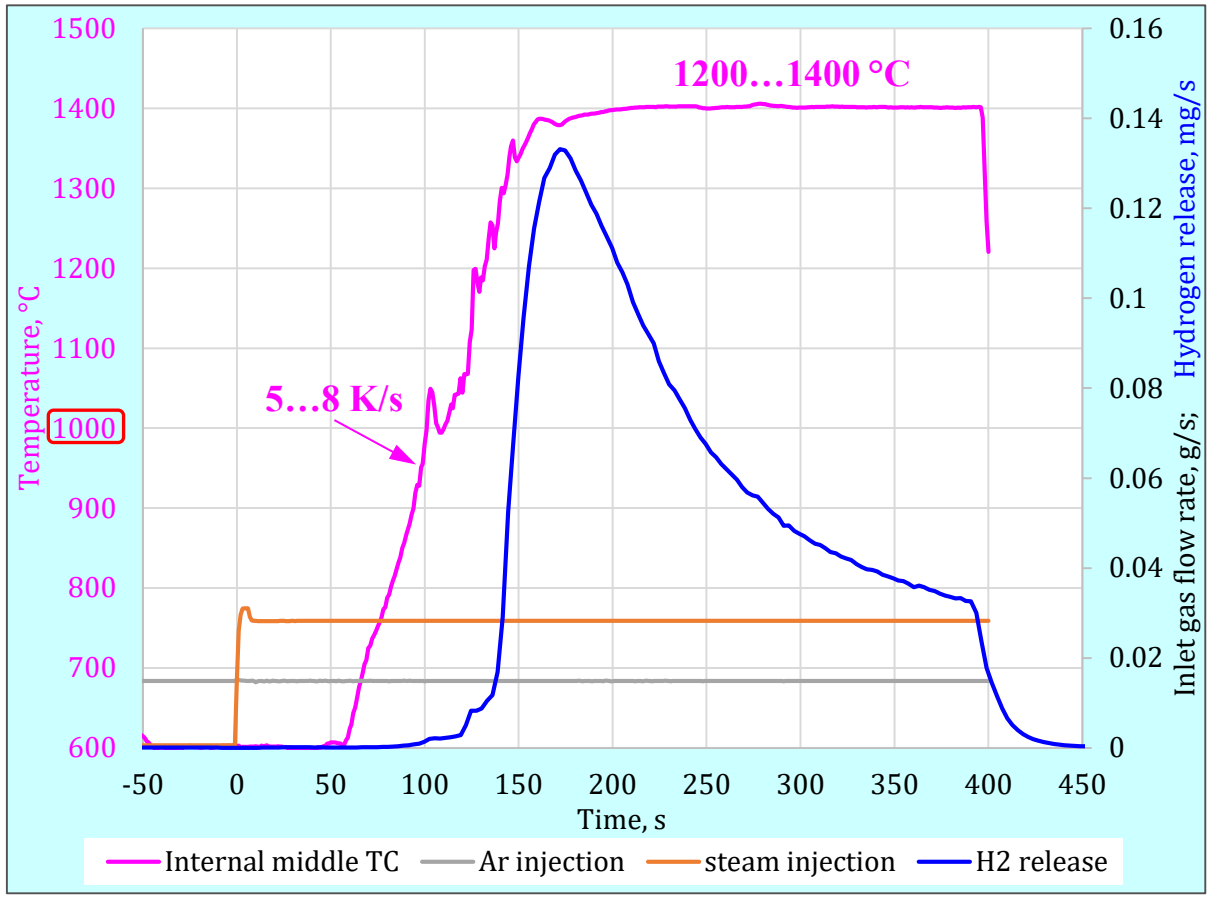

Instrumentation: 1) TC inside the sample; 2) TC at the sample surface; 3) pyrometer; 4) mass spectrometer at furnace outlet

Control of generator according to internal TC or pyrometer; oscillations above 1000 °C

Tests with 12 KIT samples coated by OERLIKON to 7 µm Cr

MC tubes: OD=10.75 mm, wall 725 µm; MCs and ZOs tubes: OD=9.5 mm, wall 570 µm

Sample	Heating rate [K/s]	Maximal clad temperature T_{max} [°C]	Duration of oxidation at T_{max} [min]	Cooldown	Comment
MC-4	7	1200	10	steam + Ar	performed
MC-5	7	1200	15	steam + Ar	performed
MC-6	8	1300	5	steam + Ar	performed
MC-7	6	1250	10	steam + Ar	performed
MCs-2	8	1360	6	steam + Ar	performed
MCs-3	8	1360	0	steam + Ar	performed
MCs-4	5	1250	6 (1250°→900°)	**water**	performed
MCs-5	5	1250	0	steam + Ar	performed
ZOs-2	5	1200	4	steam + Ar	performed
ZOs-3	5	1380	0	steam + Ar	performed
ZOs-4	5	1200	4	steam + Ar	performed
ZOs-5	5	1400	4	steam + Ar	performed

MC – for coated M5®
ZO – for coated ZIRLO™

Appearance of coated cladding samples oxidized in inductive furnace

MC-4: 1200 °C
during 10 min

MC-5: 1200 °C
during 15 min

MC-7: 1250 °C
during 10 min

MC-6: 1350 °C
during 5 min

Cladding microstructure after heating with 7 K/s and oxidation at 1200 °C

MC-4: 1200 °C during 10 min after heating

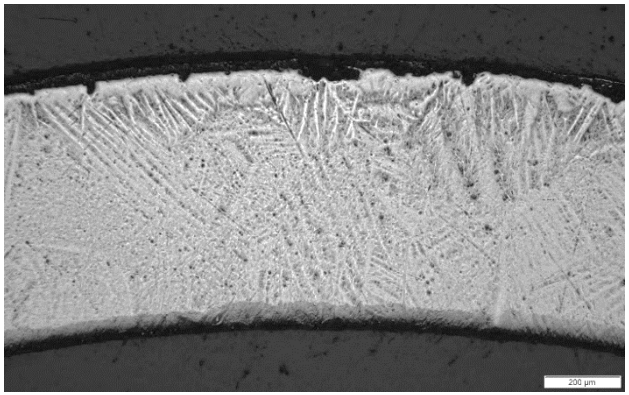

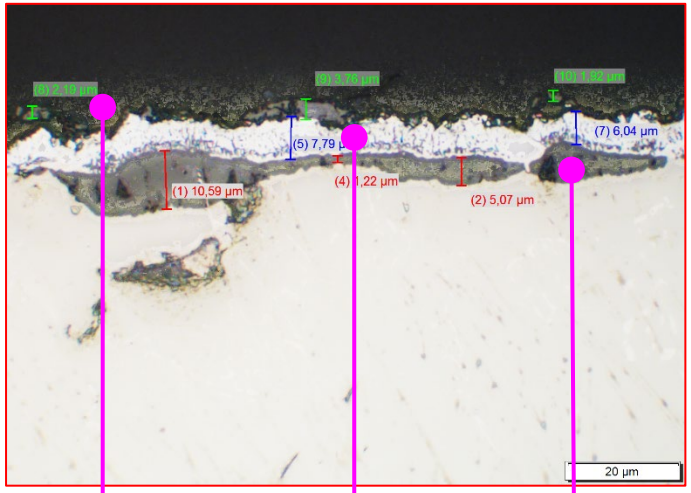

Cr_2O_3: 5µm

Cr: 5…8 µm

ZrO_2: 2…25 µm

MC-5: 1200 °C during 15 min after heating

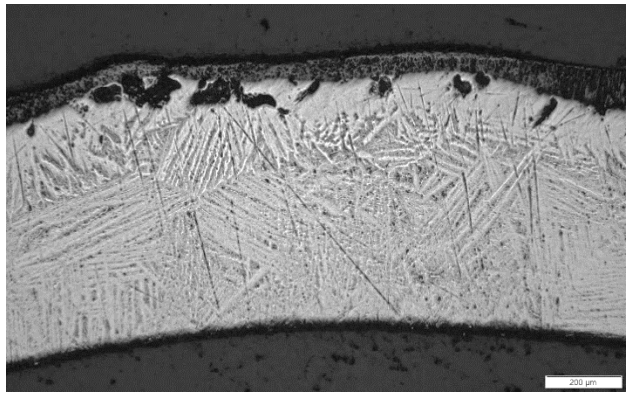

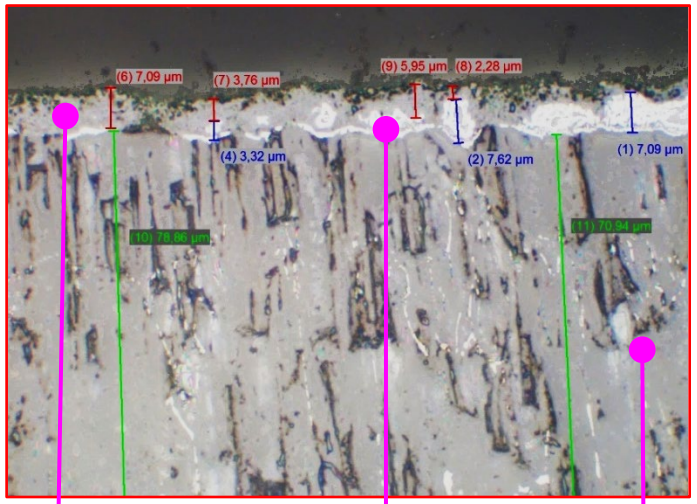

Cr_2O_3: 3…7 µm

Cr: 0…7 µm

ZrO_2: 75 µm

Influence of coating on hydrogen release (LOCA transient 5 K/s from 600 to1250 °C, then cooldown to 900 °C and quenching)

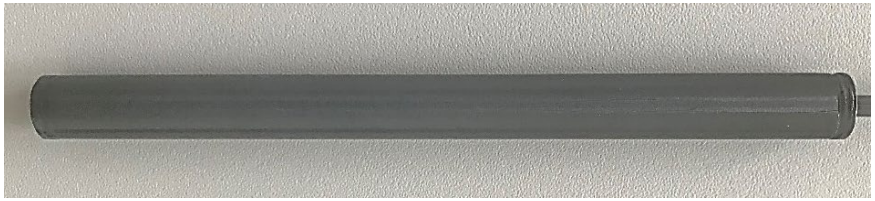

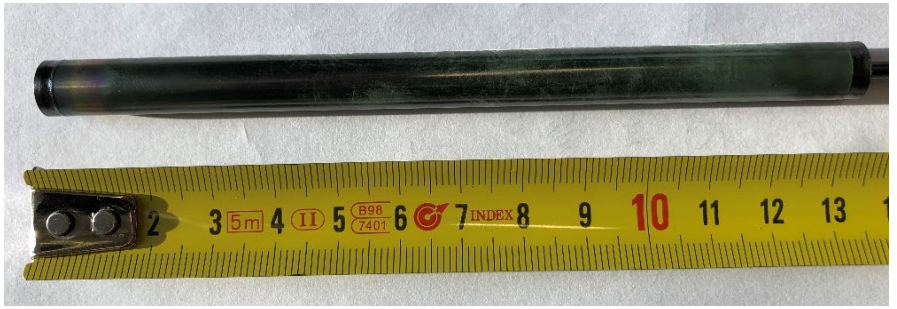

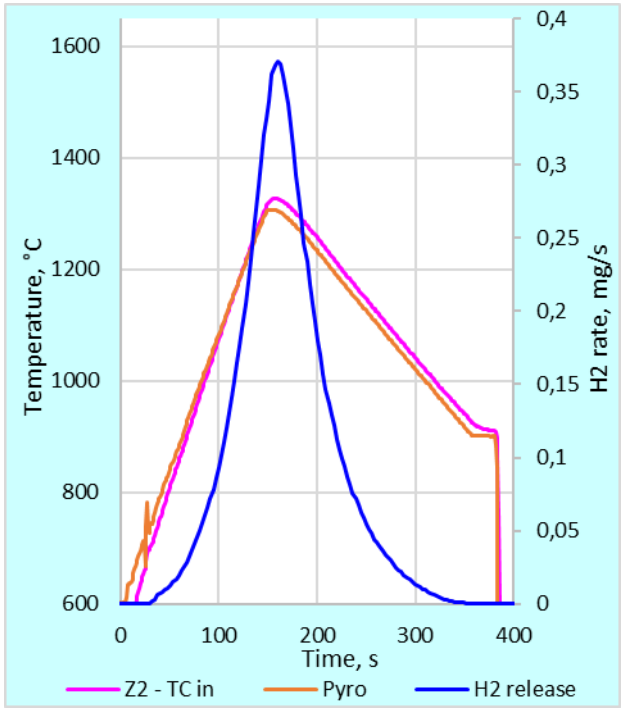

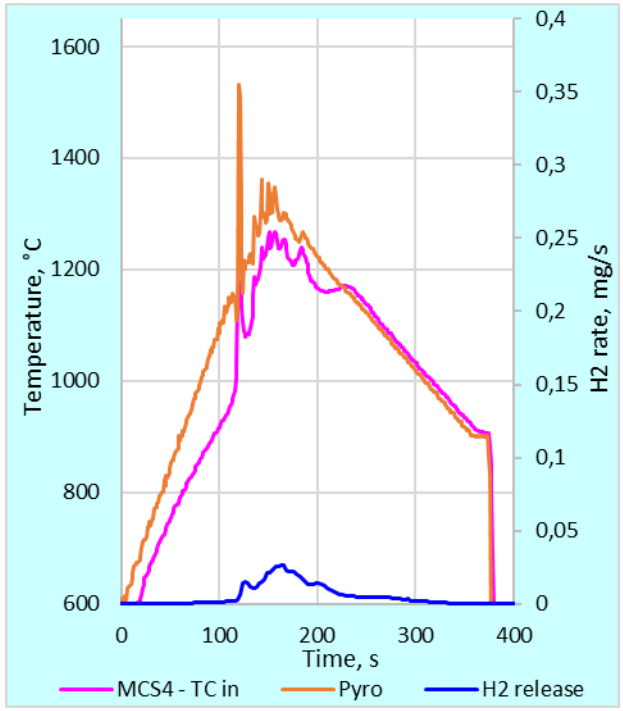

not coated sample Z2 (Zry-4): significant hydrogen release

coated sample MCs-4 (M5®): strong reduced hydrogen release (factor 15)

LOCA transient followed by a constant temperature of 1400 °C: influence of duration of oxidation in steam

sample MCs-3: transient with 8 K/s, then 1400 °C during 3 s

sample MCs-2: transient with 8 K/s, then 1400 °C during 240 s

Binary Zr-Cr phase diagram

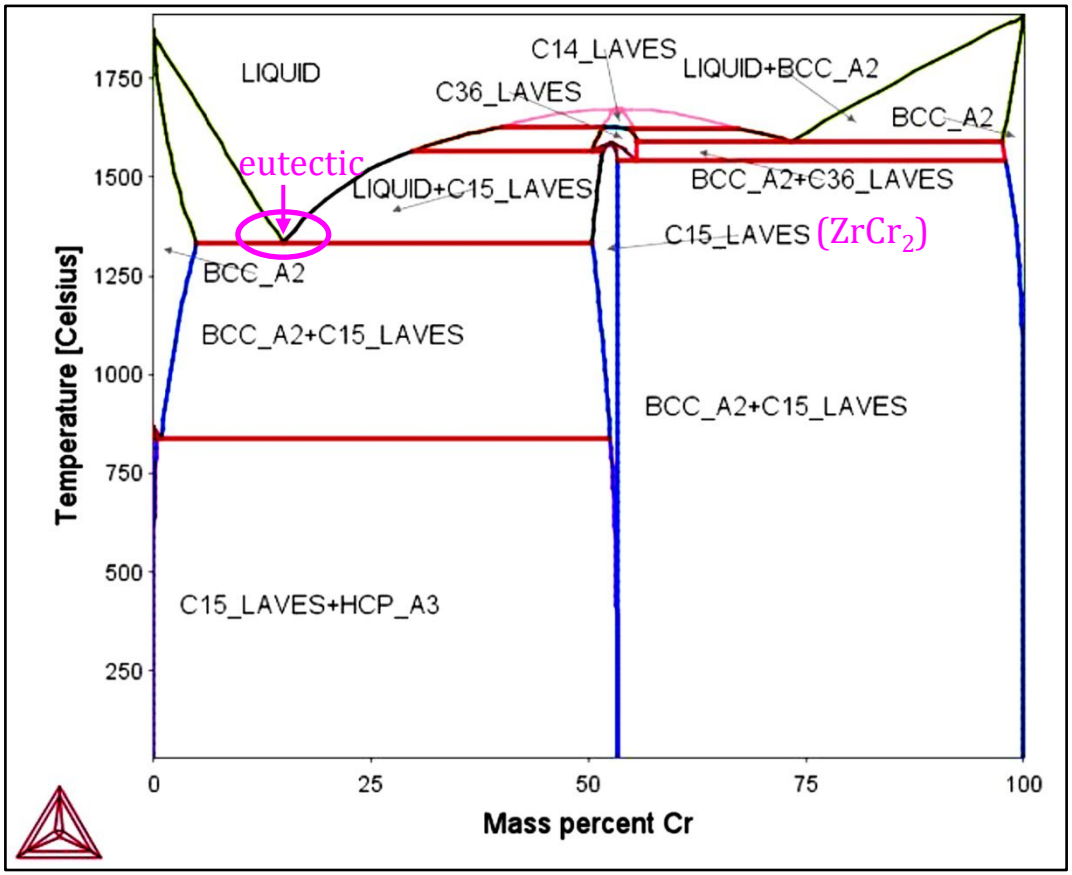

The eutectic Zr/Cr forms at ≈1330 °C

Result of SEM/EDX analysis of MCs3 sample: cladding microstructure immediately after LOCA transient from 600 to 1400 °C: formation of surface swellings containing Laves phase $ZrCr_2$

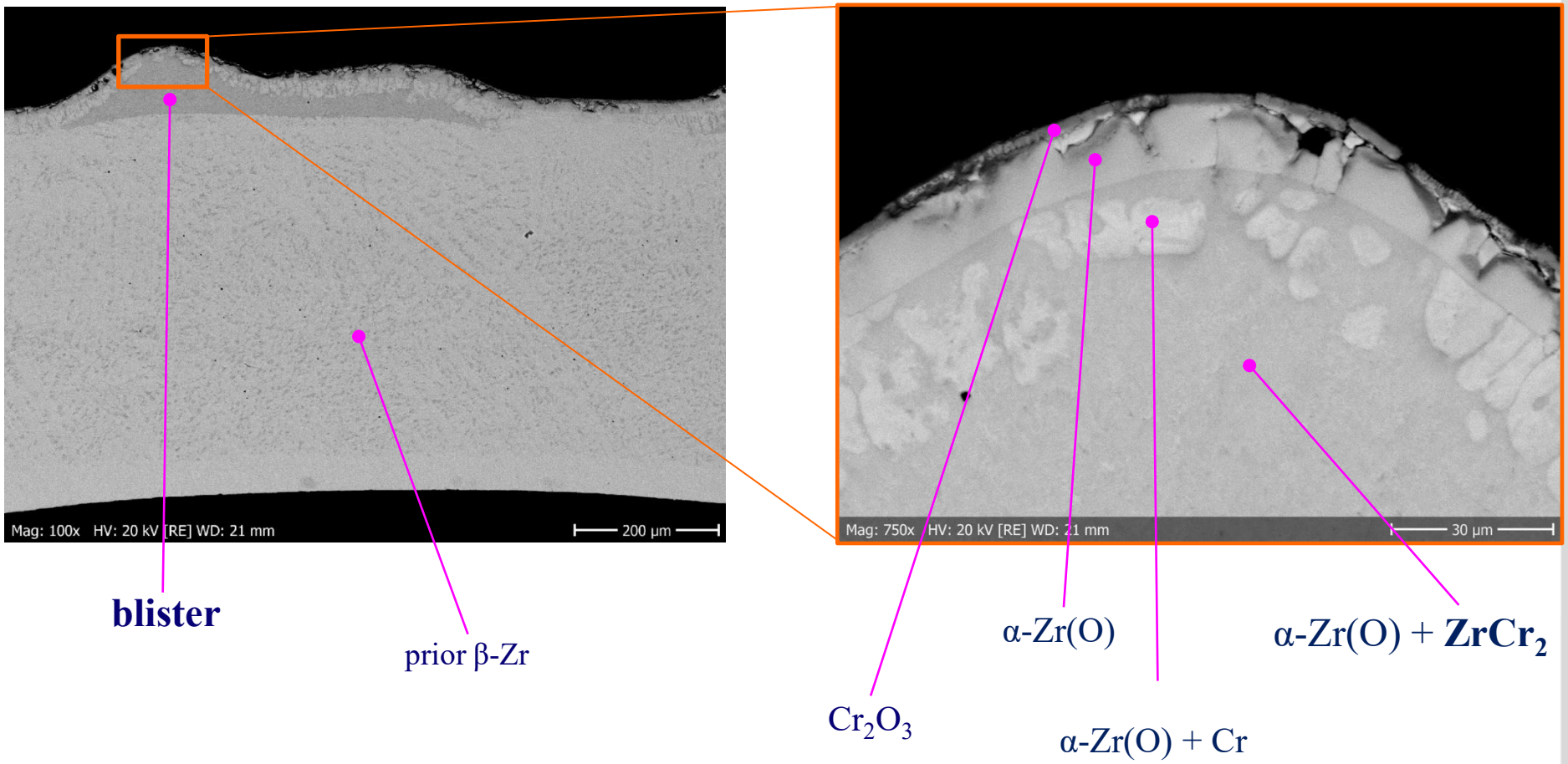

No influence of Zr alloy (as substrate) on hydrogen release for coated samples tested under similar high temperature conditions

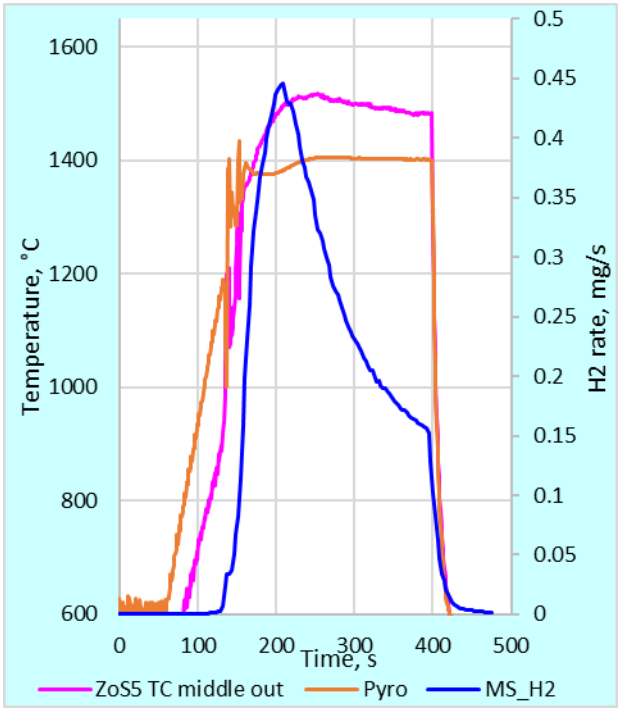

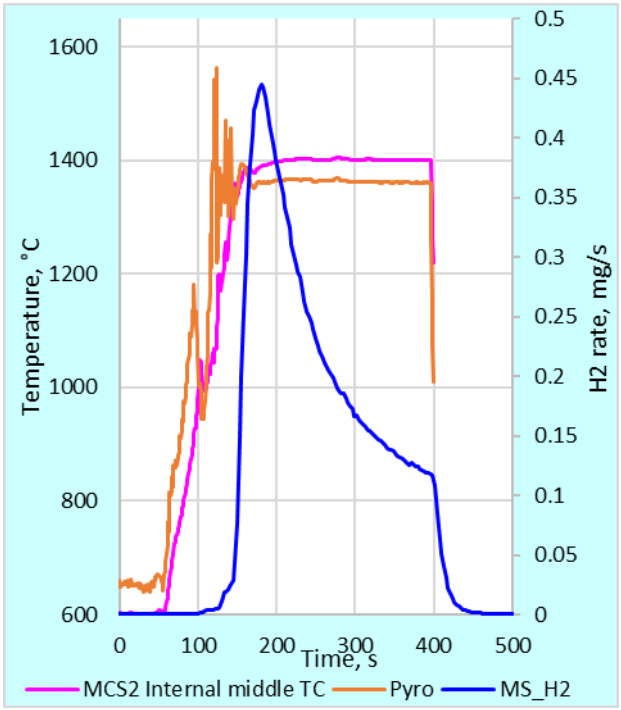

sample ZOs5 (ZIRLO™)

sample MCs2 (M5®)

Influence of peak cladding temperature on hydrogen release

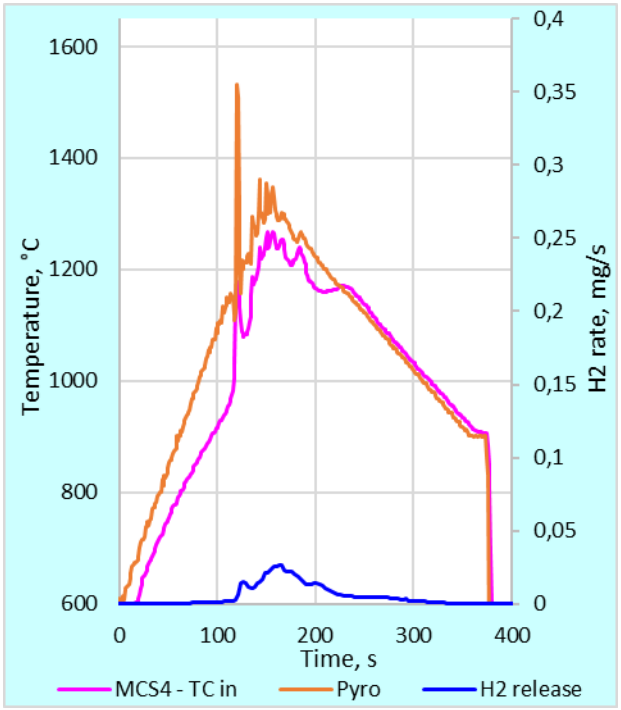

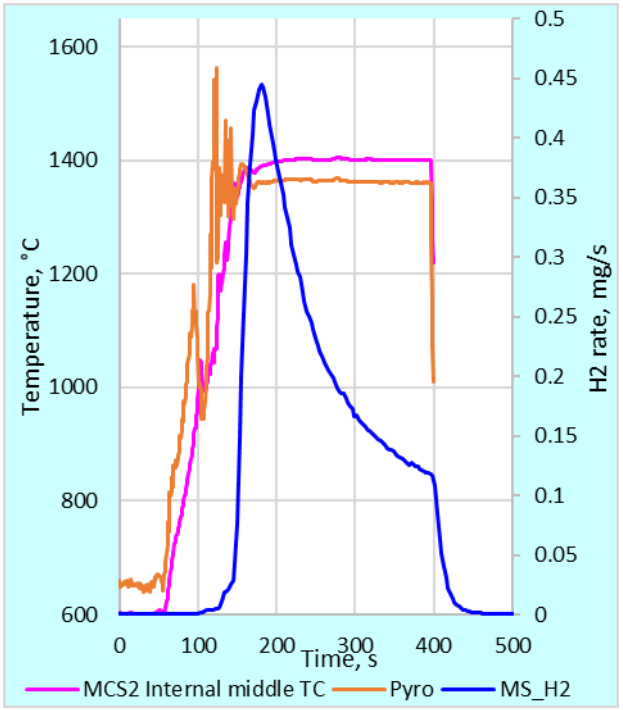

Cr coated sample MCs-4 oxidized with T_{max}=1250 °C (***only oxidation of Cr layer***)

Cr coated sample MCs-2 oxidized with T_{max}=1400 °C: factor 20 for H_2 (***additional oxidation of Zr substrate***)

Catastrophic oxidation and temperature escalation at T>1300 °C in tube furnace (without radiation heat loss)

sample MC-1: injection of oxygen at 1350°C

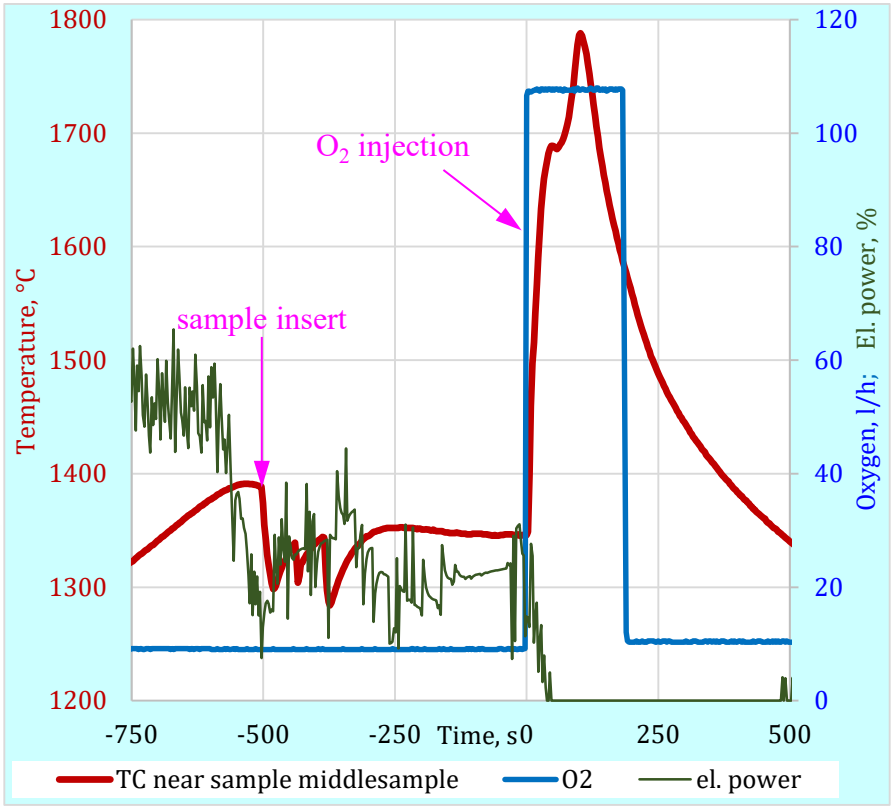

sample ZOs-1: temperature escalation in oxygen during slow transient

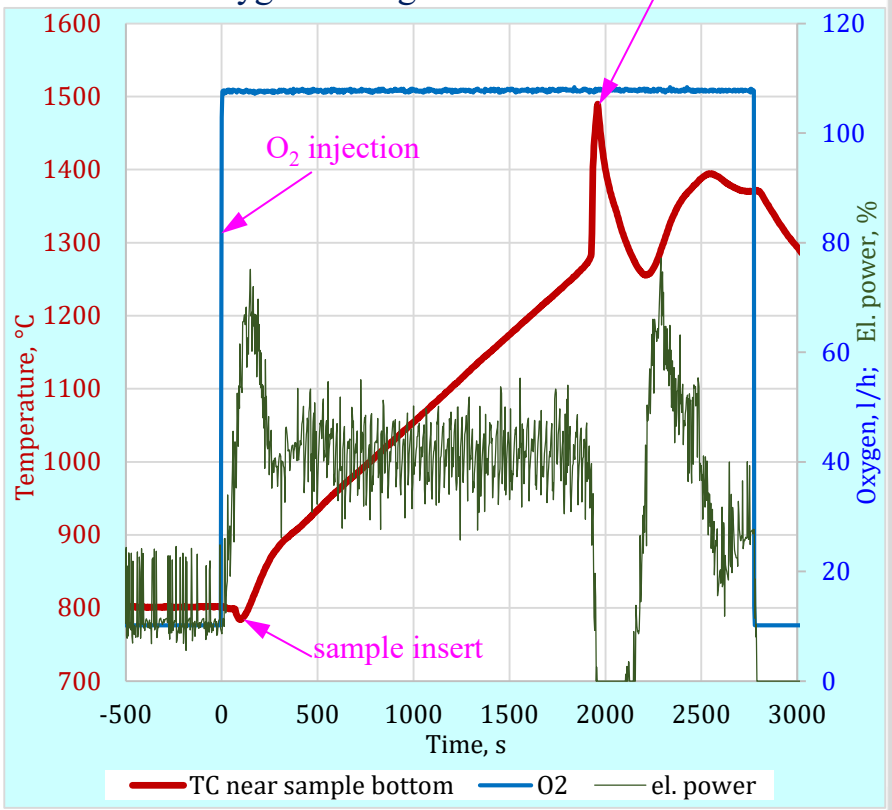

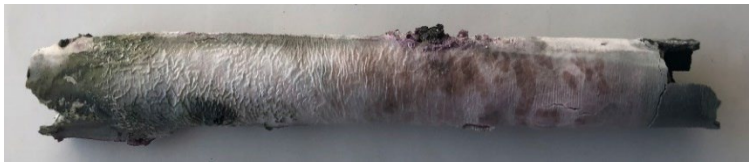

sample completely destroyed

Summary on KIT samples

➢ Inductive furnace:

1) for Tmax<1300 °C, only small oxidation of Cr layer with low hydrogen release (factor 15 in comparison to not coated claddings),

2) For higher temperatures, formation of numerous blisters (local swellings) at the outer cladding surface due to Zr-Cr eutectic at 1350 °C and significant hydrogen release due to oxidation of Zr substrate.

➢ Tube furnace: catastrophic oxidation at T>1300 °C due to the absence of radiation heat loss.

E110 sample with arc ion Cr plating (AEOI) with a layer thickness of 7…8 µm

capillary Zr tube (sample holder and pressure normalizer)

Zr plug

Zr alloy cladding coated by Cr; OD=9.14 mm ID=7.72 mm

Zr plug

coated empty sample welded at KIT and prepared for SETs

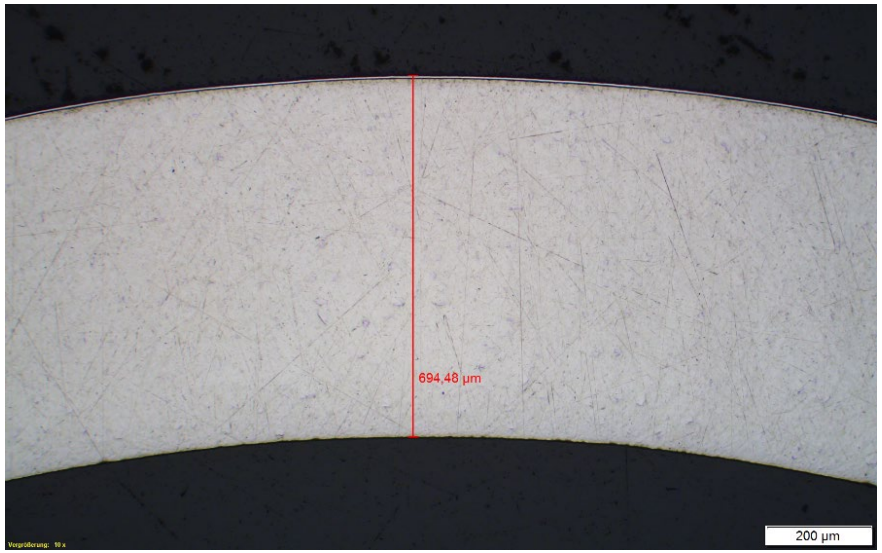

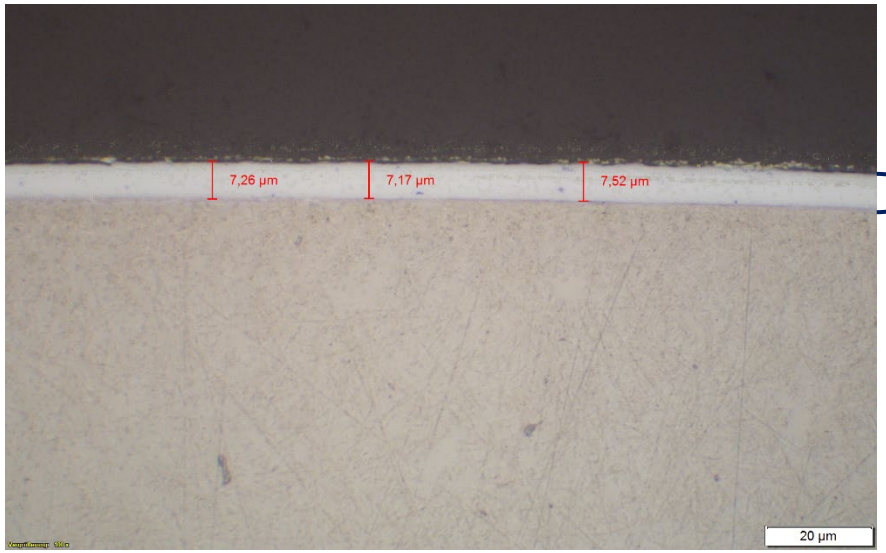

Cr layer

optical microscopy

Appearance of coated cladding samples oxidized by steam in inductive furnace

EC2: 5 K/s to T_{max}=**1250 °C**
cooldown 2 K/s, quench at 900 °C

EC4: 5 K/s to **1250 °C**,
5 s 1330 °C, imm. cooldown

EC1: 8 K/s to T_{max}=**1390 °C**,
immediate cooldown

EC3: 8 K/s to **T_{max}=1400 °C**,
240 s 1400 °C, imm. cooldown

EC4 (1250 °C, immediate cool-down), SEM/EDX

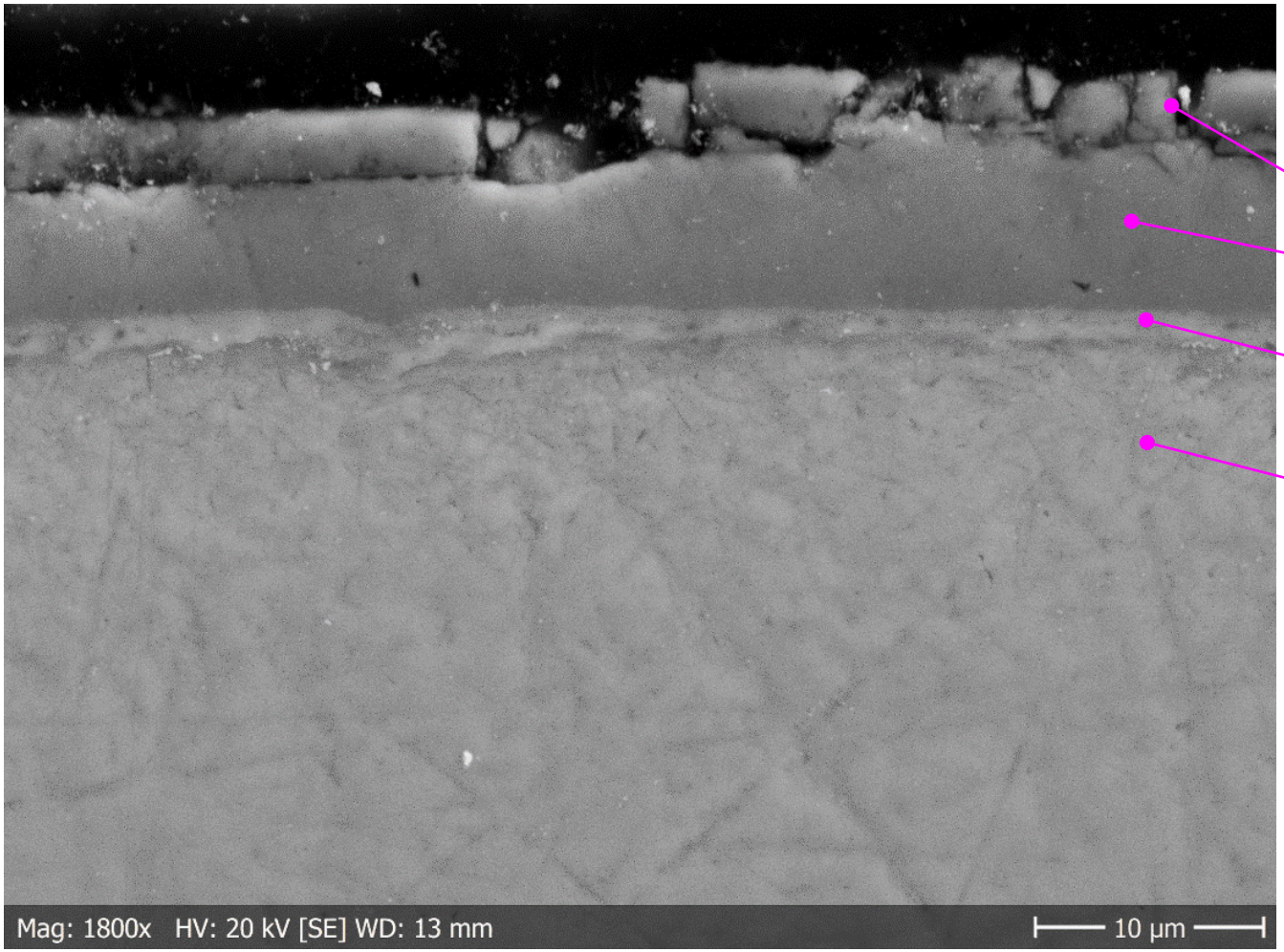

EC1 (1400 °C, immediate cool-down), SEM line scan: formation of Laves phase inside the blister

α-Zr(O) + **$ZrCr_2$**

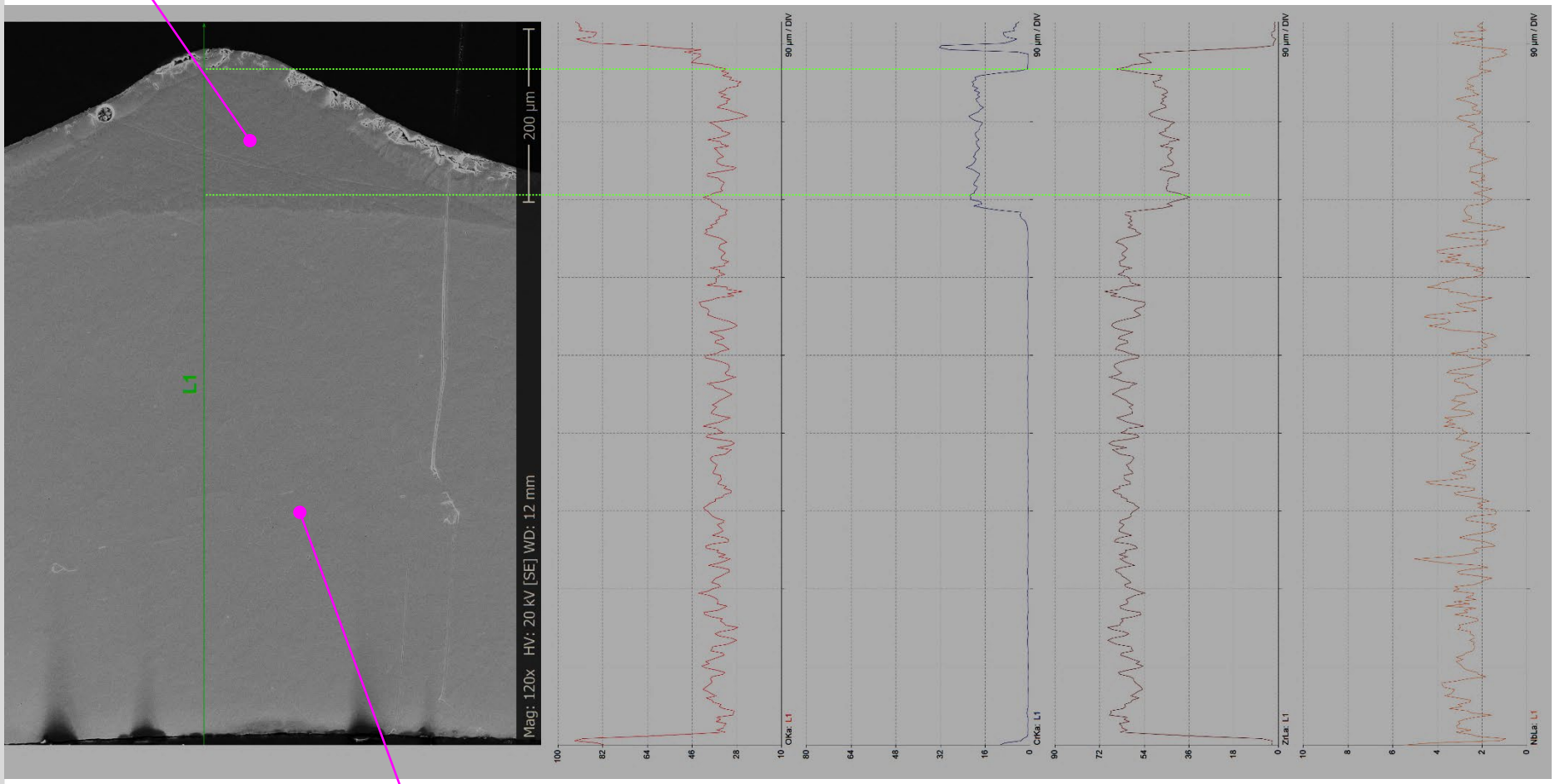

prior β-Zr

Coated AEOI samples: hydrogen release

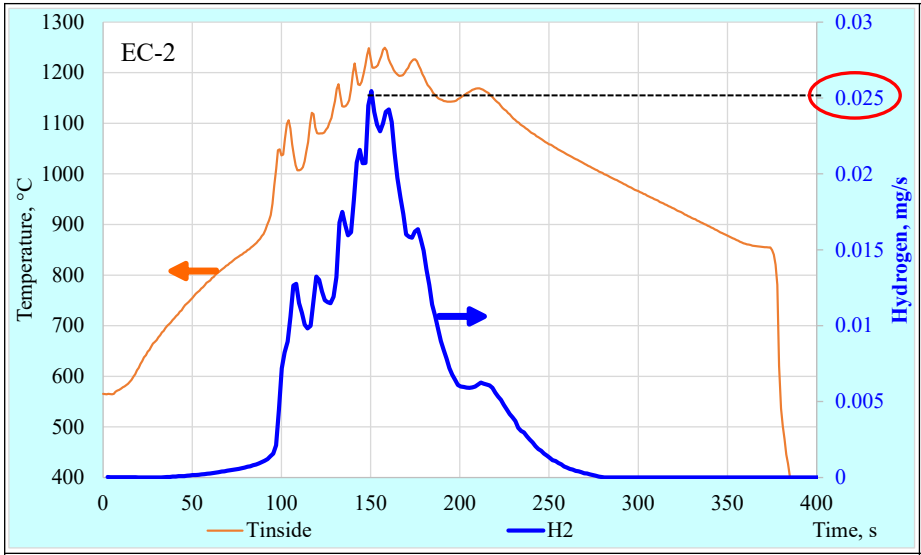

5 K/s, Tmax=**1250 °C**, cool-down 1.5 K/s to 900 °C, quench

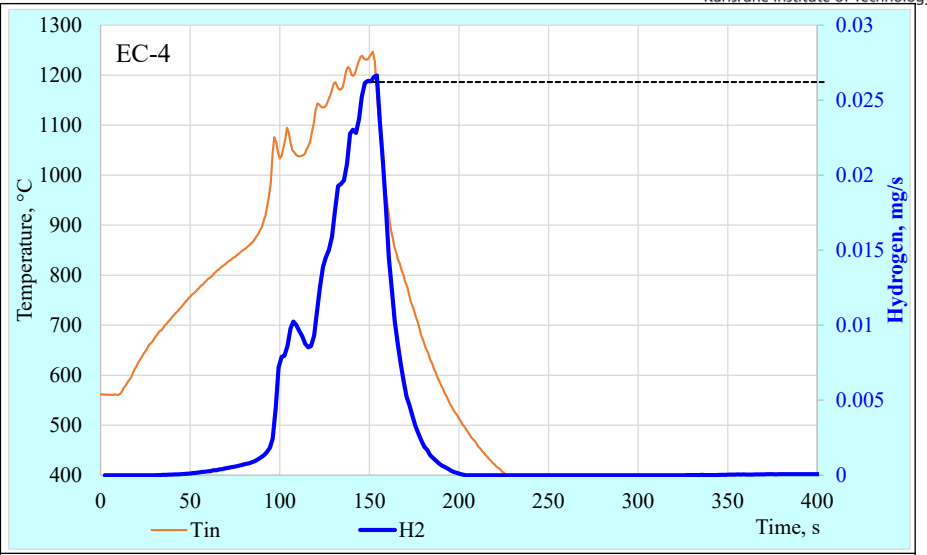

5 K/s, Tmax=**1250 °C**, immediate cool-down

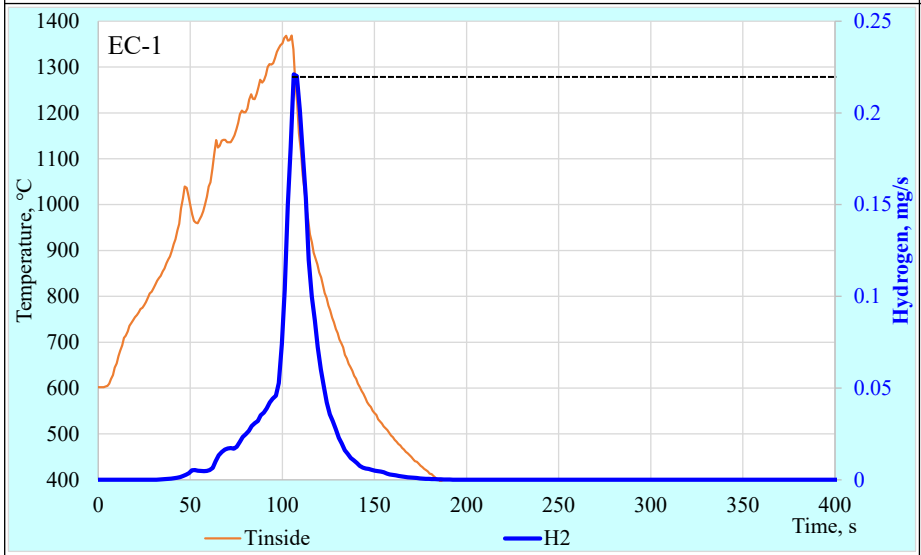

8 K/s, Tmax=**1390 °C**, immediate cool-down

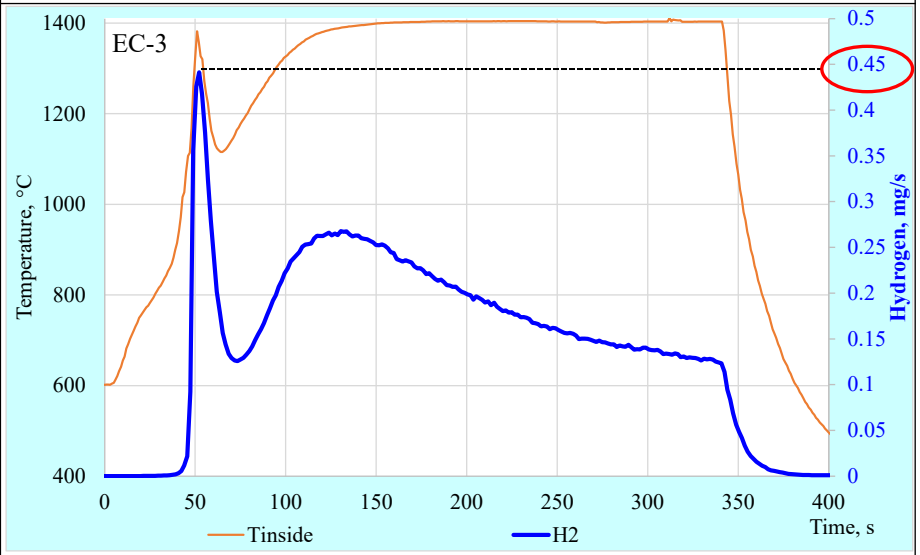

8 K/s, Tmax=**1400 °C** during 240 s, cool-down

Comparison of coated E110 (2022) and not coated Zry-4: significant lower hydrogen release for coated cladding under extended LOCA (max 1250 °C, cool-down, quench)

E110

coated E110

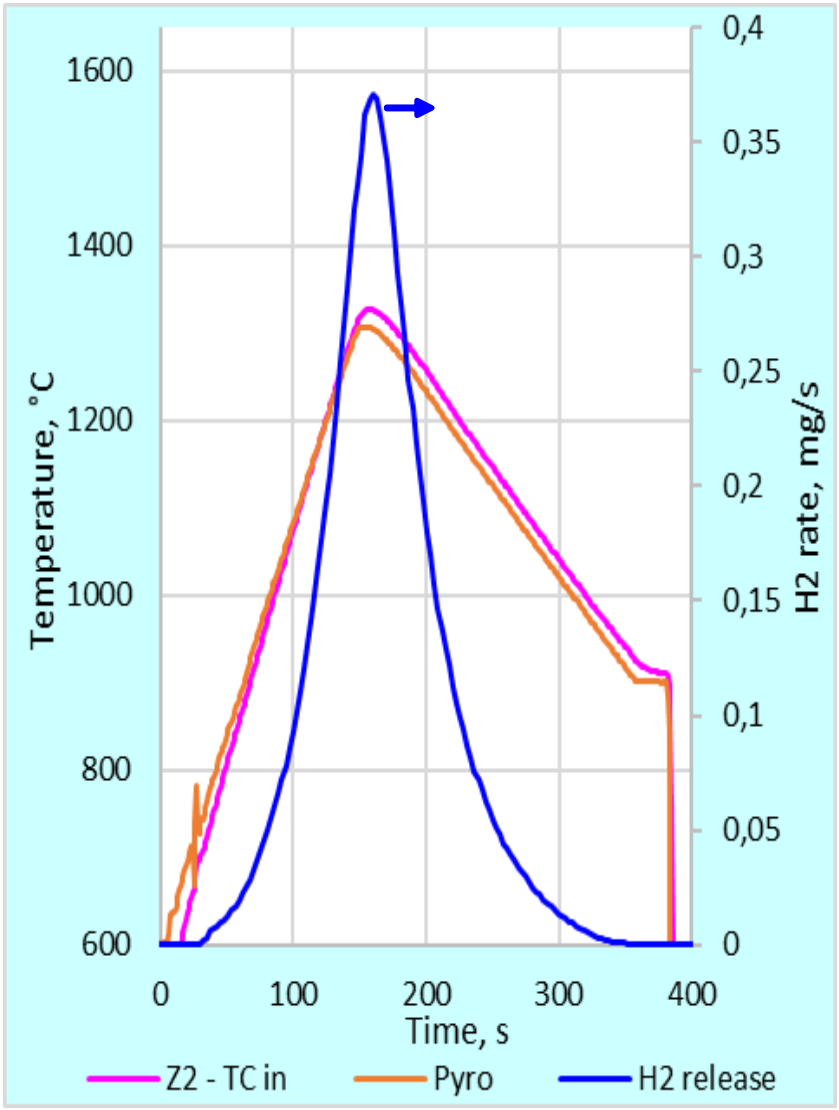

not coated Zry-4

Summary on AEOI samples

- significant decrease of hydrogen release under extended LOCA conditions (max 1250 °C) in comparison to not coated samples (factor 15).

- Numerous blisters (local swellings) at the outer cladding surface. Zr-Cr eutectic at 1350 °C and formation of Laves phase $ZrCr_2$.

Six coated (UPM/Prague) opt. ZIRLO™ samples with length 130 mm

Opt. ZIRLO claddings with OD=9.15 mm; wall thickness 650 µm:

- 2 PVD coated samples with Cr layer thickness of ≈5 µm

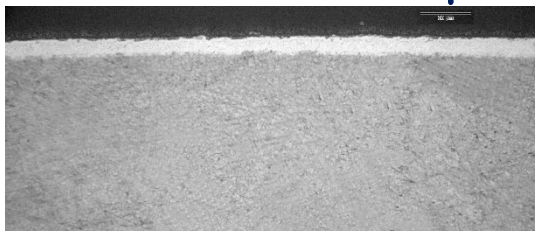

- 2 PVD coated samples with Cr layer thickness of >17 µm

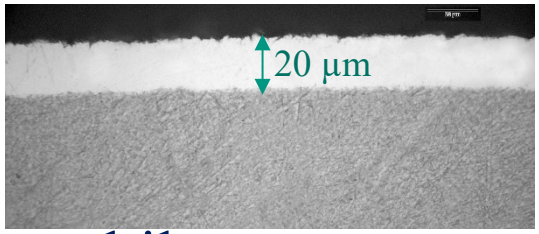

- 2 PVD coated samples with CrN/Cr multilayer

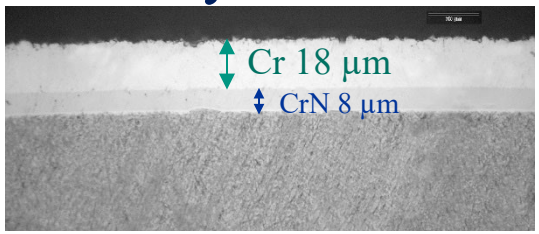

- *Samples are welded with Zr bottom and top plugs*
- *Top plug connected with Zr capillary tube*

Test matrix
and mass gains

Sample	1.1 (230418a)	1.2 (230419a)	2.1 (230419c)	2.2 (230420a)	3.1 (230421a)	3.2 (230420b)
coating	Cr 5 µm		CrN/Cr		Cr 17 µm	
heat-up, K/s	5	8	5	8	5	8
T_{max}, °C	1250	1400	1250	1400	1250	1400
oxidation duration at T_{max}, s	0	240	0	240	0	240
cool-down, K/s	1.5 to 900 °C	immediately	1.5 to 900 °C	immediately	1.5 to 900 °C	immediately
quench	water	in Ar+steam	water	in Ar+steam	water	in Ar+steam
m_0, g	26.0662	25.5293	26.2996	26.1545	26.1584	26.1517
m_{pt}, g	26.1036	26.1948	26.3287	26.3265	26.1865	26.7329
Δm, mg	**37.4**	***665.5*** - *(TC wires)*	**29.1**	***172 + (spalled scales)*** - *(TC wires)*	**28.1**	***581*** - *(TC wires)*

Outer views of samples oxidized during DBA transients (T_{max}^{surf}=1200 °C)

Karlsruhe Institute of Technology

1.1 ***pre-test***	**1.1 (Cr≈5 µm)** (sample 230418a)	*3.1* ***pre-test***	**3.1 (Cr>17 µm)** (sample 230421a)	*2.1* ***pre-test***	**2.1 (CrN/Cr; 18/8 µm)** (sample 230419c)
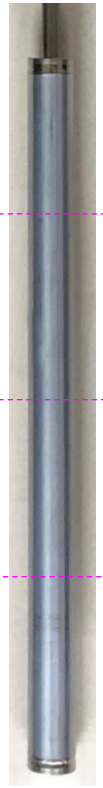		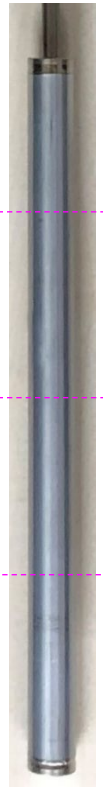	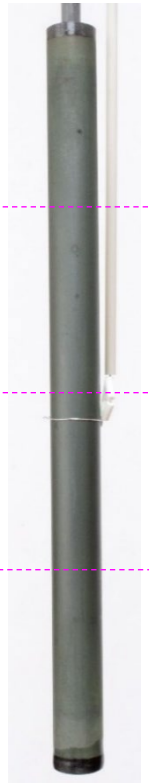	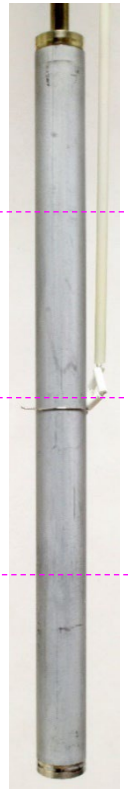	
					
	wrinkled surface		**glossy surface**		**partial oxide spalling**

IAM Institute for Applied Materials

Cross-sections (at hottest elevation of 65 mm) of samples oxidized during DBA transients (T_{max}^{surf}=1200 °C)

sample 1.1, Cr 5 µm	sample 3.1, Cr 20 µm	sample 2.1, CrN/Cr multilayer 18/8 µm
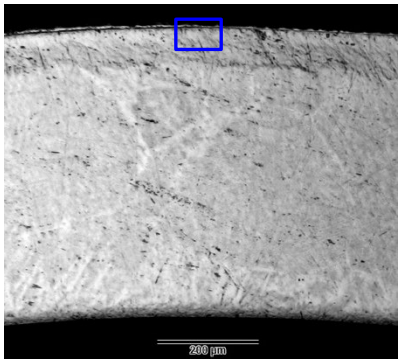	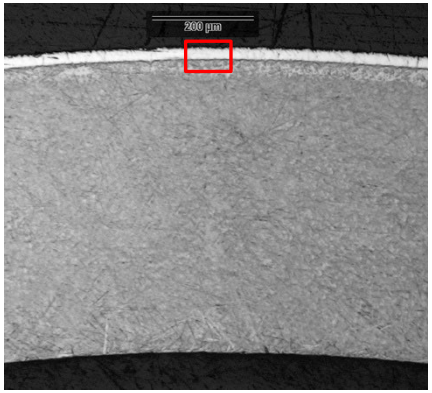	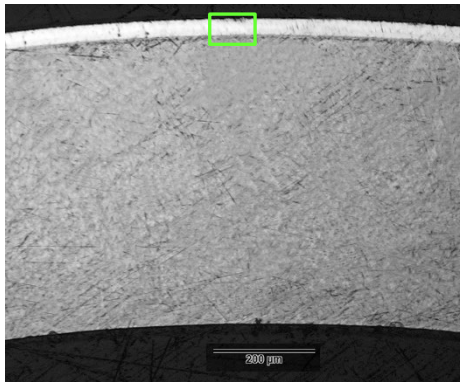
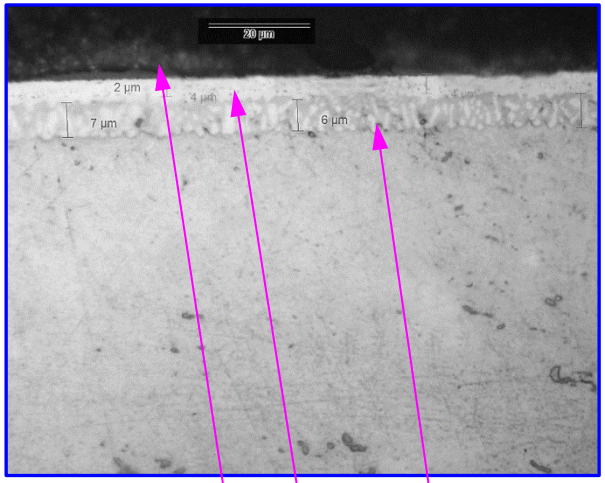	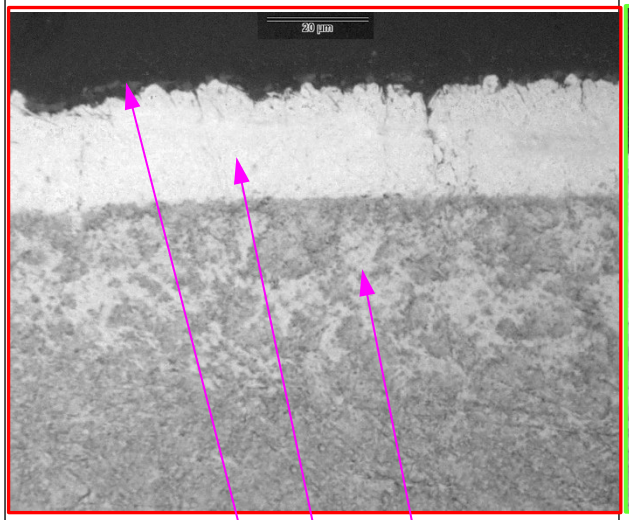	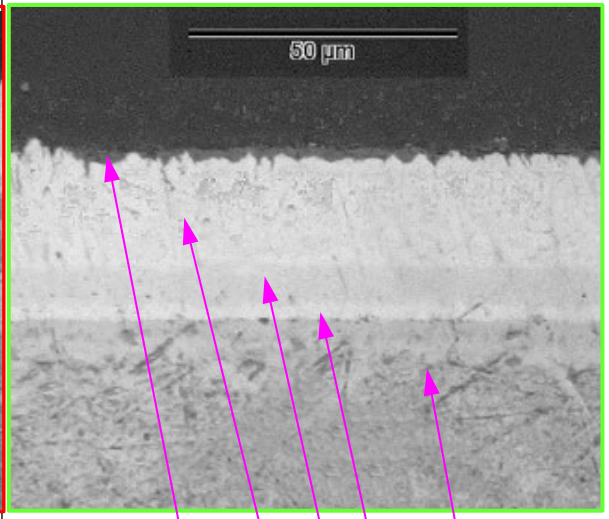
3 layers: Cr_2O_3, Cr, diffusion zone	3 layers: Cr_2O_3, Cr, diffusion zone	5 layers: Cr_2O_3, Cr, CrN, Cr, diffusion zone

Features of the behavior of the CrN/Cr sample under transient to T_{max}^{surf}=1200 °C

pre-test

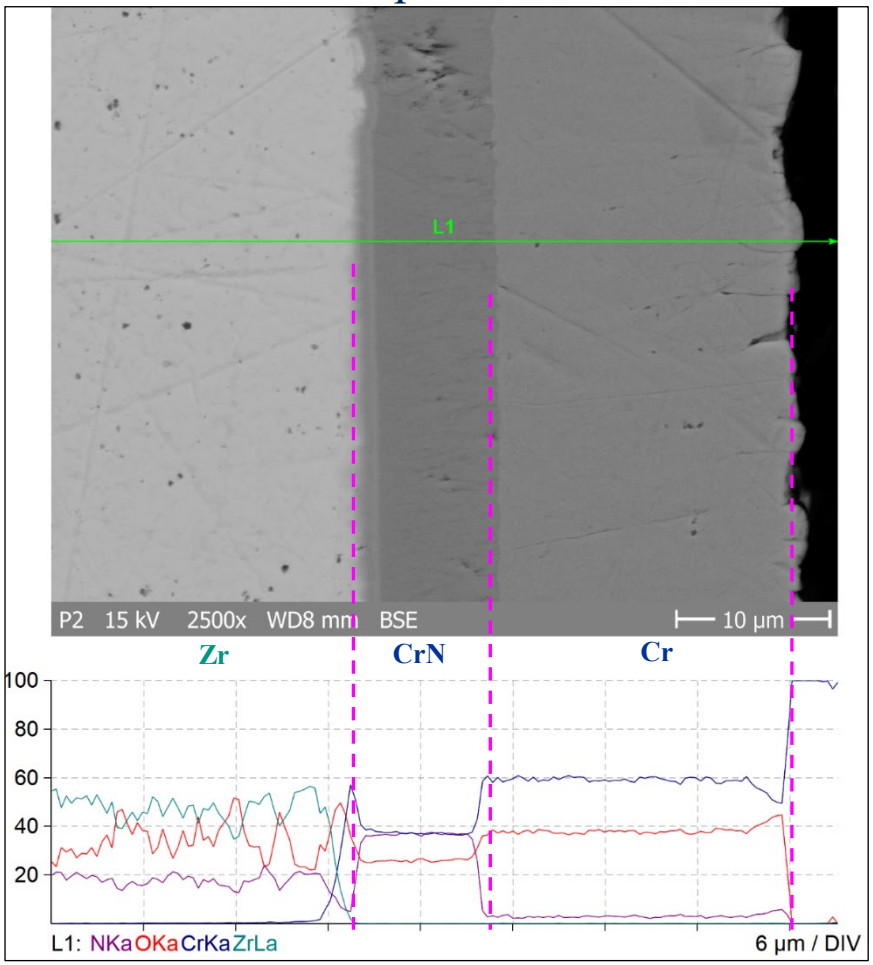

post-test

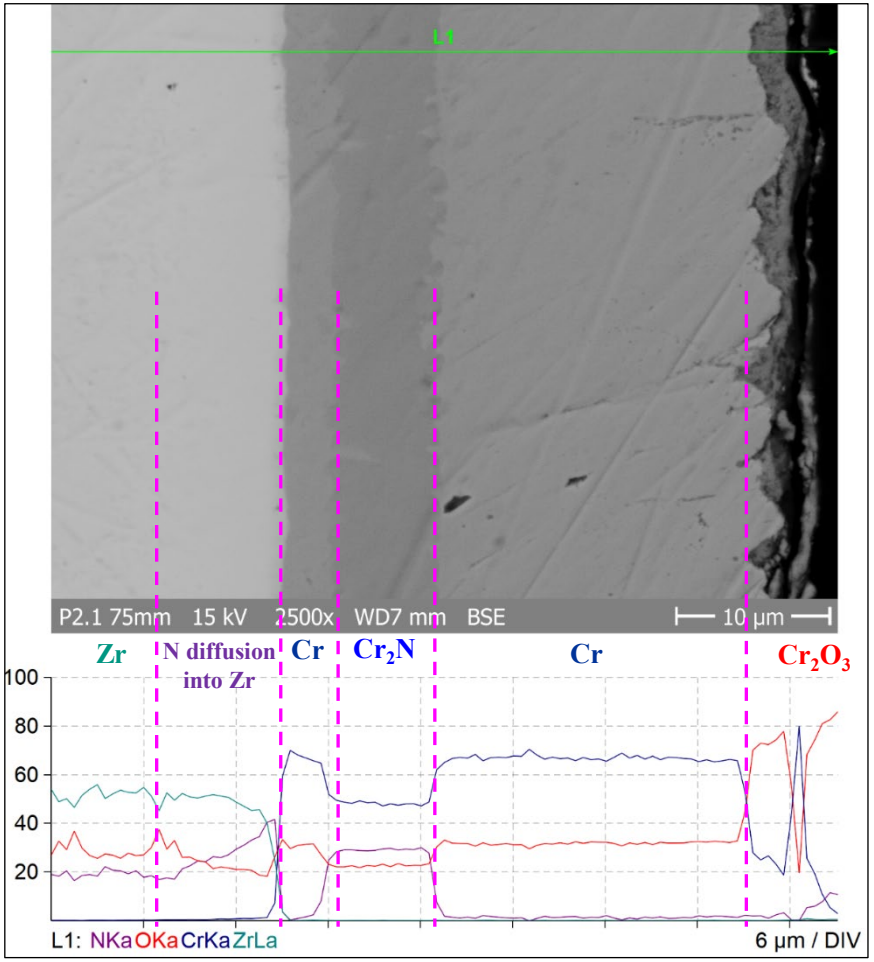

Outer views of samples oxidized at T_{max}^{surf}=1400 °C

1.1 *pre-test*	1.2 (Cr≈5 µm) (230419a)	*3.1* *pre-test*	3.2 (Cr>17 µm) (230420b)	*2.1* *pre-test*	2.2 (CrN/Cr) (230420a)
					
					
	fine surface blisters		coarse surface blisters		leaked (Zr, Cr) eutectic melt

Cross-sections of sample 1.2 (5 µm Cr) at 65 mm oxidized under BDBA conditions (T_{max}^{surf}=1400 °C)

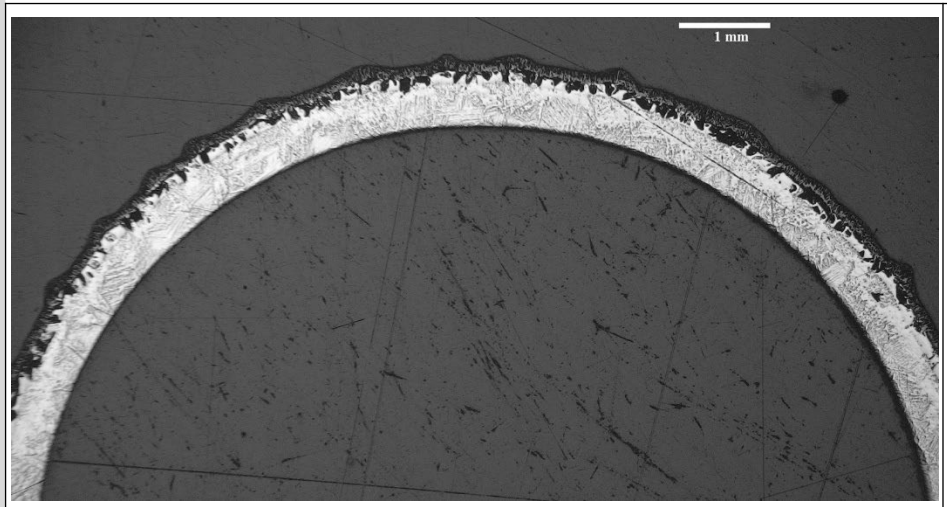

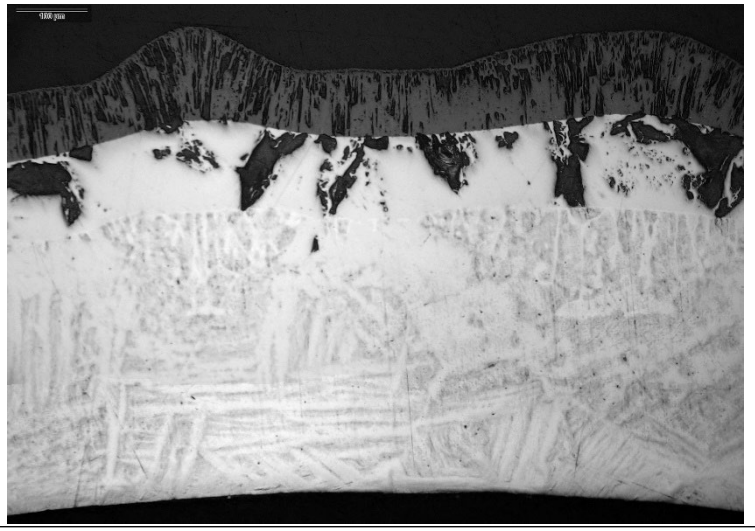

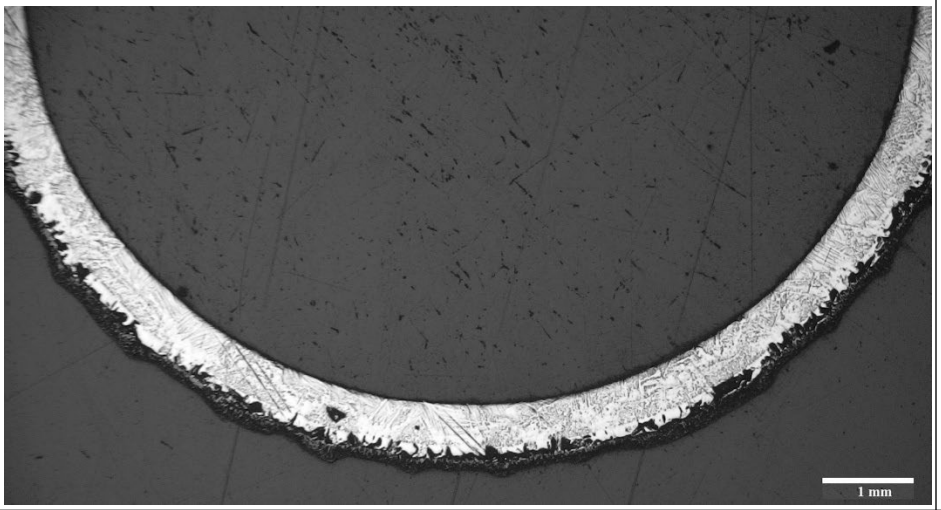

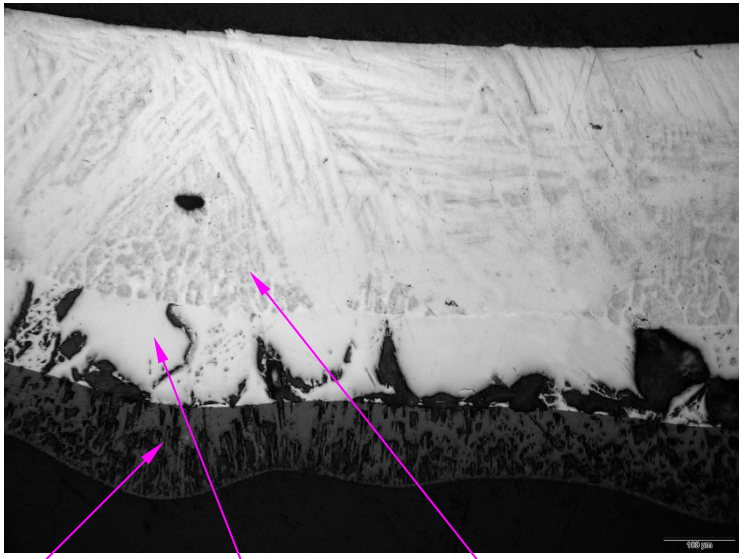

overview: ≈1.2 blisters per mm of circumference

ZrO_2 95-130 µm; α-Zr(O) 125-140 µm; $Cr_{diffusion\ in\ Zr}$

Cross-sections of sample 3.2 (>17 µm Cr) at 65 mm oxidized under BDBA conditions (T_{max}^{surf}=1400 °C)

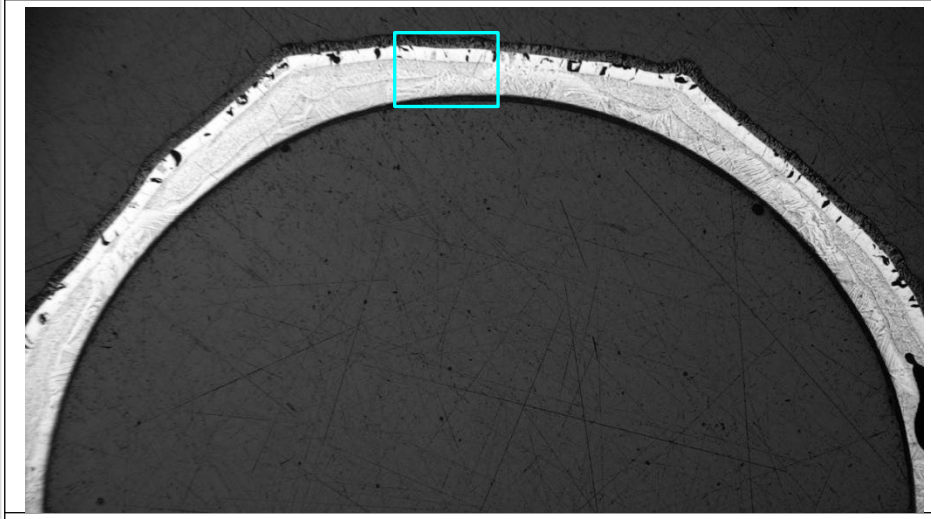

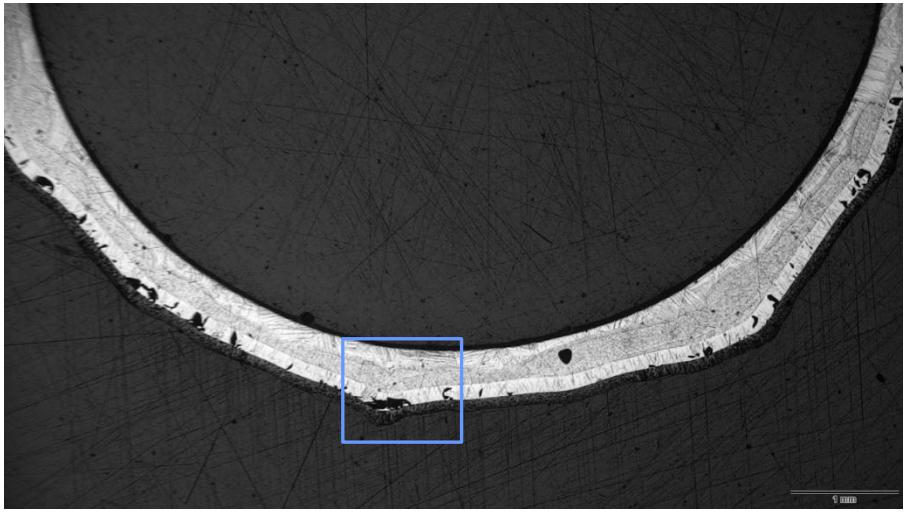

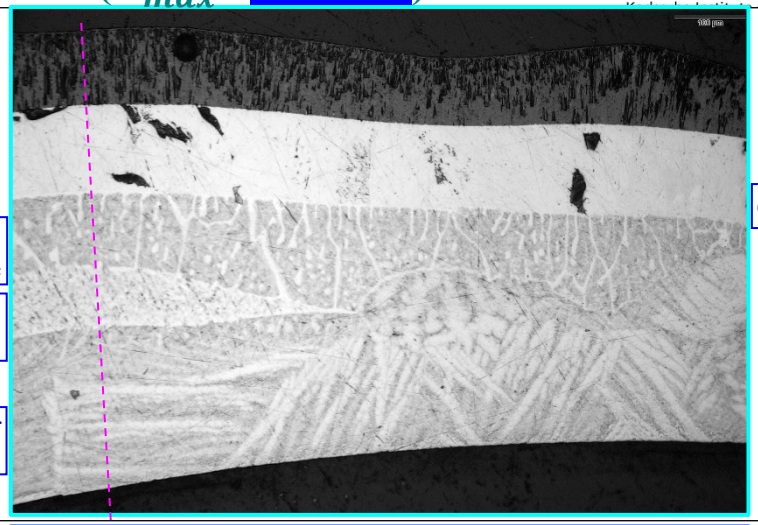

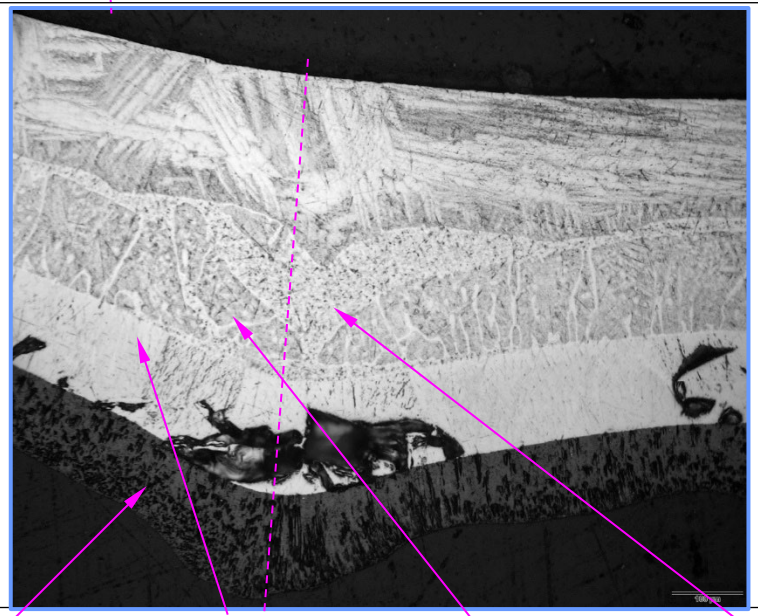

overview: ≈0.5 blisters per mm of circumference

ZrO_2 95-155 µm; α-Zr(O) 130-160 µm; $Cr_{diffusion\ in\ Zr}$ 120 µm; $(Zr, Cr)_{max}$ 120 µm

Cross-sections of sample 3.2 (>17 µm Cr) at 65 mm oxidized under BDBA conditions (T_{max}^{surf}=1400 °C)

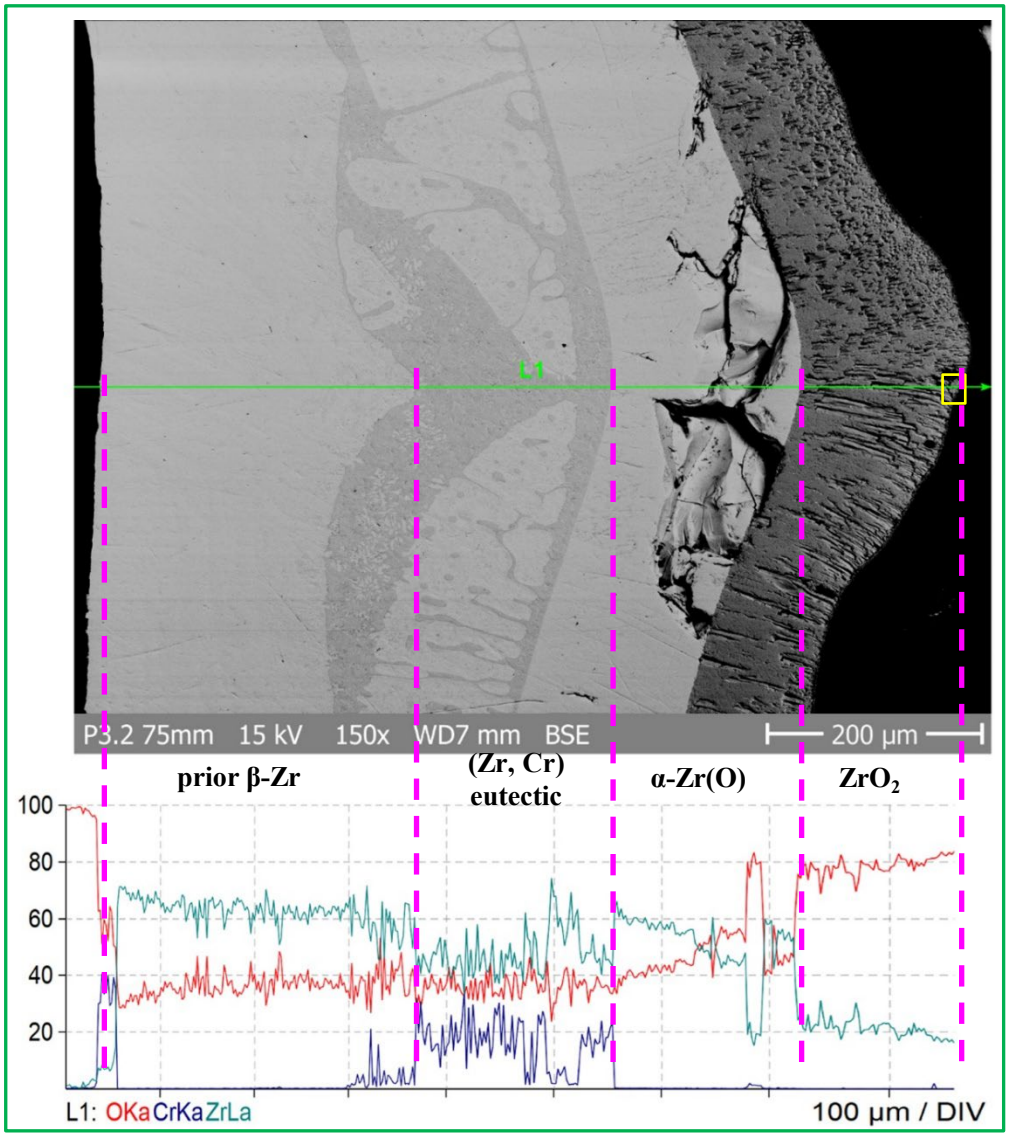

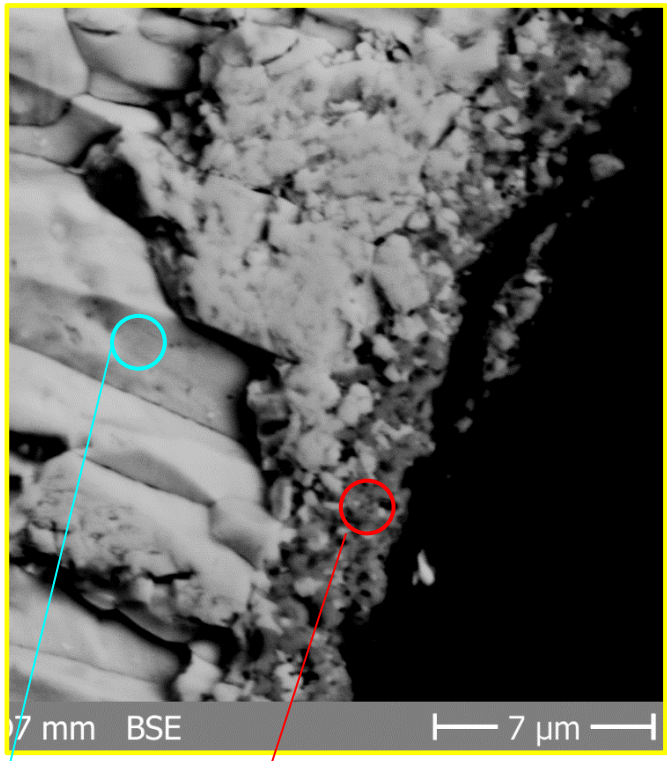

Cr_2O_3

Elt	XRay	Int	Error	K	Kratio	W%	A%
O	Ka	2563.5	64.5061	0.5452	0.4266	58.06	82.78
Cr	Ka	1630.6	1.9068	0.3948	0.3089	35.70	15.66
Zr	La	400.8	1.8673	0.0600	0.0469	6.24	1.56
				1.0000	0.7825	100.00	100.00

ZrO_2

Elt	XRay	Int	Error	K	Kratio	W%	A%
O	Ka	673.1	1.3042	0.2139	0.1256	46.00	82.91
Cr	Ka	3.0	0.1818	0.0011	0.0006	0.07	0.04
Zr	La	3508.4	6.5569	0.7850	0.4609	53.93	17.05
				1.0000	0.5872	100.00	100.00

Cross-sections of sample 2.2 (CrN/Cr) at the hottest elevation 65 mm oxidized under BDBA conditions (T_{max}^{surf}=1400 °C)

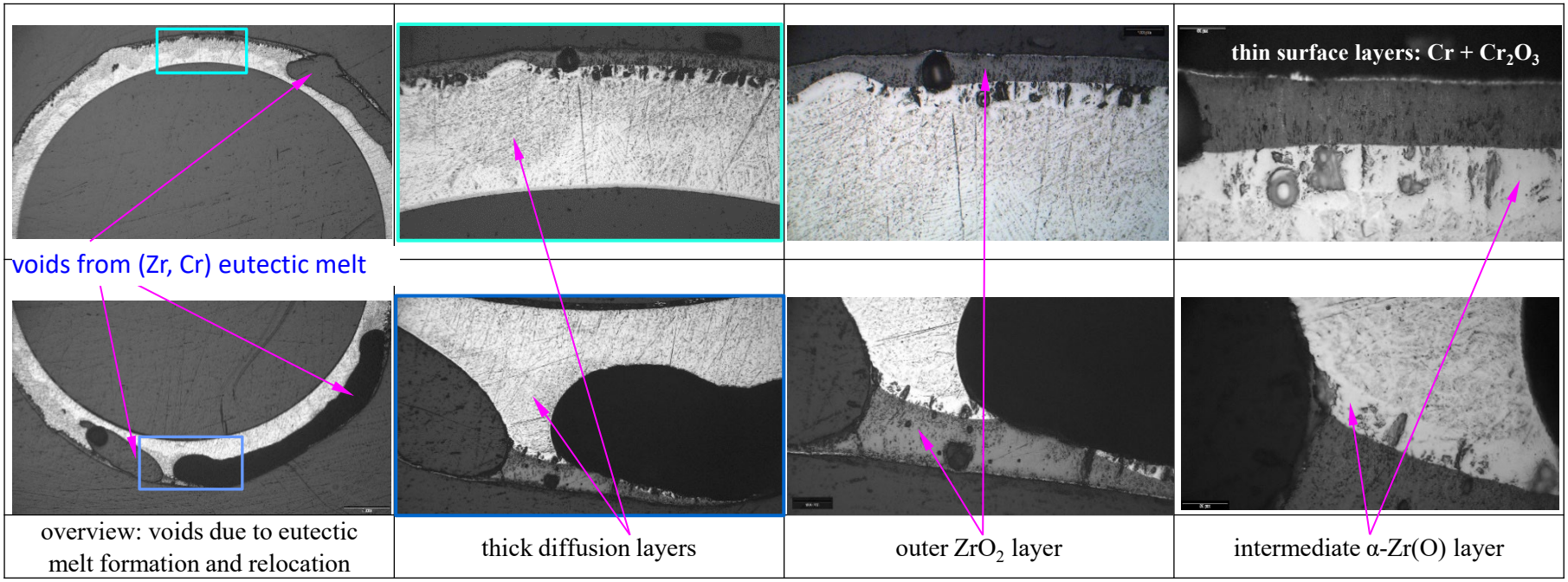

overview: voids due to eutectic melt formation and relocation	thick diffusion layers	outer ZrO_2 layer	intermediate α-Zr(O) layer

Cross-sections of the UPM/Prague samples at the hottest elevation 65 mm oxidized under BDBA conditions (T_{max}^{surf}=1400 °C)

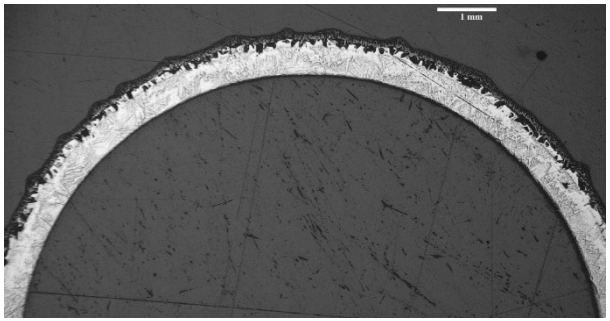	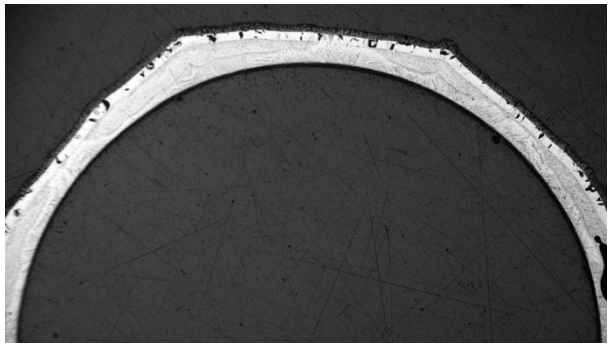	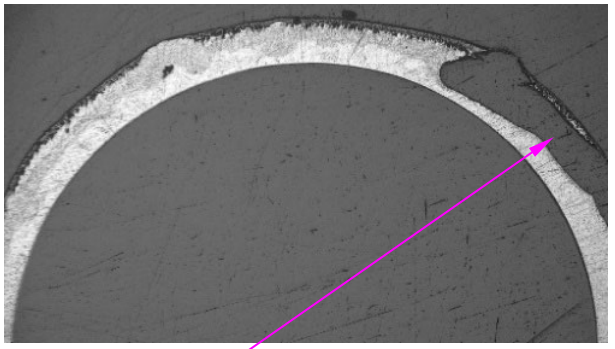
≈1.2 blisters per mm of circumference	≈0.5 blisters per mm of circumference	voids from (Zr, Cr) eutectic melt
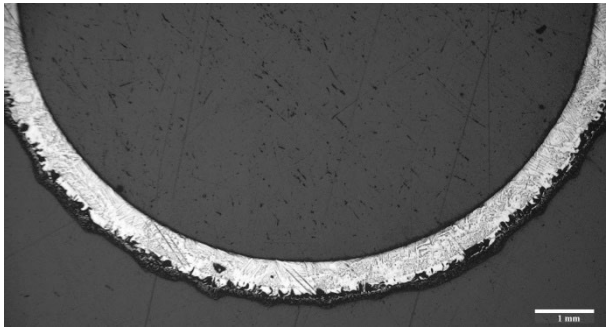	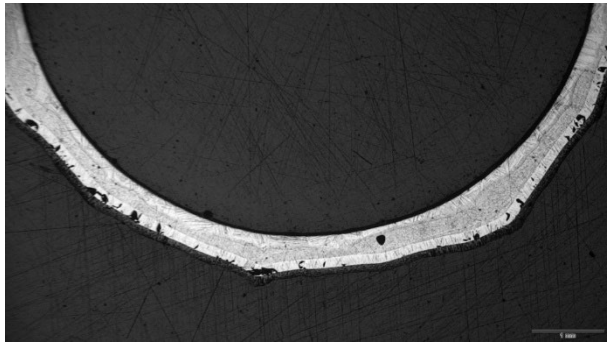	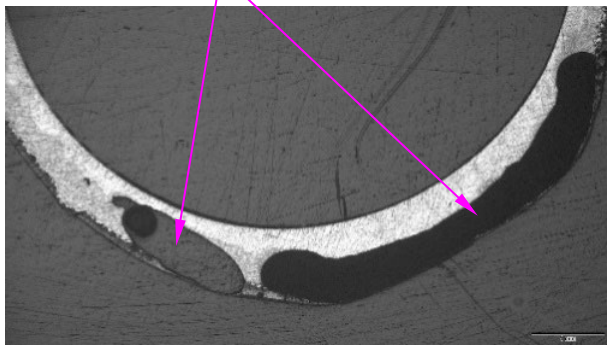
sample 1.2: 5 µm Cr	sample 3.2: >17 µm Cr	sample 2.2: Cr (18 µm)/CrN (8 µm)

- Formation and relocation of (Zr,Cr) eutectic **melt** for Cr/CrN coating perhaps due to the lack of intermediate oxidation of part of the zirconium, which could not react with steam due to the barrier effect of CrN layer.

Cross-sections of BDBA sample 2.2 (Cr/CrN) at hottest elevation of 65 mm (T_{max}^{surf}=1400 °C), circumferential position outside voids

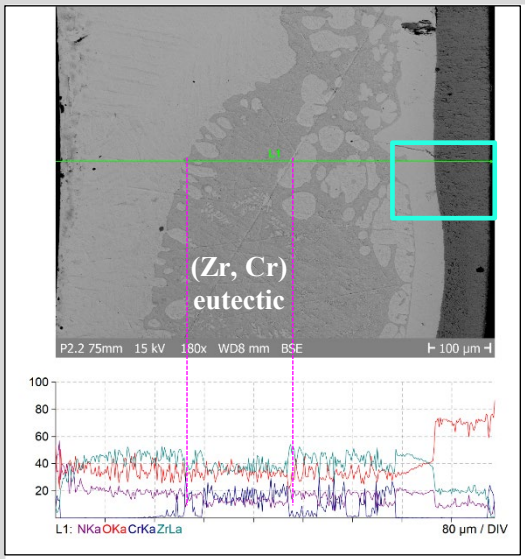

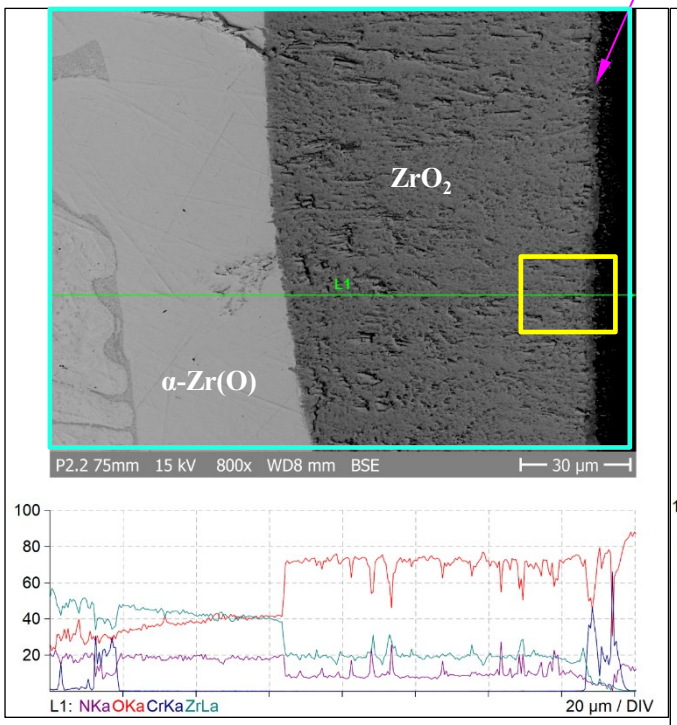

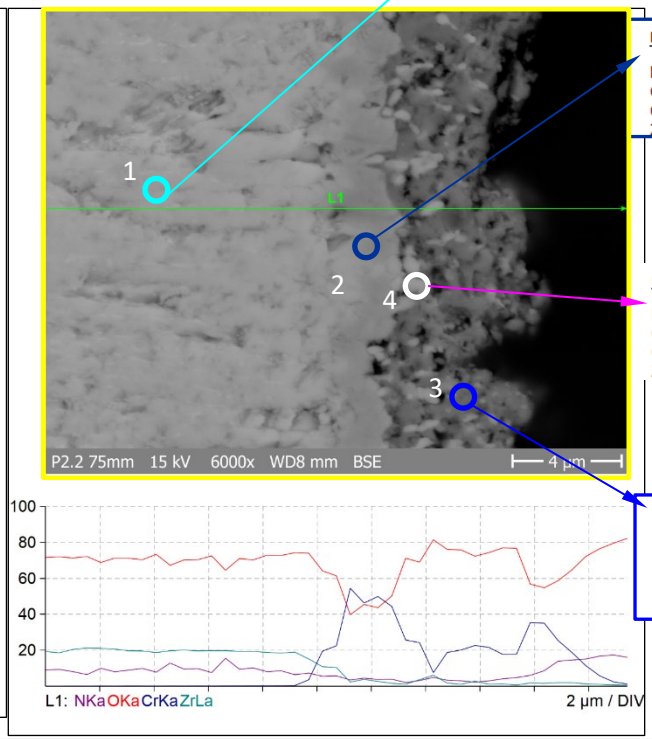

ZrO_2 with ZrN inclusions

Elt	XRay	Int	Error	K	Kratio	W%	A%
N	Ka	69.1	158.8994	0.0174	0.0103	5.37	11.41
O	Ka	866.9	158.8994	0.1519	0.0901	37.63	69.96
Cr	Ka	14.1	0.3705	0.0028	0.0017	0.18	0.11
Zr	La	6711.8	115.6367	0.8279	0.4910	56.81	18.52

Cr

Elt	XRay	Int	Error	K	Kratio	W%	A%
N	Ka	39.5	235.8792	0.0075	0.0065	1.35	3.46
O	Ka	1126.7	235.8792	0.1482	0.1299	19.46	43.74
Cr	Ka	5248.9	7.2788	0.7861	0.6889	72.62	50.21
Zr	La	629.0	11.3931	0.0582	0.0510	6.57	2.59

Cr_2O_3 with Zr inclusions

Elt	XRay	Int	Error	K	Kratio	W%	A%
N	Ka	50.5	205.6407	0.0111	0.0074	1.94	3.43
O	Ka	2452.0	205.6407	0.3755	0.2497	49.74	77.09
Cr	Ka	2351.1	1.9388	0.4099	0.2726	30.95	14.76
Zr	La	1886.9	37.5481	0.2034	0.1353	17.38	4.72

Cr_2O_3

Elt	XRay	Int	Error	K	Kratio	W%	A%
N	Ka	73.4	390.9179	0.0122	0.0098	1.69	2.88
O	Ka	4089.2	390.9179	0.4723	0.3791	50.62	75.79
Cr	Ka	3692.4	9.0070	0.4855	0.3897	44.47	20.49
Zr	La	370.5	12.8343	0.0301	0.0242	3.22	0.85

Hydrogen release during the tests with the UPM/Prague samples

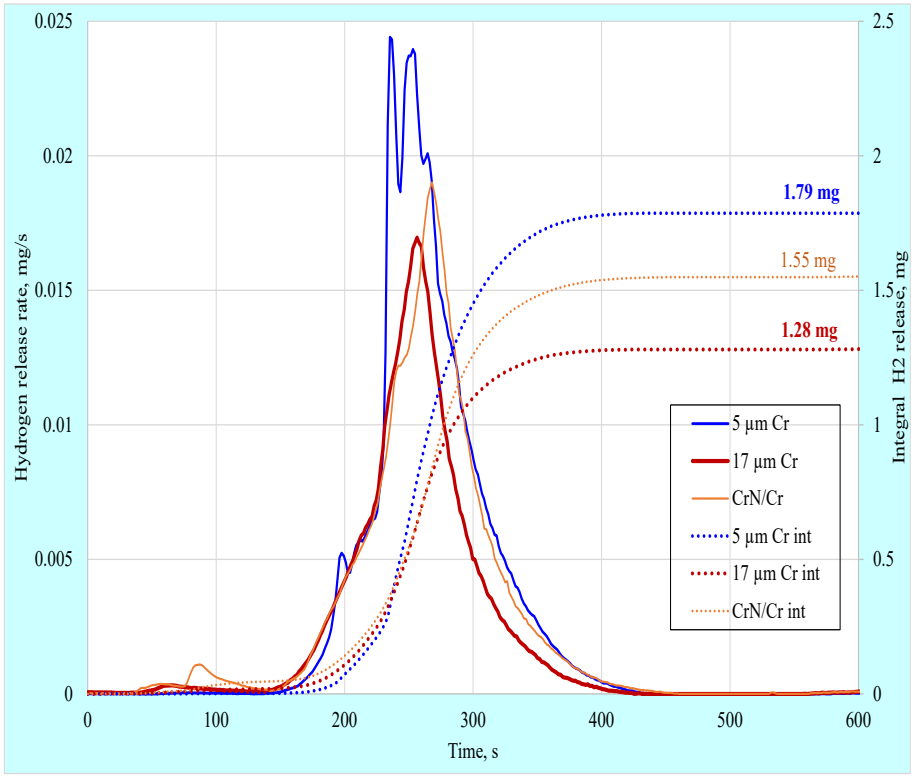

hydrogen release under DBA conditions (T_{max}^{surf}=1200 °C)

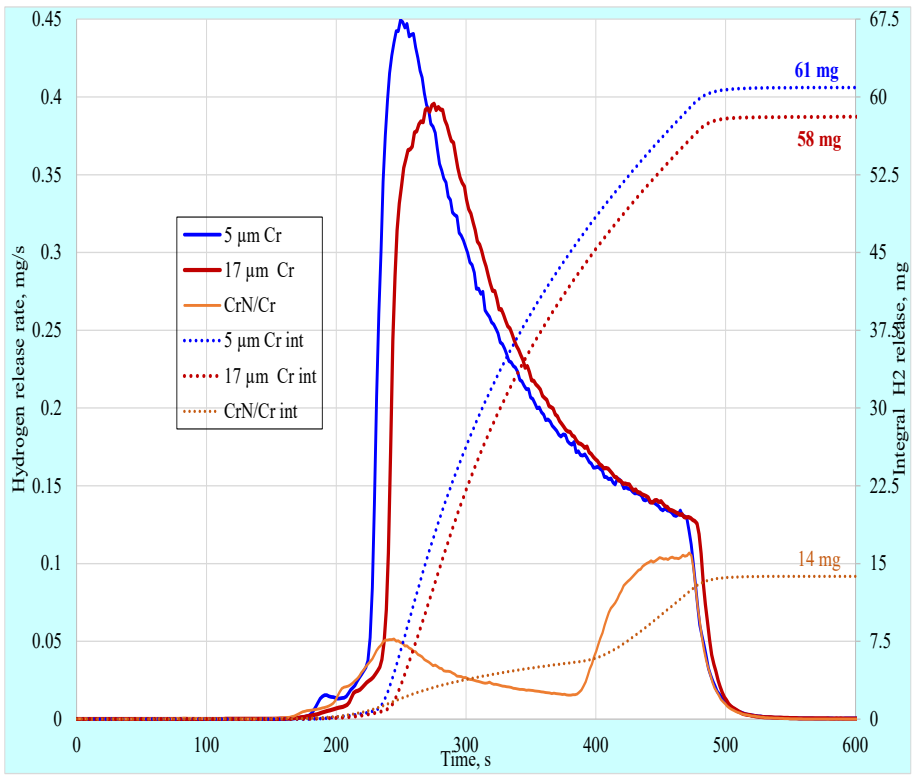

hydrogen release under BDBA conditions (T_{max}^{surf}=1400 °C)

- Increasing the thickness of the chromium layer by 3 times (from 5 to ≈17 µm) reduced the hydrogen release by 30% under DBA conditions (transient to 1200 °C), however, only by 3% under BDBA conditions (1400 °C). *The barrier CrN layer has only a moderate influence on hydrogen release under DBA, but strong reduced hydrogen release under BDBA (reduction factor 4).*

Summary on Prague samples

- an increase in the thickness of the chromium layer by 3 times (from 6 to 18 µm) reduced the hydrogen release by 30% under DBA conditions (transient to 1200 °C), however, only by 3% under BDBA conditions (1400 °C). Barrier layer CrN has only moderate influence on hydrogen release under DBA, but strong reduced hydrogen release under BDBA (reduction factor 4).
- Formation of blisters (local swellings) at the outer cladding surface under BDBA conditions (T_{max}=1400 °C): fine blisters (1.2/mm) for thin Cr layer (6 µm) and coarse blisters (0.5/mm) for thick Cr layer (18 µm).
- Cr transport from the cladding surface to the boundary of α/β-Zr phases.
- Formation and relocation of (Zr,Cr) eutectic **melt** for CrN/Cr coating perhaps due to the lack of intermediate oxidation of part of the zirconium, which could not react with steam due to the barrier effect of CrN layer.

Thank you for your attention

http://www.iam.kit.edu/awp/163.php
http://quench.forschung.kit.edu/

Alžběta Endrychová

UJP

Behaviour of Fuel Cladding with Cr Coating during LOCA and Study of Cr Diffusion into Zr-alloy

The advancement of Accident Tolerant Fuel (ATF) technologies is critical for enhancing the safety of nuclear reactors under accident conditions. Chromium (Cr) coatings on conventional zirconium alloys have been identified as the most promising near-term ATF concept due to their high-temperature resistance to oxidation. However, the presence of Cr increases the solubility of oxygen in the zirconium alloy, which can degrade the mechanical properties and potentially lead to fuel cladding failure at unanticipated temperatures.

The presentation deals with the oxidation behaviour of Cr-coated claddings under Loss-of-Coolant Accident (LOCA) scenarios, with particular emphasis on the effects of chromium diffusion into the zirconium substrate. The diffusion of Cr was studied because it can significantly influence the microstructure and mechanical properties of the cladding material. Additionally, it highlights the implications of coating defects induced by cladding deformation mechanisms such as ballooning and rupture.

Behaviour of Fuel Cladding with Cr Coating during LOCA and Study of Cr Diffusion into Zr-alloy

A. Endrychová[1,2], J. Krejčí[1], J. Kabátová[1], D. Rada[1], V. Rozkošný[1]

[1] UJP PRAHA a.s., [2] Faculty of Mechanical Engineering, CTU

QUENCH 2024

ATF cladding concepts

UJP PRAHA

- Development and testing of different concepts of **A**ccident **T**olerant **F**uels (**ATFs**) - 2 concepts:

1. Protective coatings on zirconium-based alloys (Near Term ATF)

- Cr, CrN, CrNCr
- ZrNCr
- CrNb
- CrAl

Specimen	Substrate	Coating	Thickness of coating (µm)	Method of deposition
Cr-I	Zr1Nb	Cr	7	PVD AD
CrN-I	Zr1Nb	CrN	7	PVD AD
CrN+Cr-I	Zr1Nb	CrN+Cr	6	PVD AD
CrIB1	Zircaloy-4	CrIB	17	PVD MS
Cr-KIT	ZIRLO	Cr	7	PVD MS
ZCr-KIT	ZIRLO	Cr	7	PVD MS
ZryCr-KIT	Zircaloy-4	Cr	7	PVD MS
Cr70Nb30	Zr1Nb	CrNb	7	PVD MS
Cr85Nb15	Zr1Nb	CrNb	7	PVD MS
CrAl2	Zr1Nb	CrAl	15	PVD MS

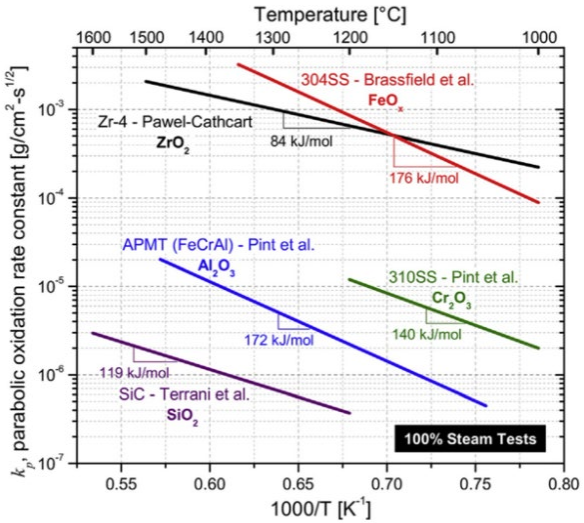

Parabolic oxidation rate constant for different ATF concepts. [1]

2. „New“ materials (Longer Term ATF Technologies)

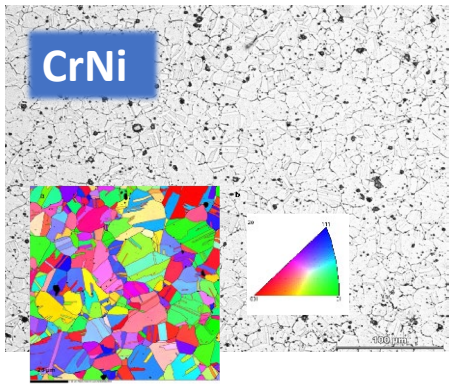

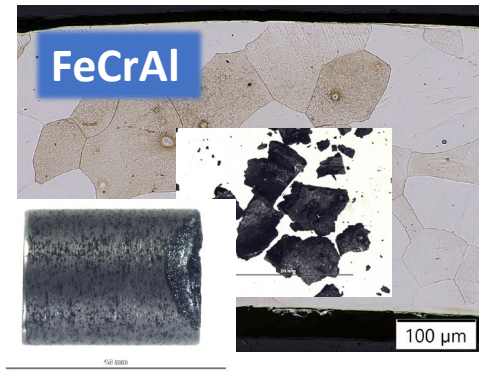

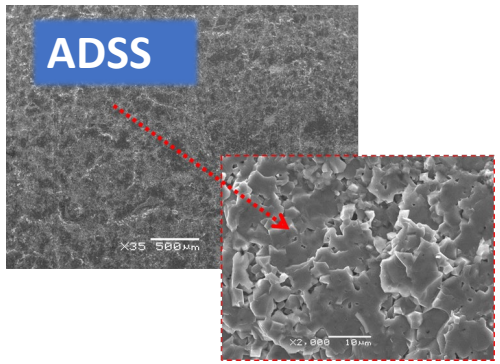

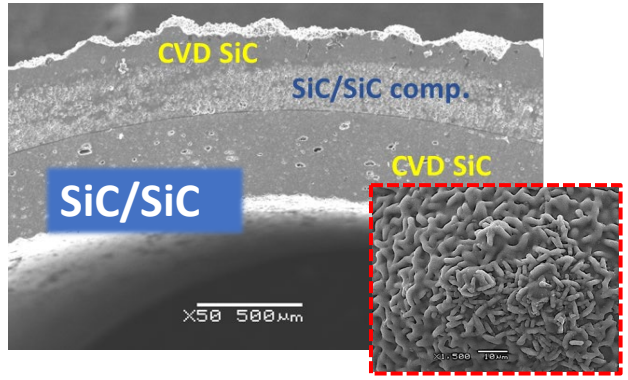

Zr-alloy with Cr coating: Diffusion

- During oxidation at high temperatures (1000–1300°C) typical for LOCA accidents, the protective coating is „consumed“:
  1. **Formation of Cr_2O_3 oxide on the outer side of the fuel cladding,**
  2. **Unwanted diffusion of chromium into the zirconium substrate.**
- Degradation of the coating due to Zr transport towards the outer interface
- Diffusion of Cr into Zr (formation of L-phase at the interface + enrichment of β-Zr Cr) – brittle phase at Cr above ~1.5 wt.%
- Rapid acceleration of kinetics after loss of Cr protective properties
- Cr is a β-stabilizer, and oxygen diffusion in β-Zr proceeds significantly faster -> **The presence of Cr increases the oxygen solubility limit in β-Zr, which can negatively impact the ductility and brittleness of the material**
  - Solution: CrN, CrN+Cr, ZrN+Cr -> microcracks

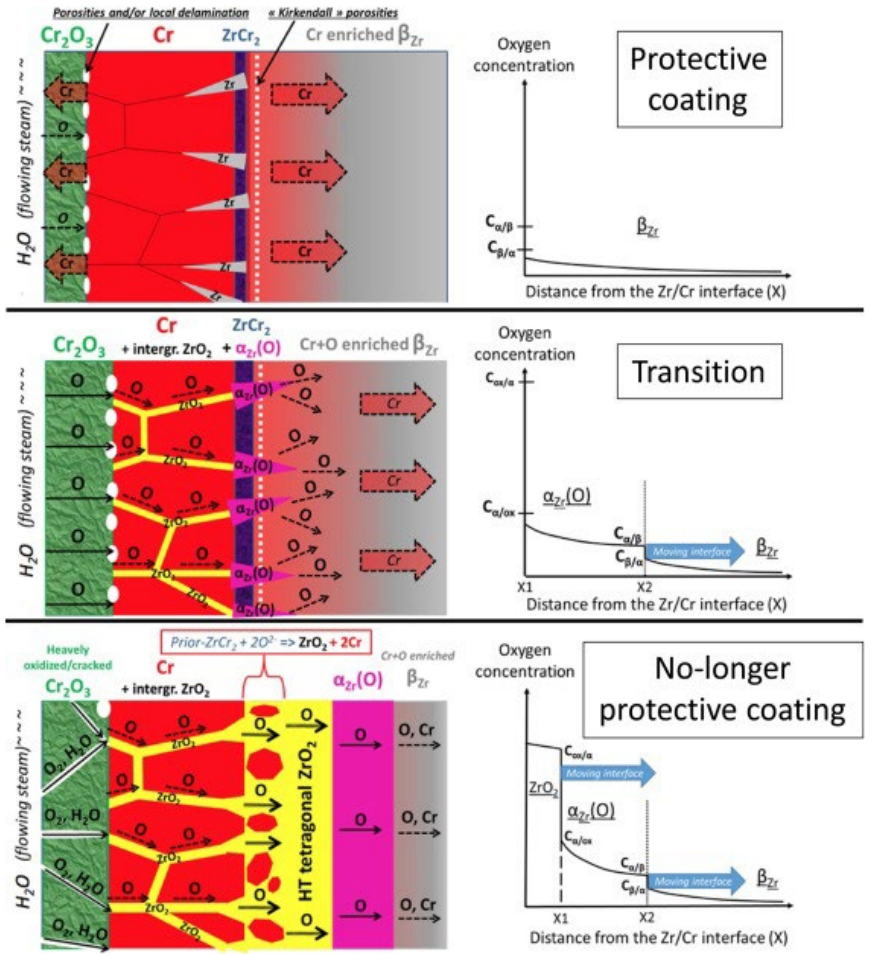

Diffusion of Cr into Zr-substrate [7]

Zr-alloy with Cr coating: Damaged coating

UJP PRAHA

- The presence of Cr leads to an increase in O solubility -> Study of the combined effects of diffusion phenomena (Cr into Zr substrate, O into Cr-enriched Zr areas) and verification of their influence on mechanical properties (mechanical testing RCT, SEM analyses - WDS).
- **Due to higher oxygen concentration, fuel cladding could fail even under conditions that are not anticipated.**
  - **Criterion "O_β" based on the critical oxygen concentration in the original beta phase, which is crucial for determining the ductility of the samples. (The limit value - 0.38 wt.%)**
  - Study of the phase diagram of Cr-coated Z1Nb-O at various temperatures.
- Most studies focus on a compact Cr layer, but regarding a **damaged coating:**
  - **Assumption: Consistently elevated Oxygen-content independant of Cr concentration** (Červenka et al. [3]).
  - A new testing methodology for „damaged coating“ will be developed -> monitoring of O and Cr diffusion.
  - Creation of a Cr-coated Zr1Nb-O diagram at various temperatures – constant temperature and varying Cr and O concentrations (Négyesi et al. [9] X classic diagram construction).

Dependance of Oxygen content to ECR [12]

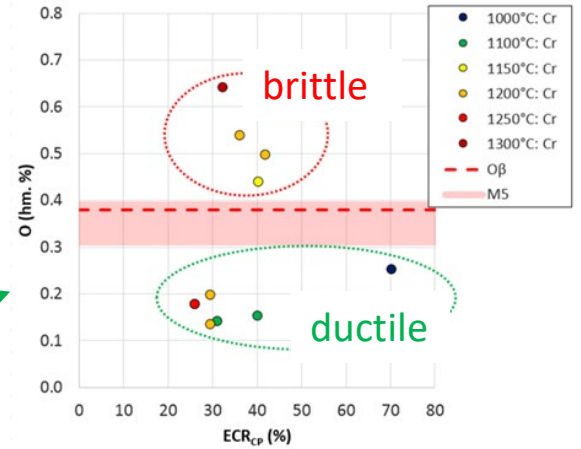

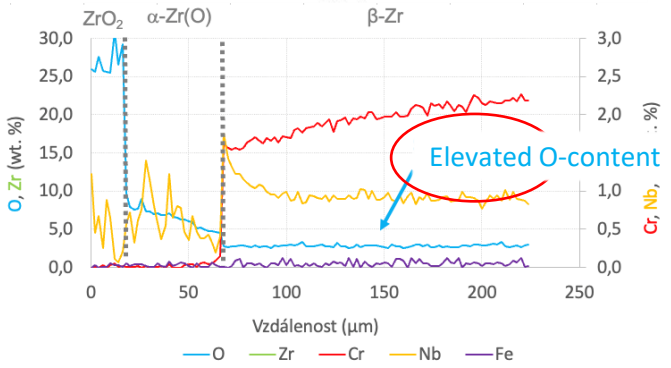

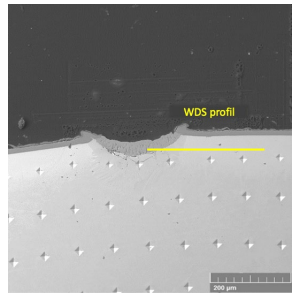

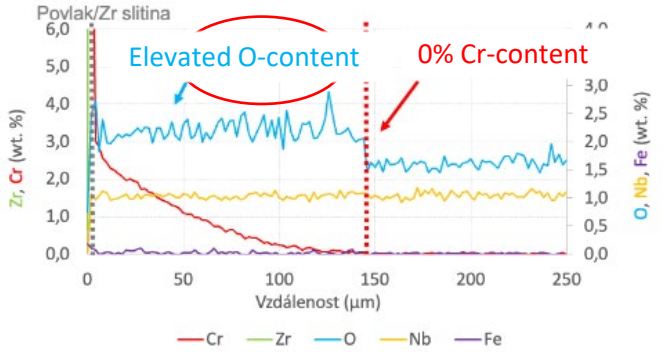

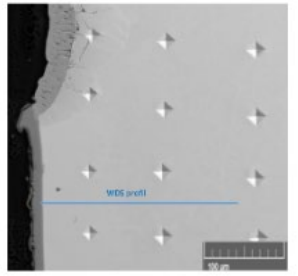

Sample with scratch after HTO 4.5 min/1200 °C; WDS [3]

EXPERIMETAL PART: High-temperature oxidation

UJP PRAHA

High-temperature oxidation in steam

- Electric resistance furnance
- Steam + Ar at atmospheric pressure
- Double-sided oxidation + direct quenching
- NRC methodology [DG-1262]
- Post-experimental examination
  - Weight gain after HTO
  - Optical and SEM analysis (EDS, WDS)

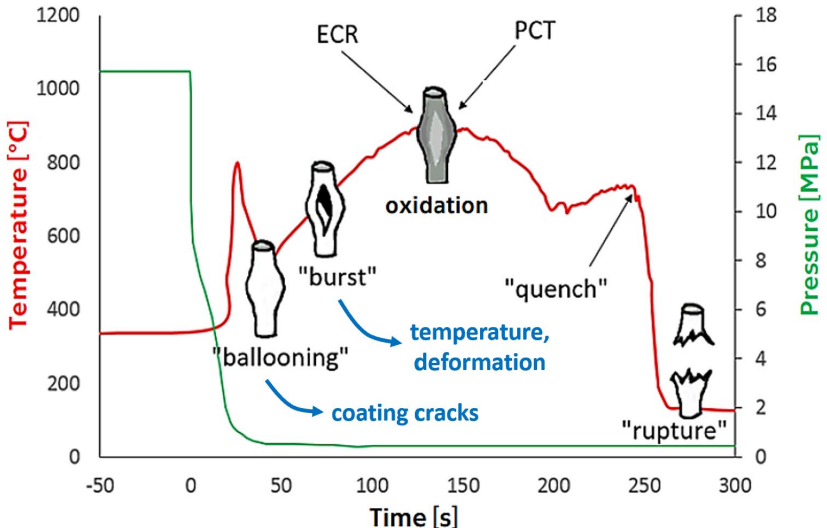

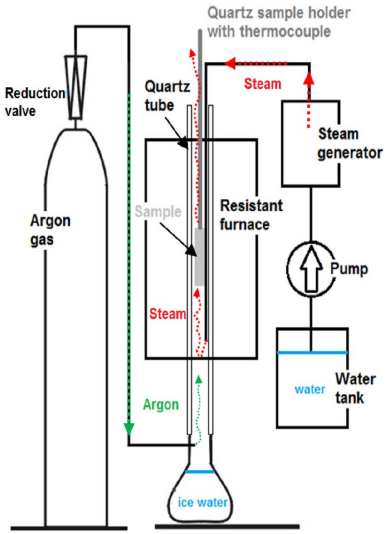

Zr-alloy with Cr coating: EDS and Diffusion

UJP PRAHA

- **Measurement of Cr concentration – pre-oxidized samples with Cr coating**
  - 1200°C – 1.5 (60 μm), 3, 4.5 (100 μm), and 9 (150 μm) min
  - 1100°C – 100 (300 μm), 30 (150 μm), 15 (115 μm), 9 (100 μm) min
- Correlation – determination of the diffusion coefficient as a function of temperature

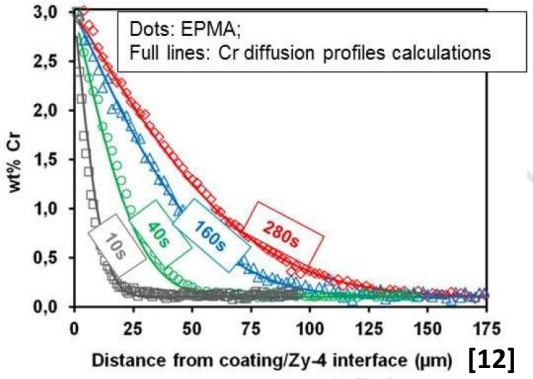

[12]

$$C(x,t) - C_0 = C - C_0 \times \left(1 - \mathrm{erf}\left(\frac{x}{2\sqrt{\boldsymbol{D}t}}\right)\right) [12]$$

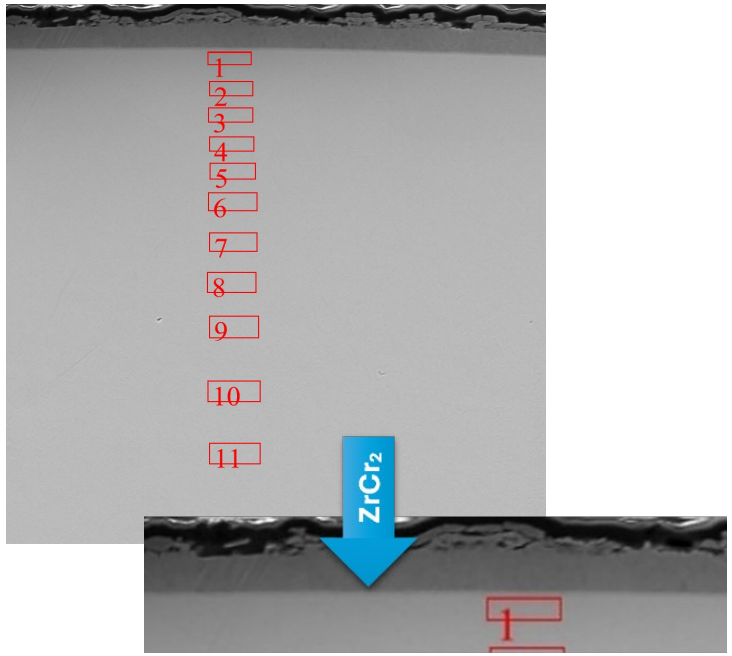

Diffusion of Cr into Zr-substrate – EDS chemical analysis (1200°C/9 min)

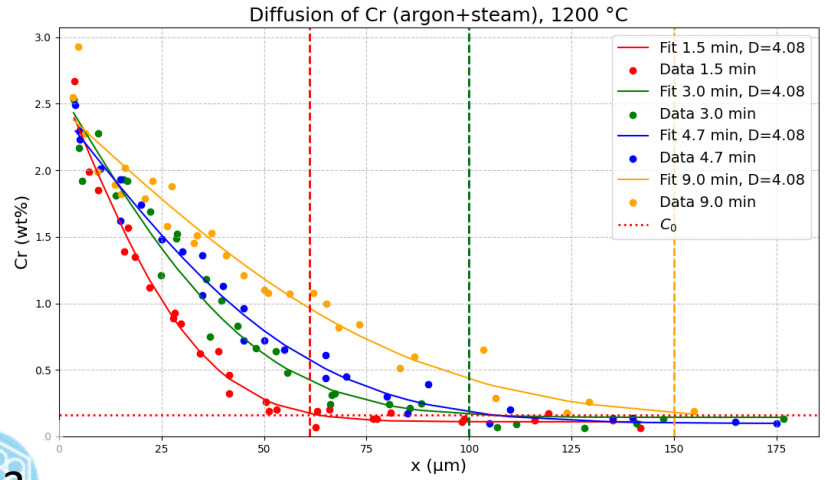

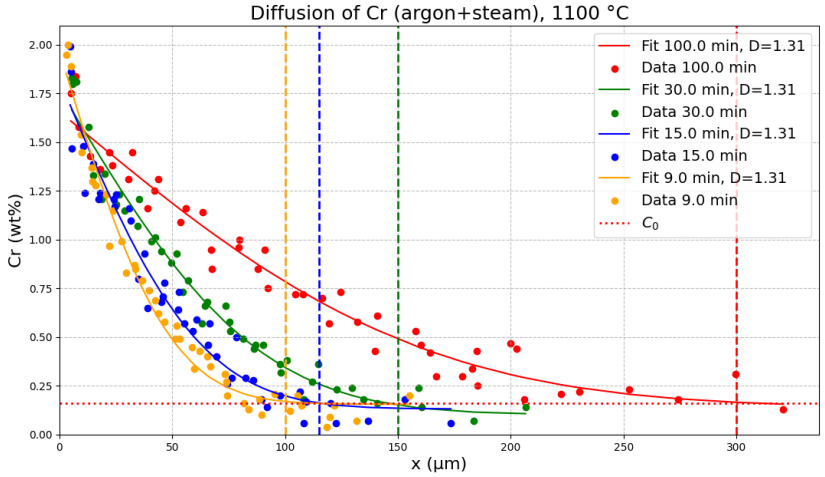

Scratch Test: Simulation of damaged coating

UJP PRAHA

- **Simulation of coating cracking due to insufficient elasticity**
- Scratch across the entire coating under different loads
  - Depth of scratch ranges from 27 to 140 μm
- Optimization of the Scratch test – ensuring a homogeneous scratch

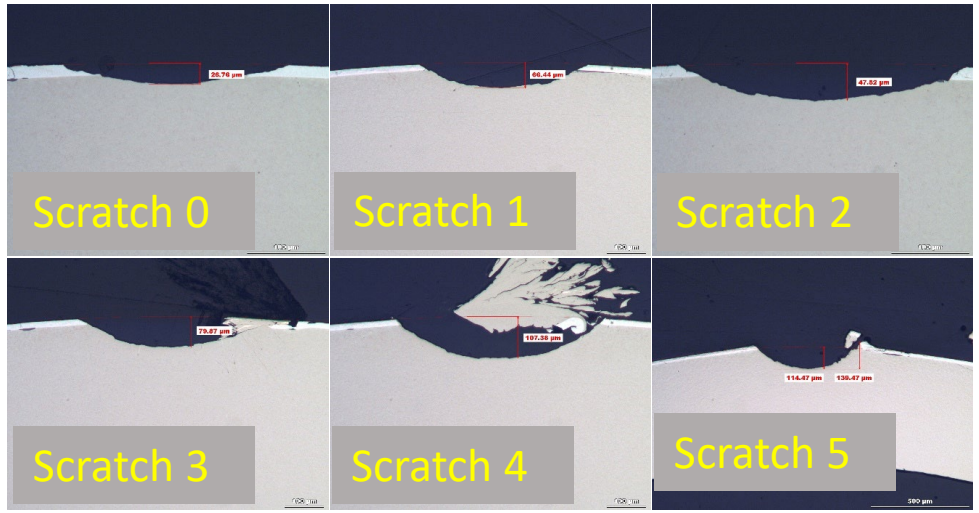

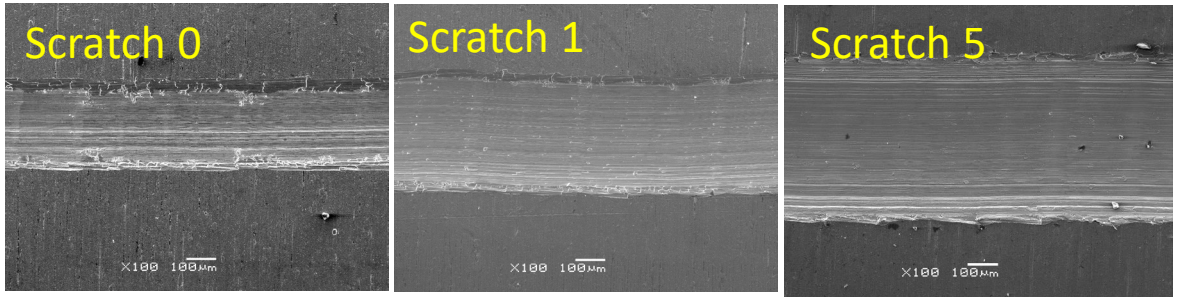

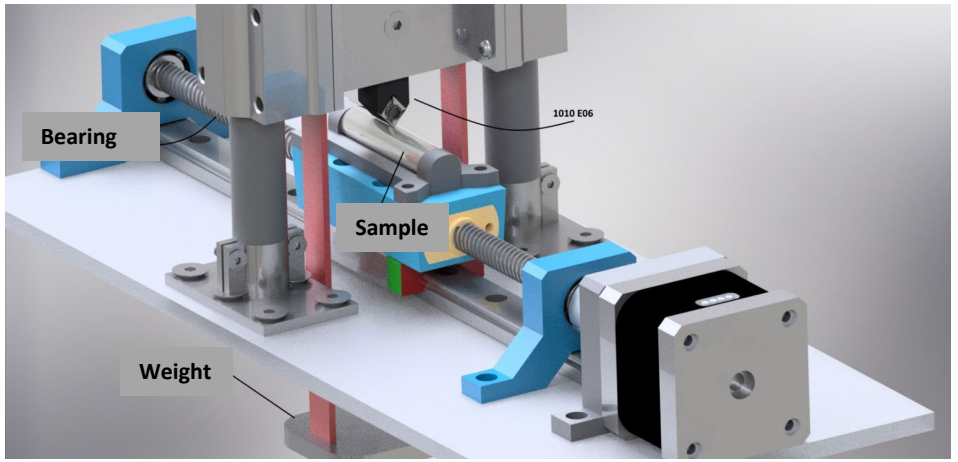

- **Stepper Motor and Lead Screw:**
  The stepper motor drives the lead screw via a coupling mechanism.
- **Linear Motion:**
  The lead screw moves the linear guide nut.
  This motion causes the carriage to travel along its path.
- **Scratch Creation:**
  A blade mounted on the carriage moves along the sample, creating the desired scratches.
- **Precision and Control:**
  The combination of the stepper motor and the mechanical guidance ensures highly precise and controllable scratches.
- **Depth Variability:**
  A weight is used to adjust and vary the depth of the scratch as needed.

Scratch Test: Results

UJP PRAHA

- **Simulation of coating cracking due to insufficient elasticity**
  - The depth of the scratch has no significant effect on the diffusion rate.

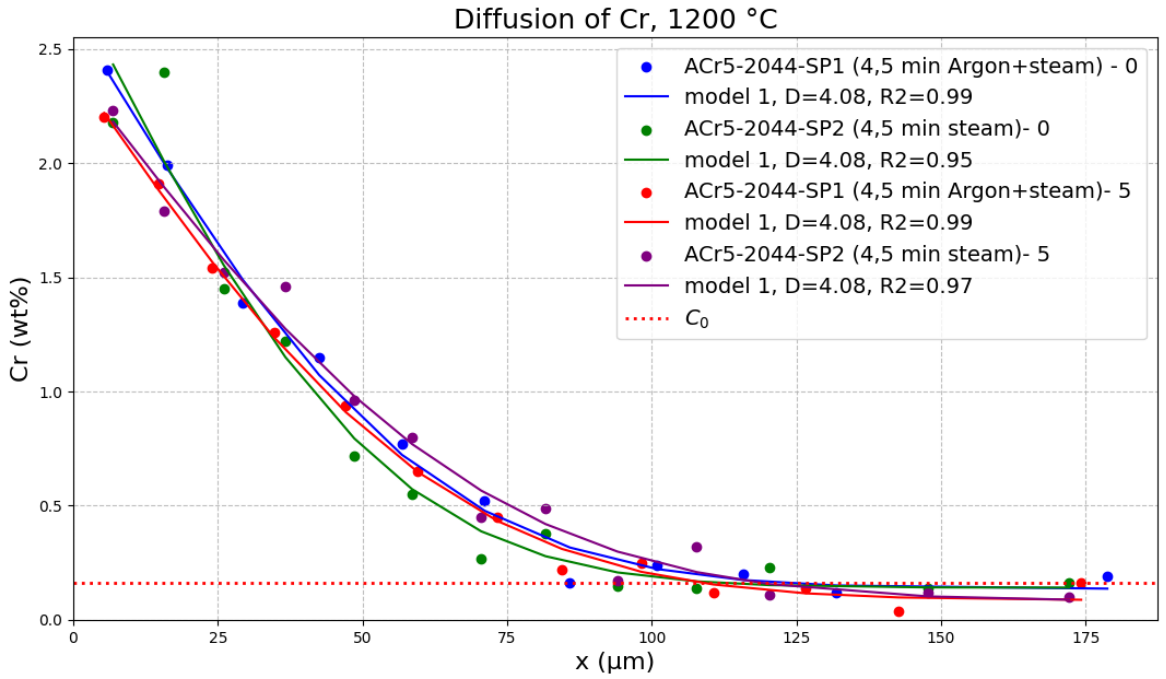

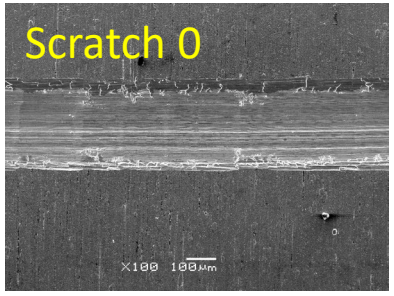

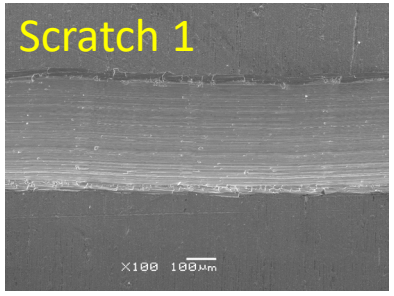

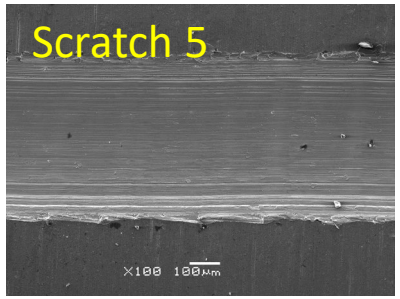

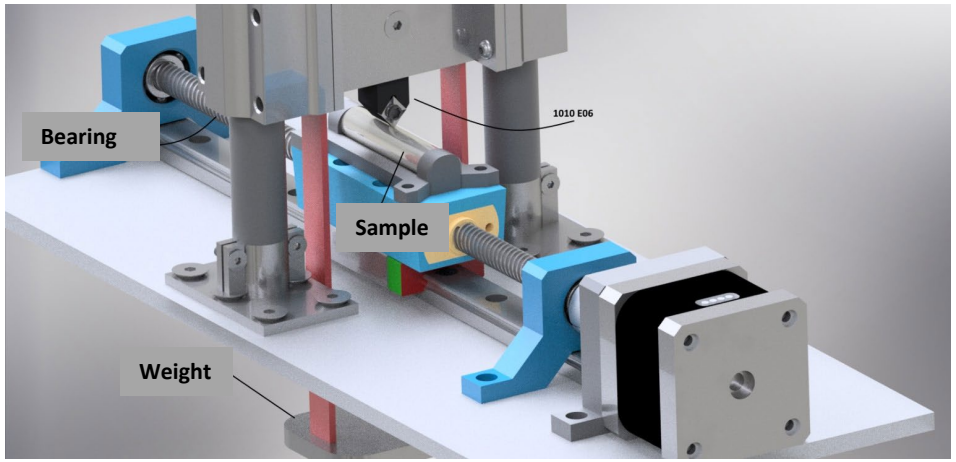

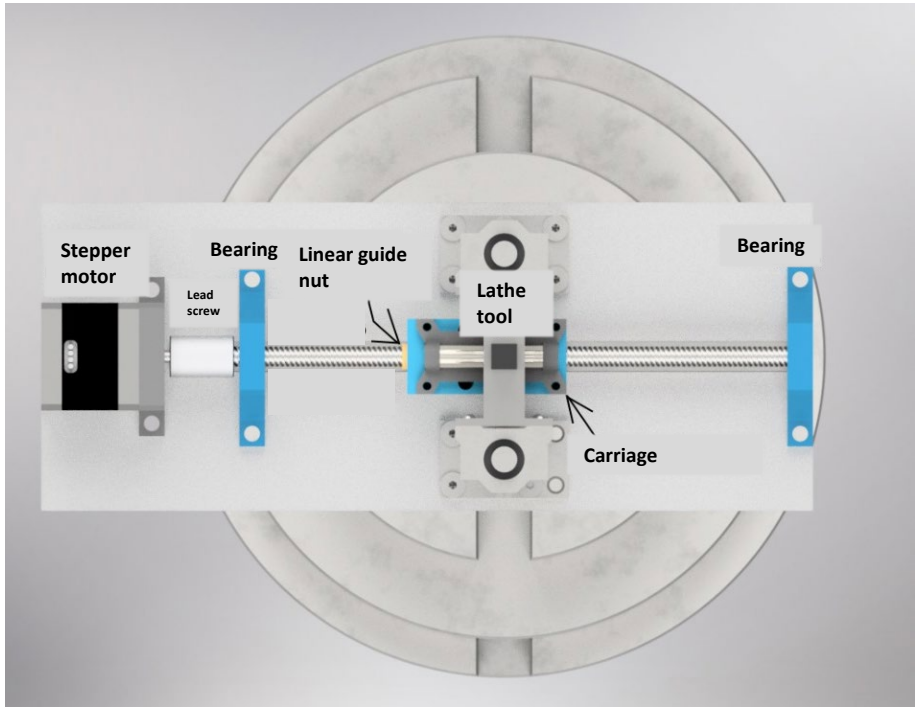

Construction of diagram (Cr-Zr1Nb)-O: WDS and Oxygen content

UJP PRAHA

- 2 types of experiment:
  - 1,5 min Argon -> 3 min steam
  - 1,5 min Argon + 3 min steam

➔ Both experiments produced similar results

➔ 0 wt% Cr-content at ~**150 µm**, **good agreement with**

Brachet et al. [13] when using **WDS**

(X Zry-4)

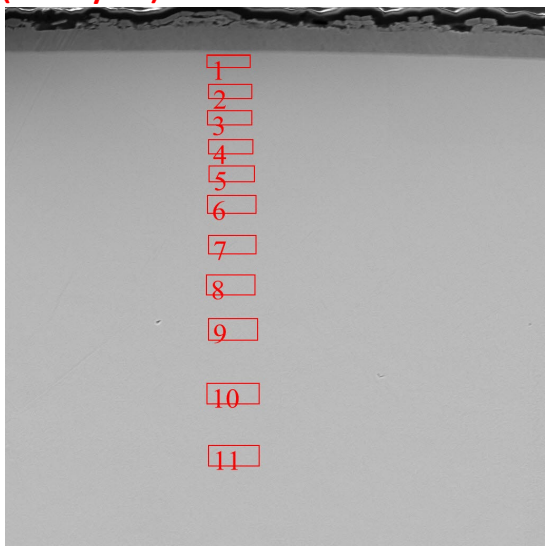

Diffusion of Cr into Zr-substrate – EDS chemical analysis (1200°C/9 min)

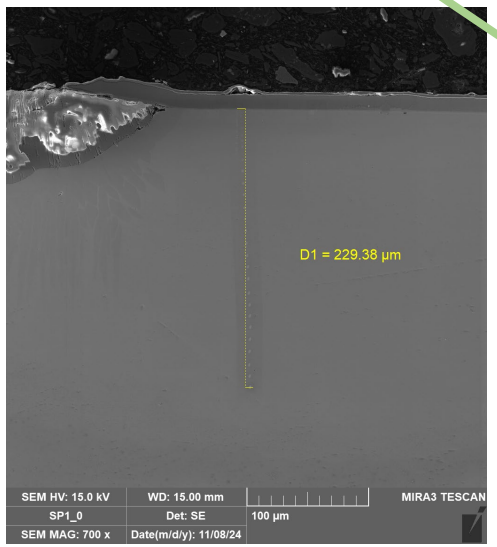

WDS chemical analysis of sample SP1 (1,5 min Argon, 3 min steam – 1200°C)

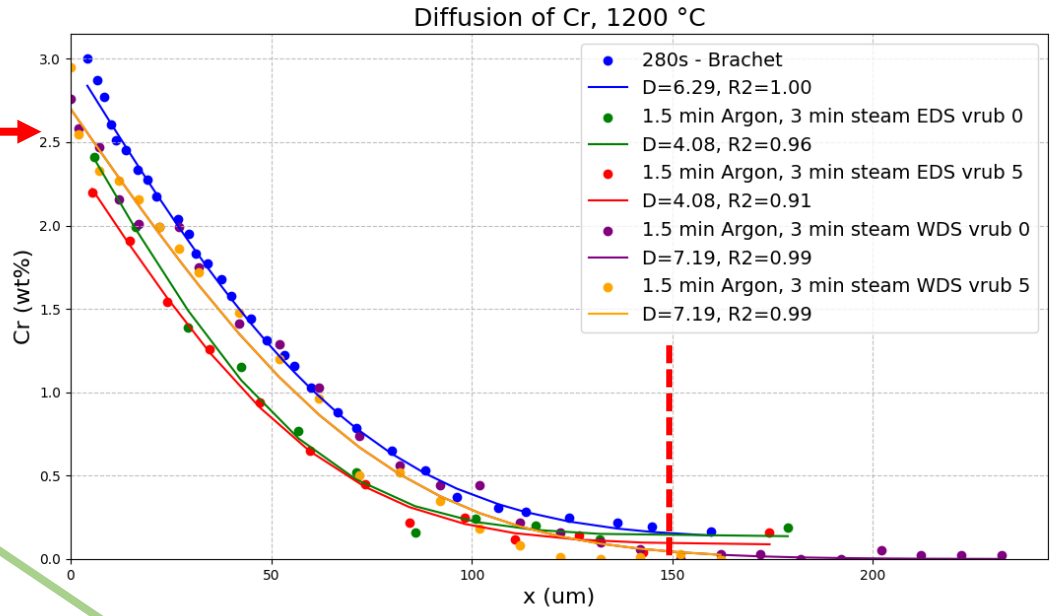

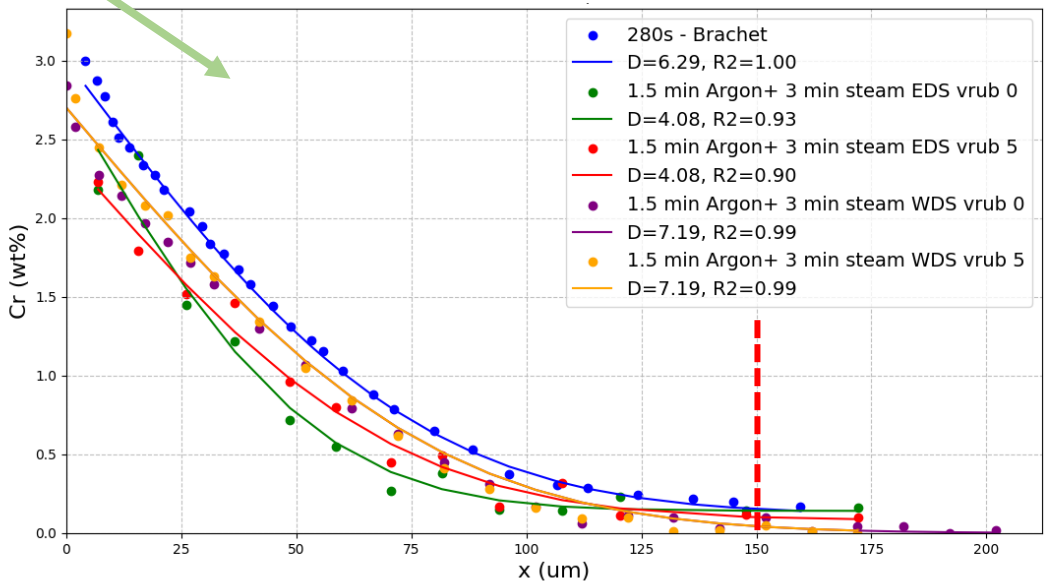

Construction of diagram (Cr-Zr1Nb)-O: Method

Classic method [11] need to produce a large quantity of samples with varying chemical compositions

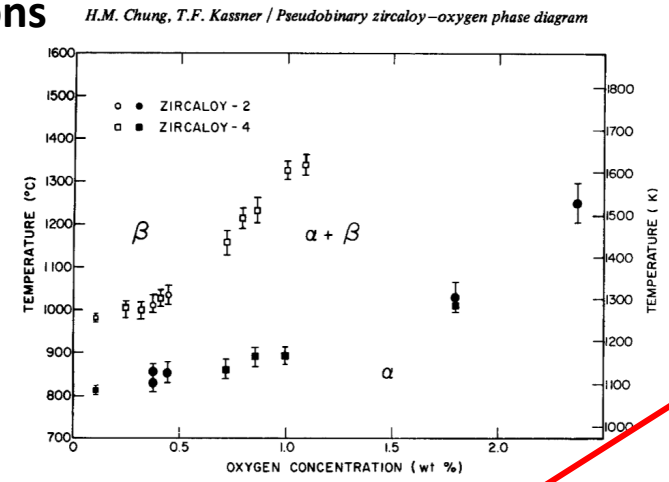

New method by Négyesi et al. [9]

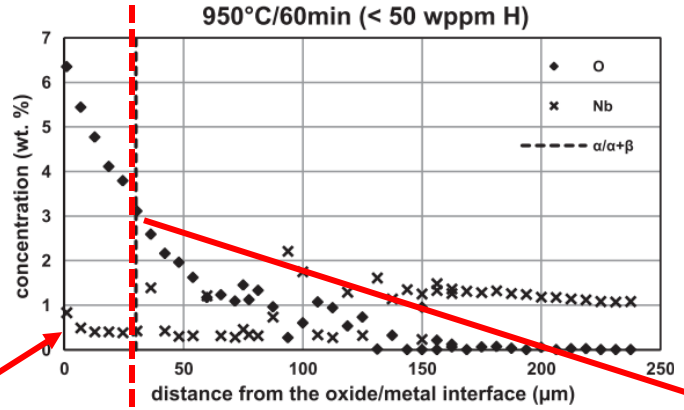

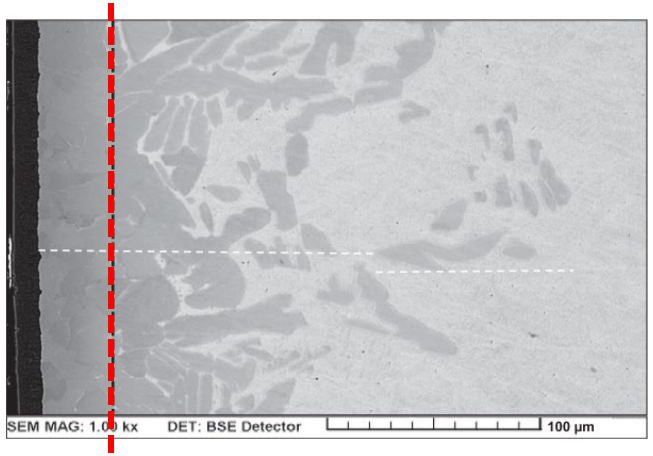

Interface of α-Zr(O)/(α+β)-Zr

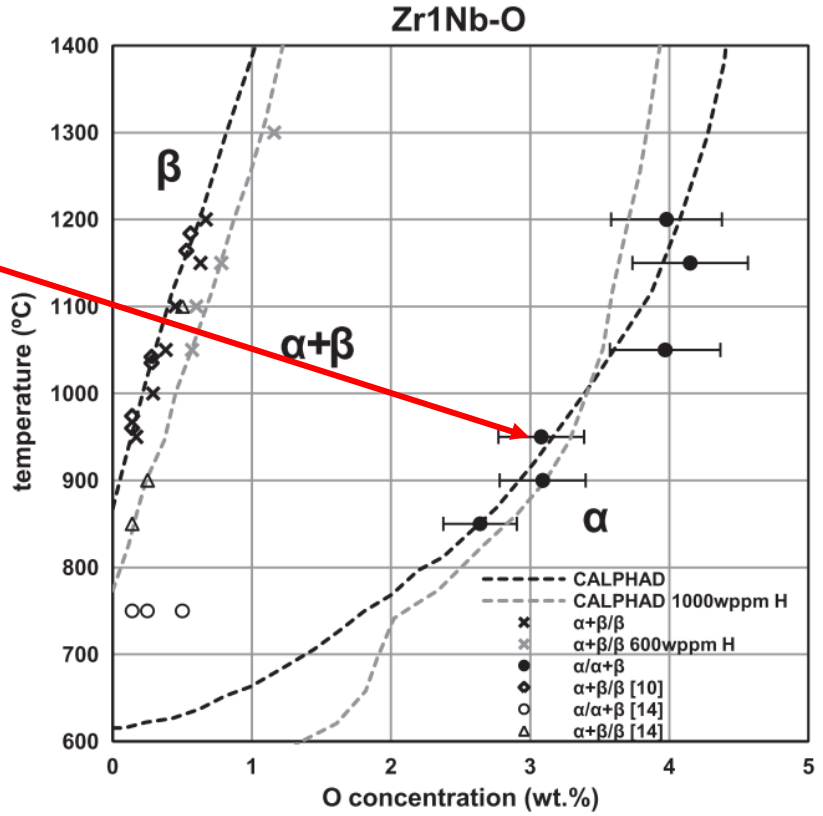

Pseudobinary Zr1Nb-Oxygen phase diagram [9]

- **The oxygen concentrations at the boundaries of the different Zr phases** (α-Zr, β-Zr, and (α+β)-Zr) were determined.
- Measurements were assumed to reflect equilibrium conditions due to isothermal oxidation followed by **rapid quenching**, which limited oxygen redistribution.

Construction of diagram (Cr-Zr1Nb)-O: Method

UJP PRAHA

- Same experiment for coated samples:
  - **Measurement of equilibrum oxygen content at phase interface (WDS)**
- For lower temperatures:
  - **Diffusion of Cr: exposition in argon, then HTO at different temperatures**

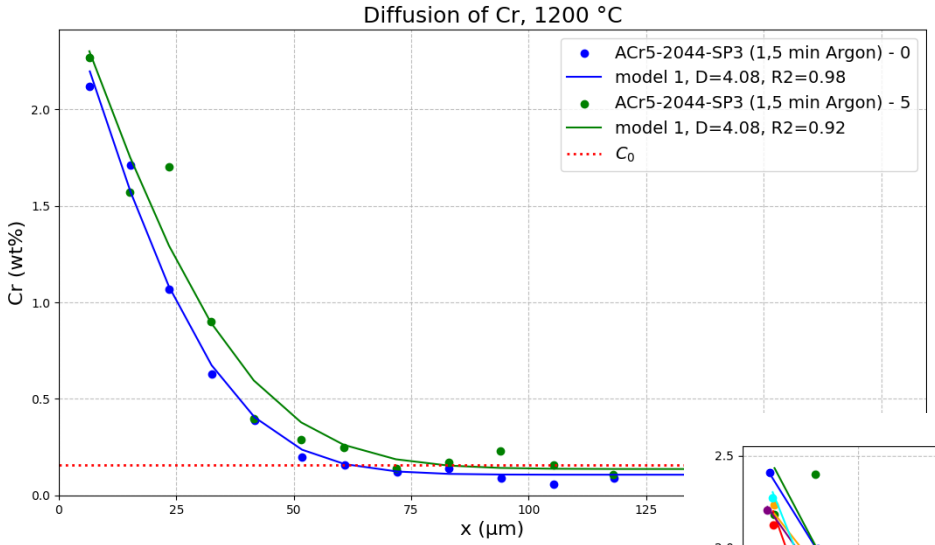

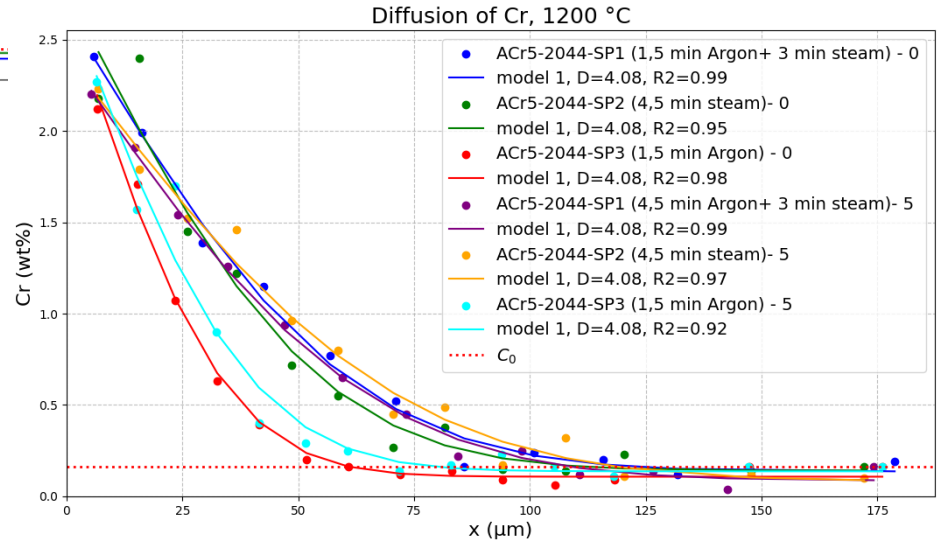

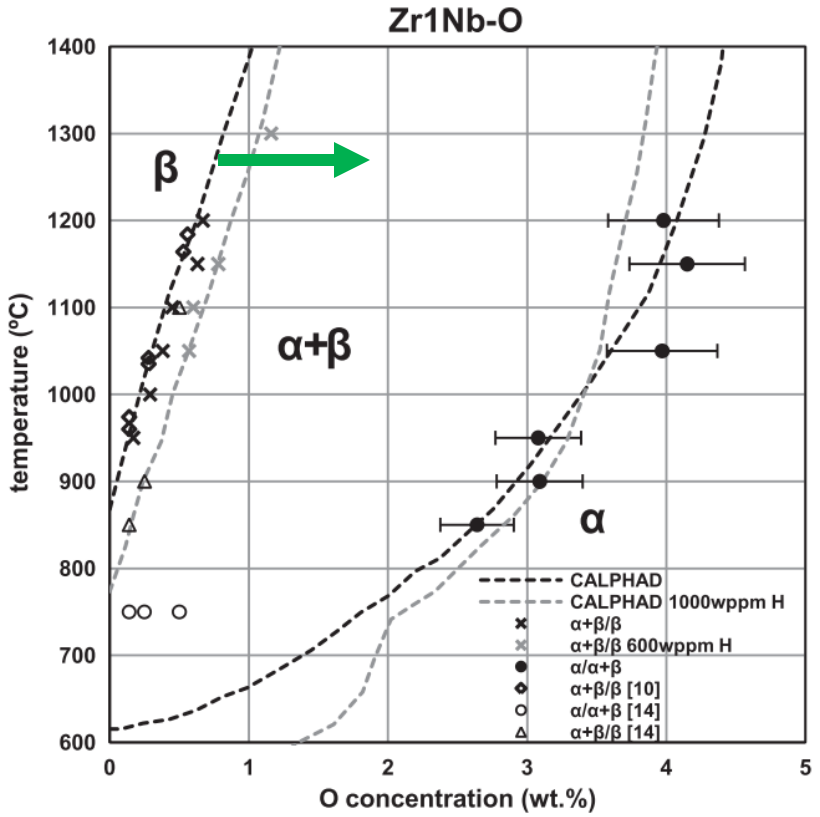

Pseudobinary Zr1Nb-Oxygen phase diagram [9]

Construction of diagram (Cr-Zr1Nb)-O: IGF and Oxygen content

UJP PRAHA

- WDS method to determine how far Cr diffused (> 150 μm)

➔ **Turn down** the outer layer and inner layer

➔ We will measure the oxygen content using **IGF (Inert Gas Fusion - G8 Galileo Brucker),** when the sample is melted in a graphite crucible at high temperatures, releasing gases that are then measured to determine their concentrations

➔ Determination of O-content in outer layer with Cr- coating and in inner layer

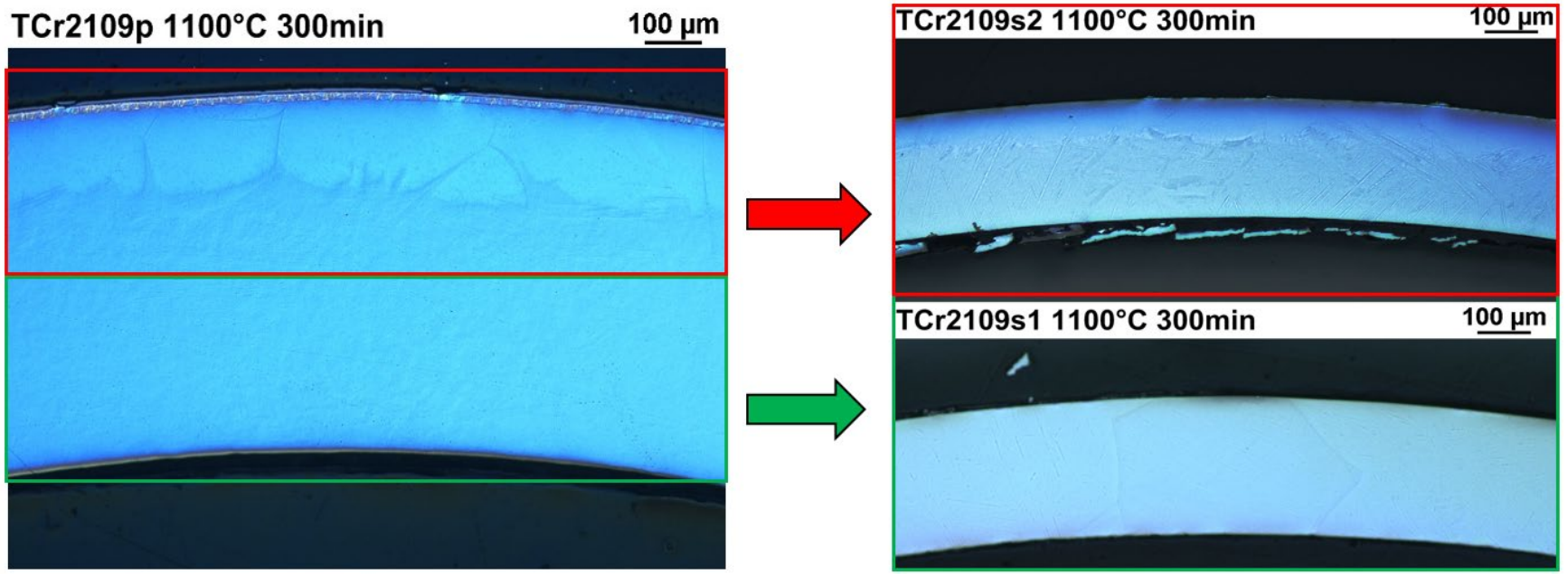

Conclusion

UJP PRAHA

- The diffusion of Cr into the Zr substrate was studied in detail.
- Scratch simulations provided insights into the effects of coating damage, highlighting **no significant impact on chromium diffusion for the tested configurations with various depths**.
- **Initial tests were conducted, showing good agreement with available literature.**
- The proposed methodologies and experiments provide a framework for studying both intact and **damaged coating** systems for zirconium alloys.

Future Work:

- **(Cr+Zr1Nb)-O phase diagram** will be constructed to provide further insights into the behavior of coated cladding under various temperature.
- The Inert Gas Fusion (IGF) method will be used to achieve more precise oxygen concentration measurements.
- Further testing will focus on **samples with scratches and studying oxygen diffusion.**
- Additional experiments will also explore **multiple scratches** on the coating to better understand its durability and performance under different conditions.

Thank you for your attention

This work was performed within
project TK04030168

Sources

1. *TERRANI, Kurt A. Accident tolerant fuel cladding development: Promise, status, and challenges. Journal of Nuclear Materials [online]. 2018, 501, 13–30. ISSN 00223115. Avaible:: doi:10.1016/j.jnucmat.2017.12.043*

2. *GOLDNER, FRANK J., MCCAUGHEY, W, WACHS, DANIEL M., KAMERMAN, D, JENSEN, COLBY, HAYES, STEVE L., NELSON, ANDREW, HARP, JASON, CAPPS, NATHAN, LINTON, KORY, PETRIE, CHRISTIAN, SALEH, TARIK A., and WHITE, JOSHUA T. Accident Tolerant Fuels Program — Update on a National Initiative. In : TopFuel. Online. United States, 2021. Available from: https://www.osti.gov/servlets/purl/1873835.*

3. *ČERVENKA, Petr, KREJČÍ, Jakub, CVRČEK, Ladislav, ROZKOŠNÝ, Vojtěch, MANOCH, František, RADA, David and KABÁTOVÁ, Jitka. EXPERIMENTAL STUDY OF DAMAGED CR-COATED FUEL CLADDING IN POST-ACCIDENT CONDITIONS. Acta Polytechnica CTU Proceedings. Online. 1 December 2020. Vol. 28, p. 1–7. [Accessed 8 August 2023]. DOI 10.14311/APP.2020.28.0001.*

4. *YANG, Jianqiao, STEINBRÜCK, Martin, TANG, Chongchong, GROSSE, Mirco, LIU, Junkai, ZHANG, Jinming, YUN, Di and WANG, Shuzhong. Review on chromium coated zirconium alloy accident tolerant fuel cladding. Journal of Alloys and Compounds. Online. February 2022. Vol. 895, p. 162450. [Accessed 8 August 2023]. DOI 10.1016/j.jallcom.2021.162450.*

5. *BRACHET, J., LEE SAUX, M., LE FLEM, M., URVOY, S., ROUESNE, E., GUILBERT, T., COBAC, C., LAHOGUE, J., ROUSSELOT, J., and TUPIN, M. On-going studies at CEA on chromium coated zirconium based nuclear fuel claddings for enhanced accident tolerant LWRS fuel. 2015.*

6. *BRACHET, Jean-Christophe, ROUESNE, Elodie, RIBIS, Joël, GUILBERT, Thomas, URVOY, Stéphane, NONY, Guillaume, TOFFOLON-MASCLET, Caroline, LE SAUX, Matthieu, CHAABANE, Nihed, PALANCHER, Hervé, DAVID, Amandine, BISCHOFF, Jérémy, AUGEREAU, Julien and POUILLIER, Edouard. High temperature steam oxidation of chromium-coated zirconium-based alloys: Kinetics and process. Corrosion Science. Online. May 2020. Vol. 167, p. 108537. [Accessed 21 August 2023]. DOI 10.1016/j.corsci.2020.108537.*

7. *KREJČÍ, J.; KABÁTOVÁ, J.; MANOCH, F.; KOČÍ, J.; CVRČEK, L.; MÁLEK, J.; KRUM, S.; ŠUTTA, P.; BUBLÍKOVÁ, P.; HALODOVÁ, P.; NAMBURI, H. K.; ŠEVEČEK, M. Development and testing of multi- component fuel cladding with enhanced accidental performance. Nuclear Engineering and Technology, roč. 52, č. 3, s. 597–609. issn 1738-5733. Dostupné z doi: 10.1016/j.net.2019.08.015.*

8. *Dongju Kim, Martin Ševeček, Youho Lee, Characterization of eutectic reaction of Cr and Cr/CrN coated zircaloy accident tolerant fuel cladding,, Nuclear Engineering and Technology, 2023, ISSN 1738-5733, https://doi.org/10.1016/j.net.2023.06.015.*

9. *NÉGYESI, M., J. BURDA, V. KLOUČEK, J. LORINČÍK, J. SOPOUŠEK, J. KABÁTOVÁ, L. NOVOTNÝ, S. LINHART, T. CHMELA, J. SIEGL a V. VRTÍLKOVÁ. Contribution to the study of the pseudobinary Zr1Nb-Oxygen phase diagram by local oxygen measurements of Zr1Nb fuel cladding after high temperature oxidation. Journal of Nuclear Materials [online]. 2012, 420(1–3), 314–319. ISSN 00223115. Avaible:: doi:10.1016/j.jnucmat.2011.10.022*

10. *ČERVENKA, Petr. KOROZNÍ VLASTNOSTI PALIVOVÉHO POKRYTÍ SE ZVÝŠENOU ODOLNOSTÍ VŮČI HAVARIJNÍM SITUACÍM. B.m.: ČVUT. 2023*

11. *Krejčí, J. Disertační práce. OXIDACE PALIVOVÉHO POKRYTÍ V TEPELNĚ-CHEMICKÝCH PODMÍNKÁCH JADERNÉHO REAKTORU, FJFI ČVUT. 2018*

12. *BRACHET, Jean-Christophe, Isabel IDARRAGA-TRUJILLO, Marion Le FLEM, Matthieu Le SAUX, Valérie VANDENBERGHE, Stephane URVOY, Elodie ROUESNE, Thomas GUILBERT, Caroline TOFFOLON-MASCLET, Marc TUPIN, Christian PHALIPPOU, Fernando LOMELLO, Frédéric SCHUSTER, Alain BILLARD, Gihan VELISA, Cédric DUCROS a Frédéric SANCHETTE. Early studies on Cr-Coated Zircaloy-4 as enhanced accident tolerant nuclear fuel claddings for light water reactors. Journal of Nuclear Materials [online]. 2019, 517, 268–285. ISSN 00223115. Avaible:: doi:10.1016/j.jnucmat.2019.02.018*

Protective coatings on zirconium-based alloys: Coating methods

UJP PRAHA

- Different coating methods (Arc Deposition, Magnetron sputtering, Coldspray)
  - **PVD MS at CTU - Department of Materials Engineering (250°C)**
  - **Ionbond Czechia s.r.o. (300°C)**
  - *HiPIMS (high power pulsed magnetron sputtering) – Faculty of Electrical Engineering (Cr - 250°C, 400°C)*
- The quality of the layer does not depend on the method used, but **on the parameters** (energy, temperature)

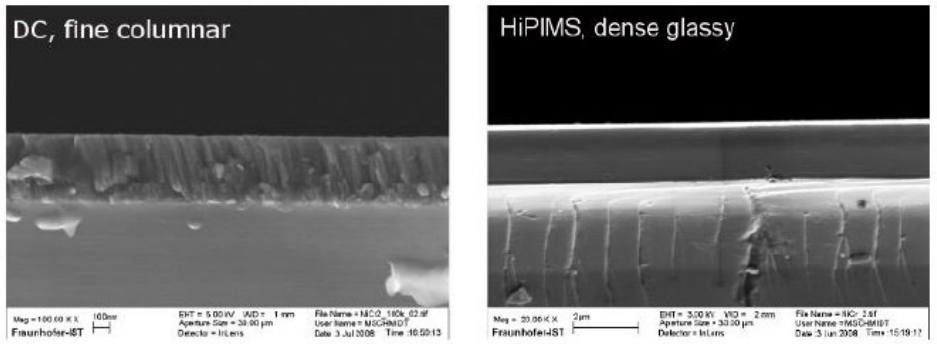

PVD MS vs. HiPIMS

The chamber of the Hauzer Flexicoat 850 coating machine – PVD, FS, ČVUT

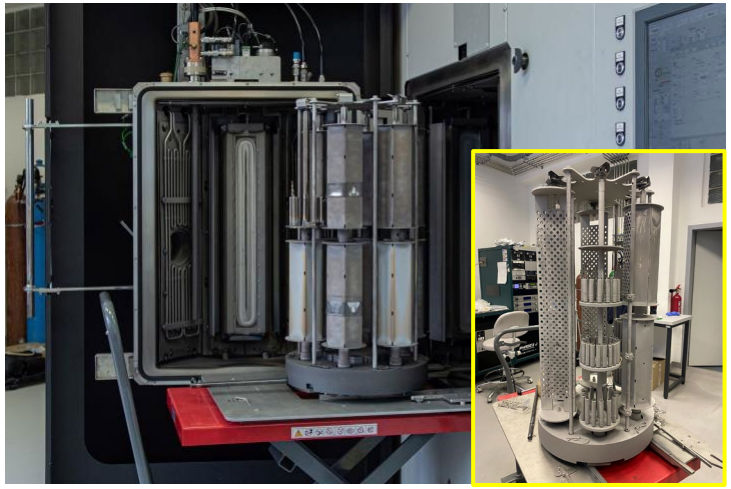

HiPIMS – FEL ČVUT

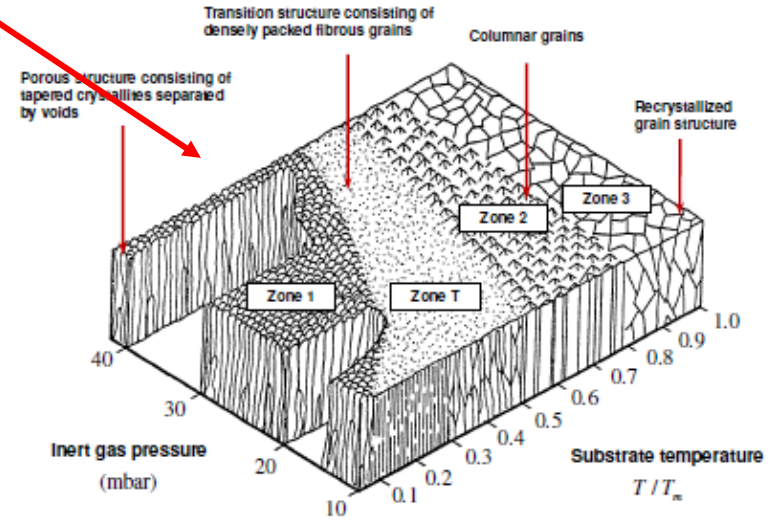

Dependence of internal overpressure, deposition temperature T and melting temperature T_m on thin film structure

FERNANDEZ, J.J. Tuning the thermal conductivity of polycrystalline films via multiscale structural defects and strain. 2015.

Martin Sevecek

CTU

Cr-Nb Coated Zr = Suitable ATF Candidate for BWRs

The coated cladding concept was originally proposed as the solution to increasing the fretting resistance of cladding materials in Boiling Water Reactors (BWRs) and it was further developed by several research groups into corrosion and fret-resistant coating. However, it has been shown that pure metallic Cr coatings developed mainly for PWR systems do not form stable oxides in BWR chemistries during normal operation. In addition, further improving the fretting resistance of Cr coating is beneficial to existing Pressurized Water Reactors (PWRs) and future Small Modular Reactors (SMRs). For BWRs, there were several predominantly ceramic materials such as ARMOR coating, CrN, CrWN, CrZrN TiN, CrxNx, and CrN-NbN proposed and studied as the coating candidates for BWRs. Ceramic coatings are very hard and improve significantly fretting resistance but at the same time brittle with limited ability to plastically deform. Fuel rod deformations during long-term operation (creep, PCMI) as well as accidental conditions (ballooning, PCMI, or axial loading during quenching) can result in excessive stresses and early fracture of the coatings so that they no longer provide the protective function. Therefore, this study focuses on a novel Cr-Nb metallic coating system and its performance in simulated BWR and VVER operational modes and accidental conditions. Two types of Cr-Nb coatings were deposited on commercial Zr-based alloys using magnetron sputtering and were tested in various separate effect tests to investigate their feasibility for BWRs and VVERs. In addition, arc-melted Cr-Nb alloys with the same composition were studied separately to provide more information about the material behavior. Standard uncoated Zr-based alloys were included in all tests as a reference to provide a baseline for the evaluation of the coated cladding concept. The out-of-pile experimental investigations includes detailed characterizations of as-received Cr-Nb coatings as well arc-melted Cr-Nb alloys, long-term hydrothermal corrosion tests, high-temperature steam oxidation tests, and thermophysical tests (thermal expansion, thermal conductivity and hardness).

Massachusetts Institute of Technology

Cr-Nb Coated Zr = Suitable ATF Candidate for BWRs

Martin Ševeček[1,2], Petr Červenka[1,2], Alžběta Endrychová[1,3], Jakub Krejčí[3], Ladislav Cvrček[1], Arunkumar Seshadri[2], Koroush Shirvan[2]

[1]Czech Technical University in Prague
[2]Massachusetts Institute of Technology
[3]UJP Praha, a.s.

29th QUENCH workshop
Karlsruhe, 30th of September 2024

Coated Zr alloys

- Motivation for application of coatings = improve material resistence in severe accidents => only **Cr-**, **Si-** and **Al**-based materials for LWRs
- High TRL or pure Cr coatings applied by various methods. Cr-coated Zr has been accepted as the main product by major fuel vendors (WEC, Framatome, KNF, TVEL, CGN) for **PWRs** with LTAs and LTRs in several NPPs around the world.
- Cr coatings form stable protective Cr_2O_3 in PWRs with minor volatilization, ~100x slower HT oxidation rate; ~50x lower H pickup; HT mechanical strengthening (ballooning/burst); potentially reduced CRUD deposition and fretting resistance
- Pure Cr seem unsuitable for BWRs due to Cr_2O_3 dissolution that accelerates with irradiation. Several candidates (mostly ceramics) proposed in the past, low TRL technology, optimization is still ongoing, e.g.:
  - HRP – CrN, TiAlN, AlCrN
  - GE – ARMOR coating,…
  - Westinghouse Sweden – CrN-CrNbN, CrWN,…

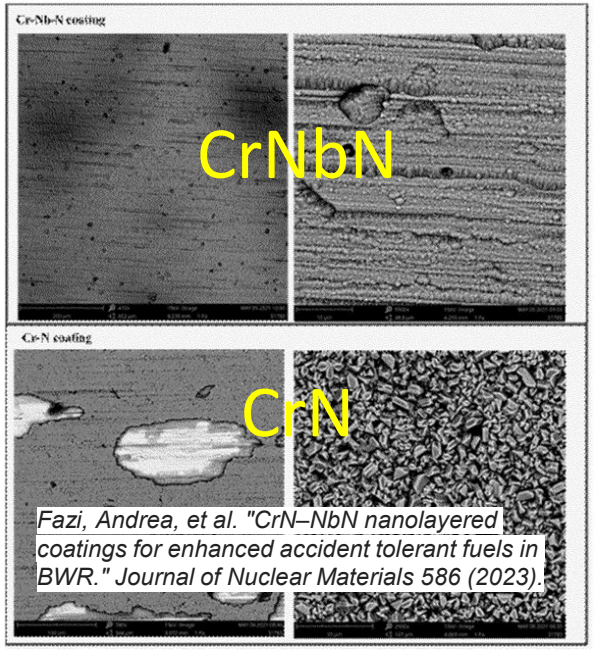

Fazi, Andrea, et al. "CrN–NbN nanolayered coatings for enhanced accident tolerant fuels in BWR." Journal of Nuclear Materials 586 (2023).

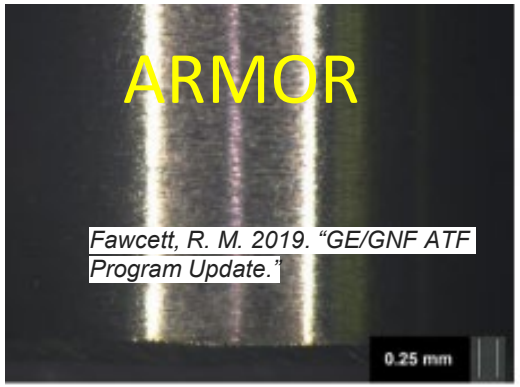

Fawcett, R. M. 2019. "GE/GNF ATF Program Update."

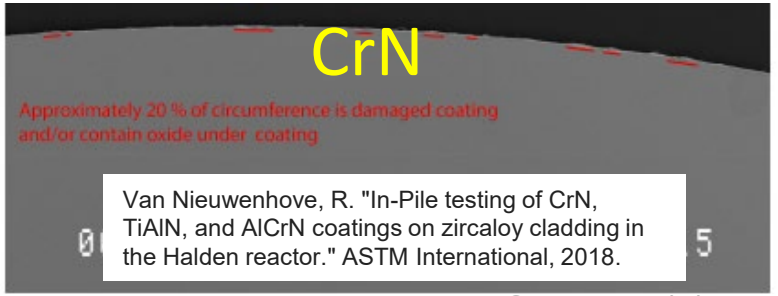

Van Nieuwenhove, R. "In-Pile testing of CrN, TiAlN, and AlCrN coatings on zircaloy cladding in the Halden reactor." ASTM International, 2018.

BWR Cladding Corrosion Testing - Motivation

- Long-term corrosion (and the accompanying H absorption) is of prime interest for new cladding materials – especially in-pile data
- Corrosion is an electrochemically-driven process affected by:
  - microstructure and microchemistry of the alloy surface
  - nature of the oxide layer that forms
  - temperature at the metal/oxide interface
  - chemistry and thermohydraulics of the coolant
  - effects of irradiation
  - effects of time
- Out-of-pile corrosion tests allow to:
  - ✓ Downselect the candidate materials and deposition methods before moving to expensive in-pile testing
  - ✓ Understand the in-pile results by providing continuous reference data for future comparison
- Uniform corrosion (normal mode) – 5-10x higher for irradiation-assisted corrosion

	PWR/VVER	BWR
Operational PCT [°C]	325-350	285-305
Oxygen [ppb]	< 0.05	2000 (NWC); 200-400 (HWC)
Hydrogen [ppm]	2-4	0.05-0.3
Chemical additions	Boric acid + Plant-specific (LiOH, KOH, NaOH, NH3)	Plant specific (e.g. Zn injection) but generally limited
Fast flux [n/cm²*s]	6-9E13	4-7E13

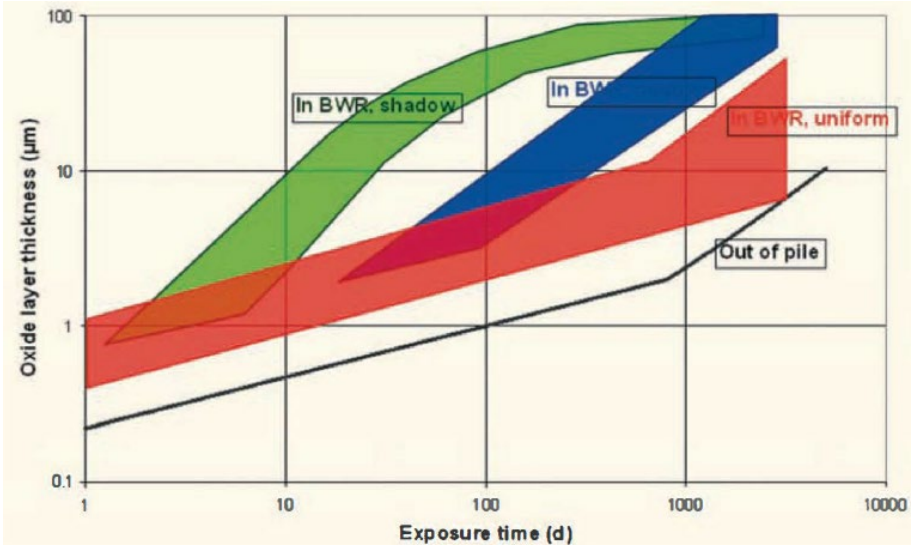

Cr/Nb-based Coatings – New Coating Design

- Cr oxides formed on Cr or CrN coating show appreciable solubility in BWR-NWC condition
- SS as chromia-forming material does not dissolve due to the presence of Fe and Ni that form less soluble compounds which motivates further studies of Cr-based coatings
- Pourbaix diagram at 300 °C indicates the equilibrium between $Cr_2O_3/HCrO_4^-$ is indicated to be at approximately 80 mV (SHE) whereas the Electro-Chemical Potential (ECP) of stainless steel under BWR-NWC conditions is in the range of 100 to 200 mV
- New coating design needed for BWR fuel rods. Idea is based on:
  - Westinghouse Sweden patent – “A nuclear fuel rod cladding tube and a method for manufacturing a nuclear fuel rod cladding tube” from June 2023: one of the candidates - Cr-Nb-N – 4-15µm with Nb between 5-35at.% (ceramic coatings)
  - MIT patent “OXIDATION AND SULFIDATION RESISTANT CHROMUM-NIOBIUM ALLOY” - Cr preferably 38-60 wt.% and Nb 40-62 wt.% (60/40wt.% = 73/27at.%)

Cook, William G., and Robert P. Olive. "Pourbaix diagrams for chromium, aluminum and titanium extended to high-subcritical and low-supercritical conditions." *Corrosion science* 58 (2012): 291-298.

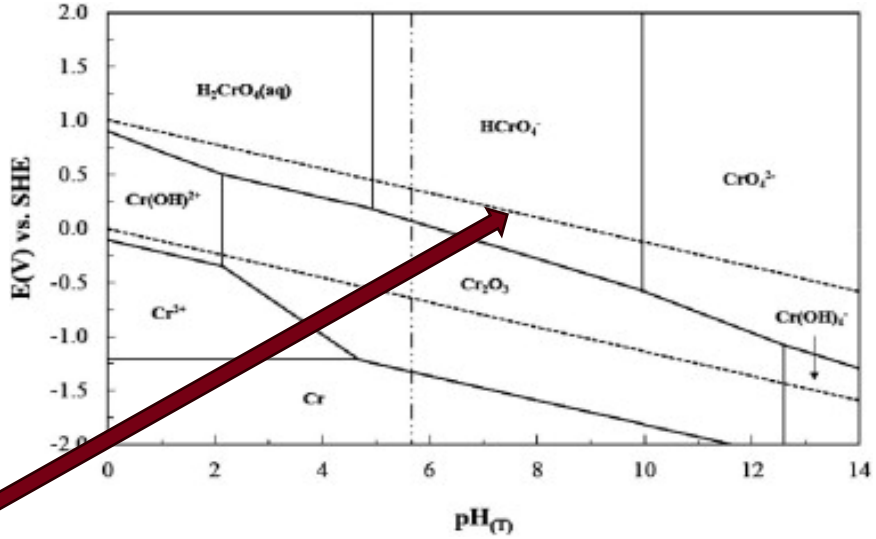

OXIDATION AND SULFIDATION RESISTANT CHROMIUM-NIOBIUM ALLOY

Inventors: **Linn W. Hobbs**, Belmont; **Chuxin Zhou**, Lexington; **Julia C. Duncan**, Somerville, all of Mass.

Assignee: **Massachusetts Institute of Technology, a MA Corp.**, Cambridge, Mass.

Appl. No.: **65,437**

Filed: **May 24, 1993**

As-manufactured Cr-Nb

Cr-Nb Metallic Coatings

- **Two types of Cr-Nb coatings produced by unbalanced magnetron sputtering at CTU – goal 85/15 and 70/30**
  - 82/18 (±3)at.% - high alloy
  - 67.5/32.5 (±3)at.% - low alloy
- **Three substrates used:**
  - Zry-4 (MIT), E110 (UJP), LK3 (Westinghouse Sweden)

	Zircaloy-4	LK3	Zr1Nb
Sn [wt.%]	1.34-1.36	1.2-1.45	-
Fe [wt.%]	0.21	0.15-0.2	-
Cr [wt.%]	0.11-0.12	0.05-0.15	-
Ni [wt.%]	-	0.03-0.08	-
O [ppm]	1150	-	-
Nb [wt.%]	-	-	1
Zr	balance	balance	balance
OD [mm]	9.5	9.84	9.1
Wall thickness [mm]	0.575	0.44	0.57

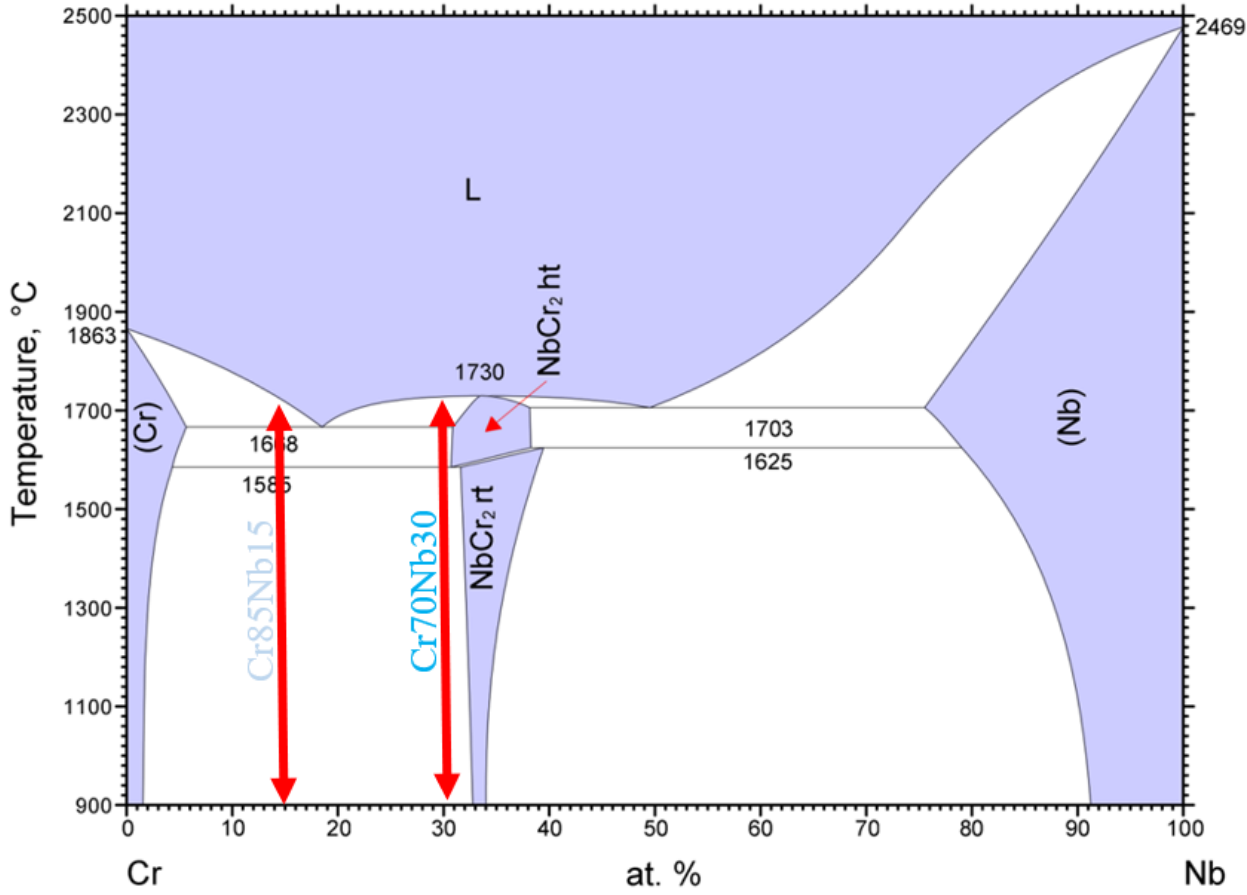

	Cr70Nb30	Cr85Nb15
Composition measured by EDX [at.%]	67.5/32.5 (±3)	82/18 (±3)
Composition measured by WDS [at.%]	75.9/24.1 (±1)	86.3/13.7 (±1)
Thickness measured by Calotest [µm]	7.0	6.2
Thickness measured on SEM micrograph [µm]	8-8.2	6.9-7.0
Thickness measured on the LOM micrograph [µm]	8.6-9.2	7.2-7.9

Cr70Nb30

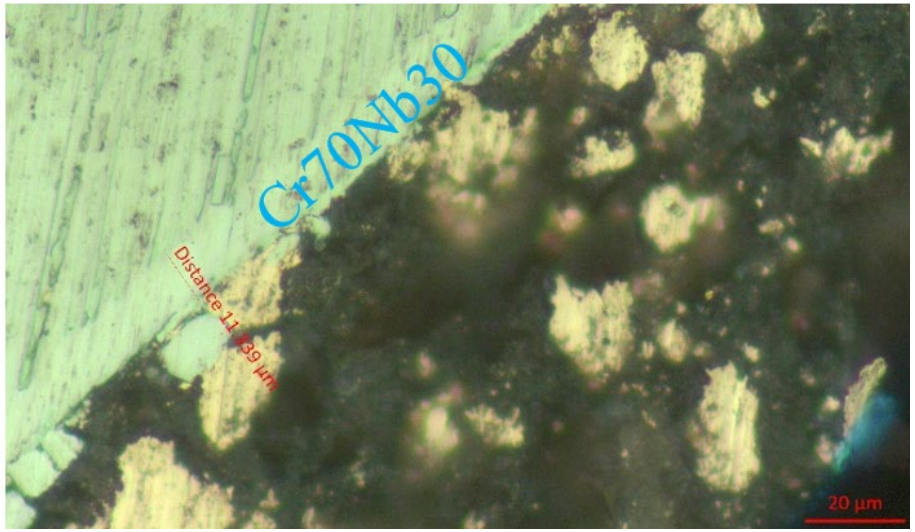
Cr70Nb30
Distance 11.89 µm
20 µm

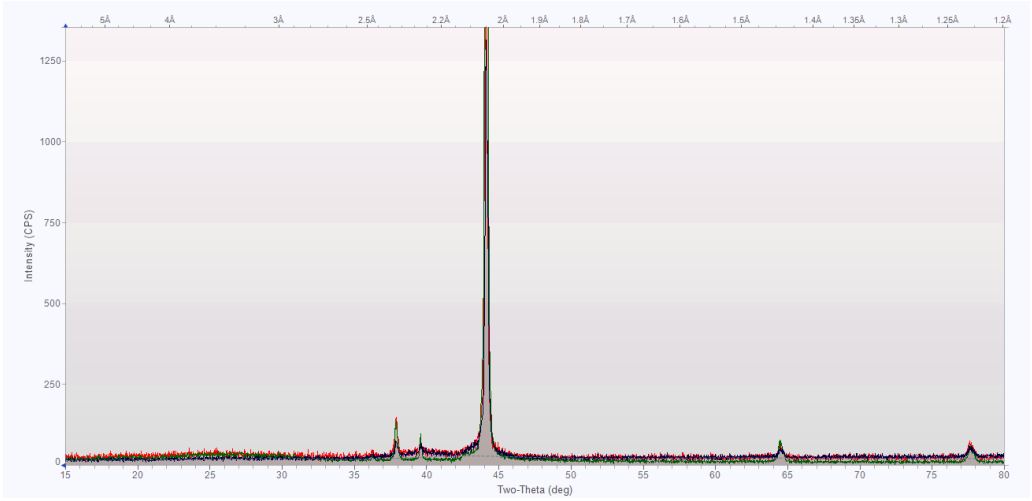
Intensity (CPS)
Two-Theta (deg)

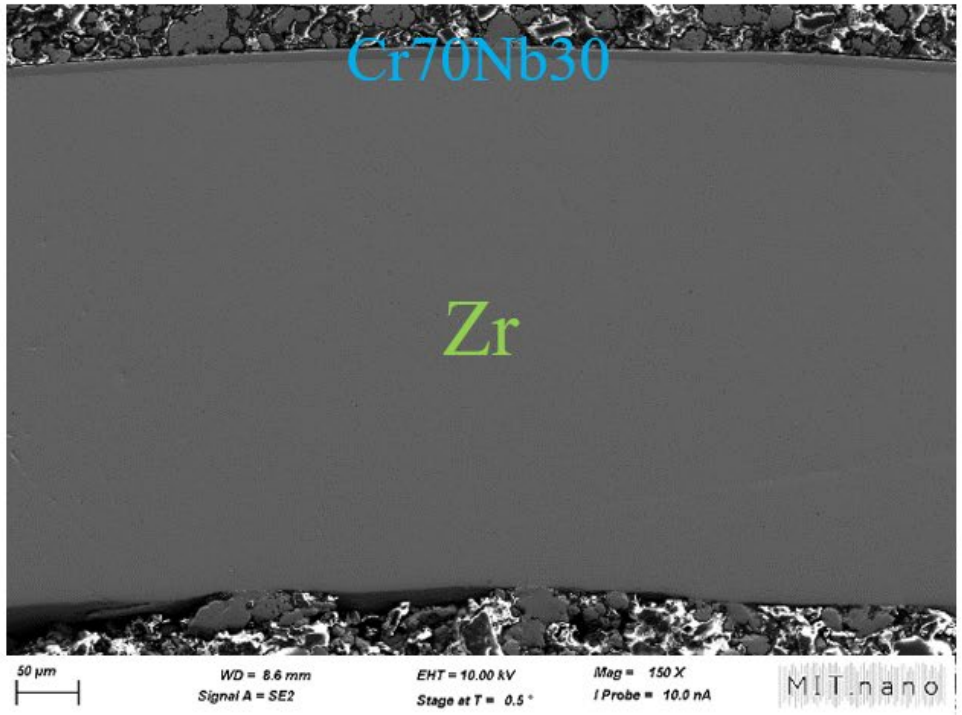
Cr70Nb30
Zr
50 µm
WD = 8.6 mm
Signal A = SE2
EHT = 10.00 kV
Stage at T = 0.5 °
Mag = 150 X
I Probe = 10.0 nA
MIT.nano

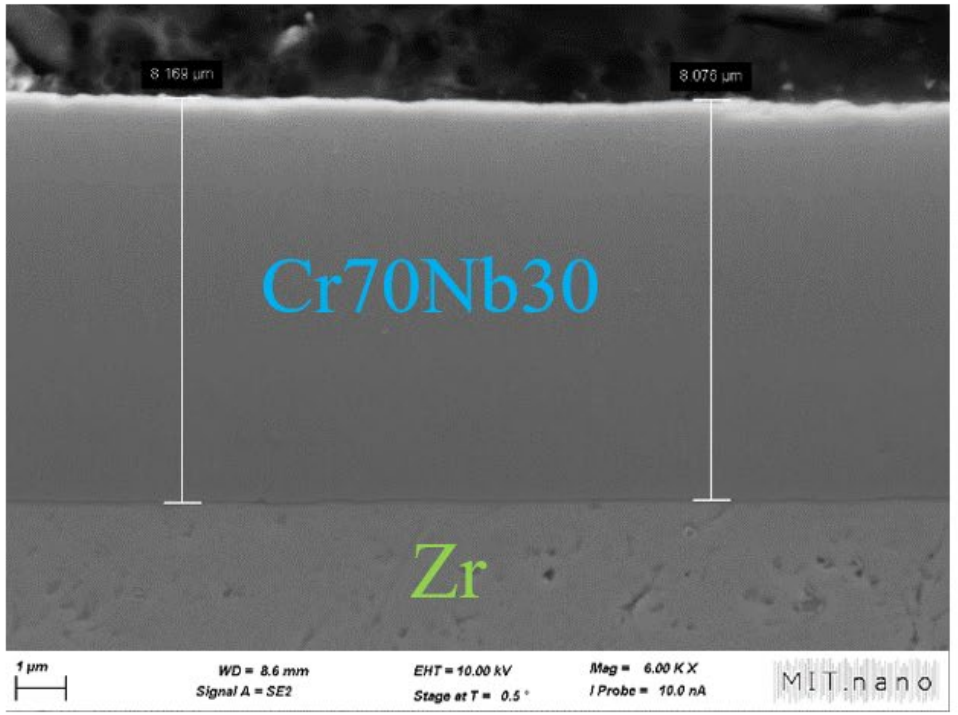
8.168 µm
8.076 µm
Cr70Nb30
Zr
1 µm
WD = 8.6 mm
Signal A = SE2
EHT = 10.00 kV
Stage at T = 0.5 °
Mag = 6.00 K X
I Probe = 10.0 nA
MIT.nano

Cr85Nb15

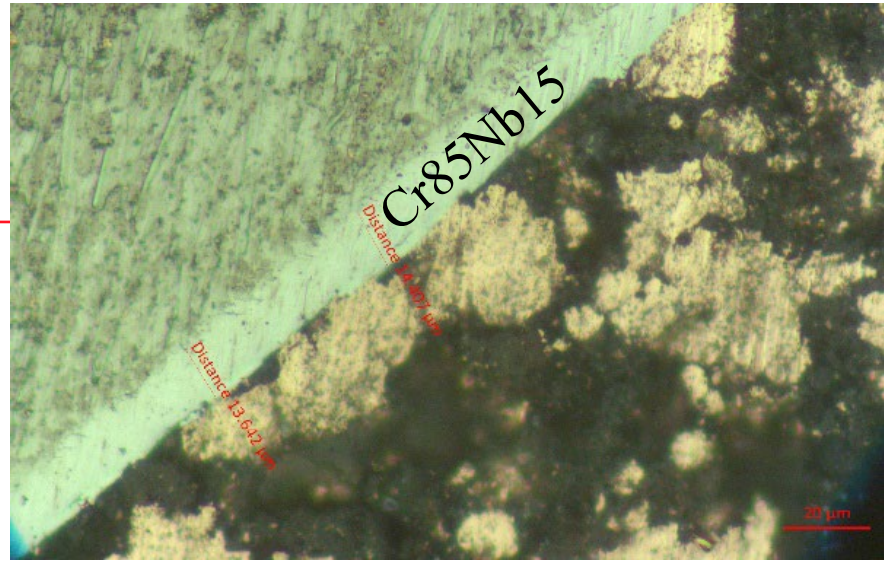
Cr85Nb15
Distance 14.497 µm
Distance 13.642 µm
20 µm

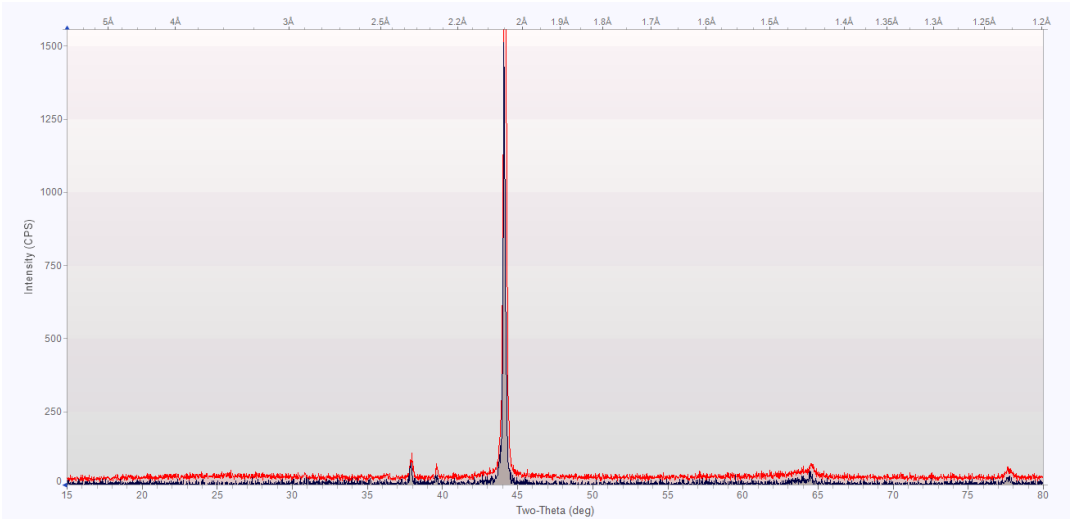
Intensity (CPS)
Two-Theta (deg)

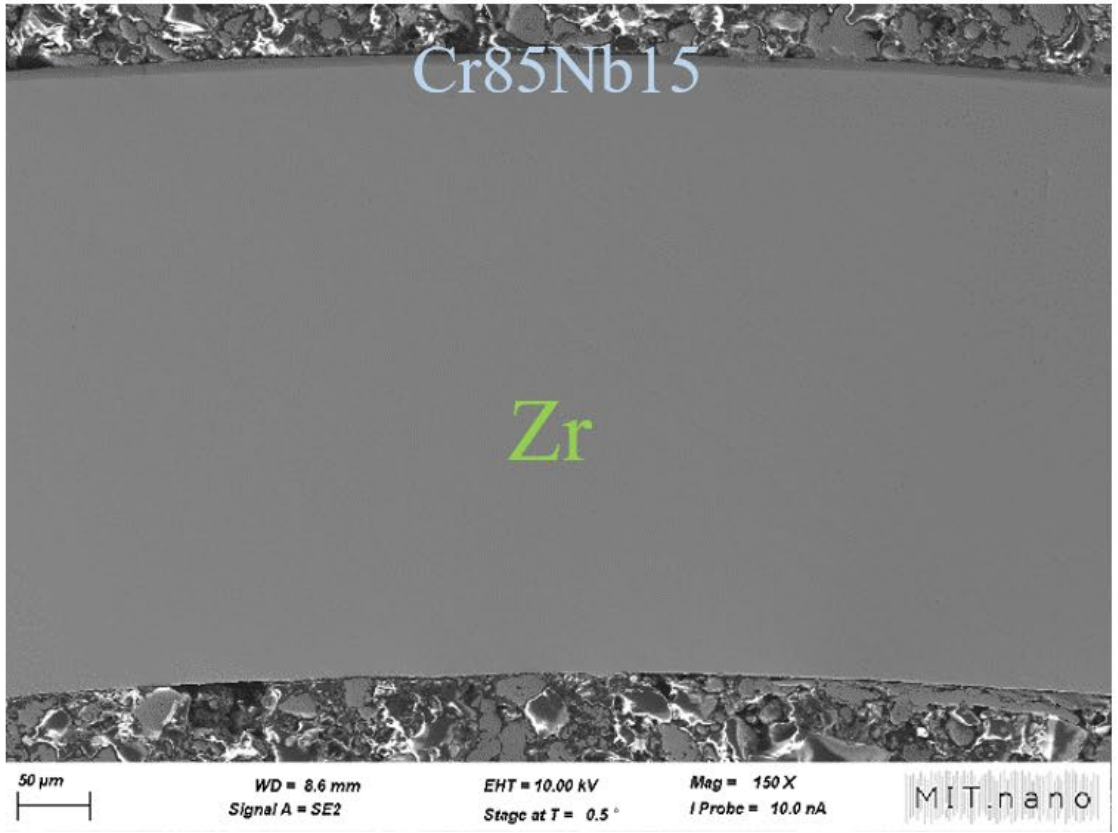
Cr85Nb15
Zr
50 µm
WD = 8.6 mm
Signal A = SE2
EHT = 10.00 kV
Stage at T = 0.5 °
Mag = 150 X
I Probe = 10.0 nA
MIT.nano


7.101 µm
6.945 µm
Cr85Nb15
Zr
1 µm
WD = 8.6 mm
Signal A = SE2
EHT = 10.00 kV
Stage at T = 0.0 °
Mag = 5.00 K X
I Probe = 10.0 nA
MIT.nano

(b)

Cr-Nb Model Alloys

- Three Binary Cr-Nb model alloys arc melted using pure commercial Cr and Nb
- Target composition, but large uncertainty was discovered on EDX analysis with higher Nb concentrations:
  - Cr85Nb15
  - Cr70Nb30
  - Cr50Nb50

- Solid solutions for Cr85 and Cr50; significant share of Cr_2Nb intermetallic for Cr70Nb30

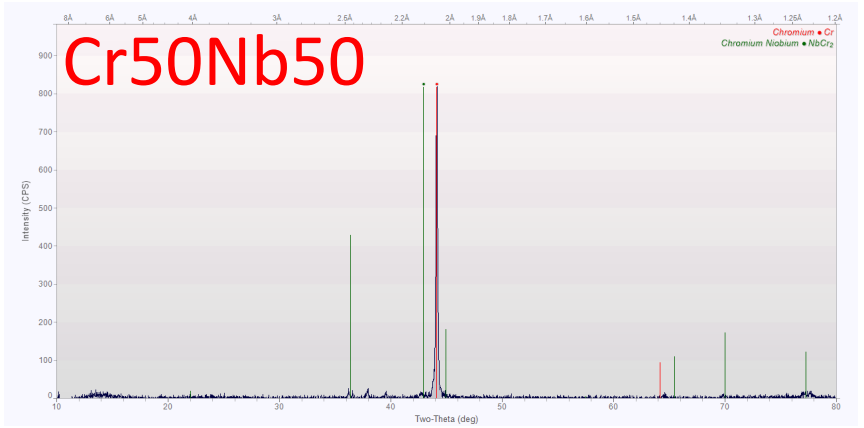

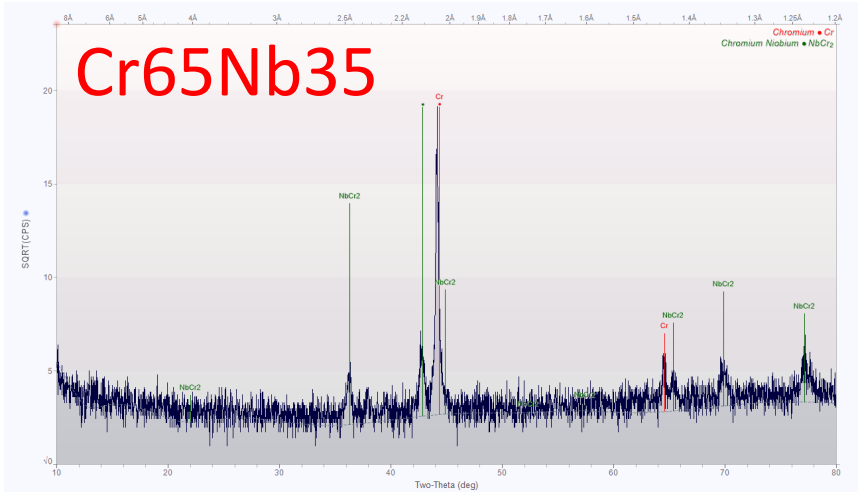

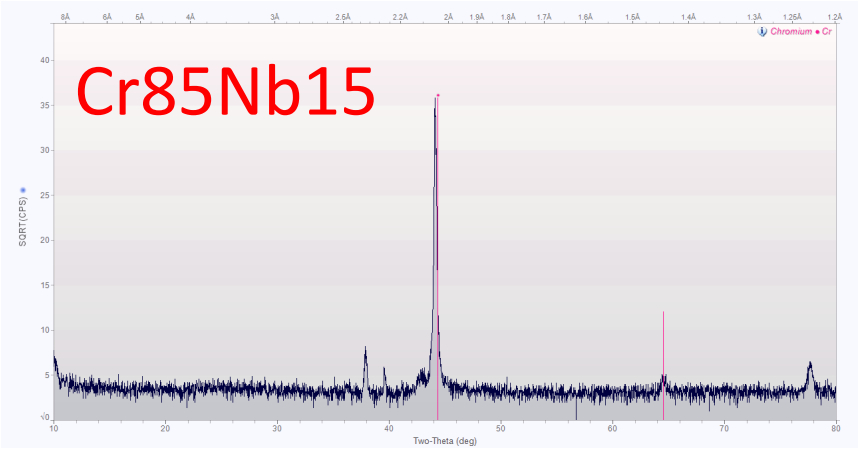

Long-term Corrosion Tests

Methodology

MITR BWR loop
in-pile tests since spring 2024

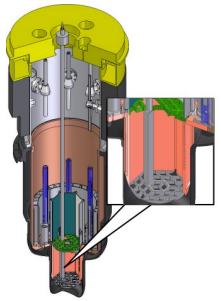

CRUD loop
flow accelerated corrosion in BWR environment

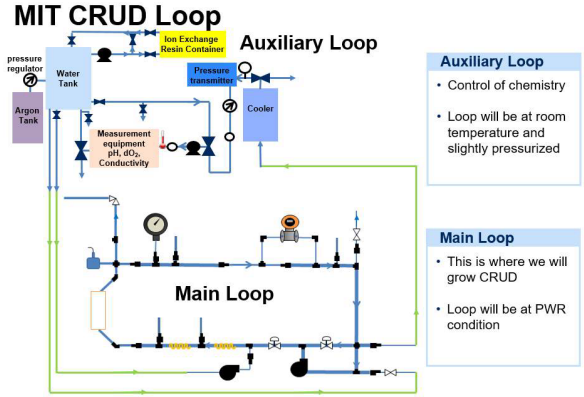

BWR dynamic loop – continuous water exchange (BWR-NWC chosen)

- pH_{RT}~6.5-7, dissolved oxygen ~2.5-5 ppm, inlet water conductivity ~0.06 µS (purified water), autoclave outlet water conductivity ~0.5-1.1 µS (corrosion products of autoclaves and other samples placed in the same test run), temperature 289-297°C, pressure around 7 MPa

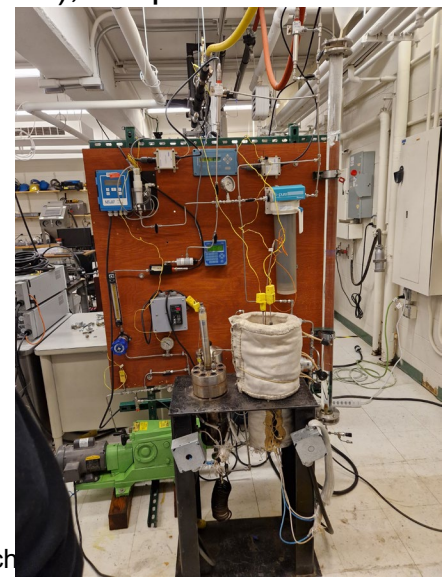

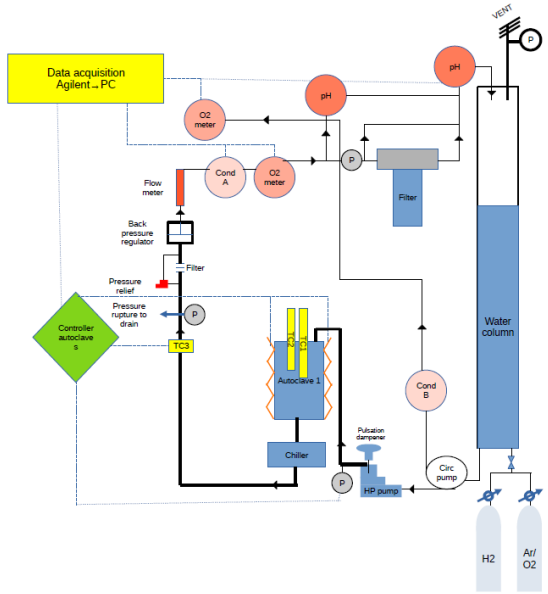

VVER static autoclave – water exchange every 21 days with well known ECP during the 21-day cycle

- 1050 ppm B, 15.9 ppm K, and 1 ppm Li => KOH chemistry in some US PWRs

Long-term corrosion results – double-sided corrosion

Contribution of the inner uncoated surface, the contribution of the coated side is only the difference between the theoretical internal surface WGs and dashed lines.

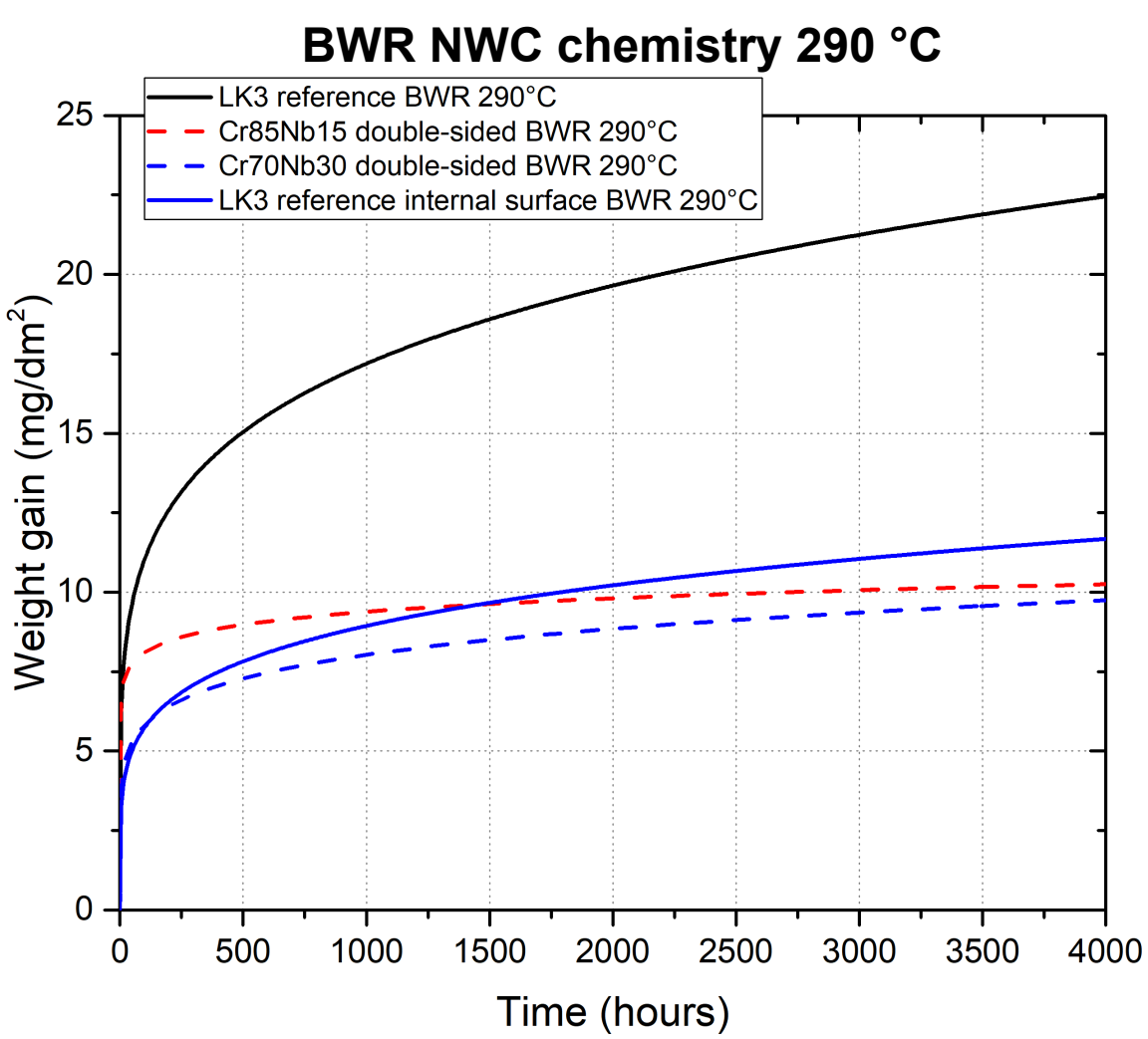

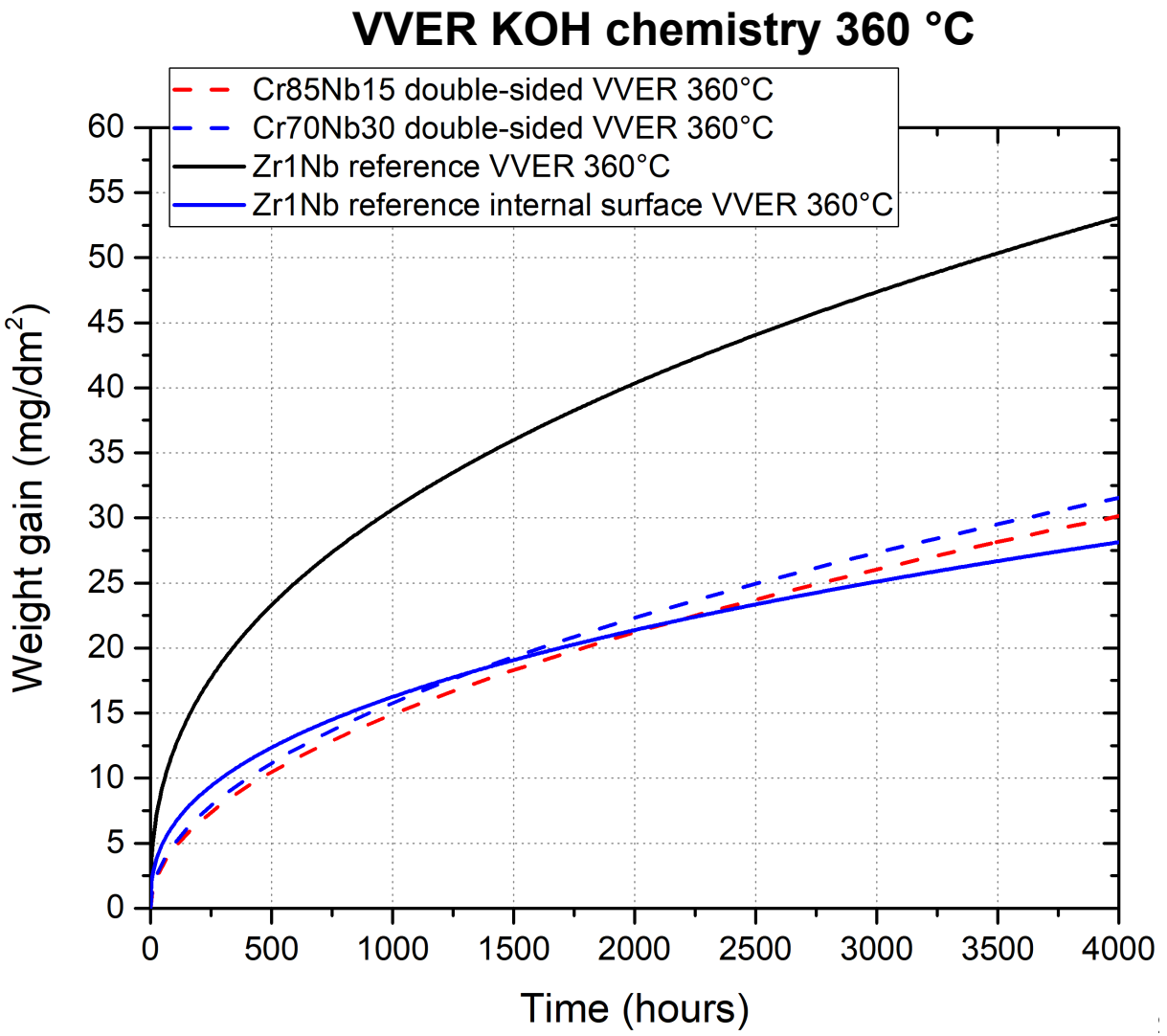

BWR corrosion – alternative coatings (CrAl, CrC and Cr)

Alternative Cr-based coatings tested in BWR. Accelerated degradation for all types. No effect of substrate or coating thickness was observed.

Cr PVD – two types, two substrates

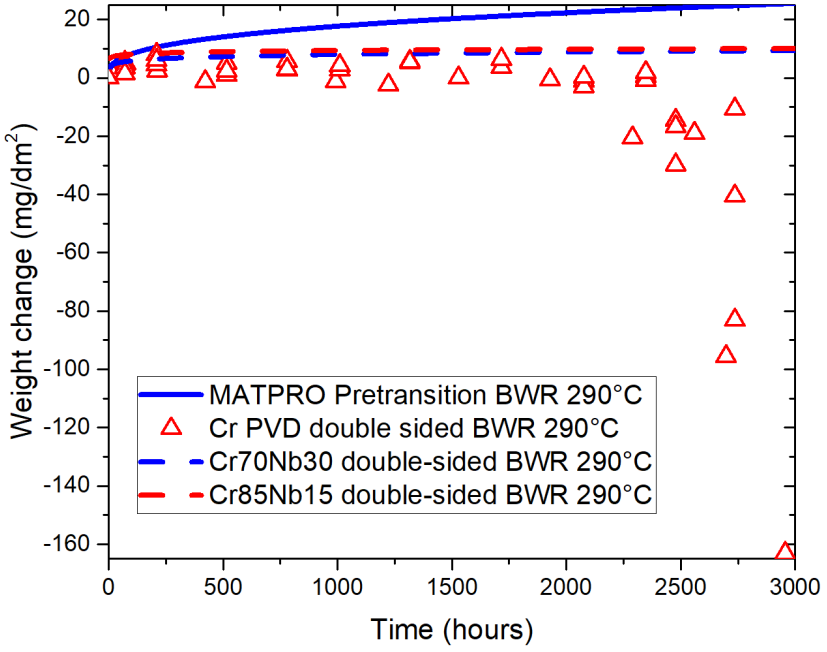

CrAl PVD

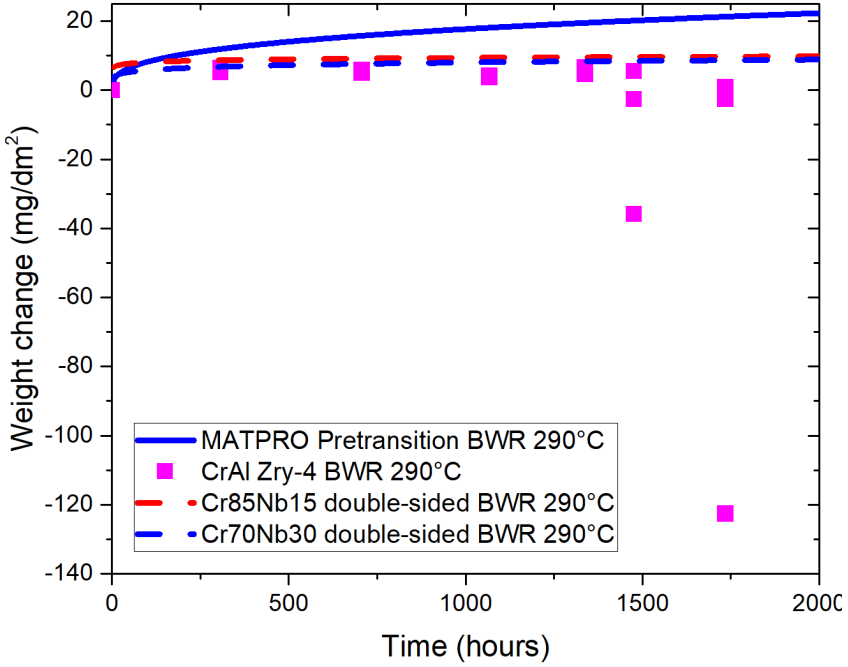

CrC PVD

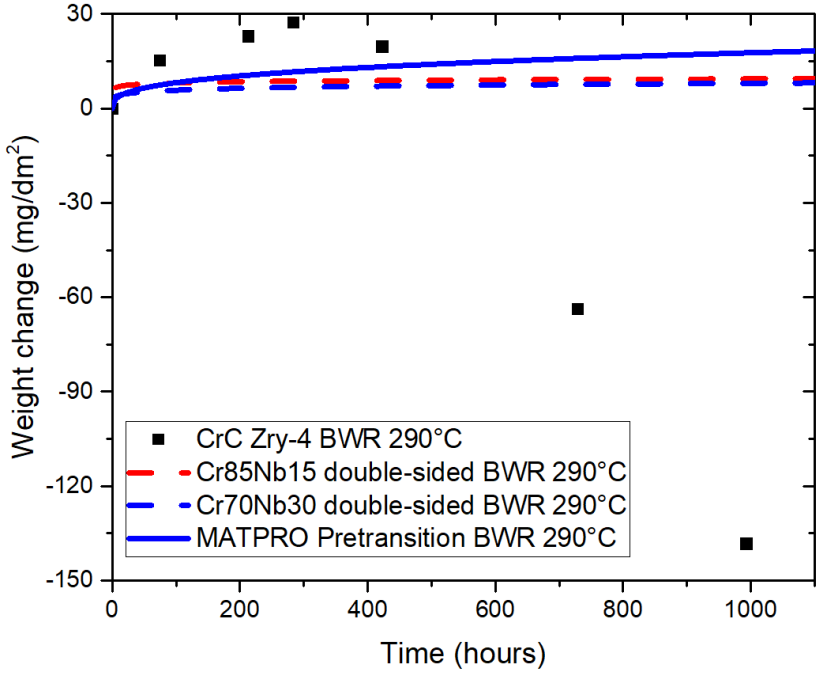

BWR-NWC 290°C LK3

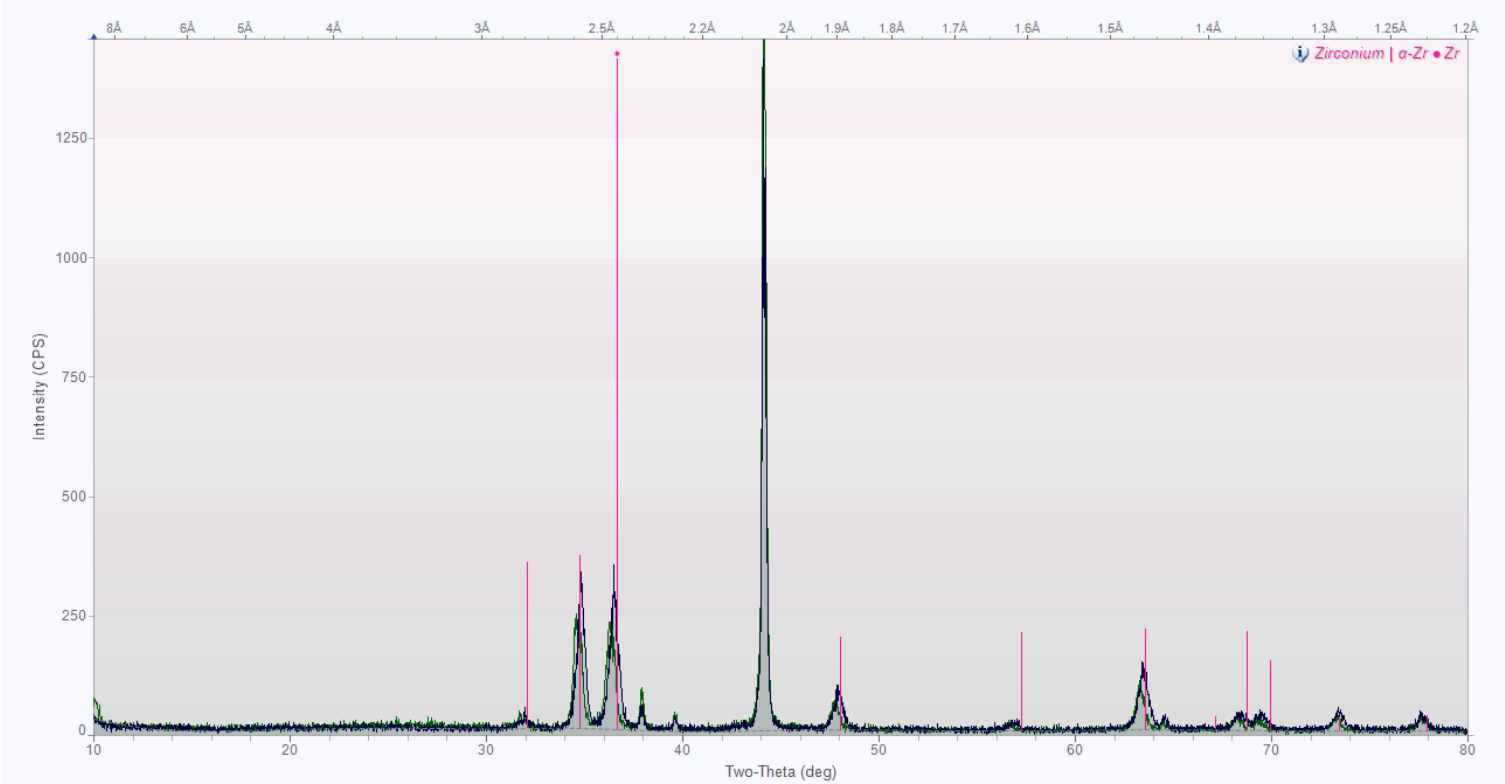

LK3

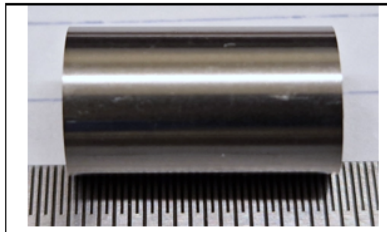	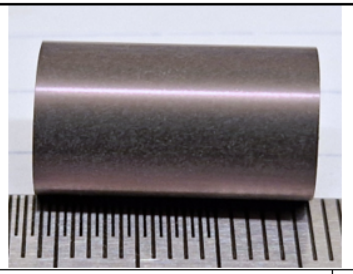	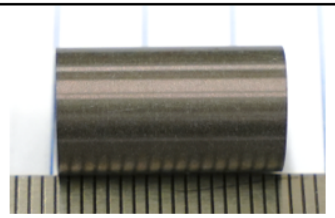	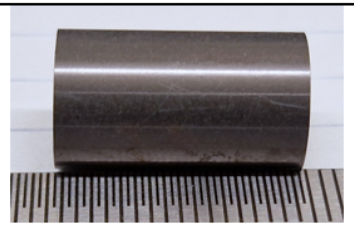	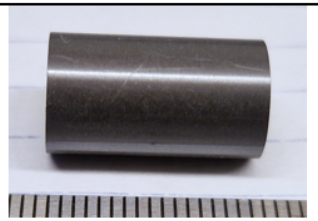	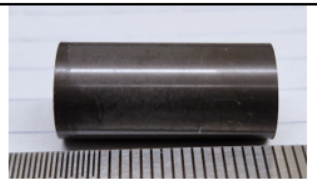	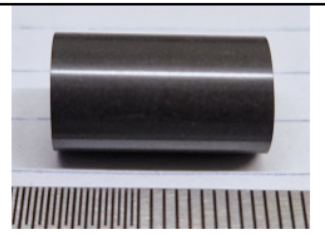
As-received	74.5 hours	212.5 hours	283.5 hours	422.5 hours	728.5 hours	992.5 hours
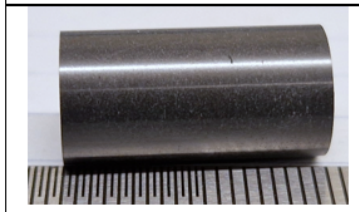	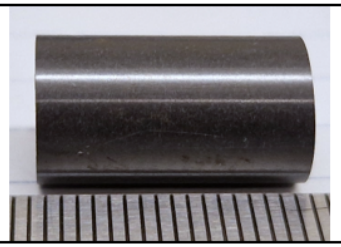	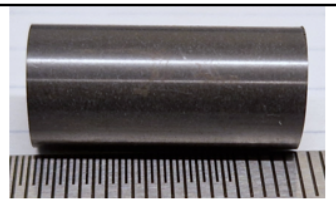	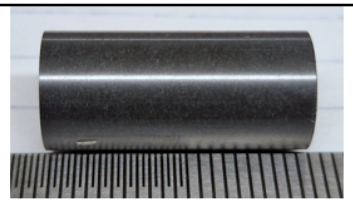	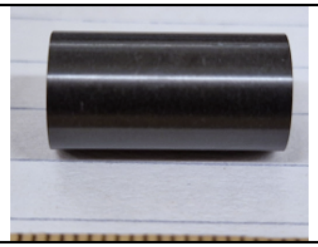	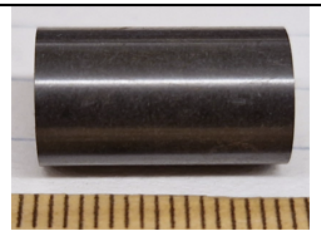	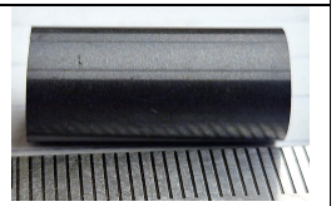
1106.5 hours	1222.5 hours	1529 hours	1929 hours	2137.5 hours	2560 hours	2698 hours

Cr85Nb15 coated LK3

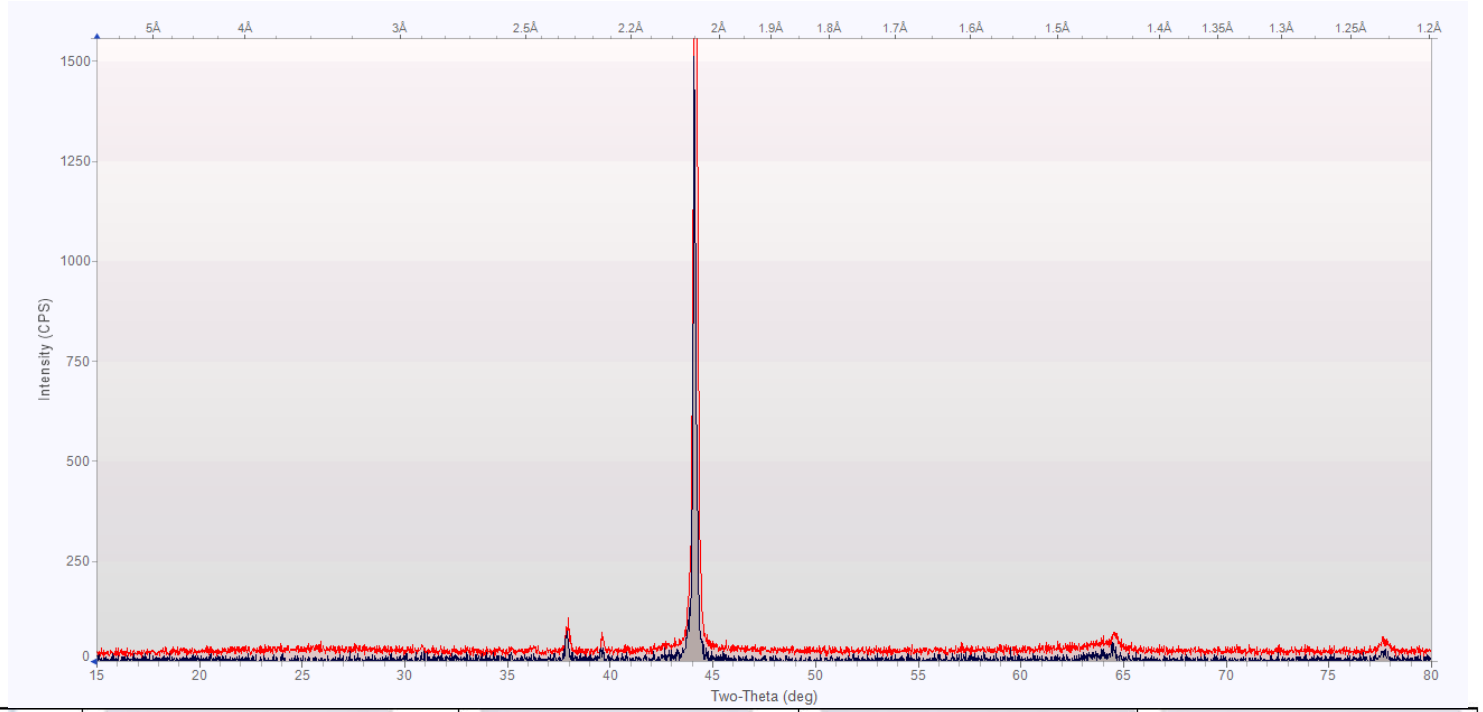

Cr85Nb15

	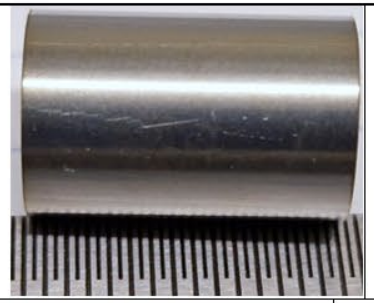	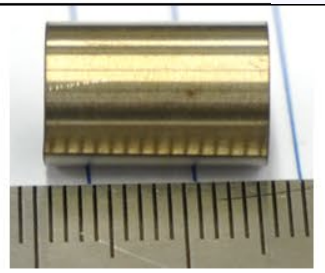	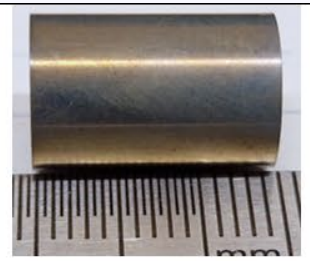	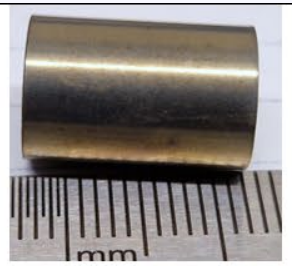	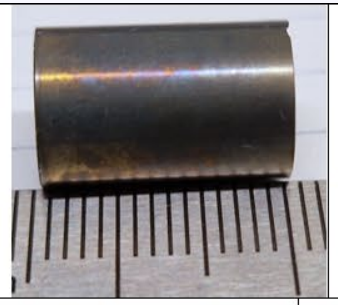	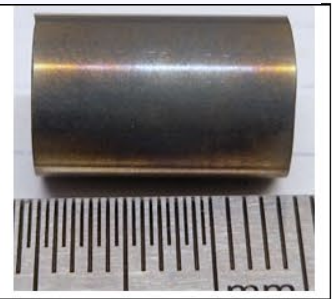
As-received	74.5 hours	212.5 hours	283.5 hours	422.5 hours	728.5 hours	992.5 hours
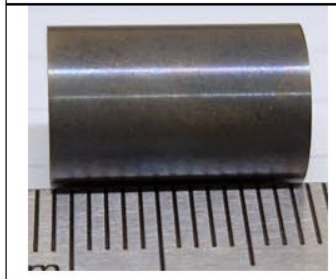	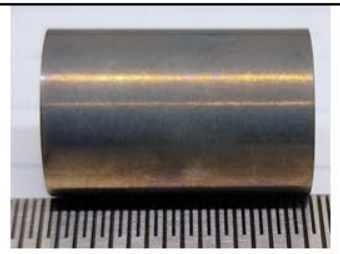	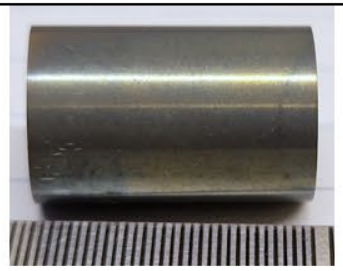	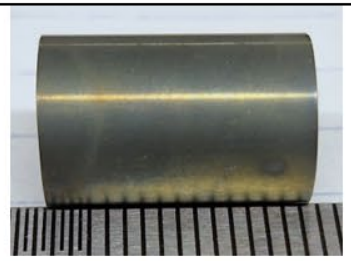	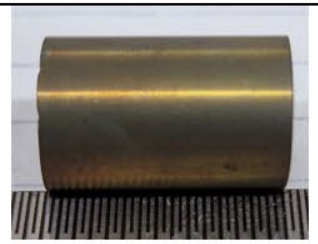	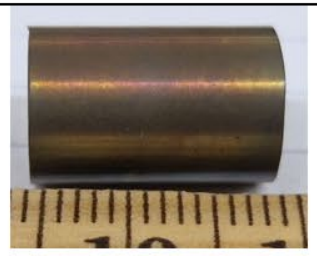	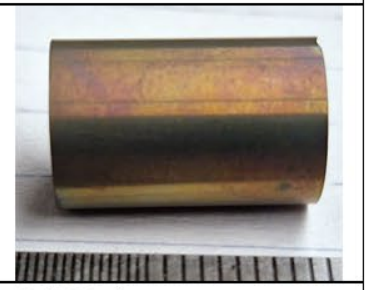
1222.5 hours	1316 hours	1529 hours	1929 hours	2289 hours	2560 hours	2698 hours

Cr70Nb30 coated LK3

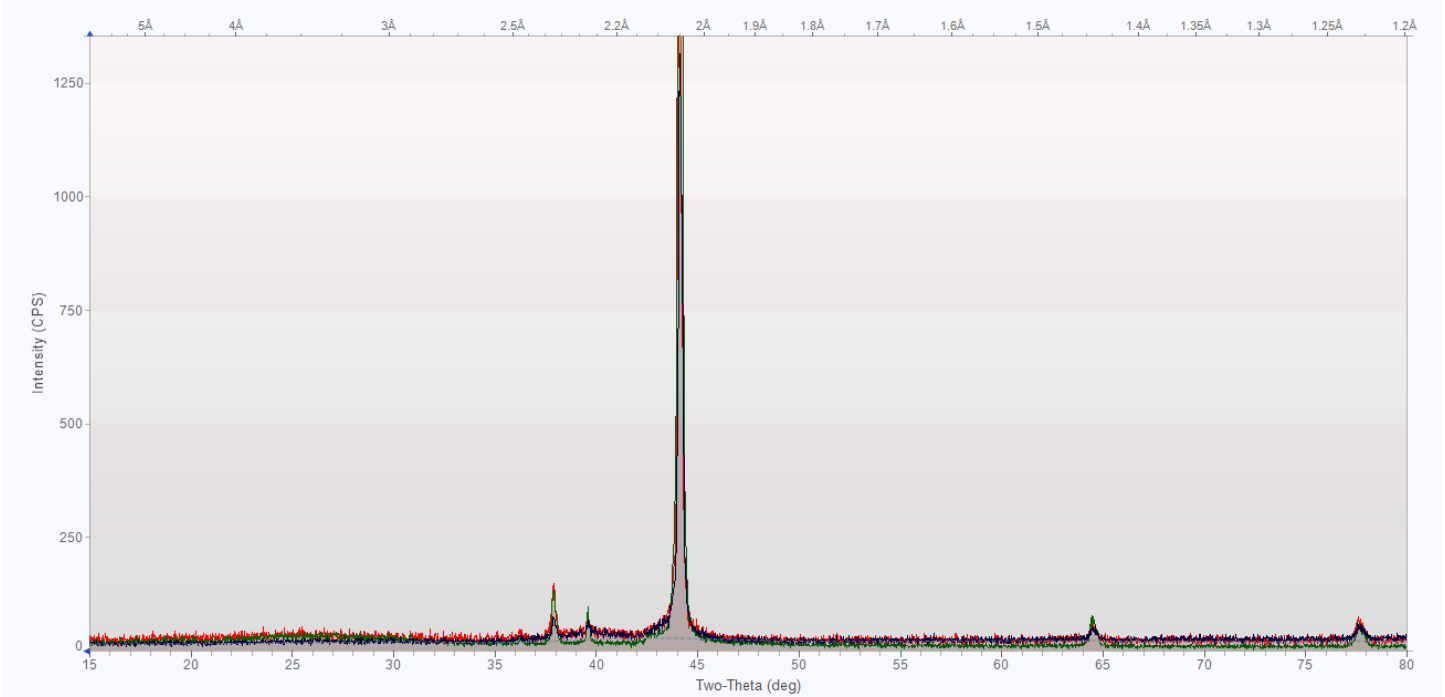

Cr70Nb30

	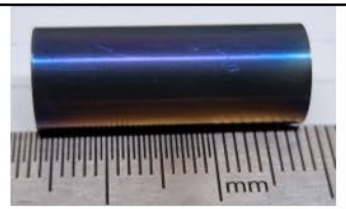	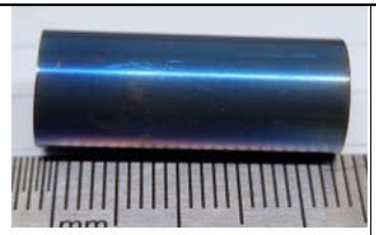	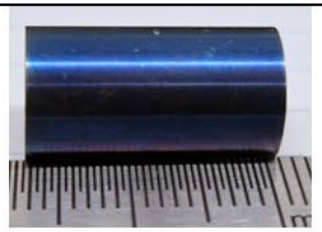	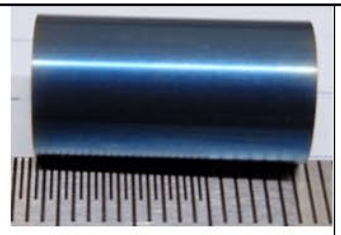	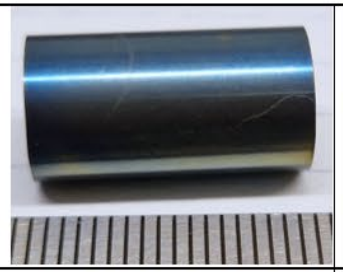	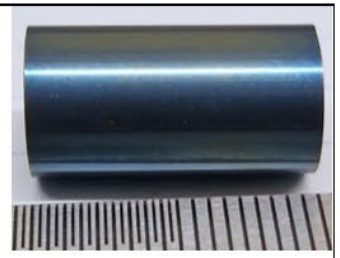
As-received	74.5 hours	212.5 hours	283.5 hours	422.5 hours	728.5 hours	992.5 hours
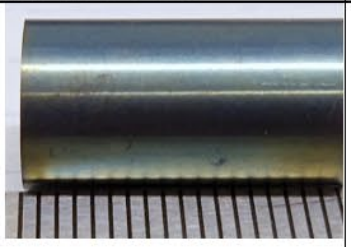	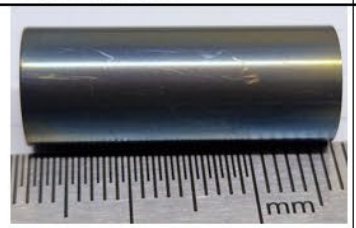	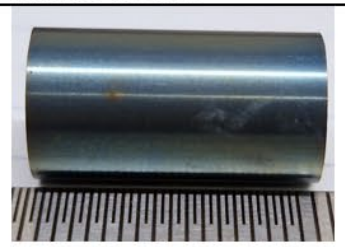	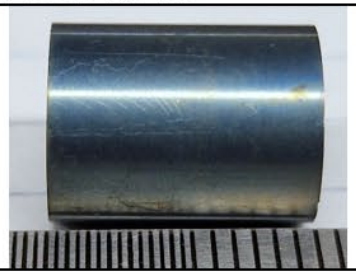	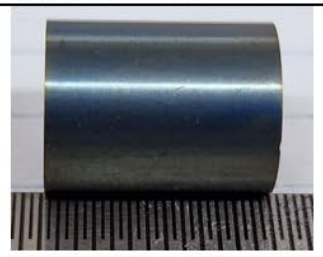	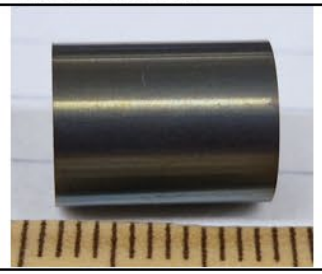	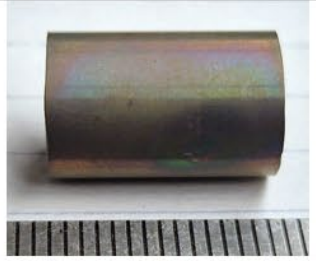
1222.5 hours	1316 hours	1529 hours	1929 hours	2289 hours	2560 hours	2698 hours

Cr PVD coated Opt. ZIRLO and Zircaloy-4

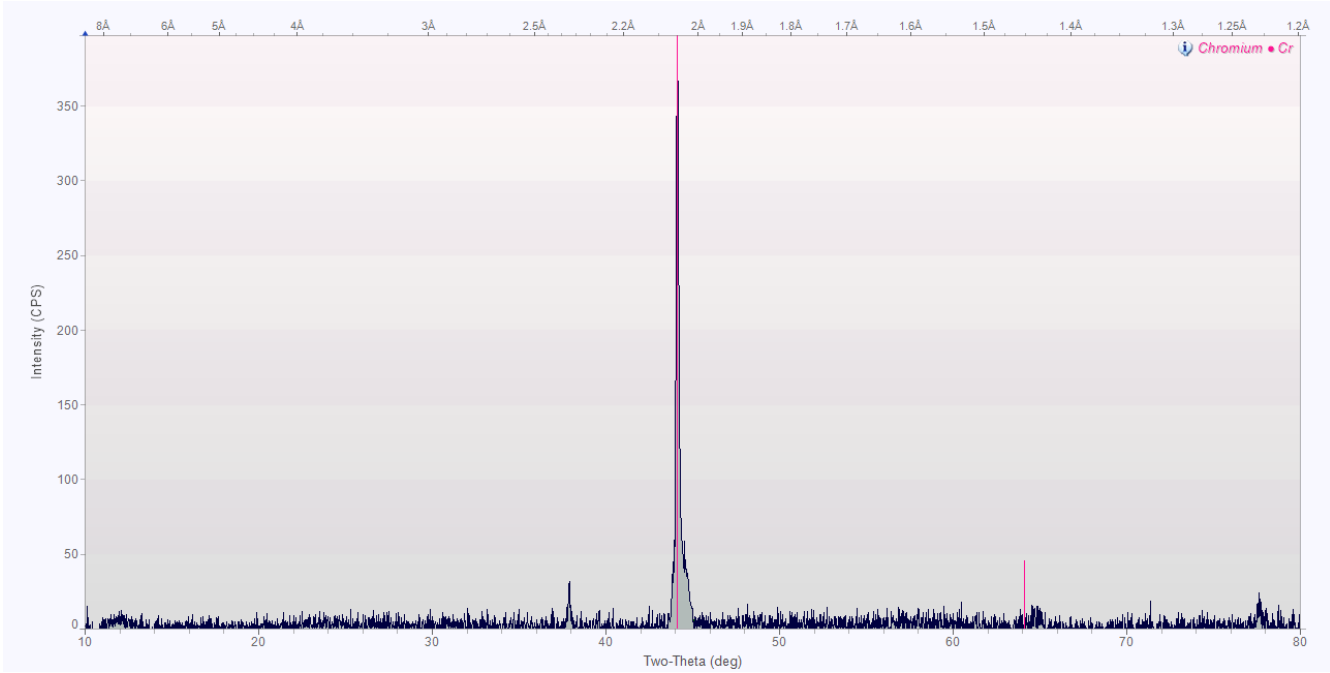

Cr PVD

	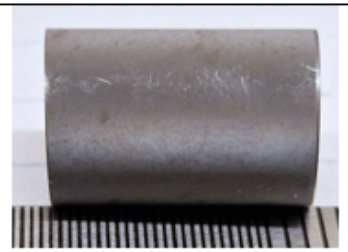	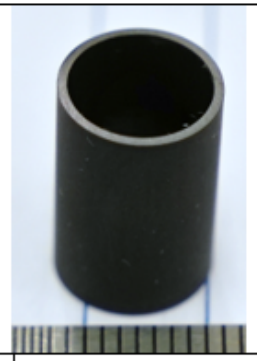	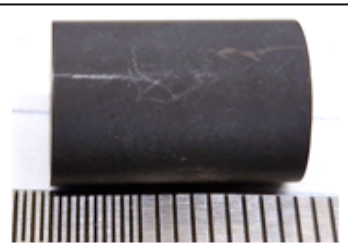	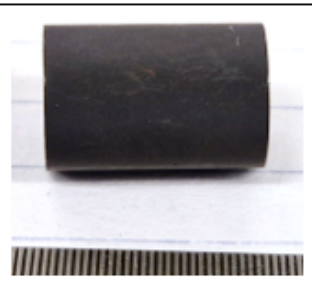	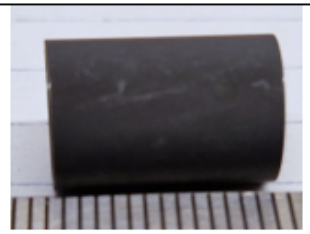	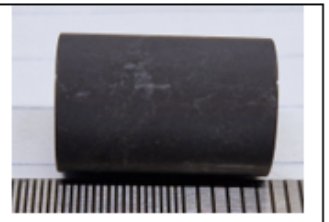
As-received	74.5 hours	212.5 hours	283.5 hours	422.5 hours	728.5 hours	992.5 hours
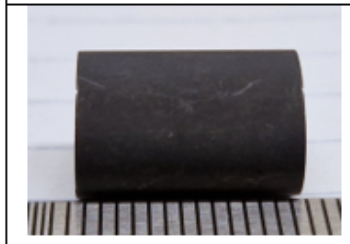		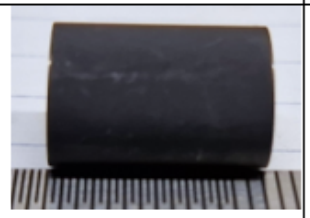	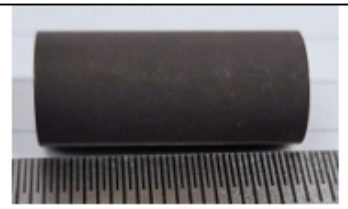	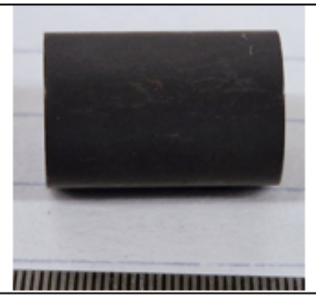	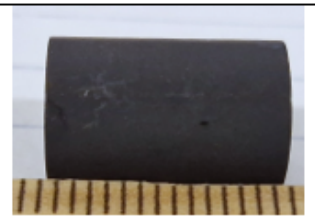	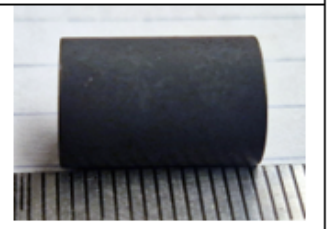
1222.5 hours	1316 hours	1529 hours	2076.5 hours	2289 hours	2560 hours	2698 hours

CrAl PVD coated Zircaloy-4

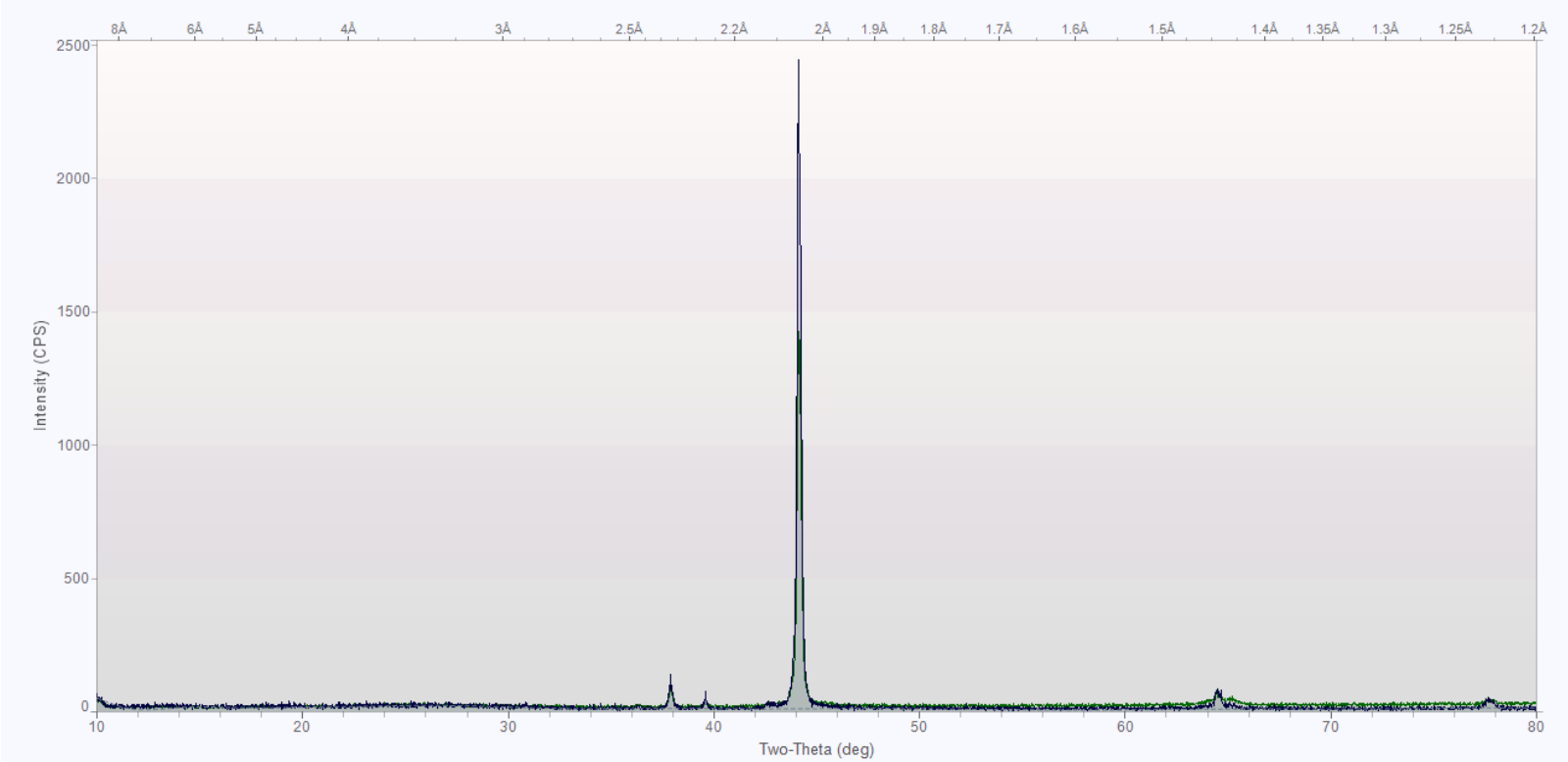

CrAl

As-received	306.5 hours	706.5 hours	1066.5 hours	1337.5 hours	1475.5 hours
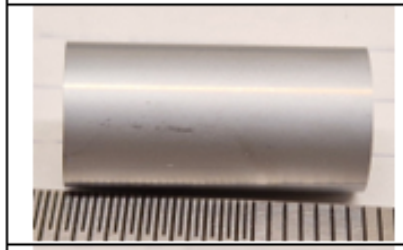	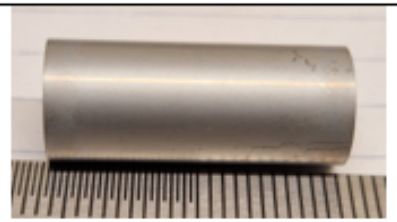	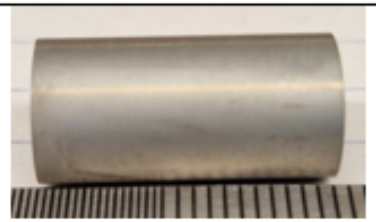	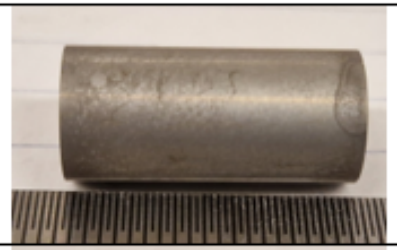	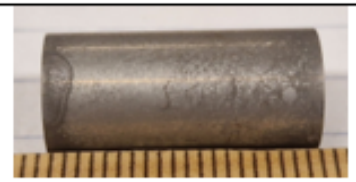	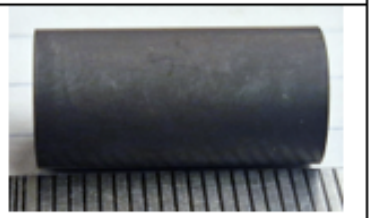
	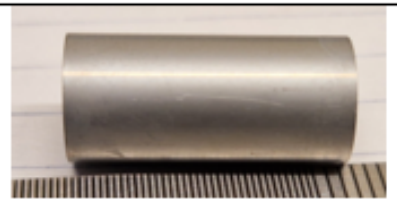	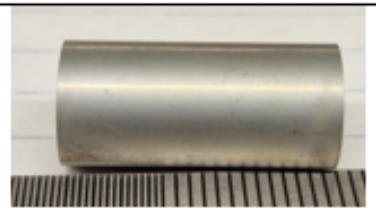	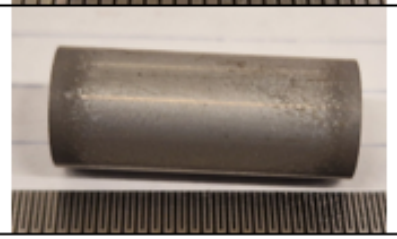	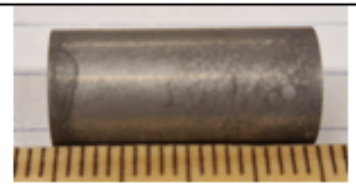	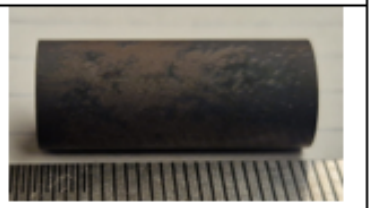

CrC PVD coated Zircaloy-4 and SiC

As-received	74.5 hours	212.5 hours	283.5 hours	422.5 hours	728.5 hours	992.5 hours

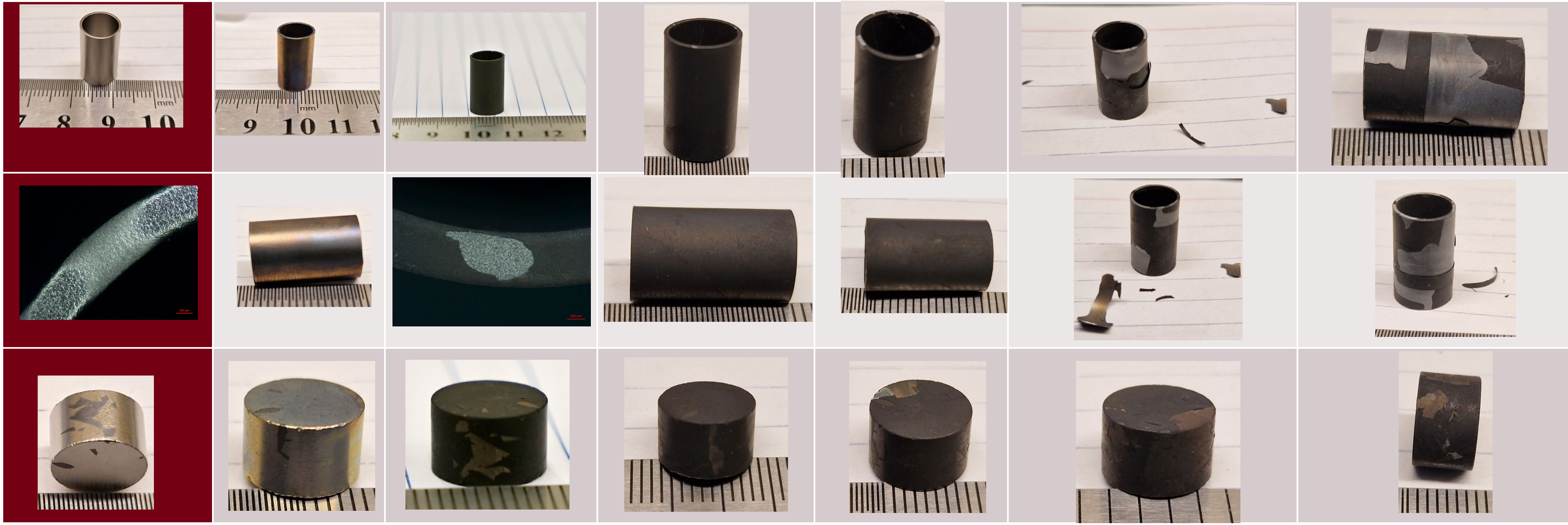

CRUD loop – Flow Accelerated Corrosion

- BWR chemistry, 290 °C – similar conditions to the BWR corrosion loop but higher flow = flow accelerated corrosion
- Flow accelerated corrosion with longer periods.
- Only one sample tested in the CRUD loop, data available up to 1700 hours
- Fully consistent trend between the BWR and CRUD loop regarding weight changes.
- Post-test analysis will focus on CRUD formation as well as oxide formations

- *PIE results from in-pile tests will be available in spring 2025*

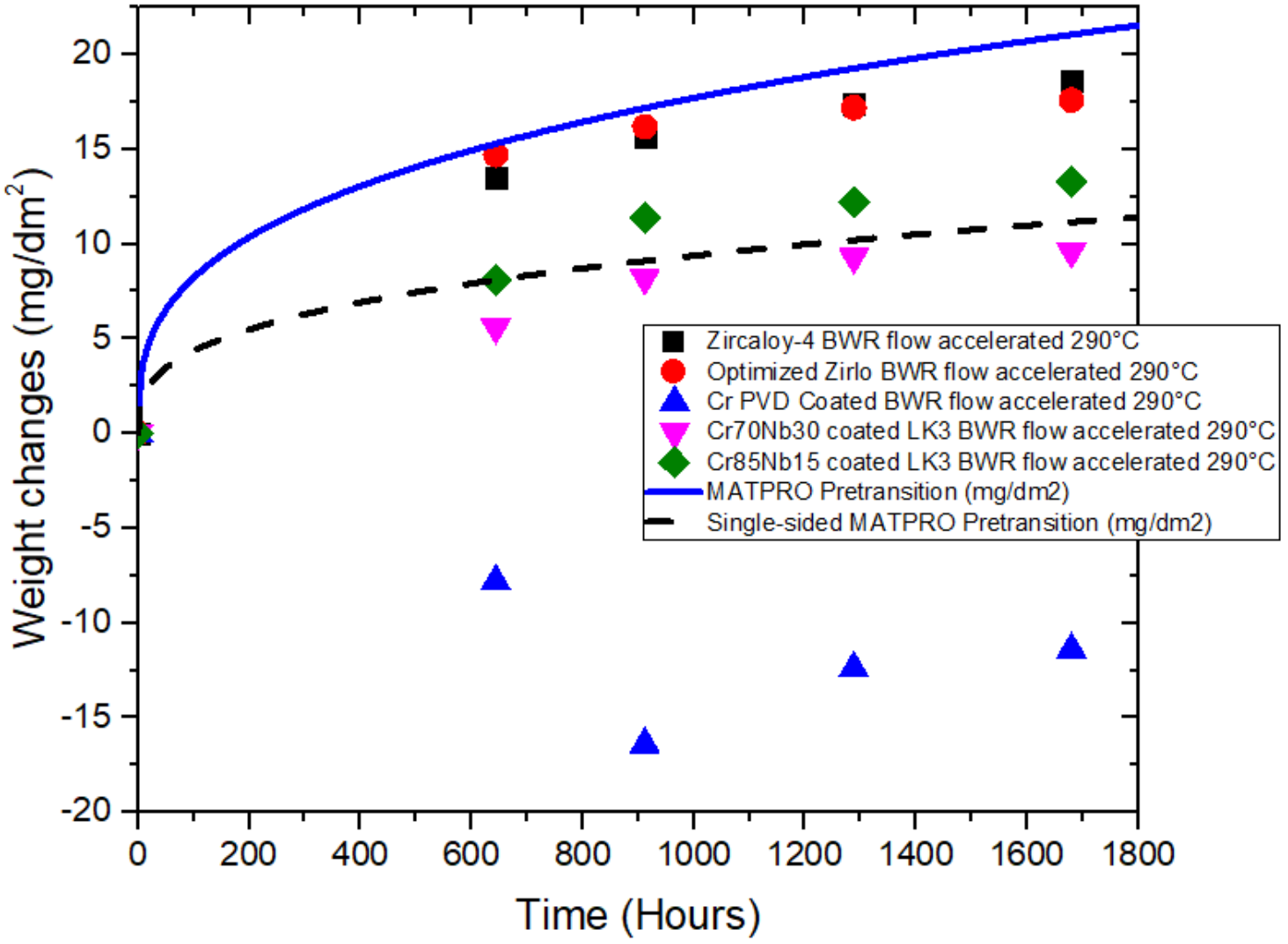

High-temperature steam oxidation tests

HT steam oxidation – double-sided tests

- Two independent experimental setups used => consistent results => validation of methodology
- Zircaloy-4 and LK3 cladding segments used for reference – good agreement with C-P correlation
- Focus on DBA and post-CHF c

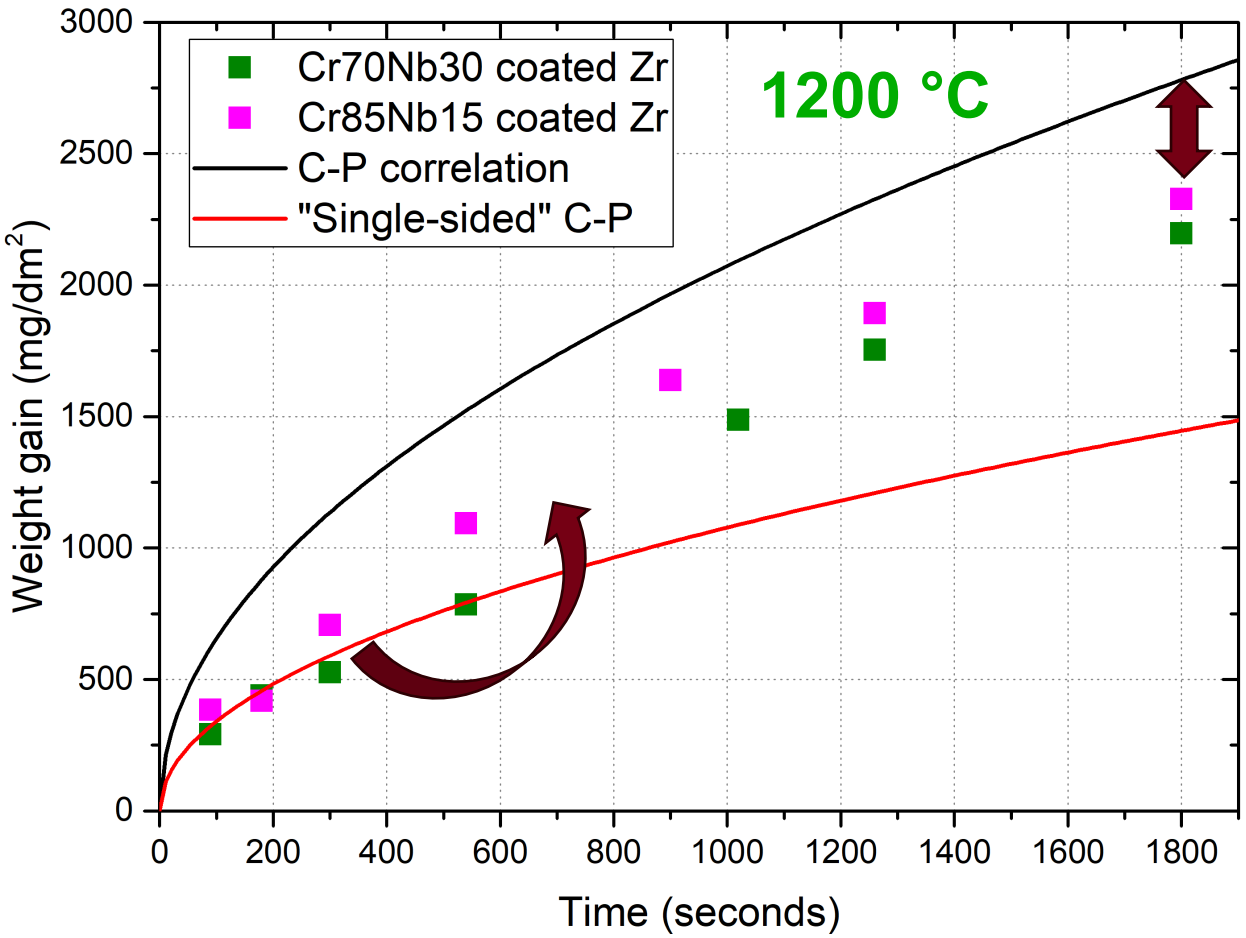

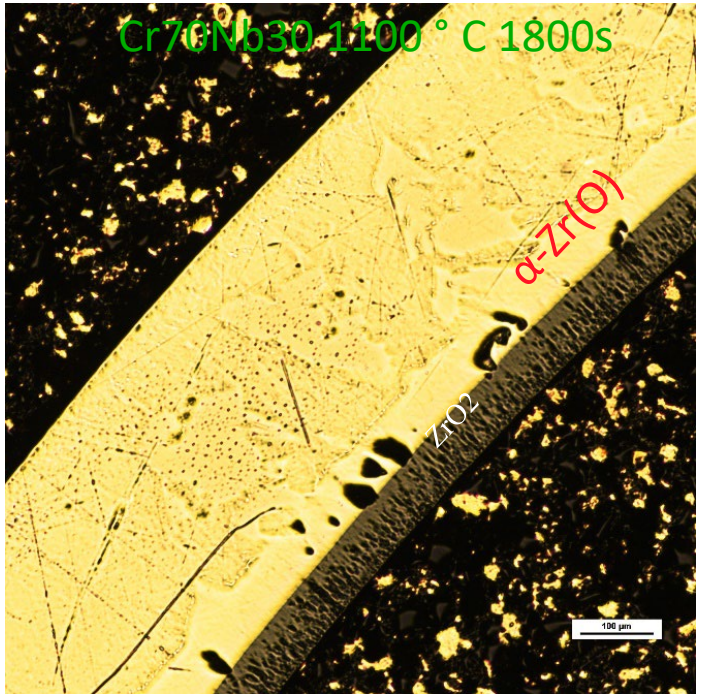
Cr70Nb30 1100 ° C 1800s
α-Zr(O)
ZrO2

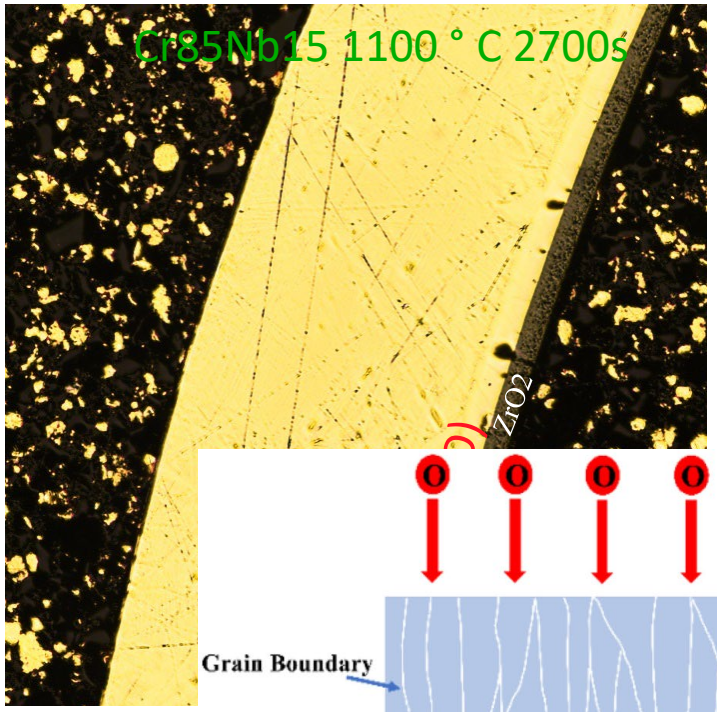
Cr85Nb15 1100 ° C 2700s
ZrO2

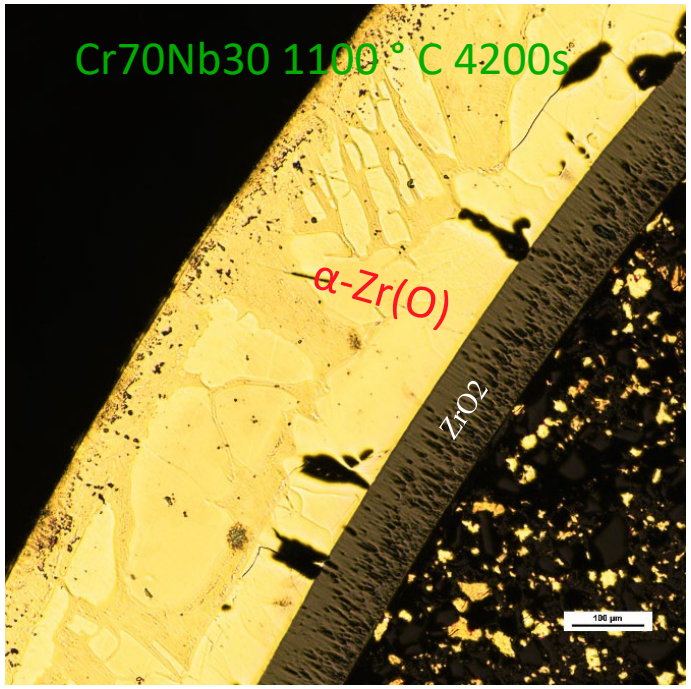
Cr70Nb30 1100 ° C 4200s
α-Zr(O)
ZrO2

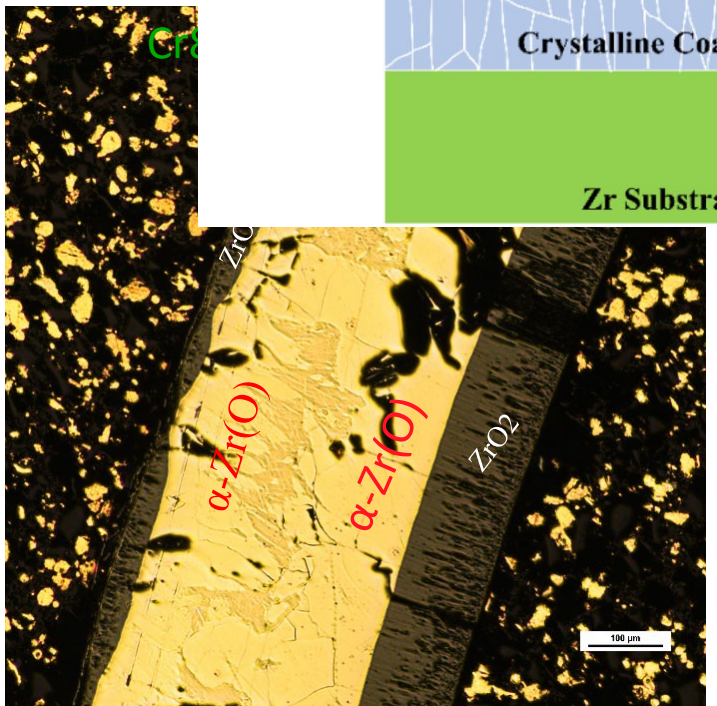
α-Zr(O)
α-Zr(O)
ZrO2

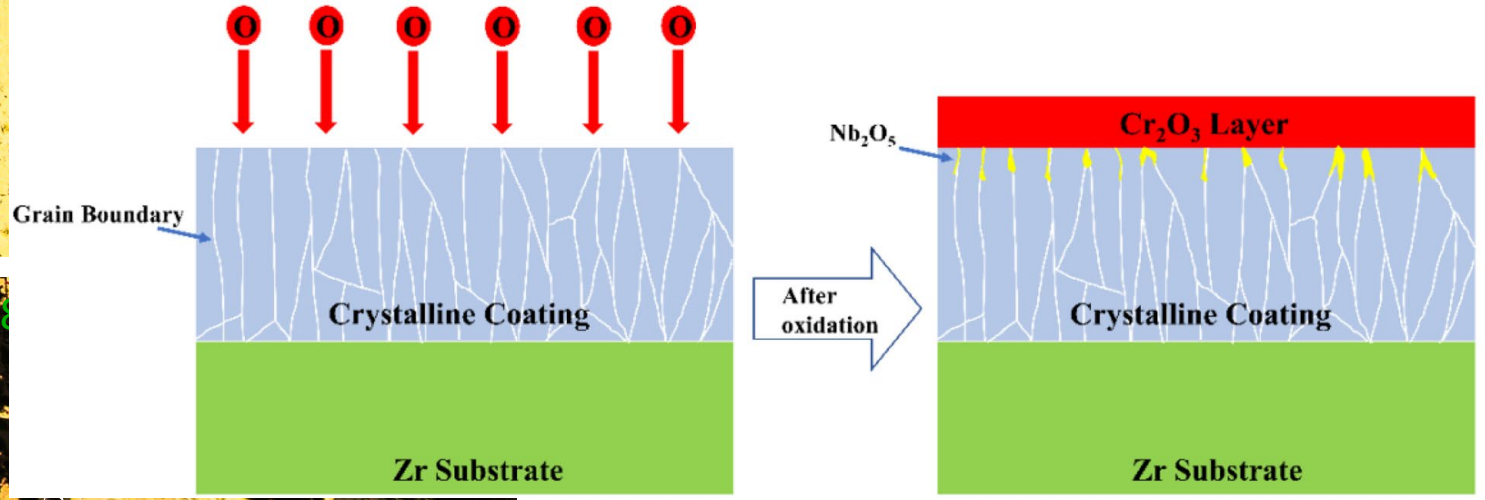
O
Grain Boundary
Crystalline Coating
Zr Substrate
After oxidation
Nb2O5
Cr2O3 Layer
Crystalline Coating
Zr Substrate

HT steam oxidation – hydrogen uptake

- Excessive hydrogen absorption especially after oxidation kinetics transition = non-protective coating?

- Old Zr1Nb alloy – breakaway oxidation, oxide spallation and H absorption in certain temperature range – effect of fluorine impurities in Zr – 4-5 ppm

- Residual fluorine in the deposition chamber? Breakaway on the inner uncoated surface due to fluorine impurities in the chamber during the argon etching?

  - Need more investigations, any feedback welcome

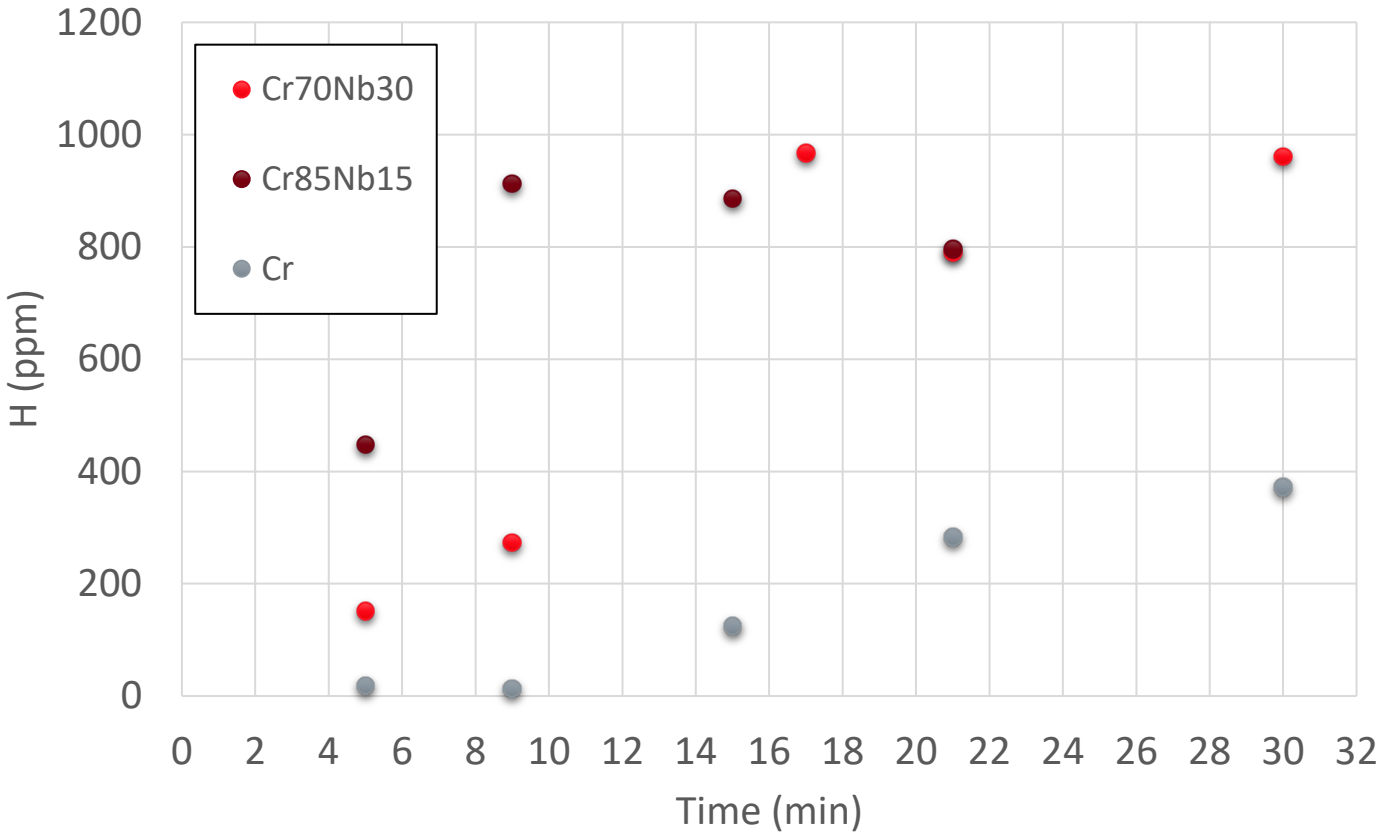

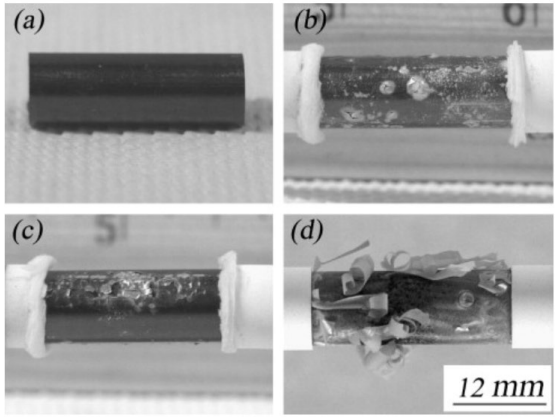

Cr-Nb characterization

Emissivity

- Fourier-Transform Infrared Spectroscopy - Bruker VERTEX 70 FTIR spectrometer
- Five repeats for each sample, average values and standard deviation reported

- LK3 – 0.42±0.02; 0.84±0.04; 0.92±0.05;
- Cr70Nb30 - 0.61±0.02; 0.92±0.03; 0.93±0.03;
- Cr80Nb20 - 0.43±0.01; 0.92±0.03; 0.95±0.03;

- Benefit - Higher emissivity for both coated samples compared to reference LK3.

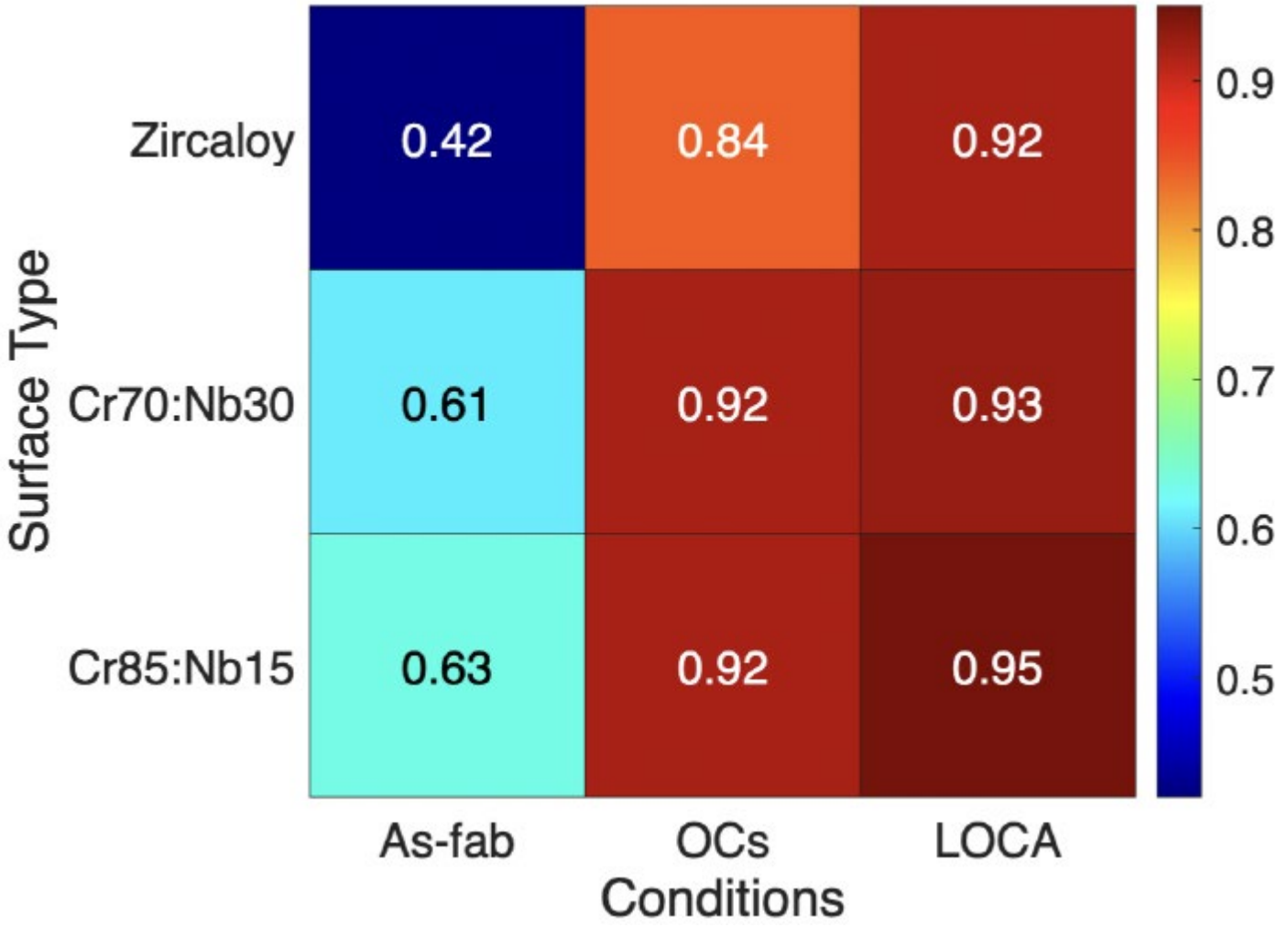

Conclusions

- Pure Cr coatings are well developed for PWRs but the search for suitable BWR coatings that would provide benefits in both accidental scenarios and normal operation continues.
- Cr-Nb system showed promise for high-temperature applications including LWR environment. Metallic coatings are ductile which is required for nominal operation and accidental conditions.
- Two novel Cr-Nb metallic coatings were successfully deposited by unbalanced magnetron sputtering on three Zr-based alloys. In addition, CrAl, CrC and pure Cr-coated Zr and SiC were tested.
- HT steam oxidation tests – protective behavior at low ECR values => accelerated degradation of the Cr/Nb coating compared to pure Cr degradation due to the presence of Nb but still a significant improvement compared to uncoated Zr.
- Long-term corrosion tests show auspicious results (low flow BWR-NWC, high flow BWR in CRUD loop, and VVER/PWR KOH). Methodologies were validated by older models/data and the tests will continue for several more months.
- Negligible corrosion rate of both Cr85Nb15 and Cr70Nb30, no spallation or delamination, excellent visual appearance.
- Cr and CrAl dissolution observed, after ~100 mg/dm2 weight loss spallation starts. CrC promising for a short time but needs improvement of deposition parameters and adhesion.
- In-pile tests in MITR ongoing with detailed PIE planned at INL in spring 2025.

Mirco Grosse

KIT

High Temperature Steam Oxidation Tests in the Framework of the SCORPION Project

In order to reduce the corrosion and high temperature oxidation, bulk silicon carbide was improved by grain boundary alloying and grain boundary engineering. Samples of these materials were investigated in slow transient tests from 500 to 1600°C in steam with heating rates of 4 K/min.

Most of the samples improve the high temperature oxidation behavior of pure SiC. However, the grain boundary engineered samples using YAG (SiC-15 wt.% (Y_2O_3-$Al_2O_{3)}$), the YbAG (SiC-15 wt.% (Yb_2O_3-Al_2O_3)) and neodymium oxide SiC15 wt.% (1 mol Nd_2O_3+1mol SiO_2)) show a relevant higher oxidation rate (two orders of magnitude and even higher than the one for pure SiC) and macroscopic material degradations.

The reason for the worse behavior of the alumina containing samples was the formation of eutectic melt at temperatures of about 1570°C. This melt has a high wettability and could be found even in cracks of the sample holder plate made of yttrium oxide. It results in breaking this plate in one of the tests. The reasons for the sample engineered by neodymium oxide are on the one hand that neodymium oxide is an oxide ion conductor and at the other hand, three different neodymium silicates are formed at about 975, 1070 and 1120°C resulting in the formation of a more porous material.

A conclusion of these results is rejecting these alloys for further and costly investigations like irradiation tests.

SCORPION

Karlsruhe Institute of Technology

SiC Composite Claddings: LWR Performance Optimization for Nominal and Accident Conditions

High Temperature Steam Oxidation Tests in the Framework of the SCORPION Project

Mirco Grosse, Martin Steinbrueck (KIT IAM/AWP),
Shuigen Huang, Jef Vleugels (KU Leuven),

Cédric Sauder (CEA Saclay),

Konstantina Lambrinou (Univ. Huddersfield, IIT Milan)

This project has received funding from the Euratom Research and Training Programme 2021-2025 under Grant Agreement No 101059511

The SCORPION project

- SiC/SiC CMC is a rather revolutionary ATF cladding material concept
- Must overcome
  - Incompatibility to the coolant (Strong corrosion in water)
    - $SiC(s) + 2H_2O(aq) = SiO_2(s) + CH_4(g)$
    - $SiC(s) + 2H_2O(aq) = SiO_2(s) + 2H_2(g) + C(s)$
    - $SiC(s) + 3H_2O(aq) = SiO_2(s) + 3H_2(g) + CO(g)$
    - $SiC(s) + 4H_2O(aq) = SiO_2(s) + 4H_2(g) + CO_2(g)$
    - $SiO_2(s) + 2H_2O(aq) = Si(OH)_4(aq)$
  - Reaction at very high temperature
    - $2SiO_2(l) + SiC(s) = 3SiO(g) + CO\ (g)$
  - Radiation-induced swelling until a dose rate of ~ 2 dpa
  - Lack of ductility
- Porosity needed for quasi ductile behaviour and to compensate irradiation induced swelling, but porosity can increase the corrosion/oxidation due to larger surface.
- Influence of water chemistry on the corrosion and high temperature steam oxidation (influence of the hydrogen partial pressure).

HORIZON SCORPION

(SiC Composite Claddings: LWR Performance Optimisation for Nominal and Accident Conditions)

***Prof. Konstantina Lambrinou**, UoH (UK) & IIT (Italy)*

HORIZON European Research & Innovation Action (RIA)

Goal: Improving SiC CMC´s for application as nuclear fuel cladding tubes

Partners: 16 organizations from D, I, F, B, S, EU, UK, CH, J, USA

Grain boundary engineered & doped SiC

- **Bulk protection by grain boundary engineering, i.e. the addition of hydrothermally stable rare-earth mono- and di-silicates or garnets at the SiC grain boundaries**

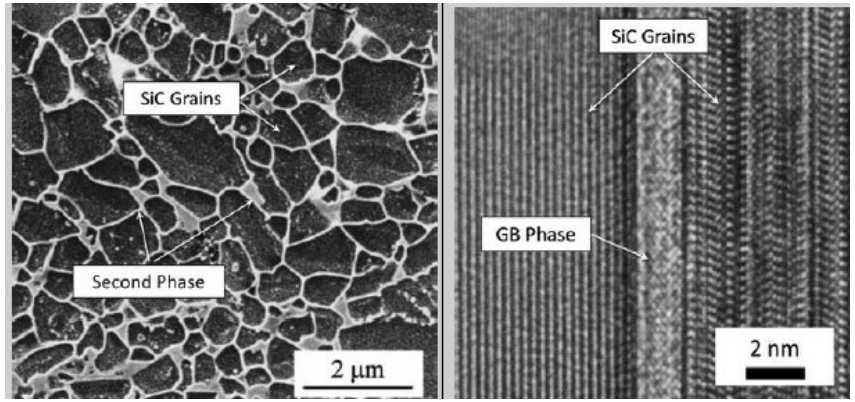

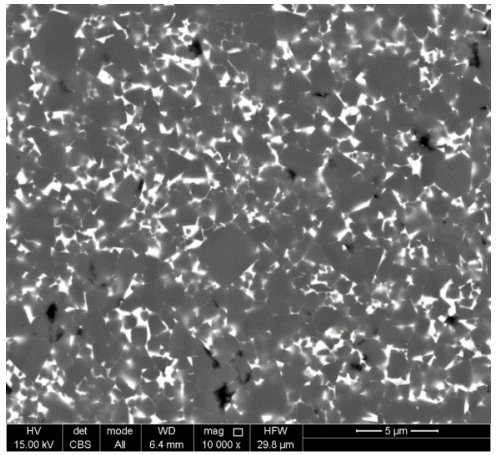

- **Grain boundary doping by the selective addition of a limited amount of atoms along the grain boundaries**

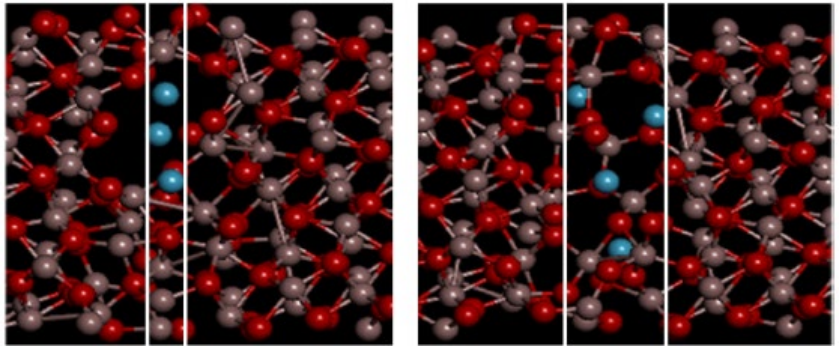

Addition of large or small cations at the GB

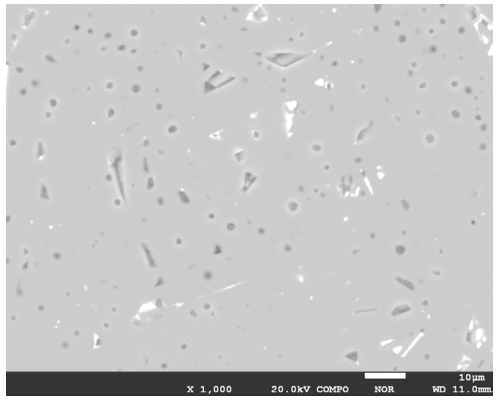

Grain boundary engineered SiC & doped SiC

- Due to the multiple phase transitions, $RE_2Si_2O_7$ are more difficult to synthesize than RE_2SiO_5

→ Two-step synthesis process:
- Solid state bulk synthesis of oxide powder, followed by
- Spark plasma sintering of the SiC + oxide mixture

- **Solid state bulk synthesis** of $RE_2Si_2O_7$, RE_2SiO_5, YAG and YbAG

CS furnace

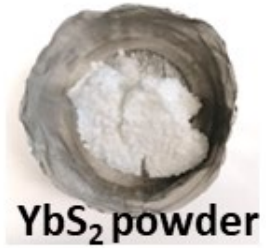

CS at 1600°C for 4 h in air

Crushed RE_2SiO_5, $RE_2Si_2O_7$, YAG or YbAG powder is added to SiC and consolidated by spark plasma sintering

Grain boundary engineered SiC & doped SiC

- Spark plasma densification of SiC powder mixtures with $RE_2Si_2O_7$, RE_2SiO_5, YAG or YbAG & grain boundary doped SiC

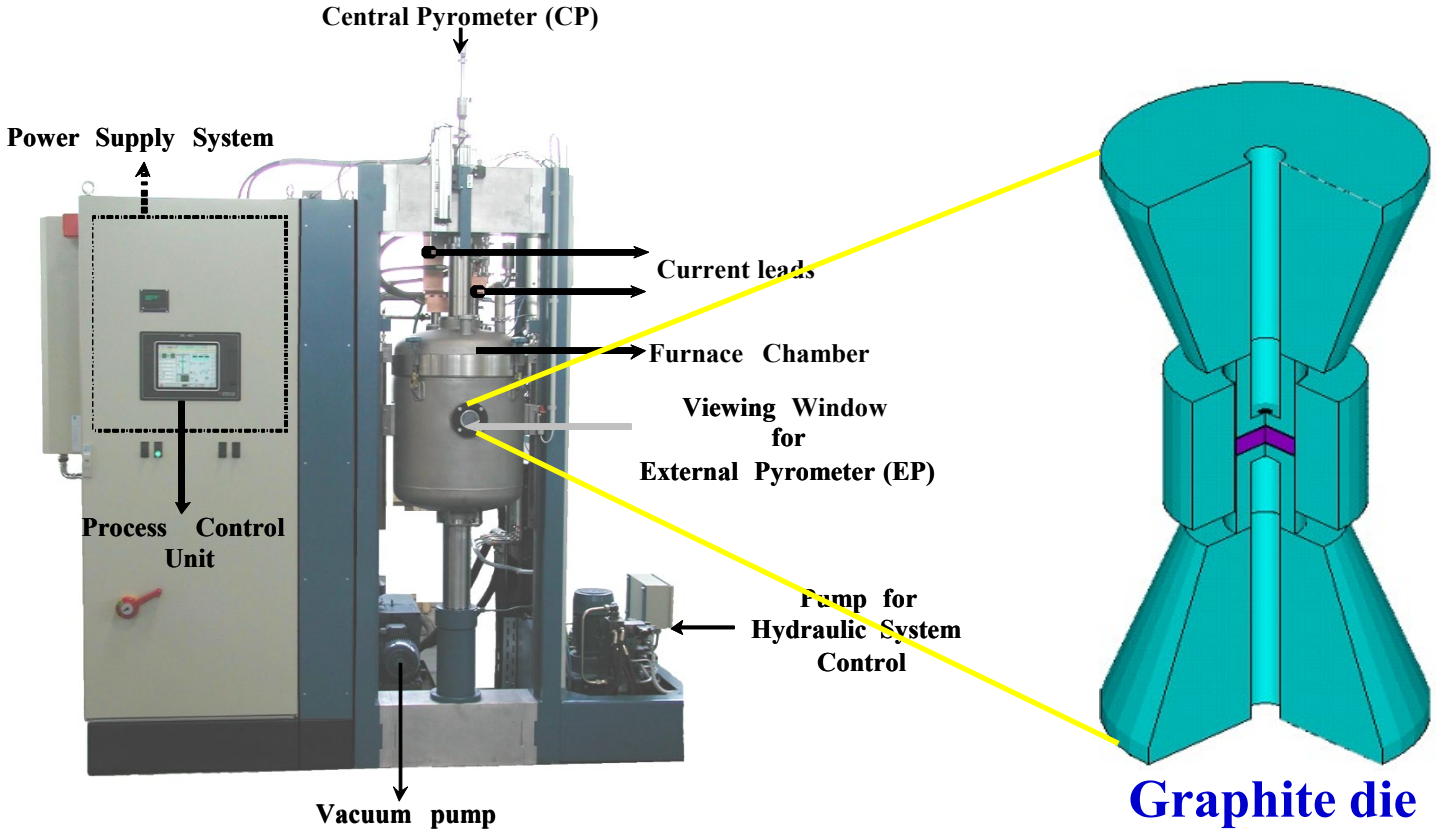

Graphite die set-up

SPS at 2000°C in 30, 40 or 56 mm diameter graphite dies at 30 MPa

High temperature oxidation tests at grain boundary engineered SiC

Slow transient tests of doped SiC from 500 to 1600°C

(heating rate of 4 K/min) in steam

Sample	Symbol	Composition (wt%)	Starting materials
SiC1	SiC-15YS1	SiC-15 wt% (1 mole Y_2O_3+1 mole SiO_2)	SiC, Y_2O_3, SiO_2
SiC2	SiC-15YS2	SiC-15 wt% (1 mole Y_2O_3+2 mole SiO_2)	SiC, Y_2O_3, SiO_2
SiC3	SiC-15YAG	SiC-15 wt% (3 mole Y_2O_3+5 mole Al_2O_3)	SiC, Y_2O_3, Al_2O_3
SiC4	SiC-15YbS1	SiC-15 wt% (1 mole Yb_2O_3+1 mole SiO_2)	SiC, Yb_2O_3, SiO_2
SiC5	SiC-15YbAG	SiC-15 wt% (3 mole Yb_2O_3+5 mole Al_2O_3)	SiC, Yb_2O_3, Al_2O_3
SiC6	SiC-15YbS2	SiC-15 wt% (1 mole Yb_2O_3+2 mole SiO_2)	SiC, Yb_2O_3, SiO_2
SiC7	SiC-15LaS1	SiC-15 wt% (1 mole La_2O_3+1 mole SiO_2)	SiC, La_2O_3, SiO_2
SiC8	SiC-15NdS1	SiC-15 wt% (1 mole Nd_2O_3+1 mole SiO_2)	SiC, Nd_2O_3, SiO_2

Grain boundary doped SiC

Sample	Symbol	Composition (wt%)	Starting materials
GS1	SiC	Pure SiC	SiC
GS2	SiC-0.5Y	SiC-0.5 wt% Y_2O_3	SiC, Y_2O_3
GS3	SiC-0.5Yb	SiC-0.5 wt% Yb_2O_3	SiC, Yb_2O_3
GS4	SiC-0.5Nd	SiC-0.5 wt% Nd_2O_3	SiC, $Nd(NO_3)_3.6H_2O$
GS5	SiC-0.5La	SiC-0.5 wt% La_2O_3	SiC, $La(NO_3)_3.6H_2O$
GS6	SiC-0.5AlN	SiC-0.5 wt% AlN	SiC, AlN

Transient tests

Symbol	m_0, g	m_{PT}, g	Δm, mg	Δm, %
SiC-15YS1	0.5207	0.5235	2.8	0.538
SiC-15YS2	0.7464	0.7470	0.6	0.080
SiC-15YAG	0.8920	0.8819	-10.1	-1.13
SiC-15YbS1	0.6110	0.6118	0.8	0.131
SiC-15YbAG	0.4942	0.4947	0.5	0.101
SiC-15YbS2	0.8014	0.8021	0.7	0.087
SiC-15LaS1	0.5736	0.5733	-0.3	-0.052
SiC-15NdS1*	0.2603	0.2660	5.7	2.19
SiC	0.4302	0.4312	1.0	0.232
SiC-0.5Y	0.4590	0.4593	0.3	0.065
SiC-0.5Yb	0.6581	0.6581	0	0
SiC-0.5Nd	0.5284	0.5285	0.1	0.019
SiC-0.5La	0.5563	0.5564	0.1	0.018
SiC-0.5AlN	0.5334	0.5535	0.1	0.018

* Test was stopped at 1140°C

Transient tests

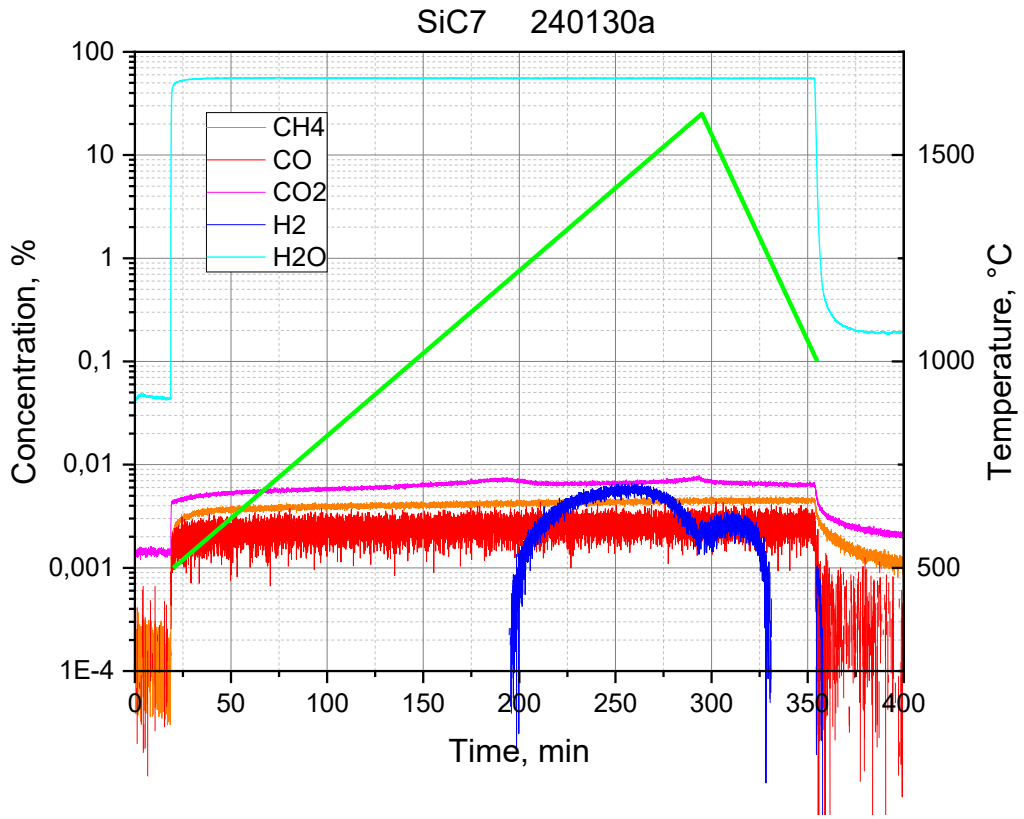

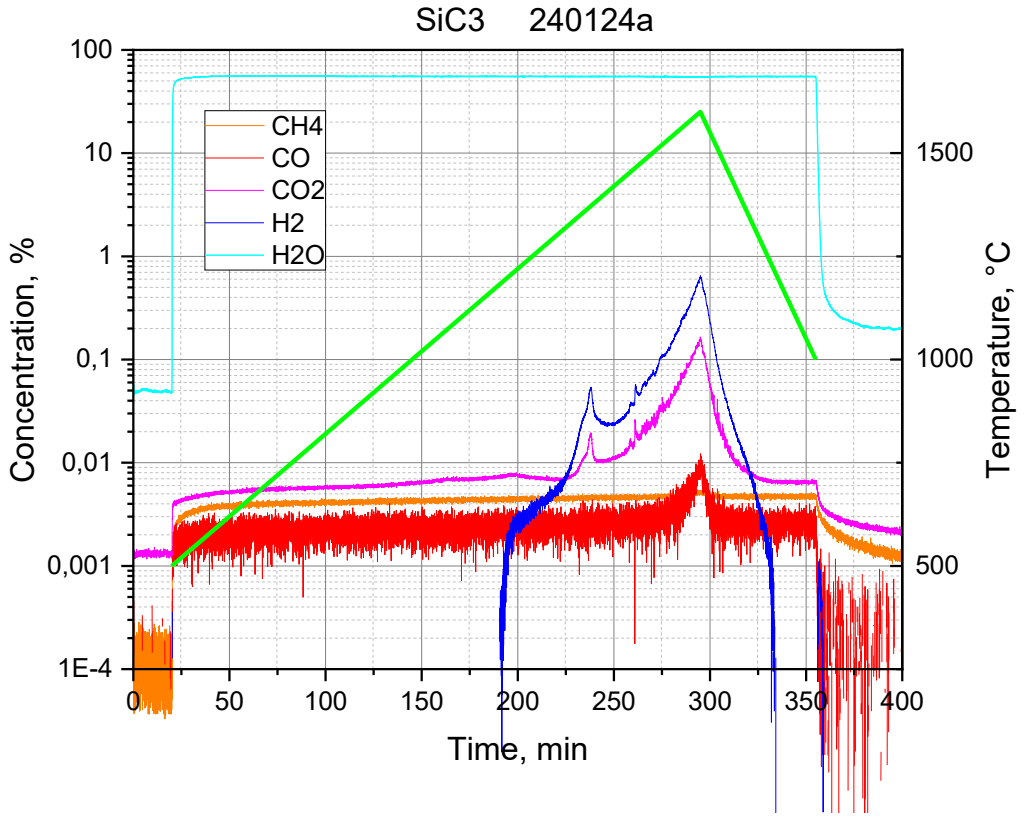

Transient tests

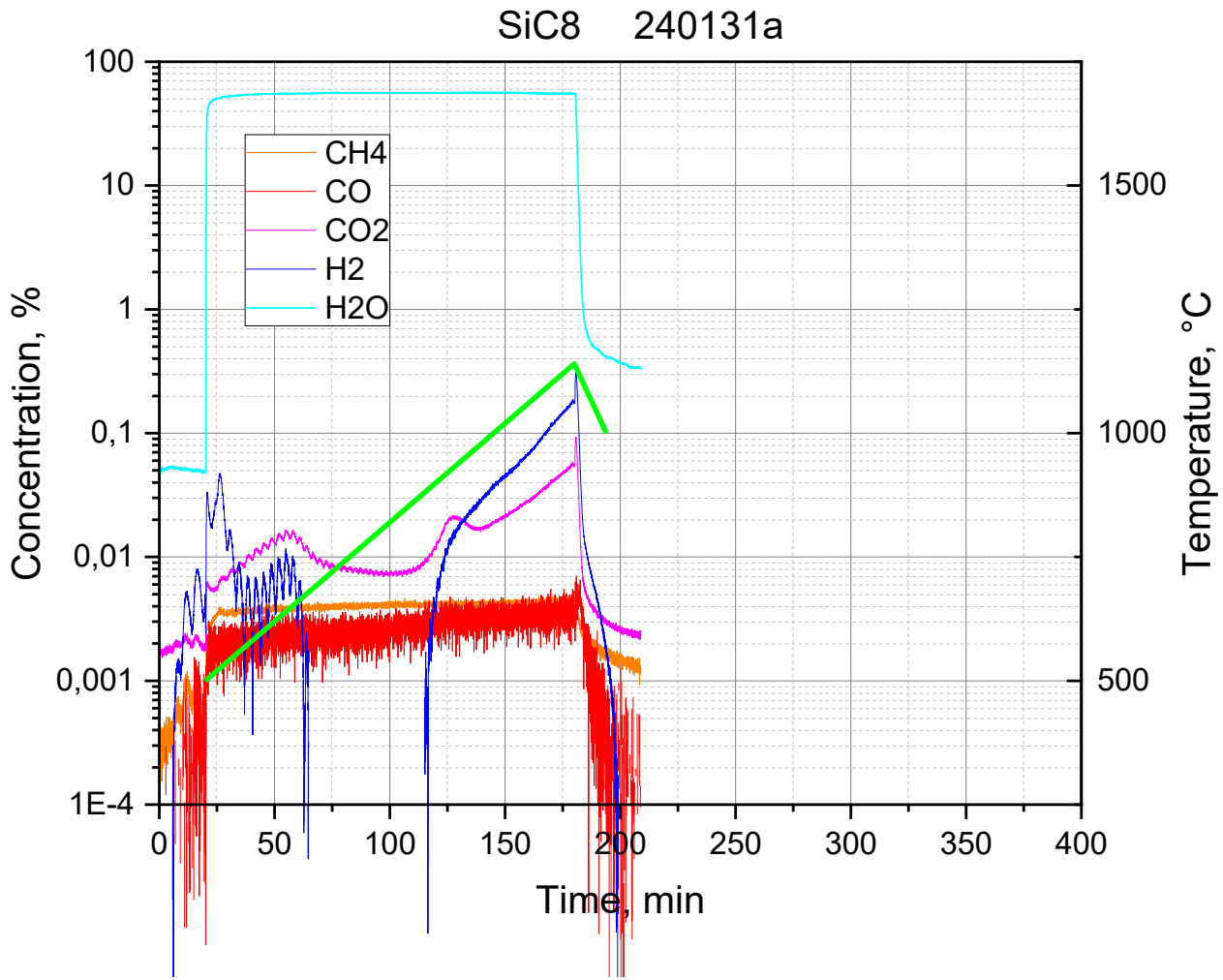

Transient tests

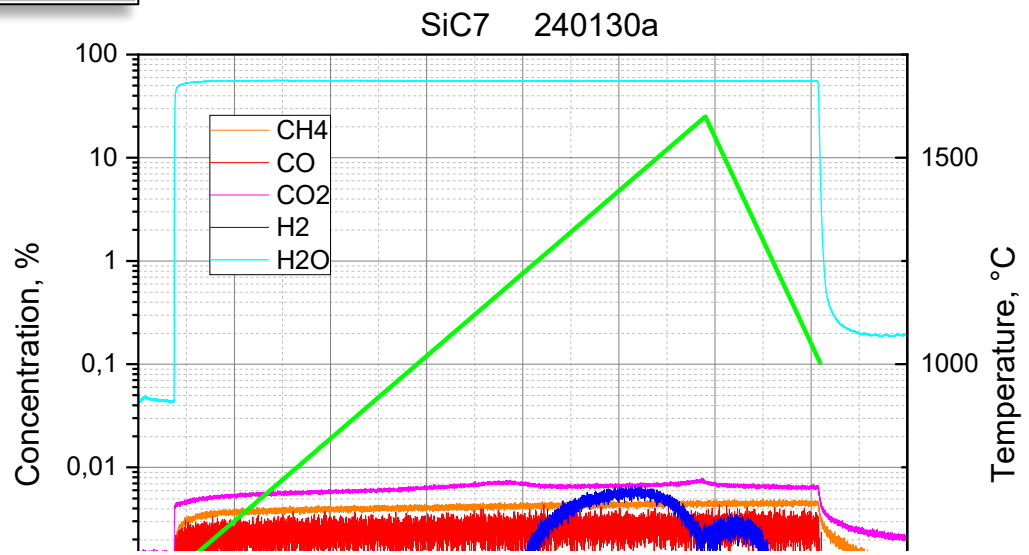

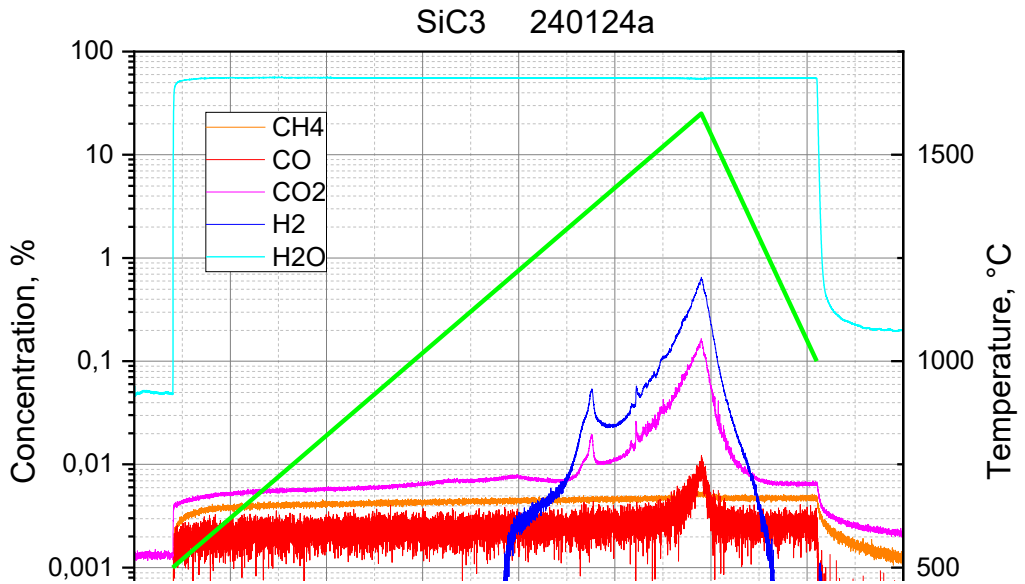

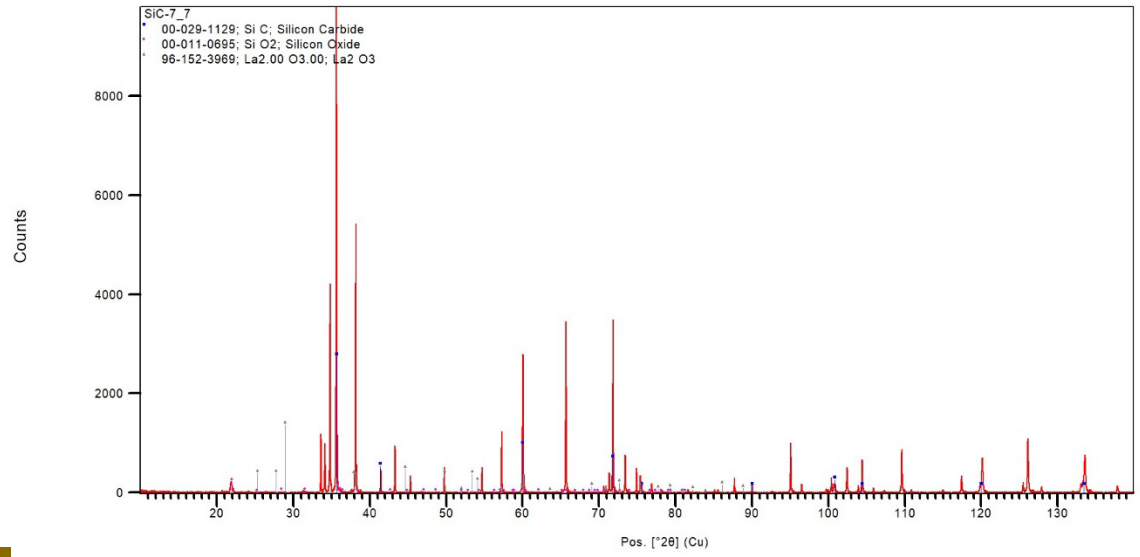

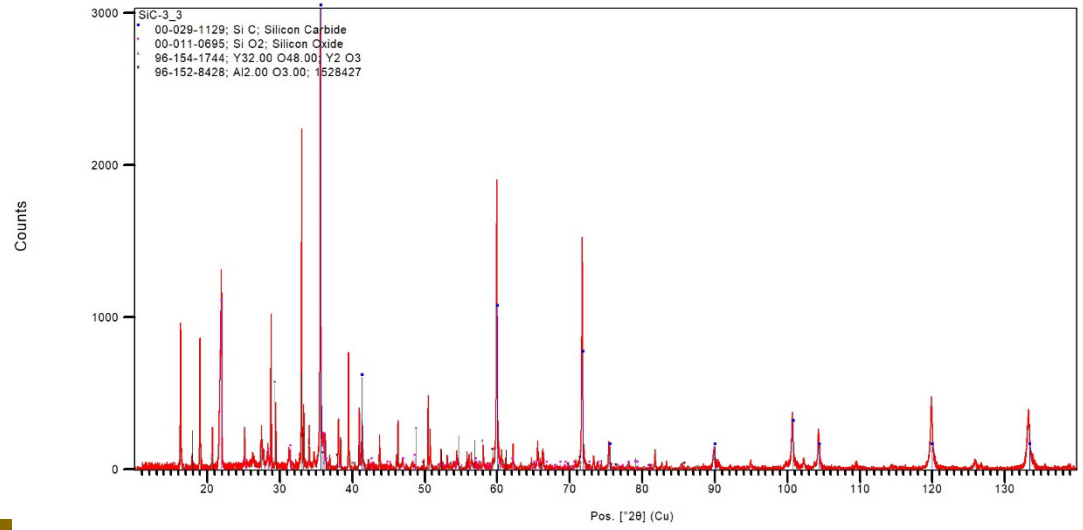

Transient tests

Sample GS1 SiC

Before the test

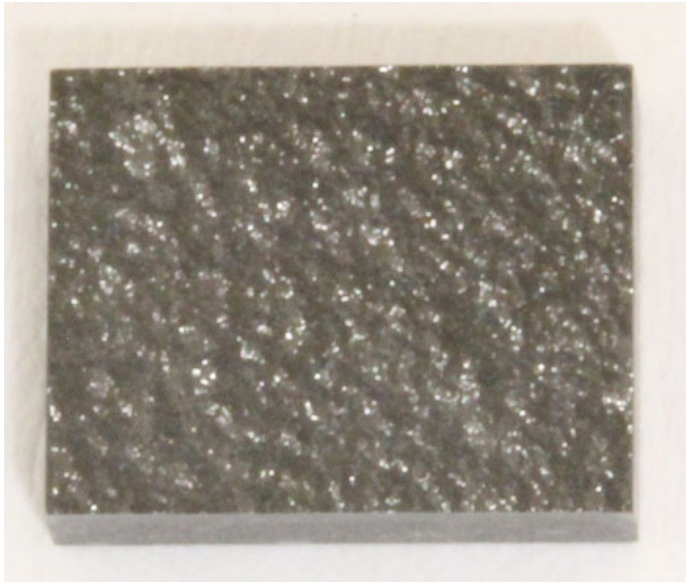

after the test upper side

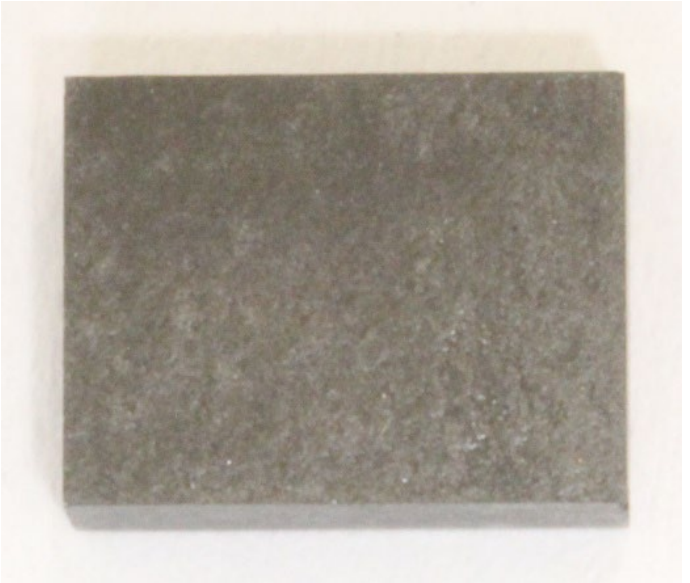

lower (contact) side

Transient tests

Sample SiC3

Before the test

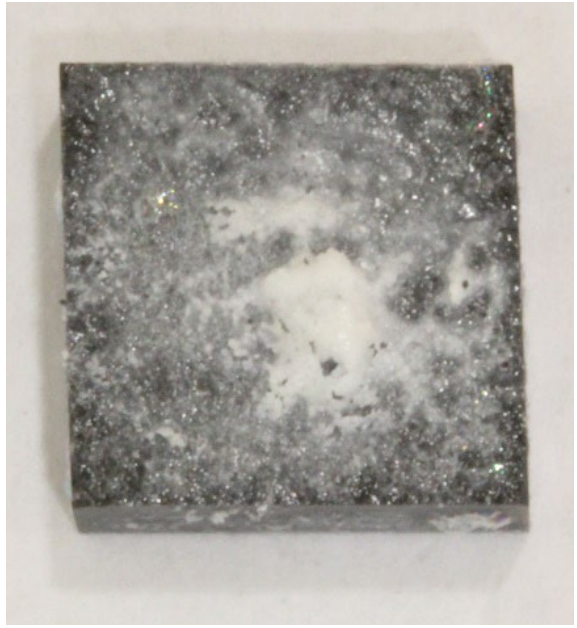

after the test upper side

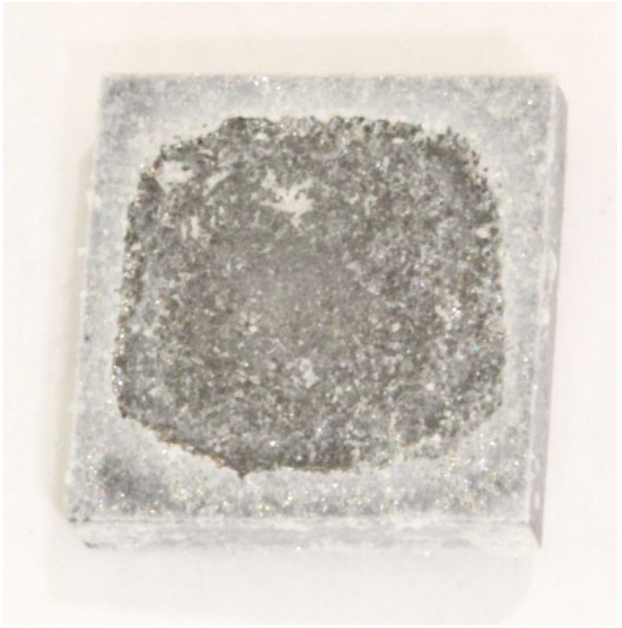

lower (contact) side

Transient tests

Sample SiC8

Before the test

after the test upper side

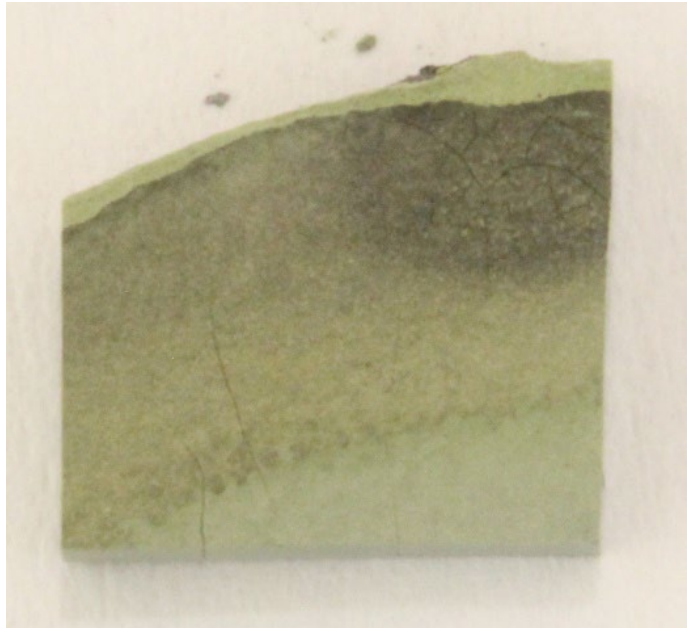

lower (contact) side

Results/Discussion

GS1 SiC

Top

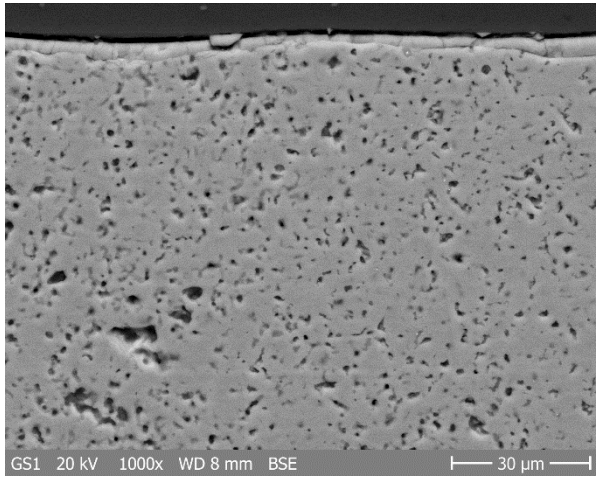

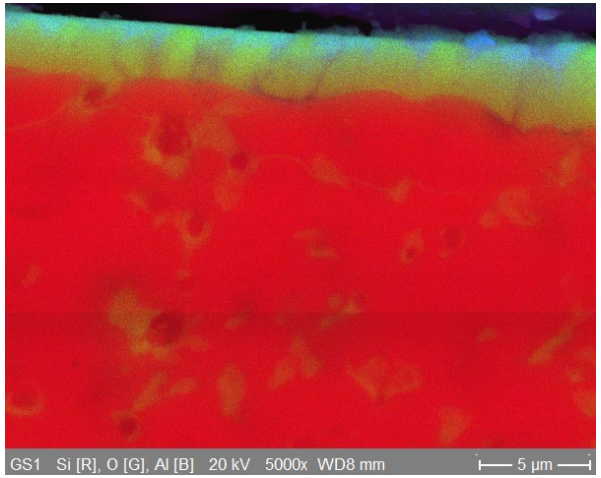

Bottom

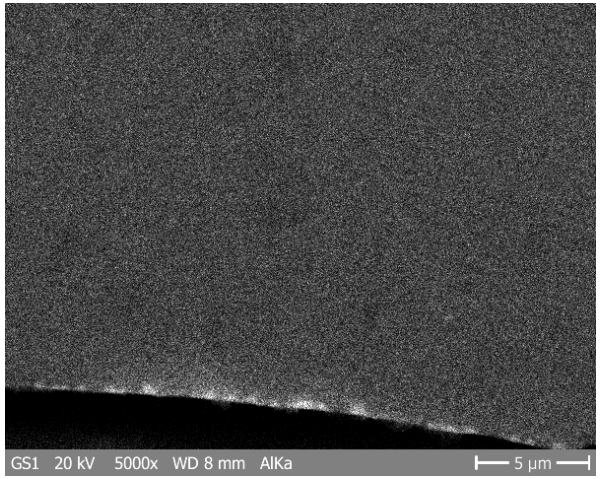

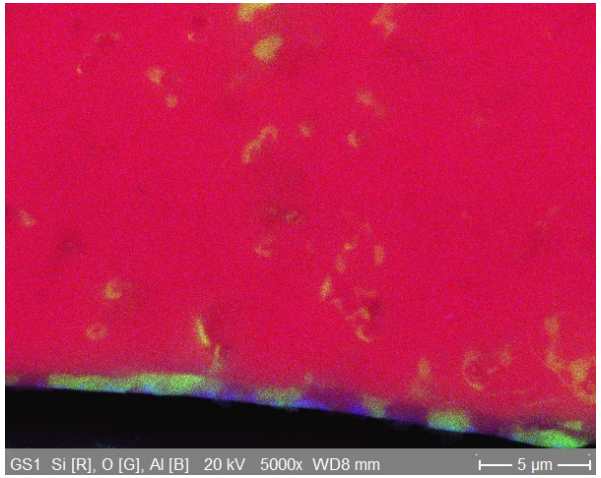

Surface

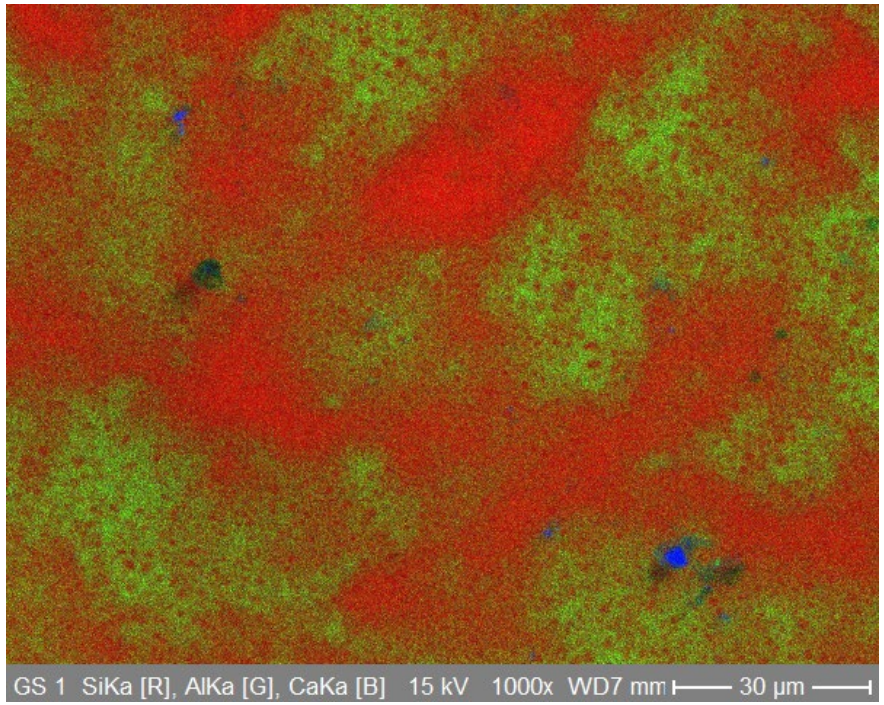

Results/Discussion

SiC3 SiC-15YAG

Top

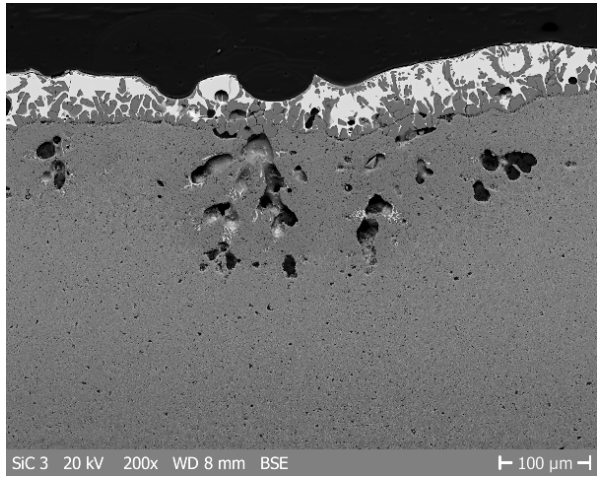

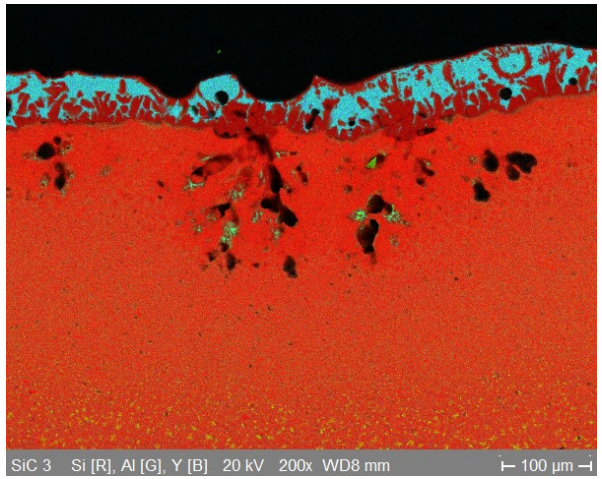

Bottom

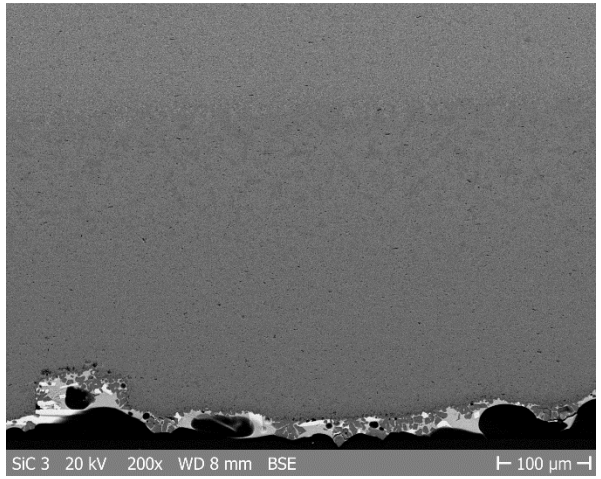

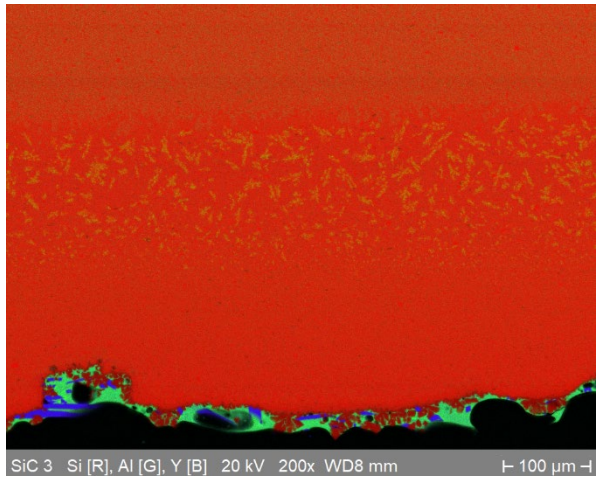

Surface

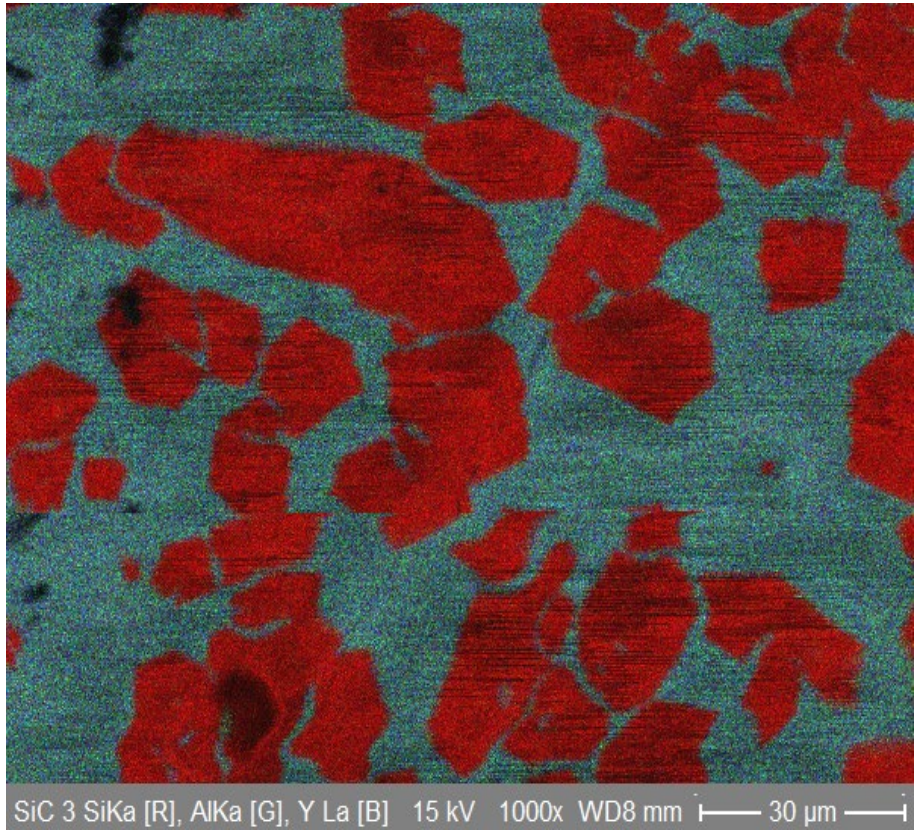

Results/Discussion

SiC5 SiC-15YbAG

Top

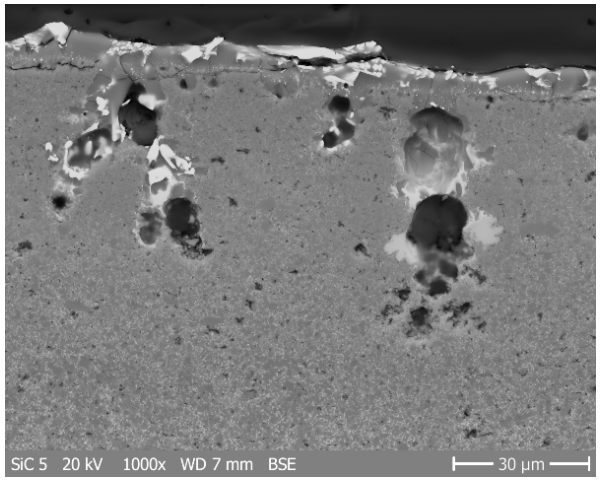

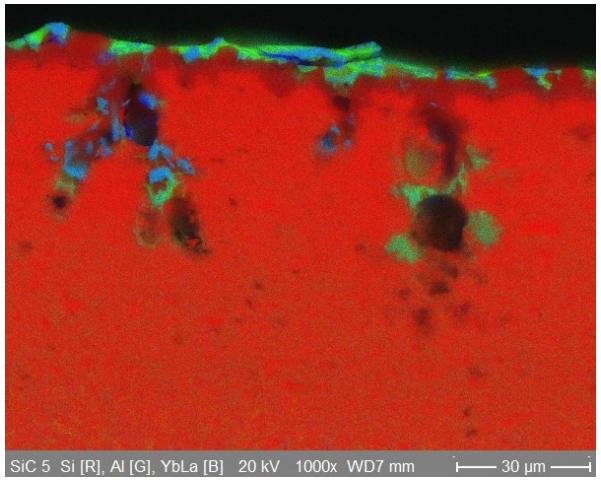

Bottom

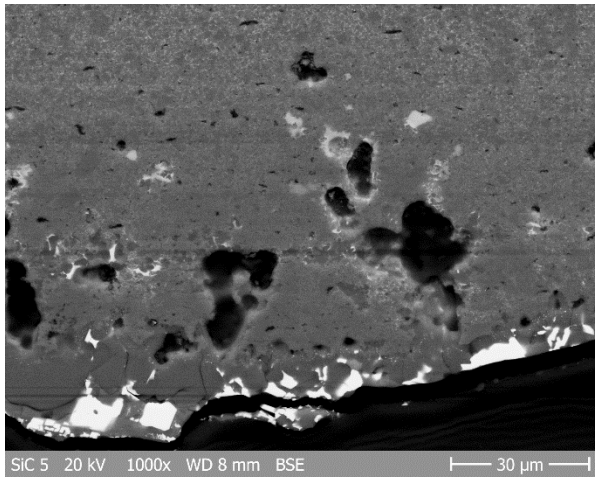

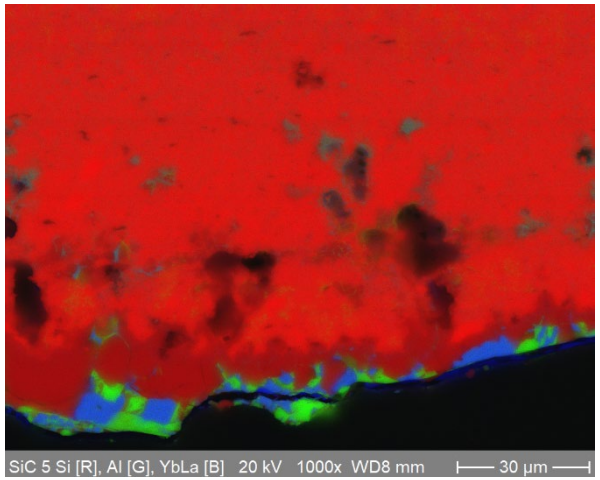

Surface

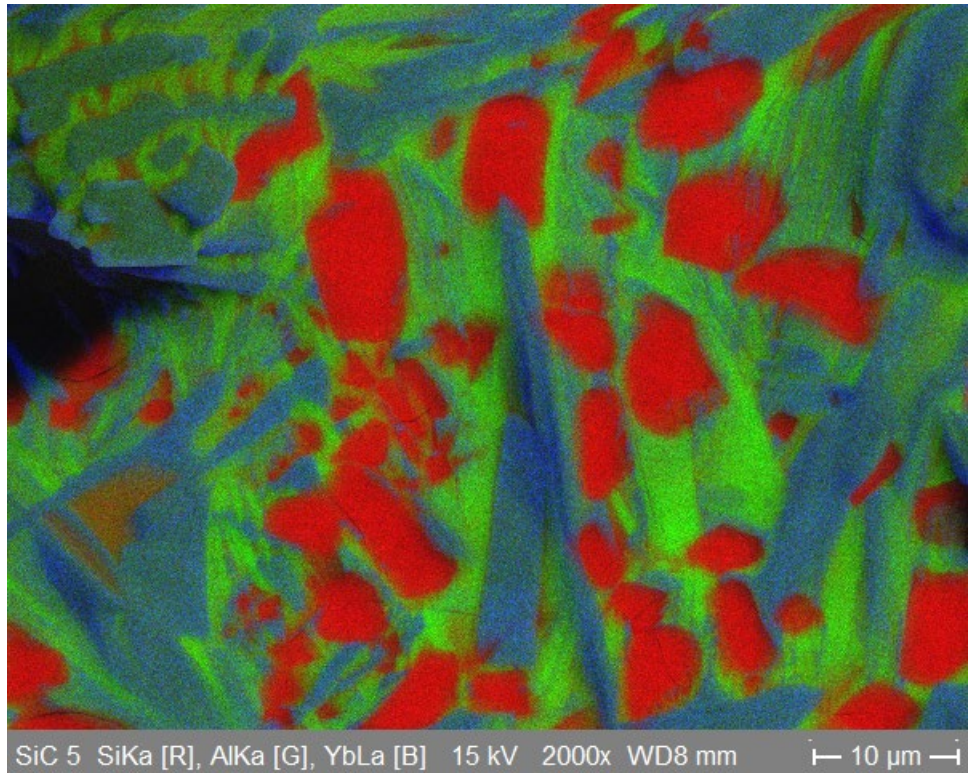

Results/Discussion

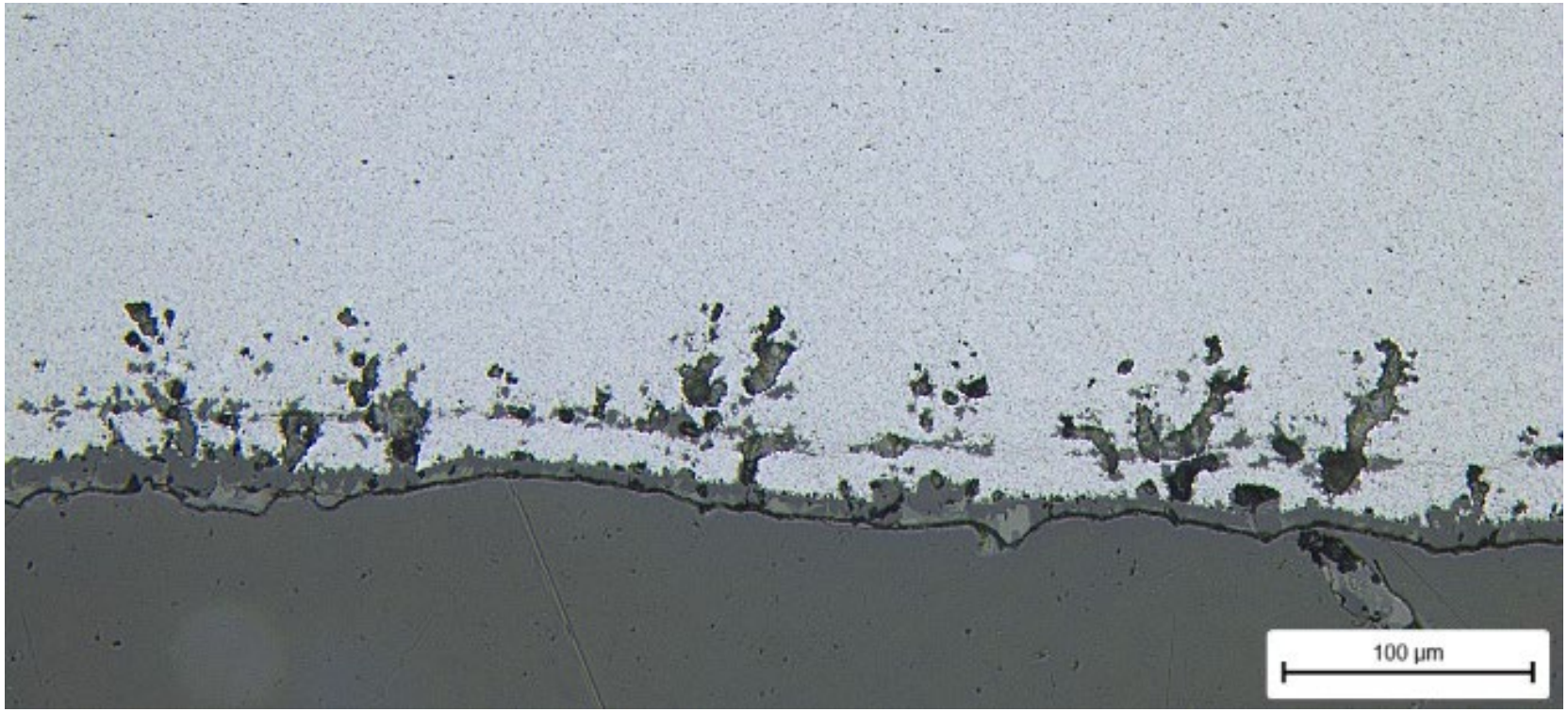

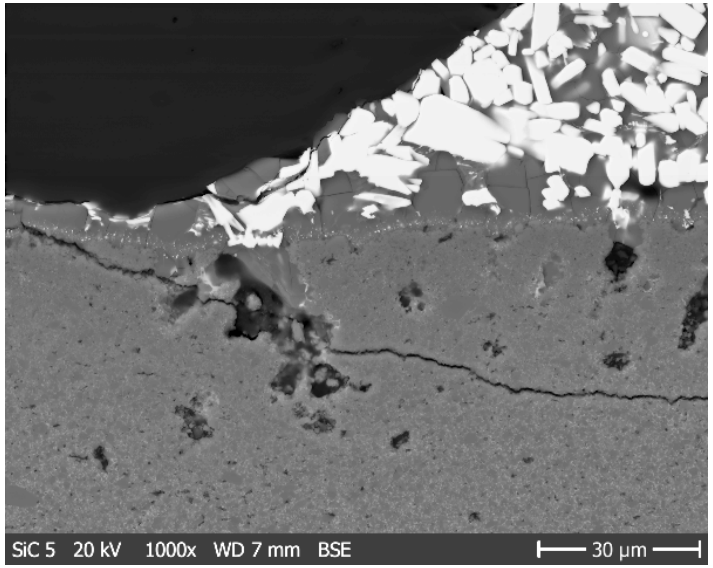

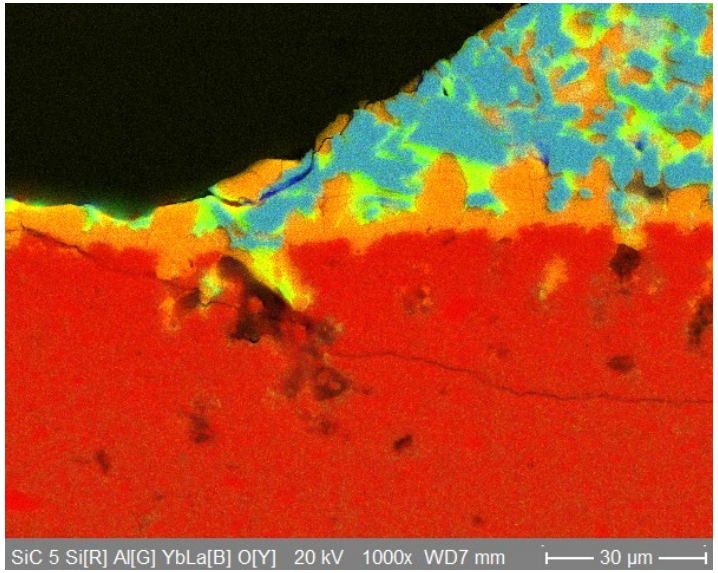

Results/Discussion

Yttria plate of SiC3

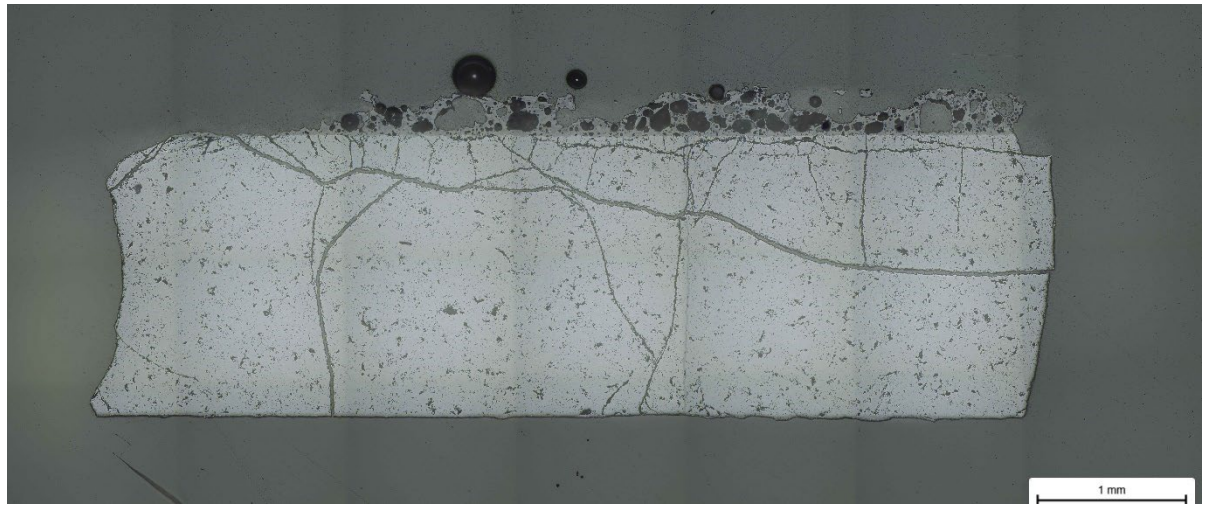

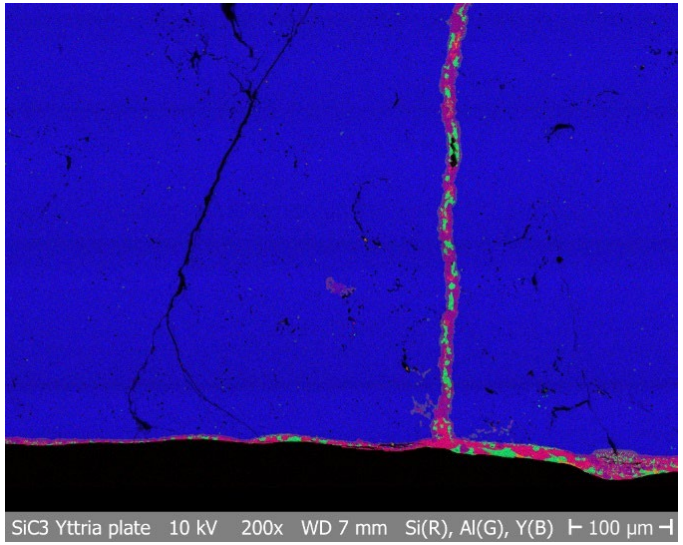

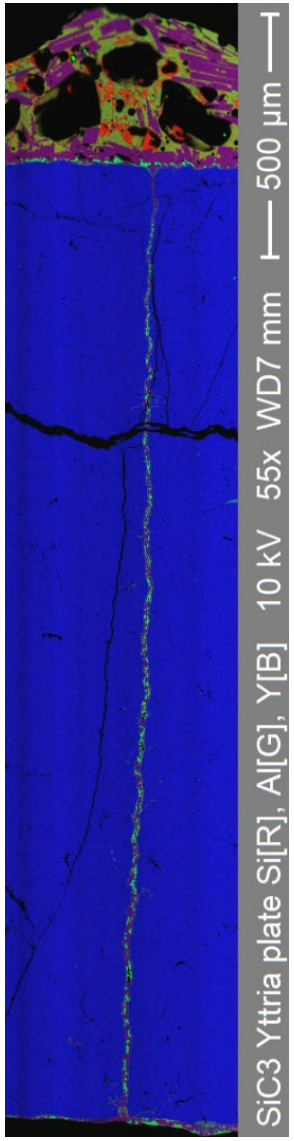

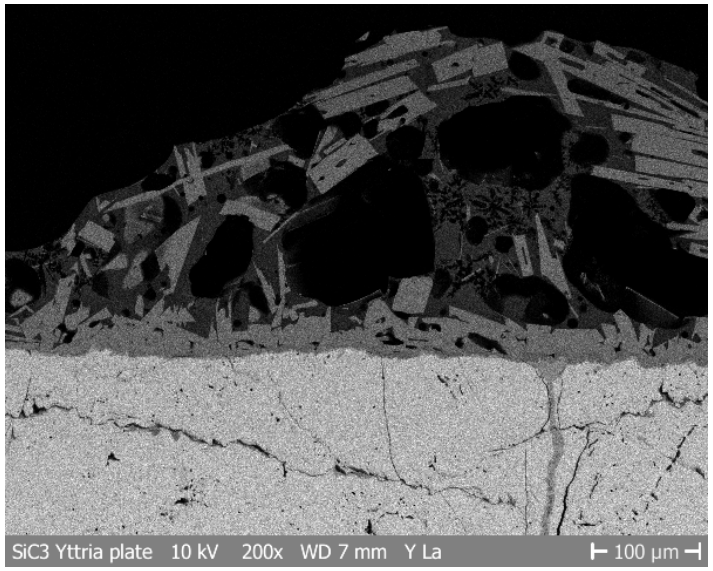

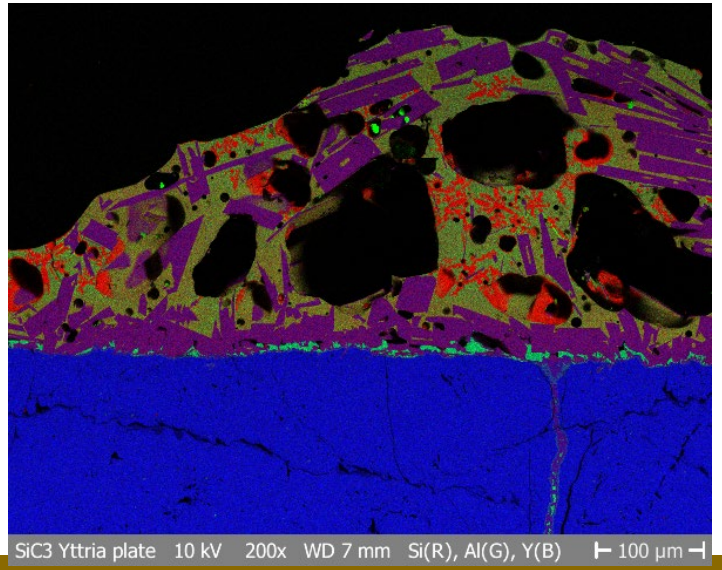

Results/Discussion

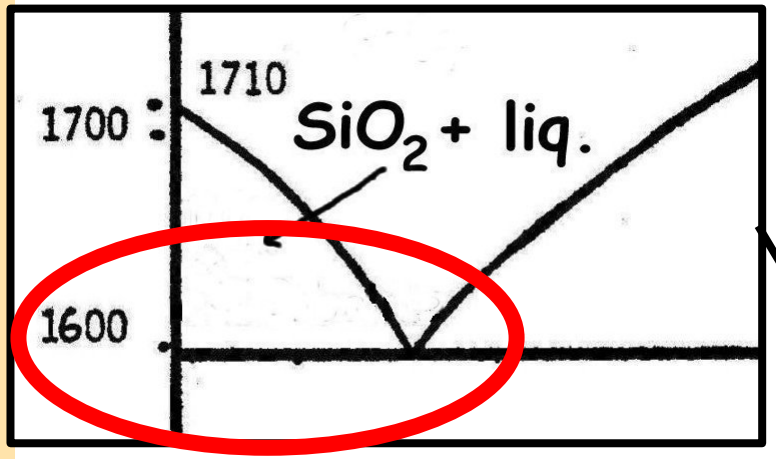

Diagramme de phases du système silice-alumine

ccd = composé chimiquement défini

s.s. = solution solide (composition chimique variable)

α-Al_2O_3 = corindon

2100
2000
1900
1800
1700
1600
1500
1400
1710
SiO_2 + liq.
liquide
liquide + mullite ccd
1595
SiO_2 + mullite ccd
mullite s.s.
1850
mullite s.s. + liquide
liq. + α-Al_2O_3
2040
1840
mullite s.s. + α-Al_2O_3
SiO_2
10
20
30
40
50
60
70
80
90
Al_2O_3 (% masse)
mullite ccd
($3Al_2O_3.2SiO_2$)

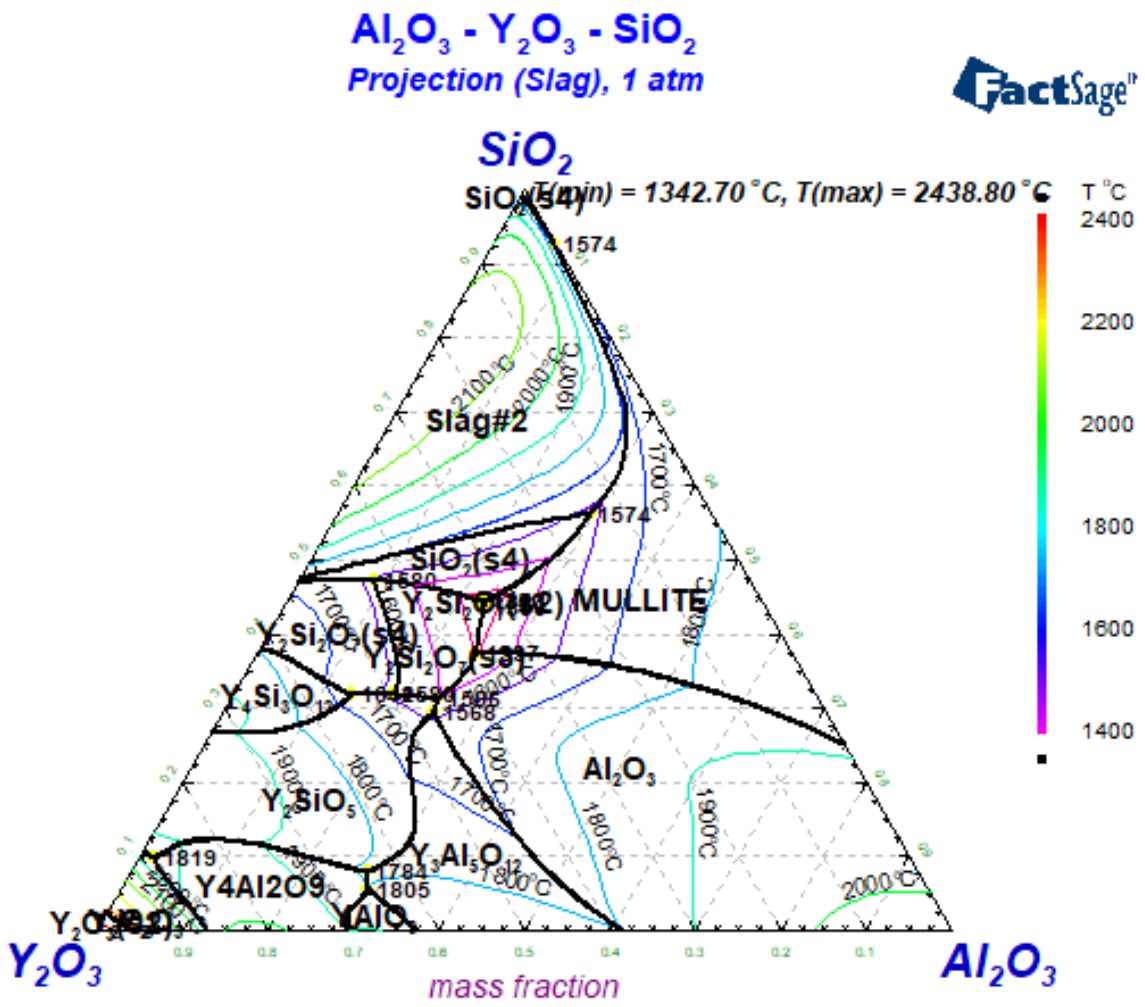
Al2O3 - Y2O3 - SiO2
Projection (Slag), 1 atm
FactSage
SiO2
T(min) = 1342.70 °C, T(max) = 2438.80 °C
T °C
2400
2200
2000
1800
1600
1400
SiO2(s4)
1574
Slag#2
2100 °C
2000°C
1900°C
1700°C
SiO2(s4)
1580
Y2Si2O7(s2)
MULLITE
Y2Si2O7(s3)
Y4Si3O12
1568
Al2O3
Y2SiO5
1819
Y4Al2O9
Y3Al5O12
1784
1805
YAlO3
1800°C
2000 °C
Y2O3
Al2O3
mass fraction

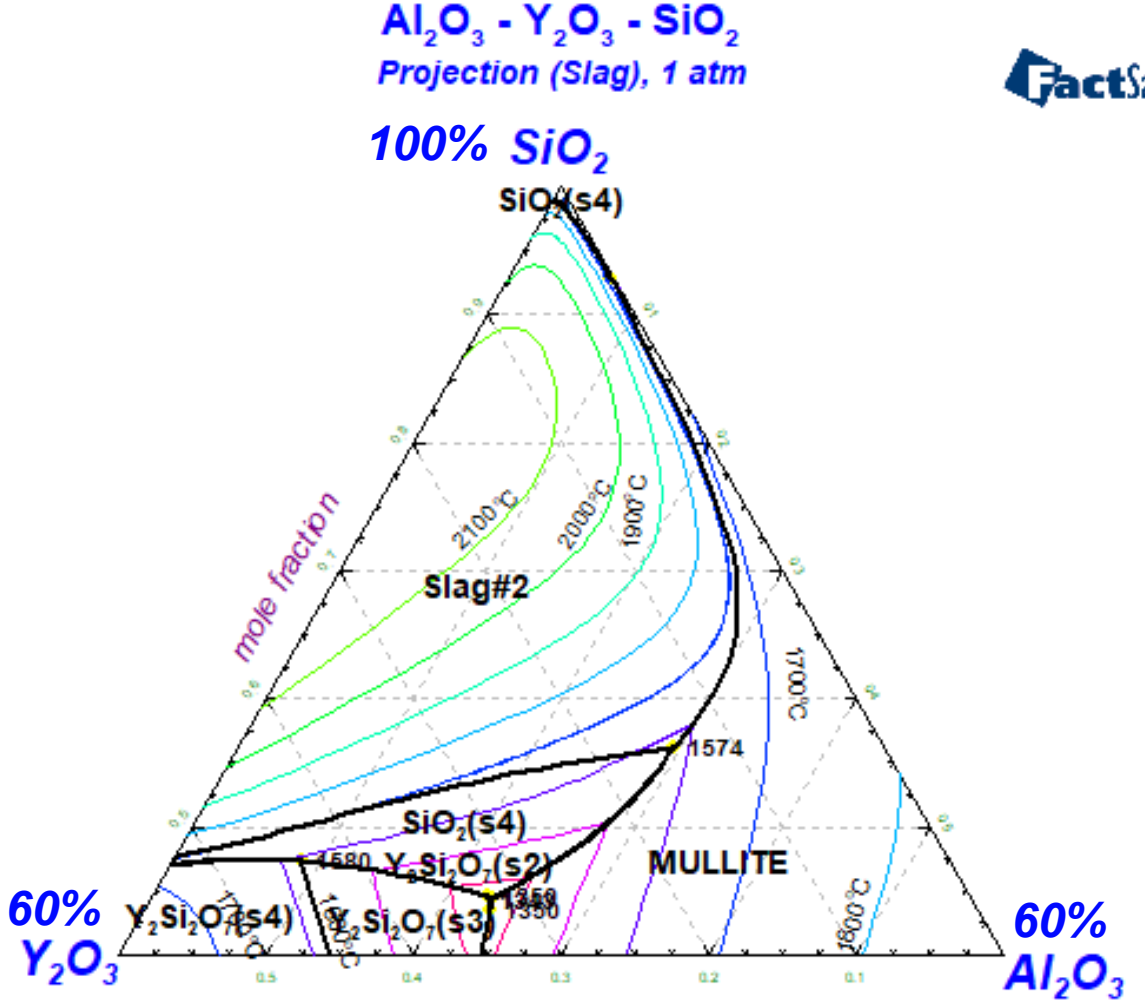
Al2O3 - Y2O3 - SiO2
Projection (Slag), 1 atm
FactSage
100% SiO2
SiO2(s4)
mole fraction
2100 °C
2000°C
1900°C
Slag#2
1700°C
1574
SiO2(s4)
1580
Y2Si2O7(s2)
MULLITE
Y2Si2O7(s4)
Y2Si2O7(s3)
1350
1800°C
60%
Y2O3
60%
Al2O3

Results/Discussion

SiC8 SiC-15NdS1

Top

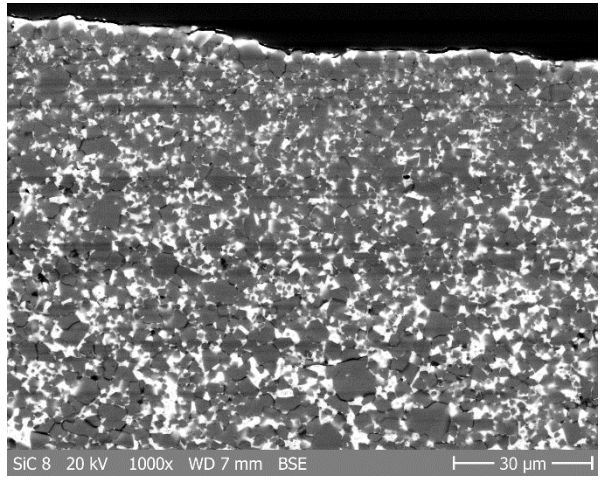

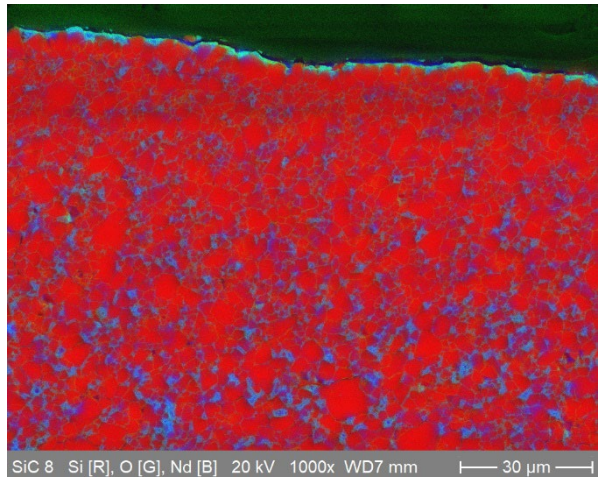

Bottom

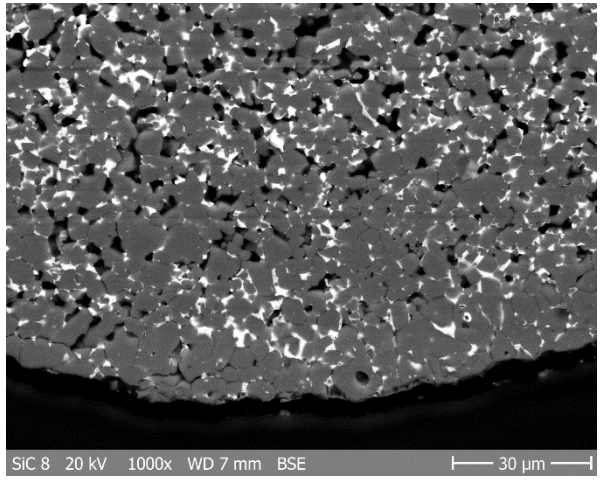

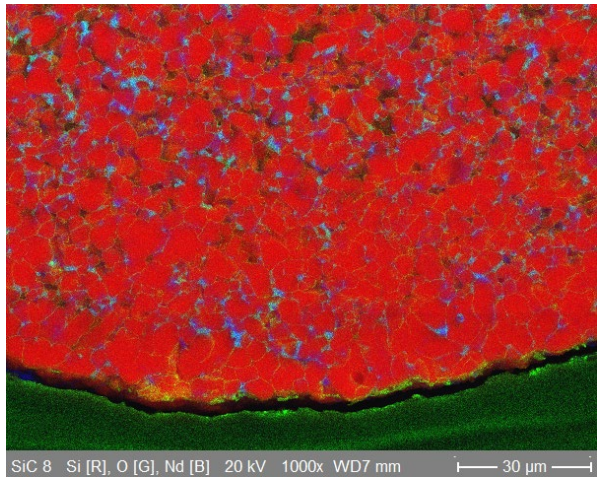

Surface

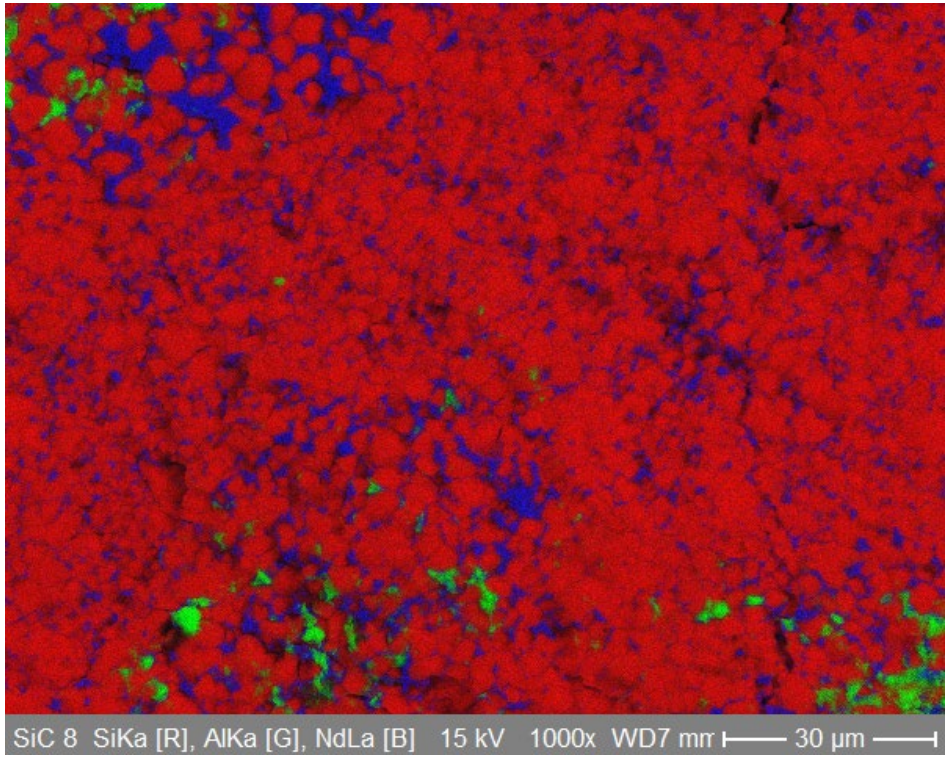

Results/Discussion

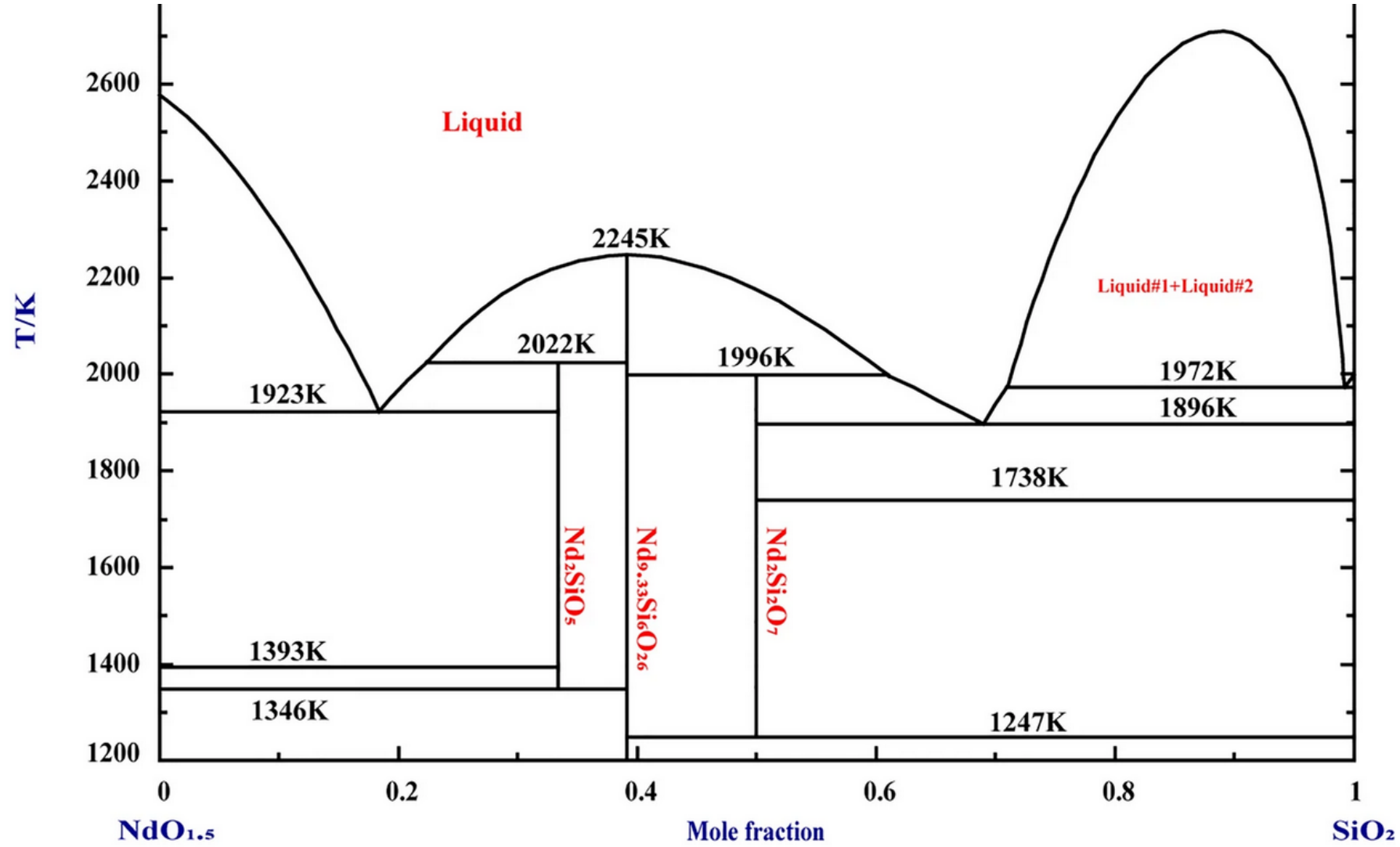

Transient tests

- Alumina alloyed SiC samples and the sample alloyed with neodymium oxide show significantly stronger reactions starting at about 1250°C (alumina alloyed samples) and already at 800°C (neodymium oxide alloyed sample)
- All other show only low reaction rates even at 1600°C.
- Eutectic SiO_2-Al_2O_3 melt is formed at T < 1600°C. Therefore, SiO_2-Al_2O_3 perform well only until 1550°C and are not much better than FeCrAl´s.
- Decomposition of SiC and Nd_2O_3.

- Conclusion: skip out aluminum and neodymium oxide as alloying substances in further R&D efforts

Outloock and Acknowledgement

Next steps:

- Very high temperature SiC oxidation tests in steam with varying hydrogen partial pressures
- HT and VHT tests on demand of the SCORPION partners

Thanks to KU Leuven for providing the samples and to U. Stegmaier (KIT) for performing the tests and the PTE.
Thanks to the sponsor.

EU Horicon 2020
Grant number **101059511**

Thank you for your attention

SCORPION

Karlsruhe Institute of Technology

SiC Composite Claddings: LWR Performance Optimization for Nominal and Accident Conditions

Status of WP5 – Cladding/coolant interaction tests
Very High Temperature Oxidation Tests

Mirco Grosse

KIT

Email Mirco.Grosse@KIT.edu

This project has received funding from the Euratom Research and Training Programme 2021-2025 under Grant Agreement No 101059511

Youho Lee

SNU

Integral LOCA Experiment to Investigate Comprehensive Accident Behavior of Cr-Coated Accident Tolerant Fuel (ATF)

This talk introduces the *i*-LOCA facility at Seoul National University, designed to investigate the integral accident behavior of a fuel rod during a Loss of Coolant Accident (LOCA). The facility enables research on various phenomena, including (1) ballooning and burst, (2) fuel dispersal using surrogate fragmented pellets, (3) oxidation of the inner wall through the burst hole and outer wall through cracked coatings, (4) hydrogen generation, (5) formation of secondary hydrides, and (6) post-LOCA ductility along the axial positions. Key assessment results and insights into each of these phenomena are discussed. This comprehensive analysis of fuel accident behavior allows for evaluating the potential benefits of Cr-coated ATFs and, importantly, assessing whether the developing regulatory framework adequately addresses the safety-limiting factors of Cr-coated ATFs.

Integral LOCA Experiment to Investigate Comprehensive Accident Behavior of Cr-Coated Accident Tolerant Fuel (ATF)

2024. 11. 19.

Youho Lee, SungHoon Joung, Hyunwoo Yook, Boyeon Kweon,
Dongju Kim, Dahyeon Woo, Donghyeon Son, Dongki Lee, Seungri Hong

Department of Nuclear Engineering,
Seoul National University, Korea

leeyouho@snu.ac.kr

Contents of the Presentation

- **Introduction of the i-LOCA facility**
- **Integral LOCA behavior of Cr-coated ATF**
  - ▷ Ballooning and burst
  - ▷ Fuel dispersal using surrogate pellets
  - ▷ Oxidation through cracked Cr-coating
  - ▷ Secondary hydrides and PQD
  - ▷ Post-eutectic hydrogen generation
- **Conclusion**

Schen A facility)

Cyl

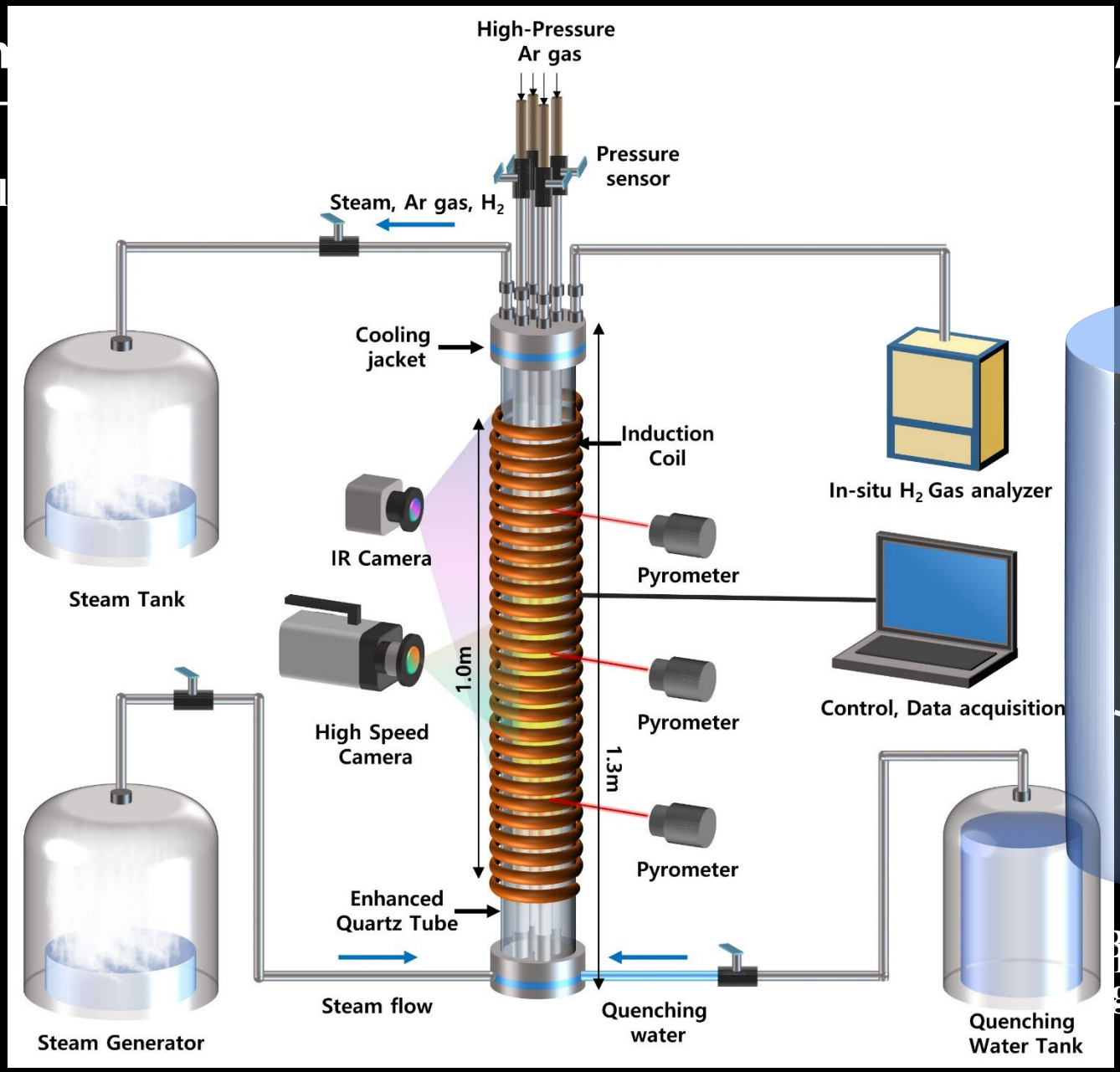

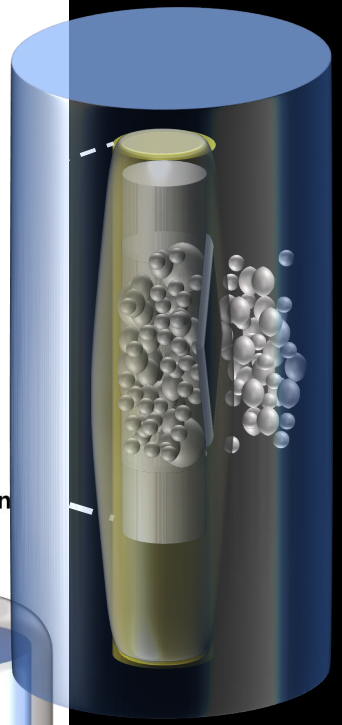

Burst & Fuel
Ballooning
gment Dispersal

Integral LOCA experiment at Seoul National University (*i*-LOCA facility)

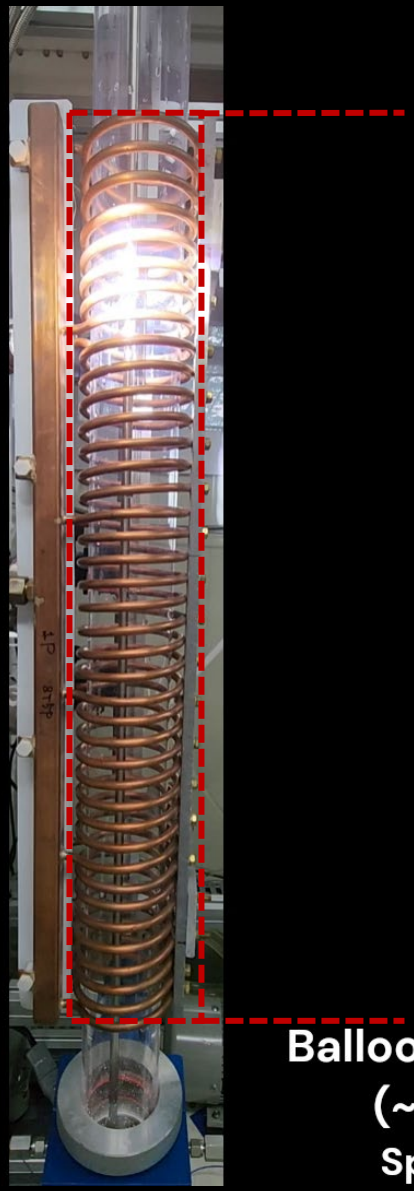

Ballooning&Burst
(~800°C)
Speed x10

<Digital camera> <IR camera>

<LOCA scenario>

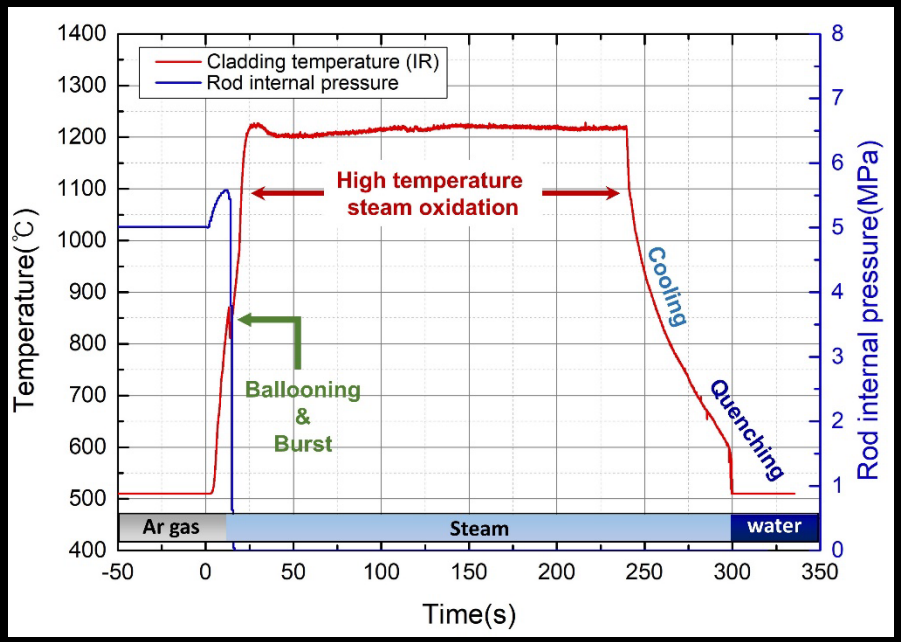

Integral LOCA experiment at Seoul National University (i-LOCA facility)

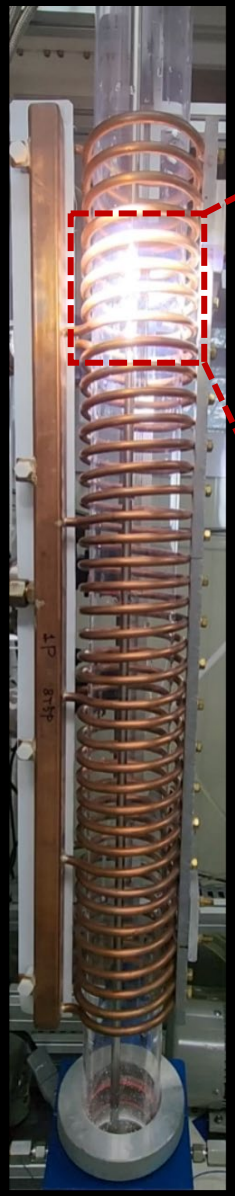

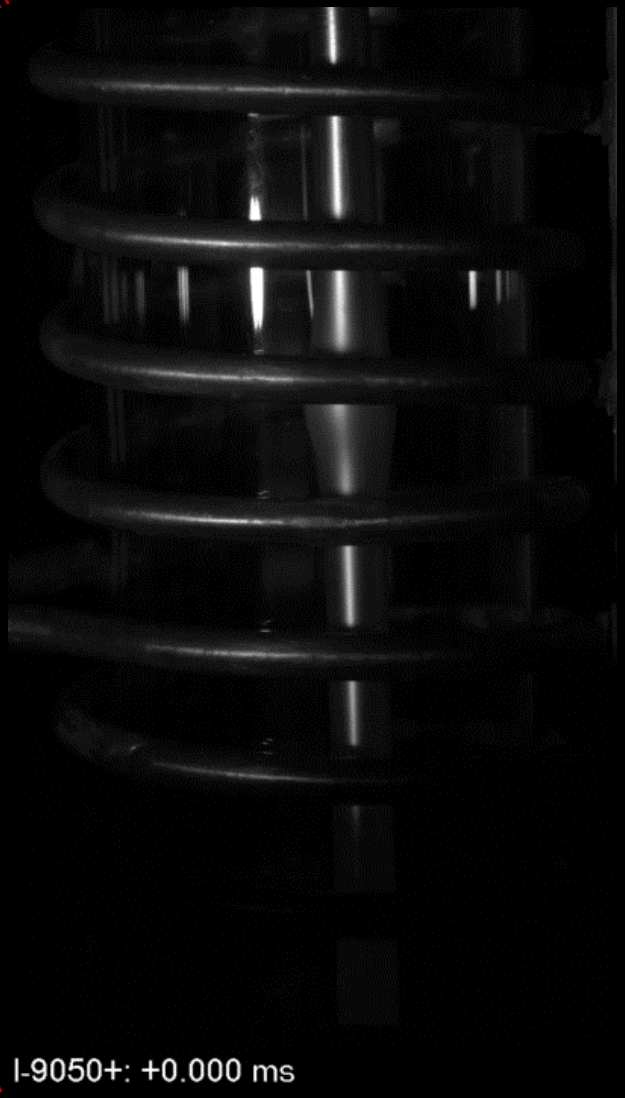

<Digital camera>

<High speed video camera>

Surrogate pellets to study dispersal behavior

Surrogate ZrO_2 pellet and powder simulating fragmented pellets [1]

① Cylinder Pellet
Bu < 55 GWd/MTU
(d=8.192mm)
Packing fraction : 96%

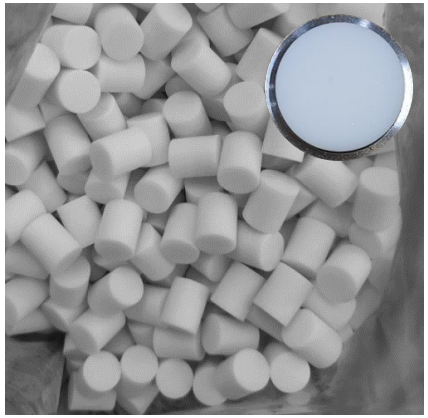

② Mixed Powder Pellet[2]
Bu ≈ 68 GWd/MTU
(d=0.3,0.5,1,2,3,5 mm
with the same mass fraction)
Packing fraction : 62.5%

<Referring to the fuel size distribution of NRC-Studsvik LOCA Program (Burnup 60~75 GWd/MTU) [1,2]>

③ Single Powder Pellet
Bu ≈ 94 GWd/MTU
(d=0.5mm)
Packing fraction : 62.1%>

Test rod condition for burst experiments

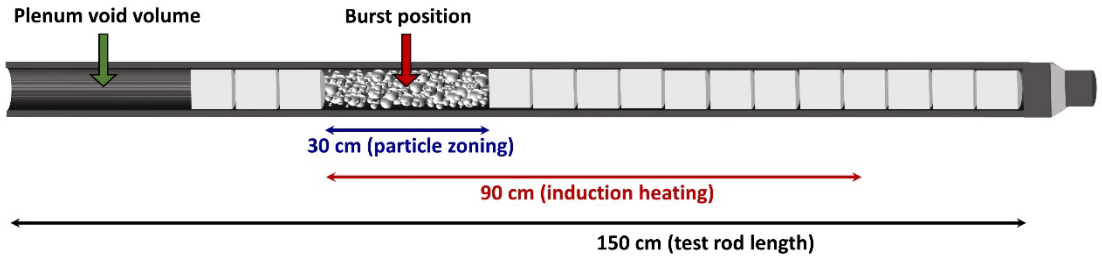

Cladding : HANA-6, Cr-HANA-6 (15μm, AIP), ZIRLO

Rod internal pressure : 1-7 MPa

- **Rod cold void volume : 30** cm^3
- **Powder pellet zoning length : 30 cm**
- **Heating rate : 60-80 ℃/s** (simulating LBLOCA)

[1] Sonnenburg, H., et al. "Report on fuel fragmentation, relocation and dispersal." Nuclear Energy Agency Committee on Safety of Nuclear Installations (2016).
[2] Flanagan, M. (2013). Post-test examination results from integral, high-burnup, fueled LOCA tests at Studsvik Nuclear Laboratory, 2013. Report NUREG-2160, US Nuclear Regulatory Commission, Washington, DC, USA, U.S.NRC.

Post-burst characterization using 3D scanner

HANA-6

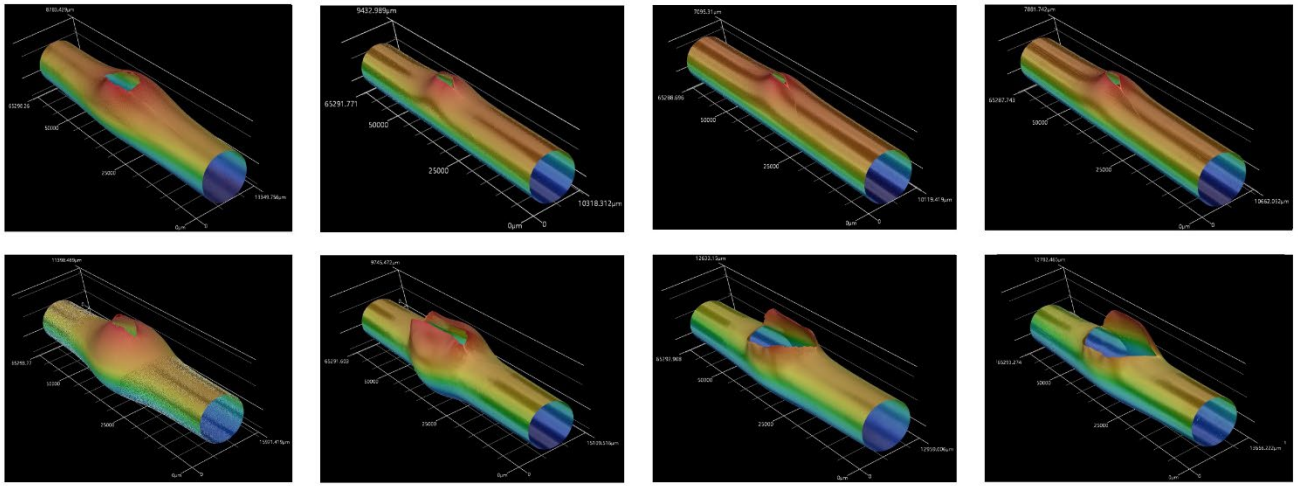

Cr-coated HANA-6

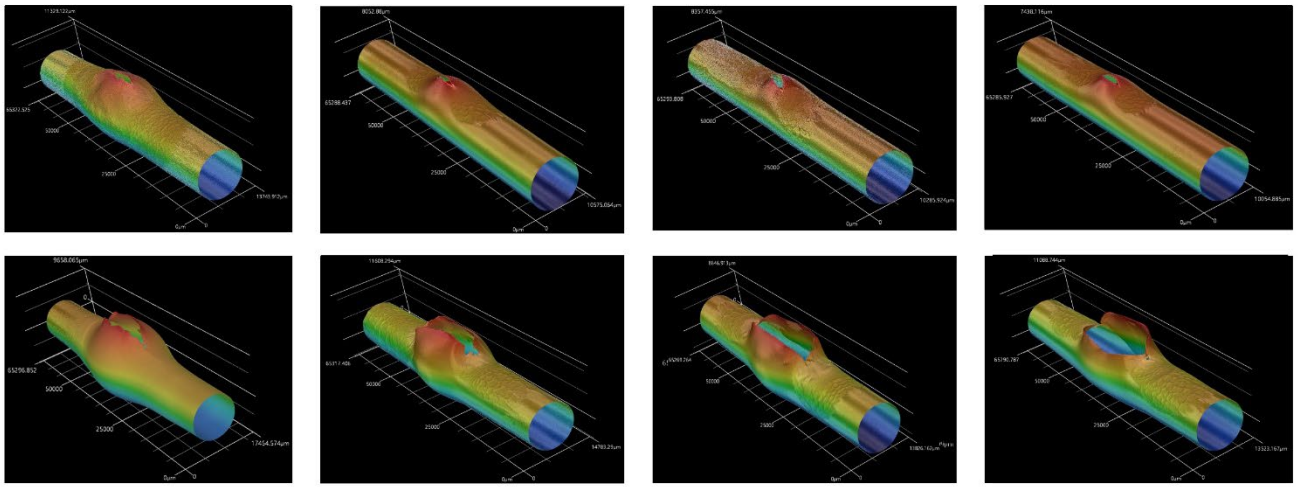

SNU burst result comparison with references

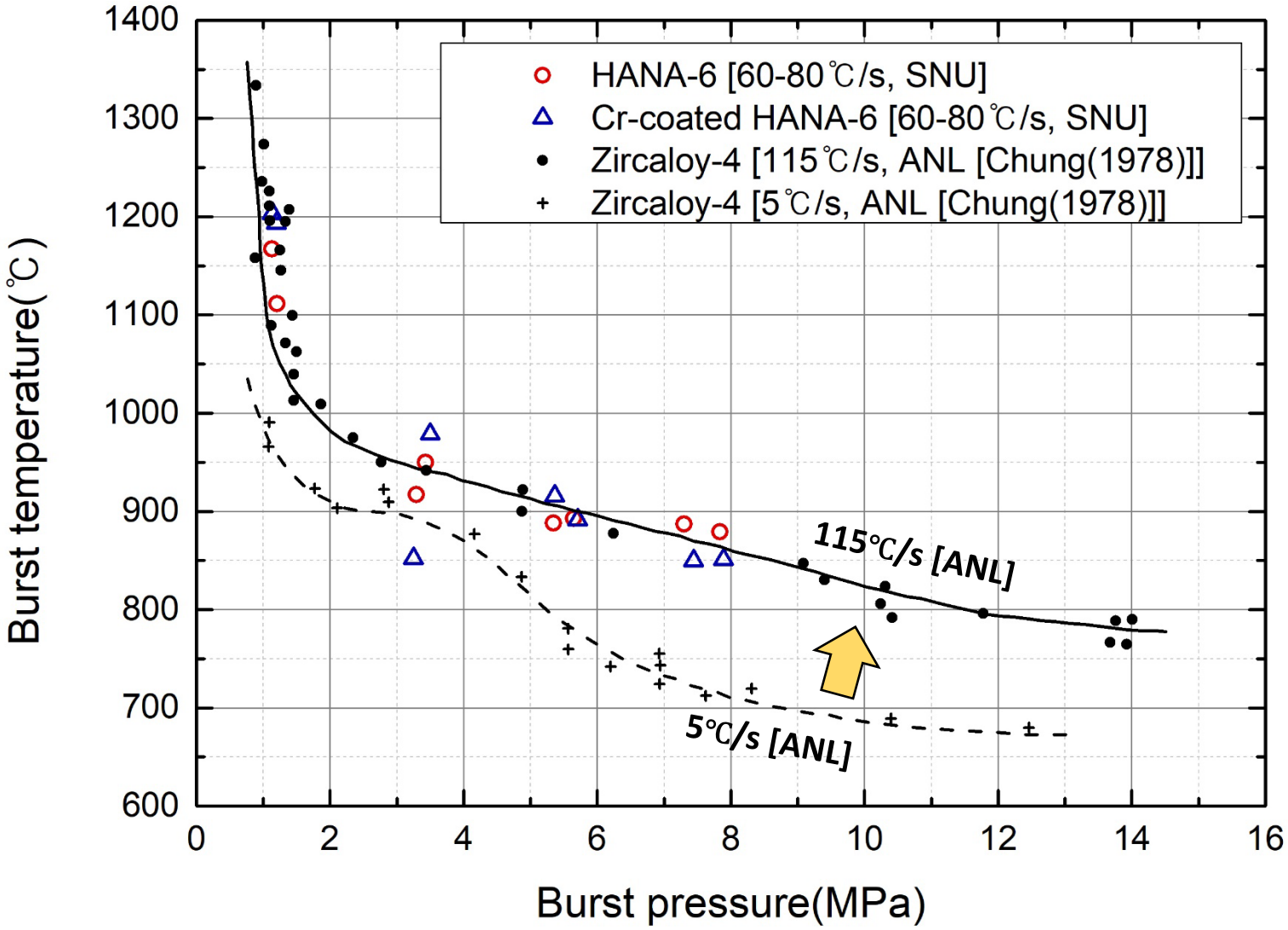

Burst shape of post-LOCA specimens

HANA-6	Cylinder pellet 	Single powder 
1 MPa	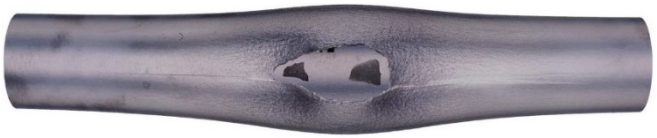	
5 MPa	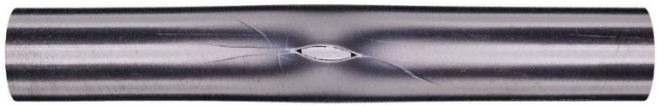	

Cr-coated HANA-6	Cylinder pellet 	Single powder 
1 MPa	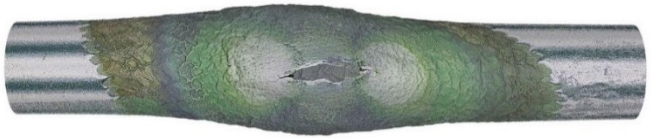	
5 MPa		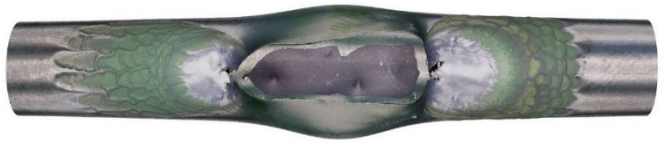

Cladding ballooning & burst is significantly affected by the inner surrogate pellets

Temperature distribution at burst

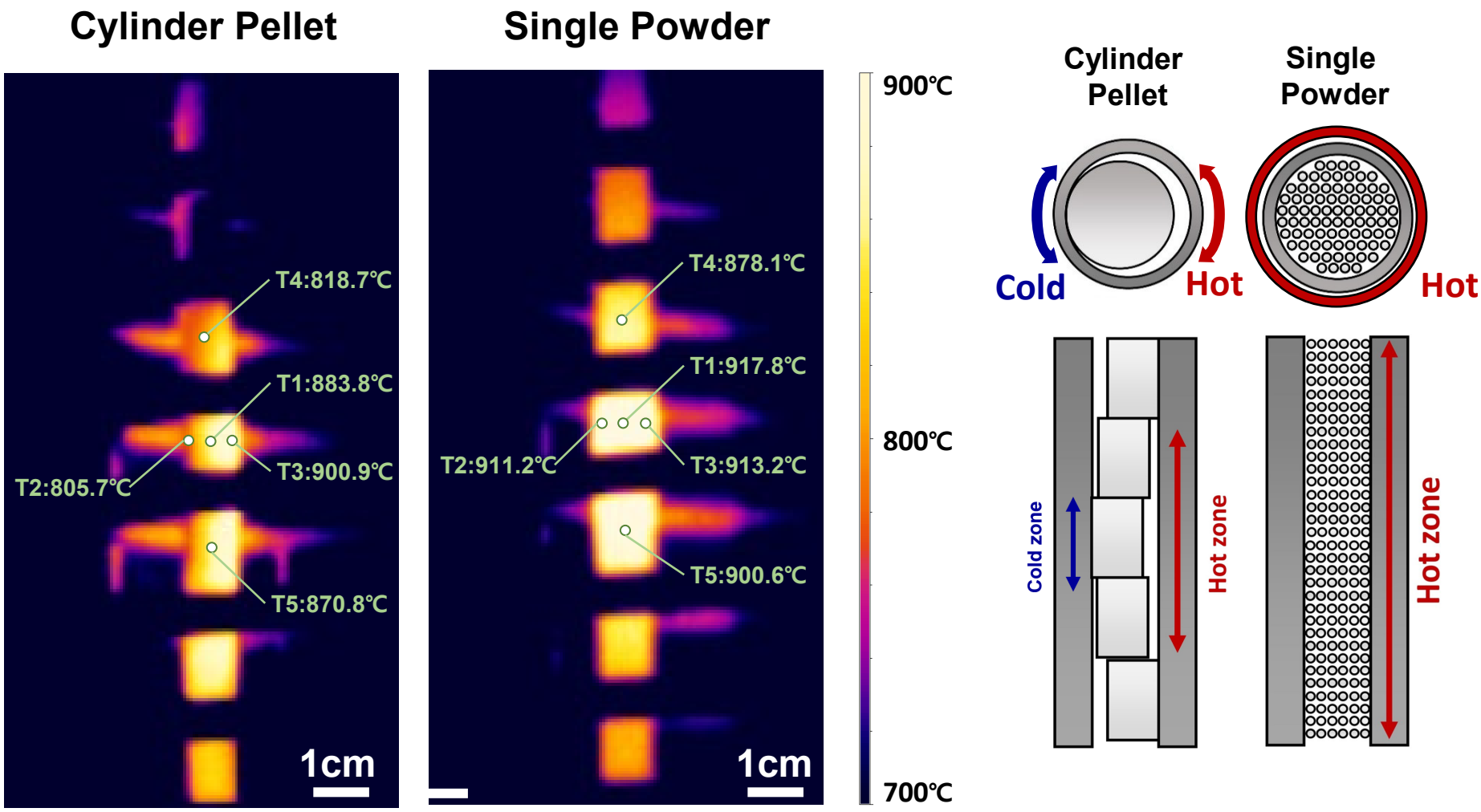

Temperature uniformity : Cylinder pellet < Single powder

**The smaller the particle size,
the more uniform the temperature distribution**

Fuel dispersal of high burnup fuels

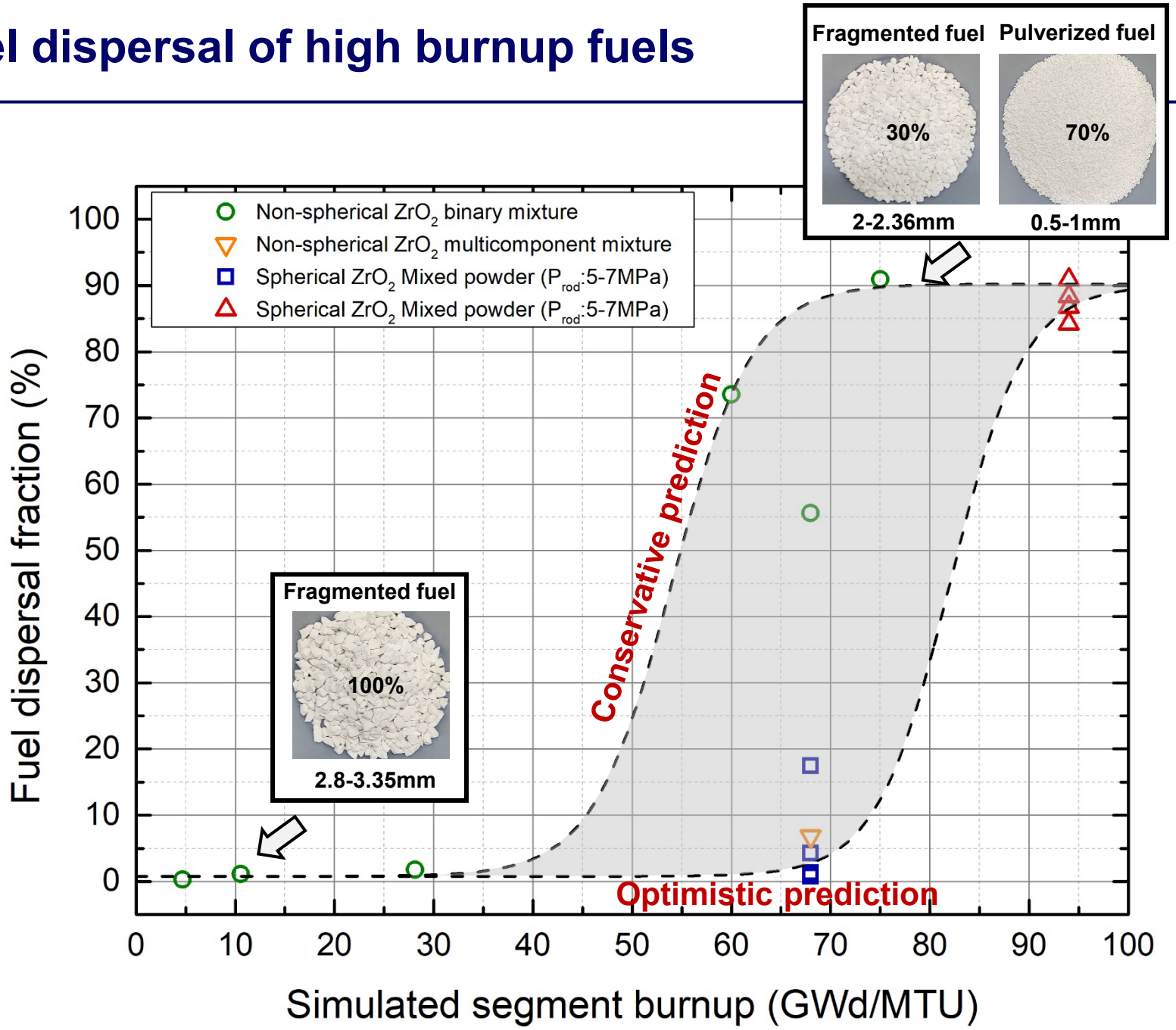

Fragmented fuel mixture determined by FRAPCON-FRAPTRAN simulation

Coating cracks due to ballooning and outer oxidation

- **Test protocol**

Cr-coated cladding

i-LOCA

Ballooning & Burst in Ar environment

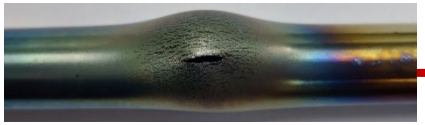

Burst pressure : 1-5 MPa

Cutting

3D scan

Steam furnace

Steam Oxidation

1200℃, 600 sec

3 inch : Double-sided oxidation range (U.S.NRC, appendix K to part 50)

Circumferential strain	8.35%	14.01%	27.96%	40.97%	75.89%
Post-burst specimens					
Post-oxidation specimens					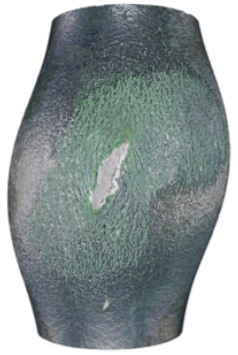

ECR due to ballooning and cracked Cr coating

$$ECR_{Reference} = 87.8 * \frac{\Delta Wg}{\delta_{cladding}}$$

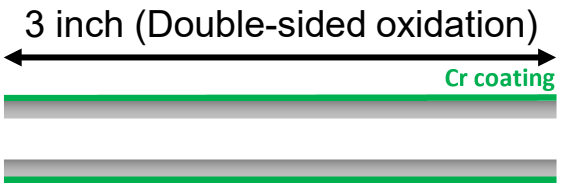

$$\boldsymbol{ECR_{Ballooned}} = 87.8 * \frac{\Delta Wg(1 + \boldsymbol{\gamma_{inner}} + \boldsymbol{\gamma_{outer} f_{crack}})}{\boldsymbol{\delta_{3\ inch-averaged}}}$$

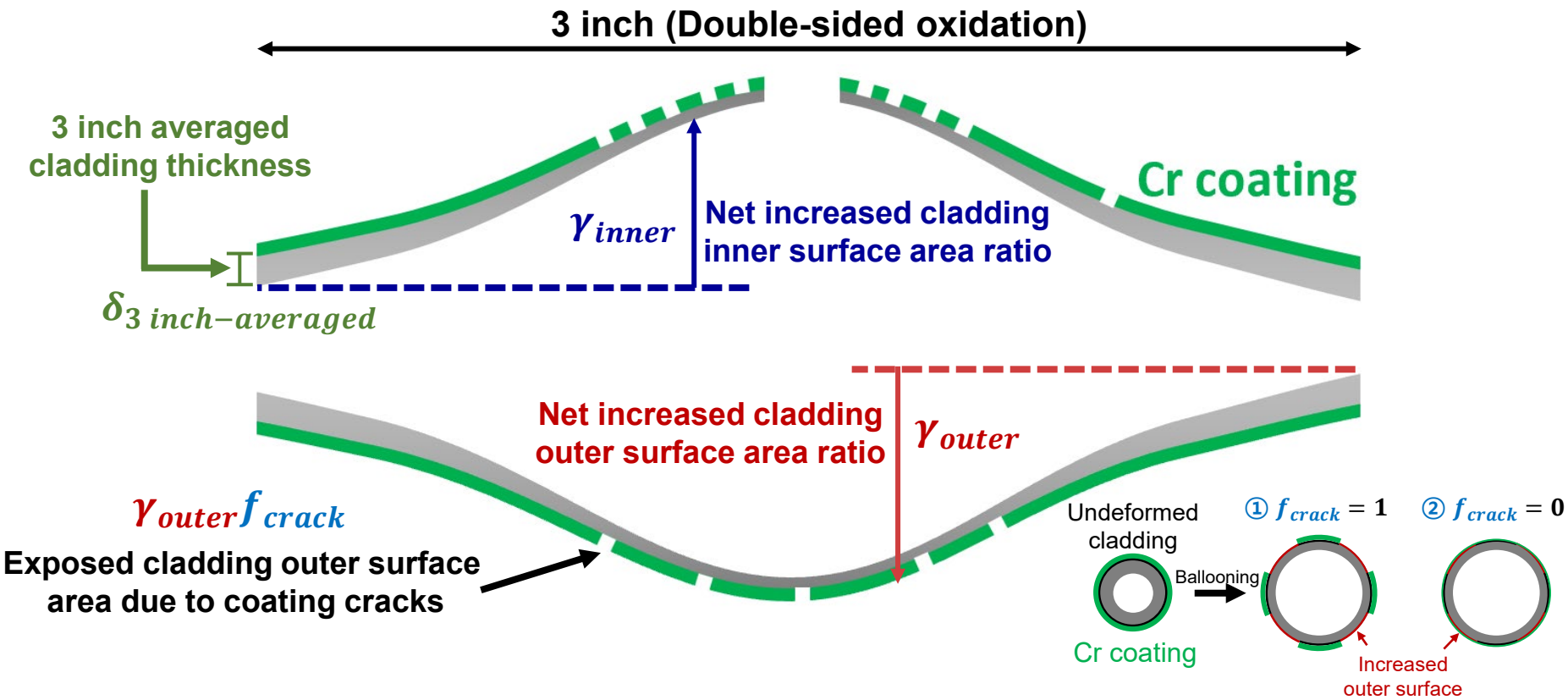

Individual factors for advanced ECR model: cladding thinning

$$ECR_{Ballooned} = 87.8 * \frac{\Delta W g(1 + \gamma_{inner} + \gamma_{outer} f_{crack})}{\delta_{cladding,\,3\ inch.avg}}$$

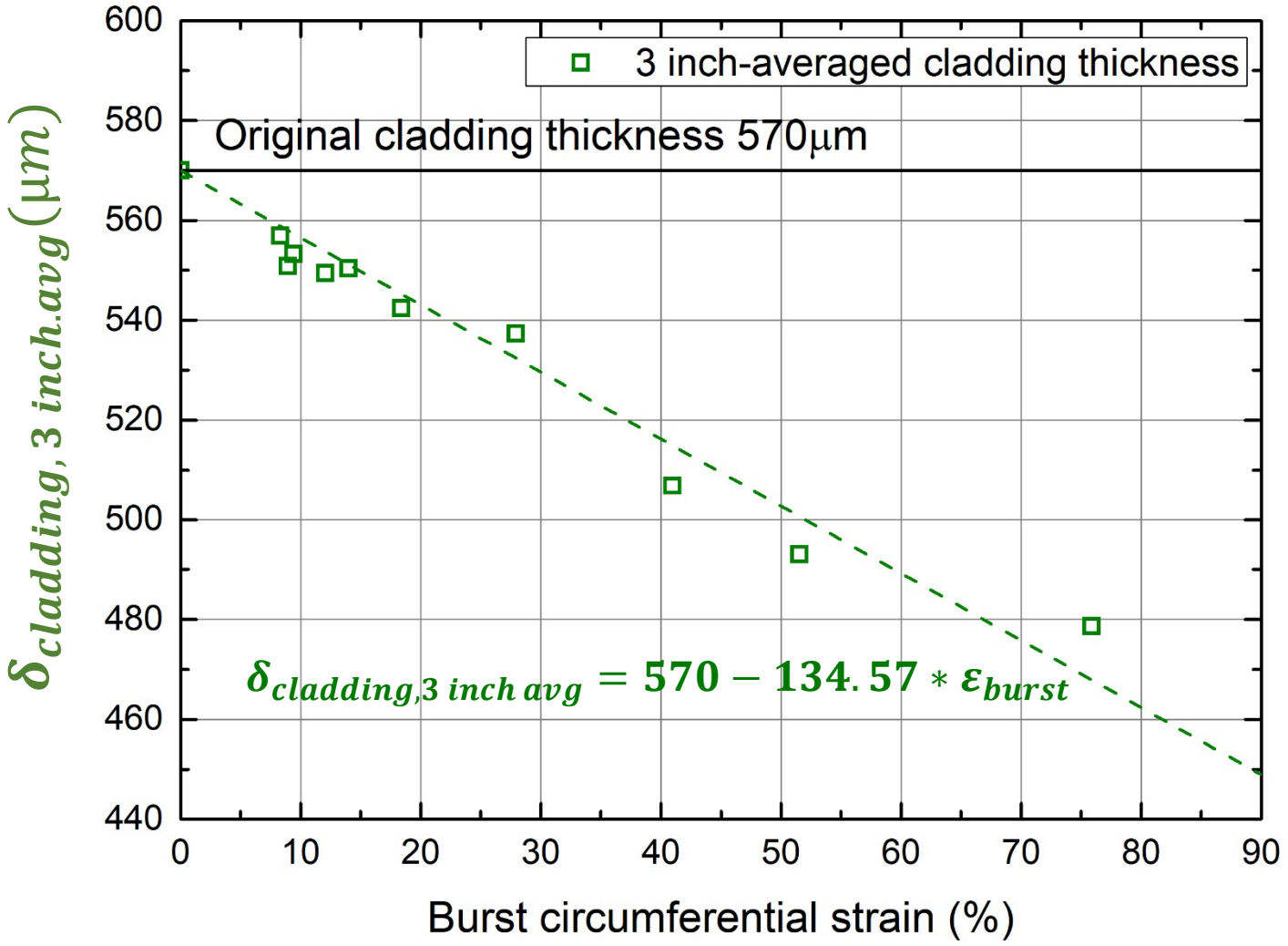

Individual factors for advanced ECR model: increase of oxidation area

$$ECR_{Ballooned} = 87.8 * \frac{\Delta W g(1 + \gamma_{inner} + \gamma_{outer} f_{crack})}{\delta_{cladding,\,3\,inch.avg}}$$

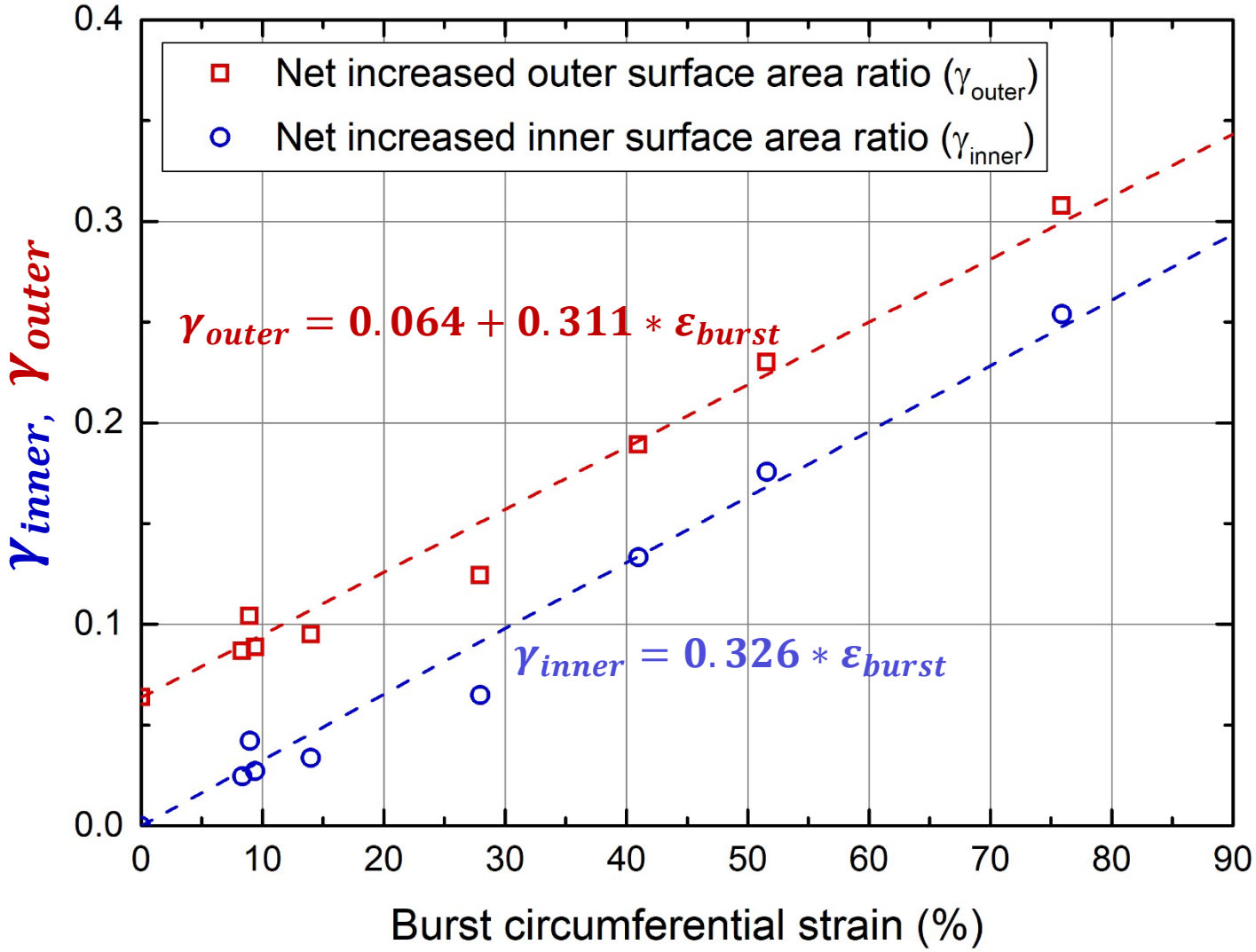

Individual factors for advanced ECR model: crack factor

$$ECR_{Ballooned} = 87.8 * \frac{\Delta W g(1 + \gamma_{inner} + \gamma_{outer} f_{crack})}{\delta_{cladding,\,3\ inch.avg}}$$

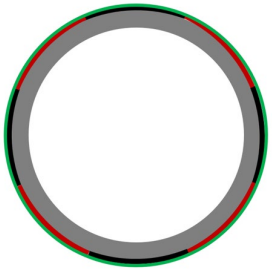

$f_{crack} = 0.0$

Coating retains '**complete**' protectiveness by fully accommodating imposed strain

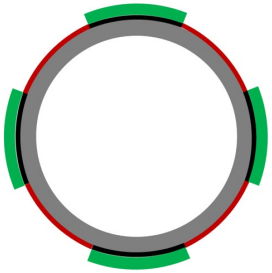

$f_{crack} = 1.0$

Coating gives '**nil**' protectiveness by not accommodating practically any imposed strain

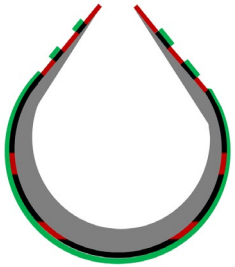

$f_{crack} = 0.5 - 1.0$

Coating gives '**partial**' protectiveness by partially accommodating some of imposed strain

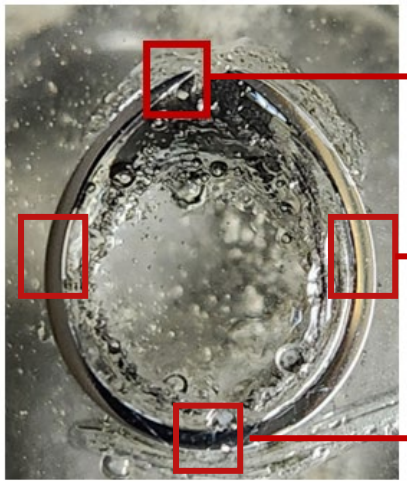

$f_{crack} = 0.0 \sim 1.0$

$f_{crack} = 0.0$

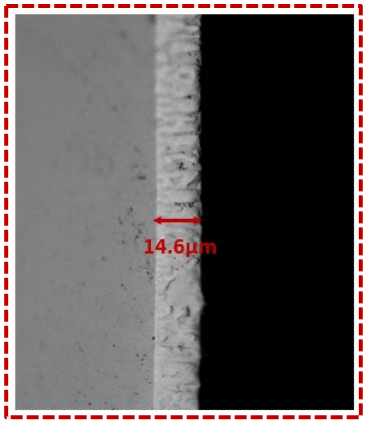

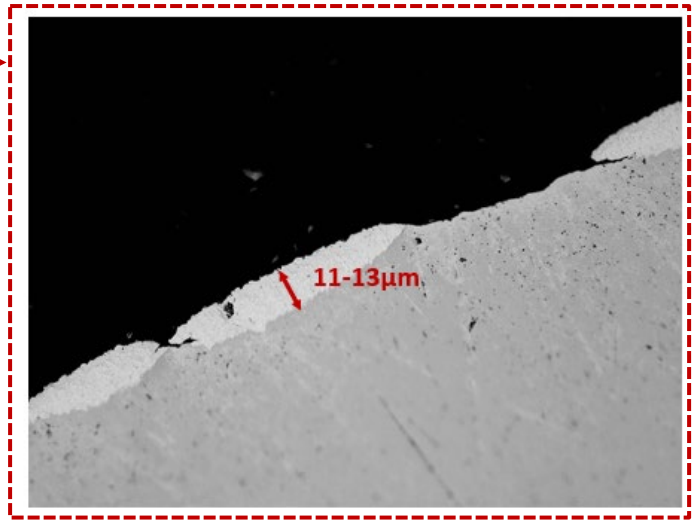

Individual factors for advanced ECR model: crack factor

$$ECR_{Ballooned} = 87.8 * \frac{\Delta W g(1 + \gamma_{inner} + \gamma_{outer} f_{crack})}{\delta_{cladding,\,3\,inch.avg}}$$

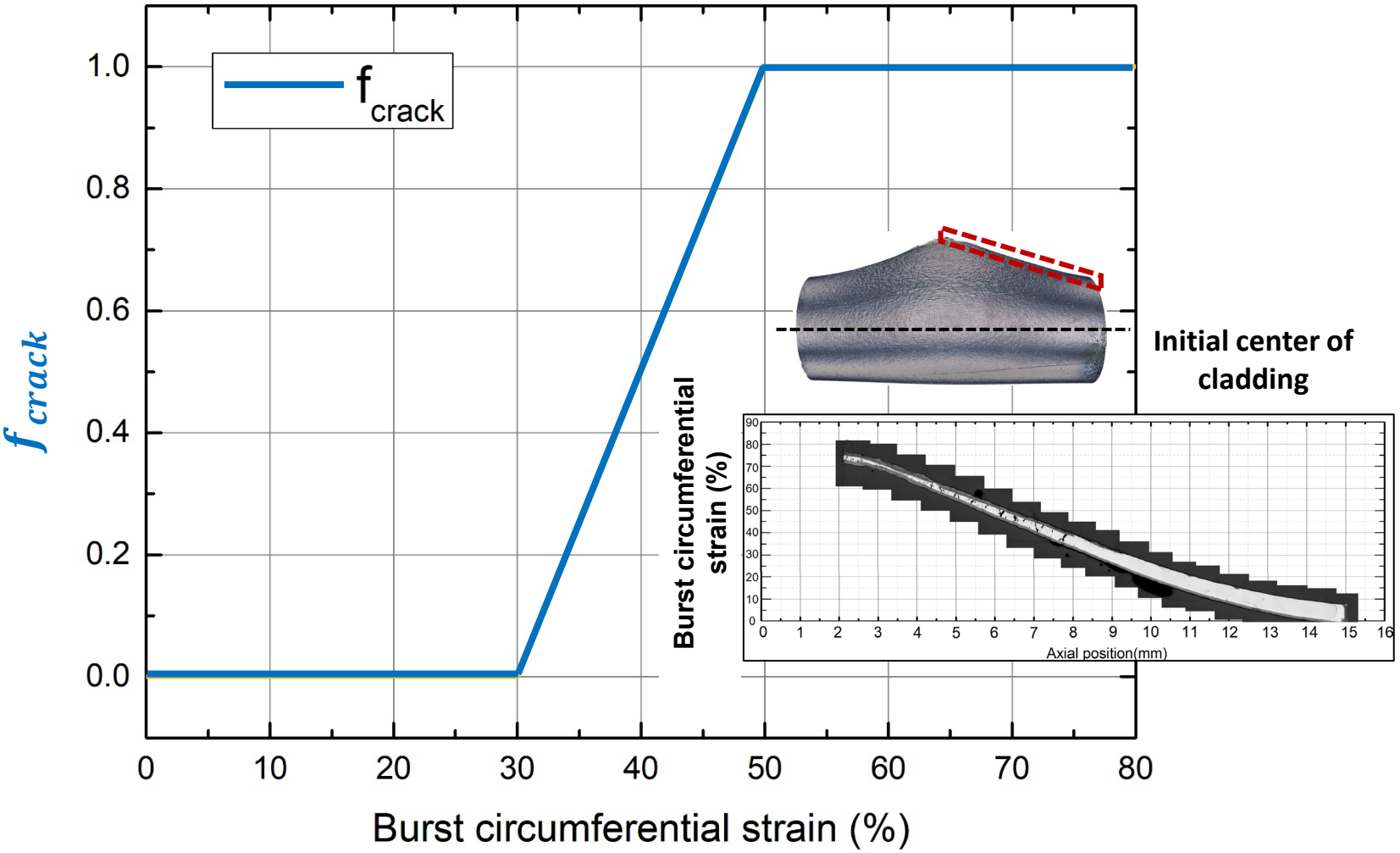

Validation of the advanced ECR model: predictability of total weight gain

$$ECR_{Ballooned} = 87.8 * \frac{\Delta Wg(1 + \gamma_{inner}(\varepsilon) + \gamma_{outer}(\epsilon) f_{crack}(\epsilon))}{\delta_{3\ inch-averaged}(\epsilon)}$$

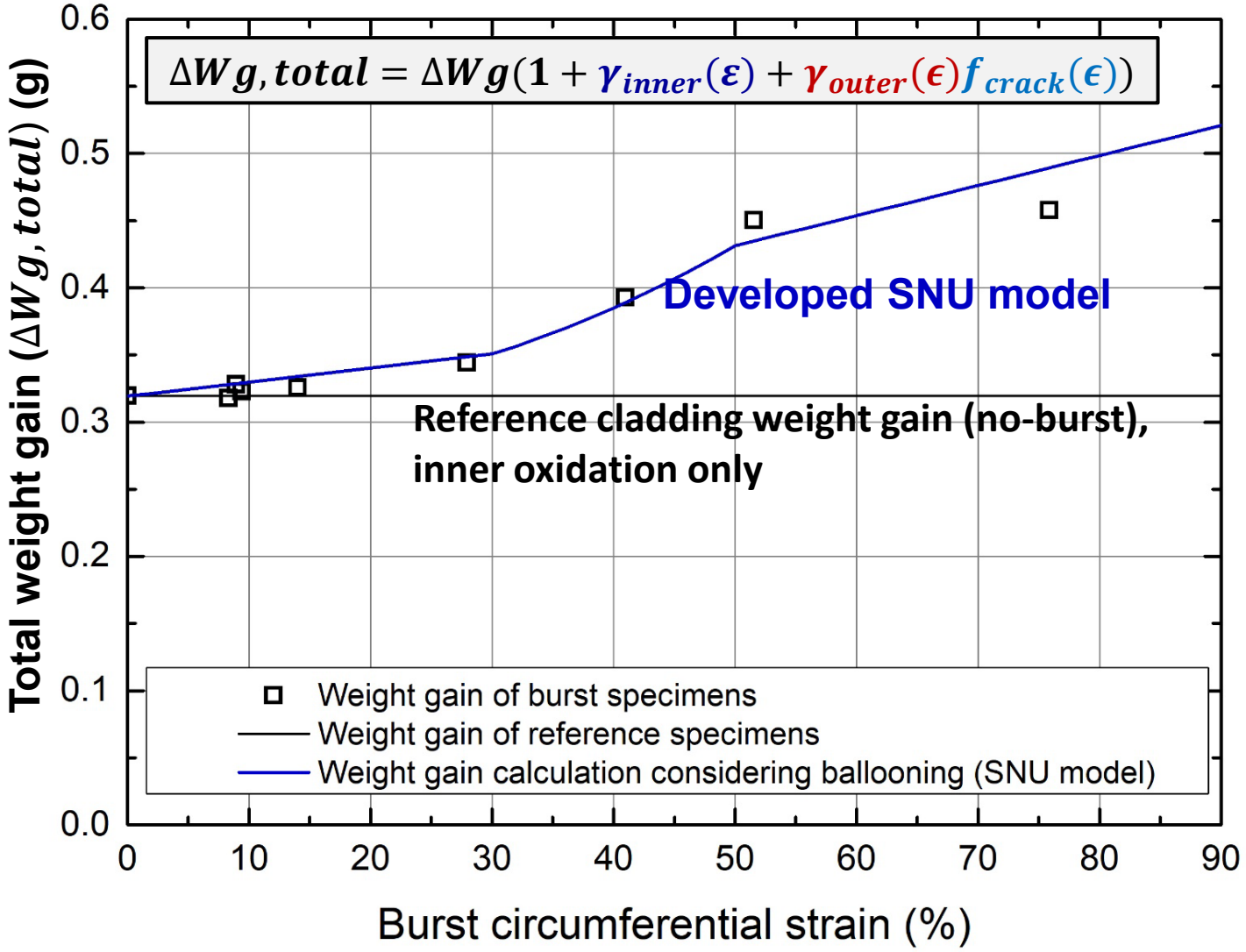

Improved ECR model near burst hole for safety code implementation

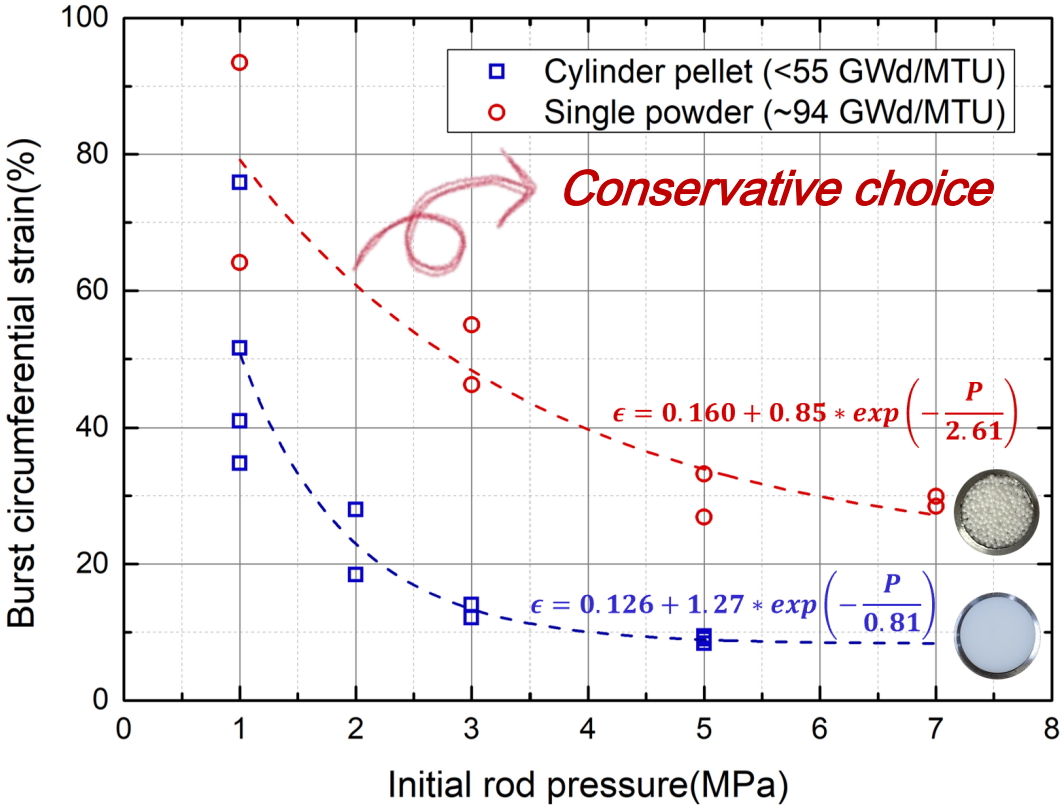

Conservative analysis: $\varepsilon(P, \dot{T}, Bu) \rightarrow \varepsilon(P)|_{\dot{T}max,\, single\ powder}$

Then, apply following equation

$$\boldsymbol{ECR_{Ballooned}} = 87.8 * \frac{\Delta W g[1 + \boldsymbol{\gamma_{inner}(\epsilon)} + \boldsymbol{\gamma_{outer}(\epsilon) f_{crack}(\epsilon)}]}{\boldsymbol{\delta_{3\ inch-averaged}(\epsilon)}}$$

Characterization of secondary hydrides

As well anticipated, secondary hydride peaks commonly occur to Cr-coated cladding via inner-wall oxidation via burst hole

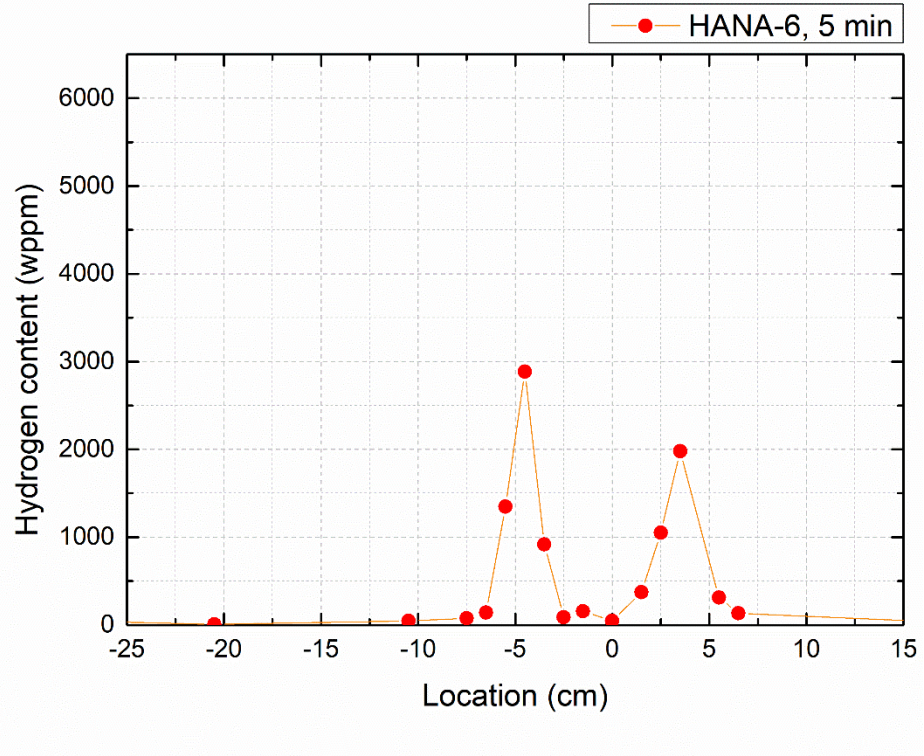

HANA-6
(PCT ~1100℃)

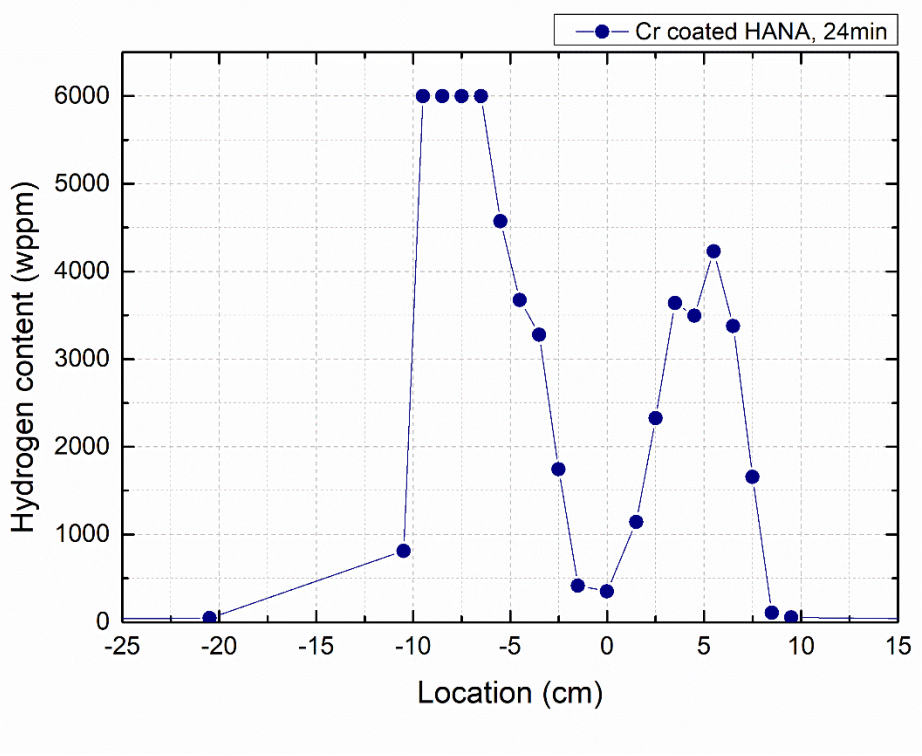

Cr-coated HANA-6
(PCT ~1360℃)

*The presented difference is primarily attributed to the different PCT and exposure time. The used ONH machine for hydride detection is limited to ~6000 PPM.

PQD of Cr-coated Zr with Secondary hydrides

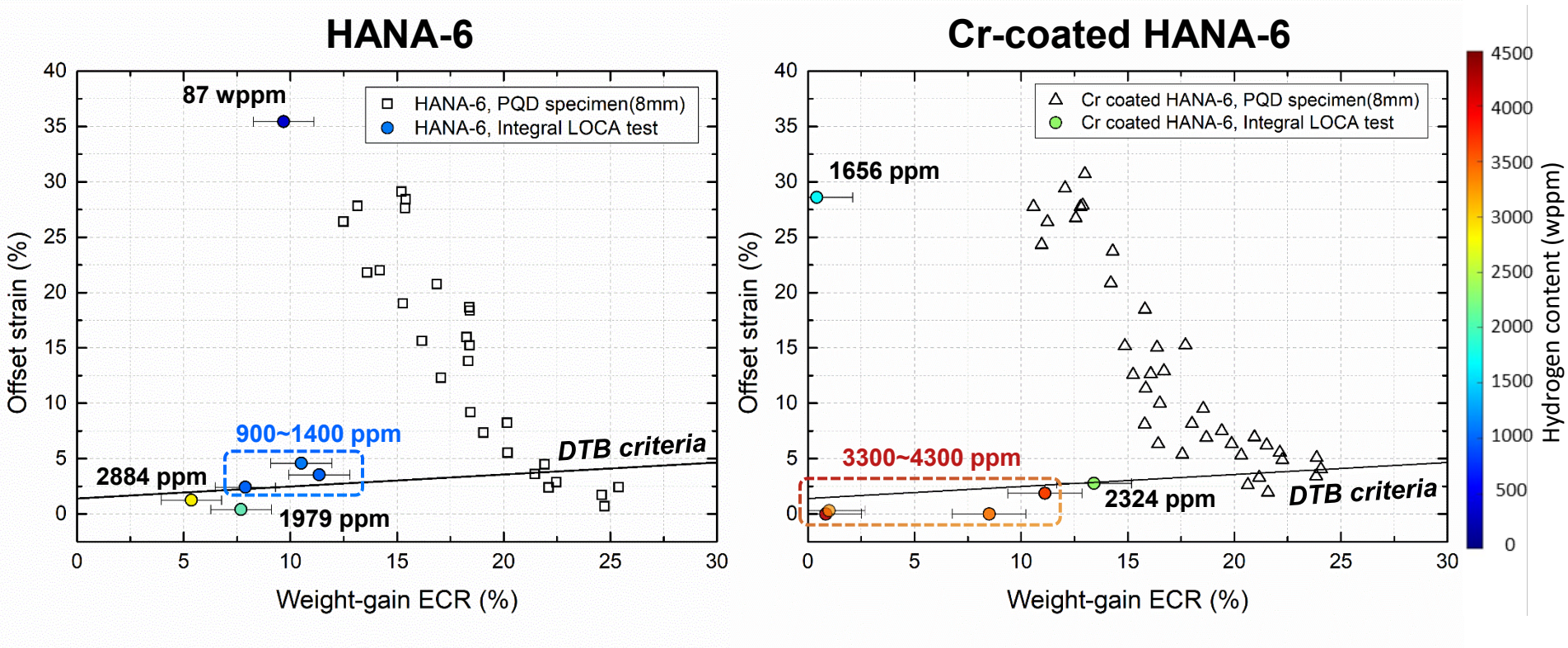

Safety implications (Food for thoughts):

1. Benefit of Cr-coating disappears in the presence of secondary hydrides

2. In a more general perspective, the current PQD criteria irrespective of secondary hydrides do not fully address all safety-challenging phenomena. It undermines the physical sanity of the current PQD criteria.

EBSD characterization of secondary hydrides

- **Hydrogen content**

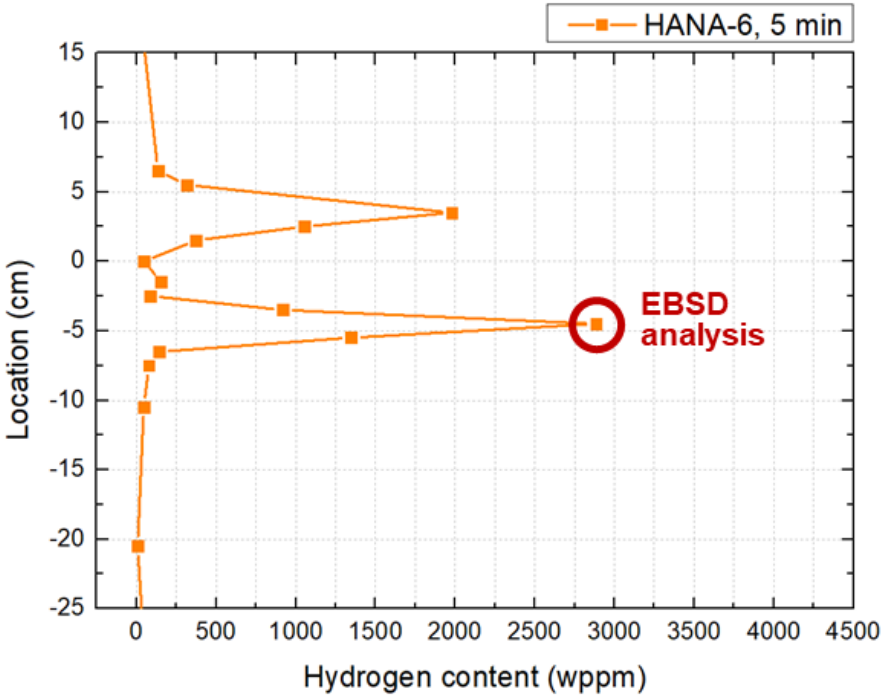

- **Temperature (cooling) history**

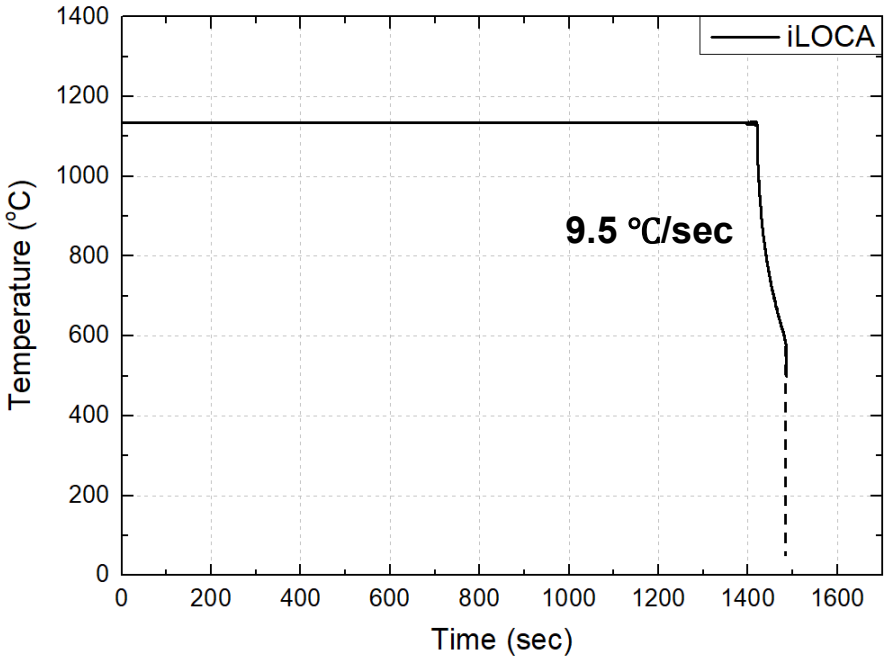

EBSD characterization of secondary hydrides

- Inverse pole figure

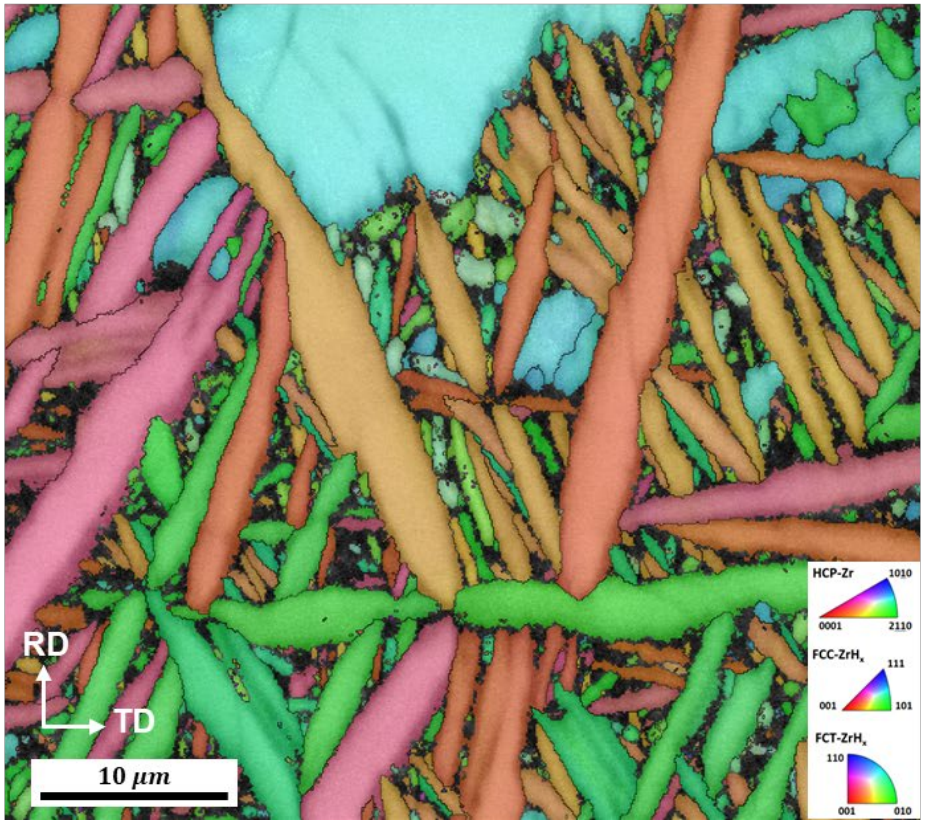

- Phase map

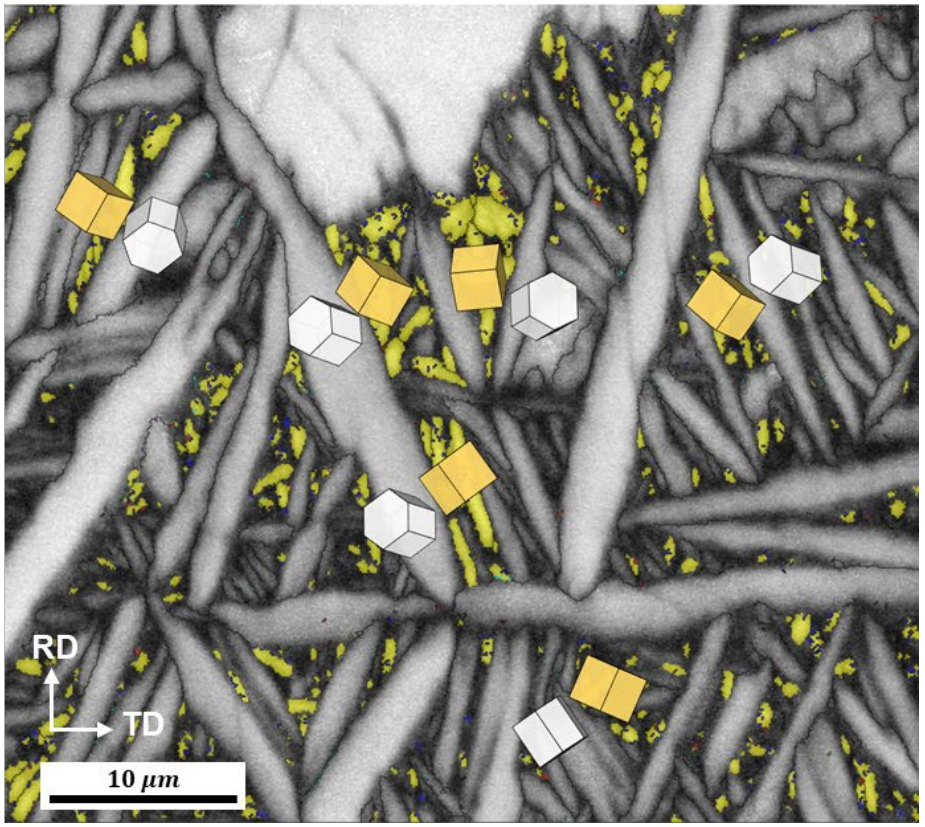

Orientation relationship of δ-hydride and Zr

- **Typical hydrides (<400℃) (180 wppm)**

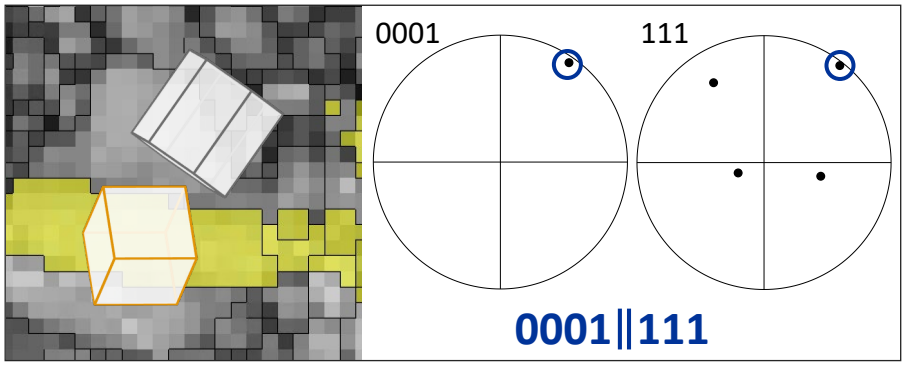

- **LOCA test (4000 wppm)**

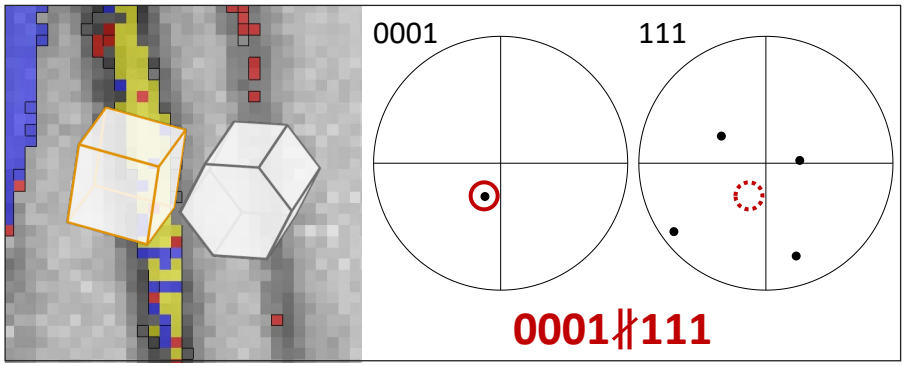

- ***i*-LOCA test (3000 wppm)**

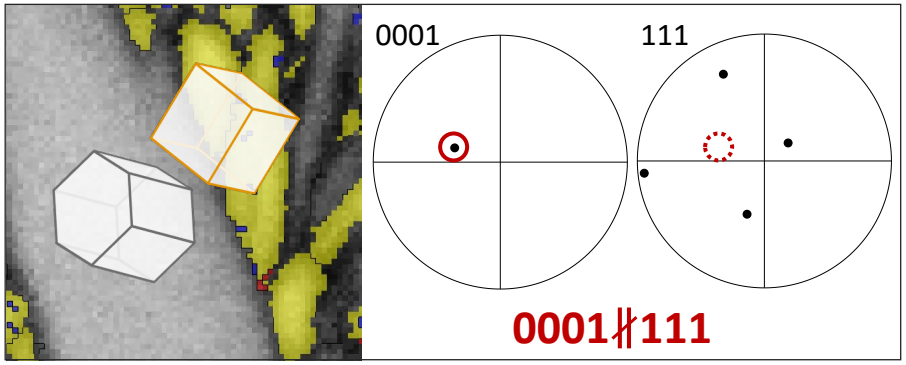

- ***i*-LOCA test (3000 wppm)**

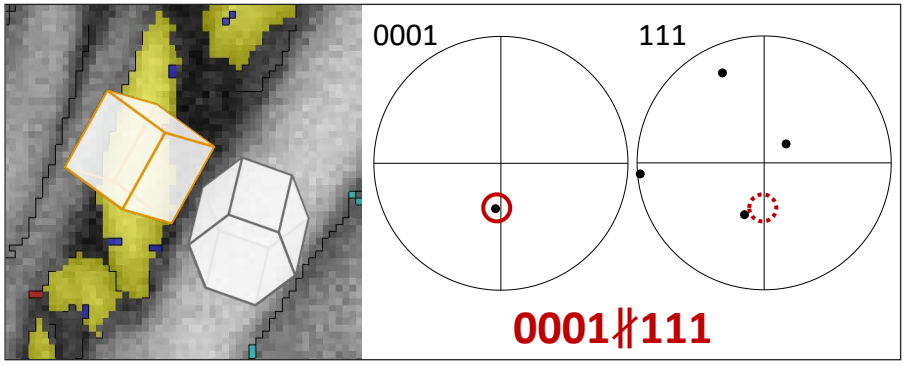

Orientation relationship analysis result

Typical hydrides (<400℃) (180 wppm)

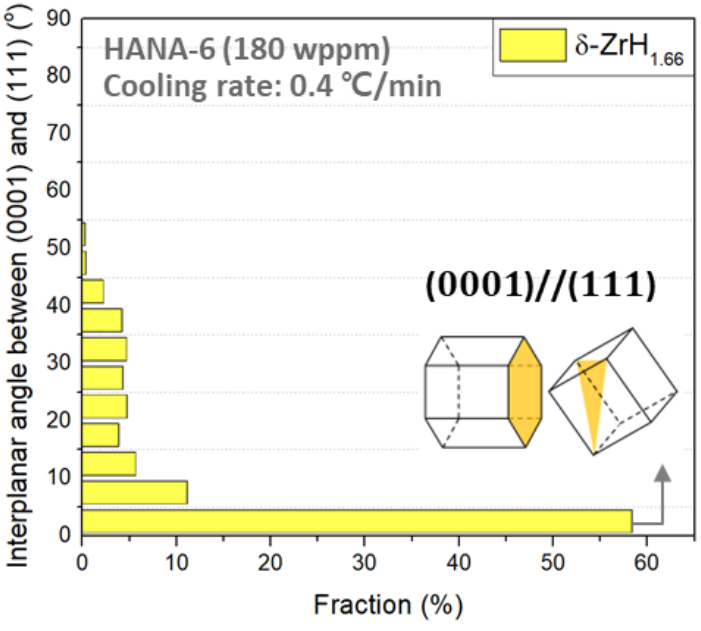

Secondary hydrides

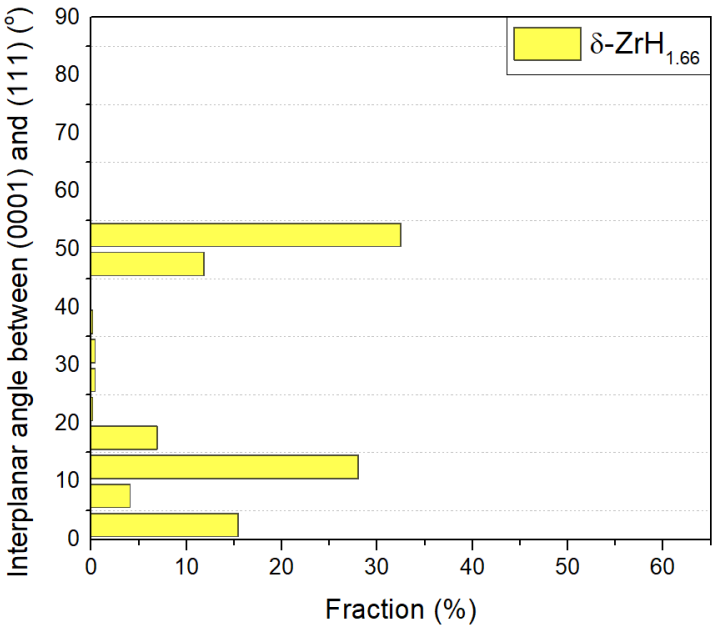

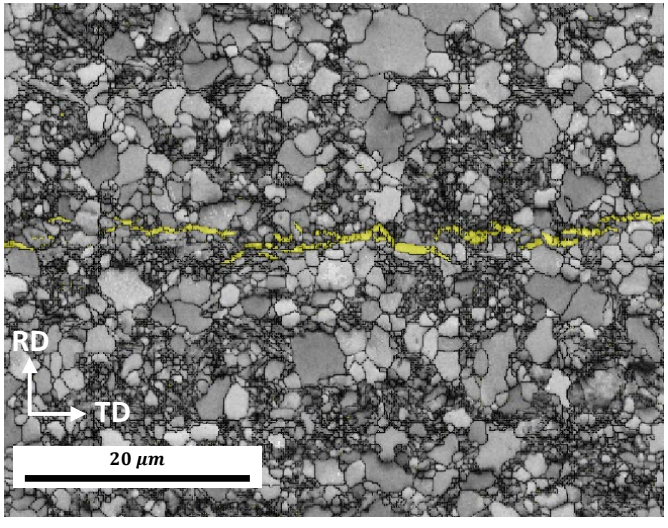

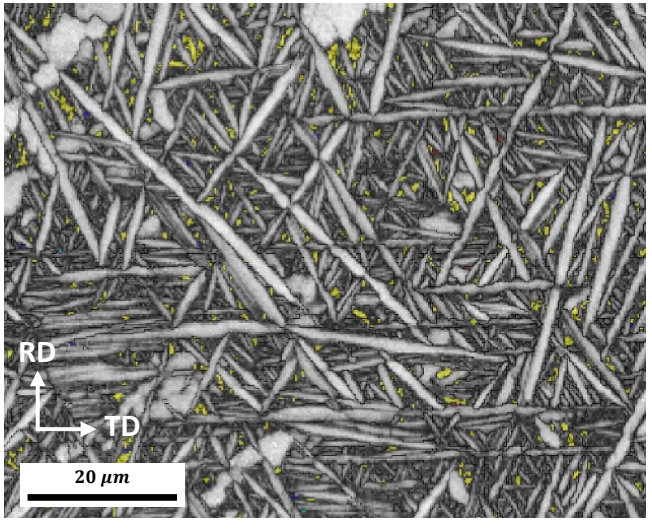

Some preliminary results on mimicking secondary hydride distribution using smaller (10cm) tube

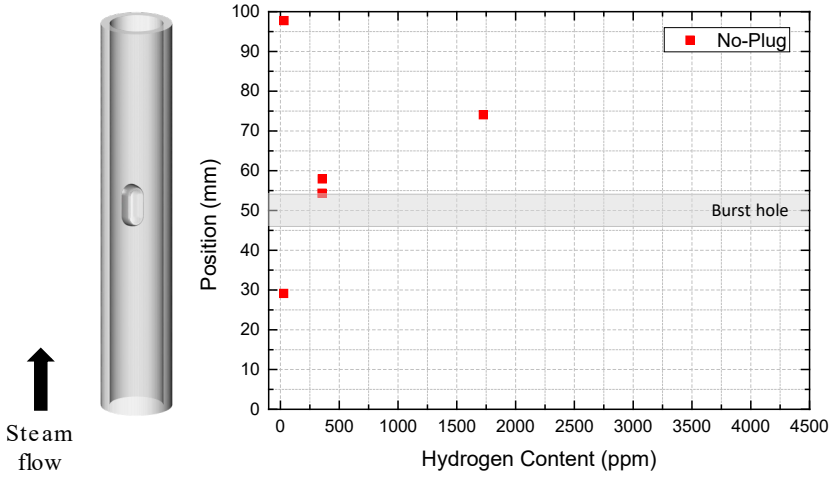

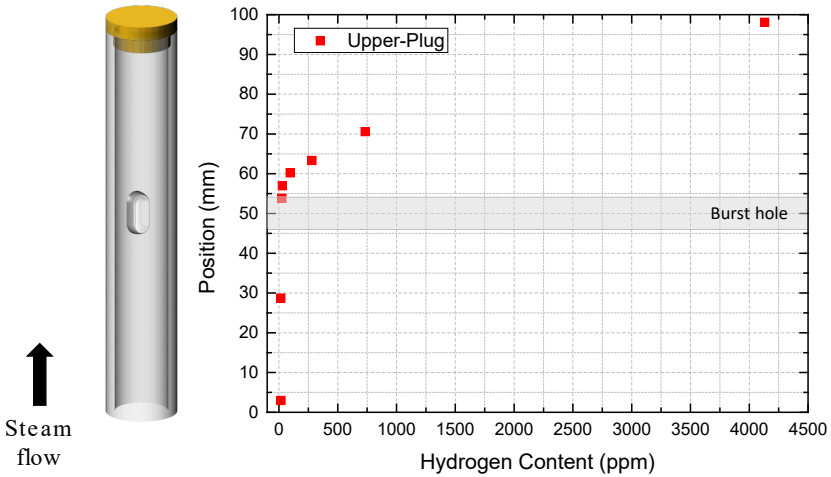

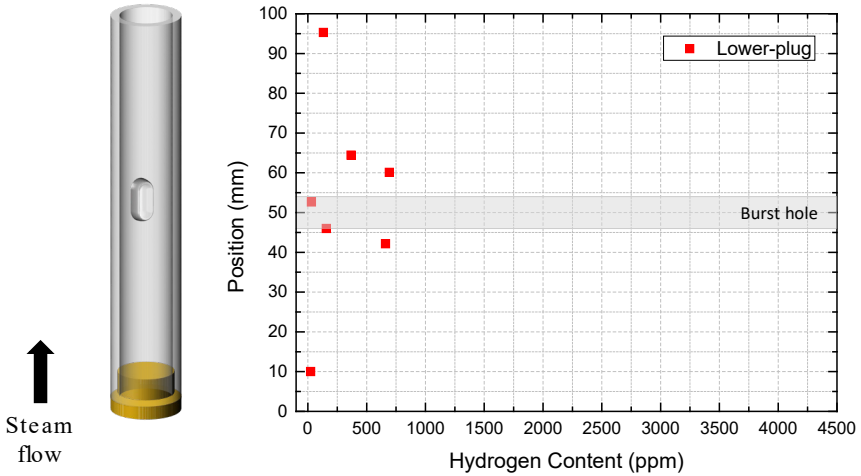

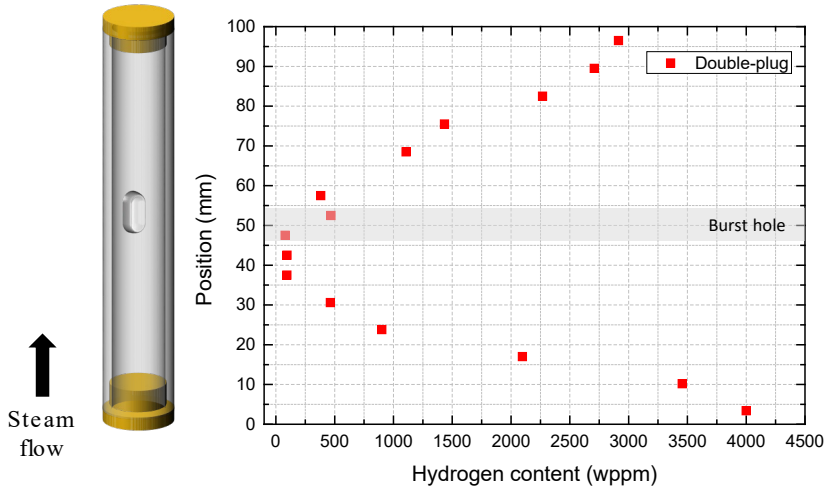

Some preliminary results on mimicking secondary hydride distribution using smaller (10cm) tube

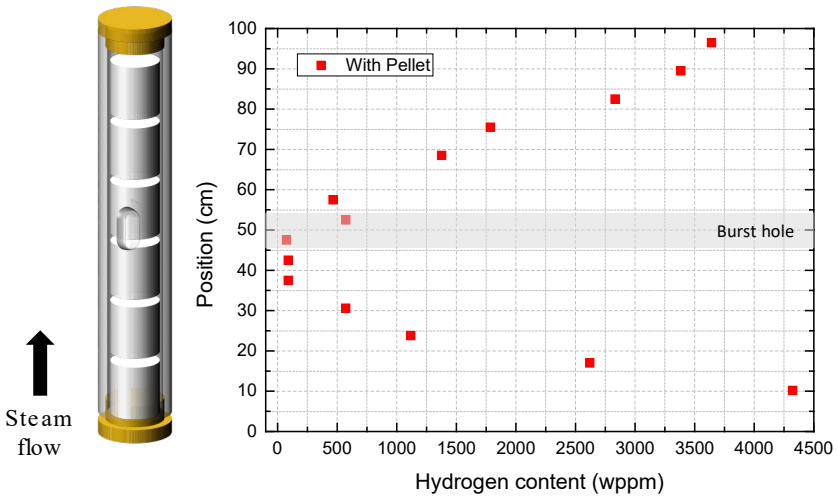

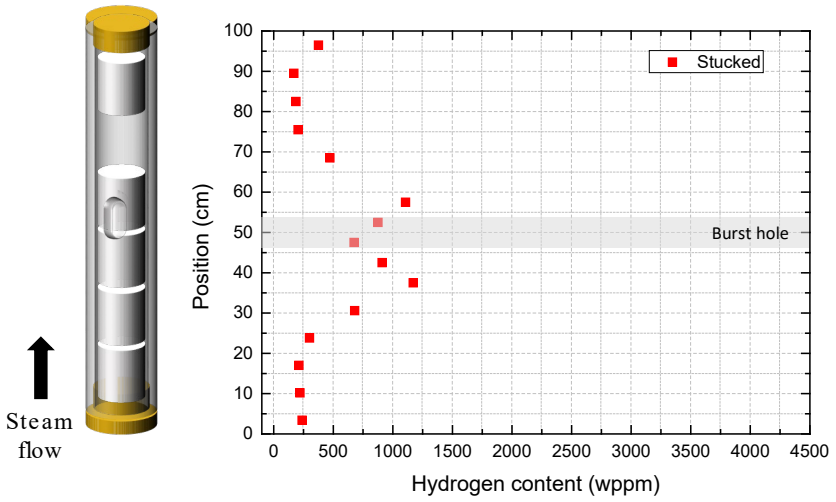

Hydrogen generation: validation of the facility

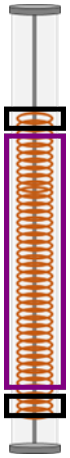

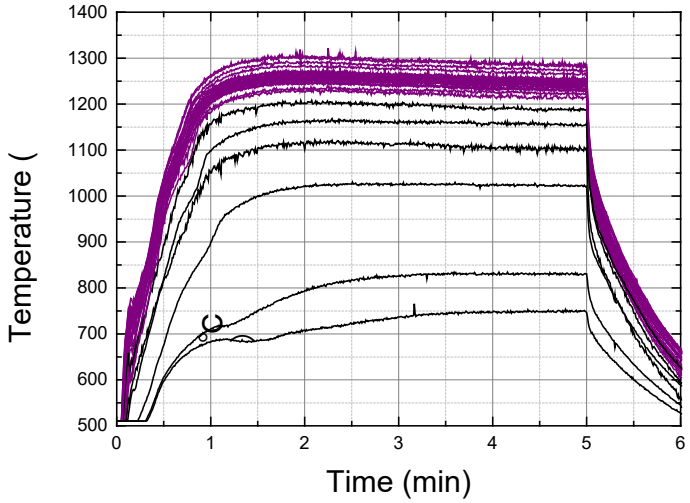

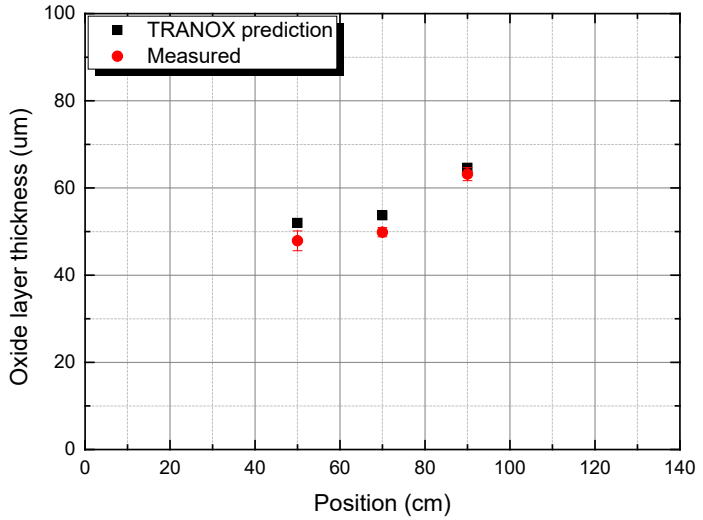

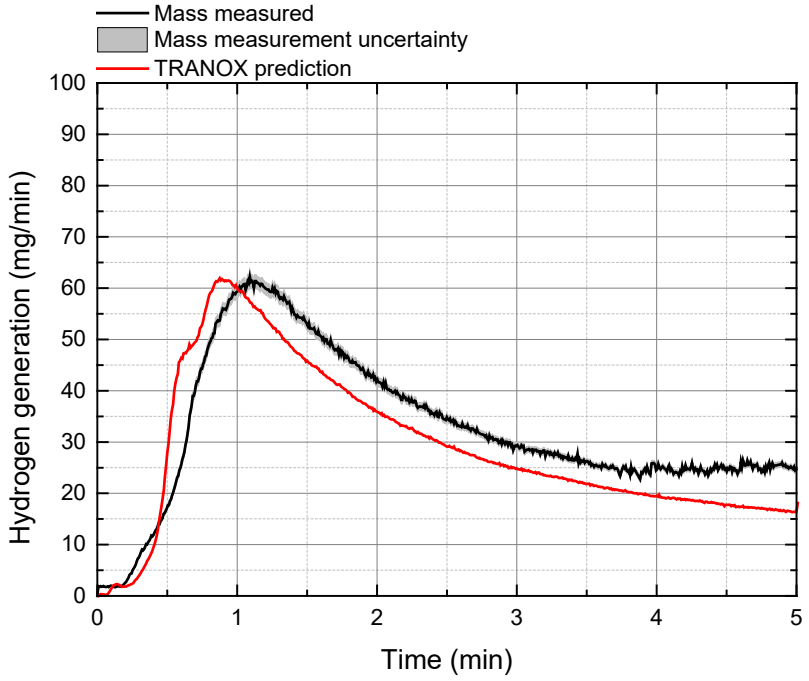

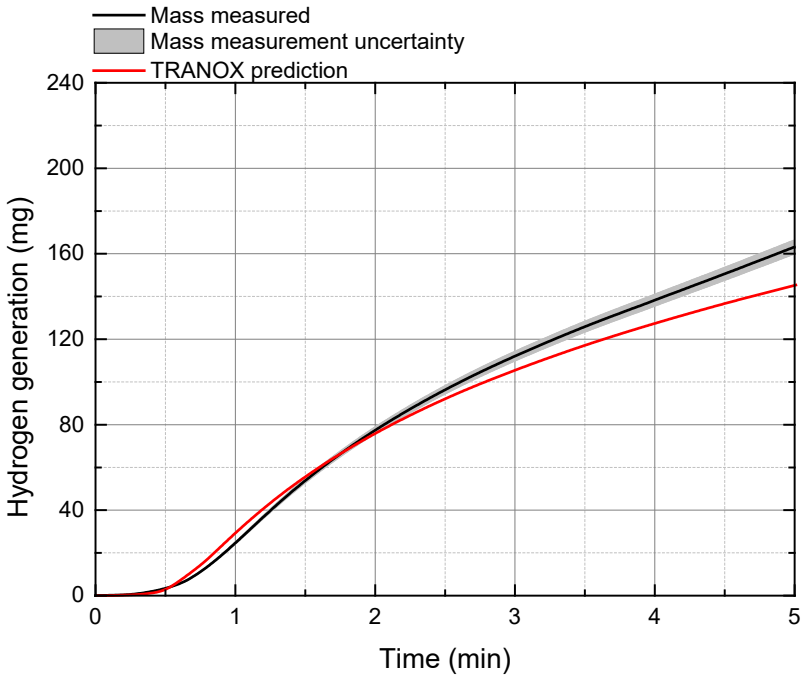

Eutectic formation on hydrogen generation

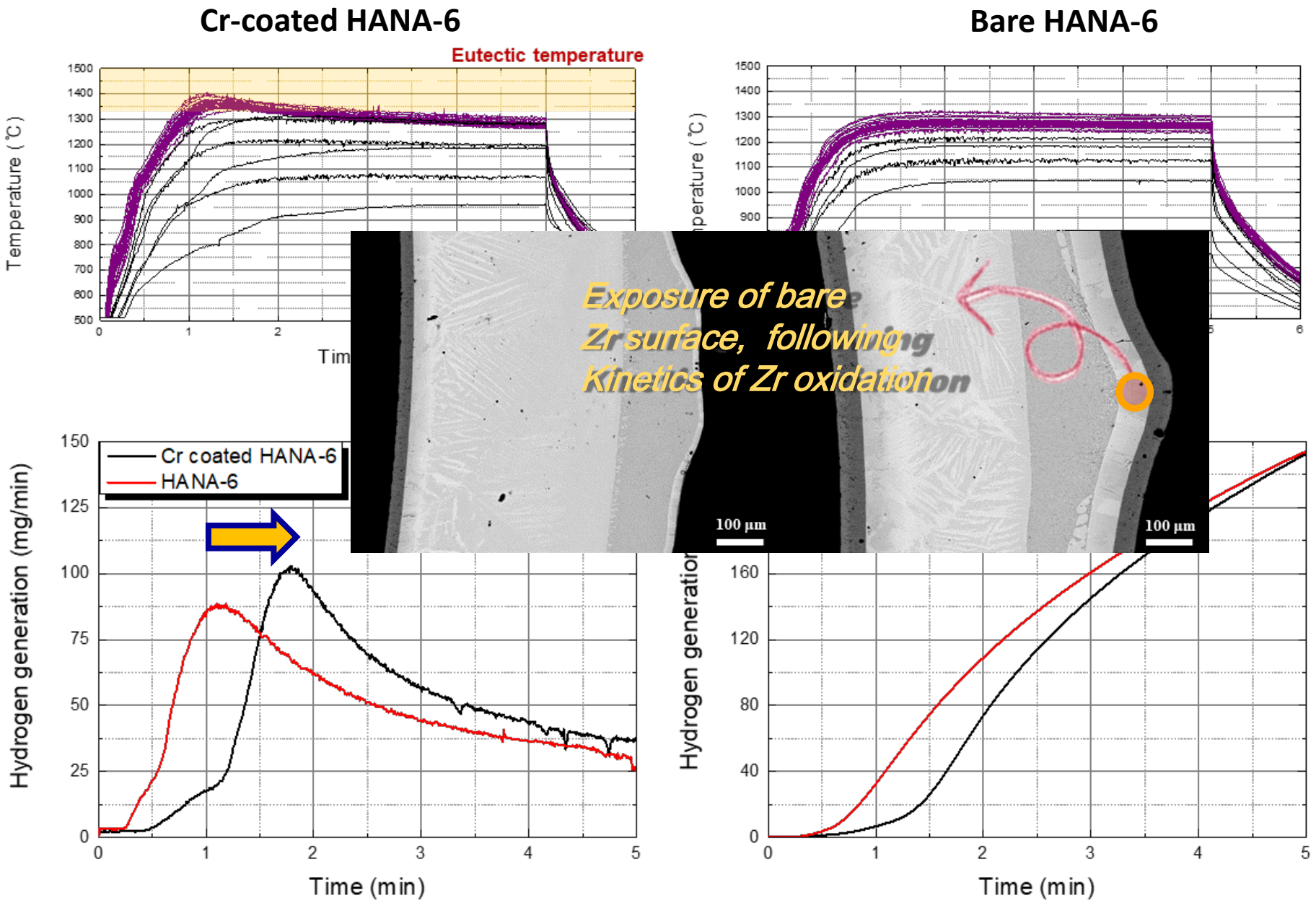

Conclusion I: The ATF emperor has no clothes

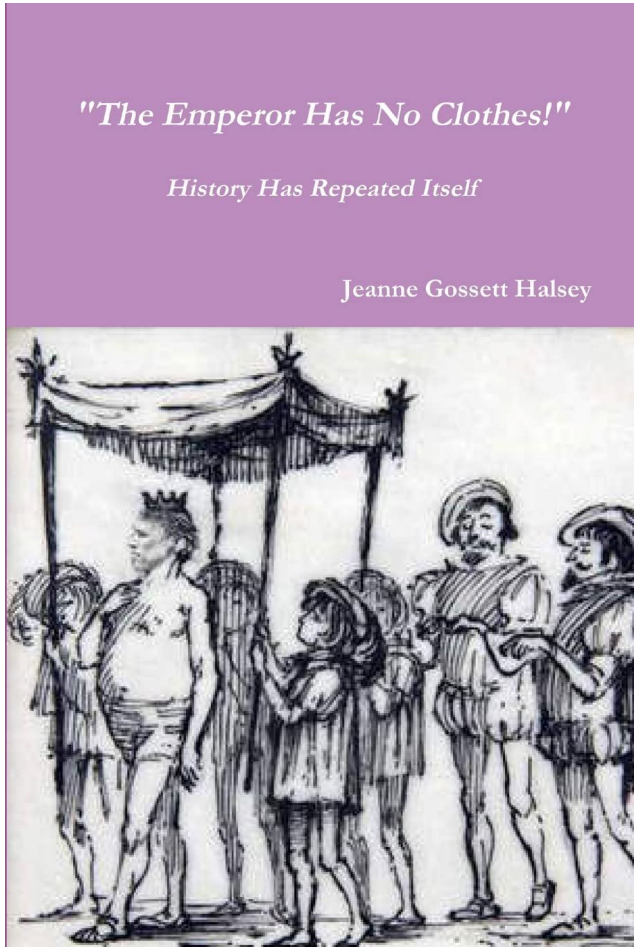

- **Ballooning and Burst:**
  Practically the same as bare Zircaloy.
  Or at best it is not significantly different.

- **Fuel Fragmentation Relocation Dispersal (FFRD):**
  Practically the same as bare Zircaloy – key limiting factor for burnup extension.

- **Inner wall oxidation:**
  Practically the same as bare Zircaloy

- **Secondary hydrides:**
  Practically similar to bare Zircaloy. The benefit of Cr coating in terms of PQD limit disappears with secondary hydrogen.

- **Outer wall oxidation through cracked coating:**
  Oxidation limitedly occurs through cracked coating in the outer wall near the burst region.

- **H_2 generation :**
  The same or can be worse

Conclusion II: BUT, the naked emperor better be appreciated

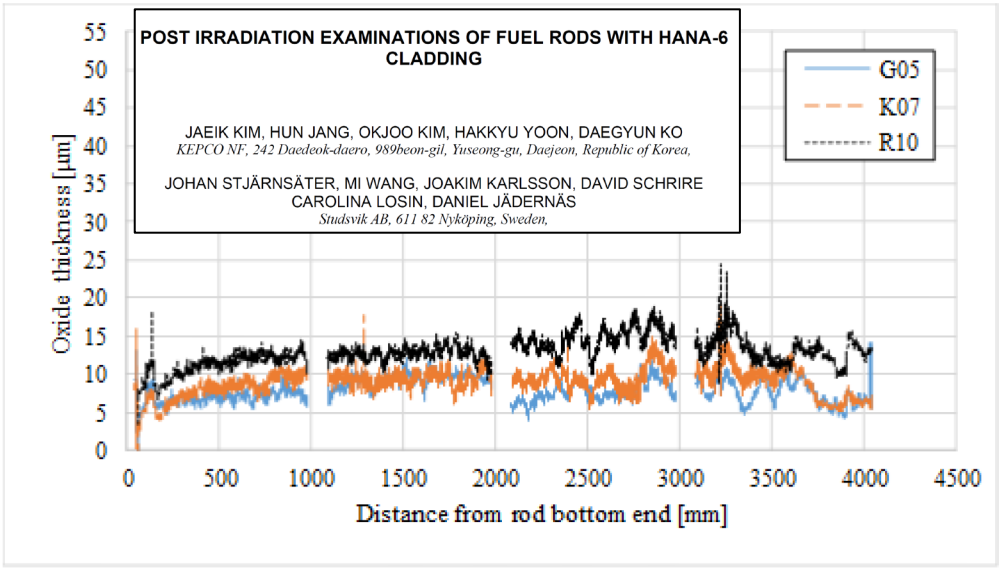

Figure 1. Oxide Layer Thickness measured in Hot Cell with EC for HANA-6 fuel rod average burnups of 46.8 ~ 64.1 MWd/kgU.

Commercial cladding tubes
Zircaloy-4
Zirlo/ Optin Zirlo
M5
HANA-6

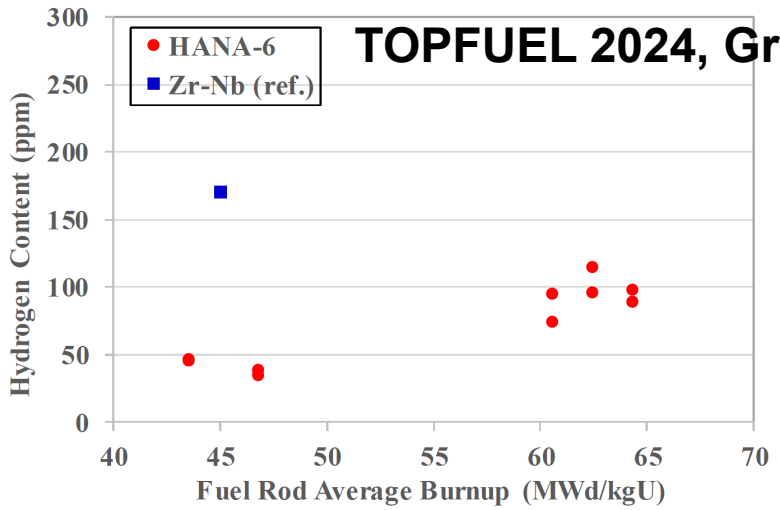

Figure 5. HANA-6 hydrogen content as a function of fuel rod average burnup versus the reference rod (R15).

Understanding what limits us from increasing burnup with LEU+

- **The problem is the design of the fuel**

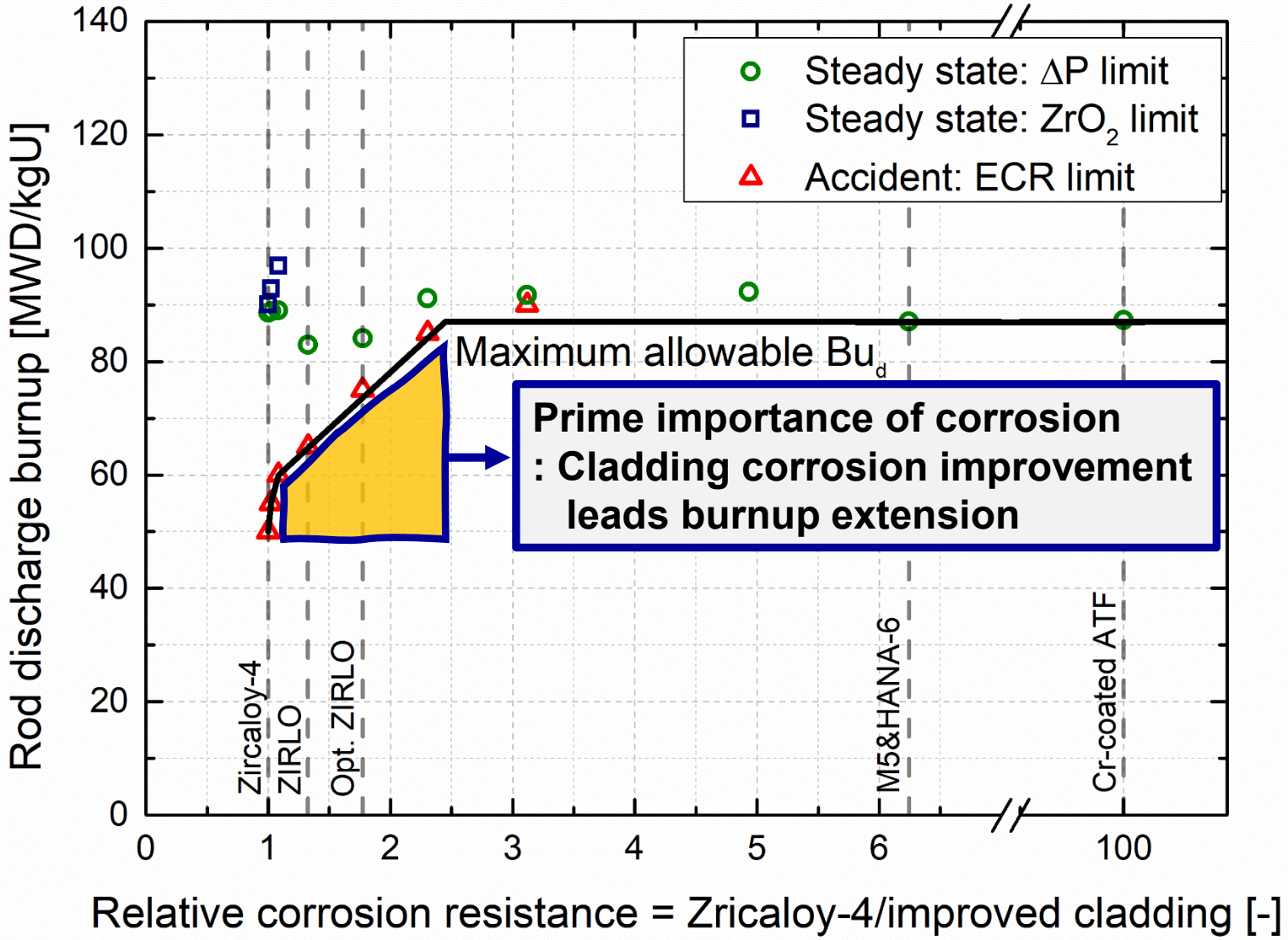

Understanding what limits us from increasing burnup with LEU+

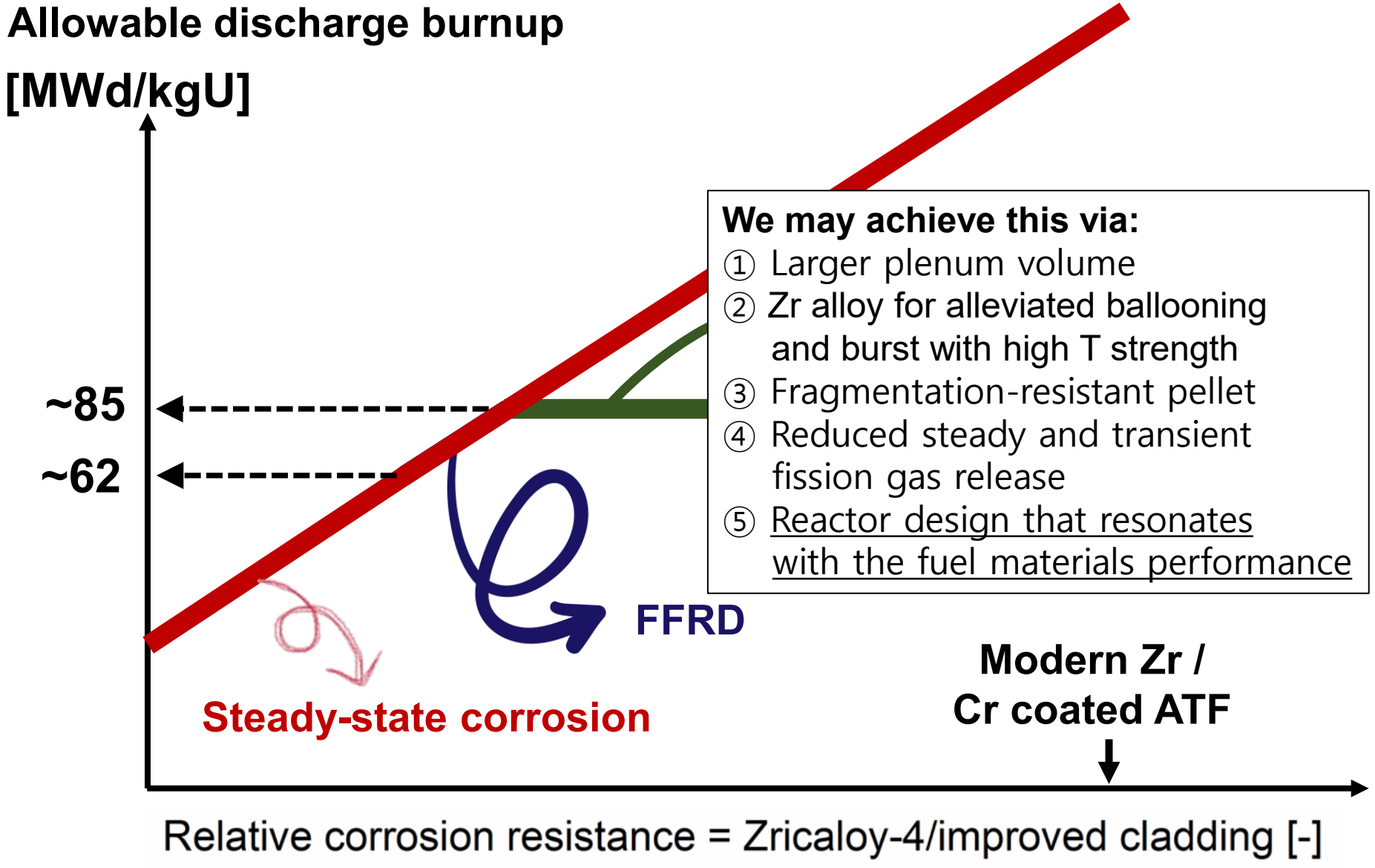

Modern Zircaloy and ATF may be best capitalized in SMRs

- **SMR offers ideal environments to fully capitalize on LEU+ and modern Zircaloy performance**

Ultra-high burnup, Ultra-long cycle length for various applications

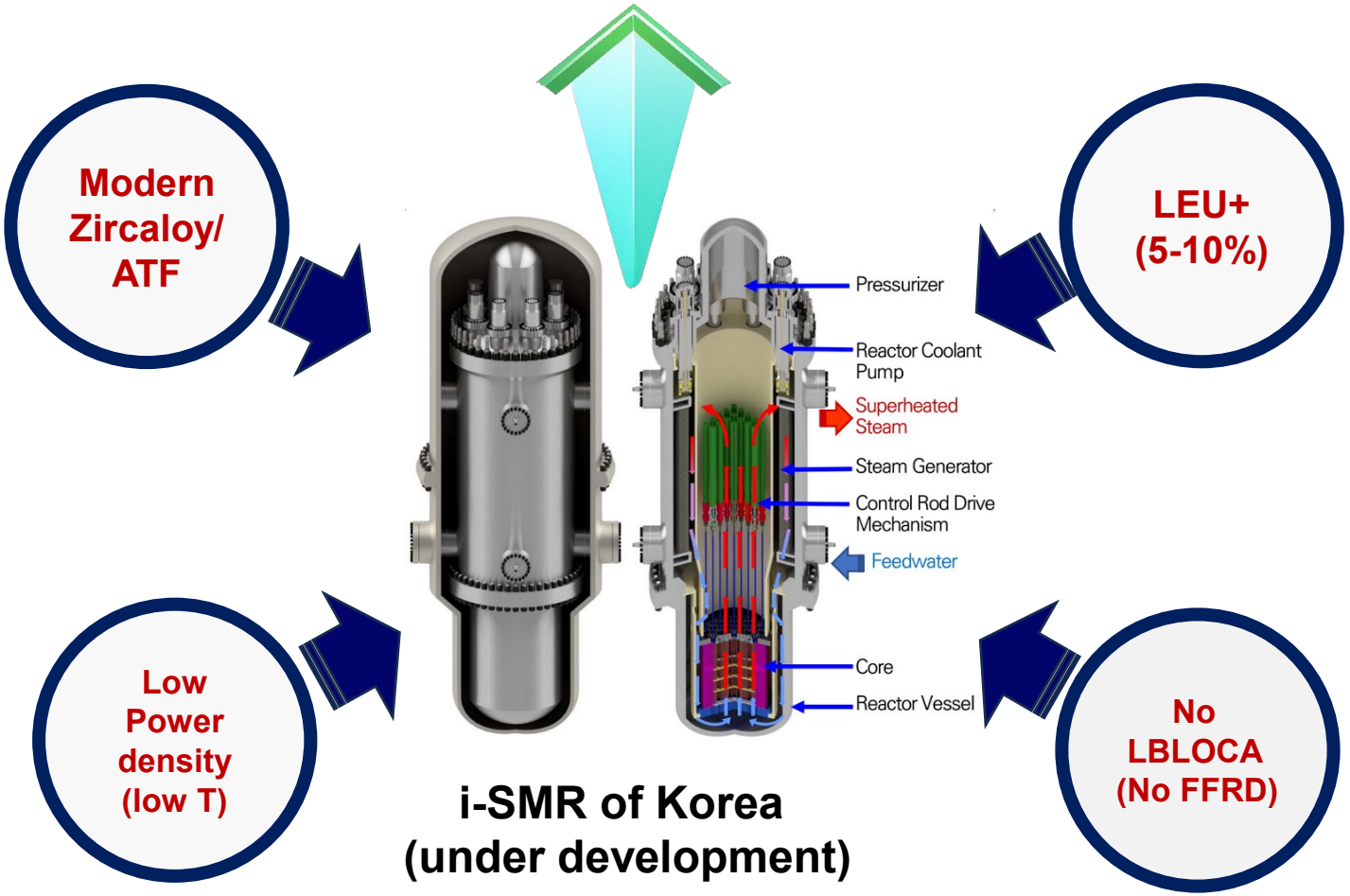

i-SMR of Korea (under development)

Thank you for listening

Simulating high burnup fuels : FRAPCON-FRAPTRAN

FRAPCON-4.0

Fuel design of conventional PWR (~1400MWe)

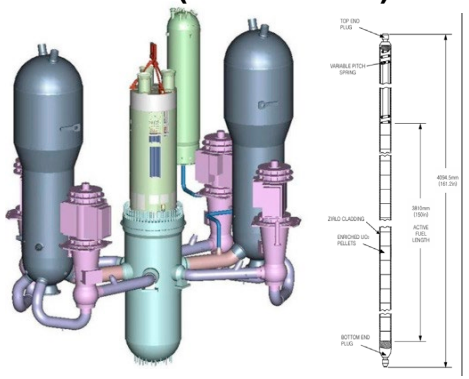

Power history for high burnup (18month → 24month)

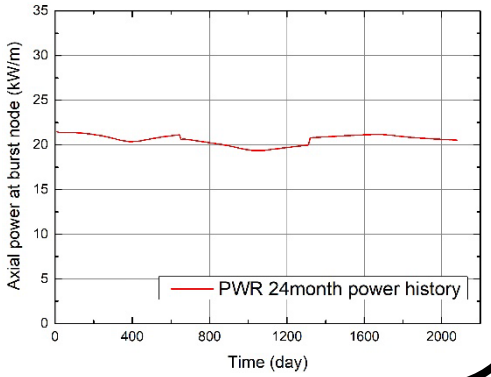

Rod pressure and void volume at target burnup (~90GWd/MTU)

FRAPTRAN-2.0

Fuel fragmentation (>1mm)[3]

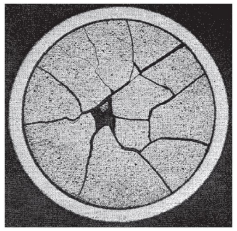

Fuel pulverization (<1mm)[2]

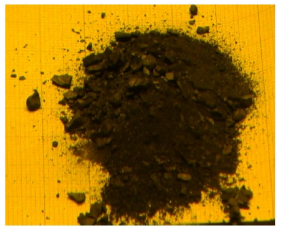

Pellet size and distribution at target burnup (~90GWd/MTU)

Required input for burnup-effect experiment

1. $P_{rod}(Bu)$
2. $Void_{rod}(Bu)$
3. $\bar{D}_{frag}(Bu)$
4. $F_{pulv}(Bu)$

[2] Flanagan, M. (2013). Post-test examination results from integral, high-burnup, fueled LOCA tests at Studsvik Nuclear Laboratory, 2013.
[3] Jernkvist, L.O., & Massih, A. (2015). Models for axial relocation of fragmented and pulverized fuel pellets in distending fuel rods and its effects on fuel rod heat load

Simulating high burnup fuels : FRAPCON-FRAPTRAN

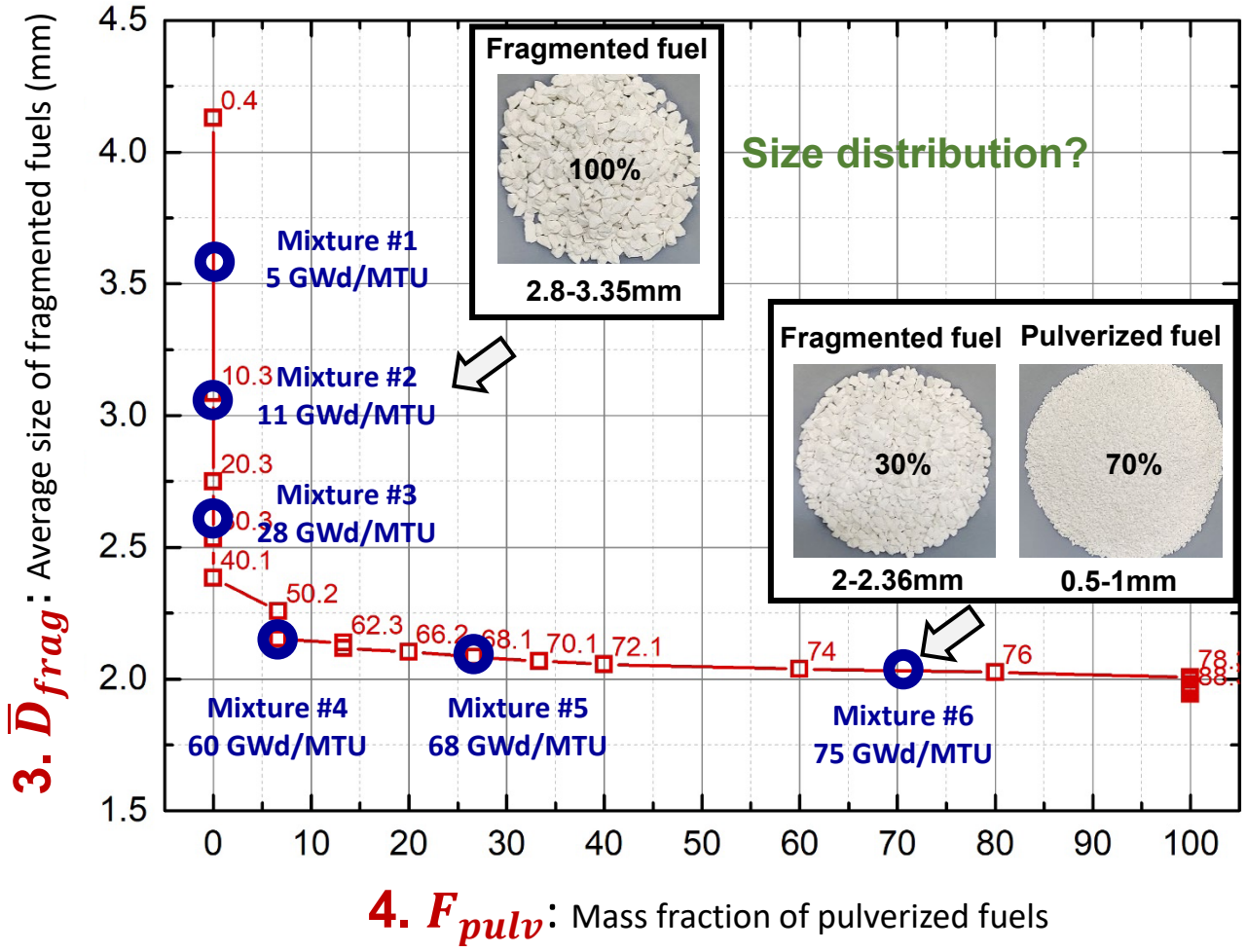

Required input for burnup-effect experiment

1. $P_{rod}(Bu)$

2. $Void_{rod}(Bu)$

3. $\bar{D}_{frag}(Bu)$

4. $F_{pulv}(Bu)$

Hydrogen generation in Burst

- **Pellet**

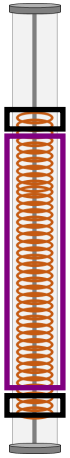

[Cr coated HANA-6]

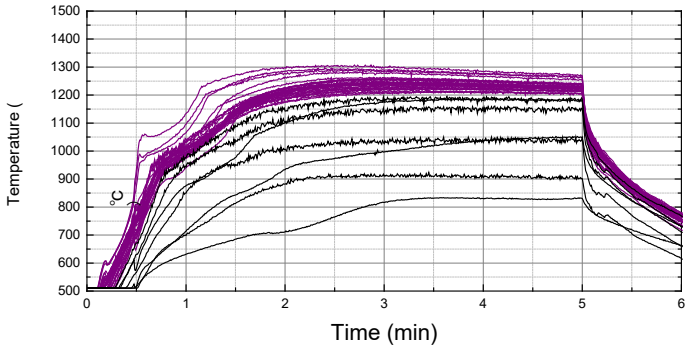

[HANA-6]

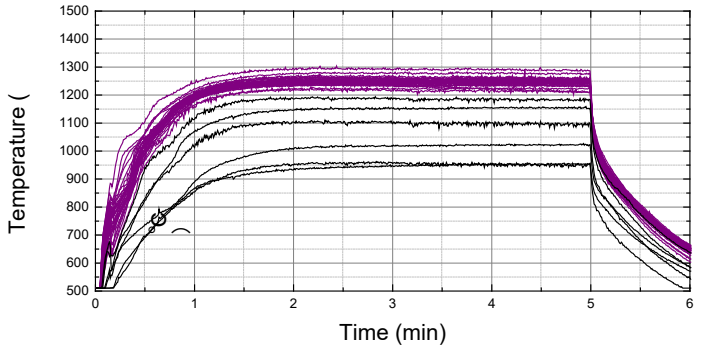

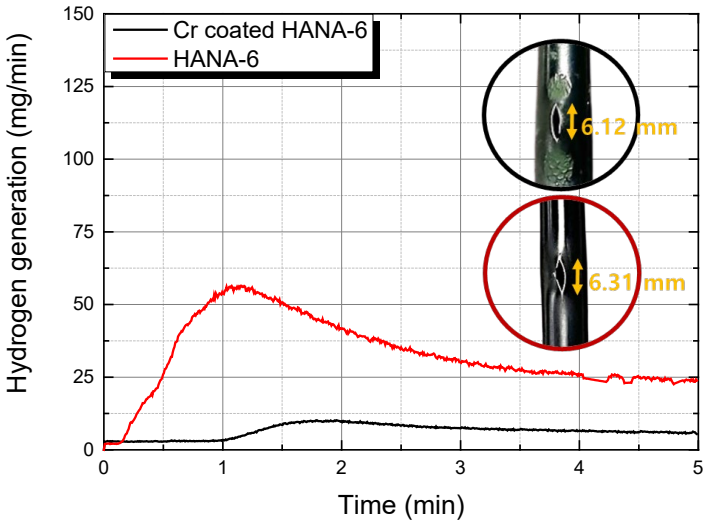

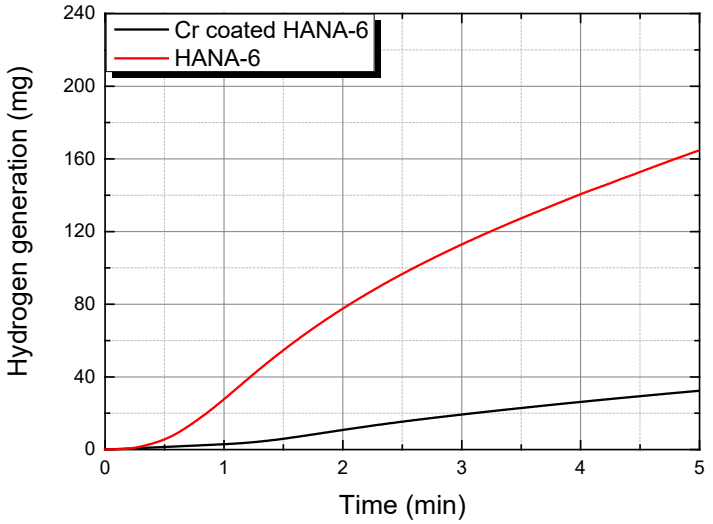

Hydrogen generation in Burst

- **Single**

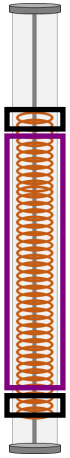

[Cr coated HANA-6]

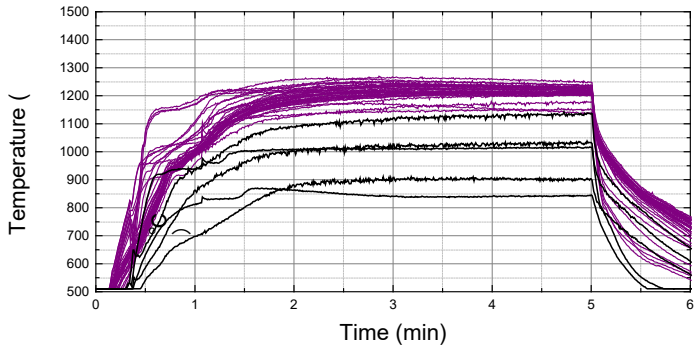

[HANA-6]

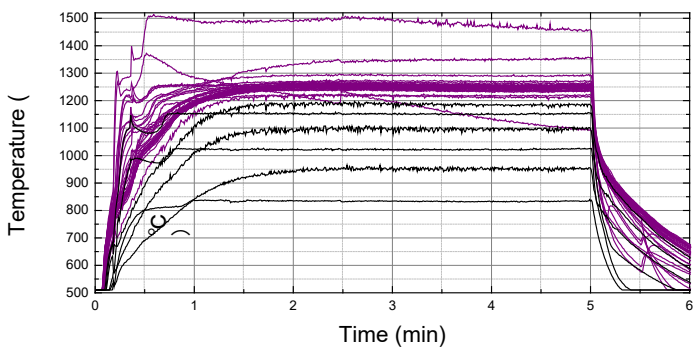

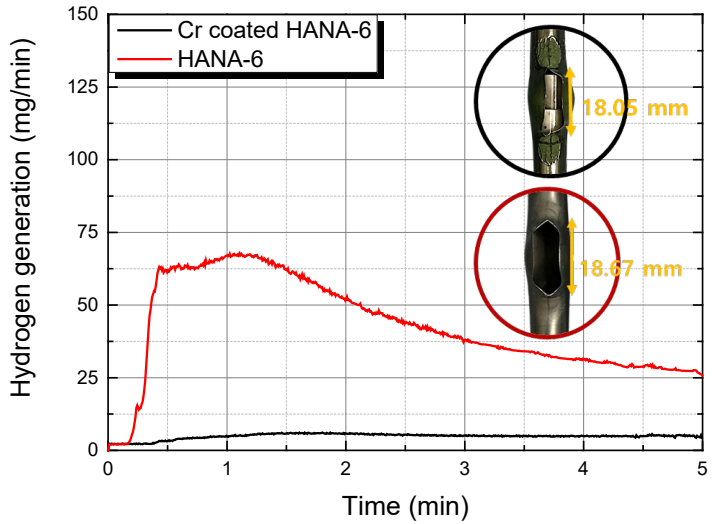

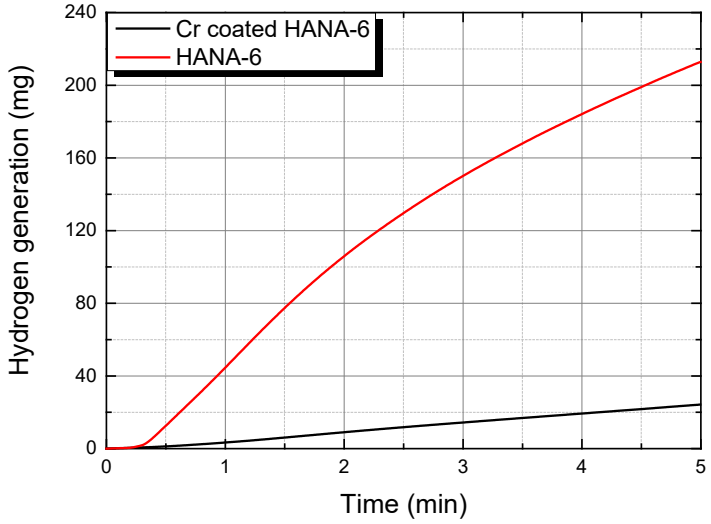

Nano-indentation and EBSD characterization of Zirconium

▪ Nano indentation

- Material: 650℃ 28h annealed HANA-6

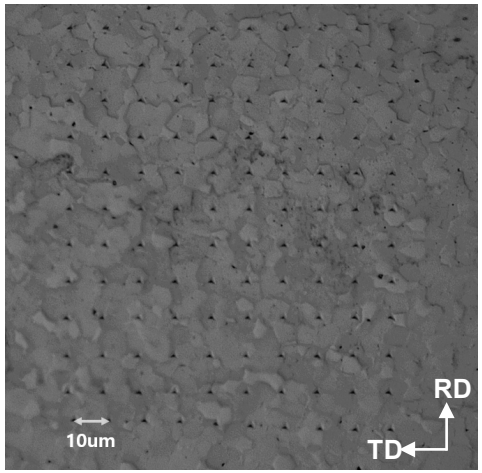

Berkovich tip

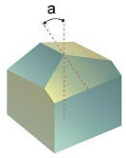

Indentation axis

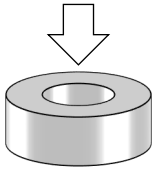

<100x12 indentation>

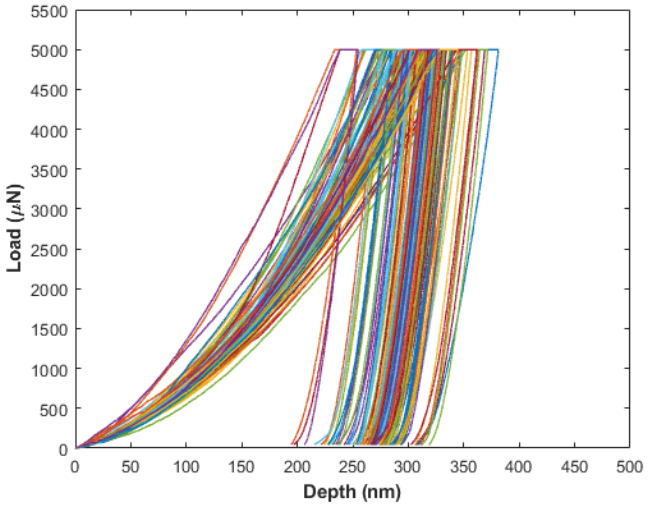

<Load-Depth curves>

▪ EBSD characterization

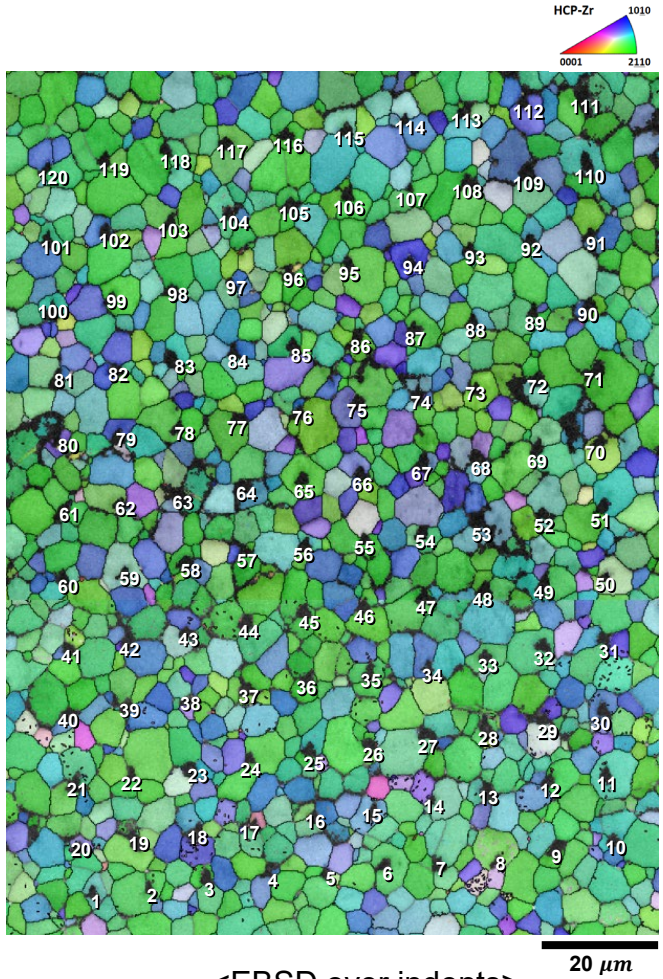

<EBSD over indents>

- Correlating nano-mechanical properties with orientation information

압입 번호와 IPF 이미지와 분리되어 있습니다. 필요에 따라 번호 삭제가 가능합니다

Orientation relationship analysis result

- **Hardness depending on the orientation**

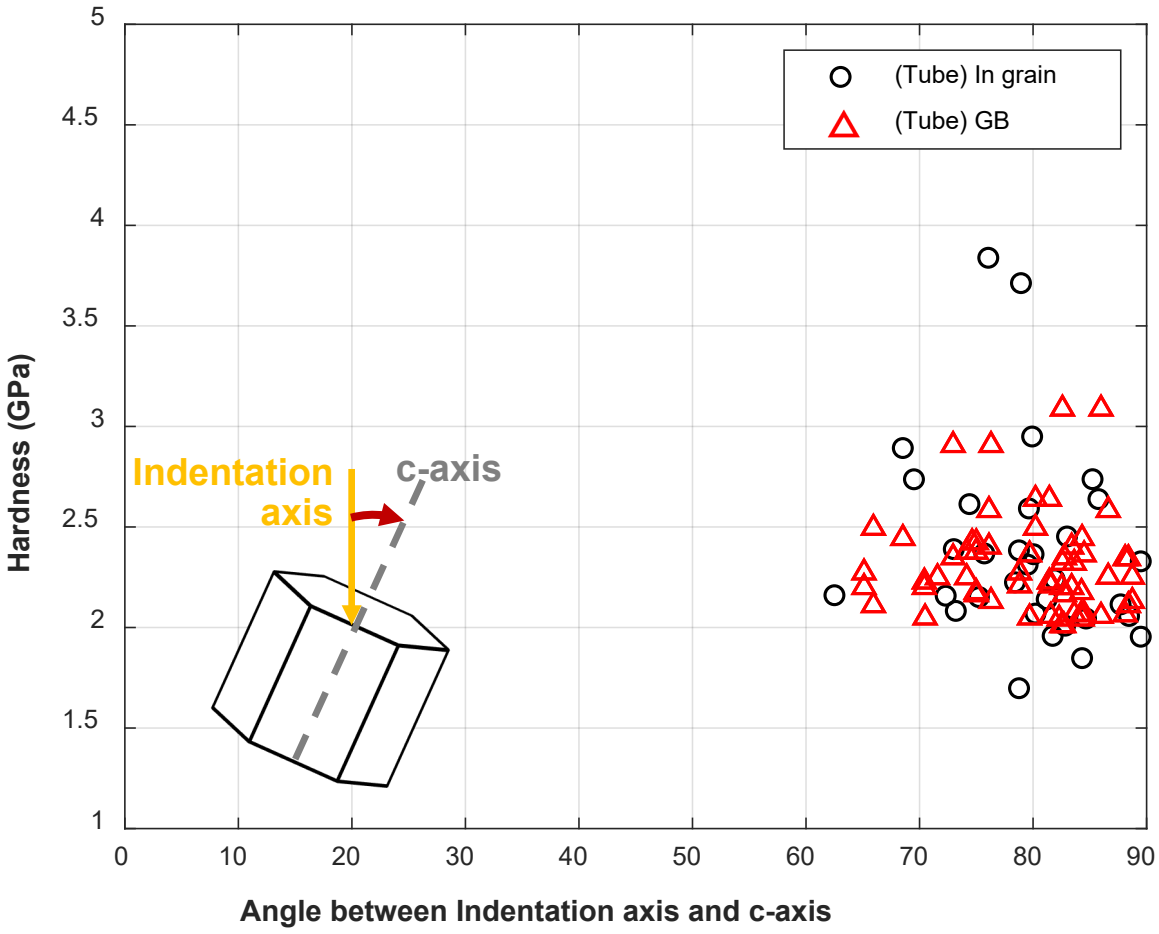

- **Indentation in Grain**

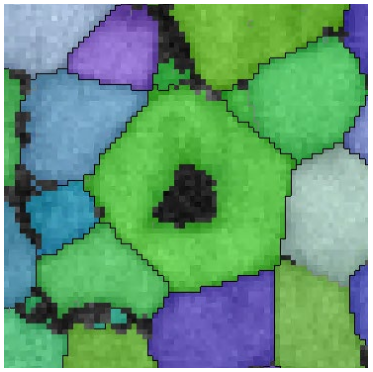

- **Indentation at GB**

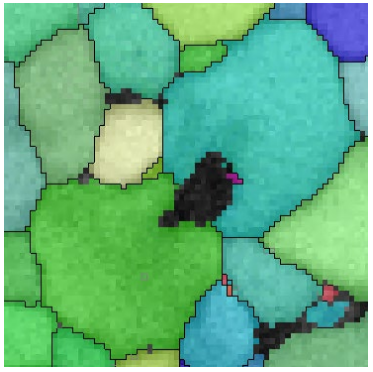

Orientation relationship analysis result in plate specimen

- **Hardness depending on the orientation**

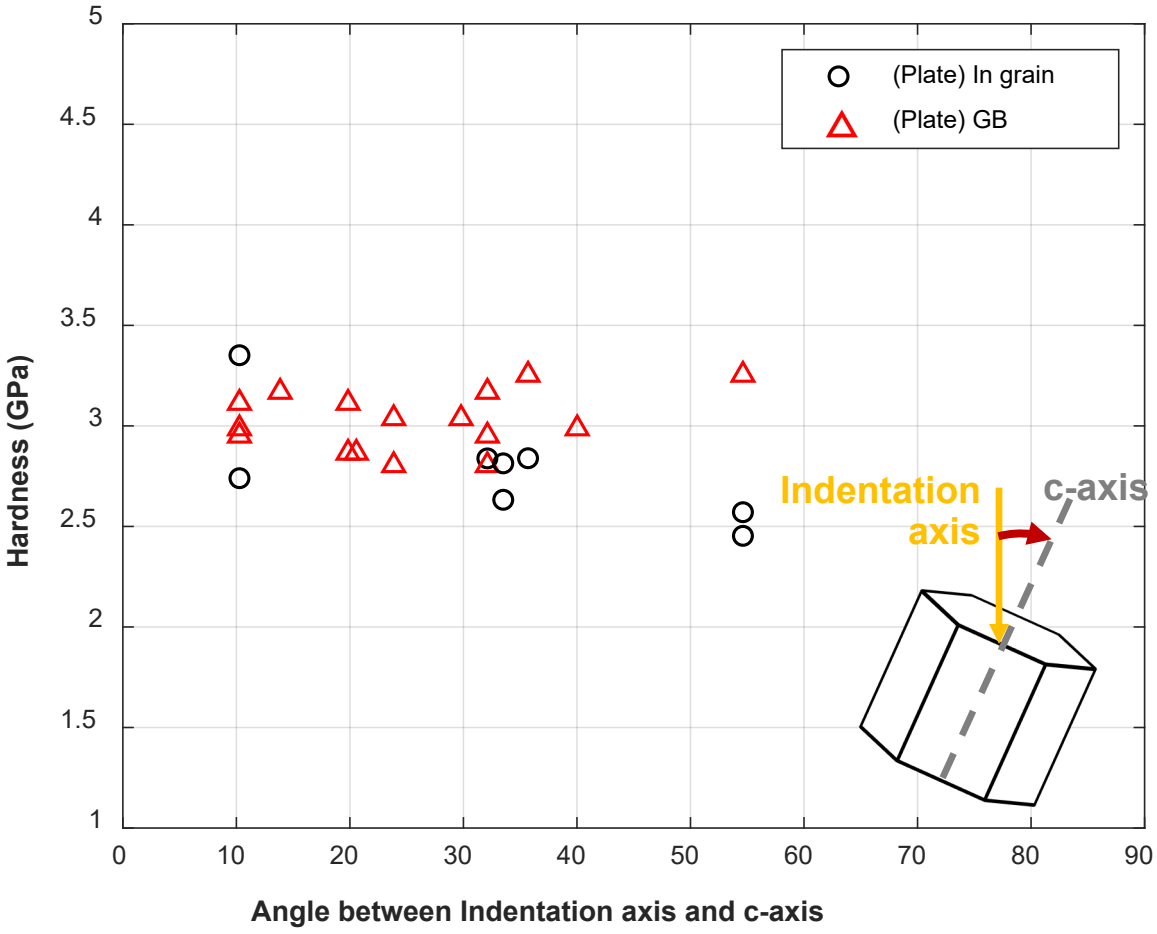

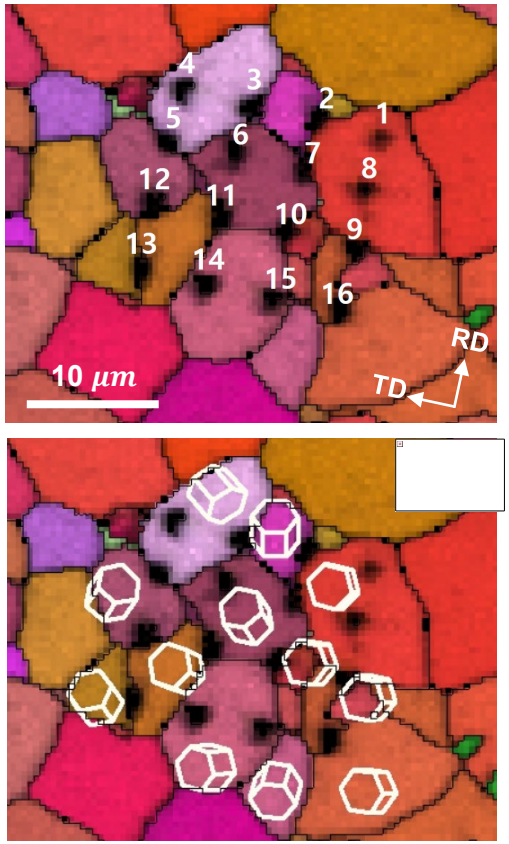

Applying the Cr-coated limits for DBA safety analyses

- **Oxidation (ECR) Limits**

Uncoated Zr-based alloys (near the burst hole):

$$ECR_{double-sided} = 87.8 * \frac{\Delta W_{CP,double}}{F_{thinning,avg}\left(\delta_{cladding} - \frac{ZrO_2}{1.56}\right)} \geq ECR_{limit}(\mathrm{H})$$

Metal substrate consumed by pre-transient oxidation [Pilling Bedworth ratio =1.56]

f(Bu) (i.e. 3.8% for 60MWd/kgU)

Cladding thinning factor due ballooning (average wall thickness reduction factor)

Metal substrate thickness after pre-transient oxidation

Cr-coated Zr-based alloys (near the burst hole):

$$ECR_{single-sided} = 87.8 * \frac{\Delta W_{CP,single}}{F_{thinning,avg}\delta_{cladding}} \geq 18\%$$

Assumption: pre-transient consumption of metal substrate via steady-state corrosion is nil.

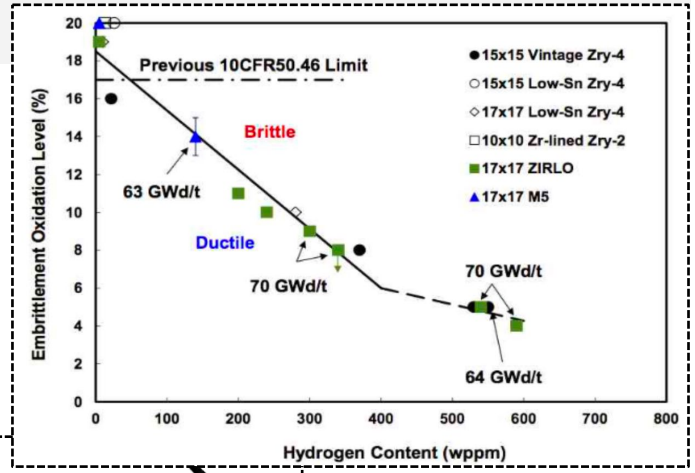

- **PCT Limits**

Uncoated Zr-based alloys: 1204℃

Cr-coated Zr-based alloys: 1204℃

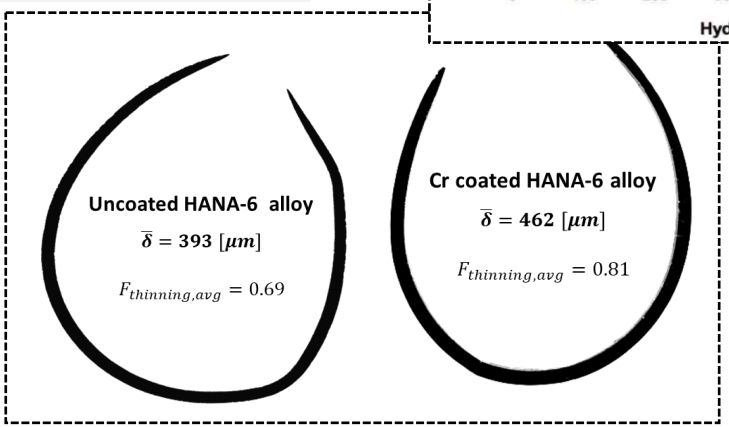

$F_{thinning,avg}$

Applying the Cr-coated limits for DBA safety analyses

- **Burnup-dependent LBLOCA progression for various claddings**

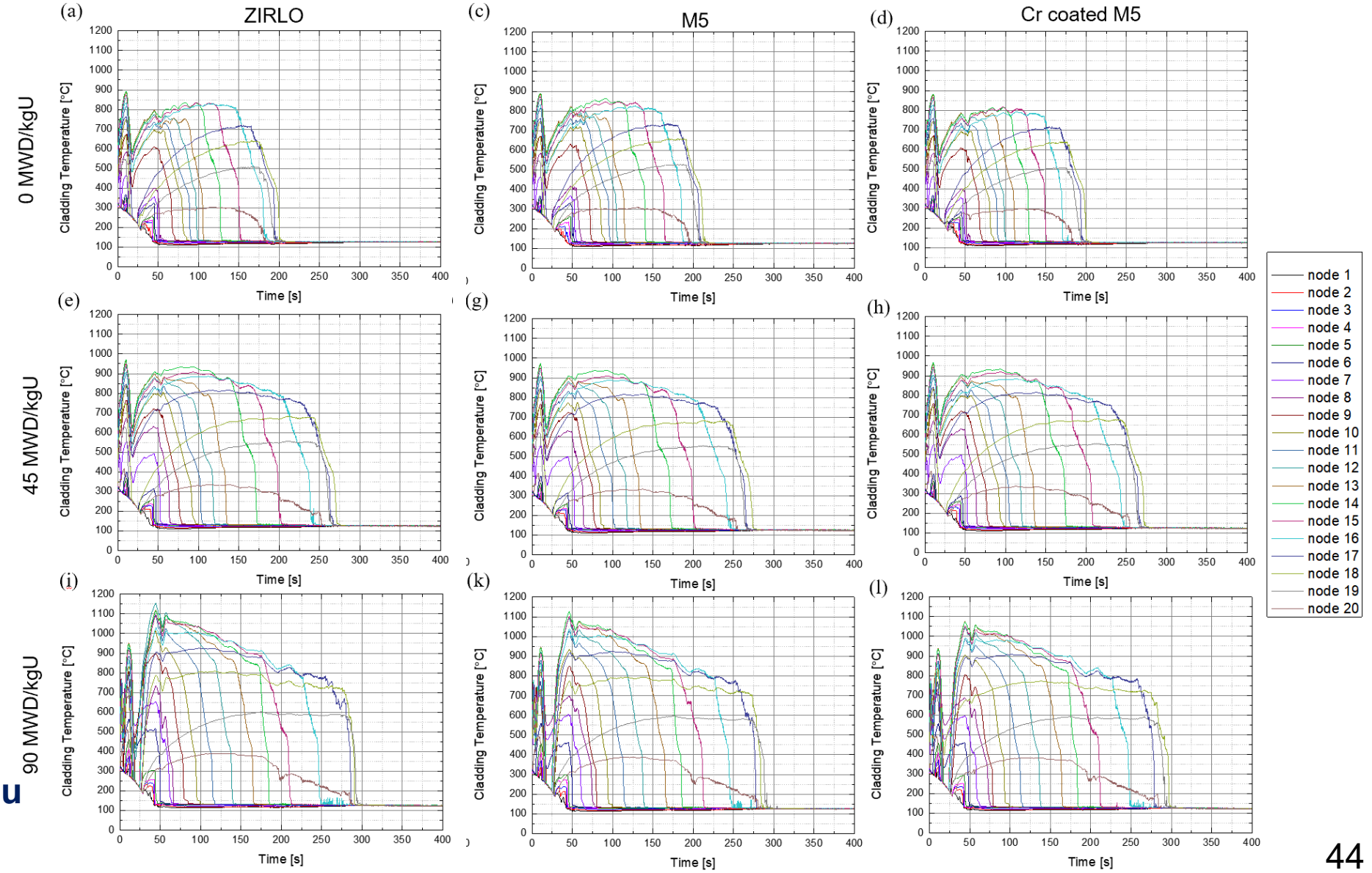

Applying the Cr-coated limits for DBA safety analyses

- Allowable discharge burnup from the safety assessment

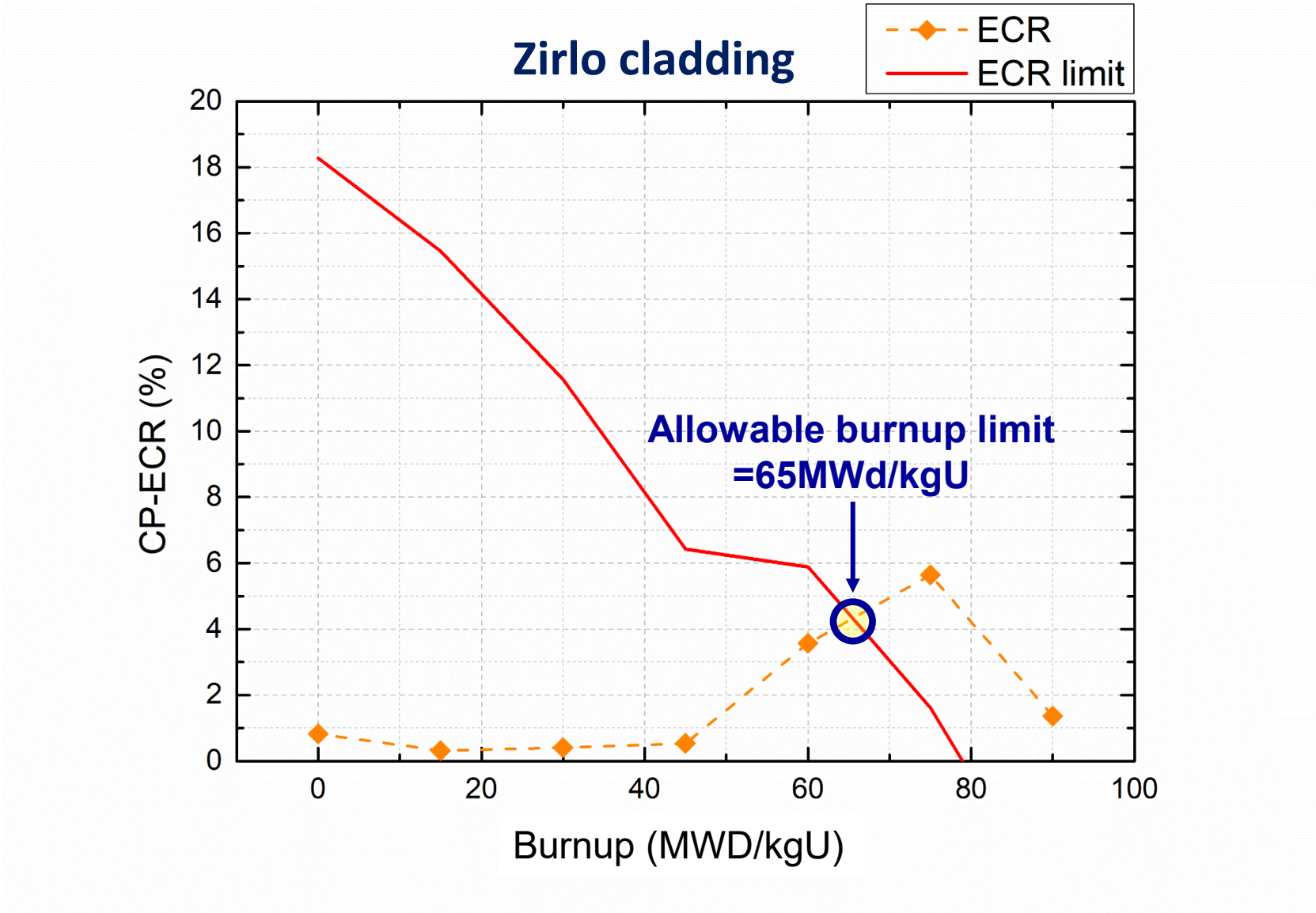

Applying the Cr-coated limits for DBA safety analyses

- **Allowable discharge burnup from the safety assessment**

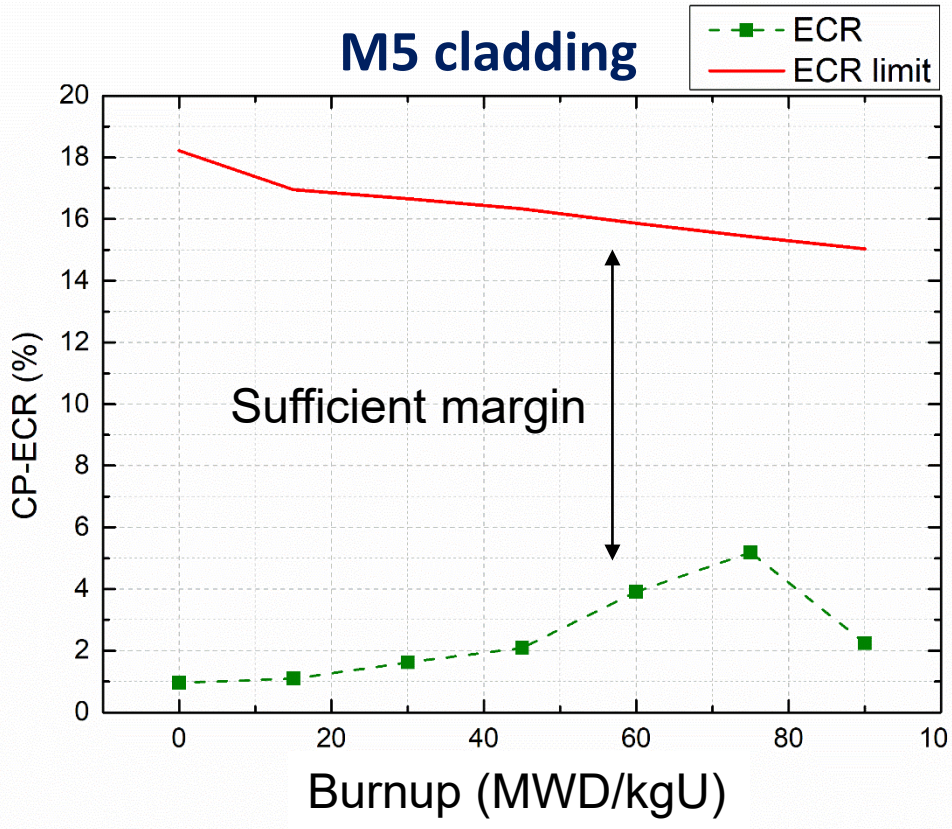

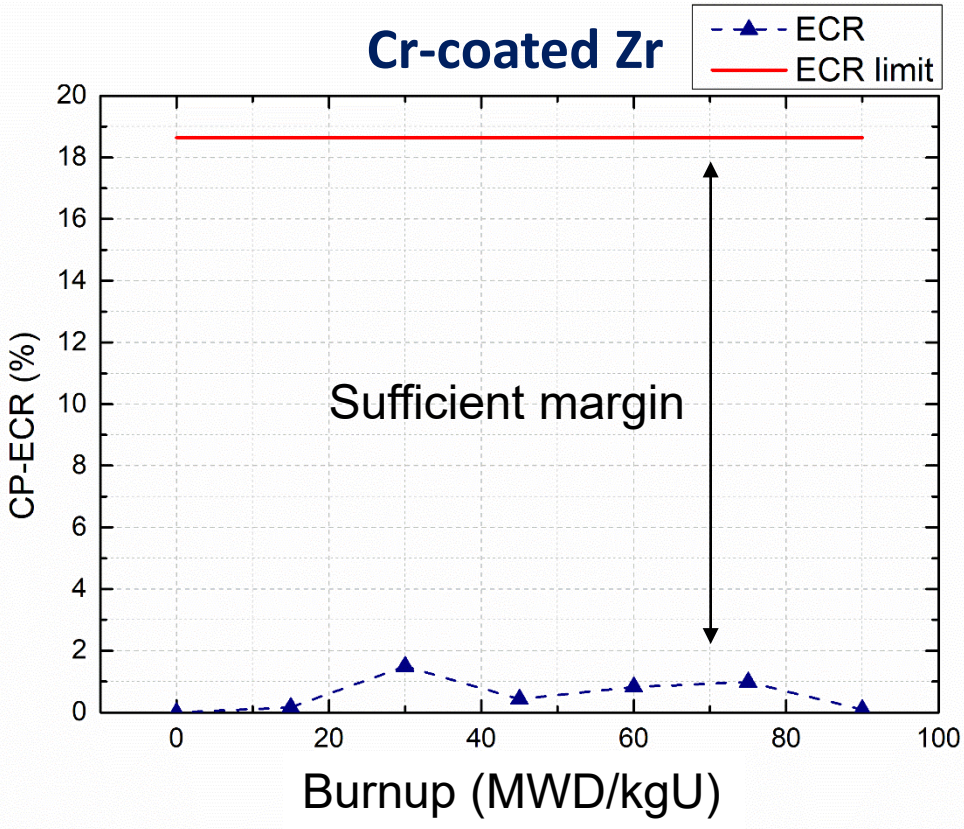

- **Modern Zircaloy (i.e., M5 and HANA-6) is almost as accident tolerant as Cr coated ATF**
- **Accident tolerance comes from steady-state corrosion resistance.** Modern Zircaloy is quite corrosion–resistant under the typical LWR operating conditions, offering sufficient safety margin.

Understanding material-limited Burnup

- **Individual limiting factors**

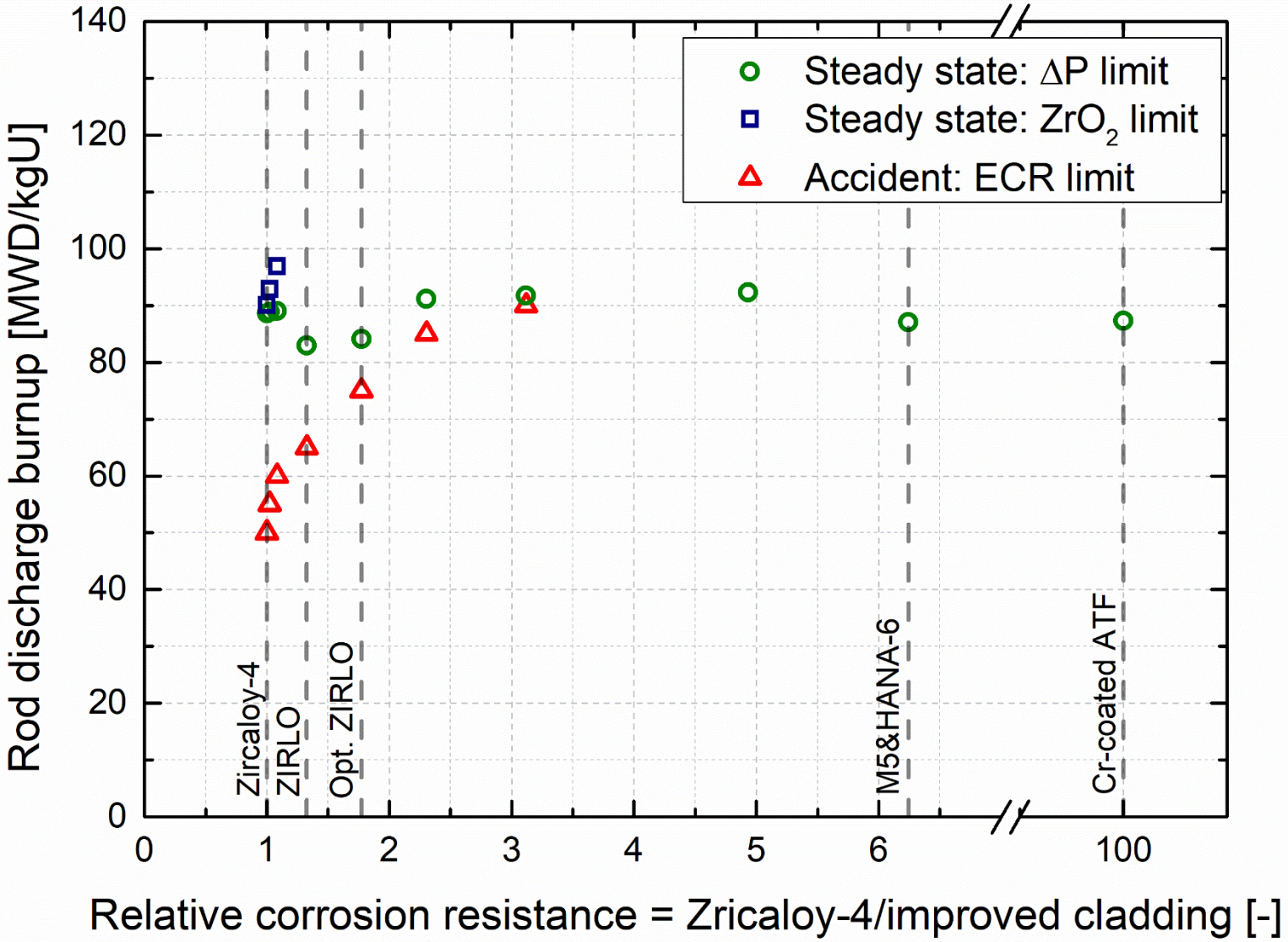

Understanding material-limited Burnup

- **Individual limiting factors**

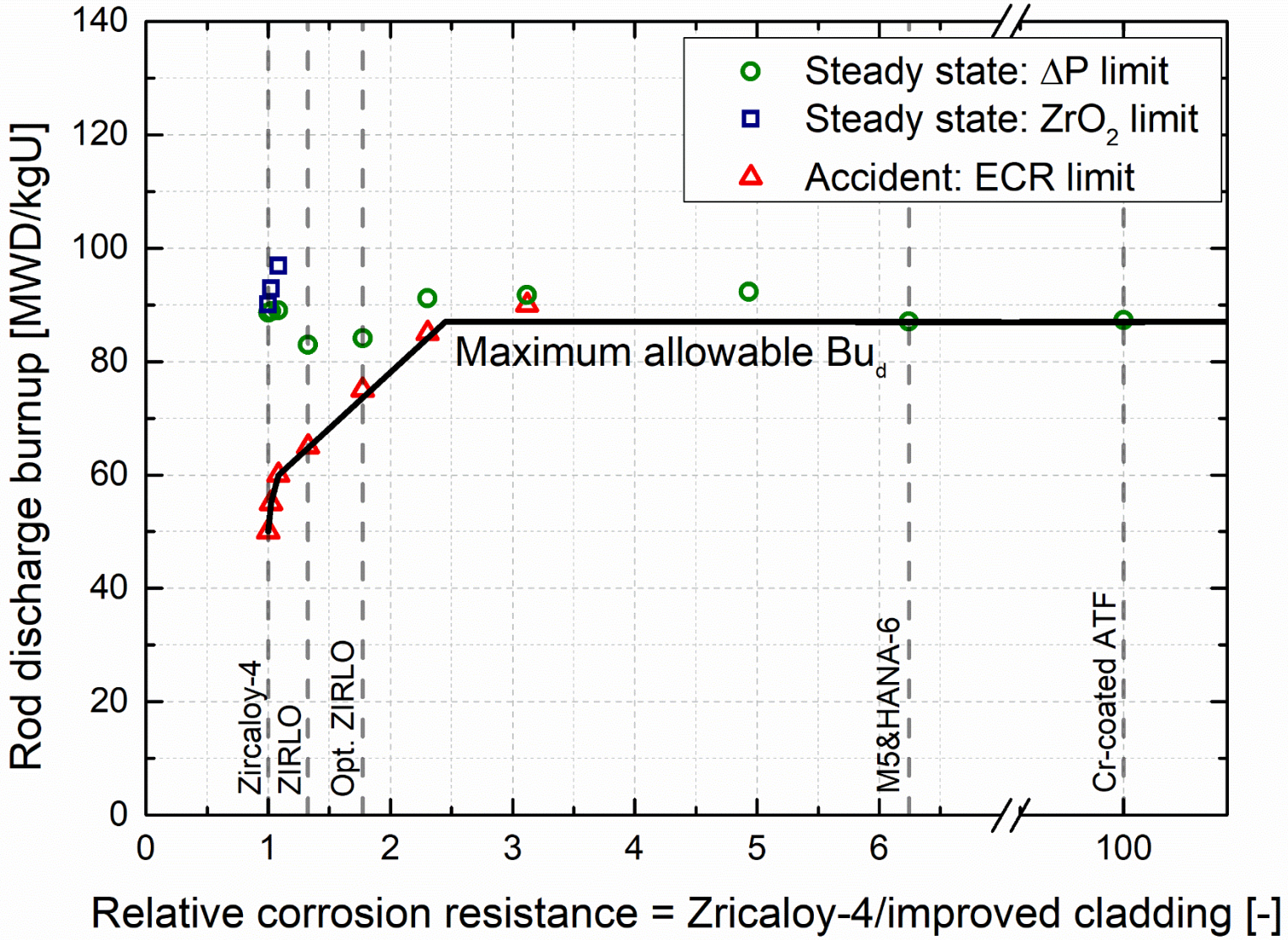

Jakub Krejci

UJP

High temperature creep during LOCA conditions

During loss of coolant accident the fuel cladding is exposed to high temperature and inner pressure, which may lead to fuel rod ballooning followed by its rupture and/or blockage of the emergency core cooling system coolant. The accident in the Fukushima nuclear power plant, in particular, showed that it is worth investigating accident-tolerant fuels, including fuel cladding, which should fulfil its role as a barrier between radionuclides and the environment better and for a more extended period in extreme conditions. This contribution focuses on the behaviour of fuel cladding samples with Cr, CrN and CrN+Cr multi-layer coating. Ramp and isothermal tests were performed for several coated cladding variants, and different behaviours depending on coating quality were observed.

The methodology with a constant amount of gas was used. Modifying the burst test setup to observe the pressure drop within the cladding can overcome the limitations of commonly used methods that only assess the total deformation after rupture. A coupled experimental and numerical approach was developed to determine the primary, secondary creep and ballooning parameters. Ballooning tests were performed on tubular specimens, and resulting deformation kinematics were measured using internal pressure drop measurements. The following methodology better describes creep mechanisms as a function of stress and thermal conditions. The standard dimension measurements were used as well.

High temperature creep during LOCA conditions

J. Krejčí[1], A. Prítrský[2], M. Svatošová[1,2], M.Ševeček[2]

[1] UJP PRAHA a.s., [2] Czech Technical University in Prague

29th International QUENCH Workshop

19-21 November 2023

Content

1) Burst-tests
2) Ramp-test data
3) Constant temperature: closed specimen
4) Summary

1

Burst-tests

Burst-tests

- Simulation of LOCA
  - Ballooning and burst
  - Resistant furnace up to 1100 °C (no video possible)
  - Inner pressure up to 16 MPa
- Experimental procedure:
  - Two temperature scenarios (Ramp-test, Isothermal test)
  - Two pressure scenarios (constant, decrease due to deformation)

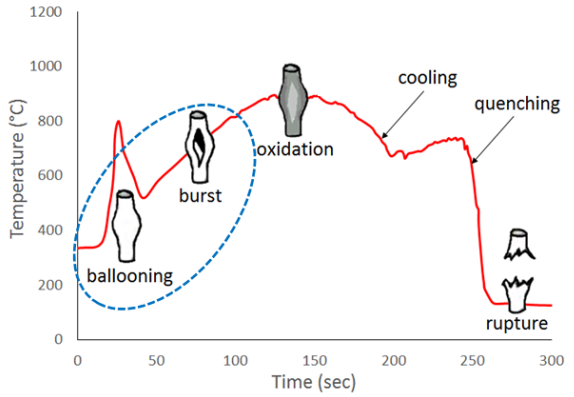

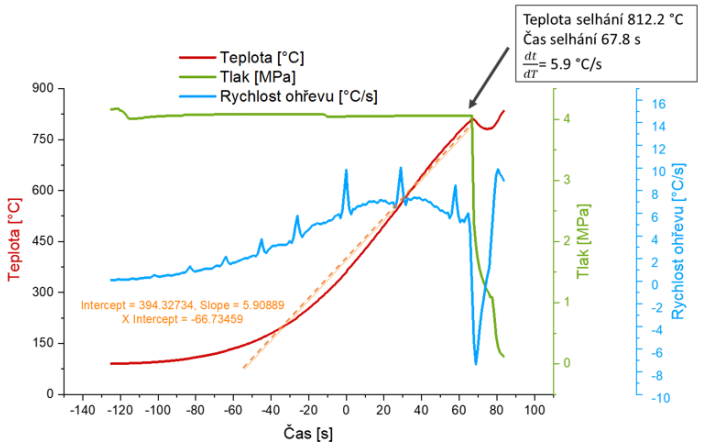

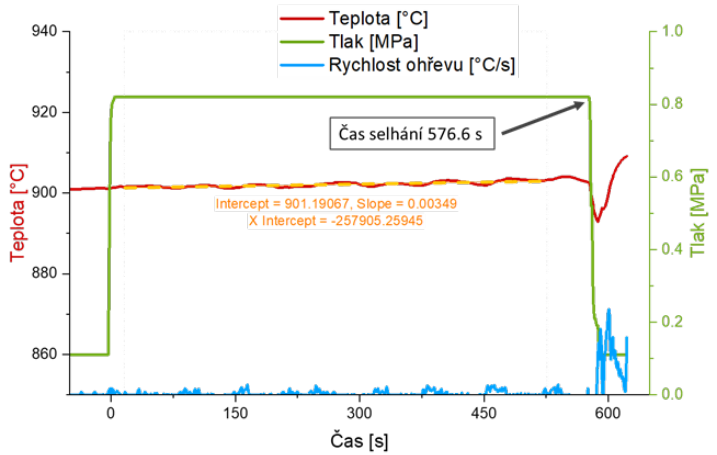

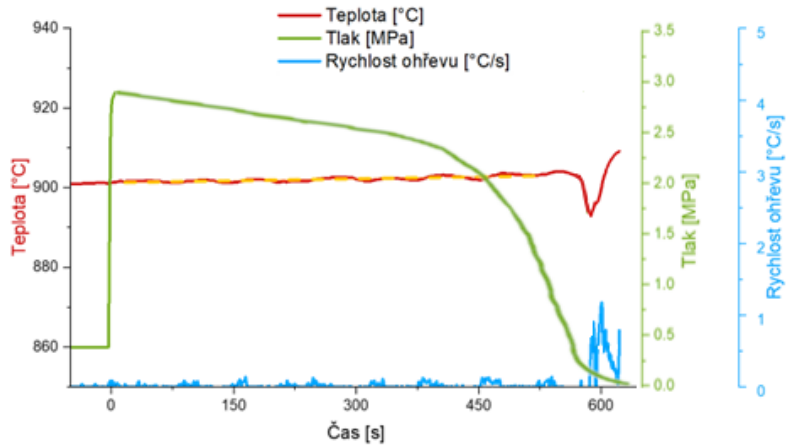

Tested materials

- Materials provided in the frame of IAEA project ATF-TS
  - PVD-Cr coated (sputtering) Opt. ZIRLO
  - PVD-Cr coated (arc-deposition) Zr1Nb
  - Uncoated Zr1Nb
  - Uncoated Opt. ZIRLO
  - Uncoated Zry-4
- Specimens
  - 110-130 mm tubes
  - Ends closed using swagelok

Burst-tests data

- Available data:
  - Ramp-tests (0.7°C/sec, 5-7°C/sec)

  ⇒ **deformation criteria**
  - Isothermal test at 750 °C (α-Zr region: constant pressure, constant volume/pressure decrease)
  - Isothermal test at 950 °C (β-Zr region: constant pressure)

  ⇒ **creep rate**
- Evaluation:
  - Ex-situ: maximal strain, uniform (20 mm) strain, rupture size
  - In-situ: temperature, pressure
  - **Deformation calculation**

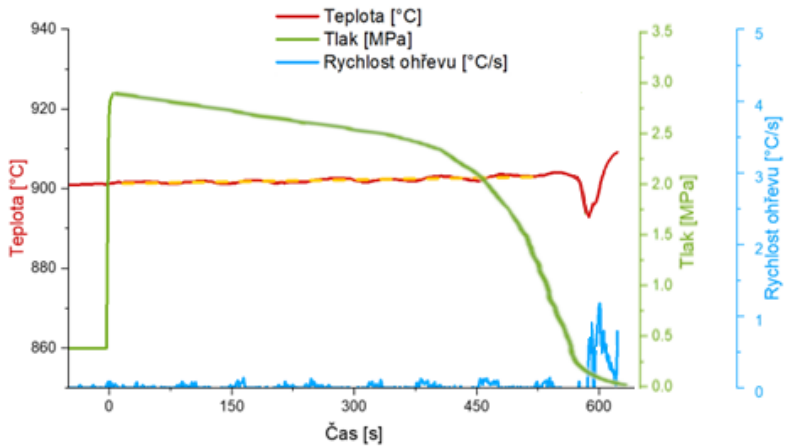

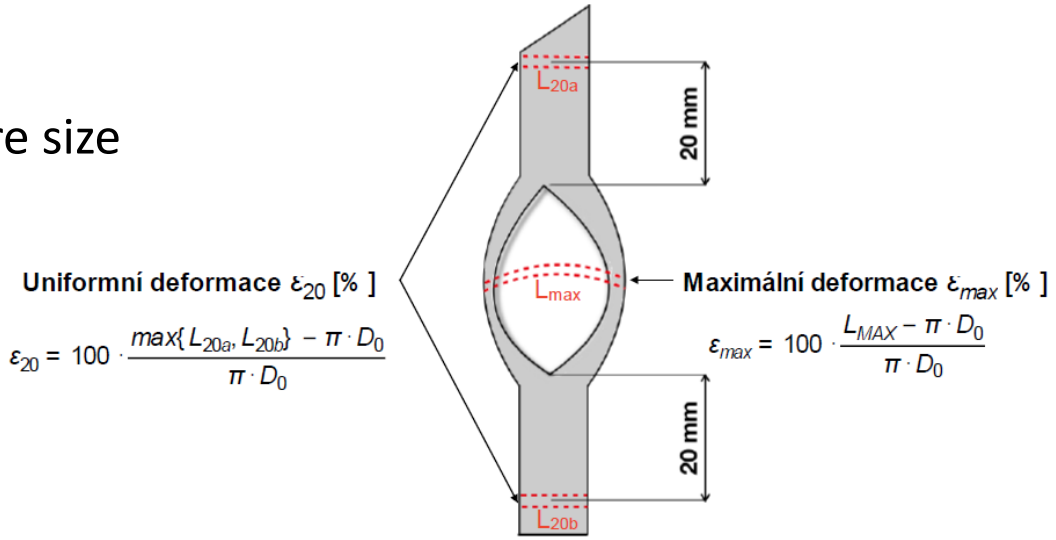

2

Ramp-test

Ramp results (1)

- Engineering stress (Barlow): σ_0=(OD-TH)/(2*TH)
- Criteria: Eng.stress/Temperature at burst
  - NUREG-0630 criteria (e.g. TRANSURANUS)
- Criteria: Maximal deformation/Temperature at burst
  - NUREG-0630, BALON 2 criteria (FRAPTRAN)
- Cr-coating on Zr1Nb specimens significantly better quality than on Opt.ZIRLO: **<u>butst temperature, crack amount</u>**

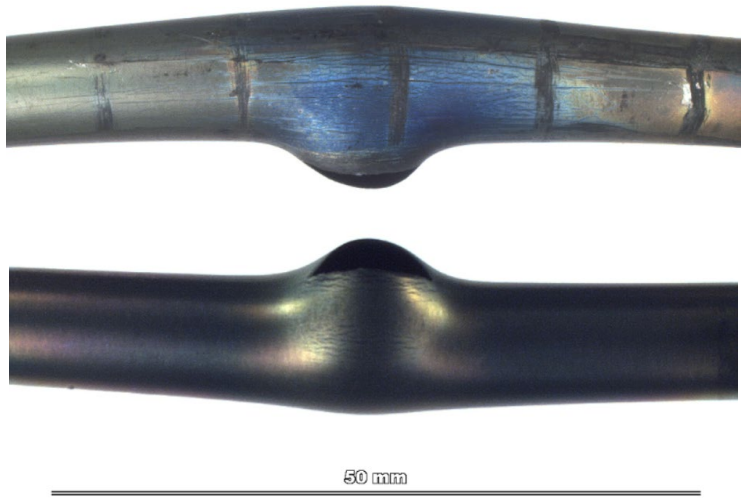

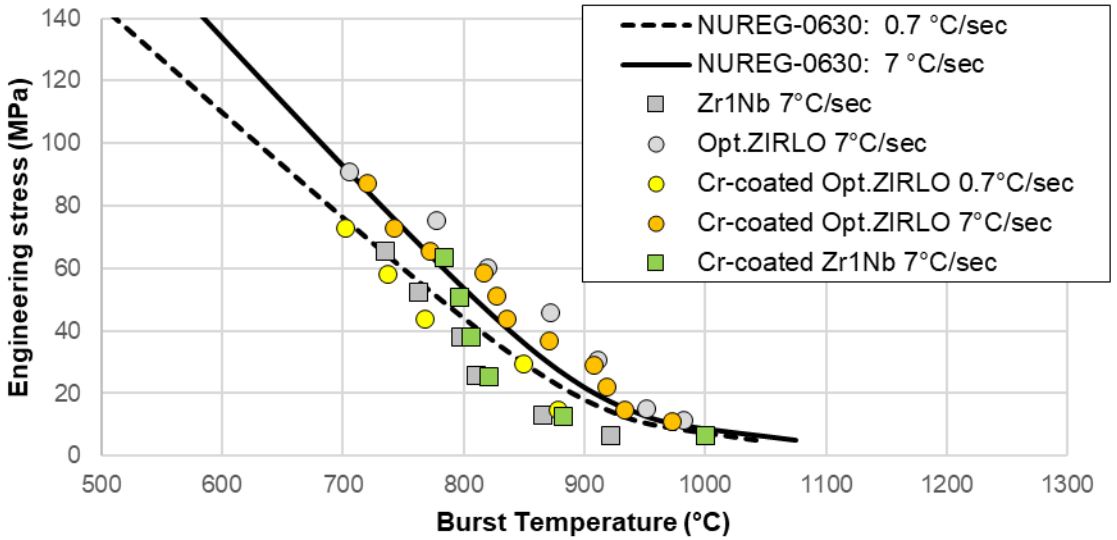

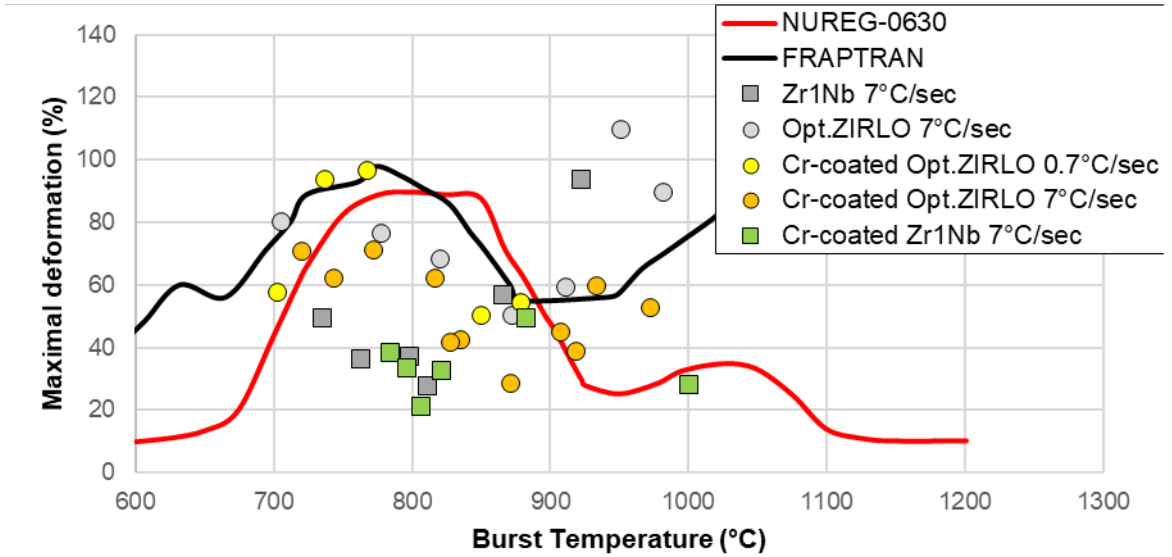

Ramp results (2)

- Burst stress: $\sigma_B = \sigma_0 * (1+\varepsilon)^2$
- Criteria: Burst.stress/Temperature at burst
  - TRANSURANUS (does not count BALLOONING) => ε_{2cm}
  - FRAPTRAN/BALON 2 (count BALLOONING)
- Cracks and thinner wall chalanging for description (make sense to use criteria like this???)

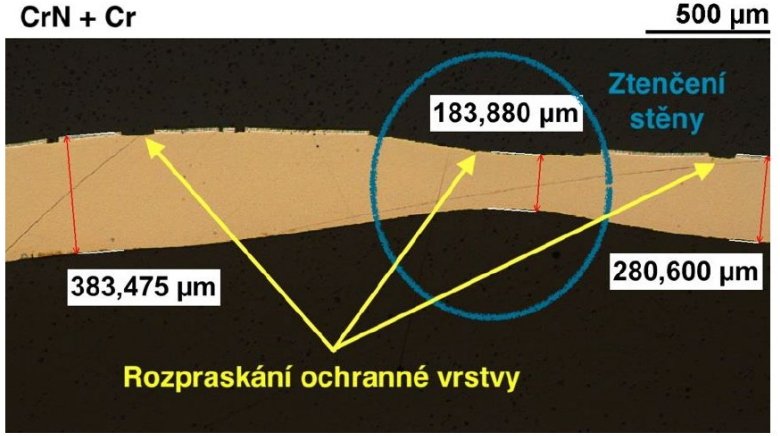

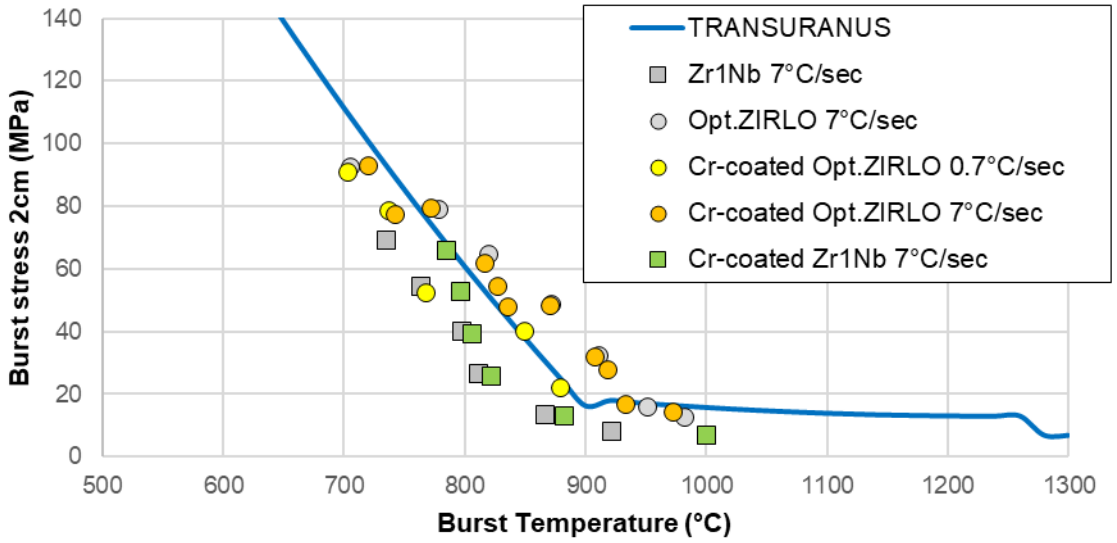

3

Constant temperature: closed specimen

Closed specimen test

- Pressure evaluation methodology => deformation reconstruction
  1) Calculating specimen's internal volume increment from pressure drop
  2) Calculating deformation using geometrical model
  3) When criterion is reached the balloon occurs
  4) From geometry and pressure, the in-wall stress is calculated

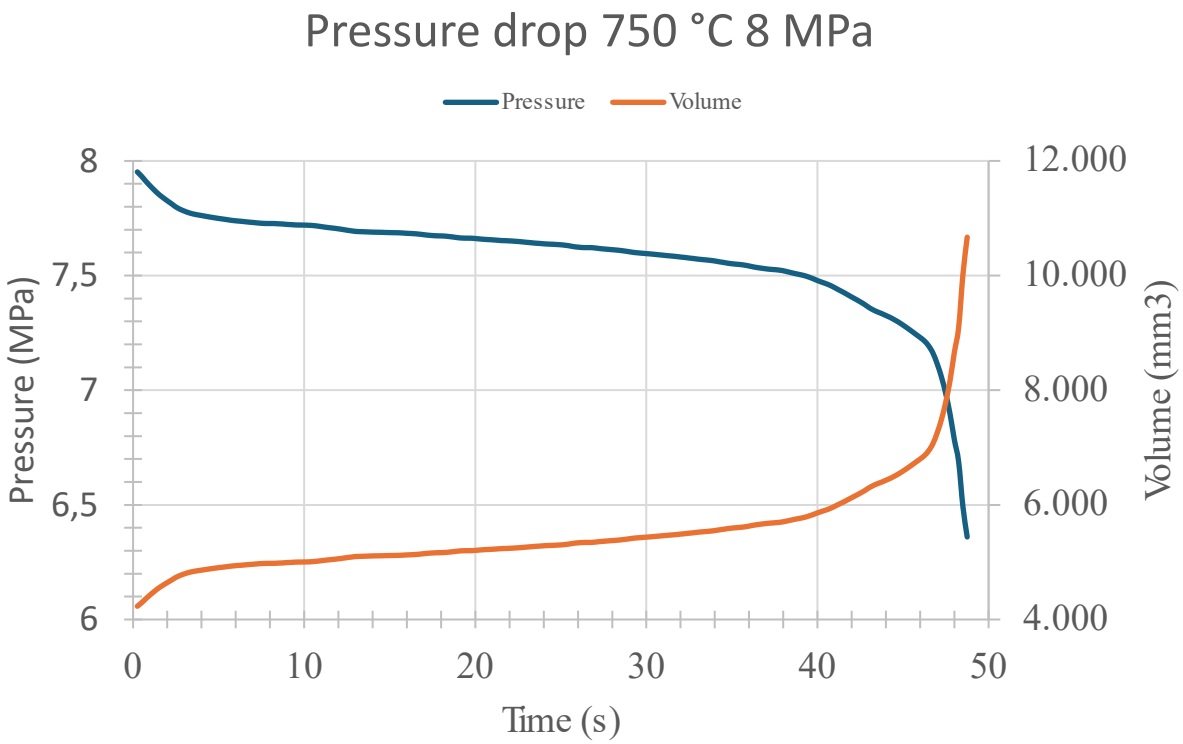

Uniform deformation

- Thermal expansion + elastic deformation + uniform plastic deformation
- Radially growing uniform cylinder
- Calculation of the deformation rate and the deformation acceleration

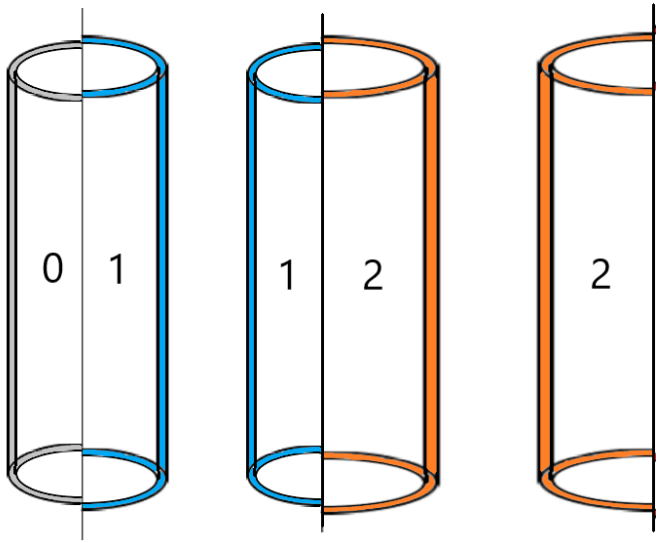

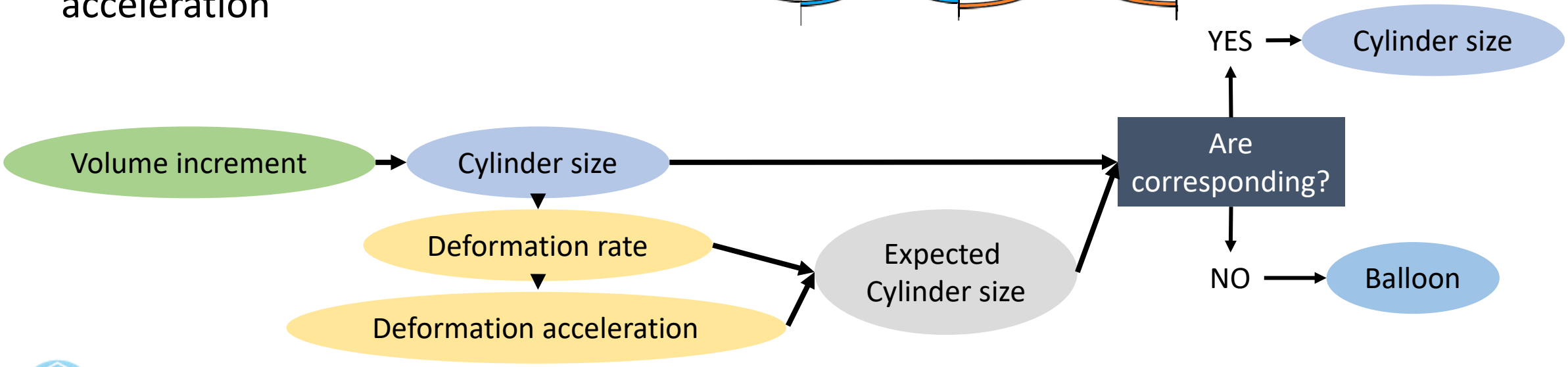

Balloon deformation

- Calculating uniform cylinder size under the balloon zone from def. rate from pre-balloon state
- Uniform cylinder is constantly growing
- Volume difference is accumulated in balloon
- Balloon geometry description based on accumulated volume
- Finding the size of balloon at burst

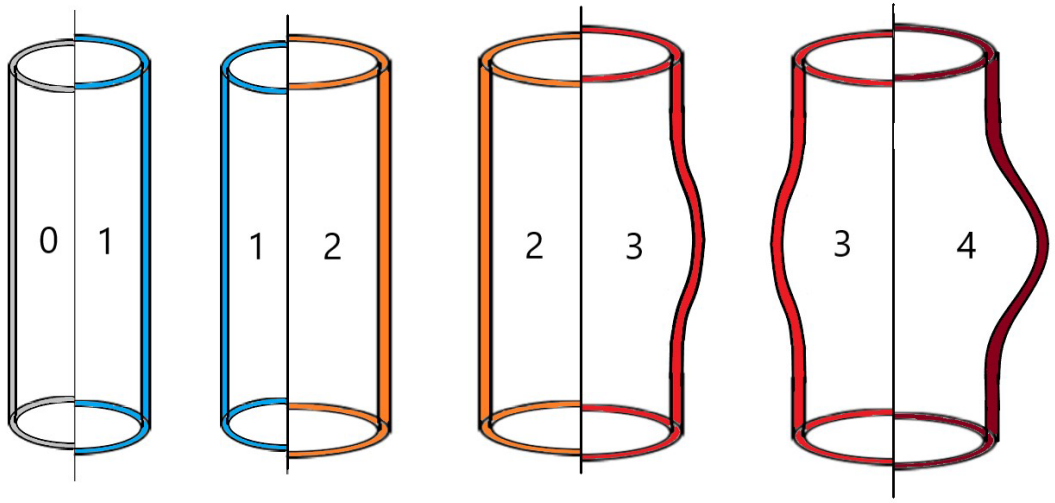

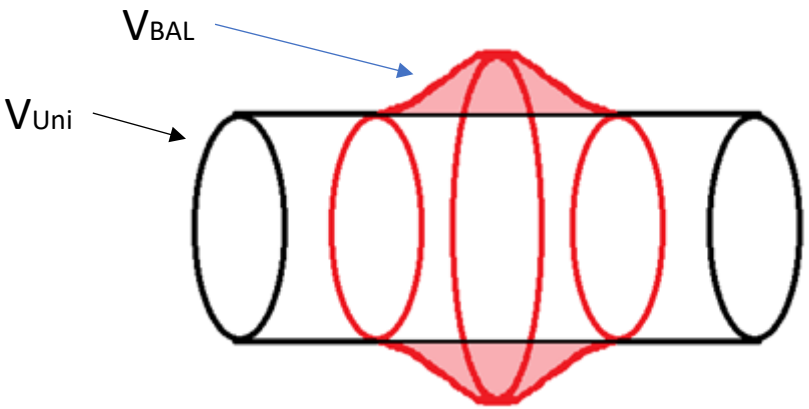

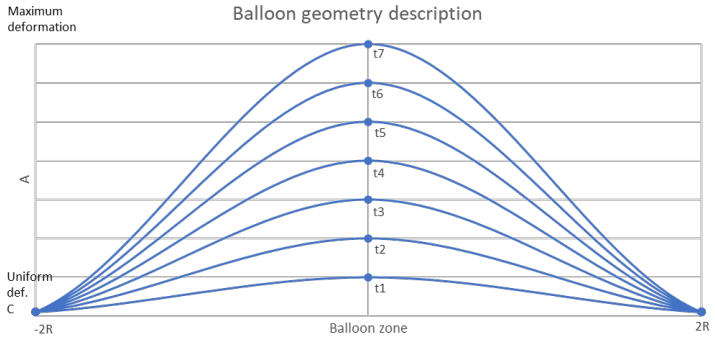

Pressure evaluation outputs

- Deformation in time
- Strain rate: 3 creep stages
- 3 axis stress in time, thick wall cylinder

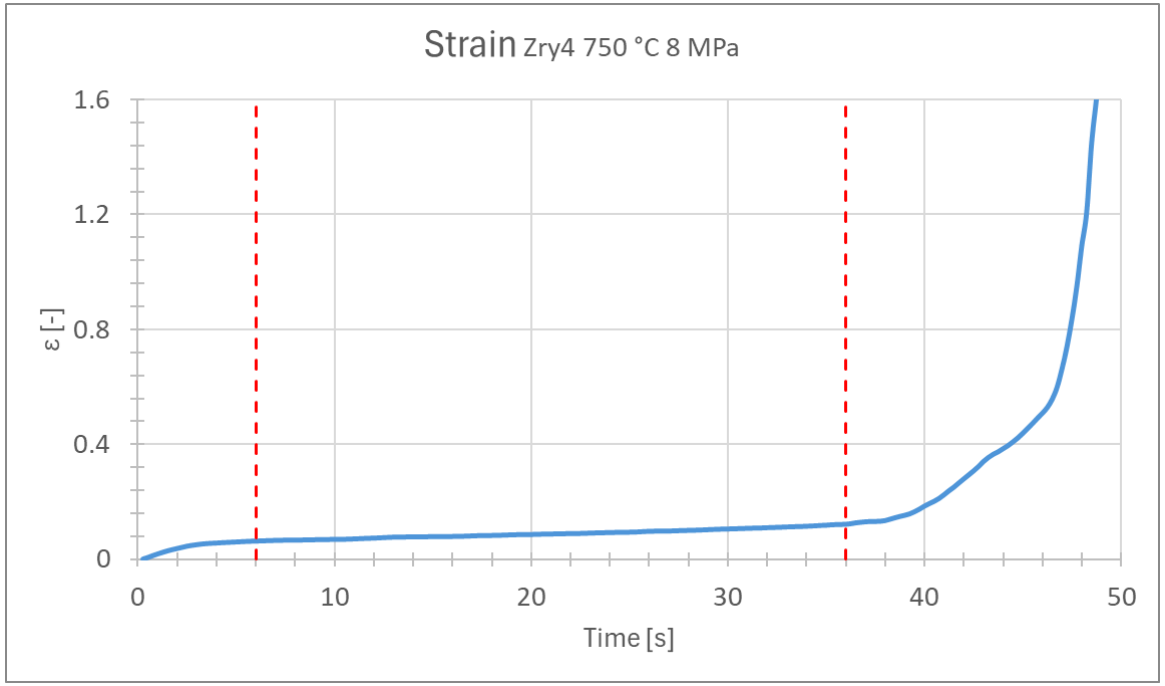

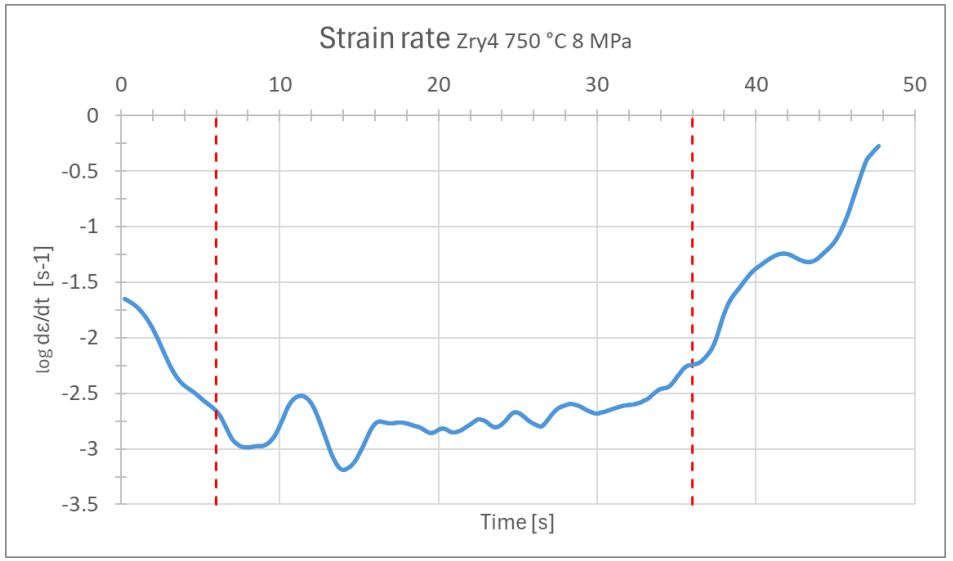

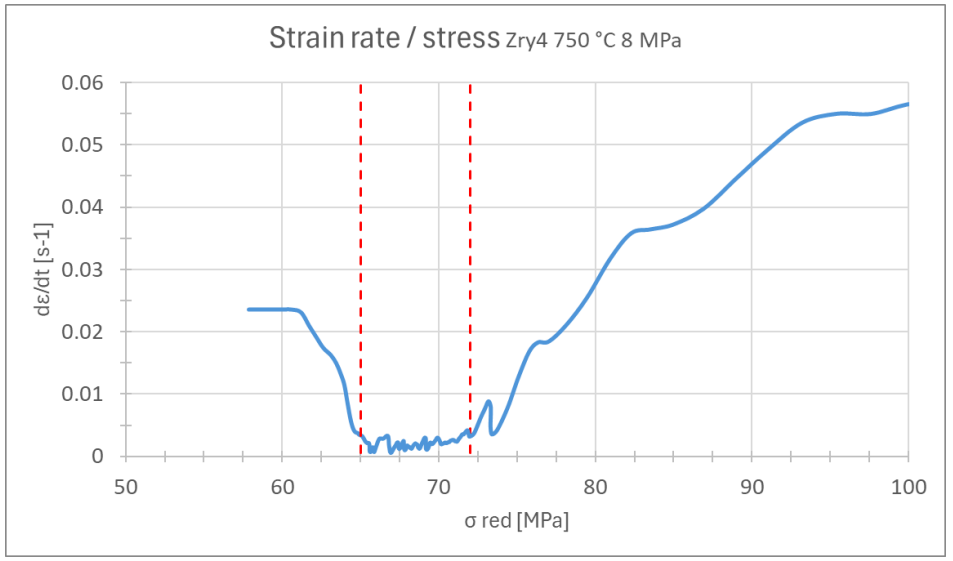

Comparison model and experimental data

- Maximal and uniform strain comparable
- Significant difference between creep rate
- Slight difference in stress during test
- Additional information about primary creep phase (ε_0)

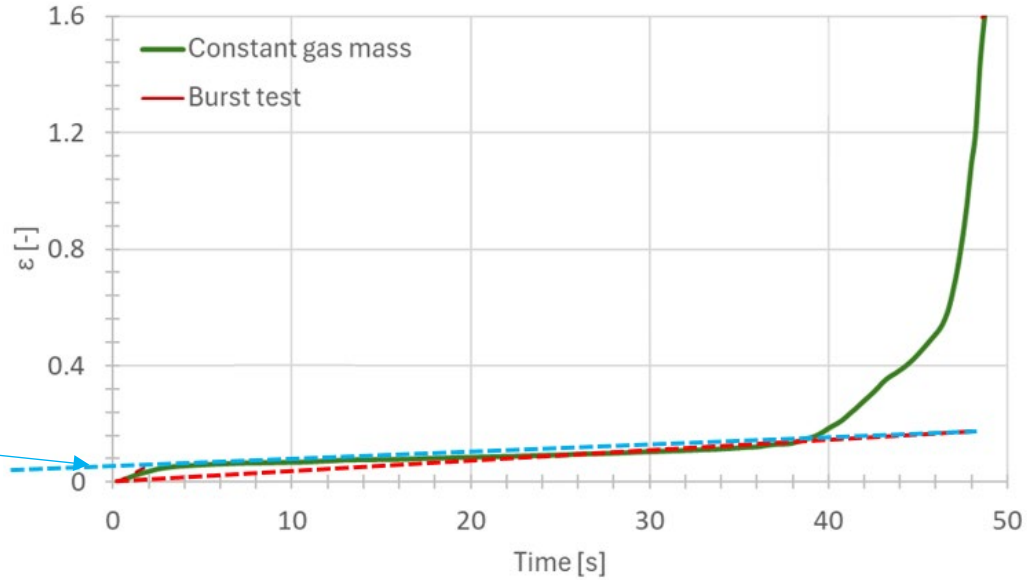

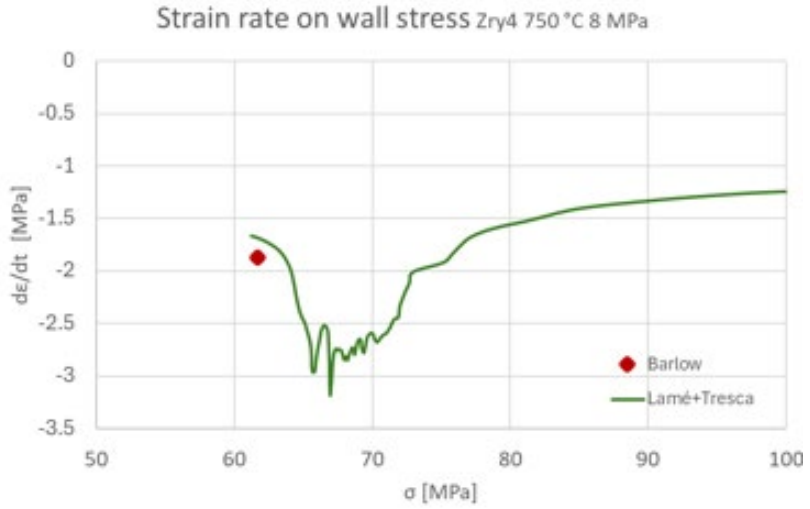

	Experiment	Model
Maximal Strain (-)	1.65	1.6
Uniform strain (-)	0.15	0.17
Primary creep strain (-)	???	0.05
Creep rate (1/s)	0.0039 ($\varepsilon_{20mm}/\tau_{BURST}$)	0.00150 (AVE: 6 – 36 s)
Stress (MPa)	60 (Barlow)	66 (Lame+Tresca)

4

Summary

Summary

- Ramp tests results
  - Significant differences between coatings
  - Burst-temperature: higher for Cr-Zr1Nb, lower for Cr-Opt.ZIRLO
  - Burst-deformation lower for coated
- Isothermal creep constant volume (closed specimen)
  - Time to burst longer for coated
  - Lower maximal deformation and creep rate for coated
  - Methodology for strain reconstruction (including ballooning model)
- Further steps for closed specimen methodology
  - Comparison with axial creep data (constant stress, in-situ strain measurement)
  - Comparison with video
  - Prediction model (based on in-situ pressure measurement)
  - Acoustic emission implementation

Thank you for your attention

Acknowledgements

- This project is supported by Technology Agency of the Czech Republic
- Project No. TK04030168, TM04000018, TS01020133

Balloon deformation

- Calculating uniform cylinder size under the balloon zone from def. rate from pre-balloon state
- Uniform cylinder is constantly growing
- Volume difference is accumulated in balloon
- Balloon geometry description based on accumulated volume
- Finding the maximum size of balloon

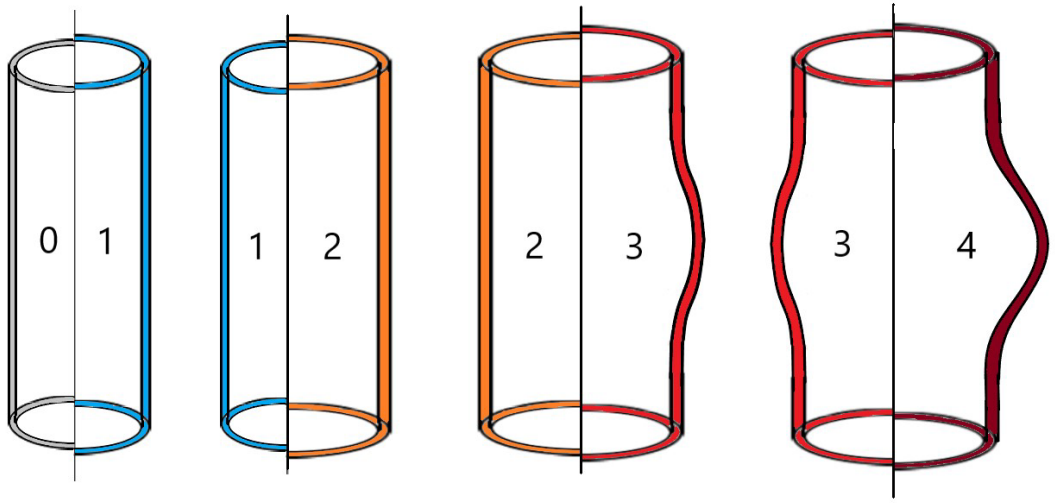

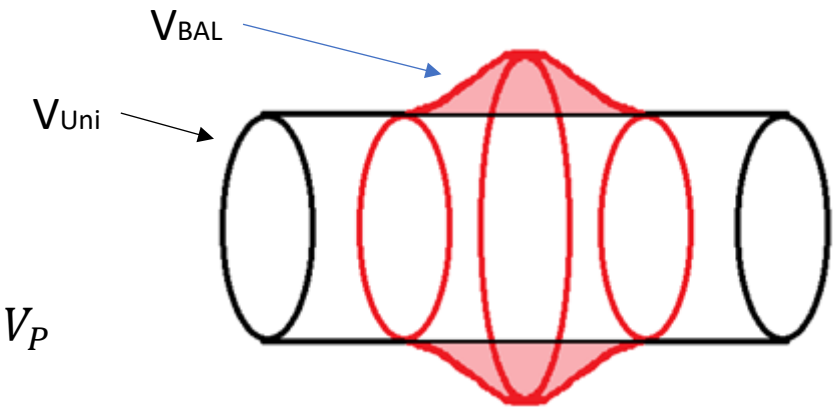

$$V = V_{Uni} + \left[\frac{\Delta V_{Uni}}{\Delta t} + \frac{\Delta^2 V_{Uni}}{\Delta^2 t} \cdot \Delta t\right] \cdot \Delta t + V_{BAL} + V_P$$

V – total volume, Vuni – volume of uniform cylinder Vbal – Volume of balloon, Vp – volume decrease from elastic deformation

Balloon geometry

- Based on post-experimental measurements
  - W is rupture length
  - C is uniform cylinder radius
  - A is function maximum corresponding to the balloon volume

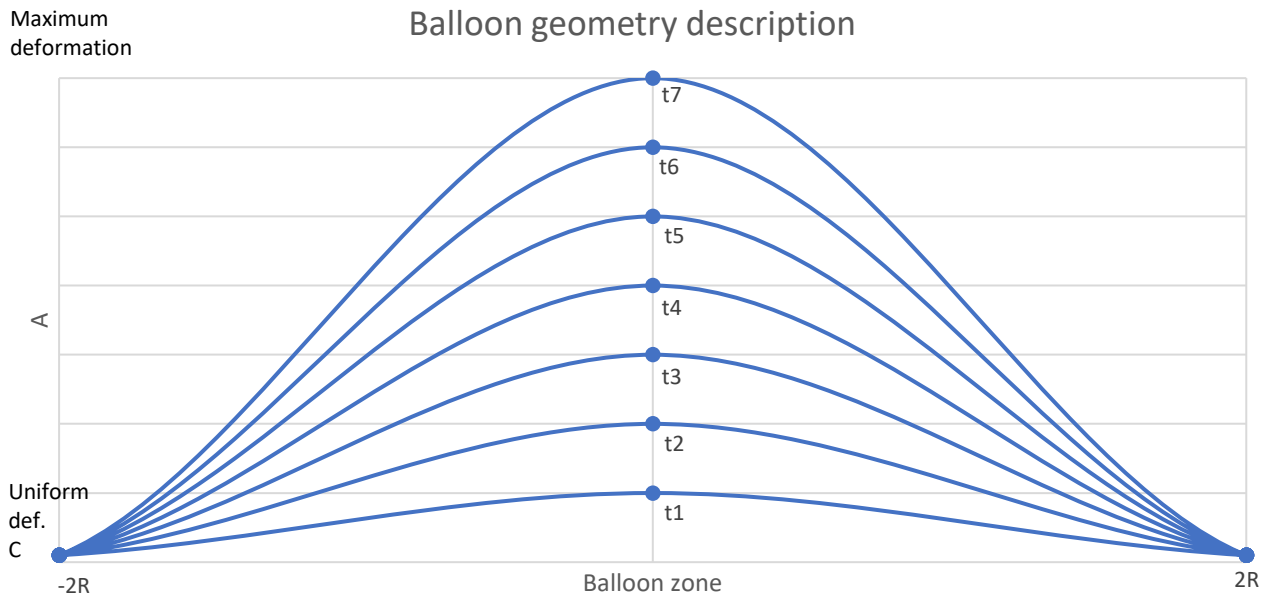

$$V_{BAL} = 2\pi \cdot \int_{-2R}^{2R} \left[\arctan\left(\frac{x \cdot R}{f} - f\right) \cdot 1.1 \cdot \left(\frac{A - C}{\pi}\right) + \left(\frac{A + C}{2}\right) \right]^2 dx \; - 8\pi \cdot R \cdot C^2$$

$$f = \sqrt{\frac{5 \cdot R}{3}} \qquad R = \frac{\frac{W}{2} + 20}{4}$$

t1..t7 symbolizes function change over time
Every dimension is in [mm], volume is in [mm3]

Stress calculation

Tri zložky napätia v stene vzorky sú [12],[4]:

$$\sigma_t(r) = 2 \cdot \frac{p(r) \cdot r^2 - p_{atm} \cdot r_{out}^2}{r_{out}^2 - r^2} + p(r) \tag{9}$$

$$\sigma_o = \frac{p_{in} \cdot r_{in}^2 - p_{atm} \cdot r_{out}^2}{r_{out}^2 - r_{in}^2} \tag{10}$$

$$\sigma_r(r) = -p(r) \tag{11}$$

kde σ_t je tangenciálne napätie v stene vzorky na danom polomere a p je tlak na vnútornom polomere alebo atmosférický vonkajší tlak, σ_o je osové napätie a σ_r je radiálne napätie.

Celkové napätie sa zo zložiek napätia sčíta pomocou teorém von Mises (12) a Tresca (14). Obe teorémy spájajú smery napätí a vyjadrujú redukované napätie v stene vzorky, ktoré sa následne využíva v analýzach bezpečnosti. Napätie von Mises sa využíva najmä v analýzach a modeloch postavených na základoch metódy konečných prvkov, kedy je jednoduché vyjadriť orientácie jednotlivých napätí. Na druhú stranu využitie Trescovho teorému je jednoduché aj pre prípad cylindrických vzoriek. Hlavnou výhodou Trescovho teorému je jeho konzervatívnosť proti von Misesovmu teorému, pretože pri zaťaženiach s vysokým šmykovým napätím vykazuje vyššie redukované napätie, preto skôr dosiahne limitnú podmienku [6],[12],[23],[46].

$$\sigma_{red} = \sqrt{\frac{1}{2} \cdot [(\sigma_{11} - \sigma_{22})^2 + (\sigma_{22} - \sigma_{33})^2 + (\sigma_{11} - \sigma_{33})^2 + 6 \cdot (\sigma_{23}^2 + \sigma_{31}^2 + \sigma_{12}^2)]} \tag{12}$$

kde σ_{red} je redukované napätie v stene vzorky a σ_{ij} sú smerové napätia.

V literatúre často používaným výpočtom napätia je takzvané efektívne napätie [40]. Proti Trescovej teoréme vykazuje mierne nižšie hodnoty $\sigma_{eff} < \sigma_{red}$.

$$\sigma_{eff} = \sqrt{\frac{(\sigma_t - \sigma_o)^2 + (\sigma_o - \sigma_r)^2 + (\sigma_r - \sigma_t)^2}{2}} \tag{13}$$

kde σ_{eff} je efektívne napätie v stene vzorky, σ_t je tangenciálne napätie, σ_r je radiálne napätie a σ_o je axiálne napätie.

$$\sigma_{red} = \sigma_t(r_{in}) - \sigma_r(r_{in}) \tag{14}$$

kde σ_{red} je redukované napätie v stene vzorky, σ_t je tangenciálne napätie na vnútornom polomere steny a σ_r je radiálne napätie na vnútornom polomere steny.

Isothermal test, Acoustic emission

- Cooperation with DAKEL company
  - Not included in the project
- One test with Cr-coated
  - More test should start in 2025

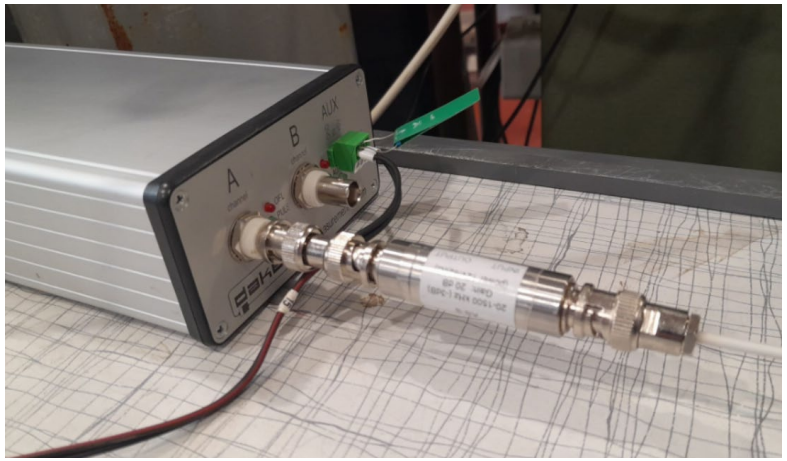

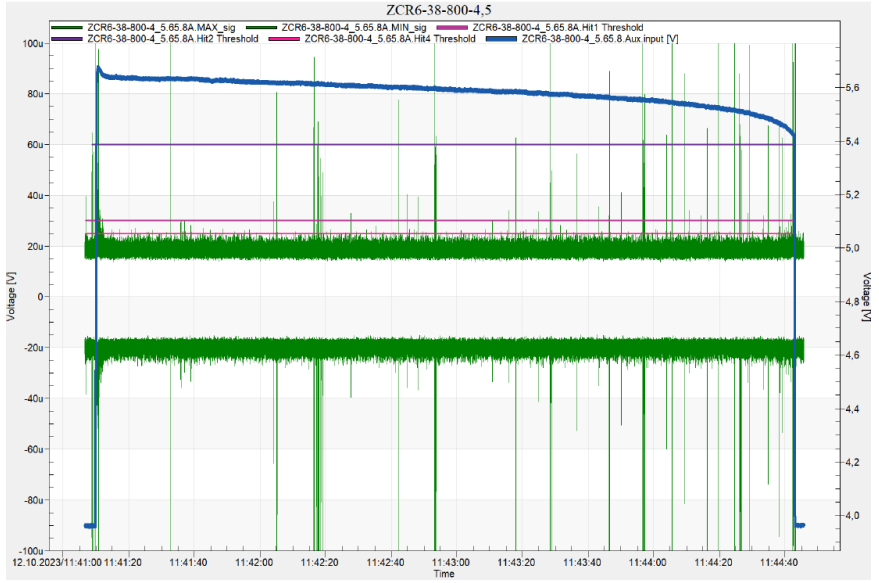

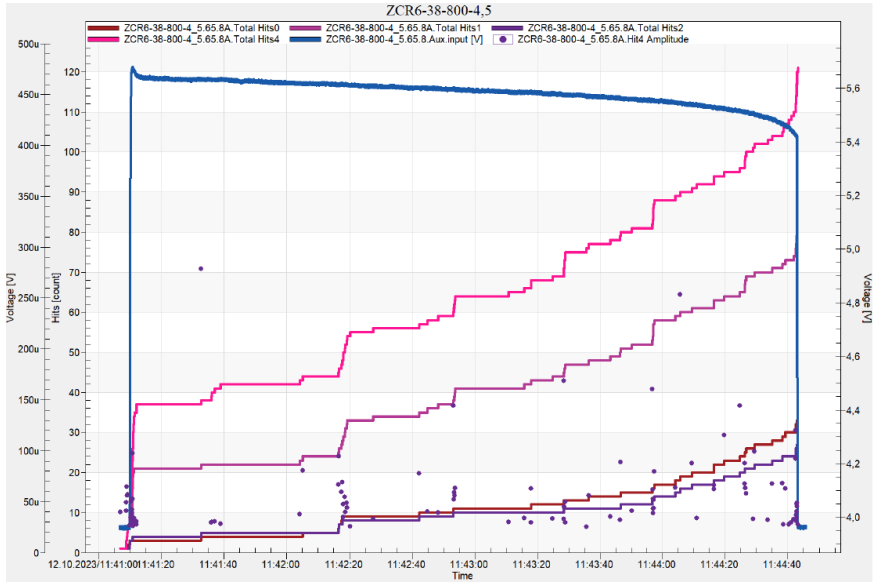

Tong Liu

SJTU

A Visual Experimental Study on Fuel Cladding Integrity under coolant loss accident (LOCA) conditions

Cladding tubes serve as critical structural components in nuclear power plants, where they are subjected to complex thermomechanical loading conditions. Understanding and predicting the behavior of these tubes is essential for maintaining their integrity and extending their operational lifetime. Traditional experimental methods often rely on Invisible systems, limiting the observation of critical intermediate processes. This study presents an innovative visual experimental approach that utilizes real-time, in-situ, full-field, and non-contact observation techniques to facilitate comprehensive data collection and validation, yielding valuable insights into cladding material performance. A series of experiments were conducted to assess the integrity of fuel cladding under Loss of Coolant Accident (LOCA) conditions, including high-temperature oxidation, ballooning burst tests, quench thermal shock, and mechanical property evaluations. High-speed cameras and digital image correlation (DIC) techniques were employed to analyze the cladding materials' responses to coupled radiation, thermology, mechanical and chemical effects. DIC data revealed uneven oxidation patterns and a significant presence of white spots in the zirconium alloy cladding under simulated LOCA conditions, with quenching contributing to the formation of these anomalies. These findings support the development of advanced predictive models for cladding behavior, optimize material selection and design, reduce failure risks, and enhance reactor safety during LOCA scenarios.

29th International QUENCH Workshop, Karlsruhe , Germany, 19-22 November 2024

A Visual Experimental Study on Fuel Cladding Steam Oxidation and Balooning

Tong Liu
Shijie Wang
Yi Li
Beiqi Wang
Shengjia Zhao

Shanghai Jiao Tong University, China

Content

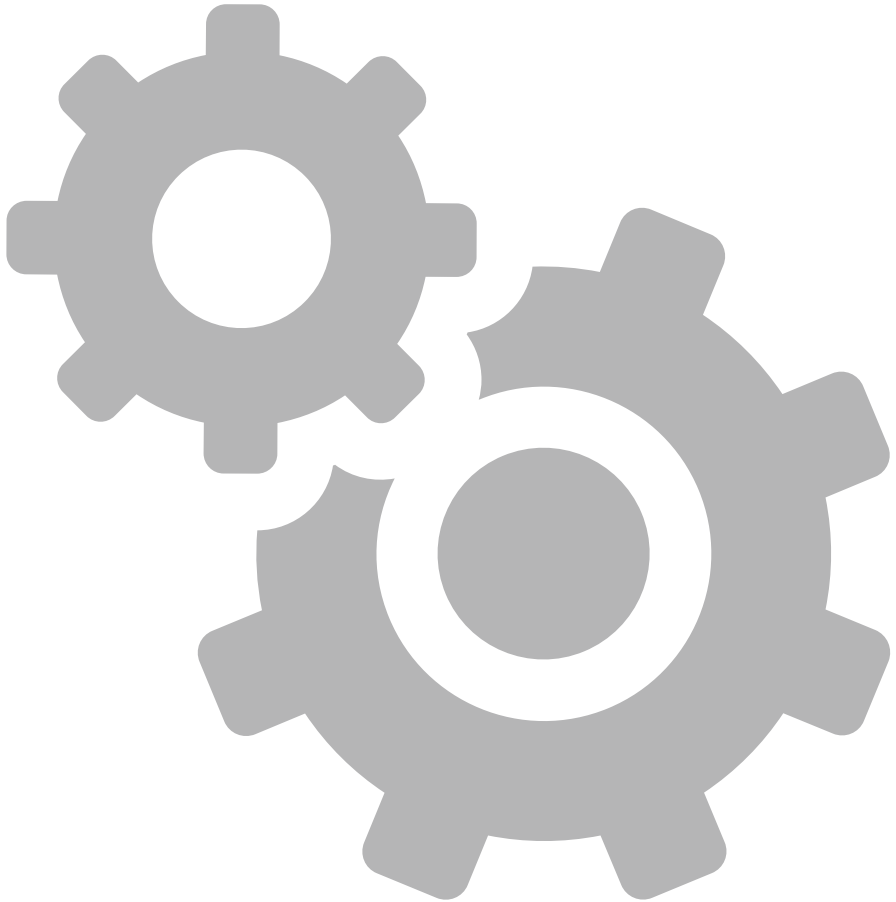

Background

The structural integrity of fuel cladding is essential to the safety and economic efficiency of nuclear reactor

Nuclear plant

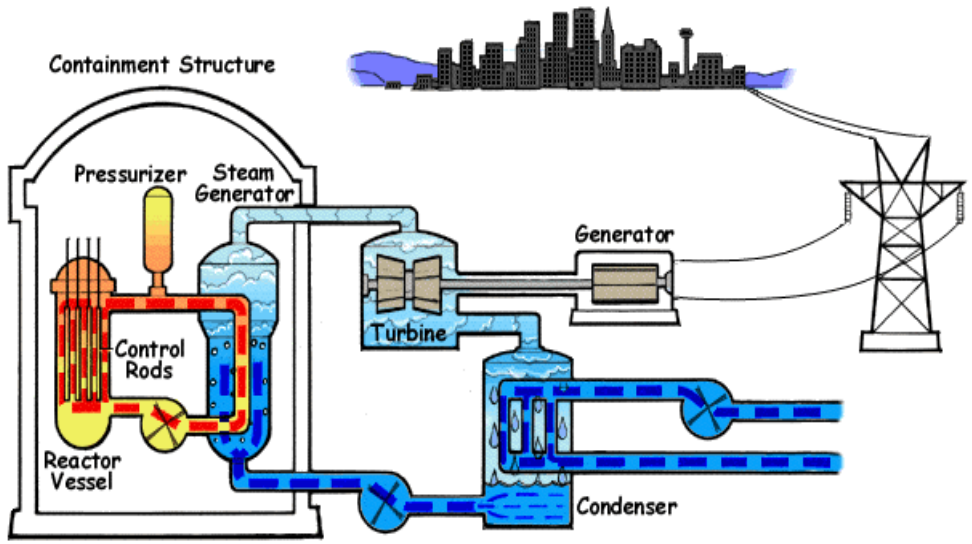

Nuclear fuel

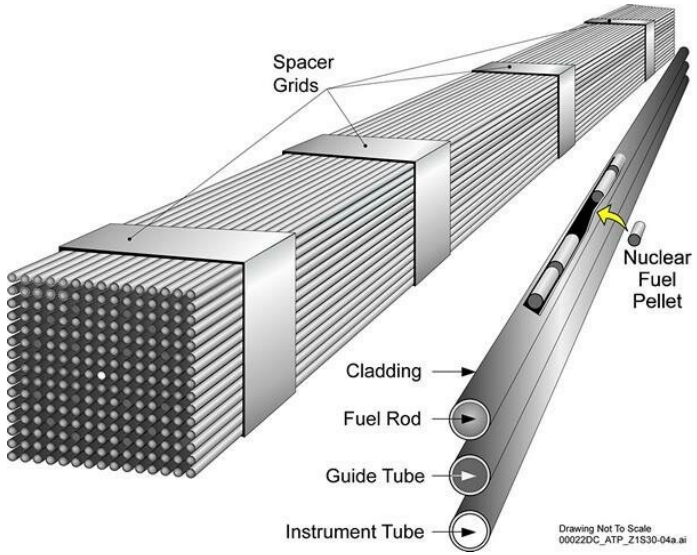

Fuel cladding

A barrier between coolant and fuel pellets

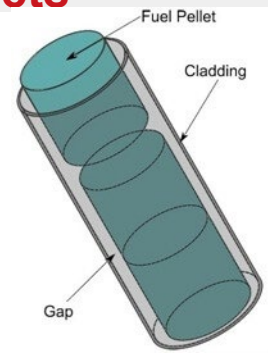

Fuel cladding constitutes one of the barriers in the ‘defense-in-depth ‘approach of NPP

Loss of Coolant Accident (LOCA)

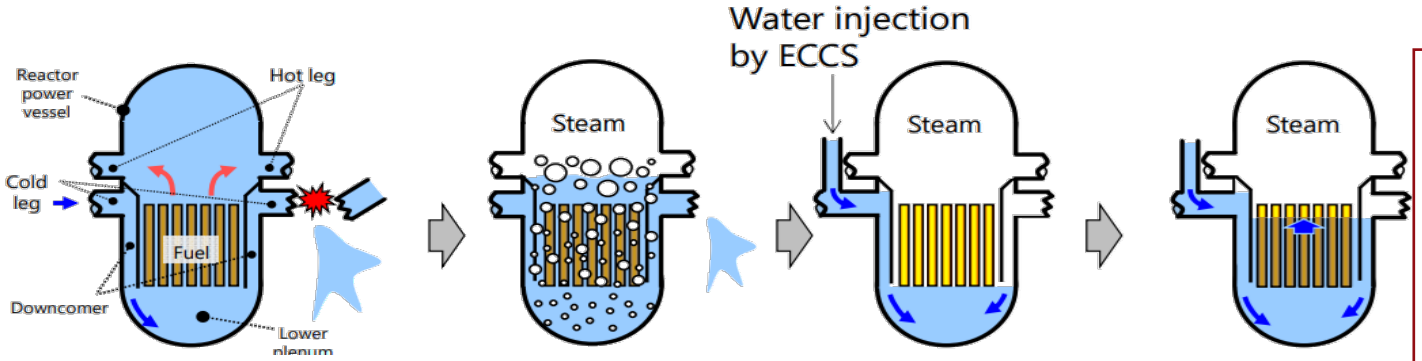

Cold Leg Break　Blowdown　Refilling　Reflood

§ 50.46 Acceptance criteria for emergency core cooling systems for light-water nuclear power reactors

(a)(1)(i) Each boiling or pressurized light-water nuclear power reactor fueled with uranium oxide pellets within cylindrical zircaloy or ZIRLO cladding must be provided with an emergency core cooling system (ECCS) that must be designed so that its calculated cooling performance following postulated loss-of-coolant accidents conforms to the criteria set forth in paragraph (b) of this section. ECCS cooling performance must be calculated in accordance with an acceptable evaluation model and must be calculated for a number of postulated loss-of-coolant accidents of different sizes, locations, and other properties sufficient to provide assurance that the most severe postulated loss-of-coolant accidents are calculated. Except as provided in paragraph (a)(1)(ii) of this section, the evaluation model must include sufficient supporting justification to show that the analytical technique realistically describes the behavior of the reactor system during a loss-of-coolant accident. Comparisons to applicable experimental data must be made and uncertainties in the analysis method and inputs must be identified and assessed so that the uncertainty in the calculated results can be estimated. This uncertainty must be accounted for, so that, when the

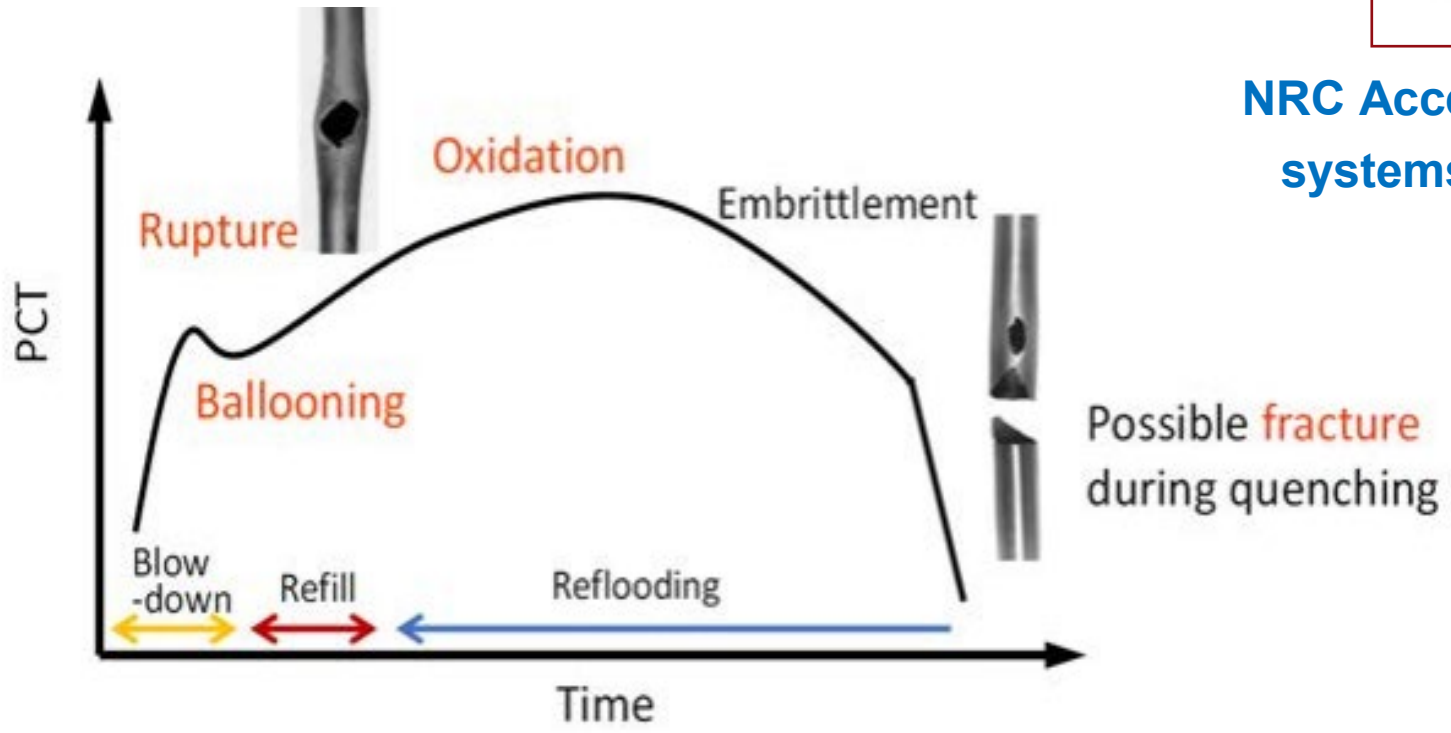

Fuel Behavior and Peak Cladding Temperature during LOCA[1]

NRC Acceptance criteria for emergency core cooling systems for light-water nuclear power reactors[2]

- Peak cladding temperature $<$ 1204℃
- Maximum cladding oxidation $<$ 17%
- Maximum hydrogen generation $<$ 1%
- Coolable geometry
- Long-term cooling

[1] JAEA-Review, 2020-076; [2] NRC, 10CFR50.46

Cladding transient experimental facilities

Karlsruhe Institute of Technology (KIT)[1]

✓ BOX : SR **Oxidation kinetics**

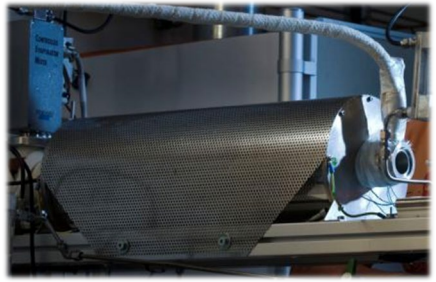

✓ QUENCH/LICAS :
Bundle **HTO+QUENCH**

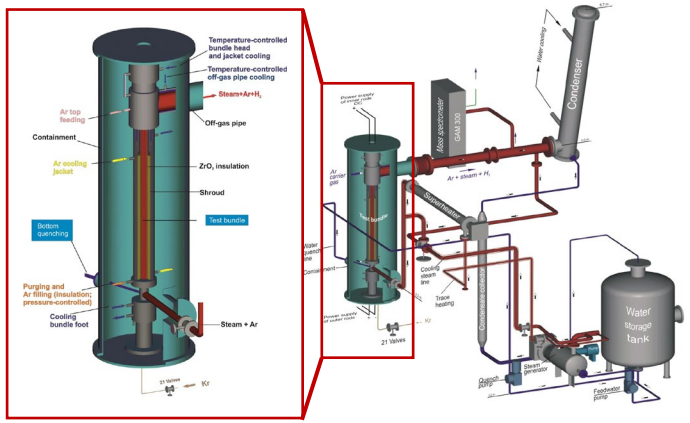

Oak Ridge National Laboratory (ORNL)[2]

✓ Severe accident test station:
SR **HTO+QUENCH**

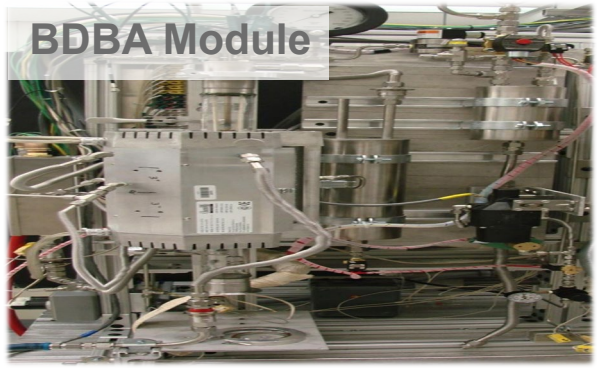

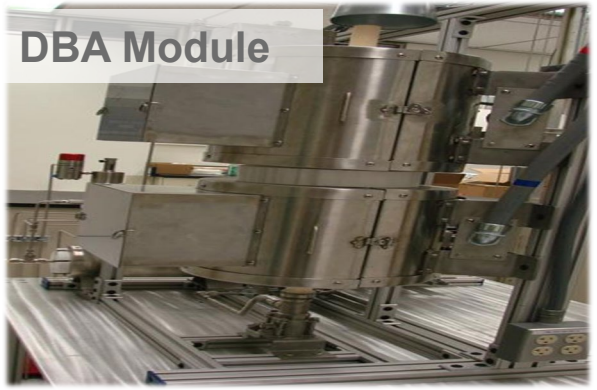

Argonne National Laboratory (ANL)[3]

✓ LOCA apparatus :
SR **HTO+QUENCH**

[1] J. Stuckert et al. Nuclear Engineering and Design 255 (2013): 185-201. [2] M. Snead et al. Severe Accident Test Station Design Document. 10.2172/1252142.
[3] Mika Helin et al. Design and construction of test train device and tests with unirradiated cladding material, Studsvik Report N-11/130, 2011.

Limitations of traditional experimental methods

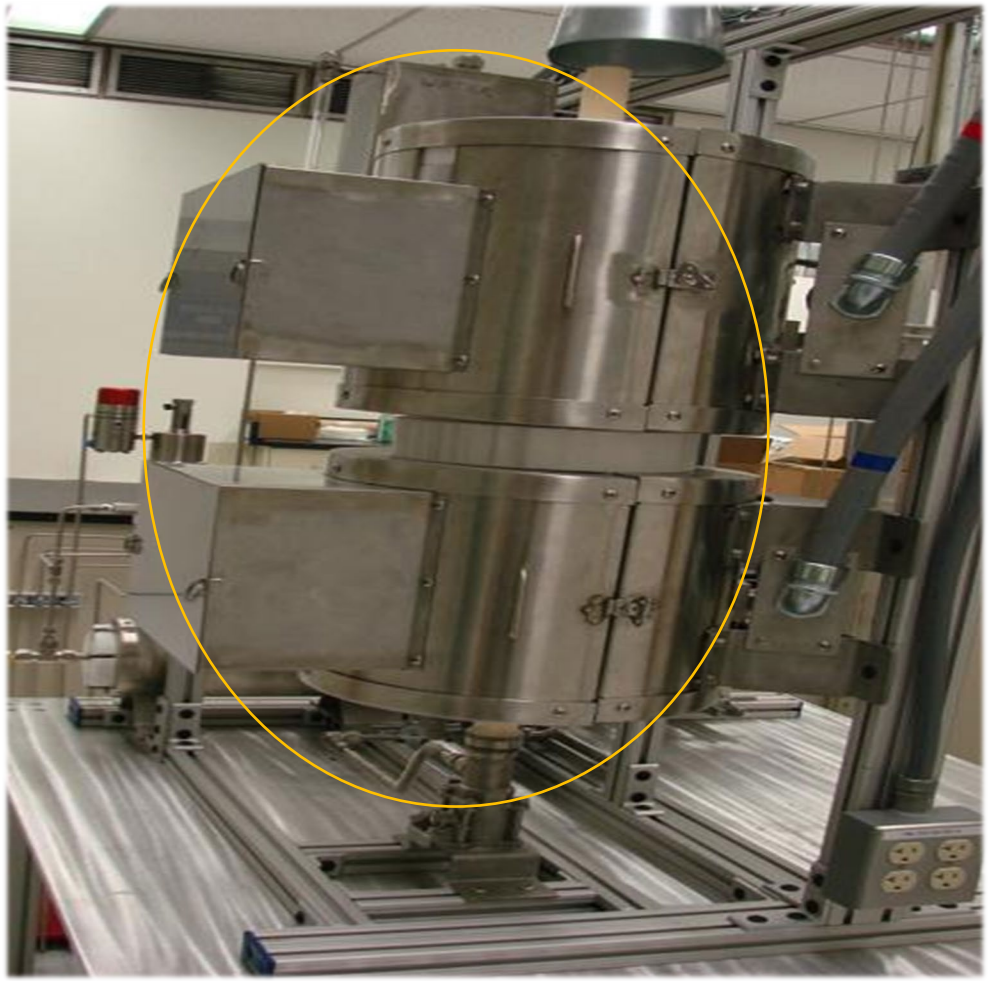

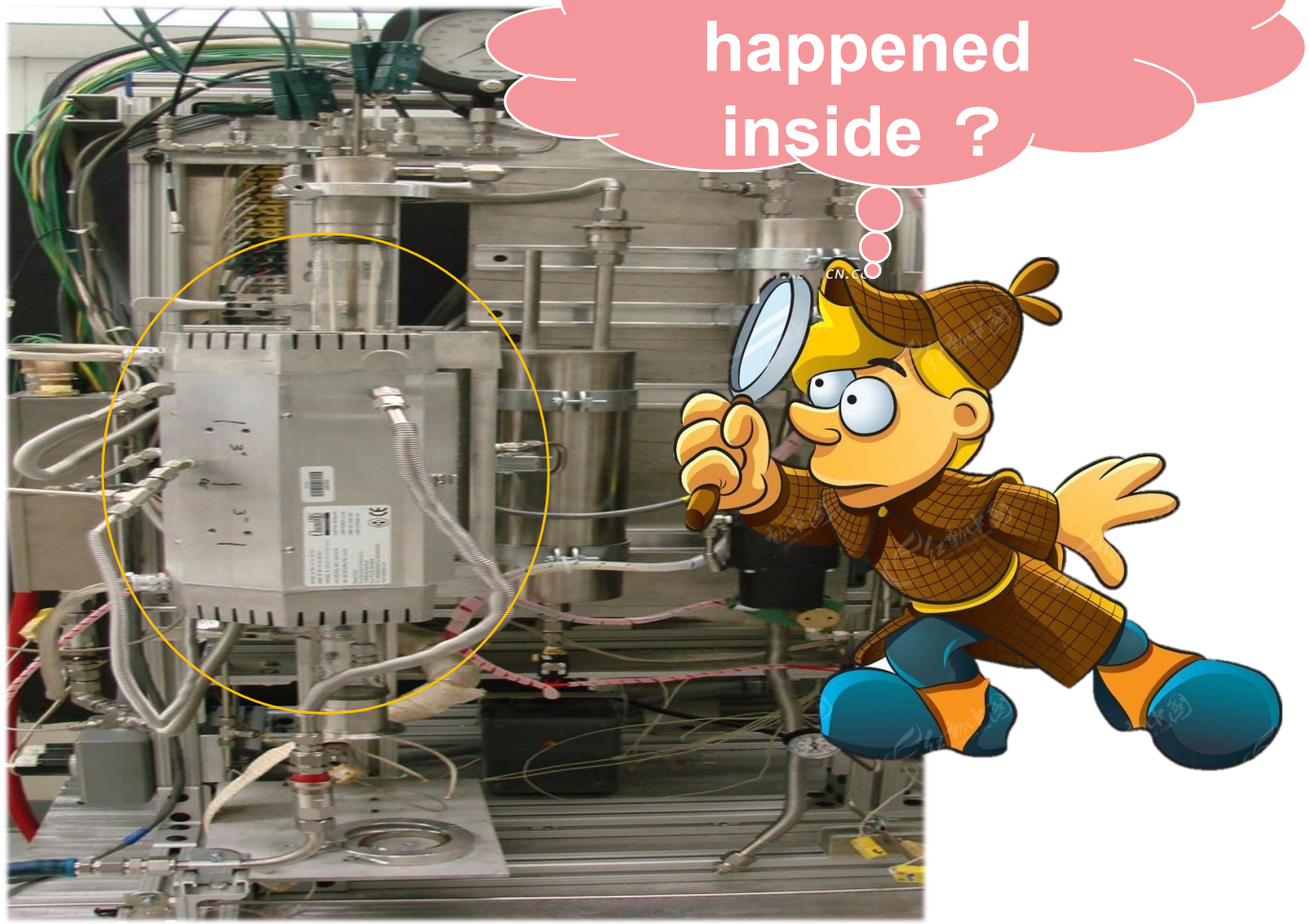

Invisible devices, very limited data obtained by TCs and SGs

Limitations of traditional experimental methods

Only the initial and final status can be observed, while the intermediate process is unknowable

Limitations of traditional experimental methods

The maxmum local strain data is missing due to limited SGs deployment

≈ 10^4 ~10^6 data points

≈ 3data points

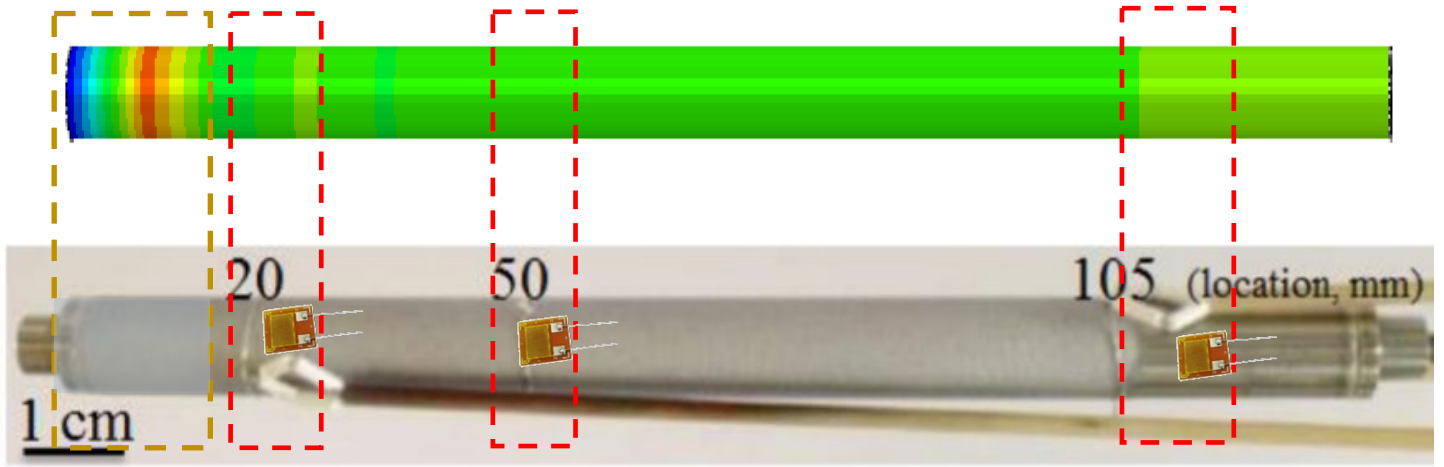

Numerical simulation

Experimental

Temperature,stress,strain and corrosion of cladding samples are interfered by SGs and TCs

Content

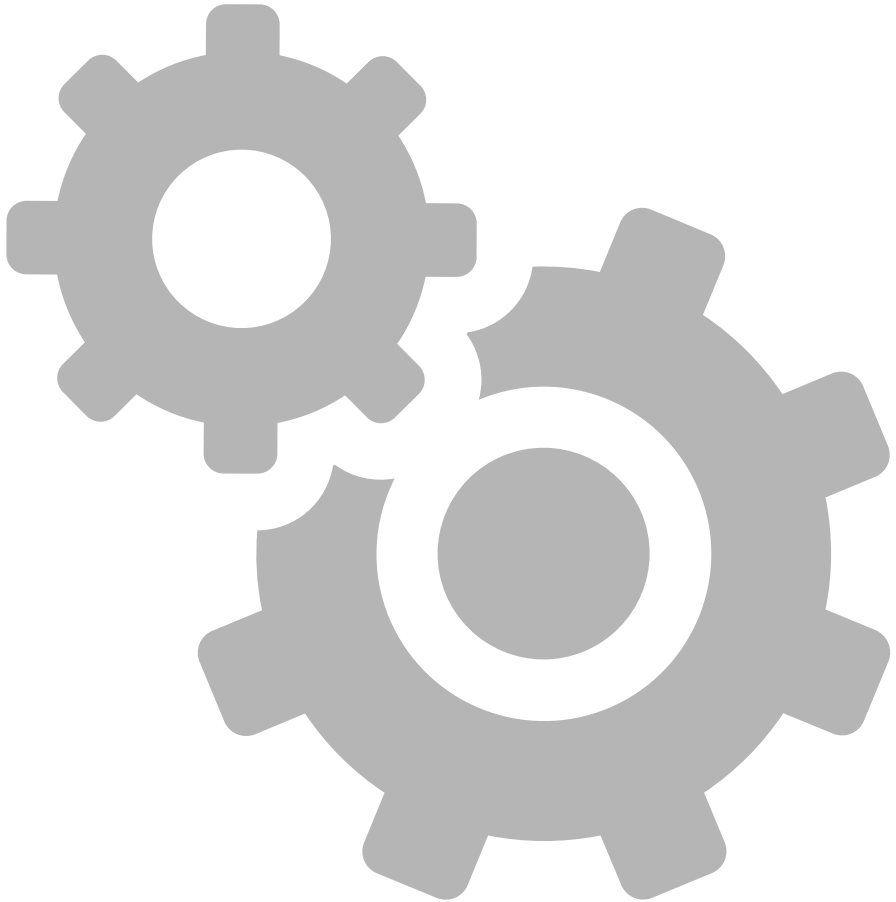

Visual experimental method

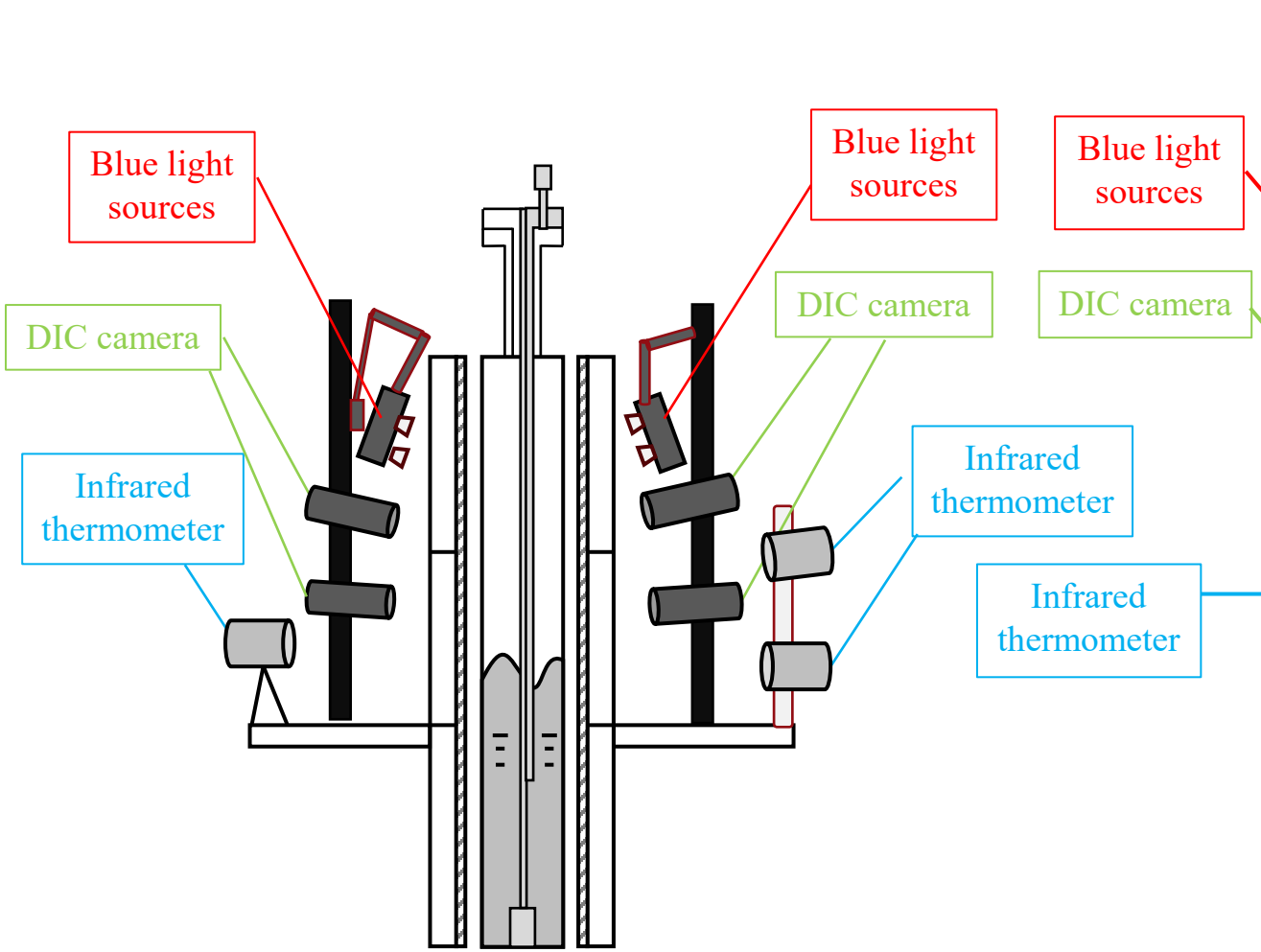

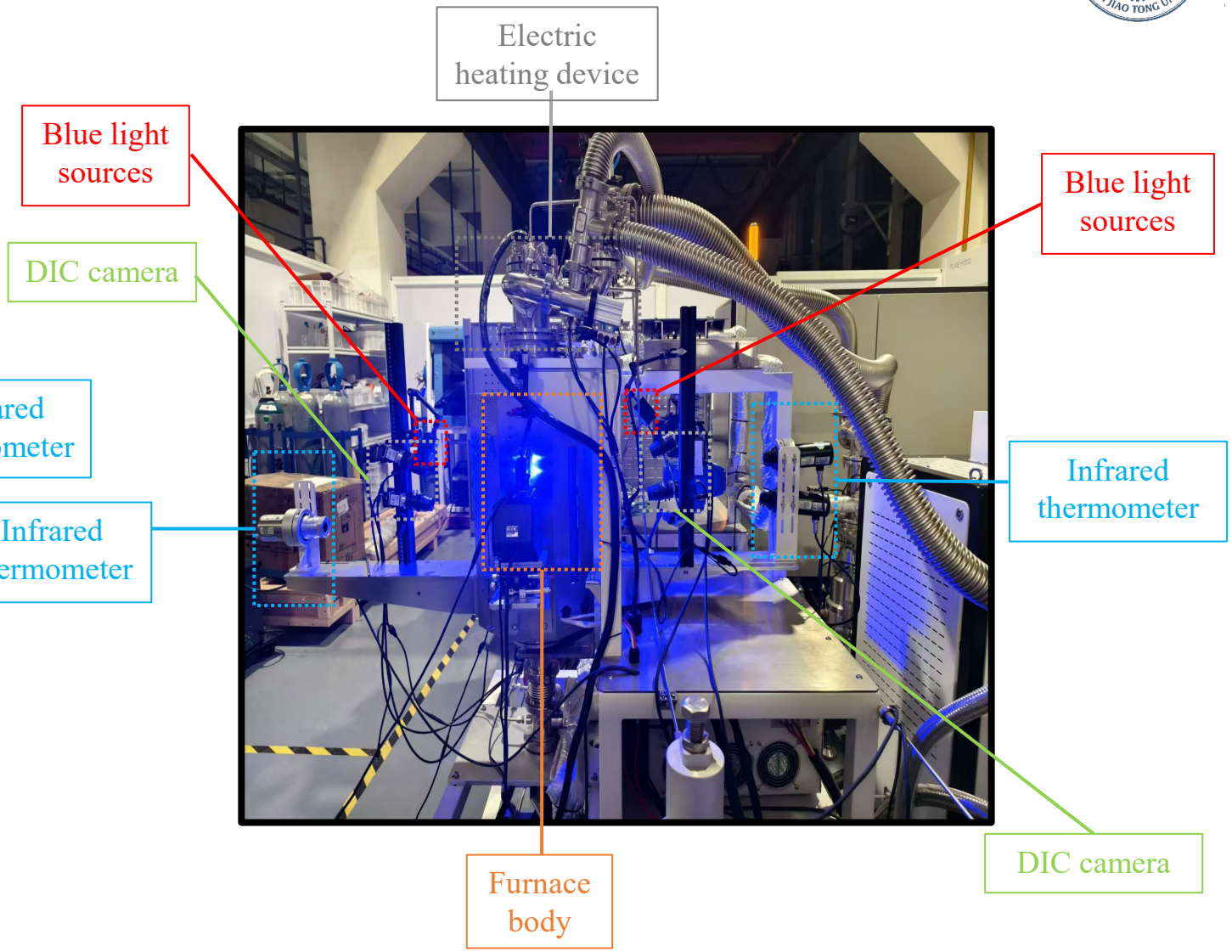

DIC based visual experimental method

Traditional methods

Experimental data — **Verification of data in time and space is not available** — **Numerical simulation results**

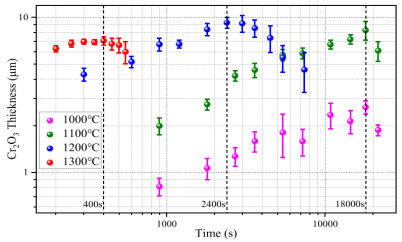

Oxidation Kinetics

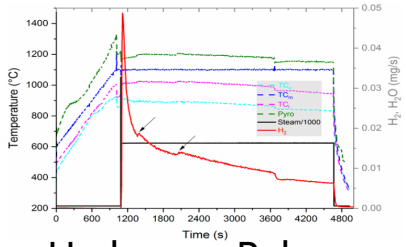

Hydrogen Release

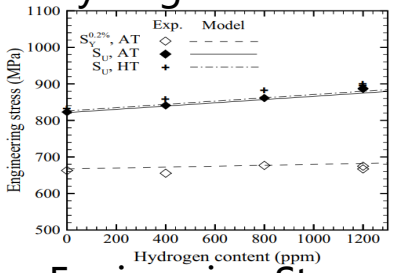

Engineering Stress

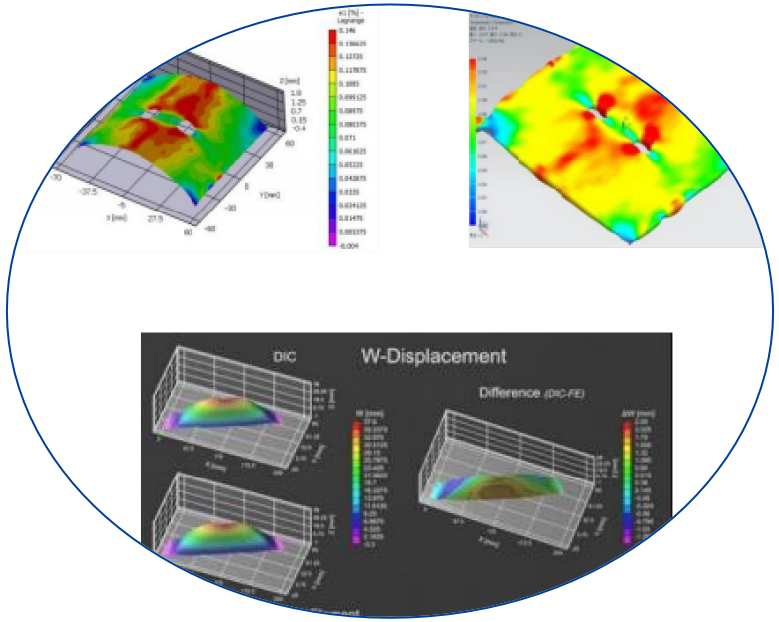

Digital Image Correlation (DIC)

Realize two-way connection
of experimental and theoretical simulation data

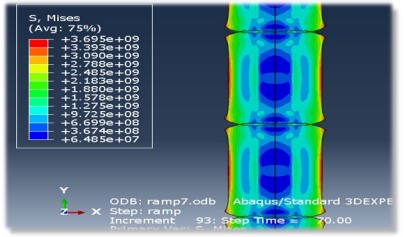

Stress Distribution

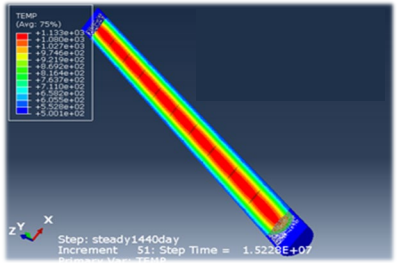

Temperature Distribution

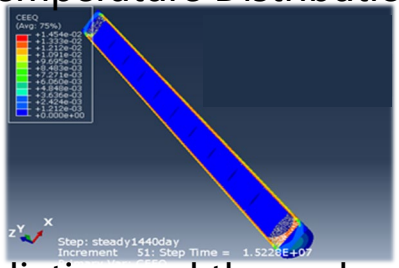

Irradiation and thermal creep

Visual Experimental Facilities

SJTU in-Service performance and safety behavior research platform

Modular Subsystems

- High-temperature heating
- Pressure Control System
- Steam Generator
- Vacuum System
- Quenching device
- Data Acquisition and Control System

Key Parameters

Heating power	135 kW
Power Voltage	380V
Vacuum	≤1.0× 10^{-4}Pa
Steam flow rate	0~30mL/min

Visual Experimental Facilities

Ultra-high temperature LOCA visual experimental device

Online Projection Image Measuring Instrument

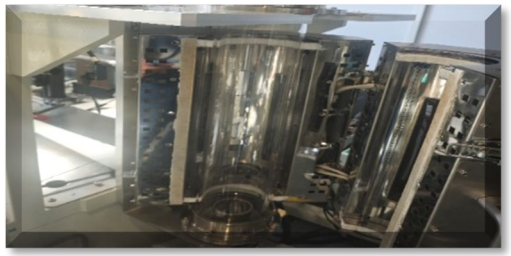

Furnace

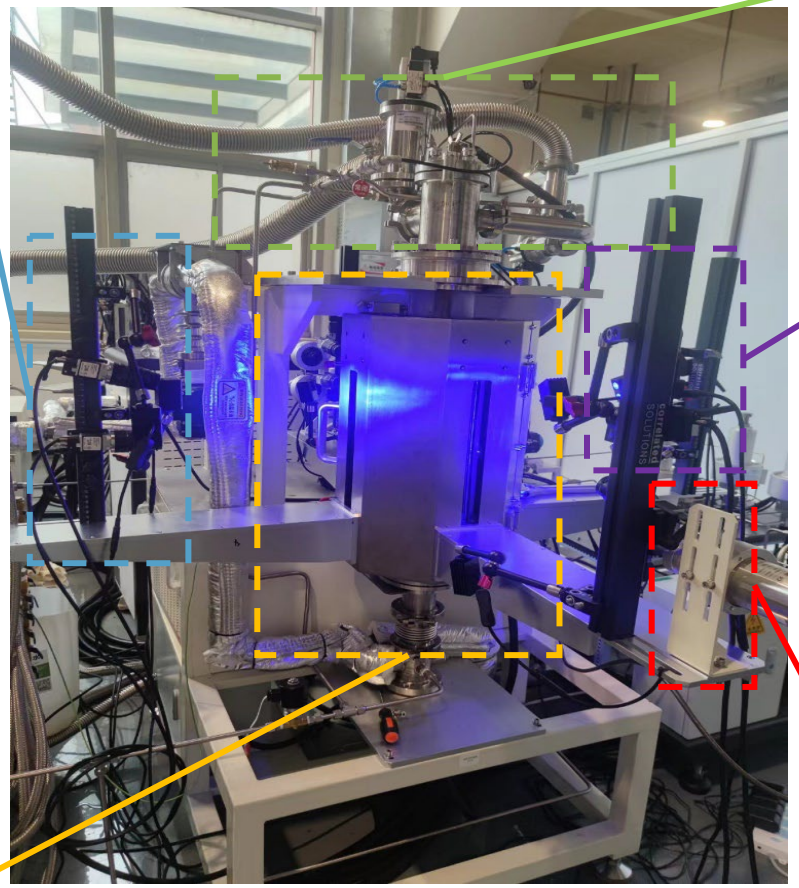

Pressure control system

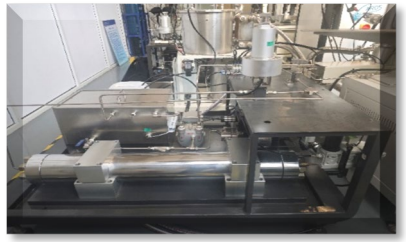

DIC system

Temperature measurement and control system

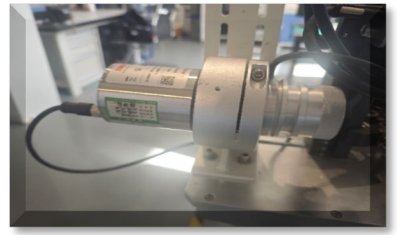

- ✓ Maximum heating temperature 2300 ℃
- ✓ Maximum heating rate 300 ℃/s

Visual Experimental Facilities

High speed camera with DIC tech.

Real-time, in-situ, and full field non-contact measurement

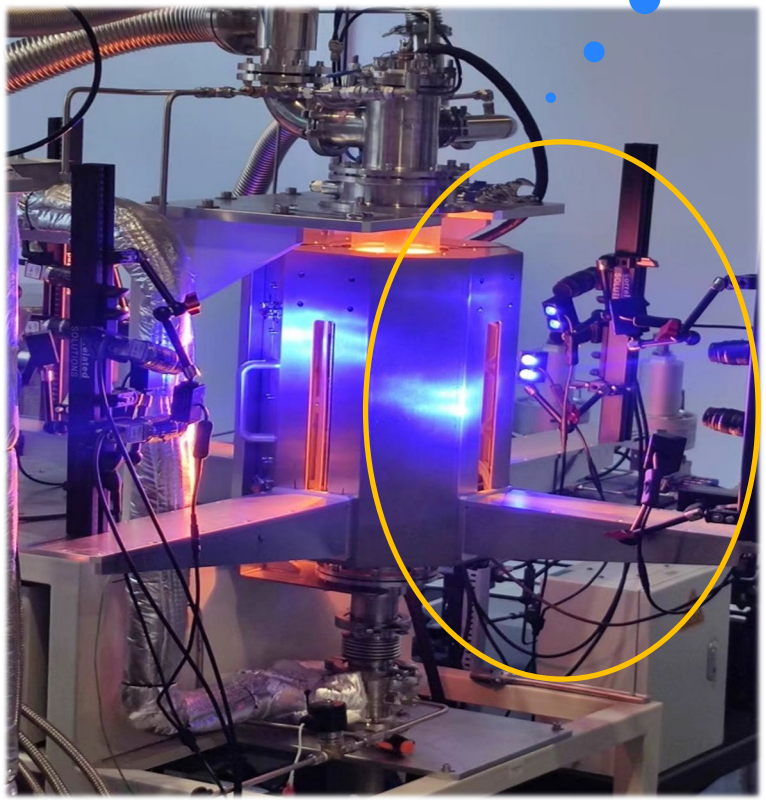

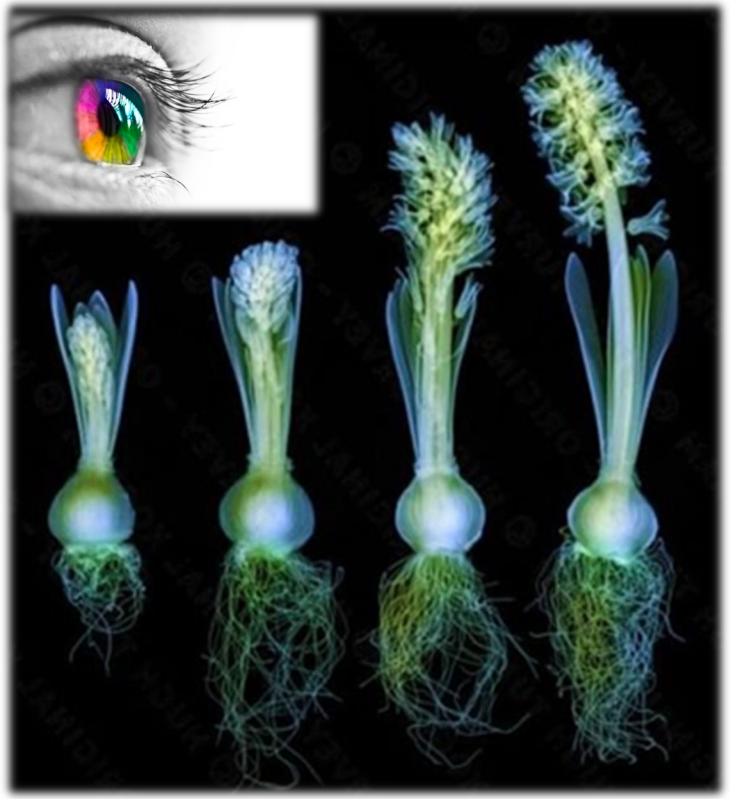

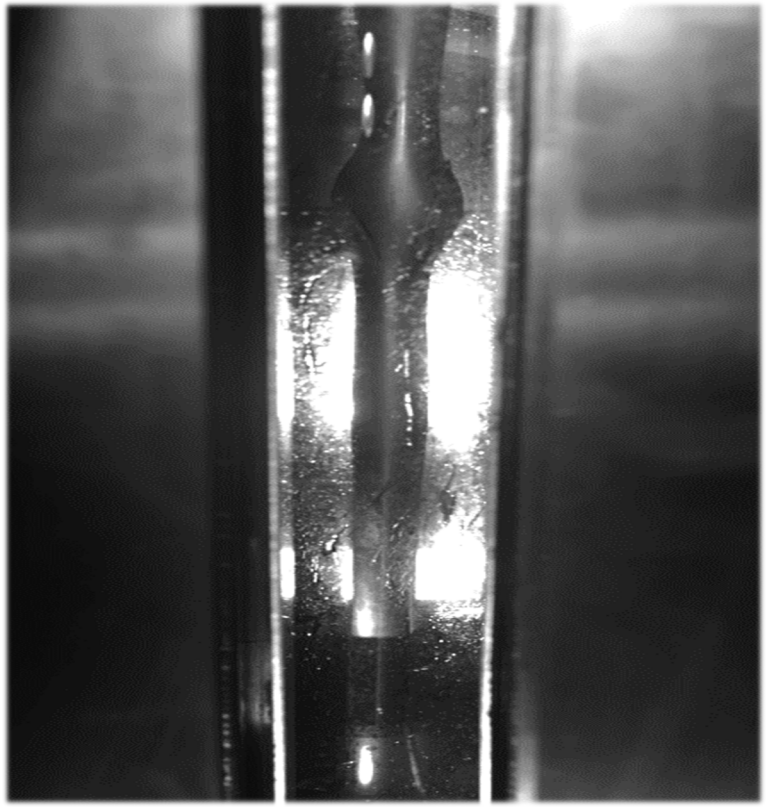

Experimental Facilities

Long time creep and LOCA visualization experiment device

Conditions

- **External**:
- Vacuum/Steam/Inert gas
- **Internal**: Long-term pressure stabilization without fluctuations **(up to 10,000 hours)**

Vacuum extraction module

Temperature Range	＞1200℃
Pressure Range	1-70MPa
Pressure rise rate	0.5-8MPa/min

Functions

Fuel Cladding After Creep Test

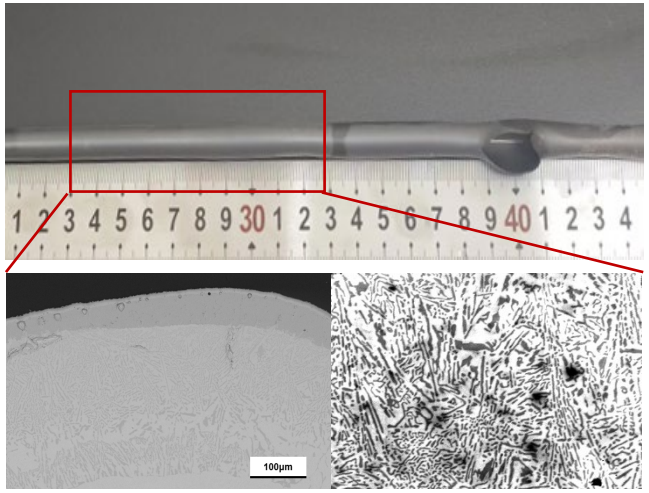

- Ultra-long time internal pressure creep
- Thermal-Mechanical-Chemical Coupling
- Separation effect

SAFCPD

Experimental Facilities

Determining Post Quench Ductility

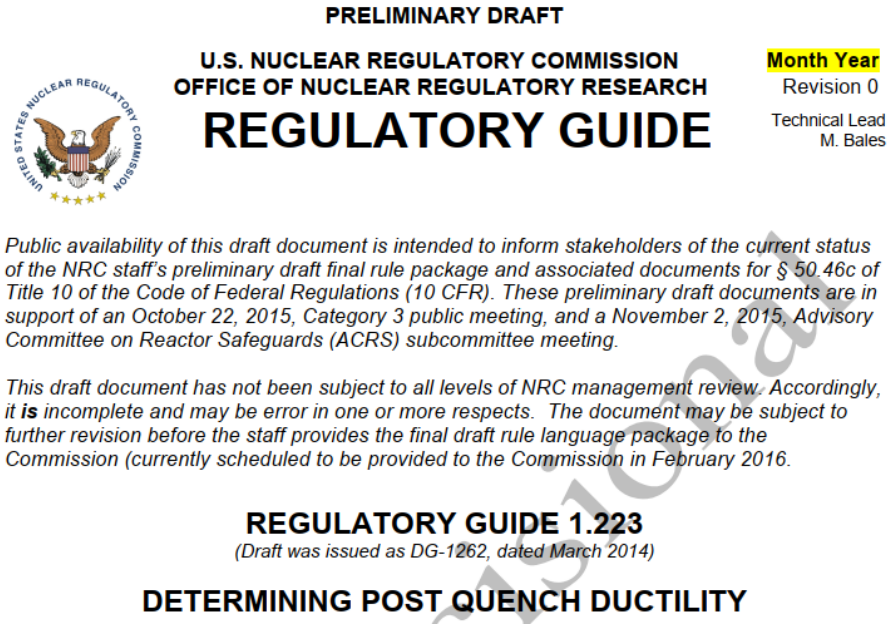

PRELIMINARY DRAFT

U.S. NUCLEAR REGULATORY COMMISSION
OFFICE OF NUCLEAR REGULATORY RESEARCH

Month Year
Revision 0

Technical Lead
M. Bales

REGULATORY GUIDE

Public availability of this draft document is intended to inform stakeholders of the current status of the NRC staff's preliminary draft final rule package and associated documents for § 50.46c of Title 10 of the Code of Federal Regulations (10 CFR). These preliminary draft documents are in support of an October 22, 2015, Category 3 public meeting, and a November 2, 2015, Advisory Committee on Reactor Safeguards (ACRS) subcommittee meeting.

*This draft document has not been subject to all levels of NRC management review. Accordingly, it **is** incomplete and may be error in one or more respects. The document may be subject to further revision before the staff provides the final draft rule language package to the Commission (currently scheduled to be provided to the Commission in February 2016.*

REGULATORY GUIDE 1.223

(Draft was issued as DG-1262, dated March 2014)

DETERMINING POST QUENCH DUCTILITY

NRC Regulatory Guide 1.223 Determining Post Quench Ductility (PQD)

Mechanical Test System (MTS)

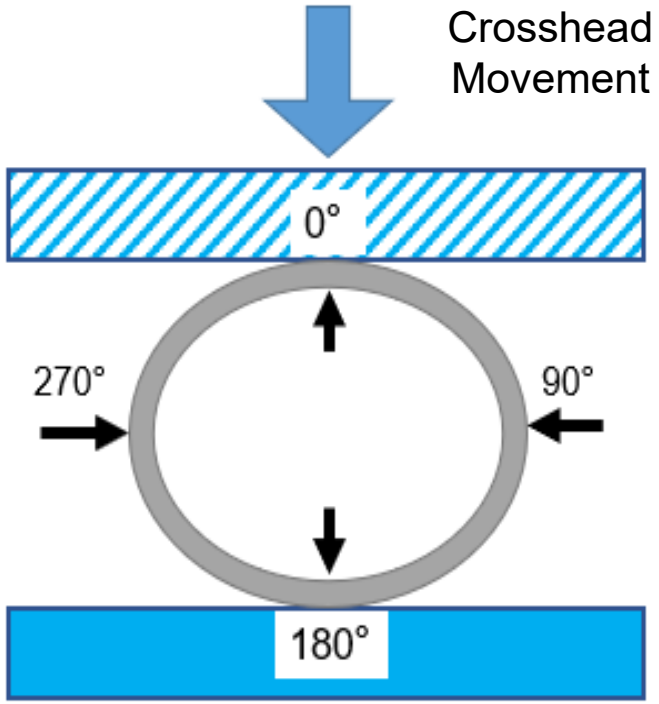

Schematic of simulated Ring Compression Test (RCT)

Content

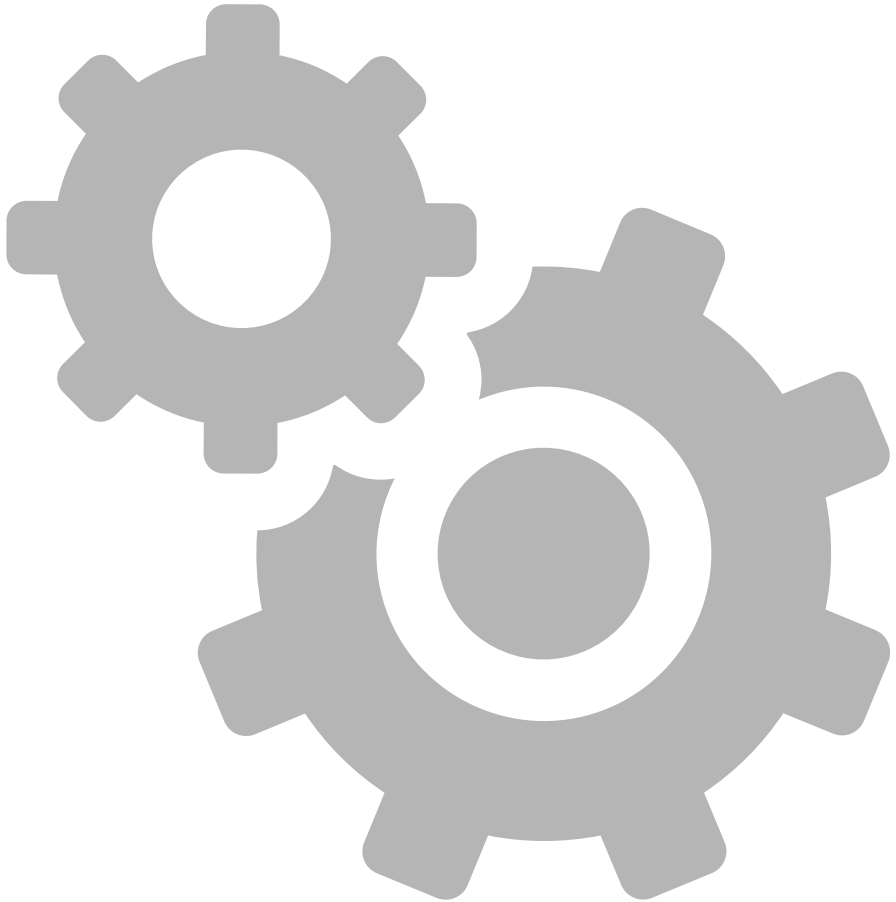

HTO and reflooding process

Ultra-high temperature LOCA visual experimental device

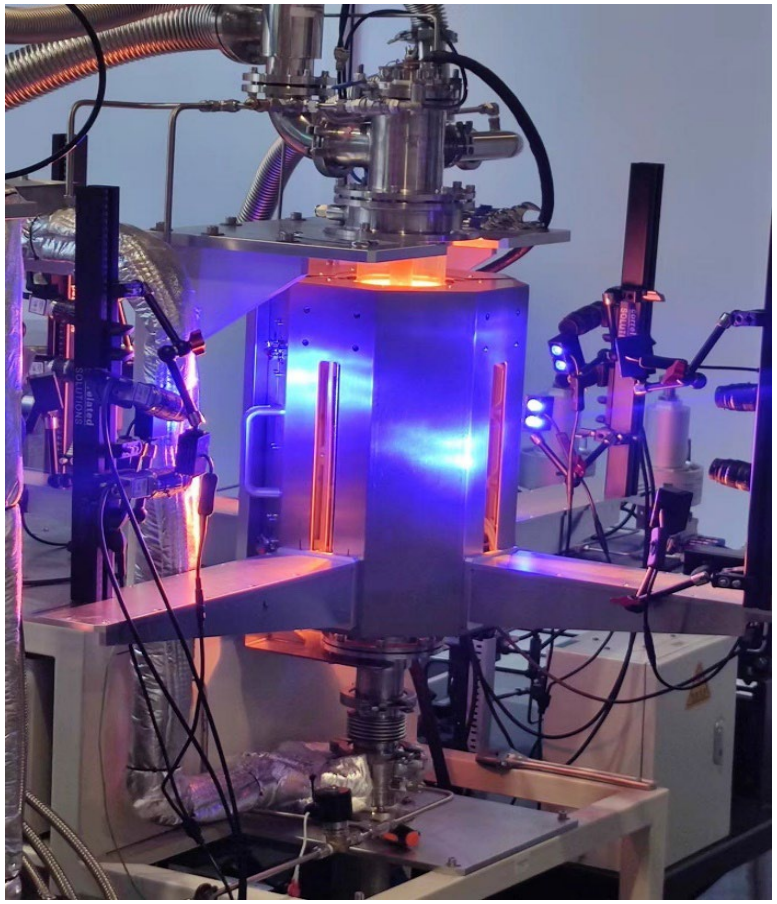

SJTU LOCA Simulation Facility

Simulating the reflooding process

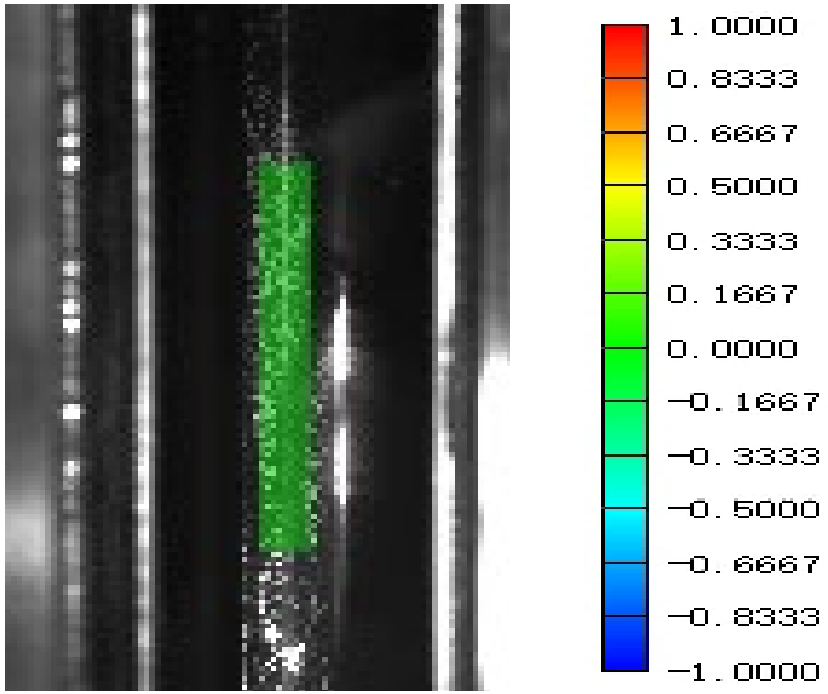

Real-time and in-situ strain distribution

High Temperature-steam Oxidation: Uncoated

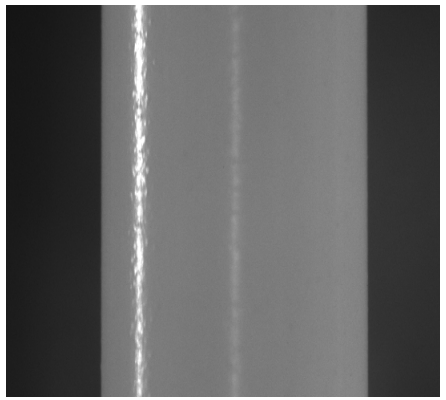

0s

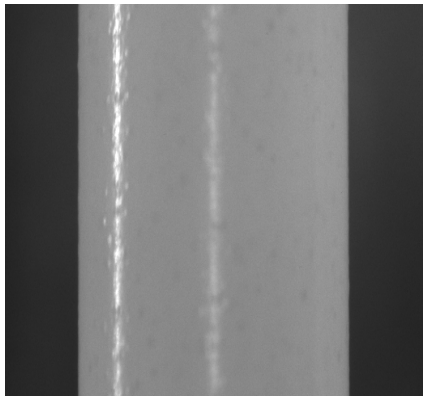

50s

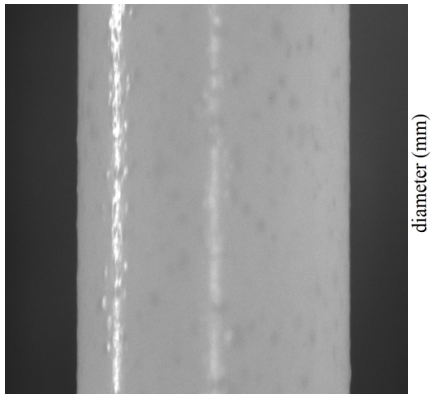

100s

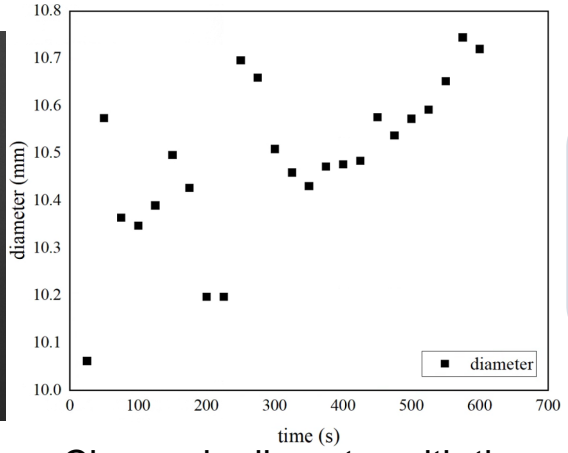

Change in diameter with time

The diameter of the cladding increased but varied

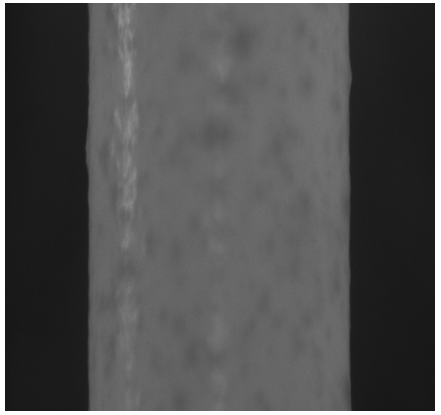

400s

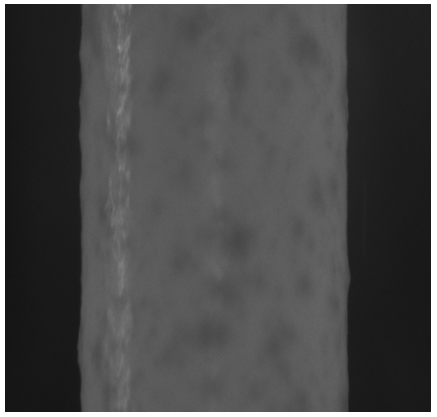

500s

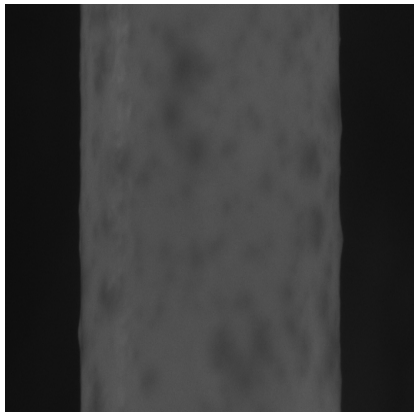

600s

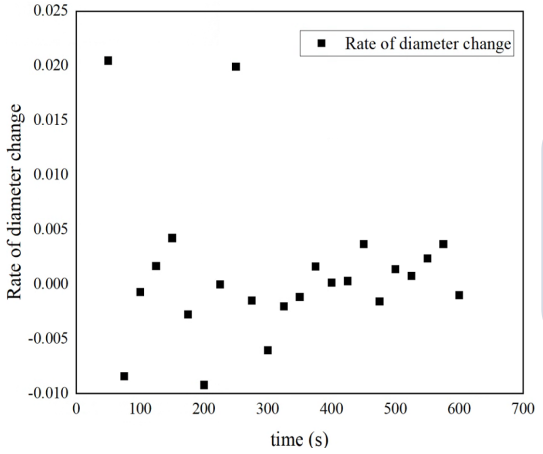

Rate of diameter change

The change rate of diameter is relatively stable

In the process of steam oxidation upto 1350℃, the surface of zircalloy appeared sand-like or granular spots , which growed up gradually.

High Temperature-steam Oxidation: Uncoated

Macroscopic morphology of cladding tube after high-temperature steam oxidation

Zr tube as received

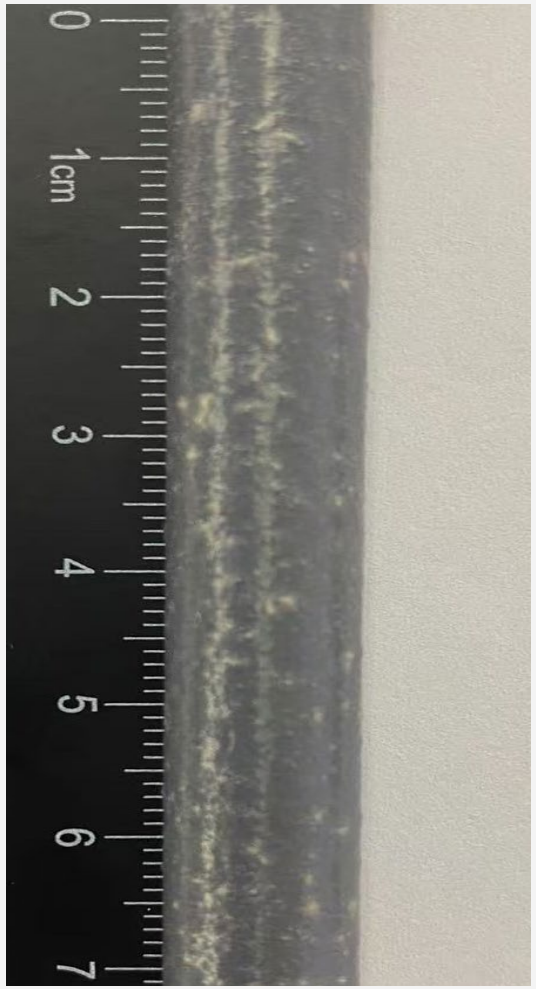

Zr tube post-oxidation

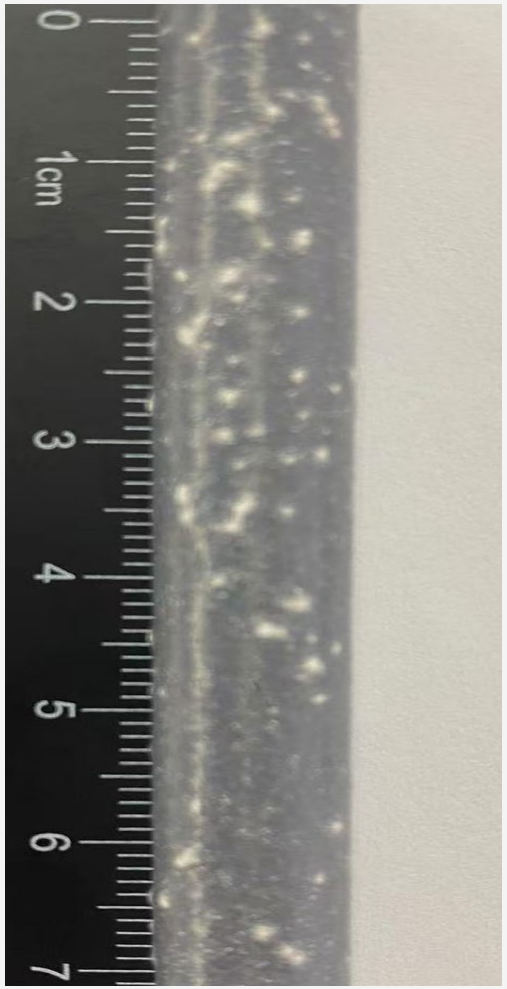

Zr tube post-oxidation & quench

- **As received:** smooth surface, appears metallic luster
- **post-oxidation:** rough surface, black oxidation film (ZrO_2), a small number of white spots(localized pitting)
- **post-oxidation & quench :** rough surface, black oxidation film, a large number of big white spots,

High Temperature-steam Oxidation: Cr -coated

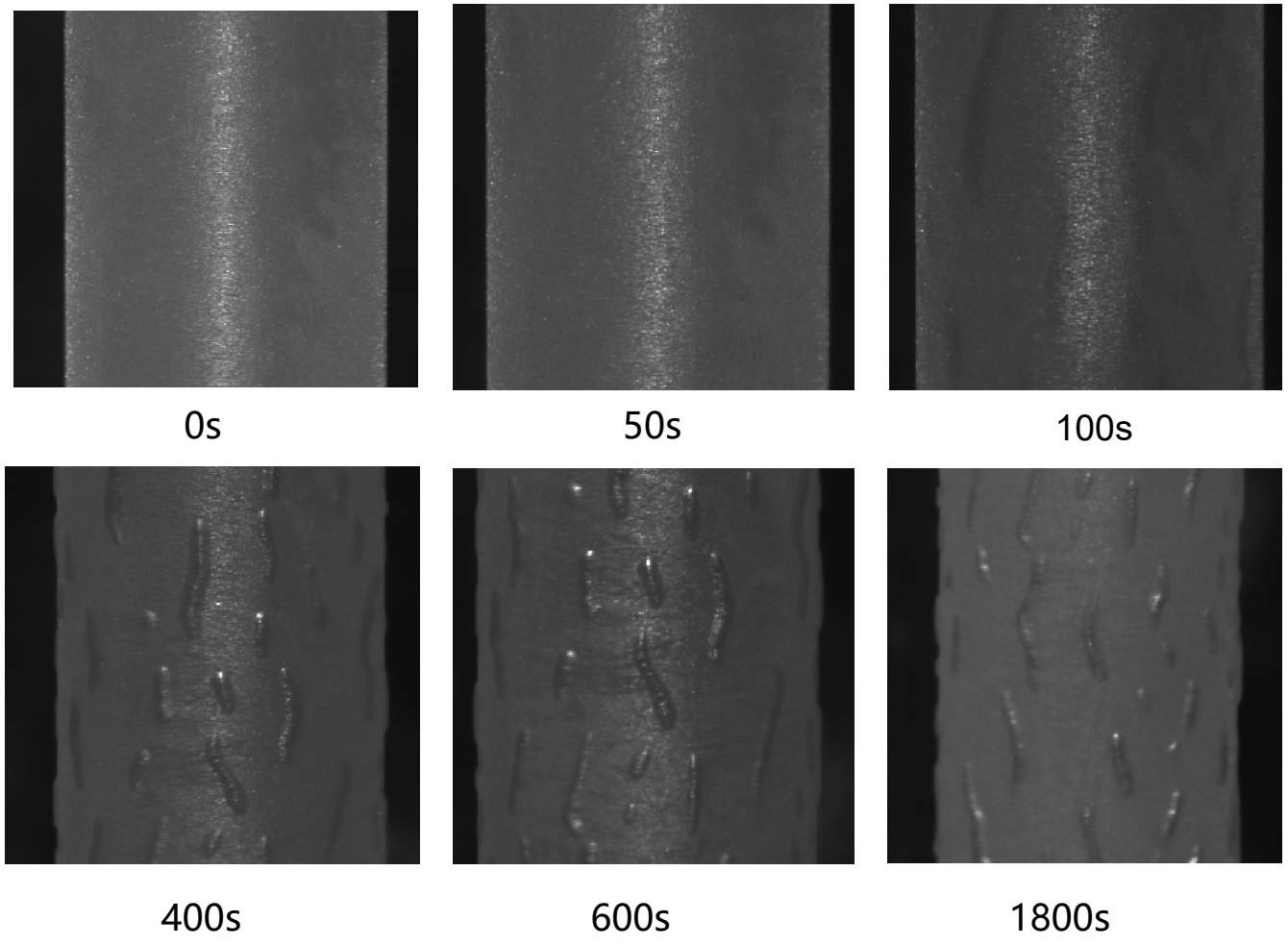

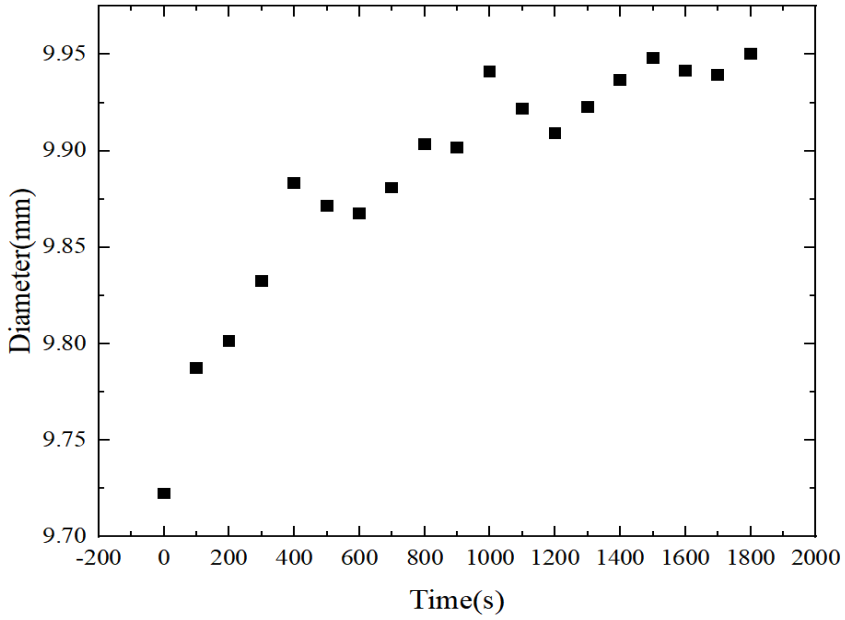

Change in diameter with time

In the process of steam oxidation up to 1200℃, large number of striped ridges appeared gradually on the surface of Cr-coated Zr alloy

Mechanical property Testing -As-received

- Compression experiments were carried out on as-received cladding ring samples pre- HTO

RCT at 135℃: As-received

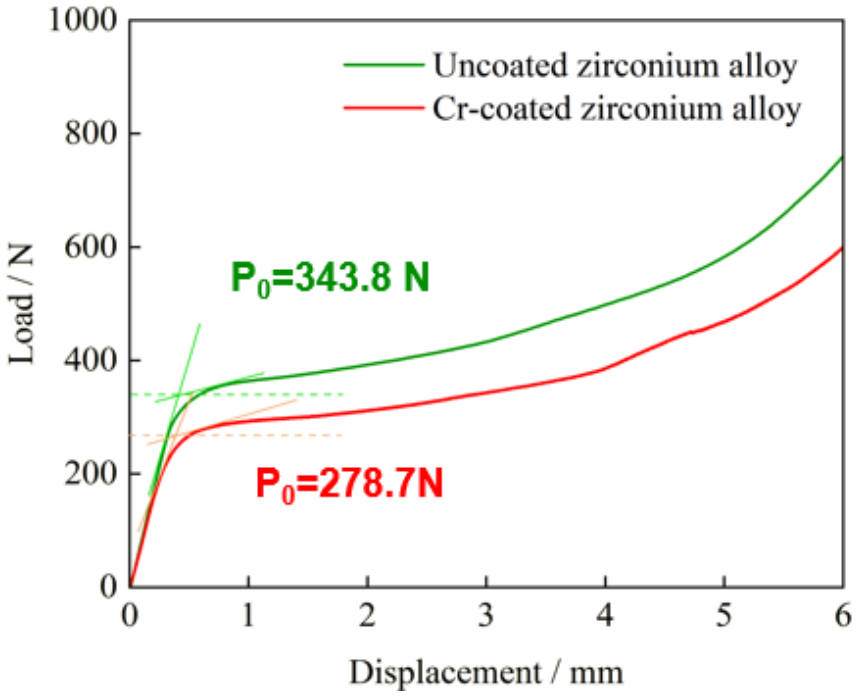

Experimental results of ring compression of two as-received cladding samples

Parametric model $\sigma_0 = \frac{\alpha P_0 R}{t^2 L}$ $E = \frac{24\beta P_e R^3}{\delta_e t^3}(\frac{\pi}{8} - \frac{1}{\pi})$

	Zr-Nb alloy	Cr-coated Zr-Nb alloy
Collapse Load (N)	343.8	278.7
Young's modulus (GPa)	99.0	81.2
Ultimate tensile strength (MPa)	628.3	509.3

Comparison of Initial Important Parameters

The addition of chromium coating decreased the mechanical properties of zirconium alloy cladding.

Mechanical property Testing- post-HTO

- The failure mode of the oxidized cladding changes from ductile to brittle fracture

RCT at 135℃: 1200℃-30min HTO

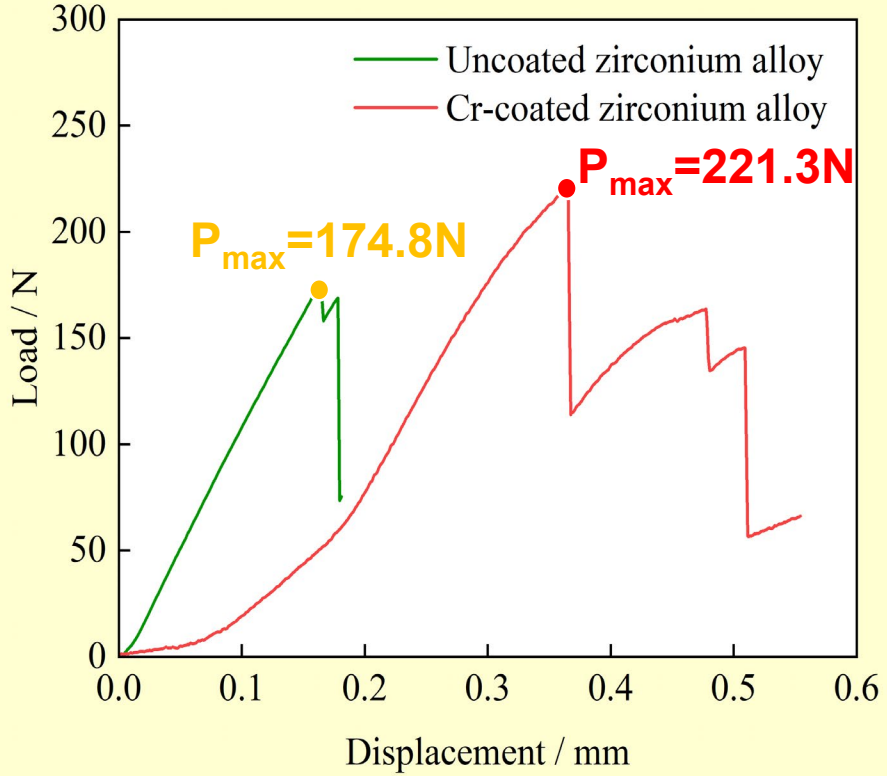

Unoxidized samples - Ductile fracture

As-received Vacuum heated

Post-HTO samples - Brittle fracture

Before compression After compression

The addition of chromium coating decreased the mechanical properties of zirconium alloy cladding.

Mechanical property Testing- post-HTO

- The thermal shock during quench could cause the cladding to fracture prematurely

RCT at 135℃: 1200℃-30min oxidized-quenched

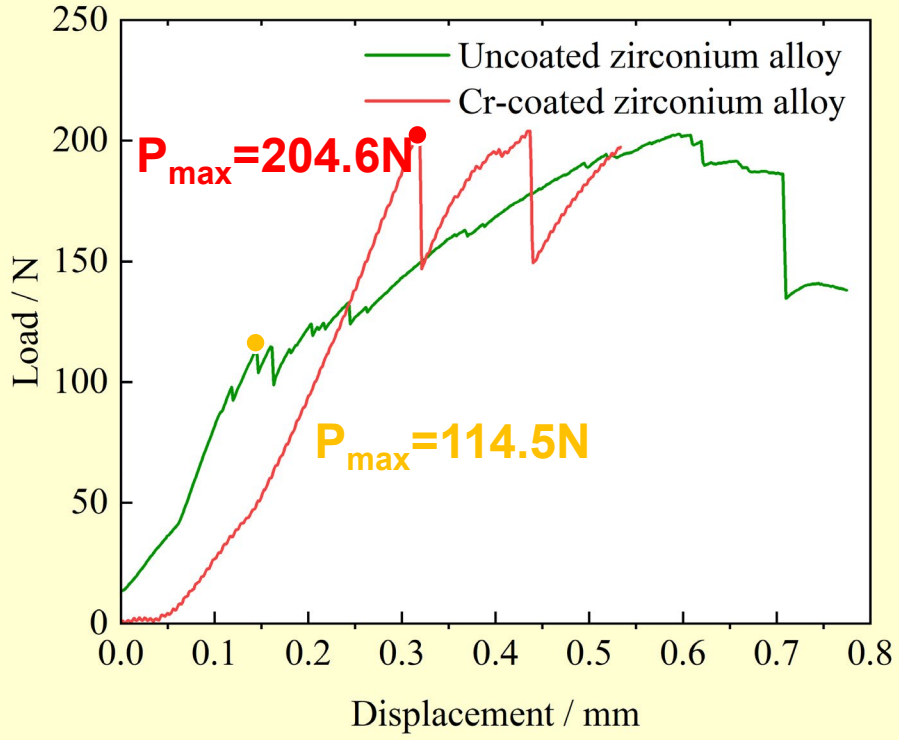

Decreased fracture stress

Fracture stress (N)	Zr-Nb alloy	Chromium coated Zr-Nb alloy
Oxidized	174.8	221.3
oxidized-quenched	114.5	204.6

The addition of chromium coating decreased the mechanical properties of zirconium alloy cladding.

Ballooning and Burst Tests

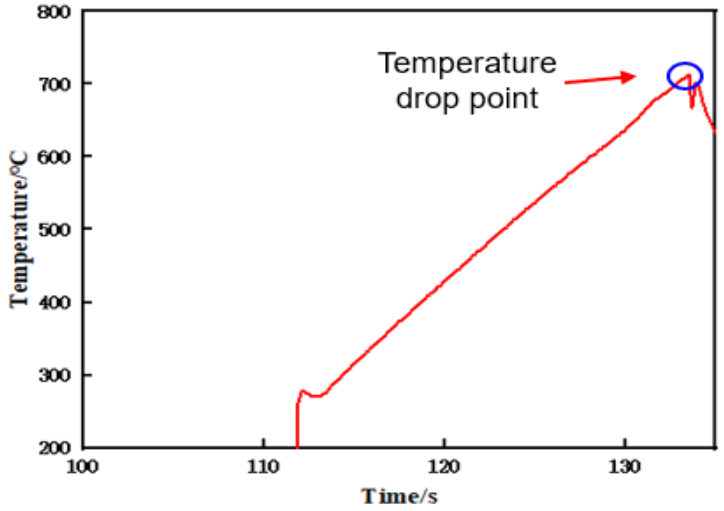

Temperature vs Time

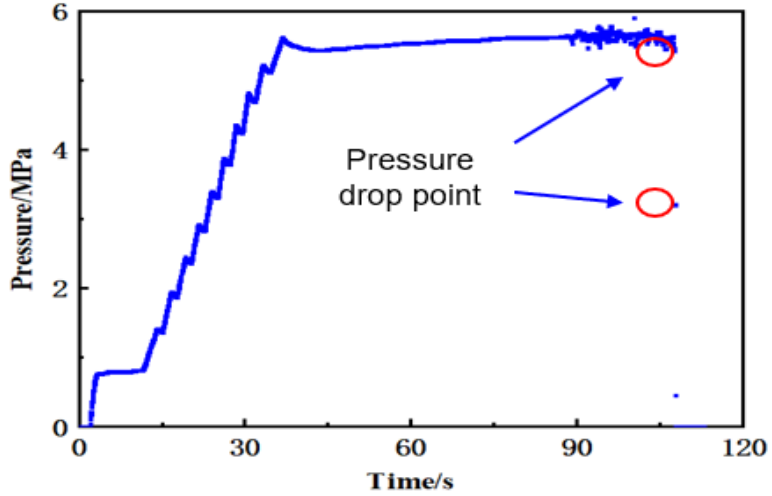

Pressure vs Time

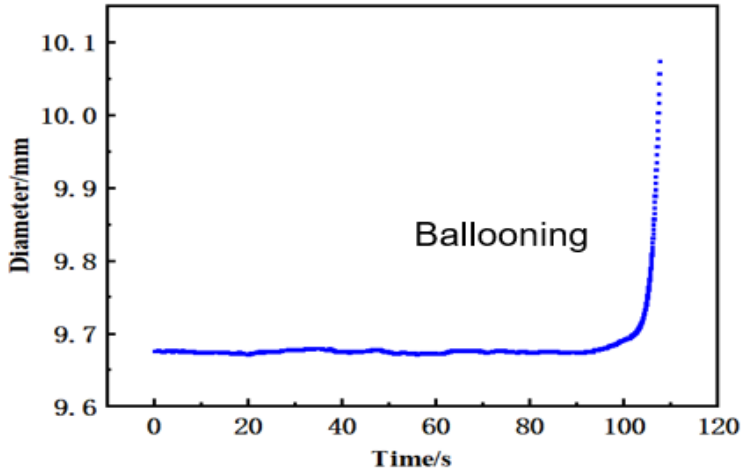

Diameter vs Time

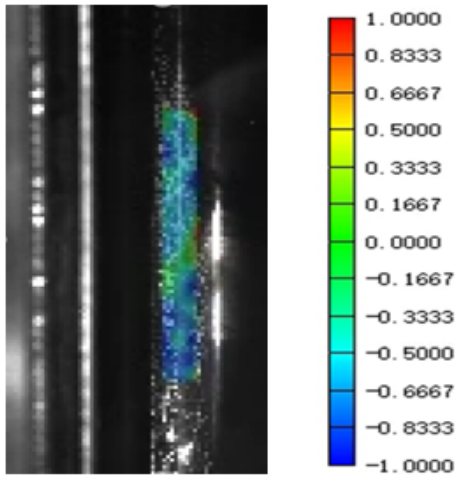

Full-field Strain Acquisition

Real time, in-situ T, OD, IP, and Stain data

Ballooning and Burst Tests

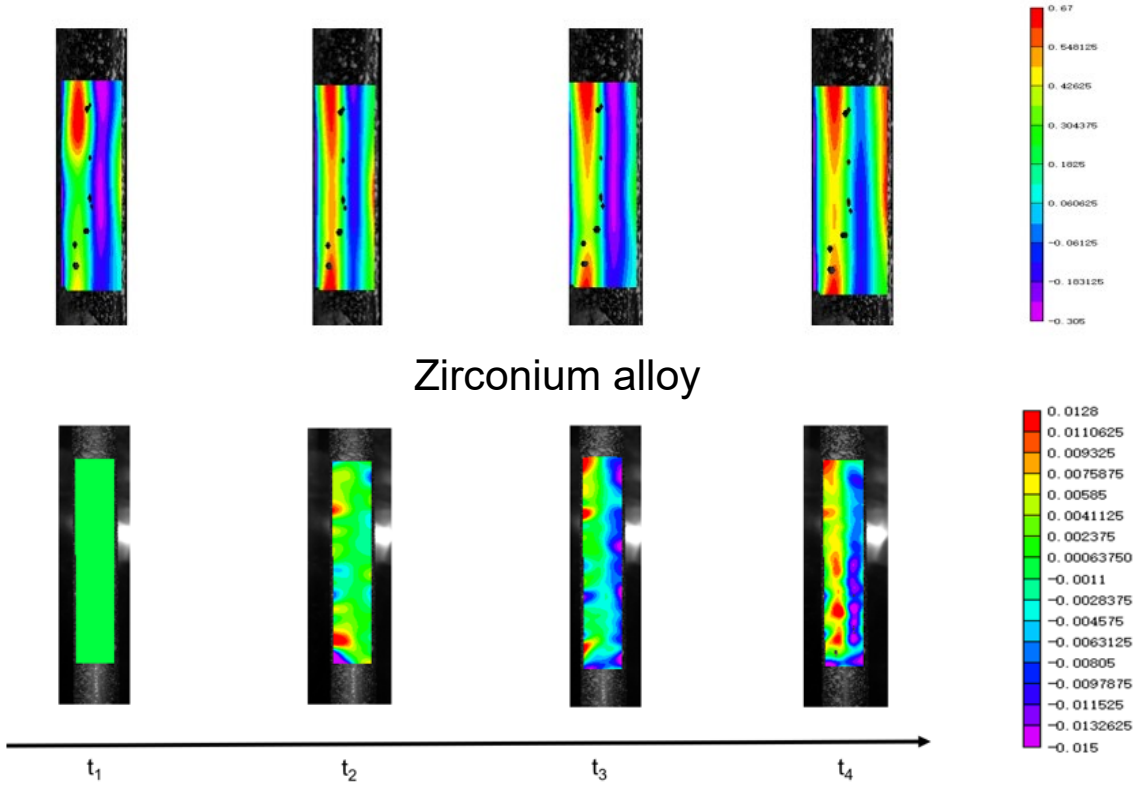

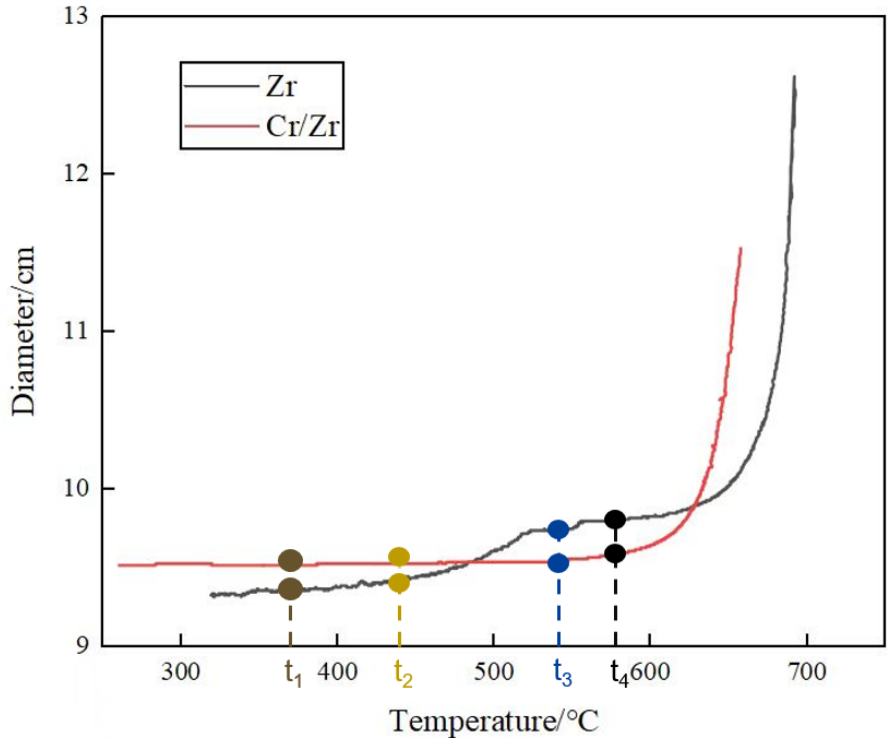

Real-time, in situ, 2D cladding surface strain

At the same internal pressure and heating rate, the strain rate of Cr-coated zirconium alloy cladding is relatively low, and the stress concentration phenomenon is significantly reduced.

Ballooning and Burst Tests: Cr coated

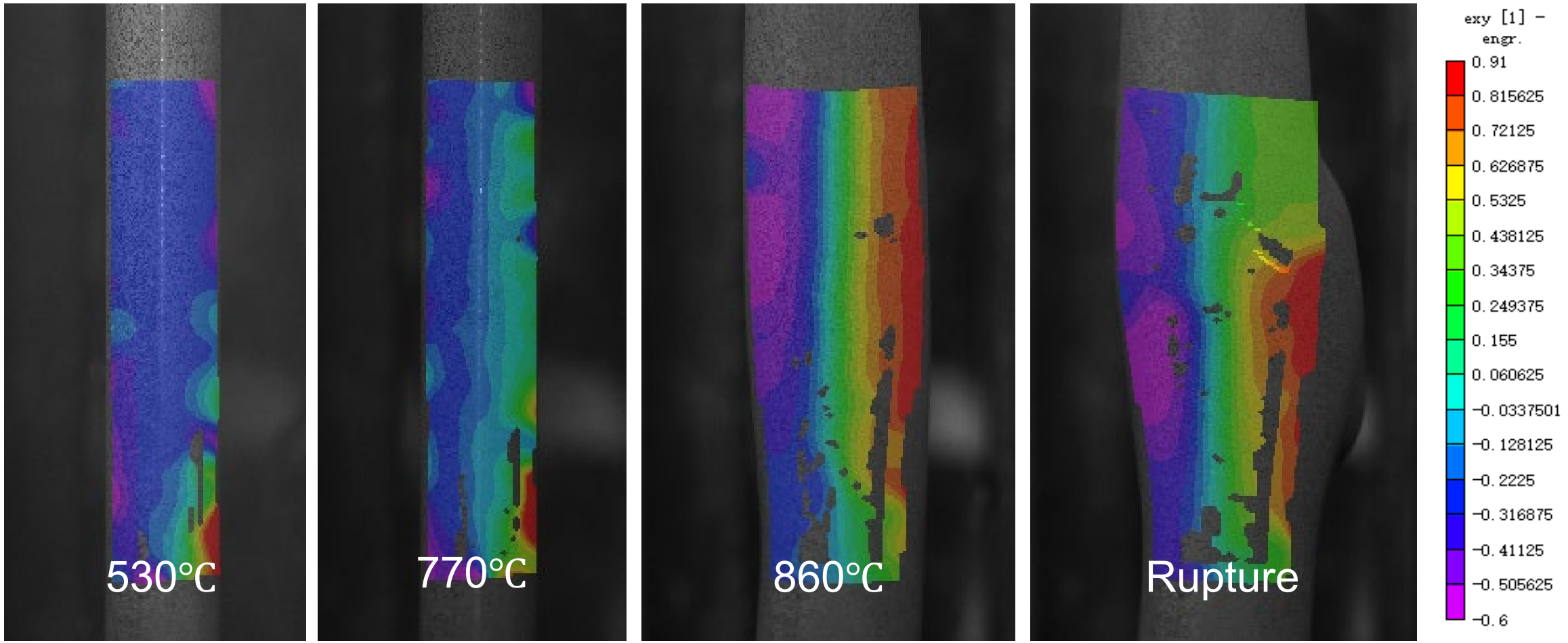

Ballooning and Burst Tests

- **Rupture temperature of new type of zirconium alloy cladding varied with internal pressure was investigated.**

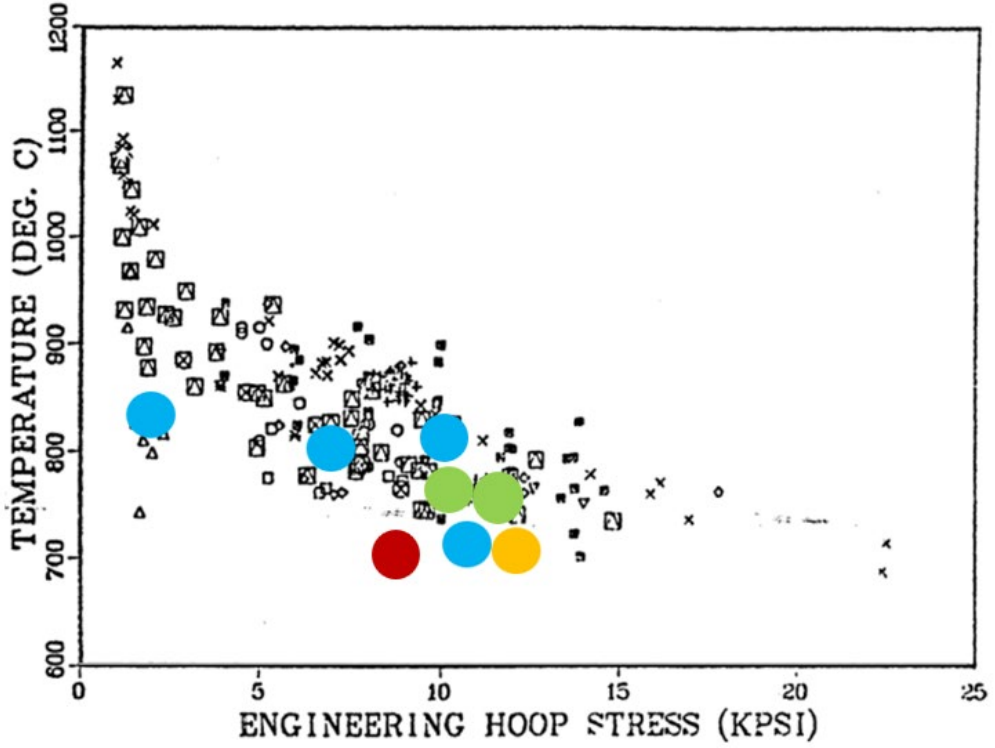

Rupture temperature as a function of engineering hoop stress [1]

Engineering Hoop Stress

$$\sigma = (d/2t)\Delta P$$

a —— engineering hoop stress

d —— undeformed cladding mid-wall diameter

t —— undeformed cladding thickness

ΔP——differential pressure across the cladding wall at the time of rupture

Rupture Temperature

$$T_R = 3960 - \frac{20.4\sigma}{1+H} - \frac{8510000\sigma}{100(1+H)+2790\sigma}$$

T_R —— rupture temperature in ℃

a —— engineering hoop stress in kpsi,

H —— the ratio of the heating rate in ℃ /s to 28℃/s (H varies from 0 to 1).

[1] NUREG0630 Cladding Swelling and Rupture Models for LOCA Analysis

Ballooning and Burst Tests

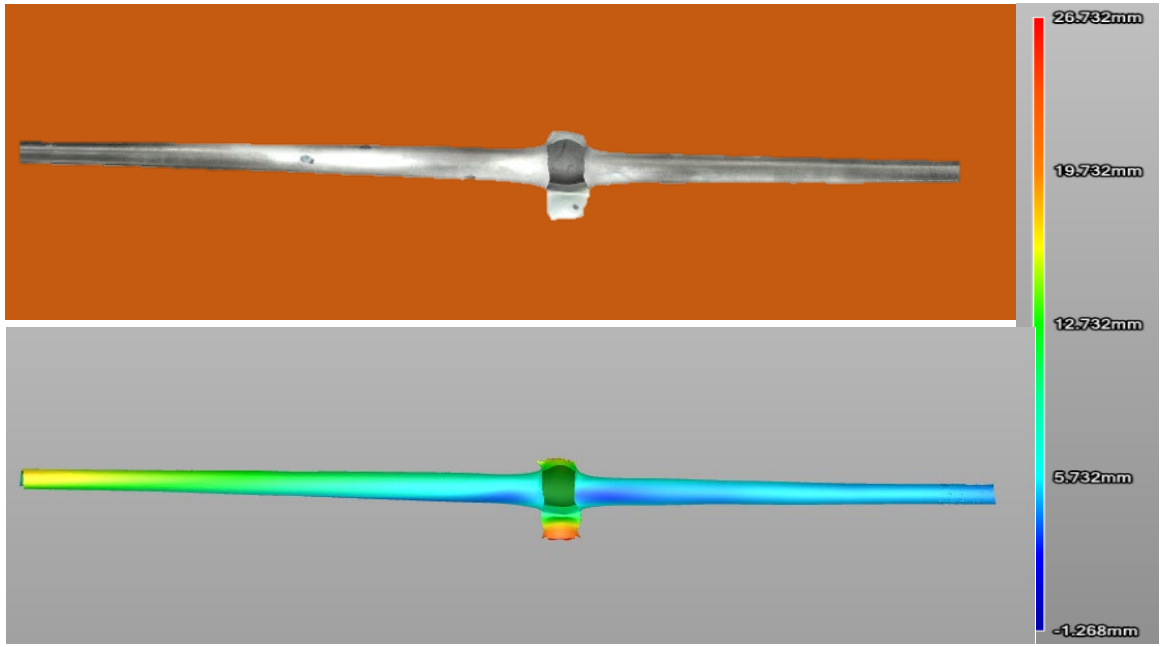

Optical scan image of uncoated cladding

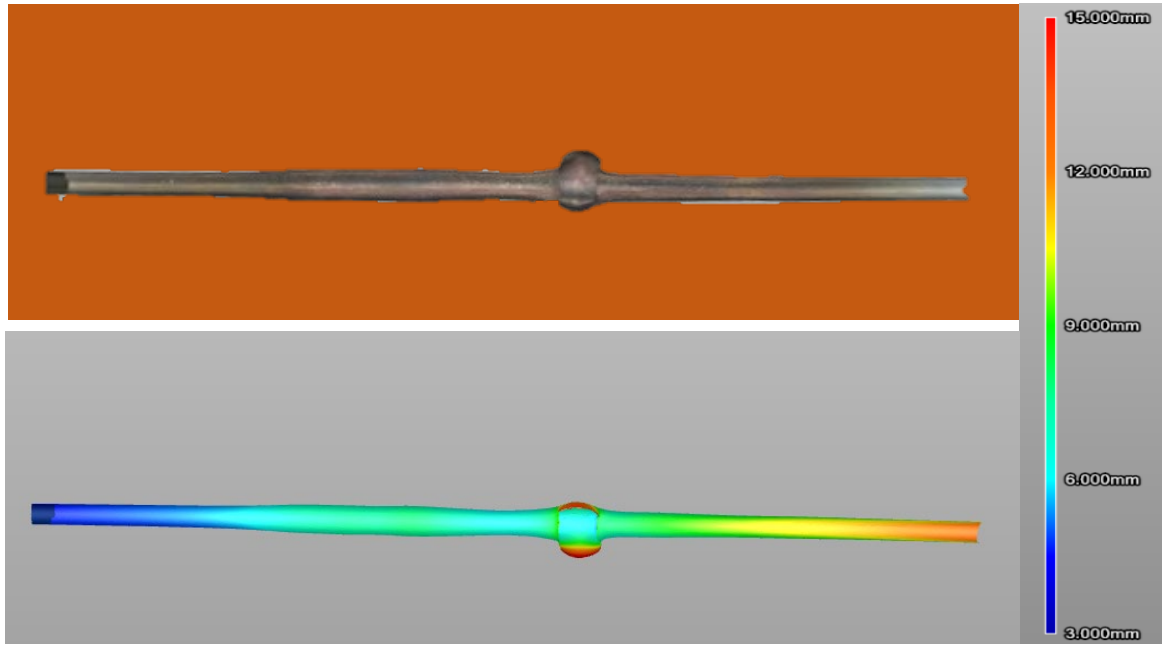

Optical scan image of Cr-coated cladding

1. **Cr coating reduced the maximum deformation at the rupture of the zirconium alloy cladding tube by 43.8%.**
2. **Under the same precharge pressure and at the same heating rate, the burst temperature of the Cr coating is reduced.**

Ballooning and Burst Tests

1℃-70℃/s 1MPa-10MPa








The rupture's **location, shape, and size** varied with different heating rates and initial pressures;

Further quantitative correlation studies are worth performing in the future.

Content

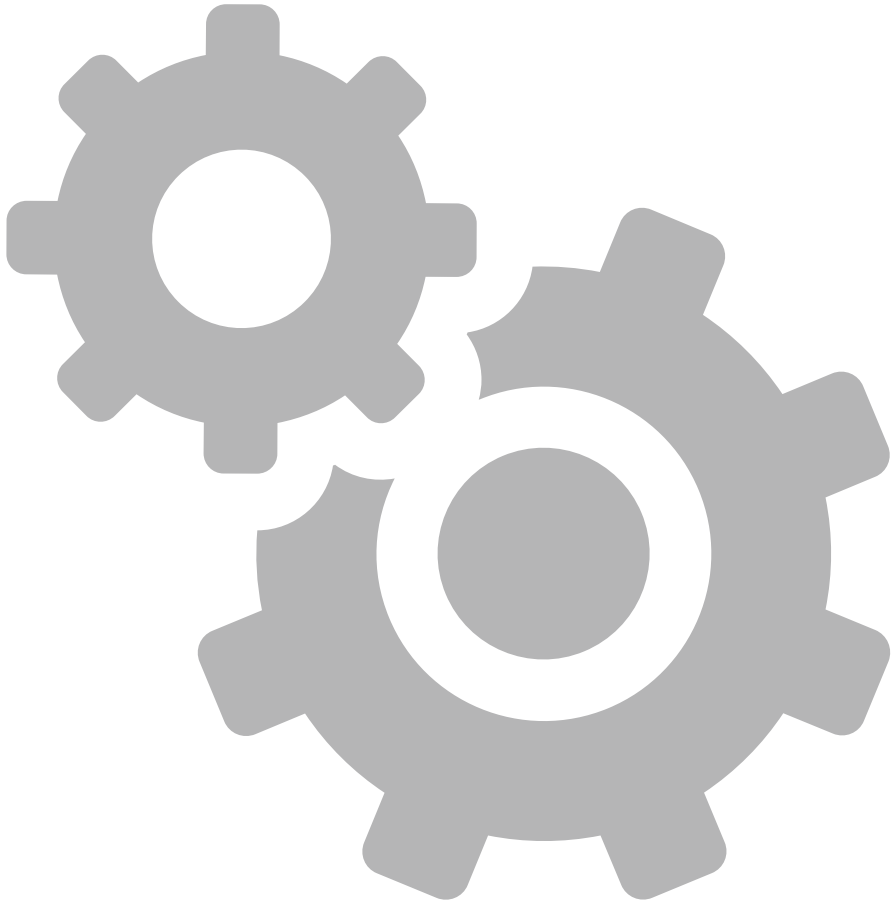

- **To investigate the behaviour of fuel cladding under LOCA conditions, a series of experiments have been carried out, including high-temperature oxidation, ballooning and burst tests, as well as mechanical property degradation evaluations.**
- **High-speed imaging and DIC techniques were used together during the experiment to process and analyze data, capturing the detailed response of cladding materials to thermo-mechanical and chemical coupling effects.**
- **The research findings contribute to the development of advanced models for predicting cladding behavior, optimizing material selection and design, reducing failure risk, and enhancing the safety of nuclear reactors under LOCA scenarios.**

(supported by HNKF202314(48) & CNNC-LCKY-202242) Project

In the history of energy development, every type of energy source has gone through a metamorphosis from *"a devil"* to *"an angel"*

Welcome to Shanghai and SJTU!

Thanks for your attention

Email: tongliu@sjtu.edu.cn

Ali Charbal

CEA

Chromium coating cracking quantification methods: some recent developments and results

Among the various potential candidates for enhanced accident tolerant fuel (EATF) cladding tubes [1], chromium coatings generated by physical vapour deposition (PVD) methods have shown some promising results [2], [3], [4], [5], [6] using separate effects studies simulating Loss of Coolant Accident conditions. Coating damage (e.g., cracking and spallation) during thermomechanical loading needs to be further studied and quantified. The effect of cracking on the coating protectiveness needs to be better understood. This presentation will illustrate some CEA's experimental developments to investigate such phenomenon.

In LOCA scenarios for instance, at temperatures above 600°C, PVD chromium-coated claddings studied at CEA seem to exhibit significant ductility. Negligible cracking (and no coating spallation) has been observed even in cases of significant ballooning and burst [6]. Post-mortem analyses such as metallographic observations or X-Ray tomography help to correlate the crack density (if any) and cladding tubes circumferential deformation. Analyses on a same sample, that has experienced an important ballooning, have shown no cracking below 37 % of circumferential hoop strain. This shows a clear gain of ductility of the chromium coating with the increase of temperature.

In order to investigate the coating ductility gain, and potential better resistance to cracking, mechanical testing on chromium-coated tubes, monitored by acoustic emission (AE), were performed at temperatures between 20°C and 540°C. Results were in good agreement with the post-mortem observations on samples tested at higher temperatures (LOCA testing). The "critical" strain level, to generate first cracks, increases with temperature. Above 400°C, no cracking is detected even for large level of strain [7].

To better understand the intrinsic behaviour of the chromium coating, micromechanical set of testing has been initiated. Additionally to micropillar compression testing, microcantilever bending testing coupled with EBSD examinations have been carried out [8] with the aim at determining the nature of crack generation and propagation. Such technique could also provide fracture toughness of the chromium layer.

References:

[1] AEN, « State-of-the-Art Report on Light Water Reactor Accident-Tolerant Fuels ». 2018. Disponible sur: https://www.oecd-ilibrary.org/content/publication/9789264308343-en

[2] I. Idarraga-Trujillo *et al.*, « Assessment at CEA of coated nuclear fuel cladding for LWRs with increased margins in LOCA and beyond LOCA conditions », *Top Fuel*, vol. 2, p. 15-19, 2013.

[3] F. Schuster *et al.*, « On-going studies at CEA on chromium coated zirconium based nuclear fuel claddings for enhanced accident tolerant LWRs fuel », in *TopFuel 2015-Reactor Fuel Performance Meeting*, 2015.

[4] J. C. Brachet, « Behavior of Cr-coated M5TM claddings under LOCA conditions », in *Proceedings of 2017 Water Reactor Fuel Performance Meeting,(Sept. 10-14, 2017), Jeju Island, Korea*,

[5] J.-C. Brachet *et al.*, « Early studies on Cr-Coated Zircaloy-4 as enhanced accident tolerant nuclear fuel claddings for light water reactors », *J. Nucl. Mater.*, vol. 517, p. 268-285, 2019.

[6] M. Dumerval, Q. Houmaire, J.-C. Brachet, H. Palancher, J. Bischoff, et E. Pouillier, « Behavior of chromium coated M5 claddings upon thermal ramp tests under internal pressure (loss-of-coolant accident conditions) », in *Topfuel 2018-Light Water Reactor (LWR) Fuel Performance Meeting 2018*, 2018.

[7] Y. Taïbi *et al.*, « In-situ chromium coating cracking investigation up to 500°C on zirconium based nuclear fuel cladding substrate, using tensile tests monitored by acoustic emission », *Oral presentation*, Singapore, octobre 2024.

[8] Y. Taïbi *et al.*, « Multi-scale approach applied to the micro/micro-mechanical characterization of chromium-coated Zr-based nuclear fuel claddings », *Poster*, Singapore, octobre 2024.

Chromium coating cracking quantification methods: some recent developments and results *,**

A. Charbal[1], J-C. Brachet[1], Y. Taïbi[1,3], G. Touze[2], S. Sao-Joao[3], S. Kalacska[3], G. Kermouche[3]

[1] Université Paris-Saclay, CEA, Service de Recherche en Matériaux et procédés Avancés, 91191, Gif-sur-Yvette, France

[2] Université Paris-Saclay, CEA, Service de Recherche en Corrosion et Comportement des Matériaux, 91190, Gif-sur-Yvette, France

[3] Mines Saint-Etienne, CNRS, UMR 5307 LGF, Centre SMS, F-42023 Saint-Etienne, France

* *The presented works are supported by the CEA-EDF-FRAMATOME triparty "Innovation COMBustible" project.*

PVD-HiPIMS Cr coating *on zirconium based-cladding substrate*

High density and thickness uniformity + strong adherence

HIPIMS PVD process

Brachet et al., 2017, WRFPM

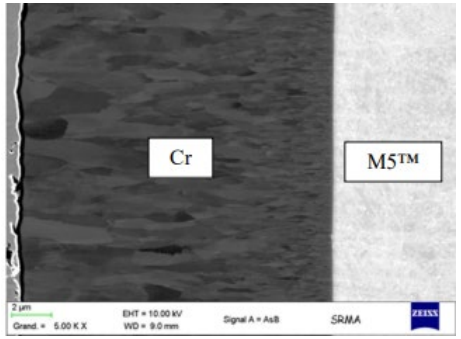

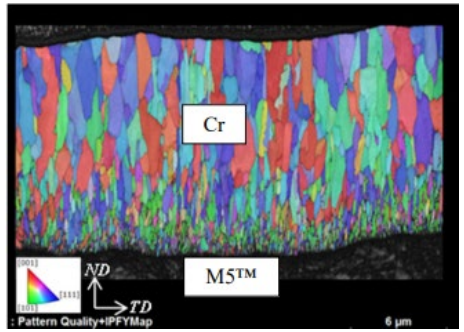

- Typical chromium coating thickness range: 5-30 µm
- Zirconium alloys substrate:
  - Diameter 9,5 mm
  - Thickness 0,580

PVD-HiPIMS Cr coating *on zirconium based-cladding substrate*

High density and thickness uniformity + strong adherence

HIPIMS PVD process

Brachet et al., 2017, WRFPM

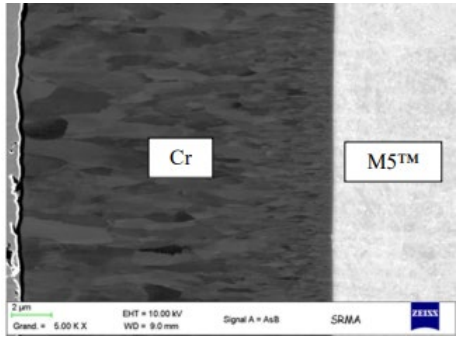

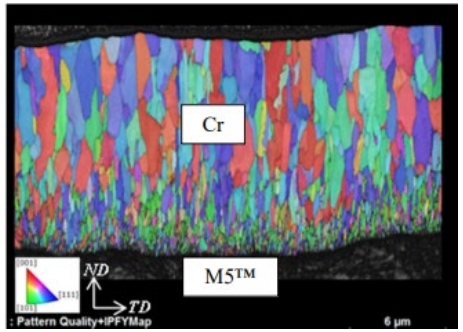

- Typical chromium coating thickness range: 5-30 µm
- Zirconium alloys substrate:
  - Diameter 9,5 mm
  - Thickness 0,580

High Temperature performances (LOCA)

Dumerval et al., 2018, Top Fuel

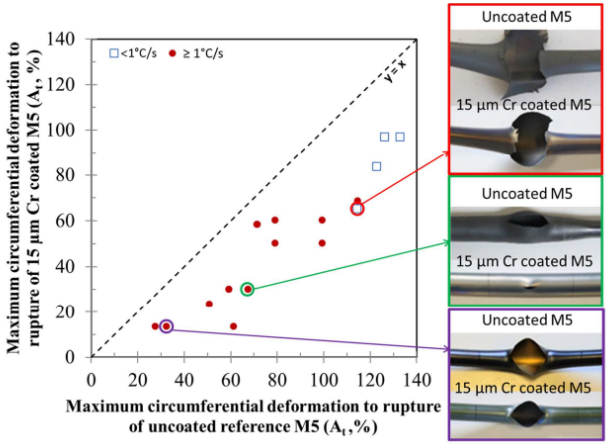

Brachet et al., 2020, Corr. Sc.

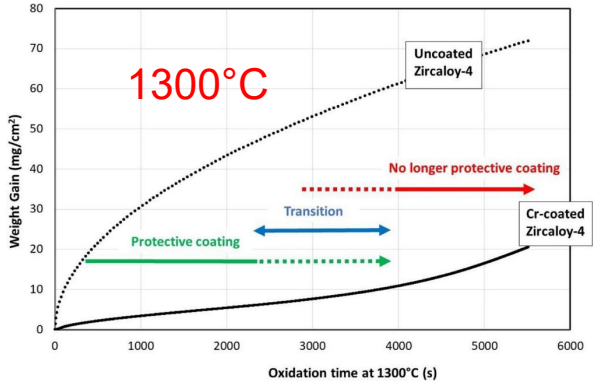

- Strengthening effect upon HT incursion + internal pressure:
  → Decrease in balloon size
- Oxidation kinetics and associated gaseous H_2 production, strongly reduced
- Enhanced quenching and post-quenching resistance

PVD-HiPIMS Cr coating *on zirconium based-cladding substrate*

High density and thickness uniformity + strong adherence

HIPIMS PVD process

Brachet et al., 2017, WRFPM

- Diameter 9,5 mm
- Thickness 0,580

High Temperature performances (LOCA)

Dumerval et al., 2018, Top Fuel

Brachet et al., 2020, Corr. Sc.

- Oxidation kinetics and associated gaseous H_2 production, strongly reduced
- Enhanced quenching and post-quenching resistance

- ❖ **Properties are process & process parameter dependent**
- ❖ **Good mastering of deposition process is key for obtaining chosen microstructure/properties**
- ❖ **Results cannot be generalized to any Cr coating deposition processes**

Cr coating *on zirconium based-cladding substrate*

How the enhanced performances could be affected by coating damage?

- **Cr-coating damaged in nominal conditions and possible consequences?**
  - Damage could be generated during in-service / post-service conditions.
  - Possibility to create localized area favorable for accelerated corrosion/hydriding and/or coating spallation?

Cr coating *on zirconium based-cladding substrate*

How the enhanced performances could be affected by coating damage?

- **Cr-coating damaged in nominal conditions and possible consequences?**
  - Damage could be generated during in-service / post-service conditions.
  - Possibility to create localized area favorable for accelerated corrosion/hydriding and/or coating spallation?
- **Cr-coating damaged during LOCA (*and other hypothetical accident scenario*) conditions and possible consequences?**
  - Ballooning of cladding can damage the Cr-coating
  - What consequences on the cladding ballooning and burst and on the protectiveness of the coating upon further high temperature oxidation?

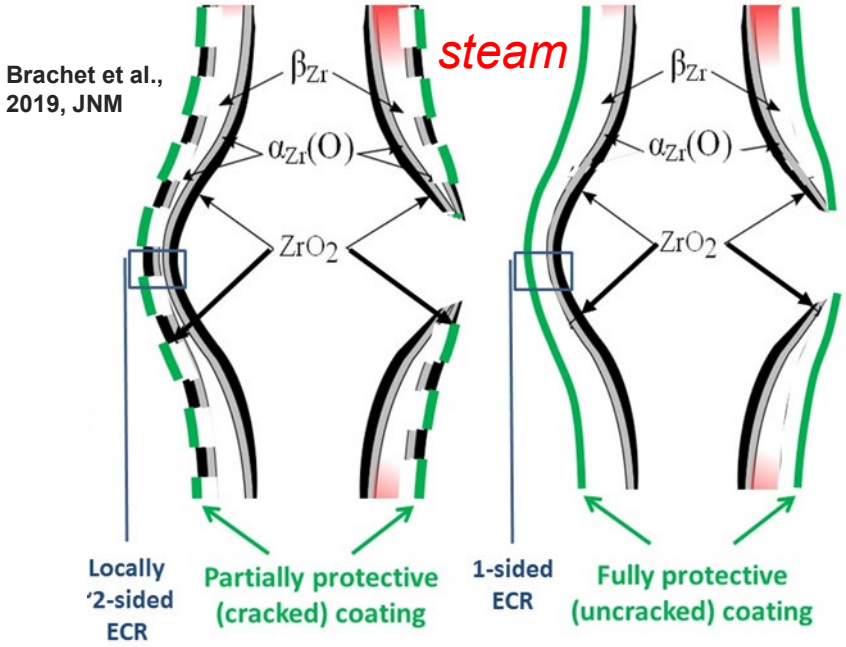

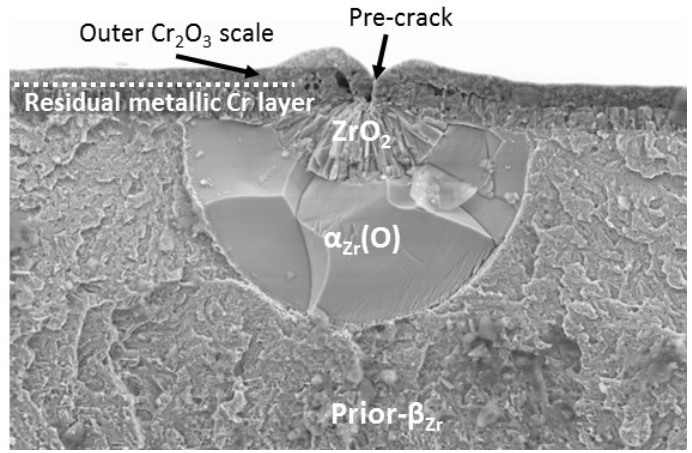

Cr coating *on zirconium based-cladding substrate*

How the enhanced performances could be affected by coating damage?

- Cr-coating damaged in nominal conditions and possible consequences?

Brachet et al., 2019, JNM

Needs for a better understanding & quantification of the Cr-coating damage upon both nominal and hypothetical accident *scenarii* (LOCA & beyond, RIA…)

- Ballooning of cladding can damage the Cr-coating
- What consequences on the cladding ballooning and burst and on the protectiveness of the coating upon further high temperature oxidation?

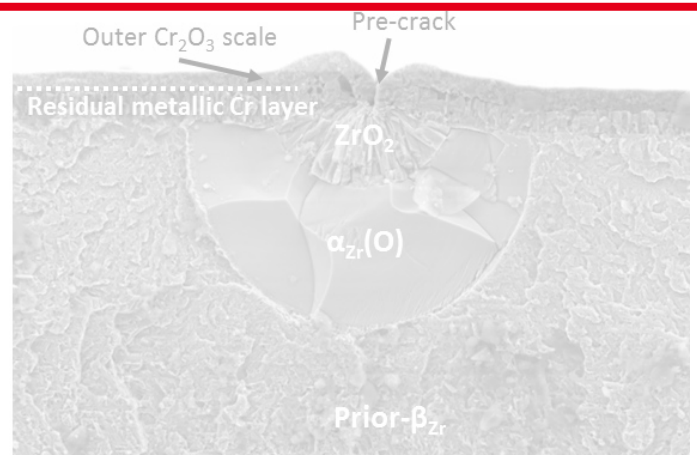

Scope of the presentation

- Focus on **CEA's current work on Cr-coating cracking under thermomechanical sollicitations**:
  - "LOCA" conditions ("EDGAR" tests under inner pressure at 600-1000°C)
  - Determination of the critical strain to cracks formation as function of temperature (tensile testing on tubes)
  - Chromium coating characterization by micromechanical testing (*collab. Ecole Des Mines de St Etiennes*)

- Provides first results and observations on Cr-coating behavior toward cracking

- Insights from several experimental technics such as:
  - Acoustic Emission (AE) for in-situ Cr cracking detection and quantification
  - *Post-mortem* analyses by optical microscopy
  - *Post-mortem* analyses by X-ray tomography

Summary

I. Introduction

II. Macroscopic approaches for coated cladding testing
   i. Ballooning/Burst testing : post-mortem methods for chromium coating cracking quantification
   ii. Tensile testing : in situ methods for chromium coating cracking evolution *(Y. Taïbi, PhD Thesis)*
   iii. Conclusions and prospects

III. Microscopic approaches for coating characterization (Y. Taïbi, PhD Thesis)
   i. Micro-cantilever testing : *toward fracture toughness measurements*
   ii. Micro-pillar testing : *toward elastoplastic behavior determination*
   iii. Conclusions and prospects

Summary

I. Introduction

II. Macroscopic approaches for coated cladding testing
   i. Ballooning/Burst testing : post-mortem methods for chromium coating cracking quantification
   ii. Tensile testing : in situ methods for chromium coating cracking evolution *(Y. Taïbi, PhD Thesis)*
   iii. Conclusions and prospects

III. Microscopic approaches for coating characterization (Y. Taïbi, PhD Thesis)
   i. Micro-cantilever testing : *toward fracture toughness measurements*
   ii. Micro-pillar testing : *toward elastoplastic behavior determination*
   iii. Conclusions and prospects

EDGAR, ballooning and burst

EDGAR 1&2 facilities:

- Designed in the late 70s, since **more than 4000 cladding tubes** have been tested
- EDGAR facilities provide the capacity to perform **thermomechanical testing under controlled inner pressure & temperature**
- **Joule effect heating**: slow and fast thermal loading can be applied (0.1°C/s to 200°C/s) up to 1200°C
- **Contactless temperature control and measurements**:
  IR pyrometers and internal thermocouple
- **Internal pressure** can be controlled up to 200 bars
- **In-situ contactless hoop-strain monitoring** (laser) during ballooning / burst
- Sample length representative of inter-grid distance in assemblies

EDGAR 1

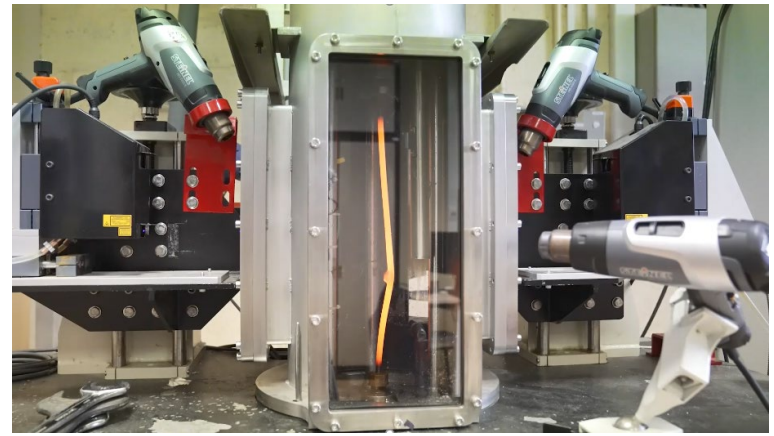

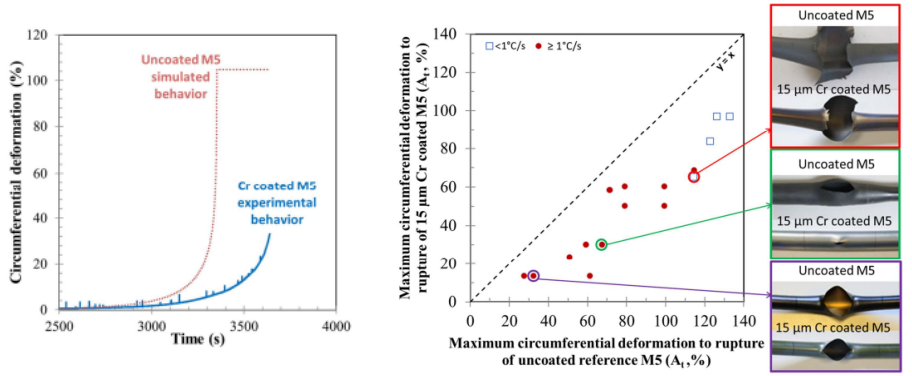

Dumerval et al., 2018, Top Fuel

Cracking generation by ballooning and burst testing

Slow thermal ramps or isothermal testing for large balloon formation

Penalizing conditions toward chromium cracking

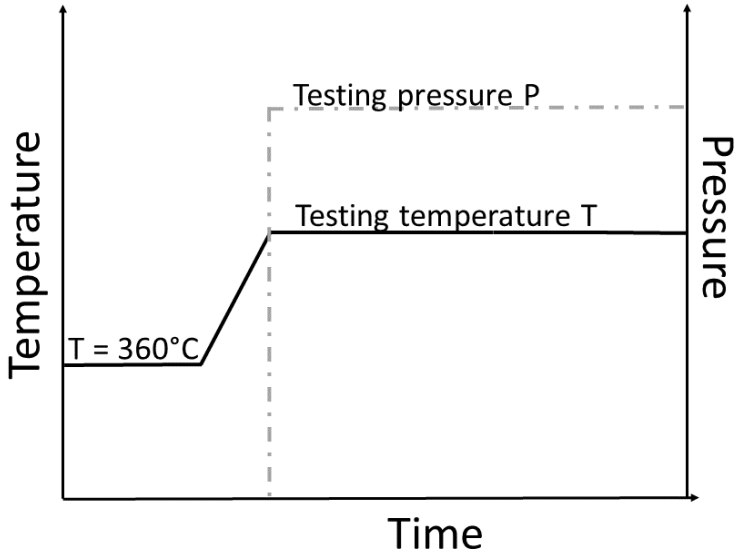

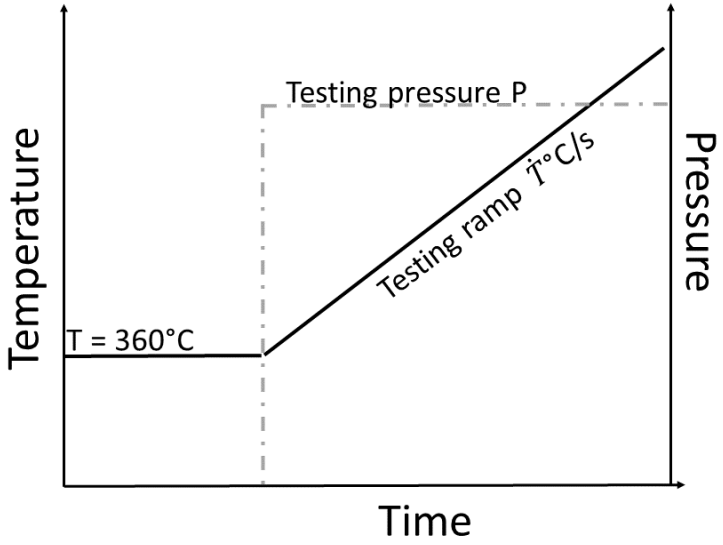

- More chance to generate chromium cracking for the purpose of the study
- Slow thermal ramps are not really representative of LOCA scenarios

Cracking quantification by optical methods

A method for marking the cracks for a better detectability!

High temperature oxidation

Charbal et al., 2024, Top Fuel

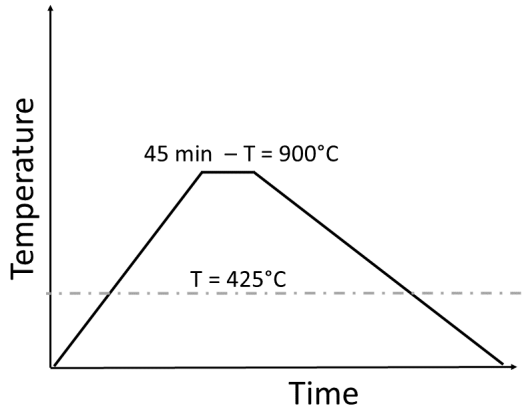

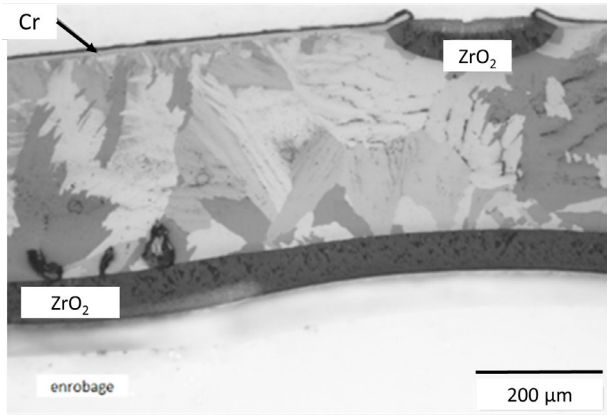

- Air oxidation in a lab furnace
- The oxidation time was estimated based on oxidation kinetics of zirconium alloy

  → Goal is to reach a thickness of ZrO2 (in the cracked areas) of about 30-40 µm

Toward a better quantification by Optical Miscroscopy

High quality images, *measurements realized at a specific height*

High resolution optical observations

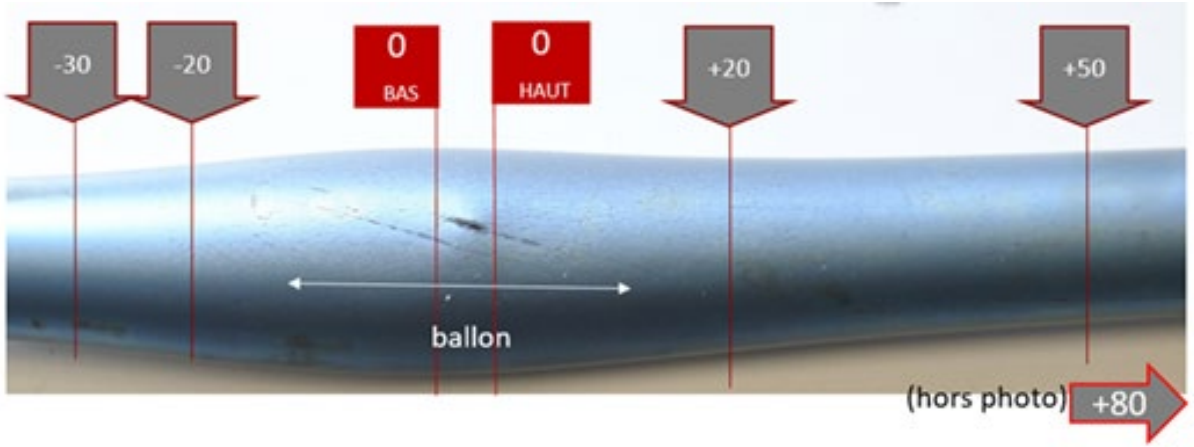

Charbal et al., 2023, QWS

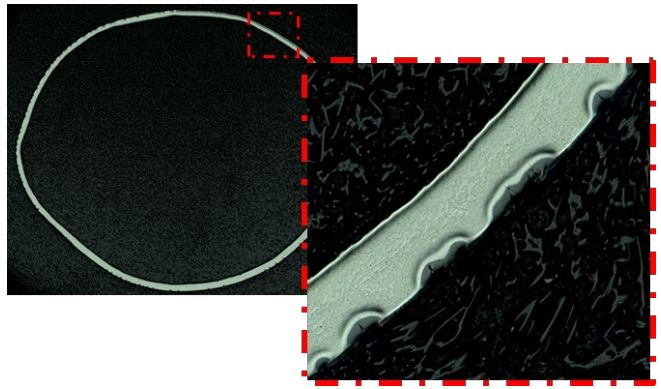

- Needs a metallographic preparation
- Resolution up to 1µm detect small cracks
- High quality image provide a good contrast for analyses
- Requires preparation efforts and can be time consuming if a large data base is needed

Toward a finer quantification by Optical Miscroscopy

High quality images, *measurements realized at a specific height*

Automated counting

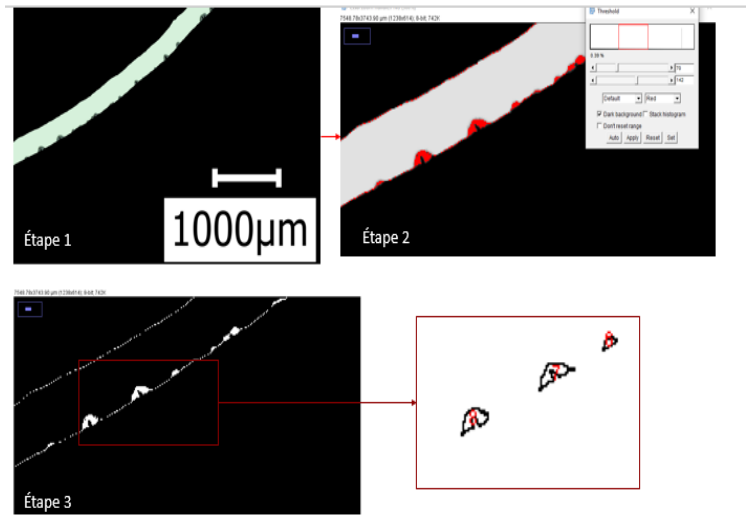

Charbal et al., 2023, QWS

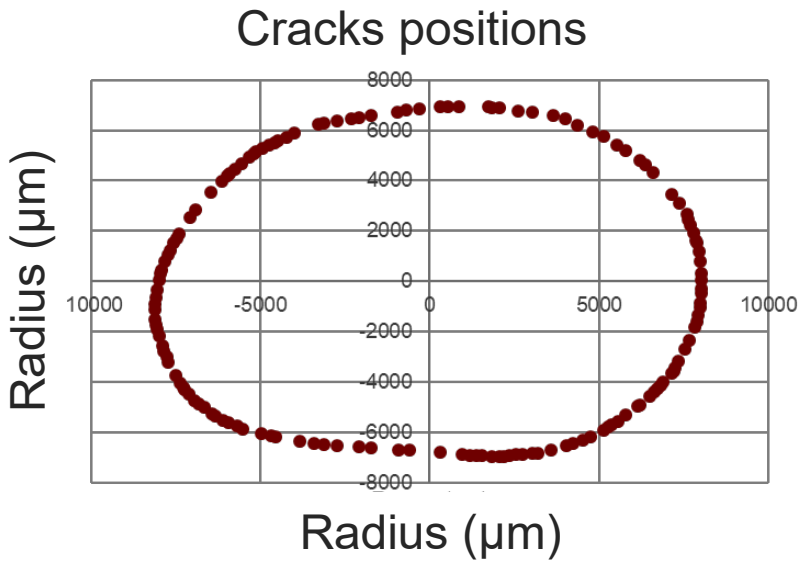

- Use of image processing and machine learning toolboxes (here Fiji & Weka plugging)
- Good detection rate of cracks on the optical images

Toward a better quantification by Optical Miscroscopy

High quality images, *measurements realized at a specific height*

Automated counting

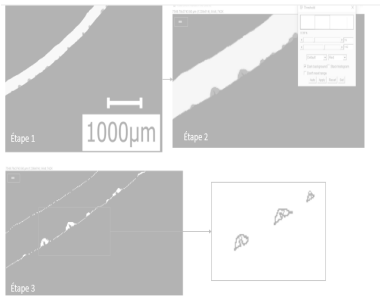

Measurement on the same cladding tube
(Tested with a heating rate of 1°C/s)

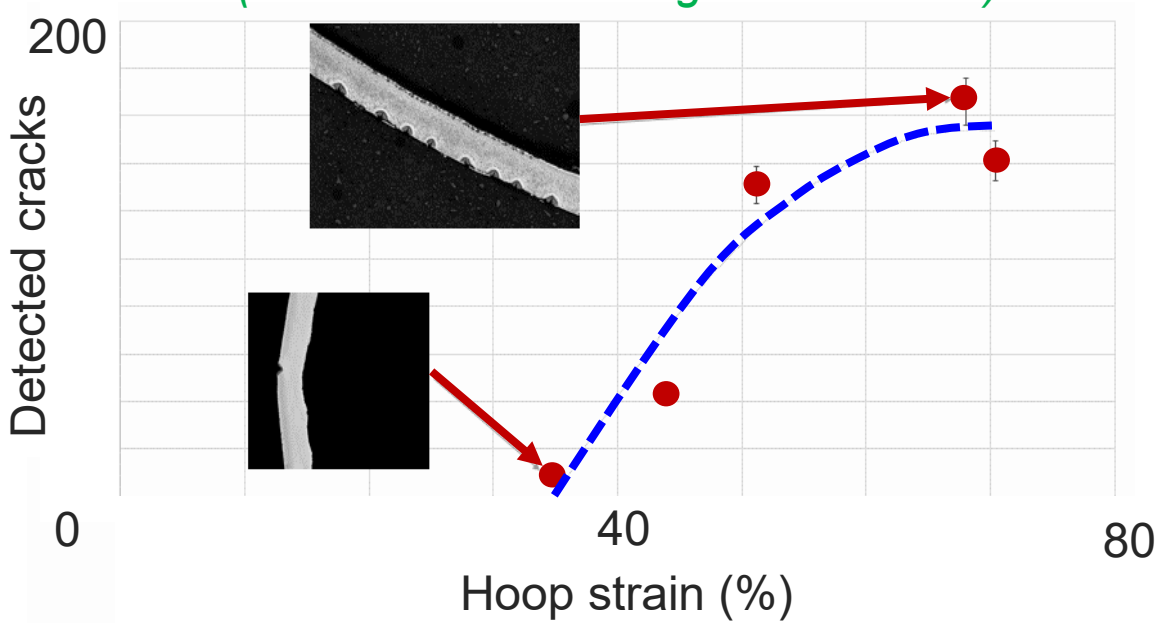

Charbal et al., 2023, QWS

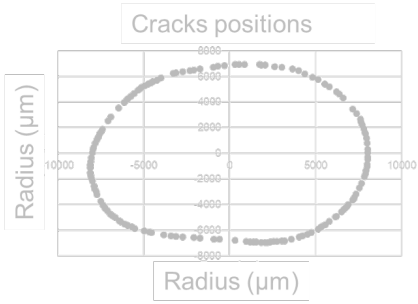

- Use of image processing and machine learning toolboxes (here Fiji & Weka plugging)
- Good detection rate of cracks on the optical images
- ***Higher Cr-coating ductility and resistance to cracking → no cracking below ~37 % of hoop strain***

→ Need to investigate a faster method to provide cracking density (to enrich the database)

Cracking quantification by X-Ray Tomography

Large amount of information is obtained with a lesser preparation effort!

Volumic observations

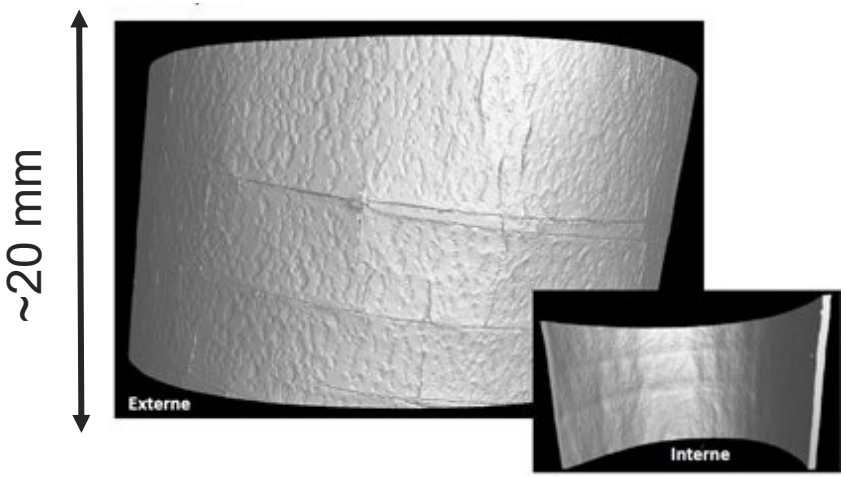

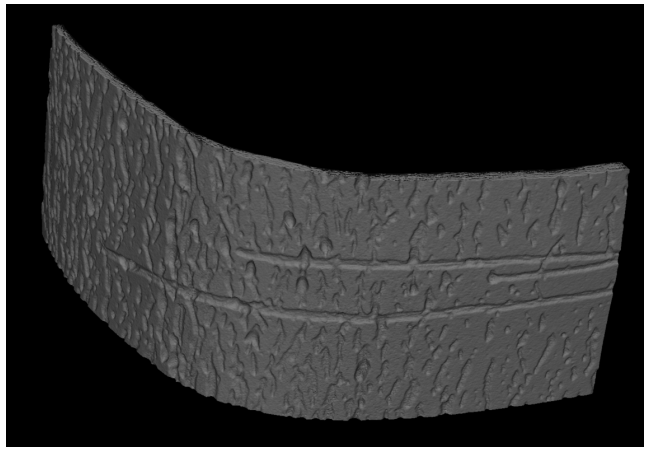

Charbal et al., 2023, QWS

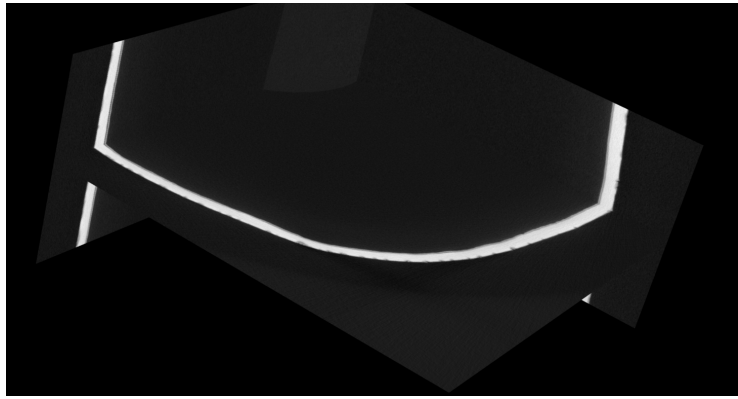

- No needs for preparation
- Large volumes can be scanned
- Resolution up to 10-15 µm per voxel
- Lower resolution and contrast than optical microscopy

Cracking quantification by X-Ray Tomography

Large amount of information could be obtained with a lesser preparation effort!

Automated counting

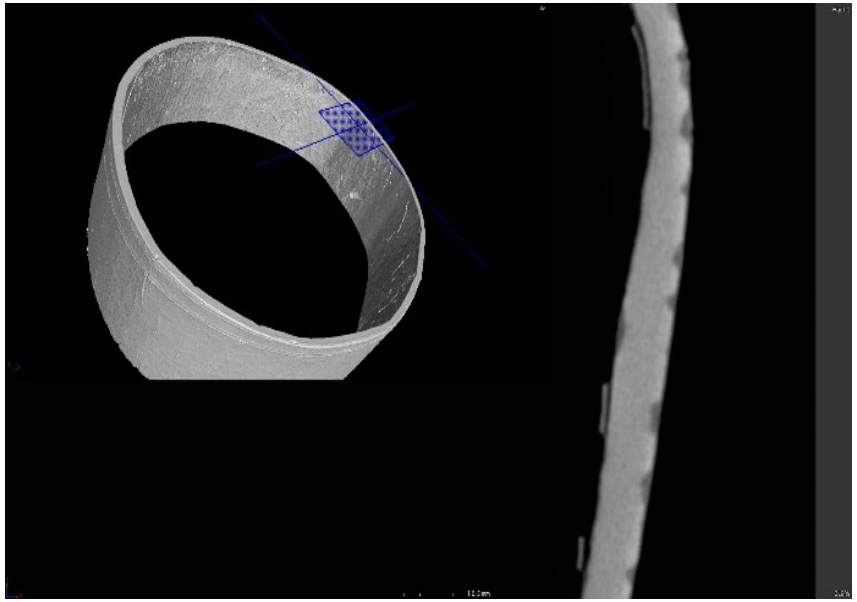

- Use of image processing (here “homemade codes” via Matlab)
- Satisfactory detection rate but still need to improvements
- Machine learning as a solution → needs extra work (vs. Optical Microscopy Images)

Cracking quantification by X-Ray Tomography

Large amount of information could be obtained with a lesser preparation effort!

Automated counting

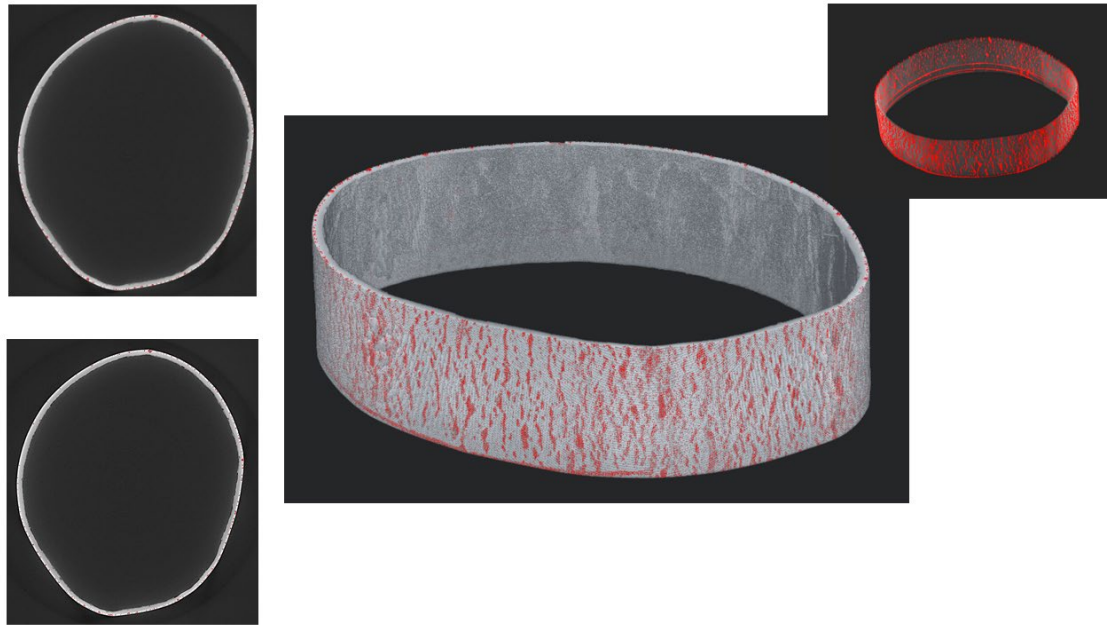

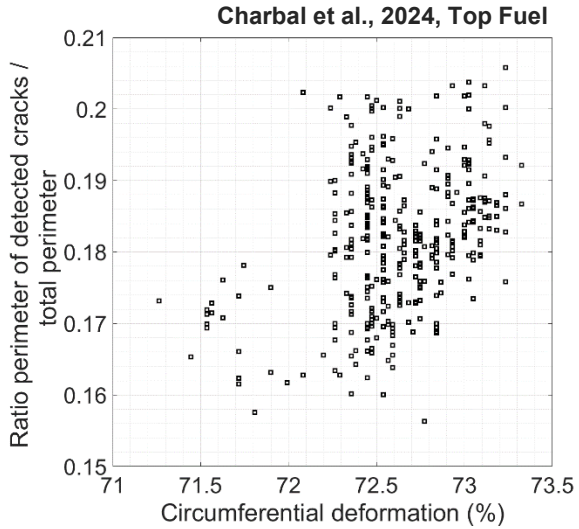

- Use of image processing (here “homemade codes” via Matlab)
- Satisfactory detection rate but still need to improvements
- Machine learning as a solution → needs extra work (vs. Optical Microscopy Images)
- Need same to perform same analysis on various hoop strain levels

Cracking quantification on larger volumes (~490 mm)

Large amount of information could be obtained with a lesser preparation effort!

Automated counting

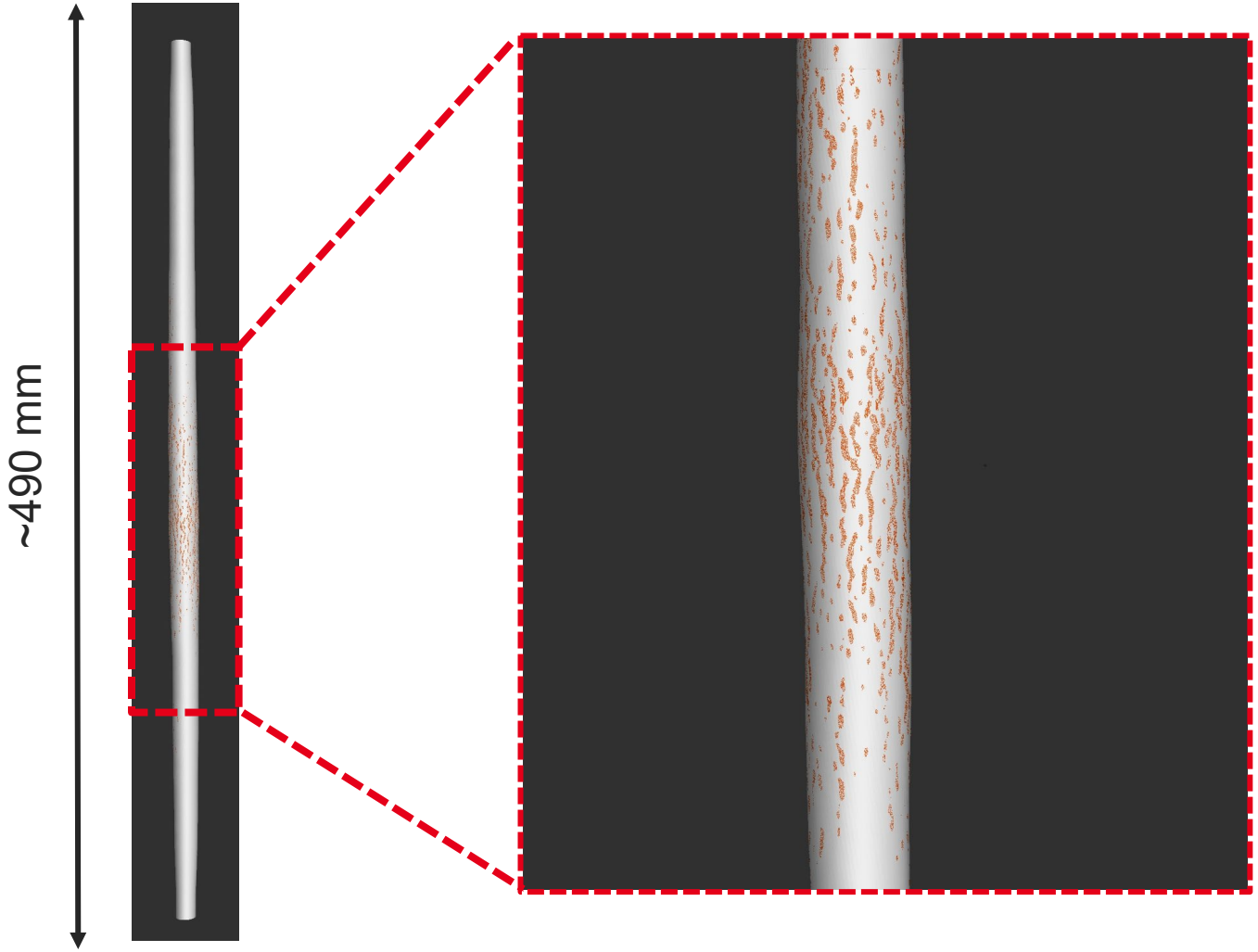

First few results show higher ductility of Cr

No cracking detected below 30-40 % at high temperatures

Automated counting

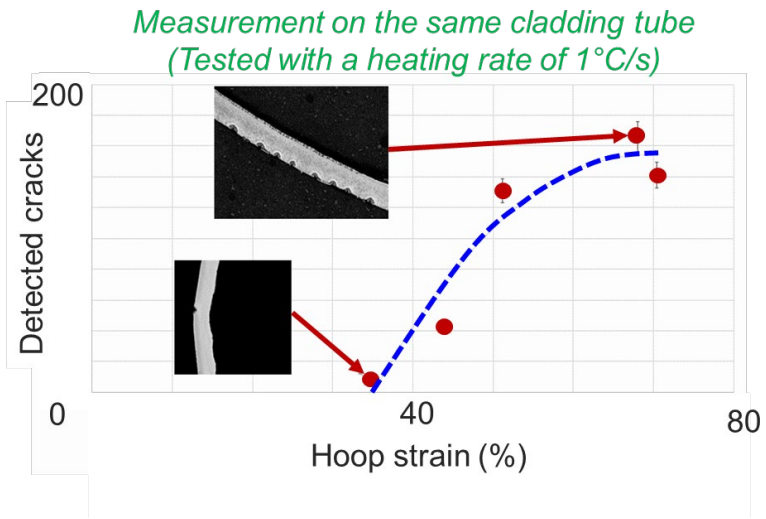

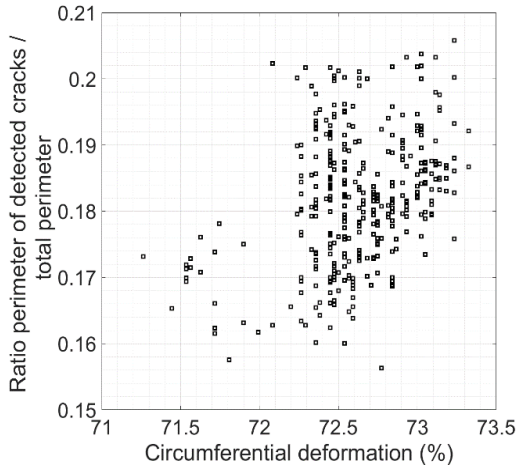

- Use X-ray tomography results to provide damage quantification as a function of hoop strain
- Clear gain in ductility is observed for the chromium coating, with no detected cracking below ~30-40 %

→ **Need to perform a parametric study to confirm the gain in ductility as a function of temperature**

Uniaxial mechanical testing on as-received samples

Temperatures range from ambient to 550 °C

Uniaxial testing machine – *non-irradiated samples*

- Facility provides the capacity to perform **uniaxial testing** (biaxality ∞) **at temperatures from -20°C to 700 °C :**
- **Extensometer:** axial extensometers for monitoring axial deformation
- **Camera with intermediate magnification lens:** capture images of the sample outer layer and determine strain fields and cracking
- **Acoustic Emission sensor** monitoring cracking by detecting the emitted sound

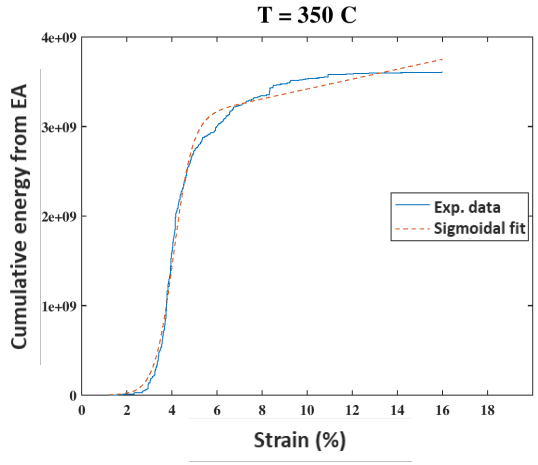

Y. Taïbi, et al. , 2024, NUMAT

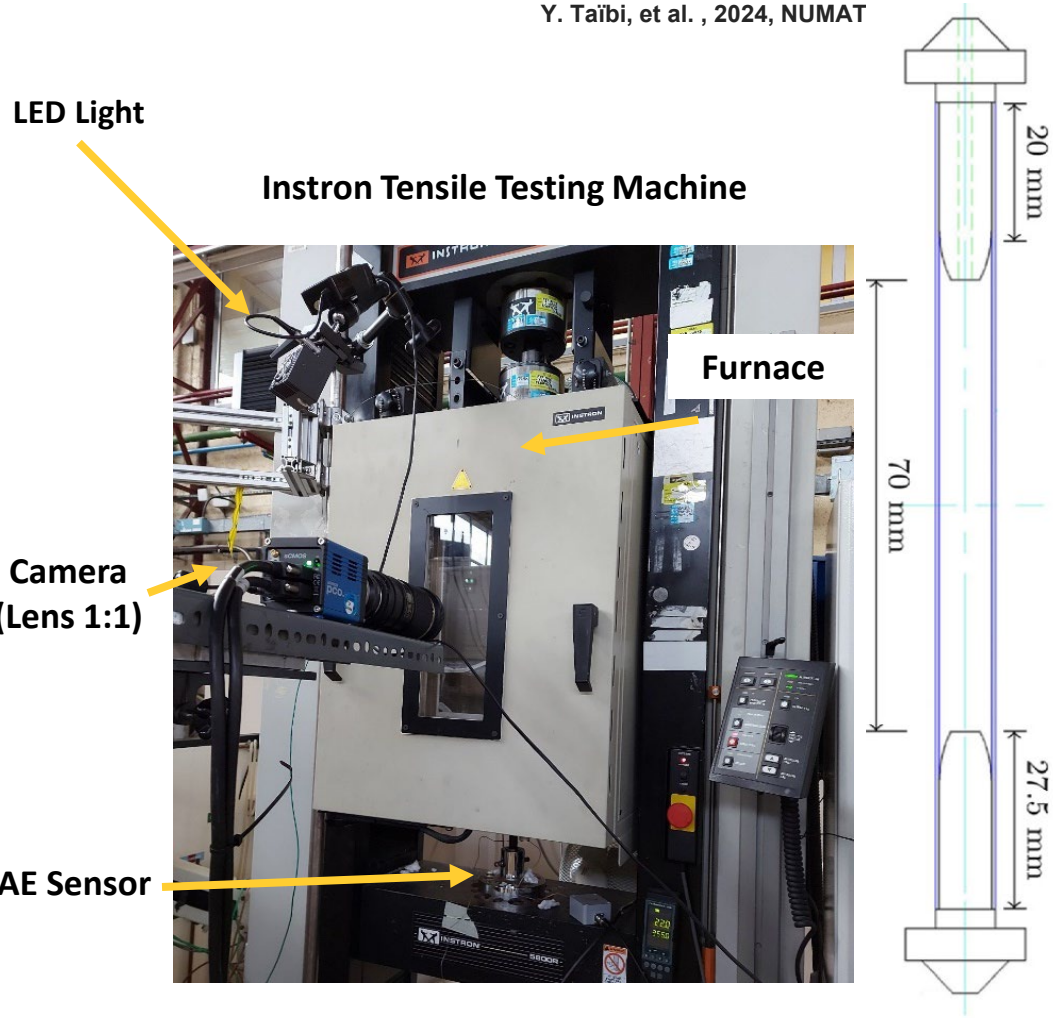

Chromium ductility increases with temperature

Cracking was not detected by AE above 410 °C (up to 20-30 % axial strain)

Critical strain vs. T

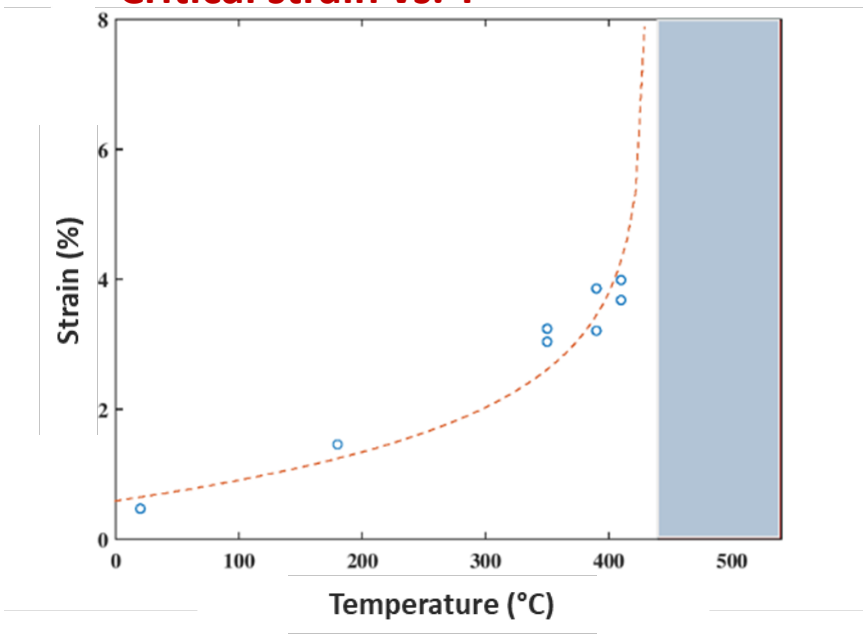

Crack density vs. T

Y. Taïbi, et al. , 2024, NUMAT

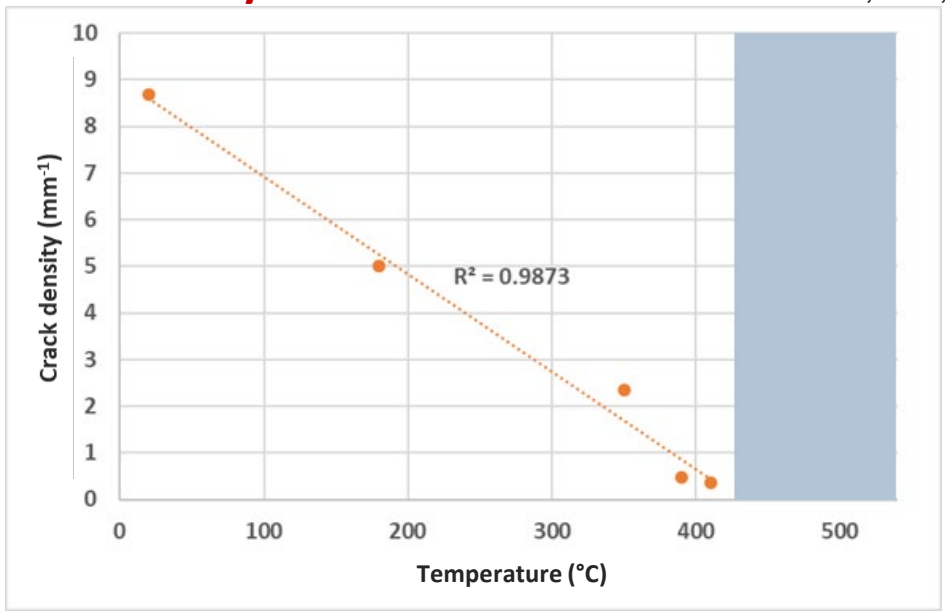

- The critical strain (to cracking) increases exponentially with temperature
- The crack density decreases linearly with temperature (up to 20-30 % axial strain)

Chromium ductility increases with temperature

No coating spallation after cracking

Y. Taïbi, et al. , 2024, NUMAT

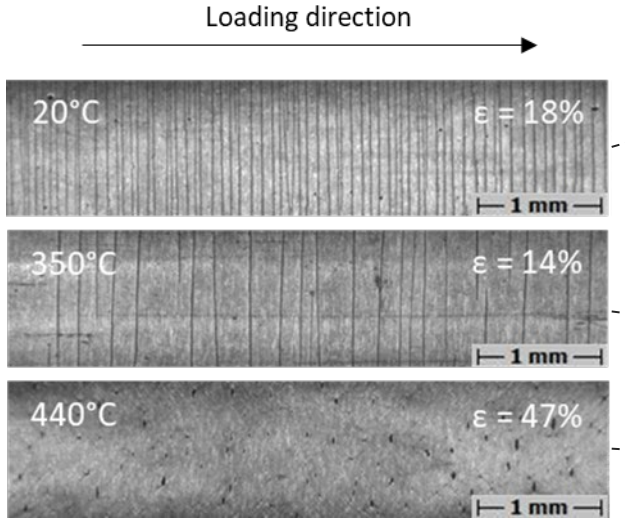

Crack density vs. T

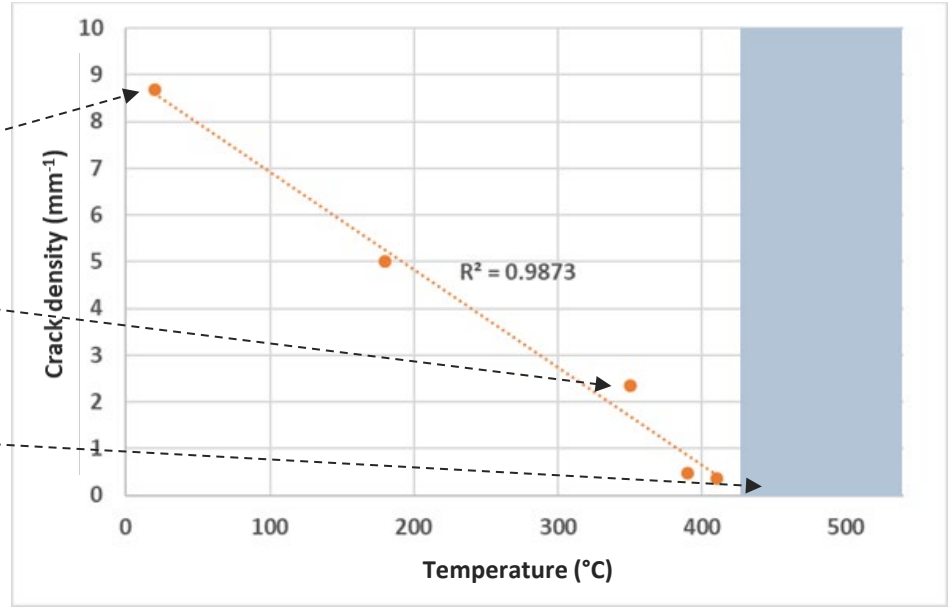

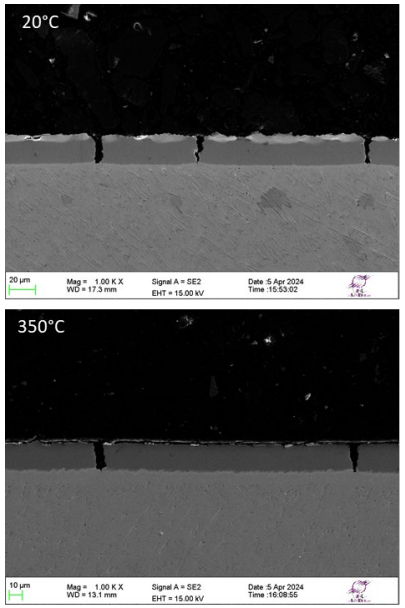

! No desquamation !

- Post-mortem observations on samples tested at 440°C shows some surface damage (crack initiation?)
- Post-mortem section analyses indicate the coating remains adherent to the substrate

Conclusions and prospects

- **EDGAR (LOCA) testing concluding remarks :**
  - ✓ Optical Microscopy provides high image quality and exploitable data for machine learning : requires preparations
  - ✓ X-ray Tomography provides lot of information at the volume scale with less preparations efforts than OM : requires more data processing due to lower spatial resolution and image quality (contrast)
  - ✓ Larger volume could be scanned (cladding tubes of ~50 cm length)
  - ✓ Post-mortem inspections indicate higher Cr-coating ductility (vs. 20° C for instance)
  - ❑ Need more volumetric analyses to enrich the database to provide crack density as a function of strain
  - ❑ Perform some comparisons with optical images (finer resolution) to determine the detection limit

Conclusions and prospects

- **EDGAR (LOCA) testing concluding remarks :**
  - ✓ Optical Microscopy provides high image quality and exploitable data for machine learning : requires preparations
  - ✓ X-ray Tomography provides lot of information in volume scale with less preparations efforts than OM : requires more data processing due to lower spatial resolution and image quality (contrast)
  - ✓ Larger volume could be scanned (cladding tubes of ~50 cm length)
  - ✓ Post-mortem inspections indicate higher Cr-coating ductility (vs. 20° C for instance)
  - ❑ Need to perform more volumetric analyses to enrich the database to provide crack density as a function of strain
  - ❑ Perform some comparisons with optical images (finer resolution) to determine the detection limit

- **Critical strain (axial) to cracking as a function of temperature (on non-irradiated sample):**
  - ✓ Uniaxial tensile testing combined with AE could be used to determine the cracks formation with applied strain
  - ✓ The critical strain to detect the first cracks increases with temperature (~3 % at 350°C vs. >20-30% at 550°C).
  - ✓ The parametric uniaxial study confirmed the gain in ductility (observed for T>550°C) of the chromium coating
  - ❑ The same methodology could be applied for various coating technologies/thicknesses
  - ❑ The same methodology could be applied to study other parameters (irradiation effects, heat treatments effects etc.)

Summary

I. Introduction

II. Macroscopic approaches for coated cladding testing
   i. Ballooning/Burst testing : post-mortem methods for chromium coating cracking quantification
   ii. Tensile testing : in situ methods for chromium coating cracking evolution *(Y. Taïbi, PhD Thesis)*
   iii. Conclusions and prospects

III. Microscopic approaches for coating characterization *(Y. Taïbi, PhD Thesis)*
   i. Micro-cantilever testing : *toward fracture toughness measurements*
   ii. Micro-pillar testing : *toward elastoplastic behavior determination*
   iii. Conclusions and prospects

Cr coating *micromechanical characterization*

Coating with particular microstructure due to deposition process

HIPIMS PVD process

Brachet et al., 2017, WRFPM

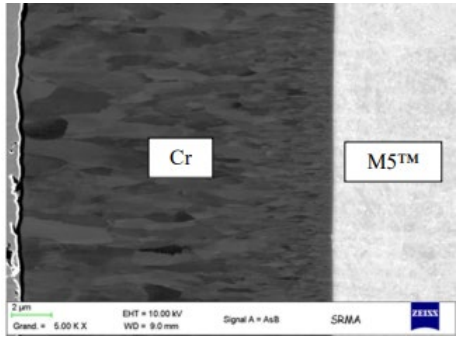

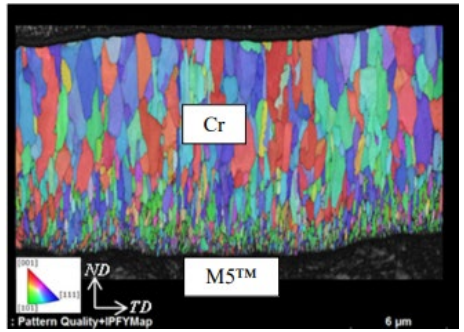

- Typical chromium coating thickness range: **5-30 µm**
- Zirconium alloys substrate:
  - Diameter 9,5 mm
  - Thickness 0,580

Cr coating *micromechanical characterization*

Coating with particular microstructure due to deposition process

HIPIMS PVD process

Brachet et al., 2017, WRFPM

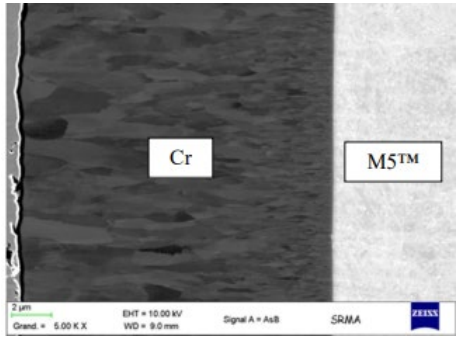

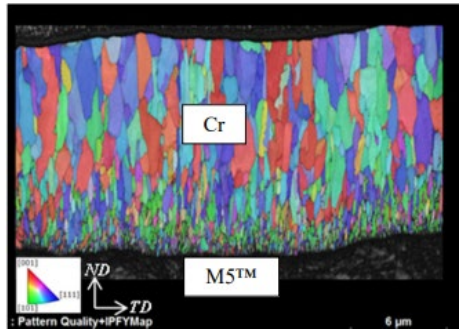

- Typical chromium coating thickness range: **5-30 µm**
- Zirconium alloys substrate:
  - Diameter 9,5 mm
  - Thickness 0,580

Microcantilever

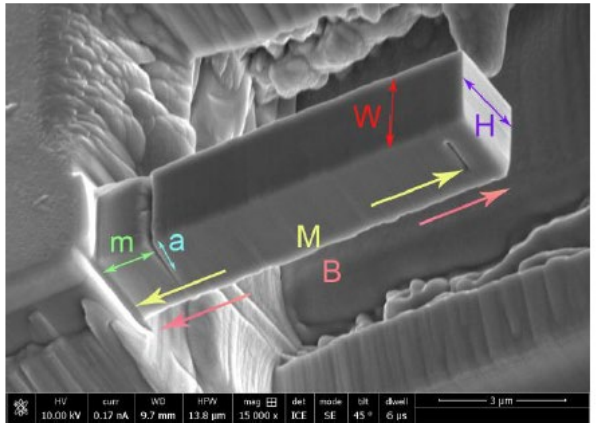

- Example of a machined cantilever within the coating thickness
- Possibility to work at temperature
- Possibility to use SEM imaging tools during the testing

Toward fracture toughness measurements

Coating tested at room temperature

Post-testing image :

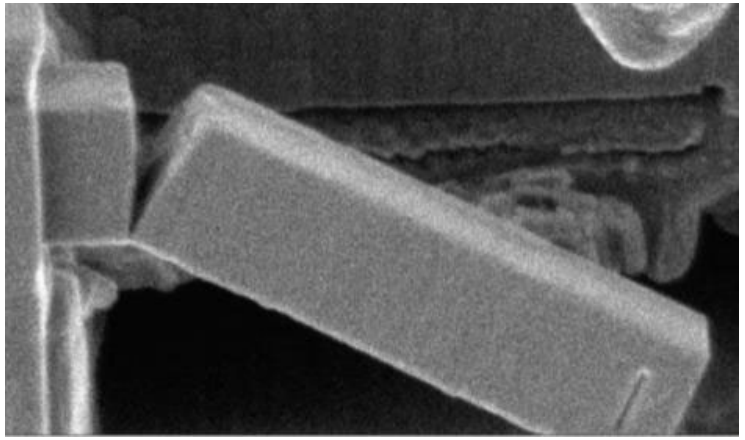

Load-displacement :

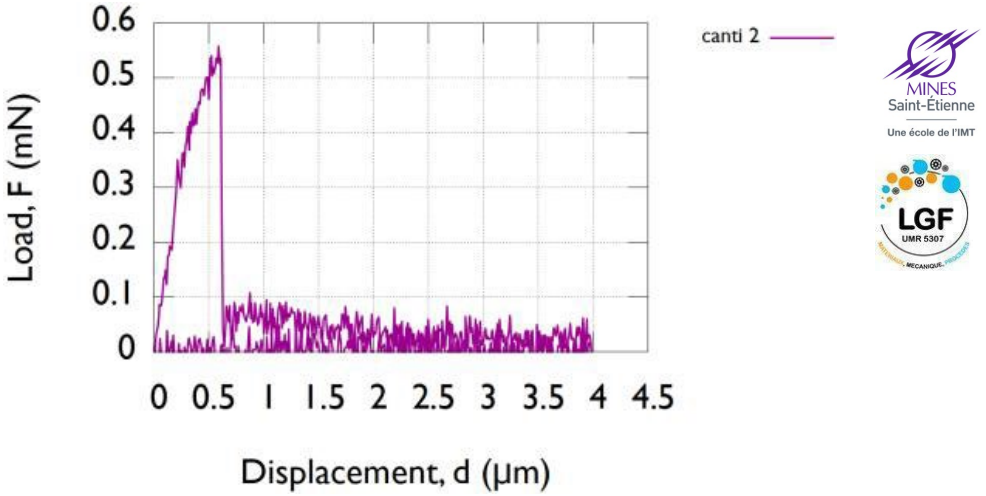

- Machining is performed using Focused Ion Beam
- Tested dimensions : ~ 10 x 2 x 2 µm3
- Pre-cracking was machined

- Load / displacement indicates quasi-brittle behavior (20°C)
- Fractured interface indicates also quasi-brittle behavior (20°C)

Toward fracture toughness measurements

Coating tested at room temperature

Images during various loading steps:

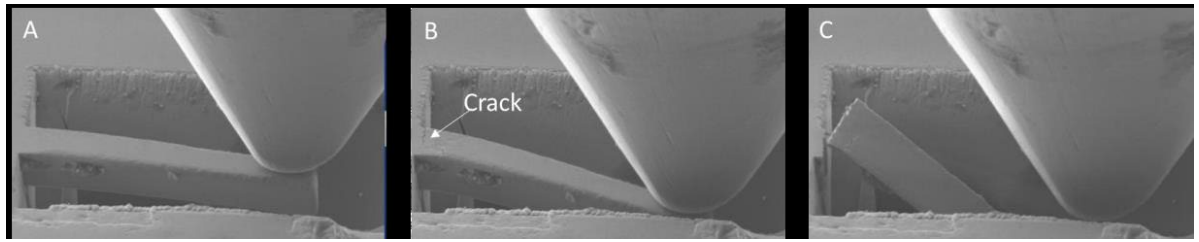

Load-displacement :

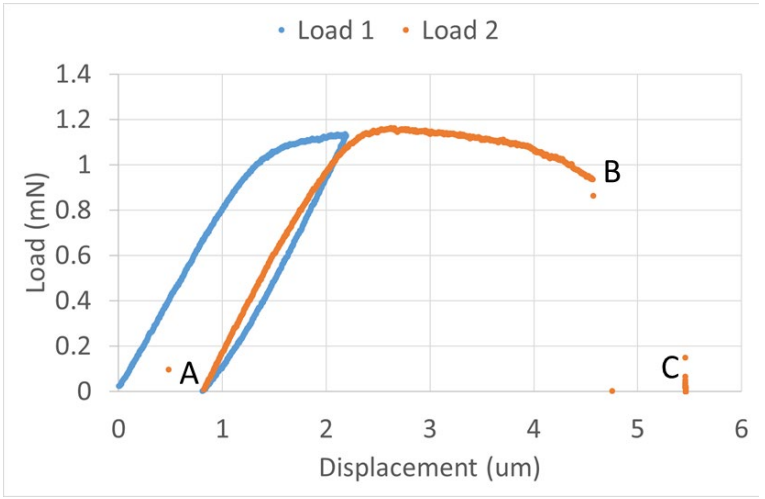

- Machining is performed using Focused Ion Beam
- Tested dimensions : ~ 10 x 2 x 2 µm3
- No - pre-cracking was machined
- Two cycles were applied

- Load / displacement indicates quasi-brittle behavior (20°C)
- Fractured interface indicates also quasi-brittle behavior (20°C)

Toward elastoplastic behaviour determination

Coating tested at room temperature and 350 °C

Post-testing image :

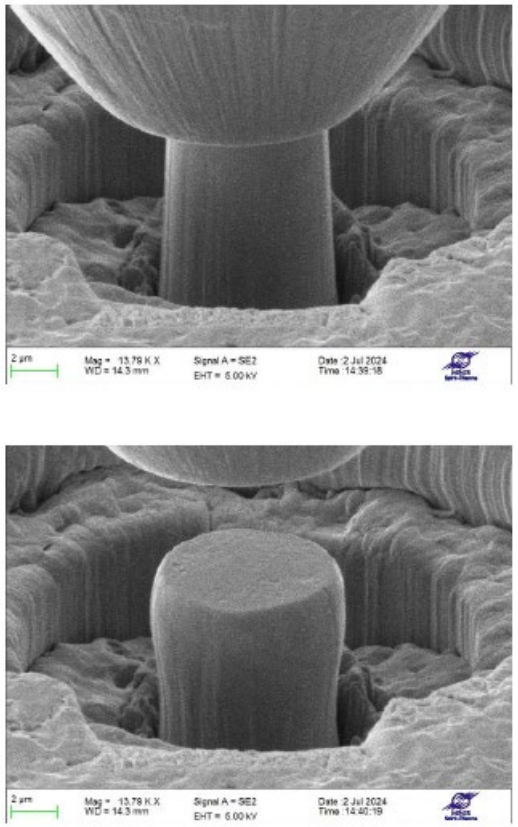

Load-displacement :

Y. Taïbi, et al. , 2024, NUMAT

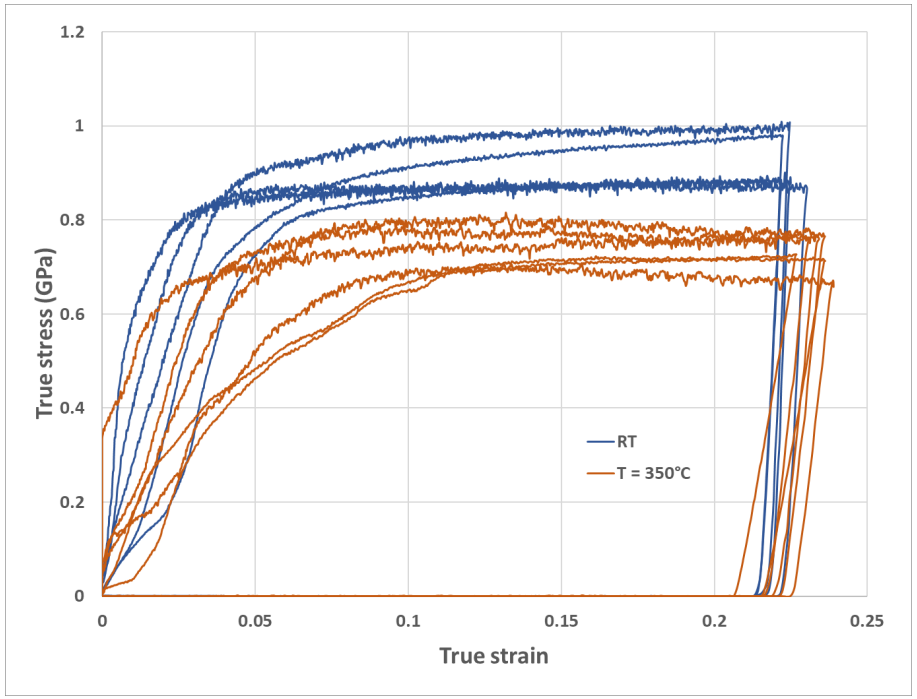

- Stress / strain curves can be derived
- Yield limit can be estimated (*not the elastic modulus*)
- Tests can be performed at various temperatures

Gregor Stahlberg

RUB

Current Progress and Testing of AC² at PSS focusing on ATF: Chromium Coating during Postulated SA within QUENCH facility and iPWR

Research indicates that alternative materials could improve safety in nuclear power plants. Current developments focus on Advanced Technology or Accident Tolerant Fuel (ATF). Particularly the coating with Chromium (Cr) of existing Zr-alloys enhances resilience during long-term operation or in the event of an accident, compared to commonly used uncoated Zr-alloys.

The main objective of the presented work is the application of a preliminary in-house model for ATF. This model specifically addresses the oxidation of Cr-coated claddings, implemented in a modified version of AC² currently being under development at the PSS Group at RUB. The code package AC² is provided by GRS gGmbH.

In the first part of this work, a large-scale bundle experiment, QUENCH-15, is investigated. It is conducted at the QUENCH test facility of KIT, considering beyond design basis conditions in light water reactors (LWR) with subsequent re-flooding. The sequence consists of pre-oxidation, stabilization, heat-up, transient, and a quench phase. Within the experiment the hydrogen source term is investigated when water or steam is injected into an uncovered and overheated core of a LWR. It is conducted with a Zr-based alloy for the fuel rod simulators, and temperatures around 1880 °C are measured. Thus, severe accident conditions are reached with temperatures beyond the eutectic melting temperature of the binary Zr-Cr system. This marks the very latest failure time for the protective chromium layer. The conducted sequence is calculated as it is. However, the new option for Cr-coating oxidation in AC² is used for fuel rod simulators and shroud, assuming a protective dense chromium layer on the Zr-alloy.

In the second part of this work, a model of a generic integral Pressurized Water Reactor (iPWR) with 160 MWth is assessed regarding the possibility of severe fuel damage during a postulated accident. Due to growing interest in building iPWRs and consequently intensified research on this reactor type, this simulation model is developed using AC² to investigate the code's capabilities for simulating Small Modular Reactor concepts. The accident tolerance during a sequence with postulated failure of selected components is analysed using Zr-alloy as core material. Within a second calculation, the oxidation kinetics of Cr-coating is applied for the same postulated accident sequence. The analyses reveal that applying slower oxidation kinetics results in a small increase in coping time. The results also indicate the need for further code improvements regarding the coating failure model and the influence of higher burn-up. Overall, the generic model of the iPWR shows plausible results.

Acknowledgement

Parts of this work are funded by the European Union. Views and opinions expressed are however those of the author(s) only and do not necessarily reflect those of the European Union or European Commission Euratom.

Neither the European Union nor the granting authority can be held responsible for them.

Parts of this work are funded by the German Federal Ministry for the Environment, Nature Conservation, Nuclear Safety and Consumer Protection (BMUV) under grant numbers 1501682A and 1501629 based on a decision by the German Bundestag. Responsibility for the content lies with the authors.

The results were obtained using the GRS software package AC² 2023 and an in-house version at PSS of the GRS software package AC² 2021.

Current Progress and Testing of AC² at PSS focusing on ATF

Chromium Coating during Postulated SA within QUENCH facility and iPWR

Gregor T. Stahlberg, Marco K. Koch

29th International QUENCH-Workshop | Karlsruhe, Germany | November, 2024

- *Stahlberg, G. T.; Koch, M. K.: Analyses of an integral Pressurized Water Reactor during postulated Accident Conditions using AC² - Extending AC² Capabilities for Accident Tolerant Fuel (ATF). NUTHOS-14, Vancouver BC, August 2024.*
- *Hollands, T.; Stahlberg, G. T.; Gabrielli, F.: Simulation of QUENCH-03 and -15 Scenarios with the Code AC² modified for Cr-coated Claddings compared with ASTEC. 28th International QUENCH Workshop, December 2023.*

PSS Plant Simulation and Safety
Prof. Dr.-Ing. Marco K. Koch

MOTIVATION AND OBJECTIVE

Postulated plant accidents with fuel damage – coping time

- Assessment of simulation models of a PWR using ASTEC and AC²
  - ↳ Unmitigated accident may lead to fuel exposure and severe damage

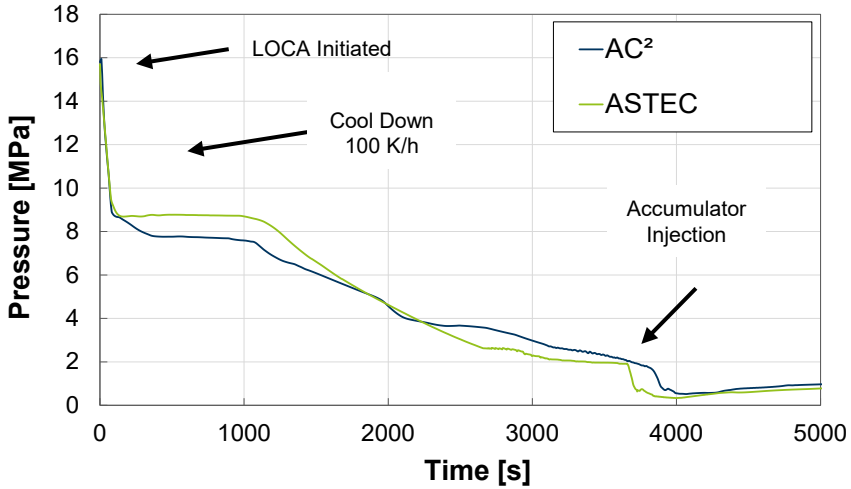

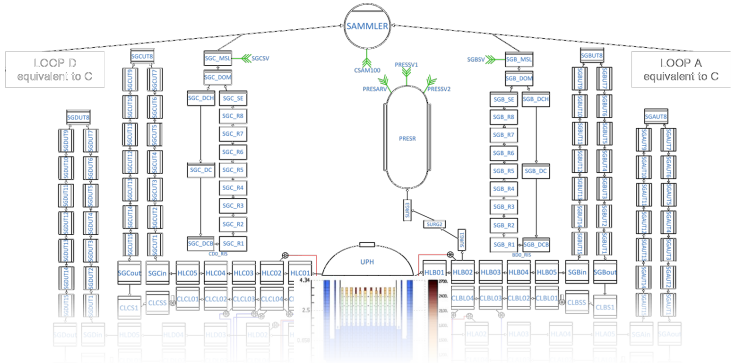

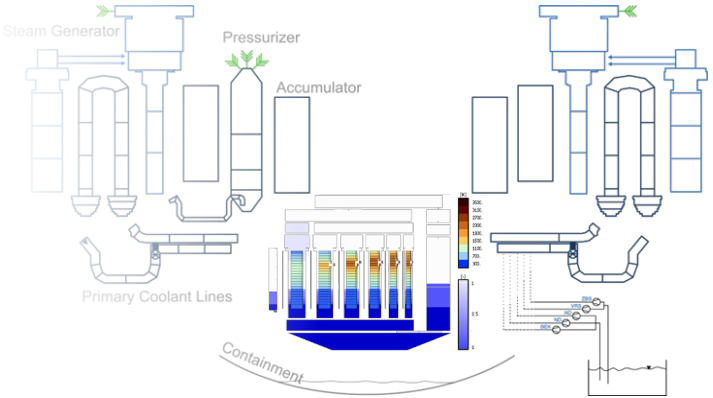

Motivation and Objective
Advanced Technology Fuel

- Analysis of technologies that specifically target improved accident behavior
- Reduce potential hydrogen and heat release, that must be removed by cooling systems (i.e. Emergency Core Cooling System) in the event of incidents or accidents → coping time!
  - Testing of new correlations for **FeCrAl alloy** based on publications by KIT
  - Development of preliminary model for oxidation of **Cr-coated claddings** available as new option for AC² at RUB PSS (ongoing development)

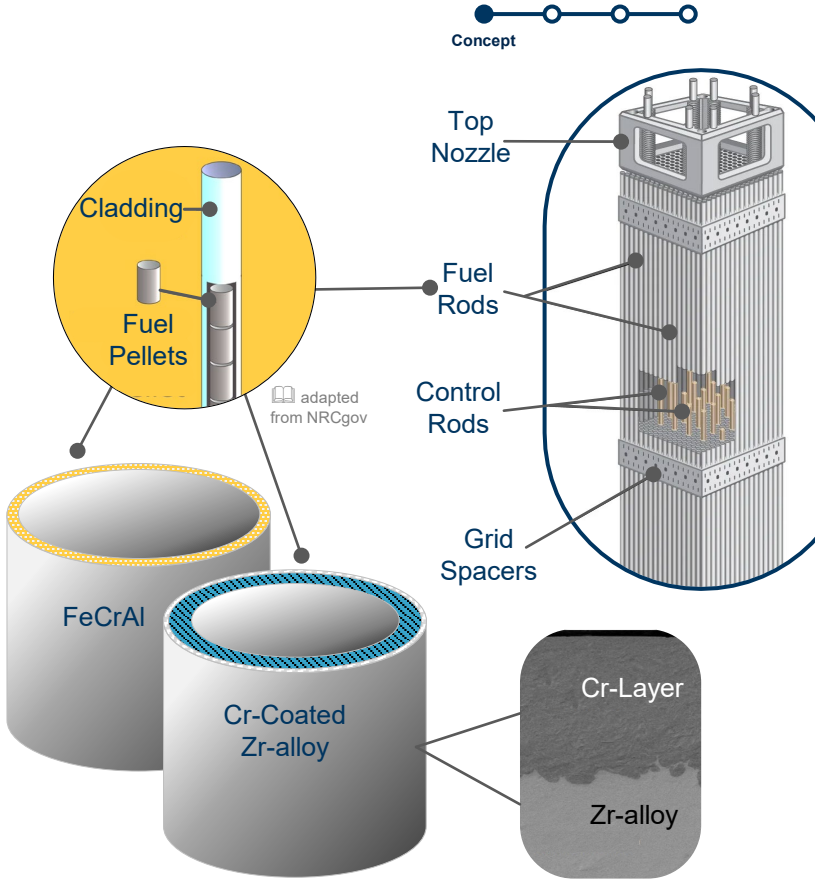

Motivation and Objective
Model Development

Current Status

ATF-Oxidation	**Model Option**
Current AC² release	
↳ Iron-Chromium-Aluminum (FeCrAl)	20/21
↳ User Input (FeCrAl-Alloys)	22
Validation: QUENCH-19	

AC² in-house version at PSS

↳ **New** Model for Chromium-Oxidation for ATHLET/CD modules

Validation: QUENCH-ATF-1 and prospectively -ATF-2
CODEX-ATF work in progress

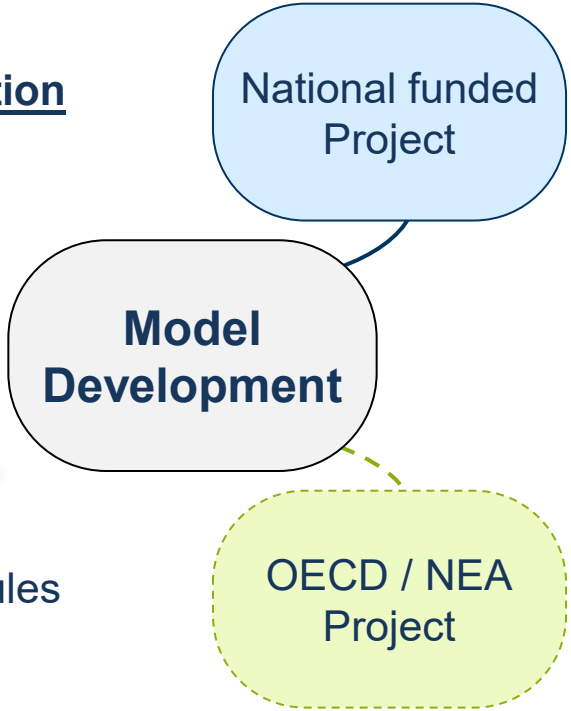

Motivation and Objective
Model Development

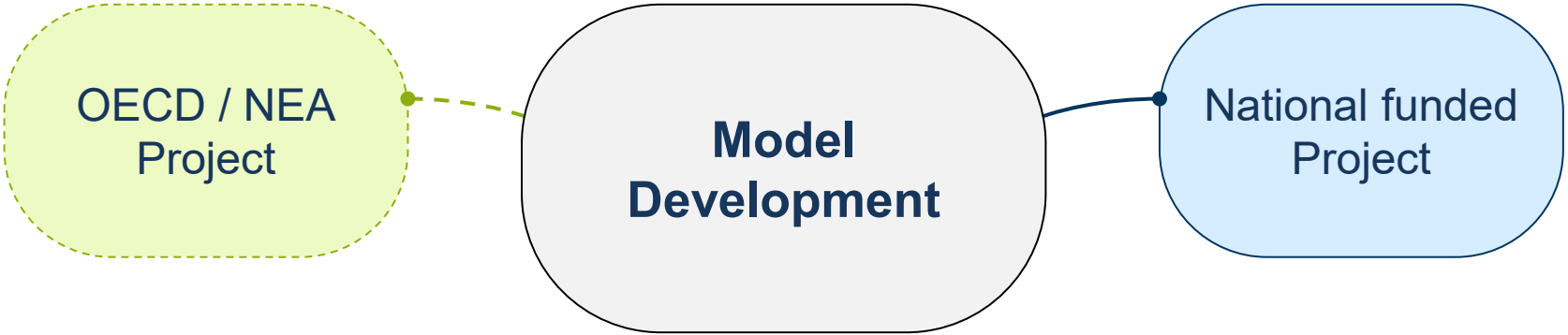

Accident-tolerant fuel (or advanced technology) concepts are presumed to increase the coping time and to reduce the load on Emergency Core Cooling Systems (ECCS) during an accident by minimizing the total amount of heat generated (e.g. through oxidation)

How to describe and model ATF behavior?

ADVANCED TECHNOLOGY FUEL

FeCrAl alloy | Cr-Coated Zr-alloy

- Coating as diffusion barrier, protecting substrate material (e.g. Zr-alloy)
- Chromium (III) oxide layer (Cr_2O_3) is characterized by low weight gain
- Corrosion resistance / protective scale influenced by several parameters
  - Microstructure (deposition technology)
  - Applied uniform layer thickness
  - Degradation mechanisms
  - **Transient Boundary Conditions**
    - Heating rate
    - Temperatures (PCT)
    - Duration

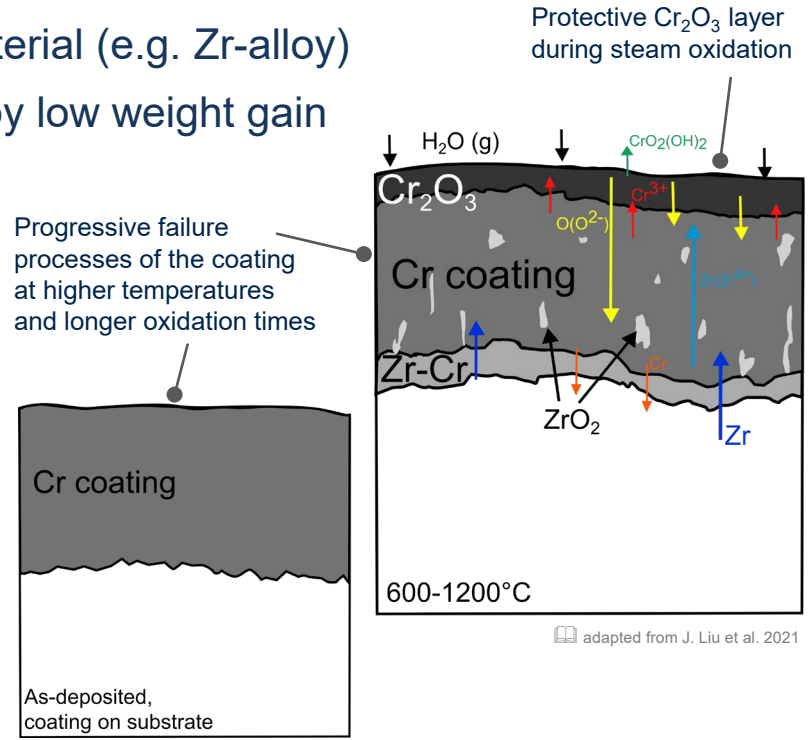

ATF FOR QUENCH TEST

FeCrAl alloy | Cr-Coated Zr-alloy

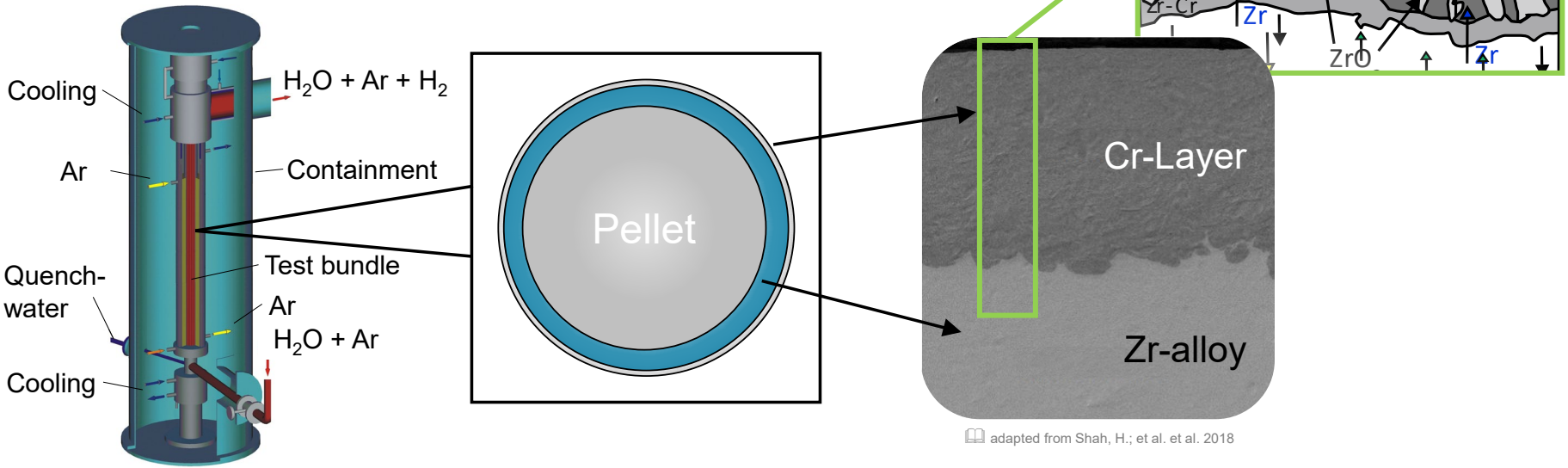

adapted from Shah, H.; et al. et al. 2018

MODELING
Current correlations under investigation

- Cr-Correlation is based on exp. data from Brachet et al. 2020, assumed to have best agreement with the behavior of current coating generations
  - Transition from Cr → Zr after asssumed coating failure at variable (user) temperature
  - Heat of oxidation depends on temperature region
  - Inner oxidation after burst under investigation

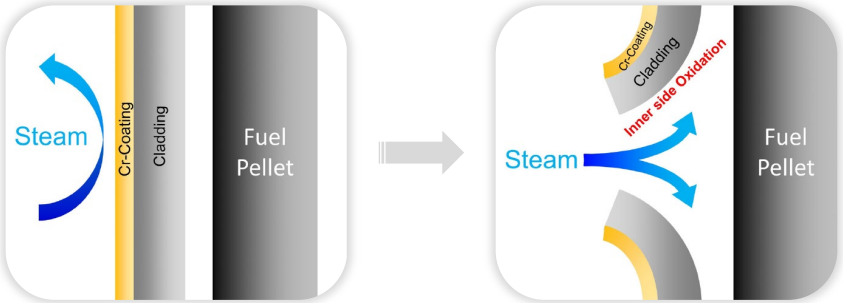

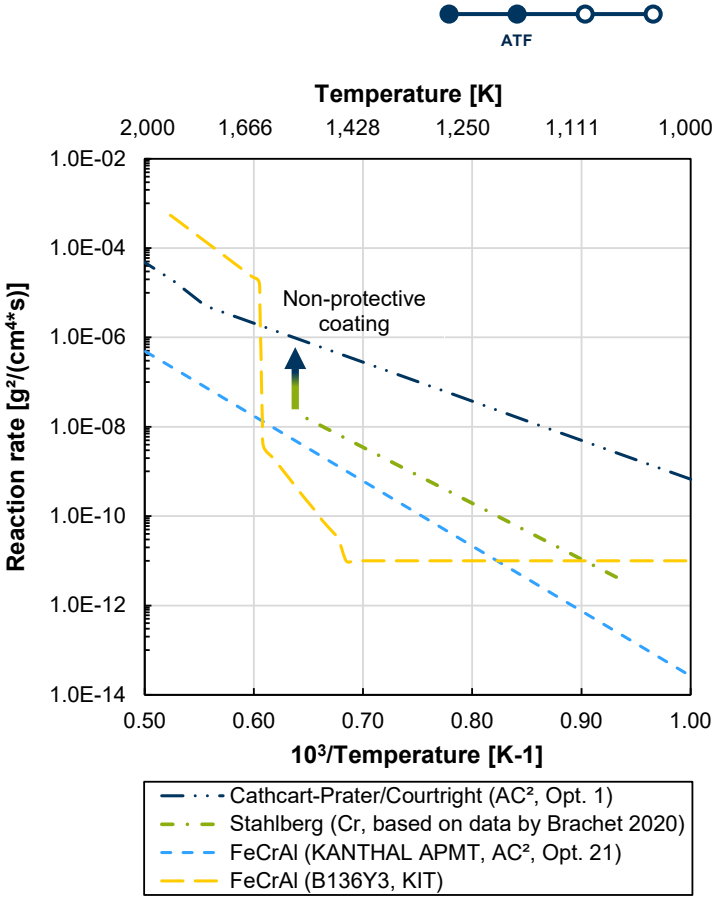

MODELING

Calculated weight gain at 1,200°C

- Calculated mass gain curve shows good agreement at 1,200°C
  - Calculated mass gain tends to be slightly overestimated; most data are captured adequately (few outliers)
  - Coating failure seems to occur for some isothermal tests around ~5,000 s

Different experimental settings and different deposition technologies may involve uncertainties.

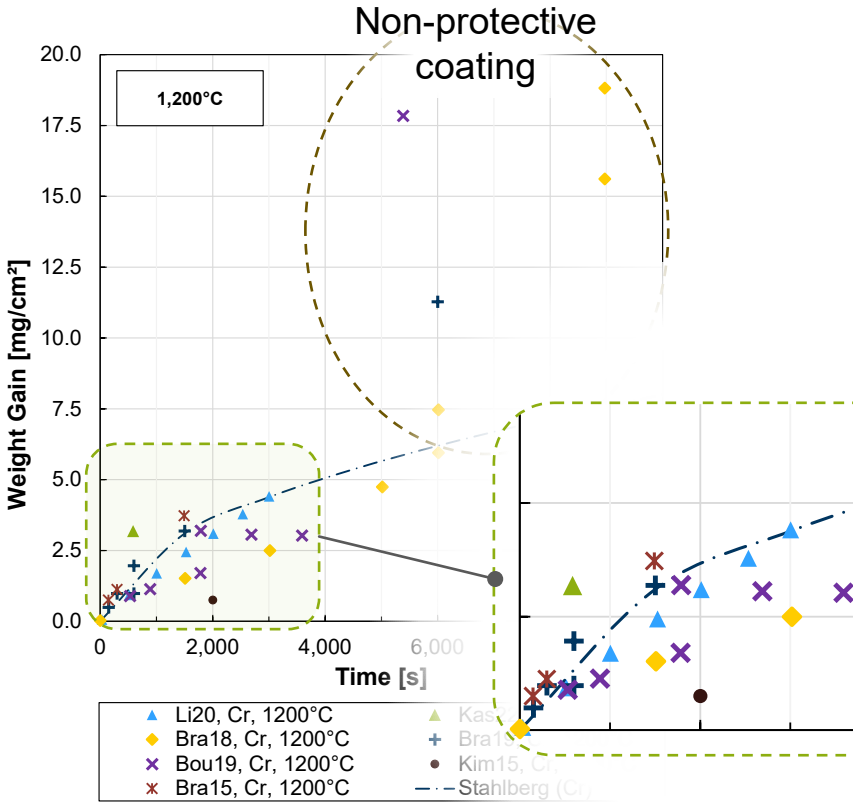

Application to QUENCH facility

MODELING
Cr-Oxidation applied to QUENCH-15 simulation model

- 1 Thermo Fluid Object as BUNDLE with 3 modelled rings as ECORE RODs (4 / 12 / 8)
- Coating applied to relevant components, Zr for spacer as well as coated components at higher temperatures (different cases with assumed failure at different temperatures)

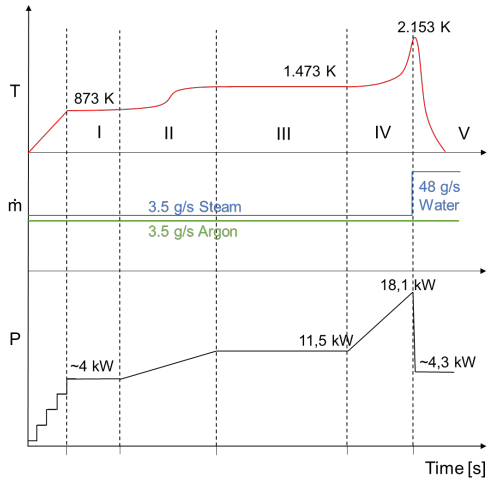

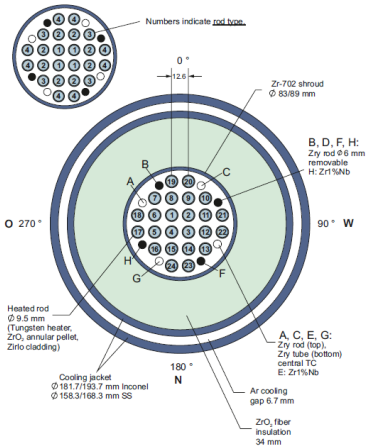

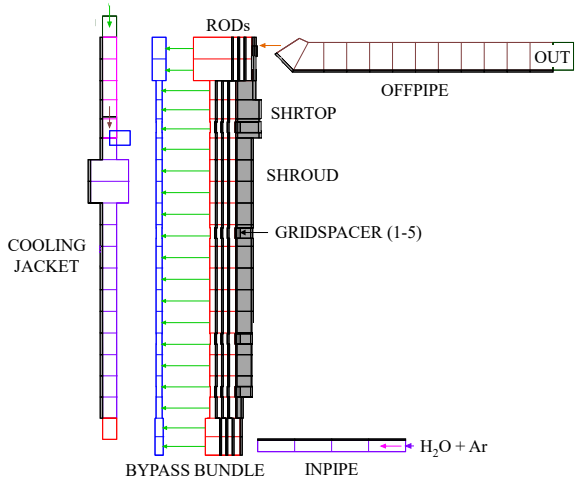

Hollands, T.; Stahlberg, G. T.; Gabrielli, F.: *Simulation of QUENCH-03 and -15 Scenarios with the Code AC² modified for Cr-coated Claddings compared with ASTEC. 28th International QUENCH Workshop, December 2023.*

RESULTS

Cr-Oxidation applied to QUENCH-15 simulation model: 850 mm

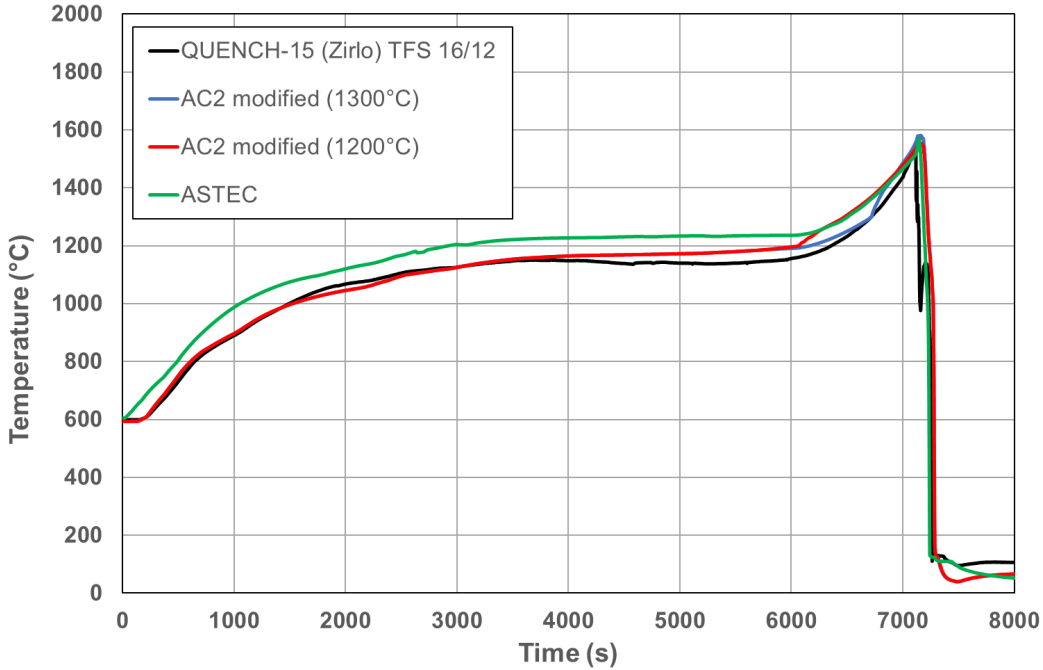

- Comparison between runs with different cladding: Zry and ATF
- All simulations reach the transition temperature to accelerated Zr oxidation
- The predicted temperatures for Cr-coating are comparable to original QUENCH-15 ZIRLO behaviour

Hollands, T.; Stahlberg, G. T.; Gabrielli, F.: *Simulation of QUENCH-03 and -15 Scenarios with the Code AC² modified for Cr-coated Claddings compared with ASTEC. 28th International QUENCH Workshop, December 2023.*

RESULTS

Cr-Oxidation applied to QUENCH-15 simulation model: Hydrogen

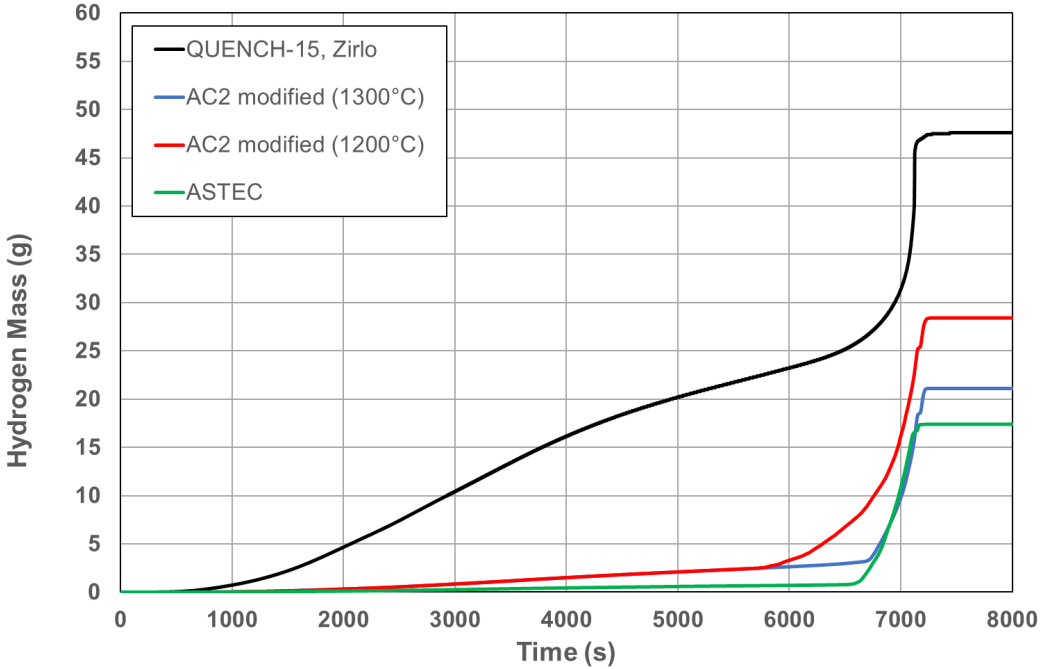

- H_2 mass lower than QUENCH-15 despite similar temperature evolution
- Pre-oxidation: less H_2 generated with Cr-coated components
- H_2 increase closely linked to transition temperature in simulations
- Post Cr-coating failure: higher H_2 generation vs pre-oxidized ZIRLO

📖 Hollands, T.; Stahlberg, G. T.; Gabrielli, F.: *Simulation of QUENCH-03 and -15 Scenarios with the Code AC² modified for Cr-coated Claddings compared with ASTEC. 28th International QUENCH Workshop, December 2023.*

RESULTS
Current Results (2024): Hydrogen

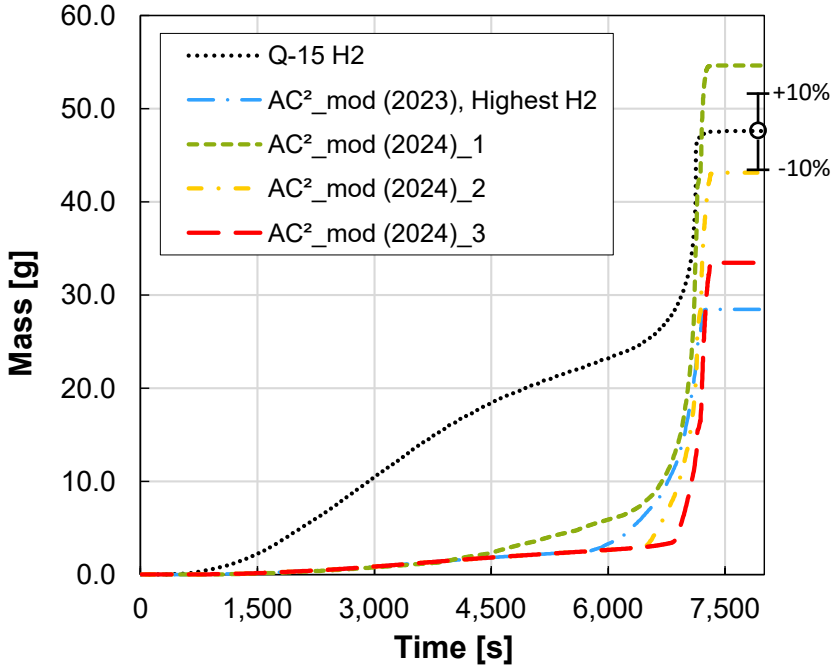

- Failure of the coating at > 1250°C is realistic considering experimental data (however strongly connected to coating condition, i.e. quality, so it depends…)
- H_2 masses varying from 14% more to -30% less than QUENCH-15, still similar temperature evolution
- Still, less H_2 generated with Cr-coated components during pre-oxidation and linked to transition temperature
- Post Cr-coating failure: very intense H_2 generation vs QUENCH-15 with Zry

Plant Application

MODELING
Plant Modeling: using AC² TFD module

- Simulation model of a generic integral PWR modelled with AC² based on public information

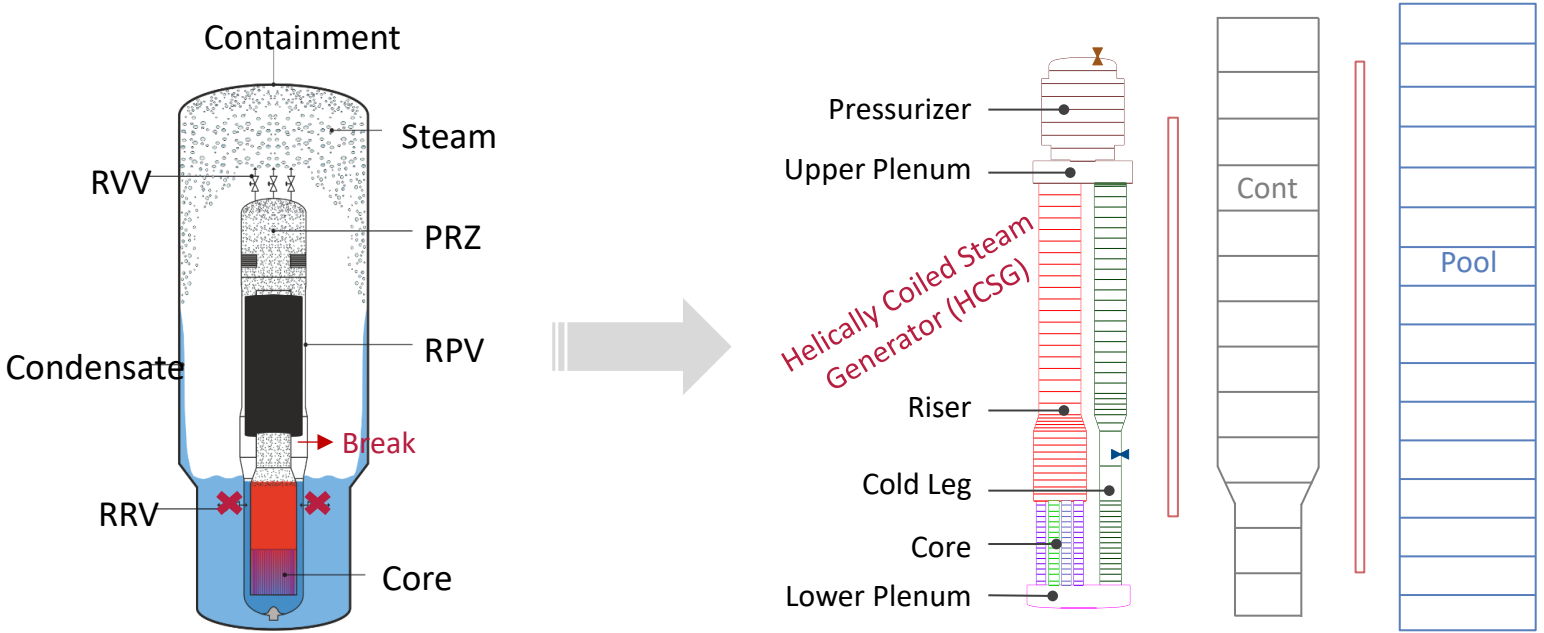

MODELING

Plant Modeling: using AC² Core Degradation module

AC² modeling

- Four Thermo Fluid Objects as radial rings (fractions of CR/FR assigned to sections)
- Modules for nuclide inventory / decay heat and FP behavior (+ transport)
- Late phase phenomena, melt
- *Containment phenomena (thermal hydraulics, fission products)*

AC² modules

ECOREMOD

OREST/FIPISO

AIDA

COCOSYS

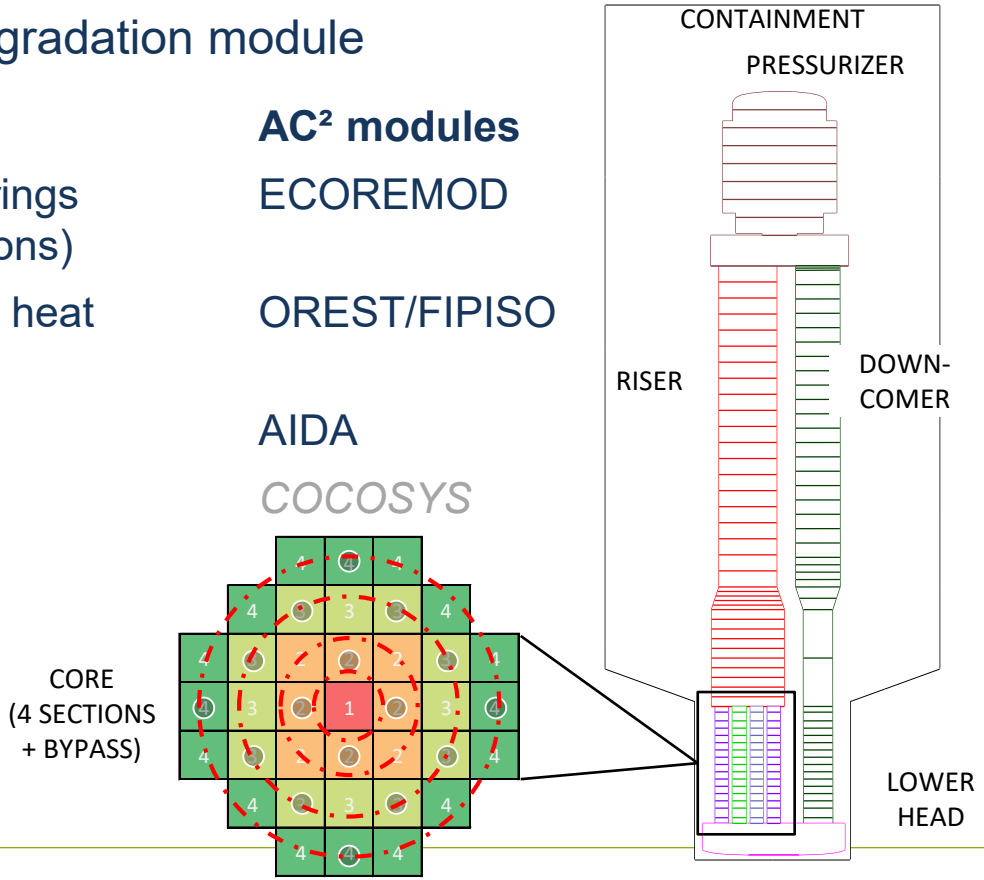

RESULTS

Postulated Severe Accident in integral PWR: Cr-coated Zry

- Stationary phase calculated plausibly, 160 MW_{th}
- Comparison between runs with different cladding: Zry and ATF
- Blowdown Phase after break opening leads to immediate pressure drop
- Pressure alignment in compart-ments through break: containment and primary circuit

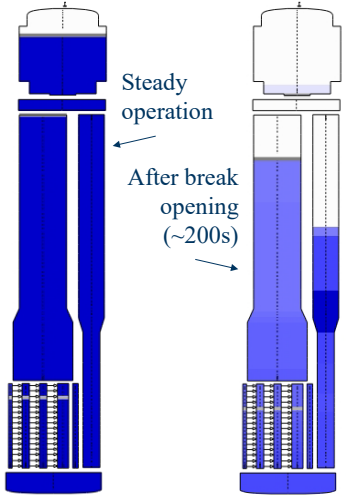

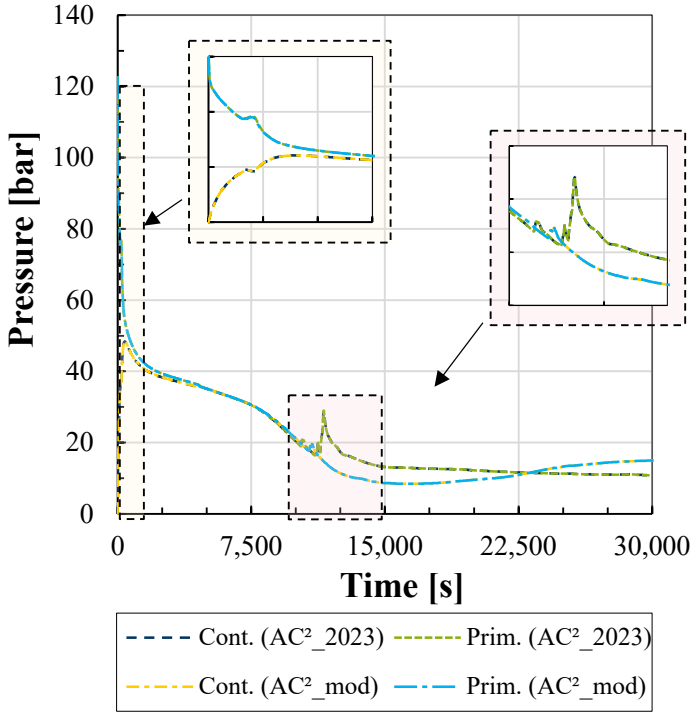

RESULTS

Postulated Severe Accident in integral PWR: Cr-coated Zry

- Evaporation increases as oxidation heat is absorbed by the coolant
- ATF results in less evaporation and faster pressure decrease
- Heat release start is delayed in run with Cr-coated cladding
- Zr-based cladding calculations show higher heat release compared to Cr-coating
- Oxidation-generated heat flow depends on the oxidized metal mass

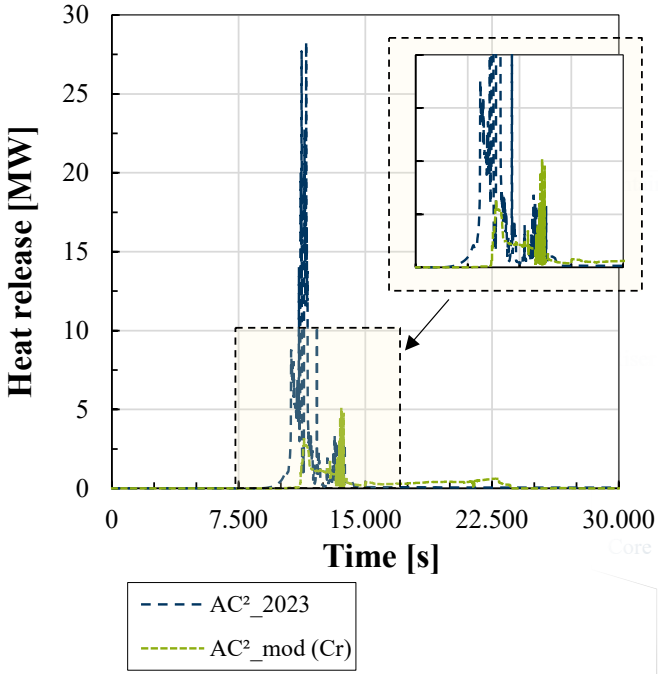

RESULTS
Postulated Severe Accident in integral PWR: Cr-coated Zry

- Preliminary results with new option for Cr-coating

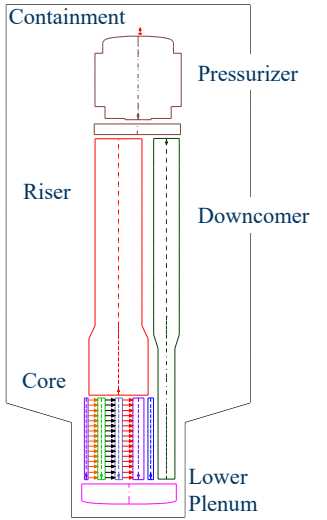

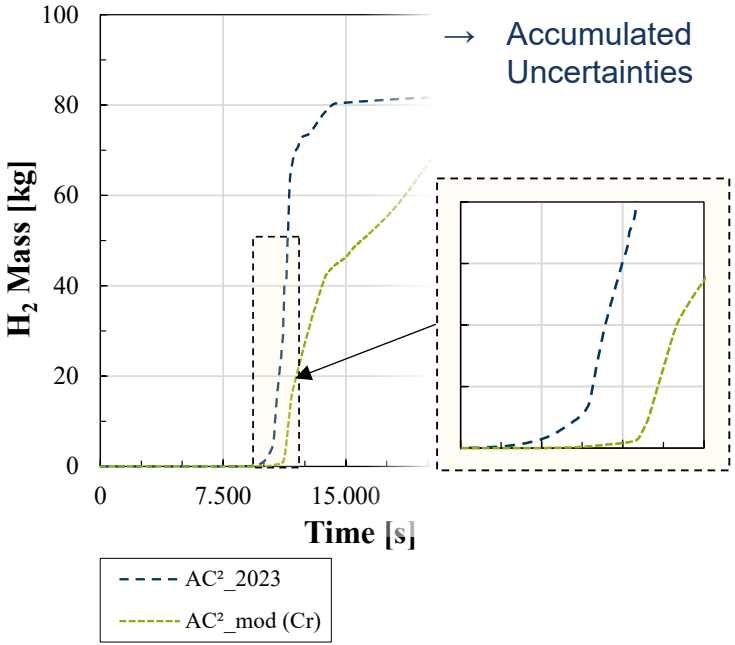

- Protection against oxidation under normal operating conditions by forming dense oxide layer
- Delayed onset of fuel degradation
- Interaction Cr/Zr and transient conditions can cause early failure
- Further research is needed to address challenges like the eutectic reaction and early failure
- Analyses regarding hydrogen mass in containment under investigation (afterwards)

Thank you for your attention!

Gregor T. Stahlberg
Stahlberg@pss.rub.de

RUHR-UNIVERSITÄT BOCHUM
PSS Plant Simulation and Safety
Prof. Dr.-Ing. Marco K. Koch

Building: IC | Floor 2
Universitätsstr. 150
D-44801 Bochum

pss.rub.de

ACKNOWLEDGEMENT

Parts of this work are funded by the European Union. Views and opinions expressed are however those of the author(s) only and do not necessarily reflect those of the European Union or European Commission Euratom.

Neither the European Union nor the granting authority can be held responsible for them.

Funded by the European Union

Parts of this work are funded by the German Federal Ministry for the Environment, Nature Conservation, Nuclear Safety and Consumer Protection (BMUV) under grant numbers 1501682A and 1501629 based on a decision by the German Bundestag. Responsibility for the content lies with the authors.

The results were obtained using the GRS software package AC² 2023 and an in-house version at PSS of the GRS software package AC² 2021.

Supported by:

Federal Ministry
for the Environment, Nature Conservation,
Nuclear Safety and Consumer Protection

based on a decision of
the German Bundestag

Liviusz Lovasz

GRS

ATF Modelling with AC2

The code system AC2 has been developed and optimized for the simulation of processes during normal operation, DBA and BDBA in nuclear power plants using zirconium alloys as cladding material in order to perform safety analysis. In the recent years the interest of using different accident tolerant fuel (ATF) materials to mitigate or eliminate the consequences of a nuclear accident increased. The usage of ATF materials in the core can have a significant impact on the evolution of the accident. To assess the impact of these materials on the accident evolution and thus for safety of the nuclear power plant AC2 had to be extended with dedicated models that consider the effects of ATF materials.

Recent model developments focused on taking the impact of two specific ATF cladding materials into account, chromium-coated zirconium and FeCrAl cladding. The presentation gives a short overview on the changed/improved models for oxidation, material interactions and mechanical fuel rod behaviors, as well as shows some initial validation results of these models. Simulation results of QUENCH-19 experiment are compared and presented to measured values for FeCrAl cladding, while the simulation results of the recently conducted CODEX-ATF-AIT experiment are also presented for the chromium-coated zirconium cladding. There were only small differences between the simulated and measured results of the QUENCH-19 experiment using the improved models of AC2 for FeCrAl cladding material. The experimental results of the CODEX-ATF-AIT test were qualitatively well reproduced with AC2, some quantitative differences were, however, observed.

A short outlook is also given about the future development plans.

ATF Modelling with AC²

Liviusz Lovasz
Gesellschaft für Anlagen- und Reaktorsicherheit (GRS) gGmbH Germany

Quench Workshop, Karlsruhe, Germany
19-21.11.2024

What is AC²?

- AC²= **A**THLET + ATLHET-**C**D + **C**OCOSYS
- Covers the whole spectrum of fault sequences in nuclear reactors

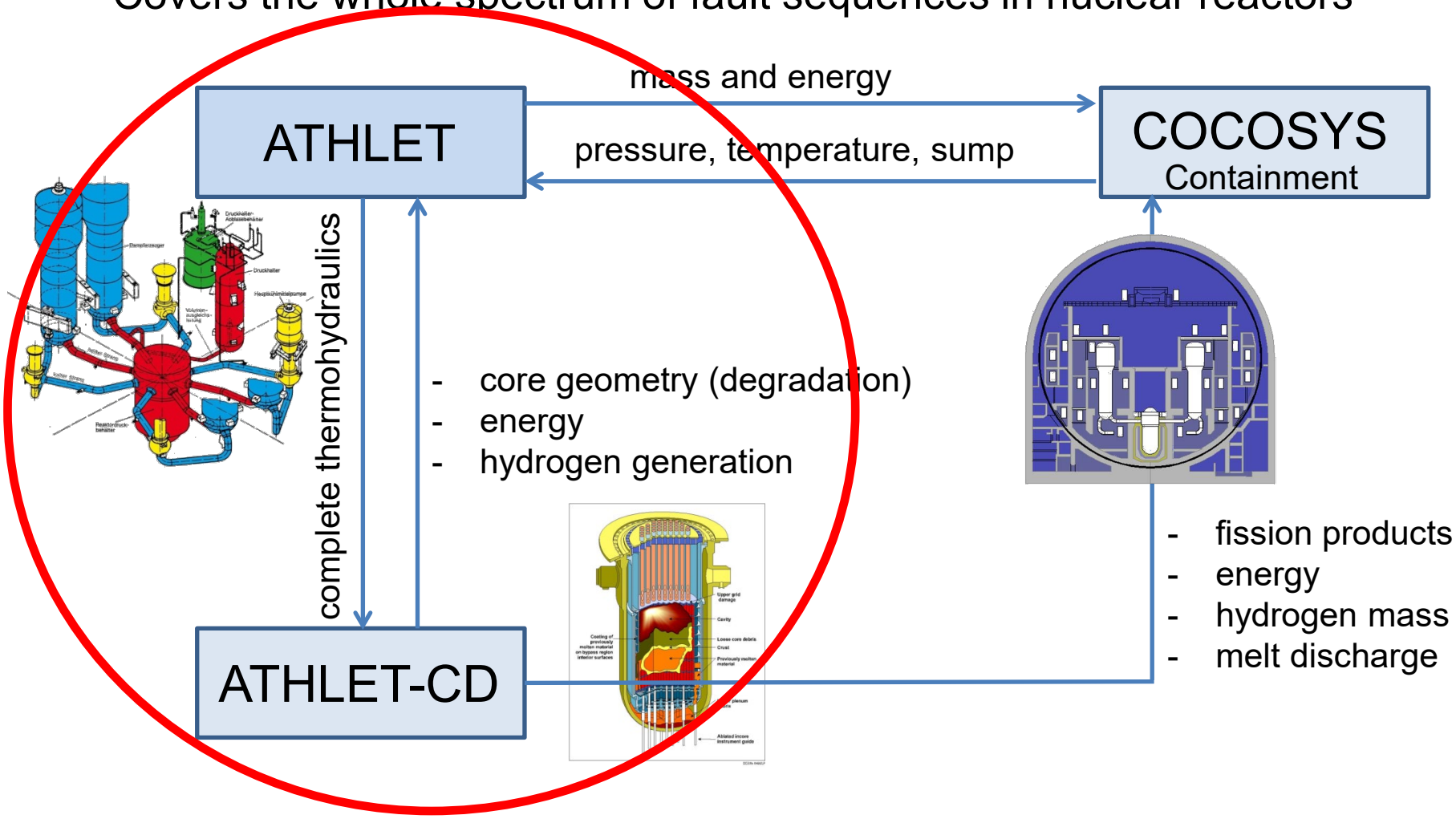

ATF simulation capabilities of AC2

- AC2 was optimized and developed for U-Zr systems
  - Including most phenomena related to ballooning, oxidation, melt relocation, fission product release and transport, lower plenum phenomena
- Using ATF materials can have an effect on all of these phenomena

- Recent developments towards materials of:
  - FeCrAl (GRS)
  - Cr coated Zr (RUB)

- Effects of ATF in AC2:
  - Simple material properties
  - Oxidation
  - Melt formation and relocation

  } These were in the main focus of development

  - Ballooning / mechanical rod behaviour
  - Lower plenum phenomena
  - Burn-up / Fission product release

AC²/ATHLET-CD – FeCrAl Oxidation Model

- Example for user input correlation for B136Y3 material:

$$K = \begin{cases} 9.62 \times 10^{-12}\,[\mathrm{g}^2/\mathrm{cm}^4\mathrm{s}], & T \le 1473\ \mathrm{K} \\ A_B \exp\left(\dfrac{-E_B}{RT}\right), & 1473\ < T < 1648\ \mathrm{K} \\ A_{Fe} \exp\left(\dfrac{-E_{Fe}}{RT}\right), & T \ge 1648\ \mathrm{K}\ (melting\ point\ of\ FeO) \end{cases}$$

A_B=3×10⁹ g2/cm4s
E_B=594354 J/mol

A_{Fe}=2.4×10⁶ g2/cm4s.
E_{Fe}=352513 J/mol.

based on

C. Kim et al.: Oxidation mechanism and kinetics of nuclear-grade FeCrAl alloys in the temperature range of 500–1500 °C in steam, Journal of Nuclear Materials Volume 564,2022,153696, ISSN 0022-3115

- Achieves acceptable results in simulating QUENCH-19 experiment

Simulation of Q-19 Experiment

- Without going into details, Q-15 experiment was the reference for Q-19
  - Cladding: FeCrAl
  - Reduced H2 production compared to Q15
- Simulation with AC2:
  - Slight overprediction of H2 production
    - Small deviations in temperatures
    - Steam starvation model needs update
    - Correlations are not fitting perfectly
  - Transition ranges could be smoother

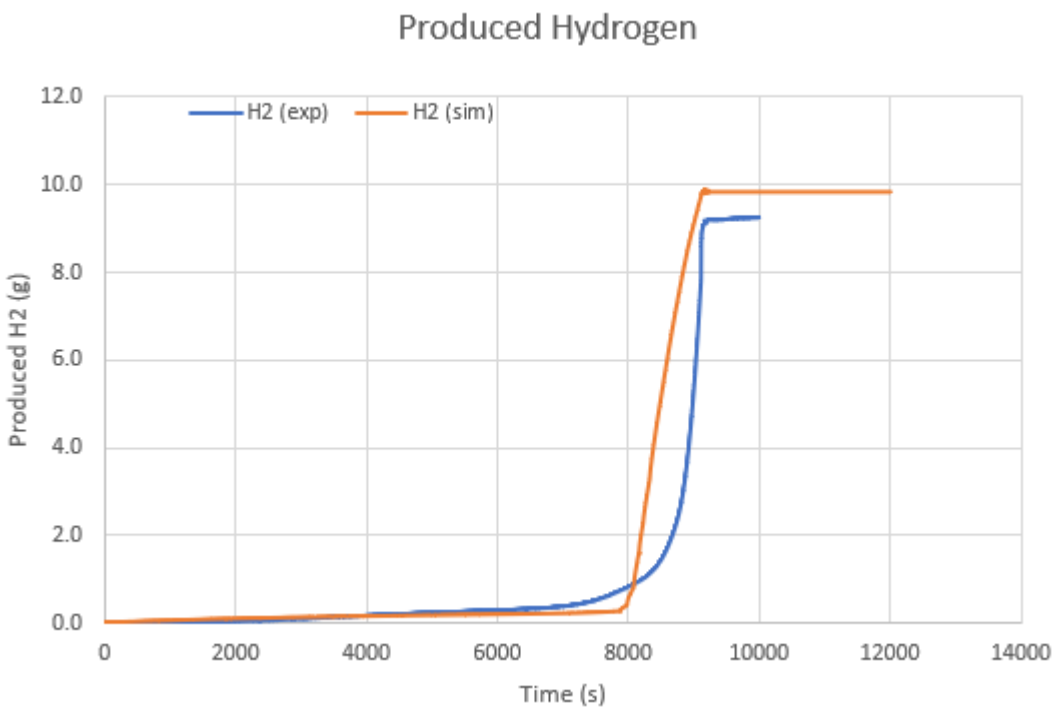

Material interaction FeCrAl-UO2

- Hard coded Zr-UO2 interaction turned off
- Material interaction between FeCrAl-UO2 based on preliminary data provided from OECD-NEA project called TCOFF-2
- Oxidized FeCrAl (Fe) reacts with UO2
  - Dependent on the average oxidation state of cladding
  - Reaction almost instant
- Competing phenomena: oxidation vs melt relocation
- Still in continuous development
  - Exact data not shown here
- Material interaction only between not relocated materials

AC²/ATHLET-CD – Cr-coated Zr Oxidation Model

- Mainly developed by RUB for steam oxidation
  - For details see presentation and publications of the previous presenter Gregor Stahlberg (RUB)

- Minor adjustments for air oxidation of Cr-coated Zr
  - Mainly to do pre and post test calculations for CODEX-ATF-AIT experiment

- Up until Cr coating failure the same correlation is used for steam AND air
  - Until Cr coating is intact, no large differences between air and steam oxidation is to be expected

- Enthalpy of reaction changed, as well as amount of H2 produced (for steam)

- Cr coating is assumed to fail at T=1600 K
  - Failure mechanism is not modelled in detail (yet)

- After failure is assumed, standard air and steam oxidation models are used

Codex-AIT-ATF Experiment

- Experiment: oxidation behaviour of Cr-coated Zr under severe accident conditions with air ingress
  - For experiment details see presentation of Nora Ver, HUN-REN

- Facility modelled and experiment simulated with AC2
  - Bundle divided into two rings
  - Axially into 18 nodes (5 cm) over the heated length

- All relevant phenomena modelled
- Typical shortcomings of the ring-like nodalization:
  - Uniform parameters along the ring

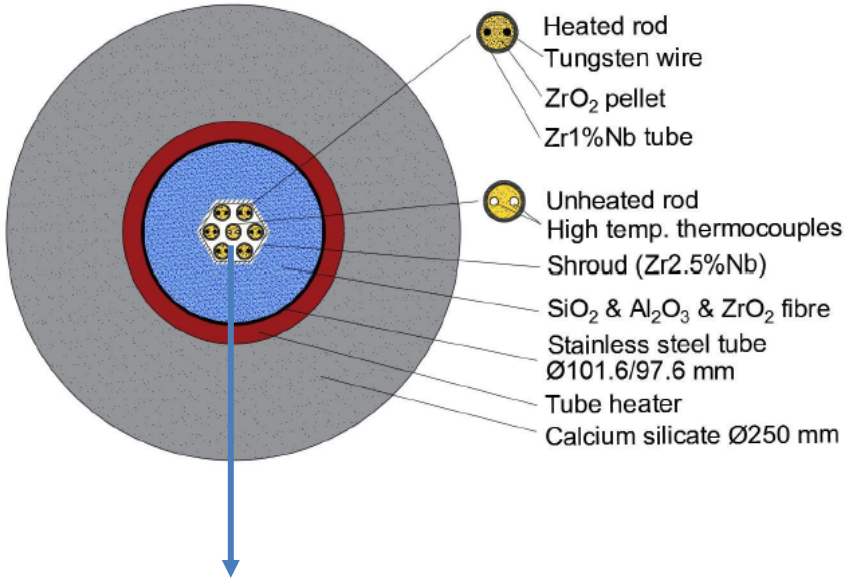

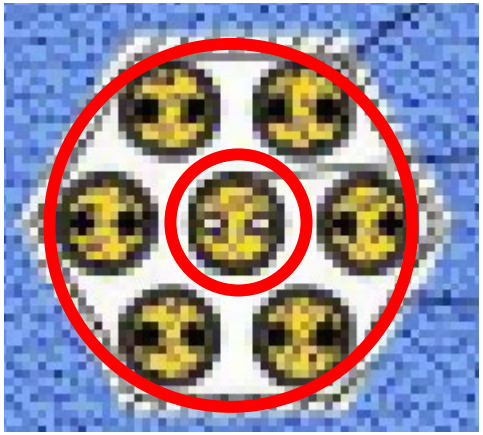

Preliminary post test simulation results at H=150 mm

- Temperature evolution
  - First slight overprediction
  - Smaller peak temperature
    - Not due to oxidation

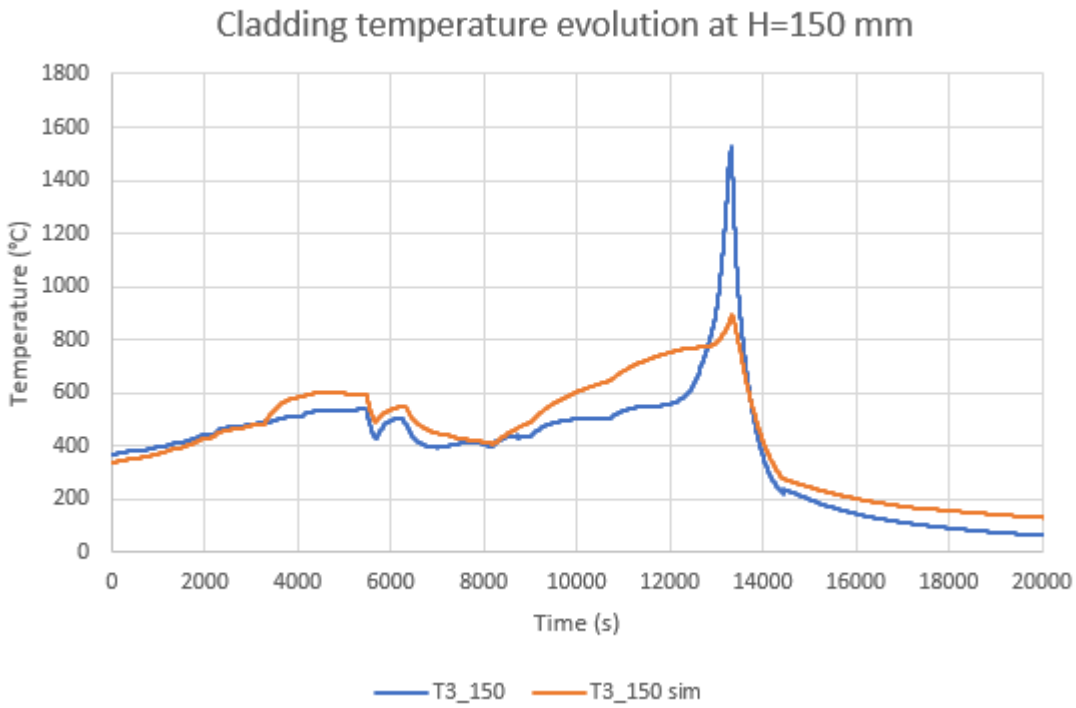

Preliminary post test simulation results at H=500 mm

- Temperature evolution:
  - First slight overprediction
  - Similar temperature heat-up
  - Oxidation escalation well predicted
  - Peak temperature comparable with measured values
    - Failure of thermocouple

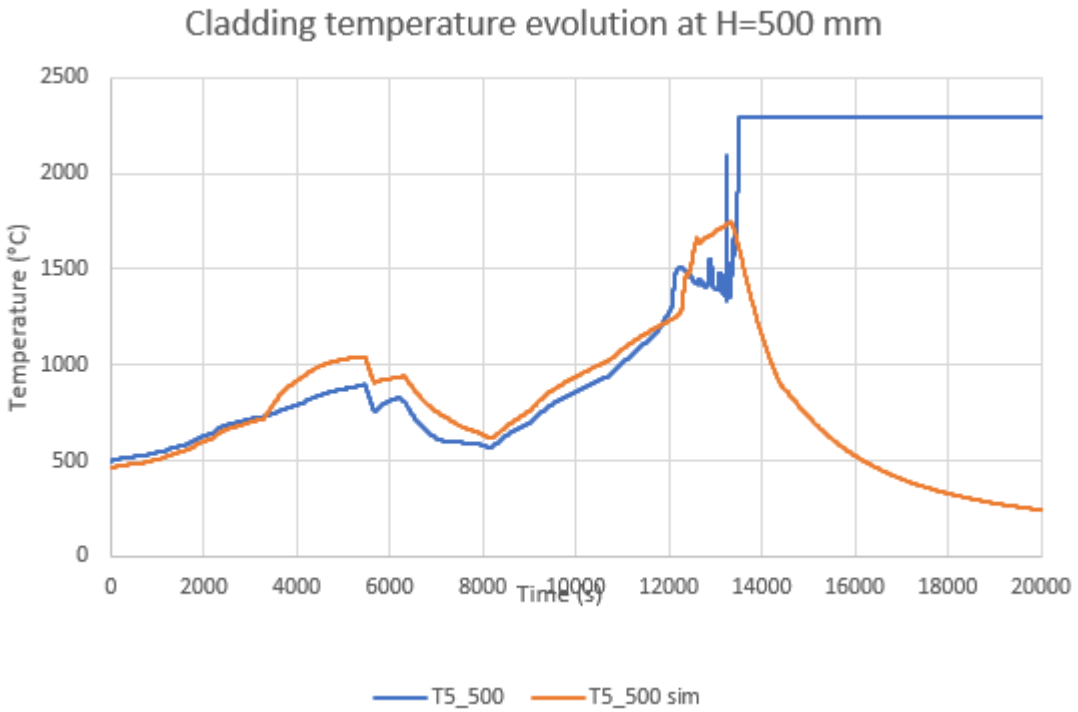

Preliminary post test simulation results at H=650 mm

- Temperature evolution:
  - Early phase similar as at other elevations
  - Similar temperature heat-up
  - Overprediction of the peak
    - Stronger oxidation

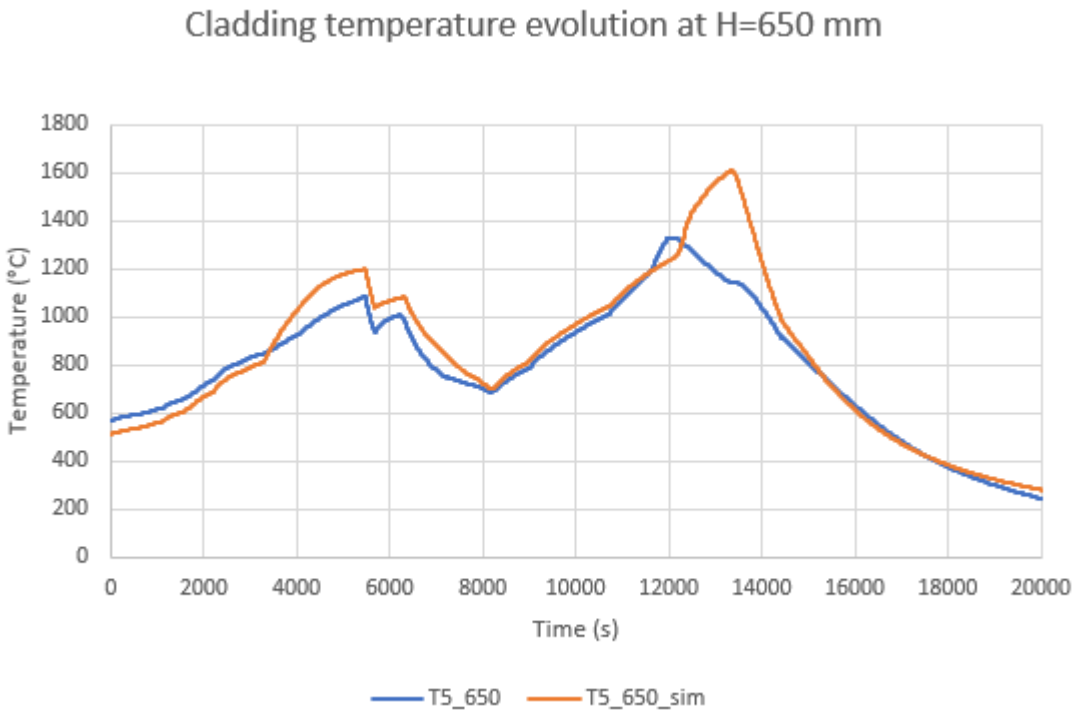

Preliminary post test simulation results at H=750 mm

- Temperature evolution:
  - Early phase similar as at other elevations
  - Similar temperature heat-up
  - Peak temperature is similar
    - Shifted in time
    - Larger steam/o2 starvation
    - Stronger oxidation in areas below

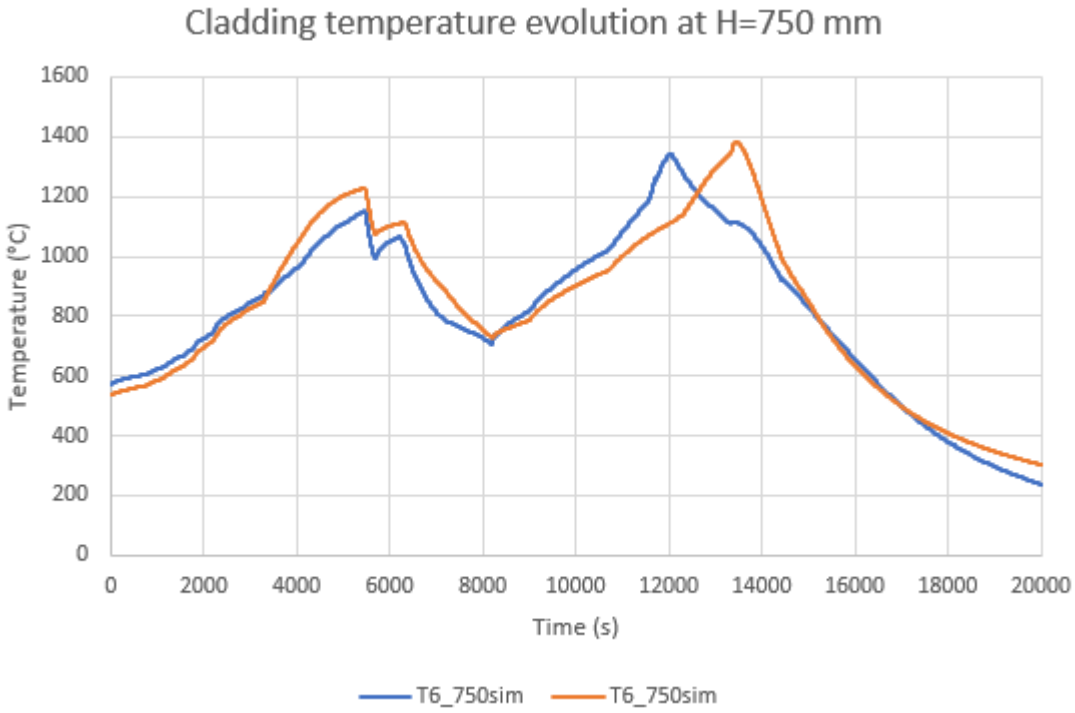

Preliminary post test simulation results at H=500 mm

- Temperature evolution of shroud:
  - First slight overprediction
  - Similar temperature heat-up
  - Oxidation escalation well predicted
  - Peak temperature comparable with measured values
    - Failure of thermocouple

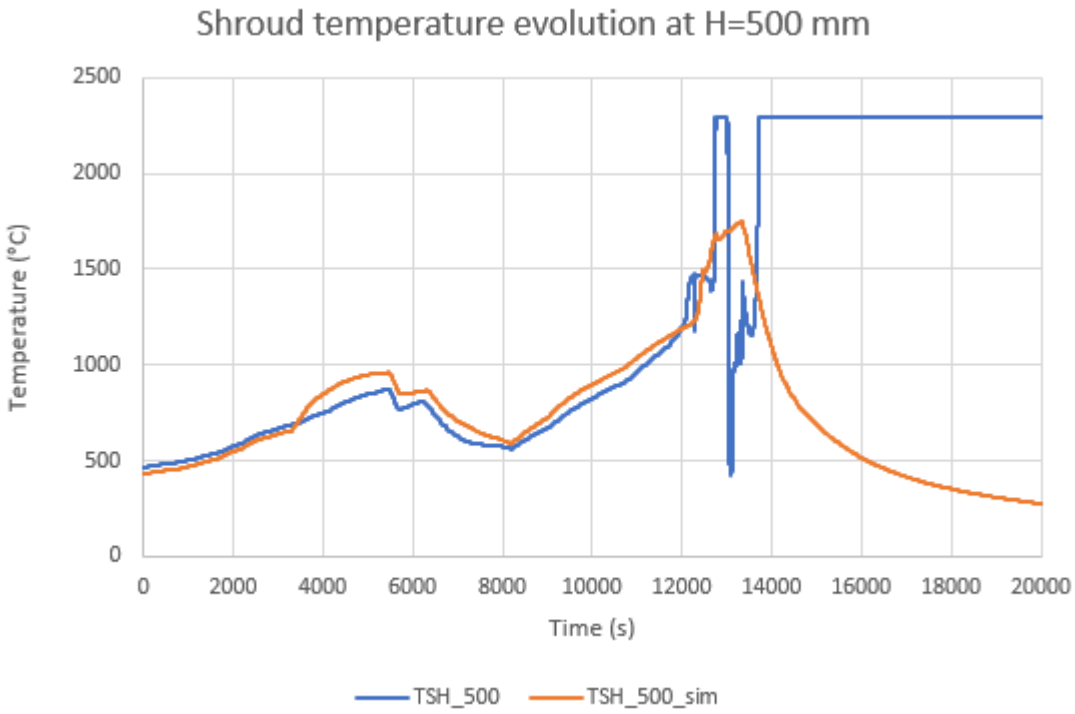

Measured values

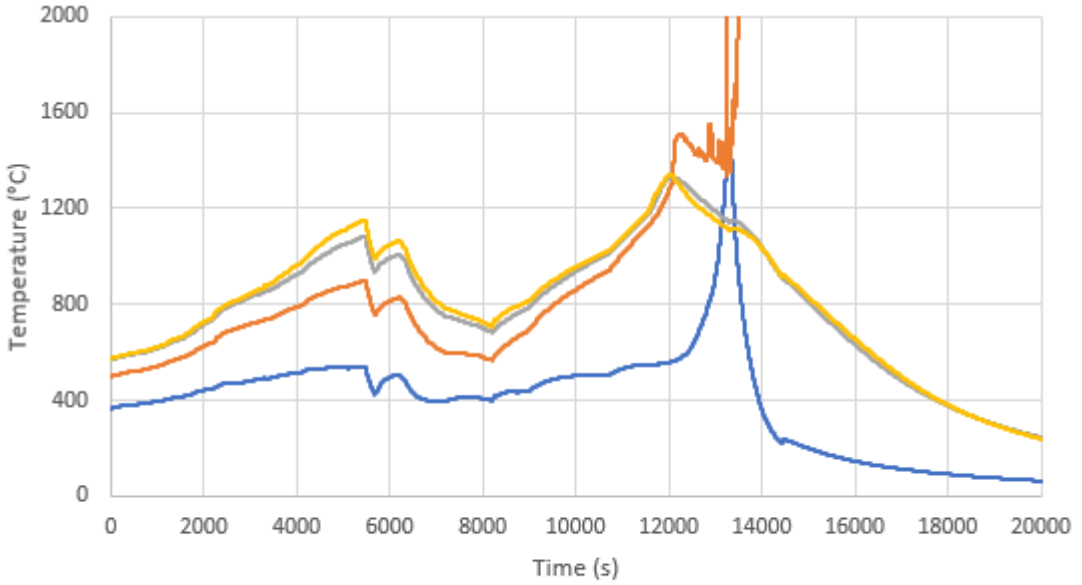

- Evolution of temperatures at different elevations:
- Location of max temperature shifts downward

Simulated values

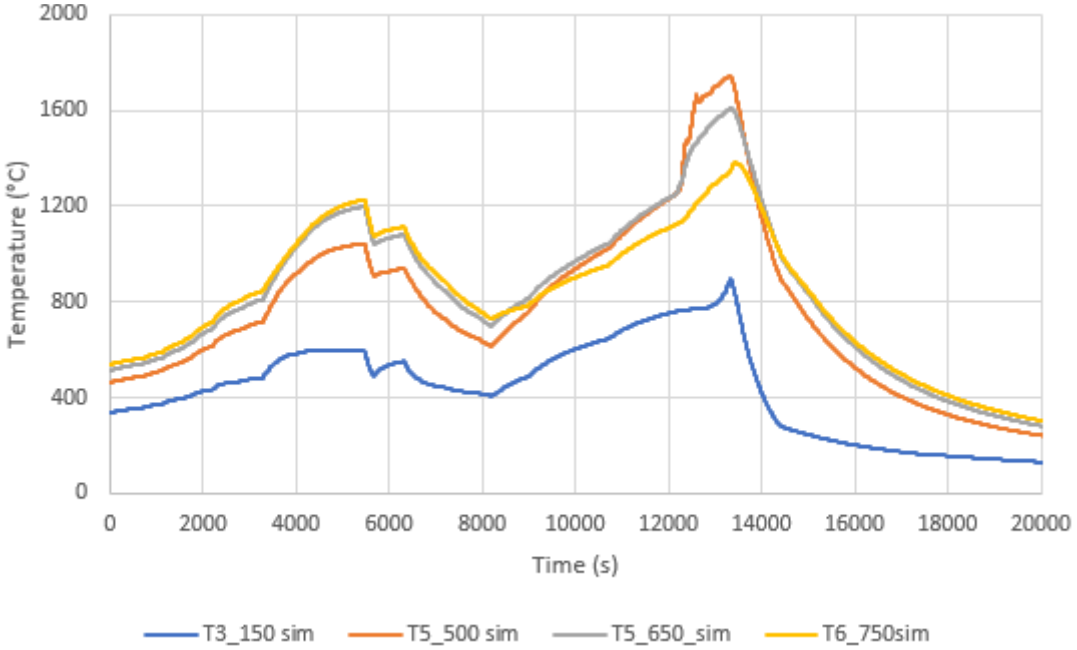

Shifting of maximum temperature downwards

- First oxidation peak in the upper third of the bundle
- Lower elevations reach the eutectic temperature
  - Starvation above

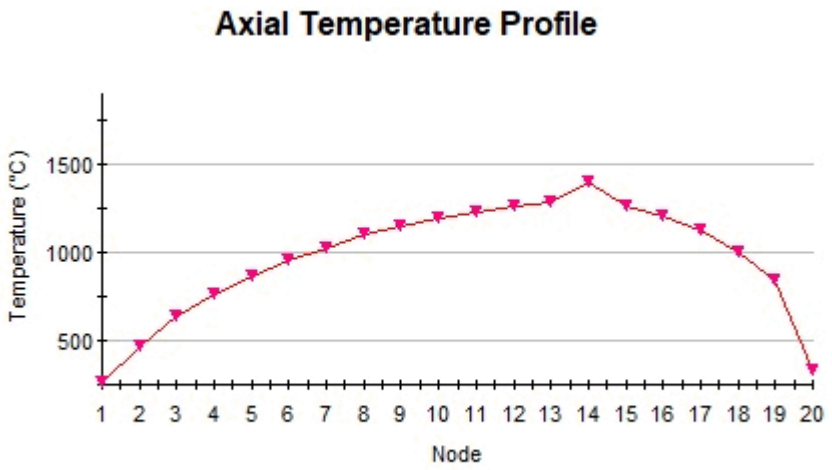

H2 production

- Underprediction during pre oxidation phase
  - 0.4g vs 1.4g
  - No oxidation of TC considered
- Underprediction during air ingress:
  - 2.4 g vs 3.3 g
  - Localized oxidation
  - Lower regions remained cold

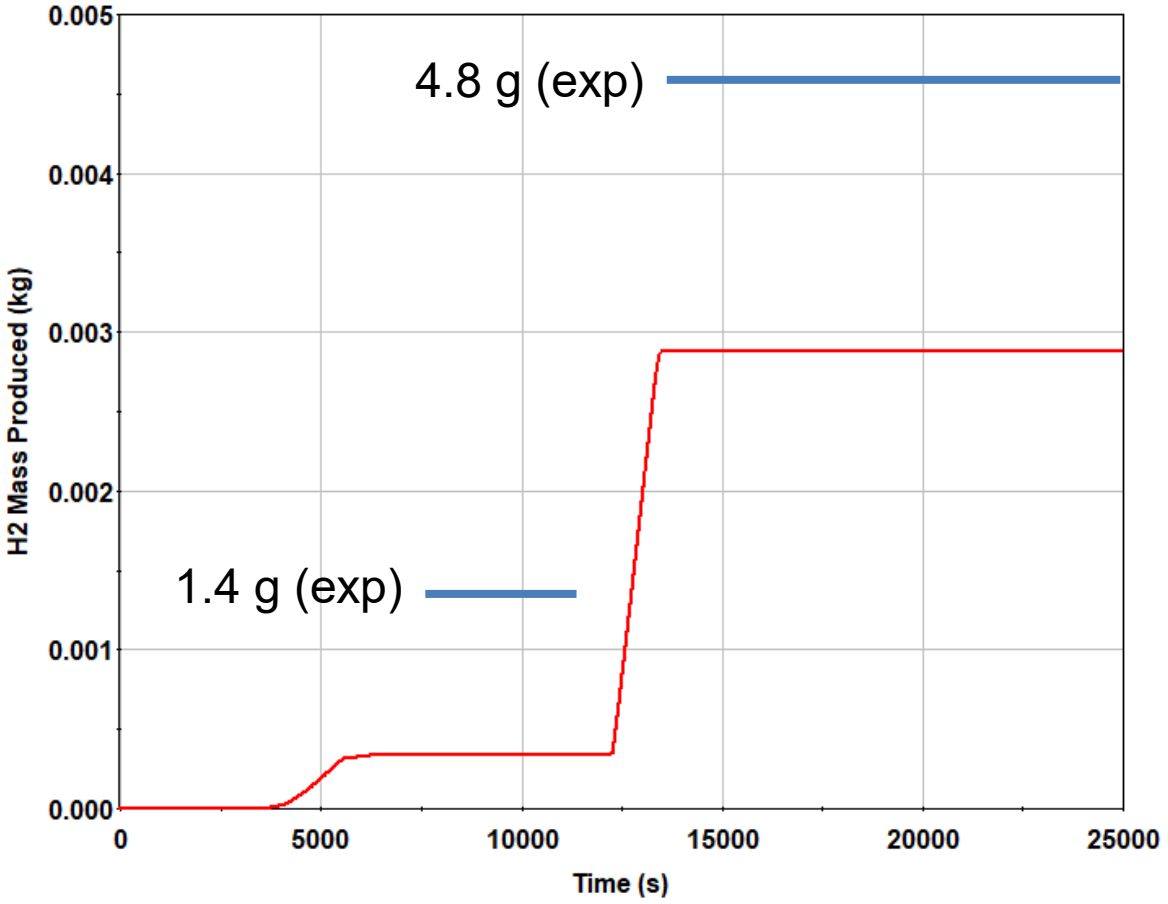

Conclusions

- AC2 currently has limited capabilities to model the influence of ATF
  - Models have been developed and used for FeCrAl and Cr-coated materials
  - Main focus is on the modelling of the changed oxidation behaviour

- Using the developer version of AC2
  - Previous activity: Simulation of QUENCH-19 experiment (FeCrAl)
  - Current activity: Simulation of CODEX-AIT-ATF experiment (Cr-coated Zr)
    - Focus on this work in this presentation

- Simulation show qualitatively good results in both cases, but
  - Further information from experiment needed
  - Models need further fine tunings and improvements
    - Ballooning, FP release, further material interactions

- Models need further validation

Thank you for your kind attention

Zaira I. Jiménez Balbuena

KIT

FeCrAl Oxidation Model Development on the ASTEC Code and Preliminary Validation Against QUENCH Experiments

Accident Tolerant Fuels (ATF) offer a promising alternative for mitigating severe accidents in nuclear reactors due to their excellent characteristics. Conducting a comprehensive study of these innovative materials' physical and chemical processes is crucial to understand and accurately predict their behavior under different conditions. Integral codes are currently being developed to effectively apply and comprehend these processes and their potential outcomes in small modular reactors (SMR). An intensive study is underway on the oxidation process resulting from an innovative cladding of iron, chromium, and aluminum alloy (FeCrAl) in a steam environment. Simultaneously, a model that considers different oxidation kinetics - transient alumina, α-alumina, and iron oxide - is being carefully developed and implemented in an integral code called Accident Source Term Evaluation Code (ASTEC) developed by IRSN. The aim is to include an appropriate model in this code to predict hydrogen production in a nuclear reactor under severe accident conditions and to rigorously assess the behavior of the innovative material, physical models to evaluate oxygen mass gain and oxide layer thickness are key to achieving this goal. The accuracy of the model approximation is important, since hydrogen production has the potential to trigger an accident. To ensure the utmost accuracy, experimental tests such as separate effects tests or QUENCH-19 have been rigorously conducted by KIT and were used to validate this model. So far, some results indicate that ASTEC effectively predicts experimental data for the single-effect test in terms of weight gain, oxide layer thickness, and hydrogen production at temperatures ranging from 873 K to 1573 K. In addition, it accurately reproduces the experimental temperatures and hydrogen production up to 1500 K in the case of the QUENCH-19 bundle test.

Karlsruhe Institute of Technology

FeCrAl Oxidation Model Development on the ASTEC Code and Preliminary Validation Against QUENCH Experiments

Z. I. Jiménez, F. Gabrielli, M. E. Cazado, V.H. Sanchez-Espinoza, L. Laborde, L. Carenini, P. Drai.

Institute for Neutron Physics and Reactor Technology

Content

- Motivation
- The ASTEC code
- Accident Tolerant Fuels
- ASTEC code improvement for FeCrAl
- FeCrAl Oxidation Model
- Model Implementation
- Model Validation
- Conclusion
- Outlook

Motivation

- KIT strategy for severe accident (SA) analyses → continuous improvement of the codes to evaluate the progression and the radiological consequences of SA in current and innovative NPPs
- ATF claddings have the potential to mitigate the progress of hypothetical severe accident scenarios, e.g., delayed hydrogen onset timing, reducing the hydrogen production, compared with Zr cladding
- A KIT/INR and IRSN shared activity is going on to improve the ATF-related modelling capabilities (cladding) of the ASTEC* code
- Goals of the work
  - Improvement and implementation of the ASTEC modelling for predicting the hydrogen generation and mass gain by the oxidation of FeCrAl under steam atmosphere
  - ASTEC validation against the SETs and QUENCH-19 bundle test performed at the KIT QUENCH large-scale facility

*CHATELARD, P., et al., “Main modelling features of the ASTEC V2.1 major version”, Annals of Nuclear Energy 93 (2016) 83–93.

The Accident Source Term Evaluation Code (ASTEC)

- Developed by IRSN (IRSN all rights reserved, [2024])
- Simulating the entire Severe Accident (SA) sequence from the initiator up to the fission product release to the environment
- ASTEC models all the physical phenomena that occur during a core meltdown accident
- ICARE module describes the in-vessel degradation phenomena
- Chemistry model: Oxidation of cladding material by steam or O2

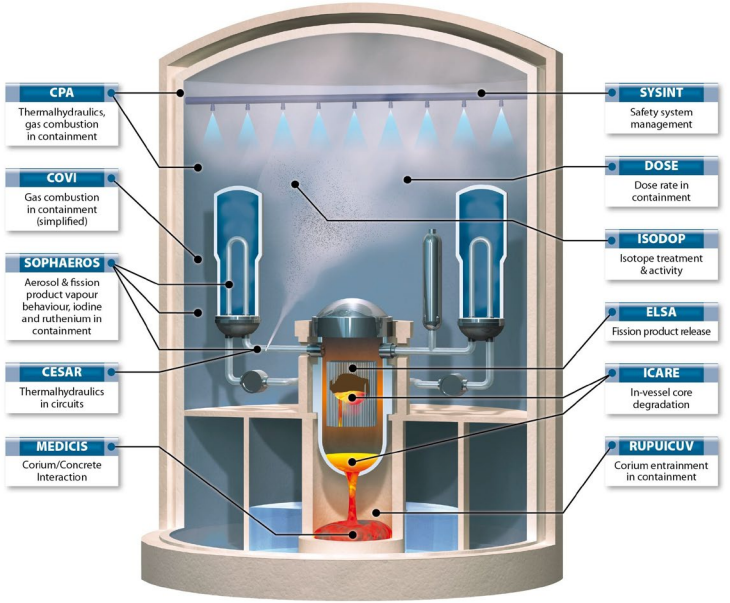

Accident Tolerant Fuels (ATF)

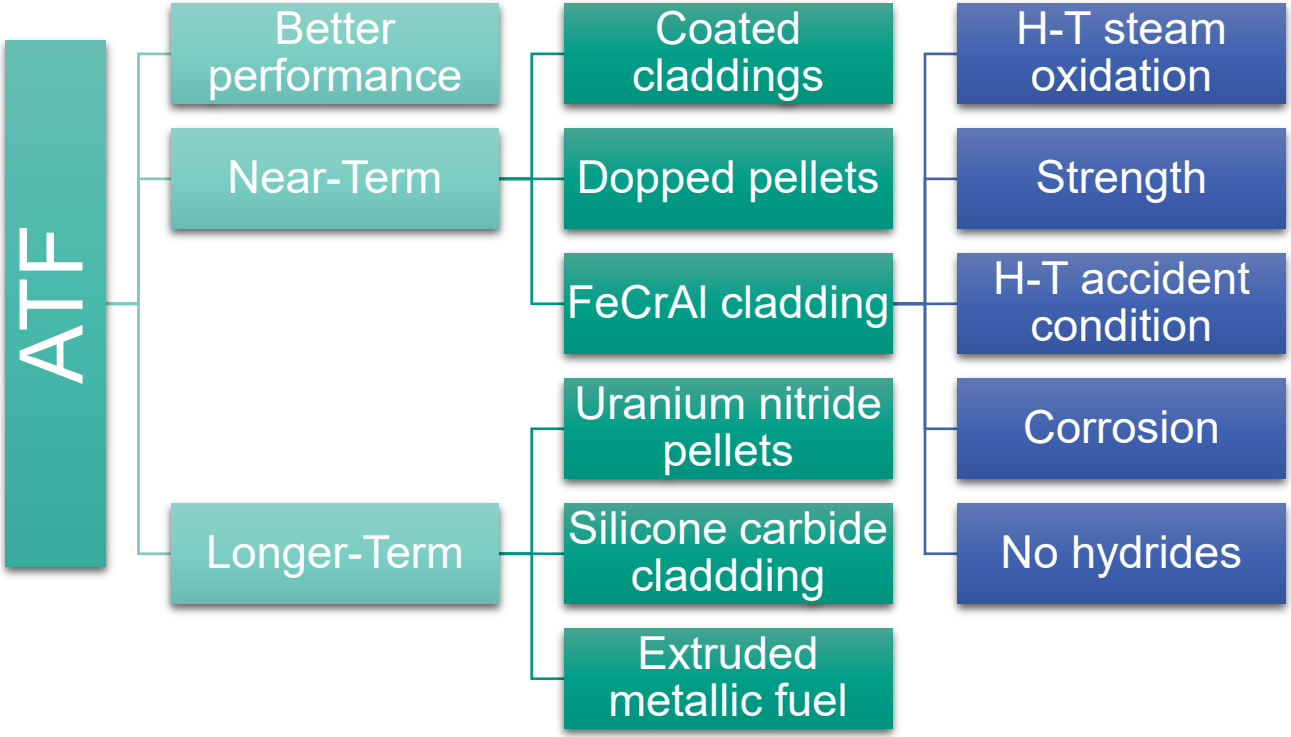

B136Y3

- Fe
- 12.97 Cr
- 6.19 Al
- 0.03 Y
- <0.01 C

C26M2

- Fe
- 11.87 Cr
- 6.22 Al
- 1.98 Mo
- 0.03 Y
- <0.01 C
- 0.2 Si

ASTEC code improvement for FeCrAl: approach

- Based on the experimental data from the QUENCH team…
- Simplification of the FeCrAl oxidation process in steam environment
- Implementation of the oxide kinetics physical models
- Implementation of the physical models for the mass gain and thickness oxide layer evaluations
- Use of the FeCrAl thermophysical properties, i.e. specific enthalpy, density, heat capacity

FeCrAl Oxidation Model

- **Steam oxidation reaction**

$$3\,FeCrAl_{(s)} + 4H_2O_{(g)} \rightarrow Fe_3O_{4(s)} + 3\,Cr_2O_{3(s)} + 4\,Al_2O_{3(s)} + 6\,H_{2(g)}$$

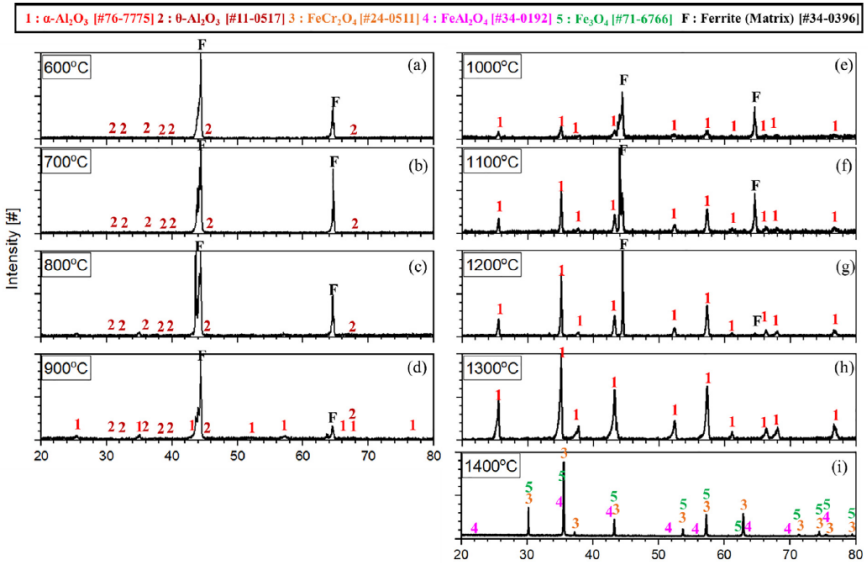

- **Single oxide layer model**

$$2\,Al_{(s)} + 3\,H_2O_{(g)} \rightarrow Al_2O_{3(s)} + 3H_{2(g)}$$

- **Composition**

80.8%Fe12.97%Cr6.19%Al

Fig. 1 Oxidation kinetics present in the FeCrAl alloy oxidation process from: Kim, C., Tang, C., Grosse, M., Maeng, Y., Jang, C., & Steinbrueck, M. (2022). Oxidation mechanism and kinetics of nuclear-grade FeCrAl alloys in the temperature range of 500–1500 C in steam. *Journal of Nuclear Materials*, *564*, 153696.

Oxidation kinetics

$873 < T < 1173$	$1173 \leq T \leq 1273$	$1273 < T < 1648$	$T \geq 1648$
Transient Alumina	Alumina	α-Alumina	FeO-Oxide

- **Oxygen Mass Gain**

It evaluates the rate of aluminum oxide mass gain

- parabolic correlation
- different coefficients according oxidation kinetics

$$\frac{dm_{O_2}^2}{dt} = K_p \qquad (1)$$

$$K_p \left[\frac{kg^2}{m^4 \cdot s}\right] = A_{gain} e^{\left(-\frac{B_{gain}}{RT}\right)} \qquad (2)$$

- dm_{O_2}: mass gain
- K_p: rate constant for mass gain
- A_{gain}: pre-exponential constant
- B_{gain}: energy activation
- R: ideal gas constant
- T: temperature
- dt: time

Oxidation kinetics implementation

Transient Alumina

$873 < T < 1173$

$A_{gain} = 5.37582 \cdot 10^{-3}$

$B_{gain} = 1.84730 \cdot 10^{5}$

Alumina

$1173 \leq T \leq 1273$

$A_{gain} = 4.69155 \cdot 10^{-12}$

$B_{gain} = 0.00000 \cdot 10^{0}$

α-Alumina

$1273 < T < 1648$

$A_{gain} = 5.01760 \cdot 10^{0}$

$B_{gain} = 2.87748 \cdot 10^{5}$

FeO-Oxide

$T \geq 1648$

$A_{gain} = 2.39940 \cdot 10^{8}$

$B_{gain} = 3.52514 \cdot 10^{5}$

ASTEC equation

- $\frac{dm_O{}^2}{dt} = K_p \rightarrow m_O^{i+1} = \sqrt{\left\{\left(m_O^{i+1}\right)^2 + \left[A_{gain} e^{\left(\frac{-B_{gain}}{RT}\right)} \Delta t\right]\right\}}$

```
STRUCTURE PROPERTY NAME "SteamOxidation"
    STRU TEST X 1000. END

    HELP "Oxygen mass gain obey to the following law :"

    HELP "m_O   (t+dt) = S ((m_O   (t)/S)**(1/model) + AGAIN EXP(-BGAIN/(R.T)) * dt )**model"

    STRUCTURE MODEL NAME 'ATFKIT' LAW 'COEFF' VARIABLE 'T' VUNIT 'K' RUNLOW 0. RUNUPP 5000.
       SRG VALUE AGAIN 5.0176000D0 BGAIN 2.8774800D5  MODEL 0.5 TERM
    END

    STRUCTURE MODEL NAME 'ATF-KIT' LAW 'COEFF' VARIABLE 'T' VUNIT 'K' RUNLOW 0. RUNUPP 5000.
       SRG VALUE AGAIN 5.3758224D-3  BGAIN 1.8473000D5  MODEL 0.5 TERM
       X  1172.9K
       SRG VALUE AGAIN 4.6915560D-12 BGAIN 0.0000000D5  MODEL 0.5 TERM
       X  1273.K
       SRG VALUE AGAIN 5.0176000D0   BGAIN 2.8774800D5  MODEL 0.5 TERM
       X  1652.9K
       SRG VALUE AGAIN 2.3994010D8   BGAIN 3.5251400D5  MODEL 0.5 TERM
    END

END
```

Fig. 2 FeCrAl oxidation kinetics implementation on ASTEC code

Thickness Oxide Layer

$$2\,Al + \frac{3}{2}\,O_2 \rightarrow Al_2O_3$$

$$m_{Al_2O_3} = m_{O_2}\,\frac{MM_{Al_2O_3}}{f_s MM_{O_2}} \qquad (3)$$

$$\delta_{Al_2O_3} = \frac{m_{Al_2O_3}}{S}\left[\frac{1}{\rho_{Al_2O_3}}\right] \qquad (4)$$

$$\delta_{Al_2O_3} = m_o\,\frac{MM_{Al_2O_3}}{f_s MM_{O_2}}\,\frac{1}{\rho_{Al_2O_3}} \qquad (5)$$

Hydrogen Production

$$2\,Al_{(s)} + 3\,H_2O_{(g)} \rightarrow Al_2O_{3(s)} + 3H_{2(g)}$$

$$mH_2 = \frac{3m_{Al_2O_3} MMH_2}{PM_{Al_2O_3}} \qquad (6)$$

Implementation

$$\frac{m_{O_2}^{i+1}}{S} = \sqrt{\left\{\left(m_{O_2}^{i+1}\right)^2 + \left[A_{gain}e^{\left(\frac{-B_{gain}}{RT}\right)}\Delta t\right]\right\}} \qquad (7)$$

$$\frac{m_{Al_2O_3}^{i+1}}{S} = \frac{m_{O_2}^{i+1}}{S}\,\frac{2MM_{Al_2O_3}}{3MM_{O_2}} \qquad (8)$$

$$\delta_{Al_2O_3}^{i+1} = \frac{m_{Al_2O_3}^{i+1}}{S}\,\frac{1}{\rho_{Al_2O_3}} \qquad (9)$$

$$m_{Al_2O_3}^{i+1} = \frac{m_{Al_2O_3}^{i+1}}{S}(S) \qquad (10)$$

$$m_{H_2}^{i+1} = \frac{3m_{Al_2O_3}^{i+1}\cdot MM_{H_2}}{PM_{Al_2O_3}} \qquad (11)$$

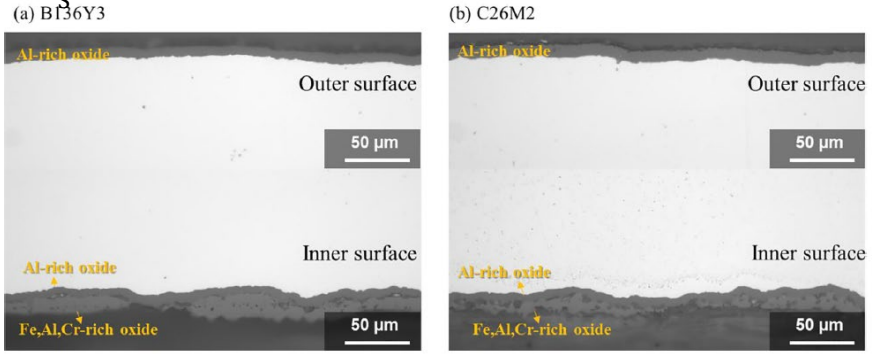

Fig. 3 Thickness oxide layer for FeCrAl alloys from*

*Kim, C., Tang, C., Grosse, M., Maeng, Y., Jang, C., & Steinbrueck, M. (2022). Oxidation mechanism and kinetics of nuclear-grade FeCrAl alloys in the temperature range of 500–1500 C in steam. *Journal of Nuclear Materials*, *564*, 153696.

Single effect test

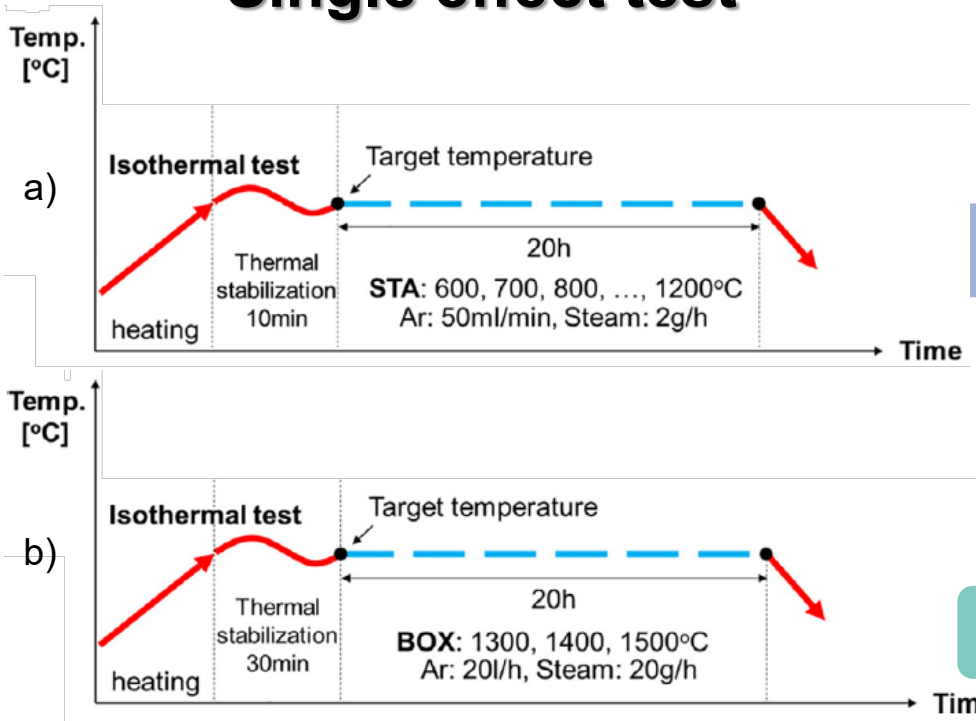

873K-1473K
L: 10 mm

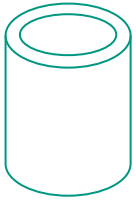

1573K-1773K
L: 20 mm

Fig. 4. The test schedules for the isothermal steam oxidation in (a) STA and (b) BOX facilities edited from*

Fig.6 Sample before isothermal test from*

- Validation data
  - Weight gain $\left(\frac{mg}{cm^2}\right)$
  - Thickness oxide layer (m)
  - Hydrogen production (gr)

*Kim, C., Tang, C., Grosse, M., Maeng, Y., Jang, C., & Steinbrueck, M. (2022). Oxidation mechanism and kinetics of nuclear-grade FeCrAl alloys in the temperature range of 500–1500 C in steam. *Journal of Nuclear Materials*, *564*, 153696.

Mass gain

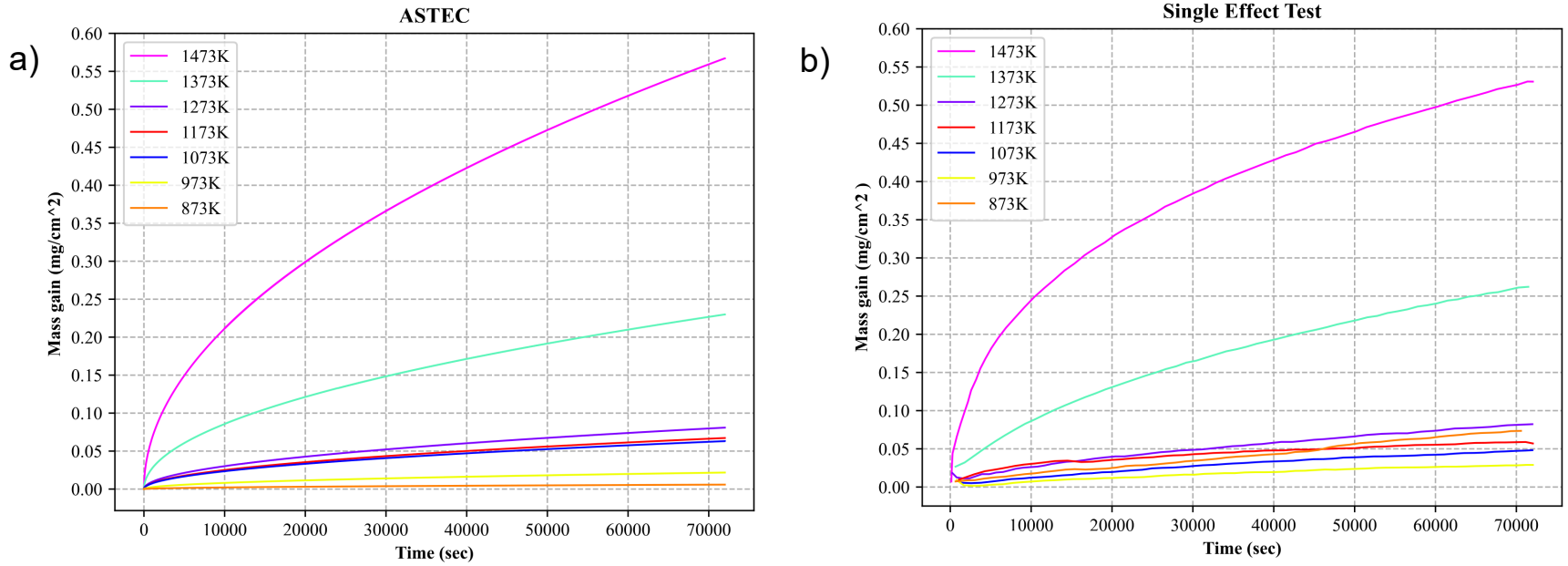

Fig. 5 Weight gains a) obtained from ASTEC b) from isothermal single effect test (extracted data from*)

*Kim, C., Tang, C., Grosse, M., Maeng, Y., Jang, C., & Steinbrueck, M. (2022). Oxidation mechanism and kinetics of nuclear-grade FeCrAl alloys in the temperature range of 500–1500 C in steam. *Journal of Nuclear Materials*, *564*, 153696.

ASTEC vs. Experiments Comparison

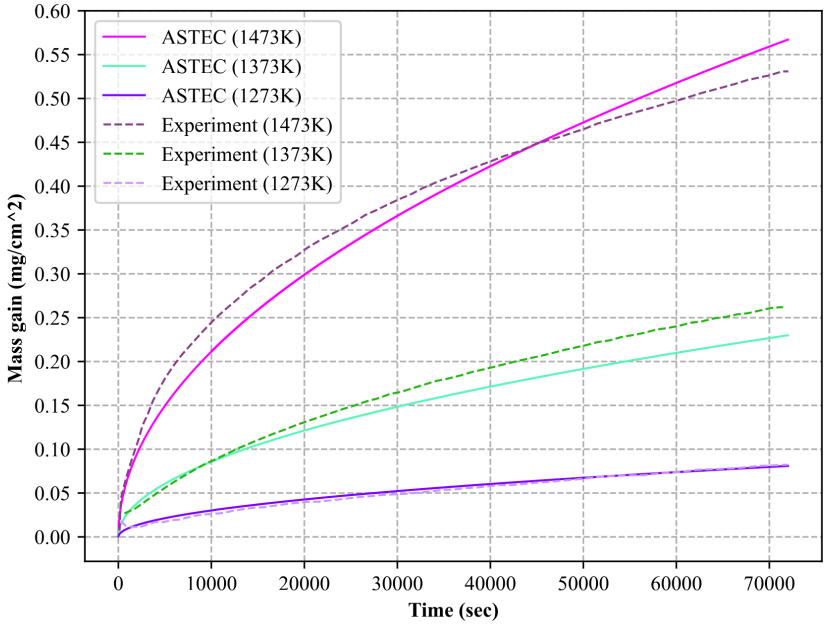

Fig. 6 Weight gains comparison Isothermal single effect test vs ASTEC

- The improvements allow ASTEC to reasonably well predict the experimental results.

Total Mass Gain 'ASTEC'

- 1373K
  $\Delta m = 0.567$
- 1473K
  $\Delta m = 0.229$
- 1573K
  $\Delta m = 0.080$

Thickness oxide layer

T (K)	Experiment Inner Surface (µm)	ASTEC Inner Surface (µm)	Difference Inner Surface (µm)	Experiment Outer Surface (µm)	ASTEC Outer Surface (µm)	Difference Outer Surface (µm
873	Nodular oxides	0.047	---	Too thin	0.047	---
973	Thin thickness	0.017	---	Thin thickness	0.175	---
1073	Thin thickness	0.509	---	Thin thickness	0.509	---
1173	Thin thickness	0.543	---	Thin thickness	0.543	---
1273	Thin thickness	0.654	---	Thin thickness	0.654	---
1373	~2.000	1.864	0.136	~1.500	1.864	0.364
1473	~4.000	4.605	0.605	~3.000	4.608	1.608
1573	~6.500	8.258	1.758	~6.500	8.258	1.758

- ASTEC results are in reasonable agreement with the experimental data

Hydrogen production

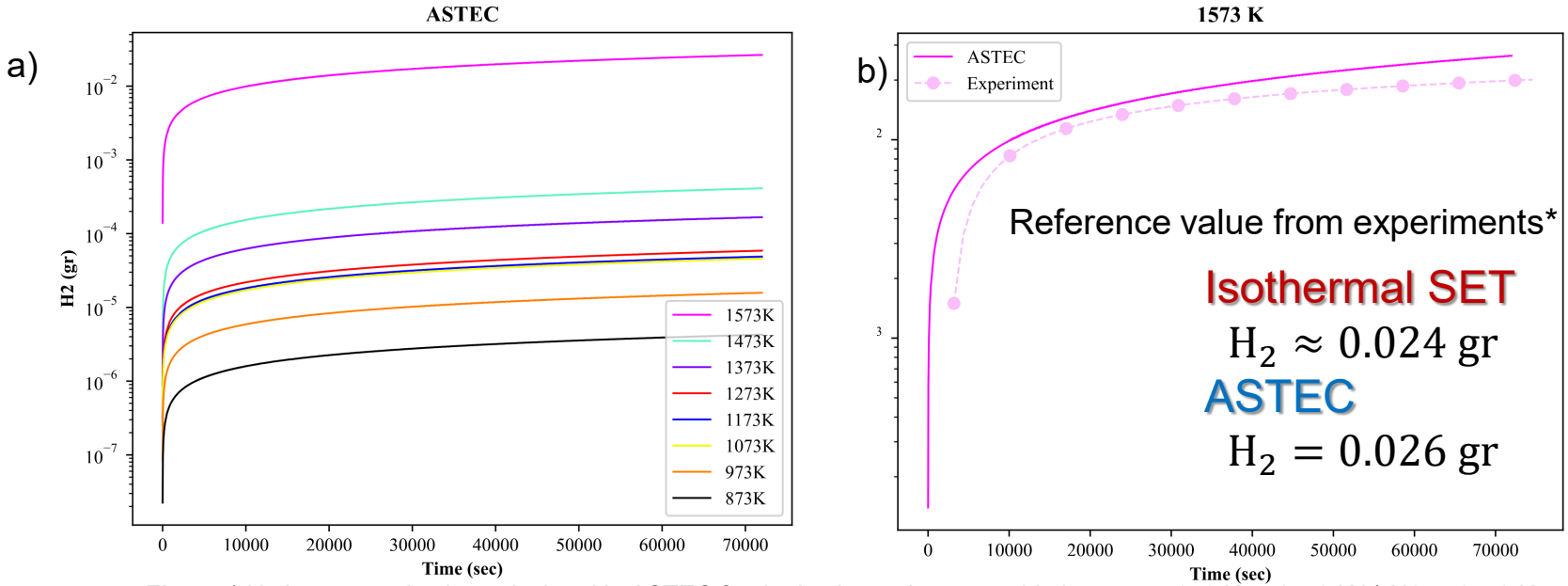

Fig. 7 a) Hydrogen production calculated in ASTEC for the isothermal steam oxidation test at 873 K to 1573 K b) H2 at 1573 K

*Kim, C., Tang, C., Grosse, M., Maeng, Y., Jang, C., & Steinbrueck, M. (2022). Oxidation mechanism and kinetics of nuclear-grade FeCrAl alloys in the temperature range of 500–1500 C in steam. *Journal of Nuclear Materials*, *564*, 153696.

QUENCH 19 test conduct

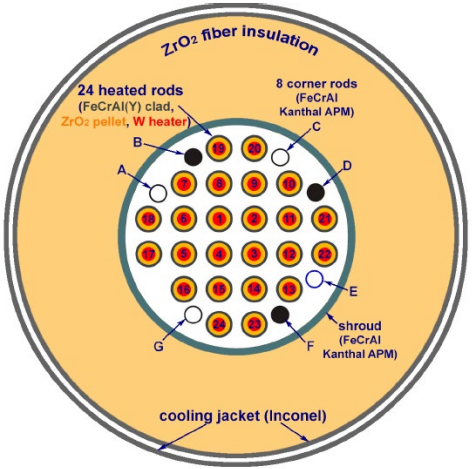

Phase 1	Heating up to ~600 °C (4 kW).
Phase 2	Power increase up to 11.5 kW (pre-oxidation).
Phase 3	Power increased up to 18.12 kW (5 W/s) (T_{pct}~1500 °C).
Phase 4	Phase 4: power reduced to 4.1 kW.

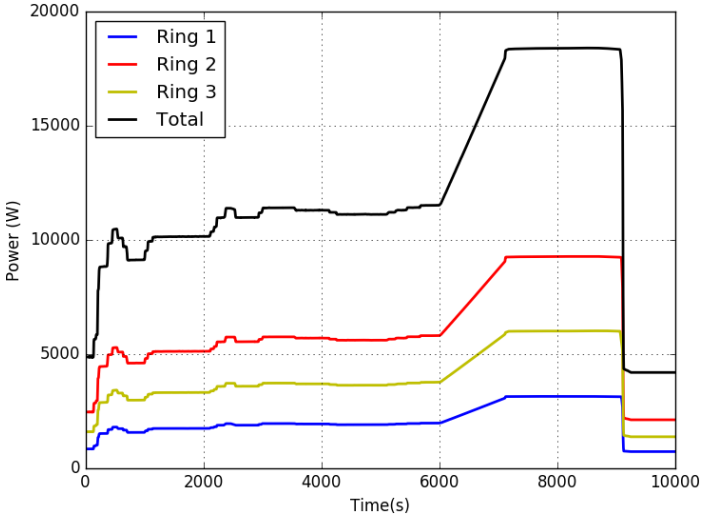

- Atmosphere of Ar (3.45 g/s) and superheated steam (3.6 g/s).
- Reflooding at ~9100 s
  - Fast initial injection of 4 L of water
  - Slow injection 48 ~ g/s of water

ASTEC model of QUENCH 19

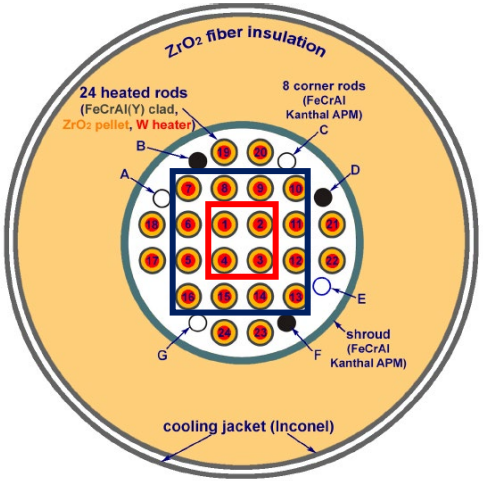

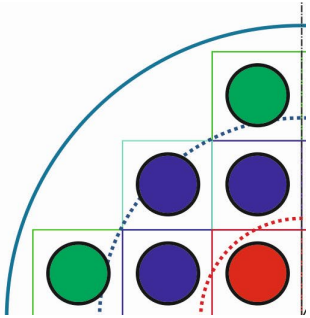

Ch. 3, 8 rods, r_{ext}= 41.5 cm

Ch. 2, 12 rods, r_{ext}= 28.4 cm

Ch. 1, 4 rods, r_{ext}=14.2 cm

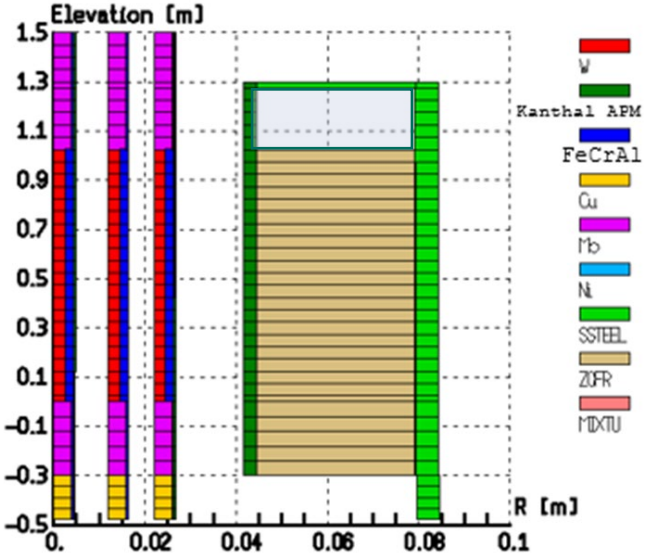

- Accidental presence of 4 l of water in the gap between the shroud and the cooling jacket modelled (J. Stuckert).

Cladding temperature

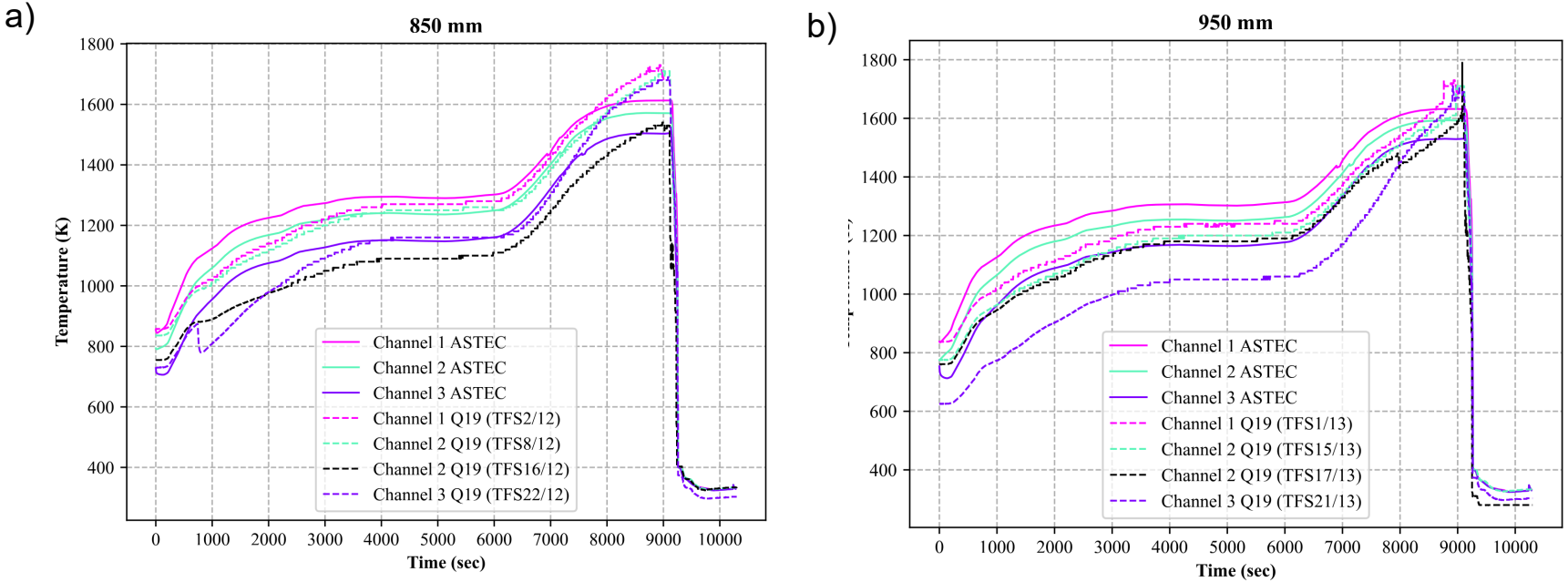

Fig. 8 Comparison Clad Temperature ASTEC vs bundle test a) 850 and b) 950 mm

- Higher temperatures from ASTEC
- Different behavior of temperature curves

Hydrogen production

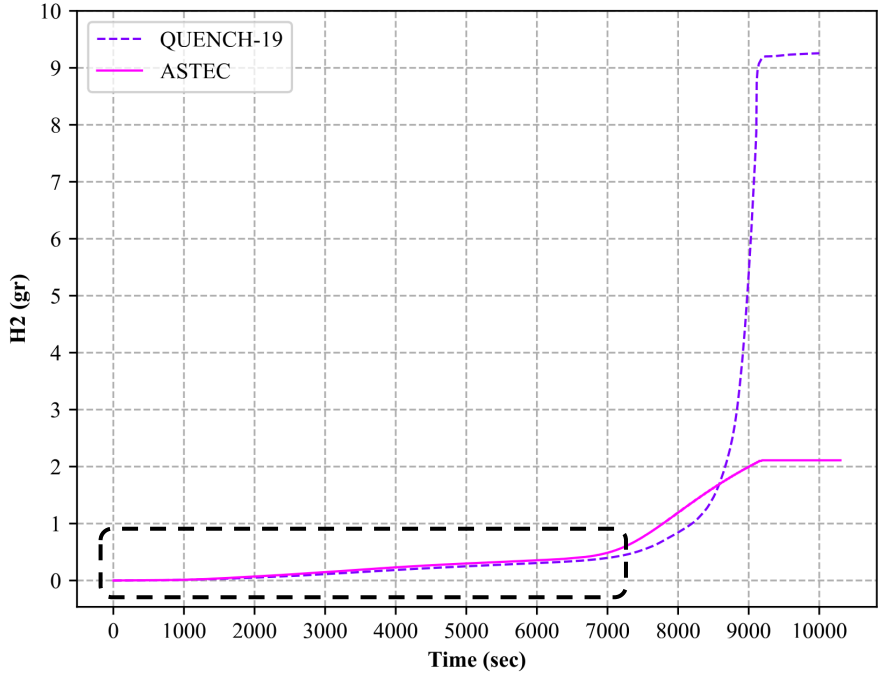

- **Experiment**
  $H_2 = 9.3$ grams
- **Cladding oxidation process**
  $H_2 = 7.2$ grams
- **ASTEC**
  $H_2 = 2.1$ grams

Fig. 9 Comparison total amount of hydrogen production from ASTEC vs bundle test QUENCH-19

Conclusion

- A KIT/INR and IRSN shared activity has been going on to improve the ASTEC modelling for FeCrAl cladding behavior in steam environment at low and moderate temperatures
- Modelling extensions have been implemented in ASTEC also based on the physical models resulting from the experimental investigations by the QUENCH team
- Validation of the improved ASTEC FeCrAl modelling has been performed
- QUENCH SETs:
  - ASTEC rather well predicts the experimental data with respect to Weight gain, Thickness oxide layer, and Hydrogen production in the experimental temperature range (873 K – 1573 K)
- QUENCH-19 bundle test
  - ASTEC well reproduces the experimental temperatures and hydrogen production as long as T<1500K
  - At very high T, important deviations appear in temperatures and H2 production, due to current model limitations:
    - Oxidation of Al only in the model overestimates Al_2O_3 layer and leads to a too strong stable protective role
    - Real Fe oxidation must be included in the modelling, with corresponding oxide layers

Outlook

- Application of the improved ASTEC modelling capabilities to postulated accidental scenarios in a generic SMR

- Application of ASTEC to the activities on the Cr-coated cladding materials in the frame of the OECD/NEA QUENCH-ATF project

Thank you for your attention

Chris Allison, pres. by Victor Martinez

ISS, ENSO

FeCrAl Oxidation Model Development on the ASTEC Code and Preliminary Validation Against QUENCH Experiments

RELAP/SCDAPSIM and ASYST are detailed BEPU codes being developed though two collaborative international programs, ADTP and SDTP (ASYST/SCDAPSIM Development and Training Programs, respectively). These two codes share many common features including detailed SCDAPSIM LWR/HPWR transient fuel assembly and reactor material behaviour models, MATPRO-based material property library, integrated uncertainty analysis options, and advanced interactive desktop simulator environments. The original development of the LWR fuel assembly behaviour models and MATPRO materials property library was started in the early 1970s by the U.S. Nuclear Regulatory Commission for use in their steady state and transient fuel behaviour codes for normal and design basis accident (DBA) conditions using UO2 fuel and Zircaloy cladding. In the 1980s, it was extended for beyond design basis (BDBA) conditions with additions of material properties for a variety of LWR core and reactor vessel materials including {U-Zr}-O2, stainless steel, Inconel, B4C, and Ag- In-Cd. In the 1990s, they were extended by Innovative Systems Software (ISS) to include Zr-Nb cladding material properties developed for VVERs for DBA and BDBA conditions. In the 2000s, the transient fuel assembly models were extended for DBA and early BDBA conditions for HPWRs. In 2019, in support of IAEA ATF-TS (collaborative research project, implementation of ATF (Accident Tolerant Fuel) models and correlations into SCDAPSIM and MATPRO was started. Descriptions of the implementation and assessment of preliminary models and correlations for FeCrAl (2022) and Cr-coated-Zr (2024) are now published in the open literature. Independent assessment of the models and correlations is now underway. Updated models and correlations will be released in 2025 once the IAEA published the final documentation for their ATF-TS project. *Please note: - separate effects and integral bundle experiments performed and described as part of the IAEA ATF-TS project are limited to DBA and early phases of BDBA conditions.*

The presentation for this meeting will focus on comparisons on the differences between the original Zr cladding and Cr-coated-Zr behavior using a reference Quench-06 input model developed originally for an international standard problem exercise and now used as a standard model for SCDAPSIM user training and certification. Similar comparisons were made for a variety of historic experiments including the PBF SFD-ST and SFD-1-4, also used in user training and certification.

Development and Assessment ATF cladding materials for DBA and BDBA conditions using SCDAPSIM

Presented
Dr. Victor Martinez-Quiroga, Energy Software, Ltd

Materials Prepared by
Dr. Chris Allison, Innovative Systems Software
Dr. Sarah Khalil, Alexandria University
Dr. Marina Perez-Ferragut, UPC / Energy Software, Ltd

Focus on assessment of Cr-coated-Zr oxidation models developed and implemented by ANT group in UPC

Two modelling options added to RELAP/SCDAPSIM

* **Bounding model** [$T_{threshold}$] simplified model that simulates the effect of the coating by turning off the Zr oxidation below a threshold temperature.
* **Cr-oxidation model** [$Cr_{thickness}$] modifies the zircaloy oxidation based on (1) T_{Cr}, (2) time from the onset of Cr oxidation, (3) Cr oxide thickness.

Phase	Conditions	Cr oxidation	Zr oxidation
#1	$T_{Cr} < 1000K$	$\delta_{C_{r_2O_3}} = w_{C_{r_2O_3}} = 0$	$\delta_{C_{r_2O_3}} = w_{C_{r_2O_3}} = 0$
#2	$1000K \le T_{Cr} < 1586K^{(*)}$, $\delta_{Cr2O3} < \varepsilon_1$, $t(T_{Cr} \ge 1000K) < 1.5h$	$\delta_{C_{r_2O_3}}$ $w_{C_{r_2O_3}}$	$\delta_{Zr_{O_2}} = 0.0 \cdot \delta_{Zr_{O_2}}^{non-coated}$ $w_{Zr_{O_2}} = 0.0 \cdot w_{Zr_{O_2}}^{non-coated}$
#3	$1000K \le T_{Cr} < 1586K^{(*)}$, $\delta_{Cr2O3} < \varepsilon_1$, $1.5h > t(T_{Cr} \ge 1000K) \le 3h$	$\delta_{C_{r_2O_3}} = 10\ \% \delta_{C_{r_2O_3}(t=1.5h)}$ $w_{C_{r_2O_3}} = 10\ \% w_{C_{r_2O_3}(t=1.5h)}$	$\delta_{Zr_{O_2}} = 0.1 \cdot \delta_{Zr_{O_2}}^{non-coated}$ $w_{Zr_{O_2}} = 0.1 \cdot w_{Zr_{O_2}}^{non-coated}$
#4	$1000K \le T_{Cr} < 1586K^{(*)}$, $\delta_{Cr2O3} < \varepsilon_1$, $t(\text{from } T_{Cr} \ge 1000K) > 3h$		$\delta_{Zr_{O_2}} = 0.25 \cdot \delta_{Zr_{O_2}}^{non-coated}$ $w_{Zr_{O_2}} = 0.25 \cdot w_{Zr_{O_2}}^{non-coated}$
#5	$\delta_{Cr2O3} \ge \varepsilon_1$	$\delta_{C_{r_2O_3}} = 0; w_{C_{r_2O_3}} = 0; \frac{dw_{C_{r_2O_3}}}{dt} = 0$	$\delta_{Zr_{O_2}} = \delta_{Zr_{O_2}}^{non-coated} + \varepsilon_1$ $w_{Zr_{O_2}} = w_{Zr_{O_2}}^{non-coated} + w_{Cr_2O_3}(\varepsilon_1)$
#6	$T_{Cr} \ge 1586K$	$\delta_{C_{r_2O_3}} = 0; w_{C_{r_2O_3}} = 0; \frac{dw_{C_{r_2O_3}}}{dt} = 0$	$\delta_{Zr_{O_2}} = \delta_{Zr_{O_2}}^{non-coated} + \varepsilon_1$ $w_{Zr_{O_2}} = w_{Zr_{O_2}}^{non-coated} + w_{Cr_2O_3}(\varepsilon_1)$

Focus on assessment of Cr-coated-Zr oxidation models developed and implemented by UPC Barcelona

Models assessed using TH conditions from historical bundle experiments

* QUENCH - 06: out-of-pile experiment conducted at the Karlsruhe Research Center in 2000.
* PBF SFD ST and 1-4: in-pile experiments conducted at the Idaho National Engineering Laboratory in the 1980s.

These experiments have been thoroughly analysed with RELAP/SCDAPSIM in the past as they served as benchmarks for validating the code.

QUENCH – 06 RELAP/SCDAPSIM nodalization

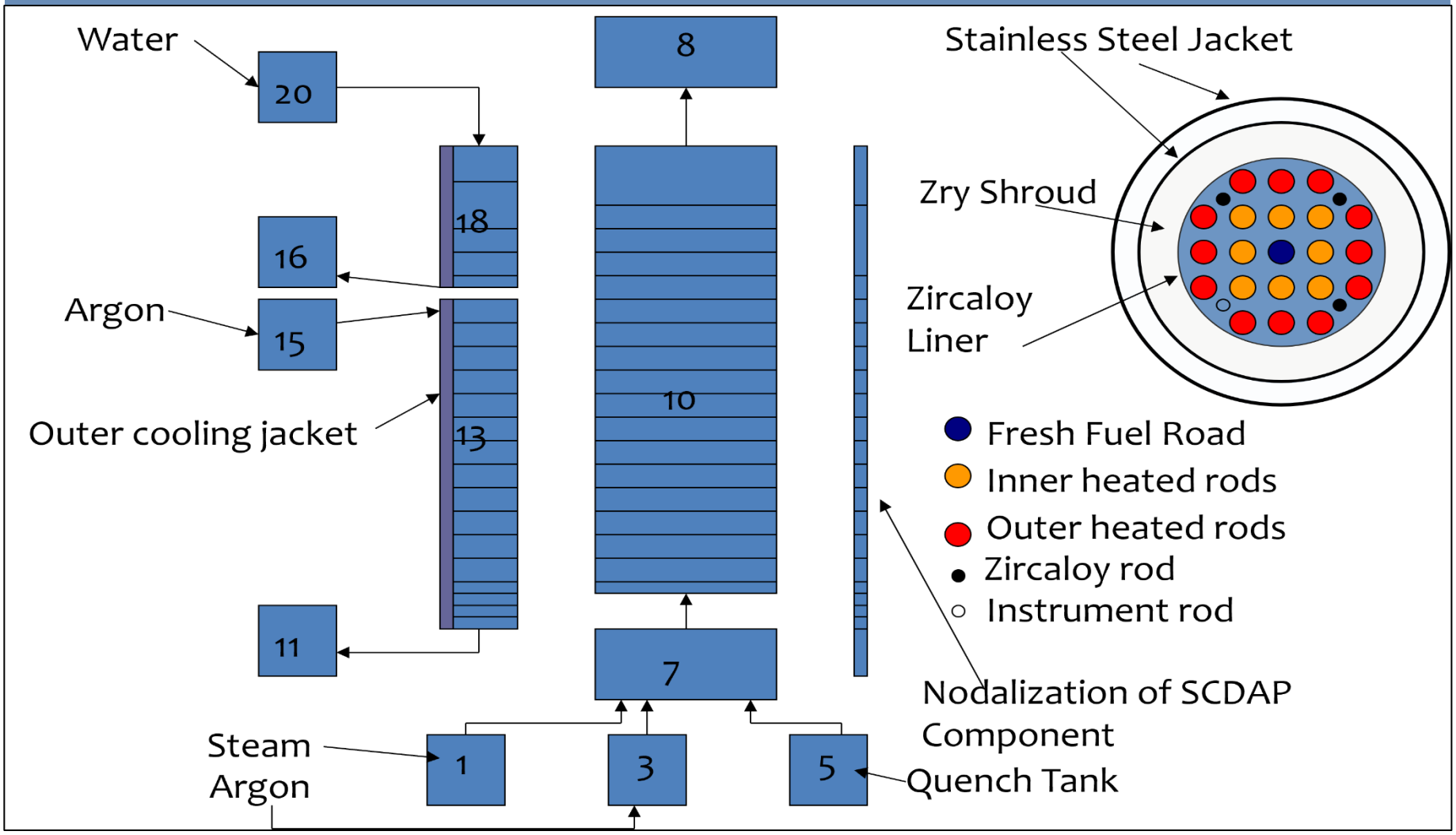

QUENCH – 06 bundle input description

- **Five SCDAPSIM core components used to model Quench -06 bundle**
  - Fuel rod component (Comp 1) – 1 center unheated rod
  - Electrically heated simulator components (Comp 2 & 3)
    - Inner ring of 8 electrically heated rods
    - Outer ring of 12 electrically heated rods
  - Fuel rod component with cladding only (Comp 4)
    - Corner rods of 4 unheated solid rods (used for oxidation sampling)
  - Shroud component (Comp 5) – outer insulated shroud with Zr liner to simulate additional ring of rods
- **Components 1-4 used Cr-coating or Zr models**
- **Component 5 used Zr liner**

QUENCH – 06 TH boundary conditions

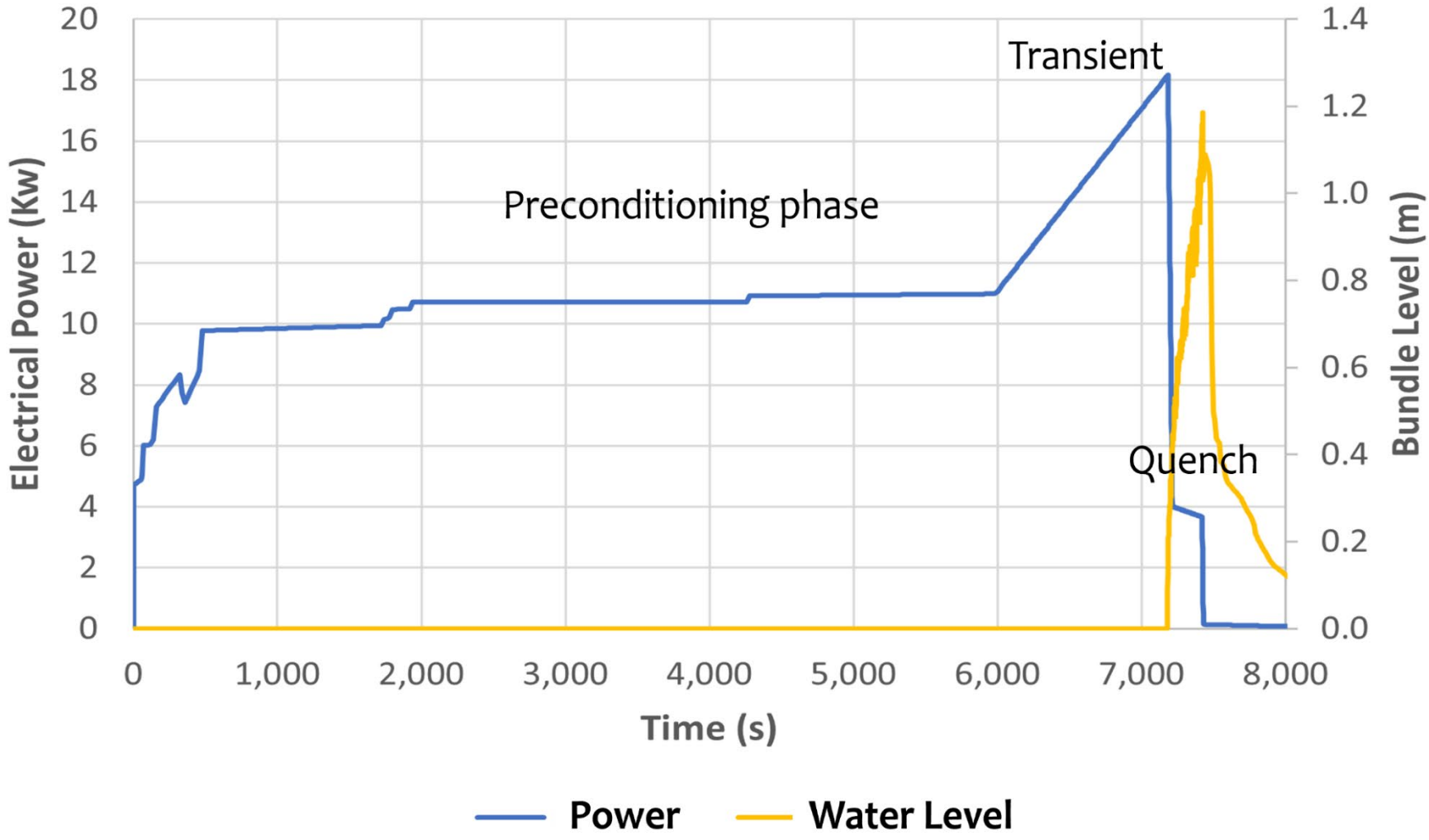

Historic presentation of RELAP/SCDAPSIM comparisons with experimental results **(Zr only)**

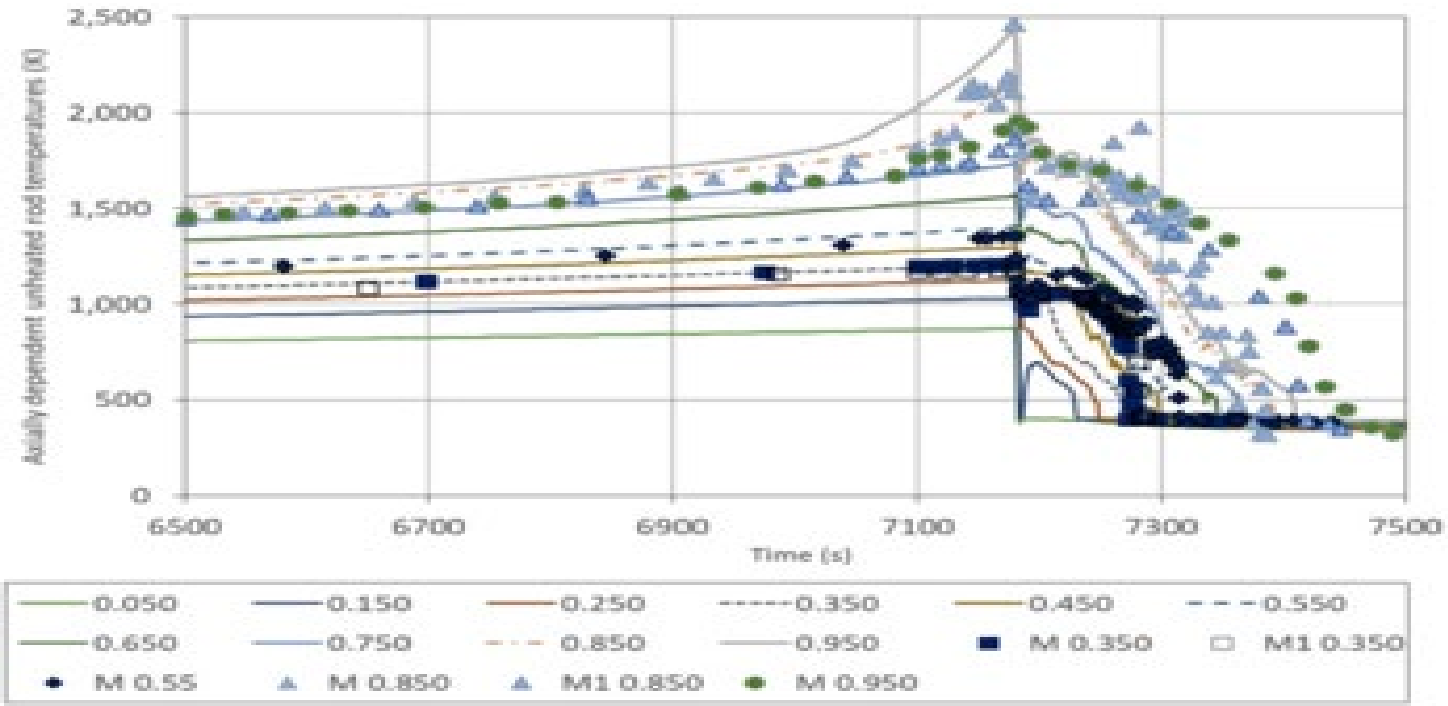

Figure 9 – Calculated bundle temperatures as a function of elevation (solid lines) in comparison to measured bundle temperatures at elevations of 350mm, 550mm, 850mm, and 950mm elevation (symbols).

emperature tion

Phase	Conditions	Chromium oxidation	Zirconium oxidation
#1	$T_{Cr} < 1000K$	$\delta_{c_{r_2O_3}} = w_{c_{r_2O_3}} = 0$	$\delta_{c_{r_2O_3}} = w_{c_{r_2O_3}} = 0$
#2	$1000K \le T_{Cr} < 1586K^{(*)}$, $\delta_{Cr2O3} < \varepsilon_1$, $t(T_{Cr} \ge 1000K) < 1.5h$	$\delta_{c_{r_2O_3}}$ $w_{c_{r_2O_3}}$	$\delta_{zr_{O_2}} = 0.0 \cdot \delta_{zr_{O_2}}^{non-coated}$ $w_{zr_{O_2}} = 0.0 \cdot w_{zr_{O_2}}^{non-coated}$
#3	$1000K \le T_{Cr} < 1586K^{(*)}$, $\delta_{Cr2O3} < \varepsilon_1$, $1.5h > t(T_{Cr} \ge 1000K) \le 3h$	$\delta_{c_{r_2O_3}} = 10\ \% \delta_{c_{r_2O_3}(t=1.5h)}$ $w_{c_{r_2O_3}} = 10\ \% w_{c_{r_2O_3}(t=1.5h)}$	$\delta_{zr_{O_2}} = 0.1 \cdot \delta_{zr_{O_2}}^{non-coated}$ $w_{zr_{O_2}} = 0.1 \cdot w_{zr_{O_2}}^{non-coated}$
#4	$1000K \le T_{Cr} < 1586K^{(*)}$, $\delta_{Cr2O3} < \varepsilon_1$, $t(\text{from } T_{Cr} \ge 1000K) > 3h$		$\delta_{zr_{O_2}} = 0.25 \cdot \delta_{zr_{O_2}}^{non-coated}$ $w_{zr_{O_2}} = 0.25 \cdot w_{zr_{O_2}}^{non-coated}$
#5	$\delta_{Cr2O3} \ge \varepsilon_1$	$\delta_{c_{r_2O_3}} = 0; w_{c_{r_2O_3}} = 0; \frac{dw_{c_{r_2O_3}}}{dt} = 0$	$\delta_{zr_{O_2}} = \delta_{zr_{O_2}}^{non-coated} + \varepsilon_1$ $w_{zr_{O_2}} = w_{zr_{O_2}}^{non-coated} + w_{Cr_2O_3}(\varepsilon_1)$
#6	$T_{Cr} \ge 1586K$	$\delta_{c_{r_2O_3}} = 0; w_{c_{r_2O_3}} = 0; \frac{dw_{c_{r_2O_3}}}{dt} = 0$	$\delta_{zr_{O_2}} = \delta_{zr_{O_2}}^{non-coated} + \varepsilon_1$ $w_{zr_{O_2}} = w_{zr_{O_2}}^{non-coated} + w_{Cr_2O_3}(\varepsilon_1)$

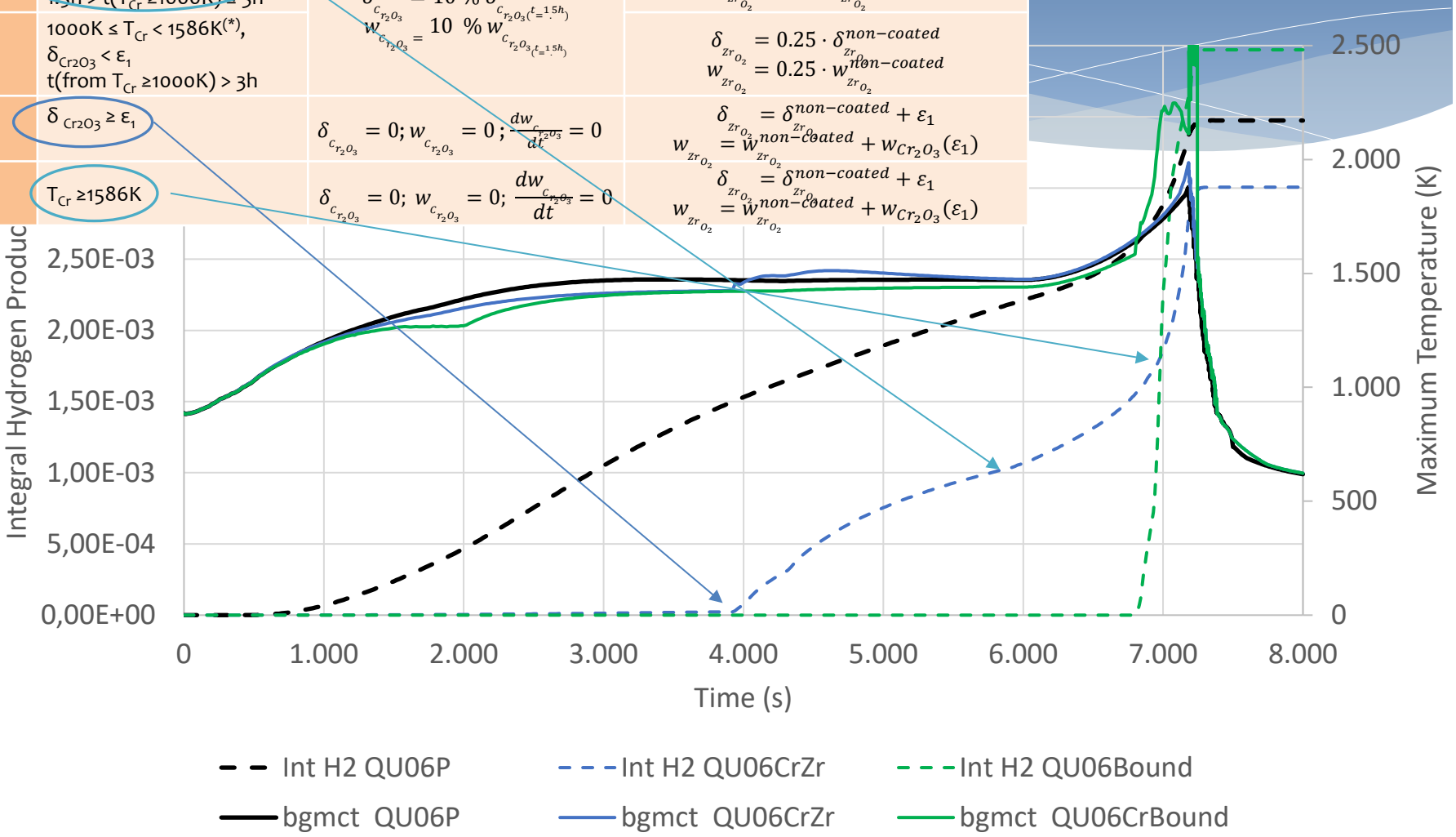

Temperature distribution of SCDAPSIM core components – 7180 s (Max. Power)

Note – Shroud used Zr liner

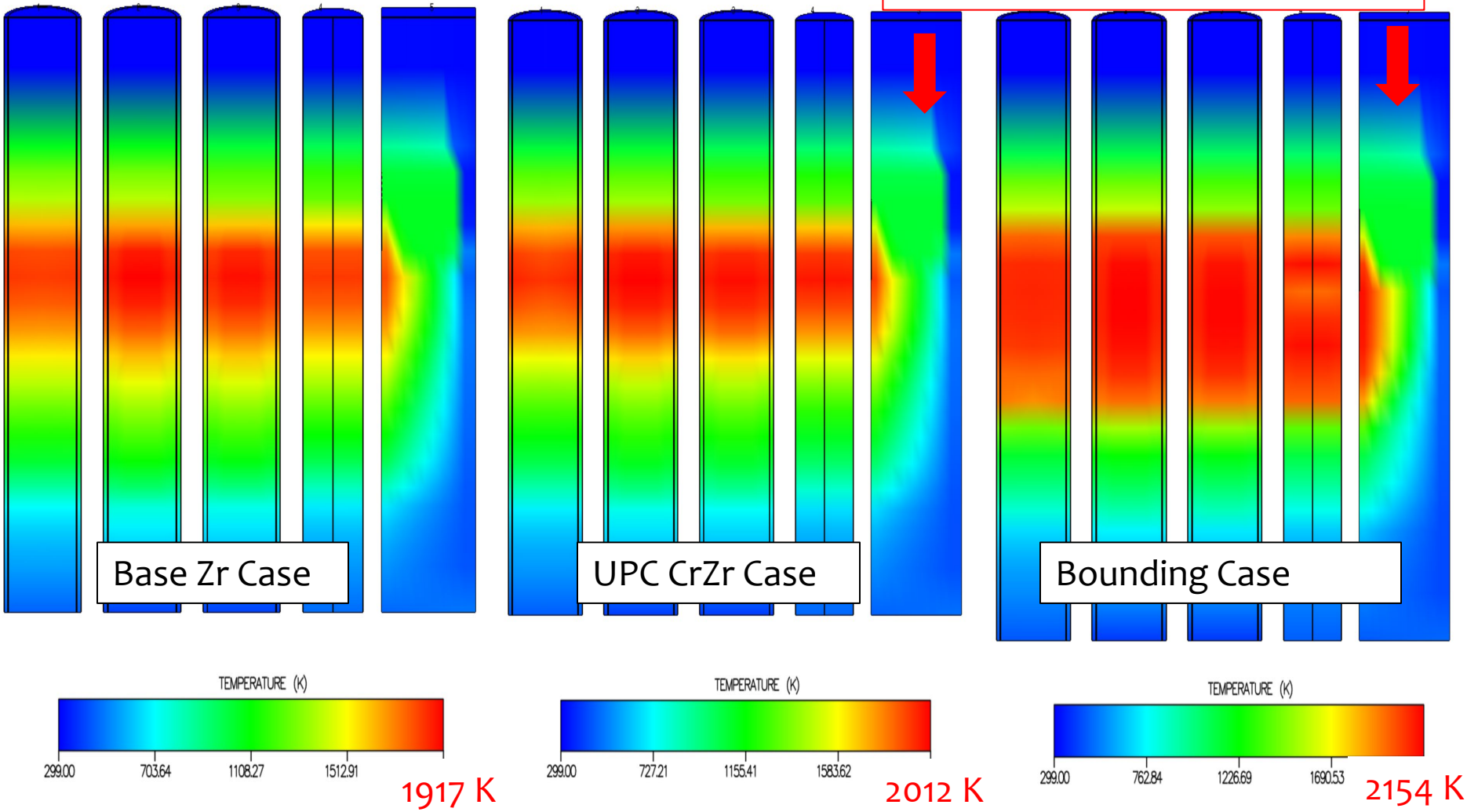

Oxide thickness distribution of SCDAPSIM core components – 7180 s (Max. Power)

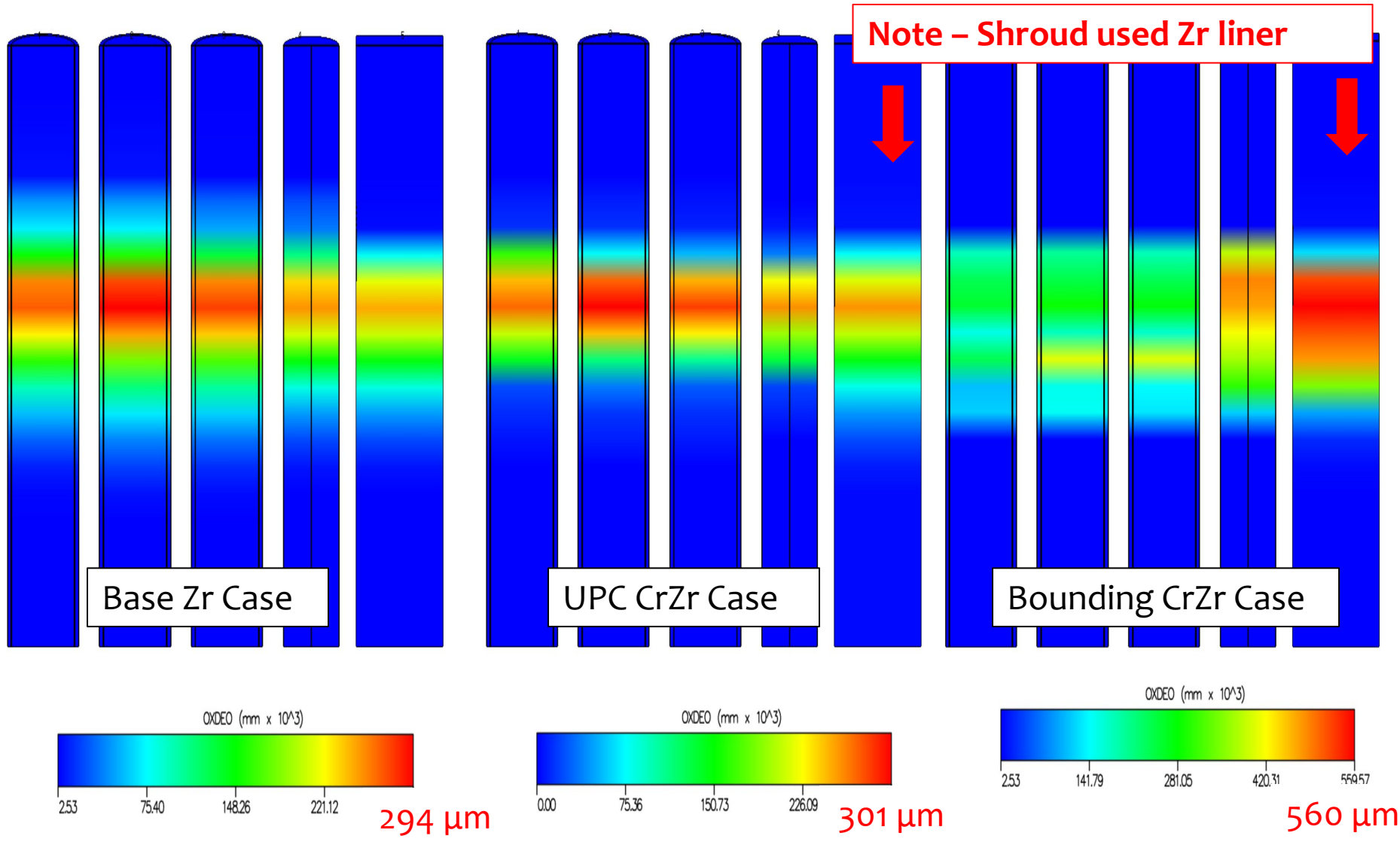

Preliminary Conclusions

Regarding the simulation results:

* Cr-coated-Zr fuel rod cladding materials is very effective in reducing hydrogen production relative to Zr where temperatures remain below 1500 K
  * Results are similar to FeCrAl cladding reported in previously published materials
* Comparison of such ATF cladding materials for wide range of experimental conditions used to assess the behavior when temperatures exceed 1500 K show oxidation can increase significantly as the Cr coated starts to degrade
  * Experimental conditions such as those occurring in Quench-06 and PBF SFD-ST where the Cr-coated-Zr fuel bundle is quenched may result in hydrogen generation rates exceeding those of Zr

Preliminary Conclusions

Regarding the Cr-coating-Zr oxidation model:

* Next step is to validate the model with experimental data
* The model contains limitation and could be improved: complete local failures when reaching the 1586 K, reduction of chromia thickness may be calculated as a function of the Cr-thickness, …

Thank you for your attention

PBF SFD TH BCs and Bundle Nodalization

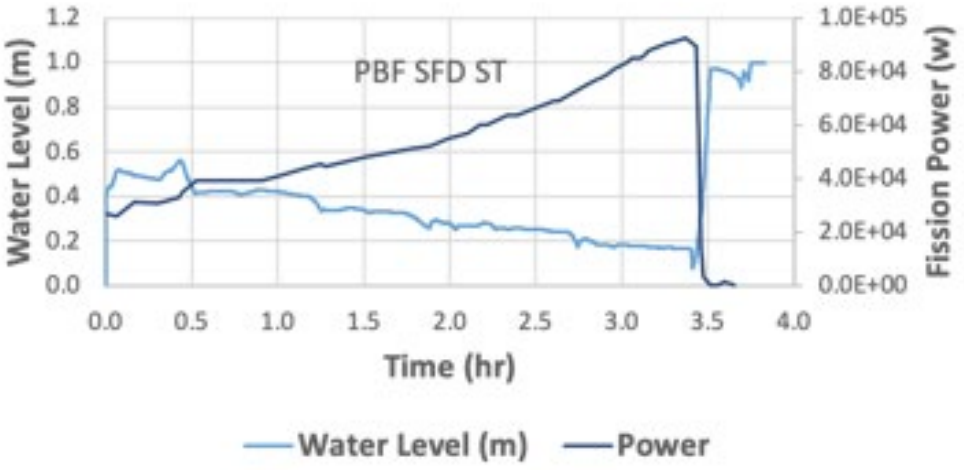

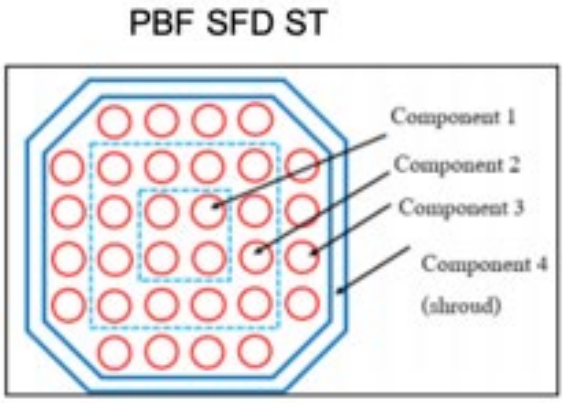

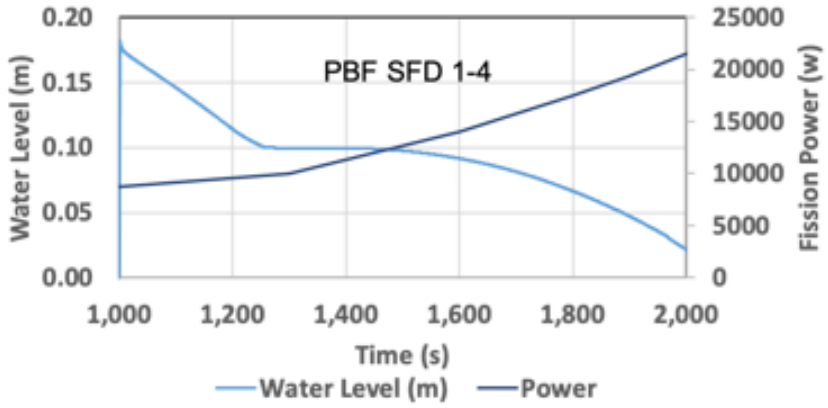

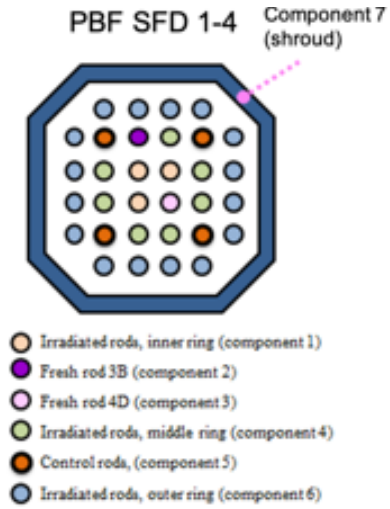

Comparison of Maximum Bundle Temperature and Integrated H2 production – PBF SFD ST

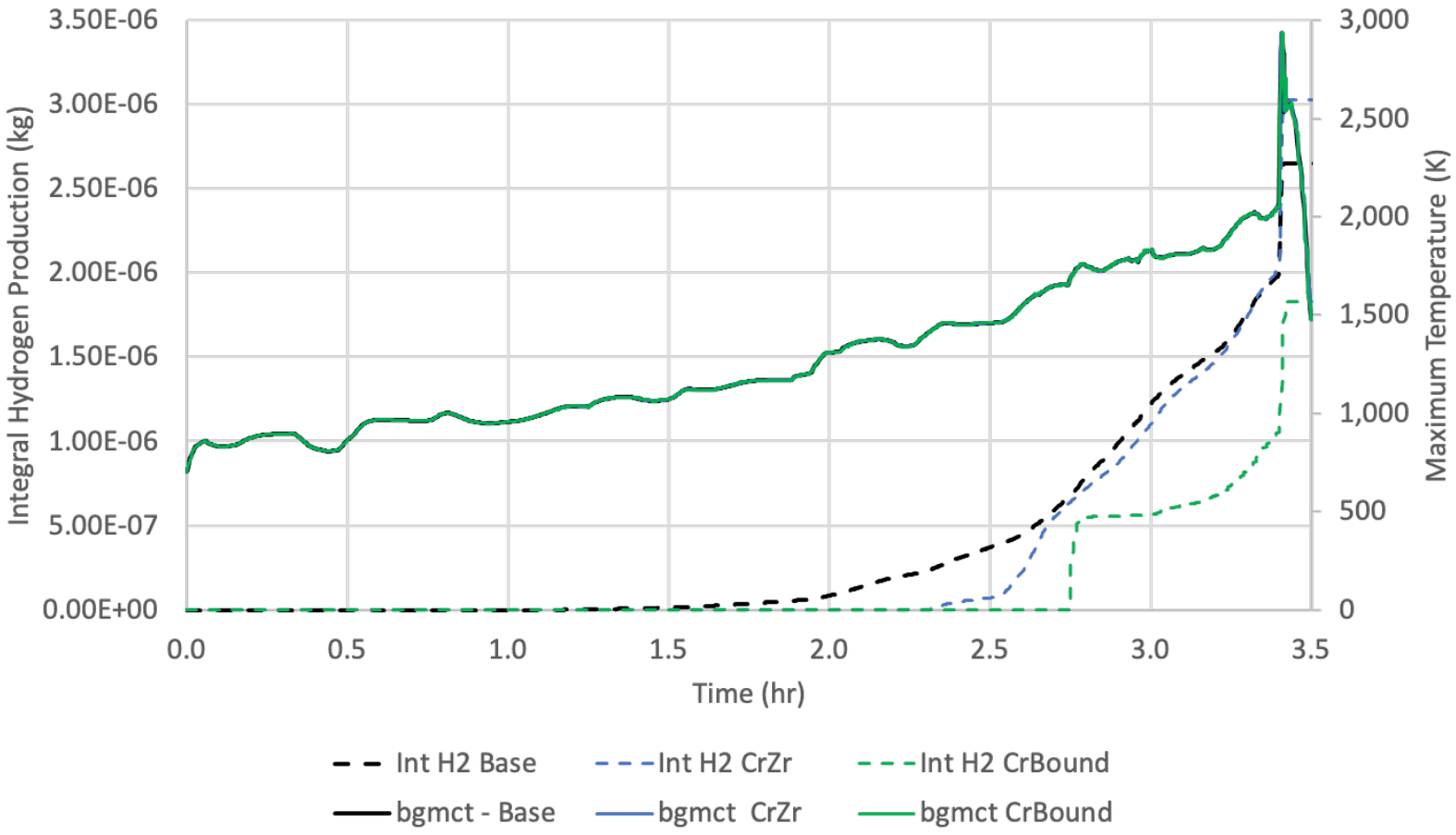

Comparison of Maximum Bundle Temperature and Integrated H2 production – PBF SFD 1-4

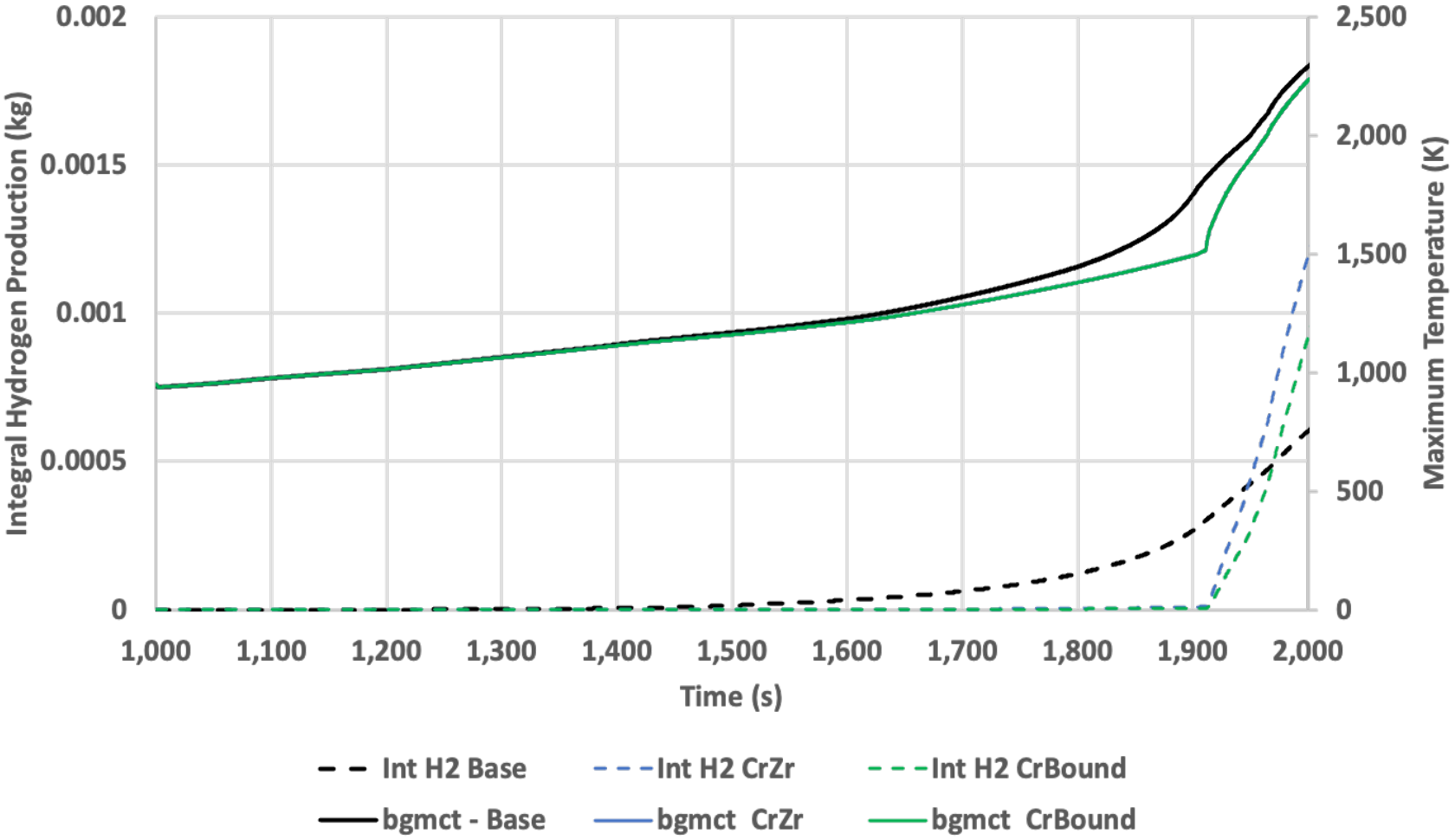

Cr-coating-Zr oxidation model

QU06_igb-4withonApr.o + (~\Desktop\RS\RS_TopFuel2024) - GVIM1

File Edit Tools Syntax Buffers Window Help

```
16718   3500.000      0.50239      6.03700E-03   0.0000      2.55484E-09  2.55108E-09  2.55132E-09  2.55367E-09
16719   3520.000      0.50239      6.03700E-03   0.0000      2.55485E-09  2.55107E-09  2.55132E-09  2.55366E-09
16720   3540.000      0.50238      6.03700E-03   0.0000      2.55485E-09  2.55107E-09  2.55131E-09  2.55366E-09
16721   3560.000      0.50238      6.03700E-03   0.0000      2.55485E-09  2.55106E-09  2.55131E-09  2.55366E-09
16722   3580.000      0.50238      6.03700E-03   0.0000      2.55485E-09  2.55106E-09  2.55131E-09  2.55365E-09
16723   3600.000      0.50238      6.03700E-03   0.0000      2.55485E-09  2.55106E-09  2.55130E-09  2.55365E-09
16724   3620.000      0.50237      6.03700E-03   0.0000      2.55485E-09  2.55105E-09  2.55130E-09  2.55365E-09
16725   3640.000      0.50237      6.03700E-03   0.0000      2.55485E-09  2.55105E-09  2.55129E-09  2.55364E-09
16726   3660.000      0.50237      6.03700E-03   0.0000      2.55485E-09  2.55105E-09  2.55129E-09  2.55364E-09
16727   3680.000      0.50236      6.03700E-03   0.0000      2.55485E-09  2.55104E-09  2.55129E-09  2.55364E-09
16728 crcoated croxth>e1   5.00004E-06  5.00000E-06  3.92730E+03  2 14
16729 ///// tcr   1.42417E+03
16730 ///// croxth,croxwg,dcroxwg,qoxcr=   5.00004E-06  0.00000E+00  0.00000E+00  0.00000E+00
16731 crcoated croxth>e1   5.00003E-06  5.00000E-06  3.95370E+03  1 14
16732 ///// tcr   1.42532E+03
16733 ///// croxth,croxwg,dcroxwg,qoxcr=   5.00003E-06  0.00000E+00  0.00000E+00  0.00000E+00
16734 crcoated croxth>e1   5.00014E-06  5.00000E-06  3.98430E+03  3 14
16735 ///// tcr   1.42419E+03
16736 ///// croxth,croxwg,dcroxwg,qoxcr=   5.00014E-06  0.00000E+00  0.00000E+00  0.00000E+00
16737 1RELAP5/SCDAP 3.4.0 BUILD 05/2024        Reactor Analysis Program
16738     QUENCH 06 with CrZr updates Comp 1-4                                    2024/09/18   10:27:15
16739 0MAJOR EDIT !!!time=    4000.00     sec
16740 0 attempted adv: tot.=  50126   edit=  40064   min.dt=   6.250000E-03 sec   last dt=   5.000000E-02 sec   ms.red=  -2.339690E-04 kg
16741    repeated adv: tot.=     17   edit=      6   max.dt=   5.000000E-02 sec   crnt.dt=   1.808146E-02 sec   tot.ms=    7.31135     kg
16742  successful adv: tot.=  50109   edit=  40058   avg.dt=   4.992760E-02 sec   err.est=   4.486489E-06       m.rato=  -3.110375E-05
16743   requested adv: tot.=  50000   edit=  40000   req.dt=   5.000000E-02 sec       cpu=    39.3281     sec     time=    4000.00     sec
16744 0System  1   exper    mass=  8.05555E-03 kg    mass error= -2.67544E-04 kg    err.est.=  4.48649E-06
16745 0    Vol.no.  pressure      voidf        voidg        quala         tempf      tempg     satt-part   uf          ug       vol-flag
16746               (Pa)                                                (K)        (K)       (K)      (J/kg)      (J/kg)     tlpvbfe
                                                                                                                  16728,1       37%
```

Cr-coating-Zr oxidation model

QU06_igb-4withonApr.o + (~\Desktop\RS\RS_TopFuel2024) - GVIM1

File Edit Tools Syntax Buffers Window Help

```
19661   5420.000      0.50425      6.03700E-03   0.0000      2.55444E-09  1.38548E-04  1.30032E-04  2.55262E-09
19662   5440.000      0.50423      6.03700E-03   0.0000      2.55445E-09  1.39404E-04  1.30857E-04  2.55263E-09
19663   5460.000      0.50420      6.03700E-03   0.0000      2.55445E-09  1.40250E-04  1.31672E-04  2.55264E-09
19664   5480.000      0.50417      6.03700E-03   0.0000      2.55445E-09  1.41087E-04  1.32479E-04  2.55265E-09
19665   5500.000      0.50415      6.03700E-03   0.0000      2.55445E-09  1.41916E-04  1.33277E-04  2.55266E-09
19666   5520.000      0.50412      6.03700E-03   0.0000      2.55445E-09  1.42736E-04  1.34067E-04  2.55267E-09
19667   5540.000      0.50410      6.03700E-03   0.0000      2.55445E-09  1.43547E-04  1.34848E-04  2.55268E-09
19668   5560.000      0.50407      6.03700E-03   0.0000      2.55445E-09  1.44351E-04  1.35621E-04  2.55268E-09
19669   5580.000      0.50405      6.03700E-03   0.0000      2.55445E-09  1.45147E-04  1.36387E-04  2.55269E-09
19670   5600.000      0.50403      6.03700E-03   0.0000      2.55445E-09  1.45935E-04  1.37145E-04  2.55270E-09
19671   5620.000      0.50400      6.03700E-03   0.0000      2.55445E-09  1.46715E-04  1.37896E-04  2.55271E-09
19672   5640.000      0.50398      6.03700E-03   0.0000      2.55446E-09  1.47489E-04  1.38640E-04  2.55272E-09
19673   5660.000      0.50396      6.03700E-03   0.0000      2.55446E-09  1.48255E-04  1.39376E-04  2.55272E-09
19674   5680.000      0.50394      6.03700E-03   0.0000      2.55446E-09  1.49014E-04  1.40106E-04  2.55273E-09
19675 crcoated dt>5400, dt=  5.40000E+03 at node  12 component   2.  3.14637E-07  3.14637E-06
19676 crcoated 1.5h<dt<3h dt=  1.50000E+00  5.93640E+03  2 12
19677 ///// tcr   1.35629E+03
19678 ///// croxth,croxwg,dcroxwg,qoxcr=   3.14637E-07  5.03635E-04  9.22884E-06  3.46305E+06
19679 crcoated dt>5400, dt=  5.40000E+03 at node  12 component   3.  2.76837E-07  2.76837E-06
19680 crcoated 1.5h<dt<3h dt=  1.50000E+00  5.99700E+03  3 12
19681 ///// tcr   1.34479E+03
19682 ///// croxth,croxwg,dcroxwg,qoxcr=   2.76837E-07  4.43270E-04  8.20870E-06  3.46645E+06
19683 1RELAP5/SCDAP 3.4.0 BUILD 05/2024        Reactor Analysis Program
19684     QUENCH 06 with CrZr updates Comp 1-4                              2024/09/18   10:27:15
19685 0MAJOR EDIT !!!time=    6000.00     sec
19686 0 attempted adv: tot.=  90272   edit=  40146   min.dt=   6.250000E-03 sec   last dt=   4.999999E-02 sec   ms.red=  -2.127377E-04 kg
19687    repeated adv: tot.=     33   edit=     16   max.dt=   5.000000E-02 sec   crnt.dt=   1.764877E-02 sec   tot.ms=    7.23283     kg
19688  successful adv: tot.=  90239   edit=  40130   avg.dt=   4.983803E-02 sec   err.est=   8.176706E-06       m.rato=  -2.828126E-05
19689   requested adv: tot.=  90000   edit=  40000   req.dt=   4.999999E-02 sec       cpu=    69.8281     sec     time=    6000.00     sec
/5400,                                                                                                          19675,13      44%
```

Cr-coating-Zr oxidation model

QU06_igb-4withonApr.o + (~\Desktop\RS\RS_TopFuel2024) - GVIM1

File Edit Tools Syntax Buffers Window Help

```
24413   6780.000      0.51059      6.03705E-03   0.0000      1.40510E-05  1.99302E-04  1.87621E-04  1.94773E-05
24414   6790.000      0.51077      6.03705E-03   0.0000      1.42498E-05  2.00254E-04  1.88500E-04  1.97335E-05
24415   6800.000      0.51097      6.03705E-03   0.0000      1.44514E-05  2.01229E-04  1.89400E-04  1.99930E-05
24416   6810.000      0.51117      6.03705E-03   0.0000      1.46558E-05  2.02229E-04  1.90322E-04  2.02559E-05
24417   6820.000      0.51138      6.03705E-03   0.0000      1.48632E-05  2.03253E-04  1.91266E-04  2.05221E-05
24418   6830.000      0.51161      6.03705E-03   0.0000      1.50735E-05  2.04304E-04  1.92234E-04  2.07920E-05
24419   6840.000      0.51184      6.03705E-03   0.0000      1.52869E-05  2.05381E-04  1.93226E-04  2.10656E-05
24420 crcoated dt<1.5h dt=  1.38346E-05  6.84550E+03  3  7
24421 ///// tcr   1.00001E+03
24422 ///// croxth,croxwg,dcroxwg,qoxcr=   5.71278E-11  9.28183E-08  1.86365E-06  3.58183E+06
24423 crcoated dt>5400, dt=  5.40000E+03 at node   9 component   1.  3.90450E-08  3.90450E-07
24424 crcoated 1.5h<dt<3h dt=  1.50000E+00  6.88000E+03  1  9
24425 ///// tcr   1.18453E+03
24426 ///// croxth,croxwg,dcroxwg,qoxcr=   3.90450E-08  6.31930E-05  1.17024E-06  3.51691E+06
24427 crcoated T>1586  1.78656E+00  6.96800E+03  2 12
24428 ///// tcr   1.58600E+03
24429 ///// croxth,croxwg,dcroxwg,qoxcr=   0.00000E+00  0.00000E+00  0.00000E+00  0.00000E+00
24430 crcoated T>1586  1.77596E+00  6.99045E+03  3 12
24431 ///// tcr   1.58603E+03
24432 ///// croxth,croxwg,dcroxwg,qoxcr=   0.00000E+00  0.00000E+00  0.00000E+00  0.00000E+00
24433 1RELAP5/SCDAP 3.4.0 BUILD 05/2024        Reactor Analysis Program
24434     QUENCH 06 with CrZr updates Comp 1-4                                  2024/09/18   10:27:15
24435 0MAJOR EDIT !!!time=    7000.00     sec
24436 0 attempted adv: tot.= 110335   edit=   7629   min.dt=   3.125000E-03 sec   last dt=   5.000000E-02 sec   ms.red=  -2.168629E-04 kg
24437    repeated adv: tot.=     46   edit=      6   max.dt=   5.000000E-02 sec   crnt.dt=   1.480342E-02 sec   tot.ms=    7.19075     kg
24438  successful adv: tot.= 110289   edit=   7623   avg.dt=   4.984914E-02 sec   err.est=   1.526809E-06       m.rato=  -2.882966E-05
24439   requested adv: tot.= 110000   edit=   7600   req.dt=   5.000000E-02 sec       cpu=    83.0469     sec     time=    7000.00     sec
24440 0System  1   exper    mass=  7.22349E-03 kg    mass error= -2.50985E-04 kg    err.est.=  1.52681E-06
24441 0    Vol.no.  pressure      voidf        voidg        quala         tempf      tempg     satt-part   uf          ug       vol-flag
/1586                                                                                                                  24427,1       55%
```

Thorsten Hollands

GRS

Results of the QUENCH-ATF-1 Benchmark within OECD/NEA QUENCH-ATF

Zirconium-based claddings have been employed for several decades due to their favourable mechanical properties, corrosion resistance, and low neutron absorption under operational conditions. However, at elevated temperatures, these claddings display negative characteristics, such as exothermic oxidation reactions in steam or air environments. Research and development of conventional cladding and furthermore Accident Tolerant Fuel (ATF) materials has been motivated by the need to establish an additional safety element in nuclear power plants.

The objective of the OECD/NEA QUENCH-ATF project is to investigate the effect of Cr-coated claddings, representing one ATF concept, on the accident progression. In addition to the three bundle experiments, the project also encompasses analytical activities, namely the simulation of the experiments with different codes for the purpose of evaluating their capabilities to model ATF-specific phenomena. The capacity to model Cr-coatings exhibits variability among severe accident codes, including AC²/ATHLET-CD, ASTEC, MAAP, SAMPSON, and MELCOR. Consequently, benchmark exercises are conducted with blind and open post-test simulations. The initial experiment, designated QUENCH-ATF-1, which addresses an extended DBA scenario, has been subjected to analysis.

The outcomes of both phases demonstrate that the codes are capable of predicting the qualitative behaviour observed in the experiment. In the blind phase, there is a notable underestimation of hydrogen generation by most codes, whereas the temperatures exhibit a satisfactory alignment with the measured data. By refining the model options and incorporating further assumptions based on an evaluation of the disclosed experimental data, the results of the open phase are brought closer to the experimental observations. However, some discrepancies remain. The application of different codes by different users revealed no code-specific weaknesses, indicating that the severe accident codes previously mentioned can predict Cr-coating oxidation and behaviour under extended DBA conditions. The capabilities will be further investigated within the QUENCH-ATF framework for the following experiments, for example, those dealing with DEC or severe accident conditions, where the transition to Zr oxidation occurs due to higher temperatures.

Results of the QUENCH-ATF-1 Benchmark within OECD/NEA QUENCH-ATF

Thorsten Hollands (GRS)

29th International QUENCH Workshop

Karlsruhe Institute of Technology, Campus North

Germany

19-21 November 2024

Outline

- Background and Motivation
- OECD/NEA QUENCH-ATF Project
- QUENCH Facility and Test Bundle
- QUENCH-ATF-1 Test Conduct
- QUENCH-ATF-1 Benchmark
  - Participants and Codes
  - ATF Modelling in Severe Accident Codes
  - Simulation Results
- Conclusion

Background and Motivation (I)

- Even before the Fukushima accident the investigations of accident tolerant fuel (ATF) and its related claddings were investigated, but afterwards the research and development were strengthened.
- Especially, for accident conditions benefit should be taken from the behavior of ATF which leads to longer grace time for accident measures, because the slower oxidation reaction kinetics would lead to slower core heat-up as long as the ATF cladding is intact. Afterwards however, the impact of the oxidation by steam could be much worse compared to classical Zr based alloys.
- Currently, two options are investigated for LWR FeCrAl alloys and Cr-coated Zr alloys with higher TRL, while SiC/SiC concepts have not that TRL.
- For FeCrAl the melting temperature is about 1500 °C and the oxidation reaction is about a factor of 100-1000 lower compared to Zr based alloys.
- Cr-coated alloys e.g., optimized Zirlo™ show orders of magnitude slower oxidation rate as long as the protective behavior of the coating is intact until app. 1300 °C. Afterwards, steam reaction with pure metallic Zr occurs, which escalates the oxidation reaction and temperature evolution. For both cases the hydrogen generation is much smaller compared to Zr steam oxidation (as long the coating is intact).

Background and Motivation (II)

- Currently, severe accident codes like AC²/ATHLET-CD, ASTEC, MAAP, MELCOR, and SAMPSON are improved for the consideration of such ATF concepts, especially for the oxidation and mechanical rod behavior.
- Complementary, several experimental campaigns are carried out for the estimation of ATF behavior on separate effect and integral test level.
- Experiments, modelling and simulations are part of running international projects like
  - IAEA ATF-TS (Testing and Simulation for Advanced Technology and Accident Tolerant Fuels) or
  - OECD/NEA QUENCH-ATF

➢ **This presentation deals with the analytical activities carried out in the OECD/NEA QUENCH-ATF project with respect to the benchmark of the first experiment QUENCH-ATF-1.**

OECD/NEA QUENCH-ATF Project

- The OECD/NEA QUENCH-ATF project was launched in 2021 to investigate the bundle behavior under DBA/DBC (design basis accident / design basis conditions) or DEC/BDBA/SA (design extension conditions / beyond design basis accident / severe accident).
- Therefore, the QUENCH facility at KIT (Karlsruhe Institute of Technology, Germany) is used which allows to consider a bundle of 24 rods with a length of 2.3 m. In the frame of QUENCH-ATF three bundle tests will be performed:
  - Optimized Zirlo with Cr-coating: LOCA conditions => Extended DBA
  - Optimized Zirlo with Cr-coating: BDBA conditions,
  - Optimized Zirlo with Cr-coating, scenario to be decided.

QUENCH Facility and Bundle

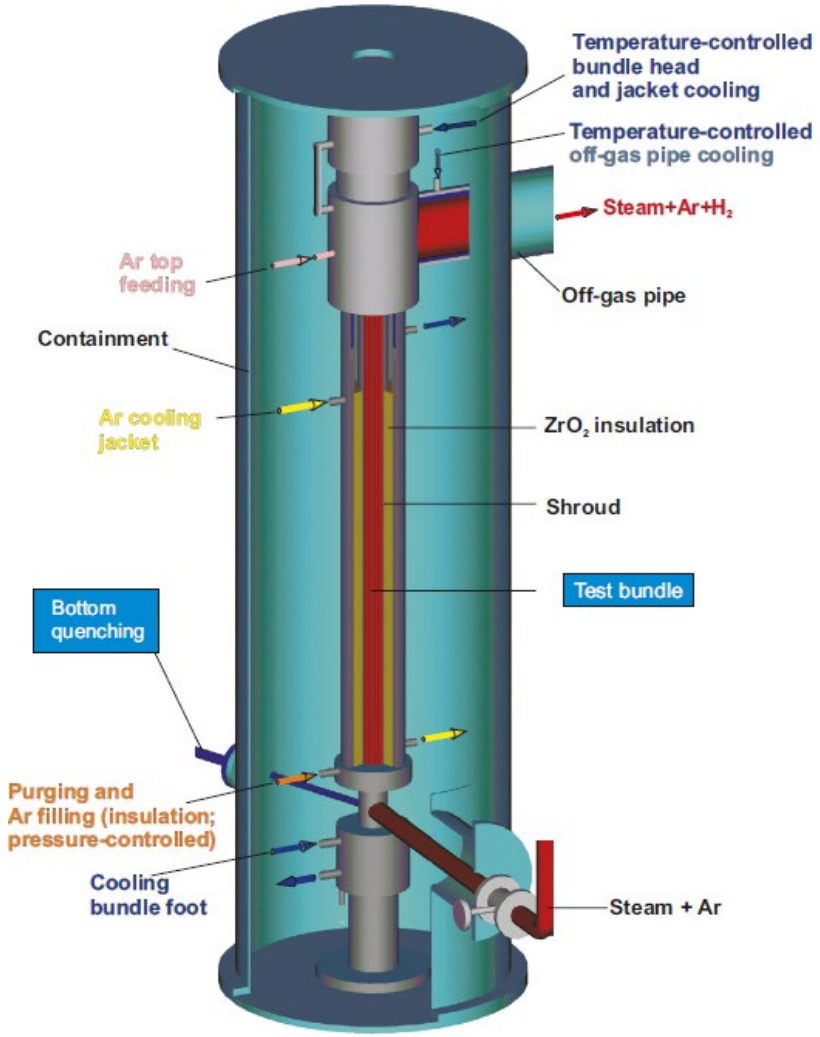

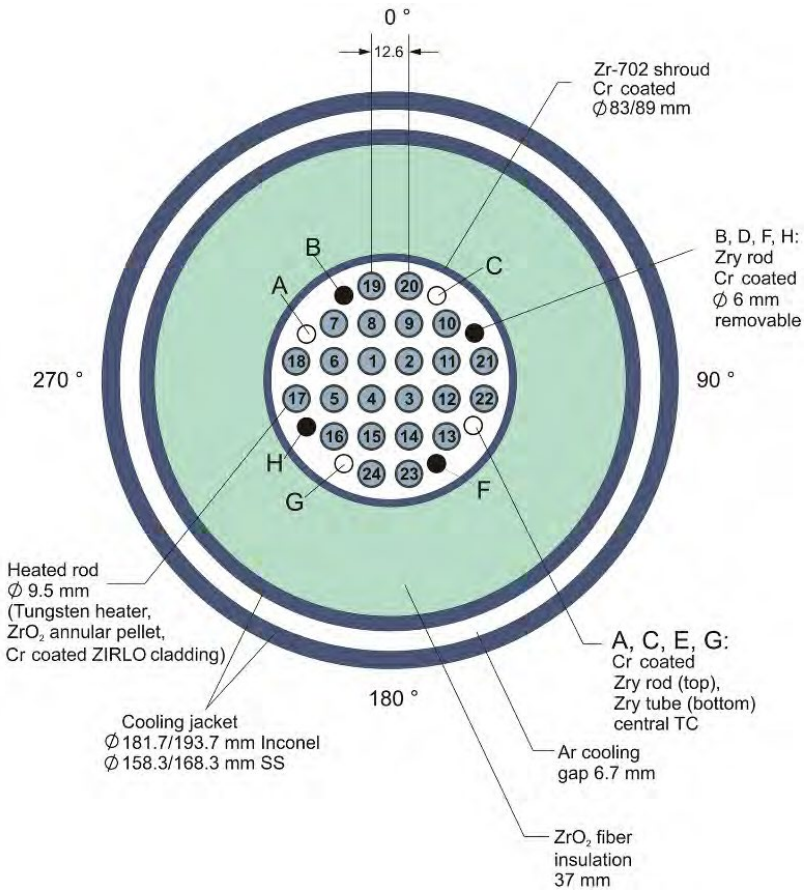

Source: KIT

QUENCH Test Conduct

- The main characteristics of the test QUENCH-ATF-1 are the following:
  - Extended LOCA conditions up to 1300 °C
  - Cr-coated optimized Zirlo claddings
  - Quenching with water
  - Reference test QUENCH-L3HT experiment

- Test Phases
  - Conditioning phase
  - Heat-up by increasing the power
  - Burst occurrence
  - Cooldown by power reduction and subsequent quenching

QUENCH-L3HT

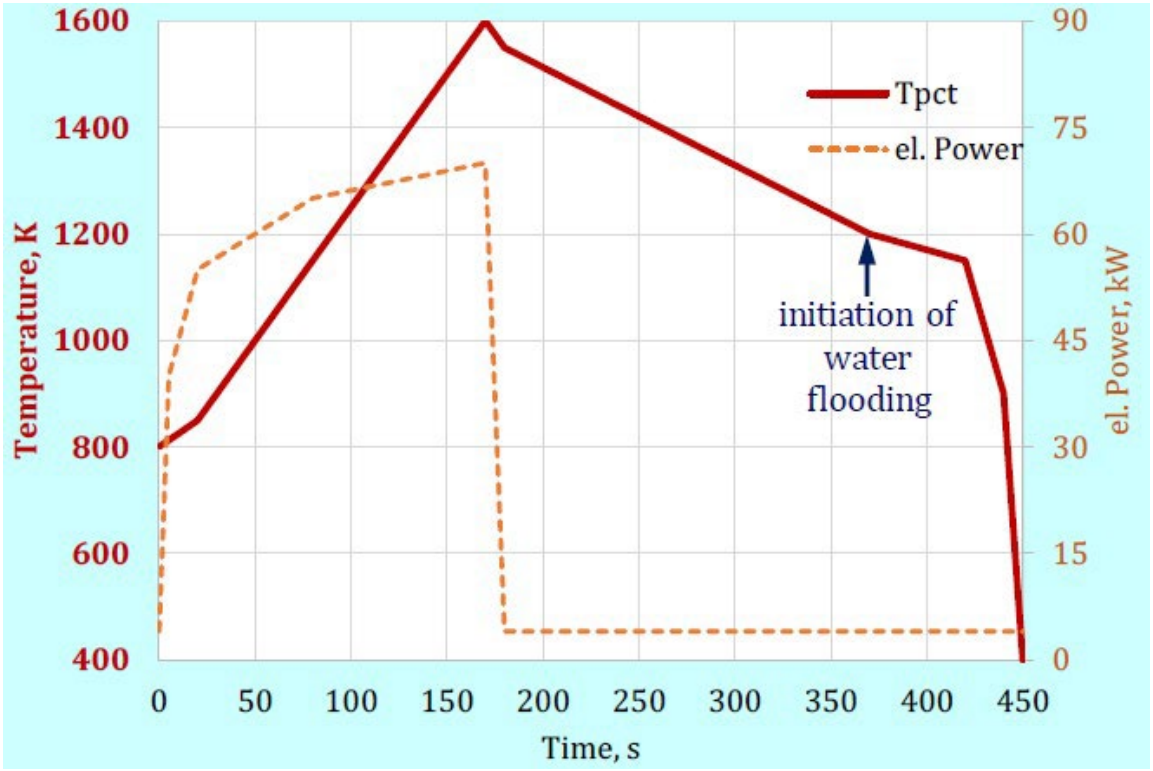

Source: KIT

Participants and Codes

- 7 Participants
- 4 Countries
- 5 Codes

This allows a detailed evaluation of the ATF models in different codes

Country	Organization	Code	Blind	Open
Czech Republic	UJV Rez	MELCOR 2.2		X
Germany	GRS	AC²/ATHLET-CD 3.3.0/ AC²/ATHLET-CD 3.3.0_mod	X	 X
	RUB	AC²/ATHLET-CD 3.3.0_mod	X	X
	KIT	ASTEC v2.2b	X	X
Japan	IAE	SAMPSON 3.0	X	X
USA	EPRI	MAAPv5.06		X
	USNRC	MELCOR 2.2		X

ATF (Cr-coating) Modelling in Severe Accident Codes

- In all codes models are available to consider Cr oxidation
- The level of detail differs and ranges from
  - a dedicated (mechanistic) model to
  - simply inserting the oxidation correlation parameter and material properties via the input deck
- As for the extended DBA scenario temperatures up to 1600 K, the transition from Cr oxidation to Zr oxidation might play a minor role, however it can be simulated by an automatic change in the code or restarts at certain points of the simulation.

Example: AC²/ATHLET-CD

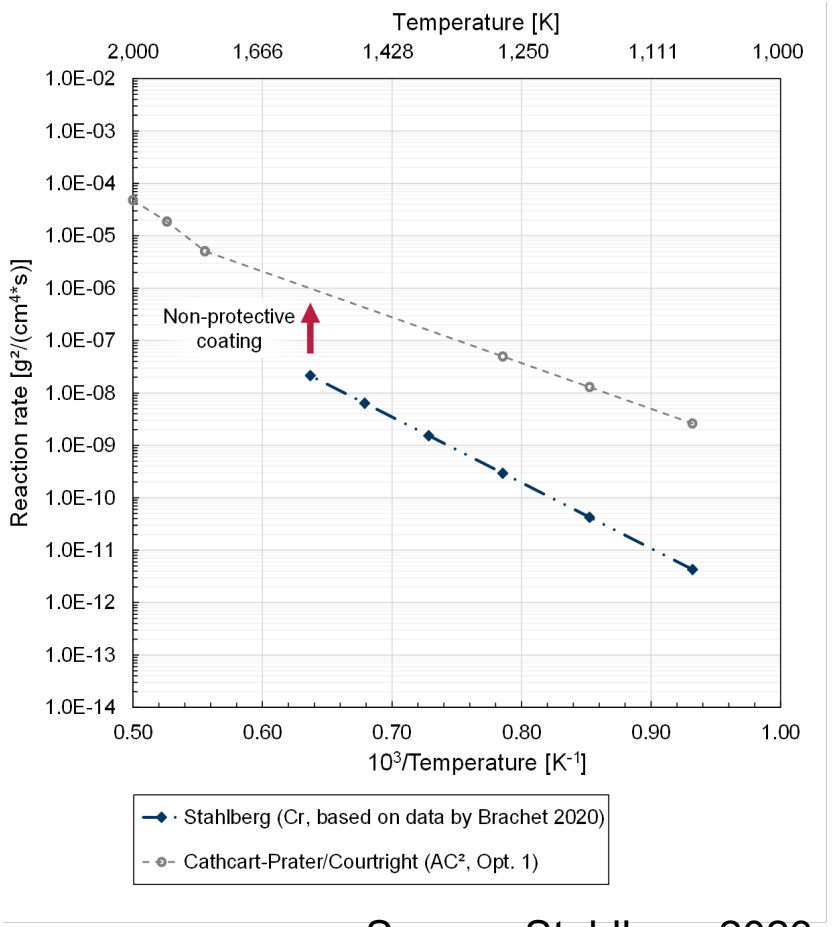

Source: Stahlberg 2023

Simulation Results
– Cladding Temperatures at 950 mm –

Blind

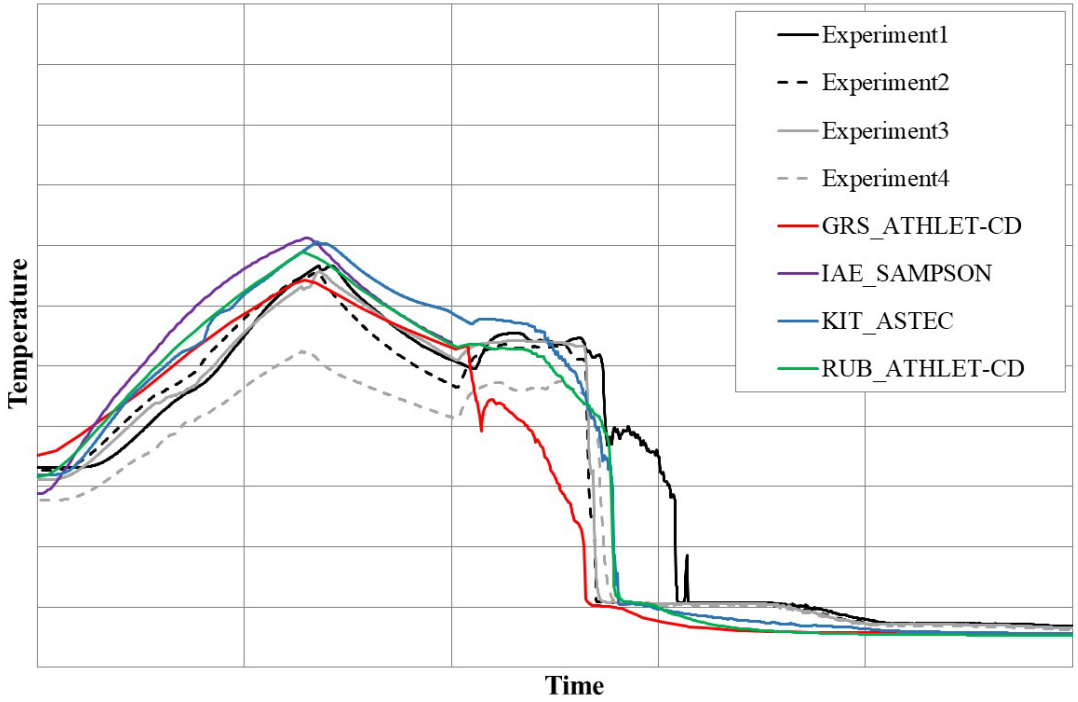

Open

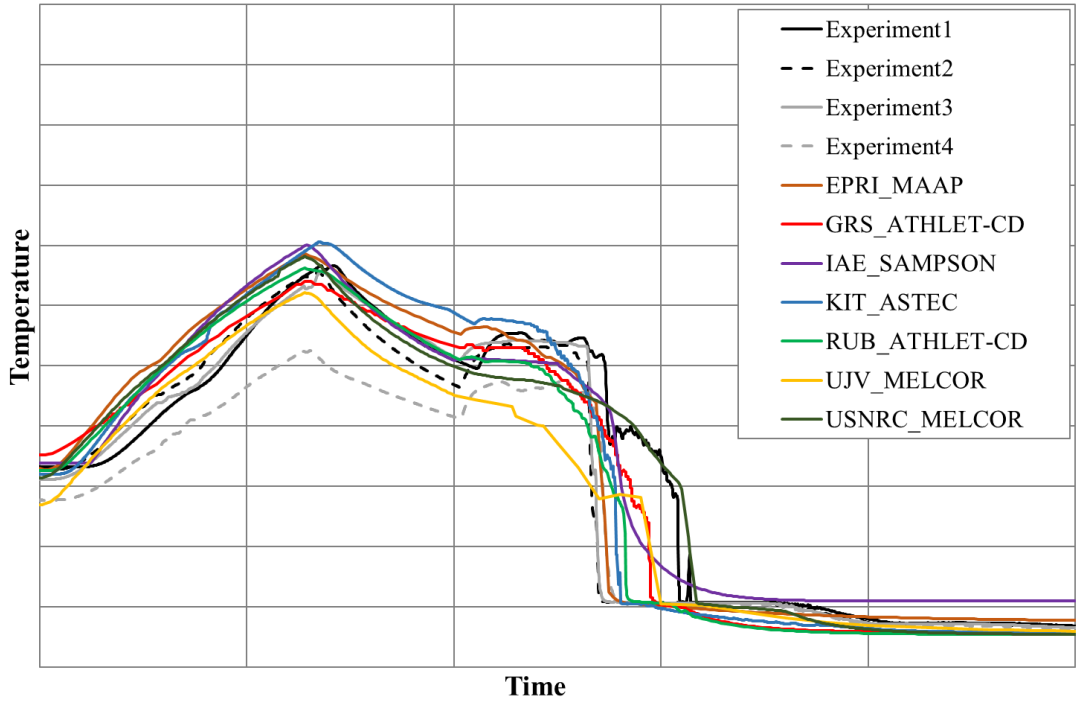

- The improved models show (significant) better results compared to the blind phase, which was in general already in good agreement to the experiment

Simulation Results
– Hydrogen Generation –

Blind

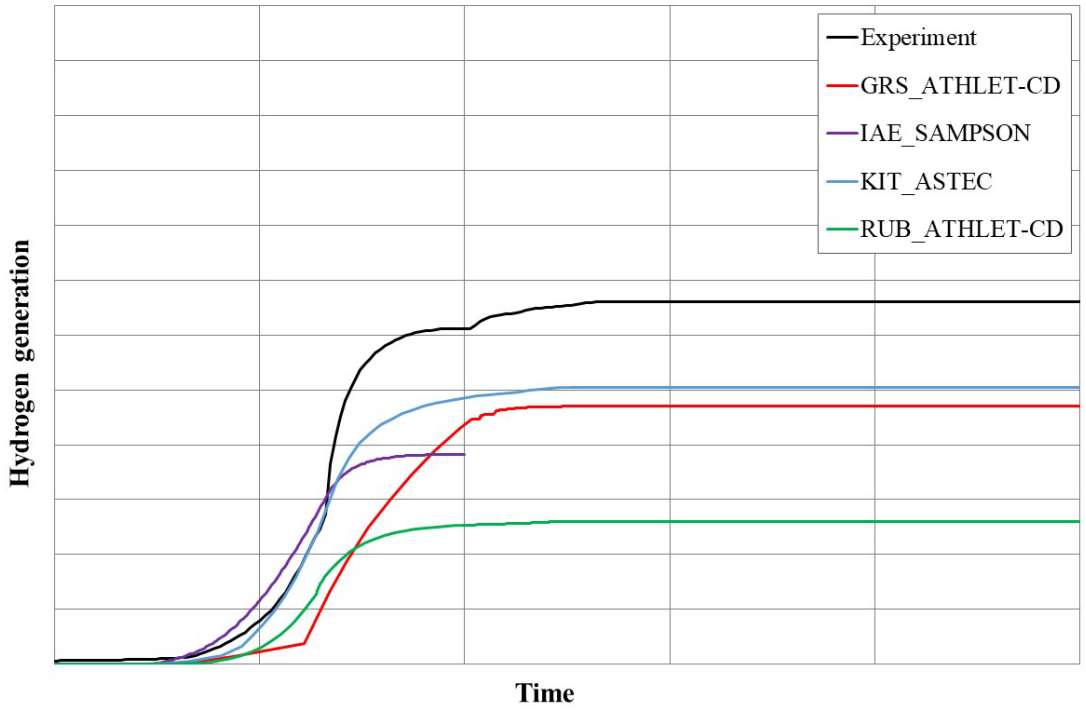

Open

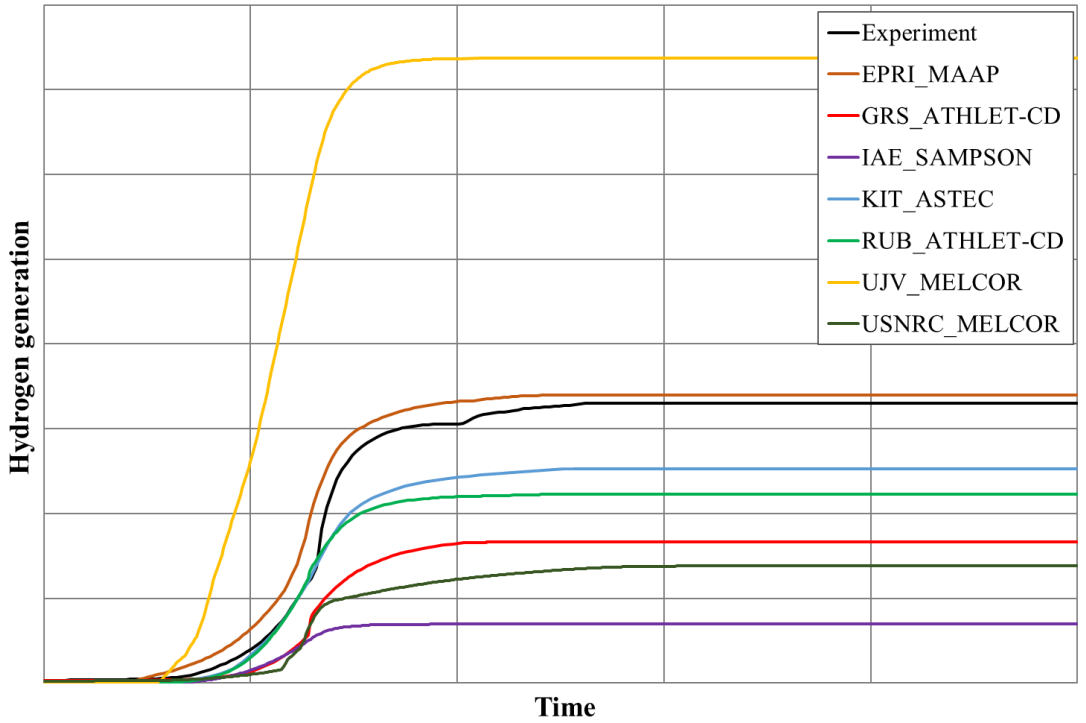

- The improved models show (significant) better results compared to the blind phase, which was in general already in good agreement to the experiment

Conclusions

- In the frame of the OECD/NEA QUENCH-ATF project benchmark exercises are carried out with blind and open post-test simulations. For the time being, the first experiment QUENCH-ATF-1 dealing with an extended DBA scenario has been analyzed.
- All codes have model options / capabilities to predict Cr oxidation, implemented in the code or as user input.
- The results of both phases show that the codes are able to predict the qualitative behavior as observed in the experiment. In the blind phase especially the hydrogen generation is underestimated by most codes, while the temperatures show a good agreement to the measured data.
- By improvement of the model options and additional assumptions based on assessment of the disclosed experimental data the results of the open phase are closer to the experimental observations, but still show some deviations.
- Different codes were applied also by different users and no code specific weakness could be identified, which leads to the conclusion that in principle the severe accident codes (AC²/ATHLET-CD, ASTEC, MAAP, MELCOR, and SAMPSON) are able to predict Cr-coating oxidation and behavior under extended DBA conditions.

Acknowledgements

- The work of GRS is sponsored by the German Federal Ministry for the Environment, Nature Conservation, Nuclear Safety and Consumer Protection (BMUV).
- The activities were performed in the frame of the OECD/NEA Joint Undertaking QUENCH-ATF.

Supported by:

Federal Ministry
for the Environment, Nature Conservation,
Nuclear Safety and Consumer Protection

based on a decision of
the German Bundestag

- The author thanks the participants of the benchmark from
  EPRI (USA),
  IAE (Japan),
  KIT (Germany),
  RUB (Germany),
  UJV (Czech Republic) and
  USNRC (USA) as well as
  KIT as operating agent for their support.

Chris Allison, pres. by Victor Martinez

ISS, ENSO

Impact of Fukushima Daiichi Decommissioning R&D on ASYST VER 3.x Late Phase SA Model Development and Assessment

ASYST VER 3.x is a detailed BEPU code being developed though two collaborative international programs, ADTP and SDTP (ASYST/SCDAPSIM Development and Training Programs, respectively). Innovative Systems Software is administrator of those programs. ASYST shares many common features with RELAP/SCDAPSIM including detailed SCDAPSIM fuel and reactor material behaviour models, integrated uncertainty analysis options, and advanced interactive desktop simulator environments. The two codes also share common I/O structures to allow continued use of the extensive RELAP/SCDAPSIM input model library and data analysis options developed over the past four decades.

ASYST VER 3.x is focused on the analysis of water-based LWR/SMR reactor designs with a shorter term goal to (a) identify and quantify the influence of the uncertainties in the system thermal hydraulic boundary conditions associated with the "real-life" events such as those occurring in Fukushima Daiichi accident, (b) address some of the flaws identified in the Fukushima Daiichi related severe accident calculations using the simplified parametric codes like MELCOR and MAAP, and (c) provide improved performance and reliability relative to the more complex modelling options used in the Japanese SAMPSON code.

The presentation for this meeting identifies and discusses some of the issues that result in wide variation for the predicted behaviour in the analysis of the later phases of severe accidents identified in the ongoing Fukushima Daiichi decommissioning R&D. Two examples are provided. First, that there are large uncertainties in the actual thermal hydraulic boundary conditions for real, rather than idealized, severe accidents that can require years to quantify. Second, there are large variations in the prediction of the timing and nature of {U-Zr}-O2, cladding, and control element material relocation into the lower plenum from widely used codes even though we have 4 decades of separate effects and integral experiments describing this process in great detail. The presentation concludes with a brief discussion on how our collaborators in the development and assessment of ASYST are addressing these issues.

Impact of Fukushima Daiichi decommissioning R&D on ASYST late phase SA model development and assessment

Assessment of FD behavior still show wide variations in predicted behavior

- **Uncertainties in system thermal hydraulic boundary conditions**
  - Timing and nature of depressurization and water addition
  - Timing and nature of channel box/control blade melting and relocation
- **Large variation between the modeling of timing and nature of fuel and structural material relocation into LP and RC**
  - Temperature and stored energy associated with fuel relocation
  - Vessel lower head failure associated with possible penetration failure
  - Relocation of molten fuel/structural material into reactor cavity

Uncertainties in system thermal hydraulic boundary conditions – ie depressurization

Depressurization likely to increase mass of {U-Zr}-O_2 relocating into LP initially

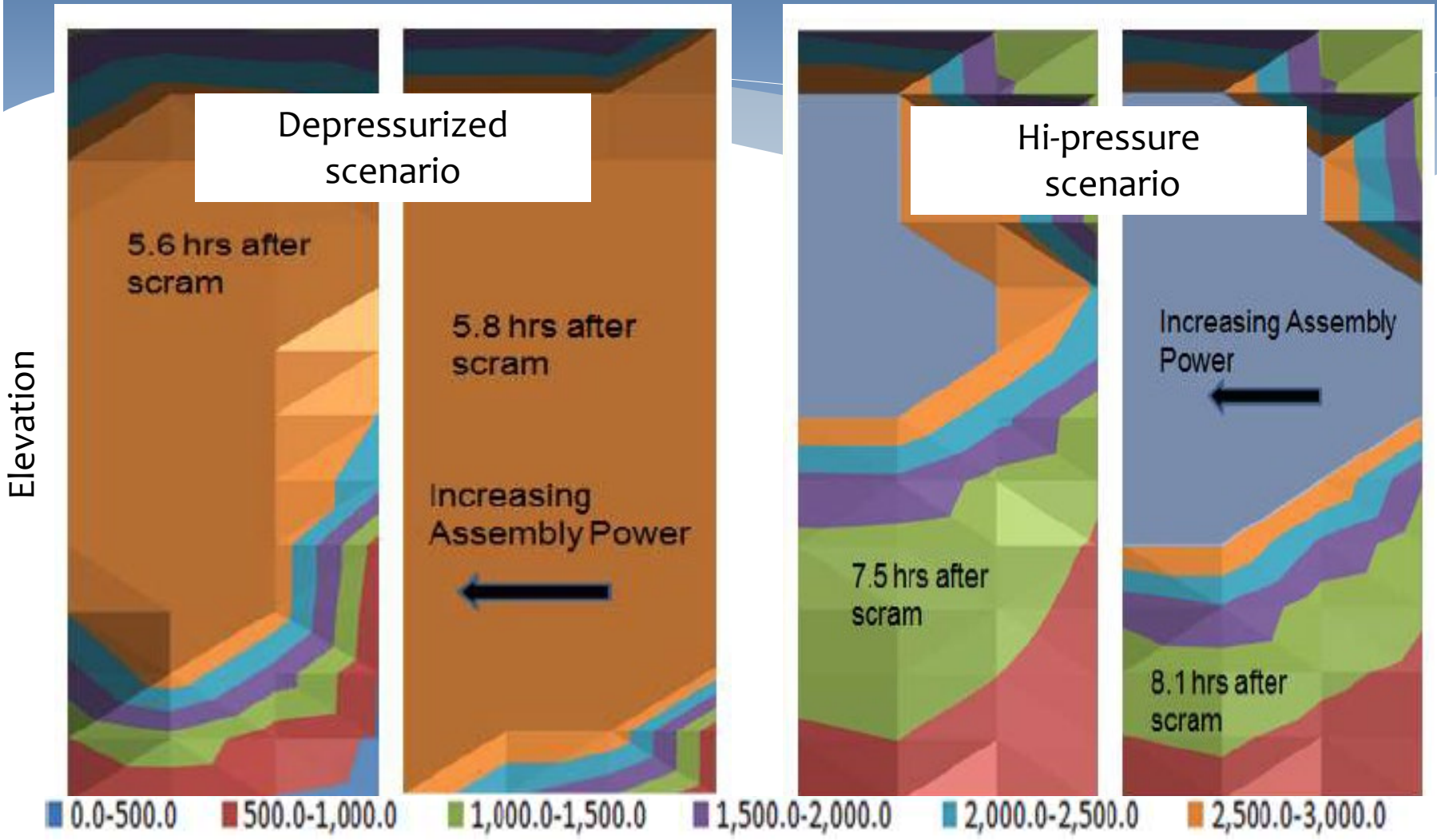

Large variation between the modeling of timing and nature of fuel and structural material relocation into LP

Integral codes MELCOR and MAAP predicted widely different results for Fukushima-Daiichi relative to SCDAPSIM and SAMPSON

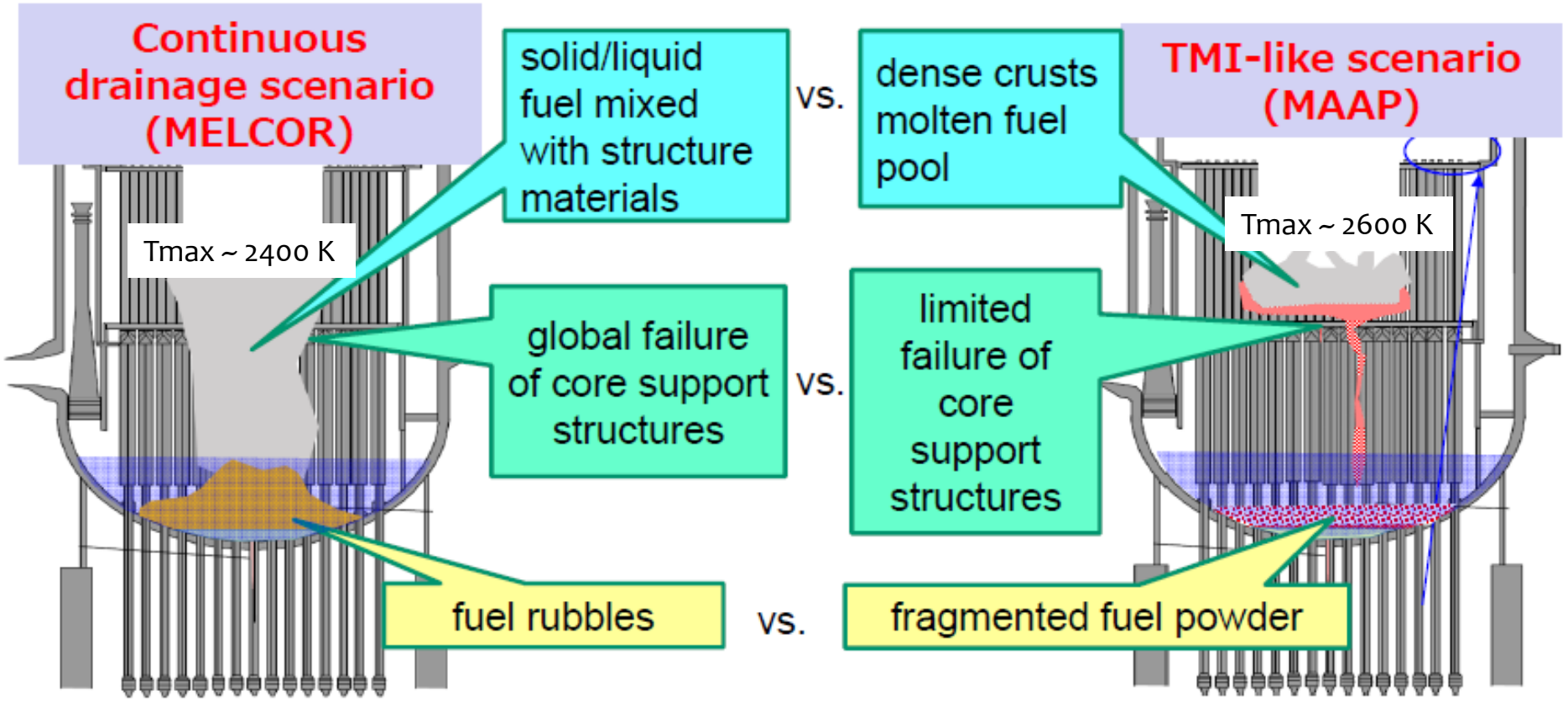

User-defined core slumping temperatures in simplified codes have significant impact on energy of molten [U-Zr] – O2

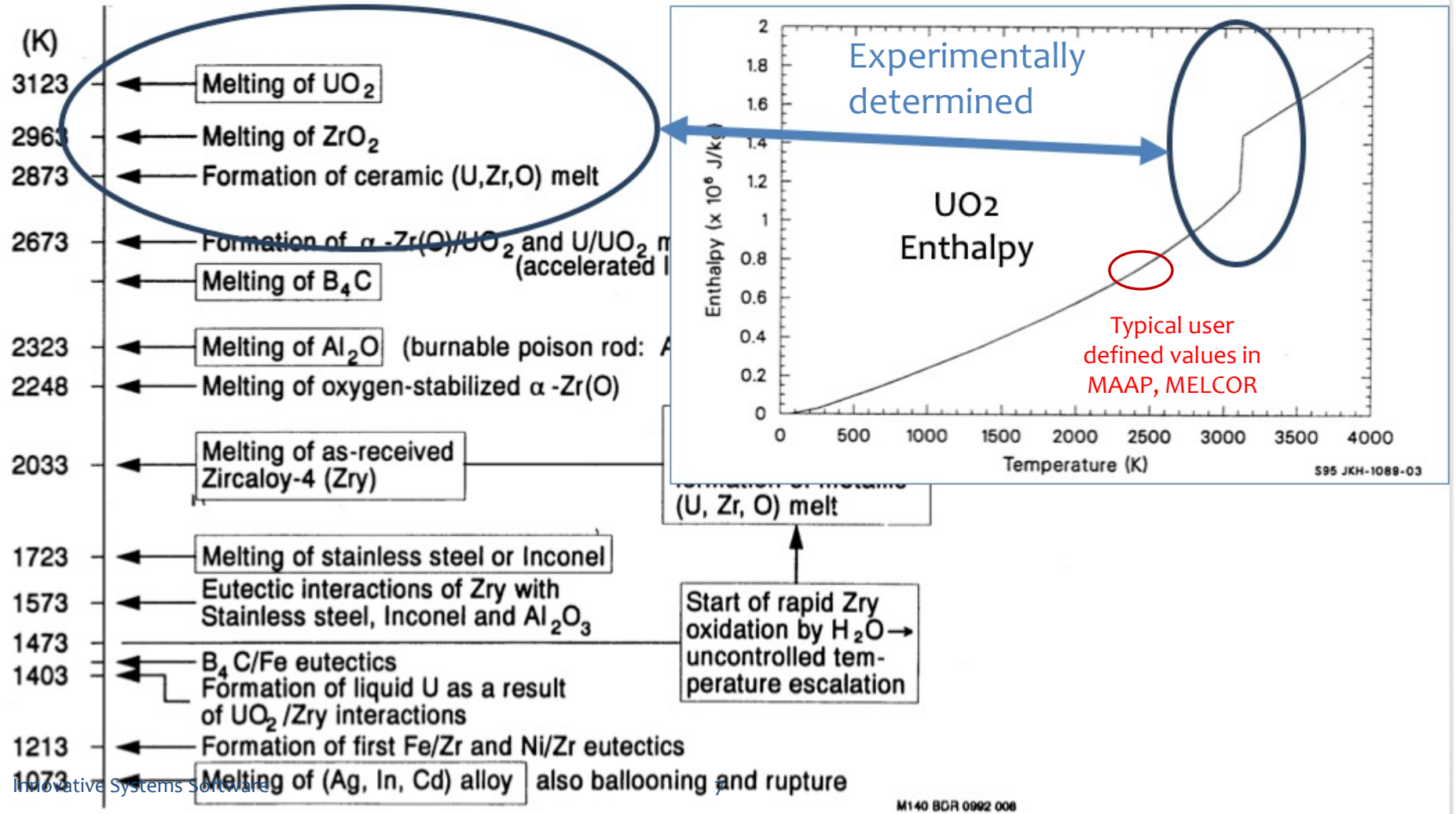

LOFT FPT -2 and PBF SFD indicate initial {U-Zr}-O2 relocation at temperatures > 2800 K

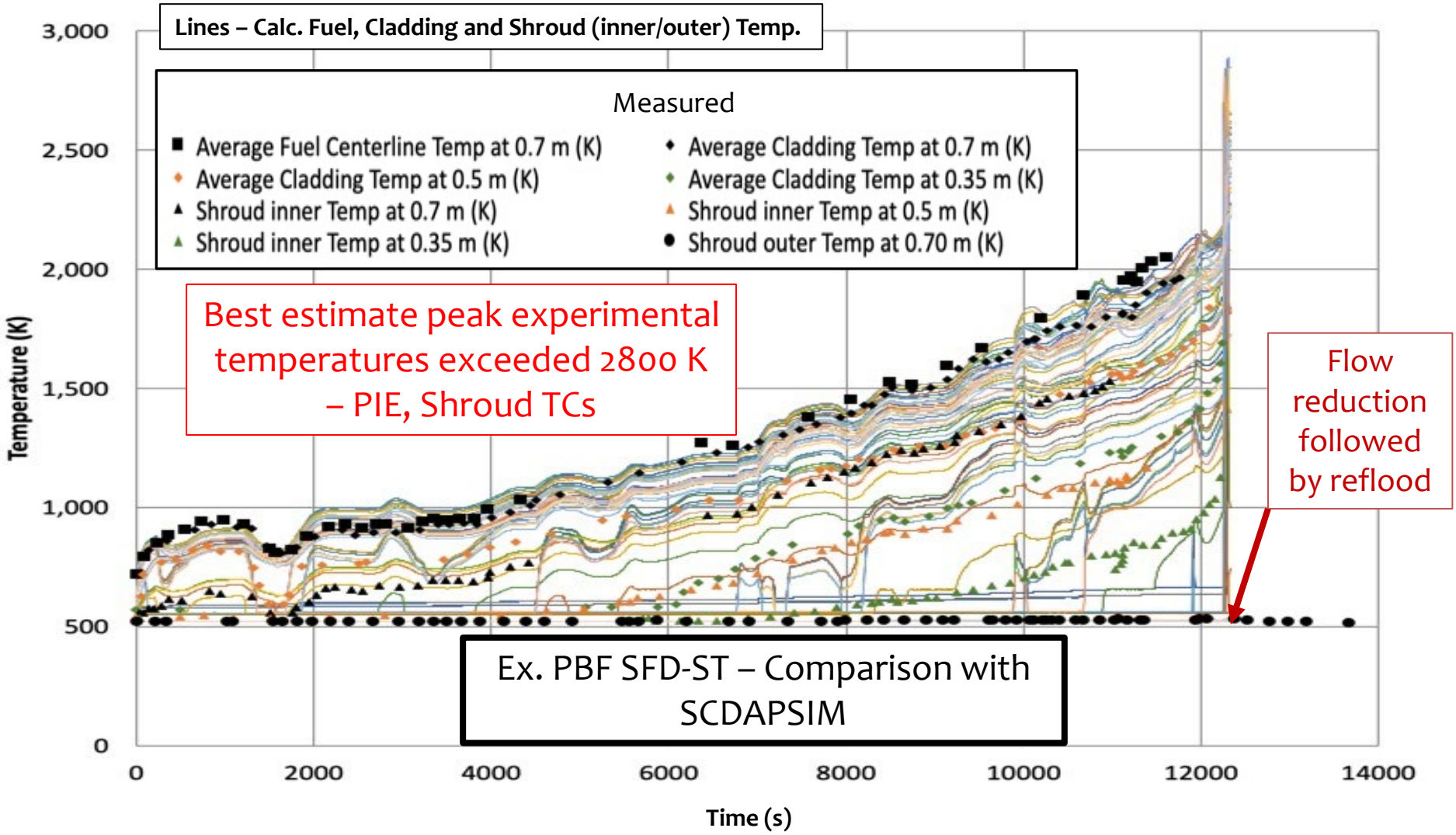

Advantages of ASYST and SAMPSON simplified integral codes

- **Backward compatible with RELAP/SCDAPSIM** used to support the design and analysis of integral SA experiments, help resolve major SA technical issues, and support accident evaluation and decommissioning of TMI-2 and Fukushima Daiichi NPPs
  - Extensive libraries of input models of historic and on-going integral experiments, and representative NPPs can be used to assess modeling improvements
- **Influence of user experience limited**
  - Modeling defaults established through extensive code-to-data comparisons
  - Input models typically easier to set up and qualify
- **Models are much more detailed** (typically 2D/3D) with integrated uncertainty analysis options

Ongoing Fukushima Daiichi decommissioning R&D guiding ASYST model development assessment activities

- **Uncertainties in system thermal hydraulic boundary conditions being reduced by** (a) expanded comparisons with limited TH measurements and (b) refinements of input models using comparisons with historic CORA BWR and in-pile experiments
  - Timing and nature of depressurization and water addition
  - Timing and nature of channel box/control blade melting and relocation
- **Uncertainties in the modeling of timing and nature of fuel and structural material relocation into LP and RC being reduced** by introducing new modeling options
  - Fuel relocation into lower plenum at later stages of core melting when water level drops below bottom of core
  - Vessel lower head failure associated with possible penetration failure
  - Relocation of molten fuel/structural material into reactor cavity
- **Improved containment modeling through links to detailed SAMPSON-based modules**

New modeling options being introduced to ASYST(SCDAPSIM) for timing and nature of fuel and structural material relocation into LP and RC and late phase containment behavior

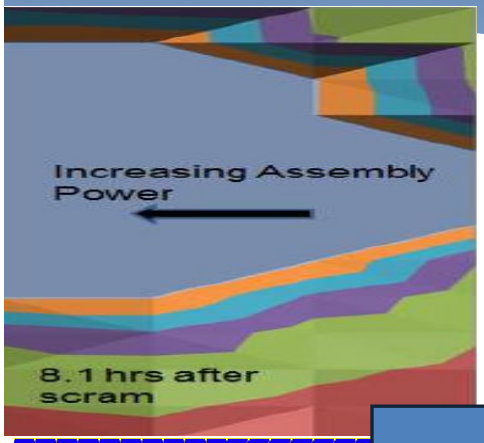

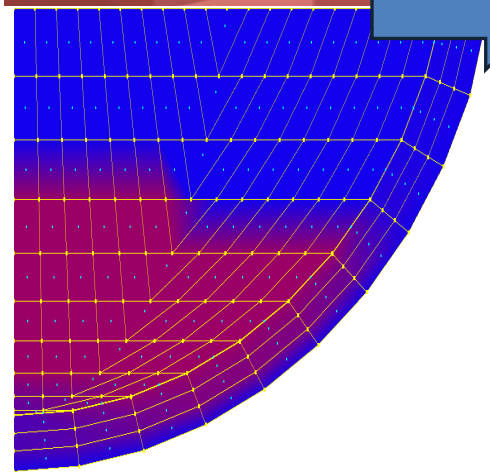

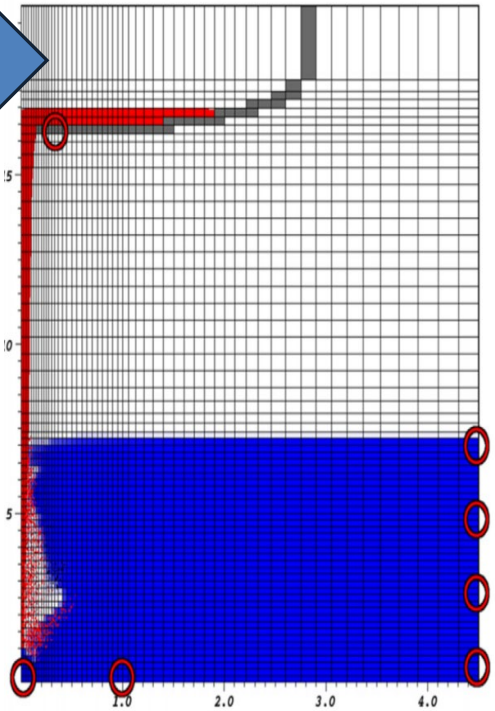

* Extend 2D FEM model to allow multiple mesh regions
  * Lower core/plate structures
  * Lower plenum/head structures
  * Reactor cavity

* Extend lower head failure models to include melt/debris relocation into reactor cavity
  * Side wall natural circulation drive creep rupture and melt relocation
  * Bottom LH penetration failure and melt relocation options

* Develop standard interfaces to more detailed SAMPSON (and other users selected) containment options
  * Melt spreading, MCCI, H2 and FP behavior

Vincenzo Anthony Di Nora

GRS

Integration and Preliminary Validation of a Thermal Mechanical Fuel Rod Model for ATHLET

The ATHLET system code, a component of the AC2 code package developed by Gesellschaft für Anlagen-und Reaktorsicherheit (GRS), is designed for the thermohydraulic safety analysis of nuclear facilities. The standalone system code can simulate scenarios ranging from normal operational conditions to design basis and extended design scenarios, all without involving core degradation. For severe accident scenarios, ATHLET is extended by its Core Degradation (CD) plug-in module forming ATHLET/CD. ATHLET/CD is capable of simulating key core degradation phenomena including fuel rod detailed thermal-mechanical behaviour until rod burst, channel blockage, and oxidation.

In ongoing ATHLET/CD development projects, GRS aims to integrate the CD module seamlessly into ATHLET to extend the applicability of CD models to scenarios where they are relevant to ATHLET and to simplify future model maintenance and development. A significant focus of these integration activities has been on incorporating complementary thermal-mechanical fuel rod models and rod bursting models from ATHLET/CD into the main ATHLET framework. This work briefly discusses the integration of these models and presents preliminary results from initial verification and validation processes.

Verification and validation activities were conducted exploiting the QUENCH-L0 bundle test conducted at the Karlsruhe Institute of Technology (KIT) as a test case. This test has been previously used for validating ATHLET/CD, providing an opportunity to leverage GRS's extensive legacy data for thorough verification and validation of the newly integrated models.

Integration & Preliminary Validation of Fuel Rod Models for ATHLET

Author: V. A. Di Nora

E-mail: Vincenzo.DiNora@grs.de

Outline

- Introduction
- Model
- Preliminary Validation
- Conclusion

Introduction

Background & Motivation

- ATHLET: GRS's thermal-hydraulics system code developed for analyses of:
  - Operational transient
  - Design & beyond-design bases accident without core degradation
- For severe accidents, ATHLET is extended by its Core Degradation (CD) module. It allows for modelling of, e.g.:
  - Rod melting, radiation phenomena in the core, &, among others…
  - Detailed Thermal-Mechanical (TM) modelling of cladding, enabling simulation of ballooning, & cladding failure
- Ongoing GRS's projects aim to seamlessly integrate CD module into ATHLET. This would:
  - Simplify future maintenance/development activities, allow for smooth transition from design basis oto design extension including severe accident conditions in simulations
  - Make available for ATHLET some models of CD that might be relevant in non-severe accident scenarios
- Examples: TM cladding models significantly affecting, e.g., via ballooning:
  - Gap size, thus gap conductance
  - Coolability of fuel rod channels

Current Status & Required Developments

- Some TM fuel rod modelling features were already implemented in ATHLET to enable better estimation of gap conductance. These include:
  - Pellet thermal expansion deformations
  - Pellet cracking[1], swelling, & densification[2]
  - Clad TM **elastic** deformations
  - Dynamic inner rod pressure model
- Models were verified & validated for open & close gap configuration[3] vs. IFA-432[4]

- Still significant & missing are models accounting for cladding creep deformations
  - Crucial at high temperatures, enabling modelling of clad ballooning, & its failure
  - Available from CD & to be integrated in ATHLET

- This presentation aims to:
  - Introduce integrated models
  - Present results of preliminary validation of integrated models, obtained by applying new ATHLET to simulation of QUENCH-L0[5] experiment

Models

Existing & New…

TM Cladding Existing Models

- Existing models[3] were simplified & mainly implemented to enable better estimation of gap size
  - $\delta_{gap} = r_{ci} - r_{fo}$ with $r_{ci} = \varepsilon_\theta \cdot \bar{r} - \delta_{clad}|_0/2$, $\bar{r}$ *mid-wall radius:*

$$\sigma_\theta = \frac{P_i r_{ci}^2 - P_o r_{co}^2}{r_{co}^2 - r_{ci}^2}$$

$$\sigma_z = \frac{P_i r_{ci}^2 - P_o r_{co}^2}{r_{co}^2 - r_{ci}^2}$$

Stress equations

$$\varepsilon_\theta = \frac{1}{E}[\sigma_\theta - \nu(\quad + \sigma_z)] \qquad + \int \alpha dT$$

Strain equation

- Suitable for scenario not involving high cladding temperature causing onset of creep effects…

TM Cladding Integrated Models

- At high temperatures creep effects become significant & are must be accounted for
  - They were modelled by following integrated equations, exploiting models from CD[6] & Lame's equations[7]:

$$\sigma_r = \frac{P_i r_{ci}^2 - P_o r_{co}^2 + \frac{r_{ci}^2 r_{co}^2 (P_o - P_i)}{\bar{r}^2}}{r_{co}^2 - r_{ci}^2}$$

$$\sigma_\theta = \frac{P_i r_{ci}^2 - P_o r_{co}^2 - \frac{r_{ci}^2 r_{co}^2 (P_o - P_i)}{\bar{r}^2}}{r_{co}^2 - r_{ci}^2}$$

$$\sigma_z = \frac{P_i r_{ci}^2 - P_o r_{co}^2}{r_{co}^2 - r_{ci}^2}$$

Stress equations

$$\varepsilon_r = \frac{1}{E}[\sigma_r - \nu(\sigma_\theta + \sigma_z)] + \varepsilon_r^P + d\varepsilon_r^P + \int \alpha dT$$

$$\varepsilon_\theta = \frac{1}{E}[\sigma_\theta - \nu(\sigma_r + \sigma_z)] + \varepsilon_\theta^P + d\varepsilon_\theta^P + \int \alpha dT$$

$$\varepsilon_z = \frac{1}{E}[\sigma_z - \nu(\sigma_\theta + \sigma_r)] + \varepsilon_z^P + d\varepsilon_z^P + \int \alpha dT$$

Strain equations

- Having defined…

$$d\varepsilon^P|_{i=r,\theta,z} = \frac{3}{2} \cdot \frac{\dot{\varepsilon}_{creep}}{\sigma_e} \cdot (\sigma_i - \sigma_m) \cdot \Delta t|_{i=r,\theta,z}$$

$$\sigma_e = \{[(\sigma_z - \sigma_\theta)^2 + (\sigma_\theta - \sigma_r)^2 + (\sigma_r - \sigma_z)^2]\}^{1/2}$$

$$\dot{\varepsilon}_{creep} = A \cdot \sigma_e^n \cdot e^{-\frac{Q_A}{RT}}$$ as in [6]

Cladding Failure & Impact of Cladding TM Deformations on TH Calculations

- Criteria for clad failure retrieved from ATHLET/CD legacy[6] were:
  - ε_θ reaches strain threshold ε_θ^{lim} (= 0.38) or alternatively…
  - Variation of ε_θ in time exceeds the threshold, $(\Delta\varepsilon_\theta)/\Delta t > \dot{\varepsilon}_\theta^{lim}$ = 0.1 1/s)

- Effects of rod deformation actually impact on hydraulic geometry quantities:
  - E.g., correction of actual hydraulic diameter, & free flow cross-sectional areas
  - Actually updated and used for thermal-hydraulics calculations (emulating e.g., flow restrictions)

Note

- Models implemented are in principle generically applicable provided cladding material properties available
  - Material properties are currently only available for Zr-2, & Zr-4…

Preliminary Validation

Validation & Test Case

- Goal: In relation to new TM modeling features, demonstrating that newly integrated ATHLET has equivalent, or improved, predictive capabilities respect to ATHLET/CD…

- Tests of QUENCH-LOCA series particularly apt for the scope:
  - As originally designed to investigate, amongst others, rod ballooning & cladding failure/burst that strongly dependent on cladding TM effects
  - Already applied successfully to validation of ATHLET/CD[8], which offers possibility to exploit available legacy data

- Among the tests available, QUENCH-L0 was selected as first case for validation purposes…

- …Beyond comparison vs experimental measurements benchmarking vs ATHLET/CD is desirable

Bundle Test Modelling

- Thermal-hydraulic modelling:
  - Two-chan. bundle representation
  - Fills & Inlet sections
  - Outlet & press. BC
  - Cooling jacket
- Simulated heat-structures:
  - Active & corner rods
  - Grids & shroud
- Models:
  - ✓ Creep, ballooning
  - ✓ TM effects on fuel rod channel
  - ✓ Oxidation
  - ✓ Dynamic inner rod pressure
  - ✗ Radiation model switched off

Pic. from [5]

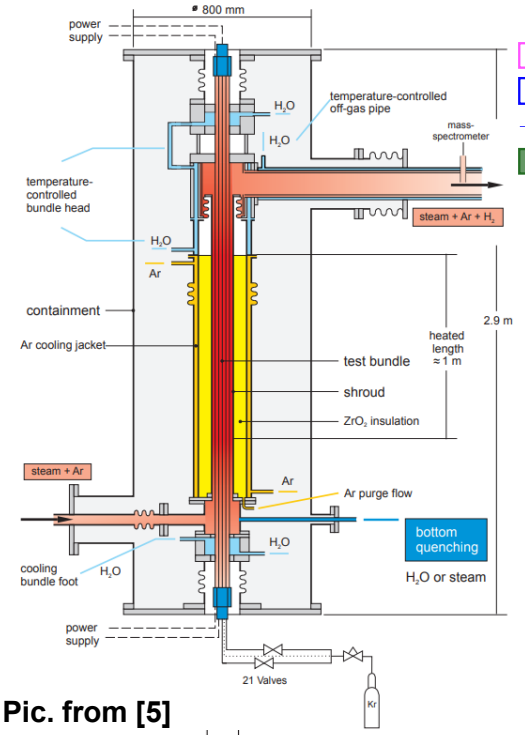

Pic. from [5]

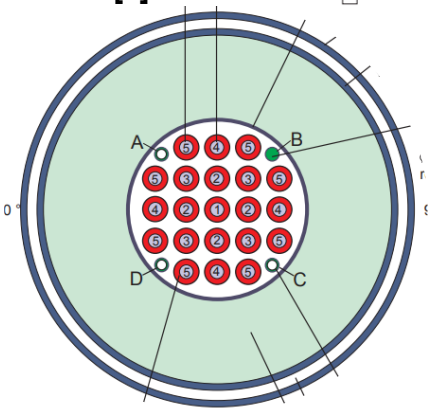

Inner rod pressure 3 to 55 bar (Kr)

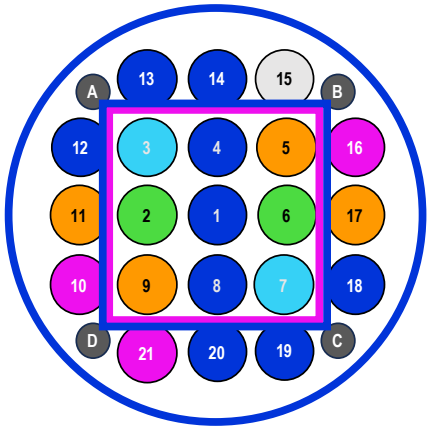

Test Conduct

Time [s]	Event
0	Transient-begin after pre-heating phase
2	Begin of heating phase, power ramp from ~ 6 to ~ 10 W/cm
187	Switch of electrical power to decay heat
215	Initiation of rapid steam supply line (50 g/s) additionally to slow steam and argon
223-225	Rapid clad cooling to ~ 400 K by entrainment of water condensed in steam supply tubes
362	Initiation of quench water supply
386	Begin of flooding phase with quench water injection (90 g/s)
1100	End of data recording

- Beyond inlet fills for Argon, steam & quench water…
- …An additional fill was simulated to inject condensed water entrained in steam supply tubes[9]

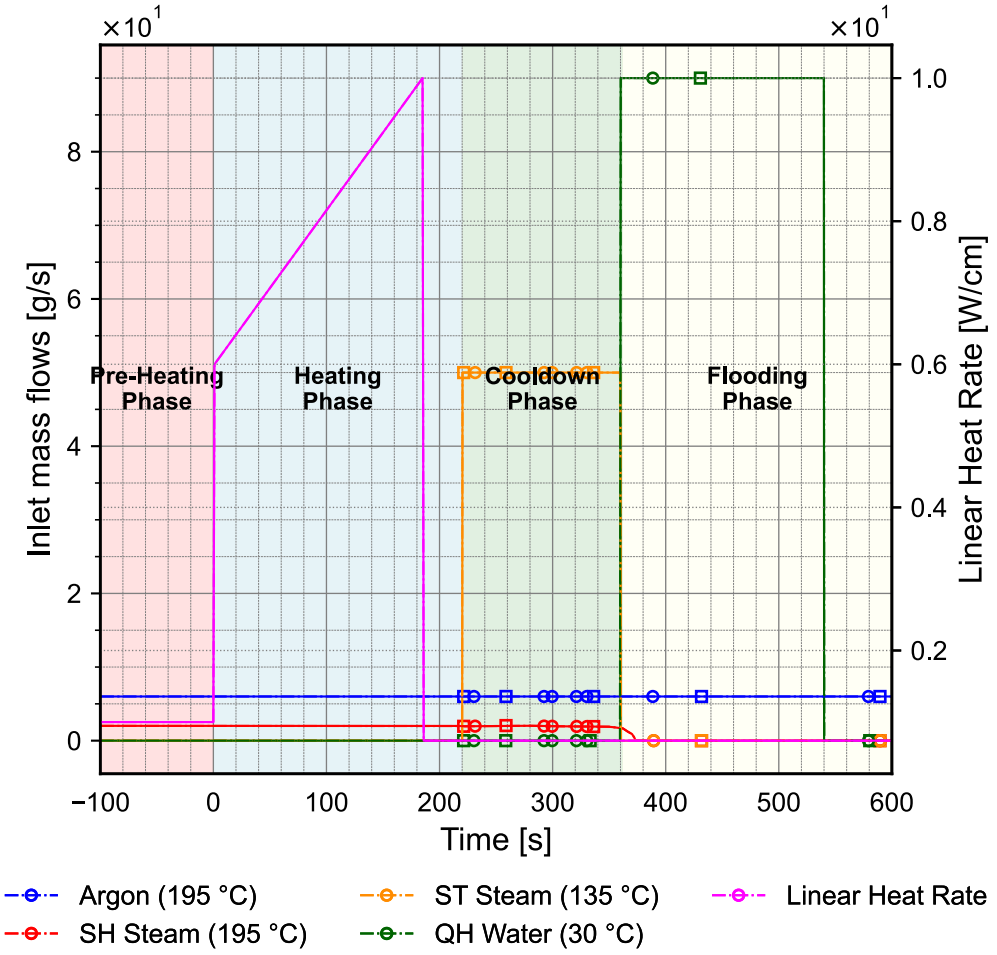

Peak Cladding Temperature (At 950 mm)

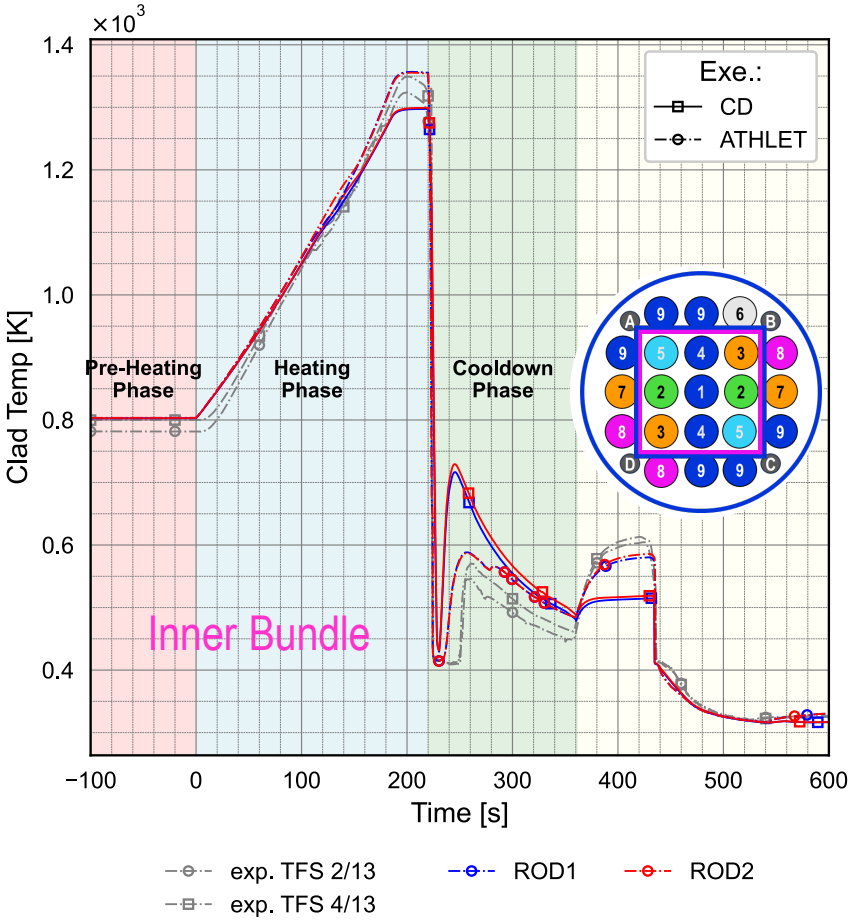

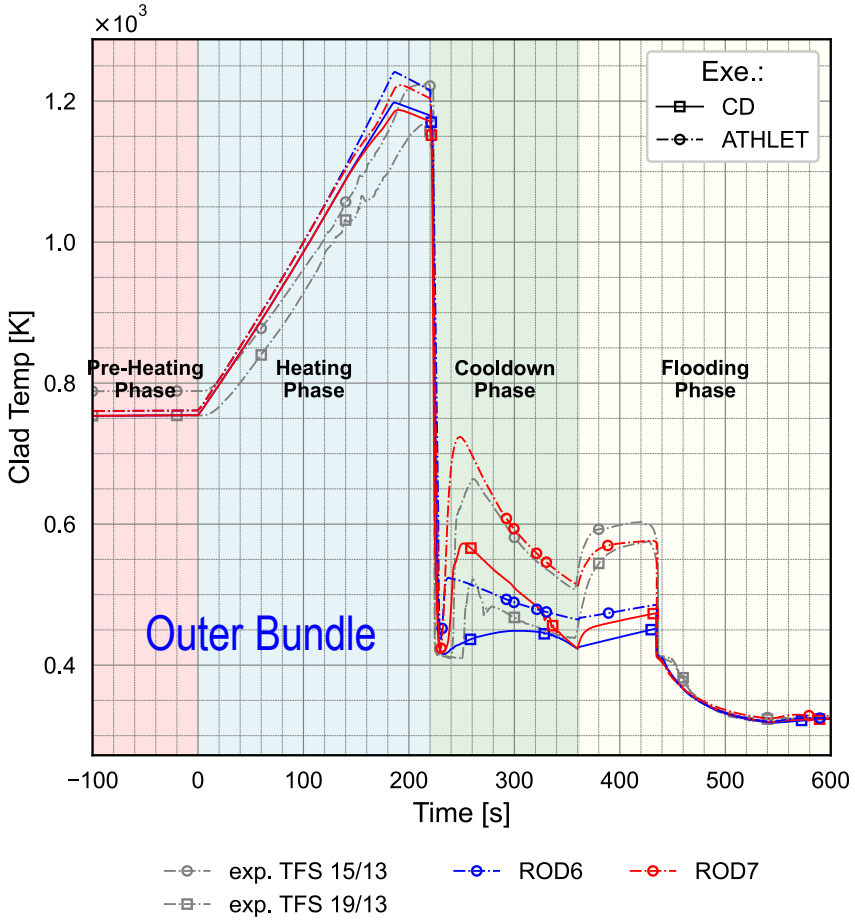

- Similar behaviour between ATHLET & ATHLET/CD found…
  - Discrepancies raise from different treatment of heat conduction/transfer… to be investigated in detail still

Rod Inner Pressure

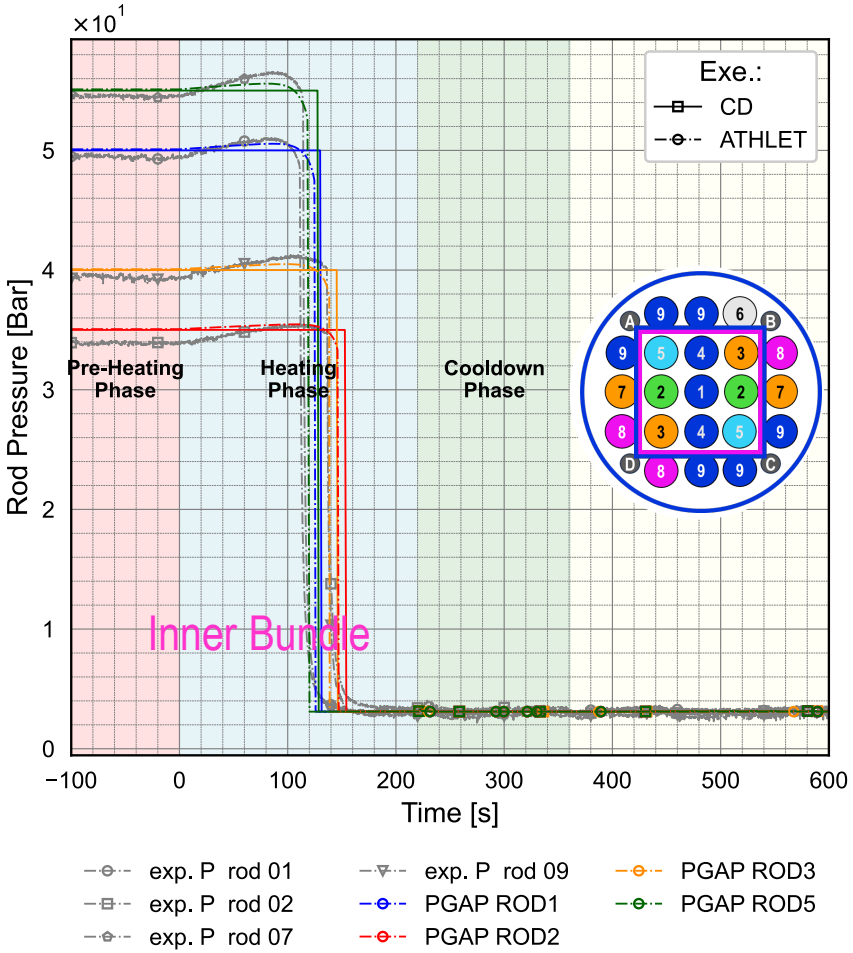

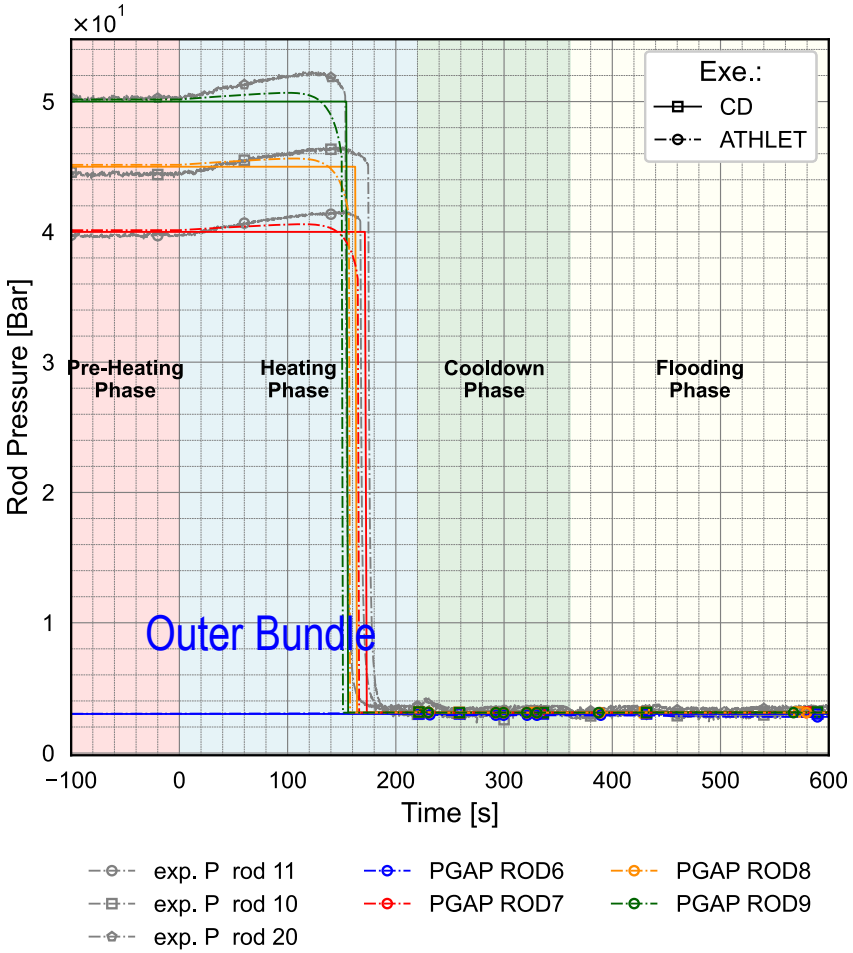

- Dynamic modelling of inner rod pressure in ATHLET enables better agreement with rod pressure measurements respect to ATHLET/CD

Burst Times

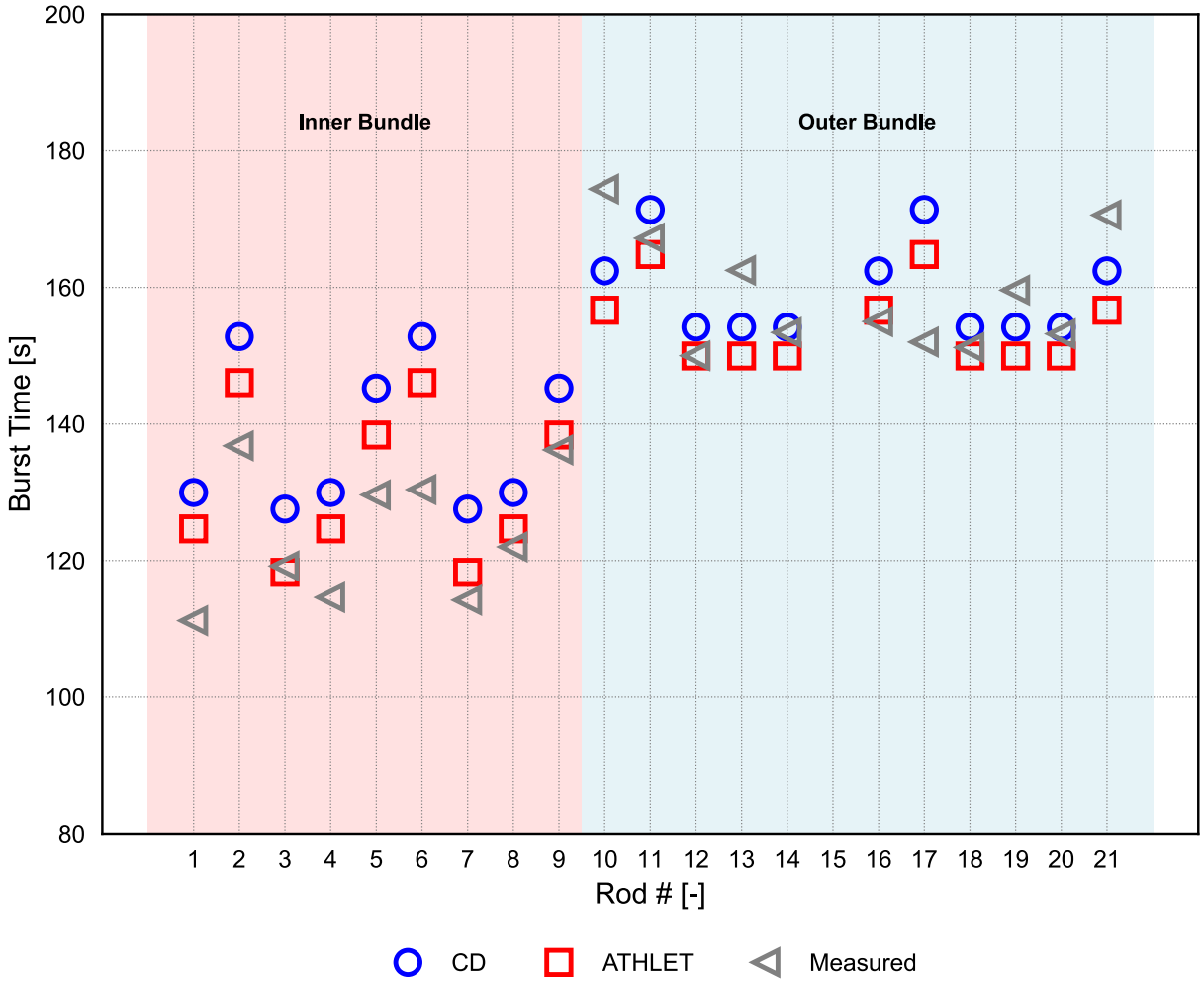

- Burst times of rods result slightly closer to experimental measurements

Azimuthal Strain

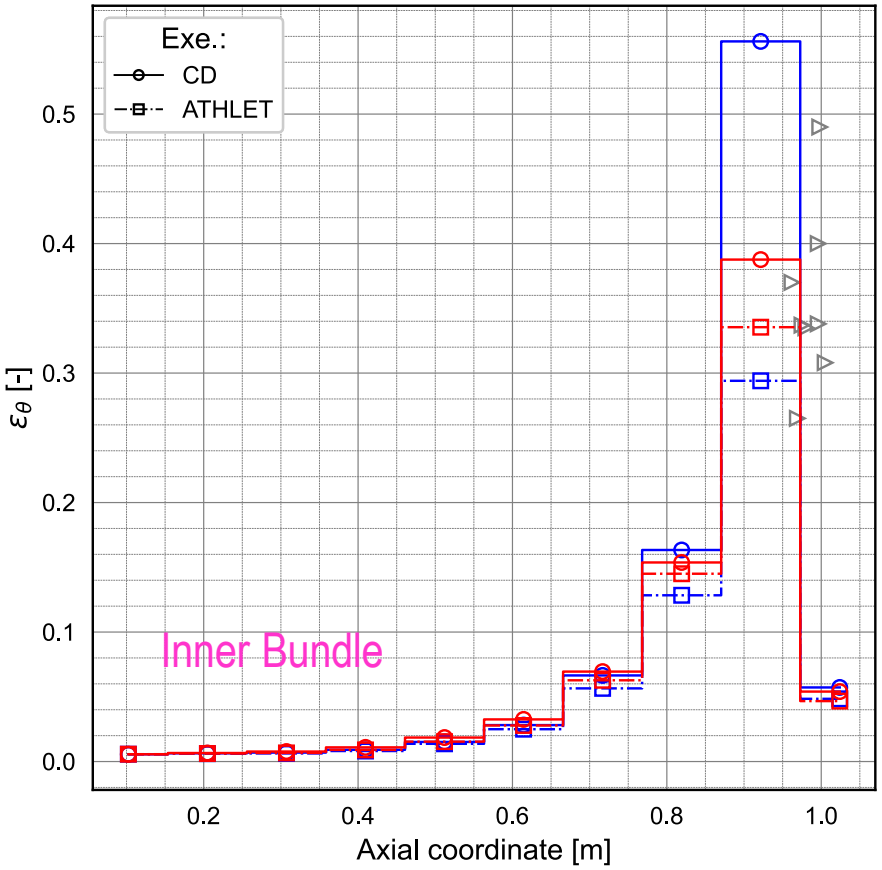

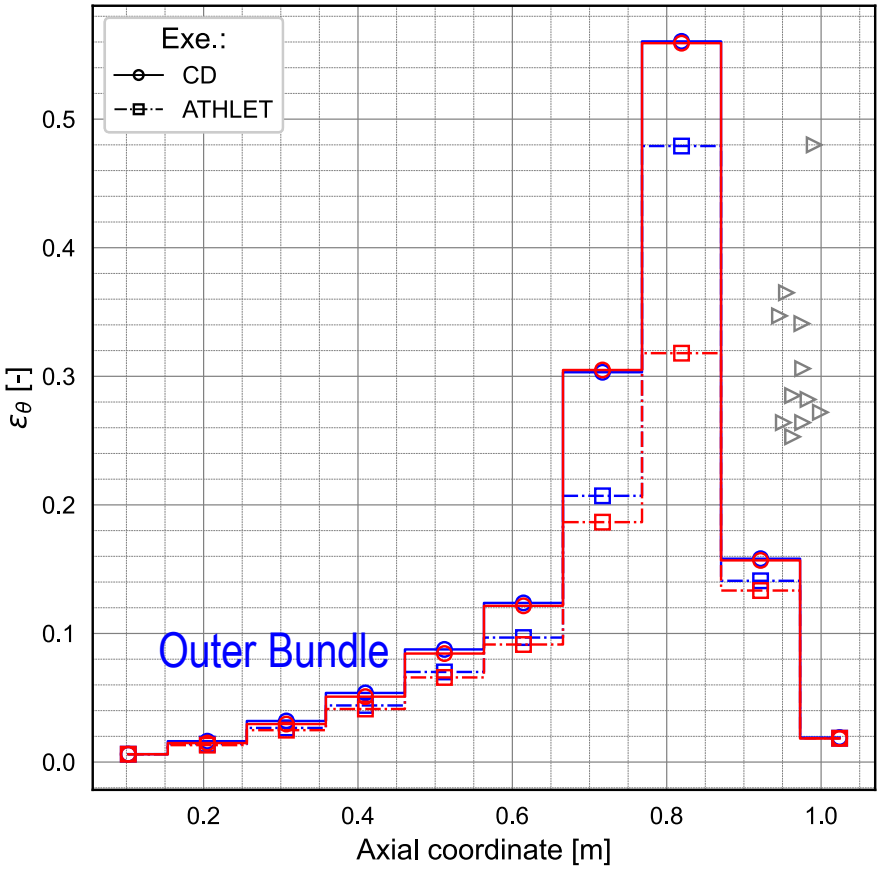

- Maximum achieved hoop strains before cladding failure differ significantly
  - This is because new TM cladding model in ATHLET detected at sub-timestep level, stronger control on error after cladding failure is achieved
  - This improves agreement vs experimental data

Conclusions

Summary & Considerations

- This work presented the integration of relevant TM cladding modelling features into ATHLET, this included among others:
  - Models accounting for TM creep deformation &
  - Cladding failure criteria

- The modelling features were validated against the QUENCH-L0 experiment & compare against available measurement & ATHLET/CD solutions

- ATHLET displayed equivalent, sometime improved, performance over ATHLET/-CD, i.e.:
  - Improved prediction of cladding peak temperatures
  - Improved dynamic pressure behaviour & burst times.
  - More realistic predictions of hoop strains with better alignment to experimental data.

Next Steps

- However, there remains significant work to be done, including several promising steps for near future, such e.g.:
  - Expanding the material properties database to encompass a broader range of materials, including high-burnup-resistant & accident-tolerant material
  - Conducting broader validations across various test scenarios & reactor types to thoroughly evaluate ATHLET's modeling features
  - Integrating a radiation heat transfer model for multi-channel hydraulic systems.

Thank You For Your Attention!

Questions?

E-mail: Vincenzo.DiNora@grs.de

References

[1] Geelhood, K. J., Luscher, W. G.: FRAPCON-4.0: Integral Assessment. Pacific Northwest National Laboratory (PNNL): Richland WA (United States), 2015.

[2] Sonnenburg, H.-G.: TESPA-ROD Code Prediction of the Fuel Rod Behaviour During Long-term Storage, AMNT 2018. Atw International Journal for Nuclear Power, No. 63 Issue 6/7, pp. 374–377, 2018.

[3] Di Nora, V. A., Schöffel, P. J., Hollands, T.: A New Gap Conductance Model for the ATHLET System Code. In: Canadian Nuclear Society (CNS) (Ed.): The 14th Topical Meeting on Nuclear Reactor Thermal-Hydraulics, Operation, and Safety. NUTHOS-14, Vancouver, Canada, 25 - 28 August 2024, 2024.

[4] Hann, C. R., Bradley, E. R., Cunningham, M. E., Lanning, D. D., Marshall, R. K., Williford, R. E.: Data Report for NRC/PNL Halden Assembly IFA-432. PNL, 1978.

[5] Stuckert, J., Große, M., Rössger, C., Steinbrück, M., Walter, M.: QUENCH - LOCA - REPORTS Nr. 1, Results of the commissioning bundle test QUENCH-L0 performed under LOCA conditions (SR-7571). KIT, DOI 10.5445/IR/1000083018: Karlsruhe, 2015.

[6] Lovasz, L., Austregesilo, H., Bals, C., D'Alessandro, C., Hollands, T., Lu, C., Pandazis, P., Tiborcz, L., Weber, S.: ATHLET-CD 3.4 Models and Methods. GRS-P-4/Vol. 2 Rev. 0, November 2023.

[7] Timoshenko, S. P., Goodier, J. N.: Theory of Elasticity. 3. ed., McGraw-Hill: Toronto, 1970.

[8] Hollands, T., Austregesilo, H., Lovasz, L., Pandazis, P., Tiborcz, L., Wielenberg, A.: ATHLET-CD 3.3.1 Validation. GRS-P-4 / Vol. 3, Rev. 2, November 2022.

[9] Gao, P., Zhang, B., Shan, J.: Study on the effect of flow blockage due to rod deformation in QUENCH experiment. Nuclear Engineering and Technology, Vol. 54, No. 8, pp. 3154–3165, DOI 10.1016/j.net.2022.03.005, 2022.

Backup Slides

Backup slides

$$P_{cont} = \frac{u_{fc} \cdot \frac{E \cdot \delta_{clad} \cdot \gamma_{clad}}{\bar{r}} + P_o \cdot r_{co} \cdot \gamma_{clad} - r_{co}^2 \cdot \delta_{clad} \cdot \nu}{r_{ci} \cdot \gamma_{clad} - r_{ci}^2 \cdot \delta_{clad} \cdot \nu}$$

Model Specifications

- Compared to previous gap conductance model, new model can account for:
  - Clad mechanical **elastic** deformations
  - Fuel pellet cracking & its radial relocation (1)
  - Fuel pellet swelling & densification effects (2)

(1)

(2)

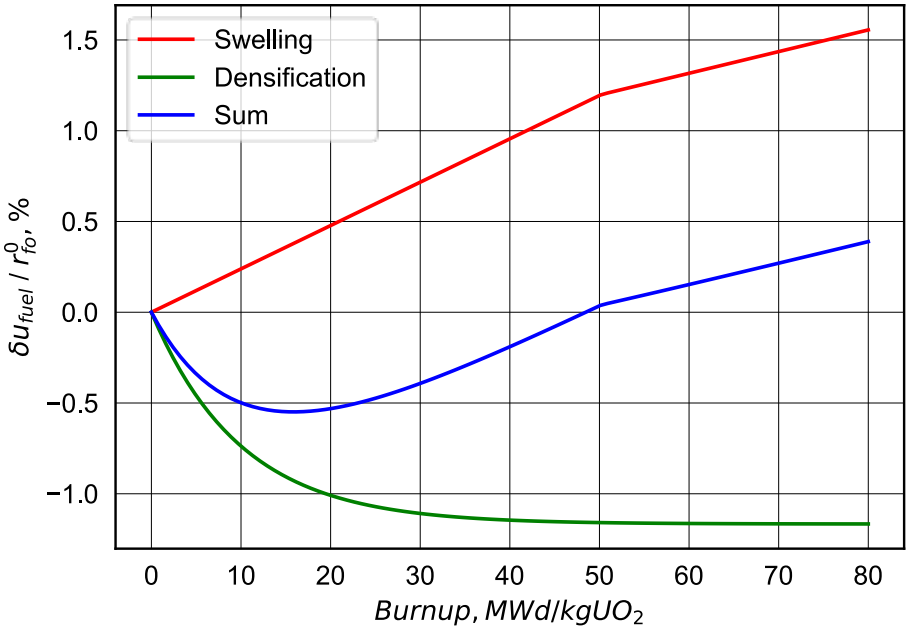

Model Details, Open Gap Configuration

Valid for UO_2 fuel only!

$$HTC_{cond.} = \frac{\lambda_{gap}}{\delta_{gap}^{eff} + 1.8(g_f + g_c) + (R_f + R_c) - B}$$

Where:

$\delta_{gap}^{eff} =$

$+\delta_{gap}^{0}$

$-(\delta u_{fuel}^{thermal} + \delta u_{fuel}^{reloc\,[3]} + \delta u_{fuel}^{dens\,[4]} + \delta u_{fuel}^{swel\,[4]})$

$+(\delta u_{clad}^{thermal} + \delta u_{clad}^{elastic\,[3]})$

With:

$$\delta u_{clad}^{elastic} = \varepsilon_\theta \cdot \bar{r}_{clad}$$

$$\varepsilon_\theta = \frac{\sigma_\theta - \nu\sigma_z}{E}$$

$$\sigma_\theta = \frac{r_i P_i - r_o P_o}{r_o - r_i},\ \sigma_z = \frac{r_i^2 P_i - r_o^2 P_o}{r_o^2 - r_i^2}$$

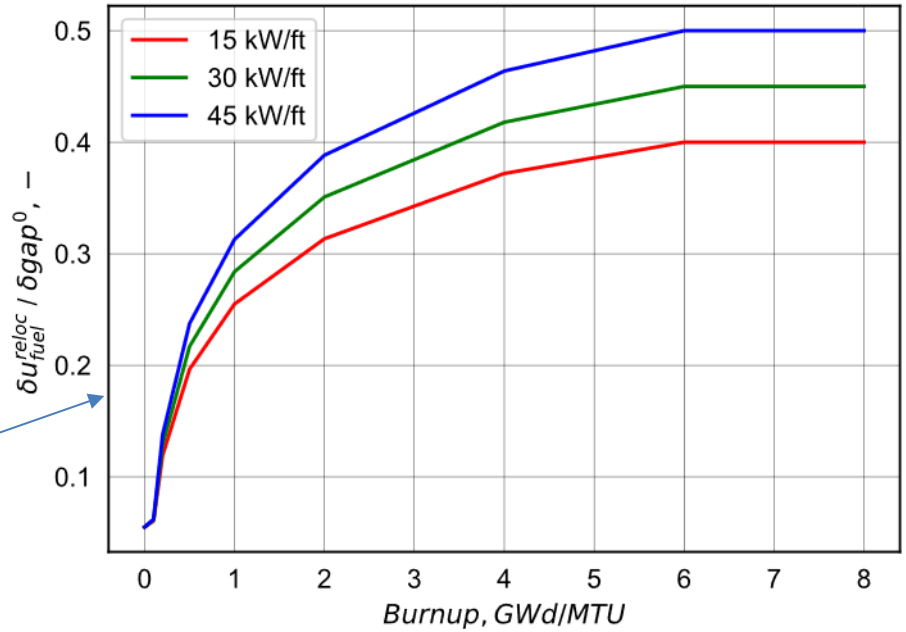

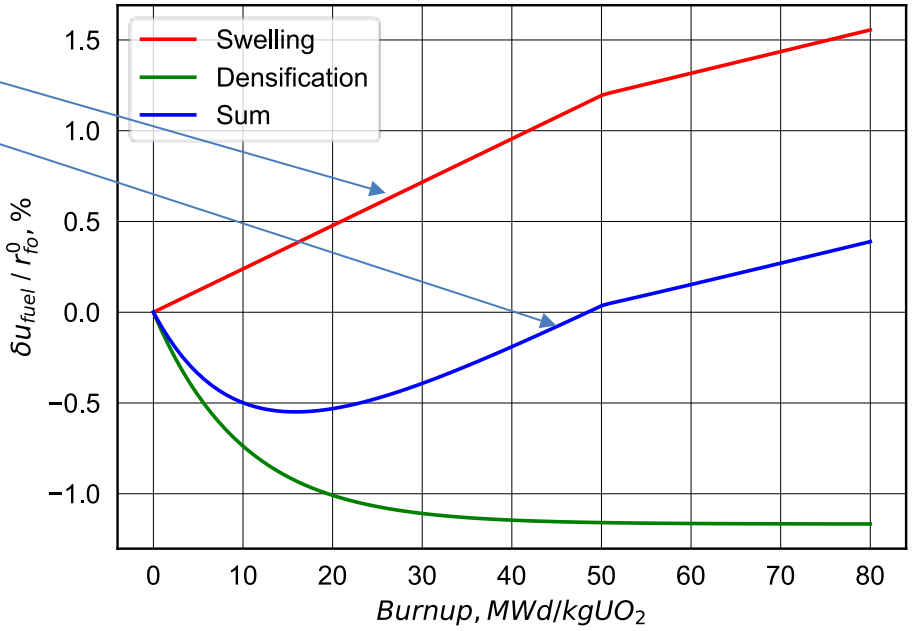

[1] FRAPCON-like
[2] /SON2/
[3] /CTF-lik/

Mauricio Exequiel Cazado

KIT

Evaluation of a BDBA Quench Sequence in a Generic iPWR with Natural Circulation: Application of the QUENCH-06 Experiment

Small Modular Reactors (SMRs) are emerging as a promising innovation in nuclear energy, offering clean, reliable, and cost-effective solutions with enhanced safety compared to traditional nuclear power plants (NPPs). Among the critical safety challenges for these reactors is the generation of hydrogen during Beyond-Design-Basis Accidents (BDBAs), which can give rise to significant risks to reactor integrity. Insights from the QUENCH-06 experiment are used in this work to evaluate the hydrogen generation and reflooding dynamics in a generic natural circulation pressurized water SMR during a quenching scenario. The generic SMR of 160 MWth consists of a compact design in which the core, pressurizer, steam generators, riser and downcomer are integrated into a reactor pressure vessel, which is located in a steel containment submerged in a pool of water. Using the ASTEC v3.1 code, this study simulates the thermal-hydraulic and core degradation phenomena that occur following a spurious valve opening at the top of the reactor vessel and subsequent loss of coolant inventory. This event initiates core uncovering and degradation, triggering hydrogen production due to oxidation reactions in the rods and structural components, and ends with a reflooding phase that quenches the core. The simulation results were evaluated against experimental data from QUENCH-06, which involved injecting water into an uncovered light water reactor (LWR) core to study quenching behavior.

Preliminary comparisons show that the ASTEC model reasonably reproduces the hydrogen generation trends, cladding temperature evolution and reflooding rates observed in the experimental setup, with deviations mainly due to model assumptions and differences between the proposed scenario and the actual conditions of the QUENCH facility. These results confirm the applicability of experimental data such as QUENCH-06 for the evaluation of degradation phenomena in SMR designs, and emphasize the role of empirical insights in improving simulation fidelity. The analysis also highlights areas for further refinement, such as accurate modeling of local cladding behavior and oxidation kinetics under transient conditions. This study contributes to the ongoing effort to establish robust safety analyses for advanced nuclear reactor designs by providing a framework for integrating experimental and computational approaches. Continued experimental validation and advanced model development are essential to address diverse accident scenarios and ensure reliable SMR deployment as a key component of future clean energy strategies.

Karlsruhe Institute of Technology

Evaluation of a BDBA Quench Sequence in a Generic iPWR with Natural Circulation: Application of the QUENCH-06 Experiment.

M. E. Cazado, F. Gabrielli, V. H. Sanchez-Espinoza

Institute for Neutron Physics and Reactor Technology

Introduction

- SMRs are a promising innovation in nuclear energy for clean, reliable, and cost-effective energy solutions.
- These advanced reactors designed are smaller than traditional NPPs with enhanced safety.
- Understanding hydrogen generation during BDBA is critical for assessing safety margins in SMRs.
- The QUENCH experiments are to investigate the hydrogen generation as results of water or steam injection in an uncovered core of a LWR: QUENCH-06 used water for cooling down the bundle.

Goal: Evaluate the applicability of QUENCH-06 data to predict the H_2 generation in a generic SMR during a quench sequence.

Introduction

ASTEC - Accident Source Term Evaluation Code developed by the French Institute for Radioprotection and Nuclear Safety (IRSN).

The code simulates the complete accident sequence in NPPs, from the initial event to the potential release of radioactive materials

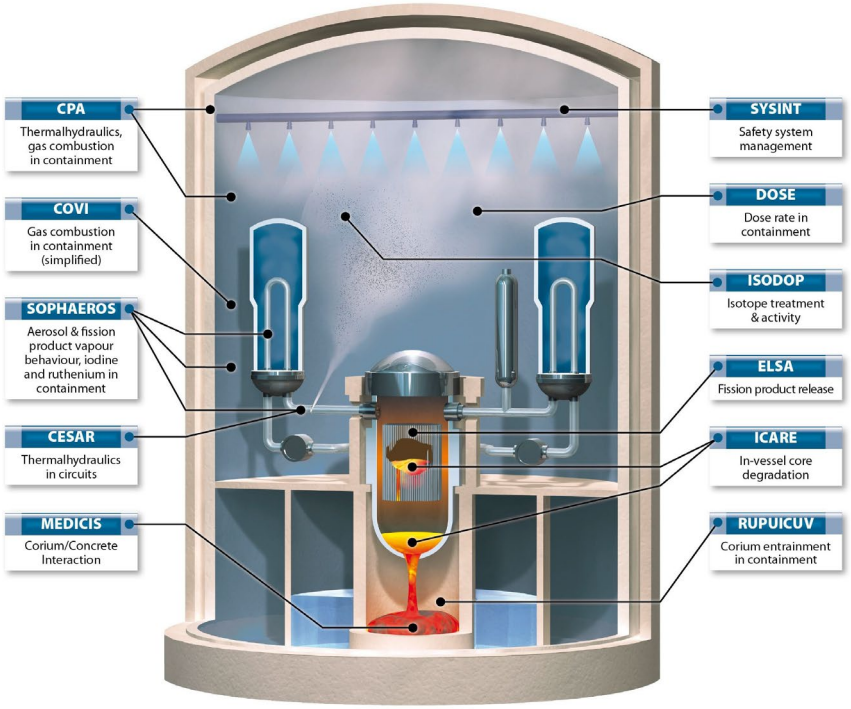

iPWR Design – General description

- Power: 45 MWe (160 MWt)
- Natural-circulation pressurized water reactor.
- Integrated reactor: core, pressurizer, helical-tube steam generators (HTSGs), Hot leg riser and Downcomer in RPV.
- RPV surrounded by Steel containment vessel immerse in a water pool.

Safety systems:

- Emergency Core Cooling Systems (ECCS): Primary coolant is collected at the Cont. and recirculation valves opens to generate a flow path.
- Containment Heat Removal System (CHRS): transfer energy to the pool by conduction and convection modes.

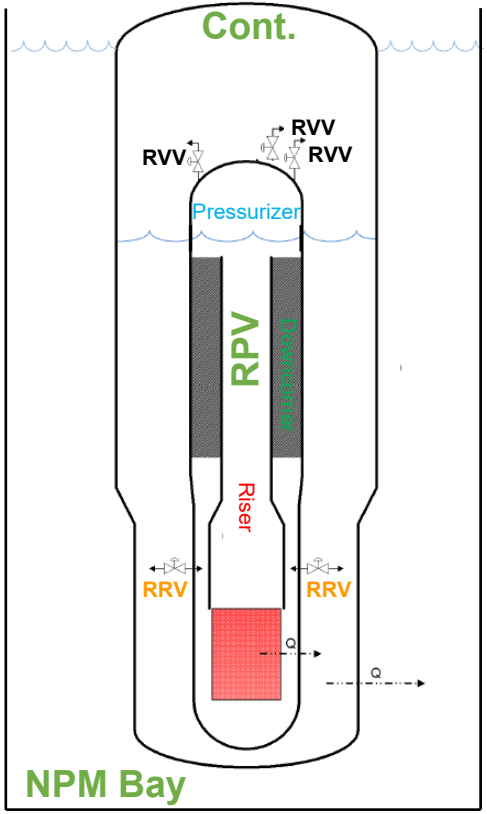

iPWR Model Nodalization

ASTEC v3.1 is employed to assess selected sequence in the generic SMR.

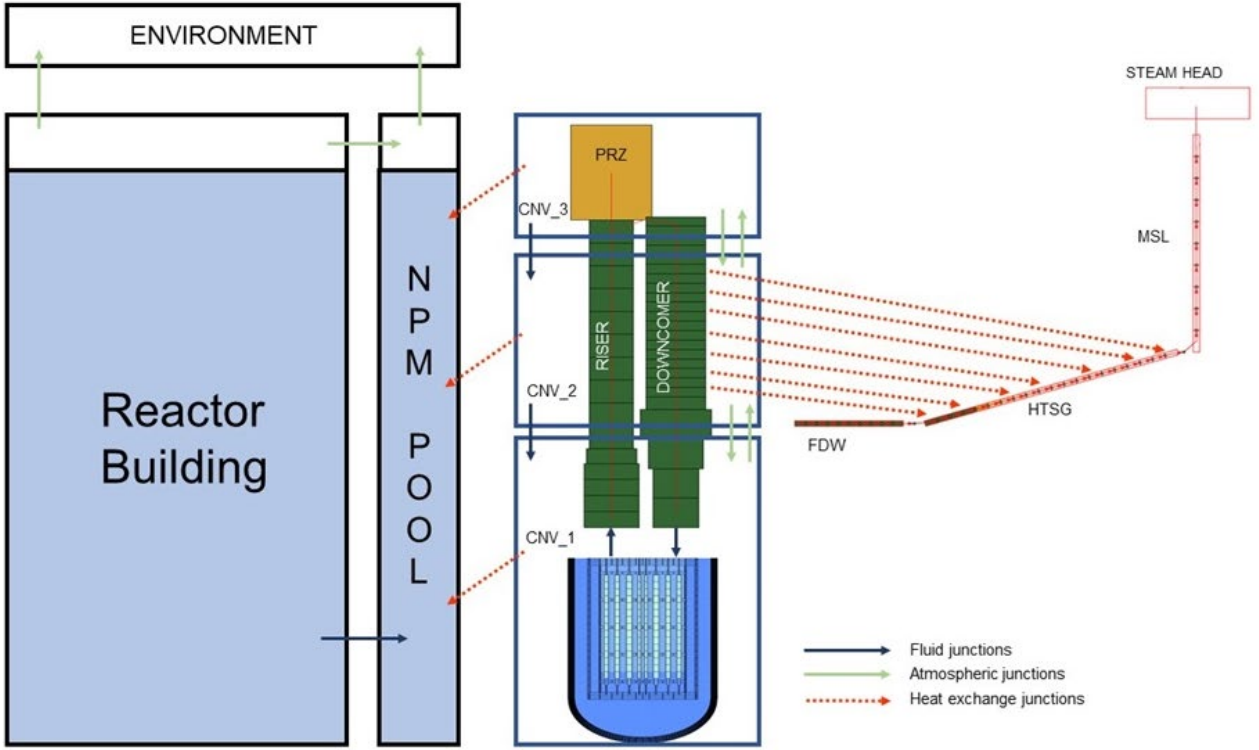

Quench Scenario Selected

2. SA Description

Spurious opening of 1 RVV.

- Loss AC (Feedwater, CVCS)
- ECCS activation ($DP_{Cont–RPV}$ < 6.9 MPa & Cont. level > 5.8 m)
- 2 RVVs available
- 2 RRVs not activated when the ECCS signal is triggered.
- After certain cladding temperature is reached the RRVs open: Tclad = 1973 [K] in the 3rd channel.

Initial Conditions

Parameter	value
Core Power [MW]	160.00
Feedwater Temperature [K]	422.0
Feedwater Pressure [MPa]	3.8
Average Core Temperature [K]	560.0
Burnup [MWd/kgU]	60.0
Containment Temperature [K]	320.0
Pool Temperature [K]	320.0
Pool water level [m]	16.8

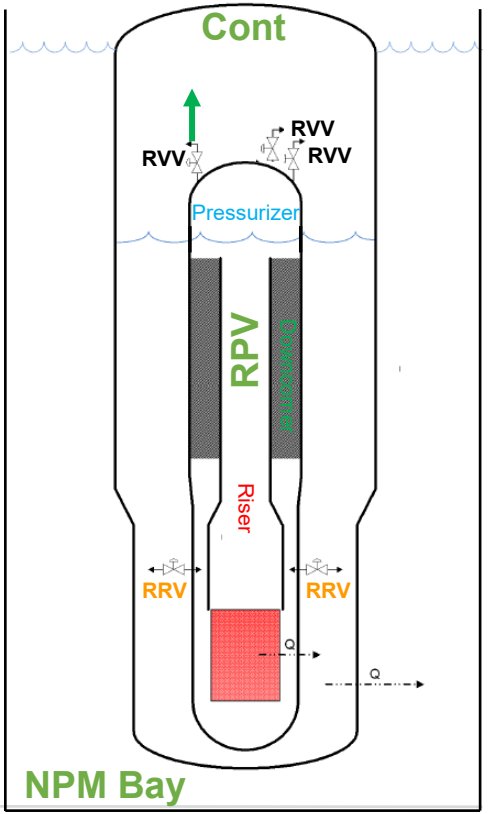

Results: Quench Scenario

Scenario Progression

key parameters	ASTEC
SCRAM time [s]	3.5
ECCS actuation time [s]	2032
Max. Press in Cont [MPa]	3.9
Max. liq. Level in Cont. [m]	8.6
Start of core uncovering [s]	~11400
Quenching Signal	17337
Start reflooding	17372
H2 onset time [s]	15102
Start of FPs release from fuel pellets [s]	16608
Total H_2 mass produced in the Vessel [kg]	7.7
Final H_2 mass in Cont. [kg]	7.1
Final aerosols mass in Cont. [kg]	6.2

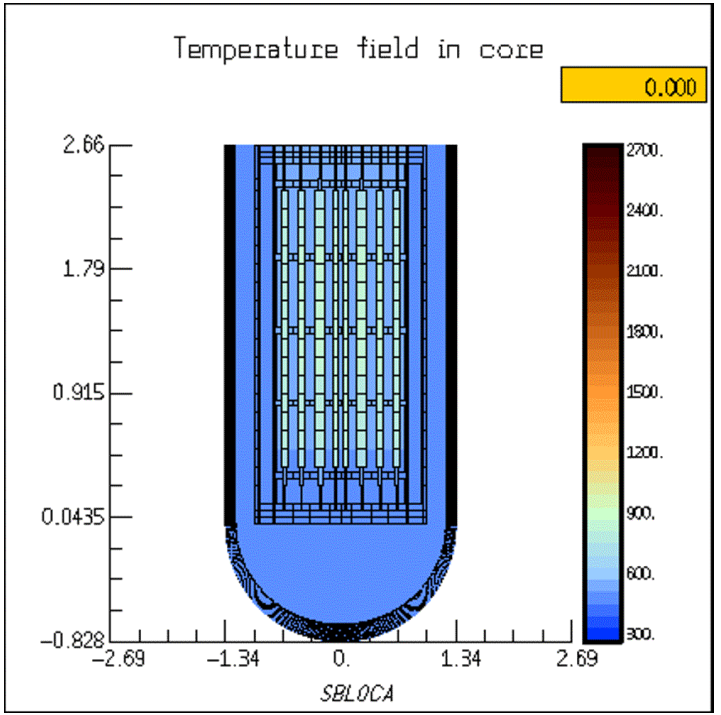

Results: Quench Scenario

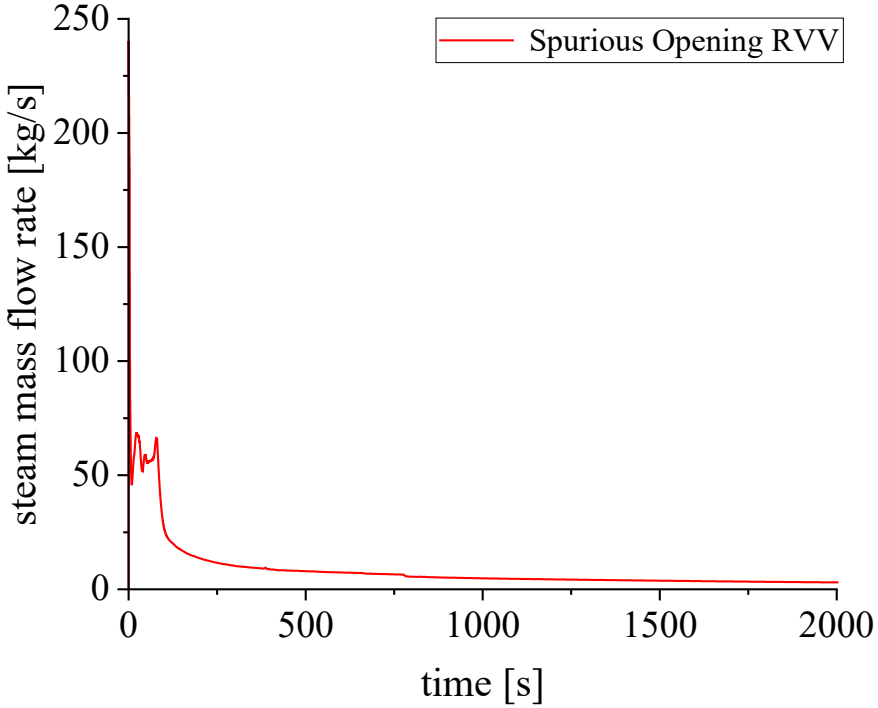

Steam mass flow rate evolution through the RVV during the scenario

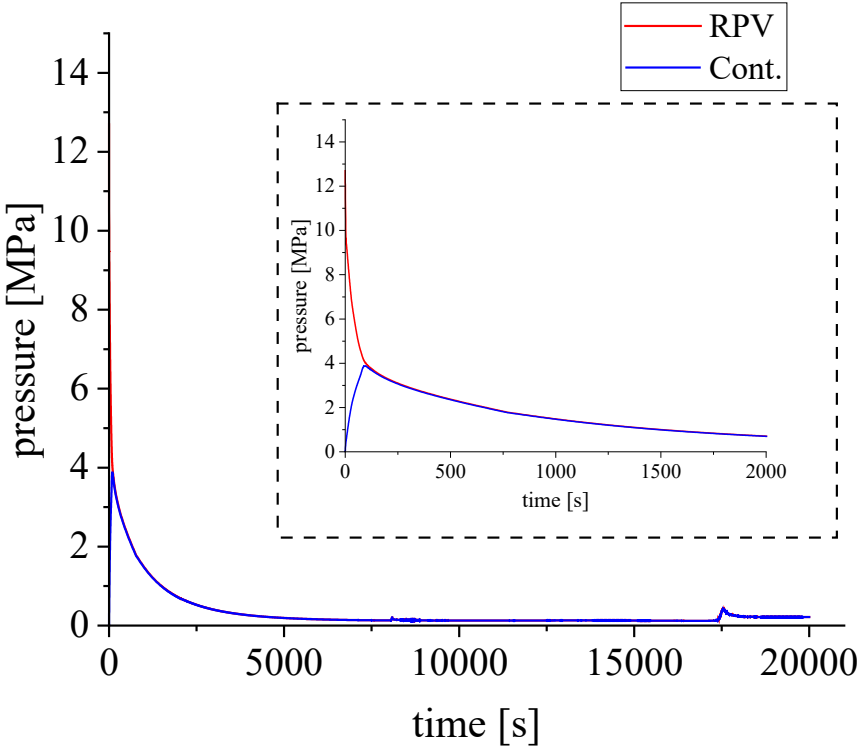

RPV and containment vessel pressure evolution

Results: Quench Scenario

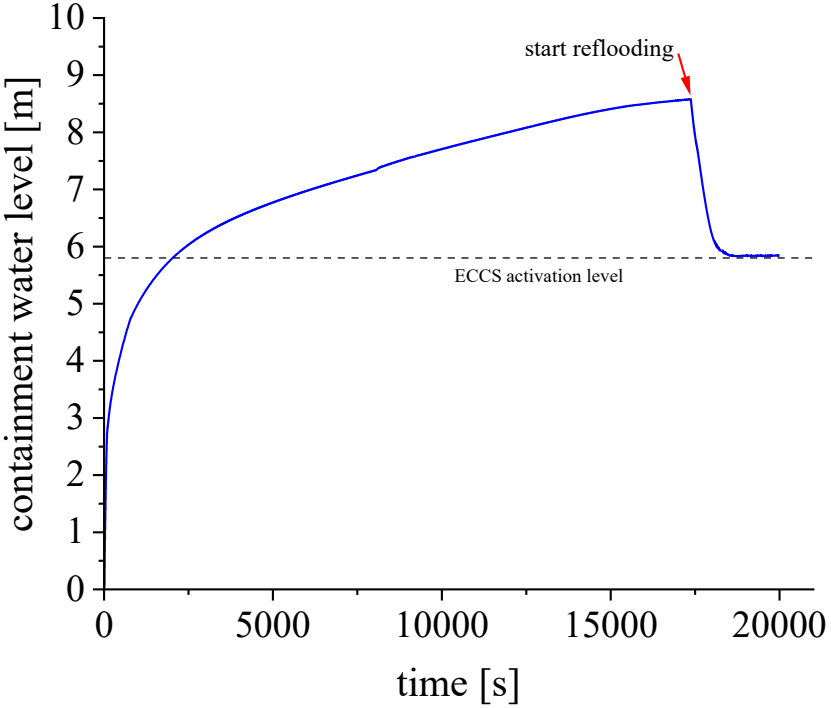

Evolution in time of water level in the containment for the BDBA case proposed.

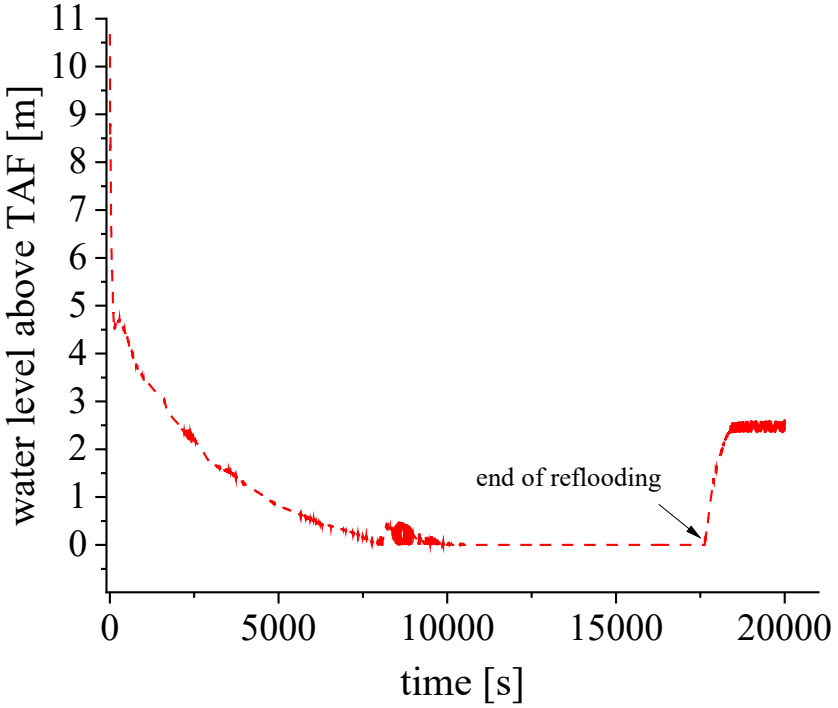

Evolution in time of water level above TAF in the Vessel for the BDBA case proposed.

Results: Quench Scenario

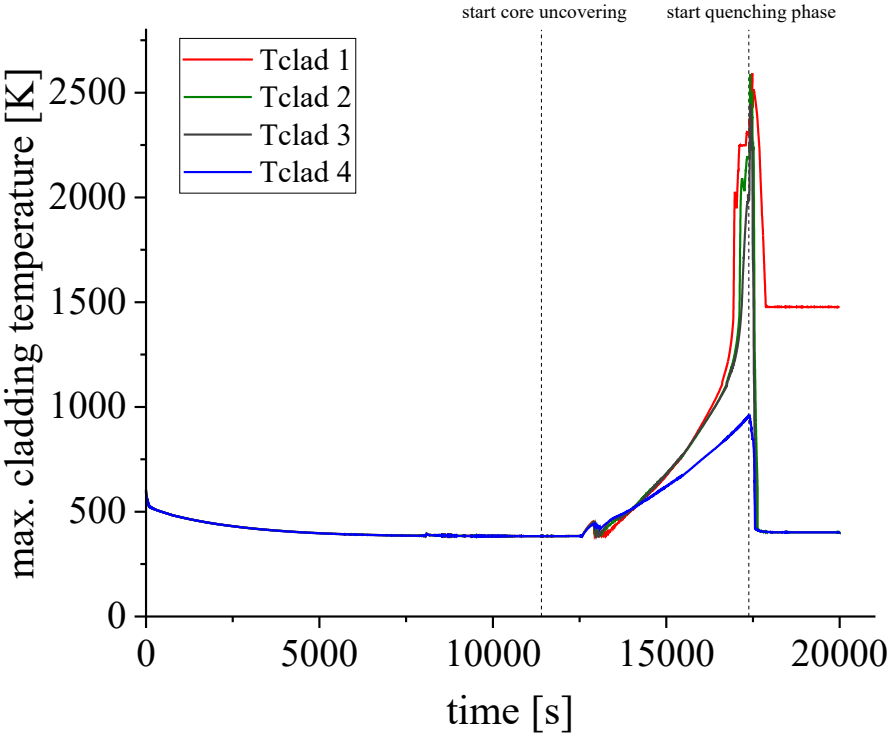

Maximum temperatura evolution for different channel during the selected BDBA scenario.

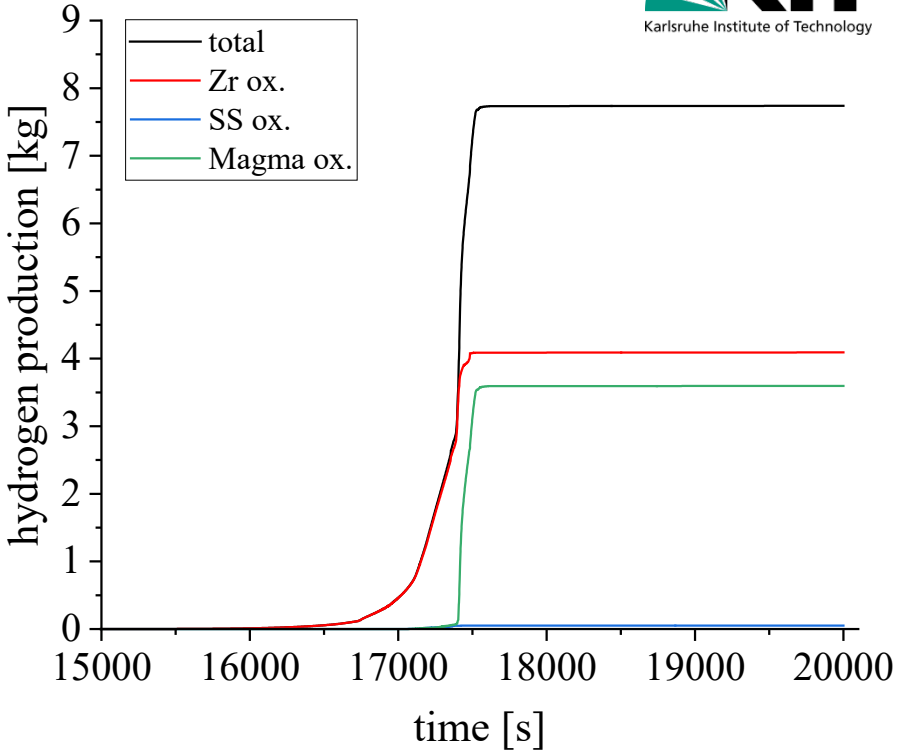

Total hydrogen generation in the RPV with different oxidation contributions during the selected BDBA scenario.

QUENCH-06: How to apply the exp. results?

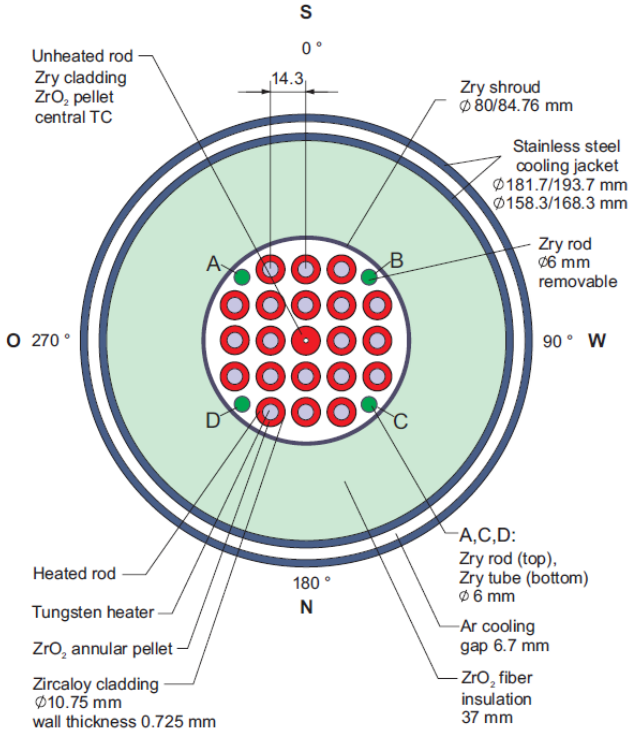

QUENCH-06; Test bundle; TC instrumentation and rod designation (Sepold et al. 2004)

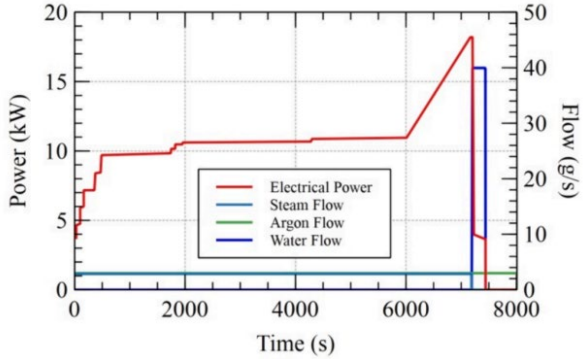

QUENCH-06 electrical power and boundary conditions (Sanchez-Mora et al. 2024)

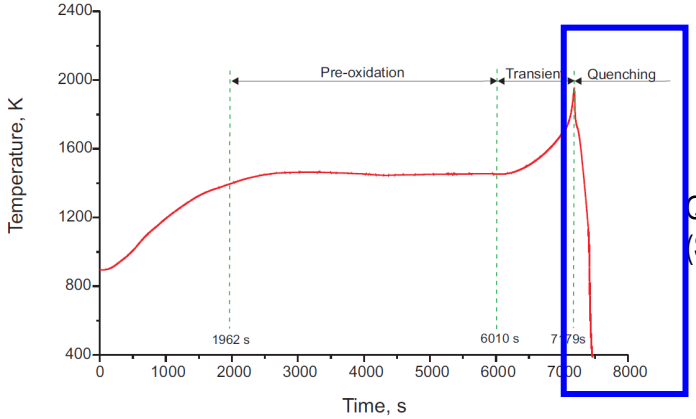

QUENCH-06; Test phases (Sepold et al. 2004)

Results: Exp. vs Sim.

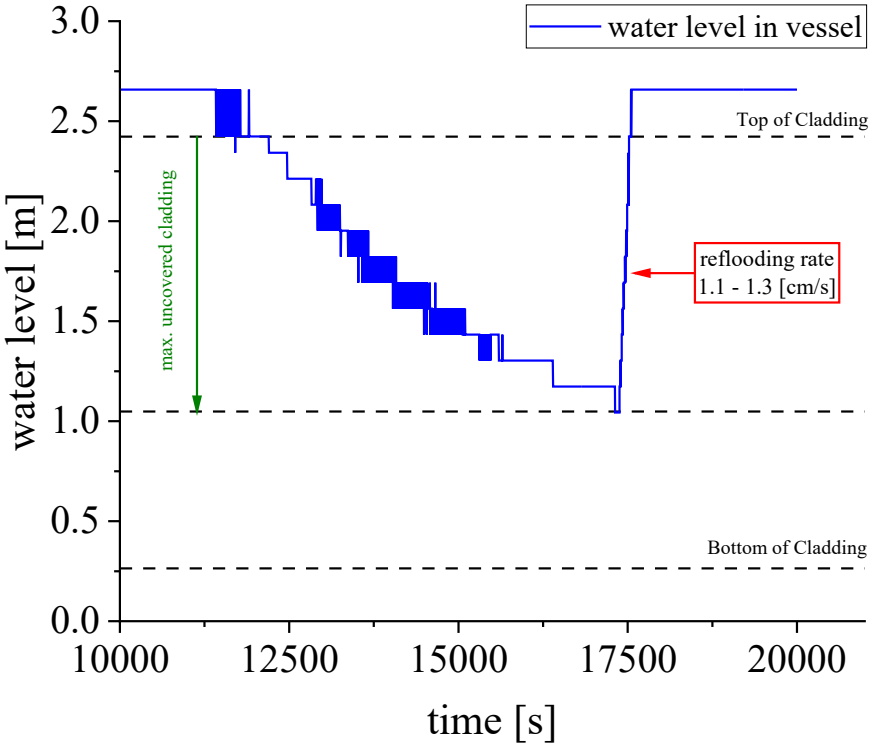

Water level evolution in the core during the selected BDBA scenario

Channel 3: Similar temperatures and less magma formation

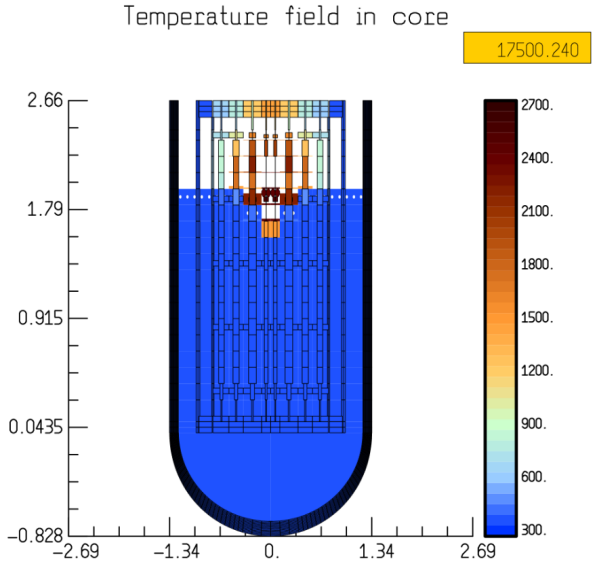

Exp. reflooding rate: ~1.4 [cm/s]

Results: Exp. vs Sim.

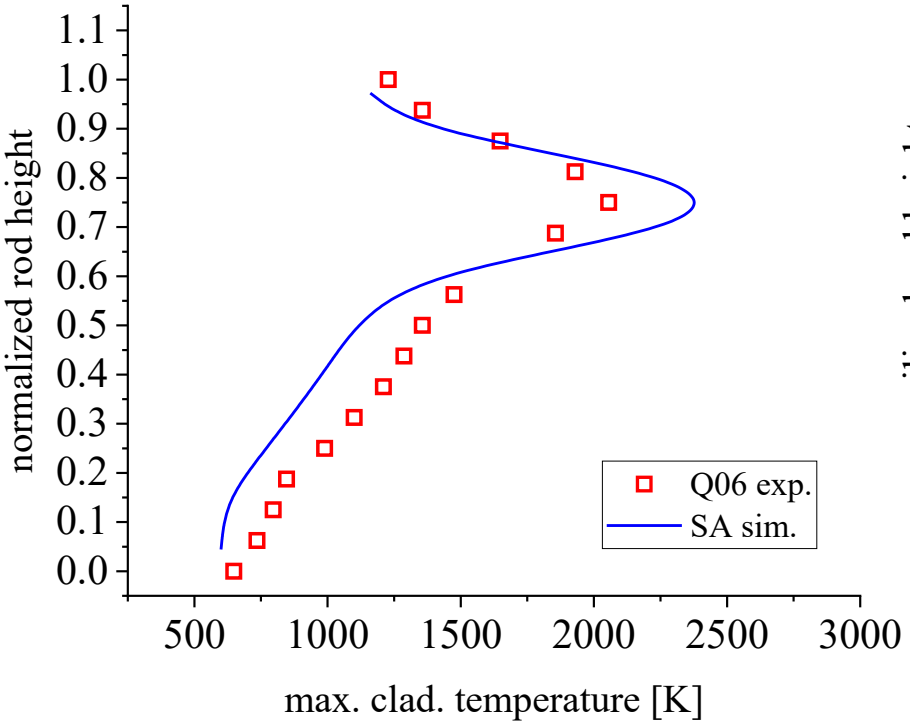

Maximum temperature profile comparison between the simulation (Claddings in channel 3) and Q06 exp.

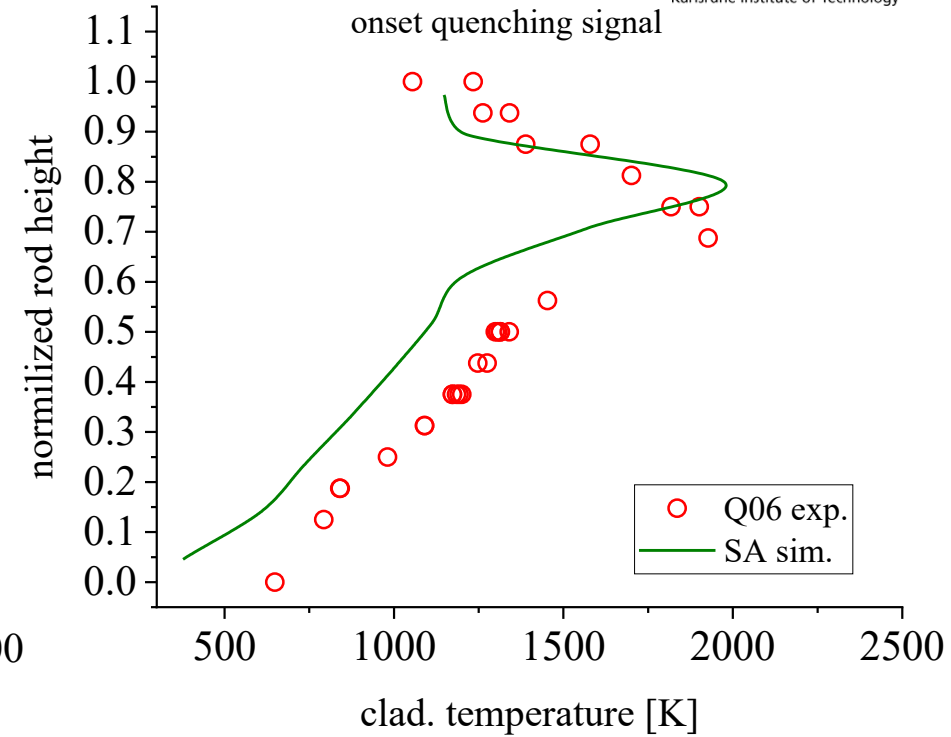

Temperatura profile comparison between the simulation (Claddings in channel 3) and Q06 exp. on the onset of the quenching signal

Results: Exp. vs Sim.

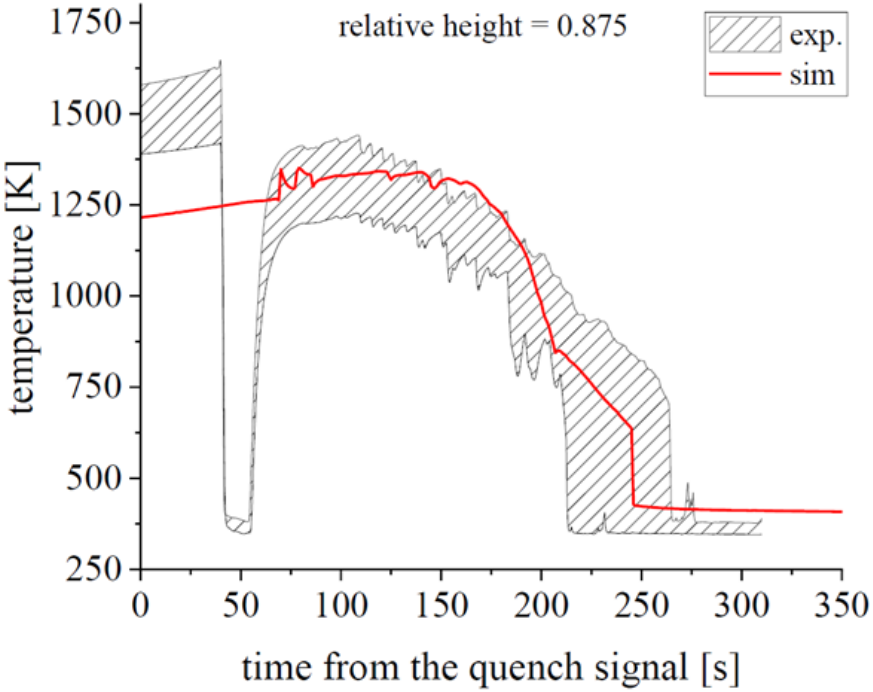

Temperature evoluation comparison between the simulation (Claddings in channel 3) and the experiment for a correspoing relative height of 0.875

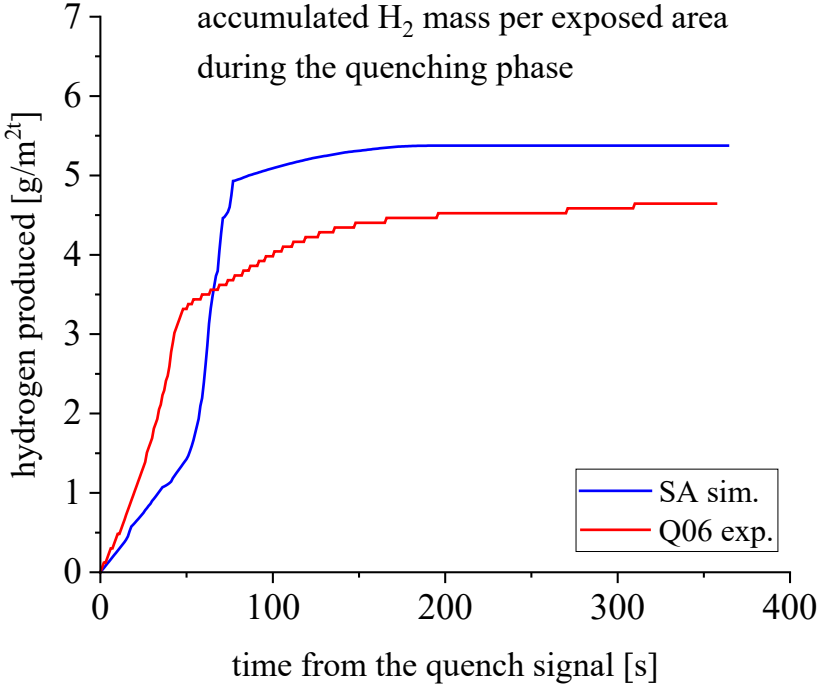

Hydrogen generation during the quenching pase for the experiment and simulation (Claddings in channel 3)

Conclusions

- A Quench scenario in a generic natural circulation iPWR was evaluated during this work showing that the ASTEC code can adequately simulate the Thermal-hydraulics and Core Degradation phenomena.
- In this analysis, the quenching phase results from the QUENCH-06 experiment showed reasonable agreement with the simulations for the hydrogen generation in the channel 3 of the core discretization in a generic SMR design during a BDBA. Some expected deviations are observed.
- These preliminary comparisons show that the QUENCH tests provide highly valuable experimental data for SMRs' safety assessments.
- Further experimental validation and simulation assessments are needed to address diverse accident scenarios and enhance predictive capabilities.

Karlsruhe Institute of Technology

Thank you for your attention

Sarah Weick

KIT

Conduction and analysis of the long-term SPIZWURZ bundle test

The orientation of hydrides in cladding tubes, circumferential or radial, depends mainly on the hoop stress. In this context, the SPIZWURZ project (Strain induced hydrogen redistribution in fuel cladding tubes during long-term interim storage) was initiated to collect relevant parameters for realistic dry storage conditions.

In this paper, the conduction and the analysis of the long-term SPIZWURZ bundle test is presented. It was the first long-term (8 month), large-scale test at the KIT's unique LICAS facility. 21 hydrided original cladding tubes from the nuclear industry of three different commercial materials (Zircaloy-4, optimized ZIRLO, Dx/D4 Duplex) were heated up under different inner pressures (106, 146 bar) with different hydrogen concentrations (100, 300 wt.ppm). Then they were cooled down to imitate dry storage conditions of spent nuclear fuel. After heating up the bundle to a maximum temperature of 409°C at the central rod, a uniform cooldown process of 1 K/day was started. The bundle test was conducted for 250 days from the 12th of May 2023 until the 17th January 2024. Since then, non-destructive and destructive analytical methods were used to investigate the post-test hydrogen concentration, hydride orientation, hydride density and cladding creep. Methods used were measurements with laser scan micrometer, ultrasonic evaluations, neutron tomography, carrier gas hot extraction (destructive) and metallography (destructive).

The different analysis revealed that the cladding materials Zircaloy-4 (and DUPLEX Dx/D4) and optimized ZIRLO behave differently under the test conditions with respect to the investigated criteria. The differences in the creep and the hydrogen re-orientation behaviour were surprisingly hight. The preliminary results will be presented and discussed in the paper. The post-test examinations are still in progress. An overview of the results will be given elsewhere.

Karlsruher Institut für Technologie

Conduction and analysis of the long-term SPIZWURZ bundle test

S. Weick, M. Grosse, C. Roessger, J. Stuckert, M. Steinbrueck

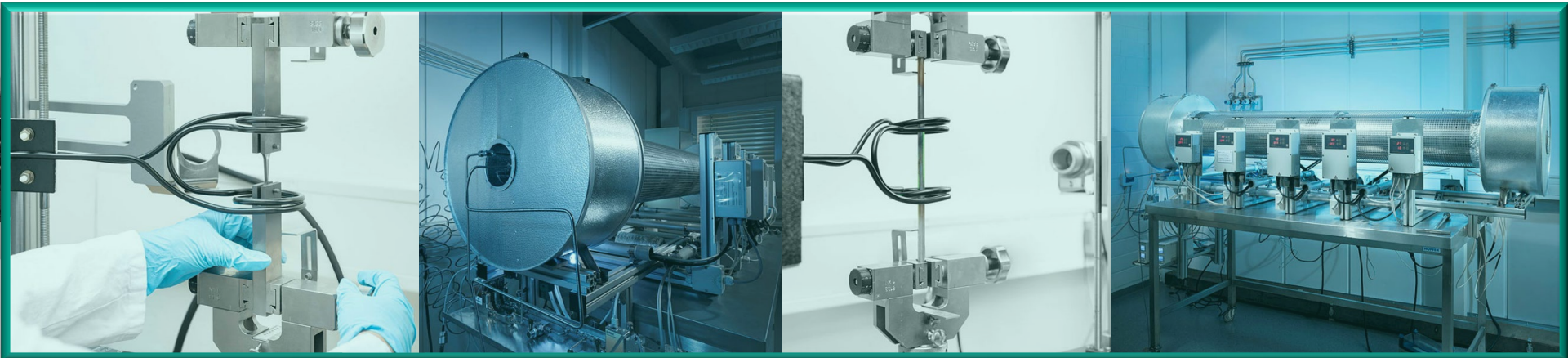

29th QUENCH workshop
19th – 21th November 2024, Karlsruhe, Germany

IAM-AWP-HTWC

Introduction

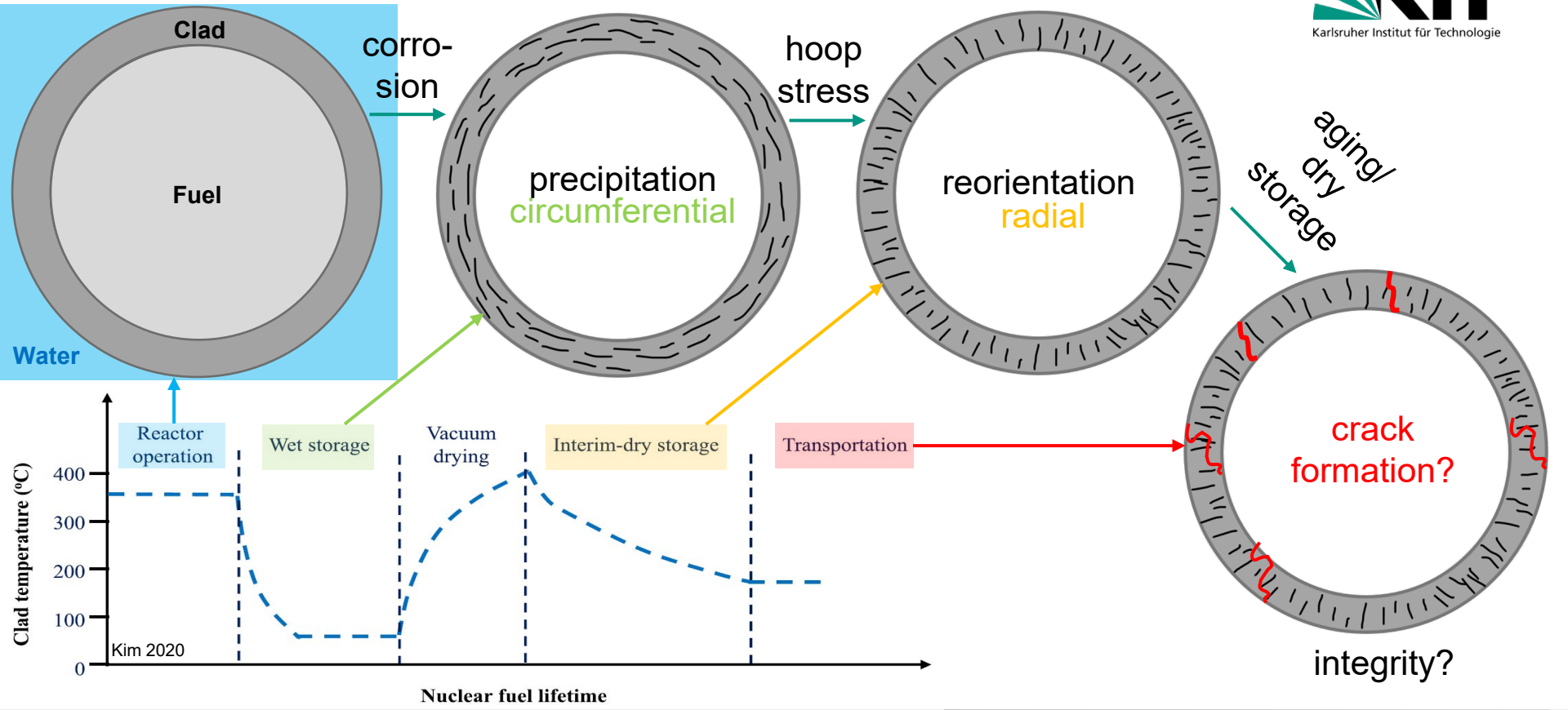

Introduction

- H dissolution-precipitation scheme with modelled **TSS** (terminal solid solubility)

→ **TSSp**: precipitation terminal solubility limit

→ **TSSd**: dissolution terminal solubility limit

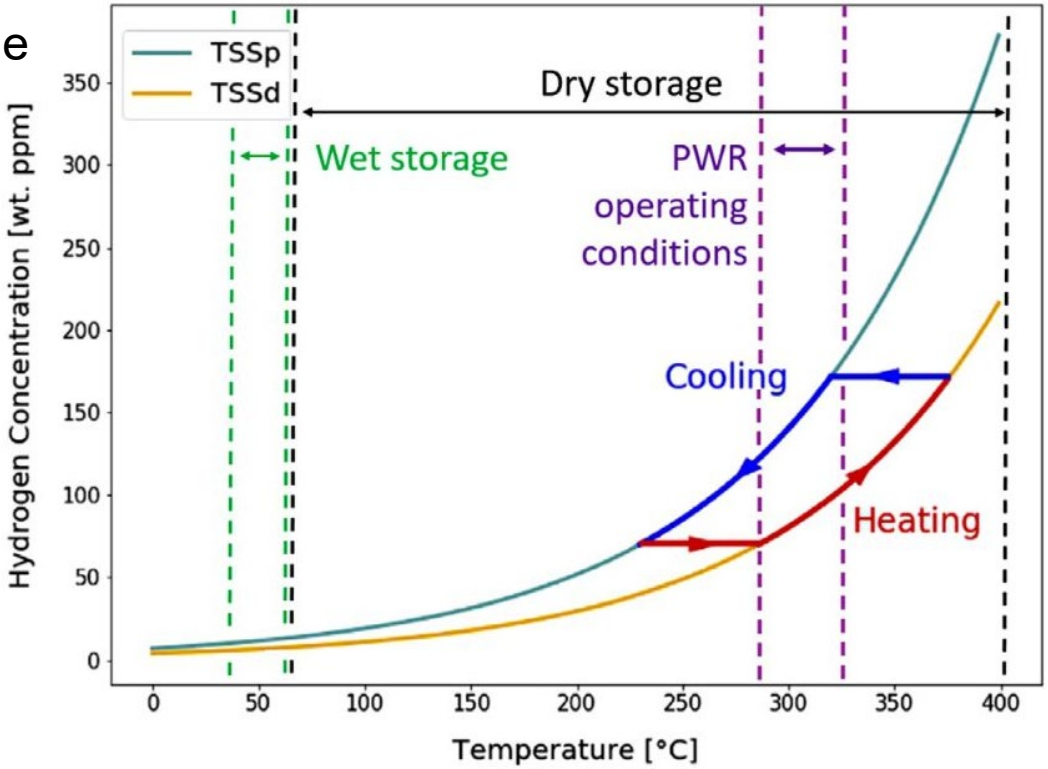

Kaufholz et al.2018, modified from Konarski 2021

Project

- **SPIZWURZ** = Spannungsinduzierte Wasserstoffumlagerung in Brennstabhüllrohren während längerfristiger Zwischenlagerung
  (Strain induced hydrogen redistribution in fuel cladding tubes during longterm interim storage)

- KIT/IAM-AWP & KIT/INE & GRS

Karlsruher Institut für Technologie

global research for safety

Bundesministerium für Umwelt, Naturschutz, nukleare Sicherheit und Verbraucherschutz

BGZ Gesellschaft für Zwischenlagerung mbH

- **Objective**: improvement & extension of experimental data base for modelling of degradation processes during dry storage

QUENCH Bundle Test

- 21 fuel rod simulators (l = 2.5 m)
- 16.05.23 – 18.01.24

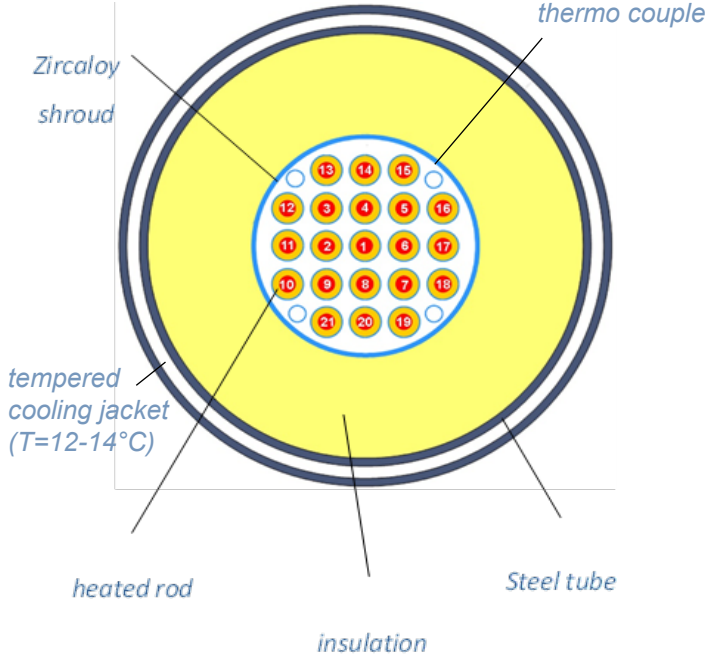

QUENCH/ LICAS facility

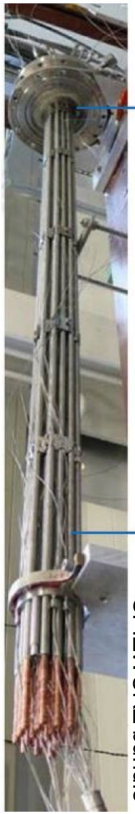

SPIZWURZ bundle

QUENCH Bundle Test

- 2 different hydrogen concentrations (100 & 300 wt.ppm)
- 2 different pressures (106 & 146 bar; approx. 68 & 96 MPa)
- 3 different cladding materials (Zry-4, ZIRLO, DX/D4)

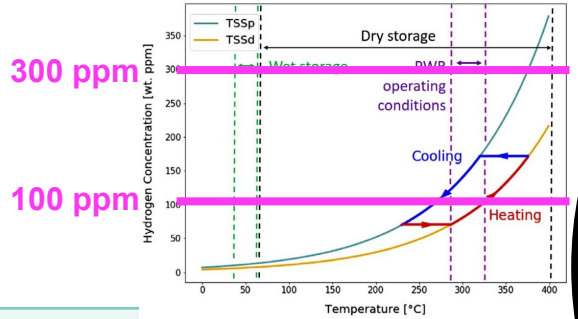

alloy	Sn [wt.%]	Fe [wt.%]	Cr [wt.%]	Nb [wt.%]	O [wt.%]
Zry-4, D4	1.3	0.2	0.1	-	0.13
Dx	0.5	0.5	0.2	-	0.14
optimized ZIRLO	0.9	0.1	-	0.9	-

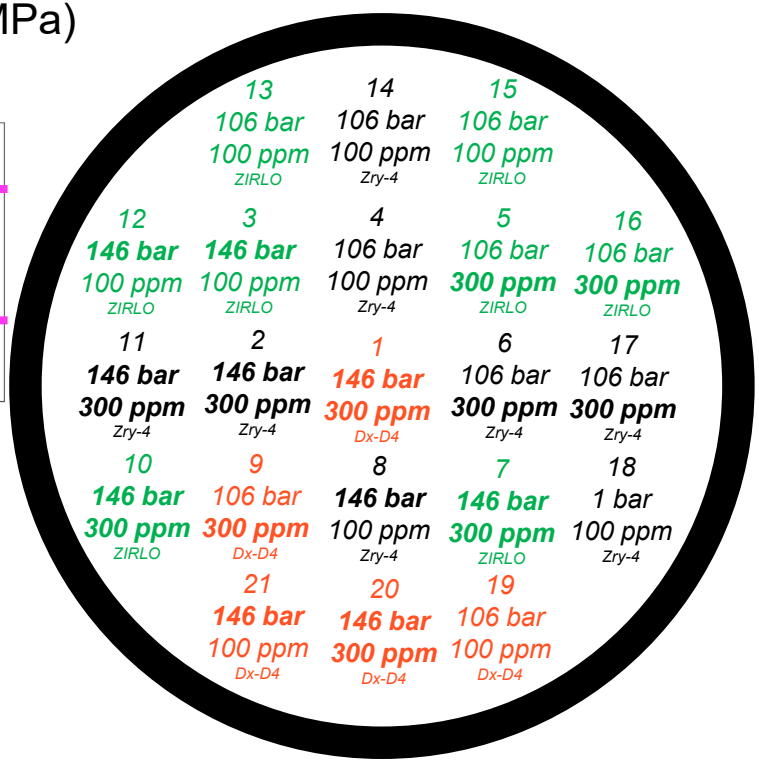

QUENCH Bundle Test

- 9 sample couples (rods with same conditions, but different positions within the bundle

→ slightly different temperatures

Sample	Cladding	c_H [ppm]	p_{inside} [bar]
Rod 1	Dx-D4	300	146
Rod 2	Zry-4	300	146
Rod 3	ZIRLO	100	146
Rod 4	Zry-4	100	106
Rod 5	ZIRLO	300	106
Rod 6	Zry-4	300	106
Rod 7	ZIRLO	300	146
Rod 8	Zry-4	100	146
Rod 9	Dx-D4	300	106
Rod 10	ZIRLO	300	146
Rod 11	Zry-4	300	146
Rod 12	ZIRLO	100	146
Rod 13	ZIRLO	100	146
Rod 14	Zry-4	100	106
Rod 15	ZIRLO	100	106
Rod 16	ZIRLO	300	106
Rod 17	Zry-4	300	106
Rod 18	Zry-4	100	146
Rod 19	Dx-D4	100	106
Rod 20	Dx-D4	300	146
Rod 21	Dx-D4	100	146

Pre-Preparation/ Hydrogenation

- H content meaured by Laser Scan Micrometer (sample diameter)

Laser scan measurement

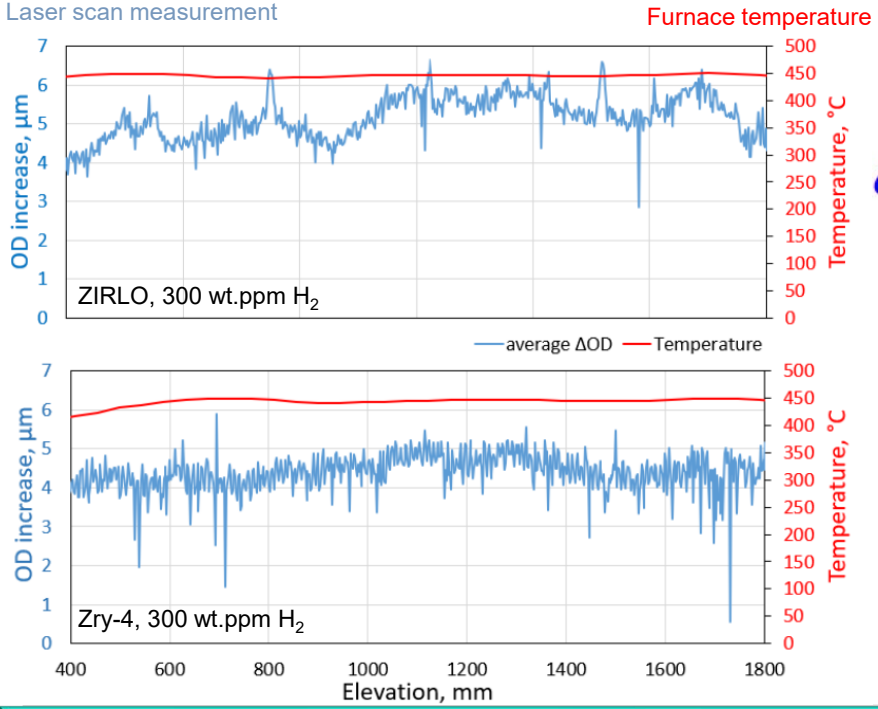

HoKi furnace at KIT

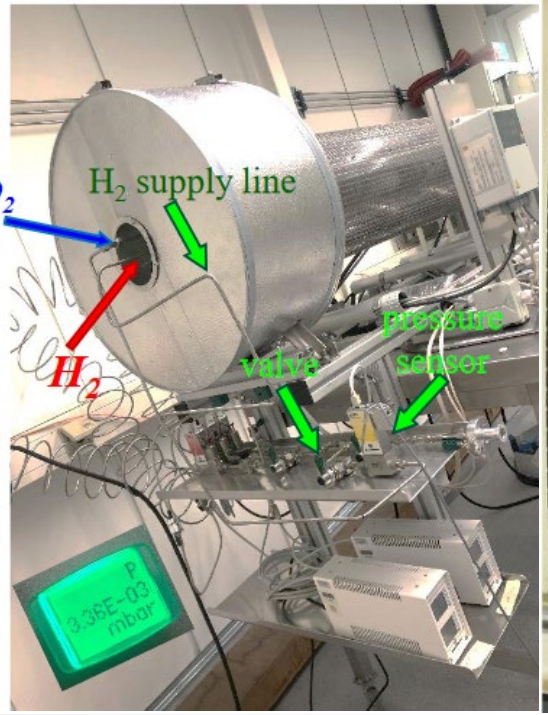

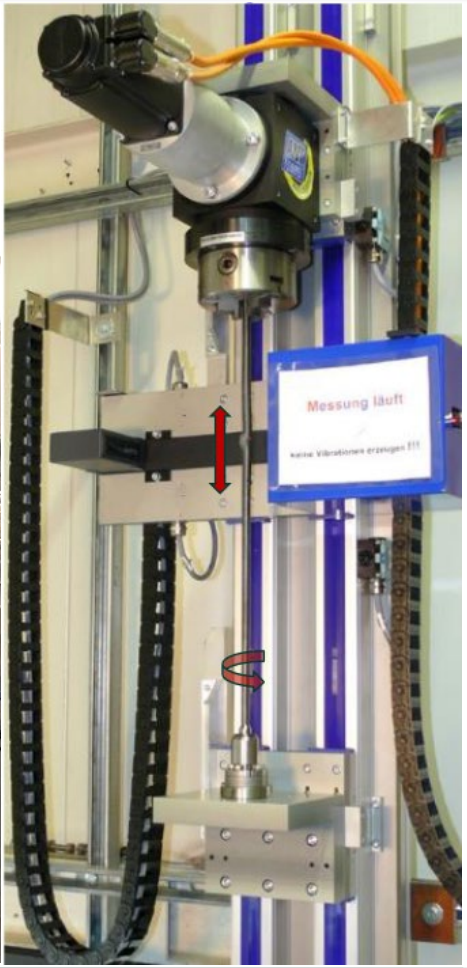

Temperature

- Start-T: 405 °C (rod centre) - 100 °C (rod ends)
- Slow cooling: 7 K/week (0.94 K/d) for 250 d (16.05.23–18.01.24)
- 405°C T_{max} (rod 1; zone 9); 165°C T_{end} (rod 1; zone 9)

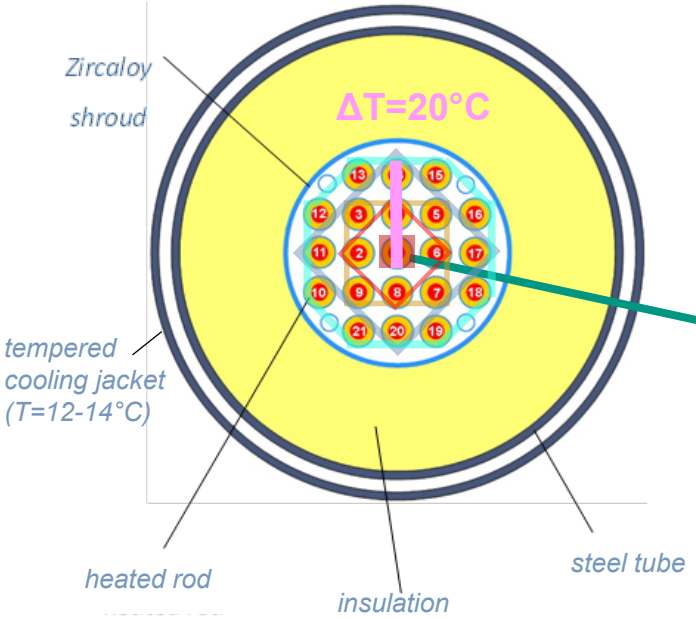

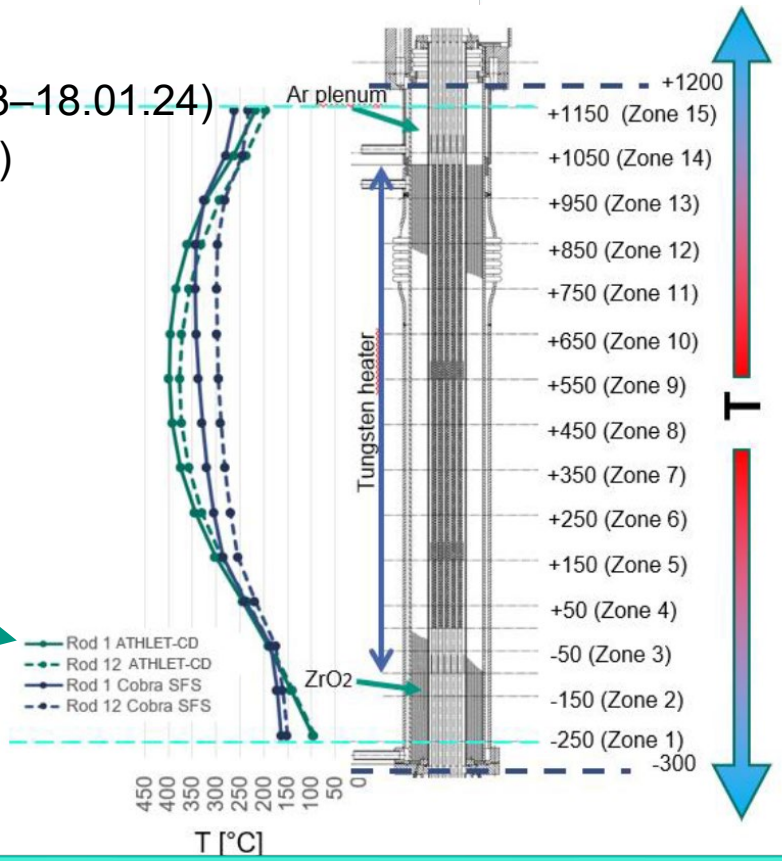

Temperature

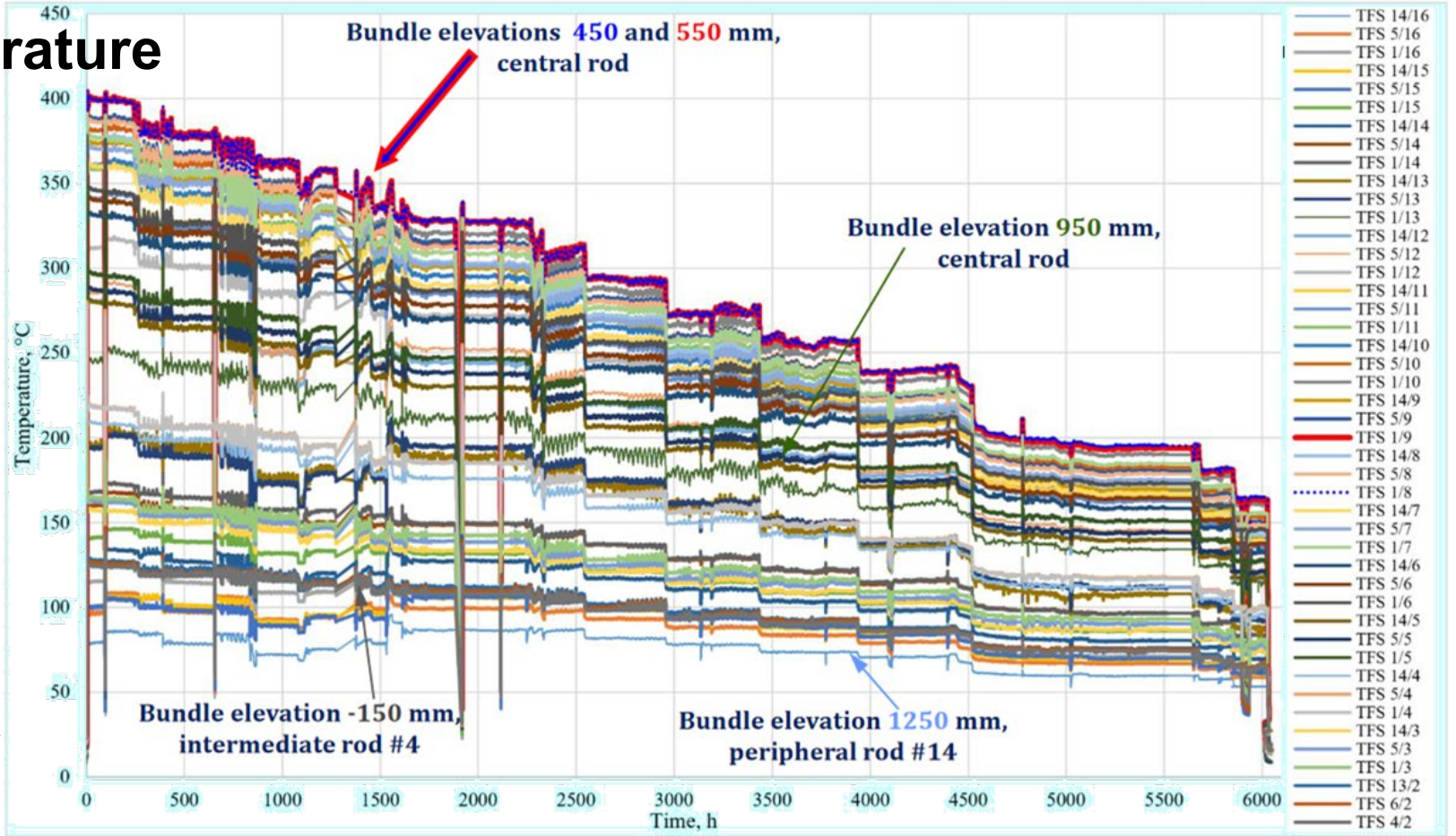

Karlsruher Institut für Technologie

Temperature

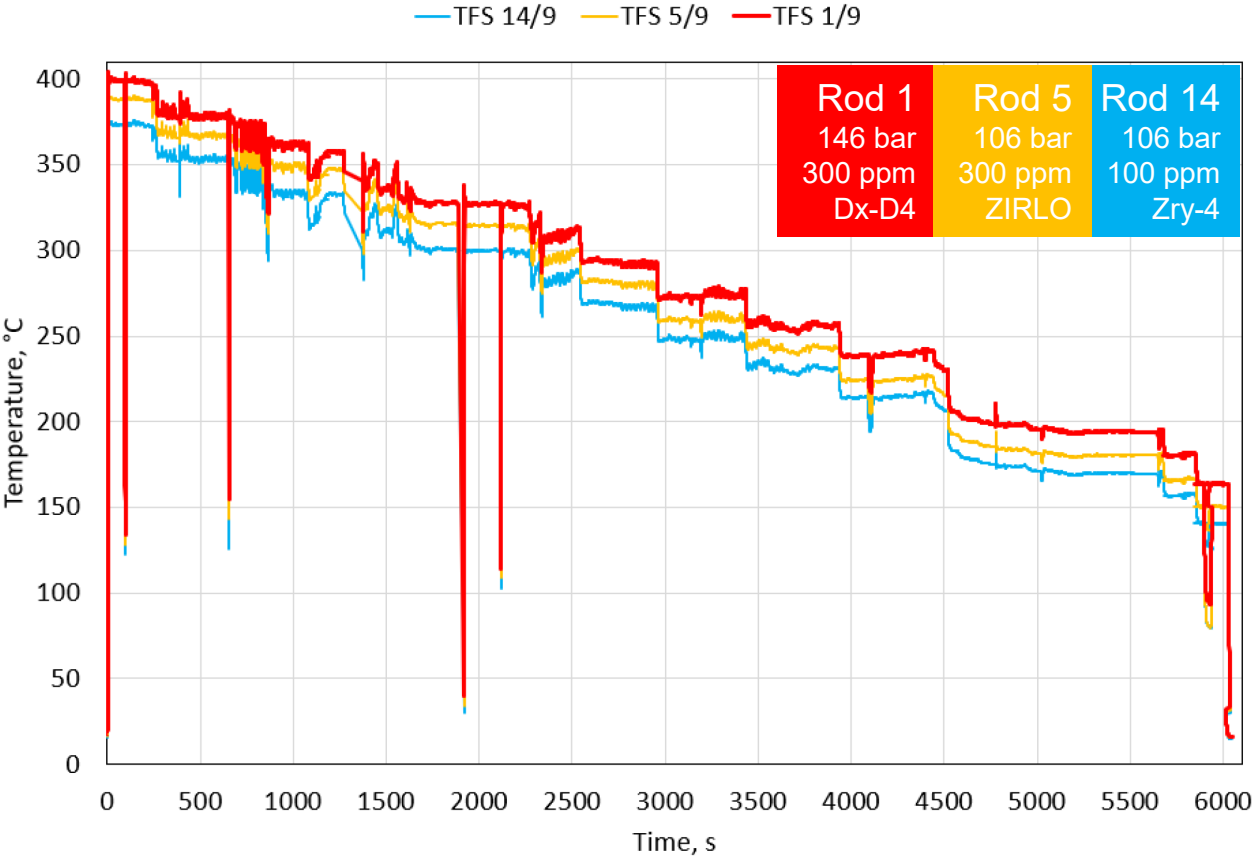

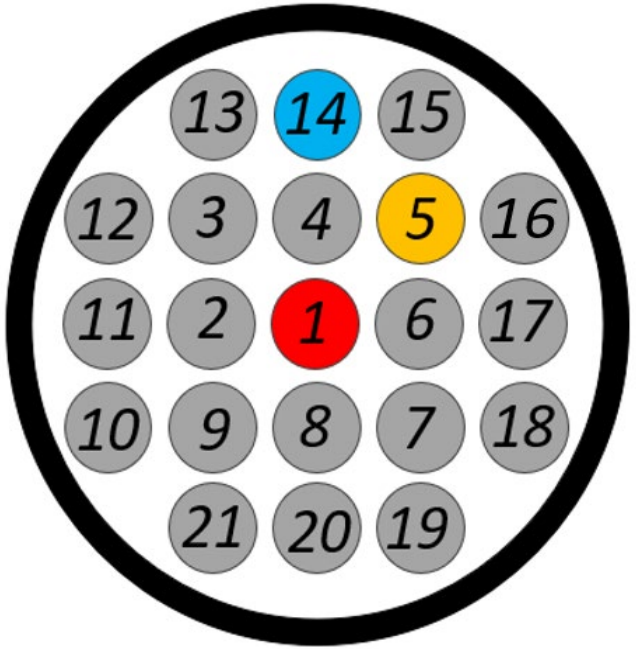

Temperature

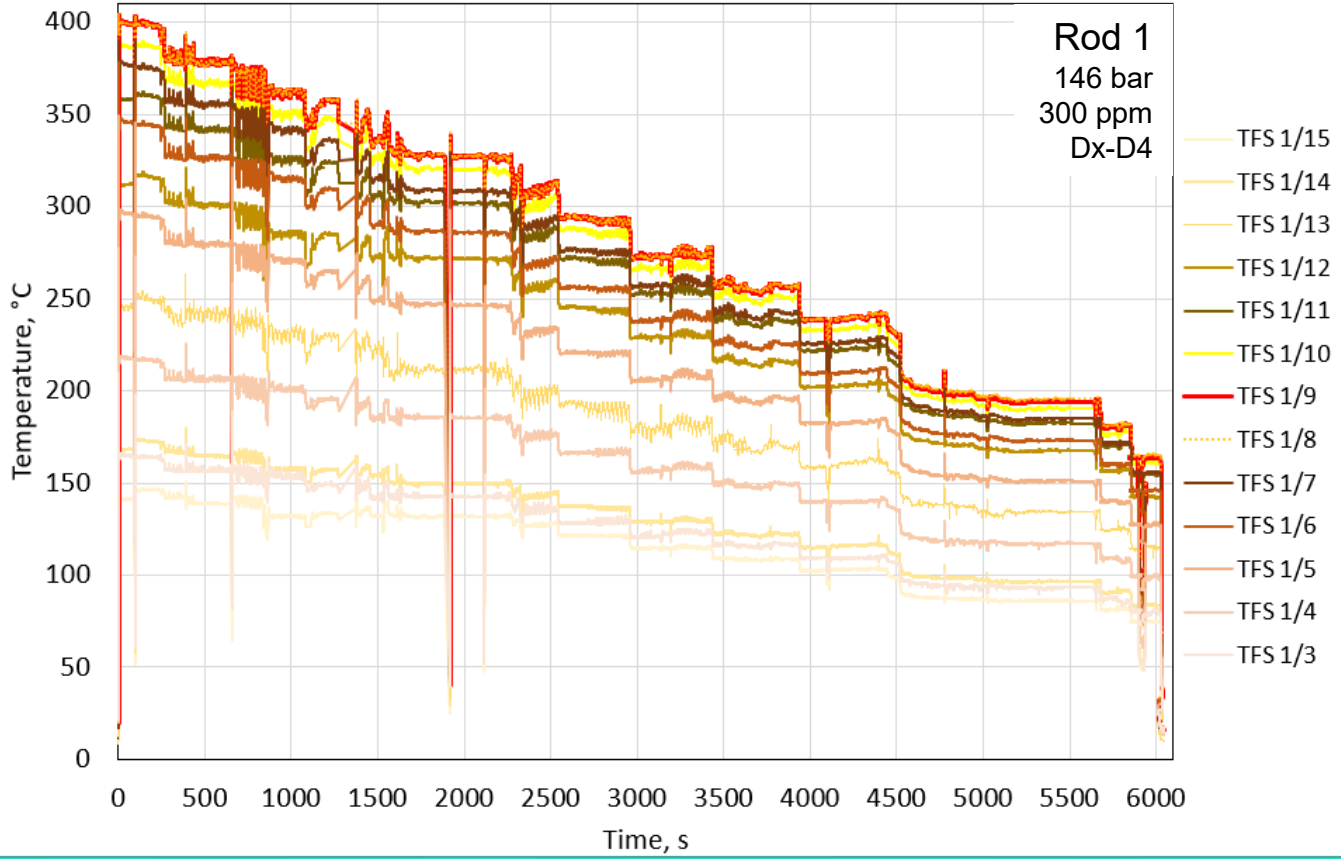

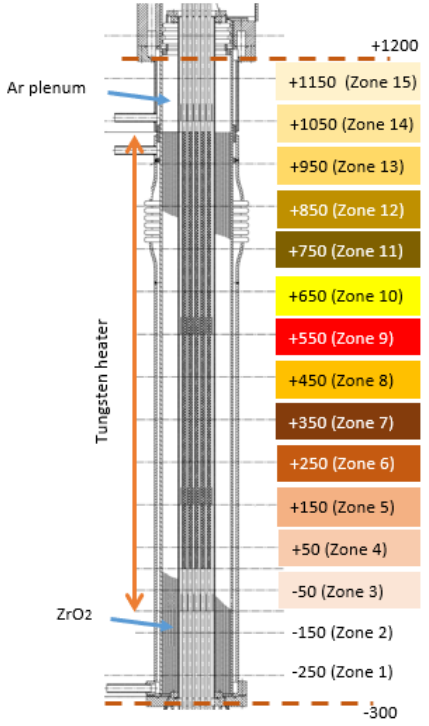

Pressure

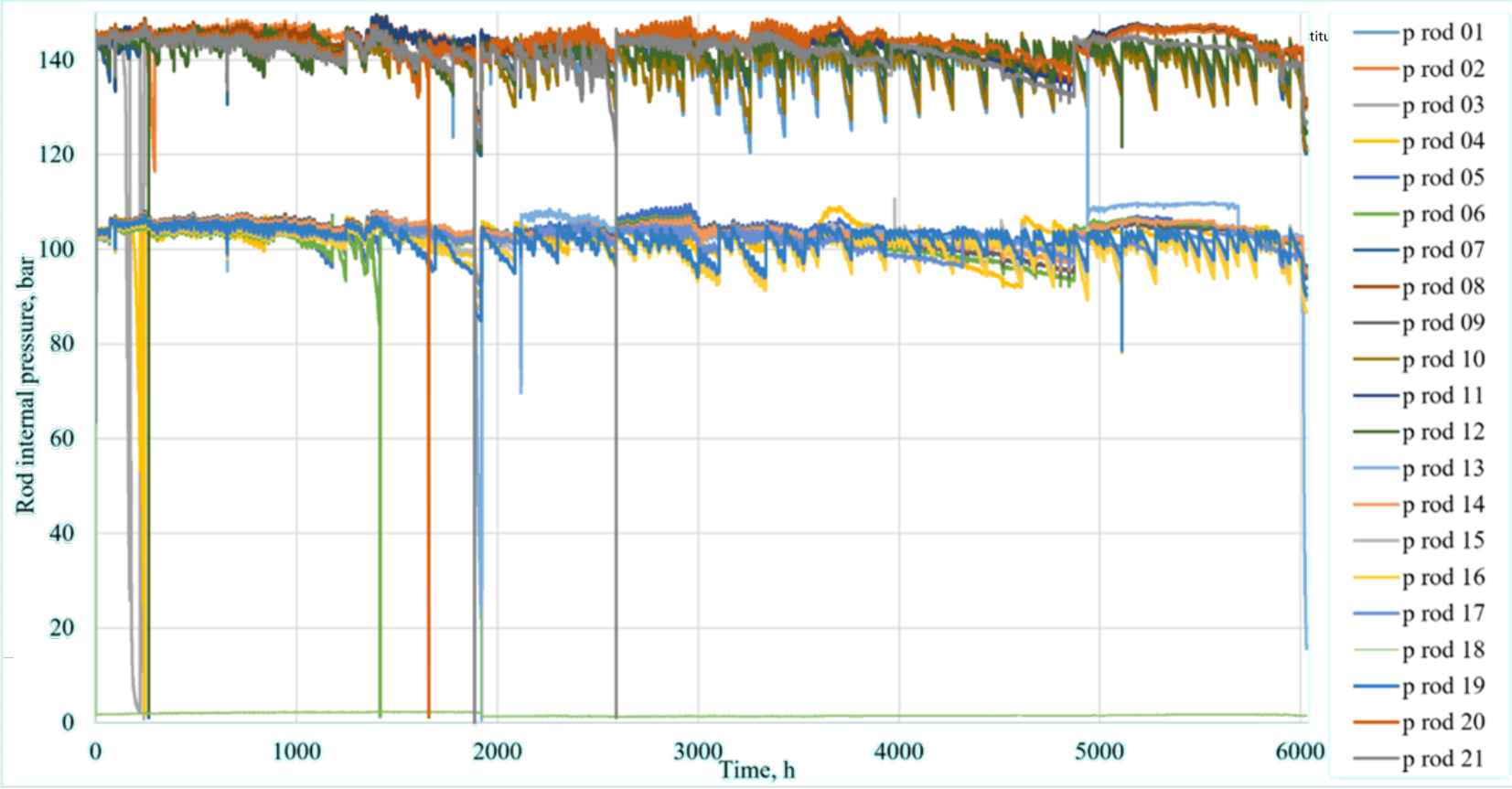

Karlsruher Institut für Technologie

Creep

- Max. creep measured at rod 7
- Diagram: same conditions (cH = 300 wt.ppm; p = 146 bar), different claddings
- Creep ZIRLO (up to 3%) > creep Zry-4 (up to 1%) = creep Dx/D4

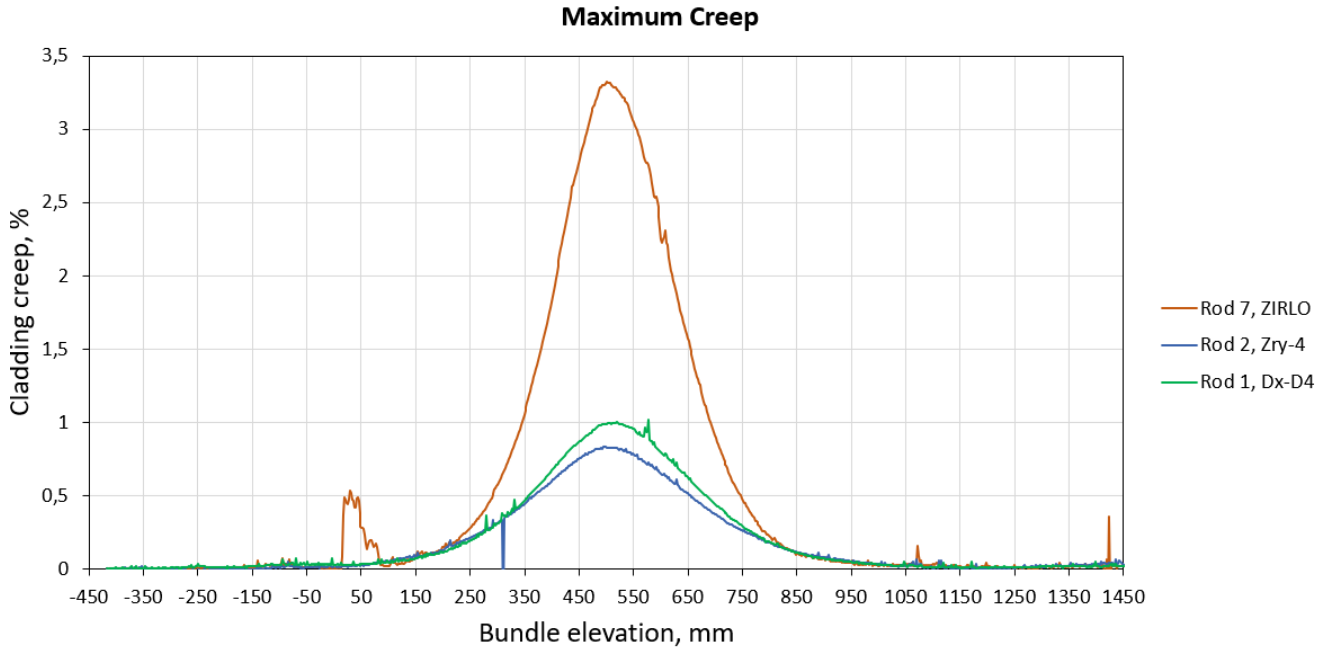

	clad	c_H	p
		ppm	bar
Rod 1	Dx-D4	300	146
Rod 2	Zry-4	300	146
Rod 3	ZIRLO	100	146
Rod 4	Zry-4	100	106
Rod 5	ZIRLO	300	106
Rod 6	Zry-4	300	106
Rod 7	ZIRLO	300	146
Rod 8	Zry-4	100	146
Rod 9	Dx-D4	300	106
Rod 10	ZIRLO	300	146
Rod 11	Zry-4	300	146
Rod 12	ZIRLO	100	146
Rod 13	ZIRLO	100	146
Rod 14	Zry-4	100	106
Rod 15	ZIRLO	100	106
Rod 16	ZIRLO	300	106
Rod 17	Zry-4	300	106
Rod 18	Zry-4	100	146
Rod 19	Dx-D4	100	106
Rod 20	Dx-D4	300	146
Rod 21	Dx-D4	100	146

H_2 analysis - Optimized ZIRLO

Δ = 146 bar

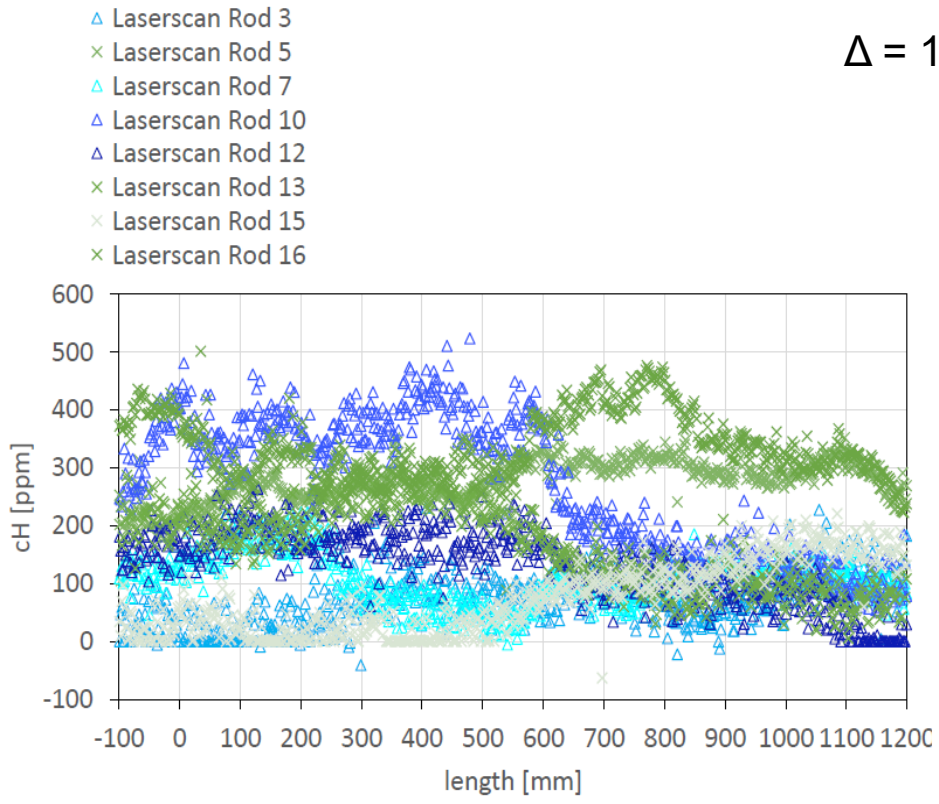

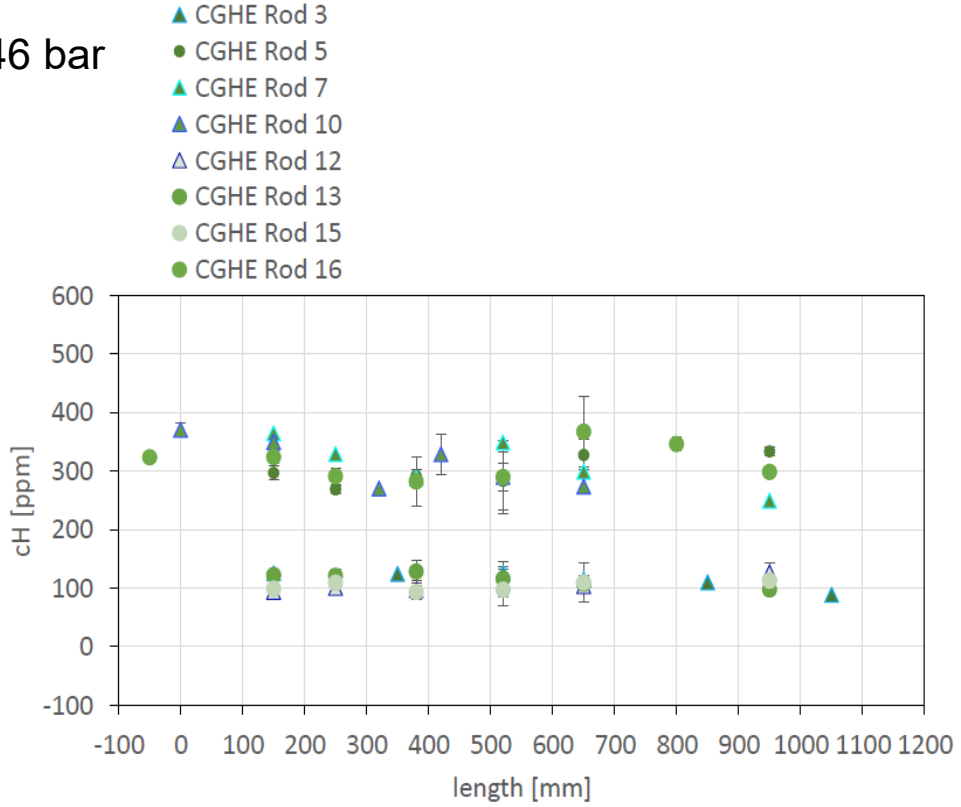

H_2 analysis - Zry-4

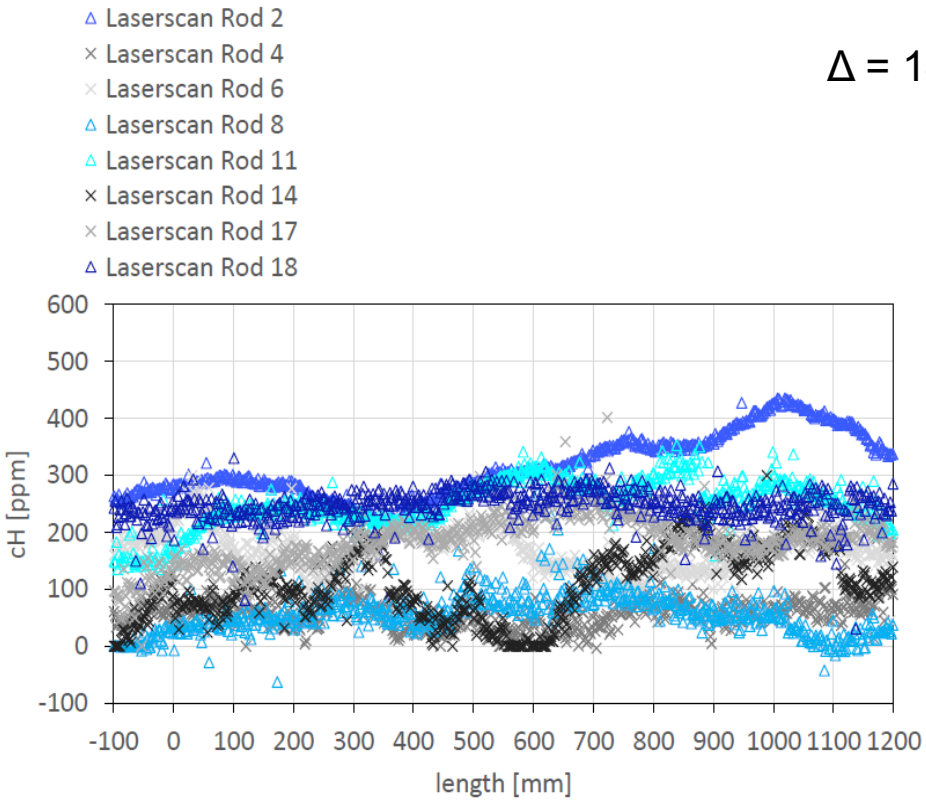

Δ = 146 bar

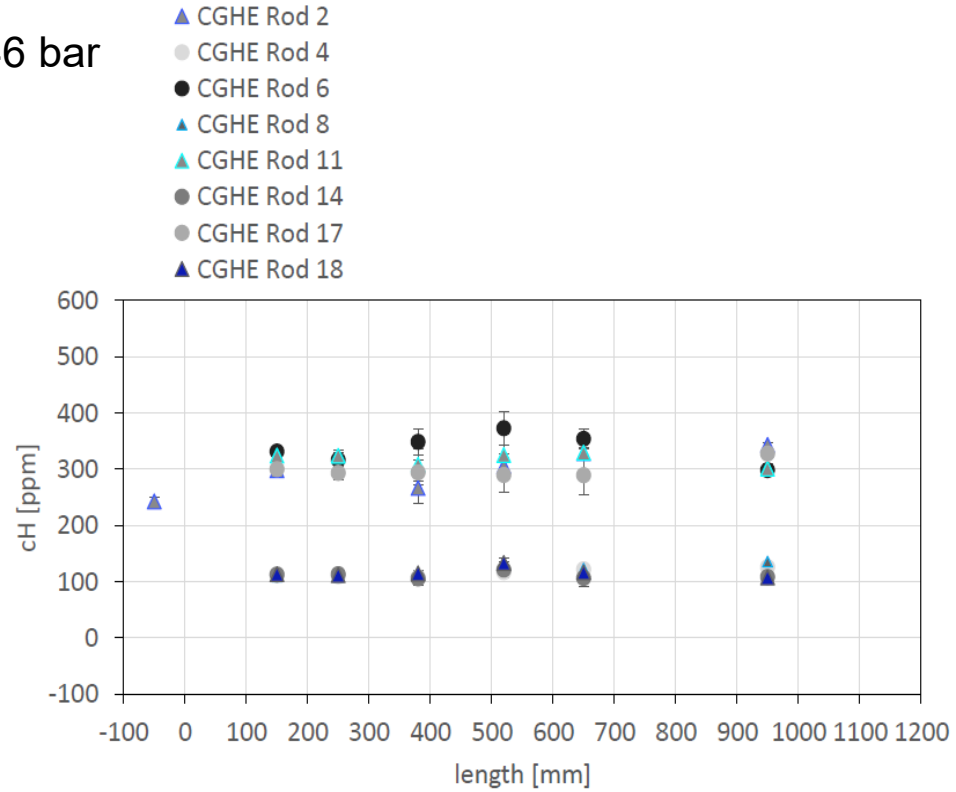

Hydrogen analysis

- Zry-4

➔ TGHE & Laserscan match

- ZIRLO

➔ TGHE & Laserscan match

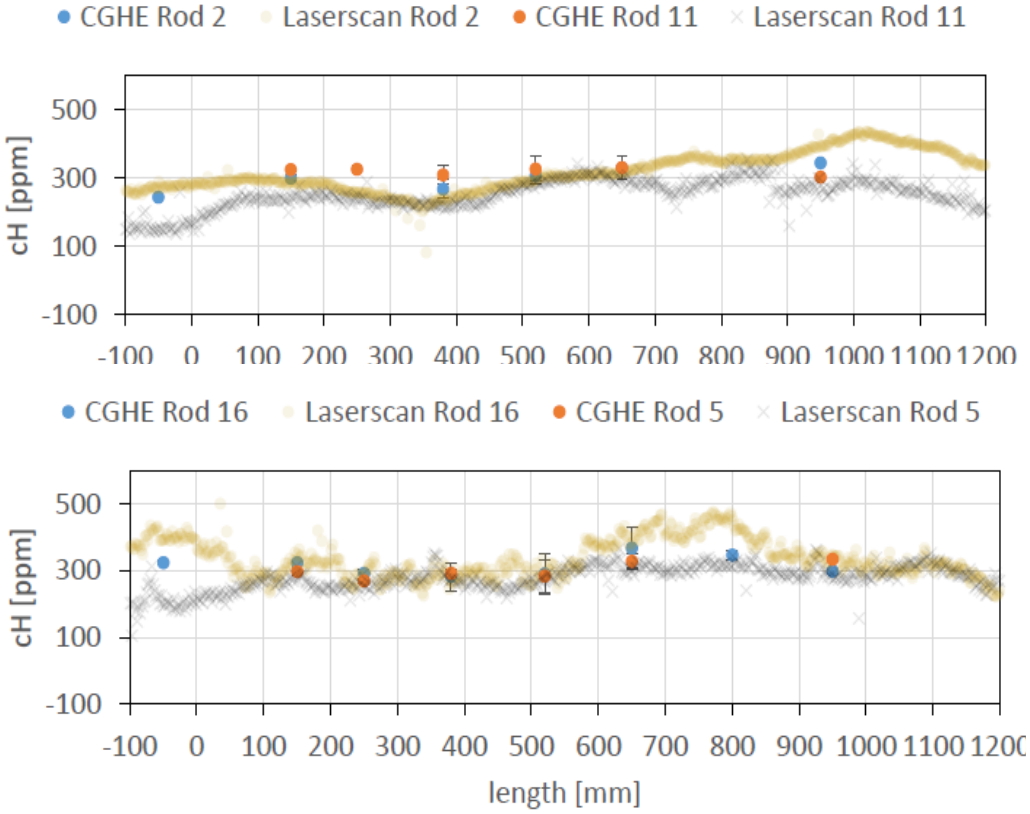

	clad	c_H	p
		ppm	bar
Rod 1	Dx-D4	300	146
Rod 2	Zry-4	300	146
Rod 3	ZIRLO	100	146
Rod 4	Zry-4	100	106
Rod 5	ZIRLO	300	106
Rod 6	Zry-4	300	106
Rod 7	ZIRLO	300	146
Rod 8	Zry-4	100	146
Rod 9	Dx-D4	300	106
Rod 10	ZIRLO	300	146
Rod 11	Zry-4	300	146
Rod 12	ZIRLO	100	146
Rod 13	ZIRLO	100	146
Rod 14	Zry-4	100	106
Rod 15	ZIRLO	100	106
Rod 16	ZIRLO	300	106
Rod 17	Zry-4	300	106
Rod 18	Zry-4	100	146
Rod 19	Dx-D4	100	106
Rod 20	Dx-D4	300	146
Rod 21	Dx-D4	100	146

Metallography

- ZIRLO –> circumferential hydrides

Rod 3	Rod 10
146 bar	146 bar
100 ppm	300 ppm
ZIRLO	ZIRLO

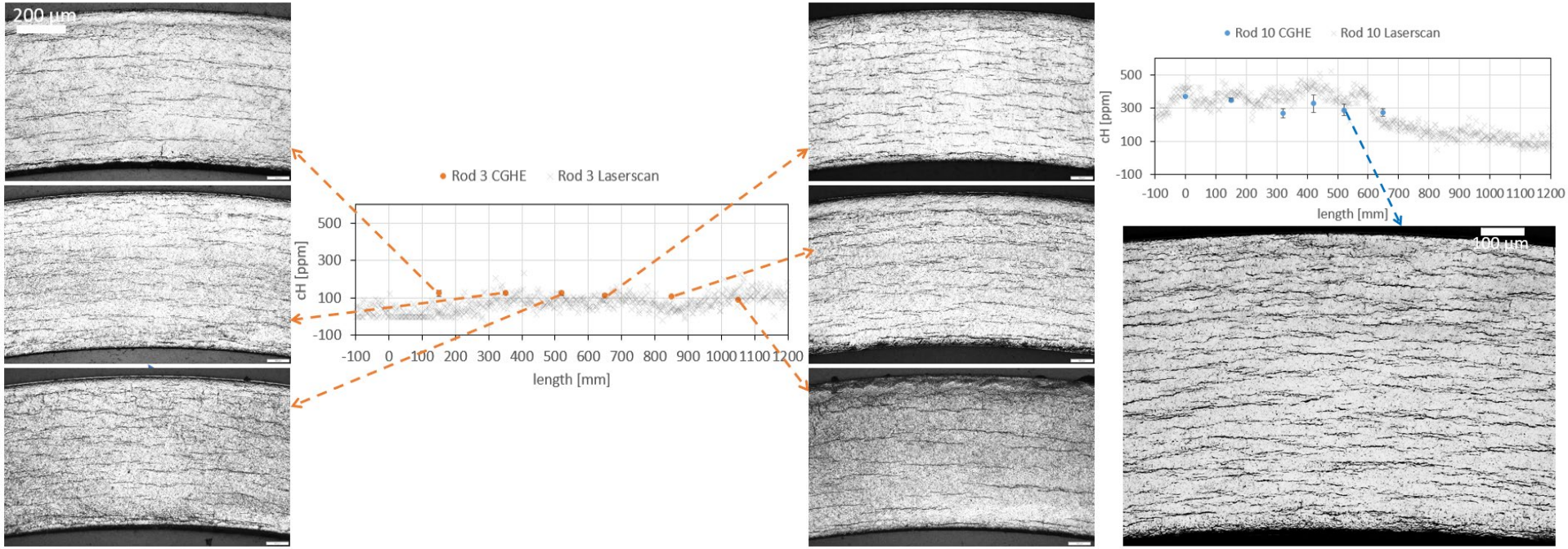

Metallography

- Zry-4 –> circumferential & radial hydrides

Rod 8	Rod 2
146 bar	146 bar
100 ppm	300 ppm
Zry-4	Zry-4

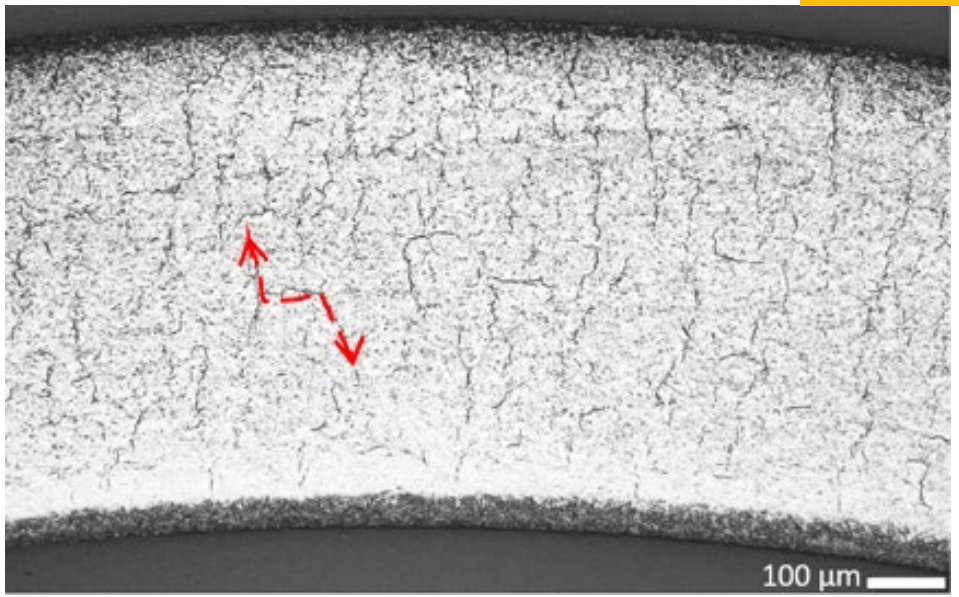

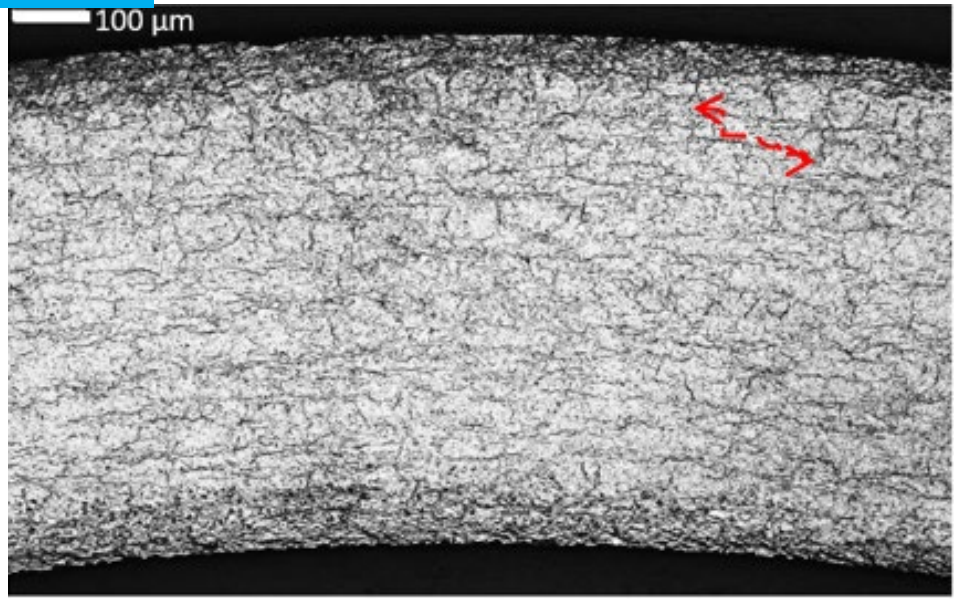

Neutron Imaging

NR = Neutron Radiography

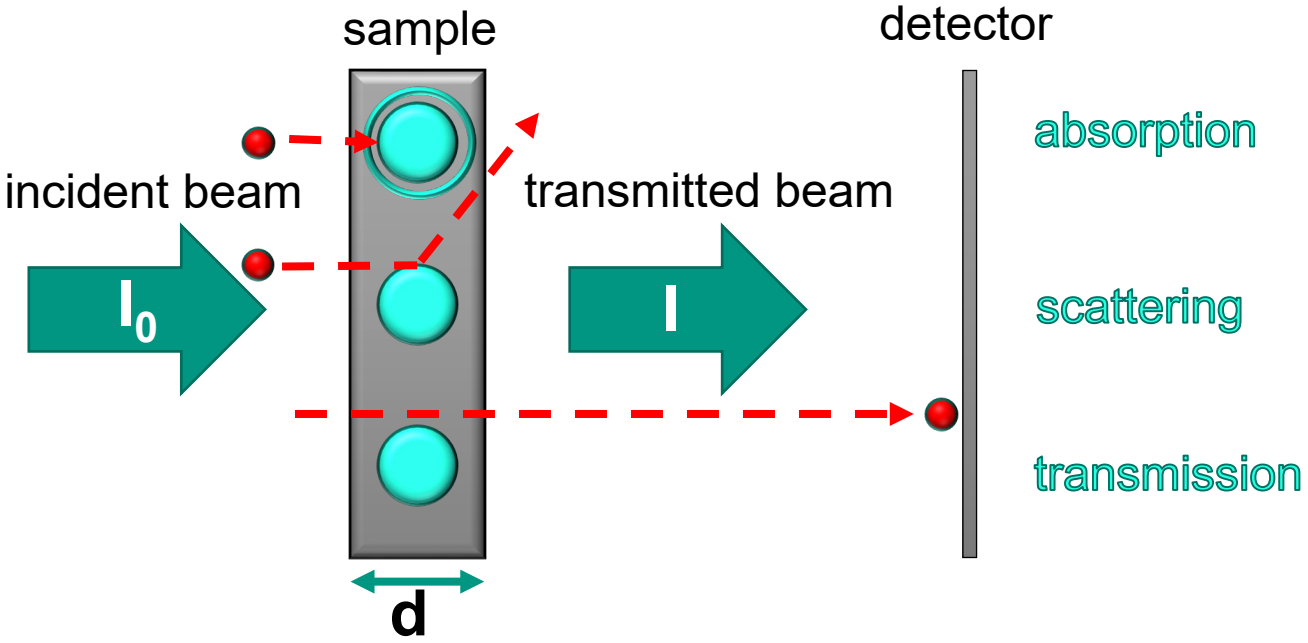

$$I = I_0 e^{-\sigma N d}$$

$$\Sigma = \sigma N$$

I: intensity
T: transmission
σ: microscopic neutron cross section
N: number density
d: sample thickness
Σ: macroscopic neutron cross section/ neutron attenuation coefficient

Neutron Imaging

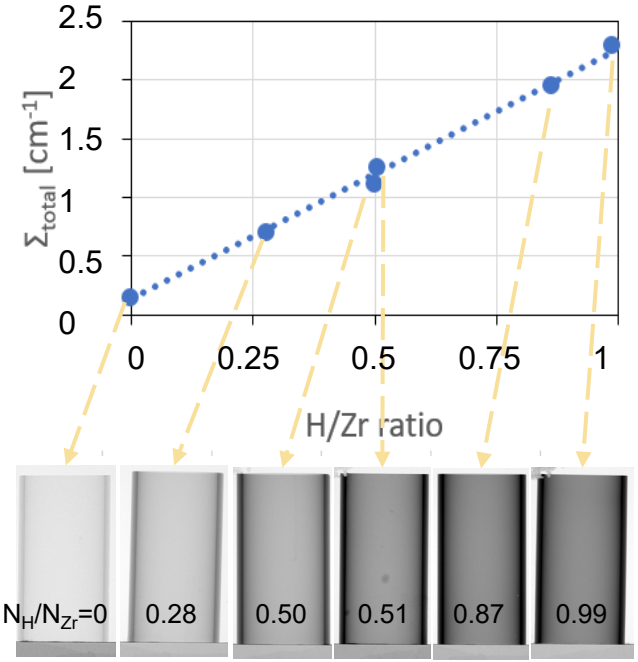

attenuation coefficients

H	Fe	Cr	Zr	Sn	O
3.44	1.19	0.54	0.29	0.21	0.17

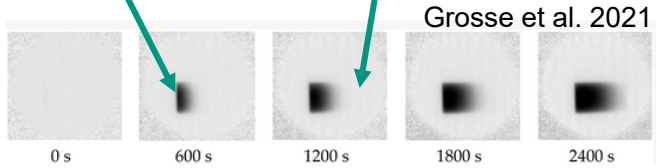

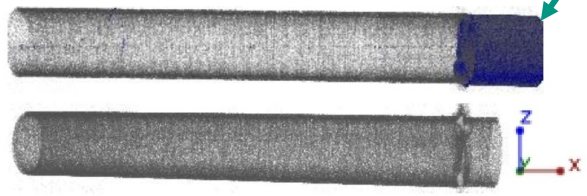

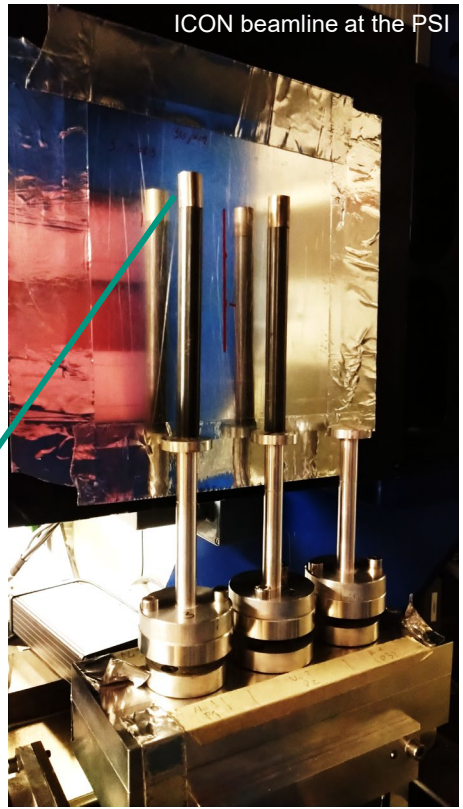

Neutron Imaging

Rod 2
146 bar
300 ppm
Zry-4

Rod 3
146 bar
100 ppm
ZIRLO

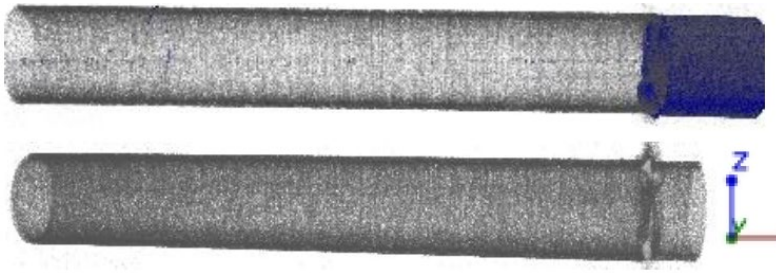

520 mm elevation

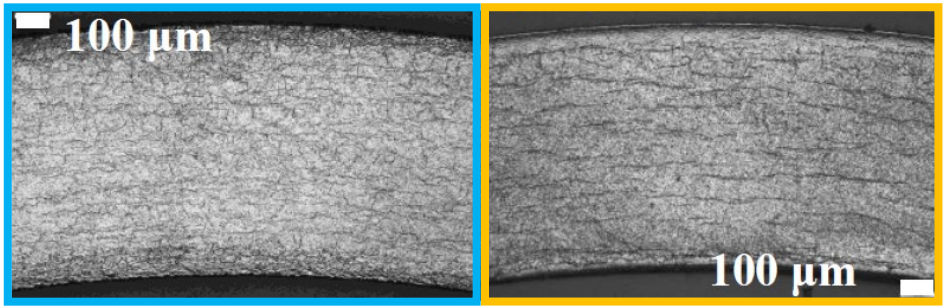

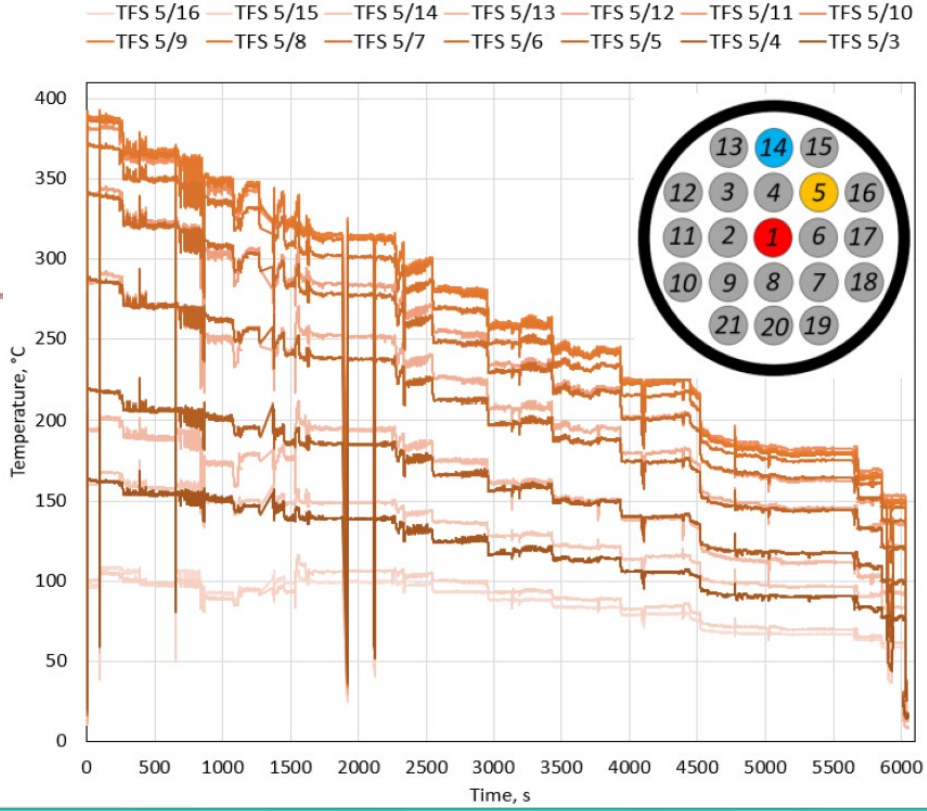

Conclusion

- QUENCH bundle test

→ LICAS facility installed with cooling mantle, new software
→ 21 cladding tubes charged with H
→ 250 d long-term test completed
→ blind benchmark ended (Apr – Oct)
→ 6 zones per rod for the analysis selected
→ analysis of first cladding tubes completed (non-destructive, destructive)
→ homogeneous hydrogen concentration in c-axis observed
→ similar behaviour Zry-4 & Dx/D4 (laserscan, CGHE, creep)
→ creep: Zry-4 < ZIRLO
→ metallography: different post-test hydride orientation observed for Zry-4 & ZIRLO

Karlsruher Institut für Technologie

Outlook




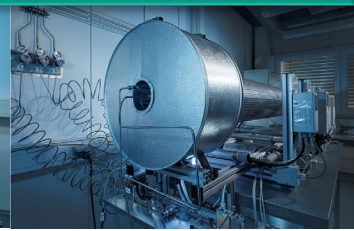

- QUENCH bundle test

→ analysis: metallography & post-test hydride orientation on-going
→ intended: more NT ex-situ investigations of the simulation rods
& NR of crosssections of Dx/D4 rods
→ open benchmark starts Jan 25
→ usage of new parameters for code validation/ modelling

→ continuing with SPIZWURZ + (optimized laboratory conditions (T decrease), new claddings, smaller diameter)

Karlsruher Institut für Technologie

Acknowledgements

- KIT/IAM-AWP
- GRS
- BGZ
- PSI
- The SPIZWURZ project (FKZ 1501609B) is funded by the Federal Ministry for the Environment, Nature Conservation, Nuclear Safety and Consumer Protection (BMUV)

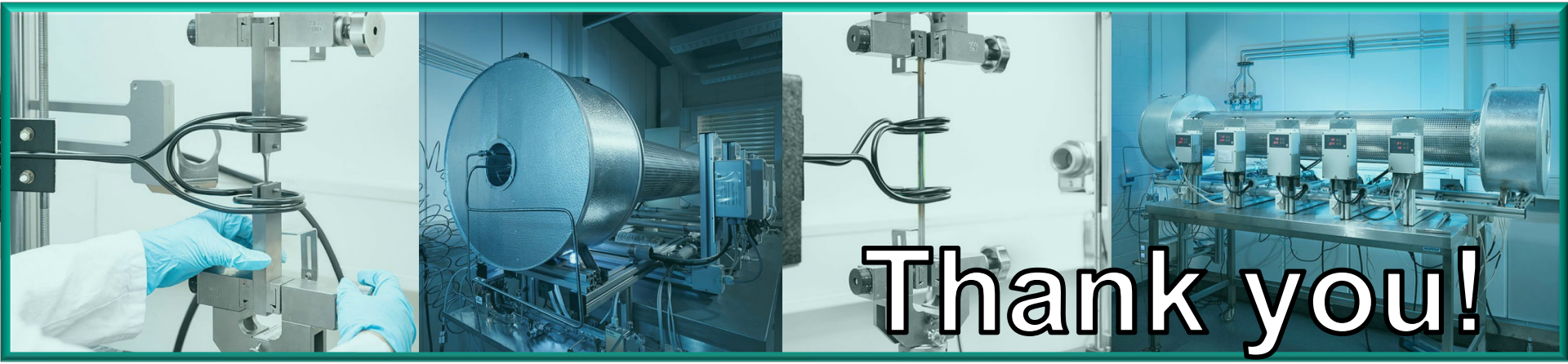

Aleksandra Rezchikova

GRS

SPIZWURZ Blind Benchmark for simulation of hydrogen and creep behaviour at dry storage relevant conditions. Preliminary results

The real long-term dry storage conditions can be reproduced experimentally only to a certain extent because of the safety issues associated with the use of irradiated materials and because of the relevant time scales. Since the fuel integrity has to be ensured during the entire storage period its assessment relies heavily on the numerical simulations. Therefore, the development of decent numerical tools is of great importance.

Reorientation of hydrides and creep can potentially lead to a degradation of the fuel rod claddings during a long-term interim dry storage. Since hydrogen and creep behaviours are not well understood yet, the collaborative project SPIZWURZ between the Karlsruhe Institute of Technology (KIT) and the Gesellschaft für Anlagen- und Reaktorsicherheit (GRS) was initiated to address these issues.

Within the frame of the SPIZWURZ project, a bundle of 21 electrically heated fuel rods was cooled down from 405°C over 250 days with a maximum average rate of 0.94 °C/day. The bundle experiment was conducted using pre-hydrogenated non-irradiated cladding tubes at the QUENCH/LICAS facility at KIT. The test matrix included 3 cladding materials (Zircaloy-4, opt. ZIRLO and Duplex Dx/D4), 2 pressurization levels (p_{min}=103 bar and p_{max}=142 bar), and 2 target hydrogen concentrations (C_{min}=100 wppm and C_{max}=300 wppm).

The SPIZWURZ Benchmark aims to validate and improve the modelling of creep and hydrogen behaviour at the interim storage conditions in the existing fuel performance codes. The benchmark is coordinated by the GRS, and its blind phase started in April 2024.

For the benchmark calculations, the participants received the temperature and pressure time histories of the bundle experiment, as well as the estimated hydrogen concentrations along the rods. The computation domain was discretized into 14 axial zones, as shown in Fig.1. The requested data included the temporal evolutions of hydrogen and hydride concentrations and the hoop strain components.

11 participants from 10 different organisations have attended the blind benchmark. The results are currently being summarized and compared against the experiments. The first comparisons show that most of the existing modelling approaches can fairly well predict the creep behaviour of the Zircaloy-4 claddings. However, some discrepancies are observed for opt.ZIRLO and Duplex claddings. The predictions concerning the reorientation of the hydrides show partly strong discrepancies, which indicates a need to revise the existing modelling approaches. Furthermore, discussions with the participants concerning the discrepancies have been started.

SPIZWURZ Blind Benchmark
Preliminary results

29th International QUENCH Workshop

November 21, 2024

Aleksandra Rezchikova

Gesellschaft für Anlagen- und Reaktorsicherheit (GRS) gGmbH

SPIZWURZ Project

„**SP**annungs**I**ndu**Z**ierte **W**asserstoff**U**mlagerung in Brennstabhüllrohren während längerfristige**R Z**wischenlagerung “

Karlsruher Institut für Technologie

English Title: “Stress-induced hydrogen redistribution in nuclear fuel cladding tubes during long-term intermediate storage”

Collaborative project between Karlsruhe Institute of Technology (KIT) and Gesellschaft für Anlagen- und Reaktorsicherheit (GRS) funded by the German Federal Ministry for the Environment, Nature Conservation, Nuclear Safety and Consumer Protection (BMUV).

Goal: experimental and theoretical investigation of hydrogen behaviour in nuclear fuel cladding tubes at microscopic and macroscopic scales during a long-term interim dry storage of spent nuclear fuel in transport and storage casks.

SPIZWURZ Benchmark: Overview

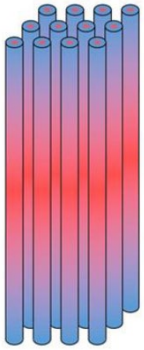

SPIZWURZ
Bundle test

May 2023 – January 2024

p, T, C_{H_2}

Blind Benchmark

April 2024 – November 2024

Open Benchmark

Anticipated start
2nd quarter 2025

Cladding tube analysis

February 2024 – March 2024

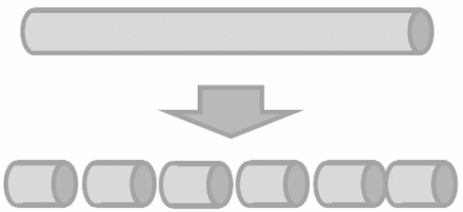

- Hydrogen concentration
- Reorientation of hydrides
- Creep

SPIZWURZ Blind Benchmark: Participation

10 Organisations are actively involved
11 Participants

Gesellschaft für Anlagen- und Reaktorsicherheit (GRS)

Comisión Nacional de Energía Atómica (CNEA)

Karlsruhe Institute of Technology (KIT)

Axpo Switzerland

Framatome Germany

Seoul National University (SNU)

Oak Ridge National Laboratory (ORNL)

Paul Scherrer Institute (PSI)

Idaho National Laboratoty (INL)

Centro de Investigaciones Energéticas, Medioambientales y Tecnológicas (CIEMAT)

EDF France

ÚJV Řež

Gesellschaft für Zwischenlagerung (BGZ)

ENUSA

SPIZWURZ Bundle experiment

Bundle long-term cooling experiment conducted at KIT using QUENCH facility

- 21 electrically heated fuel rod simulators (total length 2480 mm)
- Non-irradiated zirconium-based cladding tubes: Zry-4, ZIRLO, Dx/D4
- Cladding tubes pre-treated with hydrogen in HoKi furnace at KIT with target hydrogen concentrations $C_{MIN} = 100$ and $C_{MAX} = 300$ wppm
- Rod internal pressures $p_{MIN} = 103$ and $p_{MAX} = 142$ bar
  (hoop stresses 70 and 100 MPa approx.)
- Experiment duration 250 days
  - Maximum temperature 405 °C
  - Average cooling rate 0.94 K/d

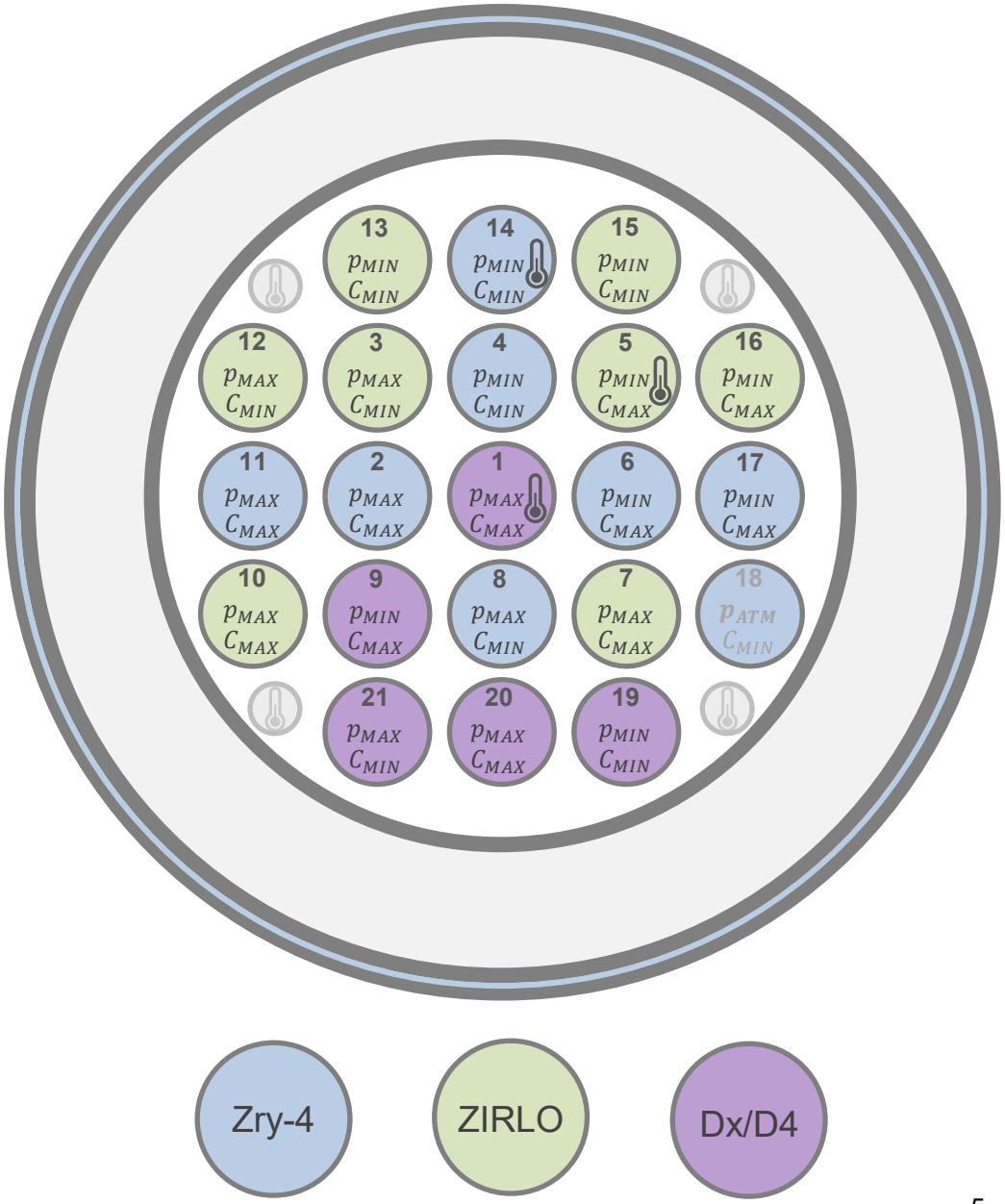

SPIZWURZ Bundle experiment

Bundle long-term cooling experiment conducted at KIT using QUENCH facility

- 21 electrically heated fuel rod simulators (total length 2480 mm)
- Non-irradiated zirconium-based cladding tubes: Zry-4, ZIRLO, Dx/D4
- Cladding tubes pre-treated with hydrogen with target hydrogen concentrations $C_{MIN} = 100$ and $C_{MAX} = 300$ wppm
- Rod internal pressures $p_{MIN} = 103$ and $p_{MAX} = 142$ bar
  (hoop stresses 70 and 100 MPa approx.)
- Experiment duration 250 days
  - Maximum temperature 405 °C
  - Average cooling rate 0.94 K/d

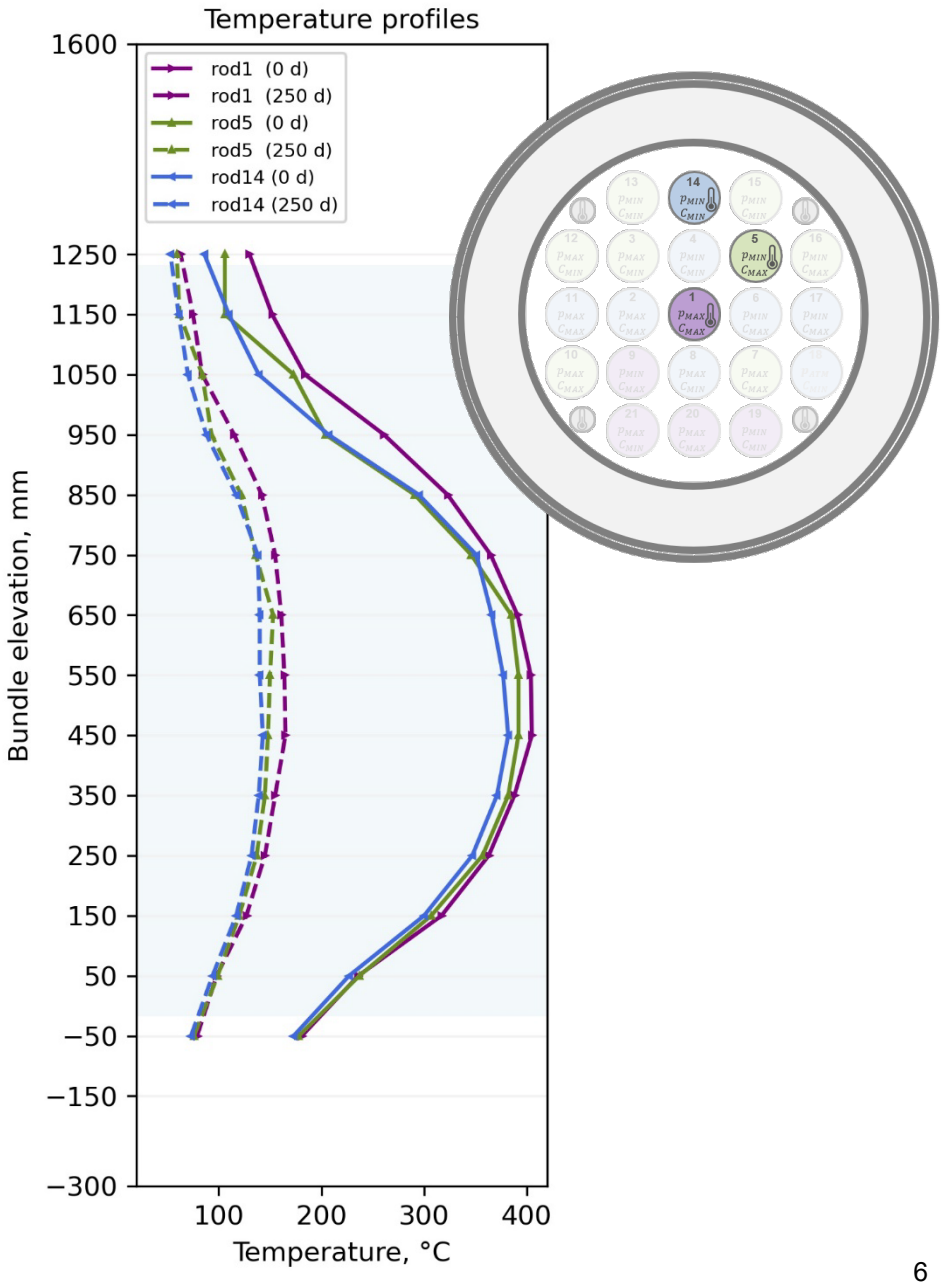

SPIZWURZ Bundle experiment

Bundle long-term cooling experiment conducted at KIT using QUENCH facility

- 21 electrically heated fuel rod simulators (total length 2480 mm)
- Non-irradiated zirconium-based cladding tubes: Zry-4, ZIRLO, Dx/D4
- Cladding tubes pre-treated with hydrogen with target hydrogen concentrations $C_{MIN} = 100$ and $C_{MAX} = 300$ wppm
- Rod internal pressures $p_{MIN} = 103$ and $p_{MAX} = 142$ bar
  (hoop stresses 70 and 100 MPa approx.)
- Experiment duration 250 days
  - Maximum temperature 405 °C
  - Average cooling rate 0.94 K/d

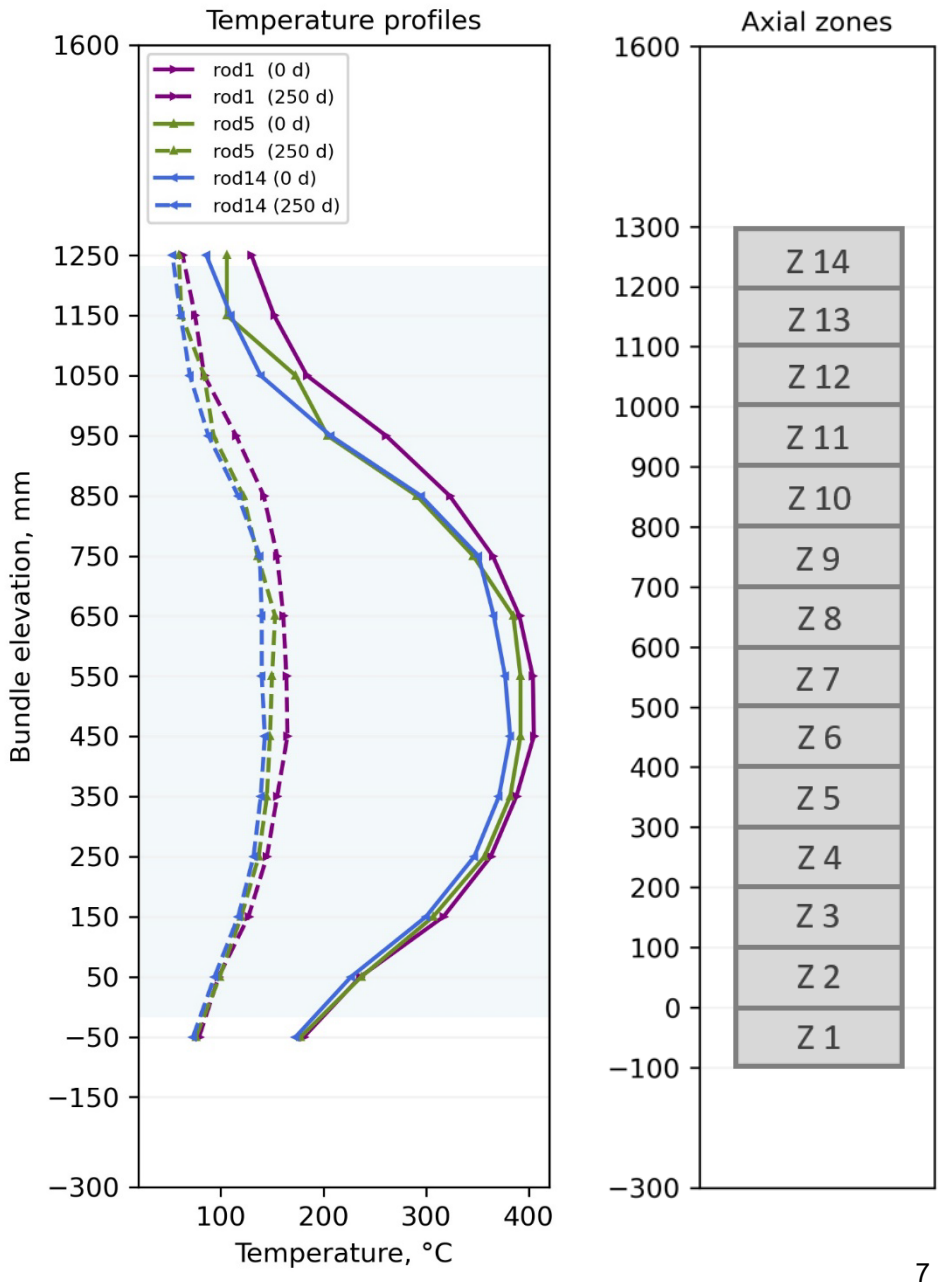

SPIZWURZ Bundle: Rod 2 Zry-4 Pmax Cmax
Computed creep VS experiment

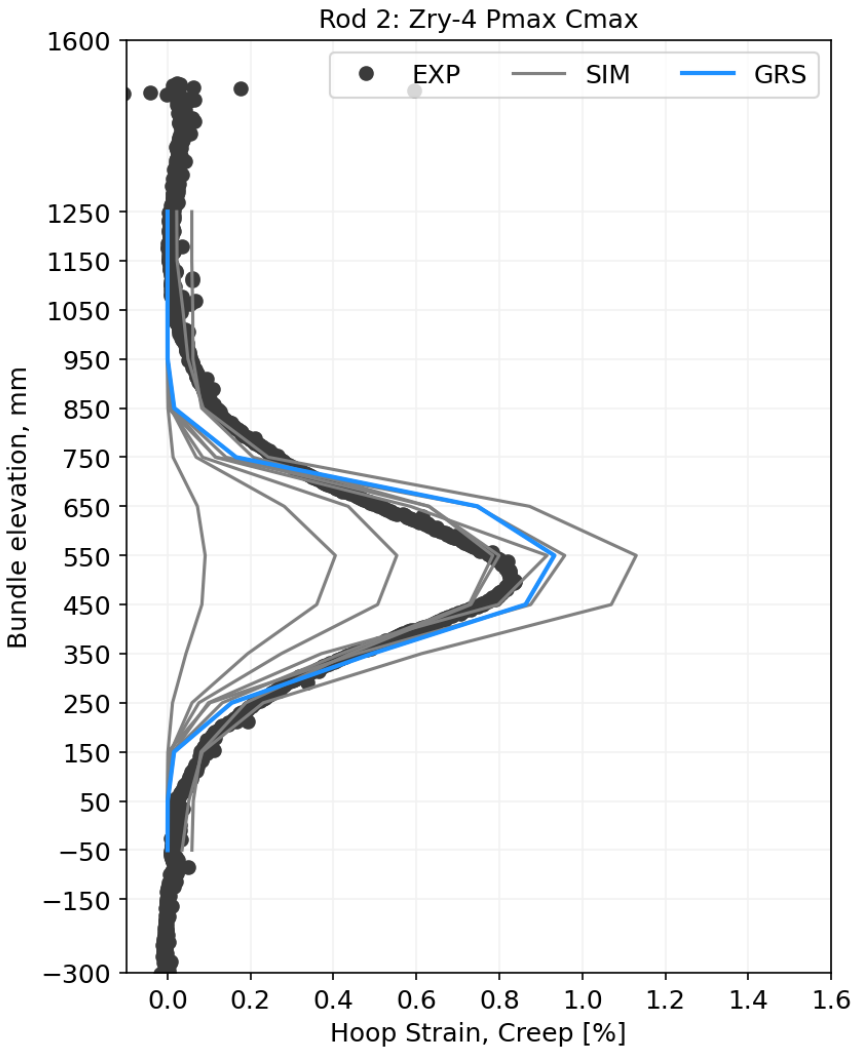

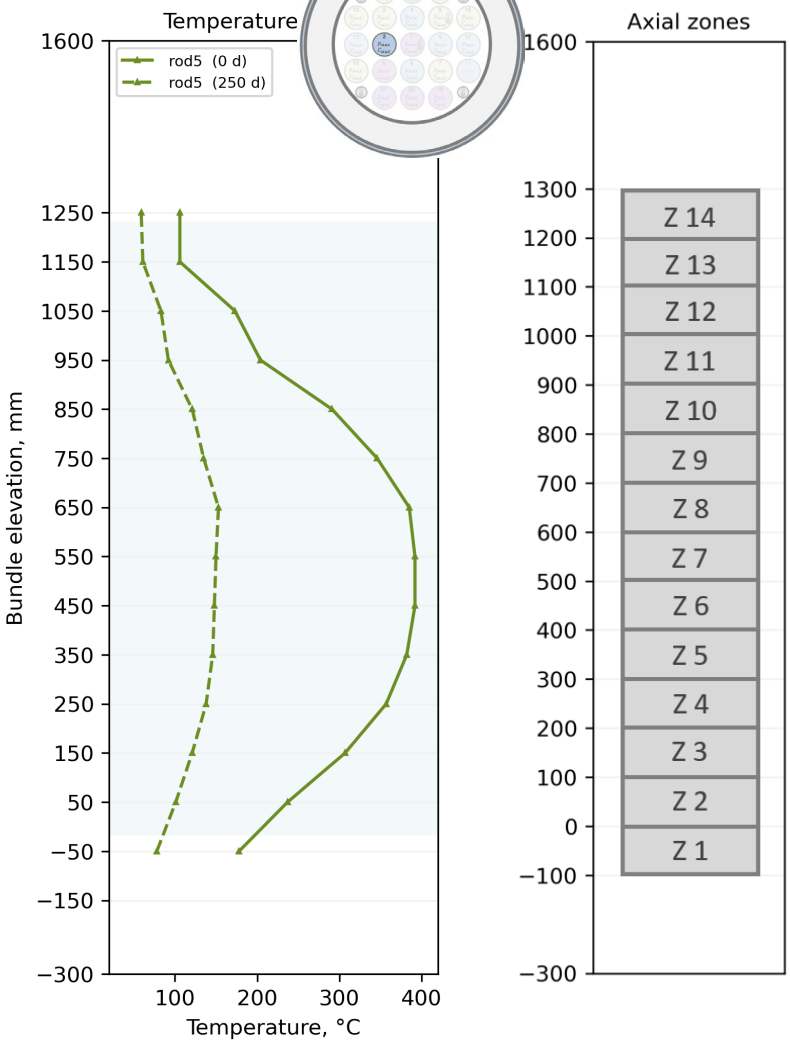

SPIZWURZ Bundle: Rod 2 Zry-4 Pmax Cmax
Computed creep VS experiment

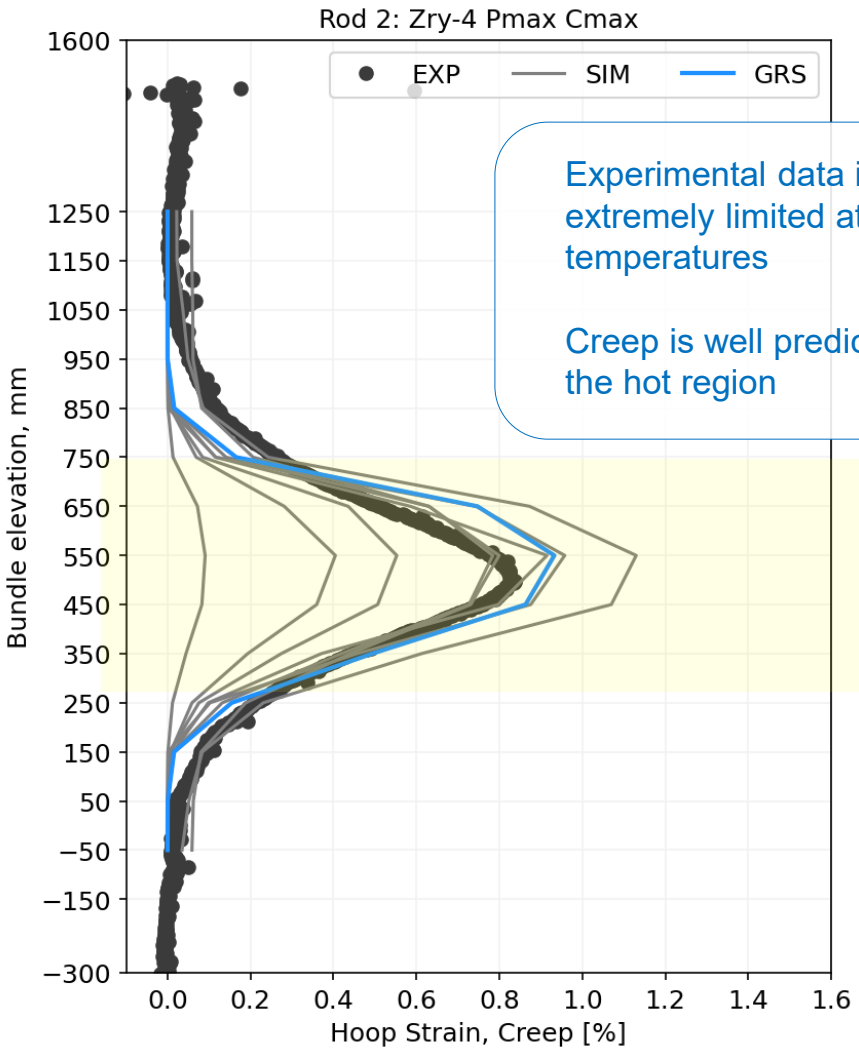

Experimental data is extremely limited at lower temperatures

Creep is well predicted in the hot region

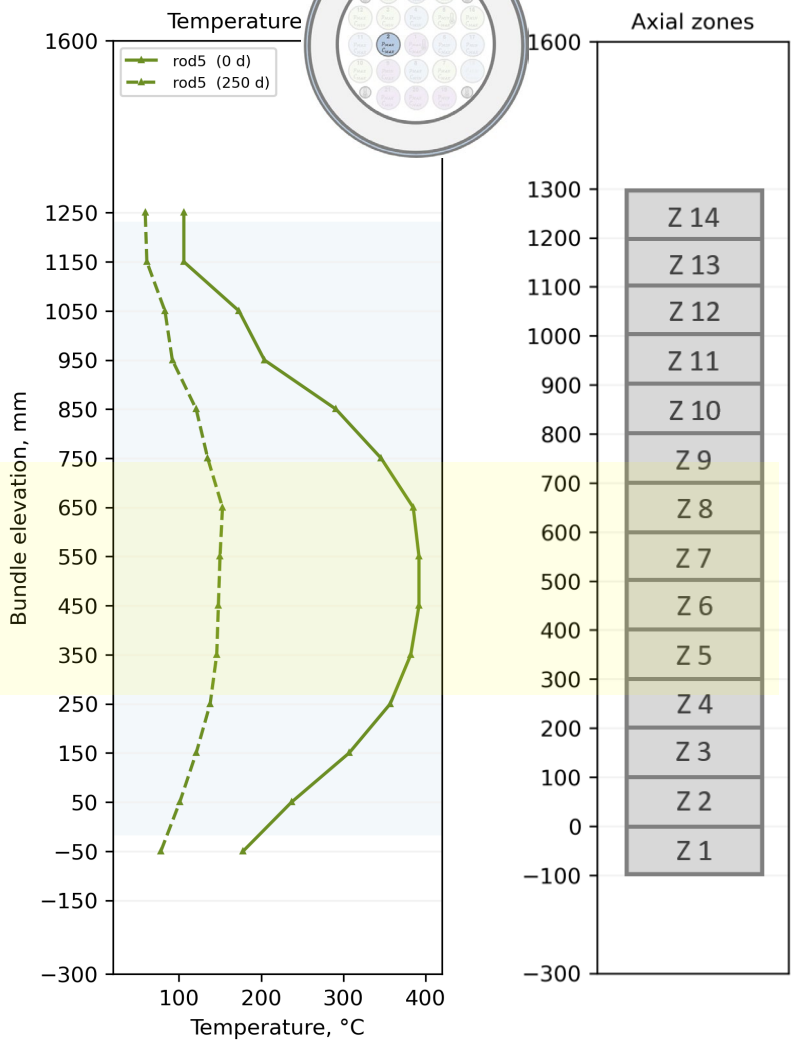

SPIZWURZ Bundle: Rod 4 Zry-4 Pmin Cmin
Computed creep VS experiment

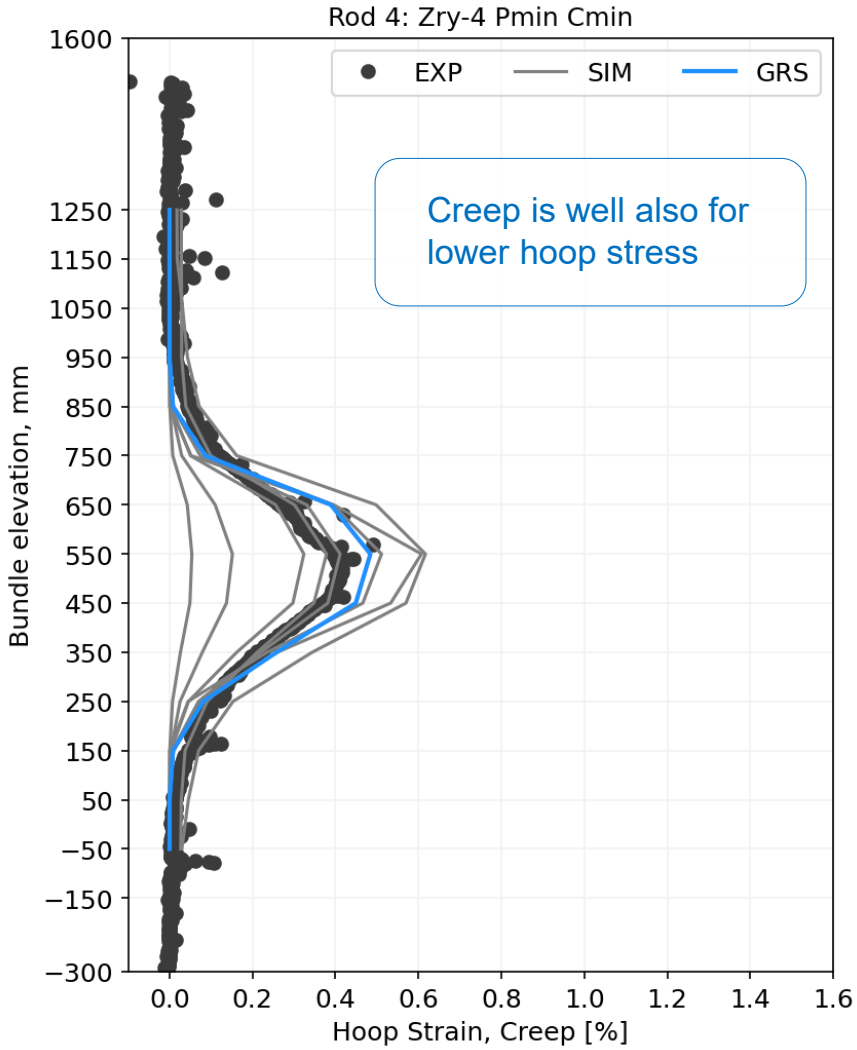

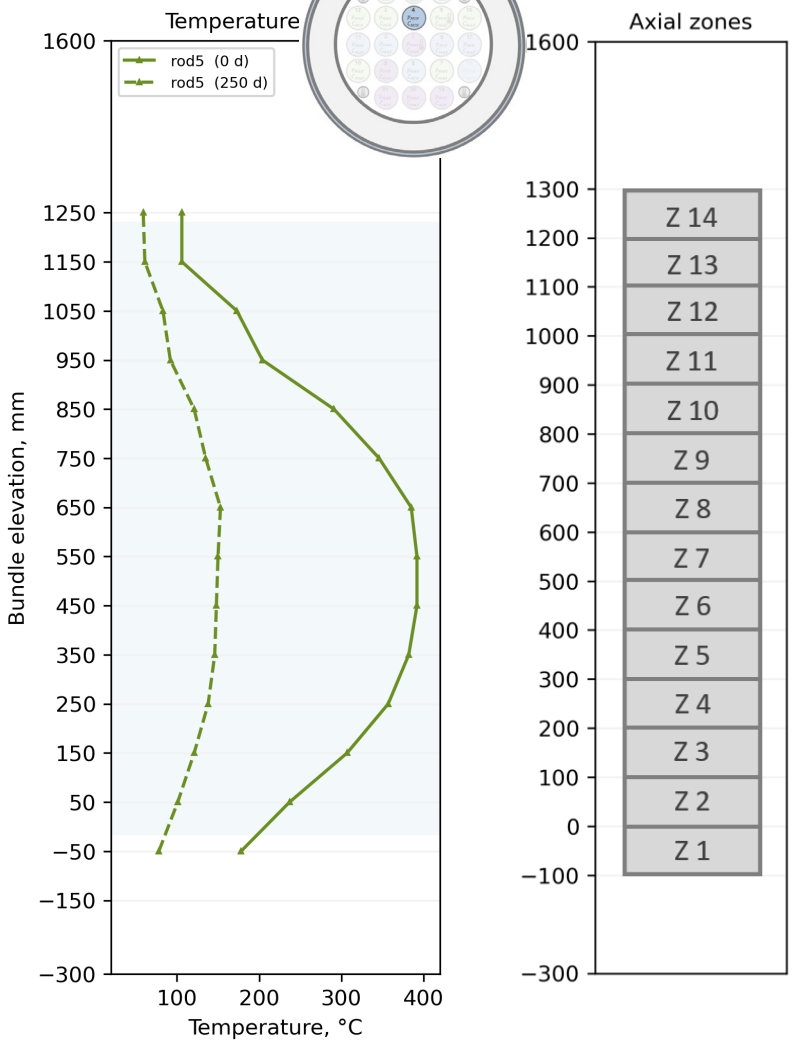

SPIZWURZ Bundle: Rod 1 DUPLEX Pmax Cmax
Computed creep VS experiment

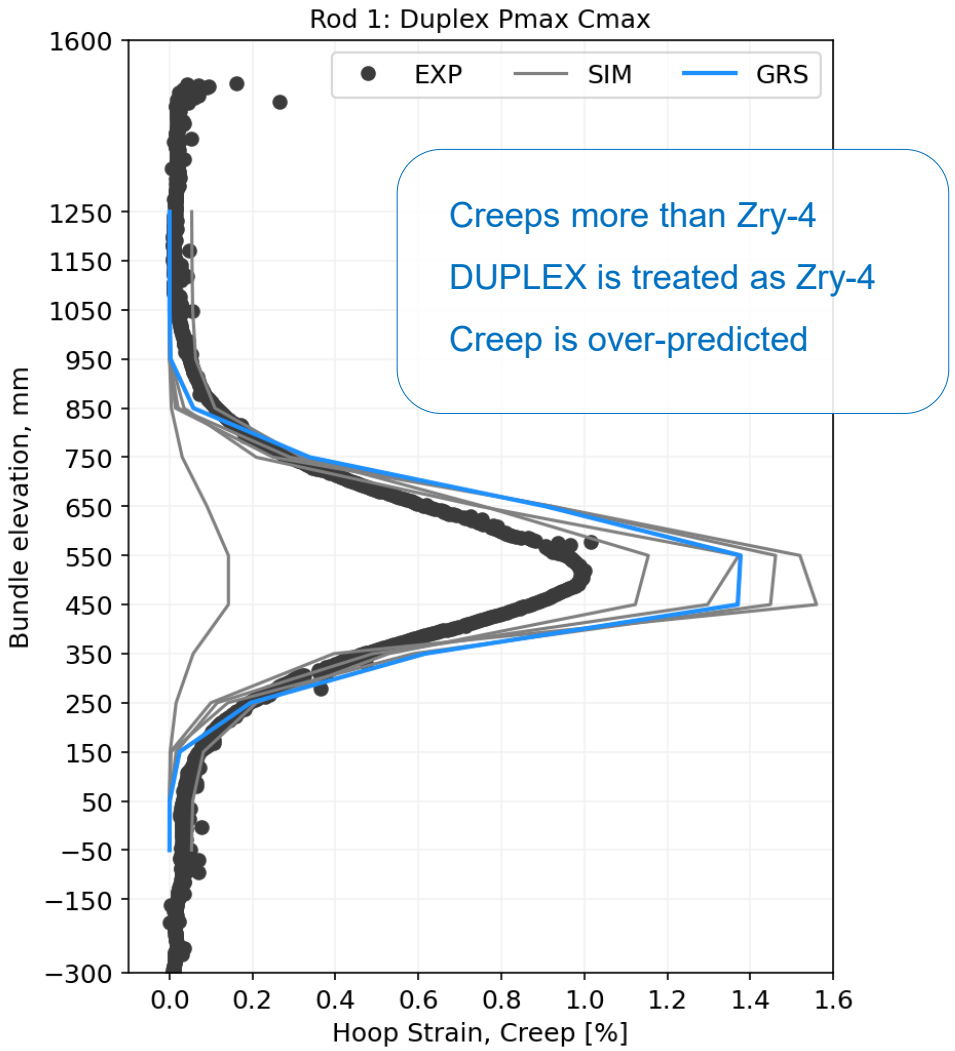

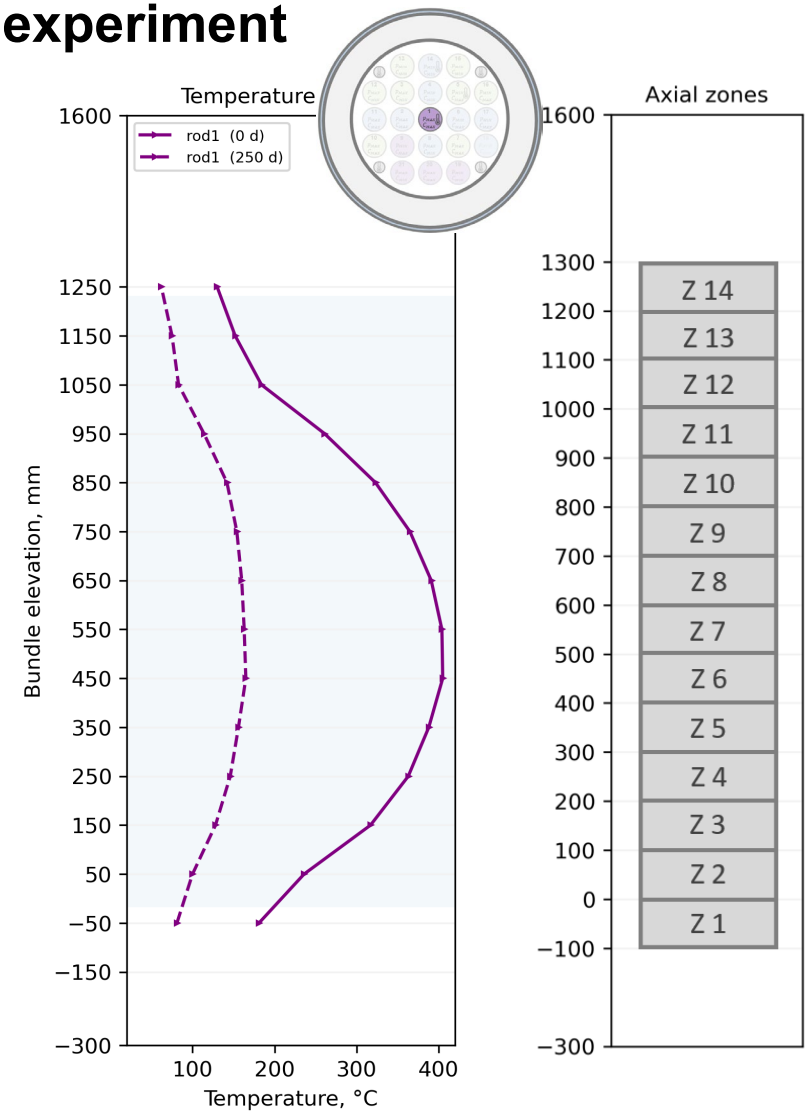

SPIZWURZ Bundle: Rod 5 opt.ZIRLO Pmin Cmax
Computed creep VS experiment

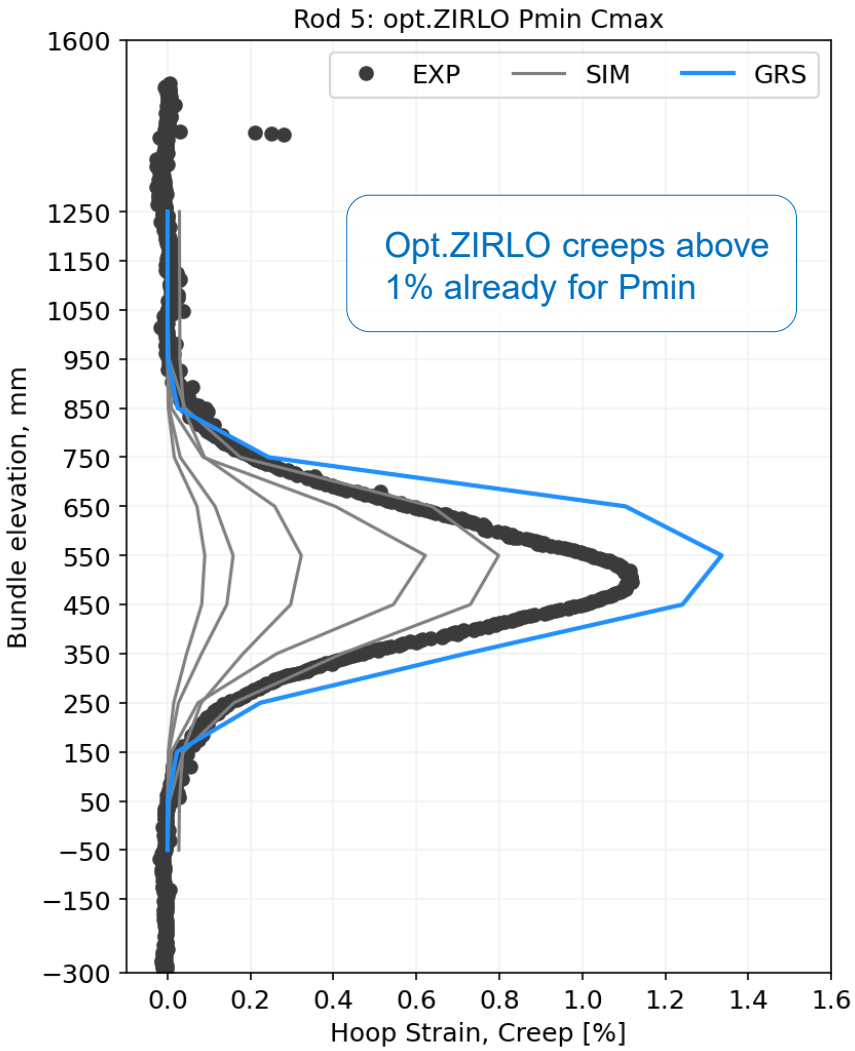

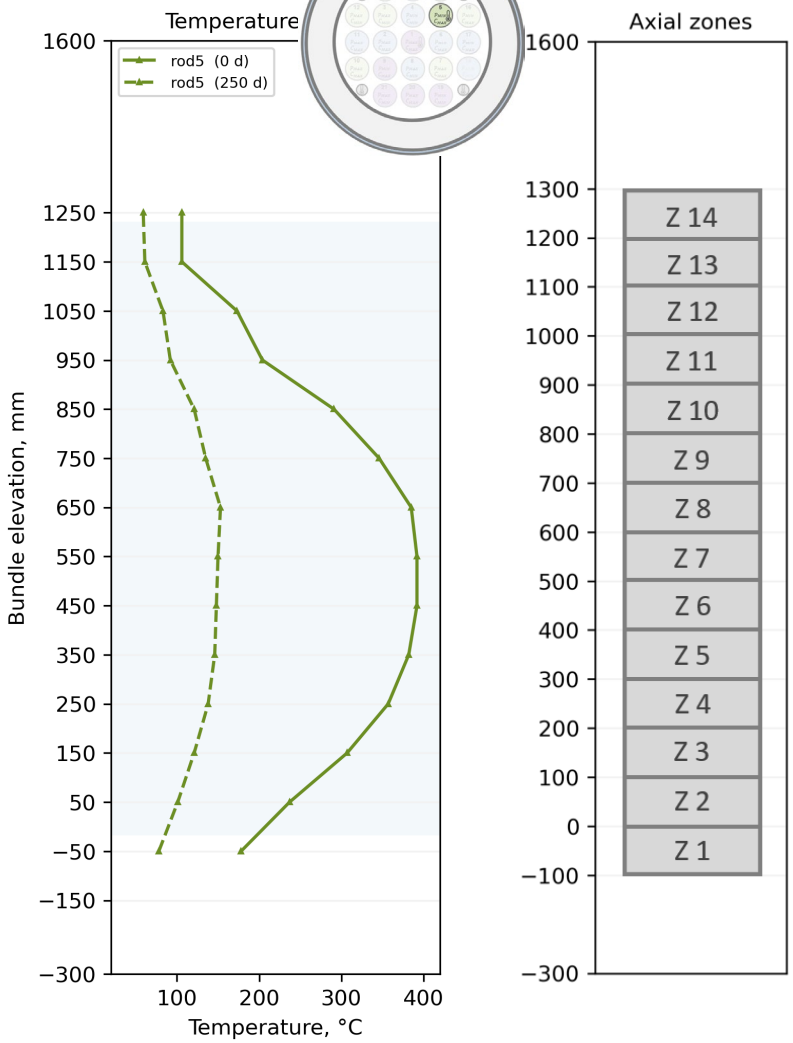

SPIZWURZ Bundle: Rod 3 opt.ZIRLO Pmax Cmin
Computed creep VS experiment

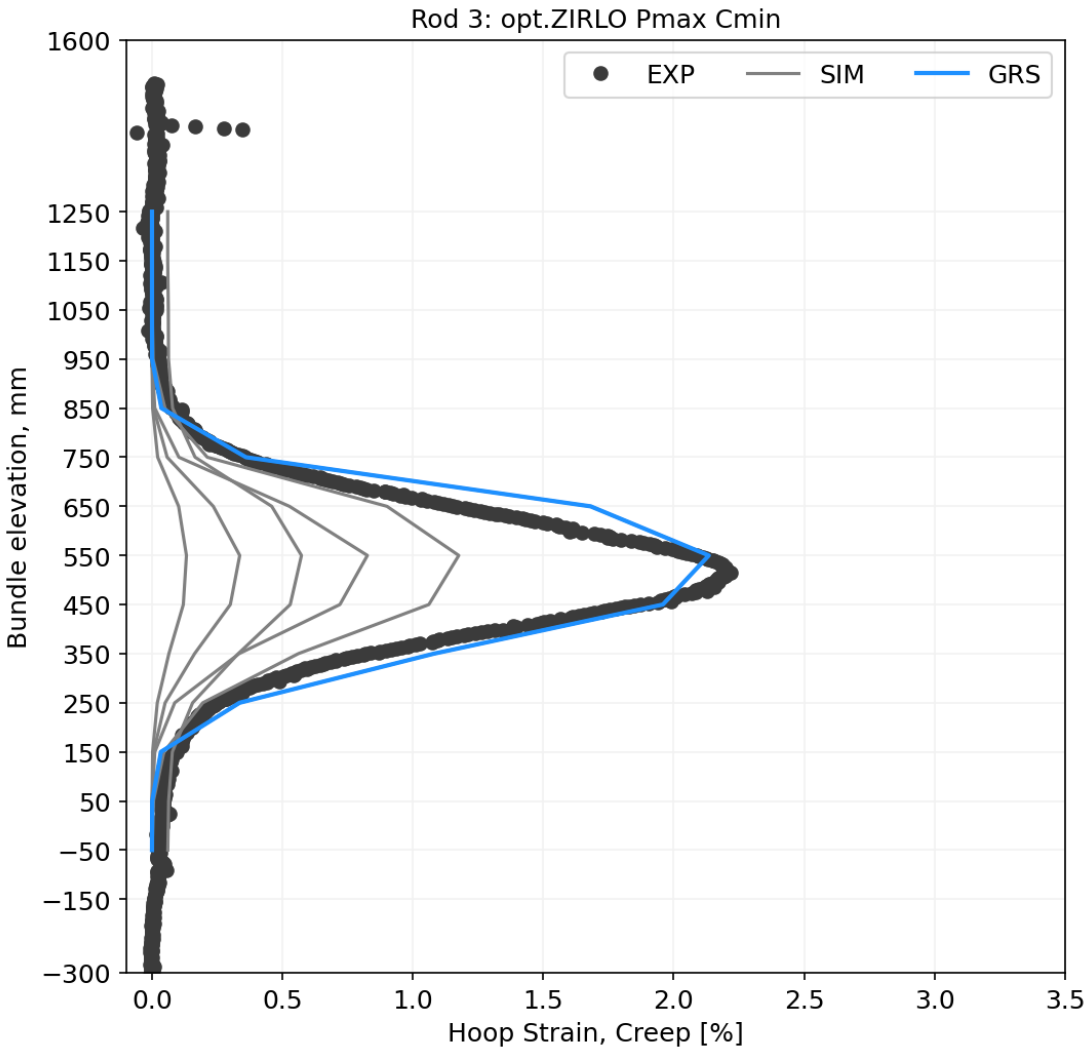

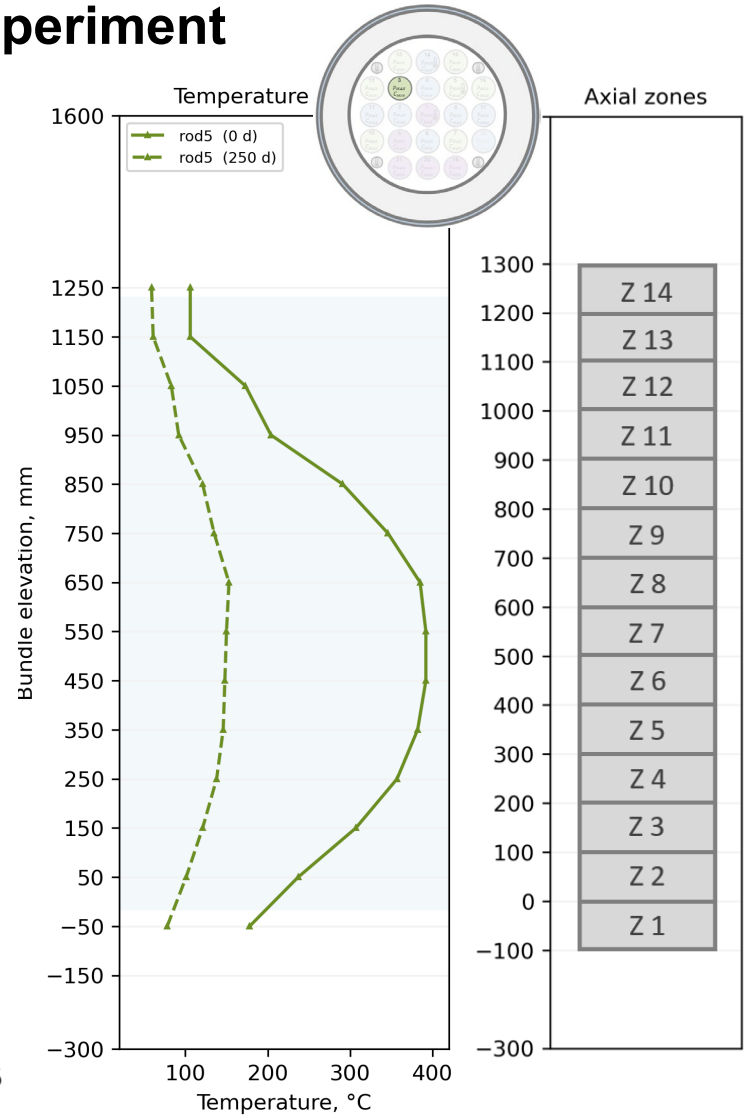

SPIZWURZ Bundle: Rod 7 opt.ZIRLO Pmax Cmax
Computed creep VS experiment

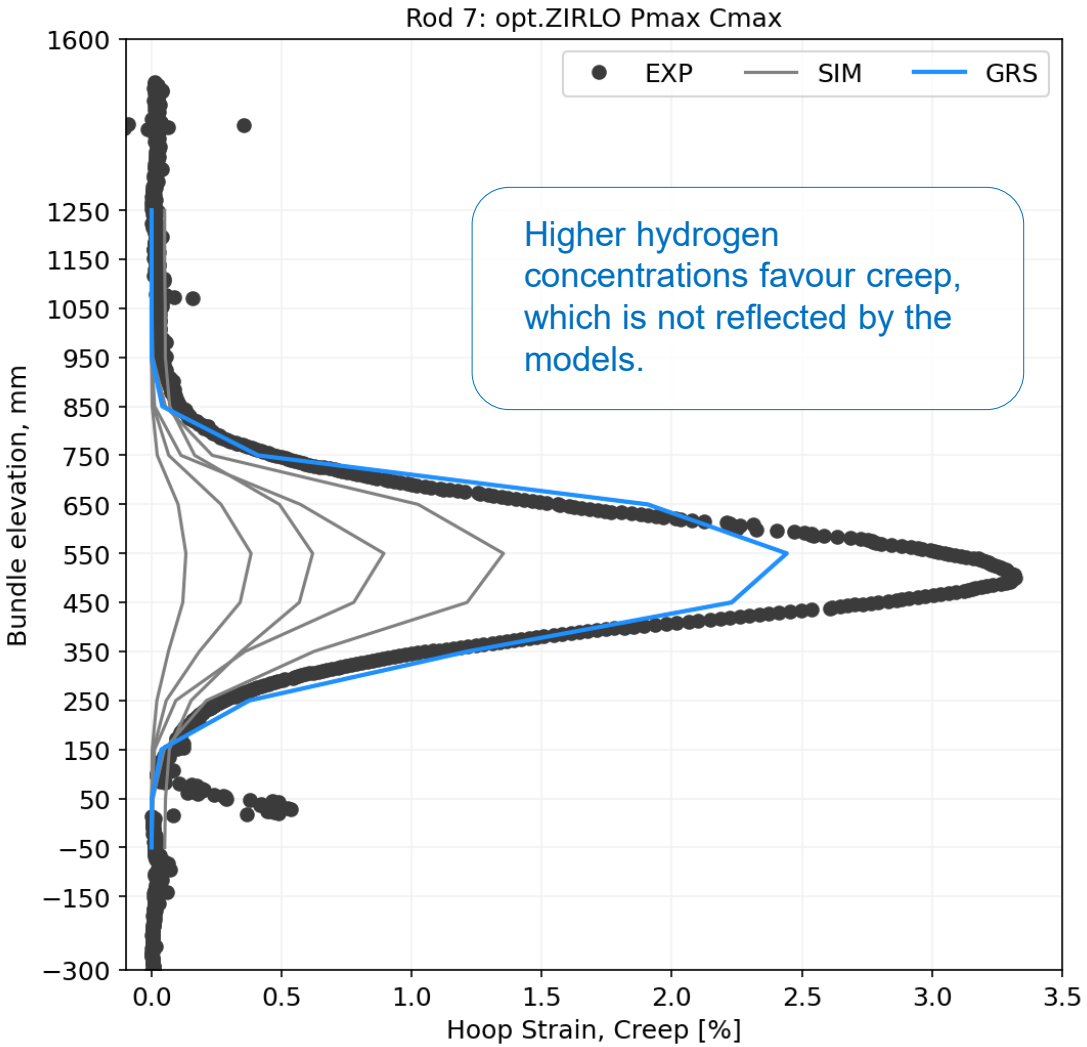

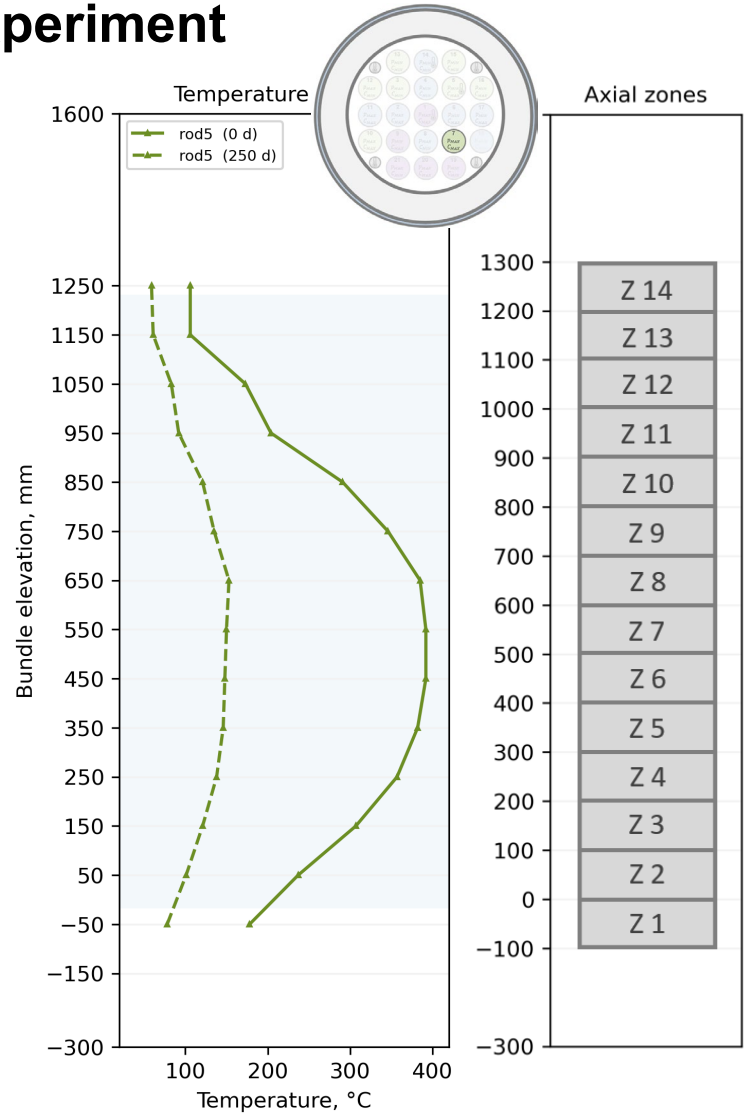

SPIZWURZ Bundle: ROD 2 Zry-4 Pmax Cmax
Reorientation of hydrides

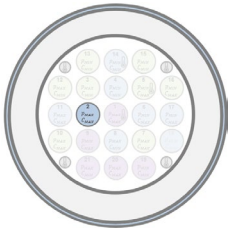

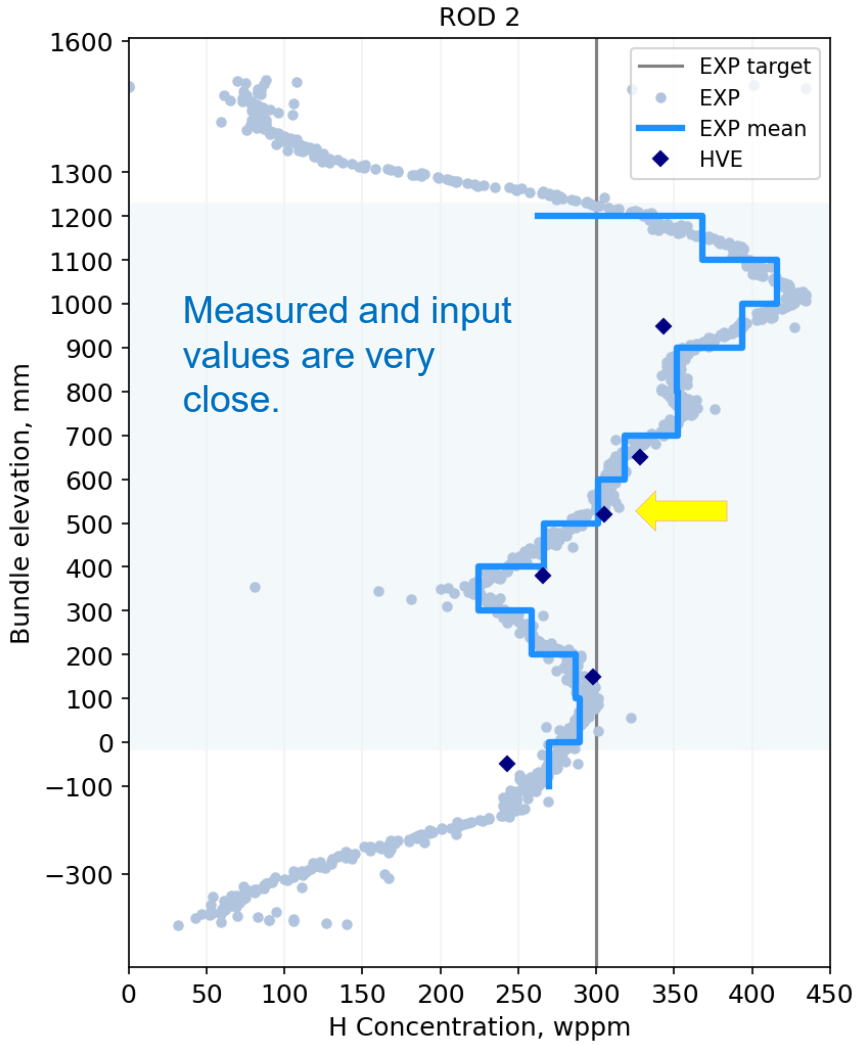

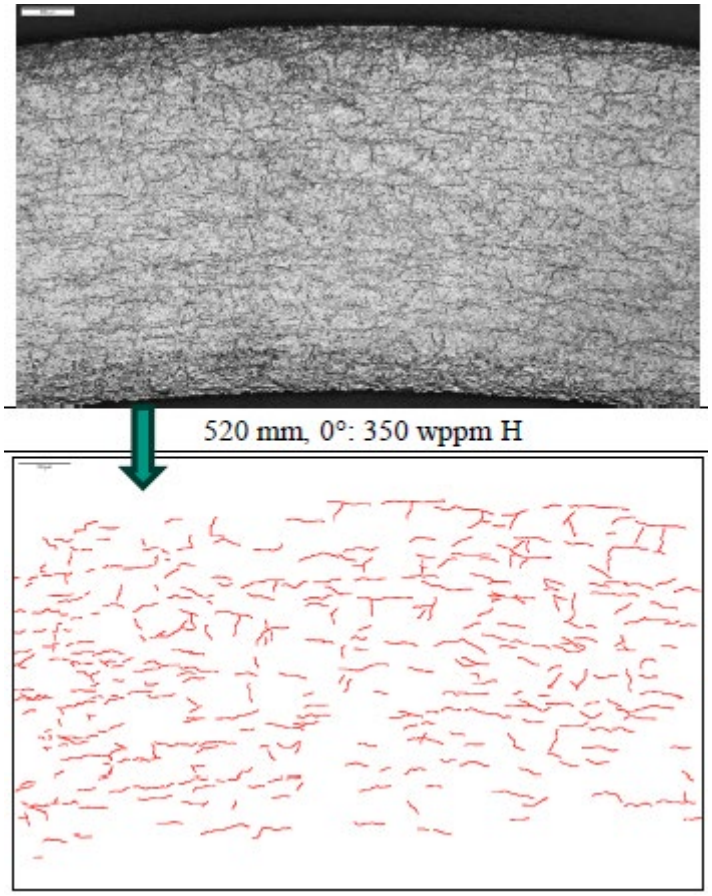

SPIZWURZ Bundle: ROD 2 Zry-4 Pmax Cmax
Reorientation of hydrides

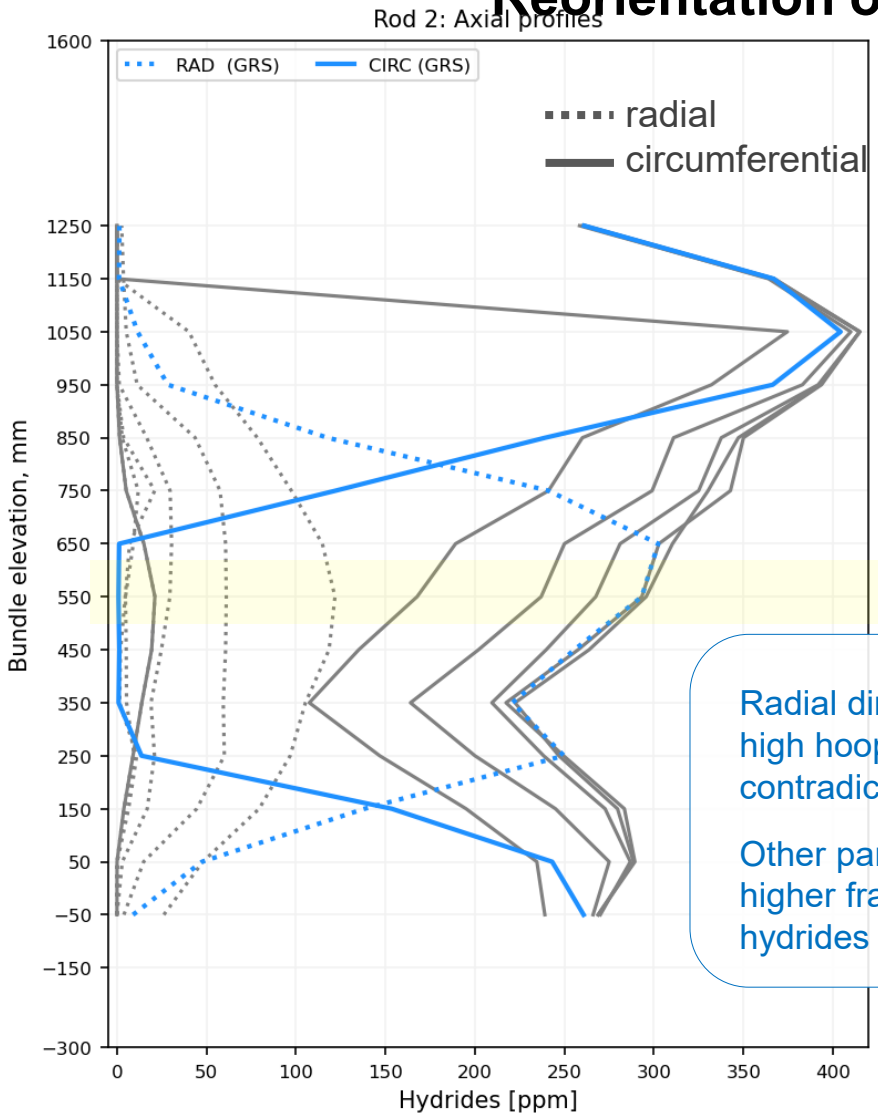

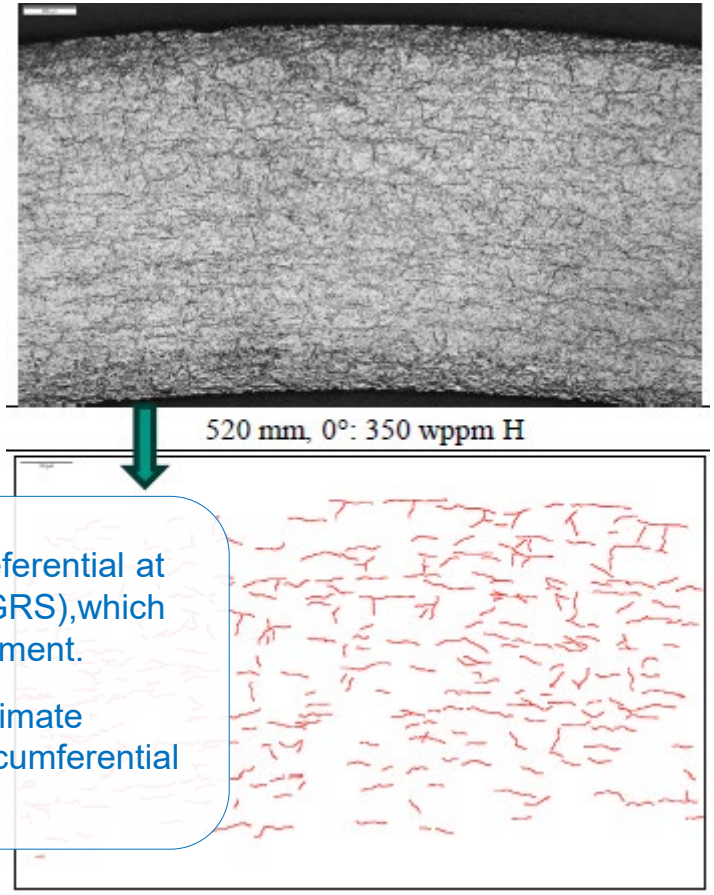

Radial direction is preferential at high hoop stresses (GRS),which contradicts the experiment.

Other participants estimate higher fractions of circumferential hydrides

SPIZWURZ Bundle: ROD 8 Zry-4 Pmax Cmin
Reorientation of hydrides

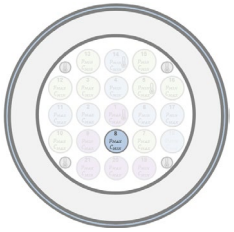

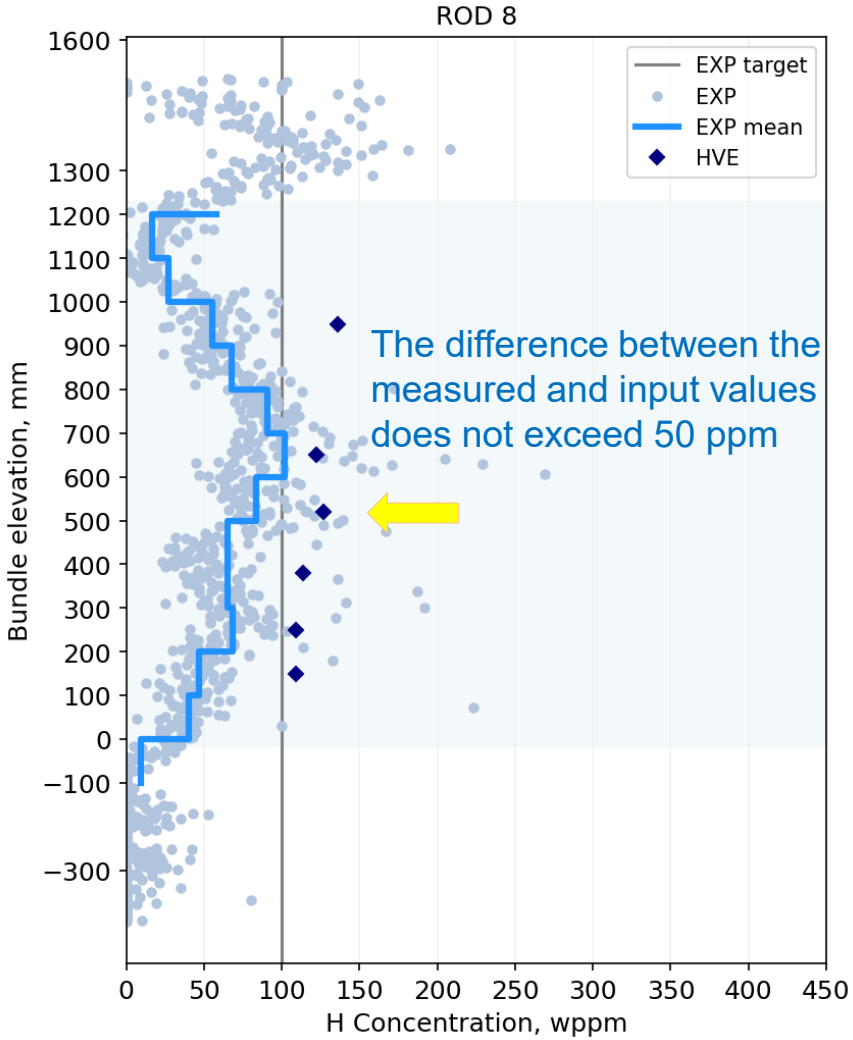

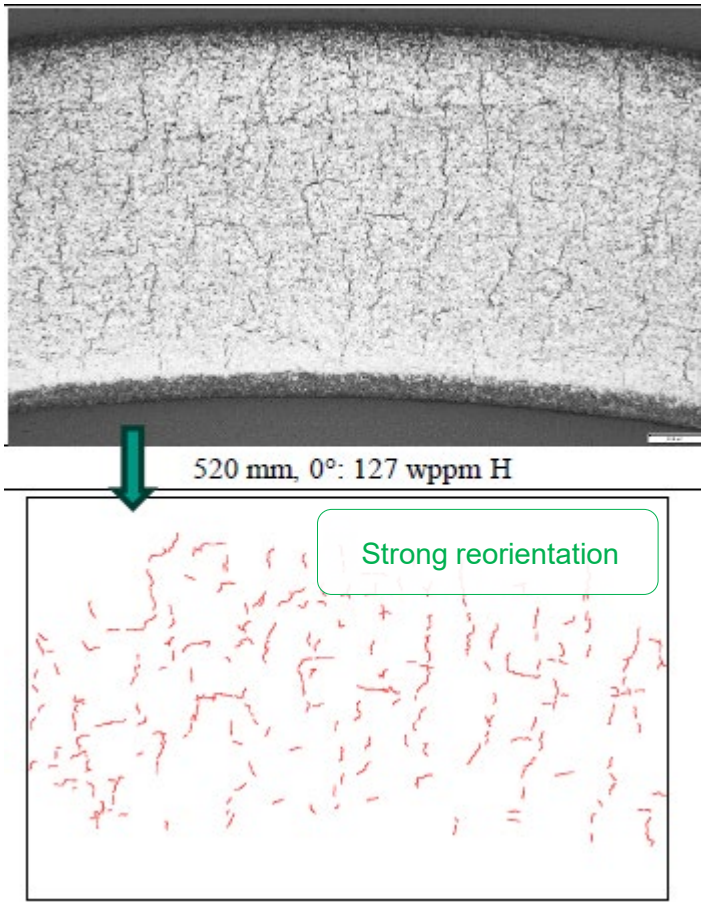

SPIZWURZ Bundle: ROD 8 Zry-4 Pmax Cmin
Reorientation of hydrides

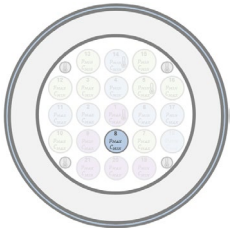

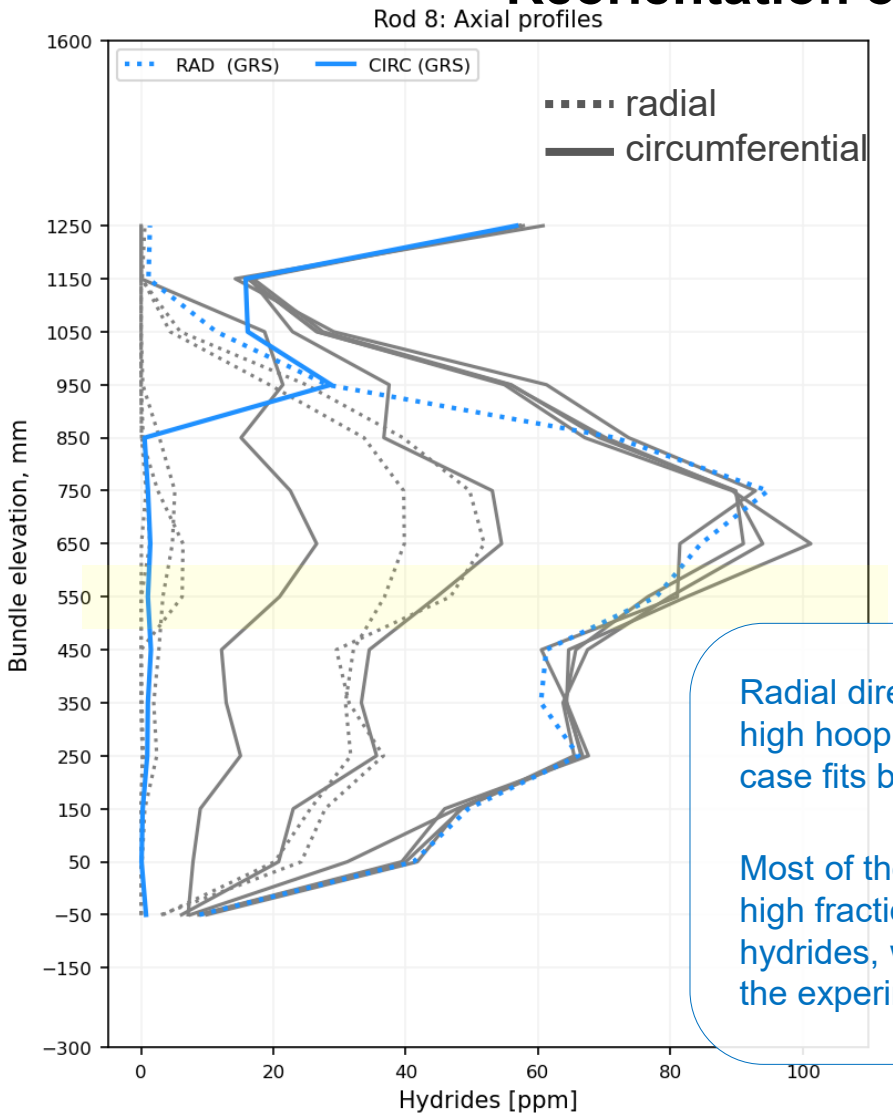

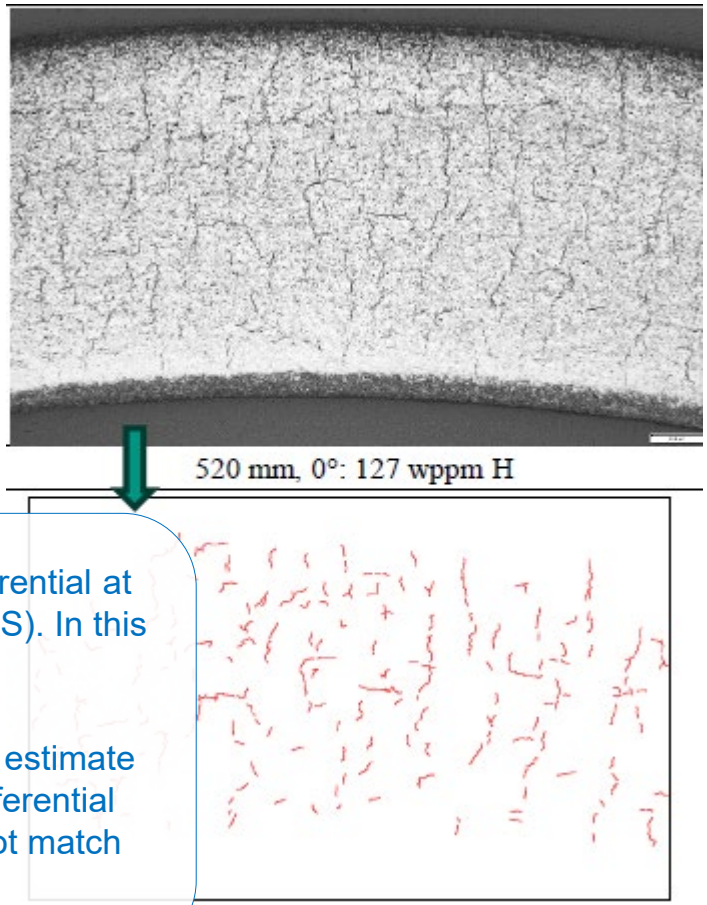

Radial direction is preferential at high hoop stresses (GRS). In this case fits better.

Most of the participants estimate high fractions of circumferential hydrides, which does not match the experiment.

SPIZWURZ Bundle: ROD 3 opt.ZIRLO Pmax Cmin
Reorientation of hydrides

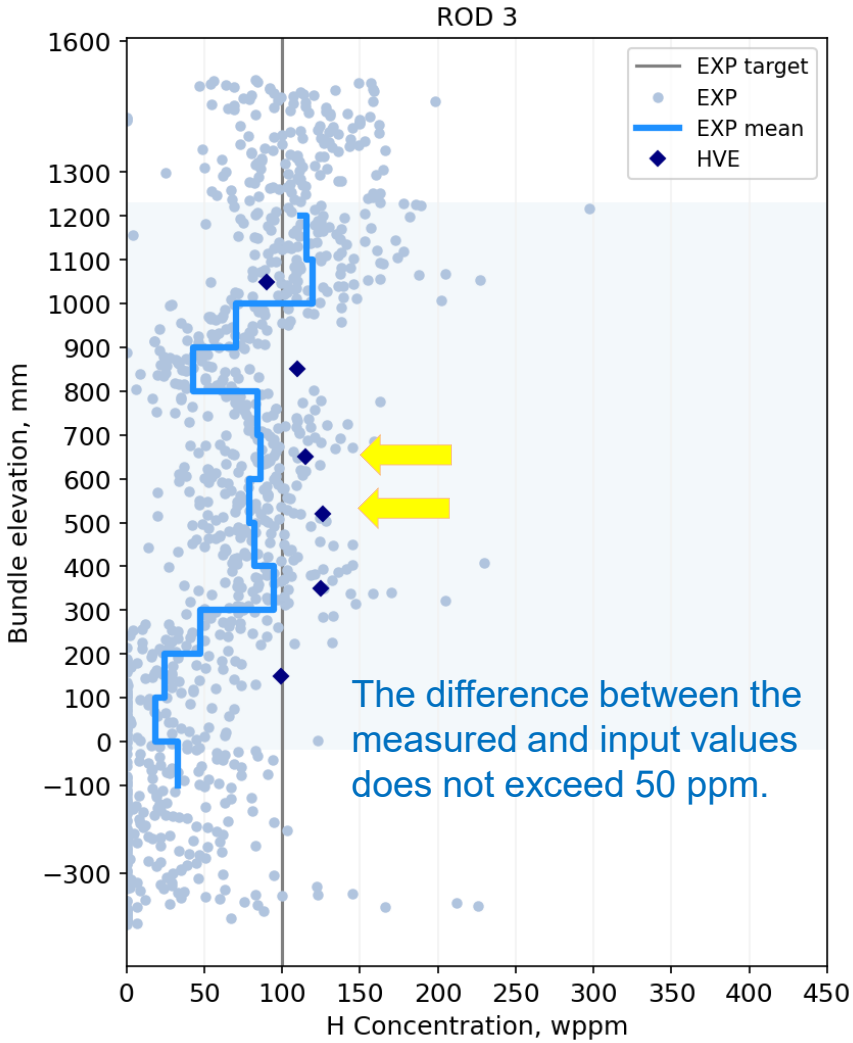

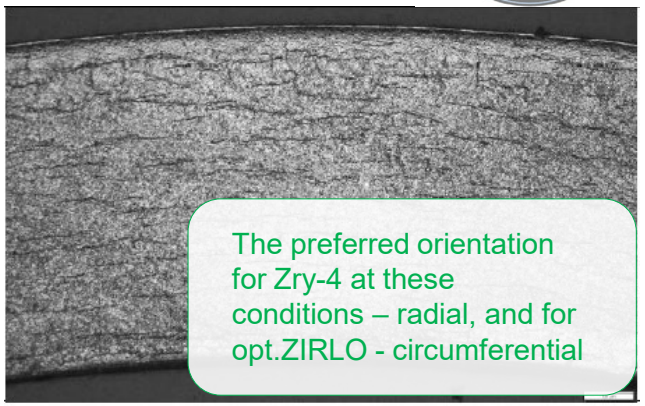

520 mm, 270°: 133 wppm H

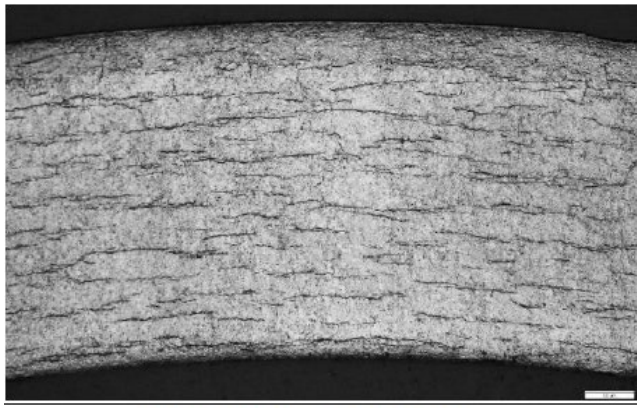

650 mm, 0°: 123 wppm H

SPIZWURZ Bundle: ROD 3 opt.ZIRLO Pmax Cmin
Reorientation of hydrides

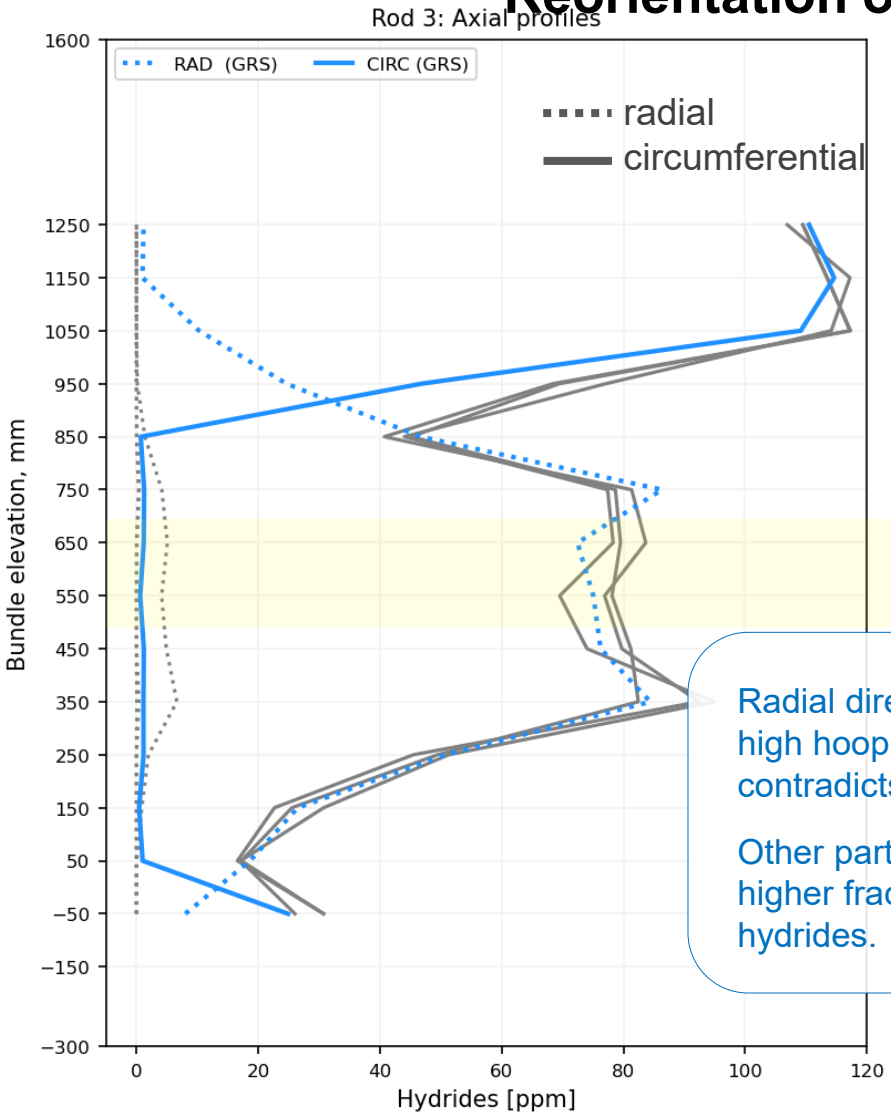

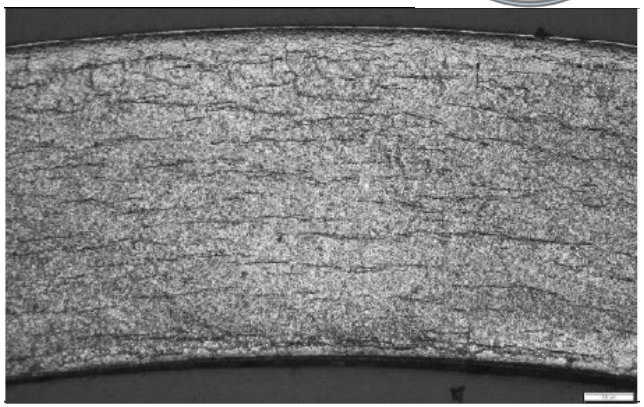

520 mm, 270°: 133 wppm H

650 mm, 0°: 123 wppm H

Radial direction is preferential at high hoop stresses (GRS),which contradicts the experiment.

Other participants estimate much higher fractions of circumferential hydrides.

Conclusions

- Preliminary SPIZWURZ Blind Benchmark results presented.
- 11 participants (10 organisations) in SPIZWURZ Blind Benchmark + 4 observers.
- Experiments show that the hydrogen and creep behaviour depends strongly on the cladding material, which is not necessarily reflected by the modelling approaches. Experimental data for the model validation is very limited.
- The start of the SPIZWURZ Benchmark open phase is anticipated for the second quarter of 2025.

- Contact person: Aleksandra Rezchikova

  aleksandra.rezchikova@grs.de

Johannes Bertsch

PSI

Hydrogen Diffusion and Precipitation – Hydrides: Do we see what has been formed and how?

Analyzing hydrides in nuclear fuel cladding is mostly based on two dimensional cuts. The question is in how far hydrides patterns represent the real distribution of hydrides in the material and their formation process. The present work concerns the detection and visualization of hydrogen and hydrides in unirradiated nuclear fuel claddings, focusing on the temporal development of hydrogen relocation and precipitation, plus the rearrangement of hydrides in three dimensions. The methods used are thermos-mechanical tests to trigger hydrogen mobility and precipitation, and thermal neutrons for imaging.

Hydrogen as by-product of fuel cladding oxidation in the hot reactor water is partially picked up into the zirconium alloy cladding, where it forms brittle hydrides. These can affect the mechanical stability of the cladding. This integrity risk is of concern during handling and transportation of spent nuclear fuel, specifically after long term intermediate dry storage during which hydrogen relocation and hydrides accumulation can occur. The characterization of hydrides distributions is important for the safety assessment. Neutron imaging is very sensitive to detect hydrogen and hydrides with a high spatial resolution in a non-destructive way.

To trigger hydrogen relocation and precipitation, we chose two approaches: (i) the hydrogen diffusion into the liner of a duplex cladding, where the liner acts as a hydrogen sink, and (ii) the hydrogen diffusion in a mechanical stress field to provoke hydrides reorientation. In both cases, the test material was slowly cooled down, to shift from a hydrogen diffusion to a precipitation mode. In the duplex cladding, hydrides gradually formed at the substrate-liner interface. Interrupted cooling allowed snapshots of the relocation. Competing attracting forces of precipitated hydrides on diffusing hydrogen and the liner could be established. In the liner-free cladding, without any stress, hydrides form according to the texture in a circumferential way. With hoop stress, hydrides form perpendicularly to the stress in radial direction, and thus deteriorate the fracture toughness of the cladding. This hydrides reorientation is typically revealed by two dimensional cuts of samples and using light optical microscopy or scanning electron microscopy. In the performed three-dimensional visualization, it turned out, that hydrides in different depths along the cladding tube axis do not necessarily show the same orientations as in a two-dimensional cut. In summary, the present work shows that conventional hydrides analyses do not reflect the complete picture and may potentially ignore parts of the temporal development of hydrides accumulation or 3D arrangement.

PSI Center for Nuclear Engineering and Sciences

Hydrogen diffusion and precipitation

Looking at hydrides ...

- Do we really see what has been formed?
- Do we see how it formed?

M. MEYER, D. MOTA, O. YETIK, L. DUARTE, P. TRTIK, R. ZUBLER, J. BERTSCH

19 – 21 Nov 2024, Quench, KIT

Introduction

- Hydrogen in zirconium claddings
- Neutron imaging

Case I

- 3D Hydrides Arrangement in Fuel Cladding Tubes

Case II

- Temporal Development of Hydrogen Relocation In Liner Cladding

Conclusion

Introduction

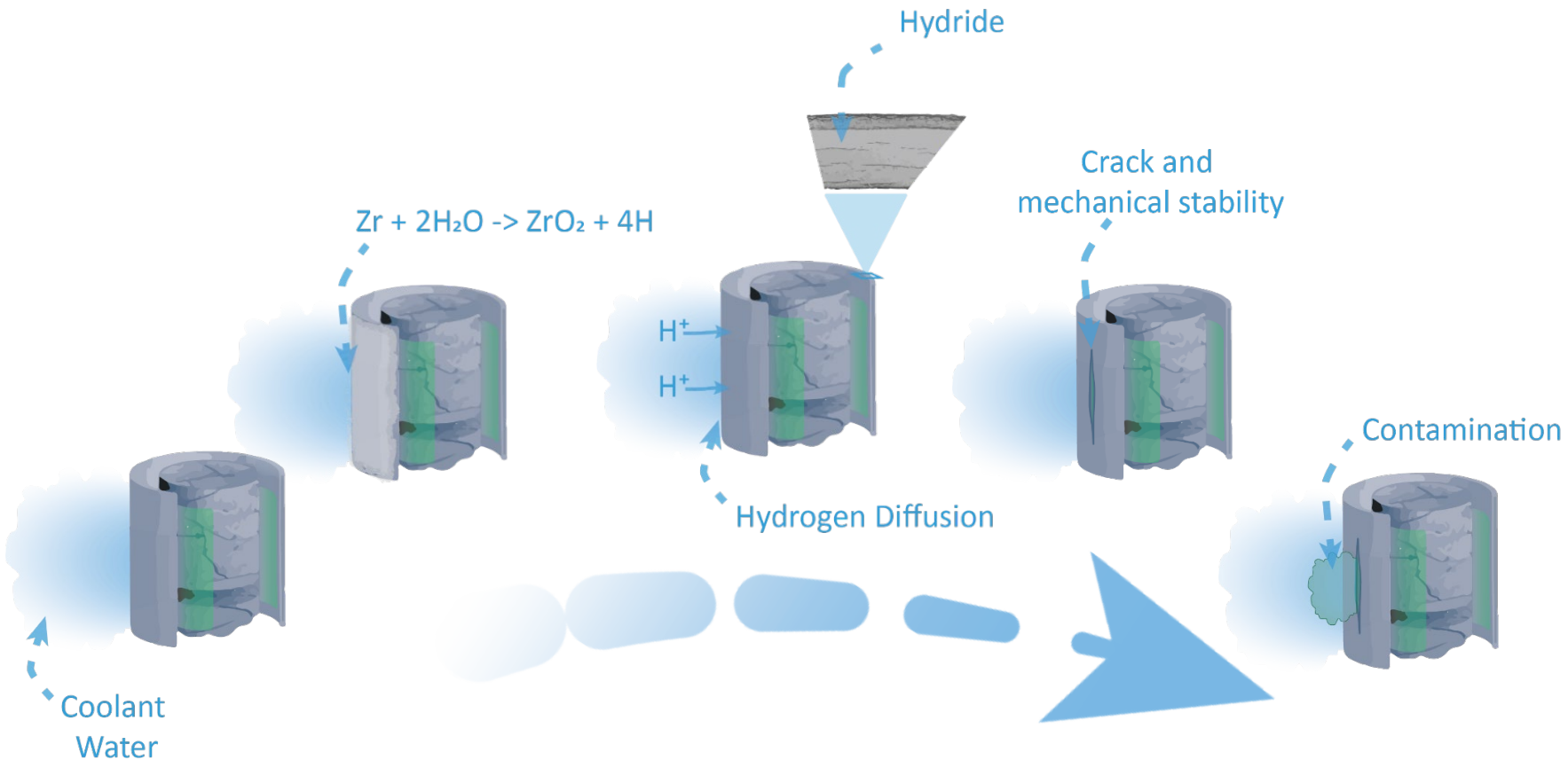

- Hydrogen and hydrides can compromise the mechanical stability of cladding materials.
- A reduction in safety, compromising cladding integrity, is undesirable!

Introduction

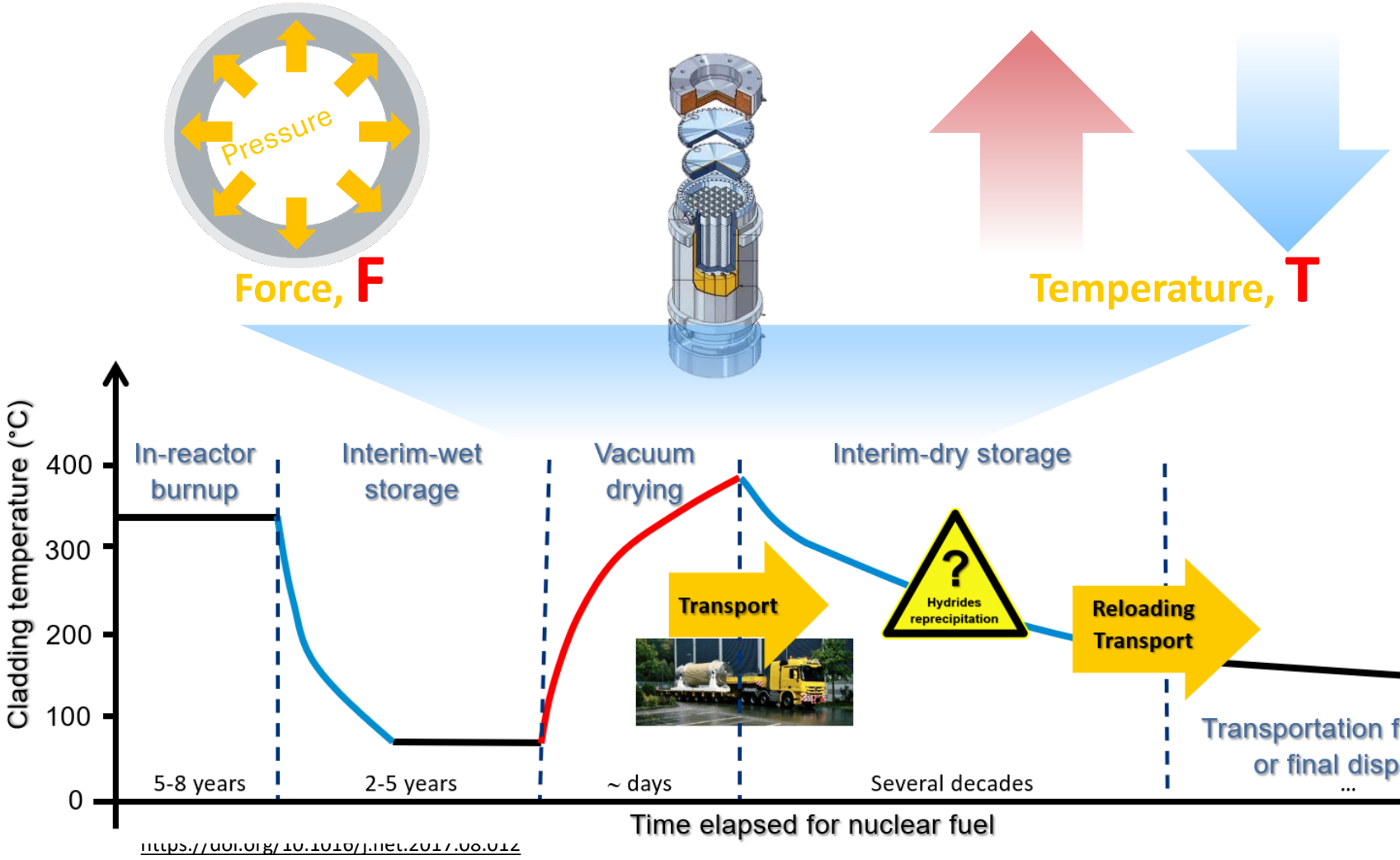

https://doi.org/10.1016/j.net.2017.08.012

- The risk to integrity may rise during handling and transportation of spent fuel.
- Accumulation of hydrides locally weakens the material.

Introduction

1 Neutron Imaging, ICON SINQ

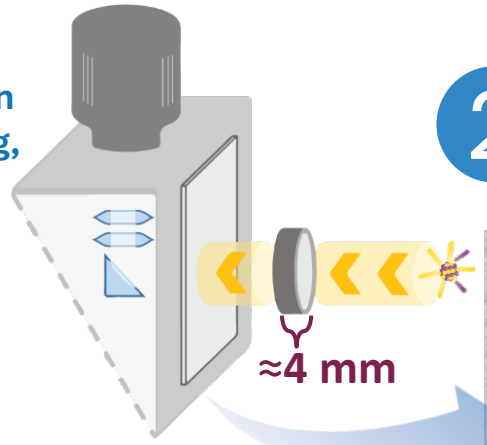

2 Image

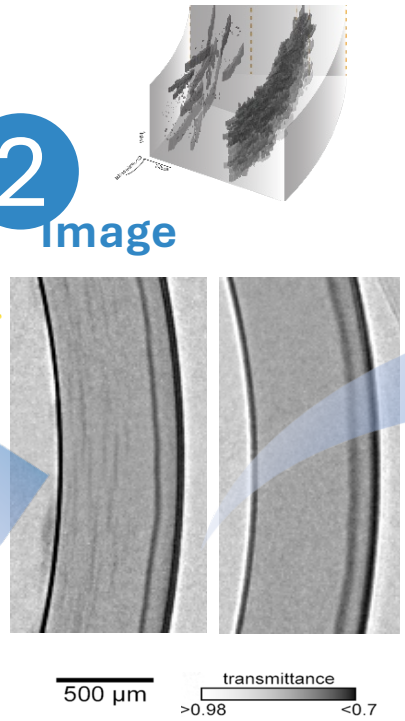

3 Quantification

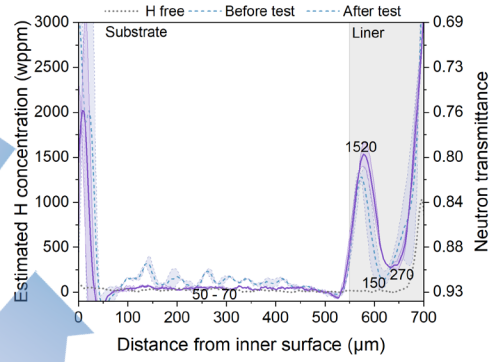

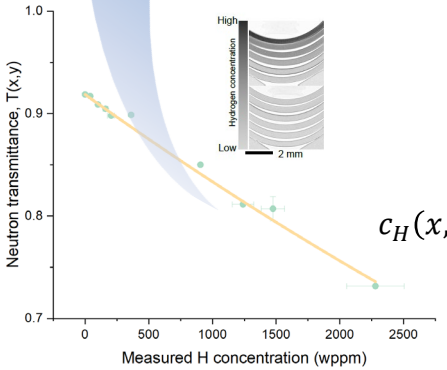

$$c_H(x,y) = \frac{\ln(\frac{T(x,y)}{0.9227})}{-9.73E-05}$$

Attenuation coefficient for neutrons

H	Zr
3.44	0.29

Neutron imaging

- quantitative analysis of hydrogen concentration distribution and hydrides packages
- high spatial and concentration resolution
- nota bene – it's radiographing

Introduction

1 Neutron Imaging, ICON SINQ

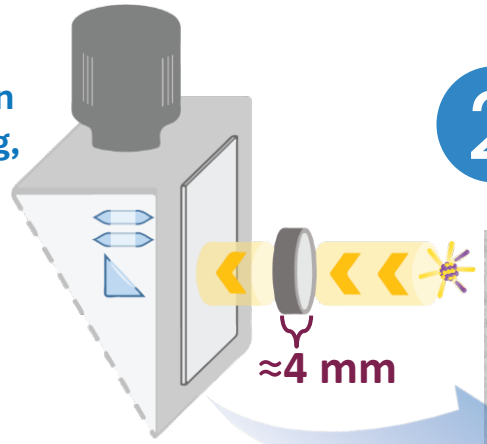

2 Image

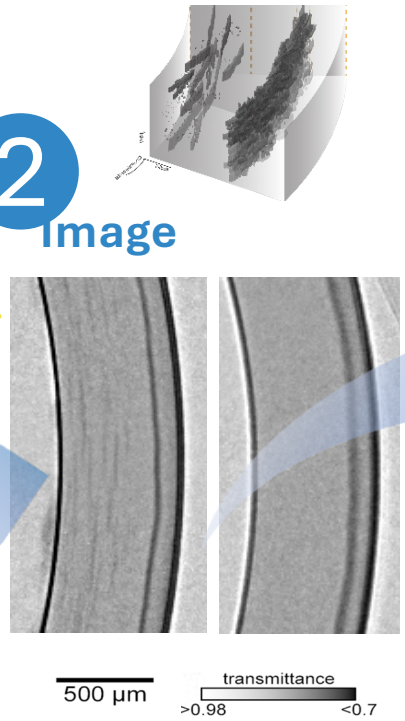

3 Quantification

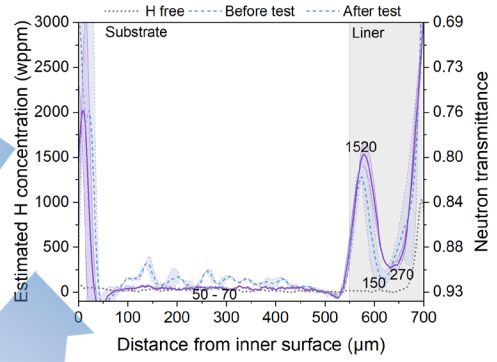

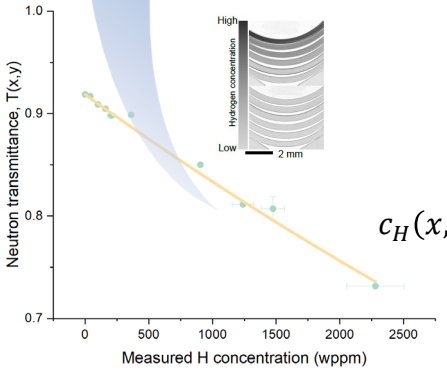

$$c_H(x,y) = \frac{\ln(\frac{T(x,y)}{0.9227})}{-9.73E-05}$$

Attenuation coefficient for neutrons

H	Zr
3.44	0.29

… thus, not considered

- Hydrides in 3D.
- Temporal development of hydrogen / hydrides distribution.

PSI Center for Nuclear Engineering and Sciences

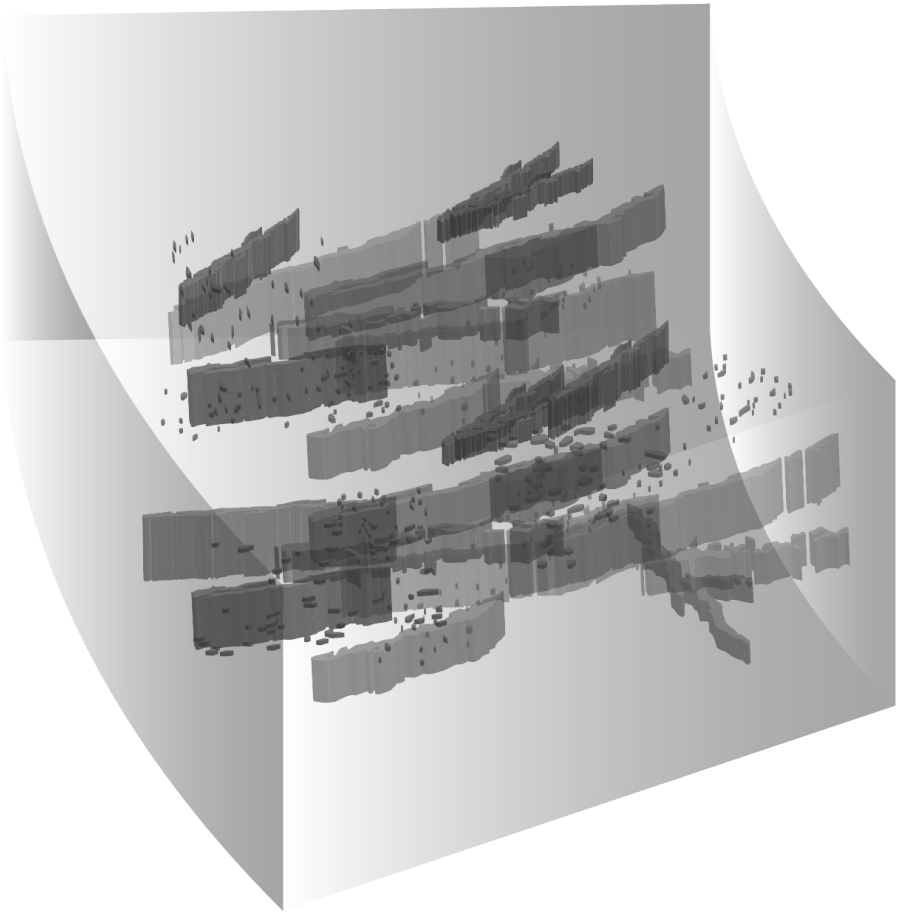

Case I

3D Hydrides Arrangement in Fuel Cladding Tubes

Motivation

Hoop stress can induce the precipitation of radially oriented hydrides.

How are the hydrides distributed and oriented in 3D after a thermo-mechanical test?

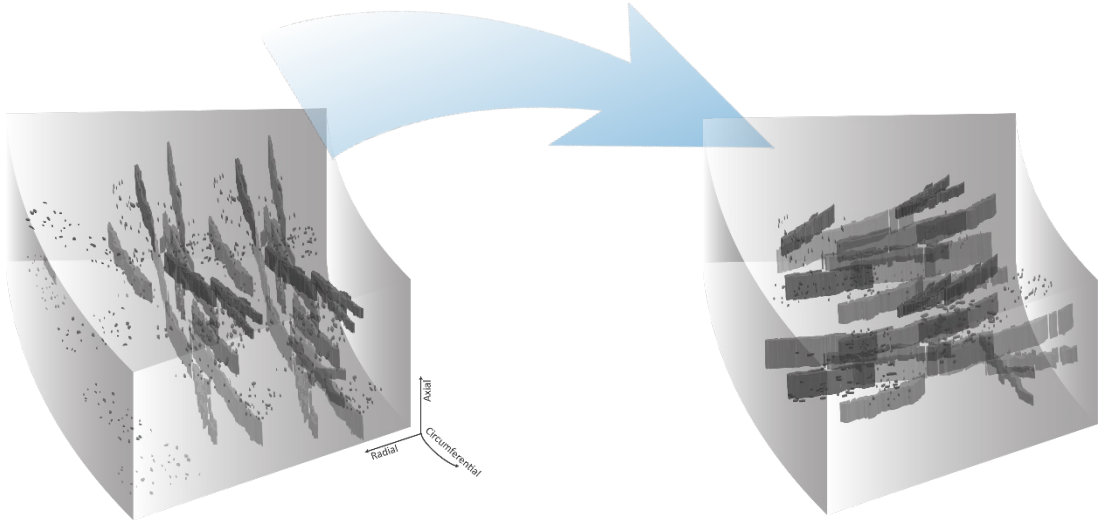

Circumferential hydride

Reorientation to radial hydride

Ref: Chengze L. et al., https://doi.org/10.1016/j.msea.2018.02.043

Material and test procedure

Test material:
Zircaloy-4 (no liner)

Hydrogen concentration:
100 wppm (nominal)

Thermo-mechanical test conditions

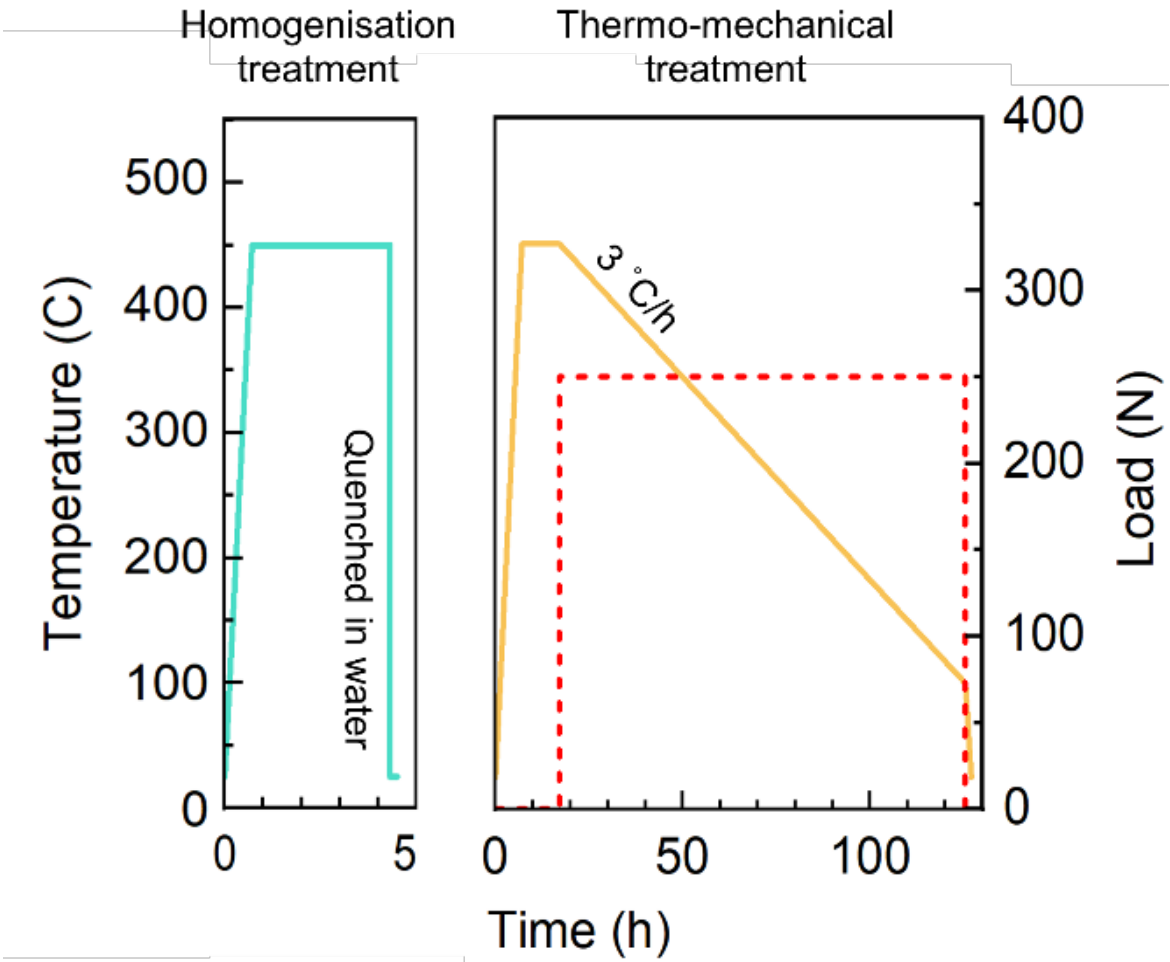

PSI

Material and test procedure

Test material:
Zircaloy-4 (no liner)

Hydrogen concentration:
100 wppm (nominal)

Test method and stress profile

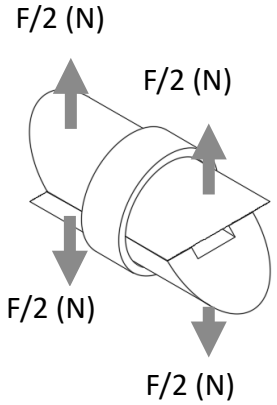

Double half cylinder test

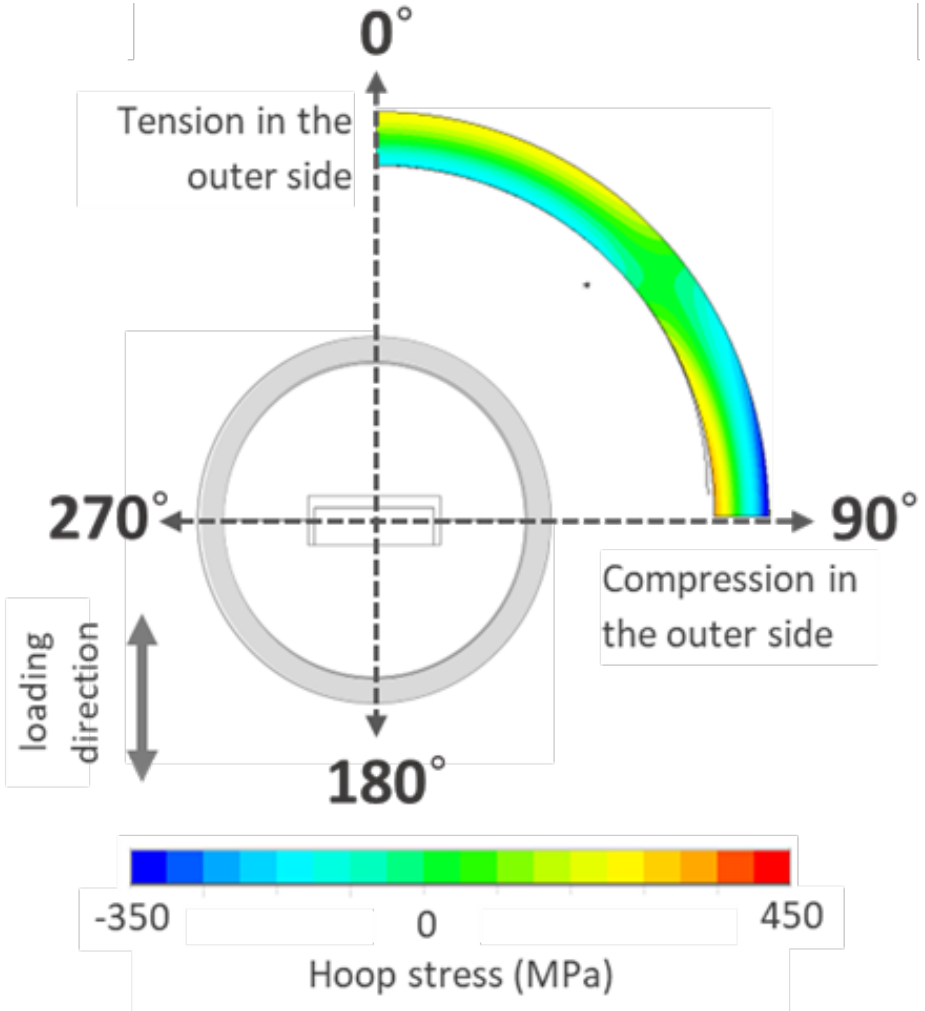

PSI

3D hydride distribution in sample T3

Long radial hydrides along axis not well displayed in projected radiography.

A significant amount of circumferentially oriented hydrides is evident in image (d).

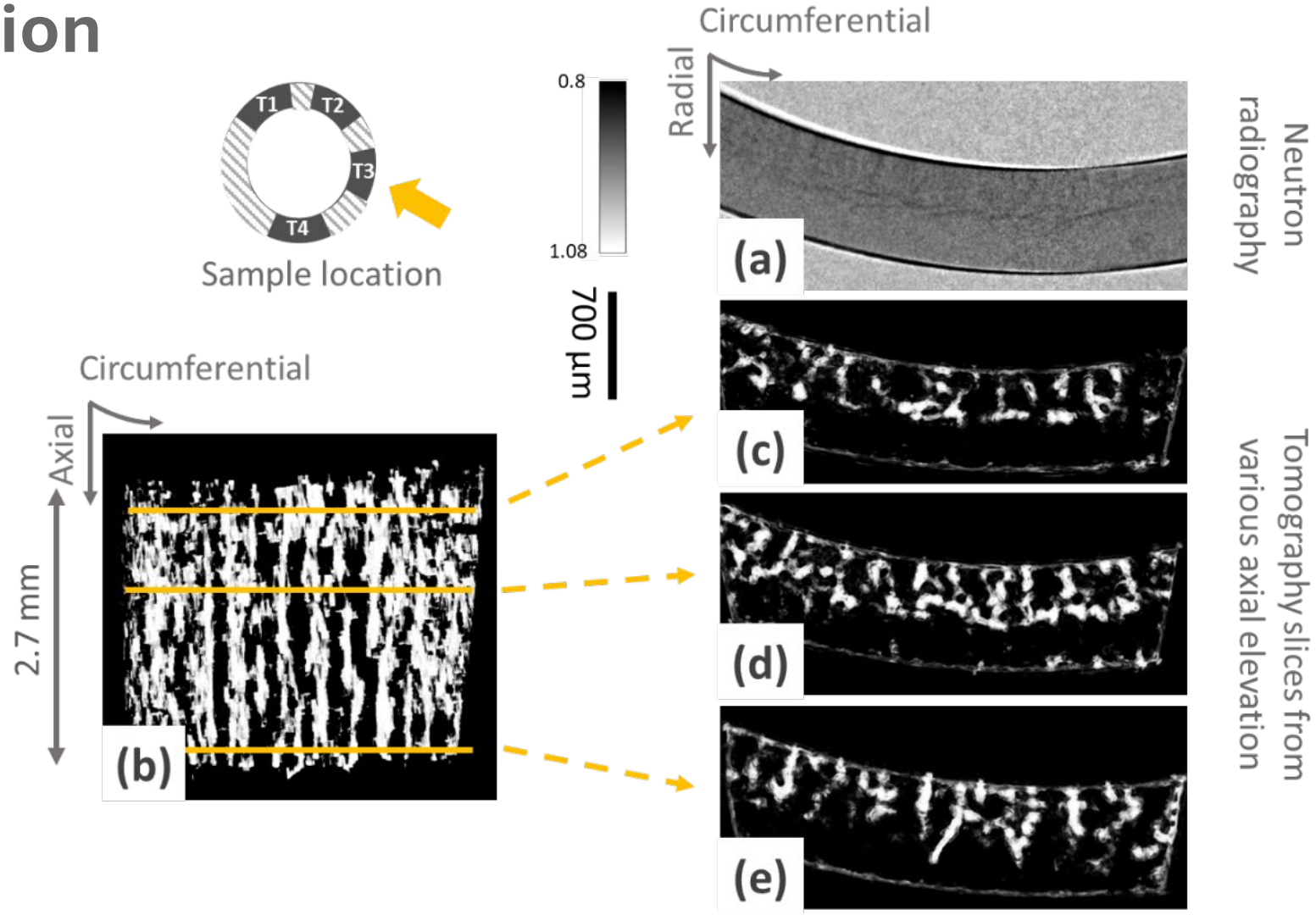

3D hydride distribution in sample T4

Although hydride re-orientation is clearly expected, the degree of reorientation varies significantly at different axial levels.

The hydrides appear shorter in the axial direction compared to those in sample T3.

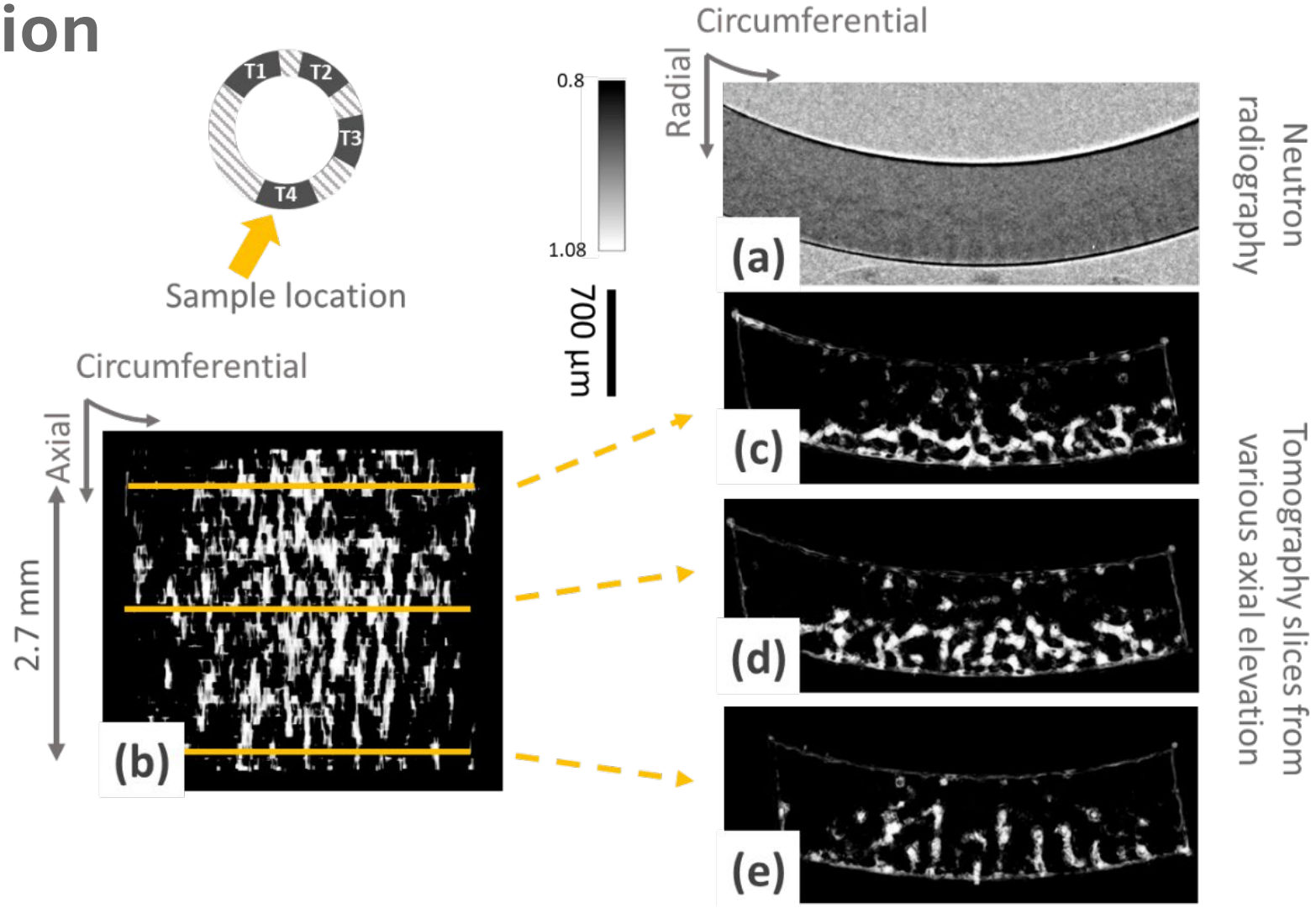

Sample T4, SEM characterisation

The widths and distances of the hydride packages are comparable across both visualizations.

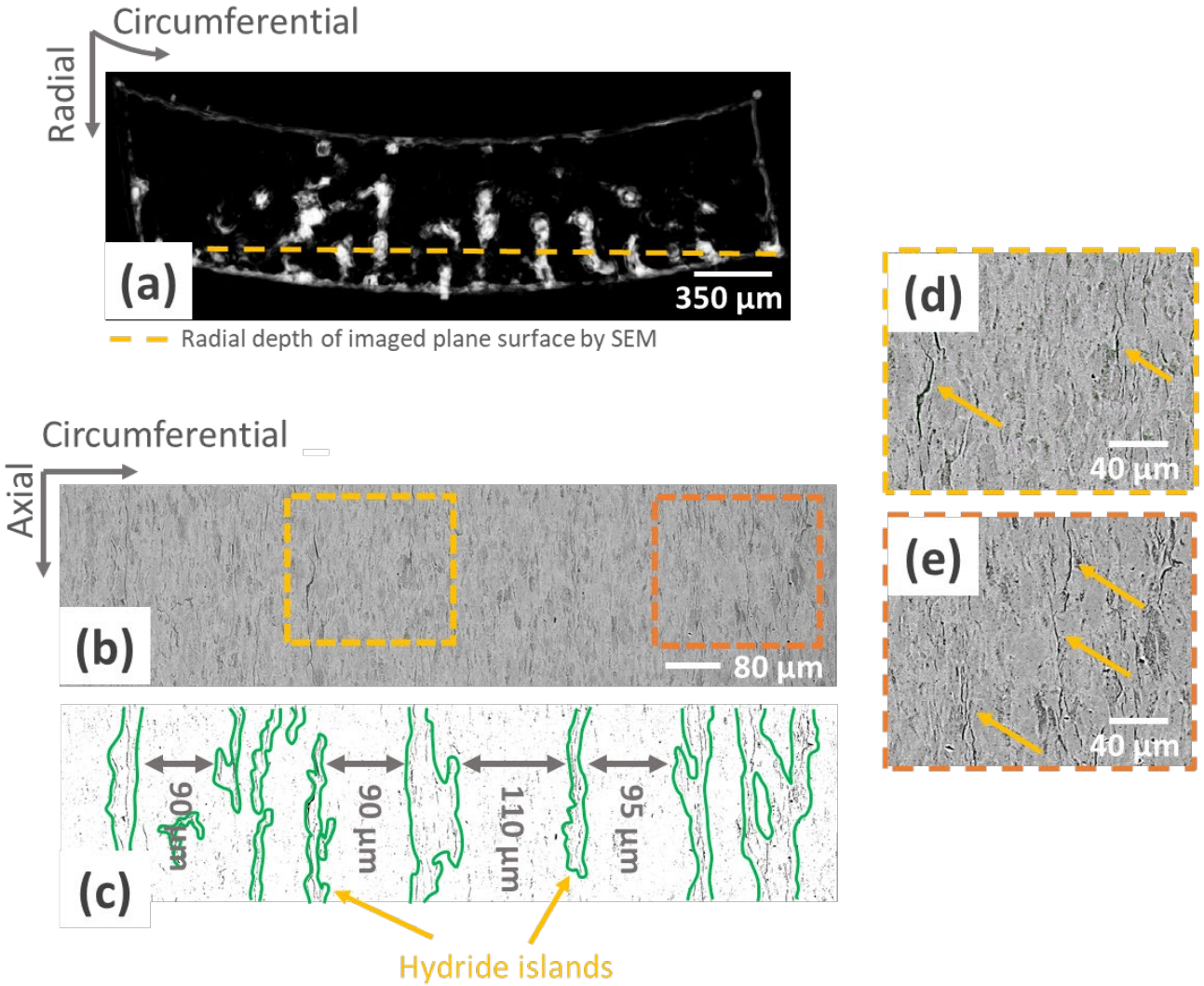

PSI Center for Nuclear Engineering and Sciences

Case II

Temporal Development of Hydrogen Relocation in Liner Cladding

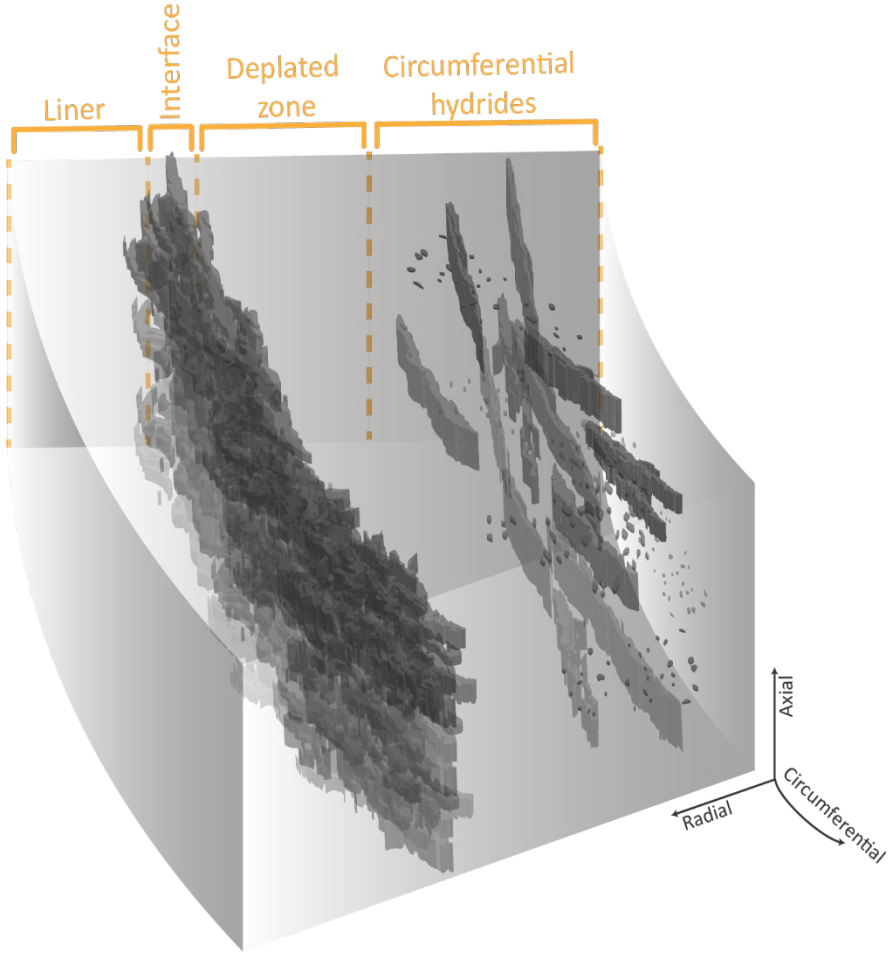

Motivation

Hydrogen diffuses into the liner of so-called duplex cladding, where the liner serves as a hydrogen sink.

How does hydrogen relocation and hydride precipitation temporally occur during cooling when competing attractive forces are present?

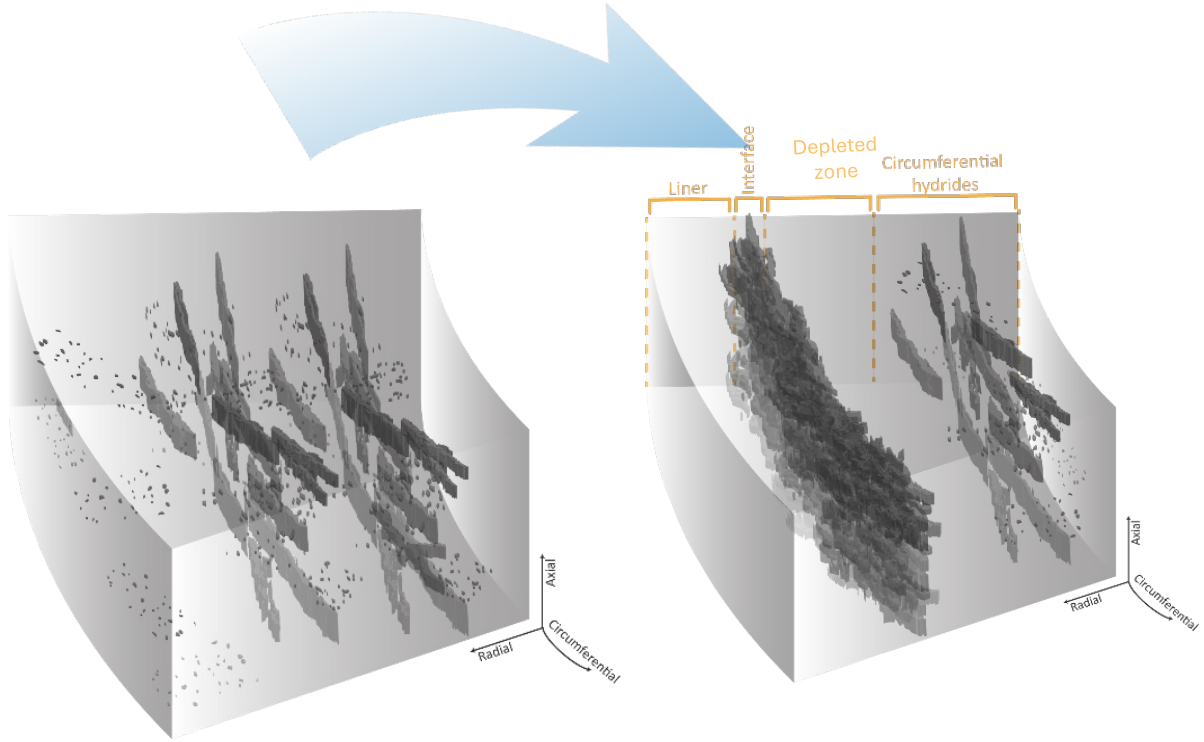

Circumferential hydrides

Hydrogen diffusion

Material and test procedure

Test material:
DXD4 (with liner)

Hydrogen concentrations:
100, 200, 400 wppm (nominal)

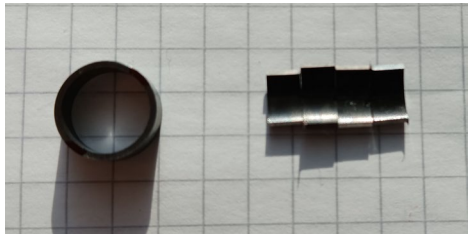

Thermal test procedure

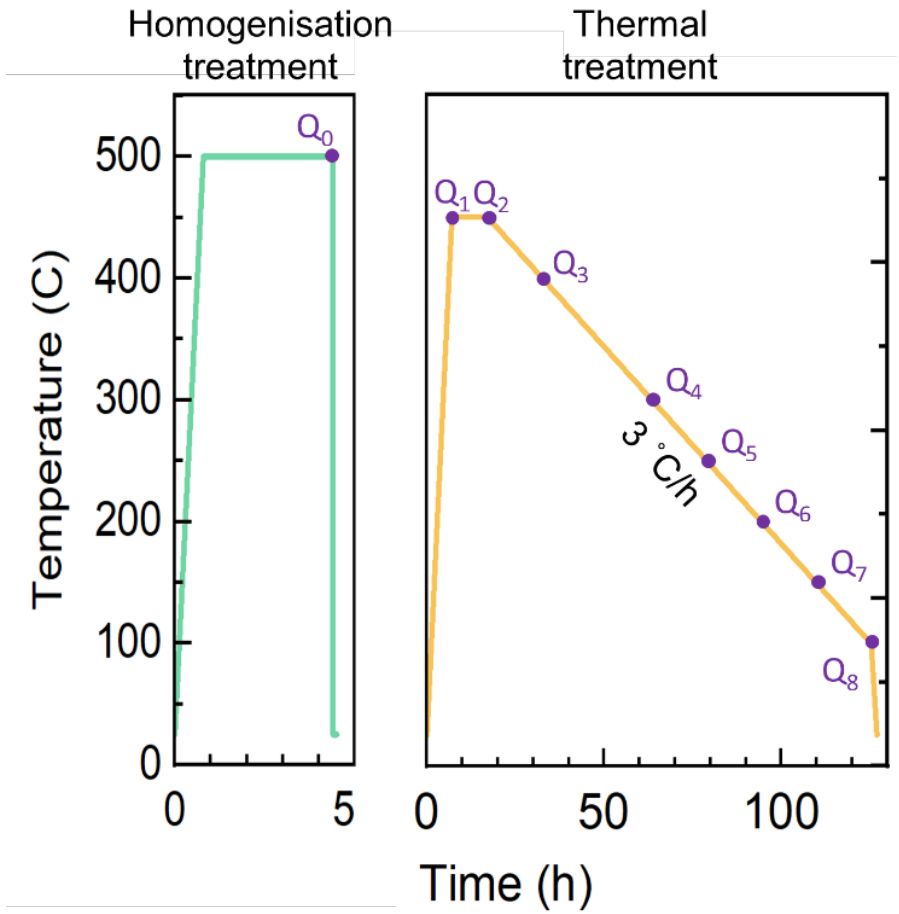

PSI

Material and test procedure

Test material:
DXD4 (with liner)

Hydrogen concentrations:
100, 200, 400 wppm (nominal)

Neutron imaging, BOA, SINQ

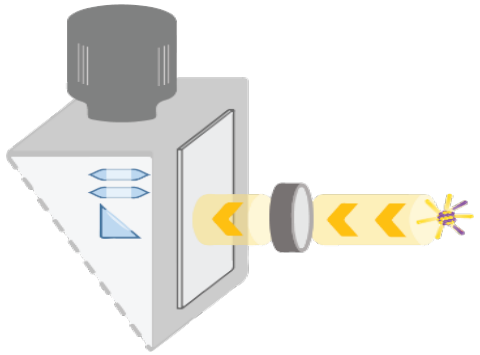

Neutron imaging

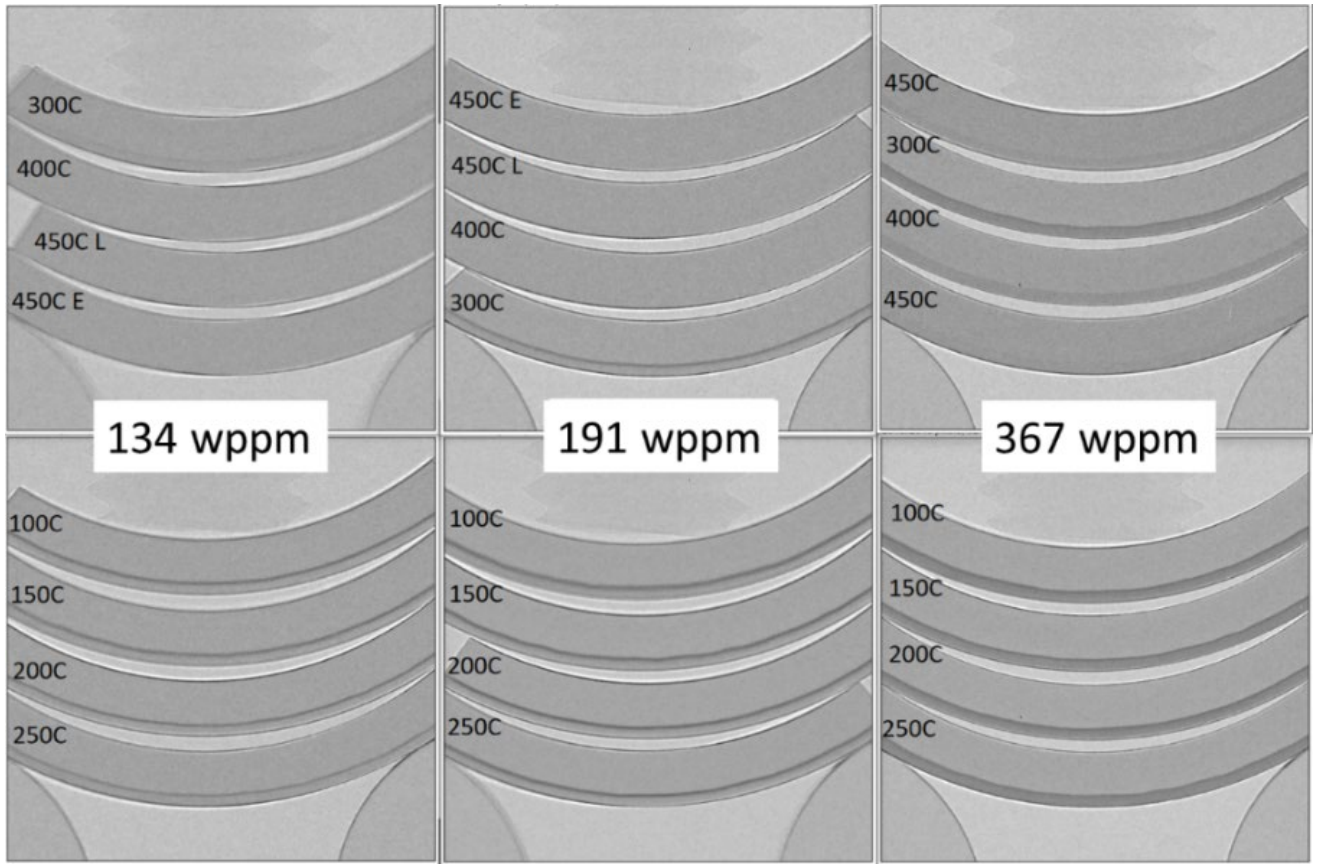

Interrupted cooling allowed snapshots of the relocation.

Hydrogen concentration profiles

The global hydrogen concentration influences the final distribution.

A peak of hydrogen/ hydrides forms in the liner near the substrate-liner interface.

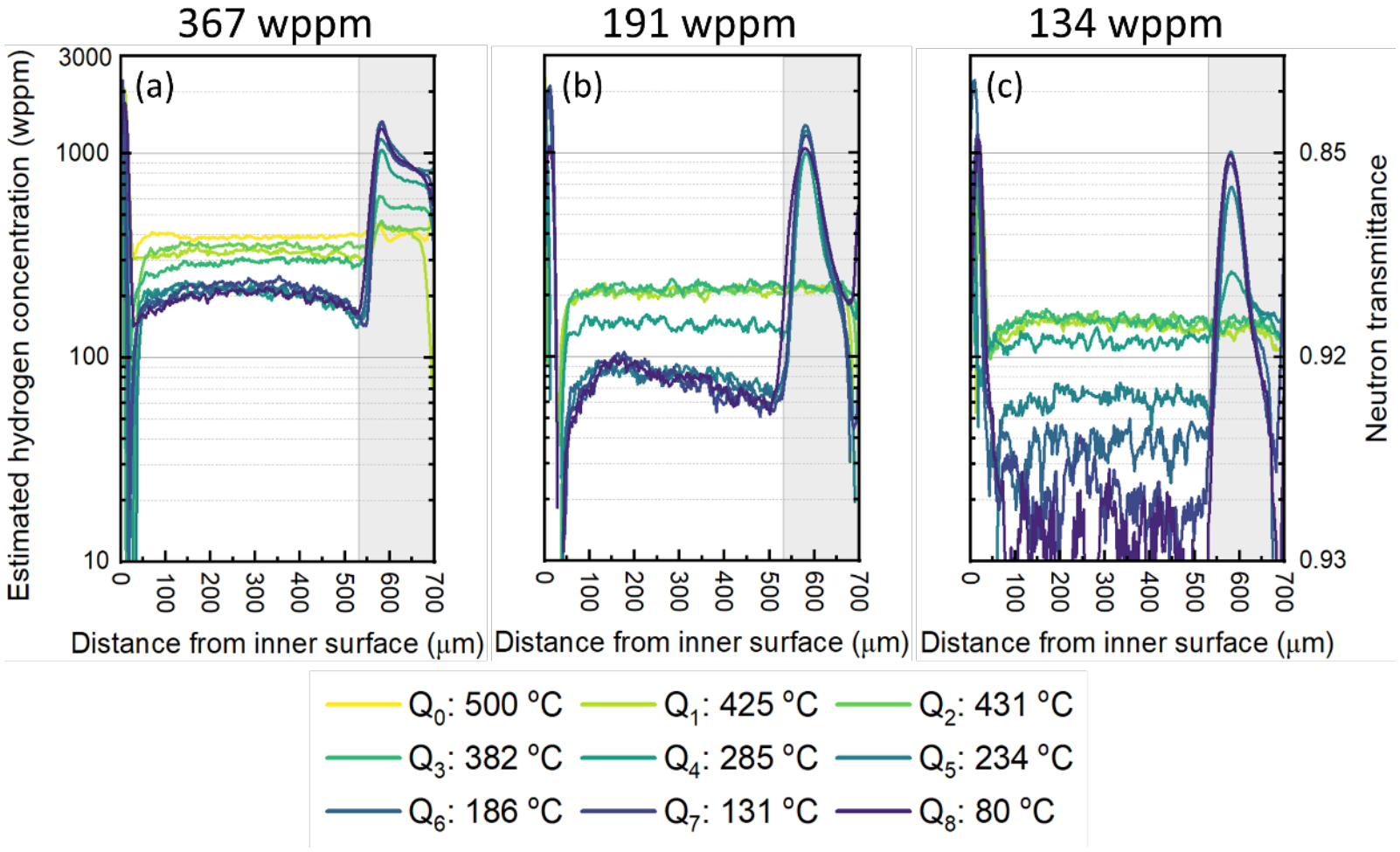

PSI

Local hydrogen changes

Hydride peak appears to have a saturation limit.

“Back diffusion” occurs at lower hydrogen concentrations.

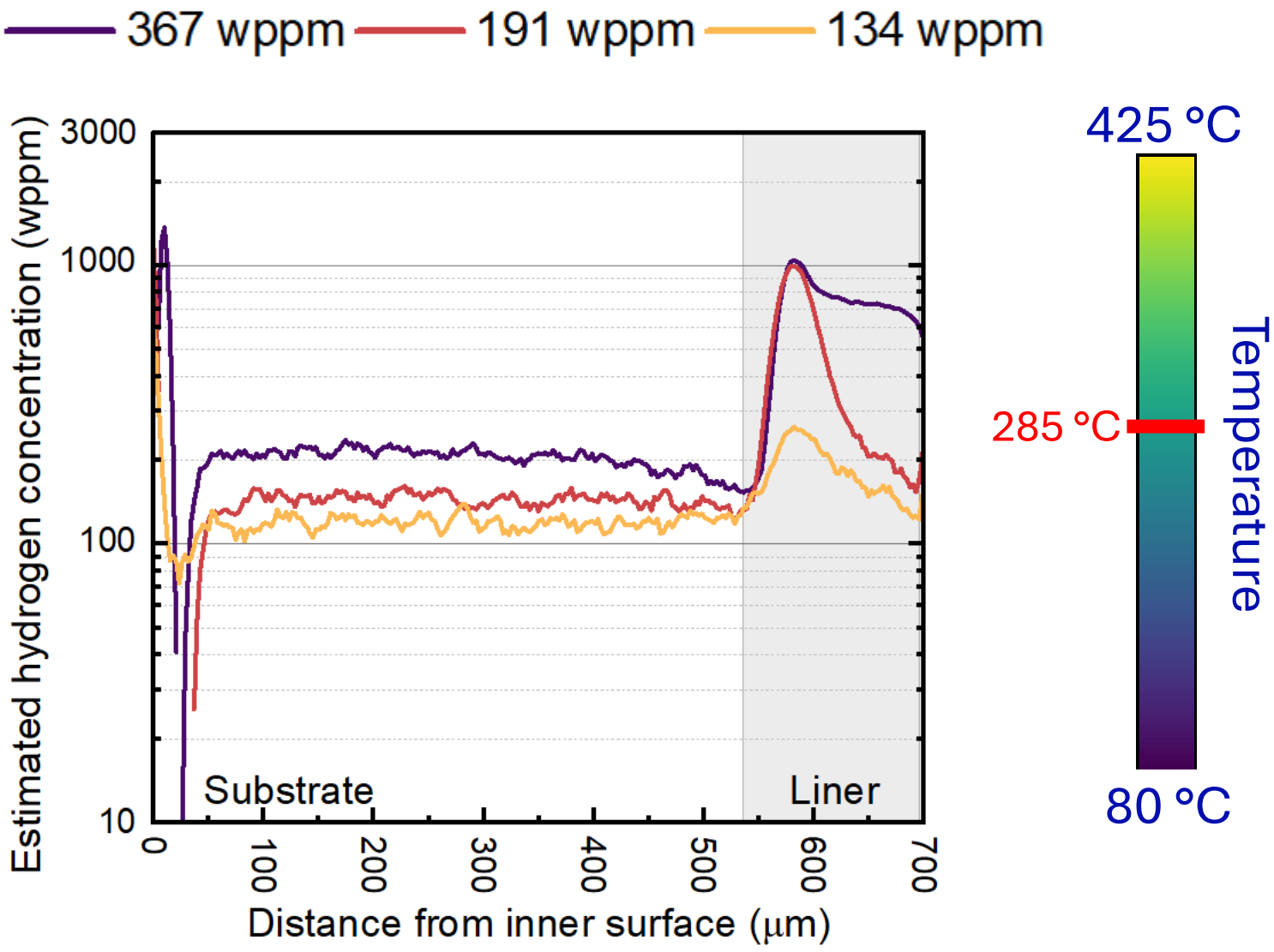

PSI

Local hydrogen changes

Hydride peak appears to have a saturation limit.

“Back diffusion” occurs at lower hydrogen concentrations.

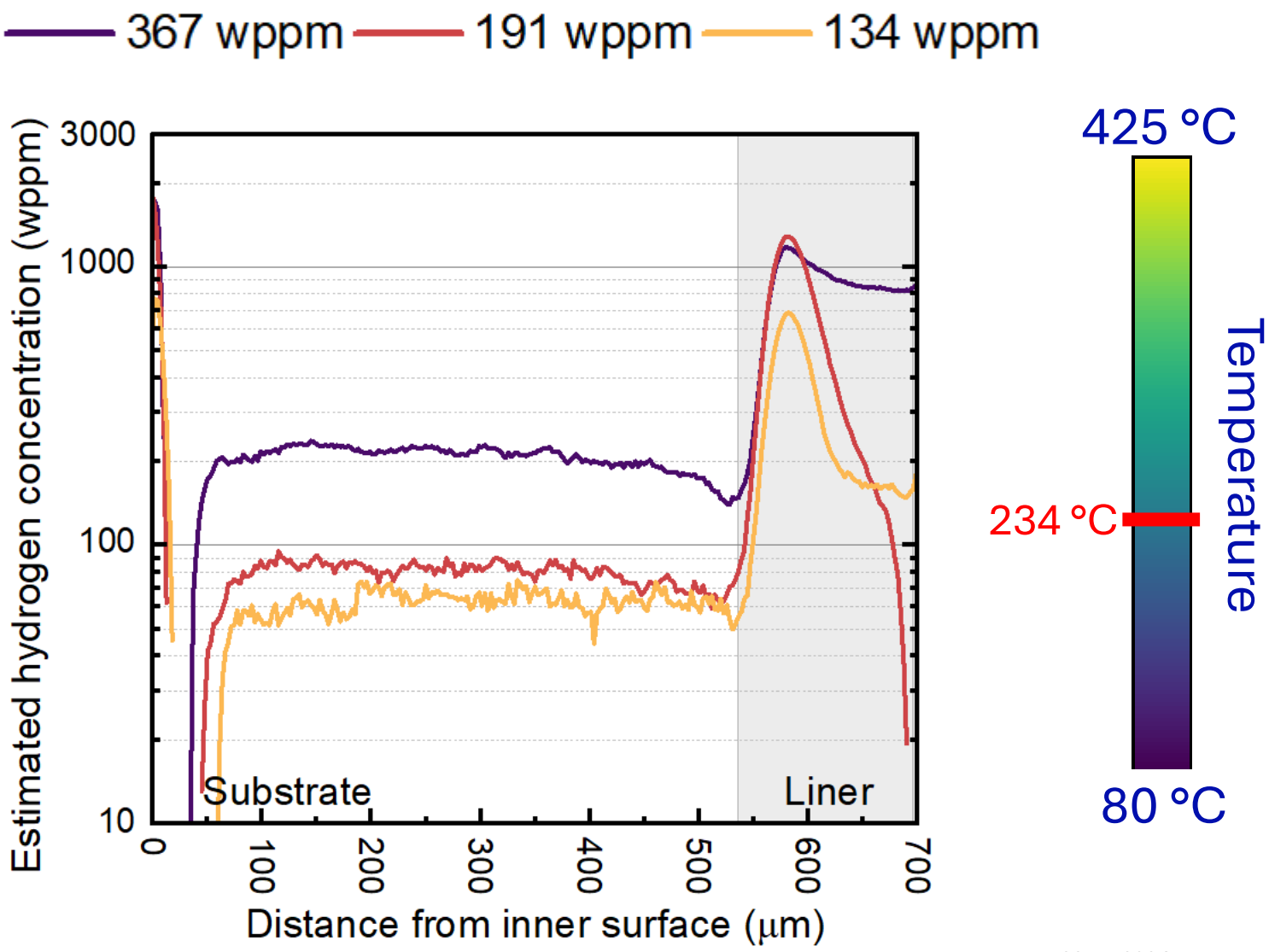

PSI

Local hydrogen changes

Hydride peak appears to have a saturation limit.

“Back diffusion” occurs at lower hydrogen concentrations.

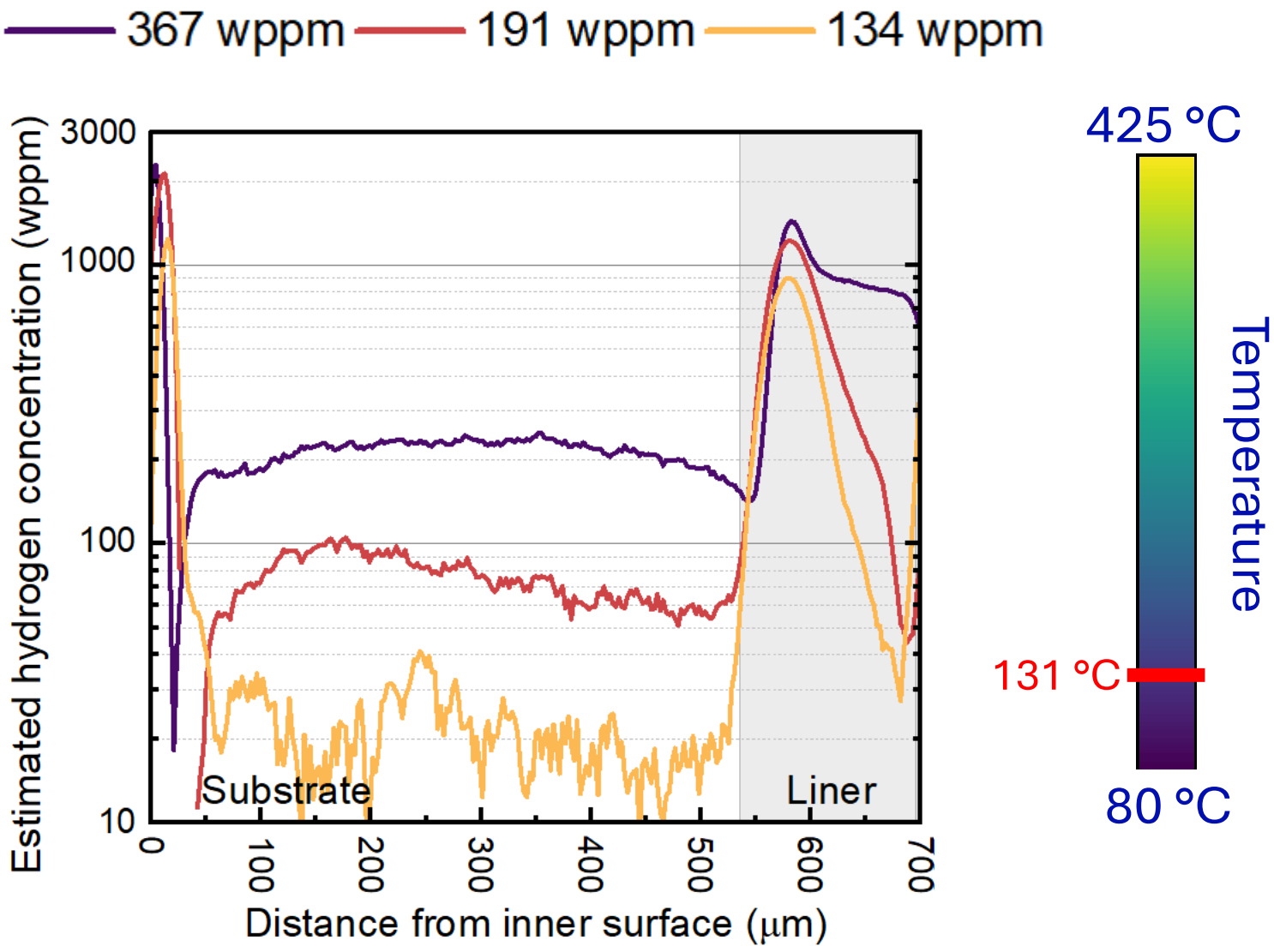

PSI Center for Nuclear Engineering and Sciences

Conclusion

- Neutron imaging was applied to 3D hydrides reconstruction, and quasi-temporal resolution of hydrogen diffusion and precipitation in zirconium-based liner cladding.
- **Neutron tomography** results showed that hydride orientation varies with depth and axial position, highlighting the limitations of 2D characterizations.
- **Interrupted diffusion experiments** revealed the temporal development of hydrogen relocation during slow cooling in duplex liner cladding, indicating a competitive interplay between hydrogen diffusion and hydride precipitation.
- Conventional 2D techniques showing final hydrides may not provide the complete picture.

Outlook:

These findings can improve models of hydrogen accumulation and hydride reorientation within cladding, thereby aiding in the assessment of failure risks during dry storage.

PSI Center for Nuclear Engineering and Sciences

Thank you for your attention

The authors would like to thank Framatome for providing the test material.

The work was cofunded by swissnuclear.

Scientific discussion and all technical support from different laboratories AHL, LNM, LNS.

Swiss spallation neutron source (SINQ) at Paul Scherrer Institute, Villigen, Switzerland.

Okan Yetik

PSI

Hydrogen Quantification in Non-irradiated Zirconium Cladding after Various Oxidation Conditions

During the operation of nuclear fuel in light water reactors, zirconium-based fuel cladding undergoes surface oxidation. As a by-product of this process, hydrogen is released, and a portion diffuses into the zirconium oxide layer and the zirconium metal matrix. The hydrogen distribution is often non-homogeneous, and when the local concentration exceeds the solid solubility limit, it precipitates as brittle hydrides. This phenomenon can compromise the mechanical integrity of the cladding. Thus, understanding the hydrogen and hydride distribution in zirconium-based claddings is critical.

This study investigates the spatial distribution of hydrogen in various zirconium microstructures and in the waterside zirconium oxide layer formed under high-temperature oxidation conditions (temperatures exceeding typical reactor operating conditions). High-resolution neutron imaging (HR-NI), a method primarily used for analyzing hydrogen in the alpha-zirconium phase, was utilized. HR-NI analyses were conducted using the PSI Neutron Microscope detector at the Swiss Spallation Neutron Source (SINQ), employing the BOA beamline. Sample microstructures were characterized using scanning electron microscopy (SEM), while hydrogen concentrations were further quantified using hydrogen gas extraction (HGE) to complement HR-NI.

The results show that zirconium oxide exhibits a higher neutron attenuation contrast compared to zirconium metal due to its greater total neutron cross-section. Challenges were experienced in some cases with HR-NI characterization due to sample deformation, severe crack formation in the oxide, and the spatial resolution limitations when analyzing thin phase layers. The hydrogen content in the oxide was measured at up to 50 wppm, regardless of the oxidation environment. However, oxides formed at 500 C and 800 °C in steam atmosphere showed higher hydrogen concentrations ranging between 100 - 300 wppm. Radial cracks in the oxide layer likely provide pathways for hydrogen to diffuse into the metal, while compact oxide layers act as barriers, reducing hydrogen diffusion into the zirconium metal. Additionally, hydrogen was observed to preferentially diffuse into β-Zr phase regions.

In conclusion, this study demonstrates the applicability of HR-NI for characterizing cladding samples oxidized under high-temperature conditions. HR-NI can be considered as a method for non-destructive and spatially resolved hydrogen determination in such cases.

PSI Center for Nuclear Engineering and Sciences

Hydrogen Quantification in Non-irradiated Zirconium Cladding after Various Oxidation Conditions*

Okan Yetik[1,2], Sarah Weick[3], Cansu Kurşun[1], Liliana Duarte[1], Pavel Trtik[2], Mirco Grosse[3], Johannes Bertsch[1]

Karlsruhe, 21 November 2024

Introduction

- Background
- Objective

Experimental method

- Test materials
- Method

Results

Summary

Hydrogen in zirconium cladding

Oxidation of cladding surface

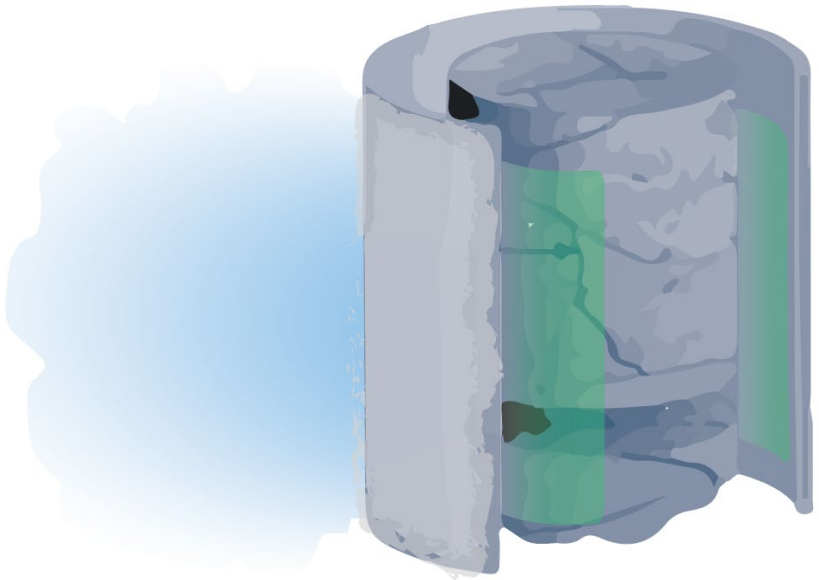

$$Zr + 2H_2O \rightarrow ZrO_2 + 4H$$

Hydrogen in zirconium cladding

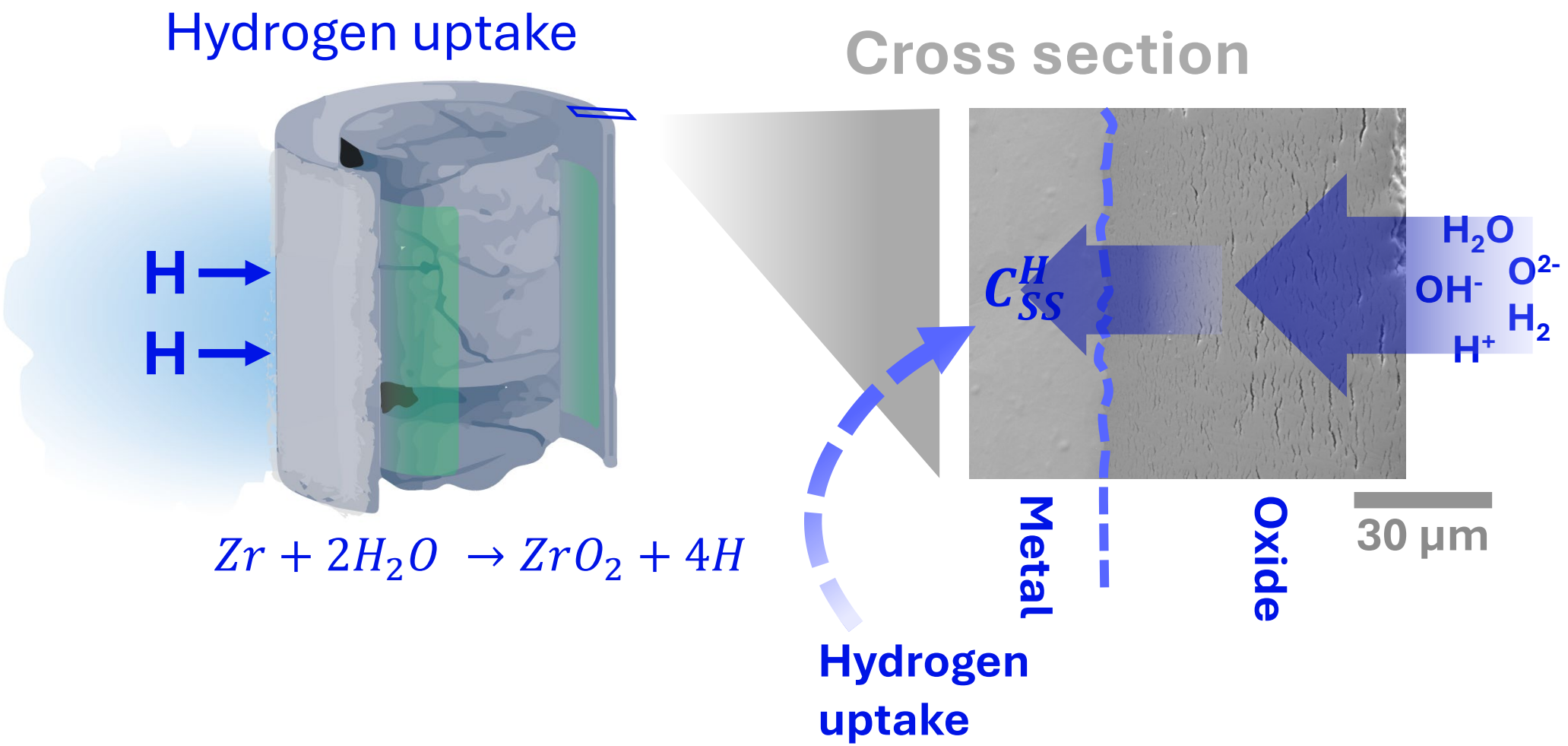

Hydrogen in zirconium cladding

- in α-Zr, hydrogen solubility is low.

- hydride precipitation.

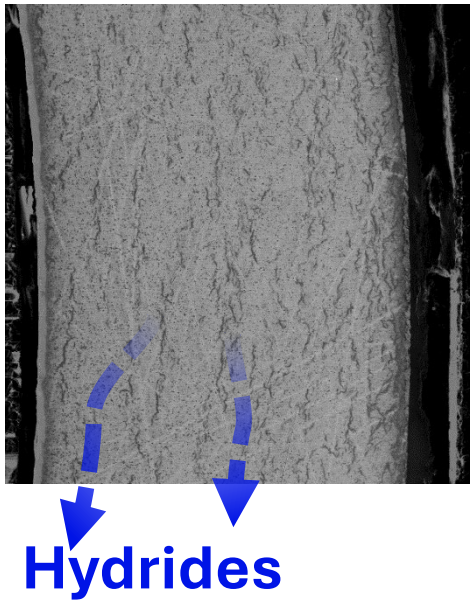

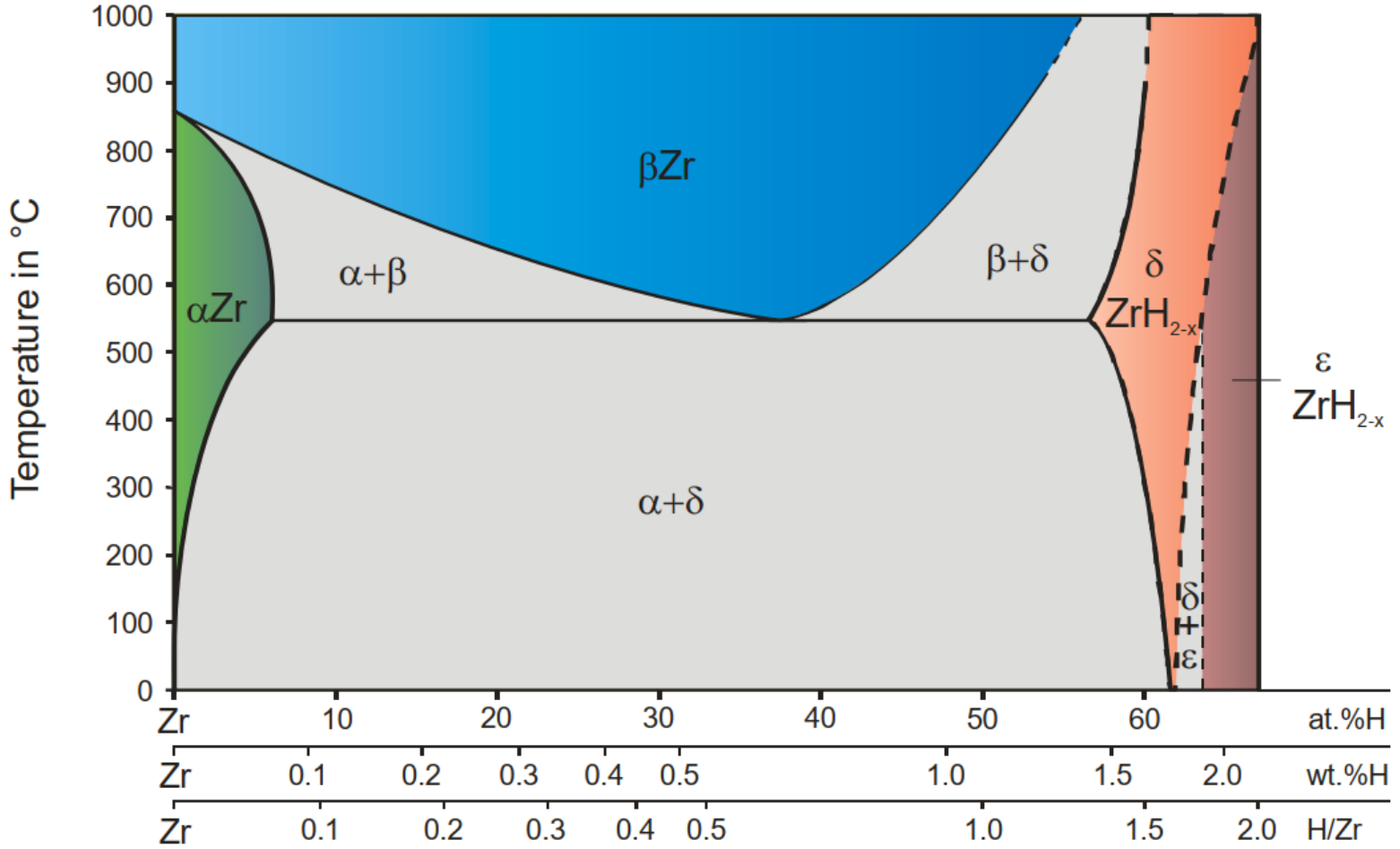

Hydrogen in zirconium cladding

- in β-Zr, hydrogen solubility is higher.

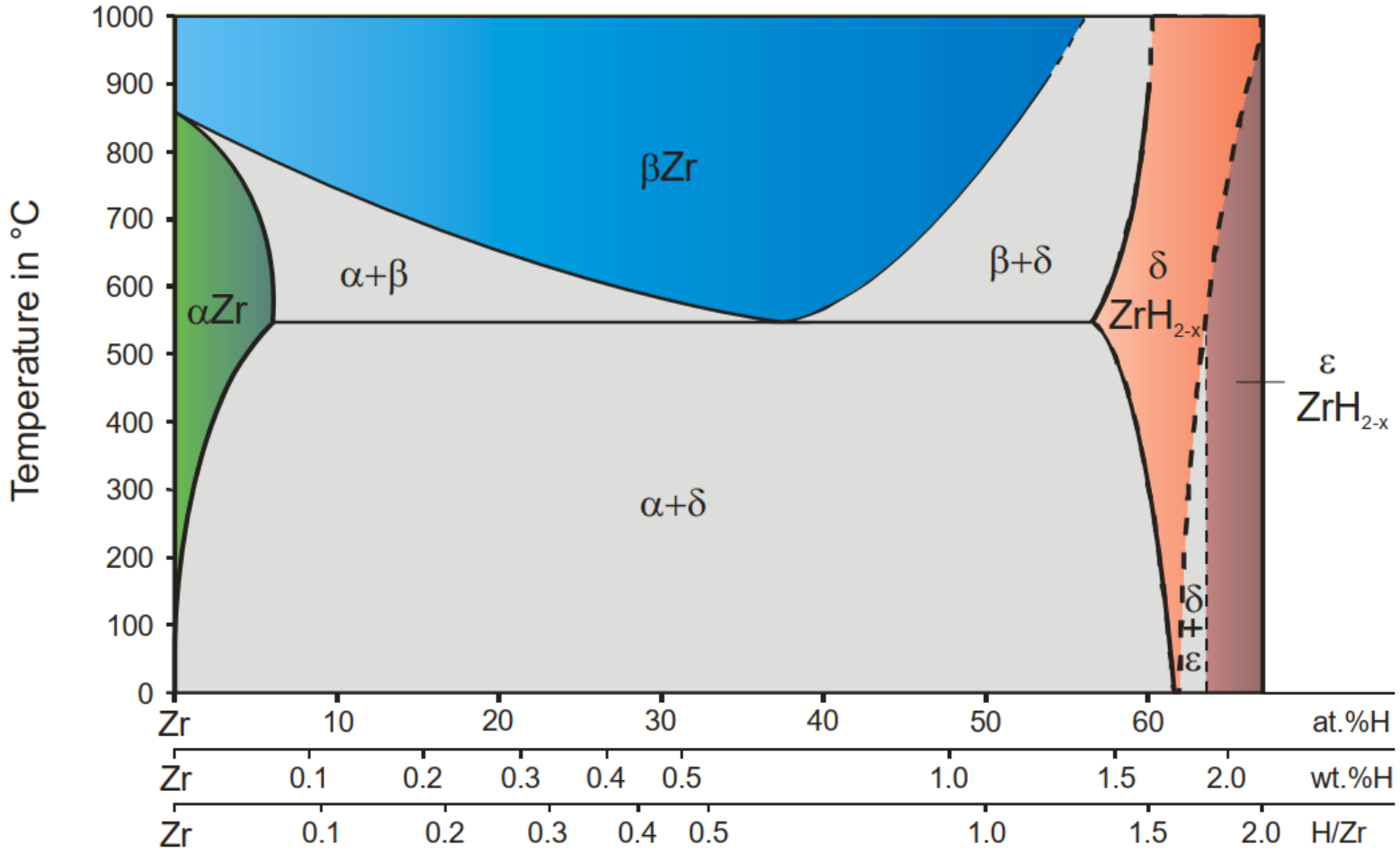

The objective of the study

High-resolution neutron imaging has been mainly limited to characterization of hydrogen in α-Zr.

The goals...

1. Is it possible to use high resolution imaging for the characterization of zirconium oxide and other Zr metal phases?

2. Quantify the hydrogen concentration in zirconium oxide and Zr metal phases after different oxidation tests.

Image credits: P. Fors - cladding

Test material

Material	Oxidation atmosphere	Oxidation temperature (°C)	Oxidation duration
Single material cladding (Zircaloy-4)	Steam	500	120h, 720 h
		800	12 h,
		1000	60 min, 90 min,
		1100	60 min, 90 min,
	Oxygen	500	120h, 720 h
		800	12 h
		1000	60 min, 90 min, 120 min
		1100	60 min, 90 min,

Test and characterization procedures

Non-irradiated Zry-4

Framatome

Oxidation tests

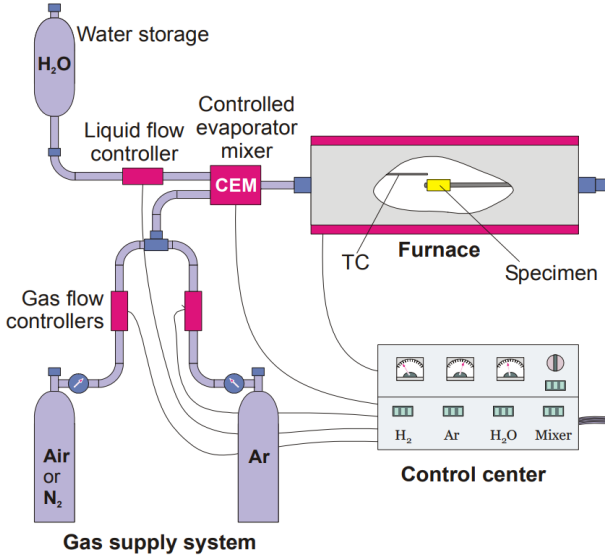

Oxidation at KIT

Experimental characterisations

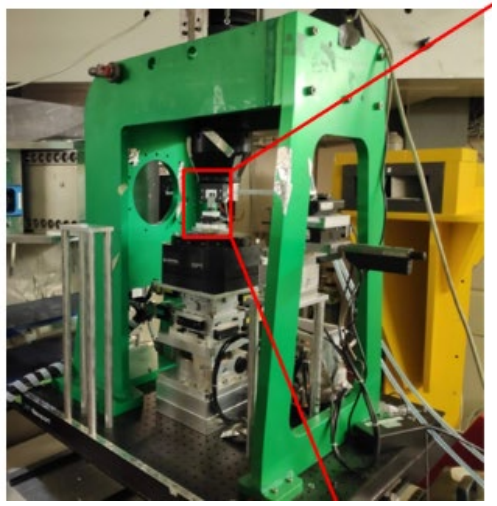

@ BOA, SINQ

Characterisations at PSI

Experimental method

Neutron imaging method

1 **PSI Neutron microscope detector, SINQ**

Spatial resolution: <10 µm

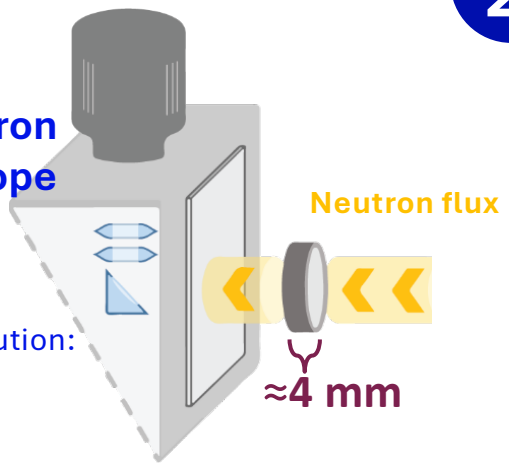

2 **Neutron image**

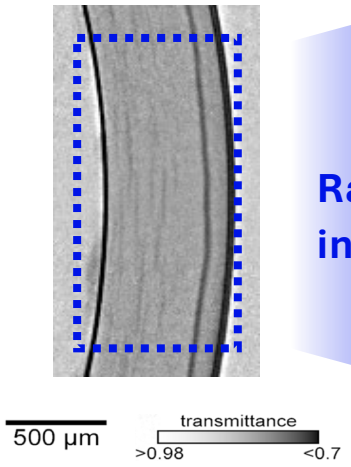

Radial integration

3 **Radial profile**

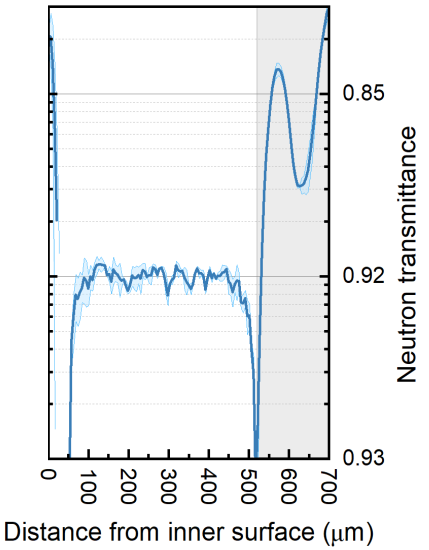

Attenuation coefficient for neutrons (25 meV), [cm^{-1}]

H	Zr
3.44	0.29

4 **Quantification**

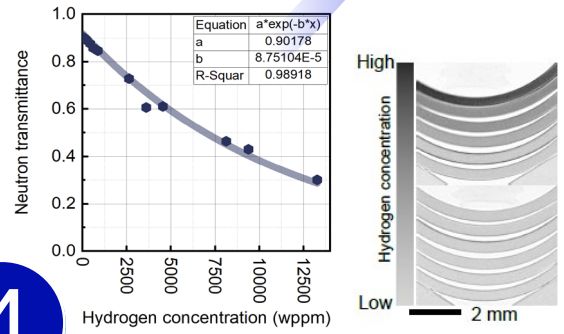

Beer-Lambert law

$$T(x,y) = \frac{I(x,y)}{I_0(x,y)} = \exp(-\sum_{total}(x,y) \cdot s)$$

$$\sum_{total}(x,y) = N_{\alpha-Zr}\sigma_{\alpha-Zr}(x,y) + N_H\sigma_H(x,y)$$

*Concentration sensitivity: ≈10 wppm

*Ref: Gong et al., 2019

Adaptation of characterization methods

1. Neutron imaging, SINQ PSI

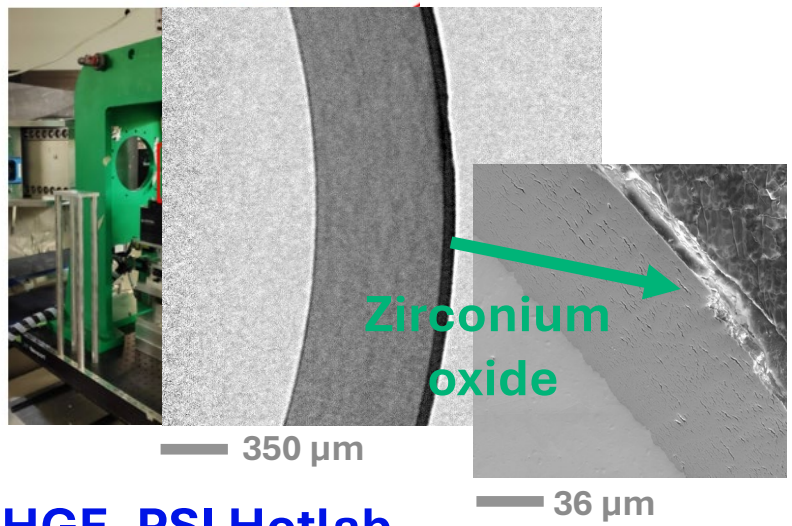

$$T(x,y) = exp(-\sum_{total}(x,y) \cdot s)$$

$T(x,y)$: *neutron transmittance*
$\sum_{total}$: *total neutron cross-section*
s: *sample thickness*

$$\sum_{total,\,oxide}(x,y) = N_{ZrO_2}\sigma_{ZrO_2}(x,y) + N_H\sigma_H(x,y) + N_{other}\sigma_{other}(x,y)$$

2. HGE, PSI Hotlab

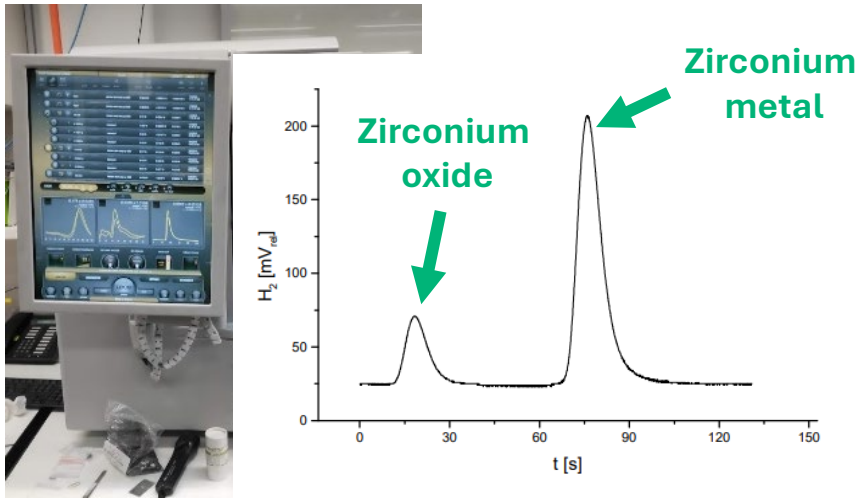

$$C_H^{sample} = (mass\ fraction).C_H^{oxide}$$

$$oxide\ mass\ fraction = \frac{\rho_{oxide}.V_{oxide}}{\rho_{oxide}.V_{oxide} + \rho_{metal}.V_{metal}}$$

Electron microscopy analysis

Phases: ZrO_2, α-Zr, α-Zr(O) α and (prior-)β Zr

Oxide formation strongly depends on temperature

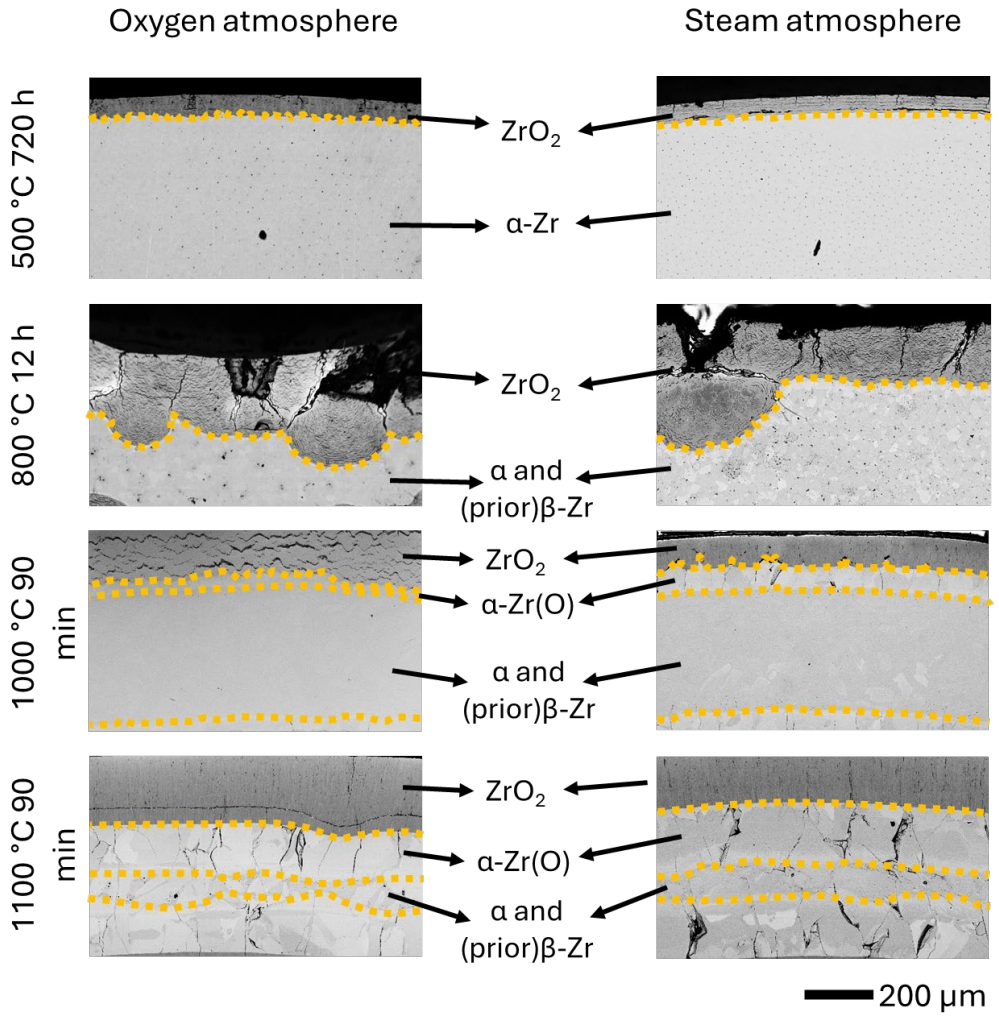

Results

Neutron radiography images

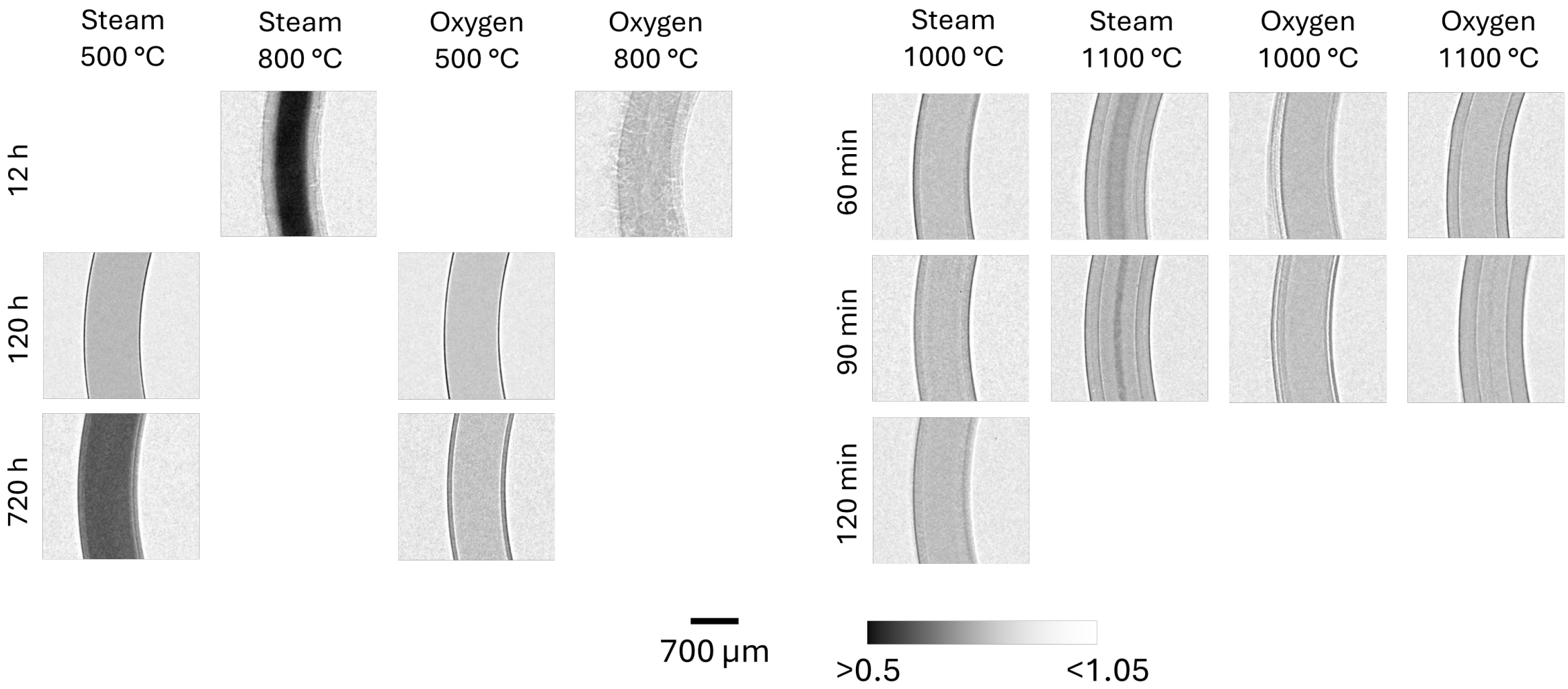

Elemental characterization of the α+(prior)β Zr phase

Diffusion of Cr and Fe into α+(prior)β Zr phase

Forms Zr (Fe, Cr)x phases

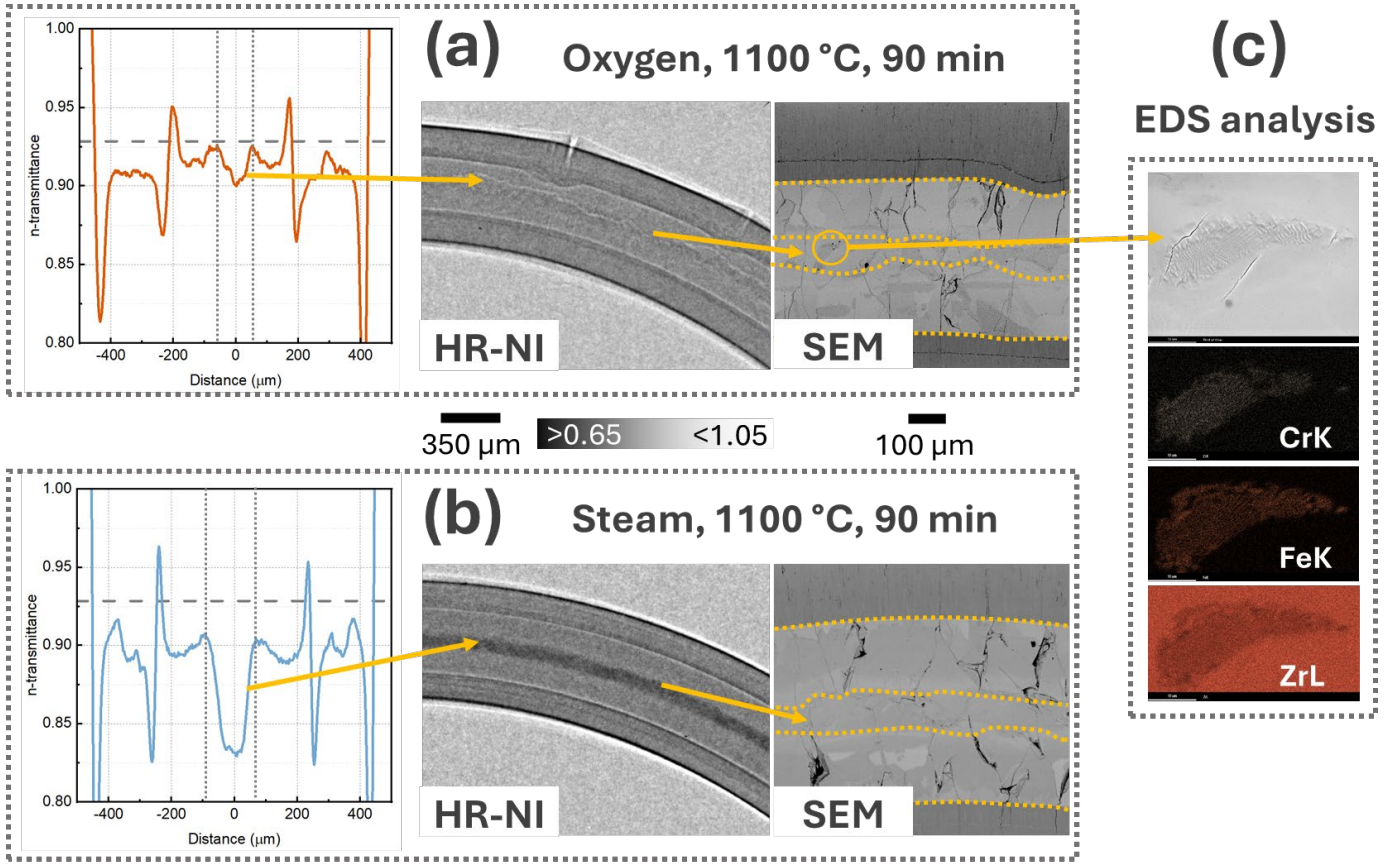

Hydrogen determination in zirconium oxide

What is the hydrogen concentration in zirconium oxide?

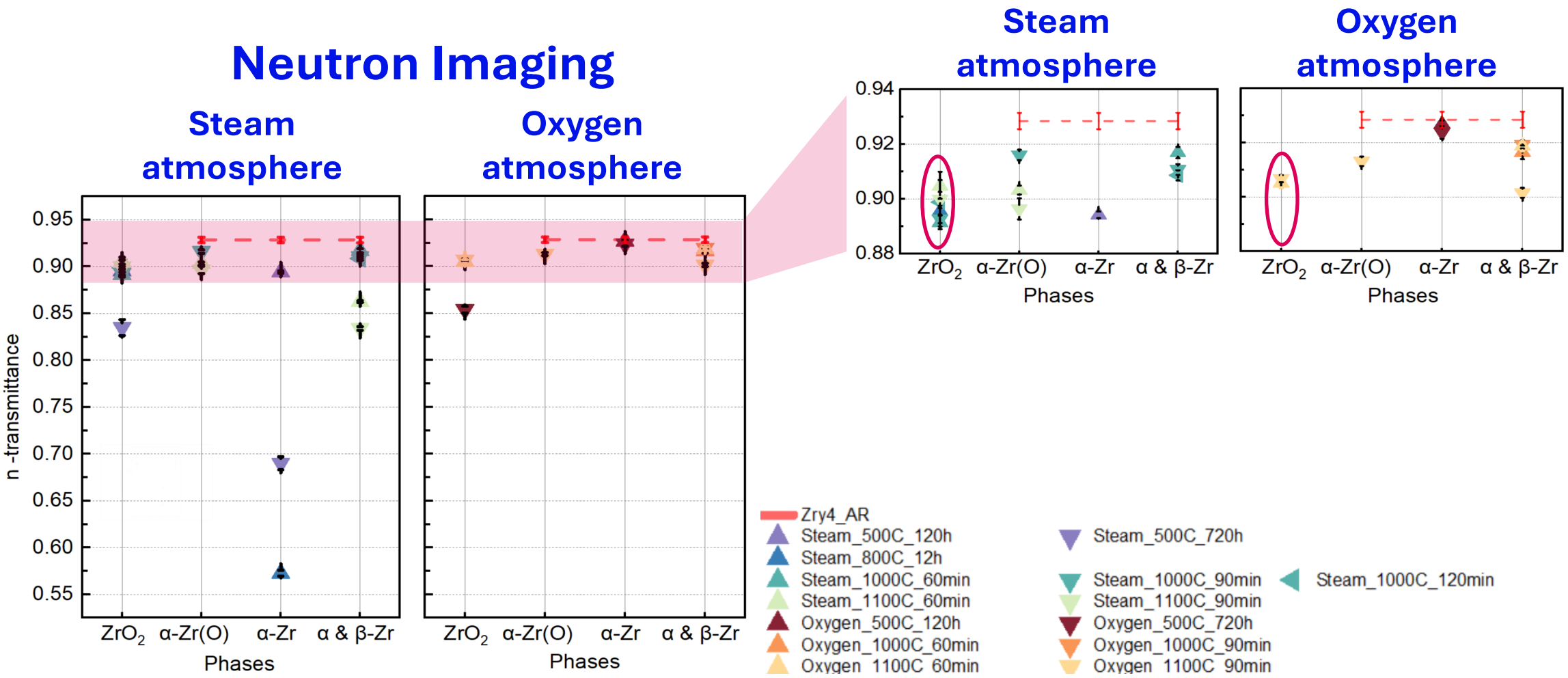

Hydrogen determination in zirconium oxide

Hot Gas Extraction

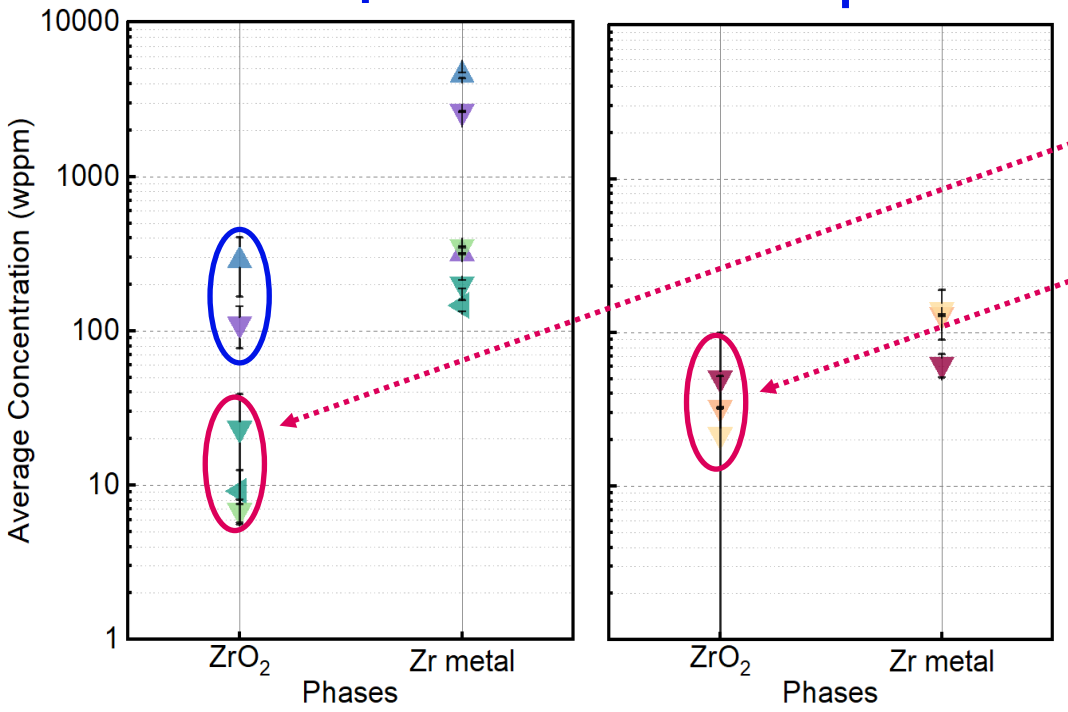

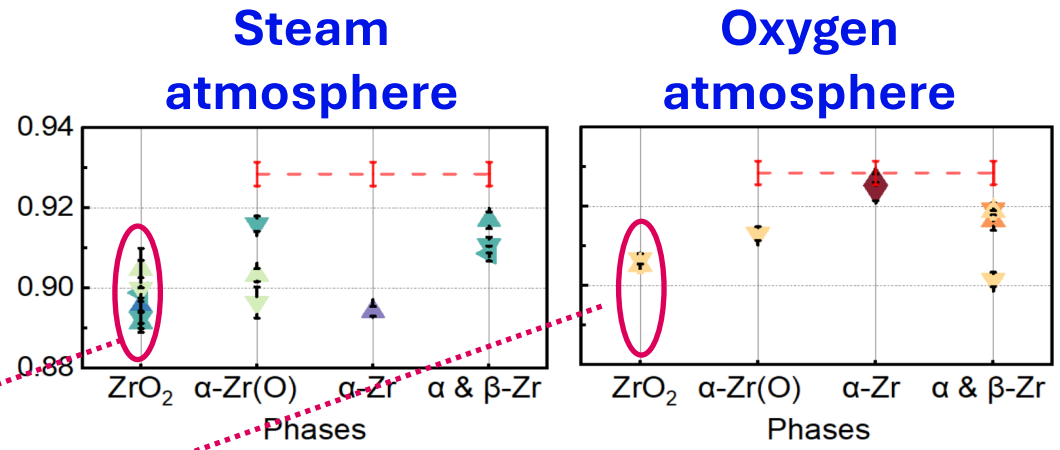

Hydrogen concentration in the oxide is typically less than 50 wppm.

At lower oxidation temperatures, hydrogen concentration in the oxide is measured higher (100 – 300 wppm).

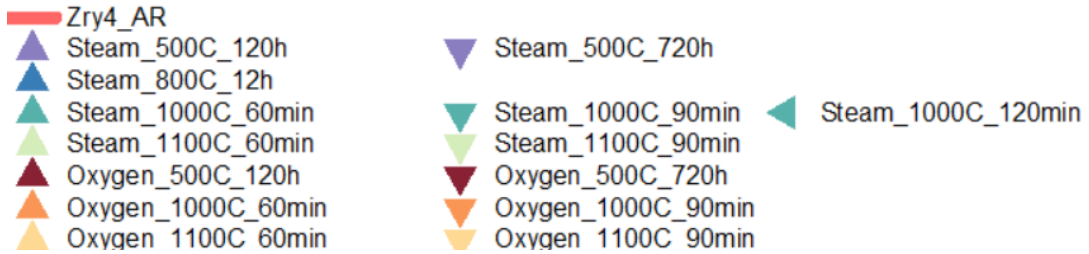

Results

Hydrogen diffusion into zirconium metal

Hot Gas Extraction

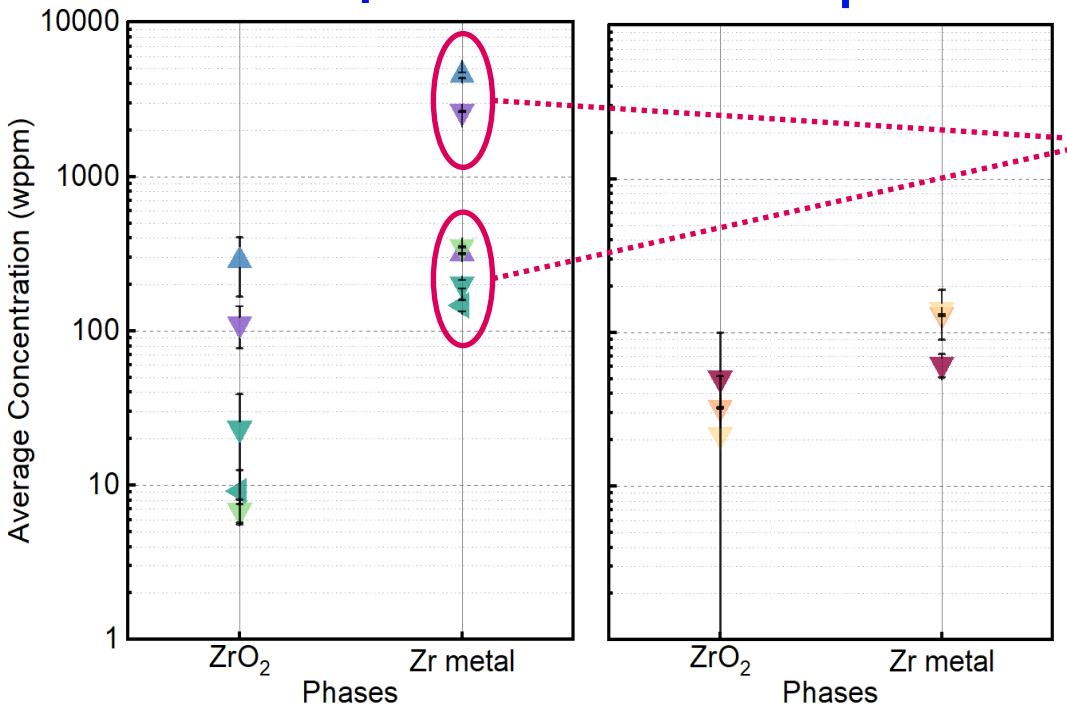

Depending on the oxide integrity:

Oxide can be a barrier

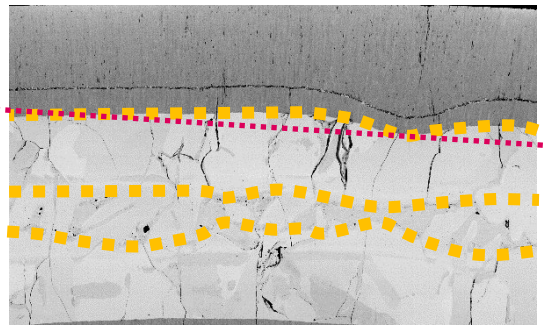

Oxide can be a highway

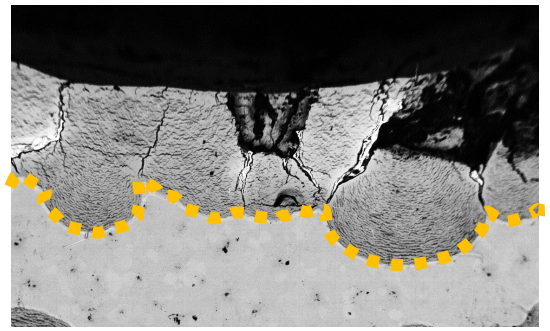

200 µm

However, hydrogen concentration was always measured higher in the metal than oxide under the given condition.

Results

Summary

1. The fraction of hydrogen concentrations at different phases by combining HR-NI and HGE methods is determined.
2. The sample deformation, large scale crack formation and phase thickness smaller than the spatial resolution limit high resolution neutron imaging.
3. For samples stored at room temperature, up to 50 wppm of hydrogen content was measured in the oxide independent to oxidation environment.
4. Higher hydrogen concentrations were measured in zirconium after oxide oxidized at 500 °C and 800 °C.
5. Radial cracks form in the oxide, acting like a path for hydrogen to reach the metal. In contrast, compact zirconium oxide layers prevent hydrogen diffusion into the zirconium metal.

PSI Center for Nuclear Engineering and Sciences

Take aways…

The application of HR-NI is extended to cladding samples oxidized at high-temperature conditions.

HR-NI can be a good complementary method for non-destructive hydrogen determination in high-temperature oxidation studies.

Acknowledgements

The authors would like to thank Framatome for providing the test material.

The work was cofounded by swissnuclear.

Scientific discussion and all technical support from different laboratories AHL, LNM, LNS.

Swiss spallation neutron source (SINQ) at Paul Scherrer Institute, Villigen, Switzerland.

okan.yetik@psi.ch

Sarah Weick

KIT

Hydrogen diffusion in dependence of the grain size of Zircaloy-4 cladding tubes

The diffusional behaviour of hydrogen in cladding tubes made of zirconium alloys during long-term dry storage of spent nuclear fuel elements in transport and storage casks are investigated in aims of the project SPIZWURZ. In order to investigate the influence of the grain size on the hydrogen diffusion within Zircaloy-4 cladding tubes, samples were pre-annealed at different T-t-conditions and then hydrogenated to investigate the post-hydride state.

This paper focuses on investigations of hydrogen diffusion dynamics in cladding tubes with regard to the grain size influence of the matrix. Zry-4 samples were pre-annealed at 400°C or 450°C for different times (1, 2, 4, 12, 24, 96h) and then hydrogenated in axial direction in contact to ZrH_2-powder for 3h at 400°C. After the hydrogenation process, the samples were analysed by metallography and then compared regarding their hydride amount, density and length. The resulting diffusion profiles and light microscopic images are presented in this paper. These reveal that the hydrogen diffusion is faster for smaller grains and that the hydride length increases and the hydride density is lowered after grain growth during the test conditions. A quantification of the diffusion will be obtained after neutron imaging investigations in December 2024.

Karlsruher Institut für Technologie

Hydrogen diffusion in dependence of the grain size of Zircaloy-4 cladding tubes

S. Weick, M. Grosse, R. Seropian, M. Steinbrueck

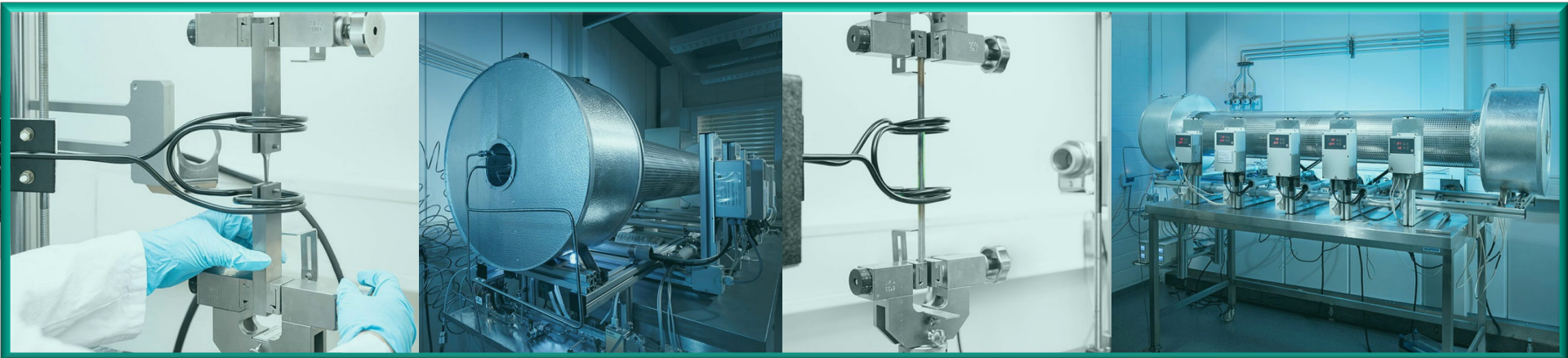

29th QUENCH workshop
19th – 21th November 2024, Karlsruhe, Germany

IAM-AWP-HTWC

Project

- **SPIZWURZ** = Spannungsinduzierte Wasserstoffumlagerung in Brennstabhüllrohren während längerfristiger Zwischenlagerung
  (Strain induced hydrogen redistribution in fuel cladding tubes during longterm interim storage)

- KIT/IAM-AWP & KIT/INE & GRS

Karlsruher Institut für Technologie

global research for safety

Bundesministerium für Umwelt, Naturschutz, nukleare Sicherheit und Verbraucherschutz

BGZ Gesellschaft für Zwischenlagerung mbH

- **Objective**: improvement & extension of experimental data base for modelling of degradation processes during dry storage

Setups

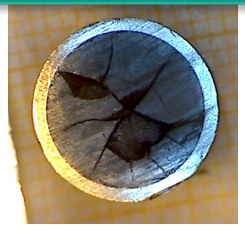

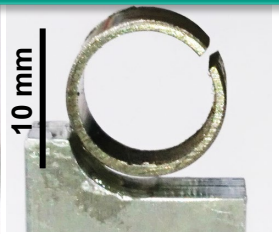

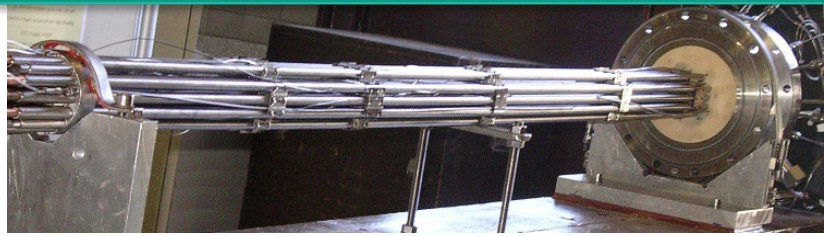

- **Single Effect Experiments**
  - → *samples*: 5 - 70 mm
  - → influences of texture & stress on H solubility & diffusion in Zry cladding tubes
  - → diffusion coefficients H

- **Fuel cladding interactions**
  - → *samples*:
    30 a dry storage; fuel rod (Zry-4 + UO_2) from PWR Gösgen, CH; 50.4 GWd/tHM
  - → elastic & residual plastic strain diameter
  - → measurements before and after defueling

- **QUENCH Bundle Test**
  - → *samples*: 2.5 m
  - → interim storage conditions (100-400°C; 70/96 MPa, 100/300 wt.ppm H)
  - → long-term 250 d (May 23 – Jan 24)
  - → modelling & code validation (benchmark)

Karlsruher Institut für Technologie

Zry-4 – as recieved

- Different grain orientation in *c*- and *a*-axis due to manufacturing
- Hexagonal Zr structure

Kim et al., 2023

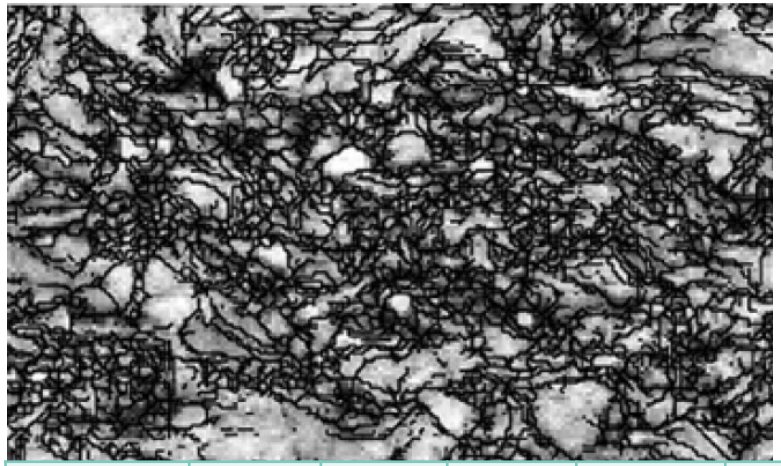

alloy	Sn [wt.%]	Fe [wt.%]	Cr [wt.%]	Nb [wt.%]	O [wt.%]
Zry-4	1.3	0.2	0.1	-	0.13

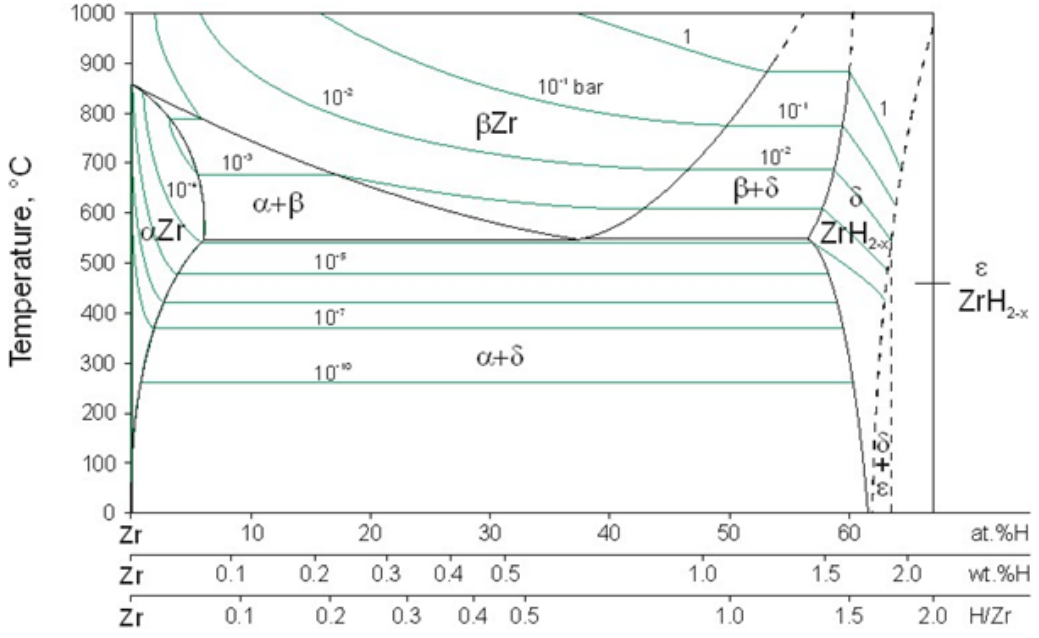

Grosse-et-al., 2020 after Steinbrück, 2004

Previous diffusion experiments

- Contact to ZrH_2 powder, Ar

$$c(x,t) = c_0\left(1 - erf\left(\frac{x}{2\sqrt{Dt}}\right)\right) + c_i$$

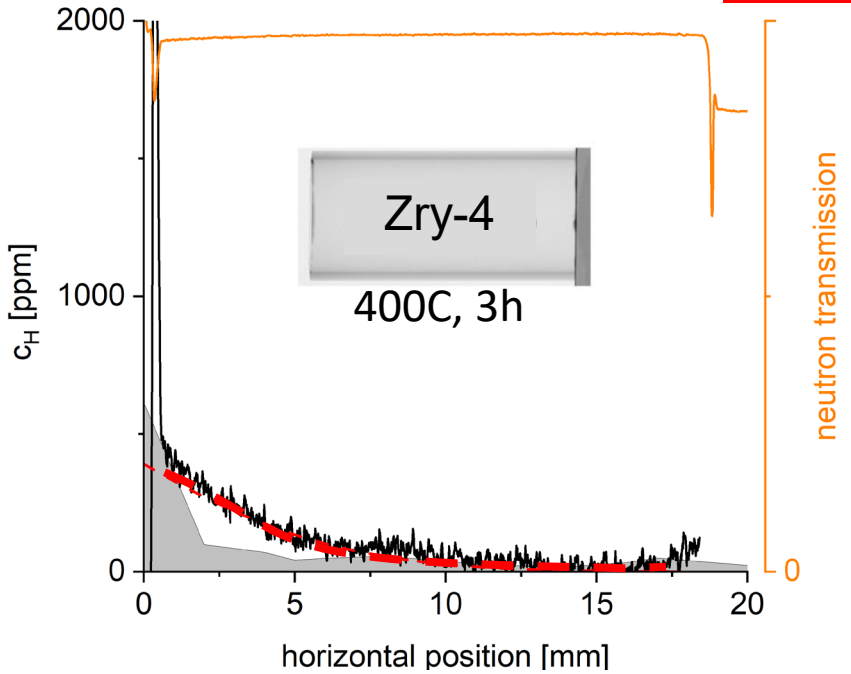

?

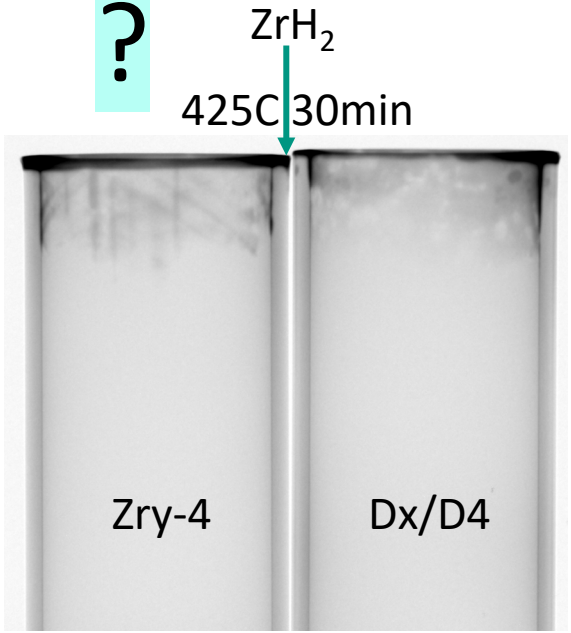

Temperature dependent grain size change

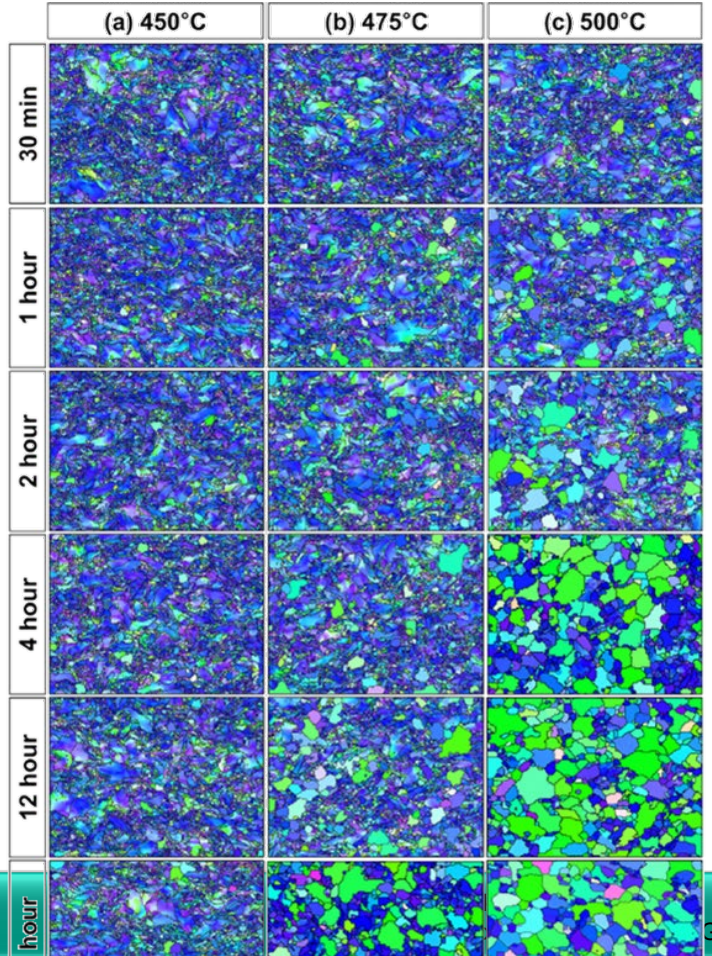

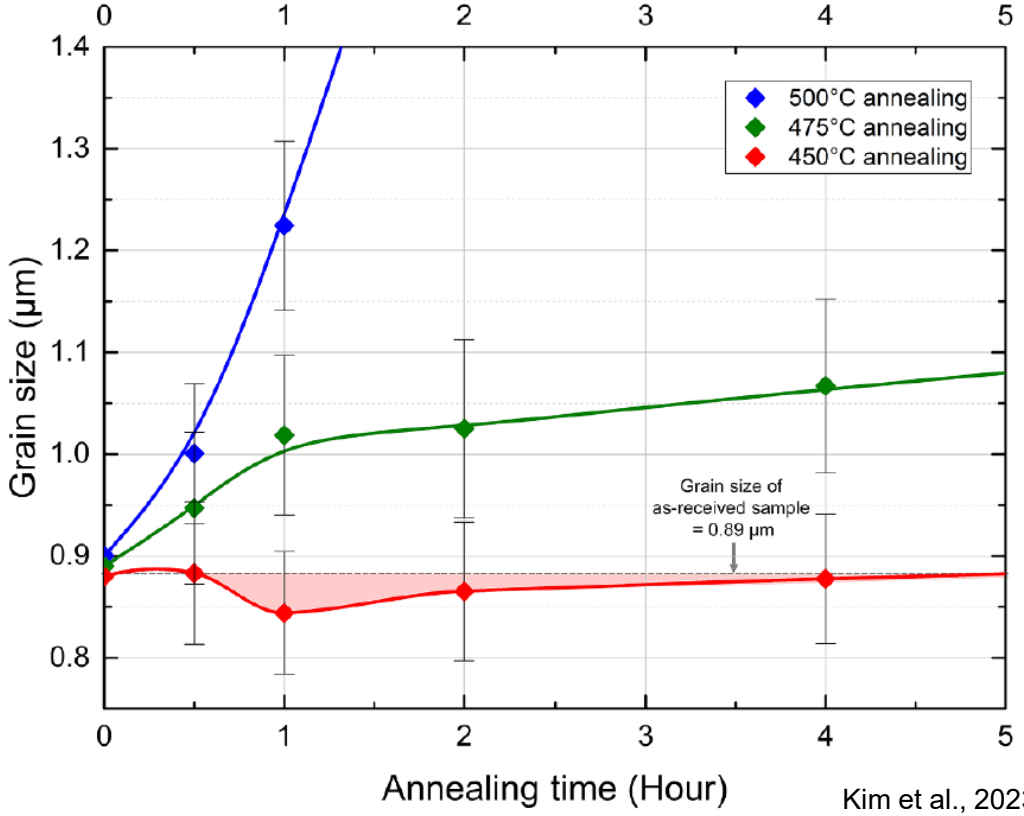

Kim et al., 2023

Hydrogenation

- Different diffusion velocities in *c*- and *a*-axis
- Hydrogenation in axial (*c*-axis) direction
- Pre-oxidation essential

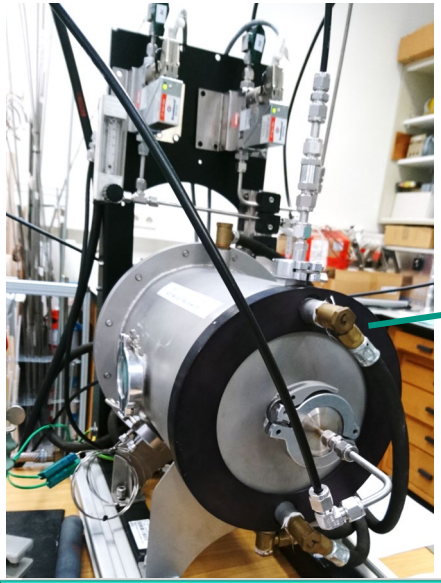

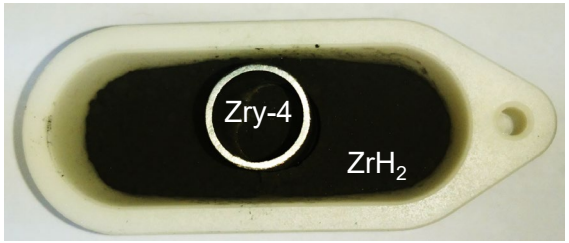

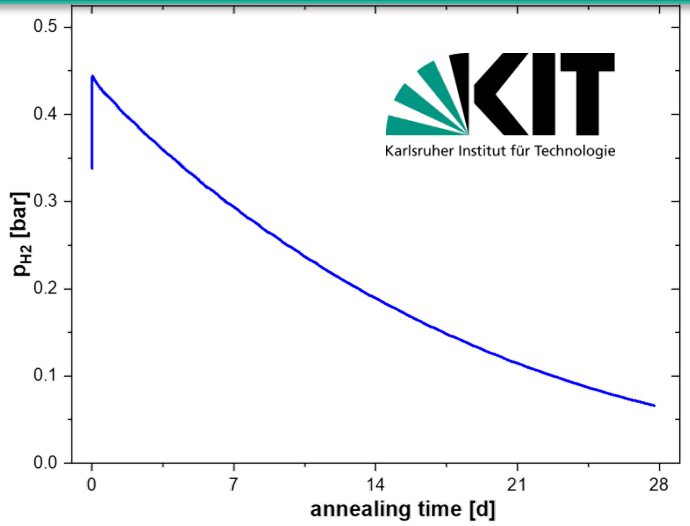

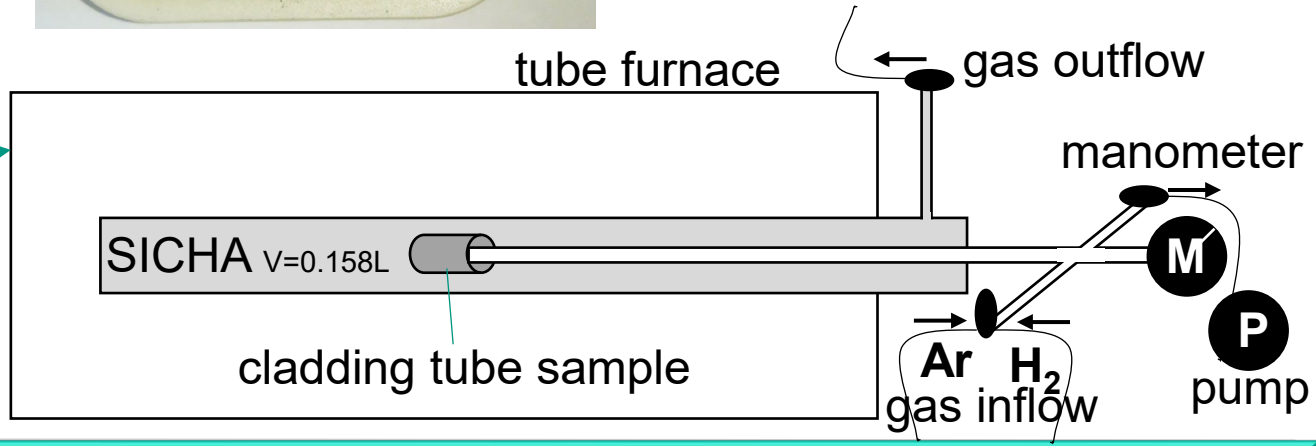

Grain size dependent hydrogen diffusion in axial direction

- Pre-annealed in Ar at 400°C or 450°C
- Hydrogenated at 400°C, 3h

Pre-annealing t [h]	400°C	450°C
1	x	x
2	x	x
4	x	x
12	x	x
24	x	x
96	x	x

ZrH_2, 400°C, 3h →

Post-hydrogenation observations
Smaller hydrides + higher hydride density
Longer hydrides + lower hydride density

Metallography

400°C, 2h

t

400°C, 96h

Longer hydrides &
lower hydride density

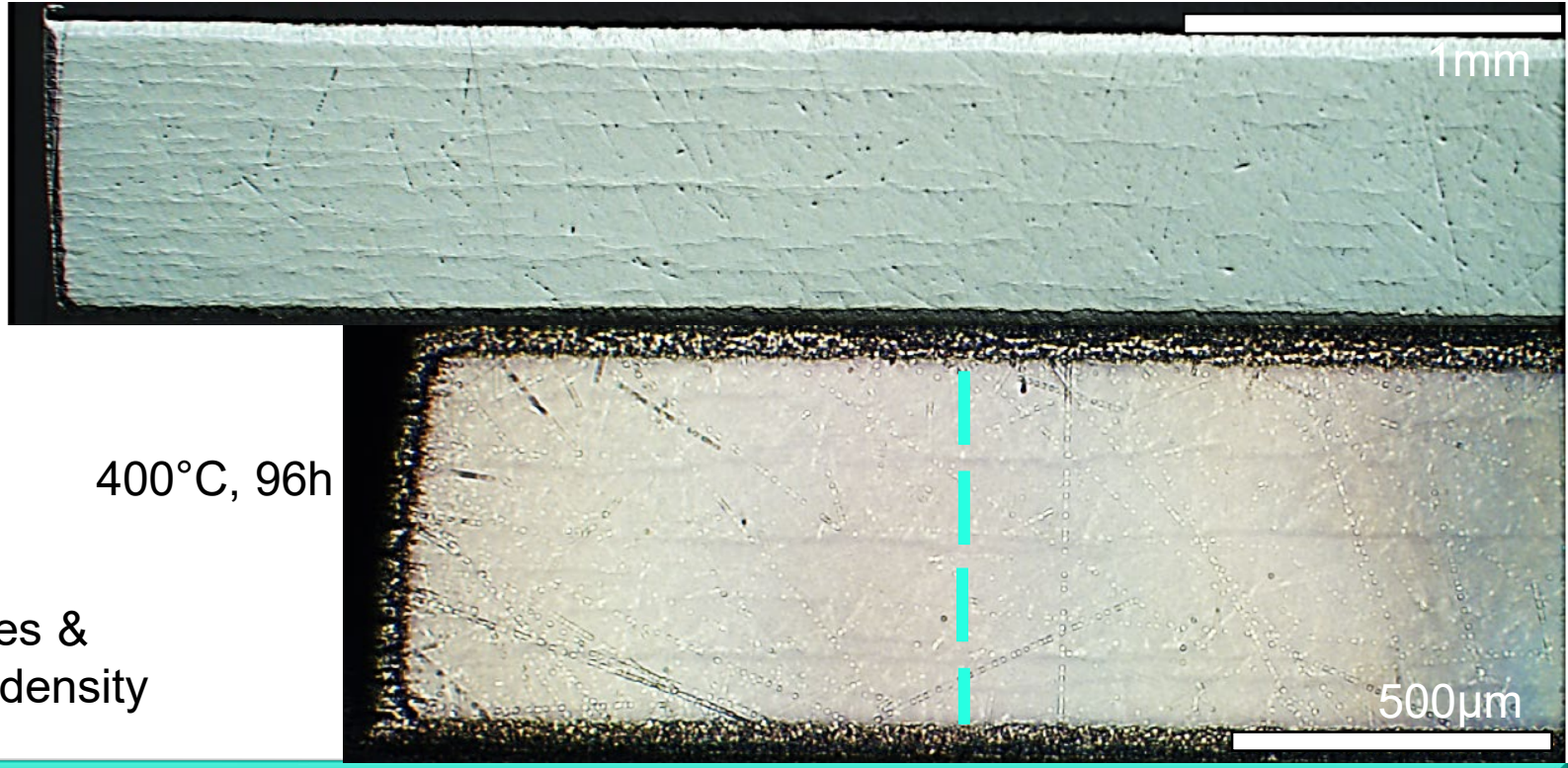

Diffusion profiles

- Faster hydrogen diffusion with 450°C pre-annealing c.t. 400°C
- Fastest/ highest hydrogen diffusion at 1h (smaller grains)

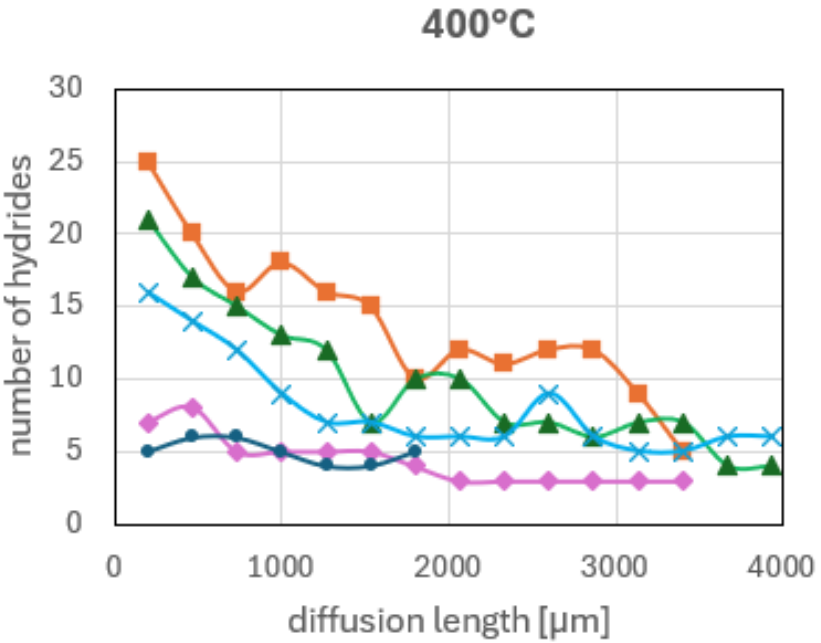

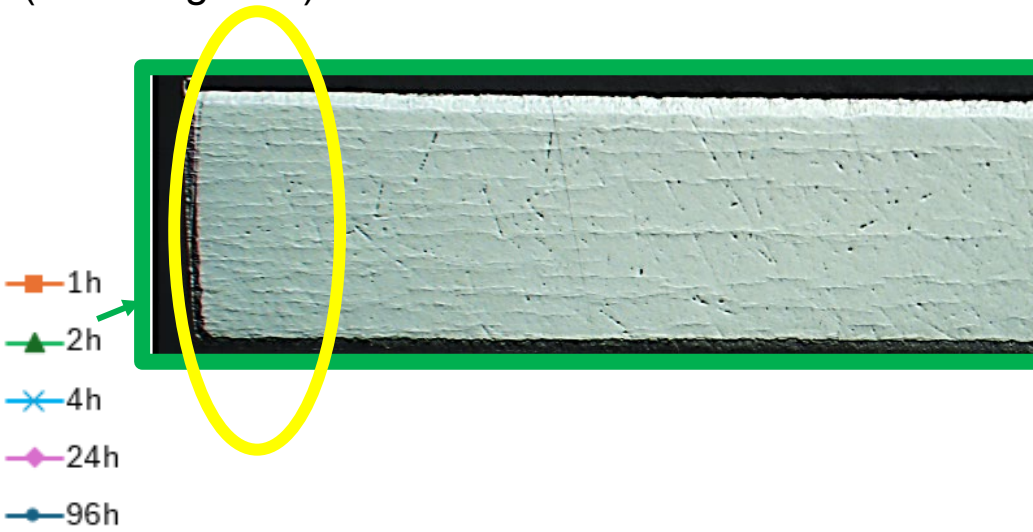

Conclusion

- Grain size dependent hydrogen diffusion in axial direction

→ Different hydrogen diffusion speed c.t. former experiments without pre-annealing
→ Faster hydrogen diffusion with 450°C pre-annealing c.t. 400°C
→ Fastest/ highest hydrogen diffusion with smaller grains
→ With increasing grain size increasing hydride length and lower hydride density

→ grain size influences hydrogen diffusion in Zry-4 strongly
(grain boundary diffusion)

Karlsruher Institut für Technologie

Outlook

- Single Effect Experiments

hydrogen diffusion
→ in axial cladding tube direction, in circumferential direction
→ in dependence of grain size (T dependent)
→ in dependence of elastic stress (in-situ)

→ in Zr single crystals
(*next beamtime: NR at IMAT, ISIS*)

Karlsruher Institut für Technologie

Acknowledgements

- KIT/IAM-AWP
- PSI
- The SPIZWURZ project (FKZ 1501609B) is funded by the Federal Ministry for the Environment, Nature Conservation, Nuclear Safety and Consumer Protection (BMUV)

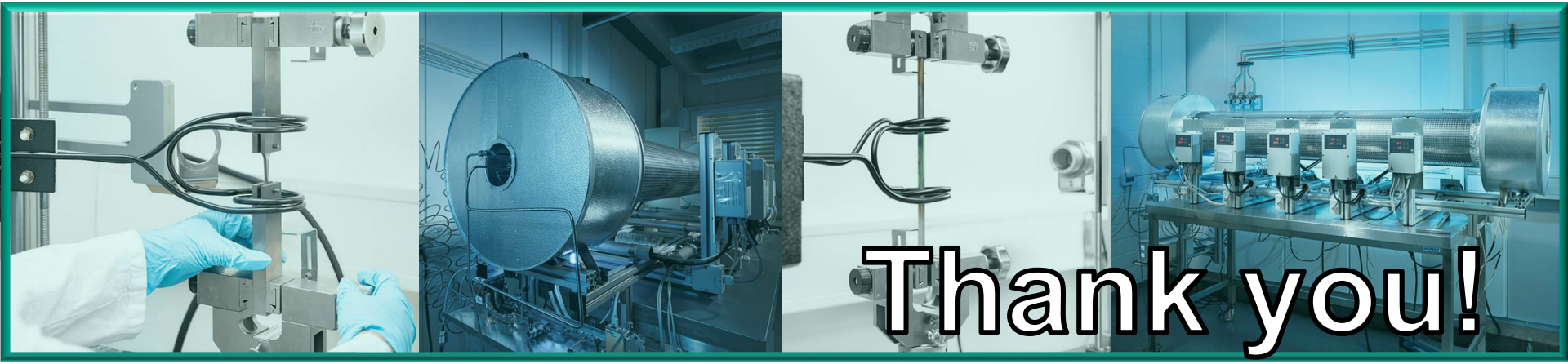

Mikhail Kolesnik

KIT

Hydride orientation in fuel rod cladding: comparison of two competing simulation approaches

Hydride embrittlement of cladding tubes is one of the most dangerous mechanisms limiting spent fuel dry storage regimes. The degree of hydride embrittlement in zirconium alloys is strongly dependent on the morphology of the plate-like hydrides, which includes orientation, length and spacing. Under certain conditions, the degree of embrittlement at the end of dry storage can be higher than before due to reorientation of hydrides as a result of the thermomechanical cycle with dissolution and reprecipitation under tensile hoop stresses in the cladding tube. Therefore, the safety justification of the thermomechanical regime during dry storage requires the estimation of the hydride morphology at the end of storage. Currently, there are two most popular approaches to simulate the orientation of hydrides developed for the needs of the nuclear industry. The first approach assumes that the growth of macroscale hydrides is predominantly due to the nucleation of new nanoscale hydrides and estimates the fraction of radially oriented hydrides based on the classical theory of heterogeneous nucleation. The second approach considers the stress threshold for the start of reorientation as a material constant which can depend on the parameters of the thermal cycle, according to engineering correlations. This discrepancy in assumptions leads to different interpretations of the role of instantaneous temperature in the orientation of precipitating hydrides. Nevertheless, both approaches are able to predict the hydride orientation with satisfactory accuracy after the typical thermomechanical cycles used in laboratory experiments. The possible effect for dry storage applications, as well as thermomechanical regimes where different approaches give different results, are discussed in the presentation.

Karlsruhe Institute of Technology

IAM
Institute for Applied Materials

Hydride orientation in fuel rod cladding: comparison of two competing simulation approaches

M. Kolesnik

29th International QUENCH –Workshop, Karlsruhe, Germany

Institute for Applied Materials; Program NUSAFE

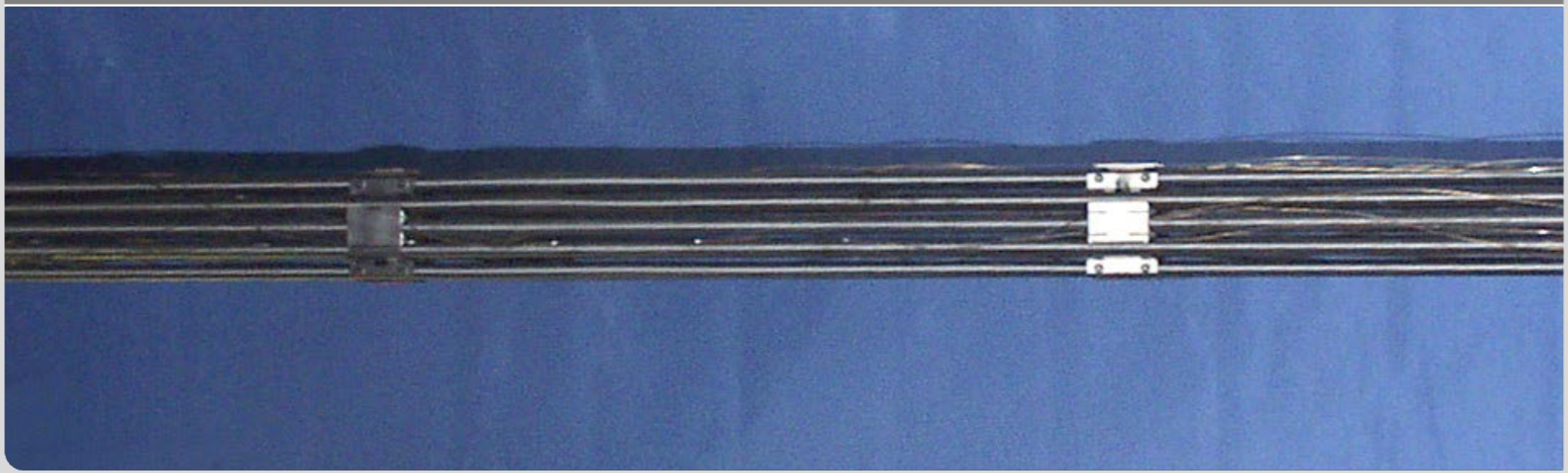

Hydride embrittlement in zirconium alloys
the role of orientation

σ

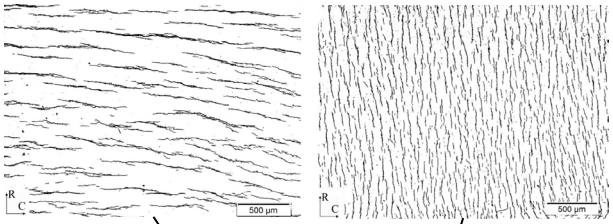

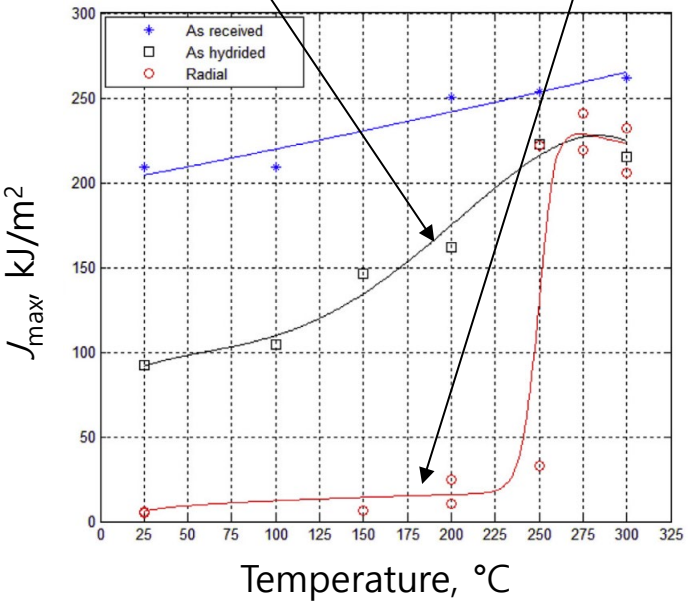

[1], Zircaloy-4

σ

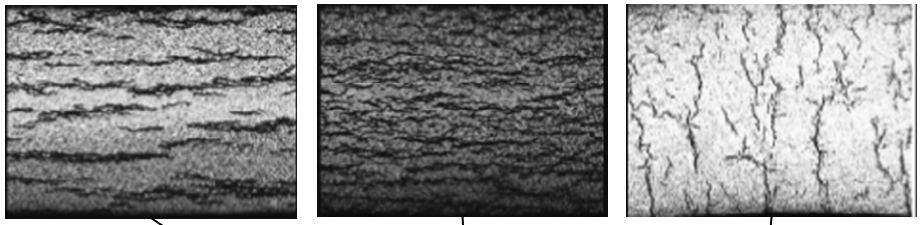

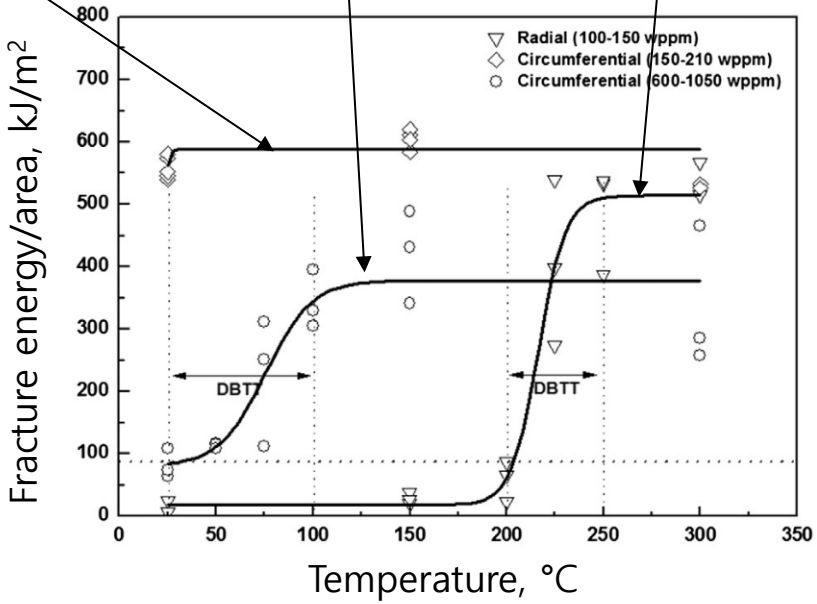

[2], Zr-2.5Nb

[1] R. Sharma *et al.*, *J. Nucl. Mat.* 488 (2017) 231 – 244, DOI: 10.1016/j.jnucmat.2017.03.025
[2] J. Kim *et al.*, *J. Nucl. Mat.* 456 (2015) 235 – 245, DOI: 10.1016/j.jnucmat.2014.09.025

Reorientation of hydrides
radial hydride fraction (RHF) and reorientation curve

Hydride reorientation requires thermal cycle with dissolution and re-precipitation of hydrides

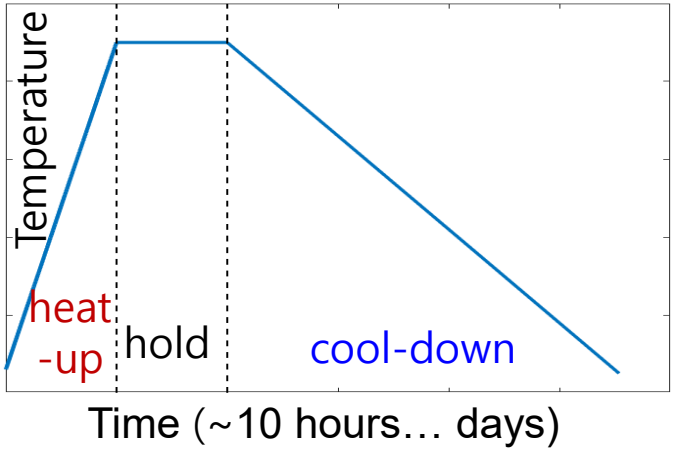

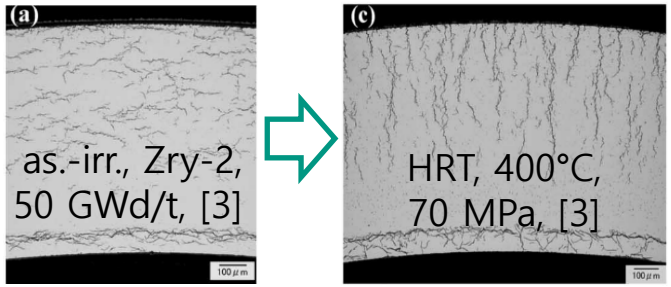

circumferential radial

Reorientation curves: the reoriented hydride fraction has a threshold dependence on the external stress applied during cooling

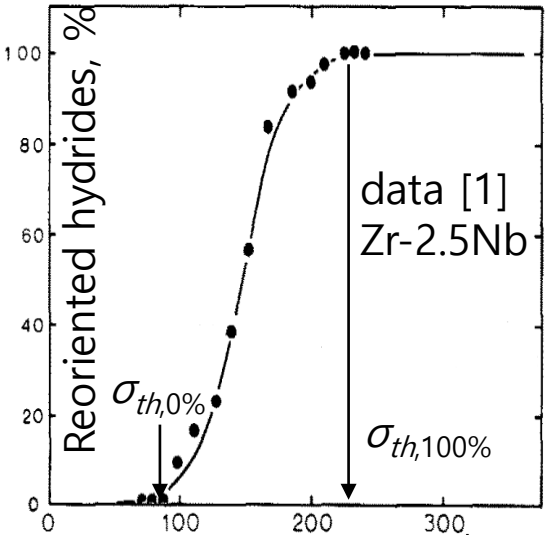

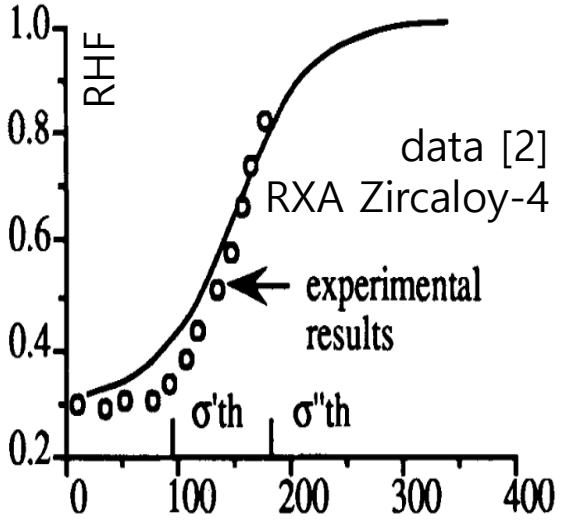

[1] D. Hardie and M. Shanahan, *J. Nucl. Mat.* 55 (1975) 1 – 13, DOI: 10.1016/0022-3115(75)90132-4
[2] J.B. Bai *et al.*, *Met. & Mat. Trans. A* 25 (1994) 1199 – 1208, DOI: 10.1007/BF02652294
[3] M. Aomi *et al.*, *J. of ASTM Int.*, 5 (2008) 651 – 673, DOI: 10.1520/JAI101262

Approach 1 overview
physically-based

Main assumptions:

- macroscale hydride consists of micro- and nanoscale ones
- macroscale hydride growth due to nucleation of new micro- and nanoscale ones

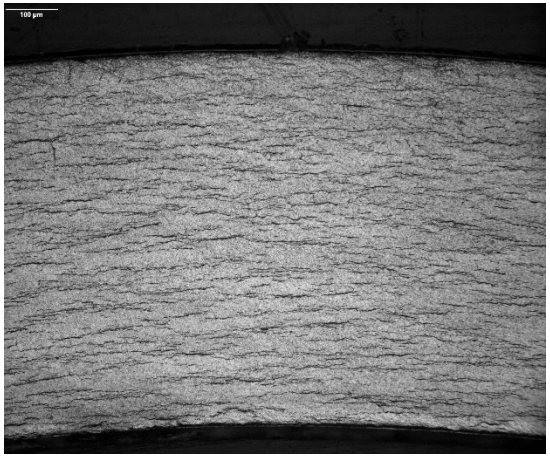

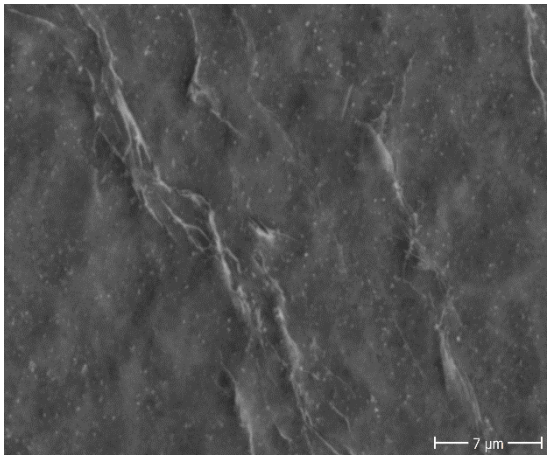

Fraction of radially-oriented hydrides:

$$F_{r1} = \frac{R_r}{R_r + R_c} = \frac{1}{1 + f_0 \cdot \exp\left(-\sigma \cdot \Omega / kT\right)}$$

where the nucleation frequency:

$$R \sim Z j_n \cdot \exp\left(-\Delta G^* / kT\right)$$

with an additional assumption: $\Delta G_c^* - \Delta G_r^* = \sigma \cdot \Omega$

Kinetic extension:

$$\mathrm{d}C_r = -F_{r1} \cdot \mathrm{d}C_s$$

The fraction of radial hydrides at the current time step is a function of the instantaneous σ/T

Approach 2 overview
based on engineering correlations

Main assumptions:

- stress thresholds are postulated as model parameters
- radial hydride fraction is a polyline function of stresses

$$F_{r2} = \begin{cases} 0, & \sigma \le \sigma_{th,0\%} \\ \dfrac{\sigma - \sigma_{th,0\%}}{\sigma_{th,100\%} - \sigma_{th,0\%}}, & \sigma_{th,0\%} \le \sigma \le \sigma_{th,100\%} \\ 1, & \sigma \ge \sigma_{th,100\%} \end{cases}$$

Thresholds can be defined as constants or correlations to thermocycle parameters:

$$\sigma_{th,0\%} = 0.02 \cdot [\mathrm{H}] + 186.9 - 0.386 \cdot \min(T_{\max}, T_{SSD})$$

$$\sigma_{th,100\%} = 110 + 65 \cdot \left(1 - \exp\left(-[\mathrm{H}]/65\right)\right)$$

Additional assumption for kinetic extension:

on the current time step F_r is the same as the cumulative reorientation curve estimated after experiment with constant stresses during cooling

$$\mathrm{d}C_r = -F_{r2} \cdot \mathrm{d}C_s$$

The fraction of radial hydrides at the current time step is a function of the instantaneous σ^*

*during cooling for a single thermomechanical cycle (i.e. for determined [H] and T_{max})

The spread of approaches

The affiliation of a model to a particular approach is related to the type of F_r function, which is the most fundamental assumption

Approach 1, $F_{r1}(\sigma/T)$

1. C.E. Ells, *J. Nucl. Mat.* 35 (1970) 306 – 315, DOI: 10.1016/0022-3115(70)90214-X
2. D. Hardie and M. Shanahan, *J. Nucl. Mat.* 55 (1975) 1 – 13, DOI: 10.1016/0022-3115(75)90132-4
3. J.B. Bai *et al.*, *Met. & Mat. Trans. A* 25 (1994) 1199 – 1208, DOI: 10.1007/BF02652294
4. K. Chan, *J. Nucl. Mat.* 227 (1996) 220-236, DOI: 10.1016/0022-3115(95)00160-3
5. J.Y.R. Rashid and A.J. Machiels, 10th ICEM05-1038, Glasgow, (2005)
6. A.R. Massih and L.O. Jernkvist, *Comp. Mat. Sci.* 46 (2009) 1091 – 1097, DOI: 10.1016/j.commatsci.2009.05.025
7. M. Kolesnik *et al.*, *Comp. Mat. Sci.* 189 (2021) 110260, DOI: 10.1016/j.commatsci.2020.110260

Approach 2, $F_{r2}(\sigma)$

1. J. Desquines *et al.*, *J. Nucl. Mat.*, 453 (2014) 131-150, DOI: 10.1016/j.jnucmat.2014.06.049
2. F. Feria *et al.*, *Ann. Nucl. En.*, 145 (2020) 107559, DOI: 10.1016/j.anucene.2020.107559
3. M. Grosse *et al.*, *Nucl. Eng. and Tech.*, (2023), DOI: 10.1016/j.net.2023.09.027
4. P. Konarski *et al.*, *Nucl. Eng. and Tech.* 56 (2024) 728 – 744, DOI: 10.1016/j.net.2023.11.012

The main goal of the current study: to investigate the pure effect of the assumption about the type of F_r function

"Basic" models
unified models used for comparison of approaches

Dissolution, $T < T_{SSD}$, $C_s < C_d$

$$\begin{cases} \dfrac{dC_s}{dt} = \dfrac{dC_d}{dt} \\ \dfrac{dC_r}{dt} = -\dfrac{C_r}{C_r + C_c} \cdot \dfrac{dC_s}{dt} \\ \dfrac{dC_c}{dt} = -\dfrac{C_c}{C_r + C_c} \cdot \dfrac{dC_s}{dt} \end{cases}$$

Precipitation, $T < T_{SSP}$, $C_s > C_p$

$$\begin{cases} \dfrac{dC_s}{dt} = \dfrac{dC_p}{dt} \\ \dfrac{dC_r}{dt} = -F_r \cdot \dfrac{dC_s}{dt} \\ \dfrac{dC_c}{dt} = -(1 - F_r) \cdot \dfrac{dC_s}{dt} \end{cases}$$

The only difference between two "basic" models – the type of the F_r function

Alloy	Appr.	Param.	Value
SRA Zircaloy-4	1	f_0	10^2
		$\Delta\Omega$	$2.3 \cdot 10^{-28}$ [m^3]
	2	$\sigma_{th,0\%}$	70 [MPa]
		$\sigma_{th,100\%}$	210 [MPa]
	both	C_d	$1.28 \cdot 10^5 \cdot \exp(-36540/RT)$
		C_p	$6.91 \cdot 10^4 \cdot \exp(-29900/RT)$

Alloy	Appr.	Param.	Value
Zr-2.5Nb	1	f_0	10^4
		$\Delta\Omega$	$4.34 \cdot 10^{-28}$ [m^3]
	2	$\sigma_{th,0\%}$	90 [MPa]
		$\sigma_{th,100\%}$	200 [MPa]
	both	C_d	$4.4 \cdot 10^5 \cdot \exp(-44606/RT)$
		C_p	$2.473 \cdot 10^4 \cdot \exp(-25840/RT)$

Comparison with experiments
a reorientation test with constant external stresses

Samples: Zr-2.5Nb plate, subjected to a thermomechanical test with constant external stresses

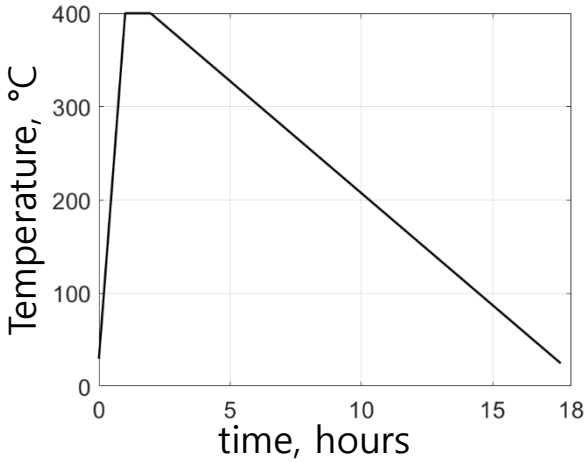

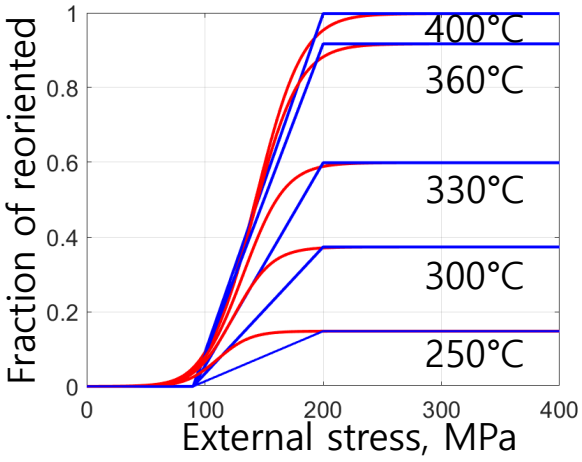

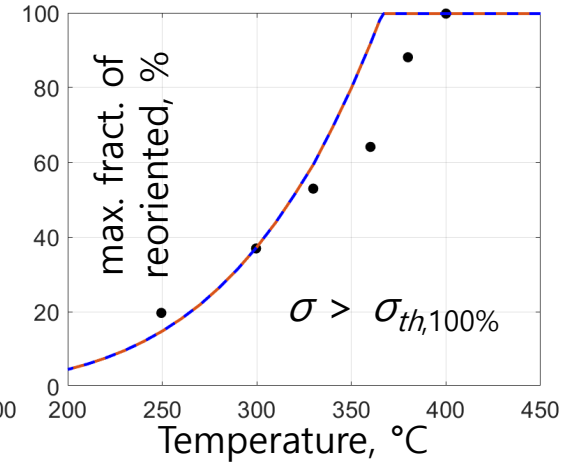

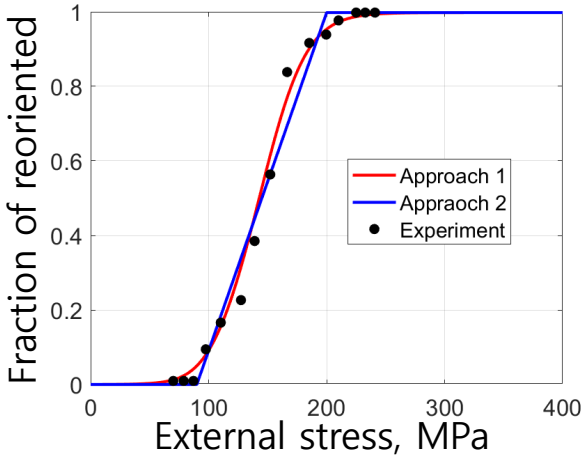

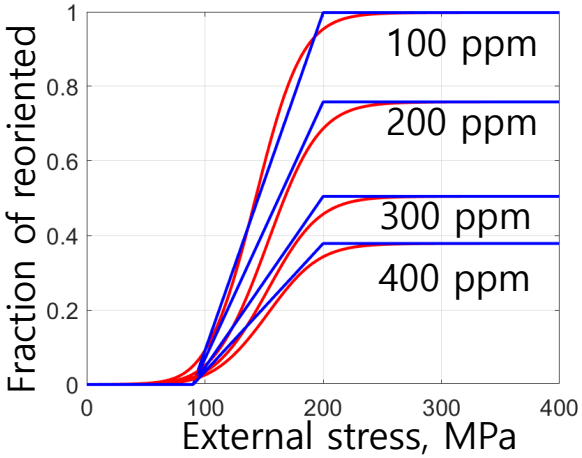

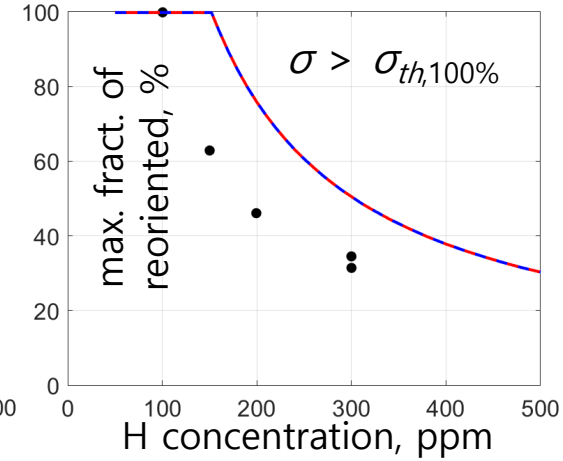

Exp. data: D. Hardie and M. Shanahan, *J. Nucl. Mat.* 55 (1975) 1 – 13, DOI: 10.1016/0022-3115(75)90132-4

Comparison with experiments
RHF dependence on decompression rate

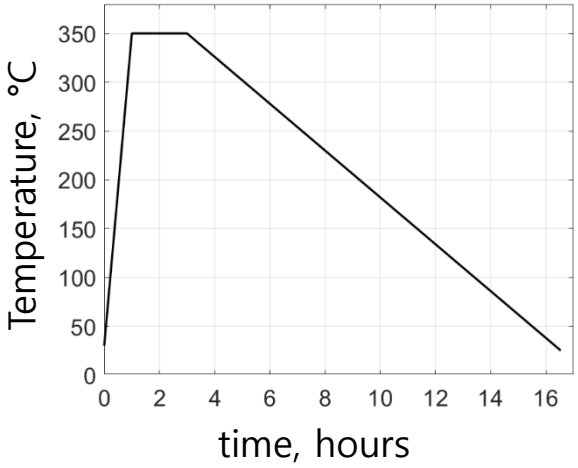

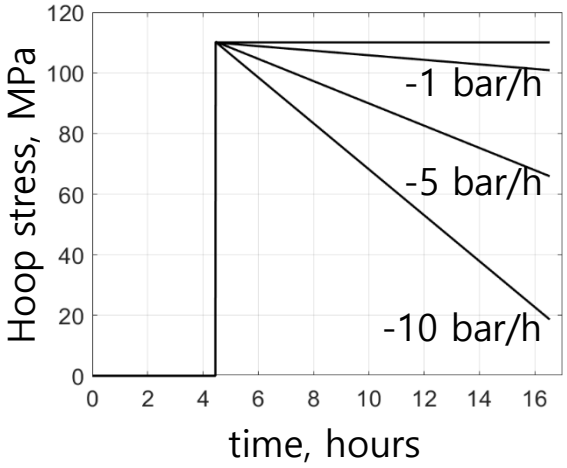

Alloy: SRA Zircaloy-4
Samples: gas-filled tubes

Feature: variation of the decompression rate

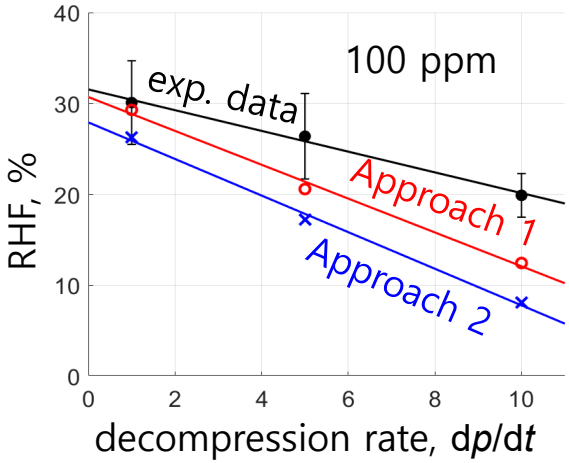

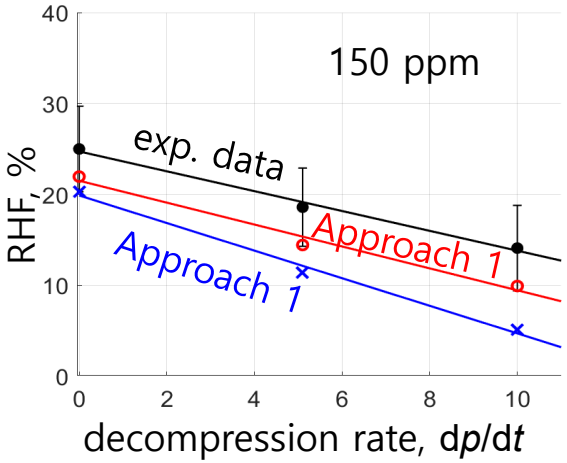

[H], ppm	Slope ΔRHF/Δ(d*p*/d*t*)		
	Exp.	Appr. 1	Appr. 2
100	1.14	1.86	2.01
150	1.09	1.20	1.52

Exp. data: J. Desquines *et al.*, *Proc. WRFPM 2023,* 80 – 86, DOI: 10.1007/978-981-99-7157-2_8

Comparison of simulation results
instantaneous parameters

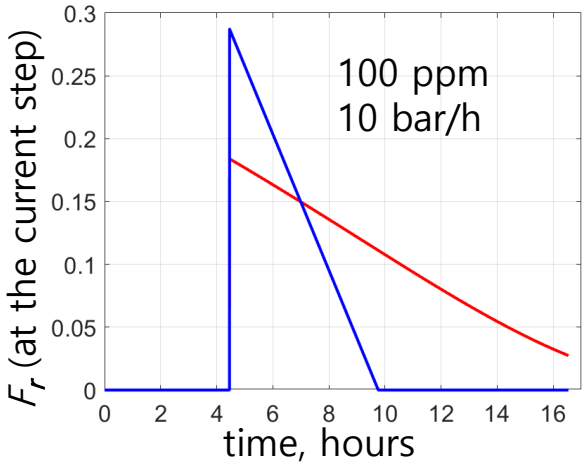

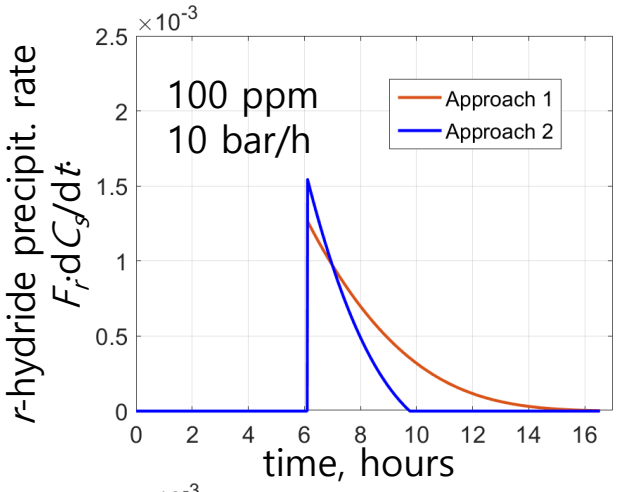

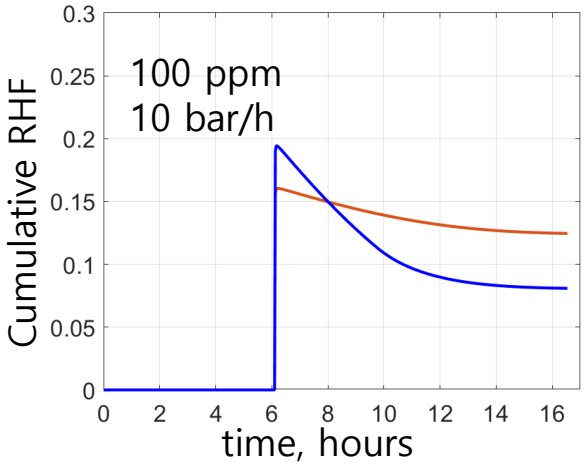

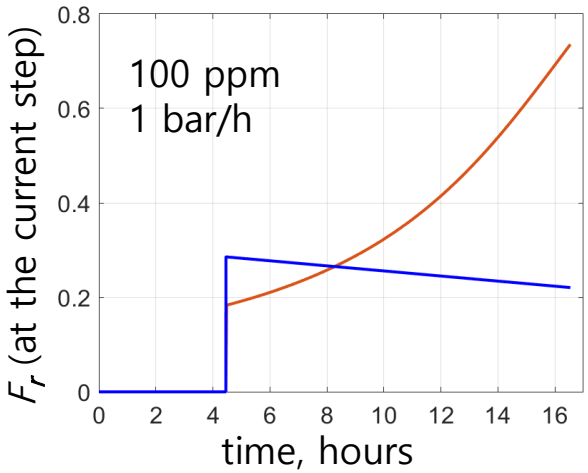

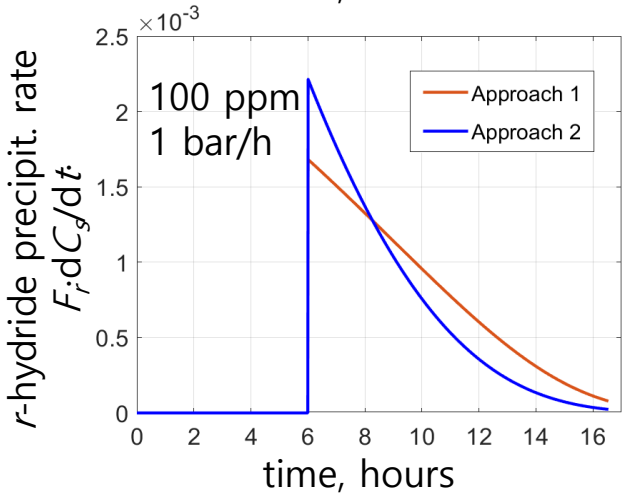

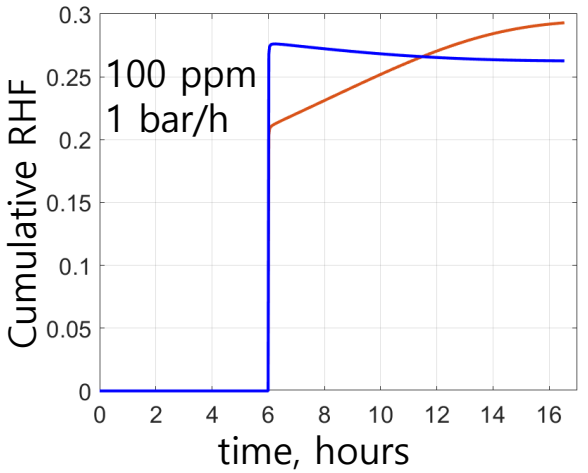

Approach 1 assumes a higher role of low-temperature precipitation in reorientation process in comparison with Approach 2

The effect of temperature on the reorientation process

scenario 1

Samples: SRA Zircaloy-4 hydrogenated up to 240 ppm

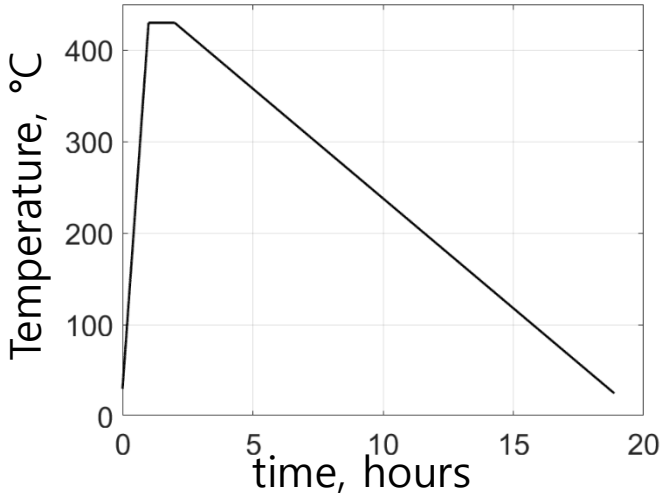

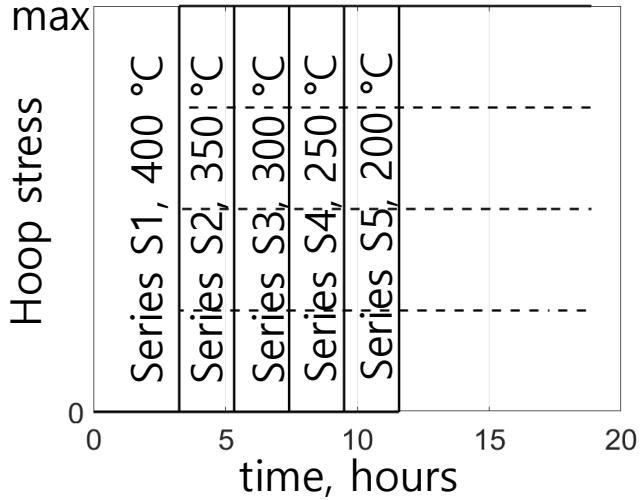

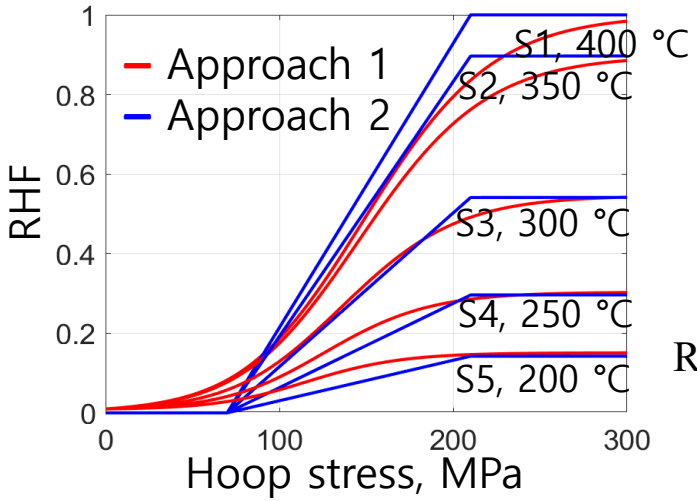

renormalization

$$\mathrm{RHF}_{\mathrm{renorm}} = \frac{\mathrm{RHF}}{\max(\mathrm{RHF})}$$

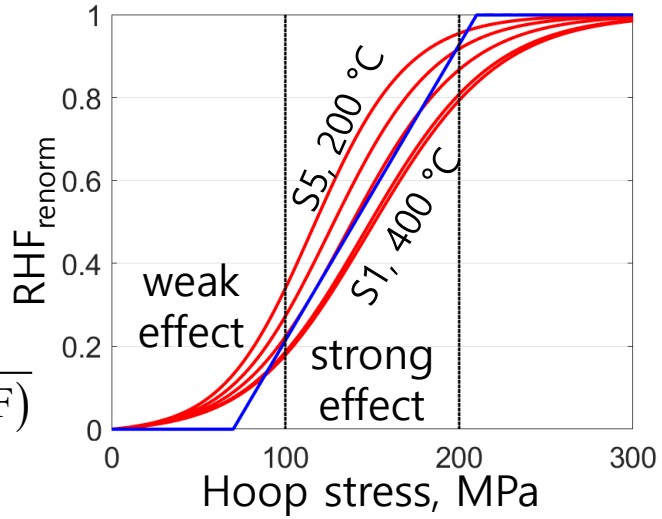

The effect of temperature on the reorientation process
scenario 2

Samples: SRA Zircaloy-4 hydrogenated up to 240 ppm

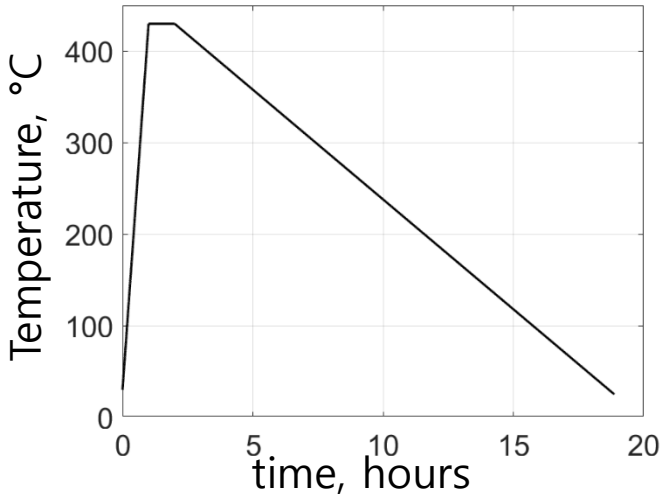

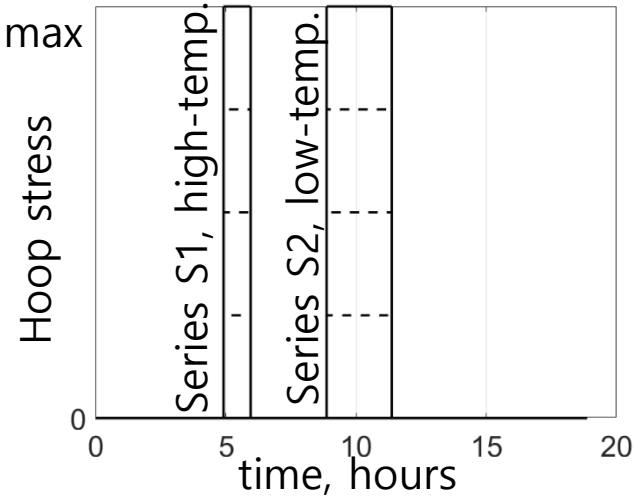

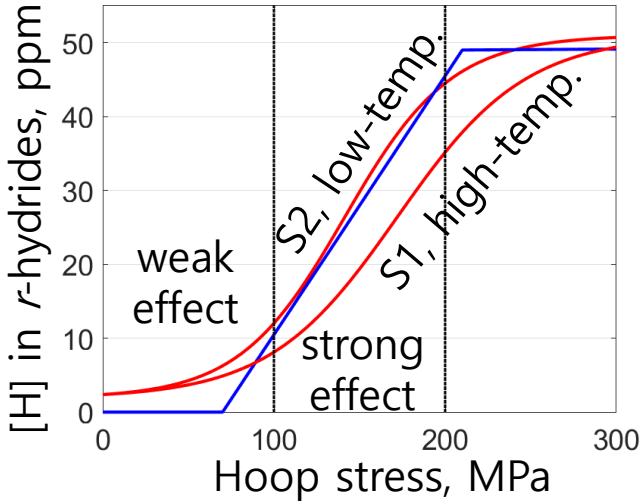

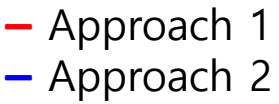

The effect for dry storage

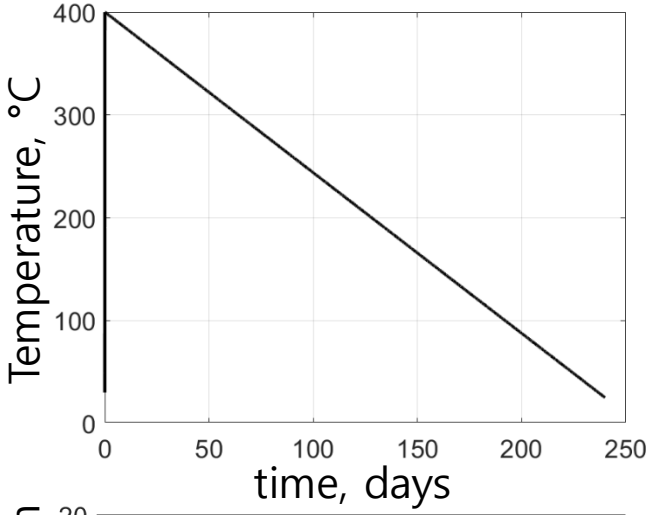

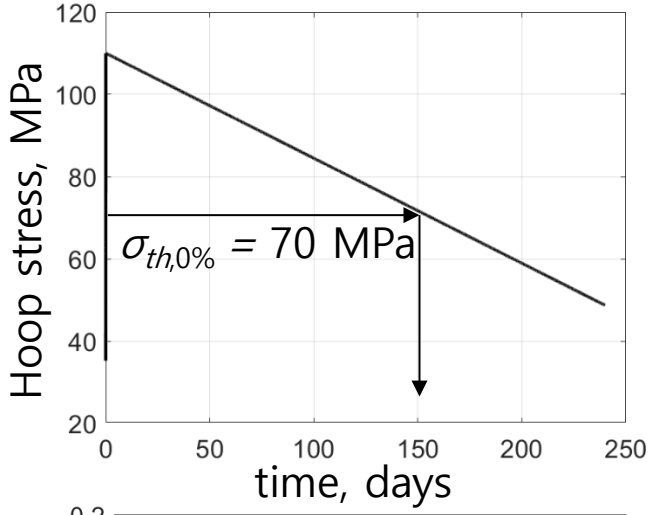

Simulation conditions:

Alloy: SRA Zircaloy-4
[H]: 100 ppm
Load: $\sigma/T = const$

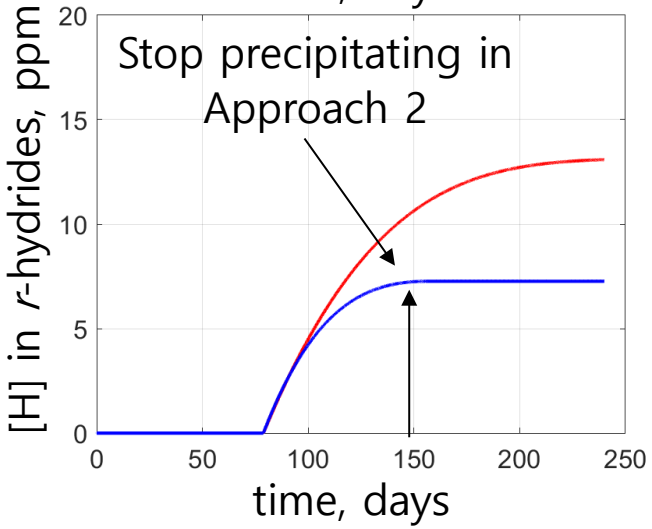

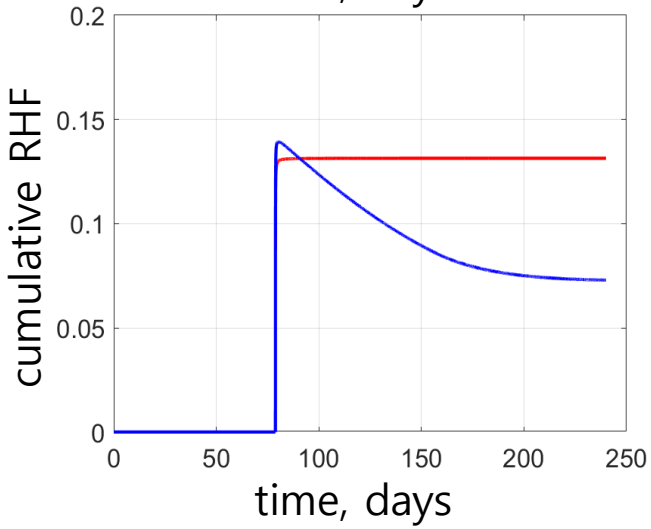

- Approach 1, $F_{r1}(\sigma/T)$
- Approach 2, $F_{r2}(\sigma)$

Approach 2 assumes that radial hydrides can stop precipitating at low temperatures, unlike Approach 1

Conclusion

- Two approaches assume different dependence of instantaneous RHF on the parameters: in Approach 1 $F_{r1} = F_{r1}(\sigma / T)$, while in Approach 2 $F_{r2} = F_{r2}(\sigma)$;
- Approach 1 assumes a higher role of hydride precipitation at low temperatures in the reorientation process compared to Approach 2.
- Both approaches are able to simulate the typical reorientation experiments with satisfactory accuracy (i.e. to predict the integral RHF after the test).
- Under dry storage conditions, Approach 2 may underestimate the amount of radial hydrides precipitated at low temperatures in the end of dry storage compared to Approach 1.
- Two thermomechanical scenarios have been proposed and can be used in experiments to compare the role of hydrides precipitated at low and high temperatures.

Thank you for your attention

https://www.iam.kit.edu/awp/english/163.php

http://quench.forschung.kit.edu/

Participants of the 29th International QUENCH Workshop
19 - 21 November 2024, KIT, Germany

29th International QUENCH Workshop - Participants

Family Name	First Name	Institution	Country	e-mail
Bae	Jaeyoon	KIT	Germany	jaeyoon.bae@partner.kit.edu
Bales	Michelle	Nuclear Energy Agency	France	Michelle.BALES@oecd-nea.org
Becker	Maarten	Institut für Umwelttechnologien und Strahlenschutz GmbH	Germany	Becker@ius-online.eu
Bertsch	Johannes	PSI	Switzerland	johannes.bertsch@psi.ch
Bochtler	Peter	Federal Office for the Safety of Nuclear Waste Management (BASE)	Germany	peter.bochtler@base.bund.de
Bottomley	Paul David William	European Commission Joint Research Centre Karlsruhe	Germany	dboksb3@gmail.com
Brachet	Jean-Christophe	CEA, Univ. Paris-Saclay	France	jean-christophe.brachet@cea.fr
Braun	Matthias	Framatome GmbH	Germany	matthias.braun@framatome.com
Brauns	Jörg	AREVA (Pensionär)	Germany	joerg@alles-fahrbar.de
Bürger	Berta	HUN-REN Centre for Energy Research	Hungary	burger.berta@ek.hun-ren.hu
Carénini	Laure	IRSN	France	laure.carenini@irsn.fr
Cazado	Mauricio Exequiel	KIT	Germany	mauricio.cazado@kit.edu
Charbal	Ali	CEA	France	ali.charbal@cea.fr

Participants of the 29th International QUENCH Workshop
19 - 21 November 2024, KIT, Germany

Family Name	First Name	Institution	Country	e-mail
Chosson	Raphael	Framatome	France	raphael.chosson@framatome.com
Di Nora	Vincenzo Anthony	Gesellschaft für Anlagen- und Reaktorsicherheit (GRS)	Germany	Vincenzo.diNora@grs.de
Dominguez	Cristina	IRSN	France	christina.dominguez@irsn.fr
Endrychová	Alžběta	UJP PRAHA, a.s.	CZ	endrychova@ujp.cz
Esmaili	Hossein	U.S. Nuclear Regulatory Commission	U.S.A.	hossein.esmaili@nrc.gov
Fargette	Andre	Framatome	France	andre.fargette@framatome.com
Farkas	Róbert	HUN-REN Centre for Energy Research	Hungary	farkas.robert@ek.hun-ren.hu
Frederick	Katerina	Westinghouse Electric Company	USA	katerina.frederick@westinghouse.com
Gabrielli	Fabrizio	KIT	Germany	fabrizio.gabrielli@kit.edu
Goebelbecker	Hans-Jürgen	KIT	Germany	h.goebelbecker@partner.kit.edu
Grosse	Mirco	KIT	Germany	mirco.grosse@kit.edu
Haste	Tim	Imperial College	England	tim.haste1@gmail.com
Hering	Wolfgang	Ingenieurbüro Hering	Germany	ib-whering@t-online.de

Participants of the 29th International QUENCH Workshop
19 - 21 November 2024, KIT, Germany

Family Name	First Name	Institution	Country	e-mail
Hollands	Thorsten	Gesellschaft fuer Anlagen- und Reaktorsicherheit (GRS) gGmbH	Germany	thorsten.hollands@GRS.DE
Hoog	Ines	Kerntechnische Entsorgung Karlsruhe GmbH (KTE)	Germany	Ines.Hoog@kte-karlsruhe.de
Howell	Jutta	KIT	Germany	jutta.howell@kit.edu
Isaksson	Patrick	Swedish Radiation Safety Authority (SSM)	Sweden	patrick.isaksson@ssm.se
Jannot	Emmanuel	Framatome GmbH	Germany	emmanuel.jannot@framatome.com
Jiménez Balbuena	Zaira Itzel	KIT	Germany	zaira.balbuena@kit.edu
Joung	SungHoon	Seoul National University	Korea	brivin5386@snu.ac.kr
Kiessling	Andreas	energy design & management consulting	Germany	ak@energy-design.info
Kolesnik	Mikhail	KIT	Germany	mikhail.kolesnik@kit.edu
Krejci	Jakub	UJP PRAHA a.s.	Czech Republic	krejci@ujp.cz
Lee	Youho	Seoul National University	Korea	leeyouho@snu.ac.kr
Litfin	Karsten	KIT	Germany	karsten.litfin@kit.edu
Liu	Tong	Shanghai Jiao Tong University	China	tongliu@sjtu.edu.cn

Participants of the 29th International QUENCH Workshop
19 - 21 November 2024, KIT, Germany

Family Name	First Name	Institution	Country	e-mail
Lovasz	Liviusz	GRS	Germany	liviusz.lovasz@grs.de
Martinez	Victor	ENSO	Spain	victor.martinez@ensobcn.com
Marx	Hermann-Josef	ehemals RWE, TÜV SÜD und HDB	Germany	hermann.josef.marx@t-online.de
Moch	Jürgen	KIT	Germany	juergen.moch@kit.edu
Nakamura	Kinya	Central Research Institute of Electric Power Industry	Japan	kinya@criepi.denken.or.jp
Nudi	Matthew	EPRI	USA	mnudi@epri.com
Peters	Ursula	KIT	Germany	Ursula.Peters@kit.edu
Rezchikova	Aleksandra	GRS	Germany	aleksandra.rezchikova@grs.de
Rössger	Conrado	KIT	Germany	conrado.roessger@kit.edu
Rouge	Emmanuel	IRSN	France	emmanuel.rouge@irsn.fr
Salnikova	Tatiana	Framatome GmbH	Germany	tatiana.salnikova@framatome.com
Sanchez-Espinoza	Victor Hugo	KIT	Germany	victor.sanchez@kit.edu
Schubert	Arndt	European Commission, Joint Research Centre, Karlsruhe	Germany	Arndt.SCHUBERT@ec.europa.eu

Participants of the 29th International QUENCH Workshop
19 - 21 November 2024, KIT, Germany

Family Name	First Name	Institution	Country	e-mail
Ševeček	Martin	Czech Technical University in Prague	Czech Republic	martin.sevecek@gmail.com
Spannagel	Gert	Ruhestand	Germany	gert.spannagel@t-online.de
Stahlberg	Gregor	RUB PSS	Germany	stahlberg@pss.rub.de
Stegmaier	Ulrike	KIT	Germany	ulrike.stegmaier@kit.edu
Steinbock	Lothar		Germany	lothar@sibex.de
Steinbrück	Martin	KIT	Germany	martin.steinbrueck@kit.edu
Stuckert	Juri	KIT	Germany	juri.stuckert@kit.edu
Sturm	Karl	KIT	Germany	karl.sturm@kit.edu
Tarumi	Naoki	Central Research Institute of Electric Power Industry	Japan	tarumi40522@criepi.denken.or.jp
Ver	Nora	HUN-REN Centre for Energy Research	Hungary	ver.nora@ek.hun-ren.hu
Wang	Shijie	Shanghai Jiao Tong University	China	pengpeng520@sjtu.edu.cn
Wang	Shisheng	KIT	Germany	shisheng.wang@kit.edu
Weick	Sarah	KIT	Germany	sarah.weick@kit.edu

Participants of the 29th International QUENCH Workshop
19 - 21 November 2024, KIT, Germany

Family Name	First Name	Institution	Country	e-mail
Yetik	Okan	Paul Scherrer Institut	Switzerland	okan.yetik@psi.ch


KIT
29th
International QUENCH Workshop
Karlsruhe Institute of Technology, Germany
19-21 November 2024
INNOVATION
LEHRE


KIT
FORSCHUNG
LEHRE
INNOVATION

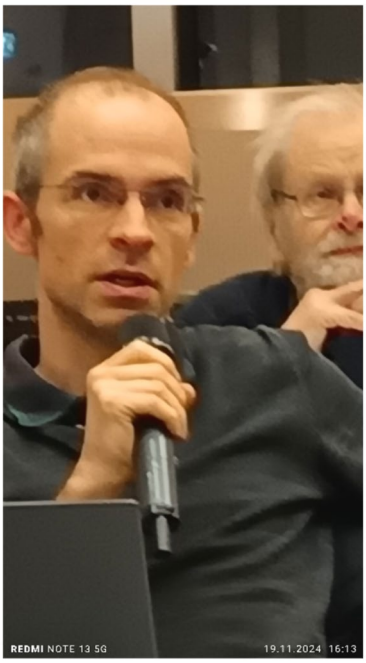
REDMI NOTE 13 5G
19.11.2024 16:13


REDMI NOTE 13 5G


20.11.2024 10:40


REDMI NOTE 13 5G
19.11.2024 16:59


REDMI NOTE 13 5G
20.11.2024 09:21


REDMI NOTE 13 5G
20.11.2024 09:28


REDMI NOTE 13 5G
20.11.2024 11:57


REDMI NOTE 13 5G


Händedesinfektion

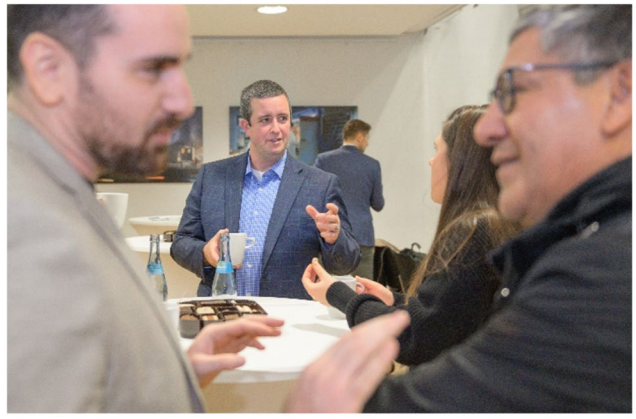

Any comments, corrections, complaints?

Please contact
martin. steinbrueck@kit.edu